TRANSACTIONS

American Society for Metals

VOL. XXXVIII 1947

TECHNICAL PROGRAM AND REPORTS OF OFFICERS AMERICAN SOCIETY FOR METALS — 28TH ANNUAL CONVENTION, ATLANTIC CITY, NOVEMBER 18 to 22, 1946

FOR purposes of record and for the benefit of members who were not in attendance at the Twenty-eighth Annual Convention of the Society, held in Atlantic City, November 18 to 22, 1946, the Programs of the Technical Papers and Educational Lectures together with the Reports of Officers for 1946 are herewith published in full.

TECHNICAL PAPERS PROGRAM

MONDAY, NOVEMBER 18

Ballroom, Municipal Auditorium—10:00 A. M.

High-Temperature Alloys

Joint Chairmen—A. E. Focke, Diamond Chain and Manufacturing Co., and M. F. Judkins, Firth-Sterling Steel Co.

The Development of a Turbosupercharger Bucket Alloy, by E. Epremian, Rensselaer Polytechnic Institute.

The Stress Rupture and Creep Properties of Heat Resistant Gas Turbine Alloys, by Nicholas J. Grant, Massachusetts Institute of Technology.

Structural Variations in Gas Turbine Alloys Revealed by the Stress-Rupture Test, by Nicholas J. Grant, Massachusetts Institute of Technology.

Room 20, Municipal Auditorium—10:00 A. M.

Magnesium Alloys

Joint Chairmen—C. F. Lucks, Battelle Memorial Institute, and W. E. Sicha, Aluminum Company of America

Some Special Metallographic Techniques for Magnesium Alloys, by P. F. George, Dow Chemical Co.

Calculation of Press Forging Pressures and Application to Magnesium Forgings, by R. L. Dietrich and G. Ansel, Dow Chemical Co.

Plastic Deformational Analyses on Pure Magnesium, by Louis A. Carapella and William E. Shaw, Mellon Institute of Industrial Research.

Room 21, Municipal Auditorium—10:00 A. M.

Stainless Steel

Joint Chairmen—Elmer Gammeter, Globe Steel Tubes, and
J. F. Kahles, University of Cincinnati

Stability of Austenite in Stainless Steels, by C. B. Post and W. S. Eberly, Carpenter Steel Co.

The Cold Work Hardening Properties of Stainless Steel in Compression, by F. K. Bloom, G. N. Goller and P. G. Mabus, Rustless Iron & Steel Div., American Rolling Mill Co.

Quantitative Evaluation of Intergranular Corrosion of 18-8 Ti, by Freeman J. Phillips, Carnegie-Illinois Steel Corp.

Room 20, Municipal Auditorium—2:00 P. M.

Steelmaking

Joint Chairmen—Horace C. Knerr, Metlab Co., and
C. G. Stephens, Gathmann Industrial Corp.

Ladle Deoxidation of Killed Steel With Silicon Carbide and Its Effect on Physical Properties and Hardenability, by E. A. Loria and A. P. Thompson, Mellon Institute of Industrial Research.

The Physical Chemistry of Acid Refining Process, by Yap Chu-Phay, National Resources Commission of China.

The Chromium-Oxygen Equilibrium in Liquid Iron, by Hsin-Min Chen, Carnegie-Illinois Steel Corp., and John Chipman, Massachusetts Institute of Technology.

Room 21, Municipal Auditorium—2:00 P. M.

Nonferrous Alloys

Joint Chairmen—Alfred Bornemann, Stevens Institute of Technology, and
W. E. Sicha, Aluminum Company of America

The Precipitation Heat Treatment of Work Hardened 61 S-W Aluminum Alloy, by J. J. Warga, Kaiser Fleetwings.

Constitution of the System Indium-Tin, by F. N. Rhines, W. M. Urquhart and H. R. Hoge, Carnegie Institute of Technology.

New Wrought Zinc Alloys Containing Small Amounts of Beryllium, by R. H. Harrington, General Electric Co.

TUESDAY, NOVEMBER 19

Ballroom, Municipal Auditorium—10:00 A. M.

Heat Treatment of Toolsteels

Joint Chairmen—Morris Cohen, Massachusetts Institute of Technology, and
A. L. Feild, Rustless Iron and Steel Div., American Rolling Mill Co.

Bainitic Hardening of High Speed Steel, by C. K. Baer and Peter Payson, Crucible Steel Co. of America.

The Tempering of High-Alloy Toolsteels, by G. A. Roberts, A. H. Grobe and C. F. Moersch, Jr., Vanadium-Alloys Steel Co.

Changes in Size and Toughness of High-Carbon High-Chromium Steels Due to Subzero Treatments, by L. E. Gippert and G. M. Butler, Jr., Allegheny Ludlum Steel Corp.

Room 20, Municipal Auditorium—10:00 A. M.

Crystal Structure

Joint Chairmen—Willard L. Hults, Schnefel Bros. Co., and
F. J. Robbins, Plomb Tool Co.

Pole Figures of the Effect of Some Cold Rolling Mill Variables on Low-Carbon Steel, by John Karl Wood, Jr., Pennsylvania State College.

X-Ray Study of the Effect of High Hydrostatic Pressures on the Perfection of Crystals, by Louis Rosen, Santa Fe, N. M.

A Periodic Chart for Metallurgists, by Carl A. Zapffe, Baltimore, Md.

Room 21, Municipal Auditorium—10:00 A. M.

Iron Alloys

Joint Chairmen—John E. Dorn, University of California, and Paul Ffield, Bethlehem Steel Co.

Formation and Transformation Studies of Iron-Carbon Powder Alloys, by J. F. Kahles, University of Cincinnati.

Carbon Concentration Control, by E. G. de Coriolis, O. E. Cullen and Jack Huebler, Surface Combustion Corp.

Decarburization During Annealing of Malleable Iron, by H. A. Schwartz and James Hedberg, National Malleable and Steel Castings Co.

Room 20, Municipal Auditorium—2:00 P. M.

Physical Properties and Testing

Joint Chairmen—L. E. Ekholm, Climax Molybdenum Co., and E. A. Snader, Westinghouse Electric Corp.

Precipitation in a Magnesium Sheet, by C. T. Haller, International Nickel Co., and C. S. Barrett, Institute for the Study of Metals, University of Chicago.

Folding in the Cupping Operation, by W. M. Baldwin, Jr., and T. S. Howald, Chase Brass & Copper Co.

Bearing Properties of 24 S-T Sheet and Shear Strength of 24 S-T Rivets at Elevated Temperatures, by A. E. Flanigan, L. F. Tedson and J. E. Dorn, University of California.

Room 21, Municipal Auditorium—2:00 P. M.

Temper Brittleness

Joint Chairmen—R. H. Aborn, Federal Shipbuilding & Dry Dock Co., and F. J. Robbins, Plomb Tool Co.

Development of Temper Brittleness in Alloy Steels, by W. S. Pellini, American Brake Shoe Co., and B. R. Queneau, Carnegie-Illinois Steel Corp.

A Metallographic Etchant to Reveal Temper Brittleness in Steel, by J. B. Cohen, A. Hurlich and M. Jacobson, Watertown Arsenal.

Electrolytic Conductivity as a Method for Studying Electronic Transitions in Elements—Application to Iron, Nickel and Cobalt, by W. R. Ham and C. H. Samans, American Optical Co.

WEDNESDAY, NOVEMBER 20

Ballroom, Municipal Auditorium—10:00 A. M.

A.S.M. Annual Meeting

Edward de Mille Campbell Memorial Lecture—

The Effect of Changes in Condition of Carbides on Some Properties of Steel, by J. B. Austin, United States Steel Corp.

Chairman—Herbert J. French, International Nickel Co.

Room 20, Municipal Auditorium—2:00 P. M.

Heat Resisting Alloys

Joint Chairmen—F. C. Lehman, Joslyn Manufacturing and Supply Co., and W. A. Mudge, International Nickel Co.

Changes in Austenitic Chromium-Nickel Steels During Exposures at 1100 to 1700 F, by Peter Payson and C. H. Savage, Crucible Steel Co. of America.

Cast Heat Resistant Alloys of the 16% Chromium, 35% Nickel Type, by Howard S. Avery and Norman A. Matthews, American Brake Shoe Co.

The Apparent Influence of Grain Size on the High-Temperature Properties of Austenitic Steels, by C. L. Clark, Timken Roller Bearing Co., and J. W. Freeman, University of Michigan.

Room 21, Municipal Auditorium—2:00 P. M.

Research and Inspection

Joint Chairmen—R. C. Dalzell, Revere Copper and Brass, Inc., and W. J. Diederichs, The Autocar Co.

A Study of Furnace Brazing as Applied to 12% Chromium Low-Carbon Steel, by T. H. Gray, Westinghouse Electric Corp.

Stress Cracking of Electroplated Lockwashers, by K. B. Valentine, Pontiac Motor Div., General Motors Corp.

Nondestructive Inspection of Mine Hoist Cable, by P. E. Cavanagh, Allen B. DuMont Laboratories, Inc., and R. S. Segsworth, General Engineering Co., Ltd.

THURSDAY, NOVEMBER 21

Ballroom, Municipal Auditorium—10:00 A. M.

Transformation of Austenite

Joint Chairmen—V. N. Krivobok, International Nickel Co., and N. I. Stotz, Braeburn Alloy Steel Co.

The Interrupted Quench and Its Practical Aspects, by Howard E. Boyer, American Bosch Corp.

Experimental Studies of Continuous Cooling Transformations, by C. A. Liedholm, Curtiss-Wright Corp.

Isothermal Transformation of Austenite, by Axel Hultgren, K. Tekniska Hogskolan, Sweden.

Room 20, Municipal Auditorium—10:00 A. M.

Copper Alloys

Joint Chairmen—H. W. Highriter, Vascoloy-Ramet Corp., and S. E. Sinclair, The Geometric Tool Co.

Influence of the Strain Rate and the Stress System on the Mechanical Properties of Copper, by D. J. McAdam, Jr., G. W. Geil and D. H. Woodard, National Bureau of Standards.

Copper-Manganese Alloys—the Properties of Cold-Worked and Annealed Alloys Containing 2 to 20% Manganese, by R. S. Dean, J. R. Long, T. R. Graham and D. P. Sugden, U. S. Bureau of Mines.

Age Hardening Copper-Cobalt-Manganese Alloys, by Jay W. Fredrickson, University of Utah.

Room 21, Municipal Auditorium—10:00 A. M.

Steelmaking

Joint Chairmen—O. W. Ellis, Ontario Research Foundation, and A. W. Grosvenor, Drexel Institute of Technology

Ingot Factors in the Production of Seamless Gun Tubes, by J. W. Spretnak, Carnegie Institute of Technology, K. L. Fetters, Youngstown Sheet & Tube Co., and E. L. Layland, Westinghouse Electric Corp.

Kinetics of Solidification of Killed Steel Ingots, by J. W. Spretnak, Carnegie Institute of Technology.

Theoretical Thermal Studies of Steel Ingot Solidification, by Victor Paschkis, Columbia University.

Room 20, Municipal Auditorium—2:00 P. M.

Hardness and Hardenability

Joint Chairmen—A. O. Crobaugh, Ingersoll-Rand Co., and J. O. Jeffrey, Cornell University

The Measured Knoop Hardness of Hard Substances and Factors Affecting Its Determination, by Newman W. Thibault and Helen L. Nyquist, Norton Co.

Determination of Knoop Hardness Numbers Independent of Load, by L. P. Tarasov and N. W. Thibault, Norton Co.

Hardenability of Shallow Hardening Steels Determined by the P-V Test, by B. F. Shepherd, Ingersoll-Rand Co.

Room 21, Municipal Auditorium—2:00 P. M.

Physical Properties

Joint Chairmen—H. I. Dixon, Sterling Alloys, Inc., and T. Holland Nelson, Consulting Metallurgist

The Effect of Composition on the Fatigue Strength of Decarburized Steel, by L. R. Jackson and T. E. Pochapsky, Battelle Memorial Institute.

Hardness Testing of Metals and Alloys at Elevated Temperatures, by Frederick P. Bens, Climax Molybdenum Co. of Michigan.

Mechanical Properties of Cast Low-Alloy Steels, by Malcolm F. Hawkes, Carnegie Institute of Technology.

FRIDAY, NOVEMBER 22

Ballroom, Municipal Auditorium—10:00 A. M.

Carburizing

Joint Chairmen—C. F. Pogacar, Mellon Institute of Industrial Research, and G. A. Roberts, Vanadium-Alloys Steel Co.

Carburized Cases of Hypoeutectoid Carbon Content, by P. C. Rosenthal and G. K. Manning, Battelle Memorial Institute.

Carbide and Oxide in Surface Zones of Carburized Alloy Steels, by Axel Hultgren and Erik Hagglund, K. Tekniska Hogskolan, Sweden.

Transformations in Krupp-Type Carburizing Steels, by A. R. Troiano and J. E. DeMoss, University of Notre Dame.

Room 20, Municipal Auditorium—10:00 A. M.

Microstructure

Joint Chairmen—A. O. Schaefer, The Midvale Co., and R. G. Spencer, Washington University Research Foundation

The Effects of Microstructure on the Mechanical Properties of Steel, by J. H. Hollomon, L. D. Jaffe, D. E. McCarthy and M. R. Norton, Watertown Arsenal.

Metallurgical and Structural Investigation of Steel Castings for Aircraft, by L. W. Smith and L. D. Morris, Cornell Aeronautical Laboratory.

Factors Influencing the Pearlitic Microstructure of Annealed Hypoeutectoid Steel, by R. A. Grange, United States Steel Corp.

Room 21, Municipal Auditorium—10:00 A. M.

Cast Steels

Joint Chairmen—D. M. McCutcheon, Ford Motor Car Co., and F. N. Rhines, Carnegie Institute of Technology

The Effect of Manganese on the Properties of Cast Carbon and Carbon-Molybdenum Steels, by N. A. Ziegler, W. L. Meinhart and J. R. Goldsmith, Crane Co.

Relation of Quenching Rate and Hardenability to the Mechanical Properties of Several Heat Treated Cast Alloy Steels, by Charles R. Wilks, Howard S. Avery and Earnshaw Cook, American Brake Shoe Co.

A Laboratory Study of Quench Cracking in Cast Alloy Steels, by M. C. Udy and M. K. Barnett, Battelle Memorial Institute.

Room 21, Municipal Auditorium—2:00 P. M.

Hydrogen Embrittlement

Joint Chairmen—M. Gensamer, Pennsylvania State College, and M. J. Stutzman, Midwest Research Institute

Practical Importance of Hydrogen in Metal-Arc Welding of Steel, by S. A. Herres, Battelle Memorial Institute.

Effect of Composition, Heat Treatment, and Cold Work on the Hydrogen Embrittlement of Stainless Steel Wire During Cathodic Pickling, by Carl A. Zapffe, Baltimore, Md., and O. George Specht, Jr., Grede Foundries.

Acid Composition, Concentration, Temperature and Pickling Time as Factors in the Hydrogen Embrittlement of Mild Steel and Stainless Steel Wire, by Carl A. Zapffe and M. Eleanor Haslem, Baltimore, Md.

Measurement of Embrittlement During Chromium and Cadmium Electroplating and the Nature of Recovery of Plated Articles, by Carl A. Zapffe and M. Eleanor Haslem, Baltimore, Md.

EDUCATIONAL LECTURES

MONDAY, NOVEMBER 18

Room B, Municipal Auditorium—2:00 P. M.

Sleeve Bearing Metals

Chairman—John K. Anthony, Metro Smelting Co.

Fundamental Considerations Concerning the Behavior of Bearings, by R. W. Dayton, Battelle Memorial Institute.

Some General Comments on Bearings, by Carl E. Swartz, Johns Hopkins University.

Cast Bronze Bushings, by Leighton M. Long, Toledo, Ohio.

Porous Metal Bushings, by A. J. Langhammer, Chrysler Corp., Amplex Division.

Room A, Municipal Auditorium—3:00 P. M.

Electronic Inspection

Chairman—J. O. Lord, Ohio State University

Electronic Methods for the Measurement of Stress in Metals, by Henry F. Hamburg, Chance Vought Aircraft Division.

Room B, Municipal Auditorium—8:00 P. M.

Sleeve Bearing Metals

Chairman—Carl E. Swartz, Johns Hopkins University

Newer Bearing Materials, by I. C. Sleight, Menasco Mfg. Co., and L. W. Sink, P. R. Mallory and Co.

Electroplated Bearings, by Ralph A. Schaefer, Cleveland Graphite Bronze Co.

Aluminum Alloy Bearings, by H. Y. Hunsicker, Aluminum Co. of America.

Room A, Municipal Auditorium—8:00 P. M.

Physical Metallurgy of Aluminum

Chairman—E. H. Dix, Jr., Aluminum Company of America

Constitution of Aluminum Alloys, by W. L. Fink, Aluminum Co. of America.

TUESDAY, NOVEMBER 19

Room B, Municipal Auditorium—2:00 P. M.

Sleeve Bearing Metals

Chairman—A. F. Underwood, General Motors Corp.

Mechanical Features of Steel-Backed Bearings, by E. Crankshaw and J. Menrath, Cleveland Graphite Bronze Co.

Moraine Durex-100 Engine Bearings, by J. A. Lignian, Moraine Products Division, General Motors Corp.
Bronze-Backed Bearings, by Bernard J. Esarey, National Bearing Division, American Brake Shoe Co.
Preparing Cast Iron Surfaces for Bonding, by J. H. Shoemaker, Kolene Corp.

Room A, Municipal Auditorium—3:00 P. M.

Electronic Inspection

Chairman—J. A. Berger, Molybdenum Corp. of America

Spectrochemical Analysis of Metals and Alloys by Direct Intensity Measurement Methods, by J. L. Saunderson, Dow Chemical Co.
Uses of the DuMont Cyclograph for Testing of Metals, by R. S. Segsworth, General Engineering Co., Ltd.

Room B, Municipal Auditorium—8:00 P. M.

Sleeve Bearing Metals

Chairman—A. J. Langhammer, Chrysler Corp.

Selection of Bearing Materials, by Arthur F. Underwood, General Motors Research Laboratories.
Selection of Bearing Materials in the Electrical Industry, by D. F. Wilcock, Thomson Laboratory, General Electric Co.
Railroad Journal Bearings, by E. S. Pearce, Railway Service and Supply Corp.

Room A, Municipal Auditorium—8:00 P. M.

Aluminum

Chairman—E. H. Dix, Jr., Aluminum Company of America

Metallography of Aluminum Alloys, by F. Keller, Aluminum Co. of America.

WEDNESDAY, NOVEMBER 20

Room B, Municipal Auditorium—2:00 P. M.

Sleeve Bearing Metals

Chairman—R. W. Dayton, Battelle Memorial Institute

Aircraft Engine Bearings, by J. Palsulich and R. W. Blair, Wright Aeronautical Corp.
British Thought and Practice: How They Differ From American, by W. H. Tait, Glacier Metals Co., Ltd.

Room A, Municipal Auditorium—3:00 P. M.

Electronic Inspection

Chairman—G. R. Fitterer, University of Pittsburgh

Supersonic Inspection of Metals, by E. O. Dixon, Ladish Drop Forge Co.
Determination of Seams in Steels by Magnetic Analysis Equipment, by Charles M. Lichy, Jones & Laughlin Steel Corp.

Room A, Municipal Auditorium—8:00 P. M.

Aluminum

Chairman—E. H. Dix, Jr., Aluminum Company of America

Commercial Cast Aluminum Alloys, by W. E. Sicha, Aluminum Co. of America.

Room B, Municipal Auditorium—8:00 P. M.

Cast Iron

Chairman—J. O. Lord, Ohio State University

Structure of Cast Iron, by Alfred Boyles, U. S. Pipe & Foundry Co.

THURSDAY, NOVEMBER 21

Room B, Municipal Auditorium—2:00 P. M.

Cast Iron

Chairman—W. J. Diederichs, Autocar Co.

Structure of Cast Iron, by Alfred Boyles, U. S. Pipe & Foundry Co.

Room A, Municipal Auditorium—3:00 P. M.

Electronic Inspection

Chairman—F. Keller, Aluminum Company of America

The Electron Microscope and Its Application to Metals, by C. S. Barrett, University of Chicago.

Room B, Municipal Auditorium—4:00 P. M.

Aluminum

Chairman—E. H. Dix, Jr., Aluminum Company of America

Commercial Wrought Aluminum Alloys, by J. A. Nock, Jr., Aluminum Co. of America.

FRIDAY, NOVEMBER 22

Room B, Municipal Auditorium—2:00 P. M.

Cast Iron

Chairman—C. O. Burgess, Union Carbide and Carbon Research Laboratories

Structure of Cast Iron, by Alfred Boyles, U. S. Pipe & Foundry Co.

Room A, Municipal Auditorium—2:00 P. M.

Electronic Inspection

Chairman—C. F. Pogacar, Mellon Institute of Industrial Research

Electronics in Liquid Steel, by Harold T. Clark, Jones & Laughlin Steel Corp.

Room 20, Municipal Auditorium—2:00 P. M.

Aluminum

Chairman—H. Y. Hunsicker, Aluminum Company of America

Thermal Treatments of Aluminum Alloys, by E. H. Dix, Jr., Aluminum Co. of America.

ANNUAL MEETING OF AMERICAN SOCIETY FOR METALS

Atlantic City, Wednesday, November 20, 1946

The meeting was called to order by President Herty, who announced that the first order of business was the President's report. He then asked Vice-President Boegehold to occupy the chair while he read his report. This is published in full beginning on the next page of this volume of TRANSACTIONS.

VICE-PRESIDENT BOEGEHOLD: You have heard the report of the President. There being no comments the report will stand as read. I now return the chair to the President.

PRESIDENT HERTY: The next order of business will be the annual report of the Treasurer, Harold K. Work.

Treasurer Work presented his report which appears in full beginning on page 13.

PRESIDENT HERTY: You have heard the report of the Treasurer. There being no objections it will stand as read. The next order of business is the report of the Secretary.

Secretary Eisenman presented his report which appears in full beginning on page 15.

PRESIDENT HERTY: You have heard the report of the Secretary. There being no objections it will stand as read. The next order of business is the election of officers. See page 22.

ANNUAL ADDRESS OF THE PRESIDENT

CHARLES H. HERTY, JR., *President*

Twenty-eighth Annual Convention, Atlantic City, November 19, 1946

AT the last annual meeting, held in Cleveland, Ohio, in February 1946, the President, Kent R. Van Horn, had the pleasure of reviewing for you the activities of your Society during the war years and he presented a story of which we all may be justly proud. At this time it is my duty to present a brief summary of the Society's activities during the reconversion year just past.

It was quite freely predicted at one time that our membership would decrease sharply following the end of hostilities, but a review of membership data for previous years shows the following: October 1, 1941, 12,684 members; on October 1, 1945, 19,629 members, and on November 1, 1946, 20,134 members. We have held all our war gains and are actually on a sound and steady increase in membership. Another interesting figure deals with the change in junior membership. On October 1, 1941, just before we entered the war, the junior membership was 790, equal to 6.3% of the total. On October 1, 1945, this had dropped to 184, equal to 0.9% of the total. On November 1, 1946, we had 425, equal to 2.1%. If the pre-war ratio

of junior members holds, we should look forward to from 1200 to 1500 junior members in the near future. This holds much promise for the continuing health and success of the Society.

We have survived the immediate past with no losses in chapters, though some have been hard pressed, and have added four members to the family—Des Moines, Los Alamos, Saginaw Valley, and Michigan College of Mining and Technology. We now have 67 chapters.

This year your president carried the secretary's suitcases to 28 chapters. Even with restrictions on Pullman reservations, uncertainties as to meetings due to strikes and the discomforts of wartime travel with which we are all familiar, the swing around the circuit was a great pleasure and I was particularly impressed with the determination of certain chapters to go through under adverse prospects, and with the enthusiasm of the members of all chapters. In talking matters over with the various executive committees and looking over the chapters' programs for the year, it was interesting to note the presence and activity of so many of the younger members. The Society is a splendid vehicle for young men in our industry to become acquainted with their fellows and to become known to the profession at large, through the media of the Metal Congress and local section meetings. Here is the place where the Society can do its best work in promoting the interests of its members, and I believe that the chapters as a whole could take advantage of the fine success that certain chapters have had with meetings where the speakers consist of a group of the younger members. More power to them.

The extraordinary advances made in all scientific fields during the war years are now beginning to be felt in our peacetime lives. Many of the developments were in the field of metallurgy, and many others will profoundly affect our metallurgical activities in years to come. We must make certain that our Society keeps abreast of the times in these matters. We have the personnel and the vehicles for so doing.

The Board of Trustees has held the customary four meetings per year and I can assure you that each meeting was full of interesting items as regards the Society's welfare. These meetings serve as an excellent clearing house for questions and suggestions from the chapters as a complete discussion can be held on matters which are brought up from time to time by the local chapter executive committees. This year a goodly proportion of the time of the meetings was taken up with educational activities. The Advisory Committee

on Metallurgical Education, under the chairmanship of Dr. R. F. Mehl, is continuing its studies of metallurgical training and educational requirements. This is necessarily a long-time effort, but progress is definitely being made. Another educational activity is the production of the "Techbooks". This project is under way with some 22 manuscripts in process and it is hoped that these will be most useful to a large section of the membership and to nonmembers in the metal industry. It might be stated here that this is a difficult task because it is generally true that a technical expert has considerable difficulty in preparing a technical subject in a nontechnical manner.

The new METALS HANDBOOK has been delayed in publication due to shortages of paper and to the tremendous demands on the printing industry. However, it is expected that the HANDBOOK will appear in the spring of 1947. In this connection it is my privilege to pay high tribute to Dr. Taylor Lyman of the home office, to G. V. Luerssen, Chairman of the Handbook Committee, and to some 2500 members of the Society who have actively and unselfishly given of their time during the past year in the revision of old articles and in the preparation of new material. I can safely predict that the new HANDBOOK will be one of the finest reference books available in the field of metallurgy.

METAL PROGRESS continues as an outstanding publication in the metallurgical field, and THE METALS REVIEW is increasing in popularity and usefulness each month. A new format for the latter will be presented soon as the result of a poll of the members.

Again in connection with education, I am pleased to report that Major Graves Taylor, after an absence of 4 years in the armed services, has returned to resume his position as Public Relations Director for the Society. The Board of Trustees feels that the matter of public relations is of vital importance to the Society's place in the metallurgical world.

You will very shortly hear the Treasurer's report, and I will only state here that the Society is on solid ground with respect to its finances.

The 1945 convention was held in Cleveland in February 1946, the postponement being due to wartime curtailment of facilities. A splendid technical program and an equally splendid metals show were heard and seen by thousands of members of the Society. At the annual dinner, the following 1945 awards were made:

The President's Medal was awarded to Dr. Marcus A. Grossmann. The Henry Marion Howe Medal was awarded to Dara P. Antia, Stewart G. Fletcher and Morris Cohen for their paper entitled "Structural Changes During the Tempering of High Carbon Steels". The Campbell Memorial Lecture was presented by Dr. Maxwell Gensamer on the subject "Strength and Ductility". The Sauveur Achievement Award was presented to Robert S. Archer for his contributions to the development of aluminum alloys. The Gold Medal of the American Society for Metals was presented to Dr. Earle C. Smith in recognition of his outstanding achievements in the field of steel production and processing. The American Society for Metals Medal for the Advancement of Research was awarded to Mr. Gerard Swope, retired President and Director of the General Electric Company, for his consistent sponsorship and influence in financing and prosecuting metallurgical research.

The 1946 Metal Congress is now upon us. There is no need to give statistics on this week's activities as all of you present can see for yourselves what a successful week this is. I believe that this week's technical program is one of the finest we have ever had, and we are highly honored by the active co-operation of the American Institute of Mining and Metallurgical Engineers, the American Welding Society, and the American Industrial Radium and X-ray Society. The co-operative efforts among such societies as are represented here made the National Metal Congress a tremendous success, and the presence of distinguished guests from across the water add an international flavor to our proceedings.

In March 1947, the Western Metals Congress will be resumed, this time at Oakland, California. This again gives promise of being an oustanding event on the West Coast, and it is particularly to be noted that the eastern and mid-western states are usually confronted with extraordinarily inclement weather at that time. The National Metal Congress for next year will be held in Chicago the week of October 20, 1947.

Finally, I should repeat what each preceding President has stated, namely, that a great part of the success of the Society and of the Metal Congress is due to the untiring activity of our Secretary—W. H. Eisenman, and his able staff. As the years go by it is more and more apparent that the strong central office which the Society maintains, and the loyal and active interest of the local chapters, are the fundamentals for our success.

TREASURER'S REPORT

HAROLD K. WORK, *Treasurer*

Your Treasurer takes pleasure in submitting this report covering the fiscal year ended August 31, 1946.

The cash balance on August 31, 1946, was $148,607.73. This figure includes advance receipts applicable to the 1946 Convention in the amount of $80,115.00.

Surplus funds were used during the past year to increase the investment portfolio in the amount of $258,189.77. Total security holdings on August 31, 1946, were $1,106,723.88.

Total assets increased from $1,155,724.43 to $1,586,315.60. Earned surplus increased from $974,289.51 to $1,223,872.60.

Accounts Receivable at August 31, 1946, amounted to $126,-387.70 which includes $87,715.00 applicable to the 1946 Convention, covering unpaid space rental billings at that date. The average age of all open accounts is considerably less than 30 days.

General Inventory has increased during the year approximately $12,000.00 while cost of paper stocks on hand is approximately $2,500.00 greater than at the close of the previous year.

Office furniture and fixtures has increased $11,000.00 due largely to the purchase of new equipment to more satisfactorily handle certain mailing and billing problems.

Improvements in the amount of $1,800.00 were made during the year to the headquarters buildings, while depreciation of approximately $3,300.00 was written off on buildings during the same period.

Close contact with the investment market is maintained by the Finance Committee, the Trustees and other officers of the Society. Frequent conferences are held with the ASM fiscal agents, The Cleveland Trust Company, to consider investment problems.

Additional purchases of securities during the year have added $259,000.00 to government holdings, while disposals effected during the year have reduced bond holdings $31,000.00, preferred stocks $10,000.00 and common stocks $11,000.00. Land Trust Certificates amounting to $49,000.00 were also acquired.

As of August 31, 1946, the total cost of securities (excluding Headquarters) was $1,100,947.71 and the market value was approximately $1,208,751.61.

CONDENSED AUDITED BALANCE SHEET
AMERICAN SOCIETY FOR METALS
As of August 31, 1946

ASSETS	
Cash	$ 148,607.73
Securities	1,106,723.88
Accounts receivable	126,387.70
Inventories	65,441.95
Other assets	7,227.63
Real estate	70,502.08
Office furniture, fixtures, and equipment	35,229.71
Deferred charges	26,194.92
	$1,586,315.60
LIABILITIES, RESERVES, AND SURPLUS	
Accounts payable	$ 59,613.00
Reserves	135,000.00
Deferred income	167,830.00
Surplus	1,223,872.60
	$1,586,315.60

AUDITED INCOME AND EXPENSE STATEMENT
AMERICAN SOCIETY FOR METALS
Year Ended August 31, 1946

INCOME		
METAL PROGRESS—monthly publication	$ 454,833.57	
National Metal Exposition—Cleveland, February 1946	212,627.28	
Memberships	127,684.62	
THE METALS REVIEW—monthly publication	16,516.70	
ASM METALS HANDBOOK	12,180.68	
TRANSACTIONS	9,427.35	
BUYERS' GUIDE	3.80	$ 833,274.50
Books published (includes sales of THE REVIEW OF METAL LITERATURE amounting to $17,998.80)		78,891.16
Interest and dividends earned		32,335.85
Profit on disposal of securities		8,199.48
General reprints and index		5,885.64
Discount earned		4,813.95
Sundry sales, etc.		2,337.41
Books purchased for resale		387.48
TOTAL INCOME		$ 966,125.47
EXPENSES		
METAL PROGRESS—monthly publication	$ 323,365.19	
National Metal Exposition—Cleveland, February 1946	110,358.97	
Books published	59,109.74	
THE METALS REVIEW—monthly publication	47,002.99	
Membership	33,068.17	
General expenses	25,462.96	
ASM METALS HANDBOOK	25,027.44	
TRANSACTIONS	24,428.13	
Secretary's office	17,948.83	
Headquarters	16,853.77	
Accounting department	10,579.95	
President's office	3,012.10	
Trustees	2,761.05	
National committees	2,703.83	
BUYERS' GUIDE	1,442.76	
Technical books	705.92	$ 703,831.80
Library salaries, supplies, etc.		6,077.90
General reprints and index		4,646.56
Miscellaneous merchandise, etc.		872.03
Lectures		525.00
Medal fund expense		413.59
Medals and awards		175.50
TOTAL EXPENSES		$ 716,542.38
Excess of Income over Expense		$ 249,583.09

The investment portfolio now shows:

Real Estate (Headquarters)	$ 70,500.00	6.0%
U. S. Government Bonds	719,710.00	61.3%
Canadian Government Bonds	10,000.00	0.9%
Railroad Bonds	13,370.00	1.4%
Industrial Bonds	18,550.00	1.5%
Common Stocks	270,720.00	23.1%
Preferred Stocks	19,550.00	1.6%
Land Trust Certificates	49,050.00	4.2%
	$1,171,450.00	100.0%

The net quick assets at August 31, 1946, amounted to approximately $1,161,500.00 which figure is 1.6 times the total operating cost of the Society and the National Metal Exposition during the year ended on that date.

The statement of income and expense for the past year is as follows in total:

Income	$ 966,125.47	
Expense	716,542.38	
Excess of Income over Expense		$ 249,583.09

Net sales of the METALS HANDBOOK amounted to $12,180.68. The sale of other technical books published amounted to approximately $61,000.00.

Gross income from membership amounted to $213,900.00 which is approximately 0.1% less than the preceding year. Of this amount $87,340.00 was returned to the chapters.

In addition to the assets of the national office, the chapters reported, at the end of the 1945-46 fiscal year, total assets of approximately $178,230.00 which is an increase over the previous year of $15,248.00.

ANNUAL REPORT OF THE SECRETARY

WILLIAM H. EISENMAN, *Secretary*

The American Society for Metals on November 1, 1946, had a total membership of 20,134. Of this number 18,285 or 91% were the member classification; 1396 or 7% were sustaining members; while 425 or 2.1% were juniors. There are 28 honorary and founder members.

On November 1, 1945, the Society had a total membership of 19,912. The membership this year showed a gain of 1%.

Transactions

Since the last National Metal Congress, Vols. 36 and 37 of the Transactions were published and distributed to the membership on request in July 1946. These two volumes total 1156 pages and constitute 35 articles with their discussions.

Vols. 36 and 37 contain all of the papers presented at the February 1946 Convention held in Cleveland and their discussion together with other interim papers received during the year. The president, secretary and treasurer's report for 1944 and other current items of record were included in Vol. 36, together with a report of the Convention.

Metal Progress

Records for Metal Progress during the fiscal year of 1946 reflect a healthy condition.

The tabulation below shows that the revenue advertising pages (2024) all but reached the record set during the preceding year. Net paid circulation (Audit Bureau of Circulation figures) has remained about stationary for two years, although it is noteworthy that the paid subscriptions for extra copies or for copies to nonmembers has increased from a relatively constant prewar figure of 500 to almost exactly three times that figure.

Fiscal Year	Editorial Pages	Revenue Advertising	Net Paid Circulation*
1941	645	1078	13,018
1942	699	1276	15,412
1943	688	1595	16,363
1944	648	1937	18,774
1945	674	2045	20,410
1946	832	2024	20,708

This tabulation shows that an unprecedented number of reading pages has been published this year. This is due to a record-breaking Annual Reference Issue for October, last, and to several unusually long and comprehensive articles about matters of interest to ASM members. These have included a condensation of the Smyth Report on the Atomic Bomb, verbatim reports of the important round table discussions held at the last convention on Nucleonics and Atomic Power and on Superalloys for high temperature services, a review of the wartime investigations of the high chromium alloys for synthetic

*Audit Bureau of Circulation figure for June. Print order is about 15% larger.

rubber plants, and the notable discussion of Science and Life in the World at the celebration of the George Westinghouse centennial.

A very large number of Society members make up the list of principal contributors to METAL PROGRESS, and the thanks of the Board of Trustees are gratefully tendered to them.

It is also my pleasant duty to record that, as a result of a little advertising campaign starting last November in METAL PROGRESS and THE METALS REVIEW, American sponsors were found for no less than 593 French metallurgists, doctors, teachers and professional men (or their war-widows), each sponsor promising to send food boxes to his protégé at monthly intervals. Names of worthy French families were secured through the American Friends Service Committee in France, French engineering societies, and the personnel departments of important French metallurgical firms. A large number of grateful letters have been received; their common tenor is gratitude and surprise that totally unknown friends have helped them through a difficult period.

METALS REVIEW

THE METALS REVIEW during the past year has continued to fulfill its three-fold function of providing news of ASM chapter and national activities, brief annotations of all published literature in the metals field in the "Review of Current Metal Literature", and descriptions of new products and processes.

During the months from October 1945 through September 1946, 251 reports were published of meetings held by the 70 chapters of the Society—a tribute to the willing efforts of the chapter publicity chairmen and the reporters.

During the same period 5500 magazine articles and books were annotated in the Review of Current Metal Literature. In the spring of 1946 Volume II for 1945 of the collected installments of the Metal Literature Review was published and found a wide sale among members of the Society who wished to retain this feature in a more permanent and well-indexed form.

The regular issues of THE METALS REVIEW carried either 20 or 24 pages, with one special issue in January of 32 pages devoted to the National Metal Congress and Exposition. Space in the 12 issues from October 1945 through September 1946 was allocated as follows:

Reports of chapter and national ASM activities and other news items	31.8%
Review of Current Metal Literature	41.5%
New Products and Catalogs	16.0%
Advertising	10.7%

METALS HANDBOOK

The manuscript for the new METALS HANDBOOK is in the hands of the editor, and at the present time is occupying the efforts of a staff of eight people in final preparation of the manuscript for the printer.

Some 1200 pages have already been forwarded to the printer to set in type, and the balance of the material is being forwarded as soon as it is ready.

It is contemplated that the METALS HANDBOOK will be on the press about February 1, and the 45,000 copies required will be completed and ready for distribution within a period of ninety days.

Every article in the METALS HANDBOOK has been revised and brought up to date; many new articles have been added; and altogether the book will undoubtedly continue as "the bible of the metal industry".

The members of the METALS HANDBOOK Committee are:

G. V. Luerssen, Chairman
Earnshaw Cook
A. J. Herzig
J. B. Johnson
J. J. Kanter
C. H. Lorig
H. W. McQuaid
H. S. Rawdon
N. E. Woldman
Lyall Zickrick, AIME Rep.
H. L. Maxwell, AWS Rep.
C. W. Obert, IAA Rep.
J. H. Romann, ASME Rep.
Taylor Lyman, Secretary

Books

During the past fiscal year, a total of 17,398 books published by the Society were sold to members and others. This figure includes 890 ASM METALS HANDBOOKS.

During this period eight new titles were added to our publication list. These are:

ASM Review of Metal Literature—Vol. 1
ASM Review of Metal Literature—Vol. 2
Cold Working of Brass
Corrosion of Metals
Heat Treatment of Metals
Induction Heating
Magnesium
Talks About Steel Making

Many of the previous titles were reprinted.

Numerous new titles are now in the process of production and will be made available during the ensuing year.

Publications Committee

The Publications Committee for the year 1945-46 was made up of the following personnel: R. M. Brick, Chairman; R. H. Aborn, R. E. Cramer, H. I. Dixon, A. L. Feild, R. P. Koehring, H. B. Osborn, Jr., R. W. Roush, E. S. Rowland, A. O. Schaefer, G. A. Sellers, Gordon Sproule, R. L. Templin, H. S. VanVleet, B. B. Wescott, and Ray T. Bayless, Secretary.

During the year and up to the present time the Committee has reviewed and approved 67 papers, 2 are now in the process of review, and rejected 7. Two manuscripts were withdrawn by the authors during their review.

The Publications Committee held one formal meeting on August 2, 1946, at which time the final arrangements for the technical program at this Convention were made. Sixty-four papers were approved and scheduled for presentation. Only 29 of the papers to be presented were prepared in preprint form due to paper shortage, printers manpower shortage and time limitations. The Committee recommended that the balance of the papers be prepared in photostat form to be sent to selected persons for the purpose of obtaining written discussion from them. It was recommended that 5 copies be prepared of each of these papers.

Preprints

Of the 64 papers being presented at this Convention, 29 were prepared in preprint form and distributed to those members of the Society who had requested them. The total number of pages for the 1946 preprints is 806. A total of 34,000 preprint copies were distributed free to the membership to date.

Educational Committee

The Educational Committee for the year 1946 was composed of the following personnel: J. O. Lord, Chairman; C. R. Austin, G. R. Fitterer, W. D. McMillan, H. B. Pulsifer, C. H. Shapiro, C. G. Stephens, R. D. Stout, and Ray T. Bayless, Secretary.

The Committee held one meeting on March 1, 1946, at National Headquarters. The main purpose of this meeting was the planning and selecting of subjects and authors for the educational lecture series

that are being presented at this Convention. The titles of the lectures are:

Three Lectures on "Structure of Cast Iron"—By Alfred Boyles, U. S. Pipe & Foundry Co.

Five Lectures on "Sleeve Bearing Metals"—

1a. *Fundamental Considerations Concerning the Behavior of Bearings*—By R. W. Dayton, Battelle Memorial Institute.
b. *Some General Comments on Bearings*—By Carl E. Swartz, Johns Hopkins University.
c. *Cast Bronze Bushings*—By Leighton M. Long, Toledo, Ohio.
d. *Porous Metal Bushings*—By A. J. Langhammer, Chrysler Corp., Amplex Division.
2a. *Newer Bearing Materials*—By I. C. Sleight, Menasco Mfg. Co. and Wayne Sink, P. R. Mallory and Co.
b. *Electroplated Bearings*—By Ralph A. Schaefer, Cleveland Graphite Bronze Co.
c. *Aluminum Alloy Bearings*—By H. Y. Hunsicker, Aluminum Company of America.
3a. *Mechanical Features of Steel-Backed Bearings*—By E. Crankshaw and J. Menrath, Cleveland Graphite Bronze Co.
b. *Moraine Durex-100 Engine Bearings*—By J. A. Lignian, Moraine Products Div., General Motors Corp.
c. *Bronze-Backed Bearings*—By Bernard J. Esarey, National Bearing Division, American Brake Shoe Co.
d. *Preparing Cast Iron Surfaces for Bonding*—By J. H. Shoemaker, Kolene Corp.
4a. *Selection of Bearing Materials*—By Arthur F. Underwood, General Motors Research Laboratories.
b. *Selection of Bearing Materials in the Electrical Industry*—By D. F. Wilcock, Thomson Laboratory, General Electric Co.
c. *Railroad Journal Bearings*—By E. S. Pearce, Railway Service and Supply Corp.
5a. *Aircraft Engine Bearings*—By J. Palsulich and R. W. Blair, Wright Aeronautical Corp.
b. *British Thought and Practice: How They Differ from American*—By W. H. Tait, Glacier Metals Co., Ltd.

Five Lectures on "Electronic Inspection"—

1. *Electronic Methods for the Measurement of Stress in Metals*—By Henry F. Hamburg, Chance Vought Aircraft Div.
2a. *Spectrochemical Analysis of Metals and Alloys by Direct Intensity Measurement Methods*—By J. L. Saunderson, Dow Chemical Co.
b. *Uses of the DuMont Cyclograph for Testing of Metals*—By R. S. Segsworth, General Engineering Co., Ltd.
3a. *Supersonic Inspection of Metals*—By E. O. Dixon, Ladish Drop Forge Co.
b. *Determination of Seams in Steels by Magnetic Analysis Equipment*—By Charles M. Lichy, Jones & Laughlin Steel Corp.
4. *The Electron Microscope and Its Application to Metals*—By C. S. Barrett, University of Chicago.
5. *Electronics in Liquid Steel*—By Harold T. Clark, Jones & Laughlin Steel Corp.

Five Lectures on "Physical Metallurgy of Aluminum"—

1. *Constitution of Aluminum Alloys*—By W. L. Fink, Aluminum Company of America.
2. *Metallography of Aluminum Alloys*—By F. Keller, Aluminum Company of America.

3. *Commercial Cast Aluminum Alloys*—By W. E. Sicha, Aluminum Company of America.
4. *Commercial Wrought Aluminum Alloys*—By J. A. Nock, Jr., Aluminum Company of America.
5. *Thermal Treatments of Aluminum Alloys*—By E. H. Dix, Jr., Aluminum Company of America.

The above four lectures will be prepared in book form and will be made available to members at an early date after the Convention.

Awards

At the annual dinner of the ASM on February 7, 1946, in Cleveland, the following awards were made:

President's Medal to Marcus A. Grossmann, twenty-fourth president, who served the ASM in 1944.

Henry Marion Howe Medal for 1945 was awarded to Dara P. Antia, Stewart G. Fletcher and Morris Cohen for their paper, *"Structural Changes During the Tempering of High Carbon Steel,"* published in Vol. 32 of TRANSACTIONS, 1944.

Albert Sauveur Achievement Award for 1945 was given to Robert S. Archer for his contribution to the metal industry in the art of fabricating, compounding, and heat treating of aluminum alloys.

ASM Medal for the Advancement of Research for 1945 was awarded to Gerard Swope, retired president and director of the General Electric Co., in recognition of his consistent sponsorship, foresight, and influence in financing and prosecuting metallurgical research, which have helped substantially to advance the arts and sciences relating to metals.

ASM Gold Medal for 1945 was awarded to Earle C. Smith, chief metallurgist of Republic Steel Corp., Cleveland, for outstanding metallurgical knowledge and great versatility in the application of science to the metal industry, as well as exceptional ability in the diagnosis and solution of diversified metallurgical problems.

Campbell Lecture was presented by Dr. Maxwell Gensamer on the subject of *"Strength and Ductility"*.

1946 (NOVEMBER) NATIONAL METAL CONGRESS AND EXPOSITION

The 1946 National Metal Congress and Exposition now in session have demonstrated to all that they are unqualifiedly successful.

The large number of papers made available for presentation here due to the release of much of the research carried on during the war

under the Government auspices, together with the educational lecture series, have all combined to make the Congress decidedly educational.

The large number of firms participating in the exposition is indicative of the fact that this event maintains its high rating as a profitable activity in which to participate.

ELECTION OF OFFICERS

PRESIDENT HERTY, *presiding:* Complying with the constitution, I appointed on March 26, 1946, the following Nominating Committee, selected from the list of candidates suggested by eligible chapters prior to March 1, 1946:

Glenn Coley, Detroit, Chairman

C. D. d'Amico, Golden Gate	O. W. Ellis, Ontario
Robert S. Lynch, Georgia	A. R. Troiano, Notre Dame
J. E. Drapeau, Jr., Calumet	R. C. Pranik, Rhode Island
D. F. McFarland, Penn State	T. G. Digges, Washington

The committee met in Chicago on May 21, 1946, and made the following nominations for national officers:

FOR PRESIDENT

A. L. Boegehold, General Motors Corp.,
Detroit—1 year.

FOR VICE-PRESIDENT

Francis B. Foley, Midvale Co.,
Philadelphia—1 year.

FOR TRUSTEES

John E. Dorn, University of California,
Berkeley—2 years.

Arthur E. Focke, Diamond Chain & Mfg. Co.,
Indianapolis—2 years.

The committee for the nomination of a Secretary for the Society was appointed by the President and consisted of the President and the six immediate Past Presidents of the Society. The report of this committee contained the nomination of W. H. Eisenman for the position of secretary of the Society for a term of two years.

A report of these nominations duly appeared in THE METALS REVIEW, June 1946.

I have been informed by the Secretary that no additional nominations were received prior to July 15, 1946, for any of the vacancies occurring on the Board of Trustees. Consequently the nominations were closed. I now call upon the Secretary to carry out the provisions of the Constitution in respect to the election of officers.

W. H. EISENMAN, *Secretary:* Conforming with the provisions and requirements of the constitution of the American Society for Metals, I hereby cast the unanimous vote of the members for the election of the aforenamed candidates who were regularly nominated May 21, 1946.

President Herty then introduced the newly elected officers, at which time President-Elect Boegehold said a few words of acceptance.

PRESIDENT HERTY: Has anyone present anything to bring before this meeting? If not, a motion to adjourn is in order. Motion duly made and carried.

Dr. Herty then introduced Herbert J. French, chairman of the Campbell Memorial Lecture meeting, who introduced the lecturer, James B. Austin, director, United States Steel Corporation Research Laboratories, Kearny, N. J., who presented his lecture entitled, *"The Effect of Changes in Condition of Carbides on Some Properties of Steel."*

ASM ANNUAL DINNER

On Thursday evening, November 21, members and guests assembled in the American Room of the Traymore Hotel for the Annual Dinner of the Society. The attendance was well over 700.

Those persons seated at the speakers' table were: Harold K. Work, Manager of Research and Development, Jones & Laughlin Steel Corp., Pittsburgh, and Treasurer of ASM; Edgar C. Bain, Past-President of ASM and Vice-President in Charge of Metallurgy and Research, Carnegie-Illinois Steel Corp., Pittsburgh, and Recipient of the Albert Sauveur Achievement Award; Kent R. Van Horn, Manager Cleveland Research Division, Aluminum Company of America, Cleveland, and Past-President of ASM; A. L. Boegehold, Head of Metallurgy Department, General Motors Corp., Research Laboratories Division, Detroit, and President of ASM; Charles H. Herty, Jr., Assistant to Vice-President, Bethlehem Steel Company, Bethlehem, Pa., and Past-President of ASM; Walter S. Tower, President of American Iron and Steel Institute and Principal Speaker at this annual dinner on the subject "The Layman Looks at Metallurgists"; A. E. White, Director, Department of Engineering Research, University of Michigan, Ann Arbor, Mich., and First President of ASM; R. E. Zimmerman, Vice-President in Charge of

Research and Technology, United States Steel Corporation of Delaware, Pittsburgh, and Recipient of the Medal for the Advancement of Research; Thomas L. Kane, Publisher of *Iron Age;* F. B. Foley, Director of Research, The Midvale Co., Nicetown, Philadelphia, and Vice-President of ASM; A. B. Kinzel, Chief Metallurgist, Union Carbide and Carbon Research Labs., Inc., New York; J. B. Austin, Director of United States Steel Corp. Research Laboratories, Kearny, N. J., and Campbell Lecturer; Axel Hultgren, Professor of Metallography, K. Tekniska Hogskolan, Stockholm, Sweden; John Chipman, Professor of Metallurgy, Massachusetts Institute of Technology, Cambridge, Mass., and Trustee of ASM; Walter E. Jominy, Chief Metallurgist, Chrysler Corp., Detroit, and Trustee of ASM; C. R. Austin, Assistant to President, Meehanite Metal Corp., New Rochelle, N. Y., and Recipient of Howe Medal; M. C. Fetzer, Metallurgical Department, Carpenter Steel Co., Reading, Pa., and Recipient of Howe Medal; L. S. Bergen, President, Bergen Precision Castings Co., Pleasantville, N. J., and Past-Trustee of ASM; A. E. Focke, Metallurgist, Diamond Chain and Manufacturing Co., Indianapolis, and Trustee of ASM; John E. Dorn, Associate Professor, University of California, Berkeley, and Trustee of ASM; W. H. Eisenman, Secretary, ASM, and Founder Member.

Presentation of President's Medal

The annual presentation of the President's Medal was made by Charles H. Herty, Jr., to Kent R. Van Horn, the twenty-fifth president, who served the Society so ably in 1945.

Presentation of Howe Medal

In honor of Dr. Henry Marion Howe, the distinguished scientist, often called the dean of American metallurgists, the Board of Trustees in 1922 established the first of its medals. The rules governing the award of this medal make the provision that it be awarded to the author or authors of the paper judged of highest merit, presented before the ASM and published during any one year in the TRANSACTIONS of the Society.

The 1946 medal was awarded to the two authors of the paper entitled "Factors Controlling Graphitization of Carbon Steels at Subcritical Temperatures" which was published in Vol. 35 of TRANSACTIONS, 1945, page 485. The authors who were honored are Charles

R. Austin and M. C. Fetzer. Each of these authors was presented a certificate, a gold medal and a bronze replica.

Albert Sauveur Achievement Award

In 1934 the Board of Trustees established an award consisting of a metal plaque and certificate in honor of Dr. Albert Sauveur, distinguished metallurgist and for many years an honorary member of the ASM. The purpose of this award is to recognize a metallurgical achievement which has stood the test of time and stimulated others along similar lines to the extent that a marked basic advance has been made in the metal arts and sciences. The 1946 candidate was Edgar C. Bain, vice-president in charge of metallurgy and research, Carnegie-Illinois Steel Corp., who was presented by Dr. Kent R. Van Horn following the reading of the citation of Dr. Bain's accomplishments. Dr. Van Horn then made the award. The citation is as follows:

Citation for Sauveur Award, 1946

Dr. E. C. Bain, among his many contributions to metallurgical science, conceived a new approach to the heat treatment of steel. Prior to this work, relatively little was known about the mechanism of the hardening of steel. True, people had known from earliest times that steel, having been heated to an elevated temperature, would become soft if cooled slowly and would be hard if cooled rapidly. When the microscope was applied to steel, it was learned that the soft material was characterized by a microscopic structure called pearlite, while the structure of the hard material was called martensite. But as to how and precisely when these structures formed, very little was known.

Bain conceived the idea that the mechanism of heat treatment might become known if each step in the cooling were investigated, examining the product formed at each temperature level during the cooling. This concept was not so simple as it might seem, for it involved the realization that the reaction below the eutectoid temperature was quite slow, whereas at some lower temperature it was probably rapid, and that consequently it might be profitable to study the times required for transformation.

The result of this concept and of the attendant research was the isothermal transformation diagram, which at one stroke placed the

science of heat treatment on a solid foundation. The basic work was performed with a simple eutectoid steel, and the significance of this single case became so apparent that a wide variety of steels was soon investigated by many workers. Indeed a recent compilation shows that transformation diagrams, or S-curves as they are colloquially known, have now been determined by various investigators for about 200 different types of steel and individual steels within each type. Probably all types of commercial heat treating steels are now understood as to their transformation characteristics, for S-curves are known for steels which range from the rapidly transforming plain carbon steels, through the automotive alloy steels which transform somewhat more slowly, to the very slowly transforming steels such as stainless steels, alloy forging-die steels and high speed steel.

The new type of attack also brought to light a new type of structure. Pearlite was shown to form in an upper range of temperature, while martensite formed in a lower range of temperature, and between the two is a range of temperature in which a hitherto unknown structure was discovered. The new structure is associated with valuable mechanical properties in the steel. Bain's associates in the work proposed that the structure be named bainite, in honor of its discoverer, and the term was at once accepted by the metallurgical fraternity and is now an established term in the literature of the subject.

A loyal associate in this work was Edmund S. Davenport. Joining in the project not long after its inception, he carried much of the burden enthusiastically and competently. Recognition for his contribution to the work has come to him and is attested by the association of his name with the basic work. It is appropriate to record his generosity in furnishing data for this award to Bain.

In the science of heat treatment, the impact of Bain's work is found not only in the newer theories but also in industrial applications. As to theory, any discussion of principles begins with a description of the isothermal transformation diagram. In practical application, industrial processes are now guided by these principles, to an extent which is ever increasing.

Conferring of the ASM Medal for the Advancement of Research

The 1946 ASM Medal for the Advancement of Research was awarded to Rufus E. Zimmerman, vice-president in charge of research and technology of the United States Steel Corp. of Delaware, in recognition of his consistent sponsorship, foresight, and influence

in financing and prosecuting metallurgical research, which have helped substantially to advance the arts and sciences relating to metals.

In making the presentation, Dr. A. E. White read the following citation that appears on the certificate of award:

Dr. Rufus E. Zimmerman entered industry primarily by way of a better preparation for a contemplated life-work in teaching and research; he remained, however, to pioneer the ways of science in industry.

From research associate in the former American Sheet and Tin Plate Laboratory, he rose through successive responsibilities to the position of Vice President, United States Steel Corporation, in 1933. Here he found the fullest scope for his talents of leadership, since, as staff officer, he acts to co-ordinate the research of a wide variety of the Corporation's enterprises in addition to iron and steel technology. In this domain is, particularly, the Corporation's Research Laboratory at Kearny, N. J., the work of which has become famous throughout the world.

Dr. Zimmerman has ever practiced the best principles of modern organization, with maximum delegation of authority, opportunity for initiative, and recognition of achievement. His publication policy, reflecting perhaps the good teacher, encourages the sharing of knowledge provided the reporting is in clear, concise language. Inevitably, he responded ably as consultant to the Services during the war and contributed his wise counsel in such capacities as President, American Standards Association; member, National Engineers Committee; member, Policy Committee on Standardization, Department of Commerce; and as a member of the boards of colleges and universities.

Dr. Zimmerman outstandingly has created the environment in which effective and fruitful research flourishes.

Address of the Evening

Walter S. Tower, president of the American Iron and Steel Institute, presented the main address of the evening entitled "The Layman Looks at Metallurgists."

THE EFFECT OF CHANGES IN CONDITION OF CARBIDES ON SOME PROPERTIES OF STEEL

(1946 Edward DeMille Campbell Memorial Lecture)

By J. B. Austin

OF those previously honored as Edward DeMille Campbell Memorial Lecturers, some, who had the good fortune to know Professor Campbell well, were able to enrich their lectures with references to personal associations. I was not so favored, yet I was privileged to have an indirect acquaintance with him through my father-in-law, James A. Evans, who, as a student at the University of Michigan, spent many hours reading to him. It was from this source that I learned much of those admirable qualities which won for Professor Campbell the esteem and respect we commemorate today. It was also thus that I first heard of his unfailing interest in the nature and constitution of carbides in steel. As I, too, have long been interested in this subject, it seems fitting to discuss today the constitution of carbides and how it may influence the properties of steel. And in keeping with the spirit of the occasion I have selected as the title of this lecture a slight modification of the title of two papers published by Professor Campbell in 1924.

Throughout most of his scientific career the constitution of cementite was a matter of speculation and debate. It was recognized that this material is a carbide of iron but there was no agreement as to its precise composition. A number of different formulas were proposed but no definite choice among them could be made on the basis of methods of investigation then used. The weight of evidence seemed to support the conclusion that cementite is Fe_3C, but a compound of this type presented many difficulties to one trained in traditional concepts of valency. That Campbell was dissatisfied is indicated not only by the direction of his investigations but also by such specific statements as:

> " . . . it is impossible for a chemist to account for all the products of solution of the carbides of iron if so simple a formula as Fe_3C is employed . . . ".

This is the twenty-first Edward DeMille Campbell Memorial Lecture presented by Dr. James B. Austin, Director, United States Steel Corp., Research Laboratories, Kearny, N. J. The lecture was presented November 20, 1946, during the Twenty-eighth Annual Convention of the Society, held in Atlantic City.

We now know that the cause of this uncertainty lay less in the experimental observations than in the narrowness of prevailing concepts of valence which, being based chiefly on the composition of simple anhydrous salts and on the structure of simple saturated organic compounds, failed to provide for the existence of less definite types of compound. In this connection, one cannot but wonder what the course of chemistry might have been had it developed from a study of intermetallic compounds or of carbides and nitrides.

The development of new methods of investigation, such as X-ray diffraction, yielded further evidence that cementite is Fe_3C so that this formula is now generally accepted; indeed, one might say, too generally accepted. For this acceptance has carried with it the tacit assumption that iron carbide conforms to the classic laws of compound formation, in particular that composition is invariant and that the ratio of iron atoms to carbon atoms is always a small whole number. As this assumption, like the concepts of valency, derives chiefly from analogy with the composition of simple salts or organic compounds, it appears high time to ask whether it is still justified.

There is, as it happens, some reason to doubt it. Thus, it is now well established that the composition of wüstite, that is, ferrous oxide, varies measurably, depending upon the conditions under which it forms, though there is always an excess of oxygen over that corresponding to the formula FeO. There is an analogous, though smaller, variation in the composition of magnetite. The sulphur content of ferrous sulphide (pyrrhotite) likewise varies but always exceeds that indicated by the symbol FeS; and many similar cases could be cited. These observations, together with the fact that it is always good scientific policy periodically to question any assumption which has come to be taken for granted, make it proper to ask: Is the composition of iron carbide invariant? If it is not, how great is the variation and what influence does this possible variation have on the properties of steels?

These are questions to which I have sought an answer. In this search I have been greatly aided by R. D. Heidenreich of Bell Telephone Laboratories and by my colleagues, R. F. Campbell, L. S. Darken, and J. R. Vilella, to each of whom I express my appreciation. My thanks are likewise due to Dr. John Johnston for his counsel and encouragement throughout the preparation of this lecture. I should also like to acknowledge my indebtedness to those investigators from whose published works I have drawn heavily and at times shame-

lessly. My apology for so doing is that though appropriation of the work of a single investigator is condemned as plagiarism, taking data from twenty is condoned as research.

The account of this search, and of the conclusions to which it leads, begins with a brief review of established principles of the structure of chemical compounds to learn what one may reasonably expect in the way of possible variation in the composition of cementite. There follows a summary of pertinent experimental evidence for the existence of such variation, particularly as it may be brought about by different heat treatments. The influence of such variation on some properties of steels is then illustrated by specific examples. Finally, inferences and conclusions drawn from these data serve as the basis for speculation as to the significance of certain features of the isothermal transformation diagrams of alloy steels. Consideration of the effect of variation in the degree or type of dispersion of carbides has, of necessity, been omitted, though in many instances it may be more significant than effect of variation in composition. Speculation as to the nature of the solid solution of carbon in alloyed ferrite is likewise avoided because it is always dangerous to draw inferences as to what is in solution from observations of what separates out under a given set of conditions.

The composition of cementite can conceivably vary in either or both of two ways: by variation in the ratio of the number of metal atoms to the number of carbon atoms, or through replacement of iron or carbon by another element. Variation of the first type, which is analogous to that observed in ferrous oxide or sulphide, is almost certain to be small and, if it does occur, is of interest chiefly from the standpoint of chemical principles. Variation of the second type is likely to be greater and of greater technologic significance.

In seeking evidence of such possible variations there are two general modes of attack. The first is direct experiment, that is, direct chemical analysis of carbides formed under controlled conditions; the second is indirect through study of the structure of carbides to see what variation is possible, or even to be expected, on the basis of established principles. The first is more definitive but likewise more difficult, especially if the variations sought are not precisely defined. The second is in part speculative but supplements the first in that it indicates the more promising fields for direct observation. It is therefore the more logical one with which to begin.

Types of Chemical Bond

Before taking up the structure of cementite, it is necessary to specify the several kinds of chemical bond as we now conceive them. There are three extreme types, electrostatic, covalent, and metallic, each of which has well-defined properties, though transition from one extreme to another is gradual, giving rise to intermediate types of bond which may possess some of the properties of each of the extremes.

The electrostatic bond, also called the ionic or polar bond, is that

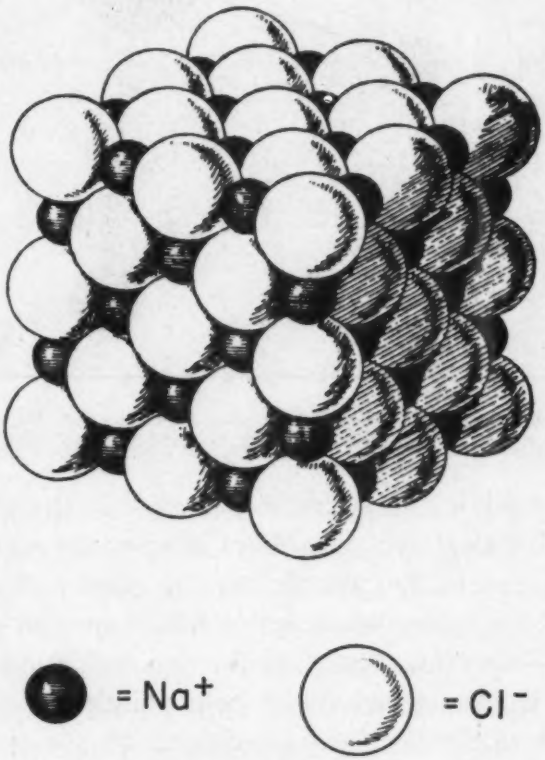


Fig. 1—Schematic Illustration of a Typical Electrovalent or Ionic Structure — Sodium Chloride.

resulting from attraction of oppositely charged ions. Atoms of a metallic element lose their outer electrons easily, whereas those of a nonmetallic element tend to take on additional electrons, thus forming stable cations or anions, respectively, which by exchange of electrons attract one another to form a stable molecule. A typical example (Fig. 1) is sodium chloride in which each sodium atom loses an electron to a chlorine atom to form a sodium cation (Na^+) and a chlorine anion (Cl^-) each strongly held by six oppositely charged

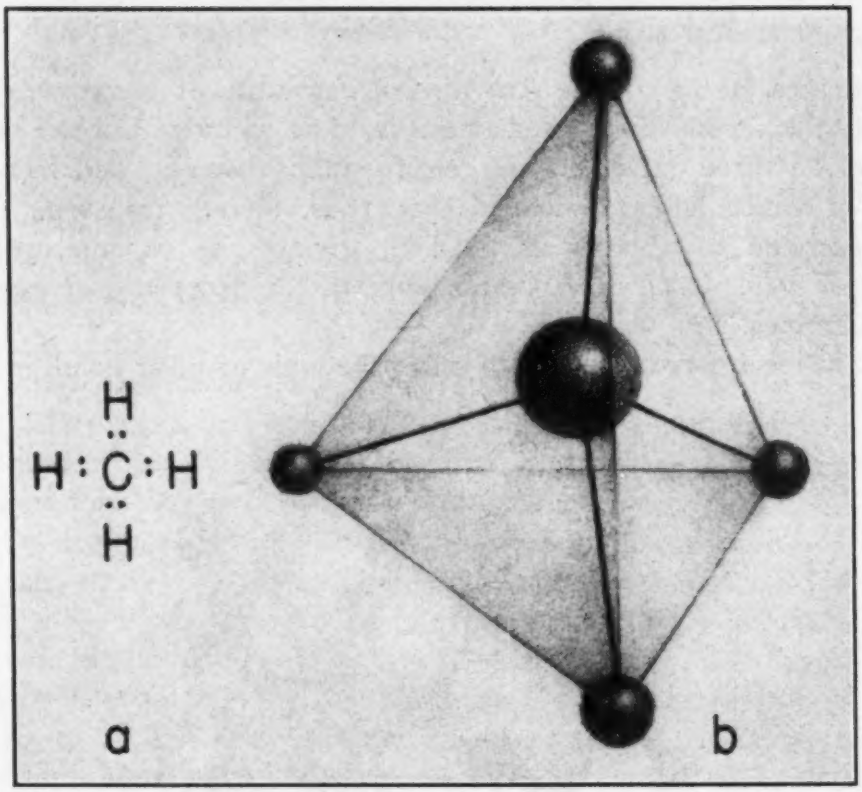


Fig. 2—Schematic Representation of the Structure of Methane; a, as Represented by a Lewis Electronic Formula; b, Arrangement in Space.

ions which surround it octahedrally. Each ion therefore forms an electrostatic bond with its six neighbors of opposite sign, these bonds combining all the ions in the crystal into one giant molecule.

The covalent, or nonpolar, bond results from the sharing of one or more pairs of electrons between the bonded atoms. A pair of shared electrons is considered to be held jointly by the two atoms and to complete a stable electronic configuration for each. A typical example is methane (CH_4) in which the carbon atom, with an inner shell of two electrons and an outer shell of eight shared electrons, assumes the stable ten-electron configuration of neon. Such an arrangement is represented by the Lewis electronic-type formula shown in Fig. 2a. Fig. 2b illustrates the spatial arrangement of the methane molecule in which the hydrogen atoms occupy the corners of a regular tetrahedron with the carbon atom at the center. I show this structure in order to emphasize two features which are significant in considering the structure of cementite. First, that the carbon atom normally has a valence of four and is therefore, when no so-called double bonds are involved, surrounded by and bonded to four neigh-

boring atoms; that is, it has a co-ordination number of four. Second, that these four bonds are normally arranged tetrahedrally as shown in Fig. 2b. Departure from this arrangement requires either serious strain within the molecule or resonance between bonds.

The concept of bond resonance, which is an essential feature of the quantum-mechanical picture of molecular structure, is analogous to resonance phenomena in classical physics. Recall, if you will, the lecture experiment with a system of two tuning forks of the same

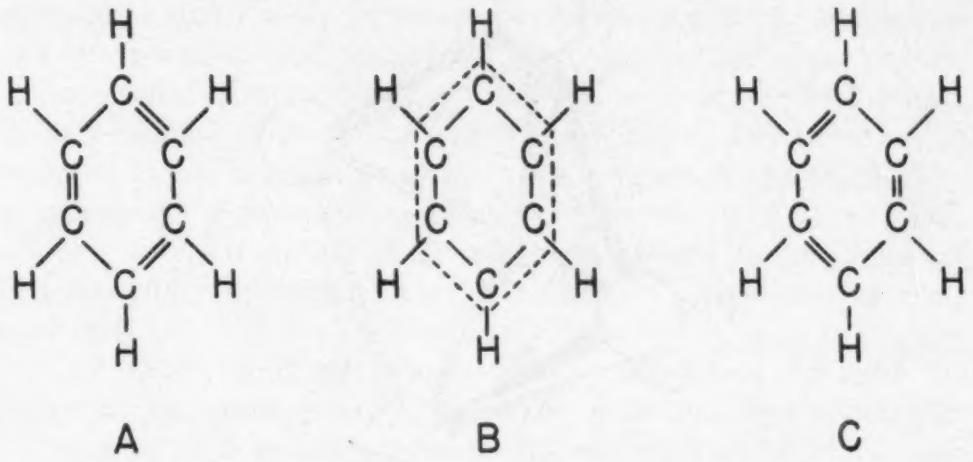


Fig. 3—Schematic Illustration of Resonance in Benzene. A and C represent the two stable Kekule configurations between which resonance (B) occurs.

characteristic frequency attached to a common base. When one fork is struck it vibrates strongly at first, then gradually ceases, transferring its energy to the other fork which now begins to vibrate; the process is then reversed so that the energy resonates back and forth between the two forks until it is dissipated by friction and other losses. The same phenomenon is observed when two similar pendulums are connected by a weak spring.

A somewhat, though not precisely, analogous resonance occurs between chemical bonds in that a molecule may resonate among several valence-bond structures. Thus there are many substances whose properties cannot be accounted for by means of a single electronic structure of the valence-bond type, such as that given for methane, but which can be fitted into the scheme of classical valence theory by assuming resonance among two or more structures. A familiar example is the structure of the benzene molecule as represented by the two Kekule formulas (A and C in Fig. 3), these being the most stable valence-bond structures which can be written for the well-established hexagonal coplanar configuration. Yet individually

they do not provide a satisfactory representation of the high stability and low reactivity of the benzene molecule. This difficulty is resolved, however, if one assumes that there is complete resonance between the two structures which, in so far as energy is concerned, are equivalent. I have attempted to indicate this resonance in rather crude fashion in B in Fig. 3. The additional energy associated with the resonance gives to the benzene molecule a greater degree of stability than it would

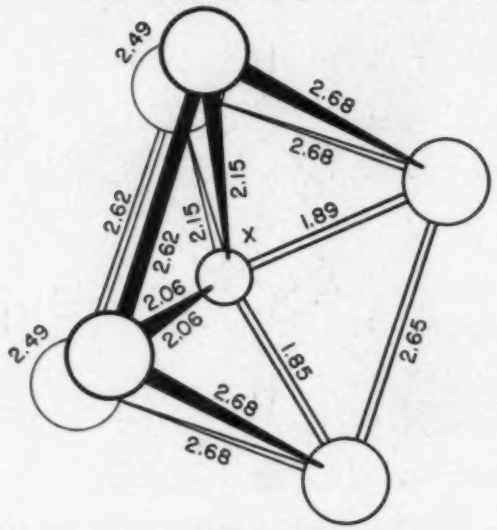


Fig. 4—Schematic Representation of the Arrangement in Space of Iron-Carbon Bonds in Cementite. (After Lipson and Petch.)

normally have; indeed, one of the significant features of resonance is that it often tends to stabilize an otherwise unstable molecule.

The metallic bond is not so simple as the other two types because the valence electrons are neither transferred to, nor shared with, another atom, but, in effect, become detached and mobile. A metal may therefore be pictured as an orderly array of positive ions with free electrons moving in the interstices. The bonds are therefore not fixed in a given direction, as in methane, but resonate among various pairs of atoms somewhat as they do in benzene. Such resonance implies that maximum stability is associated with maximum co-ordination number; that is, an increase in the number of positions among which the bonds can resonate increases the resonance energy and stabilizes the system. The typical metal structure is therefore one or the other of two types of closest-packing of spheres, namely, face-centered cubic and hexagonal with co-ordination number 12, or the body-centered arrangement with co-ordination number ap-

proaching 14. In intermetallic compounds of atoms differing in size, still closer packing with larger co-ordination number is sometimes achieved.

Structure of Cementite

With this background, we turn to consideration of the structure of cementite. I shall not give details here as the structure is complex; for those interested they are given in a paper by Lipson and Petch (1).[1] It suffices to say that there is a framework of close-packed iron atoms with the smaller carbon atoms in the interstices. Each iron atom has eleven or twelve practically equidistant neighbors, the interatomic distance being virtually the same as in metallic iron. The one element of simplicity is that each carbon atom is located at the center of a triangular prism, the corners of which are occupied by six practically equidistant neighbors, as shown in Fig. 4. This structure differs from that of the methane molecule, in that there are six instead of four neighbors so that the bond angles are far from tetrahedral.

The most significant feature of this cementite structure, as Petch (2) has pointed out, is that there must be direct bonding of iron to iron, for the molecule cannot be held together by iron-carbon bonds alone. But what is the nature of this bond between the iron atoms? Since it links atoms of the same kind, it is unlikely to be electrostatic; moreover, assuming that each atom is bonded to all its nearest neighbors, the co-ordination number is too large for normal covalent bonding. As there are no such objections to metallic bonding, it seems reasonable to conclude that the iron-iron bond is essentially metallic.

For the iron-carbon linkage (Fig. 4), electrostatic bonding again appears unlikely. It is difficult to see what ionic valency the atoms would adopt; furthermore, such a bond would require that the separation of the iron atoms correspond to the ionic radius of iron whereas the observed separation is that for metallic iron. Covalency seems improbable because each carbon atom has six virtually equidistant neighbors situated at the corners of a prism, whereas, as has been noted, the normal covalence of carbon is four with the bonds arranged tetrahedrally.

This suggests that the stability of cementite must be due to resonance among these six bonds, an inference which is supported by

[1]The figures appearing in parentheses pertain to the references appended to this lecture.

the fact that Pauling (3) has concluded that in certain other carbides—notably those of titanium, zirconium, vanadium, columbium, and tantalum—in which the carbon atoms also have six nearest neighbors, there is resonance of covalent bonds among these six positions. Such resonance is a transition of the covalent bond towards a metallic bond. As the only alternative appears to be a bond even more metallic, it is reasonable to conclude that resonance occurs in cementite.

This interpretation leads to the relatively simple picture of a structure comprising essentially a framework of close-packed iron atoms held together by metallic bonds, the smaller carbon atoms being held in the interstices by a type of bonding which involves resonance of covalent linkages and therefore has some attributes of metallic bonding. There is thus a considerable resemblance to the structure of ferrite and of austenite which suggests that although cementite is normally considered a chemical compound, it possesses, in fact, many characteristics of a solid solution. Indeed, cementite appears to be an excellent illustration of the lack of sharp distinction between a solid solution and a compound, though it might be expected to have properties which are in the main those of a compound.

On the basis of this interpretation one would expect that the carbon content of cementite might vary. But what sort of variation should one anticipate? A closer consideration of the structure supplies some clues. A structure bonded entirely by electrostatic or covalent linkages must satisfy the valency relations among the several atoms; but in a structure such as cementite with a close-packed framework of iron atoms joined by metallic bonding, it is possible that the framework may exist even if, here and there, carbon atoms are lacking. In austenite, for example, the framework of iron atoms can exist even when carbon atoms are missing. The fairly constant composition of cementite therefore requires some explanation.

Petch (2) has attempted an explanation along the following lines. Cementite, as an interstitial structure, must be considered in relation to other carbides or nitrides which have been investigated by Hägg (4) with results which indicate that in such structures the bonding forces require close packing of the metal atoms and no limitation is imposed by nonmetal atoms on their metal neighbors. Thus, the stable structure is simply that which achieves close packing and the stable composition is that required to build this structure. This is in contrast to electrovalent or covalent compounds in which

valency determines composition and the structure has then to accommodate to this composition. On this view, a stable structure results at the ratio 3Fe to 1C because with this composition close packing is possible. As this is not a valency requirement some departure from this ratio appears permissible, though great variation is not to be expected.

As replacement of one component by another is not possible, because of the great difference in atomic size of iron and carbon, the most likely variation appears to be omission of carbon atoms. The framework in cementite is, however, not the exact structure adopted by iron in the absence of carbon, so that although the framework can probably continue to exist when a certain number of carbon atoms are missing, it would be expected that this omission can take place to a limited extent only.

Petch (2) has also advanced a thermodynamic argument to show that the composition of cementite in equilibrium with ferrite or austenite may depart from the stoichiometric ratio; on this basis the composition of cementite in equilibrium with the iron solid solution in a steel would be expected to vary with temperature.

The general inferences are, therefore: (a) that minor departure from the stoichiometric ratio is to be expected; (b) that it is most likely to take the form of deficiency of carbon; (c) that it may vary with temperature.

Let us now turn to experimental observations to see to what extent they accord with these conclusions. The experimental data are, unfortunately, neither so numerous nor so precise as one might wish, yet they suffice to confirm in a general way the predictions based upon the structure of cementite.

Variation in Carbon Content

At first thought it might appear that the best means of ascertaining whether cementite does vary in carbon content is by chemical analysis of carbides extracted from samples of steel which had been subjected to different heat treatments. This is, however, not true, and although many analytical data have been published none of the methods appears capable of yielding a definitive answer. The chief difficulty is that the process of extraction itself usually alters the composition of the carbide. For example, the well-known experiments of Professor Campbell show that on solution of steel in acid some

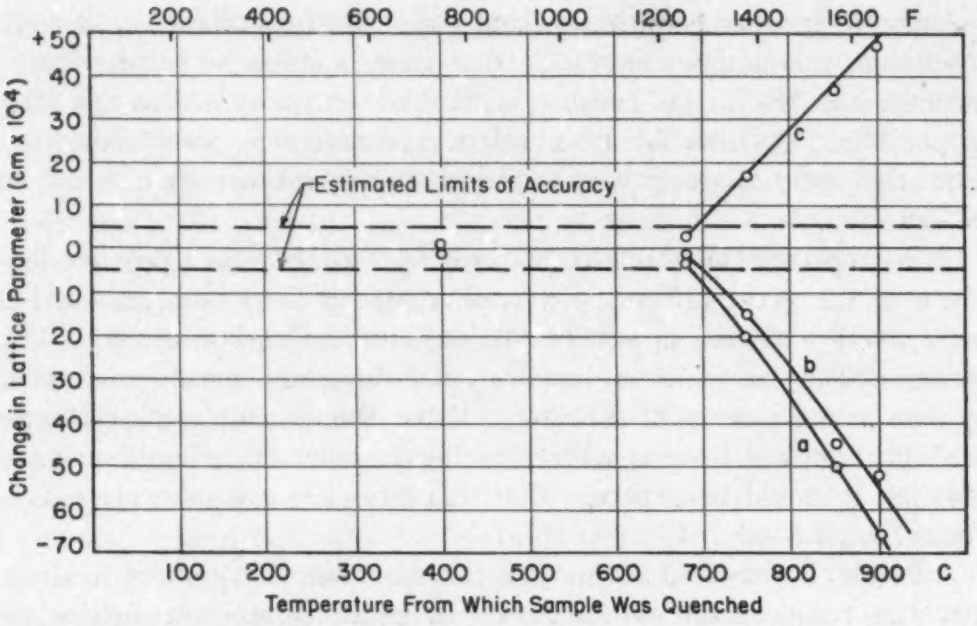


Fig. 5—Variation With Temperature of the Lattice Parameters of Cementite Isolated From 1.8% Carbon Steel Quenched After 6 Hours in Vacuum at Different Temperatures. (Data of Petch.)

carbon is evolved as hydrocarbon gases. The same is true, to a lesser extent, of electrolytic extraction. Yet all the carbide does not decompose in this fashion for the extracted particles are often contaminated by colloidal carbon. Under these conditions it is virtually impossible to obtain the precision required to establish the existence of a small variation in composition.

It is therefore necessary to use some method other than chemical analysis. Such methods are available, and results obtained by two of them are reported in the literature. In each case, they indicate a variation in the carbon content of cementite. The first, based upon a planimeter measurement of the relative area of carbide and ferrite in a photomicrograph of steel of known carbon content, has been used by Schwartz and his colleagues (5). It can hardly be considered a precision method, and one is justified in questioning the significance of the numerical results, yet it does yield qualitative evidence which Schwartz, Van Horn and Junge (5) sum up as follows: Cementite is not a definite chemical compound because its carbon content tends to decrease at temperatures above the eutectoid, this decrease being confirmed by a contraction in the dimensions of the unit cell. Moreover, cementite may possess some degree of stability even though some of the carbon atoms required by the stoichiometric formula are

missing. These conclusions accord with those derived from consideration of the structure of the carbide.

The second method, used in part by Schwartz, Van Horn and Junge, is to determine the lattice parameter rather than the chemical composition of extracted carbides. It has been refined by Petch (2) and is capable of great precision; for in this case the presence of free iron or carbon introduces no significant error. The results of Petch's careful parameter measurements on carbides extracted from purified iron-carbon alloys, which had been quenched from a series of elevated temperatures, are presented in Fig. 5. In order to make the change in parameter more evident Fig. 5 shows the difference between the three lattice constants of the quenched alloys and those for carbide extracted from an alloy which had cooled from 900 C (1652 F) to room temperature at 20 C (38 F) per hour. The estimated error of measurement is indicated in Fig. 5 by the pair of horizontal broken lines. These data indicate a systematic variation in the parameters which is quite beyond the limits of experimental error. Thus, so long as cementite is in equilibrium with ferrite the parameters remain sensibly constant, but for cementite in equilibrium with austenite there appears to be a progressive and systematic variation in the direction of a smaller unit cell at higher temperature.

It seems unlikely that these changes are due to quenching stresses. Petch reports that the X-ray patterns were so sharp that there could have been little, if any, deformation. Moreover, any effect of quenching stress should be greatly lessened by extraction from the matrix of iron. Again, the magnitude of any residual stress would depend on the orientation of the particle in the original lump. After extraction the particles are oriented at random so that each line in the X-ray pattern is due to planes which would have been subjected to a different degree of stress. If this stress were sufficient to cause significant displacement of the diffracted beam, the displacement would be different for each spot and produce diffuse lines whereas the pattern was, in fact, sharp.

It is also unlikely that these changes result from variation in amount of impurity present, since spectrographic examination of cementite extracted from steels quenched from 400 and 900 C (752 and 1652 F) indicated no significant difference. The only impurities detected were slight traces of magnesium, silicon, nickel and zinc.

It must be concluded then that there is a significant variation in the carbon content of cementite, which accords with the data reported

by Schwartz and his colleagues and with expectation based on the molecular structure.

To sum up, there is ample reason to believe that the carbon content of cementite in equilibrium with ferrite is sensibly constant at the stoichiometric ratio, whereas that of cementite in equilibrium with austenite decreases with increasing temperature. The magnitude of this variation cannot be regarded as precisely determined, but must be relatively small.

Possible Replacement of Carbon

If cementite were an electrovalent or covalent compound of the classic type, iron or carbon would be replaced only by an element with the same valence and then only if the substituent atom were of roughly the same size as the atom replaced. But resonance of covalent bonds between iron and carbon relaxes the valency limitation as far as carbon is concerned, so that the chief requirement for replacement of carbon atoms by others appears to be that they should be of nearly the same size. On this basis the element most likely to replace carbon is nitrogen.

Although direct demonstration of the presence of nitrogen in cementite is lacking, there is reason to believe that substitution or solution may occur to a limited extent. For instance, among analogous titanium compounds the existence of a cyanonitride as well as of a carbide is well established. Furthermore, Heidenreich, Sturkey and Woods (6) report that when martensite, formed in a steel containing 0.9% carbon and 0.0056% nitrogen, is tempered at a temperature above about 350 C (662 F), it yields ferrite and cementite, whereas when tempered at a lower temperature its electron diffraction pattern is identical with that of Fe_3N. Subsequent heating to a temperature above 350 C (662 F) changes this nitride pattern to that of Fe_3C, which suggests, though it does not prove, that carbon and nitrogen may be interchangeable to a significant extent.

Such replacement is difficult to establish beyond question. It seemed possible, however, that further information might be obtained by comparing the amount of nitrogen taken up by nitrided high-carbon iron with that taken up by purified iron under identical conditions. As a preliminary comparison, L. S. Darken has determined the amount of nitrogen taken up by carbonyl iron and by an iron-carbon alloy containing 4.0% carbon in equilibrium at 600 C (1112 F)

with mixtures of ammonia and hydrogen containing respectively 3, 6 and 9 volume per cent ammonia. The iron-carbon alloy was prepared by melting ingot iron in a graphite crucible and pouring the melt onto a copper plate. The chilled iron was then ground into small pieces so that equilibration would be rapid. Samples of this alloy, and of carbonyl iron sheet, were heated at 600 C (1112 F) until

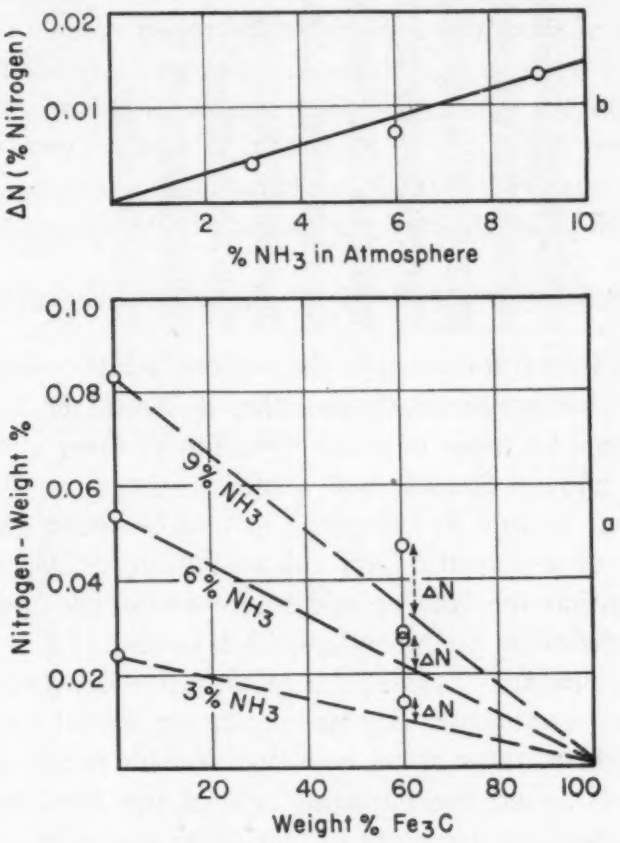


Fig. 6a—Nitrogen Content of Carbonyl Iron and of a 4.0% Carbon Alloy in Equilibrium With Different Mixtures of NH_3 and H_2 at 600 C (1110 F).

Fig. 6b—Excess Nitrogen Content Above That Required to Saturate Iron at 600 C (1110 F) as a Function of the NH_3 Content of the Atmosphere.

equilibrium had been attained, which was usually within a few hours, then quenched and analyzed for nitrogen, with results presented in Fig. 6.

The data for carbonyl iron are plotted on the left-hand vertical axis. If nitrogen neither dissolves in cementite nor displaces carbon, the amount present should decrease linearly with increasing proportion of cementite as indicated by the broken lines in Fig. 6a; that is, these lines represent the amount of nitrogen required to saturate iron

in iron-carbon alloys in equilibrium with the respective atmospheres. The points representing data for the high-carbon alloy, however, in each instance lie above the corresponding line indicating that nitrogen had been taken up in excess of the amount required to saturate the iron. Although there is some uncertainty as to the possible effect of the small amount of alloying elements present in the high-carbon iron, and although data are available for only one high-carbon alloy, it seems likely that this excess represents nitrogen taken up by cementite. Moreover, the amount of this excess nitrogen proves to be directly proportional to the concentration of ammonia in the atmosphere, as is evident from Fig. 6b. This, although hardly proof that nitrogen replaces carbon in cementite, does indicate the necessity of considering it as a possibility which deserves further investigation.*

Replacement of Iron by Alloying Elements

Since the iron framework of the cementite lattice is held together by bonds which are essentially metallic, it should be possible to replace iron atoms by those of other elements to form alloy cementites analogous to alloyed ferrites and austenites; that is, the conditions for replacement of iron in cementite should be those generally valid for formation of a substitutional solid solution. Chief among these conditions are that the solvent and solute atoms are chemically alike and that they differ by not more than 15% in size (7).

Chemical similarity is hardly a quantitative concept, yet it is the basis of several qualitative criteria which are useful for the present purposes. Clearly, there is no need to consider metals such as gold or silver which lie on the opposite side of the Periodic Table and therefore dissolve but sparingly in ferrite or austenite. The number of possibilities may be further limited by considering relative tendency of elements to form carbides. Iron carbide in a pure iron-carbon alloy is a very weak compound; indeed, it is thermodynamically unstable with respect to graphite; hence introduction of an element which is a still weaker carbide former—for instance, silicon or nickel—under most conditions merely promotes decomposition of cementite to graphite and iron, although a stable iron-nickel-cobalt carbide (cohenite) has been repeatedly observed in meteorites. On the other hand, any of those elements which form relatively stable carbides—namely, titanium, vanadium, chromium, manganese, zirconium, columbium, molybdenum, tantalum, tungsten—might be

*Recent data reported by Jack (30) appear to establish the existence of iron carbonitride.

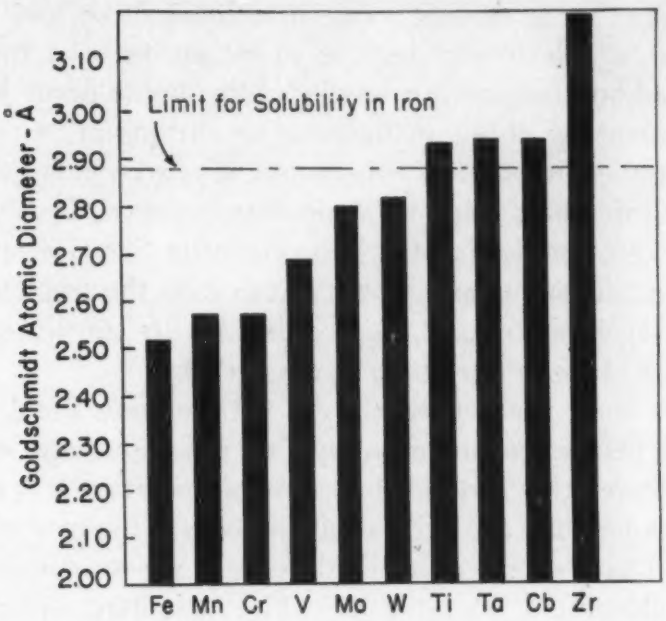


Fig. 7—Schematic Comparison of Atom Diameter of Carbide-Forming Elements.

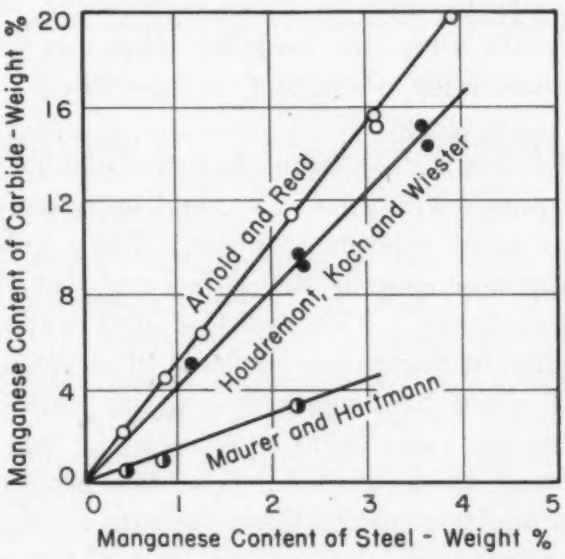


Fig. 8—Manganese Content of Carbides Extracted From Annealed Manganese Steels as a Function of the Manganese Content of the Steel.

expected to stabilize cementite if it can fit into the structure.

The relative size of the atom of these elements, expressed in terms of the Goldschmidt atom diameter (8), is indicated in Fig. 7; a horizontal line is drawn at a level 15% above that of the diameter of the iron atom to indicate the upper limit of favorable size. From

this comparison it is evident: (a) that manganese and chromium should easily be able to replace iron in cementite; (b) that replacement by vanadium, tungsten or molybdenum should occur less readily than replacement by either manganese or chromium; (c) that titanium, tantalum, columbium or zirconium atoms are too large to replace iron. These inferences must be somewhat qualified, however, by the fact that a size permitting entry into cementite likewise favors entry into ferrite or austenite; and in any given case the free-energy relations may be such as to favor the presence of the substituent element in one of these phases rather than in the carbide.

How do these inferences accord with experimental evidence? The data are neither so numerous nor so precise as one might wish and their interpretation is difficult because of uncertainty as to whether equilibrium had or had not been attained because the rate of approach to equilibrium had become exceedingly slow. Yet it appears that only manganese, chromium, molybdenum, and tungsten replace iron in cementite to a significant extent. These elements, moreover, show a marked tendency to concentrate in cementite and other carbide phases.

Pertinent data to support these conclusions are summarized below. In order to view this evidence in proper perspective it is necessary to broaden the discussion to include carbides other than cementite.

Manganese. Manganese forms an orthorhombic carbide, Mn_3C, which is isomorphous with Fe_3C (9), and apparently forms a continuous series of solid solutions with it. The equilibrium relation between the manganese content of the steel and that of the carbide is not precisely established. The available data (10), presented in Fig. 8, indicate that as manganese in the steel increases up to a gross concentration of about 5%, manganese in the carbide increases in direct proportion, the ratio being about 4 to 1; that is, manganese tends to concentrate in the carbide. The data of Arnold and Read, which extend to higher concentrations, indicate a constant content of about 22% manganese in the carbide over the range 6 to 16% manganese in the steel, but their observations are open to criticism on the ground that their photomicrographs suggest incomplete transformation of austenite in this range of composition. There is also evidence (10c) that chromium, if present, may enter cementite along with manganese.

Chromium. The behavior of chromium is more complex since in the iron-chromium-carbon system there are three stable carbides:

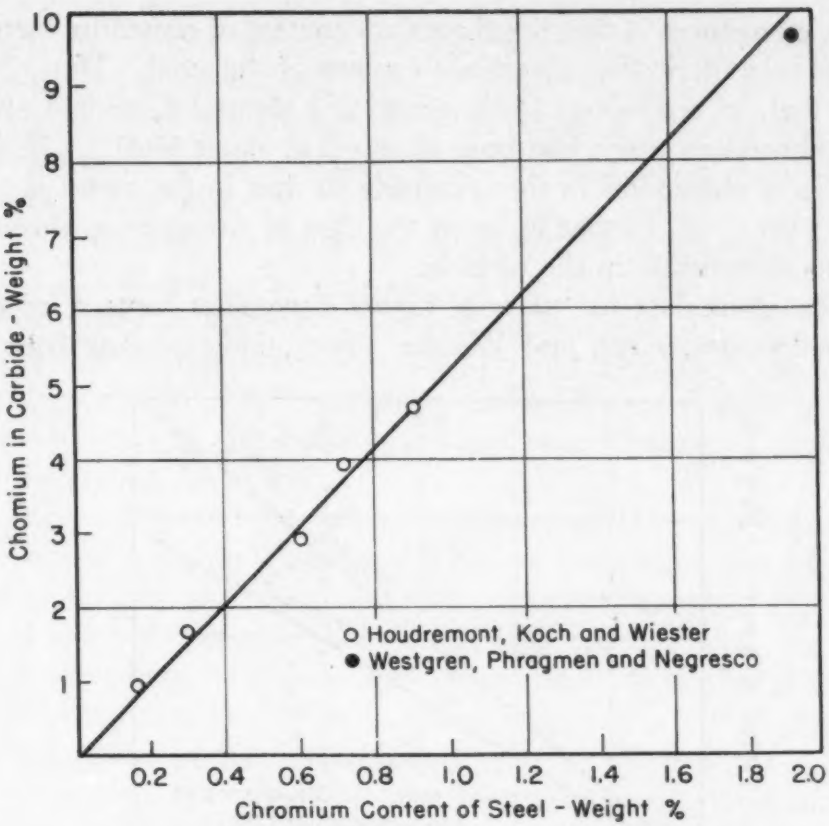


Fig. 9—Chromium Content of Carbides Extracted From Chromium Steels Containing 1.0% Carbon and Annealed at 1000 C (1830 F) as a Function of the Chromium Content of the Steel.

(a) Orthorhombic cementite $(Fe, Cr)_3C$, which may contain up to 15% chromium; it appears chiefly in alloys in which the ratio of chromium to carbon is relatively low, and predominates in chromium steels containing up to about 3% chromium.

(b) A trigonal carbide $(Cr, Fe)_7C_3$, which contains a minimum of about 35% chromium; it appears in steels containing from about 3 to 15% chromium.

(c) A cubic carbide, sometimes designated Cr_4C, though probably represented more accurately by the formula $Cr_{23}C_6$. This carbide contains a minimum of about 70% chromium and appears in high-chromium alloys such as stainless steels.

Because the composition and range of stability of each of these carbides varies with temperature and with gross composition of the steel, it is not possible to derive for chromium a simple yet generally valid relation analogous to that for manganese. Yet at a given temperature and at constant carbon content, chromium appears to behave

as does manganese in that the chromium content of cementite increases linearly with increasing chromium content of the steel. Thus, Fig. 9 shows that, in a series of steels containing about 1% carbon and up to 2% chromium which had been annealed at about 1000 C (1832 F), the ratio of chromium in the cementite to that in the metal is about 5 to 1 (10c), (11); that is, as in the case of manganese, chromium tends to concentrate in the carbide.

Analogous data for steels of higher chromium content, reported by Houdremont, Koch and Wiester (10c), indicate that both iron

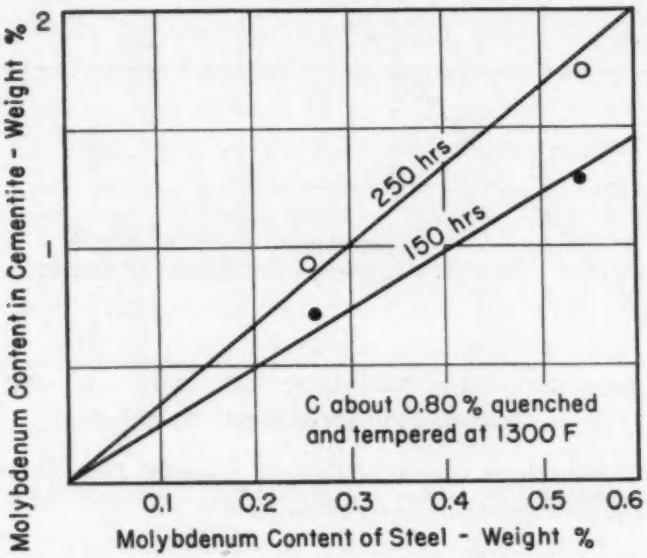


Fig. 10—Molybdenum Content of Carbides Extracted From Molybdenum Steels Containing About 0.8% Carbon and Annealed at 705 C (1300 F) as a Function of the Molybdenum Content of the Steel. (Data of Bowman.)

and manganese are present in these higher carbides of chromium, though the interpretation of their data is difficult because of the presence of more than one type of carbide.

Molybdenum. Equilibrium relations in the system iron-molybdenum-carbon are not well established, yet there seems to be no question as to the existence of at least the following carbides:

(a) Orthorhombric cementite $(Fe, Mo)_3C$, which predominates in steels in which the ratio of molybdenum to carbon is relatively low; it may contain at least as much as 3% molybdenum (12). It should be noted that, as one would expect from the greater difference in size of the atoms, iron is replaced to a smaller extent by molybdenum than by either manganese or chromium.

(b) A face-centered cubic carbide, sometimes called the double-carbide or high-speed carbide, commonly considered to be Fe_3Mo_3C

but probably more accurately represented as $(Fe, Mo)_6C$. That the composition of this carbide may vary is strongly suggested by variation in the lattice parameter reported by Adelsköld, Sundelin and Westgren (13). By analogy with the behavior of the corresponding tungsten carbide, this variation is almost certainly a replacement of molybdenum by iron.

(c) Another face-centered cubic carbide represented by $(Fe, Mo)_{23}C_6$, analogous to $(Fe, Cr)_{23}C_6$, has also been observed (14), (15) in iron-rich iron-molybdenum-carbon alloys.

(d) A hexagonal carbide, Mo_2C, which appears in the presence of a large excess of molybdenum. Although replacement of molybdenum by iron in this carbide has not been established, it must be considered as a possibility.

Although the data are scanty and the range of replacement limited, it is evident from Fig. 10 that, as is true of manganese and chromium, for a given heat treatment and carbon content the molybdenum content of the orthorhombic carbide increases linearly with that in the steel, and that molybdenum tends to concentrate in the carbide. It should be noted in Fig. 10 that a linear relationship holds even though equilibrium had not been established.

Tungsten. The system iron-tungsten-carbon is qualitatively very close to the analogous molybdenum system. Thus, there are at least four stable carbides.

(a) Orthorhombic cementite $(FeW)_3C$, which appears in steels of relatively low tungsten content; in it tungsten replaces iron to a limited extent (16).

(b) Face-centered cubic double carbide, commonly designated Fe_3W_3C but more properly represented as $(FeW)_6C$ since it has been shown that its composition may vary at least within the limits represented by the formulas Fe_3W_3C and Fe_4W_2C (17). That is, in it a substantial amount of tungsten may be replaced by iron.

(c) Another face-centered cubic carbide corresponding to the formula $(Fe, W)_{23}C_6$, analogous to $(Fe, Cr)_{23}C_6$ and $(Fe, Mo)_{23}C_6$; it is reported to occur in iron-rich iron-tungsten-carbon alloys (14).

(d) Hexagonal WC in which limited replacement of tungsten by iron appears to occur (18).

Vanadium. The phase diagram for iron-vanadium-carbon alloys (19) indicates the existence of at least two stable carbides:

(a) Orthorhombic cementite $(FeV)_3C$, in which iron may be replaced to a negligible extent by vanadium.

(b) Face-centered cubic V_4C_3 which appears in steels with a vanadium content in excess of about 0.5%.

There appear to be no precise data on the partition of vanadium between matrix and cementite, but as the alloy content of the carbide appears at best to be very small, it probably is negligible.

To sum up, the experimental data, in so far as they go, confirm predictions made on the basis of the structure of cementite, more specifically that, as equilibrium is approached, iron in cementite is replaced extensively by manganese and chromium for which the size factor is most favorable; to a more limited extent by molybdenum and tungsten, for which the size factor is less favorable; and finally to only negligible extent by vanadium for which the size factor is least favorable. Moreover, for a given temperature and carbon content, the alloying element in the carbide increases linearly with the gross content of the element in the steel, and the partition coefficient is such that at equilibrium the alloying element tends to concentrate in the carbide.

Table I
Composition of Carbides Isolated from a Steel Containing 3.3% Cr, 0.44% Mn, and 0.80% C after Quenching from 1150 C into Oil and Tempering for 4 Hours at a Series of Temperatures
(After Houdremont, Koch and Wiester)

Tempering Temp., C	Chromium %	Manganese %	Iron %	Carbon %	Type of Carbide
450	5.7	0.7	84.0	9.2	$(Fe, Cr)_3C$
	6.2	0.7	82.0	11.2	
550	14.6	1.4	76.4	7.6	$(Fe, Cr)_3C$
	13.7	1.5	77.3	7.5	
650	25.7	2.1	64.1	8.0	$(Fe, Cr)_3C$ +
	25.7	2.1	64.4	7.7	Cr_7C_3

Variation of Composition During Annealing or Tempering

Thus far we have discussed the composition of carbides which are close to equilibrium with the matrix, but in many heat treating processes equilibrium is not approached so what of the composition of carbides, particularly of cementite, resulting under these conditions?

The simplest type of such a process is equilibrating by annealing or tempering, at a given temperature, carbides formed at another temperature at which they may or may not have been in equilibrium. In general, if the temperature of annealing is higher than that of formation, the carbides tend to become enriched in alloying elements, whereas if it is lower, there is a tendency toward impoverishment.

As an example of enrichment, Houdremont, Koch and Wiester

(10c) observed that in a steel containing 2.2% manganese and 0.14% carbon, the cementite isolated after quenching from 1000 C (1832 F) and tempering for 10 hours at 400 C (752 F) contained 4.6% manganese, whereas that isolated after an additional heating at 680 C (1256 F) for 50 hours contained about 17% manganese. A comparable enrichment of chromium after analogous heat treatments was observed in steel containing 1.3% chromium and 0.36% carbon. These same investigators also present data, which are reproduced in

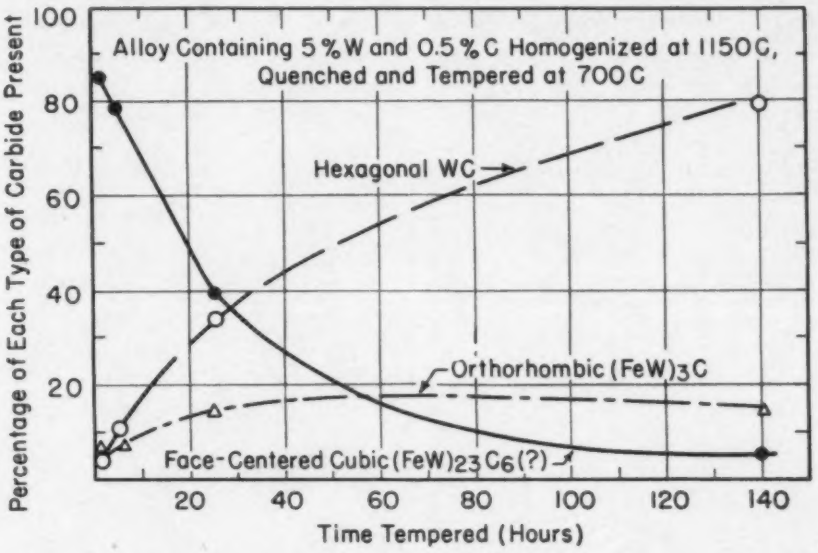


Fig. 11—Change in the Relative Amount of Different Carbides Present in a 5% Tungsten Alloy on Tempering at 700 C (1290 F). (Data of Rutherford.)

Table I, to show the increase in concentration of chromium in carbides with increasing tempering temperature. Thus, for a steel containing 3.3% chromium and 0.80% carbon quenched from 1150 C (2102 F) and tempered for 4 hours at a series of temperatures, the chromium content increased from about 6% at 450 C (842 F) to nearly 26% at 650 C (1202 F). Analogous data demonstrating the enrichment of cementite in manganese and chromium during tempering have been reported by Crafts and Lamont (27).

The formation of molybdenum-rich cementite, as well as of other carbides, on tempering quenched iron-carbon-molybdenum alloys has been reported by Bowman and Parke and by Bowman (15).

A further example of a change occurring in a more complex system in which more than one type of carbide is present is provided by some hitherto unpublished observations on a tungsten alloy made by J. J. B. Rutherford in this laboratory some years ago. Specimens

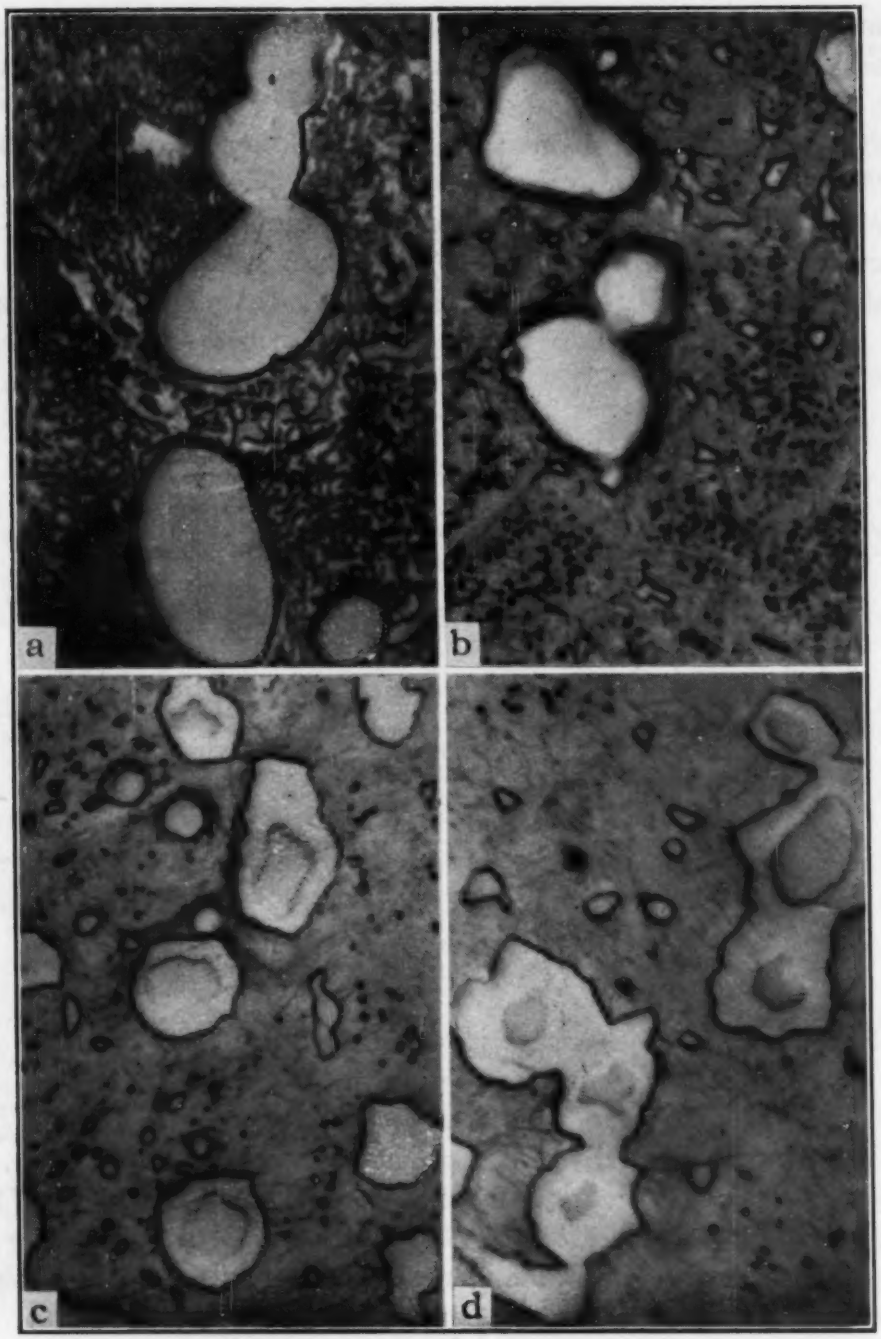


Fig. 12—Successive Stages in the Development of Cored Carbides in an Alloy Containing 6.0% Molybdenum and 1.3% Carbon on Heating at 925 C (1700 F), After 72 Hours at 1115 C (2040 F). (Photographs by R. F. Campbell.) a—After 72 hours at 1115 C (2040 F). b—After 4 hours at 925 C (1700 F). c—After 24 hours at 925 C (1700 F). d—After 72 hours at 925 C (1700 F).

of this alloy, which contained 5% tungsten and about 0.5% carbon, were first homogenized at 1150 C (2102 F), then quenched and finally

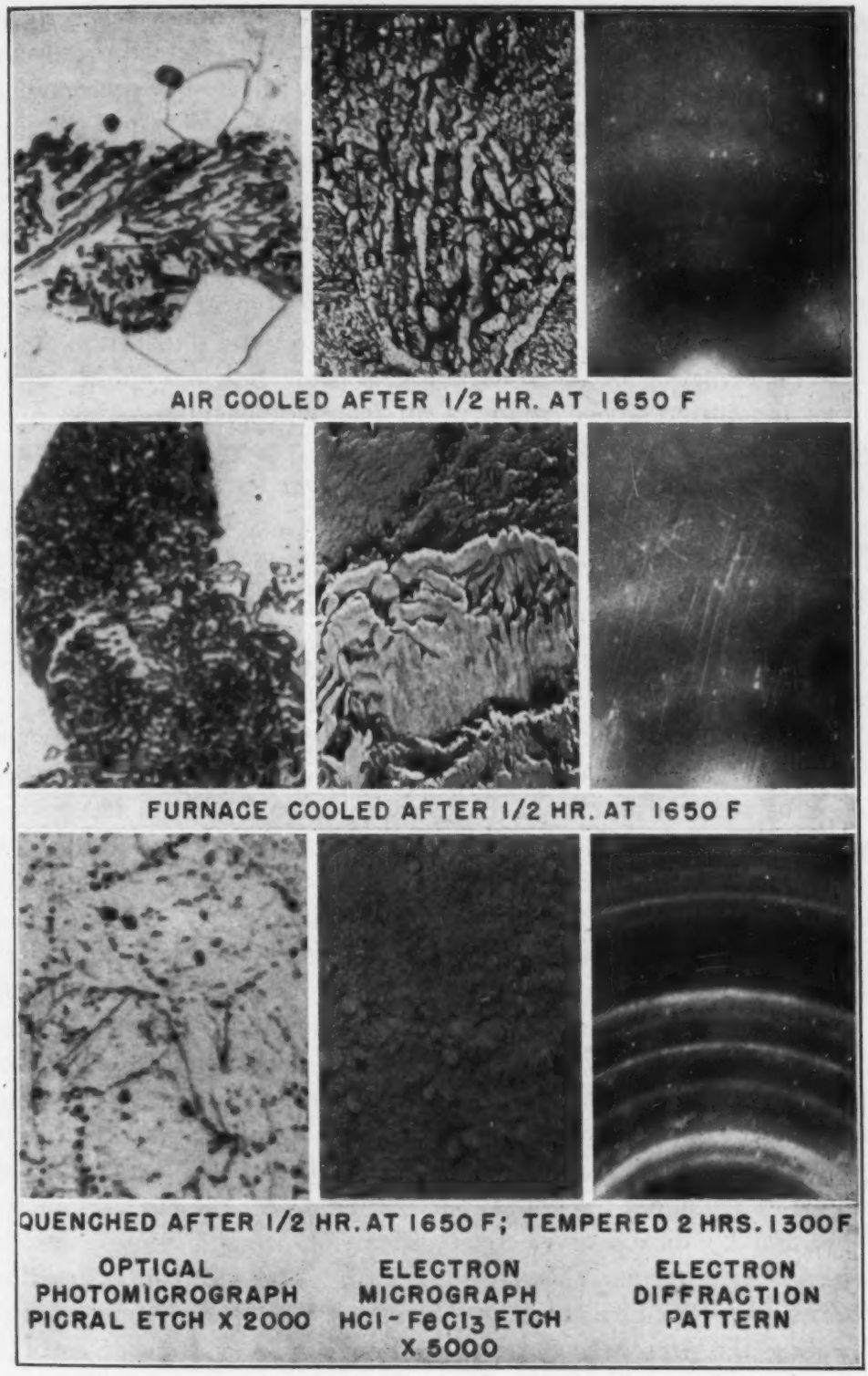


Fig. 13—Structure and Electron Diffraction Patterns of Steel Containing 1.10% Molybdenum and 0.5% Carbon After Different Heat Treatments. (Optical photomicrographs by J. R. Vilella, others by R. D. Heidenreich.)

heated at 700 C (1292 F) for 1, 5, 25 and 140 hours respectively. Carbides from each specimen were then isolated electrolytically and examined by X-rays and by other means, with results presented in Fig. 11. The carbide present after 1 hour was chiefly face-centered cubic, with only traces of cementite or hexagonal tungsten carbide, whereas after 140 hours, the double-carbide had been largely replaced by hexagonal carbide. There was also ample evidence that this change had been accompanied by a progressive depletion of tungsten in the matrix with concomitant enrichment of the carbides.

An example of the reverse change, and a good illustration of the mode of formation of cored carbides, is presented in Fig. 12, which shows the progressive change in an iron-molybdenum-carbon alloy which had been treated initially to produce a complex molybdenum-rich carbide, then subsequently held at a lower temperature, at which a carbide richer in iron, probably cementite, is more stable. This alloy, which contained about 6% molybdenum and 1.3% carbon, was first heated in an evacuated silica tube at 2040 F for 72 hours, then quenched to produce the relatively massive and hard molybdenum-rich carbide shown in Fig. 12a. Samples of the alloy in this condition were then annealed, likewise in a silica tube, at 927 C (1700 F) for 4, 24 or 72 hours, which yielded respectively the structures shown in Figs. 12b, c and d. After 4 hours, there is just visible a thin envelope of softer iron-rich carbide, which after 24 hours has grown markedly, and after 72 hours has nearly absorbed the molybdenum-rich core. On subsequent heating at higher temperature the envelope material tends to dissolve, leaving the core intact.

An example of what may happen during cooling of an alloy steel, and a good illustration of the kind of results obtainable by the electron diffraction technique developed by Heidenreich, is provided by the photographs in Fig. 13. Steel containing 1.10% molybdenum and about 0.5% carbon was heated ½ hour at 900 C (1650 F), then: (a) furnace-cooled; (b) cooled in air; (c) quenched and then tempered for 2 hours at 704 C (1300 F). The several samples were then examined under the optical microscope, under the electron microscope, and by means of electron diffraction from a heavily etched surface,* with results shown in Fig. 13. The electron diffraction patterns from the air-cooled and furnace-cooled samples are spotty, indicating the presence of a few well-developed crystals of carbide. This spottiness made it difficult to interpret the pattern, but it is

*These samples were given a rough polish, then deeply etched in HCl-$FeCl_3$. A silica replica was used for the electron micrographs.

certain that the rings observed do not coincide with those for cementite or for Mo_2C. They are, however, similar to those of a face-centered cubic structure, so that the carbide in these specimens is probably $(Fe, Mo)_{23}C_6$. The optical photomicrographs reveal the presence in the air-cooled specimens of the poorly developed pearlite characteristic of molybdenum steels, and the electron micrographs clearly show the plates of this carbide. In the furnace-cooled specimens the pearlite is better developed.

The diffraction pattern of the quenched-and-tempered specimen is quite different, showing a well-developed set of rings which correspond to those of Mo_2C. These rings indicate that these carbide particles are small and widely distributed, a conclusion confirmed by the optical and electron micrographs which show particles widely dispersed throughout the steel. The diffraction pattern also gives some indication of the presence of a small amount of the carbide found in the air- and furnace-cooled specimens. This was not evident from the optical micrographs, but occasional patches of massive plates were observed in the electron micrograph. It may be noted that the electron diffraction pattern agrees with that obtained by diffraction of X-rays from carbides isolated electrolytically.

Composition of Carbide Formed on Isothermal Transformation

There remains to be considered the constitution of carbides formed on isothermal transformation. Although the evidence is again somewhat scanty it is none the less revealing. Houdremont, Koch and Wiester (10c) have investigated the composition of a carbide, in each case cementite, formed on isothermal transformation within the range 400 to 600 C (752 to 1112 F) in both a manganese steel and a chromium steel. Their results, presented in Table II, indicate that cementite formed in the pearlite region is alloy-rich whereas that formed in the bainite region is alloy-poor. Thus, in the steel containing 0.14% carbon, 2.2% manganese and 0.18% chromium, cementite formed on transformation at 550 C (1022 F) and subsequent spheroidization at 680 C (1256 F) contains about 18% manganese and 3% chromium; on the other hand, that formed on transformation at 400 C (752 F) contains only about 4% manganese and a trace of chromium. Likewise in steel containing 0.36% carbon, 1.3% chromium and 0.31% manganese, cementite, formed at 650 C

(1202 F) and then spheroidized at 750 C (1382 F), contained 17% chromium and nearly 2% manganese, in contrast to that formed at 450 C (842 F) which contained but 3% chromium and only about 0.5% manganese.

Table II
Composition of Carbides Isolated after Isothermal Transformation in Different Temperature Ranges
(After Houdremont, Koch and Wiester)

Composition of Steel	Treatment	% Mn	% Cr
2.2% Mn, 0.14% C 0.18% Cr	Pearlite Region	18.8	2.4
	1000 C → 550 C (10 hrs.)	17.3	3.0
	+ 680 C (50 hrs.)	19.5	2.9
	Bainite Region	3.7	Trace
	1000 C → 400 C (10 hrs.)	3.9	Trace
		3.2	0.1
1.32% Cr, 0.35% C 0.31% Mn	Pearlite Region	1.9	17.1
	1150 C → 650 C (10 hrs.)	1.9	17.3
	+ 750 C (24 hrs.)	[illegible]	
	Bainite Region	0.7	2.9
	1150 C → 450 C (4 hrs.) WQ	0.6	2.6
	+ 450 C (24 hrs.) WQ		

These results are not conclusive because of the spheroidizing treatment given some of the samples, but the inference that there is a marked difference in the composition of carbides formed isothermally in the pearlite and bainite regions respectively is confirmed by data reported at this meeting by Hultgren, who suggests that the alloy content of cementite formed in the bainite region is substantially the same as the gross alloy content of the steel. Indirect evidence substantiating this conclusion has been presented by Wever and Mathieu (29). From an investigation of the saturation magnetization and Curie point of carbides in manganese steel, they concluded that the manganese content of carbides formed in the pearlite range decreases with decreasing temperature and that iron carbide formed in the bainite region contains very little manganese.

Analogous data for molybdenum steels have been reported by Bowman (15b), who concluded that in the transformation of austenite to pearlite in steels containing about 0.80% carbon and molybdenum up to 1%, the segregation of molybdenum in the carbides decreases slightly with decreasing temperature. The precise interpretation of these data is difficult because of the presence of more than one carbide, though there are indications that it is true for cementite by itself. On the other hand, subsequent data published by Bowman (12) for steels containing 0.40% carbon seem not to confirm this trend.

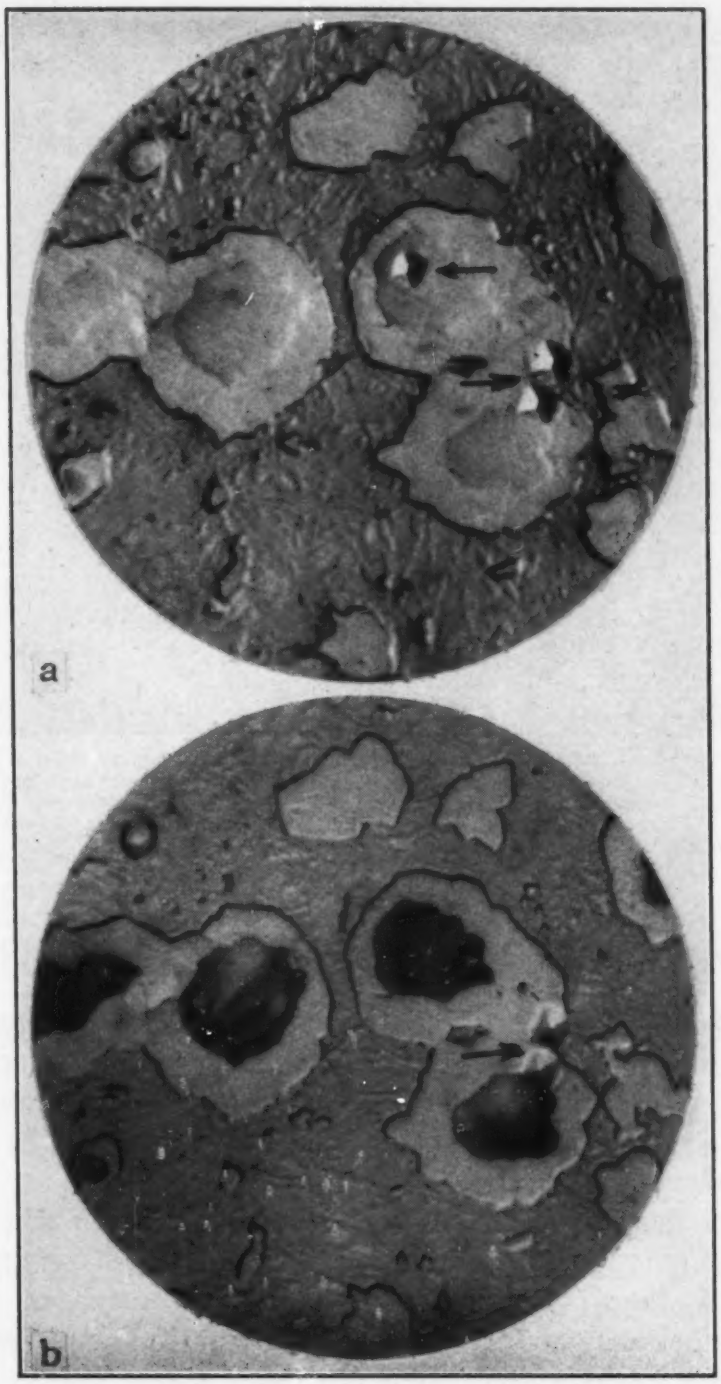


Fig. 14—Comparison of the Same Field of a Steel Containing 6% Molybdenum and 1.3% Carbon After 72 Hours at 1115 C (2040 F), Furnace Cool, 72 Hours at 930 C (1705 F) and a Brine Quench. a—Picral etch; b—Picral etch plus an electrolytic etch in alkaline chromate solution. (Photographs by R. F. Campbell.)

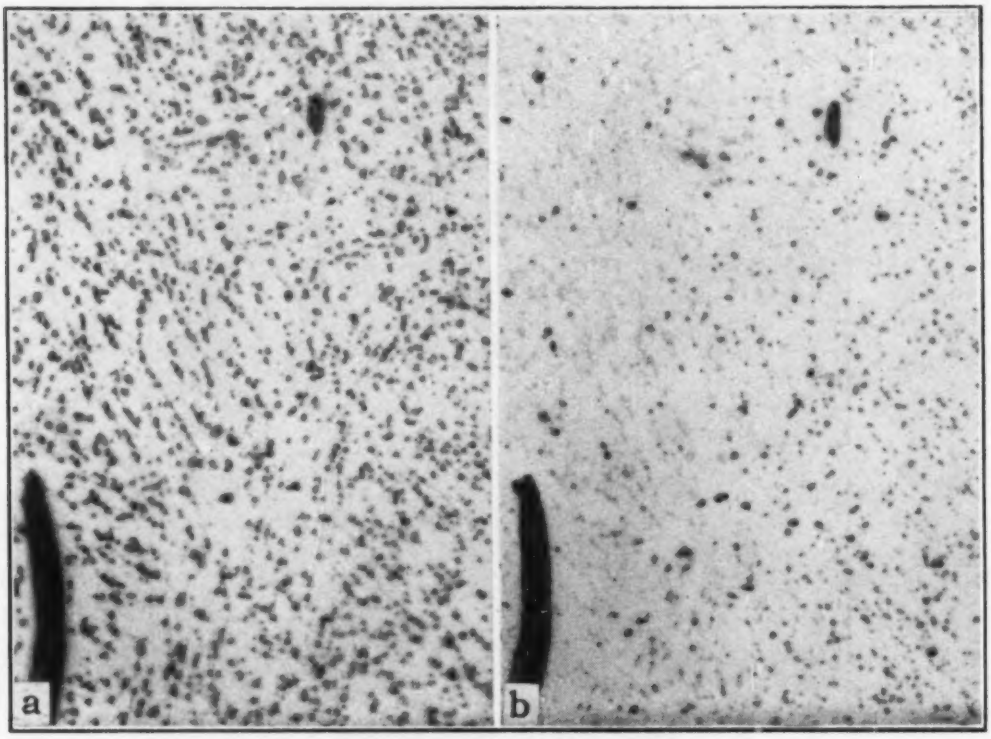


Fig. 15—The Same Field in a Steel Containing 2% Chromium and 0.35% Carbon, Quenched and Tempered for 24 Hours at 715 C (1320 F), After Different Etches; a—Etched With Picral; b—Etched Electrolytically in Alkaline Chromate Solution. (Photographs by J. R. Vilella.)

Some other interesting points brought out by Bowman and his colleagues (12), (15) are:

(a) In alloys with eutectoid carbon content, the segregation of molybdenum in the carbides is much greater at the completion of isothermal transformation, in no case more than 30 minutes, than in the same alloy quenched and tempered for as long as 250 hours at the same temperature;

(b) Orthorhombic cementite probably forms exclusively in alloys containing up to 1% molybdenum at 540 C (1000 F);

(c) In alloys containing more than 0.50% molybdenum, transformed isothermally at 650 or 705 C (1200 or 1300 F), cementite is replaced by the face-centered cubic $(Fe, Mo)_{23}C_6$;

(d) In hypoeutectoid alloys, the molybdenum concentration in cementite formed by tempering martensite can be increased to a level greater than that which results in the presence of $(Fe, Mo)_{23}C_6$, after isothermal transformation of austenite.

All these results are, in general, what one would expect in view

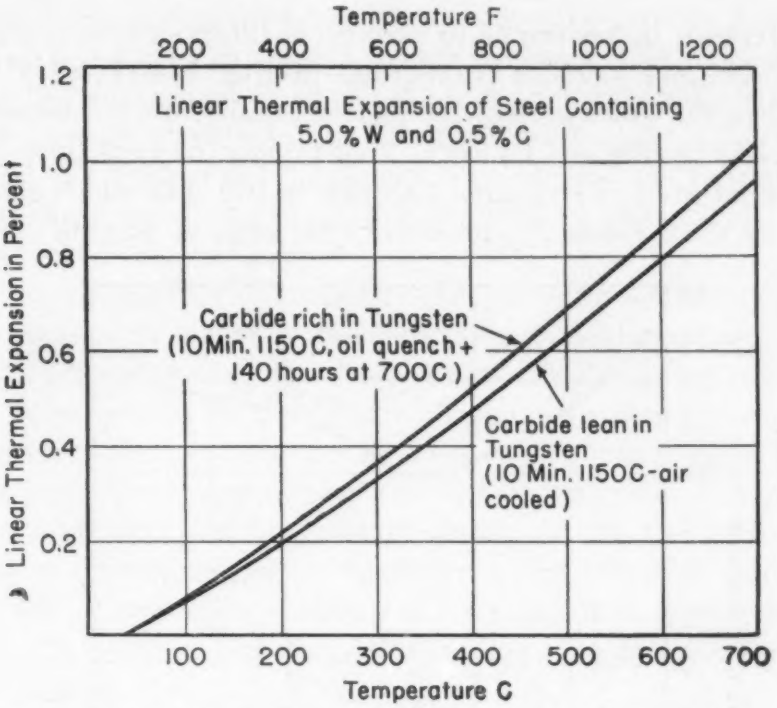


Fig. 16—Linear Thermal Expansion of an Alloy Containing 5.0% Tungsten and 0.5% Carbon When Treated so as to Put Tungsten in Solution in the Matrix as Compared With That When Tungsten is Concentrated in the Carbide Phase.

of the increasing mobility and solubility of alloying elements with increasing temperature.

Effect of Composition on Properties of Carbide and Matrix

On the basis of the foregoing data, one naturally inquires as to the significance of variation in composition of carbides on the behavior of the steel. For convenience, we shall use an admittedly arbitrary classification on the basis of the effect on the properties of: (a) the carbides themselves; (b) the matrix; (c) the steel as a whole.

Perhaps the most significant changes in the carbides themselves are in their hardness and their resistance to etching. The influence on hardness is illustrated in Fig. 14a, which shows diamond pyramid indentations made under a 2-gram load on the envelope and core of carbides in the molybdenum steel shown in Fig. 12. Although there are still some uncertainties in the extension of the Diamond Pyramid Hardness scale to such light loads, uncertainties arising in part from departure from the specified shape at the tip of the diamond, there can be no doubt that the envelope material is softer than the core, the difference being of the order of 200 DPH numbers.

Difference in resistance to etching is illustrated by comparison of Figs. 14a and b. The photograph in Fig. 14a shows a surface etched in picral which attacks the matrix rapidly, the envelopes of the carbides less rapidly and the cores least rapidly, to yield three distinct levels. Contrast this structure with that in Fig. 14b which shows the same field after a subsequent electrolytic etch in alkaline chromate

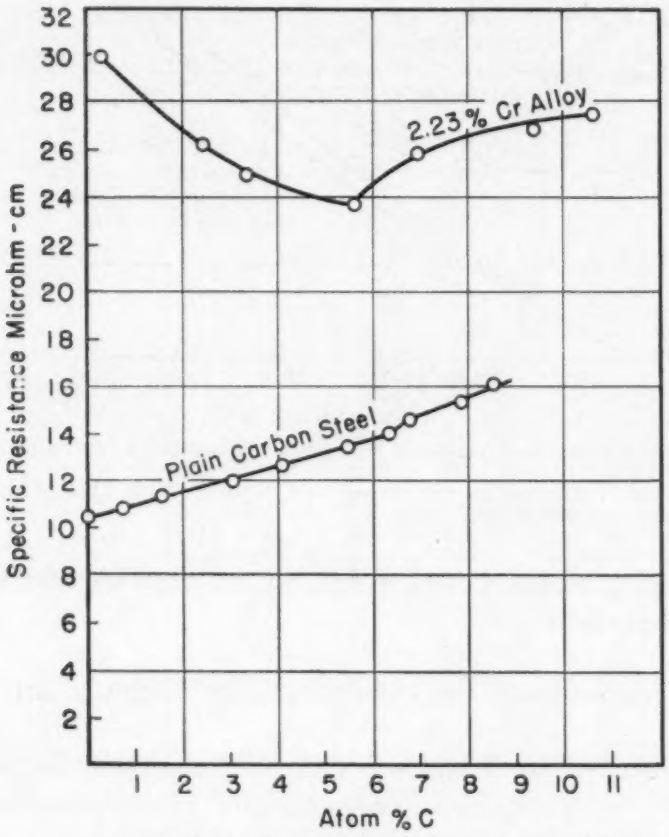


Fig. 17—Variation With Carbon Content of the Specific Resistance of Plain Carbon Steels as Compared With That of Alloys Containing 2.23% Chromium. (Data of Campbell and Whitney.)

solution which dissolves the core but leaves the envelope substantially unaltered, as is evident from the slight change in size of the diamond impressions.

Another example is presented in Fig. 15, which shows the effect of different etching reagents on the same field in a steel containing 2% chromium and 0.35% carbon, which had been quenched and tempered for 24 hours at 716 C (1320 F). Photomicrograph a shows the structure as revealed by a picral etch, b as revealed by an electrolytic etch in alkaline chromate solution. Since the phase diagram for the iron-chromium-carbon system indicates that under

these conditions cementite should be the only carbide present, the differences revealed by these reagents probably indicate a difference in the alloy content of the carbides. An analogous difference in the rate of etching of carbides in annealed ball-bearing steel has been reported by Westgren, Phragmen and Negresco (11), who demonstrated, by means of the X-ray diffraction pattern of extracted carbides, that only cementite was present.

Other properties of carbides which may be significantly altered are density, as indicated by change in lattice parameter, and magnetic susceptibility, which is influenced particularly by the iron content.

The properties of the matrix change as it becomes depleted or enriched by giving to or receiving from the carbide some of the alloying element which tends to concentrate in that phase. Thus, linear thermal expansion is significantly influenced by the effective alloy content of the matrix, as is evident from Fig. 16 which compares the expansion of a tungsten alloy after treatment to put most of the tungsten in solution with that after treatment to concentrate tungsten in the carbide.

Electric resistivity is especially sensitive to change in composition of the matrix, a good example being provided by Campbell's measurements of the resistivity of carbon and chromium steels (28), the results of which are presented in Fig. 17. The lower curve shows the increase in resistivity of a series of carbon steels of increasing carbon content, as would be expected from the formation of an increasing amount of poorly conducting carbide. The upper curve shows the change in resistance of a series of annealed steels containing 2.23% chromium. The resistivity is higher at very low carbon content because of the presence of chromium in the matrix but with increasing carbon content the formation of chromium-rich cementite so depletes the matrix that resistivity decreases up to about 5 atom per cent carbon when it begins to increase, presumably because most of the chromium is then concentrated in the carbide. It is interesting to note that from a study of the resistance of chromium steels, Le-Chatelier (20) predicted as long ago as 1898 that chromium concentrates in the carbides.

Other properties of the matrix which may be significantly altered are hardness, magnetic quality, density, lattice parameter, and corrosion resistance, of which the appearance of intergranular attack in high-chromium alloys is a good example.

Effect of Carbide Composition on the Properties of Steel

A number of properties of steel may be influenced by segregation of alloying elements in carbide phases. Some of those, such as secondary hardness, have been discussed in detail by Bain (21) and need not be considered further here. There are others, however, which should be mentioned.

The first is resistance to creep at elevated temperature. It is reasonably certain that creep strength is improved by precipitation of fine particles throughout the steel, though it has not been established that the particles need be carbides. The size and degree of dispersion of such particles may well be more significant than their composition, but one cannot ignore the possibility that progressive transfer of alloying element from matrix to carbide on holding at temperature may also be a factor.

A second is tendency to graphitize. In principle, one would expect that replacement of iron in cementite by a stronger carbide-former such as chromium or molybdenum should stabilize cementite and so lessen the tendency to form graphite; conversely, that replacement by a weaker carbide-former might enhance this tendency. The experimental evidence is difficult to interpret, in part because graphitization is influenced by many other factors and in part because of the difficulty of distinguishing between true change in equilibrium and decrease in rate of reaction. Chromium appears to stabilize cementite since, so far as I am aware, formation of graphite has never been observed in steels containing about 2% chromium. There is likewise some evidence that molybdenum is effective in preventing graphitization, yet there are well-authenticated instances of graphitization in molybdenum steels. On the other hand, it is possible that the enhanced tendency to graphitize observed in many aluminum-killed steels may be due in part to a decrease in stability of cementite resulting from the presence of aluminum.

Another example is the effect of carbide composition on susceptibility of steels to attack by hydrogen at high temperature and pressure. In the synthesis of ammonia and of certain hydrocarbons, steel is often damaged by decarburization, and by the appearance of cracks which are commonly ascribed to the formation of methane at high virtual pressure through reaction of carbide with hydrogen diffusing into the metal. Presence of alloying element in the steel, or more specifically in the carbide, appears to stabilize the carbide with conse-

quent alleviation of the attack. The influence of various alloying elements in annealed steel has been investigated by Naumann (22) with results which are summarized in Fig. 18. This chart shows the limiting temperature at which steel containing 0.1% carbon is proof against attack by hydrogen at 300 kg/cm² for 100 hours. It will be noted that the presence of silicon, nickel or copper, all noncarbide-formers, has virtually no effect. Manganese has a significant in-

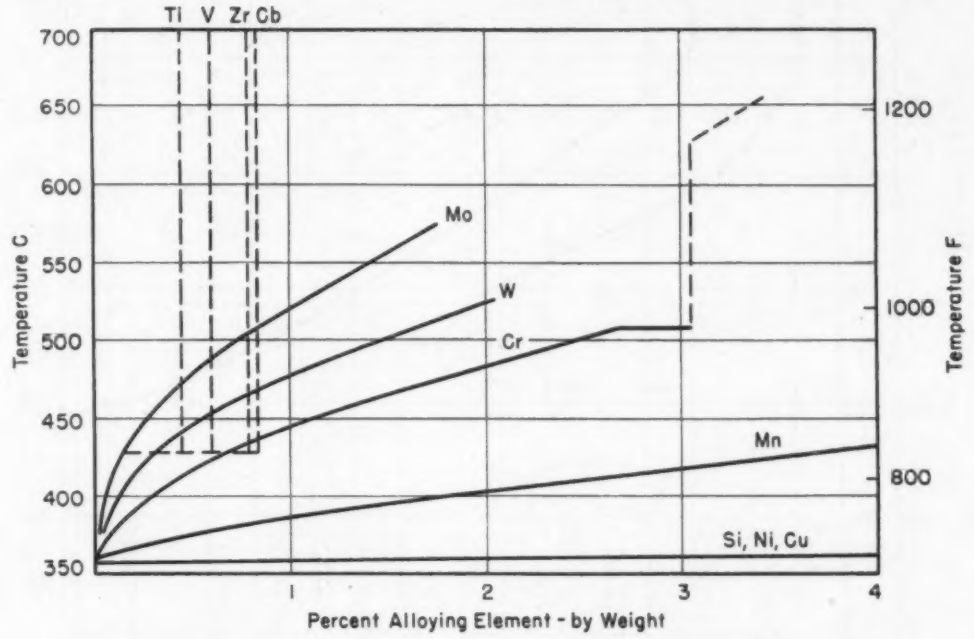


Fig. 18—Maximum Temperature at Which Different Alloy Steels, Containing 0.1% Carbon, Resist Attack by Hydrogen at 300 kg/cm² for 100 Hours. (After Naumann.)

fluence, with chromium, tungsten and molybdenum increasingly effective. All of these elements, as we have seen, concentrate in the cementite, or form higher carbides, and so become more effective as they are present in increasing concentration. Columbium, zirconium, vanadium and titanium are the most effective elements, conferring immunity to a very high temperature even when present in small concentration, because they hold the carbon as a very stable carbide.

The horizontal section in the curves for chromium, columbium, zirconium, vanadium and titanium represents the range over which two carbide phases are present. In each there is an initial range of concentration of alloying element, large for chromium, but small for the others, in which iron carbide is probably present, and in which the maximum useful temperature increases. There comes a point, however, at which another carbide appears, as indicated by the

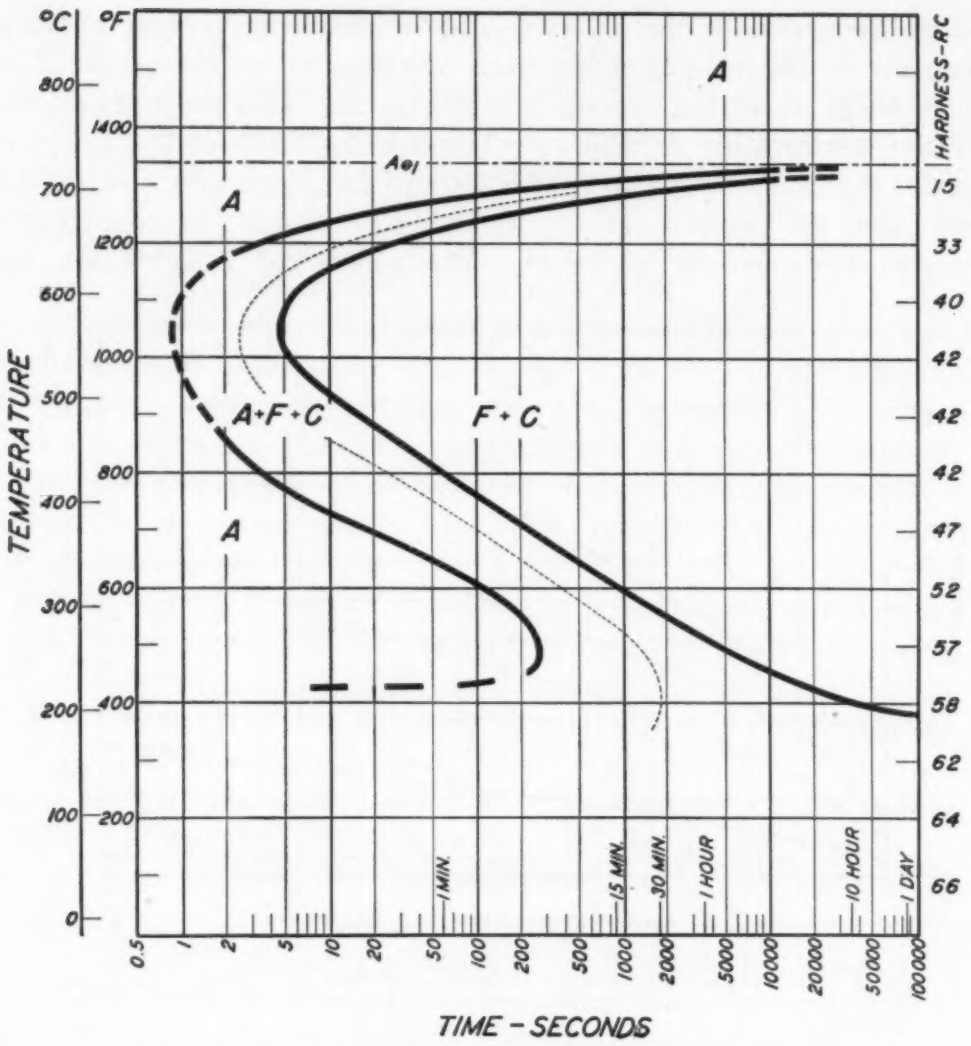


Fig. 19—Isothermal Transformation Diagram of Eutectoid Carbon Steel.

appearance of a plateau in the curve. At the concentration at which cementite disappears there is a sudden increase in the maximum temperature. The effectiveness of an alloying element in preventing attack therefore correlates directly with the degree to which it stabilizes cementite or forms a more stable carbide of its own.

These results imply that the entrance of an alloying element into cementite influences, as would be expected, equilibrium relations between iron and its carbide and a reactive gaseous atmosphere, such as hydrogen. Further evidence of this effect is found in the influence of alloying elements, especially chromium, on the rate of decarburization of steel by hydrogen, as demonstrated by Naumann (22) and by Baukloh (23). This situation is complicated by the fact that alloying

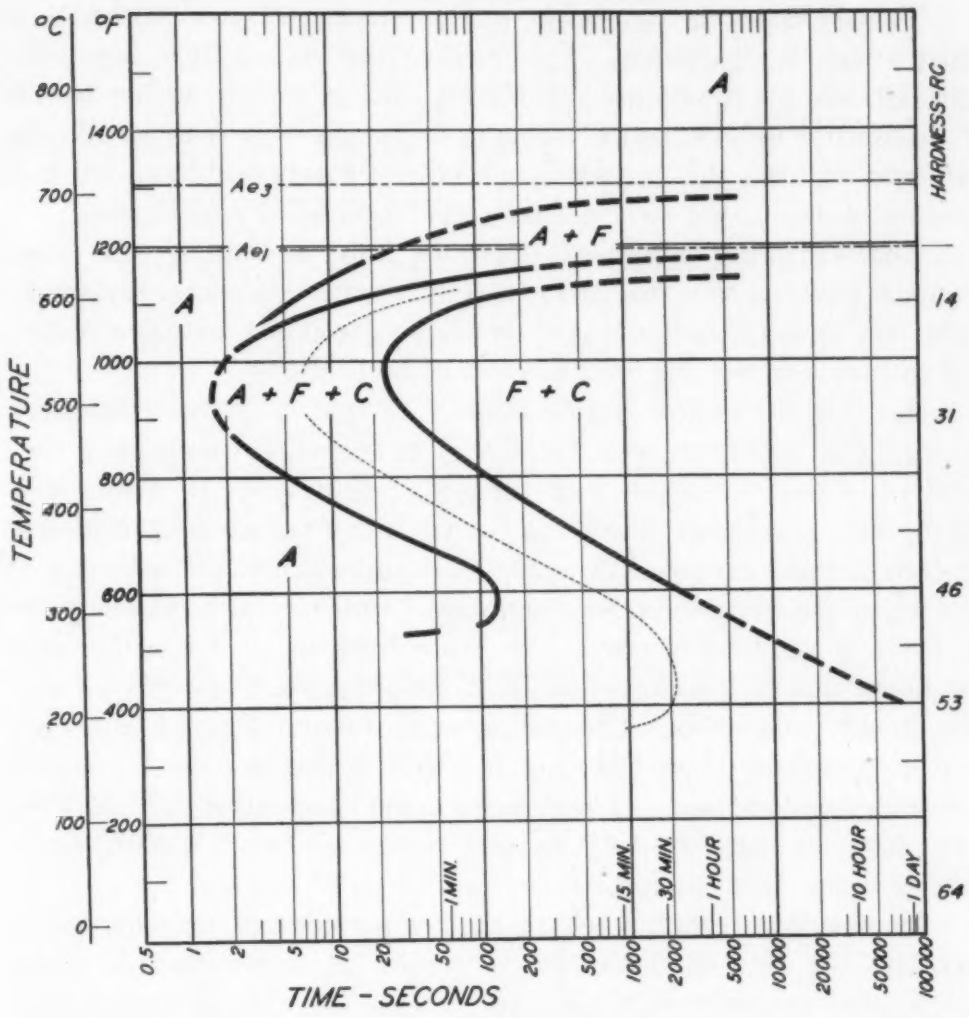


Fig. 20—Isothermal Transformation Diagram of Steel Containing 4% Nickel and 0.55% Carbon.

elements may lower the permeability of iron to hydrogen, as was demonstrated for chromium in iron by Baukloh and Guthmann (24).

If alloy steel is used in other than the annealed or tempered condition it may not, in spite of the presence of a stabilizing element, be protected. Thus, Houdremont, Koch and Wiester (10c) transformed specimens of a steel containing 3.2% chromium and 0.2% carbon in the pearlite, bainite and martensite regions respectively and exposed them to hydrogen at 500 C (930 F) at a pressure of 10,000 psi for 100 hours. Specimens transformed in the pearlite region were not attacked whereas the others were, yet subsequent annealing at 700 C (1290 F) for 24 hours rendered these specimens likewise immune.

This behavior is significant in the welding of steel which is to resist attack by hydrogen. The welding rod is usually a high-alloy material, and so commonly transforms during cooling in the bainite or martensite ranges, hence forms carbide relatively lean in alloying elements. Unless this carbide is subsequently annealed to enrich it in alloying elements, the steel is susceptible to attack by hydrogen.

The foregoing examples illustrate how misleading the usual chemical analysis of a steel may be, for in many instances, the significant fact is the distribution of an alloying element between matrix and carbide and not the total amount in both phases.

As this discussion began with a review of some established principles of chemistry and metallurgy to see what information they yield on the constitution and behavior of carbides in steel, it is appropriate now to review what we have learned about carbides to see how it bears on other principles, as, for instance, the influence of alloying elements on the rate of isothermal transformation of austenite. As there is not time to cover this entire field we shall consider only transformation to pearlite, that is, transformation nucleated by carbide, in eutectoid steels. The specific case of molybdenum has already been discussed by Ham (25) but it is instructive to treat the matter in more general terms. This requires some speculation, which, however, does no harm so long as one remembers that speculation is nothing more than opinion.

In eutectoid carbon steel, as the temperature of transformation decreases the rate of nucleation increases, as is common in many undercooled systems; this tends to increase the rate of transformation (see Fig. 19). At the same time, the diffusivity of carbon decreases, which, if the carbon gradients remain unchanged, tends to retard transformation. Yet Mehl (26) has shown that the rate of growth of pearlite nuclei increases with decreasing temperature, which indicates that the carbon gradients change in such a way as to increase the net rate of diffusion of carbon. Whether the diffusivity of carbon would, at some lower temperature, become so small as to cause a decrease in the rate of transformation to pearlite is uncertain because the nature of the reaction changes before such a temperature is attained (Fig. 19).

Addition of a noncarbide-forming element, such as nickel, silicon or copper, can conceivably influence transformation in two ways, either of which would tend to lessen its rate:

First, it may decrease the rate of the gamma to alpha trans-

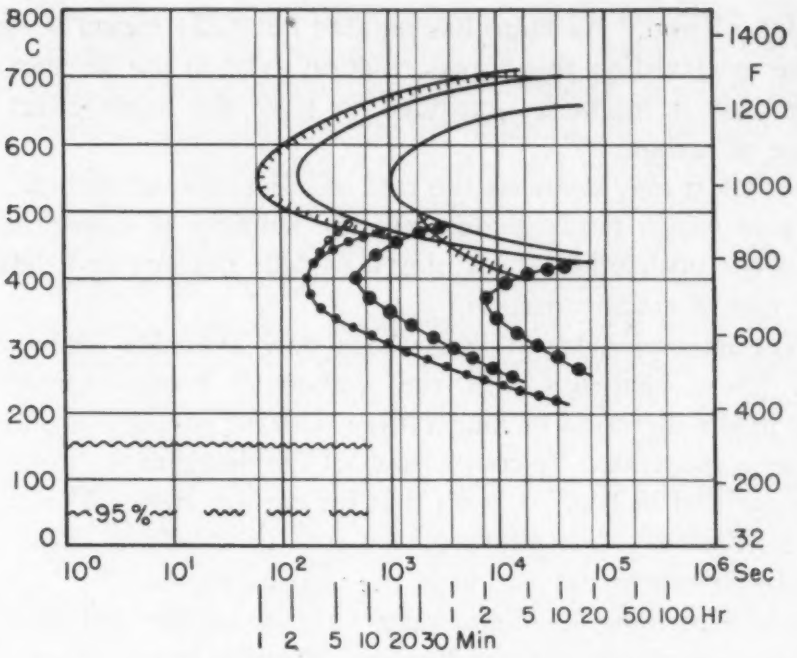


Fig. 21—Isothermal Transformation Diagram of Alloy Containing 2.90% Manganese and 0.77% Carbon Austenitized at 1300 C (2370 F). (After Hultgren.)

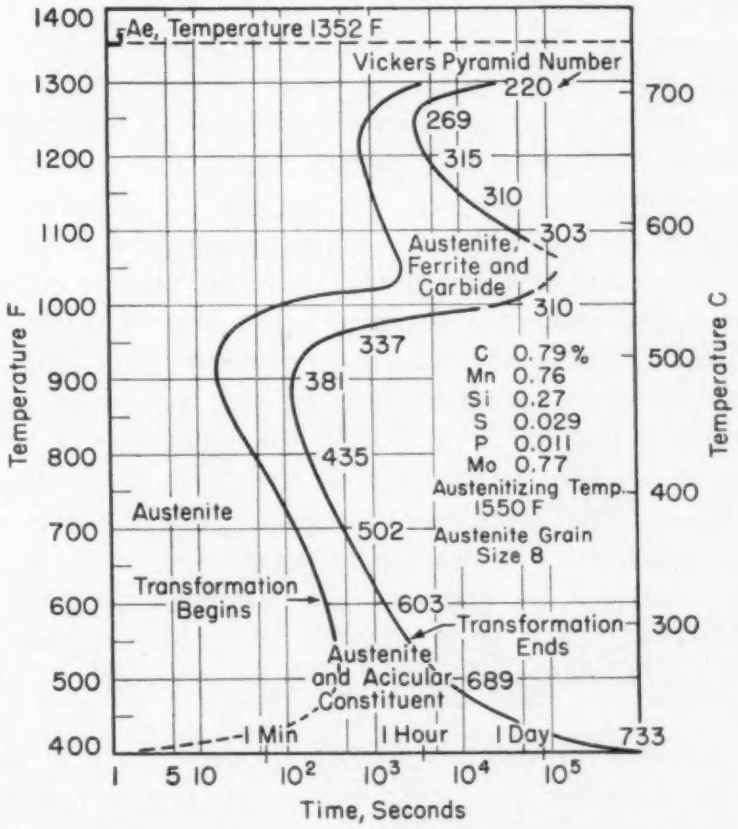


Fig. 22—Isothermal Transformation Diagram of Steel Containing 0.77% Molybdenum and 0.79% Carbon. (After Blanchard, Parke and Herzig.)

formation of iron. As Ham has pointed out (25) nickel is especially effective in retarding this transformation even in the absence of carbon, so that it might be expected to have the same effect in the presence of carbon.

Second, it may decrease the rate of nucleation of carbide. Thus, an element which tends to decrease the stability of cementite might decrease the probability of forming a carbide nucleus and thus lessen the net rate of transformation.

Experimental data, at least those now available, show that, in general, these elements shift the isothermal transformation curve slightly in the direction of longer time without essentially altering its shape, as is illustrated by comparison of the diagram for a 4% nickel alloy, presented in Fig. 20, with that for carbon steel. This suggests that the effect of such alloying elements is chiefly to slow up the gamma to alpha transformation in the pearlite region.

Carbide-forming elements may have a similar influence, since manganese and chromium are likewise effective in retarding the rate of transformation of iron, but one would also expect, since they tend to concentrate in cementite, that they would directly affect the rate of carbide formation. For instance, since manganese tends to segregate in cementite to form a continuous series of solid solutions ranging from Fe_3C to Mn_3C, the necessity for diffusion of manganese, which diffuses much less rapidly than carbon, might contribute to retarding the transformation. Moreover, the decrease in diffusivity of manganese and of carbon with decreasing temperature would seem to favor the appearance of a maximum rate in the pearlite region, unless the concentration gradients change as they appear to do in carbon steels. Most of the isothermal transformation diagrams for manganese steels thus far published show no such maximum, although in some, notably in that for SAE T-1335, the appearance of one may be foreshadowed by the promontory in the curve for completion of transformation. That there may be a definite, unmistakable maximum rate of transformation to pearlite in manganese steels is, however, amply demonstrated by some of the diagrams presented at this meeting by Hultgren, a good example being his diagram for steel containing 2.90% manganese and 0.77% carbon which is reproduced in Fig. 21.

The influence of stronger carbide-formers, such as chromium, molybdenum, tungsten and vanadium, is less simple because in the presence of these elements there is a tendency to form complex car-

bides, especially at temperatures approaching Ae_1. Thus one must take into account not only the effect of such elements on the rate of gamma to alpha transformation and the necessity for their diffusion into the carbide, but also the greater difficulty of forming a more complex nucleus. As an illustration, the unit cell of cementite contains but 16 atoms whereas that of $(Fe, Mo)_{23}C_6$ contains 116. It is only reasonable, therefore, to expect that the probability of forming such a nucleus, hence the rate of nucleation, should be markedly less than in a plain carbon steel. Combination of these three factors, all of which operate in the same direction, provides a possible explanation of the fact that the isothermal transformation curves for steels containing these elements commonly show a maximum rate of transformation within the pearlite region and that this region covers a narrower range of temperature than is found in carbon steels. A typical example of such a maximum is given in Fig. 22. It would appear that in such steels the low diffusivity of the alloying elements, together with the difficulty of forming a complex nucleus, more than offsets the influence of a change in concentration gradients.

On the basis of the foregoing speculations, it is possible to explain why these elements have relatively little effect on the position of the bainite portion of the isothermal transformation curve, since, in this range, the carbide formed is commonly alloy-lean cementite which differs but little from that formed in carbon steels.

Virtually all the data now available are for carbides which represent the end-product of isothermal transformation. It would be interesting to investigate the composition of carbides formed at the beginning and to learn how it changes during transformation, for such knowledge should increase our understanding of these processes.

In conclusion, it is now possible to answer, at least in part, the questions with which this discussion began. The composition of cementite appears to vary measurably in several different ways. When in equilibrium with austenite its carbon content may be significantly less than that corresponding to the formula Fe_3C, the deficiency increasing with increasing temperature. It is possible that carbon may be replaced to a limited extent by nitrogen. Iron atoms can be replaced by atoms of other carbide-forming elements which can fit into the cementite structure—more specifically, by atoms of manganese, chromium, molybdenum, tungsten, or vanadium. At equilibrium, on annealing, or on isothermal transformation in the pearlite region, these elements tend to concentrate in the carbide phase,

depleting the matrix and thereby altering many of the properties of the steel.

These answers are admittedly neither final nor complete. Moreover, they raise, in turn, a number of other questions; indeed, I have in this lecture probably raised more questions than I have settled. But these new questions serve to emphasize gaps in our knowledge and will, I hope, stimulate further investigation in this fruitful field in which Professor Campbell was so notable a pioneer.

Bibliography

1. H. Lipson and N. J. Petch, "The Crystal Structure of Cementite," *Journal,* Iron and Steel Institute, Vol. 142, 1940, p. 95-106.
2. N. J. Petch, "The Interpretation of the Crystal Structure of Cementite," *Journal,* Iron and Steel Institute, Vol. 149, 1944, p. 142-150.
3. L. C. Pauling, "The Nature of the Chemical Bond," 1939, Cornell University Press, p. 399.
4. G. Hägg, "Gesetzmässigkeiten im Kristallbau bei Hydriden, Boriden, Carbiden, und Nitriden der Übergangselemente," *Zeitschrift f. Physikalische Chemie,* Abt. B., Vol. 12, 1931, p. 33-56.
5. H. A. Schwartz, K. R. Van Horn and C. H. Junge, "Transformation in the Carbide Phase During Graphitization," TRANSACTIONS, American Society for Steel Treating, Vol. 21, 1933, p. 463-480.
6. R. D. Heidenreich, L. Sturkey and H. L. Woods, "Investigation of Secondary Phases in Alloys by Electron Diffraction and the Electron Microscope," *Journal of Applied Physics,* Vol. 17, 1946, p. 127-136.
7. W. Hume-Rothery, G. W. Mabbott and K. M. Channel-Evans, "The Freezing Points, Melting Points and Solid Solubility Limits of the Alloys of Silver and Copper with the Elements of the B Sub-groups," *Philosophical Transactions,* Royal Society, Ser. A, Vol. 233, 1934, p. 1-97.
8. W. Hume-Rothery, "The Structure of Metals and Alloys," Institute of Metals, Monograph No. 1, 1936, Table III, p. 40.

9a. S. Shimura, "Study of the Structure of Cementite," *Journal,* Faculty of Engineering, Tokyo Imperial University, Vol. 20, 1931 , p. 1; *Proceedings,* Imperial Academy, Tokyo, Vol. 6, 1930, p. 269.

9b. A. Westgren and G. Phragmen, "X-ray Studies on the Crystal Structure of Steel," *Journal,* Iron and Steel Institute, Vol. 105, 1922, p. 241-273.

10a. J. O. Arnold and A. A. Read, "The Chemical and Mechanical Relations of Iron, Manganese, and Carbon," *Journal,* Iron and Steel Institute, Vol. 81, 1910, p. 169-184.

10b. E. Maurer and F. Hartmann, "Über die Quantitative Bestimmung des Eisencarbids im Gewöhnlichen Kohlenstoffstahl," *Zeitschrift f. Anorganische Chemie,* Vol. 136, 1924, p. 75-89.

10c. E. Houdremont, W. Koch and H. J. Wiester, "On the Processes of Transformation in Chromium and Manganese Steels," *Archiv f. das Eisenhüttenwesen,* Vol. 18, 1945, p. 147.

11. A. Westgren, G. Phragmen and T. Negresco, "On the Structure of the Iron-Chromium-Carbon System," *Journal,* Iron and Steel Institute. Vol. 117, 1928, p. 383-400.
12. F. E. Bowman, "Partition of Molybdenum in Hypoeutectoid Iron-Carbon-Molybdenum Alloys," TRANSACTIONS, American Society for Metals, Vol. 36, 1946, p. 61.

13. V. Adelsköld, A. Sundelin and A. Westgren, "Carbide in Kohlenstoffhaltigen Legierungen . . . ," *Zeitschrift f. Anorganische Chemie,* Vol. 212, 1933, p. 401-409.
14a. F. R. Morral, G. Phragmen and A. Westgren, "Carbides of Low Tungsten and Molybdenum Steels," *Nature,* Vol. 132, 1933, p. 61-62.
14b. F. R. Morral, Discussion of article by F. E. Bowman, R. M. Parke and A. J. Herzig, "The Alpha Iron Lattice Parameter as Affected by Molybdenum . . . ," TRANSACTIONS, American Society for Metals, Vol. 31, 1943, p. 487-495, Discussion, p. 495-496.
15a. F. E. Bowman and R. M. Parke, "The Partition of Molybdenum in Iron-Carbon-Molybdenum Alloys at 1300 Degrees Fahr. and the Nature of the Carbides Formed," TRANSACTIONS, American Society for Metals, Vol. 33, 1944, p. 481-493.
15b. F. E. Bowman, "The Partition of Molybdenum in Steel and Its Relation to Hardenability," TRANSACTIONS, American Society for Metals, Vol. 35, 1945, p. 112-129.
16. S. Takeda, "On the Carbides in Tungsten Steels," Technical Reports, Tohoku Imperial University, Vol. 9, No. 4, 1930, p. 26-52, 165-202.
17. A. Westgren, "The Crystal Structure of High Speed Steel Carbide," *Jernkontorets Annaler,* Vol. 88, 1933, p. 12-14.
18. W. A. Wood, "X-ray Study of Some Tungsten Magnet Steel Residues," *Philosophical Magazine,* 7th ser., Vol. 10, 1930, p. 659-667.
19. R. Vogel and E. Martin, "Über das Ternäre System Eisen-Kohlenstoff-Vanadin," *Archiv f. das Eisenhüttenwesen,* Vol. 4, 1930-31, p. 487-495.
20. H. LeChatelier, "Electricité sur la Resistance Electrique des Aciers," *Comptes Rendus,* Vol. 126, 1898, p. 1709-1711.
21. E. C. Bain, "The Functions of the Alloying Elements in Steel," 1939, American Society for Metals, Cleveland.
22. F. K. Naumann, "Der Einfluss von Legierungszusätzen auf die Bestandigkeit von Stahl Gegen Wasserstoff unter Hohern Druck," *Stahl und Eisen,* Vol. 58, 1938, p. 1239-1249.
23. W. Baukloh, Discussion of article above, *Stahl und Eisen,* Vol. 58, 1938, p. 1249-1250.
24. W. Baukloh and H. Guthmann, "Wasserstoffdurchlässigkeit und Wasserstoffentkohlung von Stählen, Armco-Eisen, Kupfer, Nickel und Aluminium bei Höheren Drucken," *Zeitschrift f. Metallkunde,* Vol. 28, 1936, p. 34-40.
25. J. L. Ham, "The Rate of Diffusion of Molybdenum in Austenite and in Ferrite," TRANSACTIONS, American Society for Metals, Vol. 35, 1945, p. 331-361.
26. R. F. Mehl, "The Structure and Rate of Formation of Pearlite," TRANSACTIONS, American Society for Metals, Vol. 29, 1941, p. 813-862.
27. W. Crafts and J. L. Lamont, "Effect of Alloys in Steel on Resistance to Tempering," *Metals Technology,* Sept. 1946, TP2036, 21 p.
28. E. D. Campbell and G. W. Whitney, "The Effect of Changes in Total Carbon and in the Condition of Carbides on the Specific Resistance and on Some Magnetic Properties of Steel," *Journal,* Iron and Steel Institute, Vol. 110, 1924, p. 291-311.
29. F. Wever and K. Mathieu, "Ueber die Umwandlungen der Manganstähle," *Mitteilungen, Kaiser Wilhelm Institut f. Eisenforschung,* Vol. 22, 1940, p. 9-18.
30. K. H. Jack, "Iron-Nitrogen, Iron-Carbon and Iron-Carbon-Nitrogen Interstitial Alloys," *Nature,* Vol. 158, 1946, p. 60-61.

THE CHROMIUM-OXYGEN EQUILIBRIUM IN LIQUID IRON

By Hsin-Min Chen and John Chipman

Abstract

Experiments are described in which liquid iron-chromium alloys containing up to 20% chromium were brought into equilibrium with accurately controlled gaseous mixtures of water vapor and hydrogen. The relationship between the ratio $(H_2O)/(H_2)$ and the equilibrium chromium content of the bath was used to determine equilibrium constants and free energy changes in the reactions:

$$FeO \cdot Cr_2O_3\ (s) + 4H_2\ (g) = 4H_2O\ (g) + Fe\ (l) + 2\underline{Cr}\ (\text{in Fe}) \quad [1]$$

$$Cr_2O_3\ (s) + 3H_2\ (g) = 3H_2O\ (g) + 2\,\underline{Cr}\ (\text{in Fe}) \quad [2]$$

The reactions were studied in crucibles of chromite and of chromic oxide. A method was developed for manufacture of the latter.

At 1595 C, chromite is the stable solid phase in equilibrium with melts containing less than 5.5% chromium, while at higher percentages Cr_2O_3 becomes the stable phase.

The oxygen content of the metal depends upon the ratio of water vapor to hydrogen in the gas phase and the chromium content. For any given H_2O:H_2 ratio the oxygen in the bath increases with increasing chromium content. This signifies that chromium decreases the activity of oxygen in liquid steel. The effect is explained by postulating the existence of chromous oxide in solution in the metal. On this assumption the concentrations of oxygen associated respectively with chromium and with iron are calculated.

The results obtained for reaction [2] are shown to be in excellent agreement with calculated figures obtained by extrapolation of results at lower temperatures on the reduction of Cr_2O_3 by hydrogen to form solid chromium. Since the calculation involves the assumption that liquid iron-chromium alloys obey Raoult's Law for ideal solu-

This paper is based upon a thesis submitted by Hsin-Min Chen in partial fulfillment of the requirements for the degree of Doctor of Science at the Massachusetts Institute of Technology.

A paper presented before the Twenty-eighth Annual Convention of the Society held in Atlantic City, November 18 to 22, 1946. Of the authors, Dr. Chen is associated with the Metallurgical Department, Carnegie-Illinois Steel Corp., South Works, Chicago; and John Chipman is head, Department of Metallurgy, Massachusetts Institute of Technology, Cambridge, Mass. Manuscript received May 27, 1946.

tions, the agreement gives strong evidence of the validity of this assumption.

The effect of temperature on reactions [1] and [2] is established by calculations based upon extrapolation of the low temperature data. The variation of oxygen content of the melt with temperature is approximated by calculations of somewhat less certainty and the results are presented in graphs and tables covering the range 2800 to 3200 F.

THE chemical behavior of the alloying elements in molten steel varies widely among the several elements commonly employed. The reactivity toward oxygen dissolved in the bath ranges all the way from the strong affinity of the deoxidizing elements, aluminum, zirconium, etc., to the nearly complete inertness of copper and nickel. Intermediate between these two extremes lie two of the most universally used alloying elements, manganese and chromium, and it is with the behavior of the latter toward oxygen that this paper is concerned. It is known, of course, that chromic oxide is moderately stable at steelmaking temperatures; it is not stable enough to make the element a good deoxidizer but is sufficiently stable to lead to the formation of chromic oxide and chromite inclusions in most steels which contain significant amounts of the alloy.

An attempt has been made (1)[1] to calculate the free energy of formation of chromic oxide from the elements chromium and oxygen dissolved in molten steel and thus to evaluate the deoxidizing power of the element. The calculation was based upon the not very concordant experimental data at lower temperatures and the assumption that chromium and liquid iron form an "ideal" solution, i.e., a solution which conforms to Raoult's Law. Since that time, additional low-temperature data have become available which, when taken into consideration with the results of the studies to be reported in this paper, not only make it possible to describe accurately the behavior of chromium in liquid steel with respect to oxygen, but also to verify the assumption of the essential ideality of the iron-chromium liquid solution.

Studies of the nonmetallic inclusions (2), (3), (4) have indicated that there are probably two products of the reaction of chromium with dissolved oxygen; chromic oxide, Cr_2O_3, and chromite, $FeO \cdot Cr_2O_3$. The conditions which lead to the formation of the one or the other product are not clearly defined. Both products are crys-

[1]The figures appearing in parentheses refer to the bibliography appended to this paper.

talline solids and the second forms the principal constituent of chromium refractories.

The purpose of the work herein described was to observe experimentally the conditions of equilibrium in the two reactions:

$$2\underline{Cr} + 3\underline{O} = Cr_2O_3$$
$$\text{and } \underline{Fe} + 2\underline{Cr} + 4\underline{O} = FeO \cdot Cr_2O_3$$

In these equations the underscored symbols represent elements in solution in liquid steel.

The plan of attack was to melt iron-chromium alloys in chromite or chromic oxide crucibles and to bring the melt into equilibrium with a controlled atmosphere of hydrogen and water vapor, thus controlling the activity of the oxygen in the melt. It was expected that the chromium content of the bath would adjust itself to the equilibrium concentration by reacting with oxygen if it were in excess or by the solution of part of the crucible if the bath were deficient in chromium. It was further planned to secure additional data on the reaction:

$$H_2 + \underline{O} = H_2O$$

which has already been studied in pure iron (5), (6), but which up to the present has eluded attempts to obtain accurate data in the presence of alloying elements.

The essentials of the experimental method were to hold the molten alloy in the selected refractory and in the controlled atmosphere, with induction heating and its resultant stirring, long enough to attain equilibrium, to chill the melt quickly enough to avoid significant loss of oxygen by separation of slag and to analyze the resultant ingot to determine the concentration of dissolved oxygen and chromium in the melt.

Apparatus

Gas System—A diagram of the apparatus is shown in Fig. 1. Commercial hydrogen passed through a needle valve and led to the safety trap (T) which, containing mercury covered with water, was used to relieve excess tankside pressure. A by-pass (B) with stopcocks was provided so that the hydrogen could be introduced directly from the tank to the furnace when desired. The catalytic chamber (C) was used to convert any contaminated oxygen in the commercial

hydrogen into water vapor with platinized asbestos. The temperature of the catalyst was kept at about 425 C (795 F). All connections beyond the catalytic chamber were of all Pyrex glass construction, and even before it rubber tubing was used sparingly. Tubings beyond the water bath were heated to prevent the condensation of water vapor.

The gas then passed through a water bath (W), kept at desired temperature by an auxiliary heating unit, so that the gas was bur-

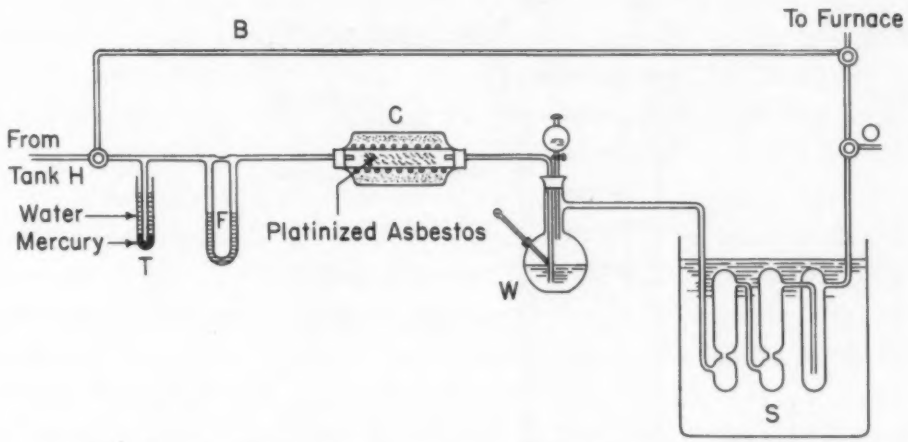


Fig. 1—Apparatus for Purification and Saturation of Hydrogen.

dened with a proper amount of water vapor before it was introduced into the saturator (S). The saturator unit was composed of three glass chambers with the first two chambers packed with glass beads and partially filled with water and the third empty as the entrainment chamber. Each tower had a glass tube with a stopper attached for the purpose of adjusting the amount of water in it. This unit was immersed in the water bath of a thermostat, the temperature of which was electrically controlled to within ± 0.05 C without difficulty and to within ± 0.02 C in certain cases.

Furnace Set-Up—The furnace set-up is shown in Fig. 2. For the first few runs a sand surface quartz tube 18 inches long and 2 inches in diameter was used, but later it was found to be permeable to hydrogen at elevated temperatures. As a result, a quartz tube with glazed surface of the same dimensions was used instead and was found to be successful.

As for the head, in the first 20 runs a brass head with a sight glass of Pyrex was used. It was found to be always a source of trouble. Neither porcelain cement nor zinc cement provided the good

gas-tight seal needed for the connection between the brass head and the quartz tube as well as that between the head and the gas inlet tube. Both these cements were sensitive to temperature changes and liable to develop small cracks. The solution was found by using a Pyrex glass head which could be directly sealed to the inlet tube. The joint with the quartz tube was made by using a pool of molten Wood's metal, kept molten at all times, as a liquid seal. Copper

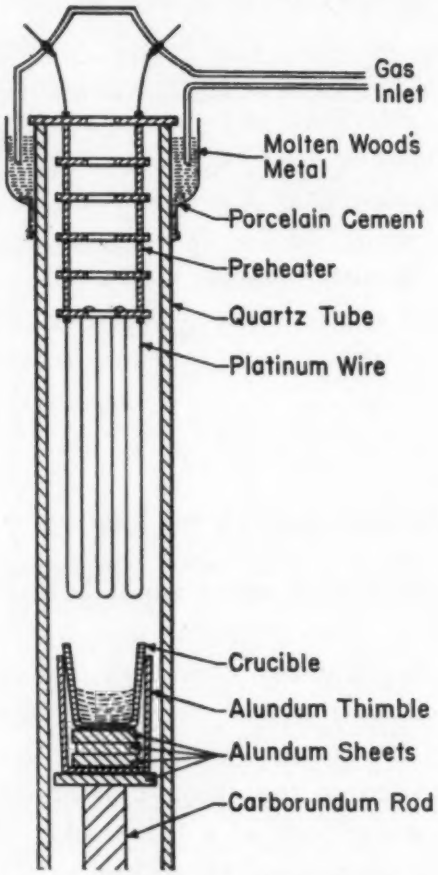


Fig. 2—Furnace Arrangement.

sheet was bent around and cemented with porcelain cement to the quartz tube to form a container for the molten metal, and nichrome wire was wound outside with asbestos paper insulation to pass electric current to supply the heat needed to keep it molten. Solidification of the metal would certainly crack the Pyrex glass head, and overheating of this low fusing metal will cause evaporation and oxidation of certain constituents of the metal as well as eventual fogging of the glass head, making the determination of the temperature inaccurate.

The crucible was rested on two or three alundum plates in an alundum crucible. This alundum crucible was in turn supported on the top of a carborundum tube, which was placed on a removable transite slide. The alundum plates were used for heat insulation. When the chromic oxide crucible was supported directly on the carborundum tube, the crucible would invariably break during the run, probably due to the high heat conductivity of carborundum and the resultant high thermal gradient through the thin chromic oxide crucible. The furnace was completed with an induction coil 2½ inches in diameter, with 12 turns of ⅜-inch copper tubing. The power was supplied by a high frequency converter. About 15 kilowatts were needed for melting, and about 9 kilowatts were enough for keeping the metal at 1600 C (2910 F).

In order to cut down the thermal diffusion (5), due to the temperature gradient of the gas mixture, a preheater was inserted as shown in Fig. 2. Platinum wire of gage No. 30 was used as the heating element, and was supported with a frame of porcelain disks and alundum tubes. The circular porcelain disks with holes for both the alundum tubes and the heating elements were made of high temperature chemical porcelain. These were designed to prevent excessive heat radiation to the top part of the furnace set-up where too high a temperature was not desired. The whole frame was supported on the top of the quartz tube with thin alundum tubes, which were cemented to the porcelain disks with porcelain cement in the lower part and bound to each other with iron wire in the upper part. The leads were made of No. 24 platinum wires sealed through the Pyrex glass head to prevent any leakage. Direct current was used for the preheater so that the resistance across it could be readily calculated by measuring the voltage across it and the current through it. The temperature of the preheater was thus estimated by the length of the platinum wire and the resistance change across it. Due to the deterioration of the platinum wire and the nonuniformity of the temperature throughout the preheater, the estimation of its temperature was only an approximation, and its temperature could not be brought much higher than an estimated average of about 1100 C (2010 F) without a rapid breakdown of the platinum wire.

Calibration and Testing of the Apparatus—The flowmeter was calibrated by passing hydrogen through the whole gas system but, instead of passing into the furnace, the gas was collected over water

through the exit in a collecting vessel. Care was taken not to disturb the pressure distribution in the gas system.

The performance of the catalytic chamber was tested by detecting the presence of any oxygen in the gas mixture by absorption in alkaline pyrogallol. It was found that the oxygen present in the system was negligible.

The performance of the saturator was tested by determining the amount of water vapor carried in a measured amount of dry hydrogen. The absorption system consisted of 3 glass-stoppered tubes. The first (a) was filled with glass wool to remove the major part of the water vapor. Tube (b) was filled with phosphorus pentoxide to remove the last trace of water vapor. The third tube (c) was filled with phosphorus pentoxide, and was used to prevent any back diffusion of the water vapor from the collection vessel into the absorption tube (b). As explained later, the gas flow rate used was sometimes very low and consequently back diffusion was not impossible. Only the increases in weight of the tubes (a) and (b) are registered as the amount of water vapor carried in the gas mixture. All the connections before tube (a) were kept hot in the same way as the main system to prevent any condensation of the water vapor. At first the whole gas current was passed through the absorption system. However, although extreme care has been taken to adjust the pressure in the collecting vessel, there was the possibility that it was not exactly equal to the atmospheric pressure due to the not-too-fine adjustment and the experimental difficulties. Later, with the main current passing into the furnace with the preheater and Wood's metal seal heated as in an actual run, a small portion of the gas mixture was led out through a side tube by adjusting the pressure in the collecting vessel. In this arrangement the situation exactly duplicated that of an actual run, but care had to be taken to remove only a small amount of gas so that no back flow from the furnace occurred. The results showed good check with the calculated results, up to 50 C for the temperature of the saturator and 430 milliliters per minute for the rate of the hydrogen flow.

Measurement of the Temperature of the Molten Bath—A Leeds and Northrup disappearing filament type optical pyrometer of recent design was used for temperature measurement. To eliminate the error introduced due to the liquid iron not being a black body and also to the absorption of part of the radiation by the glass, the optical pyrometer was calibrated by observing the melting point of electro-

lytic iron in a magnesia or alundum crucible under a gas of commercial hydrogen. It was observed repeatedly that the apparent melting point was 1335 C (2435 F). The deviation from this figure has never been greater than 2 degrees in various determinations. The melting point of electrolytic iron was taken to be 1535 C (2795 F). The equation used was

$$\frac{1}{T} - \frac{1}{T_A} = K$$

where T is the actual temperature in degrees absolute, T_A the observed temperature (also in degrees absolute) and K a constant for all practical purposes, when all the conditions were standardized and the emissivity of the observed substances did not change too much. The calculation gave the value K = —0.0000684. This value was used throughout the whole work.

Chromic Oxide Crucibles

Since it was anticipated that either chromic oxide or iron chromite would be formed in the reaction under investigation, it was desirable to use crucibles of these materials to avoid introduction of extraneous components. Fairly satisfactory chromite crucibles were obtained from a commercial source and chromic oxide crucibles were made in the laboratory by a slip-casting technique (7) which is described briefly as follows:

Three lots of chromic oxide have been used, all of technical grade. No. 1 was bought from the Baker Chemical Company. It was of dark green color and settled in water rather easily. No. 2 was bought from Merck and Company. It was light green in color and seemed to be not easily wetted with water. It tended to float on the surface of water in a thin layer, and if forced down under water by agitation, small air bubbles were always trapped and were hard to remove. No. 3 was also obtained from the Baker Chemical Company. It was different from No. 1, being light green in color and not settling so readily in water as No. 1. All three were very fine material, leaving practically no residue on a 100-mesh sieve, but their slip-forming properties were quite different from one another. No. 2 was the most plastic while No. 1 was the least. Slip made of No. 1 material showed not enough plasticity. It was thin and castings made of it cracked in the molds. No satisfactory castings

could be obtained. Slips made of materials No. 2 and 3 were sticky and rubbery, containing numerous small air bubbles, and the castings were soft and weak and stuck tightly to the mold. Very few good castings could be successfully removed from the mold. Even these had their inner surfaces scarry due to small air bubbles which could not be made to escape by any means.

Absolute alcohol and some other organic liquids were tried without success. However, crucibles which cast well and which could be dried and fired without cracking were finally obtained by using a mixture of materials and developing its plasticity by digesting with water and the use of hydrochloric acid. A mixture of 70% by weight of No. 1 material and 30% of No. 2, or one of 50% No. 1 and 50% No. 3, was found satisfactory. The mixture was digested in an excess of water for more than 2 days with occasional agitation. Then it was let settle, the superfluous liquid was decanted off, and about 0.5% of concentrated hydrochloric acid was added. The mixture was stirred gently without introducing air bubbles. The desired consistency was about that of thick cream.

The molds were made of plaster of Paris and air-dried. To make the castings, the slip was poured into the mold without splashing or entrapping air. Water was immediately absorbed by the mold. The liquid level was maintained by additions of slip until the film of solidified material reached the desired thickness. The residual liquid slip was then poured out. The time required varied greatly with the plasticity of the material, consistency and acidity of the slip, and the condition of the plaster mold. Within one-quarter of an hour, shrinkage cracks began to appear at the junction of the top of the crucible and the wall of the mold. After about 1 hour, the crucibles would be dry enough to stand gentle handling and could be removed easily from the mold. The crucibles were air-dried for 1 day, dried at 105 C for another day and then fired.

Many methods of firing were attempted before satisfactory results were obtained. A globar furnace, which reached 1500 C (2730 F) in 8 hours, and 2 gas-fired furnaces, which reached 1650 C (3000 F) in 4 and in 48 hours respectively, produced equally unsatisfactory crucibles. High-frequency firing in a graphite element produced strong dense crucibles which, however, were heavily contaminated with carbon. The final solution was obtained by induction firing, out of contact with graphite, to 1430 C (2605 F) and refiring in air in the globar furnace to 1500 C (2730 F) for 2 hours. The

crucibles had a shrinkage of 11%, were reasonably strong and showed no evidence in chemical and X-ray examinations of any constituent other than Cr_2O_3.

Experimental Work

Technique—The electrolytic iron was cleaned, pickled, washed and dried to remove any attached dust particles which might contain some carbon. Pieces with smooth surfaces would give better results since there would be less probability of introduction of carbon, which would help to make the ingot porous. Approximately 60 grams were charged into the crucible in such a manner that the upper part would not touch the wall of the crucible and, consequently, would drop down when the lower part was melted. This was to minimize the probability of arching of the charge during the melting stage. Calculated amounts of previously pickled and dried electrolytic chromium were charged at the same time. The saturator and the water bath were brought to the desired temperature, which was usually a little higher than that expected to give equilibrium condition. The whole system was flushed out with hydrogen for about three-quarters of an hour. The saturator was by-passed most of the time to prevent high water-vapor pressure in the gas, and the resultant condensation of water at the cooler parts of the furnace.

For the high chromium heats it was more advisable to melt under hydrogen since water vapor tended to form a solid film around the chromium metal, thus prolonging the time needed for melting. The preheater was started and the high frequency current was turned on. Since chromium was not so readily melted as iron, pieces of chromium would float on the surface of the melt for quite awhile. Yet it was not advisable to bring the temperature higher than necessary lest more chromium oxide be dissolved from the crucible and later manipulations would become more difficult. After the charge was melted down, the hydrogen was led to pass through the water bath and the saturator.

For the low chromium heats it was found necessary to melt under the desired gas mixture since chromic oxide dissolved rather readily under hydrogen atmosphere; the chromium content was thence higher than needed, and it would be impossible to bring it down to the desired amount without disturbing the equilibrium condition, as will be explained later. For heats with chromium content

less than 1%, no chromium was charged; for those with chromium less than 0.2%, small calculated amounts of iron oxide were charged with the electrolytic iron. After the furnace was well flushed with hydrogen, the preheater was started to bring the upper part of the furnace to a fairly high temperature. Then the hydrogen gas was led through the water bath and the saturator before entering the furnace. After about 15 minutes, the high frequency current was turned on to melt the charge.

After the charge was melted, it should be brought to the desired temperature, in this work 1595 C (2905 F), as soon as possible. After reaction for a few minutes with the desired gas mixture, solid particles began to appear floating on the surface of the melt. These would accumulate first around the rim and grow toward the center. This was an indication that under such a gas mixture the melt was too high in its chromium content. This film grew reasonably rapidly, except in the case of very low chromium or very low oxygen content, and would cover the whole melt. Since this was a solid film, it would stay on the surface and prevent exposing of the liquid metal. Even if the pyrometer reading due to the high emissivity of the solid film were corrected, it could hardly represent the temperature of the melt because the heat loss to the surroundings was so great and this solid film was so insulative to heat that the temperature of the surface would be greatly affected by the thickness of the solid film. In addition the reaction between the molten metal bath and the gas would be completely blocked, and the desired equilibrium condition would never be attained. Since raising the temperature of the melt even higher was not desirable, the temperature of the saturator had to be lowered. As it took time to get the gas composition in the furnace corresponding to that in the saturator, and also to have the formation of the solid film noticeable, the temperature of the saturator was lowered in steps of from 1 to 2 degrees instead of continuously. Yet it was practically impossible to remove the solid film which had covered the whole melt and thus prevented the transference of oxygen from the melt to the gas, which was necessary before any solid oxide could be dissolved. Dry hydrogen was usually needed in such cases, although more chromium would be introduced into the melt. Better procedure would be to lower the saturator temperature before the whole surface was covered; but in most cases the effect of the lowering of the saturator temperature was too slow to be effective, and dry hydrogen had to be resorted

to. After a few trials, a condition would be obtained in which no solid film was formed, or better in which only some isolated solid particles floated around the rim without growing inward. Everything was kept unchanged for one more hour to attain the equilibrium. At the end, the preheater was turned off first, and then the high frequency current. A strong current of gas was used to cool the melt rapidly, which was kept in its position. The solidification was rather rapid, always within 15 seconds.

The above technique was found to be the most successful and was used for the later heats. In the earlier heats, however, a charge with chromium content less than required was melted and kept at proper temperature in contact with the desired gas mixture for various lengths of time. It was thought that equilibrium should be approached from both the high chromium and the low chromium sides, but practically no reliable data could be obtained from the high chromium side due to the formation of the solid film, although it was possible to determine whether a certain melt was on the high chromium side or not. It was observed that a melt with 4% chromium could be obtained from a pure iron charge by keeping it for only 1 hour at 1595 C (2905 F). From this it could be concluded that the solution of chromic oxide was not a slow process and that equilibrium could be reached within a reasonable length of time if the chromium amount charged was not too low. With this in mind, it seemed that, although almost all the data were obtained from the lower side, they could be counted on to represent the equilibrium condition.

The ingots always adhered to the chromic oxide crucibles, while they could be separated easily from the chromite crucibles. After grinding off all the nonmetallic substances, including the crust found around the ingots as described later, the ingots were analyzed for their chromium and oxygen contents. Samples for oxygen analysis were usually cut with a cut-off wheel or a hacksaw into pie sections. Pickling and grinding were used to clean the surface, and the analyses were done by regular vacuum fusion method. Samples for chromium analysis were prepared by cutting through the vertical cross section on a shaper. The chips were cleaned with acetone and analyzed by the regular potassium persulphate method.

In material of this kind the vacuum fusion method can be depended upon to determine the total oxygen content of the sample. This will include all oxygen which was in solution in the melt and any

oxide particles which have become entrapped in the specimen. Microscopic examination showed rather frequent presence of entrapped oxide crust just beneath the surface of the ingot, and it is always possible that some of this material is not removed in grinding the sample in preparation for analysis. For this reason greater weight was attached to the lower oxygen results and, in cases where a discrepancy occurred, the average of the lowest values obtained was selected as most probable.

Experiments and Data—From a total of about 150 trials, 74 heats were successful. The others were discarded during the run due to various troubles such as the failure of some part of the apparatus, fogging of the sight glass, breaking of the crucible, bridging of the charge, covering of the whole surface with solid film, and so forth. The first two series of heats (3-4, 24-27) were made in magnesia and alundum crucibles for comparison with published data and thus to ascertain the over-all performance of the assembled apparatus. It could be seen from the data (Table I) that the performance could be considered as satisfactory. These data were entirely compatible with those of Chipman and Fontana (5).

The third series (131-189) were made in chromic oxide crucibles. For heats 131-170, the equilibrium was approached from the low chromium side and, since no information was available, the starting charge might be far from equilibrium and the results could be used only with careful consideration. Among these heats, many will be plotted along with later heats while others have been discarded. In many of the ingots, crusts containing considerable amounts of nonmetallic substances in the matrix of metallic substances were observed. These crusts were metallic in appearance after rough grinding, and could not be distinguished from the metal at that time. Fine grinding, or better, polishing, however, would show the crusts to be darker in color and also less shiny than metal. During the grinding of various ingots, streaks of two different colors, brown and green, could be observed easily and seemed to be dependent on the chromium content of the heat. The solid films formed occasionally during the heat also showed two different varieties by color, brown and green, the former in low chromium, the latter in high chromium heats. These will be discussed later in the section on the identification of the solid phase in equilibrium with the melt. Heats 171-189 were made according to the best procedure as described. These are believed to be quite reliable. However, for heats 176 and

179 it was suspected that, since the charge was not high in oxygen content, too much chromium was dissolved during the melting operation with the result that the ingots were somewhat higher in chromium and lower in oxygen than those in actual equilibrium with the gas mixture used.

The fourth series (202-206) was made in commercial chromite crucibles after burning out the carbon at 1500 C (2730 F). These crucibles were found to be rather impure, containing magnesium and aluminum among other elements. It was thought that these impurities together with iron oxides would be insignificant in their effects on the equilibrium data only if they were mixtures instead of solid solutions with the iron chromite. This might not be true, but the error would be small so long as there was an excess amount of chromite.

Due to the porosity and the nonmetallic contamination of the ingots, which seemed to be rather serious for those with higher chromium contents, the oxygen analyses of the higher chromium heats were not considered to be reliable. And, in order to ascertain the effect of chromium on the activity of oxygen, the fifth series (301-320) was made. In this series, alundum crucibles were used, but the gas composition and the chromium content of the metal were so adjusted that no chromite or chromic oxide would be present. In other words, the gas was made so as to be nonoxidizing to the chromium in that particular metal composition. Thus by varying one of the two variables, the gas composition and the chromium content, while the second variable was kept constant, the effect of these variables on the oxygen contents could be directly determined. As it is, most of the ingots of this series were sound and showed very little inclusions. The data could be regarded as reliable.

Fig. 3 is a picture showing the appearance of the crucibles and the ingots obtained.

All the observations and data of these heats are summarized in Table I.

Identification of the Solid Phase

According to the phase rule, this system consisted of four components: iron, chromium, oxygen and hydrogen, and three degrees of freedom: the temperature, the pressure and the composition of the gas phase, so that only three phases could be present in equilibrium with each other. Now that there were already a gas phase and

Table I
Experimental Conditions of the Heats

Heat No.	% Cr Charged	$\left(\frac{H_2O}{H_2}\right)$ corr.	Metal Temp. C	Time Hrs.	Rate of Gas Flow Ml. /Min.	Chromium Analysis %	Oxygen Analysis, % Data	Chosen Value	Condition of Ingots Porosity	Crust[3]
A. Magnesia Crucible										
3	0	0.1023	1592	1.6	290	....	0.0246	0.0246	Sound	.....
4	0	0.0823	1594	1.5	310	....	0.0200, 0.0201	0.0200	Sound	.....
B. Alundum Crucible										
24	0	0.0421	1592	0.75	380	....	0.0100, 0.0090 0.0116	0.0102	Sound	.....
25[1]	7.4	0.0841	1655	1.5	300	....	.....	.....	Sound	.....
26[1]	0	0.833	1597	1.6	420	....	0.224, 0.199	.....	Porous	.....
27	0	0.1247	1596	1.4	480	....	0.029, 0.031 0.030	0.030	Sound	.....
C. Chromic Oxide Crucible										
131	8.1	0.0824	1653	2.3	300	9.23	0.068, 0.083	.....	Fair	G, thick
132	5.5	0.0832	1603	1.7	350	6.09	0.068, 0.058	.....	Porous	G (?)
133	3.6	0.0832	1603	1.6	300	5.71	0.046, 0.036 0.038	0.037	Very Porous	.....
134	0	0.1259	1598	2.0	240	2.50	0.165, 0.038 0.041	0.039	Porous	B
135	2.9	0.0857	1598	1.5	500	4.37	0.061, 0.034 0.026	0.030	Fair	B
136	11.8	0.0478	1599	2.2	340	11.90	0.106, 0.104	.....	Porous	G
138[1]	5.9	0.0768	1650	2.0	340	6.71	0.076, 0.085	.....	Fair	B and G
139	3.9	0.0839	1596	2.0	260	3.99	0.034, 0.036	0.035	Sound	.....
140	1.3	0.1193	1596	1.6	320	2.27	0.051, 0.043	0.043	Porous	B
141[1]	3.0	0.0615	1594	1.7	280	4.36	0.026, 0.028	0.027	Fair	B
142	3.3	0.0623	1598	1.0	430	6.73	0.046, 0.049	0.047	Sound	G (?)
143[1]	3.5	0.0655	1597	2.0	350	5.05	0.040, 0.057	0.040	Porous	B and G
144	3.1	0.0557	1597	1.0	400	....	0.250	.....	Porous	G
151	2.4	0.0849	1597	1.4	390	4.40	0.088, 0.052	.....	Porous	.....
153	0	0.0479	1600?	1.0	370	3.92	0.034, 0.037	0.035	Porous	B
155[1]	0	0.0528	1596	2.0	320	4.06	0.034, 0.031	0.032	Sound	B
156[1]	0	0.0746	1607	2.0	250	....	.....	.....	Porous	.....
158	0	0.0747	1595	2.0	260	3.89	0.044, 0.042	0.042	Sound	.....
159	2.5	0.0744	1602	1.2	330	4.27	0.033, 0.045	0.033	Sound	.....
160	3.1	0.0625	1598	2.0	320	4.11	0.031, 0.031	0.031	Sound	.....
161	5.0	0.0625	1598	2.0	300	6.28	0.048, 0.040 0.051, 0.052	0.040	Fair	.....
162	4.3	0.0628	1601	1.6	330	4.89	0.028, 0.028	0.028	Fair	.....
165	0	0.1022	1599	2.5	360	3.28	0.036, 0.037 0.052	0.037	Porous	.....
168[1]	0	0.0892	1600	1.2	300	2.81	0.036, 0.035	0.035	Sound	B Thick
169	0	0.1449	1600	1.2	380	2.30	0.089, 0.084 0.093, 0.080	0.082	Sound	B
170	0	0.1446	1597	1.6	320	1.73	0.046, 0.049	0.047	Fair	.....
171	9.9	0.0280	1602	2.5	340	....	.....	.....	Very Porous	G Thick
172	8.0	0.0276	1596	2.0	330	8.90	0.038, 0.039 0.034, 0.029	0.034	Fair	G Thick
174	8.6	0.1162	1594	1.7	350	....	.....	.....	Fair	B Thick
175	0	0.1398	1598	3.2	340	1.55	0.040, 0.043 0.049	0.041	Sound	.....
176	0	0.2196	1598	2.1	480	0.85	0.051, 0.050	0.050	Sound	.....
177	0	0.2479	1598	1.6	410	0.47	0.047, 0.048	0.047	Sound	B
178	0	0.3189	1595	1.1	440	0.38	0.065, 0.064	0.065	Sound	.....
179	0	0.3818	1596	1.4	480	0.27	0.076, 0.074 0.078	0.075	Sound	.....
180	6.0	0.0619	1597	2.0	350	7.21	0.057, 0.061 0.031, 0.045	0.031	Fair	G
181	10.0	0.0448	1596	1.2	410	9.98	0.032, 0.029	0.031	Porous	.....
182	15.0	0.0356	1594	2.2	410	....	.....	.....	Porous	G
183	20.1	0.0280	1594	2.3	400	19.30	0.055, 0.049 0.051	0.050	Sound	.....
184	9.8	0.0462	1595	1.5	400	10.70	0.047, 0.042 0.062	0.042	Porous	G

Table I—(Continued)
Experimental Conditions of the Heats

Heat No.	% Cr Charged	$\left(\frac{H_2O}{H_2}\right)$ corr.	Metal Temp. C	Time Hrs.	Rate of Gas Flow Ml. /Min.	Chromium Analysis %	Oxygen Analysis, % Data	Chosen Value	Condition of Ingots Porosity	Crust[3]
C. Chromic Oxide Crucible										
185	7.4	0.0461	1598	1.5	400	8.29	0.039, 0.036, 0.043, 0.036	0.036	Sound	G
186	5.0	0.0591	1596	1.2	450	5.81	0.031, 0.030, 0.031, 0.031	0.031	Sound	.....
187	3.3	0.0825	1598	1.6	390	4.45	0.039, 0.036, 0.041, 0.032	0.033	Fair	B
188	12.7	0.0389	1594	1.1	390	15.13	0.042, 0.053, 0.061, 0.047	0.044	Porous	G
189	21.4	0.0257	1593	1.1	350	21.40	0.076, 0.057	0.057	Porous	G
D. Chromite Crucible										
202[2]	0	0.1180	1595	1.0	310	0.37	0.065, 0.060	0.062	Porous	.....
203[1]	0	0.789	1595	2.4	410	0.41	0.174, 0.173	0.174	Sound	.....
204[1]	0	1.033	1595	1.6	390	0.30	0.182, 0.190, 0.214, 0.186	0.184	Fair	.....
205	4.2	0.0849	1597	1.0	410	3.79	0.030, 0.030	0.030	Sound	.....
206	3.2	0.1012	1597	2.4	410	2.73	0.037, 0.032, 0.039, 0.033	0.033	Sound	.....
E. Alundum Crucible										
301	8.3	0.0262	1598	2.2	260	8.0	0.0144, 0.0130, 0.0139	0.0138	Sound	.....
302	2.0	0.0260	1595	2.0	300	1.97	0.0105, 0.0077, 0.0082	0.0080	Sound	.....
303	5.0	0.0261	1596	1.4	310	4.88	0.0122, 0.0103, 0.0113	0.0113	Sound	.....
304	10.0	0.0304	1594	2.0	270	9.63	0.0268, 0.0196, 0.0171, 0.0179	0.0175	Sound	.....
305	5.0	0.0304	1595	1.5	290	4.87	0.0138, 0.0134, 0.0121	0.0131	Sound	.....
306	2.0	0.0305	1598	1.5	290	1.95	0.0135, 0.0127, 0.0092, 0.0108	0.0100	Sound	.....
307	10.0	0.0368	1596	1.5	330	9.69	0.0260, 0.0227, 0.0214, 0.0228	0.0223	Sound	.....
308	2.0	0.0368	1595	1.0	300	1.93	0.0144, 0.0106	0.0106	Sound	.....
309	5.0	0.0369	1597	1.8	340	4.84	0.0211, 0.0181, 0.0146, 0.0146	0.0146	Sound	.....
310	5.0	0.0468	1598	1.7	320	4.83	0.0260, 0.0208, 0.0178, 0.0168	0.0173	Sound	.....
311	2.0	0.0471	1594	1.5	290	1.90	0.0161, 0.0147, 0.0137, 0.0142	0.0142	Sound	.....
312	2.0	0.0673	1596	1.5	290	1.89	0.0192, 0.0190, 0.0200	0.0194	Sound	.....
313	10.0	0.00607	1596	1.5	220	9.80	0.0069, 0.0078	0.0074	Sound	.....
314	5.0	0.00608	1595	1.7	330	4.93	0.0061, 0.0047, 0.0058	0.0055	Sound	.....
315	0.0	0.0282	1592	1.5	290	0	0.0069, 0.0068	0.0068	Sound	.....
316	0.0	0.00604	1596	1.5	340	0	0.0033, 0.0026, 0.0025	0.0028	Sound	.....
317	0.0	0.00603	1596	1.6	340	0	0.0036, 0.0024, 0.0030	0.0030	Sound	.....
318	0.0	dry hydrogen	1595	2.3	320	0	0.0018, 0.0014	0.0016	Sound	.....
320	10.0	dry hydrogen	1597	2.1	300	9.8	0.0026, 0.0025	0.0025	Sound	.....

NOTES:
[1]Preheater not used during the run.
[2]Chromite crucibles always showed some reaction with the metal, and for this one (Heat 202) it was thought that equilibrium with the gas was not attained.
[3]"G" means crust that gave green streak. "B" means crust that gave brown streak. "G (?)" means that the streak color looked like green, but not distinct. "B and G" means that green crust was found around the corner of the bottom of the ingot, while brown one was found at the bottom and the sides. This might well be explained by the difference in temperature at the various positions.
All the data lacking for crusts are due either to failure to record properly, or to the fact that the crust was so thin it could hardly be distinguished from the crucible itself.

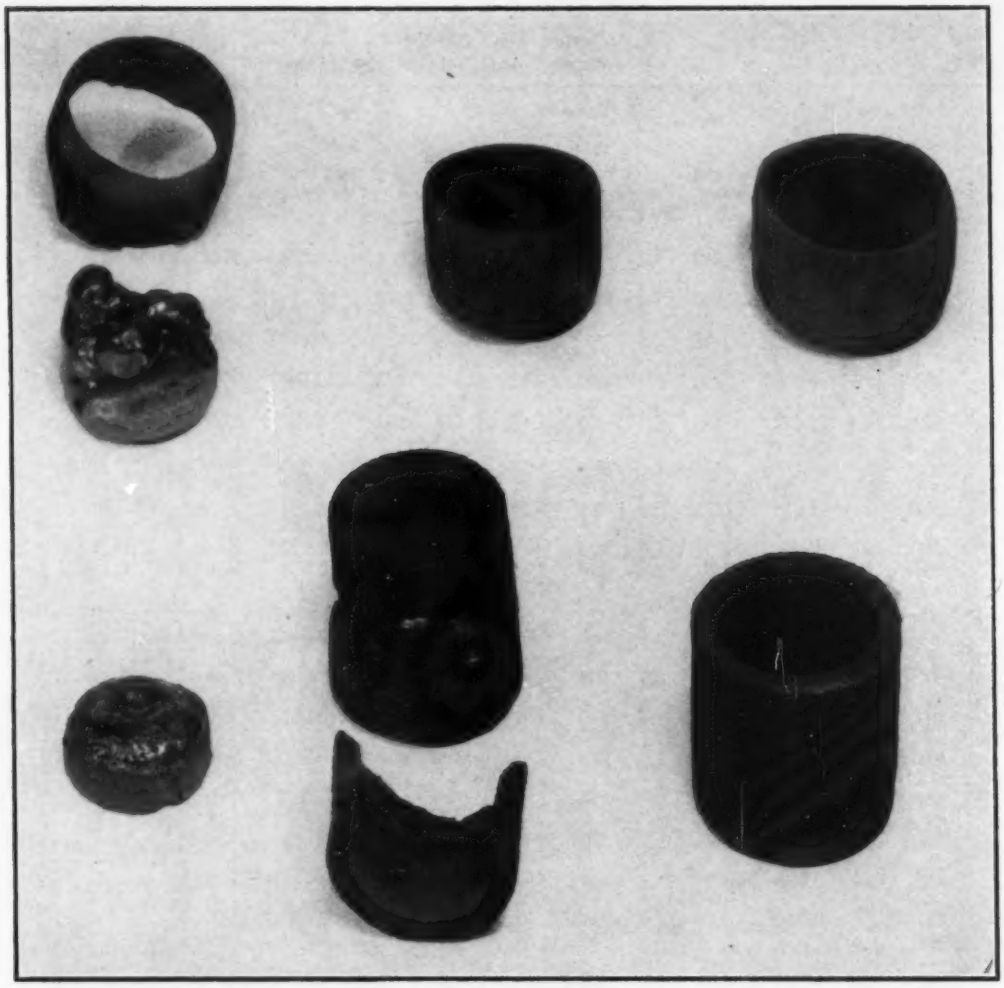


Fig. 3—Crucibles Before and After Use and Typical 60-gram Ingots. Above chromic oxide; below chromite crucibles.

a liquid phase, only one solid phase (or another liquid phase) could exist under equilibrium conditions. When a solid phase, in this case the crucible material, was introduced into the system, it might remain as such, if it were the stable solid phase under those conditions, or it might dissolve continuously into the molten metal with the precipitation of a new phase from the molten metal, also continuously. This reaction would continue to proceed until one of the phases disappeared which might be, in this investigation, the complete solution of the crucible or the complete solidification of the molten metal, and no equilibrium could be obtained before this final stage unless it was blocked. For the high chromium heats, the crucible material, chromic oxide, Cr_2O_3, was the stable solid phase and presented no problem. For the low chromium heats, iron chromite, $FeO \cdot Cr_2O_3$, was

the stable solid phase, as will be shown later. The precipitated chromite, together with the molten metal, formed a crust at the bottom of the melt which adhered to the crucible without floating up as slag. This blocked further reaction between the molten metal and the crucible, and the result would be about the same as if the melt were done in a chromite crucible.

To determine the nature of the solid stable phase, three different substances in direct contact with the melt have been studied: (a) the crust as described earlier, which consisted of nonmetallic substances in a metallic matrix and which was quite high in its content of nonmetallic substances; (b) the nonmetallic inclusions in the metal, which were present only in small amounts; and (c) the crystals, usually needles, observed on the surface of the melt, which were practically free from metal.

Microscopic Examination—Many of the ingots were cut, and both the crusts around the ingot and the nonmetallic inclusions in the metal were studied under the microscope. A few of the typical ones are shown in Figs. 4 to 10. Figs. 5 to 8 show the appearance of the crusts, and Figs. 9 and 10 that of the nonmetallic inclusions.

Fig. 4 shows one of the nonmetallic clusters inside the metal ingot, heat 185. More like this have been found in ingot 189. These, no doubt, led to the high results of the oxygen analysis and could be used to explain why some of the oxygen data were extraordinarily high. It has been observed that these clusters always contained nonmetallic substances of the green variety, and occurred only in those ingots where crusts of the green variety were found.

Fig. 5 shows the appearance of the crusts of the brown variety under the microscope. These were easily polished. The tendency to pit was small. The particles were medium gray under white reflected light, and showed some bright red internal reflection under dark-field illumination. They seemed to be fairly rounded and tended to grow into a network with the particles joining together. They did not exhibit high relief. They were almost opaque under the polarized reflected light. These observations seemed to correspond exactly with what had been observed (2), (3), (4) for the inclusion of "chromite".

Fig. 6 shows the appearance of the nonmetallic crusts of the green variety. In contrast to the brown variety they were not easily polished, always tending to pit. They were light gray in color under white reflected light. They exhibited rather high relief, and their boundaries were defined by a furrow, which appeared dark in reflected

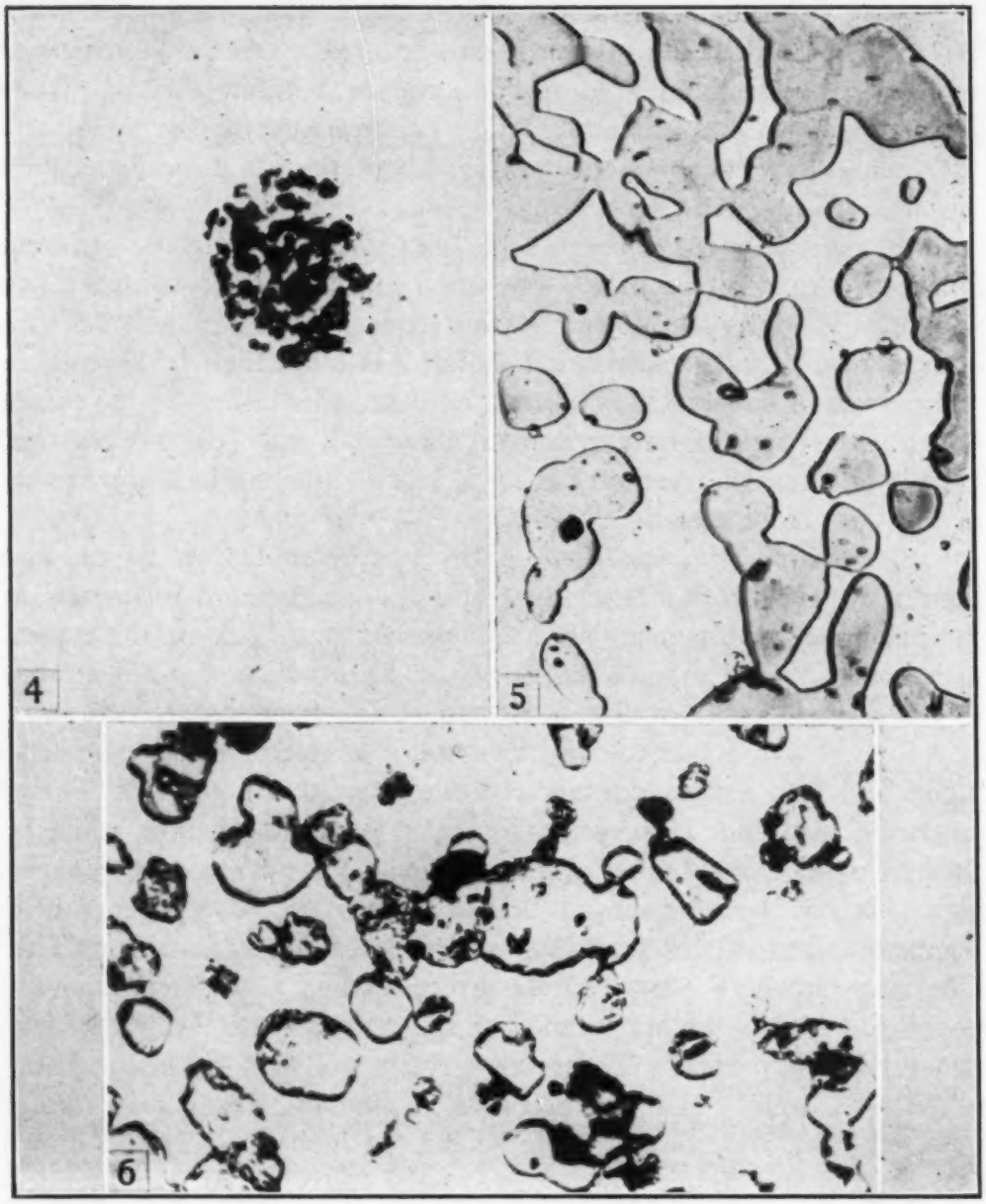


Fig. 4—Oxide Cluster Found in High Chromium Heats. × 100. (Heat No. 185, Cr 8.29%.)

Fig. 5—Microscopic Appearance of Brown Type Crust ($FeO \cdot Co_2O_3$). × 500. (Heat No. 187, Cr 4.45%.)

Fig. 6—Microscopic Appearance of Green Type Crust (Cr_2O_3). × 500. (Heat No. 180, Cr 7.21%.)

and bright in dark-field illumination. The particles seemed to be more irregular than the brown variety, and tended to remain as single particles rather than joining together. These seemed to be what is described as chromic oxide, with the exception that these particles did not exhibit green color under dark-field illumination nor aniso-

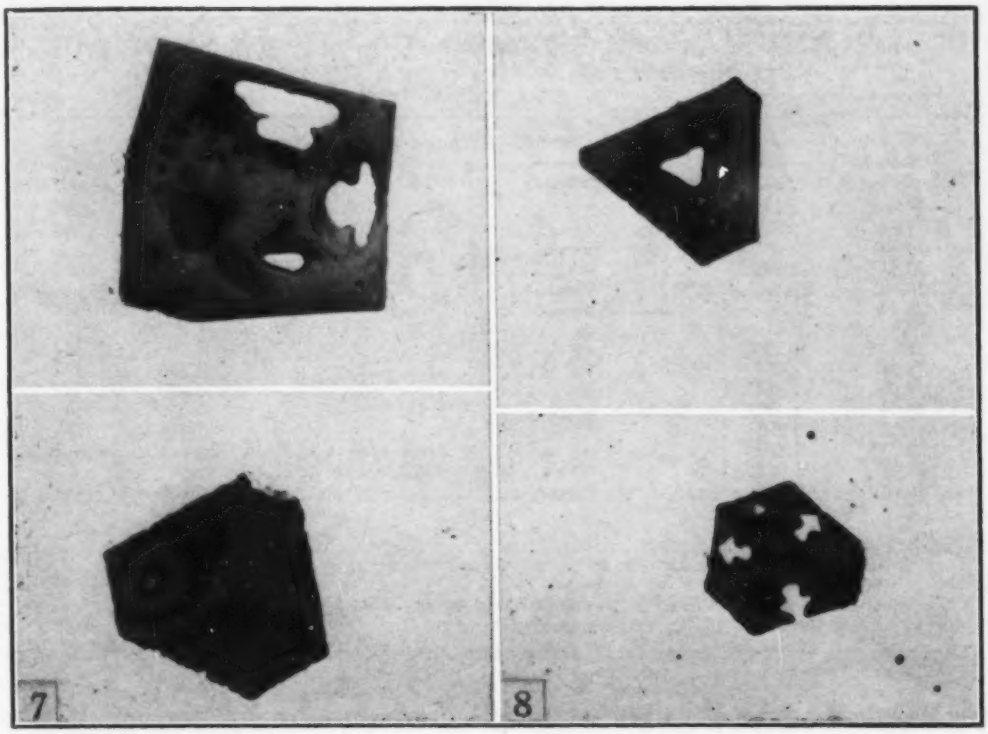


Fig. 7—Crystalline Inclusions, Probably $FeO \cdot Cr_2O_3$, in Low Chromium Heat. × 500. (Heat No. 169, Cr 2.30%.)

Fig. 8—Crystalline Inclusions, Probably Cr_2O_3, in High Chromium Heat. × 500. (Heat No. 188, Cr 15.13%.)

tropic characteristics under polarized light, and instead seemed to be opaque under those circumstances. Etching with an acid permanganate reagent attacked many of the metal ingots very rapidly and offered no opportunity for comparison.

Fig. 7 shows crystalline inclusions in the ingot 169, which had a low chromium content, and Fig. 8 those in the ingot 188, which had a high chromium content. They seemed to be fairly similar in appearance, but as Portevin and Castro (2) pointed out, octahedron and rhombohedron sections might, in fact, be very similar in appearance, and the shapes of the plane sections are not sufficient to identify their crystal systems. Both were opaque under dark-field illumination, and have not been identified.

X-Ray Examination—As the microscopic examination was not very conclusive in determining the nature of these solid phases, X-ray diffraction was resorted to. The true inclusions were too small in amount and could be separated from the metal only with difficulty; they were not examined.

Filings of the crust of the brown variety were examined with

Table II
X-Ray Diffraction Pattern of Heat No. 140 Crust Residue After Iodine Treatment

Co Radiation: $\lambda_\alpha = 1.787$ A $\lambda_\beta = 1.617$ A No Filter

Measured				Fe		$FeO \cdot Cr_2O_3$	
Corr. Angle	d_α	d_β	Intensity	d	Intensity	d	Intensity
10.98	4.69		vw	.....	....	4.82	0.2
17.62	2.92		vvw	.....	....	2.95	0.4
19.46	(2.68)	2.43	vvvw	.....	....	....	...
20.93	2.50		w	.....	....	2.52	1.0
23.92	(2.20)	2.00	vvw	.....	....	....	...
25.24	2.10		vvw	.....	....	2.08	0.4
26.45	2.01		vs	2.01	1.00	....	...
32.74	1.65		vvvw	.....	....	1.70	0.3
33.64	1.613		vw	.....	....	1.606	0.8
37.60	1.464		vw	.....	....	1.475	0.9
38.84	1.425		w	1.428	0.15	....	...
44.38	1.277		vvvw	.....	....	1.274	0.4
50.00	1.166		s	1.166	0.38	....	...
61.96	1.012		w	1.010	0.10	....	...
68.40	0.961		vvvw	.....	....	0.966	0.3

NOTES:
d_α = d calculated from λ_α; d_β = d calculated from λ_β.
v = very; w = weak; s = strong.
Fe data from ASTM X-ray diffraction data cards No. 3399.
$FeO \cdot Cr_2O_3$ data from Clark, Ally and Badger (20).

the result that the iron lines were so predominant that the other lines were too obscure. In order to separate most of the iron from the mixture so that it would be more concentrated in the nonmetallic phase, the iodine treatment for oxide inclusions as described by Cunningham and Price (8) was used. The essential part was to dissolve the metallic iron in a ferrous iodide solution with the addition of ammonium citrate, which would not dissolve the oxides. The residue after 5 hours of digesting at 0 C was filtered and washed. The measurement of the X-ray diffraction photograph of the residue from ingot 140 is tabulated in Table II. Comparison with the published data indicates that there is a good check with those of chromite, considering the inaccuracy of the measurement of the lines on a Debye-Scherrer picture, especially for the very faint lines. Table III gives the measurement and comparison of the lines for the crust of heat 182, and Table IV those for the surface condensate of heat 181. It could be seen that the last two consisted of mixtures of iron and chromic oxide, Cr_2O_3, with more iron for the crust.

Since chromium did exhibit some fluorescent radiation, using cobalt as the target, the films were somewhat fogged, and the measurements less accurate. However, the data left no doubt as to the identification of these crusts; that is, the brown variety as chromite and the green variety as chromic oxide. Slight amounts of other substances might occur in the solid phase as solid solutions, but if

Table III
X-Ray Diffraction Pattern of Heat No. 182 Bottom Crust

Co Radiation: $\lambda_\alpha = 1.787$ A No Filter

Measured			Fe		Cr_2O_3	
Corr. Angle	d	Intensity	d	Intensity	d	Intensity
20.60	2.54	vw	.....	....	2.67	0.70
21.71	2.415	vw	.....	....	2.47	0.70
26.51	2.001	s	2.01	1.00	....	....
29.85	1.795	vvw	.....	....	1.81	0.45
32.80	1.649	w	.....	....	1.67	1.00
38.95	1.421	w	1.428	0.15	1.432	0.45
50.07	1.165	s	1.166	0.38	.....	....
55.13	1.089	vvw	.....	....	1.087	0.12
58.73	1.045	vvw	.....	....	1.041	0.10
61.93	1.013	w	1.010	0.10	.....	....
71.00	0.945	vvvw	.....	....	0.946	0.06

NOTES:
Fe data from ASTM X-ray data card No. 3399.
Cr_2O_3 data from ASTM X-ray data card No. 3667.

Table IV
X-Ray Diffraction Pattern of Heat No. 181 Surface Condensate

Co Radiation: $\lambda_\alpha = 1.787$ A No Filter

Measured			Fe		Cr_2O_3	
Corr. Angle	d	Intensity	d	Intensity	d	Intensity
14.50	3.57	vvw	.....	....	3.62	0.45
19.82	2.64	w	.....	....	2.67	0.70
21.49	2.44	w	.....	....	2.47	0.70
24.47	2.16	vvw	.....	....	2.17	0.30
26.36	2.015	s	2.01	1.00	2.03	0.04
29.78	1.800	vw	.....	....	1.81	0.45
32.50	1.663	w	.....	....	1.67	1.00
34.90	1.562	vvw	.....	....	1.58	0.06
37.77	1.460	vw	.....	....	1.465	0.30
38.82	1.426	w	1.428	0.15	1.432	0.45
43.86	1.290	vvvw	.....	....	1.294	0.16
46.14	1.239	vvvw	.....	....	1.236	0.06
49.77	1.170	w	1.166	0.38	1.172	0.05
51.46	1.141	vvvw	.....	....	1.148	0.06
52.77	1.122	vvw	.....	....	1.123	0.06
55.46	1.085	vvw	.....	....	1.087	0.12
59.06	1.041	vvw	.....	....	1.041	0.10
61.73	1.016	vvvw	1.010	0.10	.....	....
71.19	0.943	w	.....	....	0.946	0.06
72.61	0.937	vw	.....	....	.....	....

NOTES:
Fe data from ASTM X-ray data card No. 3399.
Cr_2O_3 data from ASTM X-ray data card No. 3667.

the assumption that the solubility was limited was true, the activity of the solid phase could be considered as constant and equal to that of the solid chromite or chromic oxides.

Discussion—From the above observations it could be concluded that there were two different varieties of crusts, the brown chromite and the green chromic oxide. Since chromic oxide crucibles were used for all these ingots, this left no doubt that chromite was the reaction product and should be the stable solid phase under certain conditions, one of which was the low chromium content. The high-

est one where the presence of chromite could still be assured was ingot 143 with a chromium content of 5.05%. On the other hand, chromic oxide crust could be assured in ingot 180 with a chromium content of 7.21%. The presence of both the green and the brown variety in one ingot, as ingot 143, seemed to be due to incompleteness of the reaction between iron and chromic oxide.

It has been tried to obtain chromic oxide crust without using chromic oxide crucible so that it could be ascertained that the chromic oxide found was really precipitated from the ingot, and thus proved to be the stable solid phase. This attempt was not successful. First a chromite crucible with a proper chromium content was used, but the chromite acted differently from the chromic oxide in that it did not dissolve readily, and practically no crust could be found. A heat with a high chromium charge was made in an alundum crucible with a gas mixture high in water vapor content which was beyond the equilibrium point. The result was that (heat 25) the entire surface was covered with a very thin film rapidly, which could be removed only by raising the temperature or lowering the water vapor content of the gas, and that no crust could be found. Yet from the color of the film formed it looked rather certain it was of the green variety, that is, chromic oxide variety.

It seems quite safe to say that the critical chromium content, above which chromium oxide was stable and below which chromite was stable, lies between 5 and 7%. It should be emphasized that the above statement is true only when the oxygen in the metal is exactly in equilibrium with the stable nonmetallic phase. If oxygen is in much excess, the precipitation of both chromite and chromic oxide would be possible. As observed in the case of heat 174, where chromite was formed from a high chromium melt, it seemed that chromite might be precipitated more rapidly than chromic oxide. This might be one explanation of why chromite inclusions were so often found in ferrochromiums and high chromium steels.

As both chromite and chromic oxide are considerably lighter than iron (5.09 for specific gravity of chromite and 5.21 for that of chromic oxide), they were expected to float on the surface of molten iron. On the contrary, they were found at the bottom as crusts, which could be explained best by the assumption that the crusts adhered to the crucible wall. It was postulated that, owing to the porous nature of the chromic oxide crucible, the liquid iron might creep into the interstices of the crucible wall to form a crust within which the solid particles were not free to move away. In this

way the contact surface between metal and crucible was tremendously increased, and the reaction between metal and solid phase promoted. The facts that the chromic oxide crucibles always adhered to the ingots and could be removed only by grinding, while the alundum and chromite crucibles could be separated easily from the ingots, supported this postulate. The high rate of solution of chromic oxide from the crucible also supported it. As the crusts were first formed, they were composed of chromic oxide in a matrix of iron principally, but as time went on and when conditions were favorable to the formation of chromite, reaction proceeded on the surfaces of the particles with the result that some of the chromic oxide particles might be occluded without further reaction with the melt. If the conditions were favorable to chromic oxide formation, the crust will remain as such without reaction. This was considered as the reason why chromic oxide crusts remained in particles and chromite crusts tended to become a network. The strong eddy current in the melt would tend to carry these particles upward to the surface, thus explaining the occasional appearance of clusters of nonmetallic substances in the steel. While chromite crusts always tended to grow into a network, the tearing away of a part of these chromite particles would be difficult, and that might be why no cluster of chromite was found in the metal.

As this postulation could be used successfully to explain the observed phenomena, the hypothesis that the nonmetallic particles in the crust constitute the stable solid phase in equilibrium with the melt during the process, and were not produced otherwise, could be established. Chromite and chromic oxide are the stable solid phases for low and high chromium melts, respectively.

As for the nonmetallic inclusions in the metal, the most probable explanation was that most of them were produced during the solidification process. At that stage since the cooling was rapid, the equilibrium constants might drop so low that the precipitation of both solid phases would be possible. In such cases the phase which appeared in quantity would depend more on reaction rates than on equilibrium conditions, and could not be used as a criterion for the stability of the solid phase at higher temperatures. Besides, the identification was not conclusive, and it seems unwise to count heavily on those observations.

The observations on the surface film and surface condensates were very incomplete, but those available did show a good check with those based on the crusts.

The Equilibrium Data

Sources of Error

Temperature Measurement. The reading and calibration of the pyrometer were quite satisfactory and could be duplicated within two degrees. However, as the method of correction presumed that the emissivities of the molten metals of various heats were constant and equal to that of the pure iron, it was possible to introduce some error. No attempt was made to determine the emissivity of the various alloys. As pointed out by Goller (9), the chromium-iron alloy would have a higher emissivity than iron. Although his data could not be used in this investigation because other alloying elements were present in the materials he used, it is quite possible that a higher chromium alloy would have a higher emissivity. If this were true, the actual temperature of the high chromium heats would be lower than the corrected temperature as listed in the tables.

As for the individual runs, the temperature control for the earlier runs was not very good, and in some cases it had been necessary to go somewhat higher than desired, as listed in the table. Heats 174 and 177 had the metal surface covered with solid film; heat 153 showed some fogging on the sight glass due to various reasons; and heats 169 and 156 bridged. For these heats the temperature measurements might be erroneous. With these exceptions it was thought that the temperatures were accurate to at least ± 5 C, provided there was no change in emissivity. It was found to be quite possible to hold the temperature constant to within ± 5 C during an experiment.

Gas Composition. From the data obtained in the testing of the saturator, it was evident that the calculated gas composition did represent the actual gas composition up to at least 50 C. Table V gives the oxygen analysis in iron melted under definite gas composition, and the corresponding values of the equilibrium constant in the final column. The results checked very well with the data of Fontana and Chipman (5), which gave the value 3.95 at 1600 C (2910 F), and the equation of Chipman and Samarin (6), which gave the value 4.1 at 1595 C (2905 F) for the ratio $K_O = \left(\frac{H_2O}{H_2}\right)/[O]$. The average value obtained in these heats was 4.15, which will be used in later calculations. This also indicated that the performance of the saturator was excellent, provided the amount of water in the

Table V
Equilibrium of Chromium-Free Melts With Steam and Hydrogen at 1595 C

Heat No.	Crucible Used	$\left(\frac{P_{H_2O}}{P_{H_2}}\right)_{corr.}$	[O] Analysis	$\left(\frac{P_{H_2O}}{P_{H_2}}\right)/[O]$
3	MgO	0.1023	0.0246	4.16
4	MgO	0.0823	0.020	4.11
24	Al_2O_3	0.0421	0.010	4.21
26	Al_2O_3	0.8258	0.199	4.15
27	Al_2O_3	0.1243	0.030	4.14

towers and the temperature of the water bath were well adjusted as well as the temperature of the saturator. In case of very high moisture content in the gas, the deviation might be higher but, for those cases, the chromium analyses were also not too accurate, and the data could be used as references only.

Chromium Analysis and the Equilibrium. The results of chromium analyses checked very well normally. As an estimation, it could be said that for those samples with more than 10% chromium, the maximum deviation of single values from the average is $\pm 0.10\%$; for those around 5%, $\pm 0.06\%$; for those around 1%, $\pm 0.03\%$; and for those around 0.3%, $\pm 0.02\%$. As the method used was standard, there seemed to be little doubt about the validity of the results of these analyses.

As for the equilibrium, since the reaction involved the absorption or evolution of a considerable amount of oxygen from or to the gas, and since the transference of gas between liquid and gas was a slow process, the equilibrium condition was more difficult to be attained than in the case where no alloying element and only relatively small amounts of oxygen were involved, unless the amount of chromium in the charge was about equal to that needed in the final equilibrium condition. The solution of solid chromic oxide into the metal was fairly rapid, as exhibited by the rapid increase of chromium content in certain heats.

For the high chromium heats, more change in chromium concentration was generally needed for the same change of (H_2O/H_2). To dissolve more chromium from the crucible, oxygen must also dissolve into the metal from which it must be transferred to the gas before more chromium can be dissolved. This was a slow process. The effect might not be noticeable for low chromium heats, where the amounts of chromium and oxygen involved were small, but were significant for high chromium heats. If this was the case, the ingot

would be lower in chromium than it should be under equilibrium conditions.

In some low chromium heats the amounts of chromite produced were not enough to block the reaction between the melts and the chromic oxide crucibles. In those cases the solution of the chromic oxide and the precipitation of the chromite would proceed simultaneously, and the chromium contents of the melts would be intermediate between those corresponding to the chromic oxide equilibrium and those to the chromite equilibrium depending on the relative rate of these two reactions. Heats 170 and 176 could be cited as examples belonging to this case.

From the above reasoning it could be said that the chromium content in the ingot tended to be high for low chromium heats and low for high chromium heats. Therefore, more weight was put on lower chromium data for the low chromium heats, and on higher chromium data for the high chromium ones. This deviation from the true equilibrium was aggravated when the chromium content in the charge was far away from the equilibrium chromium content, and decreased when proper charge was made. On this basis the later runs, heats 171-189 and 203-206, would give better data than the earlier runs where the charges were determined by mere guesses.

In the fifth series, heats 301-320, the amount of oxygen to be transferred was much less. The ingots were sound, and very little inclusions have been found. The chromium analyses should be considered as rather reliable and true equilibrium actually reached.

Oxygen Analysis. As explained in the previous section, oxygen analyses of heats in chromic oxide or chromite crucibles tended to be lower in low chromium heats and higher in high chromium heats than they should be under equilibrium conditions, due to the heats being short of true equilibrium conditions.

However, unlike the chromium analyses, the oxygen analyses exhibited other complexities by themselves. The chief difficulty encountered was the complete removal of the crusts from the samples. This could be done by prolonged grinding, and it was advisable to do the last grinding on sandpaper (No. 1 or, better, No. 0) so the presence of any crust could be easily recognized by the difference in luster from the metal itself. This had been done for most of the samples analyzed, with special care exercised in heats 171-189 and 203-206. As stated before, the lower values of the oxygen analyses

of a single heat were considered as better representatives than the higher ones.

In several other cases, especially for high chromium heats as in heats 180 and 189, clusters of the nonmetallic crusts were found in the ingot. Doubtless this would lead to some extraordinarily high values of oxygen in the metal. This could not be removed completely, as evidenced by the fact that it was impossible to obtain check data on four oxygen samples analyzed for each of these two heats. In such cases the lowest value was chosen as the best value that could be obtained and, as a result, these values cannot be considered as reliable.

On the other hand, loss of oxygen might occur during the cooling and solidification process through (a) settling (floating-up) of the nonmetallic substances formed during cooling, and (b) evolution of gas. The absence of noticeable amounts of nonmetallic substance on the surface of the solidified ingot, and the presence of clusters of nonmetallic inclusions, in some of the ingots lent support to the assumption that the loss of oxygen (or chromium) through the removal of the nonmetallic inclusions was negligible. Nevertheless, the loss of oxygen through evolution of gas might be considerable, as indicated by the bad porosity of some of the ingots. Despite the attempts to reduce the porosity by removing all the carbon in the charge and crucible, many ingots were still porous, especially for the high chromium heats. This porosity might have two contradictory effects on the oxygen analysis. One was the loss of oxygen through formation of carbon monoxide or other gas, and the other was to occlude more of the crust into the ingot by stirring. Needless to say, the larger surface produced by porosity offered more chances to be oxidized and thus show higher oxygen content. This effect, however, was reduced by keeping all the ingots in a desiccator and by processing without quenching in water. As a conclusion, the effect of porosity was different in different cases and could not be generalized. It could only be said that oxygen data of sound ingots should be more reliable than those of the porous ones.

For the fifth series, heats 301-320 which were made in alundum crucibles, the oxygen analyses could be considered as fairly good because of the invariably sound ingots and their freedom from inclusions.

Interpretation of the Data

Chromium and the Water Vapor-Hydrogen Gas Mixture. When chromite is the stable solid phase, the reaction involved in the system is:

$$FeO \cdot Cr_2O_3\ (s) + 4H_2\ (g) = 4H_2O\ (g) + Fe\ (l) + 2\underline{Cr} \qquad [1]$$

where (s) denotes solid state, (g) gas state, and (l) liquid state, and the underscored symbol represents a substance dissolved in liquid iron. Assuming that $FeO \cdot Cr_2O_3$ is a pure solid phase, that the activity of iron is a constant, which is strictly true only when the amount of solute in the molten metal is insignificant, but which may be considered as approximately true in the case of chromium less than 5.5%, and that the activity of chromium is proportional to its weight per cent, the equilibrium constant for this reaction would be

$$K_1 = \left(\frac{H_2O}{H_2}\right)^4 [\%\ Cr]^2 \qquad [1a]$$

Similarly, when chromic oxide is the stable solid phase, the reaction and the equilibrium constant would be

$$Cr_2O_3\ (s) + 3H_2\ (g) = 3H_2O\ (g) + 2\underline{Cr} \qquad [2]$$

$$K_2 = \left(\frac{H_2O}{H_2}\right)^3 [\%\ Cr]^2 \qquad [2a]$$

In this reaction no iron is involved, and thus its activity could be changed to a greater extent without affecting the constancy of the constant K_2.

The data are plotted in Fig. 9 and also in Fig. 10 on a logarithmic scale.

The significance of the logarithmic plot becomes evident if we put equations [1] and [2] in logarithmic form and simplify to obtain the following:

$$\log\left(\frac{H_2O}{H_2}\right) = \tfrac{1}{4} \log K_1 - \tfrac{1}{2} \log [\%\ Cr] \qquad [1b]$$

$$\log\left(\frac{H_2O}{H_2}\right) = \tfrac{1}{3} \log K_2 - \tfrac{2}{3} \log [\%\ Cr] \qquad [2b]$$

From these equations it may be seen that in the range where equa-

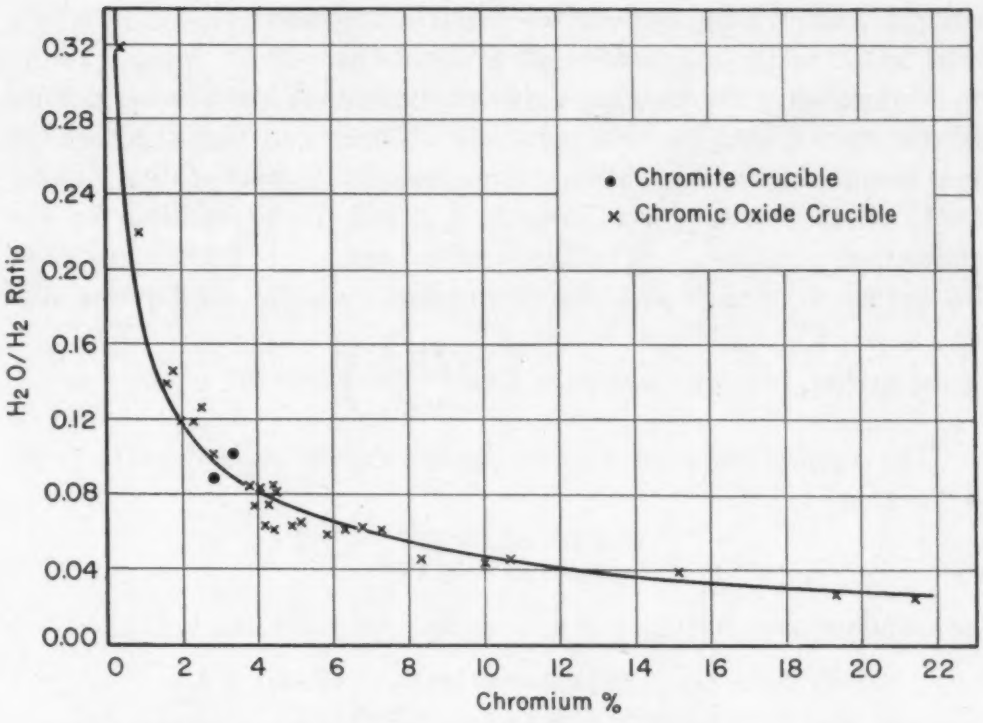


Fig. 9—Relationship Between Chromium Content of Molten Iron and Equilibrium Ratio of Water Vapor to Hydrogen at 1595 C (2903 F).

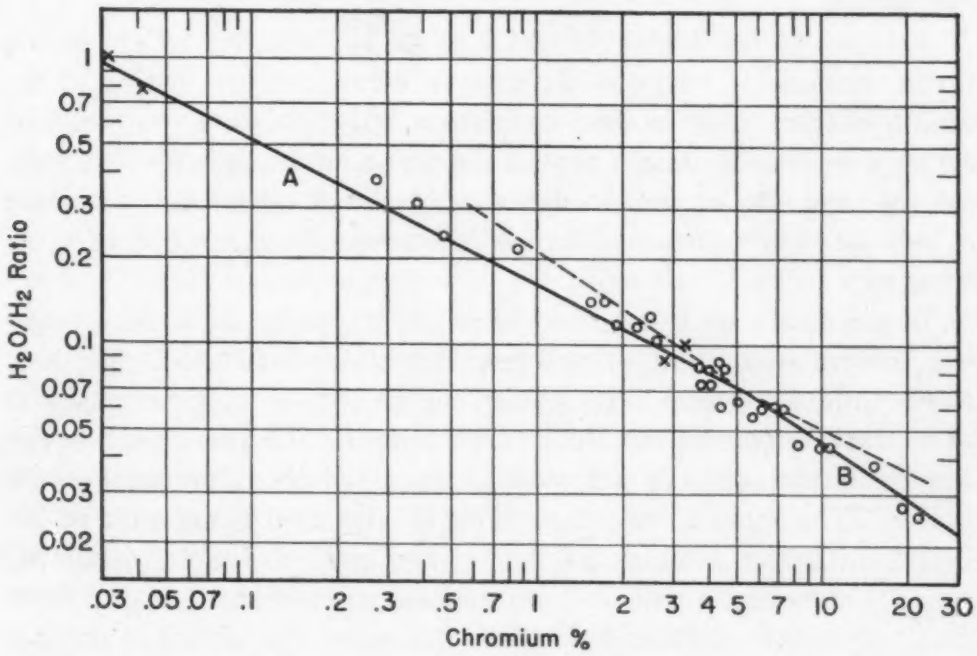


Fig. 10—Ratio $(H_2)/(H_2)$ as a Function of Chromium Content. Line A in equilibrium with chromite; line B with chromic oxide.

tion [1] pertains, the slope of the logarithmic curve should be $-\frac{1}{2}$ while in the range of equation [2] it should be $-\frac{2}{3}$.

Considering the possible experimental errors, two straight lines are drawn in Fig. 10 with their proper slopes, and almost all of the experimental points do fall on these two lines beautifully. These justify all the assumptions made in deriving the expression for the equilibrium constants. The intersection point of 5.5% chromium also agrees very well with the observations on the solid phase discussed earlier. At this point the ratio $\left(\frac{H_2O}{H_2}\right)$ is 0.070.

The equilibrium constants as defined can be read directly from the lines as

$$K_1 = 7.23 \times 10^{-4}$$
$$K_2 = 1.036 \times 10^{-3}$$

The standard free energy changes in the two reactions are:

$$FeO \cdot Cr_2O_3\ (s) + 4H_2\ (g) = 4H_2O\ (g) + Fe\ (l) + 2\underline{Cr}$$
$$\Delta F^\circ_{1595\,C} = -RT \ln K_1 = 26840 \text{ cal.} \quad \ldots\ldots\ldots [1c]$$
$$Cr_2O_3\ (s) + 3H_2\ (g) = 3H_2O\ (g) + 2\underline{Cr}$$
$$\Delta F^\circ_{1595\,C} = -RT \ln K_2 = 16960 \text{ cal.} \quad \ldots\ldots\ldots [2c]$$

The effect of temperature on these values will be discussed in a later section.

Oxygen in the Melt. In order to study the effect of chromium on the relationship between the oxygen content of the bath and the steam-hydrogen ratio in the gas, heats 301-320 were made. The data of the other heats are considered to be inadequate for this purpose, because the oxygen analyses of the high chromium heats are not reliable, while those of the low chromium ones are not very informative.

These heats were made in alundum crucibles with an insufficient amount of chromium charged so that no chromite or chromic oxide would be precipitated under the particular gas composition. There was always the possibility that some of the chromium in the form of oxide might form solid solution in the aluminum oxide crucible. The pinkish innermost layer of the used alundum crucible served as a strong evidence of the formation of such solid solutions. Naturally these solid solutions of various compositions would show various activities of chromic oxide. But since the diffusion process in the solid phase would be slow, the layer in direct contact with the molten metal could be considered to be saturated with chromic

oxide to such an extent that it was in real equilibrium with the molten metal. Thus we could eliminate the effect of the solid phase in the system and limit the system under consideration to the liquid and the gaseous phases only. In this way, through the elimination of one of the phases involved, it is possible to introduce one more

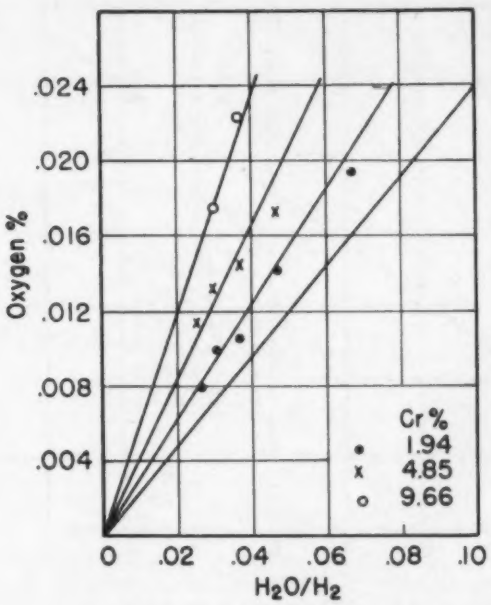


Fig. 11—Relationship Between Oxygen Content and Ratio $(H_2O)/(H_2)$ for Unsaturated Chromium-Iron Alloy Melts. Lowest line represents chromium-free melts.

independent variable. By keeping the chromium content constant we could determine the effect of the gas composition on the oxygen content in the melt at various chromium levels.

Fig. 11 gives the relationship. It is evident that the oxygen content is directly proportional to the H_2O-H_2 ratio for any particular chromium content. This is expected, yet it is interesting to note that the slopes of the straight lines are different for different chromium contents. As the oxygen and the H_2O-H_2 ratio are directly proportional and all the lines for various chromium contents in Fig. 11 converge at the origin, it is evident that for any particular chromium content the ratio $[\%\ O]/(H_2O/H_2)$ is a constant. The values of this constant are plotted against the chromium content in Fig. 12. A very good straight line is obtained, with its intercept on the ordinate at 0.241, which is exactly the value found for pure iron melts.

Fig. 12 makes it possible to calculate the oxygen content of metal of any chromium content within the range studied when in

equilibrium with an atmosphere of any H_2O/H_2 ratio. When applied to metal which is also in equilibrium with chromite or chromic oxide refractories the result is the limiting oxygen content of the metal for any chromium content at the temperature of the investigation. Table VI summarizes the results of this sort of calculation based

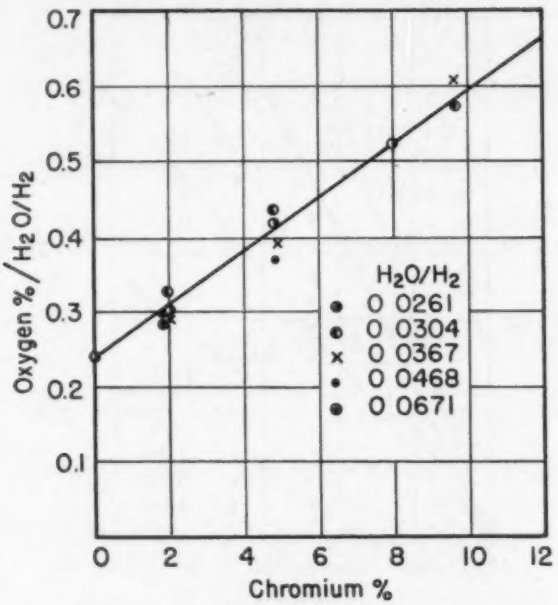


Fig. 12—Values of the Quotient [% O]/$\frac{(H_2O)}{(H_2)}$ in Chromium-Iron Alloy Melts. The characteristic value for pure iron appears at zero per cent chromium.

upon the curve of Fig. 9 and the straight line of Fig. 12, which for this purpose is assumed to continue as a straight line up to 20% chromium.

The relationship between the oxygen and chromium contents of the melt are shown in Fig. 13. Here the curve above 5.5% chromium is based entirely upon the extrapolated values of Table VI.

Table VI
Limiting Gas Composition and Oxygen Content in Chromium-Iron Alloys in Equilibrium with Chromium Refractories at 1595 C

Cr, %	H_2O/H_2	O %	a_o	f_o
0	0.930	0.224	0.224	1.00
1	0.162	0.045	0.039	0.87
2	0.116	0.036	0.028	0.78
4	0.081	0.031	0.020	0.63
5.5	0.070	0.030	0.017	0.56
8	0.056	0.029	0.013	0.47
10	0.046	0.028	0.011	0.40
12	0.041	0.027	0.010	0.37
16	0.034	0.027	0.008	0.30
20	0.029	0.027	0.007	0.26

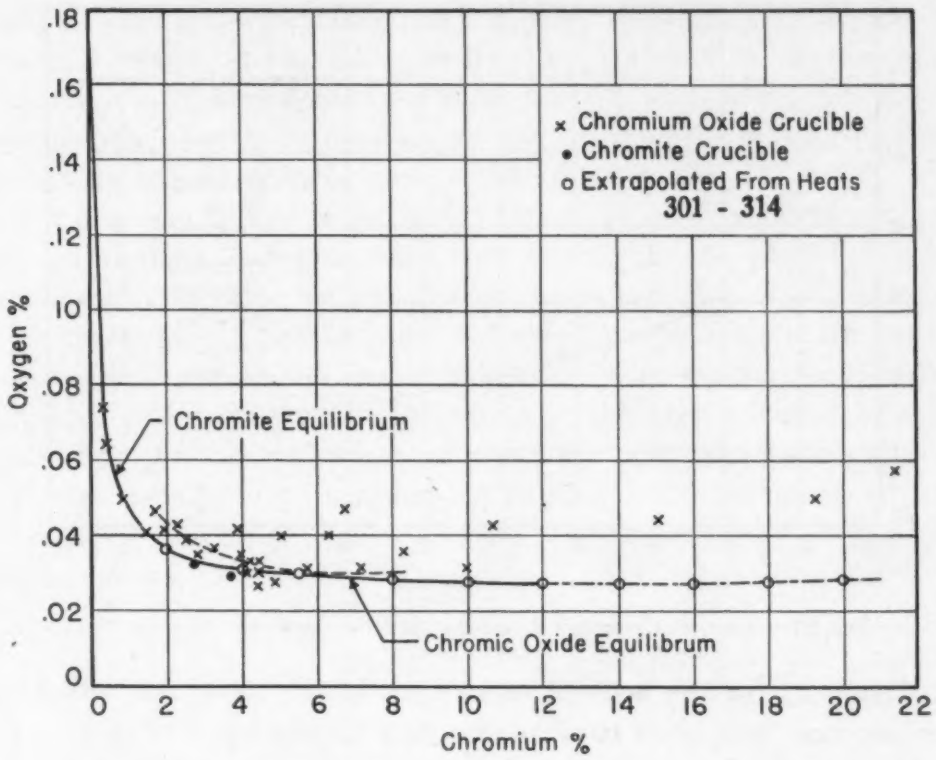


Fig. 13—Oxygen Content of Chromium-Iron Melts in Equilibrium with Chromite, X, or Chromic Oxide. Open circles indicate results extrapolated from lower chromium heats of Figs. 11 and 12.

As already pointed out, the discrepancy in the high chromium range is due to occasional suspended particles of chromic oxide and to incomplete removal of crusts from the analytical specimens.

Activity of Oxygen in Chromium-Iron Alloys. It has been well proved (5), (6) that the activity of oxygen is directly proportional to its concentration in pure iron melts. However, in the case of iron alloys, the situation might be different. Let the activity of oxygen in any melt be defined as equal to the concentration of oxygen in pure iron which would exert the same oxygen pressure or, in other words, which would remain in equilibrium with the same H_2O-H_2 gas mixture. Now it has already been established that the relationship between the oxygen concentration in pure iron and the H_2O-H_2 gas mixture at 1595 C is $(H_2O/H_2) = 4.15$ [% O], which can be used to calculate the activity of oxygen in the various heats. As shown in the preceding discussion, the activity of chromium is directly proportional to its concentration within the limits of the data and no loss of accuracy is introduced in using its concentration in per cent instead of its activity.

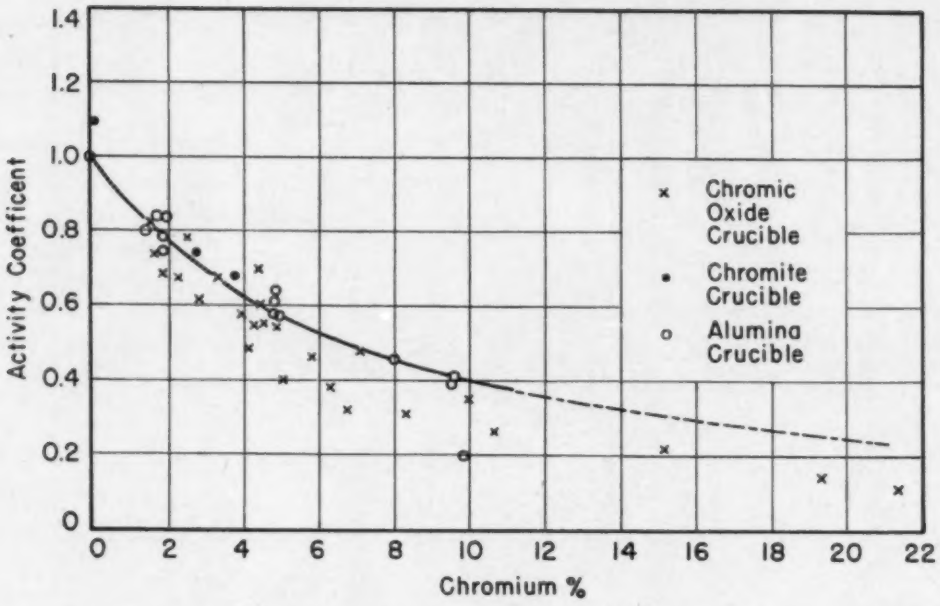


Fig. 14—Effect of Chromium Upon the Activity Coefficient of Oxygen.

Using a_o for the activity of oxygen in the melt, the following equation may be applied to all of the data obtained at 1595 C:

$$K_3 = \left(\frac{H_2O}{H_2}\right)/a_o = 4.15 \quad \ldots\ldots\ldots\ldots [3]$$

Therefore, for melts which are in equilibrium with chromite:

$$FeO \cdot Cr_2O_3\ (s) = 4\underline{O} + \underline{Fe}\ (l) + 2\underline{Cr}$$
$$K_4 = [\%\ \underline{Cr}]^2\, a_o^4 = K_1/K_3^4 = 2.44 \times 10^{-6} \quad \ldots\ldots [4]$$

And for melts in equilibrium with chromic oxide:

$$Cr_2O_3\ (s) = 3\underline{O} + 2\underline{Cr}$$
$$K_5 = [\%\ \underline{Cr}]^2\, a_o^3 = K_2/K_3^3 = 1.45 \times 10^{-4} \quad \ldots\ldots [5]$$

The above equations are valid only when the activities of oxygen instead of the concentrations are used.

Equation [3] and the data of the second and third lines of Table VI permit the calculation of the activity of oxygen in the saturated solution at any percentage of chromium. The results are shown in the fourth line of the table. The deviations of the behavior of the solution from the laws of the ideal dilute solution are best shown by the calculation of an activity coefficient, defined as the ratio of the activity to the concentration. This coefficient is tabulated in the fifth line of the table from which the great deviations from ideal behavior are obvious, since the ideal law calls for a coefficient of

unity. This is further illustrated in Fig. 14 which includes all the available data. It should be noted that the activity coefficient of oxygen is a function of chromium content and is independent of whether the heat is in equilibrium with chrome refractories or not. This is in accord with the form of the lines in Fig. 11.

Chromous Oxide in the Melt. From the strictly thermodynamic viewpoint there is no necessity for explaining the remarkably low activity coefficient of oxygen in the chromium-iron alloys, and likewise there is no proof that the following explanation is the correct one. The unexpectedly low activity coefficient results from an unexpectedly high oxygen concentration in the melt which can be explained if part of the oxygen is associated with the chromium.

The results of a considerable number of experiments on pure iron melts showed that their oxygen content at 1595 C is given by the equation:

$$[\%\ O] = 0.241\left(\frac{H_2O}{H_2}\right) \quad \ldots\ldots\ldots\ldots\ldots\ldots [6]$$

This may be regarded as the oxygen associated with the iron and, if its amount is proportional to the fraction of iron in the chromium-iron alloys, we may write:

$$[\%\ O_{Fe}] = 0.241\left(\frac{H_2O}{H_2}\right)\frac{\%\ Fe}{100} \quad \ldots\ldots\ldots [7]$$

The excess oxygen above this amount may be assumed to be associated with the chromium as some compound whose formula may for the moment be written Cr_xO_y. The oxygen present in this form is obtained by subtracting the above equation from that representing the total oxygen content of the alloys shown in Fig. 12, which is

$$[\%\ O_{total}] = (0.241 + 0.0355\ [\%\ Cr])\left(\frac{H_2O}{H_2}\right) \quad \ldots\ldots\ldots [8]$$

From which we find for O_{Cr}, the oxygen associated with chromium:

$$[\%\ O_{Cr}] = 3.79\left(\frac{H_2O}{H_2}\right)\frac{\%\ Cr}{100} \quad \ldots\ldots\ldots [9]$$

This signifies that, at any given gas composition (up to saturation) the oxygen associated with chromium is a linear function of the percentage of chromium in the bath, a result which was already obvious from Fig. 12. This could only be the case if the value of y

in Cr_xO_y is unity. Since the value of x cannot be learned from these experiments it will be sufficient to conclude that the behavior of the oxygen associated with chromium in the bath may be satisfactorily explained on the assumption that it is present as the compound CrO. This conclusion is strikingly similar to results previously reported (10) which indicated the presence of dissolved CO in iron-carbon-oxygen alloys, and is also reminiscent of earlier indications of the presence of SiO in acid melts (11).

Calculation of the Effect of Temperature

Comparison with Data at Lower Temperatures—While the thermodynamic properties of the oxides of chromium have not been established with finality even at low temperatures, it will be interesting to compare the results of the present experiments wih calculations based upon low temperature data. For this purpose we use the summary and calculations of C. G. Maier (12). He based his calculations upon Roth and Wolf's (13) value of —268,900 calories for the heat of formation of Cr_2O_3, the known entropies of the several substances involved (14) and carefully estimated, though not accurately known, values for their heat capacities at elevated temperatures. These calculations led to the following equation for the free energy change in the reduction of Cr_2O_3 by hydrogen:

$$Cr_2O_3\ (s) + 3H_2\ (g) = 2Cr\ (s) + 3H_2O\ (g) \quad \text{.....[10]}$$
$$\Delta F^\circ = 99{,}390 + 13.78\ T\ln T - 4.84 \times 10^{-3}T^2 + 0.46 \times 10^{-6}T^3 - 123.16T$$

A graph of this equation is shown in Fig. 15 along with the experimentally determined points of Wartenberg and Aoyama (15), Grube and Flad (16) and Granat (17). While the agreement is not perfect it must be regarded as quite satisfactory, in view of the entirely independent nature of the sources of data. A revision of the equation to take account of recent determinations of the heat capacity of Cr_2O_3 (18) seems unwarranted at this time in view of the greater uncertainty in the heat of formation of this compound. Maier's equation appears to represent as good a summary as can be obtained of all the data on the free energy of formation of Cr_2O_3 from solid chromium.

For use at steelmaking temperatures the equation may be simplified by calculating from it values of ΔF° and ΔH at 1600 C and using these to set up the following equation:

$$Cr_2O_3\ (s) + 3H_2\ (g) = 2Cr\ (s) + 3H_2O\ (g);\ \Delta F^\circ = +84510 - 18.75T \quad [11]$$

The remaining data which are needed in applying the above equation to reactions of chromium in liquid steel are taken from Chapter 16 of "Basic Open Hearth Steelmaking" (19). The following equation was derived to express the change in free energy when one gram atom of solid chromium dissolves in molten iron to form a 1% chromium alloy:

$$Cr\ (s) = \underline{Cr};\ \Delta F^\circ = 4350 - 11.11T \quad \ldots\ldots\ldots\ldots\ldots\ldots\ldots\ldots [12]$$

This was based upon two approximations, the first an estimate of

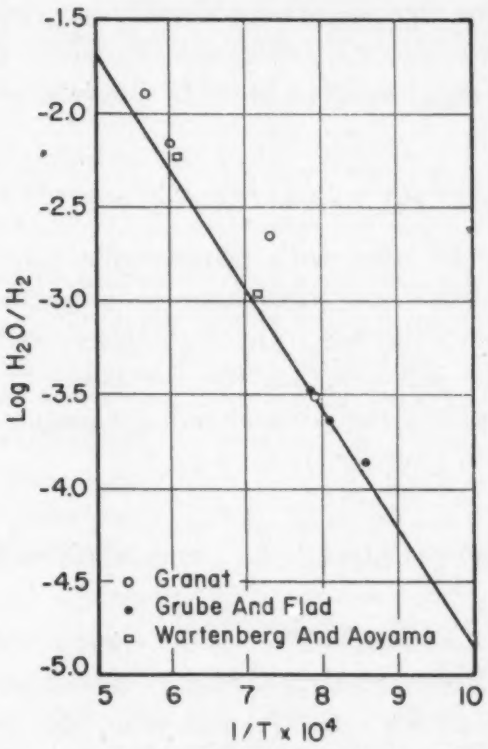


Fig. 15—Equilibrium in the Oxidation of Solid Chromium by Water Vapor at Lower Temperatures. The line represents Maier's equation based upon heat of reaction and entropy.

the heat of fusion of chromium which might introduce a minor error, and the second the assumption that chromium and iron form an ideal solution, i.e., one which obeys Raoult's Law throughout its possible range of compositions. This second assumption might introduce errors of unknown and possibly large proportions, although the physical similarity of the two elements would warrant its use as a first approximation.

The combination of these two equations leads directly to the desired result:

$$Cr_2O_3\ (s) + 3H_2(g) = 2\underline{Cr} + 3H_2O\ (g);\ \Delta F^\circ = +93210 - 40.97T \quad [13]$$

This calculated equation may now be compared with the experimental results which were summarized by Figs. 9 and 10 and by the experimental value of K_2 at 1595 C. The comparisons are shown in the following:

	Obs.	Calc.
ΔF°	16,960 cal.	16,560 cal.
K_2	1.036×10^{-2}	1.15×10^{-2}

The precision of this agreement must be, to a large degree, fortuitous since the discrepancy is considerably smaller than the uncertainties in the data employed. A minor change in the derived equation brings it into exact agreement with the data of this paper, giving us the following:

$$Cr_2O_3\ (s) + 3H_2\ (g) = 2\underline{Cr} + 3H_2O\ (g);\ \Delta F^\circ = +93210 - 40.83T \quad [14]$$

This equation may be used with considerable confidence to extend the experimental results of this paper to temperatures above and below that of the experiments. In combination with equations cited (19), this yields the following for the formation of Cr_2O_3 from the elements. This replaces the corresponding equation previously published (reference 19, page 493).

$$2Cr\ (s) + \frac{3}{2}O_2\ (g) = Cr_2O_3\ (s);\ \Delta F^\circ = -265{,}050 + 60.40T \quad [15]$$

Stability of Chromite—The free energy of formation of $FeO \cdot Cr_2O_3$ from FeO and Cr_2O_3 may be obtained from the intersection of the lines of Fig. 10. At this point the chromium content is 5.5% and the mol fraction of iron is therefore 0.94. The equilibrium gas composition is a ratio of $H_2O/H_2 = 0.070$. This establishes the equilibrium:

$$Fe\ (l) + H_2O\ (l) + Cr_2O_3\ (s) = FeO \cdot Cr_2O_3\ (s) + H_2\ (g) \quad \ldots [16]$$

$$K = \frac{(H_2)}{(H_2O)\ (Fe)} = \frac{1}{0.070 \times 0.94} = 15.2$$

or $\Delta F^\circ_{1595} = -10{,}100$ cal.

The corresponding oxidation of liquid iron is represented as follows (19):

$$Fe\ (l) + H_2O\ (g) = FeO\ (l) + H_2\ (g);\ \Delta F^\circ_{1595} = -620 \text{ cal.} \quad [17]$$

Table VII
Oxygen in Iron-Chromium Alloys in Equilibrium with Chromite or Chromic Oxide

Temp., F	2800		2900		3000		3100		3200	
				Chromite Equilibrium						
Cr, %	O_{Fe}	O	O_{Fe}	O	O_{Fe}	O	O_{Fe}	O	O_{Fe}	O
0.1	0.078	0.079	0.122	0.125	0.182	0.185	0.273	0.277	.....	.....
0.2	0.055	0.057	0.086	0.090	0.128	0.135	0.193	0.198	0.275	0.282
0.5	0.035	0.038	0.055	0.061	0.083	0.090	0.122	0.130	0.175	0.185
1.0	0.025	0.030	0.038	0.045	0.058	0.067	0.087	0.099	0.122	0.138
2.0	0.018	0.024	0.027	0.036	0.041	0.053	0.061	0.078	0.087	0.108
5.0	0.011	0.020	0.017	0.031	0.026	0.046	0.037	0.064	0.052	0.089
10.0	.....	.....	.....	.....	.....	.....	.....	.....	0.036	0.086
				Chromic Oxide Equilibrium						
5.0	0.011	0.019	0.017	0.031	(0.027)	0.047	(0.042)	0.071	(0.063)	0.103
10.0	0.0065	0.017	0.011	0.028	0.016	0.041	0.026	0.063	0.036	0.086
20.0	0.0035	0.017	0.006	0.028	0.010	0.042	0.014	0.060	0.021	0.083

Hence for the formation of chromite:

$$FeO\ (l) + Cr_2O_3\ (s) = FeO \cdot Cr_2O_3\ (s)\ ;\ \Delta F^\circ_{1888} = -9480\ \text{cal.} \qquad [18]$$

At much lower temperatures Boericke and Bangert found values of −8630 to −7800, decreasing numerically with increasing temperature. Our results thus indicate a slightly greater stability of the compound at high temperatures than would be expected from their work.

Effect of Temperature on Oxygen Content—Temperature coefficients of the various equilibria studied were not determined directly. For the principal reaction, that of Cr_2O_3 with hydrogen, the agreement with earlier data gives confidence that equations [14] and [15] are as valid over the whole range of steelmaking temperatures as at the temperature of our experiments. No such certainty may be claimed for the corresponding reduction of $FeO \cdot Cr_2O_3$ but, since it seems probable that the effect of temperature on the free energy change in equation [18] is relatively small, it will be assumed that this equation is valid over the range of steelmaking temperatures.

There is no means for calculating with certainty the oxygen content of the bath at temperatures other than that of the experiments, but the following represents an attempt to estimate the effect of temperature upon oxygen content of metal in equilibrium with chromium refractories. The temperature effect on equation [7] is represented by the following equation which is based on the observed constant of equation [7] and the heat of the reaction [19].

$$H_2O\ (g) = \underline{O}_{Fe} + H_2\ (g)\ ;\ K = \frac{[\%\ \underline{O}_{Fe}]\ (H_2)}{[\%\ Fe]\ (H_2O)};\ \log K = -5930/T + 0.556 \qquad [19]$$

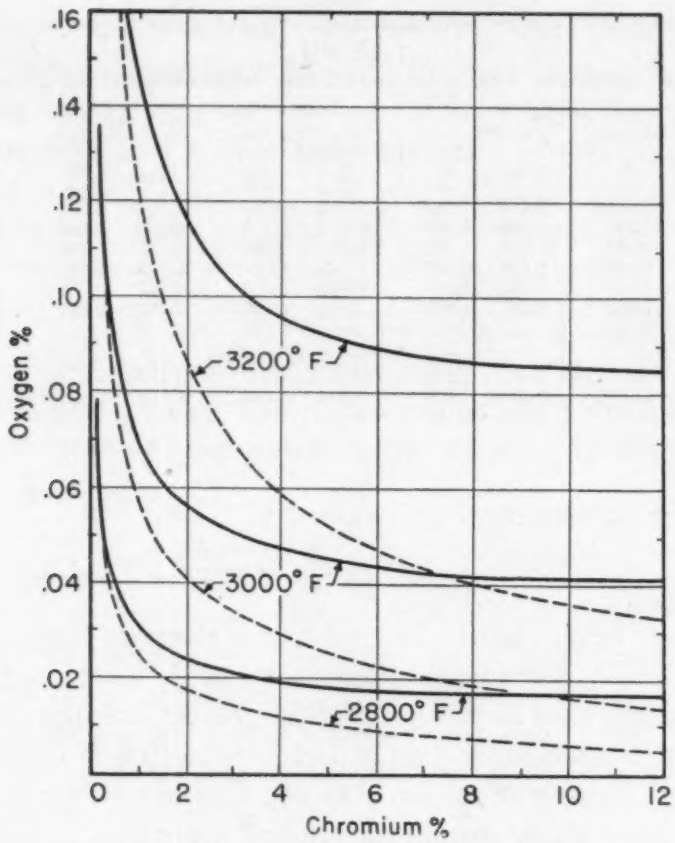


Fig. 16—Calculated Chromium-Oxygen Relationship in Molten Chromium-Iron Alloys at Several Temperatures, Estimated from Observations at 1595 C (2903 F). Solid lines, total dissolved oxygen. Broken lines, oxygen associated with iron, probably as FeO.

Now if we assume that the entropy change in equation [9] is the same as that of equation [7] we find for dissolved oxygen associated with chromium:

$$\underline{Cr} + H_2O\ (g) = \underline{O}_{Cr} + H_2\ (g)\ ;\ K = \frac{[\%\ \underline{O}_{Cr}]\ (H_2)}{[\%\ Cr]\ (H_2O)};\ \log K = -3690/T + 0.556 \qquad [20]$$

These two equations, together with equations [14] and [18], have been used to compute the data of Table VII, part of which is plotted in Fig. 16, showing the chromium-oxygen relationship at several temperatures. Table VII summarizes all of the data of this paper on the constitution of liquid iron-chromium-oxygen alloys in equilibrium with chromium refractories. It should be noted that only the column representing 2900 F has been directly determined, values for the other temperatures being calculated from these and other data.

Summary

The chemical behavior of chromium with respect to its reactions with oxygen in liquid iron-chromium alloys has been investigated in a series of experiments at 1595 C (2905 F). The experimental method involved the establishment of equilibrium conditions in the system iron-chromium-oxygen in which the oxygen pressure was controlled by means of the water vapor: hydrogen ratio of the gas phase. In the presence of chromium refractories the principal reactions were:

$$FeO \cdot Cr_2O_3\ (s) + 4H_2\ (g) = 4H_2O\ (g) + Fe\ (l) + 2\underline{Cr}\ (in\ Fe) \quad [1]$$

$$Cr_2O_3\ (s) + 3H_2\ (g) = 3H_2O\ (g) + 2\underline{Cr}\ (in\ Fe) \quad \ldots\ldots\ldots\ldots [2]$$

The equilibrium constants of these reactions at 1595 C are as follows:

$$K_1 = \left(\frac{H_2O}{H_2}\right)^4 [\%\ Cr]^2 = 7.23 \times 10^{-4}$$

$$K_2 = \left(\frac{H_2O}{H_2}\right)^3 [\%\ Cr]^2 = 1.036 \times 10^{-2}$$

A method was developed for the manufacture of small crucibles of Cr_2O_3 using slip casting and special firing techniques. For the first reaction, commercial chromite crucibles were also used.

At 1595 C, chromite is the stable solid phase in equilibrium with melts containing less than 5.5% chromium, while at higher percentages Cr_2O_3 becomes the stable phase. Calculations indicate that the quadruple point represented by this composition increases in chromium content with increasing temperature.

The oxygen content of the saturated alloys (i.e., those which were in equilibrium with chromium refractories) could not be determined accurately on account of suspended fragments and nonmetallic crusts embedded in the small ingots. For this reason a series of experiments were carried out in alumina crucibles at oxygen contents below the level required for formation of the chromic oxide. In these alloys it was found that for a given ratio, $H_2O : H_2$, the oxygen content increased with increasing chromium, being more than doubled by an increase in chromium content from zero to about 9%. This signifies that chromium lowers the activity coefficient of oxy-

gen. The effect is explained quantitatively by postulating the formation of CrO in solution in the bath.

The oxygen content of molten metal in equilibrium with chromite or chromic oxide was obtained by extrapolation of the data obtained in alumina crucibles. The result shows approximately constant oxygen content above about 6% chromium.

Thermodynamic calculations show that the results on reaction [2] are in good agreement with published data obtained at lower temperatures. Since the calculations involved the assumption that liquid iron-chromium alloys obey Raoult's Law the agreement is taken as confirmation of this assumption.

The effect of temperature upon the free energy change in the reduction of Cr_2O_3 by hydrogen to yield chromium directly as a constituent of liquid steel is:

$$Cr_2O_3\ (s) + 3H_2\ (g) = 2\underline{Cr} + 3H_2O\ (g)\ ;\ \Delta F^\circ = +93210 - 40.83T$$

The effect of temperature upon the oxygen content is also calculated, though with somewhat less certainty. Tables and graphs are presented which show the relationship between chromium and oxygen content in the range 2800 to 3200 F. Table VII and Fig. 16 give values of the percentage of total oxygen, $\underline{O}$, as well as of the ferrous oxygen, $\underline{O}_{Fe}$. The remainder appears to exist in combination with chromium, presumably as dissolved chromous oxide.

Bibliography

1. John Chipman, "Applications of Thermodynamics to the Deoxidation of Liquid Steel," TRANSACTIONS, American Society for Metals, Vol. 22, 1934, p. 385.
2. A. M. Portevin and Rene Castro, "Morphology of the Inclusions in Siderurgical Products. Part III, Chromium Alloys and Chromium Steels," *Journal*, Iron and Steel Institute, Vol. 134, No. 2, 1936, p. 213.
3. M. Baeyertz, "A Note on Chromium Oxide Inclusions in Stainless Steel and Ferrochromium," TRANSACTIONS, American Society for Metals, Vol. 22, 1934, p. 625.
4. M. A. Scheil, Mary Baeyertz and J. R. Vilella, "Identification of Inclusions in Steel by the Use of Reflected Polarized Light," TRANSACTIONS, American Society for Metals, Vol. 27, 1939, p. 479. Also ASM Handbook, 1939, p. 741.
5. M. G. Fontana and John Chipman, "Equilibrium in the Reaction of Hydrogen with Ferrous Oxide in Liquid Iron at 1600 C," TRANSACTIONS, American Society for Metals, Vol. 24, 1936, p. 313.
6. John Chipman and A. M. Samavin, "Effect of Temperature Upon Interaction of Gases with Liquid Steel," *Transactions*, American Institute of Mining and Metallurgical Engineers, Vol. 125, 1937, p. 331.
7. J. G. Thompson and M. W. Mallett, "Preparation of Crucibles from Special Refractories by Slip Casting," Bureau of Standards *Journal of Research*, Vol. 23, 1939, p. 319, R.P. 1236.

8. T. R. Cunningham and R. J. Price, "Determination of Nonmetallic Inclusions in Plain Carbon and Manganese Steels," *Industrial and Engineering Chemistry,* Vol. 5, 1933, p. 27.
9. G. N. Goller, "The Emissivity of Molten Stainless Steels," TRANSACTIONS, American Society for Metals, Vol. 32, 1944, p. 239.
10. Shadburn Marshall and John Chipman, "The Carbon-Oxygen Equilibrium in Liquid Iron," TRANSACTIONS, American Society for Metals, Vol. 30, 1942, p. 695.
11. C. A. Zapffe and C. E. Sims, *Transactions,* American Institute of Mining and Metallurgical Engineers, Vol. 154, 1943, p. 192.
12. C. G. Maier, "Sponge Chromium," U. S. Bureau of Mines, Bulletin 436, 1942.
13. W. A. Roth and U. Wolf, *Z. Elektrochem.,* Vol. 46, 1940, p. 45.
14. K. K. Kelley, U. S. Bureau of Mines, Bulletin 434, 1940.
15. H. v. Wartenberg and S. Aoyama, "The Reduction Equilibria of Cr_2O_3," *Z. Elektrochem. angew. physik. Chem.,* Vol. 33, 1927, p. 144.
16. G. Grube and M. Flad, "The Reduction Equilibrium of Chromic Oxide," *Z. Elektrochem.,* Vol. 45, 1939, p. 835.
17. I. Ya. Granat, "Reduction of Chromium Oxide," *Metallurg,* Vol. 11, 1936, p. 35.
18. K. K. Kelley, F. S. Boericke et al., U. S. Bureau of Mines, Technical Paper 662, 1944.
19. "Basic Open Hearth Steelmaking," Committee on Physical Chemistry of Steelmaking, American Institute of Mining and Metallurgical Engineers, 1944.
20. G. L. Clark, Abde Ally and A. E. Badger, "The Lattice Dimensions of Spinels," American Journal of Science, Vol. 22, 1931, p. 539.

DISCUSSION

Written Discussion: By S. F. Urban, director of research, The Titanium Alloy Manufacturing Co., Niagara Falls, N. Y.

Drs. Chen and Chipman have published an extremely worthwhile paper on a very fundamental problem that should certainly be very useful to any individual concerned with the melting of stainless steels. Though it has been known from Dr. Chipman's paper of several years back, based on thermodynamic calculations, that the temperature coefficient for chromium was extremely high, it is refreshing to have this verified so beautifully with actual data.

Consistent with the thinking in the previous paragraph, it is evident that carbon from stainless steel bonds may be reduced to appropriate values without excessive oxidation of chromium provided the carbon elimination is carried out at temperatures more elevated than normal. This, of course, presupposes that there is a means available for getting through the lower temperature range rapidly.

Written Discussion: By Shadburn Marshall, Research and Development Division, Carnegie-Illinois Steel Corp., Pittsburgh.

This paper is another example of the excellent research work in the field of steelmaking that continues to emanate from Dr. Chipman's laboratory.

At first glance, one would believe that the authors have taken a broad liberty in correcting their optical temperatures for chromium-containing melts

to the melting point of pure iron, since Goller has shown that chromium affects considerably the emissivity of pure iron. However, the close agreement with data extrapolated from lower temperatures and the fact that the extrapolation of the ratio $\frac{\%\,O}{PH_2O/PH_2}$ to chromium-free melts (Fig. 12) agrees extremely well with other published data precludes the existence of much error in temperature measurement. If, however, any check on this point is desired, it is suggested that the pyrometer could be calibrated by taking cooling curves on iron-chromium alloys and comparing with the data of Adcock,[2] obtained by thermocouple, on high purity iron-chromium melts. The maximum difference in liquidus on cooling and solidus on heating shown by Adcock in the range of compositions used by the authors is only about 18 C so that a fair check should be obtainable.

It is interesting to note that these new data show chromium to be a slightly better "deoxidizer" than previously calculated. This is in line with the observation that the product of the reaction is chromite, whereas the original calculation was based on chromic oxide as the reaction product.

Written Discussion: By Carl A. Zapffe, consulting metallurgist, Baltimore.

Of particular interest in this paper is the evidence for the existence of chromium monoxide, CrO, in liquid chromium steel. The authors refer to similar evidence published several years ago (their Ref. 11) concerning silicon monoxide, SiO—a matter which was much debated at that time. There are two subsequent papers enlarging that information on SiO which are not recognized in the present work,[3, 4] the second likewise calling attention to chromium monoxide, CrO, and, in addition, to the monoxides of certain other alloy elements in steel, such as TiO, ZrO, AlO, BO, VO, and CbO.

If CrO is a chemically identifiable constituent in Fe-Cr-O systems, as it certainly seems to be, the authors' classifications of the nonmetallic phases into Cr_2O_3 and $FeO \cdot Cr_2O_3$ seem insufficient. Indeed, in a contemporary publication[5] direct evidence is presented for the existence of a blue-black CrO slag phase as distinguished from the characteristically green Cr_2O_3 and it then follows that a protoxide chromite may also exist, possibly expressed by the formula $(FeO)_x(CrO)_y$.

One may consequently question the interpretation provided for Fig. 10. In the first place, the fit of the points is too enthusiastically described as "beautiful" by the authors. Actually, other straight lines, or a curve, could be drawn through those points. In fact, the existence of CrO should be expected to modify the Cr_2O_3 constitutional boundaries, also those of $FeO \cdot Cr_2O_3$, much as FeO modifies Fe_3O_4 in the wüstite field.

In Figs. 13 and 16 there appears exactly the type of divergence between

---

[2]F. Adcock, *Journal*, British Iron & Steel Institute, Vol. 124, 1931, p. 99-149.

[3]C. A. Zapffe and C. E. Sims, "Silicon Monoxide," *Iron Age*, Vol. 149, 1942, No. 4, p. 29-31, No. 5, p. 34-39.

[4]C. A. Zapffe, "Conversion of Certain Refractory Oxides to a Suboxide Form at High Temperatures," *Journal*, American Ceramic Society, Vol. 27, 1944, p. 293-298.

[5]C. A. Zapffe, "Dissociation Reactions Within Inclusions," Advance copy, British Iron and Steel Institute, August 1946, 5 pages.

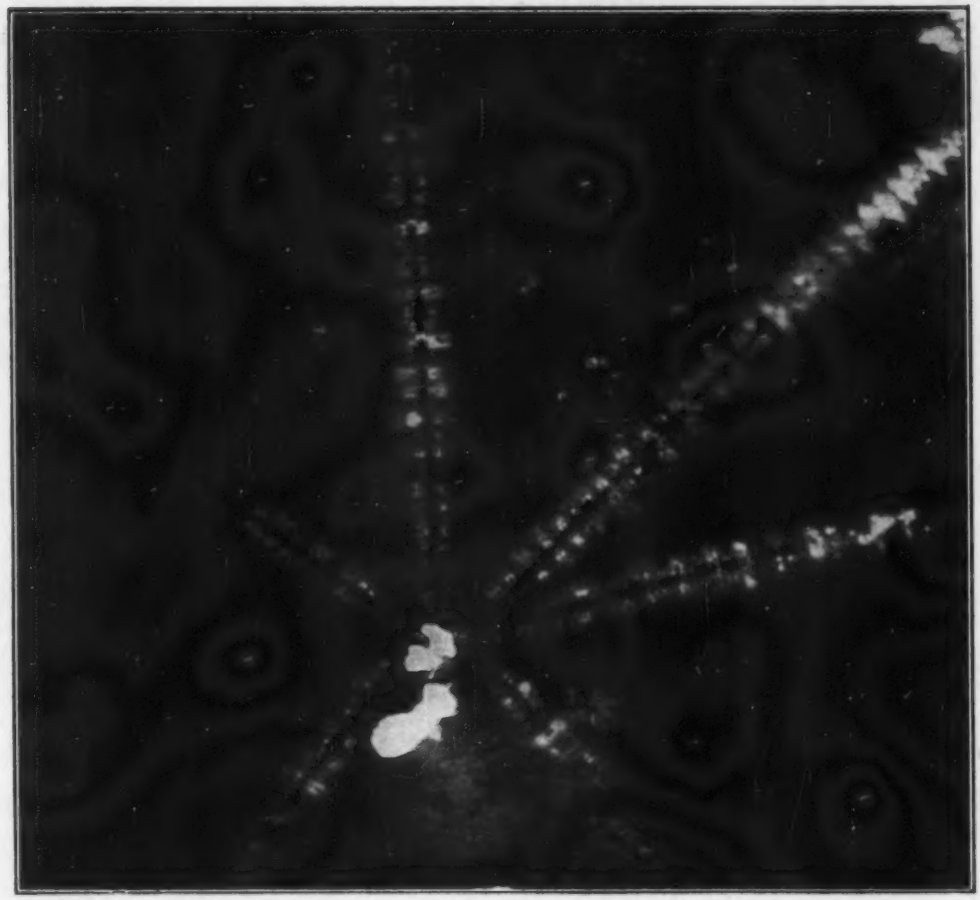


Fig. A—Blue-Black Groundmass of Chromium Protoxide Which Dissociated During Cooling to Form Green Cr_2O_3 and Metallic Cr Along Narrow Dendrite Positions. (See footnote 4.) × 2000.

theoretical and experimental curves noted in Zapffe and Sim's research with Fe-Si-O (Fig. 7 in Ref. 11). In that work the monoxide form was recognized, and consideration was given to a consequent stepwise oxidation process which seems inevitable. In the Fe-Cr-O system this becomes:

I. $$[FeO] + [Cr] \rightarrow Fe + [CrO]$$

II. $$[FeO] + 2[CrO] \rightarrow Fe + (Cr_2O_3)$$

If the activity of Cr_2O_3 is unity:

$$[CrO] = \frac{K'}{(FeO)\ 1/2}$$

Thus, as the steel is "deoxidized" with respect to FeO, its oxygen content *increases* with respect to CrO. The corollary of this statement seems more readily grasped: [CrO] increases as [Cr] increases. In the present paper there is no mention of Equation II just given; and in view of its transcending importance one should inquire why.

Still another equation of broad importance remains unmentioned. This is the "chromiumizing" reaction discussed in a contemporary paper:[5]

III. $3\,CrO = Cr + Cr_2O_3$

which liberates free Cr on cooling just as CO liberates free C in the graphitizing reaction:

$$2\,CO = C + CO_2$$

and as FeO liberates Fe in its decomposition to produce magnetite:

$$4\,FeO = Fe + Fe_3O_4$$

Figs. 7 and 8 stand as demonstrations of this "chromiumizing" reaction, for the inclusions contain metallic particles. Since either Cr_2O_3 or chromite is definitely a primary solidification entity, and of typically chunky character lacking in cavities and concavities, one cannot easily claim that these are mere cross sections of re-entrant metal arms. As demonstrated elsewhere,[5] such metallic particles probably represent Cr or Cr-Fe alloy liberated from dissociation of an original protoxide phase.

In closing, we will point to the similarity between the inclusion in Fig. 4 and the "cluster type" inclusion in Fig. 3 of Ref. 11, which was related to the dissociation of silicon monoxide. Since the dissociation product of CrO is green Cr_2O_3, an explanation results for the typical association of these inclusions with a green nonmetallic, noted by the authors. Fig. A reproduced from footnote 5 is presented as evidence of the described dissociation of blue-black groundmass CrO into dendrites of green Cr_2O_3 and metallic Cr.

Authors' Reply

Dr. Marshall's point regarding the uncertainties of optical temperature measurements is well taken. If subsequent determinations of emissivity under the conditions employed should indicate a marked effect of chromium, it will be necessary to revise the figure recorded as the average of our experimental temperatures.

With respect to the application of the data to the practical metallurgy of stainless steels, the authors have carefully refrained from attempting to draw conclusions. The presence of chromium probably affects the activity of carbon in the bath as well as that of oxygen, and experimental studies of the system iron-chromium-carbon in the liquid range might be expected to yield interesting results.

Dr. Zapffe's comments are interesting but fall short of proving the existence of CrO as a separate phase. The hypothetical presence of the compound as a constituent of the melt is in no way dependent upon its existence as a pure substance.

His equations I and II are not independent of the equations of the paper and can be deduced from the latter, along with numerical values for their equilibrium constants. Such calculations would seem redundant.

The increase in oxygen associated with chromium accompanying an increase in the chromium content, in an environment of constant oxidizing potential, was pointed out very specifically in connection with equation [9]. Similarly for saturation with chromite the increase in [% O_{Cr}] with increased chromium content is readily found by subtracting any two corresponding columns of Table VII.

THEORETICAL THERMAL STUDIES OF STEEL INGOT SOLIDIFICATION

By Victor Paschkis

Abstract

The thermal aspects of solidification are discussed in a qualitative manner and it is shown that the energy balance as well as the time-temperature characteristics of various parts of the ingots are necessarily different. The cooling rate at the center is very different from that at the surface or points in between. Mathematical analysis is impractical because of the many assumptions necessary to permit analytical solution. A relatively new method—that of electric analogy—is described and then experiments carried out by this method are described. The experiments show the beneficial influence of a carbon insert at the bottom of a mold; the freezing near the bottom becomes much more uniform. A comparison of a round and a rectangular ingot shows, as expected, the greater uniformity of the former, as far as solidification rates are concerned. Finally a comparison of two hot tops shows that both are sufficient; i.e., with neither is a bridging of the ingot below the hot top to be expected.

Qualitative Analysis of the Heat Flow Problem

THIS paper deals only with the thermal aspect of steel ingot solidification. It is recognized that the problem of solidification has many angles, but it is believed that answers can be obtained only by dealing separately with the different sides of the problem.

In considering the thermal aspect of ingot solidification the metallurgist encounters immediately a puzzling statement. The entire complex question of existence of a "mushy state" between liquid and solid, the problem of how the transition from liquid to solid steel takes place, is of no importance from a thermal viewpoint. A thermal

The experiments described in this paper are part of the work carried on by the NDRC Research Project NRC-39 in Contract OEMsr-755.

A paper presented before the Twenty-eighth Annual Convention of the Society held in Atlantic City, November 18 to 22, 1946. The author is technical director of the Heat and Mass Flow Analyzer Laboratory, Columbia University, New York City. Manuscript received July 30, 1946.

study should merely yield the answer to one or both of the two following questions:

(a) What time is required to cool the steel from the pouring temperature to any given and desired lower temperature?

(b) How much heat is extracted during this time from the steel?

The present paper deals only with the first of these two questions. Moreover, the "desired lower temperatures" are in this paper limited to the two values, represented by the liquidus and the solidus lines on the constitution diagram.

Different points in the ingot reach these temperatures at different times. Curves can be drawn, connecting all points reaching a given temperature (e.g. the liquidus), at the same time. Such curves are called "isochrons"* and need two characterizations: the time and the temperature. Thus a "20-minute isochron for 2700 F" connects all points in the ingot which cool within 20 minutes from the pouring temperature to 2700 F.

Ingot—The following considerations refer to an ingot of finite thickness, but of infinite area of contact with the mold. In other words, it refers to an infinite plate of finite thickness. Each of the two surfaces of the "ingot" plate contact another plate of finite thickness (mold), which is initially cold.

In the plate representing the ingot, three elements, the characteristics of which are characteristic of the behavior of the entire plate, will be considered. All three elements are thought of as having infinitely small thickness, so that temperature differences within each element may be neglected. It is furthermore assumed that the mold fills instantaneously, or in other words, that the pouring time is zero. Changes by slow filling will be considered later.

Element A (see Fig. 1) is located at the surface of the ingot facing the mold. Element B is located midway between the center plane and the surface, and there are of course a great number of Elements B, each of which is at a different distance from the center. Element C is located at the center plane.

Element A—Element A will freeze immediately after pouring unless the mold is covered with a heavy coating or unless the degree of superheat is unreasonably high. After solidification of Element A and possibly of immediately adjacent elements, the mold will expand and the ingot contract; consequently an air gap between ingot and

*In the NDRC Report on which this publication is based, the word isotemp had been used. However, in the literature the term isochron has been mentioned, and in order not to confuse by different terms, the word isochron is adopted in this paper.

mold is formed. This air gap offers considerable resistance to heat flow and thus the temperature of Element A may, after a short time, rise again. Schematically this is indicated in Fig. 2 which represents a temperature-time curve for Element A.

It is even conceivable that Element A could experience oscillating temperatures so that the surface would "breathe". The underlying idea is that upon contact between steel and mold the temperature of

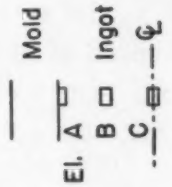


Fig. 1—Position of Elements in Ingot.

the steel drops, the steel contracts, and an air gap is formed. The air gap is bounded on one side by the mold and on the other by a thin shell containing the as yet liquid steel. The subsequent temperature rise breaks the thin solidified skin of the ingot; the liquid flows out to the mold wall so that the air gap vanishes again. When the temperature has dropped further a new air gap is formed, etc.



Fig. 2—Temperature-Time Curve for Element A (at Mold Ingot Interface).

It should be noted that this is mentioned as a possibility, and that as yet no experiments have been carried out to substantiate this theory. However, such breathing would be entirely in line with what appears to be happening at the surface.

Element B—Fig. 3a represents schematically the energy balance for Element B. The element receives heat from elements located nearer the center of the ingot and from the exothermic heat of solidification. The heat expenditure is entirely in the heat flowing toward the outside. Similar energy balances occur for any elements located between those marked A and C.

Element C—Fig. 3b represents the energy balance for this element. The only heat income is that from the exothermic heat of solidification; the only heat expenditure consists of the heat flowing to the next element.

Provided that all elements have the same size, then the following statements can be made:

(a) Depending on the superheat, a certain time will elapse before any of the inside elements (B) start to solidify.

(b) The closer an Element B is to the center plane of the ingot, the smaller the stream marked "from elements nearer to the center plane" (Fig. 3a) will be for this element at any one time.

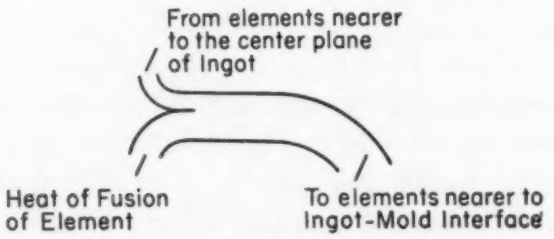


Fig. 3a.

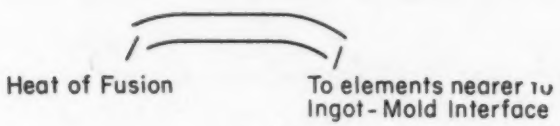


Fig. 3b.

Fig. 3a—Energy Balance for Element B (Midway Between Center and Surface of Ingot).
Fig. 3b—Energy Balance for Element C (Center of Ingot).

Mold—The mold is initially at room temperature. After the molten steel is poured the temperature of the mold will rise, and, of course, the farther away an element of the mold is from the interface, the later will the rise occur. The interface and the element close to it may first rise quickly and then drop again by the "breathing" process described above for the ingot. Eventually all parts of the mold will heat up, and after sufficient time has passed will drop again, this time along with the ingot. In practice the ingot will probably be stripped before the mold temperatures start to decrease in the final temperature drop. Fig. 4 shows schematically temperature-time curves for different parts of the mold.

Introduction of Finite Mold Size—So far it has been assumed

that the rectangular ingot is of finite thickness but infinite in both other directions. Actually the ingot is of course finite in all three directions, and therefore the rates of solidification near top and bottom are different from those at midheight. Solidification is more rapid near the bottom unless special and not conventional means are employed to delay solidification at this place. Solidification would also be accelerated near the top if no hot top were employed to cut

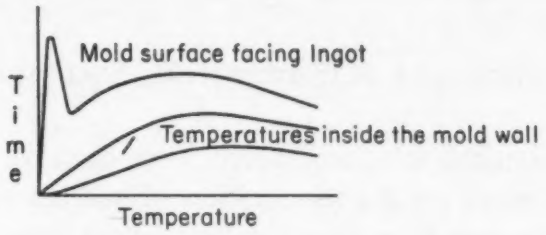


Fig. 4—Temperature-Time Curves for Mold.

down the rate of heat losses toward the top. Any element directly in contact with the surface of the mold bottom or with the covering in the hot top will act initially like Element A, described above. However, because the steel rests on the bottom it cannot shrink away from the mold as it does on the sides, and thus no air gap will form at the bottom. It is believed that the covering in the hot top will follow the metal and that therefore no air gap is formed at the top either. Hence the "breathing" of the surface will not occur at top or bottom and the temperature will drop steadily; the elements will act as those described as "Element B". The rate of heat flow to the outside will be increased. From elements at or near the bottom heat will flow in part toward the bottom, in part toward the sides. The greater the distance of any part from the bottom, the more will it approach the behavior of Element A or B, according to the distance from the side wall. Similar conditions prevail for elements near the top.

Finite Pouring Time—Another concept, which has been introduced above, should be dropped now—that of sudden pouring. Several minutes are required to fill the mold with steel. With top pouring, the flow of steel should be directed in such a way that it will not strike the side walls of the mold. In bottom pouring, the steel wells up in the mold and in that way immediately contacts the side walls of the latter. In either case there will be heat flow in the mold wall before the entire mold is filled. The heat flow will be parallel to the axis of the mold as well as perpendicular to it. The elements

of the steel which come in contact with the mold toward the end of the pouring time will find a mold wall which is warmer than when the first elements of the steel strike the mold.

Finally it should be pointed out that quite often the molds are preheated. Such preheating usually does not result in uniform temperature over the entire thickness of the mold. Depending on the methods of preheating, the outside or the inside surface of even the midthickness of the mold may be the point of highest temperature.

Review of Mathematical Solutions

All mathematical solutions which have come to the attention of the author are based on the assumption of sudden solidification: the range of solidification is replaced by one single temperature at which the metal is assumed to freeze as if it had a eutectic point. In the mathematical solutions published so far, it is assumed that the entire heat of solidification is given off at this temperature, thus maintaining the temperature constant for some time.

Beyond this basic assumption various authors make additional assumptions. It appears that three methods of mathematical approach have been developed, namely those by Schwarz (1),[1] by Saito (2), and by Roth (3). All other authors base their work on those three fundamental investigations. Exception may be made for the work by Feild (4), who does not offer any mathematical deduction or proof for his well-known formula.

Schwarz assumes that the ingot as well as the mold are infinitely thick. In the first part of his paper he assumes that there is no air gap. In the second part he uses an approximate method in which the air gap is considered, but it is assumed that liquid and solid steel have the same properties.

Saito (5), and later Lightfoot (6) in a more accessible publication, base their work on the assumption that the properties of mold and steel, liquid and solid, are identical. Several cases are investigated: one case assumes that mold and ingot are both infinitely thick, and the other assumes that the ingot is of finite thickness, facing a surrounding of constant temperature.

Roth used a step method and based his work on the assumption that the entire liquid metal is at one constant temperature throughout, thus neglecting any temperature gradient in the liquid. Both authors

[1]The figures appearing in parentheses pertain to the references appended to this paper.

neglect the influence of the air gap and assume that the steel is in continuous, complete and perfect contact with the mold.

In a publication by Tageev and Gulyaev (7), use is made of the Feild formula, and of charts similar to the Gurney-Lurie charts (8), but in the form used by Groeber (9). However, Tageev and Gulyaev do not offer mathematical deductions for their conclusions.

In view of the sweeping assumptions necessary for mathematical solutions, it is not to be expected that observed freezing times necessarily coincide with calculated values.

Electric Analogy Method

The study of heat flow by means of electric analogy has been previously described (10). It is sufficient to state here that the method is based on the setting up of an electric circuit representing the body in which heat flow occurs. On this electric circuit measurements are carried out which are later translated into heat terms. The obvious advantage of this method is the elimination of the costly and difficult bleeding experiments on ingots and the destruction of the ingot when taking samples from the inside. An advantage over the mathematical solutions discussed previously is that a number of sweeping assumptions made in the mathematical analogies may be dropped. First, the finite thickness of ingot and mold can be taken into consideration, and secondly the assumption of sudden solidification for steel need not be maintained. The experimental technique is described in Appendix I. It may be pointed out here that this method has been proved time and again to give correct results when compared with actual thermal experiments, or with calculations. Reference is made to various publications discussing such comparison (11).

Experiments on the Solidification of Ingots by the Electric Analogy Method

Problems—Three problems have been investigated:

(a) The influence of the material of the bottom on cooling, comparing a cast iron bottom with a carbon insert.

(b) The solidification at midheight of the ingot.

(c) A comparison of two hot tops.

The bottom material and solidification at midheight were analyzed

for a round as well as for a rectangular ingot, whereas the hot top problem was analyzed only for a round ingot.

Approach—As indicated in the heading, all experiments were carried out by the electric analogy method. The rectangular ingot represents a problem of three-dimensional heat flow. Thinking of the vertical axis of the ingot as the x axis of a rectangular system of coordinates, the other two axes (y and z) can be arranged so as to be parallel with the sides of the ingot. Inasmuch as the present electric equipment lends itself only to the study of one and two-dimensional problems, an approximation was made by investigating three different two-dimensional problems and combining the results proportionately. The three problems may be characterized by the three planes, xy, yz, and xz, for each of which the isochrons were determined, under the assumption that ingot and mold surface were infinite in the direction of the third axis (z, x and y respectively). The method of combining the sets of three two-dimensional tests is explained in Appendix II.

Properties and Simplifications—Various experiments were carried out: experiment numbers in relation to a description of prevailing conditions are listed in Table I.

Table I
List of Experiments

Material of Bottom and Solidification in Midheight of Ingot			
Cylindrical Ingot			
Exp. A-1	**Cast Iron Bottom**		
Exp. A-2	**Carbon Bottom**		
Rectangular Ingot			
Exp. C1-1	**Cast Iron Bottom**	**Ingot Infinite In**	**y-y axis**
Exp. C1-2	**Cast Iron Bottom**		**x-x axis**
Exp. C1-3	**Cast Iron Bottom**		**z-z axis**
Exp. C2-1	**Carbon Bottom**		**y-y axis**
Exp. C2-2	**Carbon Bottom**		**x-x axis**
Investigation of Hot Top			
Cylindrical Ingot			
Exp. A-3	**Straight Hot Top**		
Exp. A-4	**Inclined Hot Top**		

Properties—Properties of the steel and the mold were prescribed by Mr. Spretnak of Carnegie Institute of Technology, who was working on the metallurgical aspect of solidification. The properties were selected as shown in Table II.

The values of resistance to heat flow from the outside mold surface to the surroundings were selected on the basis of preliminary experiments. The resistance to heat flow per unit area and unit temperature difference is the reciprocal of the boundary conductance. The boundary conductances are listed in Table III for the various

Table II
List of Properties

INGOT		
Thermal Conductivity—Liquid	9.2	Btu/ft,hr,F
Solid	18.4	Btu/ft,hr,F
Specific Heat—Liquid	0.180	Btu/lb,F
Solid	0.144	Btu/lb,F
Density—Liquid	449.5	lb/cu ft
Solid	467.0	lb/cu ft
Heat of Fusion	126.1	Btu/lb
MOLD		
Thermal Conductivity	21.8	Btu/ft,hr,F
Specific Heat	0.152	Btu/lb,F
Density	453.0	lb/cu ft
Pouring Temperature		2845 F
Freezing starts at		2700 F
Change of Properties at		2650 F
Freezing ends at		2600 F
Preheat Temperature of mold, carbon, refractory		250 F
Ambient temperature		70 F

experiments, and are different for sides, bottom and top, because of the different surface temperatures prevailing at those points.

It has been explained above, that after the ingot shrinks away from the mold, an air gap is formed, which represents an appreciable barrier to heat flow. Heat exchange across the air gap takes place by conduction and radiation. In the present experiments only the latter mode of heat transfer has been considered, the conduction component being neglected. The radiation component is independent of the width of the air gap, whereas the amount of heat exchanged by conduction is inversely proportional to the air gap width. There seems little doubt that the air gap is so narrow that convection currents can be neglected. The relative importance of conduction has been studied by C. Schwarz (1). He proves that heat transfer by conduction amounts to only 20% of that by radiation, even with very small air gaps. With larger air gaps the resistance to heat flow by

Table III
Boundary Conductances

ROUND INGOT			RECTANGULAR INGOT		
Exp.	Boundary Conductance in Btu/sq ft,hr,F		Exp.	Boundary Conductance in Btu/sq ft,hr,F	
A1	Side	7.14	C1-1	Side	9.45
	Bottom	8.37		Bottom	8.37
A2	Side	7.14	C1-2	Side	9.45
	Bottom	4.18		Bottom	8.37
A3	Side	6.02	C1-3	Side	9.45
	Top	8.37	C2-1	Side	9.45
A4	Side	3.1		Bottom	4.18
	Top	8.37	C2-2	Side	9.45
				Bottom	4.18

conduction increases but that to heat flow by radiation remains unchanged, and therefore the importance of conduction becomes relatively smaller. Inasmuch as the mold forms a complete envelope for the ingot, the radiation can be considered to be black body radiation.

Black body radiation may be expressed by the following equation:

$$Q_r = 0.173\, \epsilon \left[\left(\frac{T_1}{100}\right)^4 - \left(\frac{T_2}{100}\right)^4 \right] = \epsilon\, 0.173\, \Xi\, (t_1 - t_2)$$

Here the following notations are used:

Q_r Heat transferred by radiation (across the air gap) where t_1 and t_2 are the interface temperatures of the ingot and mold respectively in F.
T_1 Temperature in degrees Rankine ($T_1 = t_1 + 460$) (Ingot side surface of air gap)
T_2 (Degrees Fahrenheit + 460) ($T_2 = t_2 + 460$) (Mold side surface of air gap)
ϵ Emissivity (Black body radiation; hence $\epsilon = 1$)
0.173 Radiation constant
A Area of heat transmission

$$\Xi \frac{\left(\frac{T_1}{100}\right)^4 - \left(\frac{T_2}{100}\right)^4}{T_1 - T_2} = \frac{\left(\frac{T_1}{100}\right)^4 - \left(\frac{T_2}{100}\right)^4}{t_1 - t_2}$$

The values Ξ change with temperature and therefore it might be expected at first that it would be necessary to change the values during the experiment. However, it turns out that the increase of the mold surface temperature and the decrease of the ingot surface temperature tend to balance each other, so that the values of Ξ occurring during solidification change but little and that therefore it is possible to work with a constant value of Ξ for each experiment.

For one specific experiment, namely C1-1, the values of the temperatures of both surfaces of the air gap together with the values Ξ are listed in Table IV for the entire time of solidification.

Table IV
Air Gap Temperatures and Values Ξ

Time, Min.	Exp. C1-1 Mold Side Temp., F	Ingot Side Temp., F	Ξ
0	1030	1980	325
6	1080	1920	349
12	1180	2000	358
18	1210	1880	336
24	1240	1830	327
30	1280	1830	332
36	1310	1806	335
42	1330	1770	330
48	1360	1760	330
54	1380	1750	336
60	1390	1730	332
66	1400	1720	332
72	1400	1695	325
78	1400	1673	322
84	1410	1658	320
		Average Ξ =	330.6

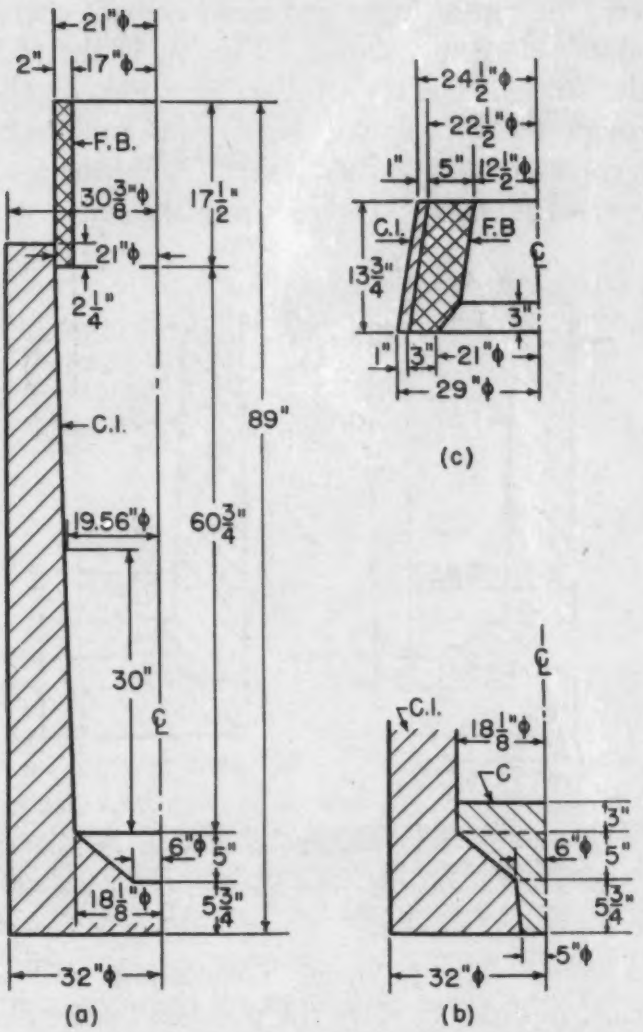


Fig. 5—Dimensions of Cylindrical Ingot: a—With Cast Iron Bottom, Straight Hot Top; b—With Carbon Bottom (Top Not Shown Because Unchanged as in a); c—Inclined Hot Top. F.B. = Firebrick; C = Carbon; C.I. = Cast Iron.

This table may serve as proof for the justification to work with constant Ξ values. The values of Ξ were determined in preliminary experiments and were selected as follows:

Cylindrical mold (Exp. A1 through A4) $\Xi = 330$
Hot top for cylindrical mold (Exp. A3) $\Xi = 1000$
Hot top for cylindrical mold (Exp. A4) $\Xi = 979$
Rectangular mold (Exp. C1 and C2) $\Xi = 471$

Dimensions—The dimensions of the ingots, molds and hot tops are shown in Figs. 5 and 6. Fig. 5 holds for the cylindrical, Fig. 6 for the rectangular ingot. In Fig. 5a the cast iron bottom, the entire ingot and the straight hot top are shown; Fig. 5b is a picture of the

carbon insert; the top of ingot and mold are not changed as against Fig. 5a and therefore not shown. Fig. 5c is the inclined hot top, replacing the straight hot top of Fig. 5a. Fig. 6a shows the cross section through the rectangular ingot with cast iron bottom, and Fig. 6b the corresponding carbon insert. Only the lower part of the rectangular ingot is shown, because only the latter has been tested.

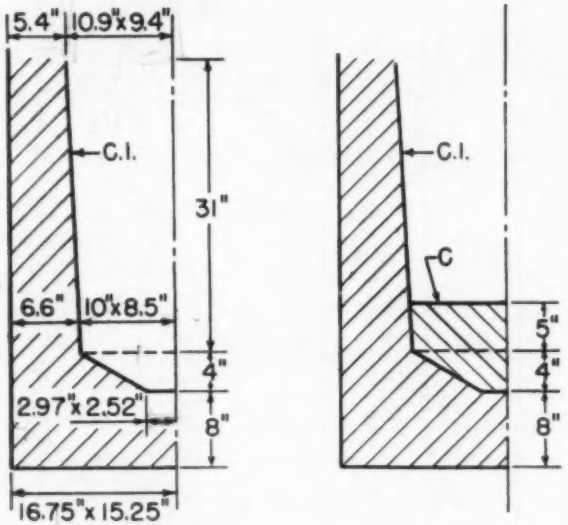


Fig. 6—Dimensions of Rectangular Ingot: a—With Cast Iron Bottom; b—With Carbon Bottom. Only the lower part of the ingot up to a total height of 35 inches is shown; no heat flow vertically through the 35-inch level. C.I. = Cast Iron; C = Carbon.

Simplifications—The following assumptions and simplifications had to be made, in order to solve the problem by the electric analogy method:

(a) Instead of the steady change of diameter or cross section, a change in steps was introduced as demonstrated in Fig. 7. It was assumed that in each step heat flowed only perpendicularly to the axis, not in the direction of the axis. This holds true for all steps on the sides but not for those on the bottom, where heat flow in both directions was introduced.

(b) Air gap time was assumed to be constant and equal to 2 minutes. The air gap resistance was constant and the Ξ values on which it was based are shown above.

(c) The pouring time was neglected. It was assumed that at time zero the entire mold is filled with steel at its pouring temperature.

(d) It was assumed that the mold was at a uniform temperature of 250 F at the beginning of mold-steel contact.

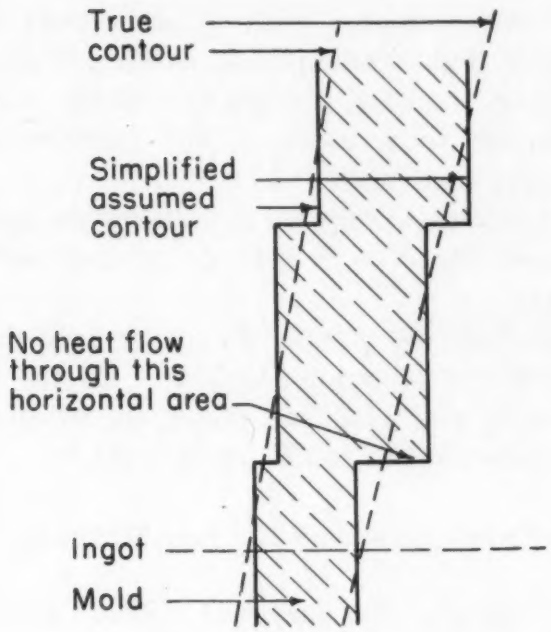


Fig. 7—Explanation of Using Steps Instead of an Incline.

(e) It was assumed that the properties are constant over the range of superheat, and that a second set of properties is constant over the entire range of "solid" temperatures. In other words, the properties were assumed to be constant between the pouring temperature of 2950 F and the mean of the solidification range, 2650 F. A second set of properties was assumed to be constant between the last-mentioned temperature and the end of the cooling period.

(f) It has been assumed that the heat of solidification is liberated over the range of solidification, following an exponential curve. This assumption simplifies the electric experiments considerably because it makes it possible to think of the heat of solidification as a temporary increase of specific heat lasting during the drop over the solidification range.

Experimental Results—All curves presented are isochrons. Two complete sets of isochrons were taken: one for 2700 F (liquidus) and one for 2600 F (solidus).

When the experiments were started, it was believed that the solidification should be considered accomplished only when the temperature at the center of the ingot has dropped to the solidus (2600 F). While the experiments were progressing, tests on solidification of castings were carried out (11c). The results of the electric

analogy tests were compared with bleeding tests of castings. It appeared probable that bleeding tests would for any prior time of solidification show solidified thicknesses which coincide with the predictions from the isochrons for 2700 F (liquidus line), found by the electric analogy method.

This hypothesis was confirmed by bleeding an ingot (12). Therefore, the isochrons for 2700 F were determined for all cases dealt with in this paper.

In order to limit the number of curves only the isochrons for 2700 F are shown, not those for 2600 F. Of the latter only two examples (Figs. 8a and 14a) are presented, to offer the reader a comparison between the two solidification times.[2]

Experiments on Bottom Material

Cylindrical Ingot—The isochrons (2700 F) for a cast iron bottom are shown in Fig. 8, those for a carbon bottom in Fig. 9. The isochrons for the cast iron bottom for a temperature of 2600 F are shown in Fig. 8a.

In all three figures it can be seen that the isochrons are practically parallel to the side wall from the midplane to a plane approximately 10 to 15 inches below the midplane. Apparently the nature of the bottom does not influence the rate of solidification at the midplane.

A comparison of Figs. 8 and 9 brings out forcefully the influence of the carbon bottom. With no carbon insert (Fig. 8) the solidification 5 inches from the bottom takes 13 minutes (on the axis); the carbon insert slows that time down to more than 40 minutes.

A comparison of Figs. 8 and 8a shows the considerable time lag between the liquidus and the solidus. For any given position the time for reaching the solidus is almost twice as long as that required to reach the liquidus. A similar relationship holds for the times shown by the isochrons for carbon insert (Fig. 9 for 2700 F; a curve not shown in this paper for 2600 F).

Rectangular Ingot—As explained above, the isochrons for the rectangular ingot were found by combining the results of three independent two-dimensional tests. The isochrons are presented for different levels (measured in inches from the bottom of the ingot). The numbers of the illustrations for the different levels may be seen from Table V.

[2]Complete curves of isochrons for 2600 F are available for inspection in the Heat and Mass Flow Analyzer Laboratory at Columbia University.

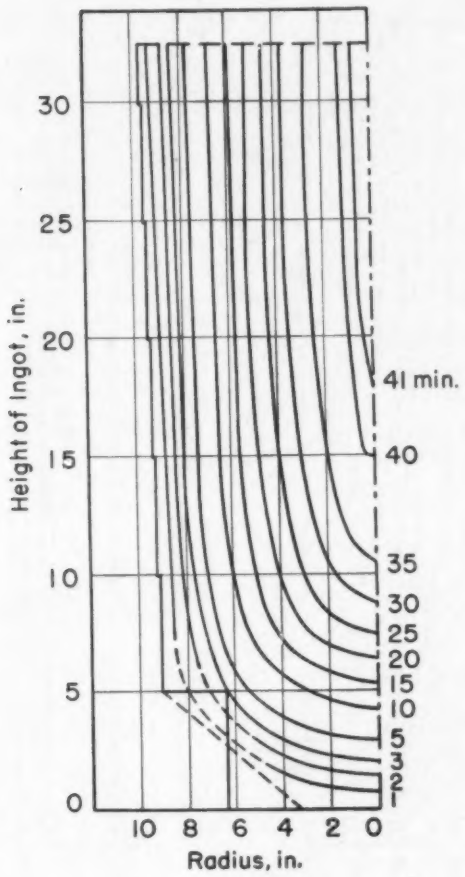


Fig. 8—Isochrons Round Ingot, Mold Bottom (2700 F).

The curves for the 35-inch level were measured directly. No influence from the nature of the bottom is to be found on this level. Therefore no separate curves are shown for the carbon bottom. The fact that there is no influence may also be expressed by saying that the isochrons in vertical planes are in the neighborhood of the 35-inch

Table V
List of Isochrons (2700 F) for Different Levels
(Rectangular Mold)

Level (Inches from Bottom)	Isochrons (2700 F) for Cast Iron Bottom Shown in Fig.	Carbon Bottom Shown in Fig.
5	10	15
10	11	16
15	12	17
25	13	18
35	14	

Fig. 14a shows the isochrons (2600 F) for the 35-inch level

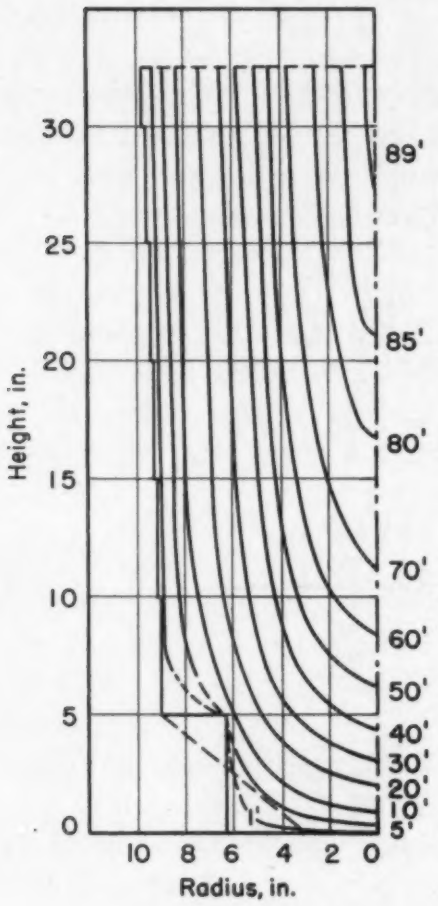


Fig. 8a—Isochrons Round Ingot, Mold Bottom (2600 F).

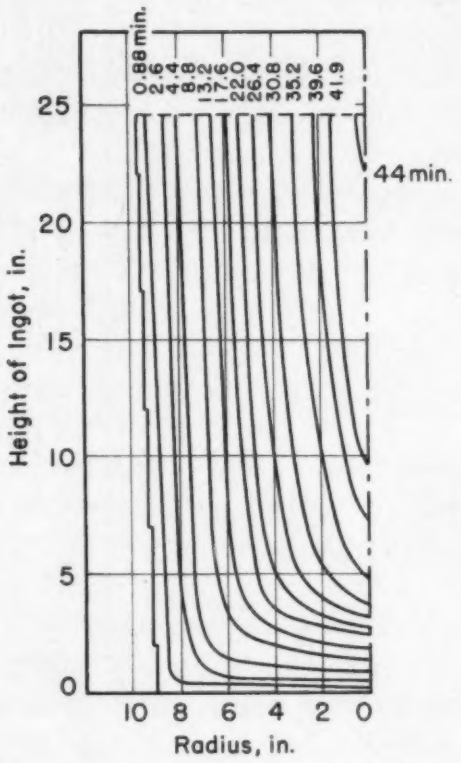


Fig. 9—Isochrons Round Ingot, Carbon Bottom.

level, parallel to the sides. Therefore no axial heat flow can occur across the 35-inch level. This was also proved by taking the isochrons separately for the 42.75-inch level. For similar distances from the surface they check well with those of the 35-inch level. The results are compared in Fig. 19. In this figure freezing times are plotted as ordinates, and distances from the vertical axis (measured in a horizontal plane) as abscissas. Four curves are shown, holding for different angles, 0 degree indicating the x-x axis and 90 degrees the y-y axis. The curves show the measured times for the 42.75-inch level; the dots are the times found by extrapolation from the values measured for the 35-inch level. Obviously measured and extrapolated curves check well. The isochrons for the levels other than 35-inch were found by interpolation as explained in Appendix II.

In all the charts the corner effect is very marked. Cooling next to the corner takes place to a much greater extent than at the two

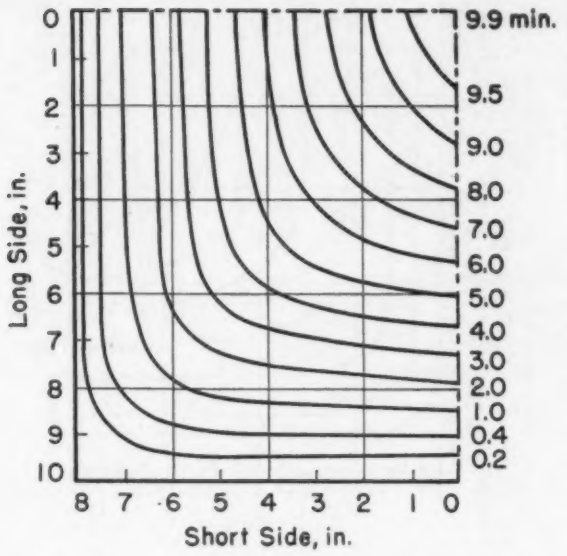


Fig. 10—Isochrons Rectangular Ingot, Mold Bottom, 5-Inch Level.

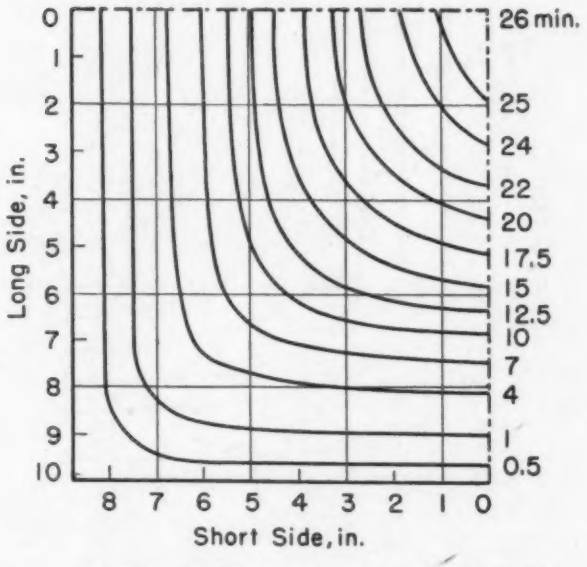


Fig. 11—Isochrons Rectangular Ingot, Mold Bottom, 10-Inch Level.

axes. The influence of the corner decreases, of course, toward the center of each side, but is noticeable roughly to a distance of 3 inches from the corner.

It has been suggested that as the solidification progresses toward the center (i.e., the vertical axis) the isochrons become more and more like circles. Undoubtedly the curves become more and more round—but even the last isochron drawn is rather an elliptic curve

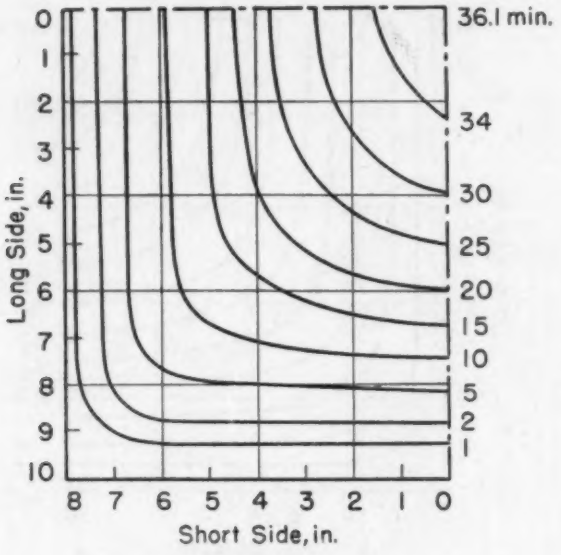


Fig. 12—Isochrons Rectangular Ingot, Mold Bottom, 15-Inch Level.

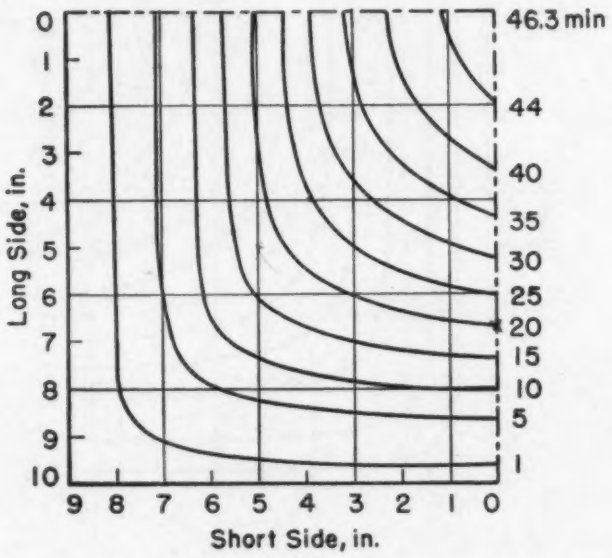


Fig. 13—Isochrons Rectangular Ingot, Mold Bottom, 25-Inch Level.

than a circle. In Fig. 10 the 9.5-minute isochron cuts off 1 inch on the short side axis, but 1.8 inches on the long side axis.

Some Comments on the Solidification Near the Bottom—In the electric experiments the incline near the bottom was replaced by rectangular steps, as shown in Fig. 7. The sections were so made as to have equal volume with the corresponding part of the incline. Reference is made to Fig. 20 where on the left side the surface in

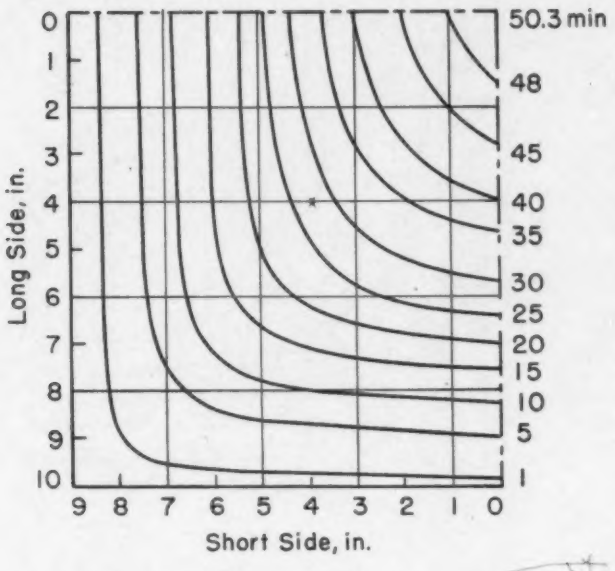


Fig. 14—Isochrons Rectangular Ingot, Mold Bottom, 35-Inch Level (2700 F).

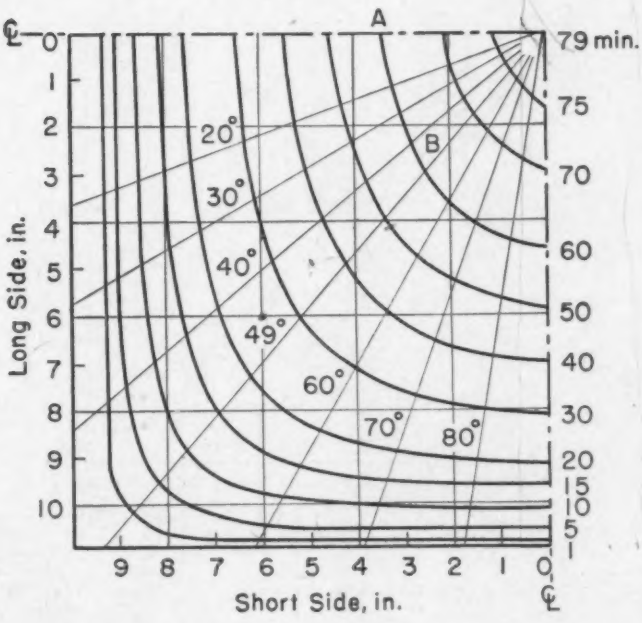


Fig. 14a—Isochrons Rectangular Ingot, Mold Bottom, 35-Inch Level (2600 F).

steps, and on the right side the incline, is shown. The shaded area proportional to the volume is equal in both cases. However, the surface area of the rectangular step is necessarily larger than that of the incline, as is obvious by comparing the circumference (heavy lines) of both parts of Fig. 20. A correction for this increased area

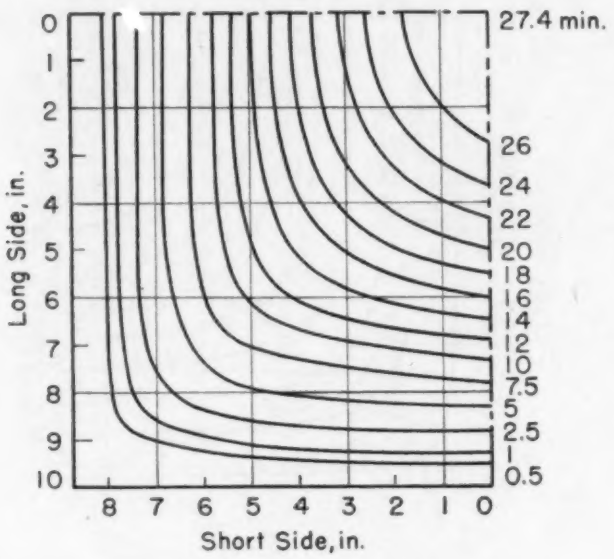


Fig. 15—Isochrons Rectangular Ingot, Carbon Bottom, 5-Inch Level.

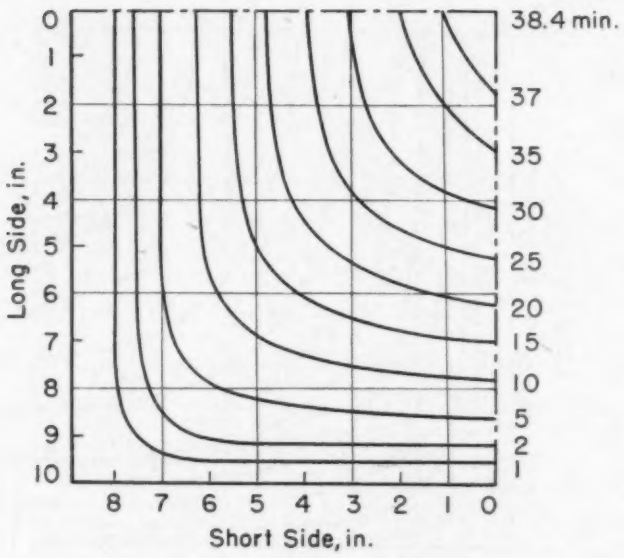


Fig. 16—Isochrons Rectangular Ingot, Carbon Bottom, 10-Inch Level.

could be applied, but this possibility was noticed only after completion of the experiments.

It is therefore to be expected that the solidification times near the bottom as shown in the charts are shorter than actual times. However, the relative magnitude of freezing times with and without carbon is still correct.

Cooling at the Midheight—Comments on this aspect are based on

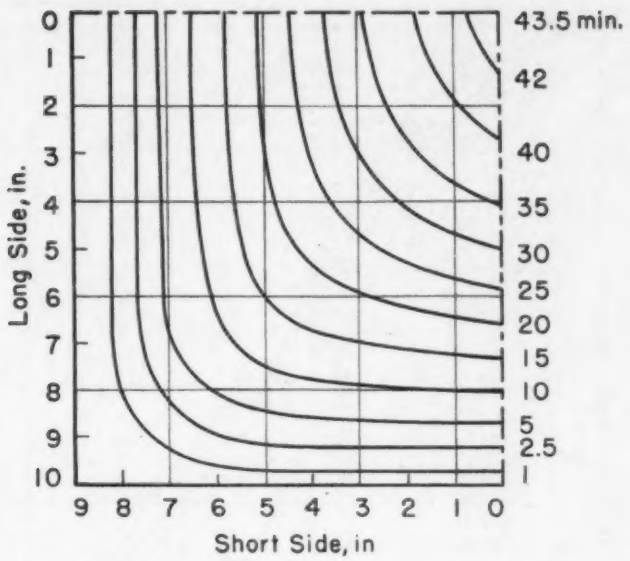


Fig. 17—Isochrons Rectangular Ingot, Carbon Bottom, 15-Inch Level.

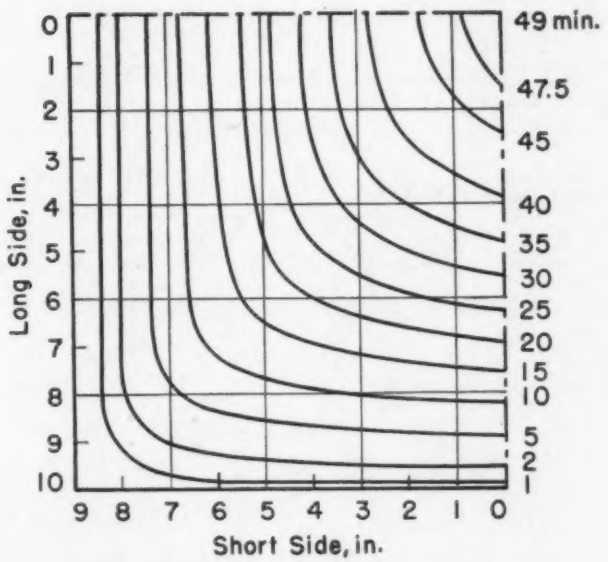


Fig. 18—Isochrons Rectangular Ingot, Carbon Bottom, 25-Inch Level.

the experimental results described before. No separate experiments were required. Complete solidification of the cylindrical ingot took 44 minutes (2700 F). The ingot mold ratio (cross sectional area of mold/cross sectional area of the ingot) at the center was 467/294 = 1.59. Compared herewith the rectangular ingot solidified in the center (2700 F) 50.3 minutes after pouring. The ingot mold ratio at this plane was 138/103 = 1.34.

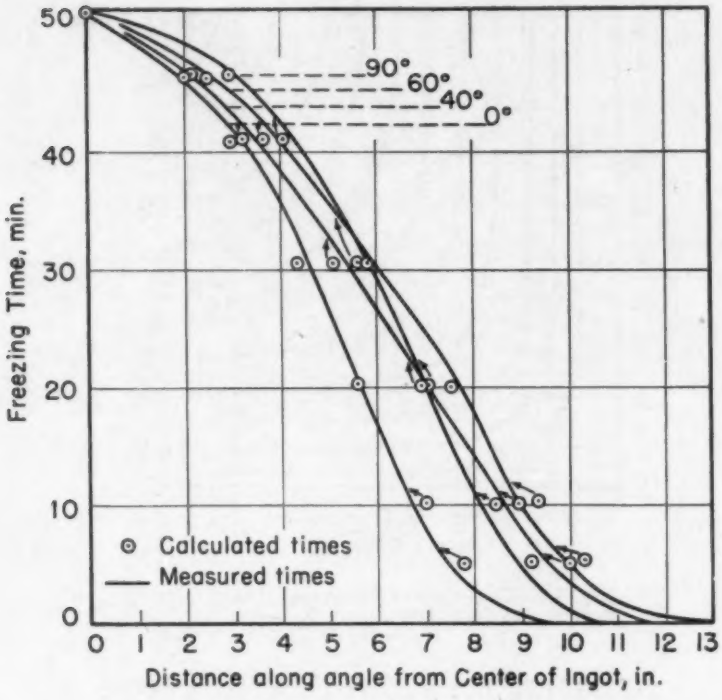


Fig. 19—Comparison of Measured and Extrapolated Solidification Times, 42.75-Inch Level.

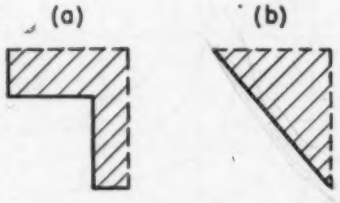


Fig. 20—Replacement of Incline by Steps—Volume and Area.

Hot Top—The isochrons (2700 F) for the hot tops are shown in Fig. 21 for the straight hot top and Fig. 22 for the inclined hot top.

As expected, the final freezing of the hot top takes place below the top surface, and in the case of the straight hot top (Fig. 21) somewhat lower than for the inclined hot top (Fig. 22) the highest isochron is for 85 minutes and embraces the 10-inch level (Fig. 21) as compared with the 7.5-inch level (Fig. 22). The complete solidification may require approximately 90 minutes. It is important to note that for both kinds of hot tops the isochrons in their lower part run parallel to the axis; with neither design is there a danger of bridging.

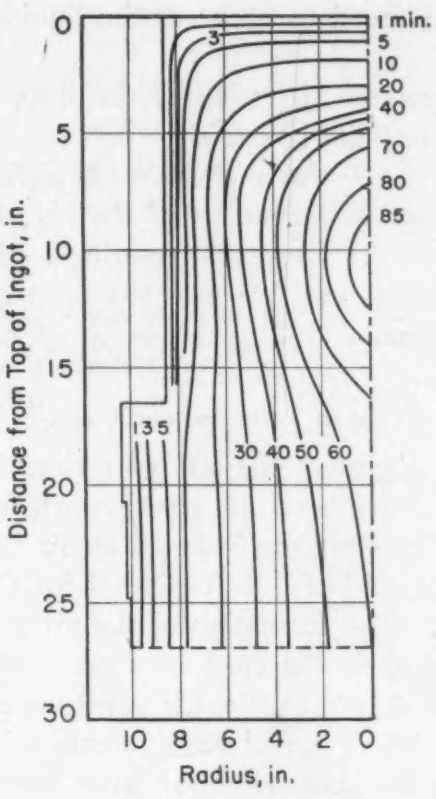


Fig. 21—Isochrons Round Ingot, Straight Hot Top.

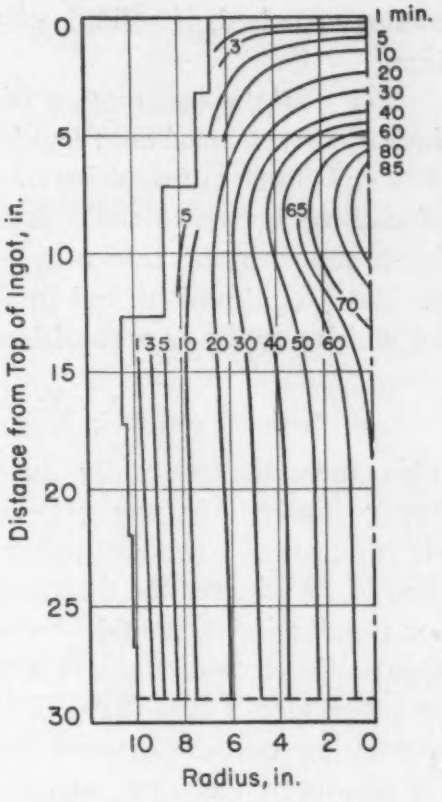


Fig. 22—Isochrons Round Ingot, Inclined Hot Top.

The 2600 F isochrons (solidus line) are entirely different in curvature. The ratio of solidification times is again approximately in the order of magnitude of 1:2.

In considering the hot top isochrons it should be kept in mind that as the steel within the mold shrinks, steel is drawn from the hot top, resulting possibly in a different shape of the top surface, which in turn might influence the cooling. In view of the limited heat losses from the surface, the error by neglecting this possible change of shape is probably small.

Further Investigation

It is believed that the study of the thermal phase of the solidification of ingots is a promising approach to the entire question of steel solidification. Among the items which should be investigated, the following seem in part controversial: (a) Is the freezing completed when the temperature of the steel reaches the liquidus line or the solidus line? The experiments carried out so far seem to prove that bleeding experiments check with heat flow studies by the electric

analogy method, if solidification is assumed to occur at the liquidus line.

(b) Is the assumption of exponential liberation of the heat of fusion correct, or should another assumption be made?

(c) Time of formation of the air gap. Work on the solidification of castings seems to show that the time of formation of the air gap increases with the thickness of the steel. For small castings, cast against a chill and backed up by sand, a tentative rule has been set up which may be expressed by the formula:

$$AT = 2.25\ L^2 \text{ sec.}$$

L= thickness of steel in inches. AT= Time of formation of air gap.

This formula apparently does not apply to the air gap time in larger ingots. In the experiments mentioned in this report, an air gap time of 2 minutes was used. Based on the formula, an air gap time of 10 minutes for the round ingot, and of 8 to 9 minutes for the rectangular ingot, would be required. The formation of the air gap apparently changes the temperature drop in the steel very markedly, and therefore it is perhaps possible to determine the air gap time by correlating the temperature-time studies in actual experiments with the results by electrical analysis. On the other side, for large ingots as considered in this report, a difference between 2 and 10 minutes would probably not be significant.

(d) The influence of superheat in the solidification time appears to be very marked in the case of castings cast against sand. Statements in literature, that superheat has no influence on solidification time when casting an ingot in a cast iron mold, appear to lack proof from a thermal viewpoint. The influence may be small but necessarily exists in order to maintain the law of conservation of energy.

(e) The question of ingot-mold ratio has not been solved satisfactorily. It is recognized that the mold thickness depends on other items besides the desired solidification time. However, the knowledge of the influence of the ingot-mold ratio on solidification time would help to make a correct decision in selecting mold size.

(f) The influence of the bottom and of various forms of hot top are also not yet solved systematically.

Acknowledgments

Thanks are due to Mr. M. P. Heisler and Mrs. George Muse for the greater part of the experimental work and help in the preparation of this paper.

Appendix I

The experimental technique applied to solidification experiments can be explained by using Figs. 23 and 24. It should be remembered that the method involves the "lumping procedure". This means that the body is thought of as divided into individual sections or lumps.

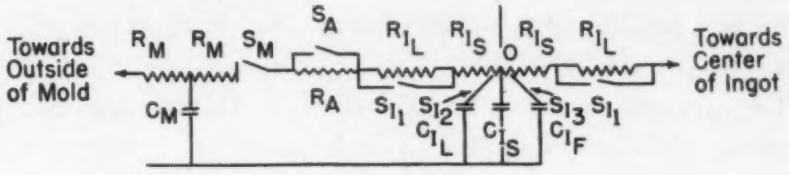


Fig. 23—Wiring Diagram—One Section.

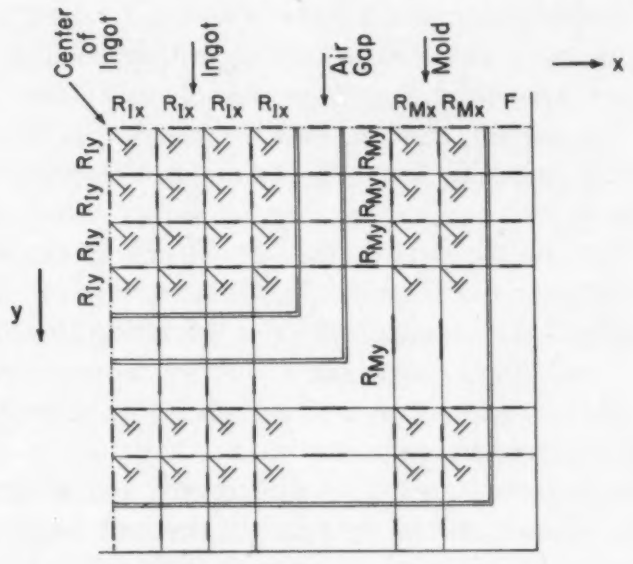


Fig. 24—Wiring Diagram—Exp. C1-1.

Fig. 21 shows an element of the circuit, comprising a section or lump of a large ingot (no end effects) next to the ingot-mold interface and an adjacent lump of the mold.

In the drawing, subscripts I are used for all elements representing the ingot, subscripts M for all elements representing the mold, and subscripts A to elements representing the air gap.

For the one ingot section four resistors are used, two marked R_{IS} and two marked R_{IL}. The former represent the resistance of the solid steel to heat flow to the left and to the right of the center of the section. As long as the steel is liquid the conductivity is lower. The resistance accordingly is higher. The additional resistances are

indicated by R_{IL}. Similarly the thermal capacitance of the section is represented by two capacitors, C_{IL} and C_{IS}, the latter representing the heat storage capacity of the solid steel, whereas C_{IL} is equivalent to the difference between liquid and solid capacity.

The capacitor C_{IF} when loaded represents the heat of solidification. Each of the resistors R_M represents one half of the thermal resistance of the mold section; and C_M the capacitance of the mold section. R_A, finally, is the equivalent of the thermal resistance of the air gap.

The procedure, now, is as follows: At the beginning of the experiment capacitors C_{IL} and C_{IS} are loaded at a voltage equivalent to the pouring temperature of the steel, capacitor C_{IF} is loaded at a voltage equivalent to the upper limit of the solidification range (solidus line) and capacitor C_M at a voltage equivalent to the preheat temperature of the mold. Switches B_1 are open, thus providing a large resistance (R_{IL} and R_{IS} in series), because the thermal conductivity of the liquid steel is low. Switch S_{I_2} is closed, thus providing for large specific heat (in liquid state). Switches S_A, S_M and S_{I_3} are open.

At the start of the experiment, switch S_M is closed, thus connecting the "ingot circuit" with the "mold circuit". The ingot is poured suddenly; i.e., the time required for filling the mold (closing the switch) is assumed to be zero. After a predetermined time (2 minutes) the air gap forms and switch S_A is opened, thus introducing the air gap resistance.

The voltage drop at point 0 is observed, and when the voltage (temperature) of point 0 has dropped to the value equivalent to the liquidus, switch S_{I_3} is closed, thus introducing the heat of fusion. The rate of voltage (temperature) drop is slowed down by this additional heat capacity. When the voltage (temperature) has dropped to the middle of the solidification range (2650 F), switches S_I are closed, thus bringing the resistance down to the value prevailing in "solid state"; and switch S_{I_2} is opened in order to bring the capacitance to the value of the solid state. These changes result in an increased rate of temperature drop. As soon as the voltage (temperature) reaches the lower limit of the solidification range, switch S_{I_3} is opened again; no additional heat comes from the solidification procedure.

The arrangement as shown in Fig. 23 is repeated in the different sections or lumps of the circuit, except that the air gap resistance R_A and the correspondent S_A switch are of course used only at the inter-

face between ingot and mold. Fig. 24 shows the circuit as used for Exp. C1-3. In the figure each section is represented only by one capacitor and two resistors (one on either side of the capacitor). In Fig. 23 are shown the additional resistors and capacitors required for representing "change of properties"; in Fig. 24 they have been left out for clarity. Subscripts x and y indicate resistors for direction x and y. Each "ingot resistor" in Fig. 24, both of the "x" and "y" type, stands for a pair, one each for solid and liquid, as explained in Fig. 23.

Appendix II

Method of Interpolation

(a) The general idea underlying the method is that the isochrons shown in Figs. 14 and 14a repeat on each level with only two modifications: first, the times assigned to each line are lower on lower levels; and second, because of the decreasing width and thickness of the ingot the geometry on each level must be slightly changed.

(b) The procedure will be explained in one example, referring to the "60-minute" curve, Fig. 14a.

The 60-minute curve intersects with the short side 3.42 inches from the center (point A). Fig. 25 shows two isochrons for the two-dimensional experiment (x-z axis) and Fig. 26 several isochrons for the two-dimensional experiment (y-z) axis. Fig. 25 reads, for a distance 3.42 inches from the center, a freezing time of 93.8 minutes on the 35-inch level. For the 15-inch level the distance is modified as explained below; the corresponding distance is 3.18 inches and for this distance Fig. 25 reads 75.6 minutes. Based on the calculations for point A the curve holding for 60 minutes on the 35-inch level would be called $\frac{75.6}{94.1} \times 60 = 48$ minutes on the 15-inch level.

The same point has the distance "zero" from the center measured on the long side.

Fig. 26 reads for the center a freezing time of 201 minutes on the 35-inch level and 137 minutes on the 15-inch level.

The fictitious chart, based on the long side, would therefore show in the place of the 60-minute curves a curve for $60 \frac{137}{201} = 40.8$ minutes.

In the further calculations the mean of 48 and $40.8 = 44.4$ minutes is introduced.

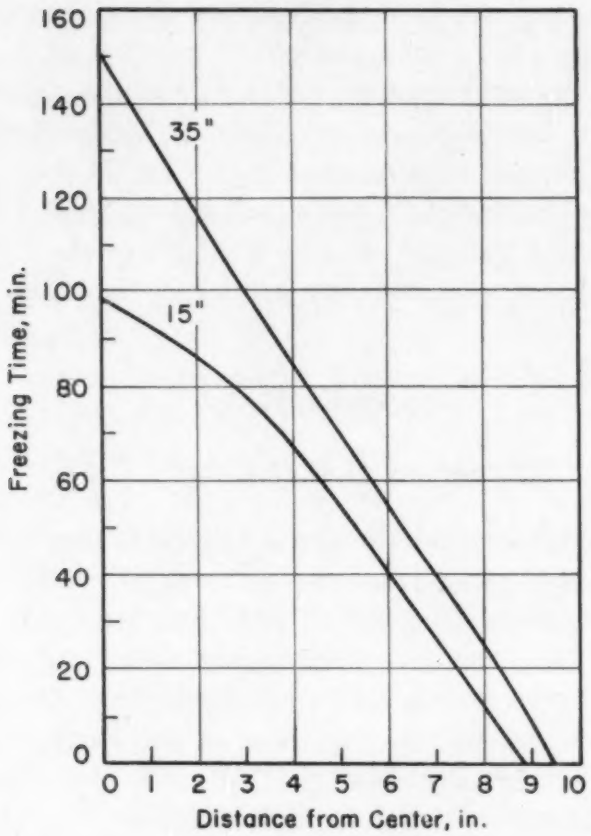


Fig. 25—Freezing Lines, End of Freeze, 2600 F, Rectangular Ingot, Mold Bottom, 35-Inch and 15-Inch Levels, Short Side, C1-2.

A similar procedure is applied to point B, located at the intersection of the "60-minute" curve (Fig. 14a), with the diagonal. On the 35-inch level the distances from the center are 2.9 inches (long side) and 2.5 inches (short side) respectively, the times are 46 and 46.2 minutes and the mean is 46.1 minutes.

Finally the same procedure is applied to the intersection of the 60-minute curve with the short side (point 6). The mean value is 44.3 minutes.

Now the average of the three times is taken: $44.4 + 46.1 + 44.3/3 = 44.9$ minutes. This is the time assigned to the new curve on the 15-inch level.

The position of the curve is found as follows: For each level all dimensions are reduced in proportion to the total length on the 35-inch level to that on the new level. This will be made clear by the example referring to the 60-minute curve mentioned above.

The short side on the 35-inch level is 9.4 inches long, on the

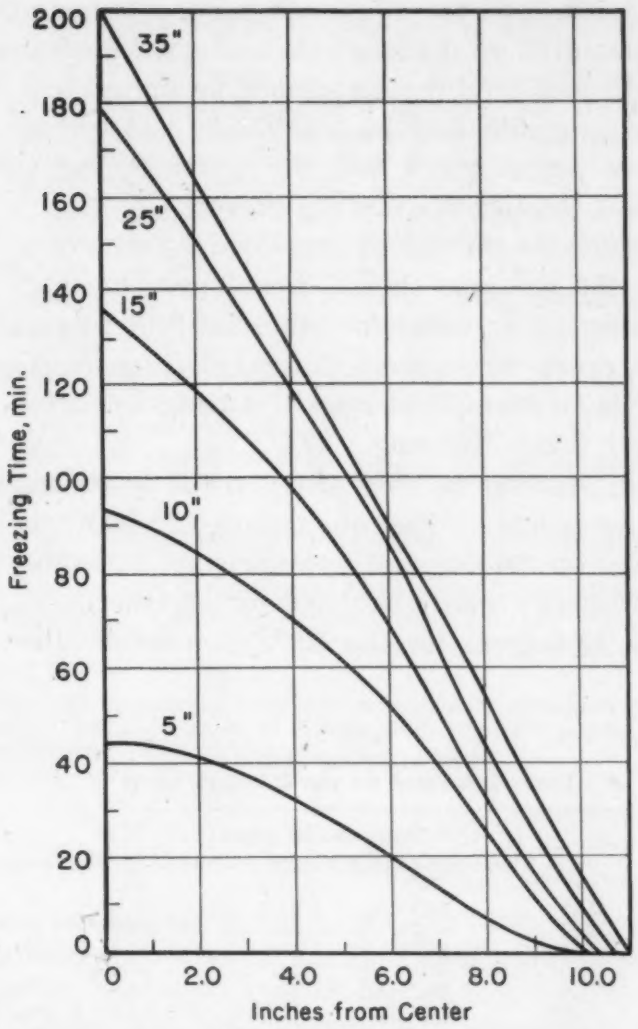


Fig. 26—Rectangular Ingot Freezing Line for Various Levels, C1-1 Long Side, Mold Bottom, End of Freeze 2600 F.

15-inch level only 8.75 inches. The correction ratio is therefore

$$8.75/9.40 = 0.931.$$

The long side on the 35-inch level is 10.90 inches long, on the 15-inch level only 10.26 inches. The correction ratio is therefore

$$10.26/10.90 = 0.941.$$

The 60-minute curve (Fig. 14a) intersects the short side at 3.44 inches, on the 35-inch level. Consequently on the 15-inch level it intersects at $3.44 \times 0.931 = 3.2$ inches.

The 60-minute curve intersects the long side at 4.6 inches on the 35-inch level. Consequently on the 15-inch level it intersects at $4.6 \times 0.941 = 4.32$ inches.

On the 35-inch level the 60-minute curve intersects the diagonal at 2.9 inches measured on the long side and at 2.5 inches on the short side. On the 15-inch level the corresponding figures are $2.9 \times 0.941 = 2.73$ for the long side, and $2.5 \times 0.931 = 2.33$ for the short side.

With three points given and the trend of the curve clearly discernible it was possible to draw the curves.

(c) The times for the curves thus obtained are not round figures but rather, as the example shows, round numbers plus a fraction (e.g., 44.9 minutes). In order to obtain the round figures shown in Figs. 10 to 18, cross curves were drawn, plotting times against distance. Fig. 25 is an example of a set of such cross curves, drawn for the 15-inch level, and of freezing (2600 F).

(d) Before starting on this procedure it was determined that taking only three points on the time curves (35-inch level), namely, on both axes and on the diagonal, is sufficient. For this purpose the times as shown in (b) were calculated for several angles, namely 0, 20, 40, 60 and 90 degrees for the 42.75-inch level. See Table VI.

Table VI
End of Freeze (2600 F)
Times Calculated for the 42.75-Inch Level

(All Times are Minutes)

Times on 35" Level	Times on 42.75-Inch Level Calculated for Following: 0°	20°	40°	60°	90°
70	72.1	72.1	72.2	72.2	72.0
60	62.3	62.2	62.5	62.3	62.0
40	41.6	41.7	41.7	41.8	41.8
30	31.3	31.6	31.7	31.7	31.9
20	21.2	21.1	21.2	21.9	22.3
10	11.08	11.49	11.05	11.9	12.17

The table shows that the values are all close together except the 10-minute value of 90 degrees which is almost 10% different from the 0 degree value. Compared with the mean value for the 10-minute curve (11.54) the maximum is 5% off, which seems acceptable.

References

1. C. Schwarz, "The Mathematical Treatment of the Cooling and Freezing Phenomena in Liquid Metal," *Archiv für das Eisenhüttenwesen,* Vol. 5, 1931, p. 139-148, 177-186.
2. S. Saito, "Distribution of Temperature in Steel Ingots During Cooling," *Science Reports,* Tohoku Imperial University, Vol. 10, 1921, p. 305-330.
3a. W. Roth, "Betrachtungen über das Erstarren von Metallblöcken," *Zeitschrift für Metallkunde,* Vol. 25, 1933, p. 134-137.
b. Dissertation, "The Cooling of Ingots in Molds, Particularly of Brass Ingots in Water Cooled Molds," Institute of Technology Aix la Chapelle, 1930.

4. A. L. Feild, "Solidification of Steel in the Ingot Mold," TRANSACTIONS, American Society for Steel Treating, Vol. 11, 1927, p. 264-276.
5. N. M. H. Lightfoot, "Effect of Latent Heat on the Solidification of Steel Ingots," *Journal,* Iron and Steel Institute, Vol. 119, 1929, p. 364-376.
6. N. M. H. Lightfoot, "Some Further Mathematical Considerations Concerning the Cooling and Freezing of Steel Ingots," Special Report No. 2, Iron and Steel Institute, 1932, p. 162-191.
7. V. M. Tageev and B. B. Gulyaev, "The Solidification of a Steel Ingot," *Metallurg,* Vol. 14, 1939, p. 23-38; Abst. in *Journal,* Iron and Steel Institute, Vol. 141, 1940, p. 235A.
8. W. H. McAdams, "Heat Transmission," 1942, McGraw-Hill, New York.
9. H. Groeber and S. Erk, "Die Grundgesetze der Waermeübertragung," 1933, J. Springer, Berlin.
10a. V. Paschkis and H. D. Baker, "A Method for Determining Unsteady-State Heat Transfer by Means of an Electrical Analogy," *Transactions,* American Society of Mechanical Engineers, Vol. 64, 1942, p. 105-112.
b. V. Paschkis, "Electrical Analogy Method for the Investigation of Transient Heat Flow Problems," *Industrial Heating,* Vol. 9, 1942, p. 1162, 1164, 1166, 1168, 1170.
11a. V. Paschkis, "Establishment of Cooling Curves of Welds by Means of Electrical Analogy," *Welding Journal,* Vol. 22, p. 462s-483s.
b. C. B. Bradley and C. E. Ernst, "Analyzing Heat Flow in Cyclic Furnace Operation," *Mechanical Engineering,* Vol. 65, 1943, p. 125-129.
c. V. Paschkis, "Studies on Solidification of Castings," *American Foundryman,* Vol. 8, Dec. 1945, p. 26-37.
d. Same as 10a.
12. J. W. Spretnak, "Kinetics of Killed Steel Ingots," TRANSACTIONS, American Society for Metals, Vol. 39, 1947, p. 569.

DISCUSSION

Written Discussion: By K. L. Fetters, special metallurgical engineer, The Youngstown Sheet and Tube Co., Youngstown, Ohio.

This paper represents a much needed contribution to the science of solidification of ingots, and although there appear to be minor differences between the curves predicted by the analog method and the experimental data they furnish a sound basis for ingot design and an explanation for some of the solidification characteristics that may be observed.

Up to the present time, ingot design has been based on a number of empirical rules and considerations, such as: size ingot desired to "cut out" to desired product multiples; size of ingot that may be heated in soaking pits; radii and general shape to minimize cracks; taper and design to minimize pipe in ingot; etc. With a thorough application of the present data and that which may be expected from additional studies that will likely be made in follow-up of this work, it should be possible to set up a sound technical basis for ingot design that would be expected to be reflected in better ingot yields and improved quality of product.

Author's Reply

The author appreciates the remarks by Dr. Fetters. He agrees with Dr. Fetters that a further investigation of the thermal behavior of ingot solidification will result ultimately in better ingots.

THE APPARENT INFLUENCE OF GRAIN SIZE ON THE HIGH TEMPERATURE PROPERTIES OF AUSTENITIC STEELS

By C. L. Clark and J. W. Freeman

Abstract

This paper presents results obtained from an investigation undertaken to determine the effect of variations in grain size on the high temperature strength characteristics of austenitic steels. Four different steels were considered and their relative high temperature properties were evaluated on the basis of short-time tensile, creep and stress-rupture tests at temperatures varying up to 1800 F (980 C).

It is shown that too broad generalizations cannot be drawn with respect to the influence of grain size variations on the high temperature properties. The 18-8 alloy behaves as would be expected in that the coarser grain structure is superior at the more elevated temperatures with the magnitude of the differences, due to grain size, being of a relatively low order of magnitude. With the three remaining steels, however, the finer grained structures were greatly inferior in their high temperature load carrying ability over certain portions of the temperature range, and this is shown to be due to the appearance of an as yet "unknown" phase. On the other hand, these finer grained steels possessed a much higher hot ductility to fracture under the more prolonged fracture times. For each of the steels the choice of the proper grain size, therefore, will depend on the proposed operating temperature and the relative importance of strength and suitable hot ductility to fracture under prolonged time periods.

WHILE the austenitic chromium-nickel steels are generally considered as being nonheat-treatable, since in the ordinary sense of the word their room temperature mechanical properties cannot be greatly varied by the usual heat treatments, their grain size can be controlled, under proper conditions. This involves cold work-

A paper presented before the Twenty-eighth Annual Convention of the Society held in Atlantic City, November 18 to 22, 1946. Of the authors, C. L. Clark is research metallurgical engineer, Steel and Tube Division, The Timken Roller Bearing Company, Canton, Ohio, and J. W. Freeman is research engineer, Department of Engineering Research, University of Michigan, Ann Arbor, Mich. Manuscript received June 1, 1946.

ing the structure, followed by recrystallization and the desired degree of grain growth at the proper temperature. Due to the pronounced strain hardening characteristics of these steels, and their high ductility in the annealed state, control of grain size by this procedure is commercially feasible.

There is at present an increasing tendency on the part of some users of the austenitic chromium-nickel seamless tubes to specify a fine grain size, one specification requiring that the grain size should be 5, or finer, on the basis of the ASTM Grain Size Classification Chart, and another, that no grains shall be coarser than 6. The desire for this finer grain size was based on service performance of 18 chromium-8 nickel rather than on laboratory data for at the time of the issuance of these specifications little if any design data were available concerning the influence of grain size on the high temperature properties of these steels. It must be recognized that, as in the case of the lower alloyed pearlitic type steels, the treatments employed to produce differences in grain size may also introduce other structural alterations and these in turn may exert a greater influence on the characteristics under consideration than the grain size variation itself. This has definitely been found to be true with certain of the austenitic steels and for this reason the influence of grain size is referred to as apparent.

Steels Investigated

Recognizing that variations in grain size, with other possible accompanying structural alterations, might not exert the same effect on the commonly used austenitic steels, four different types were investigated and each was considered in at least two different grain size conditions. In order to obtain these differences in grain size, properly cold-drawn 1-inch diameter bars of each analysis were annealed at temperatures ranging from 1700 to 2250 F (925 to 1230 C). The chemical composition, heat treatment, grain size, hardness and resulting room temperature physical properties of these steels are given in Table I.

In the given conditions of heat treatment each of the steels has very acceptable strength and ductility characteristics at room temperature and all would meet the requirements of the various specifications covering seamless tubes made from these analyses. In general, the finer grained structures (normalized) possess the higher strength

THE APPARENT INFLUENCE OF GRAIN SIZE ON THE HIGH TEMPERATURE PROPERTIES OF AUSTENITIC STEELS

By C. L. Clark and J. W. Freeman

Abstract

This paper presents results obtained from an investigation undertaken to determine the effect of variations in grain size on the high temperature strength characteristics of austenitic steels. Four different steels were considered and their relative high temperature properties were evaluated on the basis of short-time tensile, creep and stress-rupture tests at temperatures varying up to 1800 F (980 C).

It is shown that too broad generalizations cannot be drawn with respect to the influence of grain size variations on the high temperature properties. The 18-8 alloy behaves as would be expected in that the coarser grain structure is superior at the more elevated temperatures with the magnitude of the differences, due to grain size, being of a relatively low order of magnitude. With the three remaining steels, however, the finer grained structures were greatly inferior in their high temperature load carrying ability over certain portions of the temperature range, and this is shown to be due to the appearance of an as yet "unknown" phase. On the other hand, these finer grained steels possessed a much higher hot ductility to fracture under the more prolonged fracture times. For each of the steels the choice of the proper grain size, therefore, will depend on the proposed operating temperature and the relative importance of strength and suitable hot ductility to fracture under prolonged time periods.

WHILE the austenitic chromium-nickel steels are generally considered as being nonheat-treatable, since in the ordinary sense of the word their room temperature mechanical properties cannot be greatly varied by the usual heat treatments, their grain size can be controlled, under proper conditions. This involves cold work-

A paper presented before the Twenty-eighth Annual Convention of the Society held in Atlantic City, November 18 to 22, 1946. Of the authors, C. L. Clark is research metallurgical engineer, Steel and Tube Division, The Timken Roller Bearing Company, Canton, Ohio, and J. W. Freeman is research engineer, Department of Engineering Research, University of Michigan, Ann Arbor, Mich. Manuscript received June 1, 1946.

ing the structure, followed by recrystallization and the desired degree of grain growth at the proper temperature. Due to the pronounced strain hardening characteristics of these steels, and their high ductility in the annealed state, control of grain size by this procedure is commercially feasible.

There is at present an increasing tendency on the part of some users of the austenitic chromium-nickel seamless tubes to specify a fine grain size, one specification requiring that the grain size should be 5, or finer, on the basis of the ASTM Grain Size Classification Chart, and another, that no grains shall be coarser than 6. The desire for this finer grain size was based on service performance of 18 chromium-8 nickel rather than on laboratory data for at the time of the issuance of these specifications little if any design data were available concerning the influence of grain size on the high temperature properties of these steels. It must be recognized that, as in the case of the lower alloyed pearlitic type steels, the treatments employed to produce differences in grain size may also introduce other structural alterations and these in turn may exert a greater influence on the characteristics under consideration than the grain size variation itself. This has definitely been found to be true with certain of the austenitic steels and for this reason the influence of grain size is referred to as apparent.

Steels Investigated

Recognizing that variations in grain size, with other possible accompanying structural alterations, might not exert the same effect on the commonly used austenitic steels, four different types were investigated and each was considered in at least two different grain size conditions. In order to obtain these differences in grain size, properly cold-drawn 1-inch diameter bars of each analysis were annealed at temperatures ranging from 1700 to 2250 F (925 to 1230 C). The chemical composition, heat treatment, grain size, hardness and resulting room temperature physical properties of these steels are given in Table I.

In the given conditions of heat treatment each of the steels has very acceptable strength and ductility characteristics at room temperature and all would meet the requirements of the various specifications covering seamless tubes made from these analyses. In general, the finer grained structures (normalized) possess the higher strength

Table I
Composition, Heat Treatment and Room Temperature Physical Properties of Four Austenitic Steels

A. Chemical Composition

Type Steel	C	Mn	P	S	Si	Cr	Ni	Cb
18-8 (Q)	0.06	0.50	0.008	0.008	0.61	17.75	9.25	....
18-8 (N)	0.056	0.50	0.010	0.015	0.47	18.68	10.21	....
18-12 + Cb (Q)	0.07	1.68	0.013	0.014	0.55	17.78	12.70	0.88
18-12 + Cb (N)	0.08	1.72	0.011	0.008	0.58	18.25	12.93	0.88
25-20	0.11	0.58	0.009	0.010	0.75	23.60	20.65	....
25-12	0.06	1.55	0.011	0.017	0.42	24.96	13.40	....

B. Heat Treatment*, Hardness and Grain Size

Type Steel	Heat Treatment, Deg. Fahr.		Brinell Hardness	Grain Size
18-8 (Q)	Water-Quenched	2000	137	2/5
18-8 (N)	Normalized	1700	143	8+
18-12 + Cb (Q1)	Water-Quenched	1900	144	4/6
18-12 + Cb (Q2)	Water-Quenched	2250	148	2/4
18-12 + Cb (N)	Normalized	1700	163	8
25-20 (Q)	Water-Quenched	2150	143	2/4
25-20 (N)	Normalized	1700	159	8+
25-12 (Q1)	Water-Quenched	1900	183	5/7
25-12 (Q2)	Water-Quenched	2200	178	3/5

C. Room Temperature Physical Properties

Type Steel	Tensile Strength	Yield Stress 0.2% Set	Proportional Limit	Elongation in 2 In.	Reduction of Area
18-8 (Q)	85,200	27,900	12,500	61.0	74.0
18-8 (N)	87,500	33,500	15,500	54.0	75.0
18-12 + Cb (Q1)	83,350	33,500	12,500	54.0	72.5
18-12 + Cb (Q2)	81,800	32,000	12,500	54.0	73.0
18-12 + Cb (N)	91,750	41,500	22,500	46.0	66.0
25-20 (Q)	87,400	36,000	15,000	54.0	76.0
25-20 (N)	96,000	50,000	37,500	40.0	63.0
25-12 (Q1)	98,000	47,500	20,000	40.5	72.7
25-12 (Q2)	93,600	44,000	22,500	49.5	73.9

*Bars cold drawn to the desired degree before quenching or normalizing from designated temperature.

and elastic properties with the differences being the smallest with 18-8 and the greatest with 18-12 + Cb and 25-20.

Representative microstructures after each of the treatments are shown in Fig. 1. The structures shown are of completed creep specimens since the conditions of the creep tests produced an intergranular precipitation and thus permit the grains to be clearly defined. While in each of the analyses differences in grain size exist for the different treatments, the total variation is not the same for each of the steels. The 18-12 + Cb and 25-20 steels exhibit the greatest range of grain sizes and the 25-12 the least. A small amount of ferrite was present in the 25-12 alloy.

High Temperature Physical Properties—The effect of the variations in grain size on the high temperature physical properties of each of the four analyses was determined by short-time tensile, stress-rupture and creep tests over a range of temperatures of possible commercial interest.

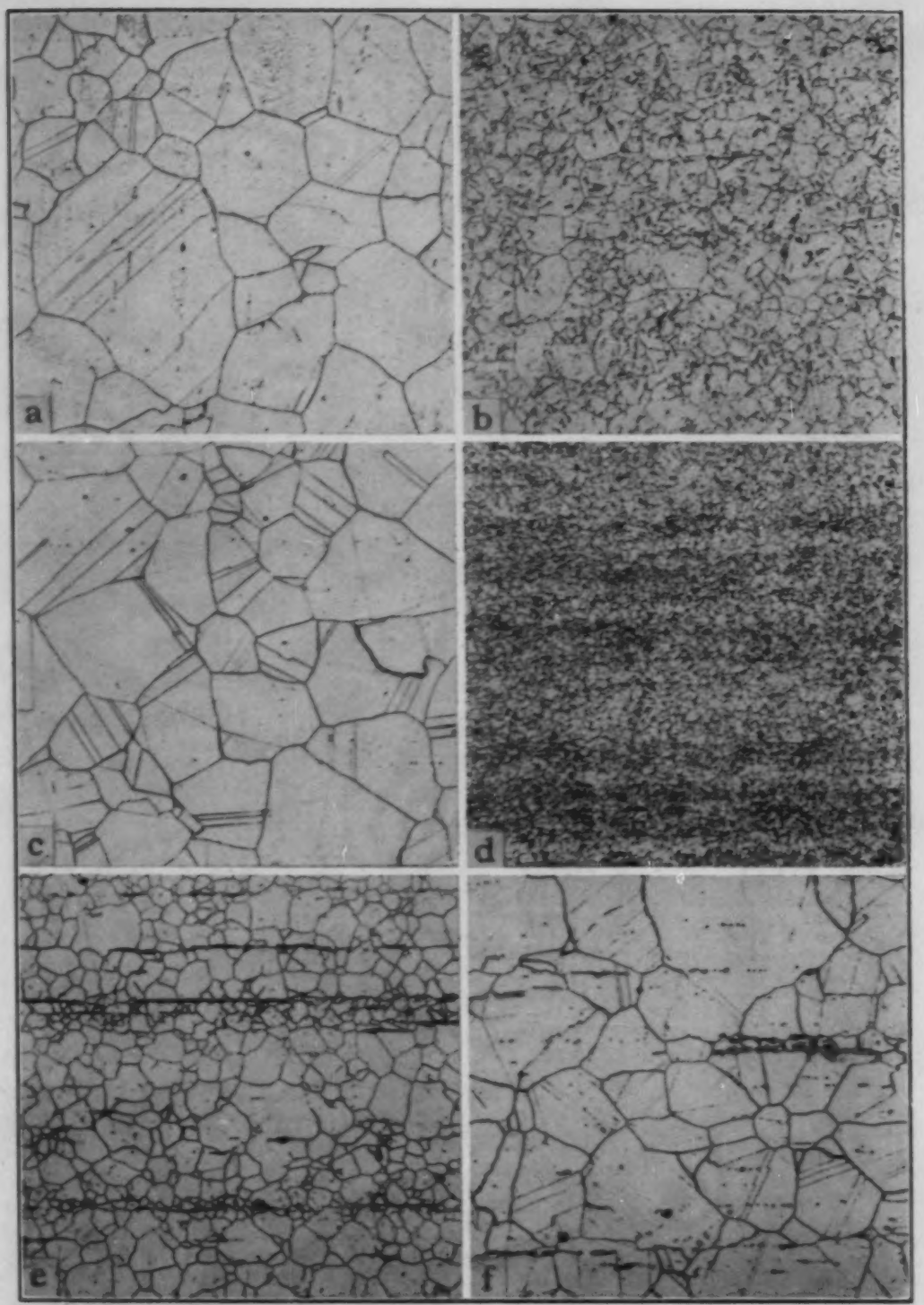


Fig. 1—Representative Microstructures Showing Grain Size of Steels Investigated; × 100. (a)—18-8(Q), water-quenched 2000 F. (b)—18-8(N), normalized 1700 F. (c)—25-20(Q), water-quenched 2150 F. (d)—25-20(N), normalized 1700 F. (e)—25-12(Q1), water-quenched 1900 F. (f)—25-12(Q2), water-quenched 2200 F.

Short-Time Tensile Properties—The apparent effect of grain size on the short-time high temperature tensile properties of 18-8,

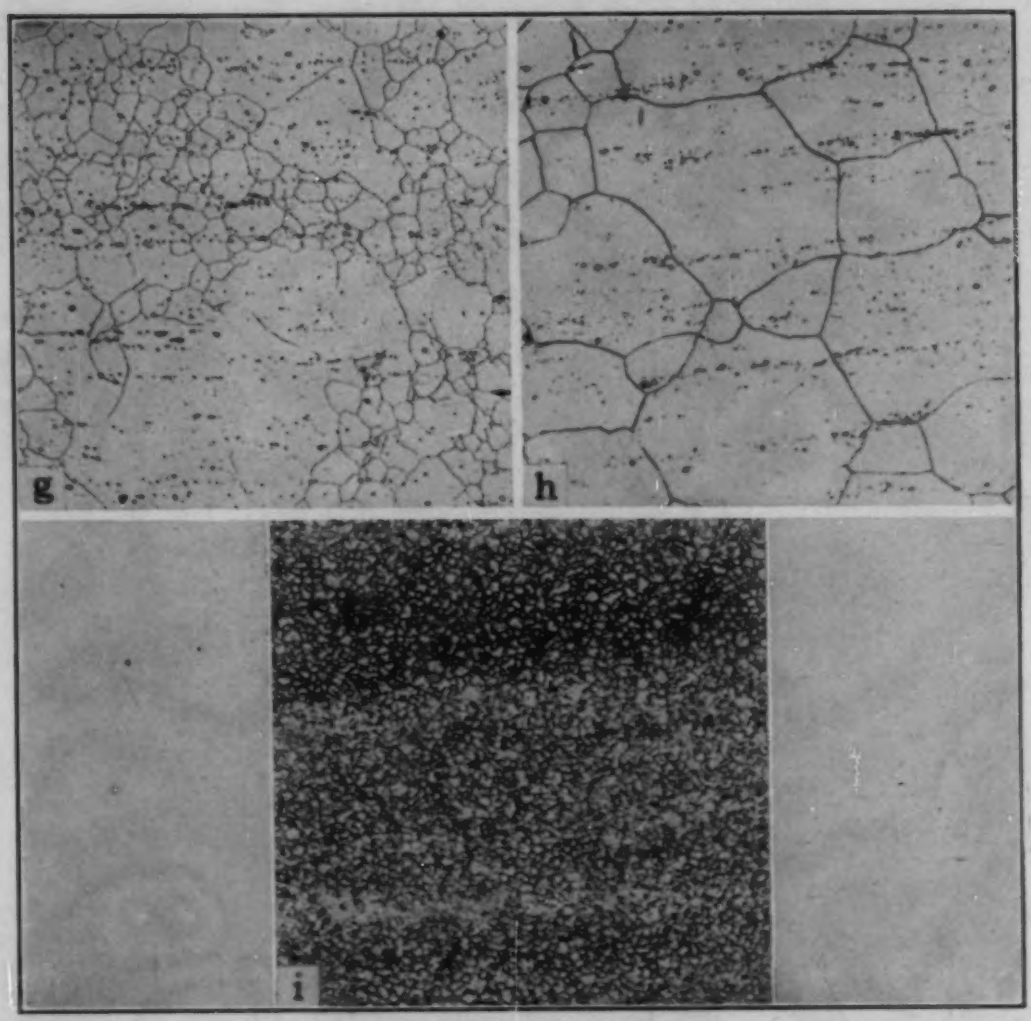


Fig. 1 (Cont.)—Representative Microstructures Showing Grain Size of Steels Investigated; × 100. (g)—18-12 + Cb (Q1), water-quenched 1900 F. (h)—18-12 + Cb (Q2), water-quenched 2250 F. (i)—18-12 + Cb (N), normalized 1700 F.

18-12 + Cb and 25-12 over the range of 1000 to 1800 F (540 to 980 C) is shown in Figs. 2, 3 and 4; with Fig. 2 giving the tensile strength properties, Fig. 3 the yield stress (0.2% set) values and Fig. 4 the elongation in 2 inches.

Insofar as the tensile strength is concerned the variations in grain size do not have the same influence on each of the four different analyses. For the temperatures considered the coarse-grained 18-8 is superior to the fine-grained at 1300 to 1500 F (705 to 815 C) while the two are equal at 1200 F (650 C). With 25-20 the coarse-grained structure is superior up to 1800 F (980 C) but the finer grained 25-12 possessed the higher strength up to 1500 F (815 C). On the other hand, with 18-12 + Cb, the coarse-grained steel is su-

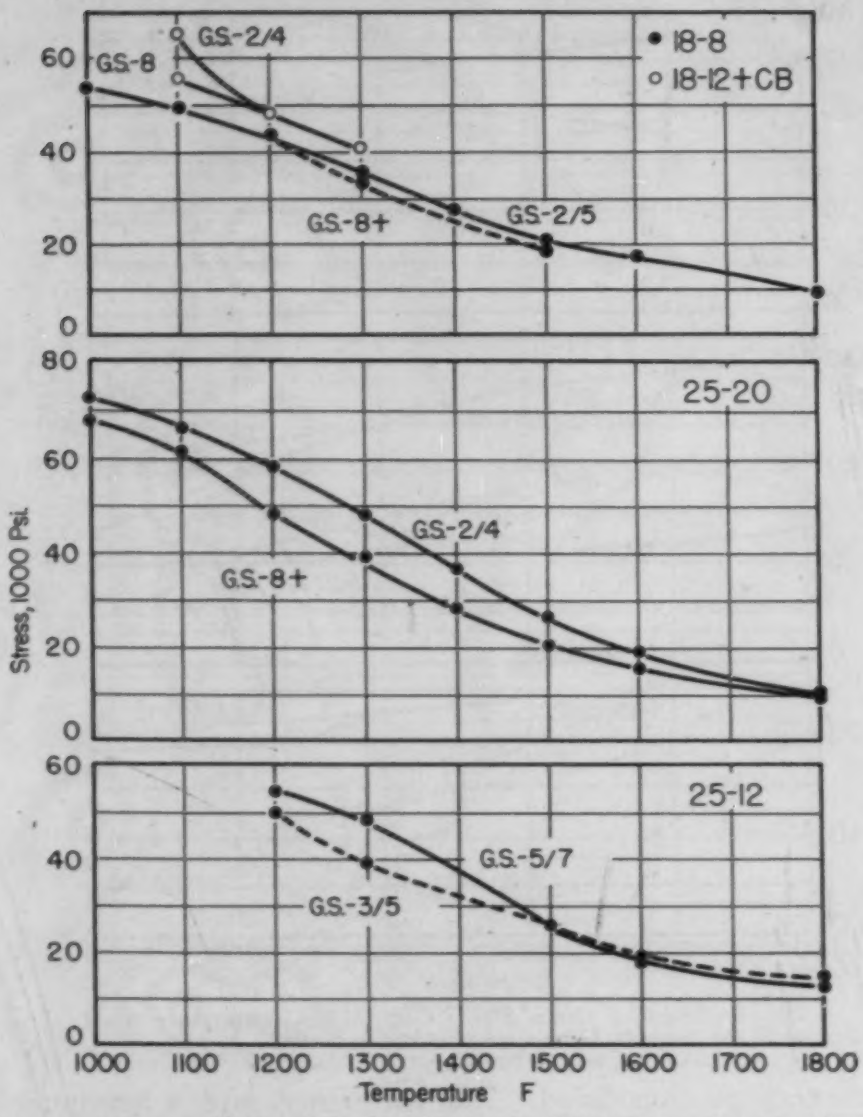


Fig. 2—Effect of Grain Size on the High Temperature Tensile Strength of Designated Austenitic Steels.

perior at 1100 F (595 C) but grain size has no influence at 1200 and 1300 F (650 and 705 C). Purely on the basis of the short-time tensile strength values the differences between the fine and coarse-grained steels are in general not of sufficient magnitude to be of much commercial interest. The only possible exceptions are 25-20 at 1000 to 1500 F (540 to 815 C) and 25-12 at 1200 and 1300 F (650 and 705 C).

The effect of apparent grain size on the yield stress values, Fig. 3. is more uniform than in the case of the tensile strength. With each of the four analyses, the fine-grained structures possess the maximum values over the complete, or at least major portion of the

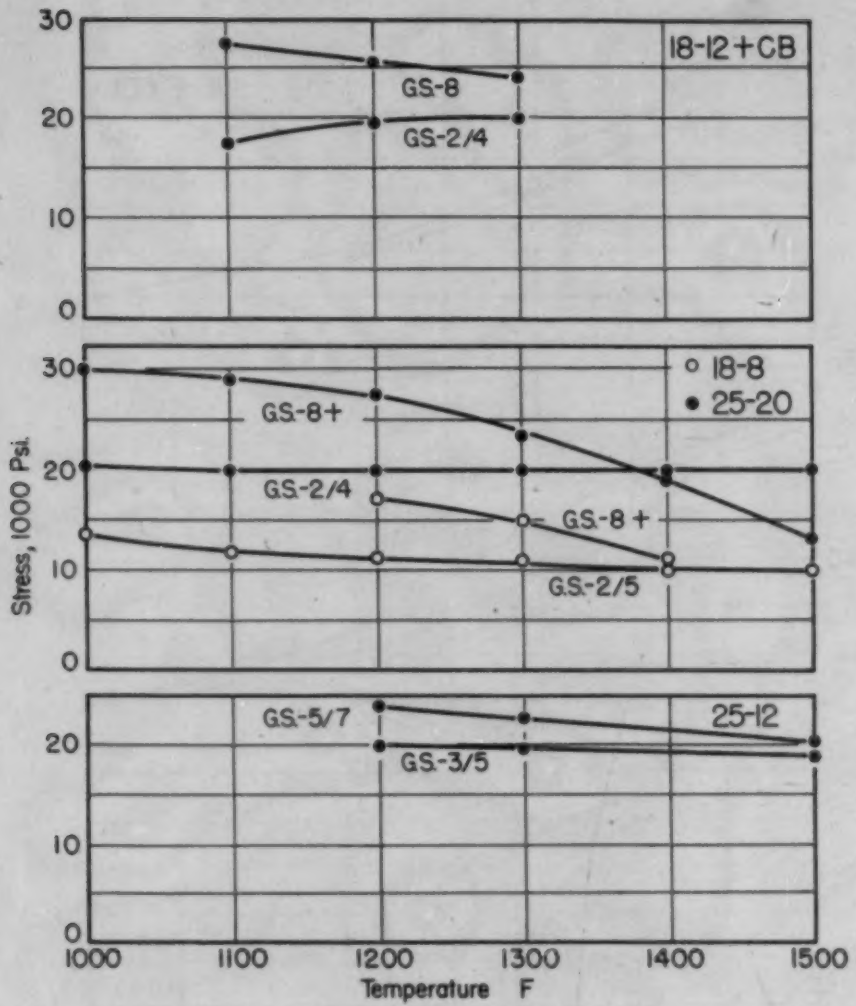


Fig. 3—Effect of Grain Size on the High Temperature Yield Stress (0.2% Set) of Designated Austenitic Steels.

temperature range considered. The differences are a maximum at the lower temperatures and are the least pronounced with the 25-12 analysis.

The elongation values, Fig. 4, are influenced to a greater degree by differences in the grain size than the other characteristics obtained from the tensile tests. At all temperatures in excess of 1100 F (595 C) the finer grained steel possesses a much higher ductility than the coarse-grained steels. In fact, the minimum elongation values obtained in the fine-grained steel was of the order of 30.0%, while with the coarse-grained steels many of the values were of the order of 10%. Only in the case of 18-8 were all of the values 30% or higher, regardless of grain size.

Therefore, on the basis of the short-time tensile properties it follows that the finer grained steels will possess the higher elastic

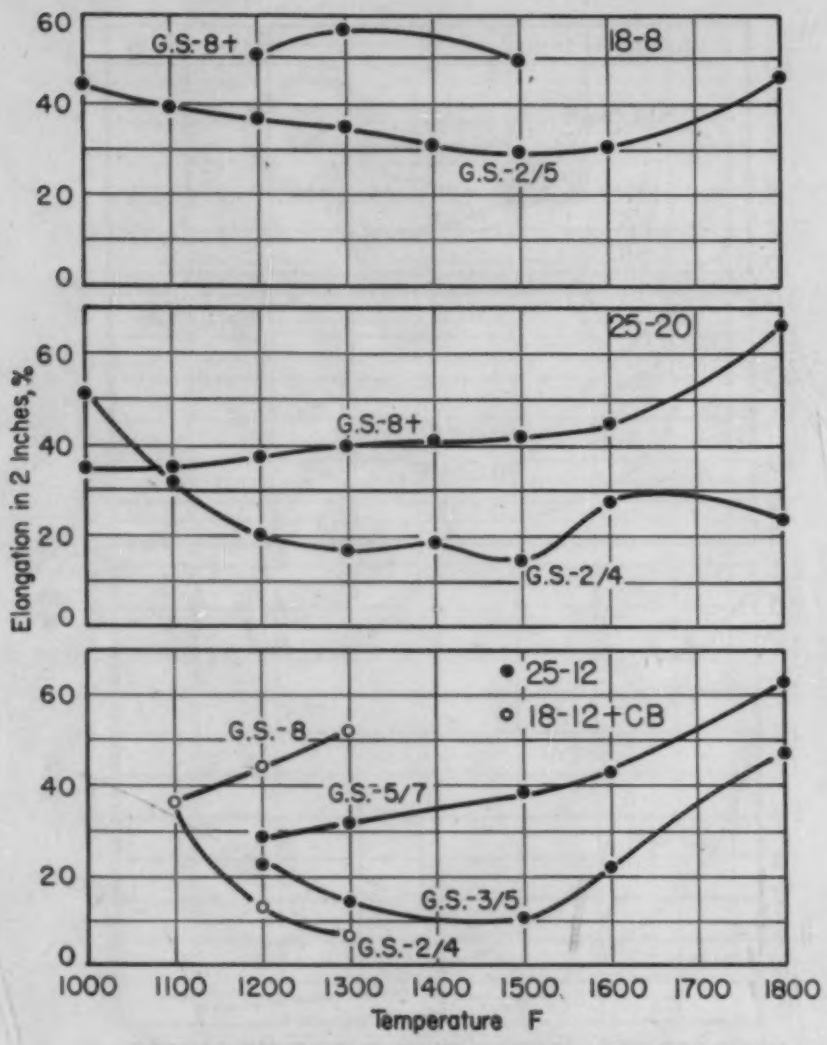


Fig. 4—Effect of Grain Size on the Short-Time High Temperature Ductility of Designated Austenitic Steels.

values and the greater ductility while in general the differences in the tensile strength values are not of sufficient magnitude to be of great importance. From this it would follow that the finer grained steels would be preferred insofar as these characteristics are concerned.

Stress-Rupture Characteristics—The results obtained from stress-rupture tests on these steels at temperatures of 1000 to 1800 F (540 to 980 C) are given in Figs. 5 and 6, with the results of the first of these figures being based on a 100,000-hour fracture time, and those of the second figure on a 10,000-hour time period. Again two different grain sizes are considered for three of the analyses, and three for 18-12 + Cb.

While variations in grain size tend to exert the same influence on the rupture strength of each of these analyses the degree of its effect

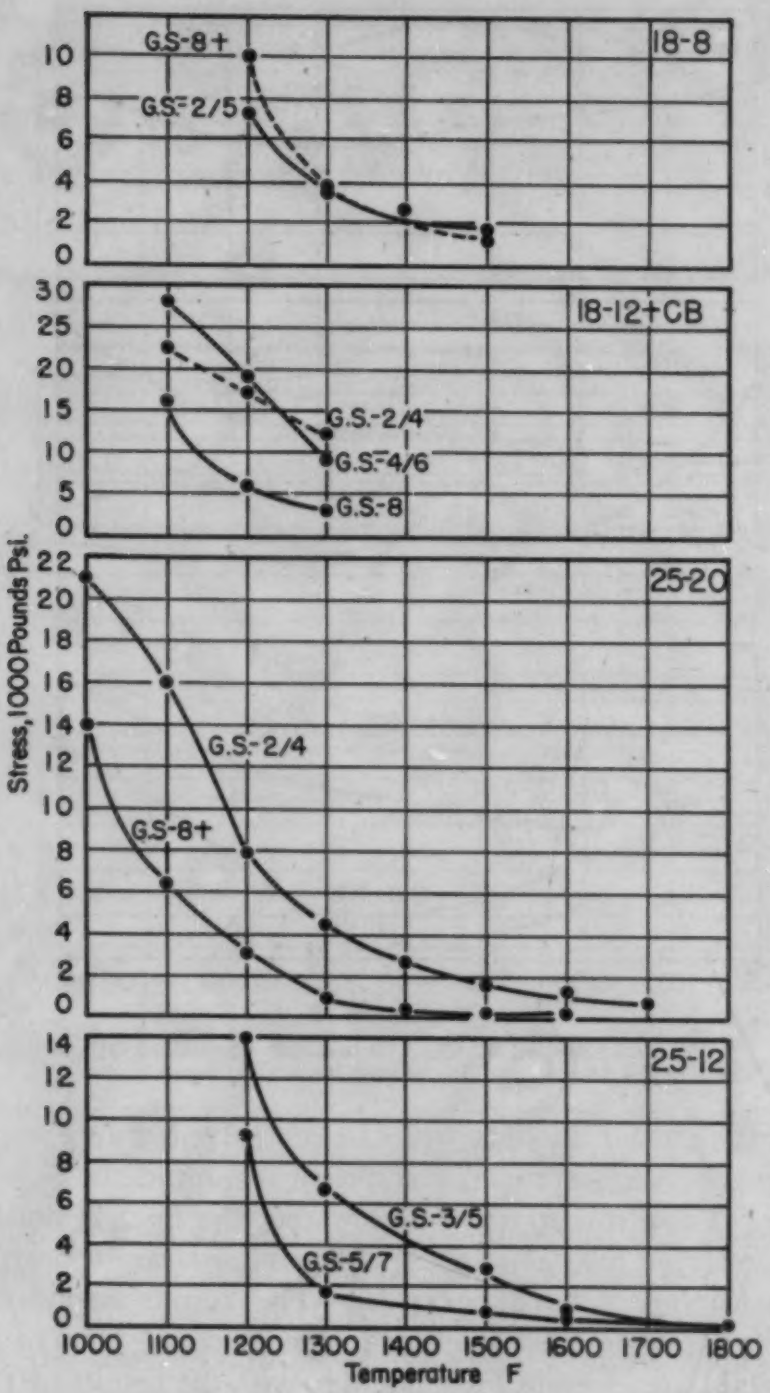


Fig. 5—Effect of Grain Size on the Rupture Strength (100,000 Hours) of Designated Austenitic Steels.

varies considerably. In the case of 18-8, the effect is not too pronounced but the finer grained structure has the greatest strength at the lower temperatures while the coarser grained steel is superior at

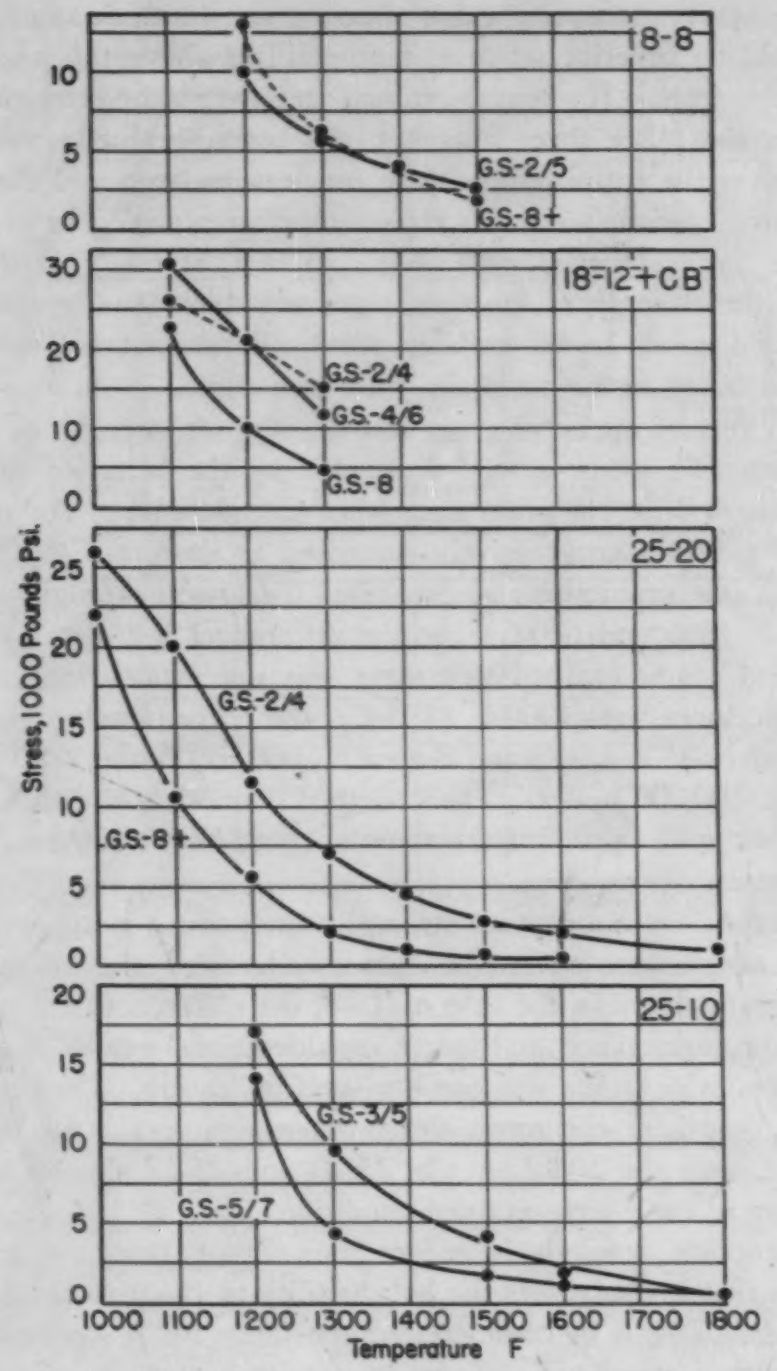


Fig. 6—Effect of Grain Size on the Rupture Strength (10,000 Hours) of Designated Austenitic Steels.

the higher temperatures. The dividing temperature is about 1350 F (730 C).

The behavior of 18-8 in this respect is typical of what should be expected on the basis of the various theories which have been advanced concerning the plastic deformation of metals. For at tem-

peratures below the equicohesive temperature the fine-grained structure should be superior while at temperatures above this apparently critical temperature the coarse-grained steel would be stronger.

With the other three analyses, the coarse-grained steels were superior over the entire temperature range considered and the differences in stress values were of a considerably greater degree of magnitude than those observed with 18-8. In fact, at many of the temperatures the strength of the coarse-grained steels was several times superior and as will be shown later, these differences are greater than can be attributed to variations in grain size alone.

The effect of apparent grain size on rupture strength of certain of the austenitic steels is well illustrated by the behavior of 18-12 + Cb. Three different grain sizes were considered and the strength at 1300 F (705 C) progressively decreased as the grain size became finer. The fine grain size also possessed the lowest strength at 1100 and 1200 F (595 and 650 C) but the differences between the intermediate and coarse-grained structures was not pronounced at these two temperatures. At 1300 F (705 C), the corresponding strengths for grain sizes of 2/4, 4/6 and 8 were 12,000, 8800 and 2800 psi for fracture in 100,000 hours. There is thus a maximum difference of over 4 times in strength for the same analysis heat treated to different grain sizes.

Therefore, from a rupture strength standpoint it is apparent that too broad conclusions cannot be drawn concerning the influence of apparent grain size. In the case of 18-8, the differences are of relatively minor importance and other considerations would determine the most desirable grain size for a given application. On the other hand, if strength at the more elevated temperatures is of primary importance, then the 18-12 + Cb, 25-20 and 25-12 should be considered only in the coarse-grained condition.

The rupture test yields information other than the rupture strength in that it also shows the hot ductility to fracture for varying time periods. This is of commercial importance for it shows the degree to which a metal will deform in service before actual fracture occurs. The ductility to fracture of these steels for a time period of approximately 1000 hours is shown in Fig. 7.

In every case the fine-grained steels have the superior ductility values, with their degree of superiority over the coarse-grained steels being especially pronounced with all of the steels except 18-8. However, even with 18-8, the coarse-grained structure possesses values as

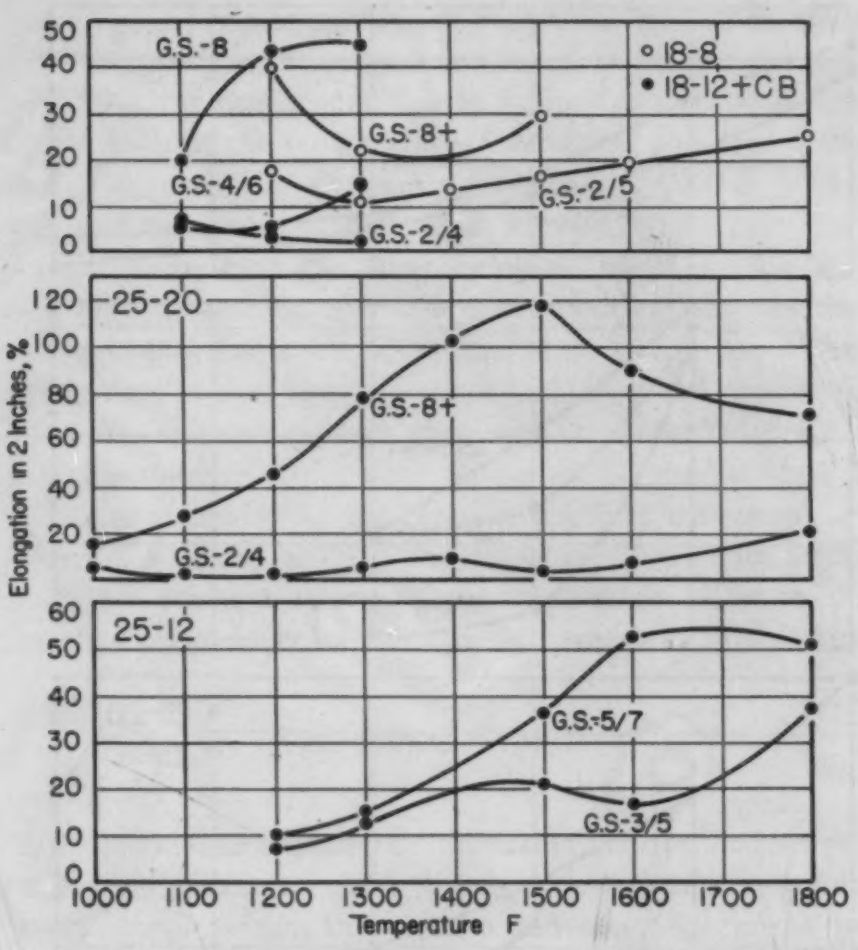


Fig. 7—Effect of Grain Size on the Hot Ductility to Fracture of Designated Austenitic Steels.

low as 11% but with the remaining three analyses certain of the elongation values are as low as 5%. The coarsest grained 18-12 + Cb steel considered not only had low ductility but was subject to premature failure under slow rates of deformation due to stress concentration brittleness in the fillets of the specimens.

From this it would follow that on the basis of hot ductility to fracture the fine-grained steels are superior but, as previously shown, a coarse grain is necessary to impart a high degree of strength. The selection of the proper grain size for these analyses will, therefore, depend on the relative importance of strength and hot ductility in any given application.

Creep Resistance—While, for most of the applications of austenitic steels at the more elevated temperatures, it is believed the stress-rupture characteristics are a more suitable basis for design than the creep strength, creep tests were also conducted on these steels at

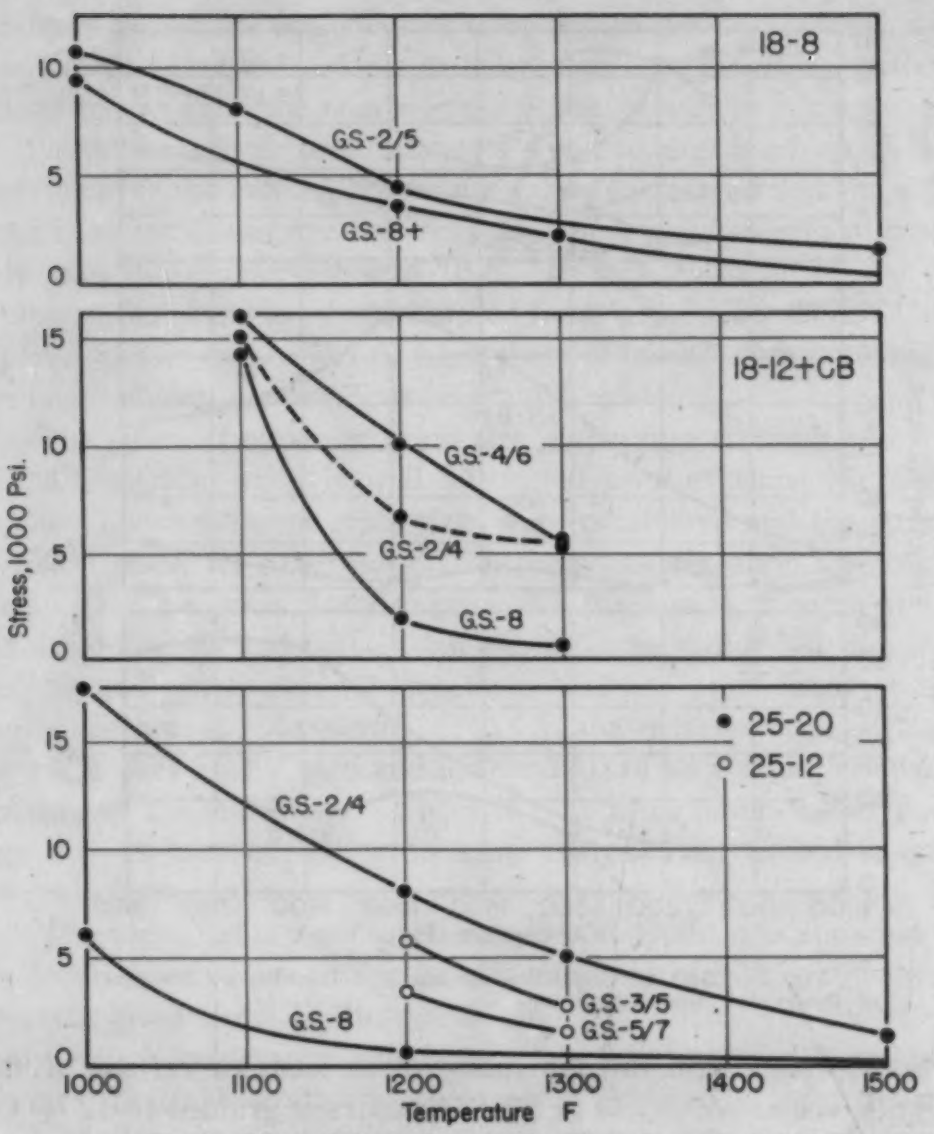


Fig. 8—Effect of Grain Size on the Creep Strength (0.01% Per 1000 Hours) of Designated Austenitic Steels.

temperatures up to 1500 F (815 C) and the results obtained are given in Fig. 8. The stresses given are those required for a creep rate of 0.01% per 1000 hours (1.0% per 100,000 hours).

As in the case of the stress-rupture characteristics, the apparent grain size has a marked influence on the creep strength with the coarse-grained steels having the higher values in every case, except with the intermediate-grained 18-12 + Cb. The magnitude of the difference, however, varies with the temperature and with the type steel, being the most pronounced with 18-12 + Cb at 1200 and 1300 F (650 and 705 C) and with 25-20 at 1000 to 1300 F (540 to 705 C) inclusive.

At certain of the temperatures with these two steels the coarse-grained structure is superior by many times to the fine-grained steels. Yet with 18-8, the differences, due to grain size variations, are fairly constant at each of the temperatures considered and are of the order of 600 to 1300 psi. For all temperatures except 1500 F (815 C) this amounts to a difference of only from 12 to 21%.

As an example of the other extreme, 18-12 + Cb at 1200 F (650 C) may be considered. The corresponding stresses for grain sizes of 2/4, 4/6 and 8 are 6500, 10,000 and 1750 psi. The maximum difference is thus nearly 6 times and, as in the case of the rupture strength, is much greater than can be accounted for by grain size variations alone.

Therefore, insofar as the creep strength is concerned, a coarse grain size is required to give the maximum resistance and should be specified if strength is of primary importance. The results from the creep and rupture tests are thus in agreement in this respect.

Structural Stability

In an attempt to explain the unusual effect of apparent grain size on the high temperature strength properties of 18-12 + Cb, 25-20 and 25-12 samples from the rupture and creep specimens were examined microscopically and certain of the completed creep specimens were subjected to room temperature tensile and impact tests.

Insofar as the structural changes were concerned, 18-12 + Cb, 25-20 and 25-12 all behaved similarly in that heating at the elevated temperatures caused a new constituent or phase to appear in the fine-grained steels but not in the coarse-grained materials. This constituent precipitates in isolated areas at first with the number and size of these particles increasing rapidly with increasing temperature. This phase etches very rapidly and while its exact identity is not known it is believed to be a carbide phase but not sigma.

This phase has not been found in 18-8, regardless of the grain size, nor in coarse-grained 18-12 + Cb, 25-20 or 25-12. All of these steels do, however, undergo structural alterations in that carbide precipitation occurs in the grain boundaries. It is the appearance of this carbide intergranular network, or structural changes which precede or accompany this precipitation, which is believed to account for the decreased hot ductility of the coarse-grained steels. When the so-

called unknown phase appears this intergranular precipitation either does not occur or is not as pronounced.

The appearance and characteristics of the structural changes which occurred in the fine and coarse-grained 18-12 + Cb, 25-20 and 25-12 are illustrated by the microstructures of Fig. 9 which, while they are for the 25-20, are also representative of the other two steels. Likewise, the structural alterations of the coarse-grained 25-20 are typical of those for both the fine and coarse-grained 18-8.

The appearance of the "unknown" phase is believed to account for the marked decrease in the strength of the fine-grained steel. This is substantiated by the fact that, (1) pronounced differences, due to apparent grain size, exist only at those temperatures at which this phase appears, (2) the differences in the strength of the fine and coarse-grained steels become greater as the amount of this phase increases, and (3) 18-8, which does not develop this phase, behaves according to accepted theories with respect to the influence of grain size on the creep and rupture strength.

In order to determine the effect of the appearance of this "unknown" phase on room temperature physical properties, tensile and impact tests were conducted on the completed creep specimens. The changes, due to the conditions of the creep tests, were of the same type and order of magnitude for 18-12 + Cb, 25-20 and 25-12 and consequently only the results for 25-20 are summarized in Table II.

The conditions of the creep tests at temperatures up to 1500 F (815 C) had little influence on the room temperature strength characteristics of the fine-grained steels but they did tend to increase those of the coarse-grained steels. With both grain sizes the room temperature ductility characteristics decreased with the degree of decrease tending to increase with increasing temperatures of the creep test. The magnitude of the changes in the ductility values are of the same order of magnitude for both the coarse and fine-grained structures and thus it would follow that the appearance of the "unknown" phase has little if any influence on this decreased ductility.

However, the results from the modified Izod impact tests on the completed creep specimens do indicate the finer grained steels to have undergone a greater degree of decrease and consequently the appearance of the unknown phase may be a contributing factor in this respect. This is substantiated by the corresponding results obtained on 18-8, Table III, which show the decrease in the room temperature impact resistance, due to the conditions of the creep tests, to be of the

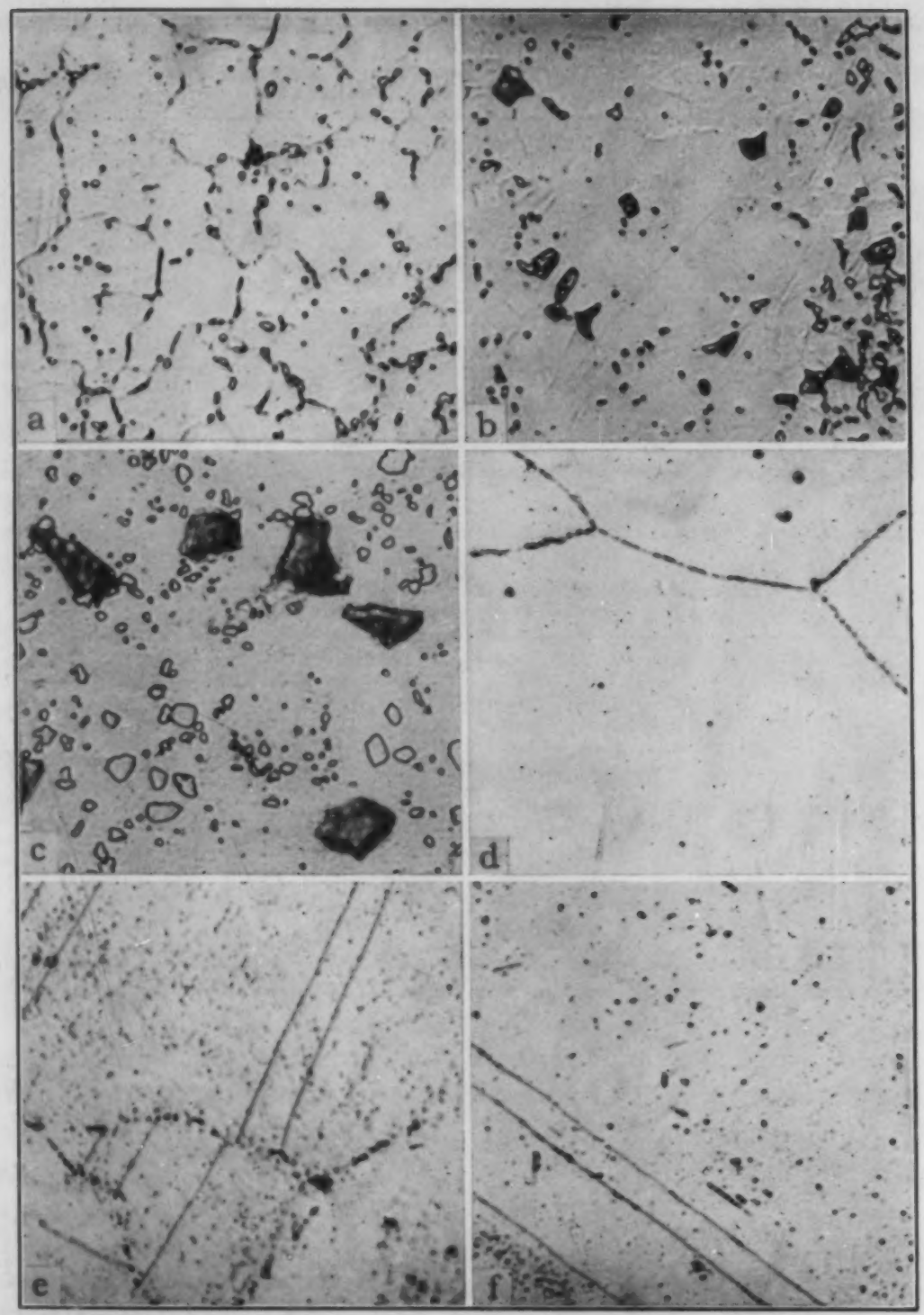


Fig. 9—Typical Microstructures of Fine-Grained and Coarse-Grained 25-20 Steels After Creep Testing; × 1000. (a)—25-20(N) after 1200 hours at 1000 F under 10,000 psi. (b)—25-20(N) after 1480 hours at 1200 F under 5000 psi. (c)—25-20(N) after 1070 hours at 1500 F under 780 psi. (d)—25-20(Q) after 1055 hours at 1000 F under 25,000 psi. (e)—25-20(Q) after 1080 hours at 1200 F under 17,500 psi. (f)—25-20(Q) after 1005 hours at 1500 F under 1750 psi.

Table II
Effect of Creep Test Conditions on the Room Temperature Physical Properties of 25 Cr-20 Ni Steel

Creep Test Temperature	Tensile Strength	Yield Stress 0.2%	Proportional Limit	Elongation in 2 In., %	Reduction of Area, %	Izod* Impact
		Fine Grain Size				
Original	96,000	50,000	37,500	40	63	79
1000	96,500	49,000	27,500	37	62	72
1200	94,000	46,000	27,500	33	48	35
1300	95,000	47,000	30,000	29	39	25
1500	95,000	49,000	30,000	30	40	24
		Coarse Grain Size				
Original	87,400	36,000	10,000	54	76	100
1000	92,750	43,500	27,000	49	69	97
1200	101,750	55,500	32,500	31	47	62
1300	100,000	50,000	30,000	30	44	62
1500	93,350	38,000	10,000	37.5	55	62

*Impact Specimens Smaller than Standard: 0.365 In. Sq. with 0.050-In. V-notch.

Table III
Effect of Creep Test Conditions on the Room Temperature Physical Properties of 18-8 Steel

Creep Test Temperature	Tensile Strength	Yield Stress 0.2%	Proportional Limit	Elongation in 2 In., %	Reduction of Area, %	Izod* Impact
		Fine Grain Size				
Original	88,100	33,500	15,000	57	74	100
1000	91,000	34,500	15,000	52	72	98
1200	90,000	32,000	16,500	53	70	86
1300	88,000	31,500	15,000	53	70	89
1500	89,750	33,000	19,000	52	71	80
		Coarse Grain Size				
Original	82,500	30,500	12,000	61	74	92
1000	85,500	29,000	15,000	67	76	91
1100	92,500	27,500	15,000	65	70	91
1200	89,000	27,500	12,500	60	69	91
1500	92,500	25,000	12,000	60	66	84

*Impact Specimens Smaller than Standard: 0.365 In. Sq. with 0.050-In. V-notch.

same order of magnitude for both of the grain sizes considered. As has previously been shown, this "unknown" phase does not appear in 18-8, regardless of the grain size.

Nature of the Unknown Phase

The exact nature of the phase or constituent which forms in fine-grained 18-12 + Cb, 25-20 and 25-12 at the higher temperatures has not as yet been ascertained. While some believe that it may be a complex carbide, or carbide plus nitride, the large amount appearing in 18-12 + Cb under certain conditions would indicate that it is not a carbide, or carbide-rich area, since theoretically the carbon is

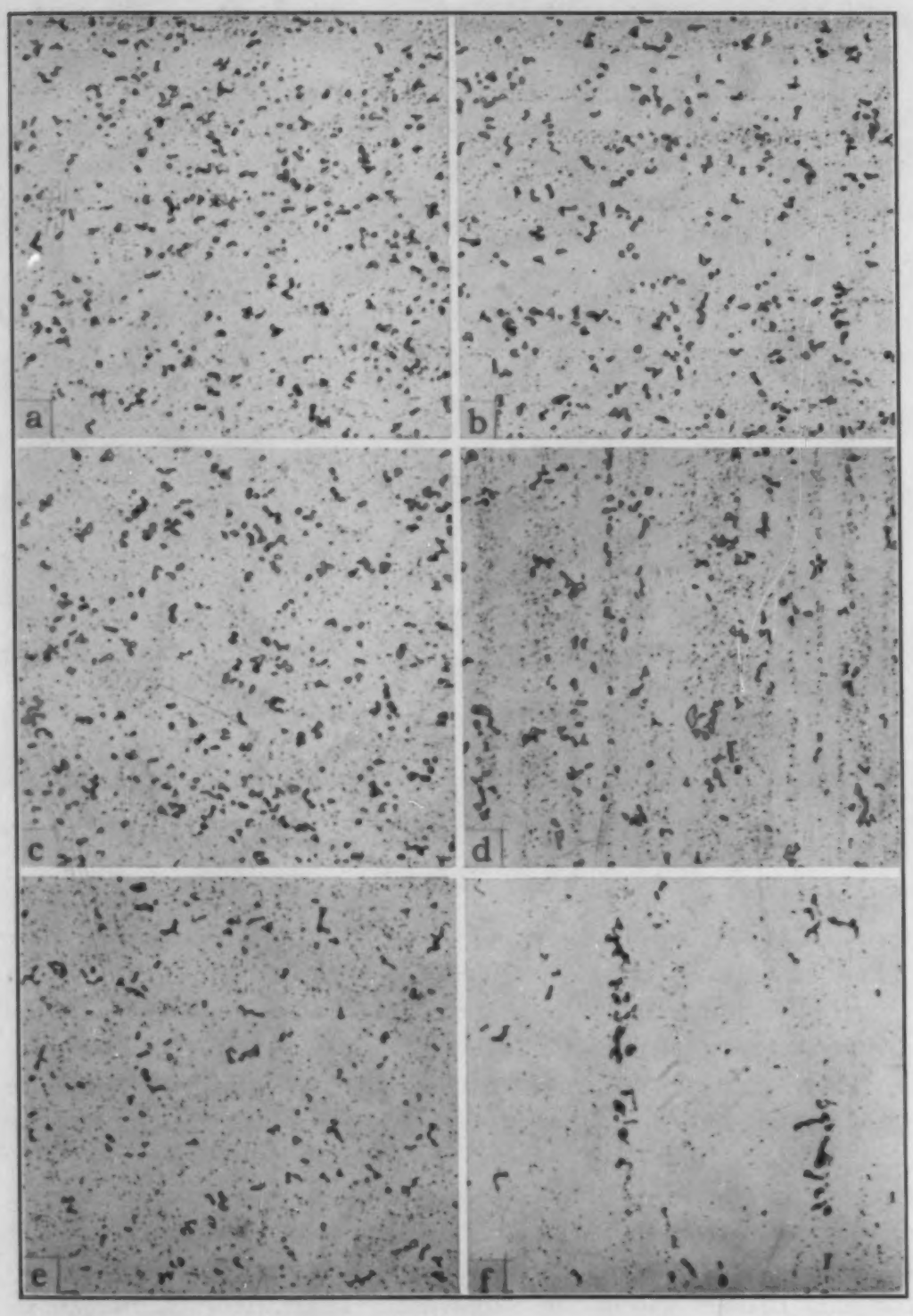


Fig. 10—Amount of Unknown Constituent Formed in 25-20 Steel in 1300 Hours at 1500 F After Heating 1 Hour at Indicated Temperatures and Air Cooling; × 100. (a)—1650 F. (b)—1750 F. (c)—1800 F. (d)—1900 F. (e)—1950 F. (f)—2000 F.

removed from solution prior to testing by being combined with the columbium. On the other hand, it cannot be a direct function of the

columbium content for it forms just as readily in fine-grained 25-20 and 25-12.

In order to obtain further information with respect to the characteristics of this constituent a series of heating tests were undertaken to determine the effect of time and temperature on its appearance. In one series of tests originally cold-worked specimens of 25-20 were heated to temperatures ranging from 1650 to 2150 F (900 to 1175 C), inclusive, held 1 hour, and air-cooled. In another

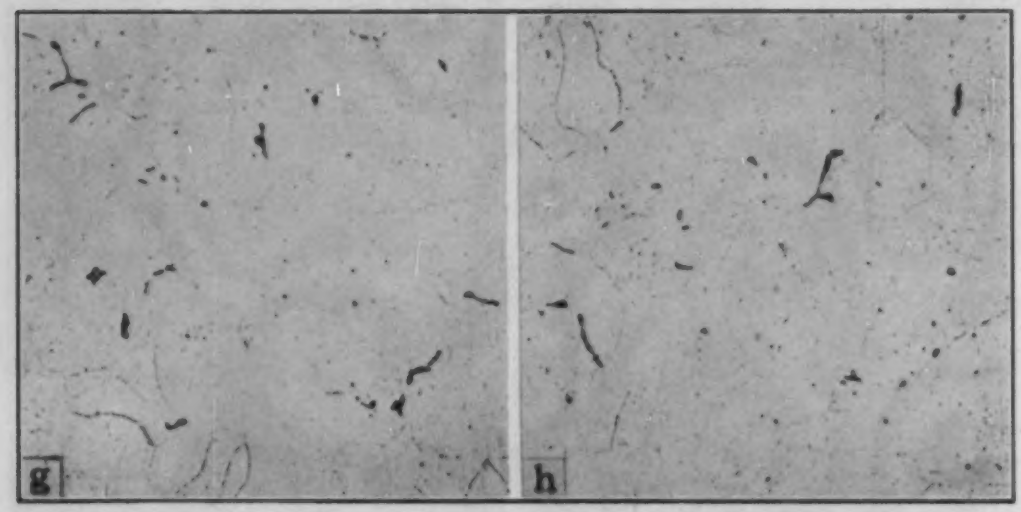


Fig. 10 (Continued)—Amount of Unknown Constituent Formed in 25-20 Steel in 1300 Hours at 1500 F After Heating 1 Hour at Indicated Temperatures and Air Cooling. (g) 2100 F. (h) 2150 F.

series of tests, specimens originally cold-worked and air-cooled after 1 hour at 1700 F (925 C) were held for varying time periods at a range of temperatures. Representative results are shown in the microstructures of Figs. 10 and 11.

The results of the tests in which the normalizing temperature was the variable, Fig. 10, indicate that with 25-20 a treatment of at least 2150 F (1175 C) is required to prevent its appearance. This temperature, likewise, results in a coarse grain size and on the basis of the results from the creep and rupture tests on coarse-grained 25-20, it is evident that this constituent does not reappear when heated for long periods within the temperature range of 1000 to 1800 F (540 to 980 C).

These facts suggest the following possibilities as to the structural stability differences between fine and coarse-grained 18-12 + Cb, 25-20 and 25-12:

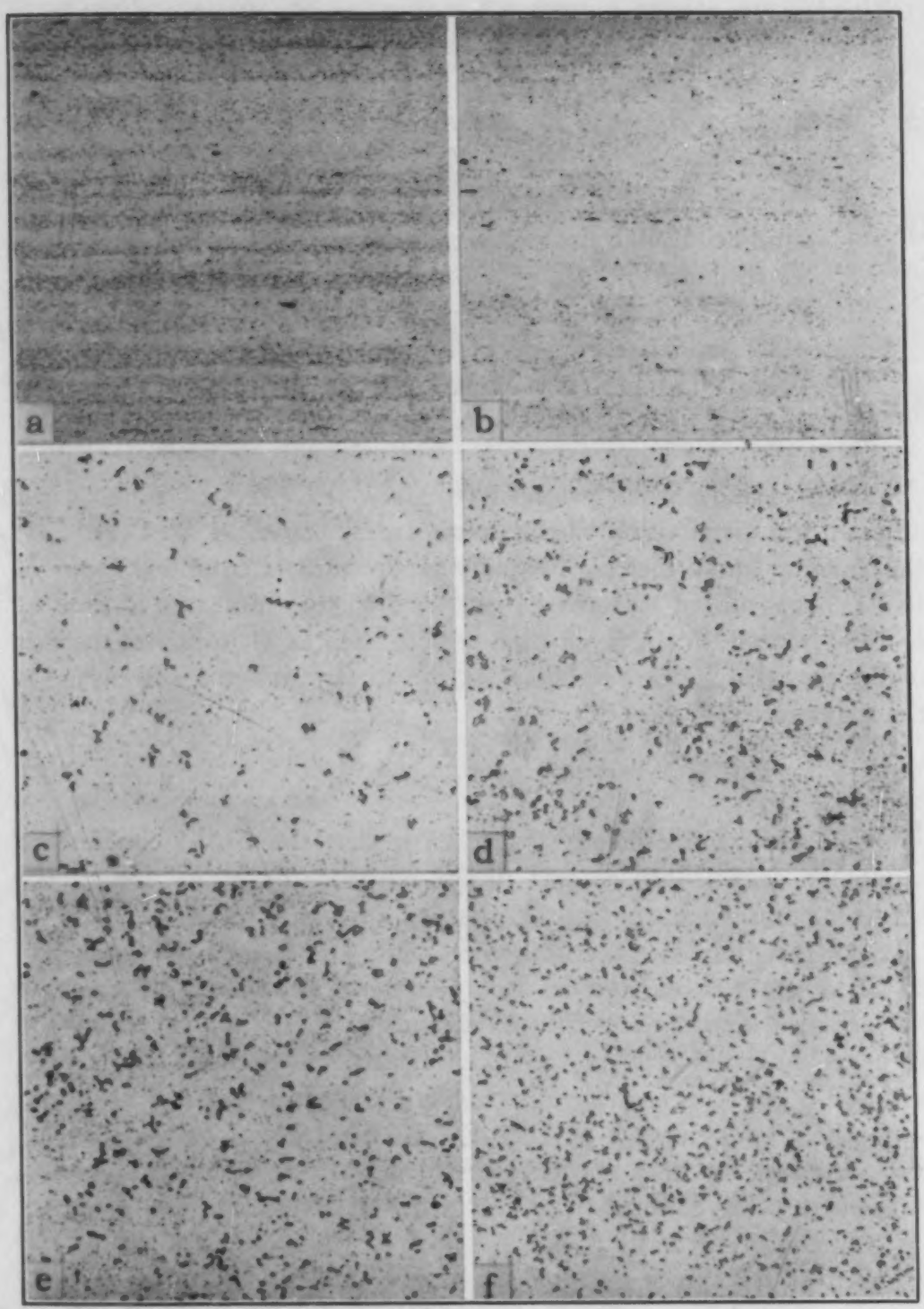


Fig. 11—Effect of Time and Temperature on the Amount of Unknown Constituent Formed in 25-20 Steel Originally Air-Cooled After 1 Hour at 1700 F; × 100. (a)—original. (b)—24 hours at 1500 F. (c)—100 hours at 1500 F. (d)—500 hours at 1500 F. (e)—1300 hours at 1500 F. (f)—1300 hours at 1300 F.

1. This constituent may exist, regardless of grain size, but to be distributed differently, as for example, in the grain boundaries of the coarse-grained steels. The low ductility of these coarse-grained steels in the rupture tests may be due to this cause.
2. High temperature annealing treatments may change the phase equilibrium in a manner which prevents the formation of this constituent.
3. High temperature annealing treatments may destroy nuclei which have been set up by the hot or cold deformation.
4. There is a possibility that the stability of the fully annealed coarse-grained steel is much greater due to the sluggishness of the reactions.

Fig. 11 is included primarily to show the effect of time on the amount and distribution of the unknown phase. At 1500 F (815 C) the amount found increases rapidly as the time is extended from 24 to 100 hours and at a decreased rate with further increases in time up to 1300 hours. For a given time period, such as 1300 hours, the size of the particles appears to be a function of temperature, increasing as the temperature is raised.

Conclusions

The results presented clearly show that too broad conclusions cannot be drawn with respect to the influence of grain size on the high temperature strength properties of austenitic steels.

Of the four steels considered, 18-8, 18-12 + Cb, 25-20 and 25-12, only 18-8 behaved in accordance with the accepted theories concerning the high temperature behavior of steels and especially the influence of grain size on these characteristics. This is true, since with 18-8 the coarse-grained structure possesses the higher creep strength at temperatures of 1000 F (540 C) and above, and the superior rupture strength at the higher temperatures, but with all of the differences being of a relatively low order of magnitude.

On the other hand with the 18-12 + Cb, 25-20 and 25-12 the strength of the coarse-grained steels at certain of the temperatures, at least, is very many times stronger than that of the fine-grained steels due to the extreme low strength of the fine-grained structure. It has further been shown that the low strength of these fine-grained steels is due to the appearance of a constituent whose identity has not yet been completely established.

On the basis of these results, the most desirable grain size for any given application will depend on the proposed operating conditions and the relative importance of strength and ductility. In the case of 18-8, even though the coarse grain structure produces the slightly higher creep and rupture strength, other considerations might justify the use of a fine grain size even when strength is of importance.

However, with 18-12 + Cb, 25-20 and 25-12, a coarse grain size should be specified if strength is of primary importance but, if good hot ductility is required, then a fine grain size should be used.

As more information is acquired with respect to the characteristics and nature of the as yet unknown phase it may be possible to so adjust the analysis and treatment of 18-12 + Cb, 25-20 and 25-12 to assure a more suitable combination of strength and ductility at elevated temperatures.

DISCUSSION

Written Discussion: By G. W. Watts, director of engineering, Standard Oil Co., Chicago.

Austenitic 18-8 and other stainless alloy steels are used extensively in refineries for tubing, flanges, valves, vessel linings, vessels, headers, furnace castings, etc., where heat resistance is a principal or major consideration. Although these steels are among the best, and in many cases actually are the best, commercial heat resistant alloys for the high temperature range of refinery operations, failures of such materials are experienced occasionally, and these failures are often difficult to explain in the light of existing theories. The authors of this paper are to be commended for the work they have done and are doing in advancing the metallurgy of such heat resistant alloys. Their present paper brings out facts which are important to an ultimate understanding of the behavior of the austenitic alloy steels in high temperature service. In this connection perhaps it would be instructive to consider briefly the failure of a number of cast 18-8 columbium-stabilized alloy steel gate valves.

These valves were used in our refinery in an application where the temperature oscillated between 600 and 1050 F (315 and 565 C). The atmosphere in contact with the valves consisted approximately of 70% hydrogen and 30% low molecular weight hydrocarbons. These valves failed after about 8 months' service by developing circumferential as well as longitudinal network-like cracks on their interior surfaces. Microscopic examination revealed that a phase similar to the unknown phase described by the authors was present in the microstructure of the used valves as well as in the coupons originally cast with these valves. However, this phase, and the one described by the authors, may or may not be identical, and it is not known whether the condition is deleterious in certain applications. Hence there is need for much more knowl-

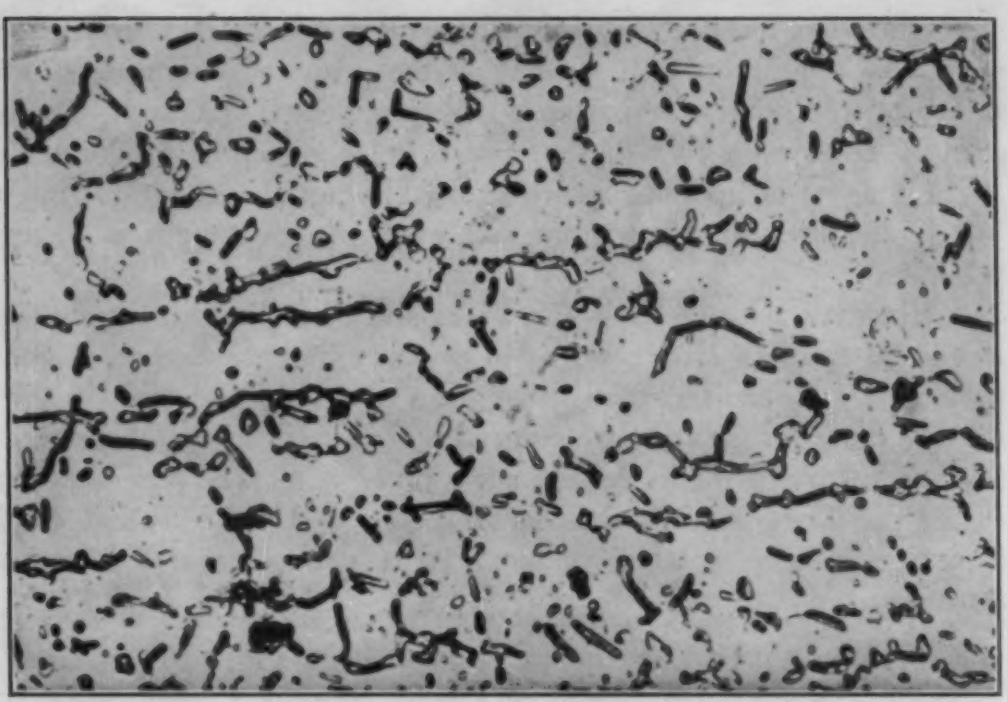


Fig. A—Microstructure of the Heat-Affected Parent Metal Adjacent to Gas Weld. Parent metal is AISI 321 steel containing 18.67% chromium, 9.60% nickel, 1.26% manganese, 0.07% carbon and 0.60% titanium. Electrolytic 10% sodium cyanide etch. × 500.

edge concerning the character of these phases, and the degree to which they influence the properties of some of our supposedly stable austenitic chromium-nickel alloys. The research conducted by the authors, and that of other investigators presenting papers at this time at the ASM Convention, appears to be definitely in the direction of supplying information which we feel certain eventually will create a better and more complete understanding of the chromium-nickel alloys.

No mention is made by the authors of the possibility that their unknown phase may be alpha ferrite. For purposes of comparison, a microstructure is shown in Fig. A which represents the heat-affected parent metal adjacent to a gas weld made by joining AISI 321 (18-8) titanium-stabilized 0.053-inch thick alloy steel sheets. The microstructure is a duplex one consisting of austenite and a phase which is believed to be high temperature ferrite (delta ferrite). Although it is recognized that the ferrite shown in Fig. A formed at a temperature of about 2400 F (1315 C) and the authors' unknown phase at lower temperatures in the 1000 to 1500 F (540 to 815 C) range, it is believed that they can be compared on the basis that they are commonly thought to be identical because of their similarity in crystalline structure and other properties.[1] It is to be noted in this connection that titanium, a vigorous ferrite former, is probably responsible for the relatively large amount of ferrite present in the Fig. A microstructure which bears some resemblance to that of Fig. 9a of the authors' paper. It is to be further noted we observed that the

[1] "The Book of Stainless Steels," American Society for Metals, Cleveland, Ohio, 1935, p. 21.

ferrite of Fig. A, like the unknown structure described by the authors, etched very rapidly, and in this connection it was found that an electrolytic sodium cyanide etch was more satisfactory than an electrolytic oxalic acid or an electrolytic chromic acid etch.

The fact that the 25-12 alloy steel used by the authors was partly ferritic before testing may indicate that this alloy, and the others that developed the unknown phase when heated in the 1000 to 1500 F (540 to 815 C) range, are in a zone where austenite and ferrite coexist, and that prolonged heating is necessary to produce a state of equilibrium. However, such a hypothesis does not account for the described structural stability differences between fine and coarse-grained steels. A very small clue to the latter, probably of little importance, was suggested by the photomicrographs of the authors' Fig. 10. Microstructures a, b, c, d and e thereof seem to indicate that the unknown phase has been precipitated generally throughout the austenite grain, showing no preference for the grain boundaries, and it is noted that this apparent mode of precipitation prevails until a heat treatment temperature of about 2000 F (1095 C) is reached. This manner in which the unknown phase is distributed in the austenite matrix of the 25-20 alloy steel when it is heat treated for 1 hour at temperatures below 2000 F (1095 C), and held 1300 hours at 1500 F (815 C), suggests a similarity to the precipitation of carbide from a cold-worked austenitic 18-8 alloy steel where instead of carbide appearing in the grain boundaries, as it would if the material were fully annealed, it is precipitated upon the slip planes, and is distributed throughout the austenite grain. The microstructure of the authors' Fig. 10f, representing heat treatment at 2000 F (1095 C), is of special interest, because the unidentified constituent does not choose now to precipitate as it did before at lower treating temperatures, but appears in bands apparently in the direction of working. This is significant since it suggests that all the nuclei or heterogeneities, that were instrumental in causing the unknown phase to precipitate in a general pattern, have disappeared, and only the very persistent inherent nuclei or heterogeneities, similar to those that are associated with the familiar banding in ordinary SAE carbon and low alloy steels, remain to nucleate the unknown phase. It is well known that banding in the low alloy SAE steels will often remain even when high temperature homogenizing treatments are used. As the treating temperature rises, further changes appear to take place, and at 2100 and 2150 F (1150 and 1175 C), the condition responsible for the unknown phase precipitating in a straight line has been destroyed, and the unknown phase is found only in the grain boundaries. The small amount of unknown phase present tends to suggest that when nuclei or heterogeneities have been removed, and when transformation is restricted to the austenite grain boundaries, the time required for beginning of transformation is greatly increased.

The preceding behavior confirms somewhat the explanation offered by the authors that high temperature annealing treatments may destroy nuclei which have been set up by hot and cold deformation. The possible relationship between cold working and the unknown structure becomes more evident when one considers the very strong influence cold working exerts on the decomposition of what are usually assumed to be stable phases. This is exem-

plified by the decomposition of some chromium-nickel austenites to ferrite when subjected to cold working at room temperature, and by the experiments of Austin and Norris[2] who showed that residual strain in certain steels is related to susceptibility to graphitization.

While the nature of the unknown phase awaits further investigations for its determination, we agree with the authors that the importance of the unknown phase may overwhelm that of the effect of grain size.

Written Discussion: By W. L. Fleischmann, Turbine Generator Engineering Division, General Electric Co., Schenectady, N. Y.

The authors have written an excellent paper showing that austenitic steels are greatly influenced in their creep and rupture behavior at high temperatures by grain size and heat treatment. In the conclusion, the statement is made that "only one steel, that is 18-8, behaved in accordance with the accepted theories concerning the high temperature behavior of steels and especially the influence of grain size on these characteristics."

The authors' interpretation of accepted theory is not stated at length in their paper and presumably it is always permissible to review the data on their own merits.

The alloy which does not follow the trend of the majority of the steels investigated here is 18-8. It behaves in contrast to the other three alloys like a solid solution alloy in which precipitation appears, perhaps to a very limited extent, in the temperature range between 1200 and 1300 F (650 and 705 C). According to Fig. 7 of the authors' paper, a drop in the high temperature ductility appears which perhaps can be explained by precipitation. At higher temperatures, rediffusion might take place. It would be interesting to learn if the authors have made Strauss tests to show what is happening in that particular temperature range.

It is a valuable contribution to prove so conclusively that the so-called columbium stabilized type 347 and the other two so-called fully austenitic steels are not so stable as it might be assumed, but that an unknown phase precipitates. The microstructures of Fig. 9 show that the precipitates in the fine-grained material are much coarser. Can one not assume that the high temperature properties in the fine-grained materials are decreased by having precipitation take place along grain boundaries while in large grains precipitation takes place along slip planes, thus strengthening the alloy? Perhaps if the authors would quote the data which show the effect of time on the fracture strain, this point could be clarified.

From a user's point of view, it would be interesting to learn if the type 347 steel can still be considered stabilized or better resistant to intergranular corrosion if the steel is exposed to corrosive media after exposure to temperatures at which the unknown phase precipitates; also, if a difference in corrosion resistance can be detected between the fine-grained, which probably is commercially the more common grain size in type 347, and the coarse-grained steel.

Written Discussion: By S. F. Urban, director of research, The Titanium Alloy Manufacturing Co., Niagara Falls, N. Y.

---

[2]C. R. Austin and B. S. Norris, "Effect of Small Amounts of Alloying Elements on Graphitization of Pure Hypereutectoid Steels," TRANSACTIONS, American Society for Metals, Vol. 30, 1942, p. 425-457.

Drs. Clark and Freeman are again to be complimented on their timely paper dealing with the effect of grain size on four commonly used austenitic-type stainless steels. Their results, though very enlightening, are a bit disconcerting in the sense that it is difficult to make up one's mind with respect to ductility and maximum strength. This is in no way a criticism but is merely an observation that is evident from the fine data.

The only real question that the writer has on this paper has to do with the basis for the reasoning that heat treatments above approximately 1900 F (1040 C) involve a water quench, whereas those below require an air quench. The writer finds this somewhat disturbing in that his knowledge of processing of such steels tells him that they are all water-quenched beyond a certain maximum section and are all air-quenched below a certain section, regardless of quenching temperature. Stated in another manner, it would be enlightening to know if the authors have any data indicating their reason for this specific choice which they have made.

Written Discussion: By Charles H. Savage, Eastern Research Laboratory, Crucible Steel Co. of America, Harrison, N. J.

We would be interested in knowing what etching reagent the authors used since it is evident from their photomicrographs that the particles of the "unknown" phase are severely attacked by this reagent, while the characteristic precipitation of carbides is not fully revealed by their etching technique. This difference in resistance to attack may serve as a clue to the identity of this "unknown" phase. In the work that we have done on heat resistant austenitic steels,[3] we have found that Vilella's and Marble's reagents are preferable to the other reagents used for the austenitic chromium-nickel steels. We have found that Vilella's reagent is more easily controlled than Marble's reagent on samples which have been reheated for comparatively long times at those elevated temperatures where carbides precipitate and sigma forms from the austenite. Chrome regia, aqua regia, aqua regia in glycerol, and 10% oxalic acid have all been found to be inferior to Vilella's and Marble's reagents because they are more difficult to control. Aqua regia is the only one of these solutions which severely attacks the massive particles of sigma phase in high-silicon types 309 and 310.

Written Discussion: By E. Gammeter, chief metallurgist, Globe Steel Tubes Co., Milwaukee.

The authors are to be congratulated on the contribution of these data on high temperature properties of austenitic steels. The emphasis on apparent influence appears very much in order as the grain size in austenitic steels is influenced by many factors and conditions whch may be more directly responsible for changes in properties than the grain size as such.

It is noted that the 18-8 studied consisted of two heats of appreciably different analyses. In the case of the 18-12 + Cb, two heats are also used although having somewhat lesser variations in analyses. This appears rather unfortunate as different heats with even very slightly different practice, particularly deoxidation practice, might easily change the resultant grain size and

[3]Peter Payson and Charles H. Savage, "Changes in Austenitic Chromium-Nickel Steels During Exposures at 1100 and 1700 F," TRANSACTIONS, American Society for Metals, Vol. 39, 1947, p. 404.

properties. It would appear that more accurate comparisons might be made if the same heats were used and the grain sizes developed by heat treatment. For this reason the differences observed may be more associated with other variables than grain size. In this respect it is noted that the properties of the 18-12 + Cb in grain sizes 2/4 and 4/6 (which represent the same heat) do not show much deviation. The heat studied as grain size of 8, which represents a different heat, shows marked deviation from both grain size conditions of the other heat.

The grain size as produced in the individual heats of 25-12 and 25-20 appear to correlate with variation in properties. This variation also appears associated with the amount of the unknown phase. The authors feel that this phase is not sigma. It would be interesting to know what methods were used that brought this conclusion as the phase does seem to have some of the characteristics of sigma. In this connection the authors do not state what etchant was used for any of the photomicrographs. It would be helpful to know this, especially in the cases where the unknown phase appears. The identification of this phase may throw considerable light on further studies of these variations in properties.

In an effort to establish identity of some phases, the writer has recently had some success by examining metallographic samples after carefully magnafluxing the sample using a liquid suspension of the powder. Evidence of partial transformation of alpha (magnetic) to sigma (nonmagnetic) was clearly shown by this method.

The writer also would like to take exception to the use of "normalized" as defining the air-cooled samples. The term, by definition, is not intended to cover the austenitic grades and has been the source of much confusion and its use should be discouraged.

The authors state the microstructure of Fig. 9 is representative of 18-12 + Cb. They also state that 18-12 + Cb undergoes structural alterations in that carbide precipitation occurs in the grain boundaries. The writer would like to ask if this has been found to any extent and especially to the amount as shown in Fig. 9d, which appears as a rather complete network. We have not encountered this extensive precipitation in 18-12 + Cb in heats adequately stabilized such as the authors used, even after 1000 hours in the sensitizing range.

The writer does not feel that the work done on this subject has been sufficiently complete and conclusive to justify the conclusion that implies commercial materials of 18-12 + Cb, 25-20 or 25-12 should be specified fine or coarse-grained, depending on the high temperature properties expected. The present paper represents a great deal of work but this is a very involved subject and little would be gained by too hasty conclusions that will involve specifications governing commercial materials.

It is hoped the authors' presentation will be supplemented with additional studies and will likewise stimulate work by other investigators.

Written Discussion: By L. V. Horne, Union Oil Company of California, Los Angeles.

The complex alloy analyses required to withstand destructive effects en-

countered in modern chemical processes have brought in their train problems of selection and application which in themselves are far from simple. Economic use of these relatively expensive materials can only be fully realized when their respective reactions to different operating environments are known, and unfortunately such knowledge is too often confined to the metallurgist rather than shared, as it should be, by the prospective user. The authors are to be commended for their contribution in this paper of data concerning the behavior of a class of material widely used over a great variety of operating conditions and in this respect alone the paper is a definite step toward the goal of applying the correct material in its proper physical condition to any specific installation.

It has been the writer's belief for a long time that acceptance specifications for the majority of metallic materials should base upon, or at least emphasize, microstructure limitations rather than to rest, as so many do, either upon destructive tests made under conditions in no way comparable to those under which the material is expected actually to perform or upon analysis requirements concerning which the metallurgical stability factor has been more or less ignored. The fact that our approach to optimum control procedures has to keep pace with metallurgical developments is once more demonstrated by the authors of the subject paper.

The application of the austenitic type of steels to high temperature oil heater tubes makes the authors' findings concerning the 18-8 and 18-8 + Cb analyses of great interest, particularly the opposite hot-ductility-to-fracture tendencies of the two analyses in the fine-grained condition as compared with their respective reductions in long-time rupture strength. Considering Figs. 5 and 6, it is noted that at 1200 F (650 C) the 10,000-hour rupture strength of both analyses in the fine-grained condition corresponds quite well although a wide difference exists after 100,000 hours at this temperature. It would be interesting to know if the rupture strength of the 18-8 + Cb material decreases linearly with time—in other words, if it can be considered as a gradual depreciation effect rather than as an abrupt rate change at some critical temperature level due to appearance of the unknown phase. Offhand, the former would seem to be the case. As the hot-ductility-to-fracture property has, up to a certain point, its advantage in furnace tube application in that some prior warning of failure (provided to a far less extent by the higher strength structures) is afforded, the rate (or critical point, if one exists) of accelerated rupture-strength loss seems an important factor.

The use of 18-8 material in high temperature tubes has sometimes been discouraged because of service failures occurring without warning, tubes of lower alloy content usually giving some prior notice of failure by swelling or bulging, although this has by no means precluded the possibility of actual rupture during operation. The 18-8 failures are undoubtedly due to intergranular precipitation and considering the general susceptibility of 18-8 (without the stabilizer) to this condition, it is possibly not the best for high temperature tube application. The authors have shown the disadvantageous effect of columbium on creep and stress-rupture qualities over a long period of time in the fine-grained steels; however, it appears that precipitation effects are at the same time largely inhibited in grain structures of any size.

From the data given it would seem that considering a reasonable balance of desired properties, the optimum selection for high temperature tube material would be the 18-8 + Cb material in the medium grain size since this appears to combine fair creep and hot-ductility-to-fracture properties with resistance to intergranular effect to be expected from inclusion of the stabilizer. However, the writer wonders how effective the stabilizing element really is in the case of medium and coarse-grained steels and whether in such case there is much practical advantage over a fine-grained 18-8 containing no columbium at all, since grain size in that material is such a minor factor. Previous published work has shown precipitation in stabilized steels at high temperature at relatively short periods under high stress. Is magnitude of stress a factor in microstructural stability at high temperature levels and what is considered to be the mechanism involved in the reduction of creep strength, etc., by inclusion of the columbium?

With respect to the 25-12 and 25-20 materials, it is noted that the carbon contents of the specimens tested are much lower than certain commonly used analyses, particularly in the cast form. Have the authors developed data concerning effects of varying the carbon upward or downward? The writer understands that sigma phase was not in evidence at any time during the tests although temperatures reached 1800 F (980 C). However, since this constituent appears in the cast form of certain austenitic analyses within the test temperature range cited, the questions arise as to (a) whether carbon content directly influences the formation of either sigma or the "unknown" phase, and (b) why sigma was not in evidence in these tests for those analyses ordinarily considered as subject to it.

In view of the apparently beneficial effects of nitrogen in 25-12 cast material for high temperature applications it would be interesting to know if inclusion of the same element has any effect in suppression of the weakening unknown phase described in this paper.

The writer would like to know if the manufacturers of tubular goods and castings for high temperature use and other products made from the austenitic family of steels intend to give effect to these and similar data in the form of recommendations as to the optimum microstructural condition in which the product should be furnished for any given analyses and service conditions.

Written Discussion: By E. R. Wilkinson, Standard Oil Company of New Jersey, Louisiana Division, Baton Rouge, La.

The developments accomplished in the preparation of this paper by Drs. Clark and Freeman are a real contribution to the many users of austenitic steel tubing for high temperature service. The authors have taken a most practical point of view throughout the discussion of their experiments, and this is the type of discourse which is of most value to the engineers who are specifying materials for various operations.

For some years now we have been specifying fine-grained 18-8 chromium-nickel steel tubes for operating temperatures up to 1600 F (870 C) and higher, and have received very good service from them. This experience, it seems, would generally bear out the conclusions given concerning this particular material. Other austenitic steel tubing has generally been specified to be fine-

grained also, but it appears from the data given that we might expect better service from the coarse-grained material. For instance, the impact values at low temperature are quite important from a practical viewpoint because of the shock to which furnace tubing is subjected when being mechanically cleaned. The impact tests on 25-20 show that the coarse-grained material is generally superior to the fine-grained and although the authors appear to place more credit for this with the unknown transformation or phase which the metal structure undergoes, the grain size may still be a very important factor. This conclusion is based on the fact that the unknown phase seems to appear more pronounced in the lower range of high temperatures whereas the impact values decreased from 1000 to 1200 F (540 to 650 C) creep temperature and then leveled off. If the unknown phase were the more important factor for this consideration, it seems that it would naturally follow for the impact value to improve with the higher creep test temperature. Thus, we might conclude that the use of coarse-grained 25-20 is even more important than the authors claim.

One interesting factor that has been noted, however, and the authors are no doubt aware of it, is the fact that the fine-grained material seems almost invariably to react more uniformly to various treatment than the coarse-grained materials. This is disclosed in the results of most of the tests and manifests itself in the smoothness of most of the curves in the charts and particularly in the tensile strength figures for 25-20 steels in Table II. We are not exactly sure what this might indicate, but it may mean that a fine-grained structure is more reliable or dependable than a coarse-grained one.

In connection with fine-grained structures, the fact that grain growth occurs during operating service at high temperature is worthy of mention. For instance, experience with 18-8 has shown that the grain size increased from about 6/8 to about 3/4 after some 20 to 25 thousand hours of operation at 1500 to 1700 F (815 to 925 C) with spot temperature conditions considerably in excess of 1700 F (925 C). Data are not available here to show that the same is true of the other austenitic steels referred to in the paper, but if it is, this may influence the grain size specification.

The authors may feel that too broad generalizations are made in these comments. It must be remembered, however, that unless there can be certain generalizations of these data, then the data become less practical due to the fact that when tubes are specified for a given temperature condition, that condition may actually vary over a range of several hundred degrees Fahr.

The authors of this paper are to be commended for their presentation which is just another example of their fine work.

Authors' Reply

Our comments with respect to the various questions raised by Mr. Horne are as follows:

1. The decrease in the strength of the fine-grained 18-12 + Cb steel, as well as the 25-20 and 25-12, is believed due to the precipitation of the unknown phase and is also believed to be a linear function with time. Results to date would indicate the effect of stress to be a minor factor.

2. Sigma phase was not observed in the 18-12 + Cb steel since the analysis was balanced with respect to the ferrite and austenite formers to prevent its appearance.

3. In this same connection nitrogen was added to both the 25-20 and 25-12 to help stabilize the austenite.

4. The effect of pronounced variations in carbon content has not been investigated, for it is believed this element should be held below at least 0.10% in wrought austenitic steels in order to improve stability of structure and corrosion resistance.

5. Grain size can be controlled in wrought austenitic products by cold working followed by recrystallization but this procedure cannot be readily followed in the case of castings.

6. It is not believed that the results presented preclude the use of 18-8 for high temperature service. This alloy has rendered excellent service in many applications, and while it often tends to fail with a brittle-type failure (as do many other type austenitic steels), these fractures can be largely eliminated by using the stress-rupture data for determining the available service life.

The precipitation effects appear to be just the opposite of those postulated by Mr. Fleischmann. That is, in the coarse-grained steels precipitation occurs largely within the grain boundaries while in the fine-grained steels it tends to have random distribution. With 18-12 + Cb both the fine and coarse-grained steels were immune to the Strauss corrosion test under all conditions. However, in the case of 25-12 and 25-20, the fine-grained structure, after the precipitation of the unknown phase, was more immune than the corresponding coarse-grained steels.

In reply to Mr. Savage the unknown phase was readily attacked by any of the etching reagents used but the microstructures shown were etched with electrolytic sodium cyanide.

The question raised by Dr. Urban should have been clarified in the paper. In the lower temperature treatments for fine grain size control the specimens were air-cooled, for in this case it was not a question of retaining carbides in solution. These specimens could just as well have been water-quenched and it is believed this would not have influenced the results. On the other hand, since 1-inch diameter bar stock was used, a water quench was believed desirable from the higher temperature treatments in order to retain the carbides in solution.

We cannot agree with Dr. Gammeter that the differences observed in the high temperature strength values of 18-8 and 18-12 + Cb may be due to the slight variations in chemistry more than to the appearance of the unknown phase resulting from differences in heat treatment and grain size. If this were true then the users of high temperature steels have been very fortunate, to say the least, in being able to design on the basis of creep and rupture data, for the differences in chemistry are all well within the limits of the various specifications. This belief is further substantiated by the fact that in the case of 25-12 and 25-20 only single heats were used and the effect of variations in grain size and heat treatment were the same as with 18-12 + Cb. However, it is true, as Dr. Gammeter states, that the precipitation in the grain

boundaries of the coarse-grained 18-12 + Cb is slight as compared to the other steels considered and the network is not as continuous.

While we agree that the microstructure given in Mr. Watt's discussion does show ferrite to be present, this constituent was not observed in any of the steels considered except 25-12. Again it is a question of properly balancing the analysis to prevent the formation of ferrite and in this connection it should be noted that our type 347 actually is of the 18-12 + Cb type rather than of the 18-8 + Cb type. Small amounts of ferrite were present in both the fine and coarse-grained 25-12 steel but since this alloy behaved the same as 25-20 and 18-12 + Cb, in which ferrite was not present, it must follow that the presence of ferrite is not the main contributing cause to the low strength at high temperatures of the fine-grained austenitic steels.

The comments of Mr. Wilkinson have added to the value of this paper for as he states it is true that coarsening of the fine grain structure will occur under prolonged times at temperatures of the order of 1700 F (925 C) or higher, as this was the temperature employed to cause only sufficient recrystallization of the cold-worked structure to produce the desired fine grain size. However, this tendency for grain growth will be more pronounced in 18-8 than in the other steels considered.

Likewise, as Mr. Wilkinson states, consideration must be given to other factors such as impact resistance and the ability to reproduce the given structures not only from heat to heat but likewise in the individual tubes from any given heat. With proper processing control it should be possible to produce with equal ease either a fine or a coarse-grained structure in these austenitic steels.

EXPERIMENTAL STUDIES OF CONTINUOUS COOLING TRANSFORMATIONS

By C. A. Liedholm

Abstract

This paper demonstrates methods, results, and applications of direct experimental studies of continuous cooling transformations including some data on their effect on subsequent isothermal reactions in hypoeutectoid steel of high pearlite and bainite hardenabilities. Experimental results are presented on mechanical and physical properties of partly transformed or slack-quenched and drawn structures in such materials. It is demonstrated that the time required by the S-curve to complete an isothermal reaction in the bainite region is lengthened, in some instances more than 2000%, by ferrite rejection during continuous cooling preceding the isothermal transformation.

It is hoped that this contribution will stimulate interest in direct experimental studies of transformations of the types which probably are encountered most frequently in industrial heat treating operations.

Introduction

ISOTHERMAL transformations lend themselves most readily to scientific studies of the fundamental principles of the pearlite and bainite reactions in steel. S-curves also provide the practical metallurgist with a handy and popular method of comparing the transformation characteristics of one steel with those of another, or the effect of various alloy additions on these characteristics.

But strictly isothermal transformations occur comparatively seldom or perhaps even rarely in industrial heat treating processes; a 30-ton annealing charge or even one of a few hundred pounds weight can hardly be transformed in a strictly isothermal fashion, because the essence of isothermal transformation is rapid quenching to the isotherm; nor can a gun tube, or a propeller hub of 50 to over 100 pounds weight, or a propeller blade, or a weldment, unless it be relatively small in mass or thickness.

A paper presented before the Twenty-eighth Annual Convention of the Society held in Atlantic City, November 18 to 22, 1946. The author, C. A. Liedholm, is chief engineering metallurgist, Curtiss-Wright Corp., Propeller Division, Caldwell, N. J. Manuscript received June 27, 1946.

The Jominy test gives a rather accurate representation of the cooling cycles occurring during industrial quenching operations permitting, by hardness correlation, the indirect interpretation of a cooling cycle in terms of distance from the quenched end of a Jominy bar. One of its limitations is that of giving hardness values only, but since other physical properties may be different for one and the same hardness, it is not always possible to predict them accurately on the basis of hardness alone.

It is hoped that this introduction suffices to justify the statements that the S-curve sometimes fails to predict accurately the results of industrial heat treating cycles, and on occasion may lead to quite erroneous conclusions; and that the information obtainable from the Jominy test often forms an inadequate basis for accurate heat treating recommendations.

The intention of this paper is to demonstrate engineering information obtained by methods devoloped or used to supplement S-curves and standard Jominy tests in order to predict and control practical heat treating results or evaluate materials for proposed applications. Experimental procedures will be briefly discussed. The supporting data represent a limited selection from laboratory results whose unabridged inclusion would make the paper excessively lengthy. The work whereon this report is based is still in progress.

For convenient discussion, the subject matter will be grouped under the following headings:

Continuous cooling transformation diagrams
Flat end-quench method
Isothermal reactions preceded by gradual cooling

Each interrelated topic will include the experimental procedure and results, and a discussion of the practical applications or significance of the results.

Continuous Cooling Transformation Diagrams

Procedure and Results

The major part of these studies has been based on partial continuous cooling transformation diagrams obtained by a technique combining Jominy's end-quench test (1)[1] with Bain's method of developing S-curves (2) by arresting transformations at various stages through quenching, thus exposing their progress to metallographic

[1]The figures in parentheses pertain to the references appended to this paper.

observations. The details of the experimental procedures employed to develop these partial continuous cooling transformation diagrams have been described elsewhere (3), but will be reviewed briefly in the following.

Cooling curves are obtained for a sufficient number of positions on a ½-inch diameter by 4-inch long end-quench bar with a fast recording potentiometer such as the Speedomax. The recommended practice is to take duplicate curves for each typical material (chosen to represent a specified analysis range) and each hardening temperature at twelve positions along the bar—namely, at ⅛-inch intervals from the quenched end to the 1-inch station, and at 1¼, 1½, 2, and 2½ inches from the end. These curves are plotted in ink on a large, thin graph paper so that black and white work prints can be obtained easily. At least twenty-four specimens are required with this procedure for the basic step of the program.

To obtain the experimental data for each individual diagram requires an additional twenty-one ½-inch diameter end-quench bars. These specimens are protected by a controlled atmosphere or by partial embedding in cast iron borings or any other suitable method during heating to the hardening temperature (we have used 1700 F (925 C) in most of our work). The specimens then are end-quenched for various selected intervals, e.g., 10, 15, and 20 seconds; beyond that the successive test pieces can be timed in the jig with 10 to 20-second increments up to 200 or 300 seconds, which period usually is long enough to permit all-over quenching of most steels without any appreciable effect on the form of the normal Jominy curve. Each selected end-quench period is terminated by the rapid quenching of the entire specimen, preferably in ice water.

All the structural changes associated with the various cooling cycles existing throughout the length of the Jominy bar, therefore, are "frozen" at various time intervals from the beginning of the end quenching and can be studied metallographically. The time and place of birth of each new microconstituent is plotted on the time-temperature curves obtained previously for successive positions of the end-quench bar. (Obviously, it is often necessary to interpolate between the various end-quench periods and cooling curves.) All points on the cooling curves denoting the beginning of the same transformation are next connected by a faired curve which, therefore, will indicate the time and temperature of the beginning of the observed reaction—such as ferrite, pearlite, or bainite—during progressively slower cooling cycles.

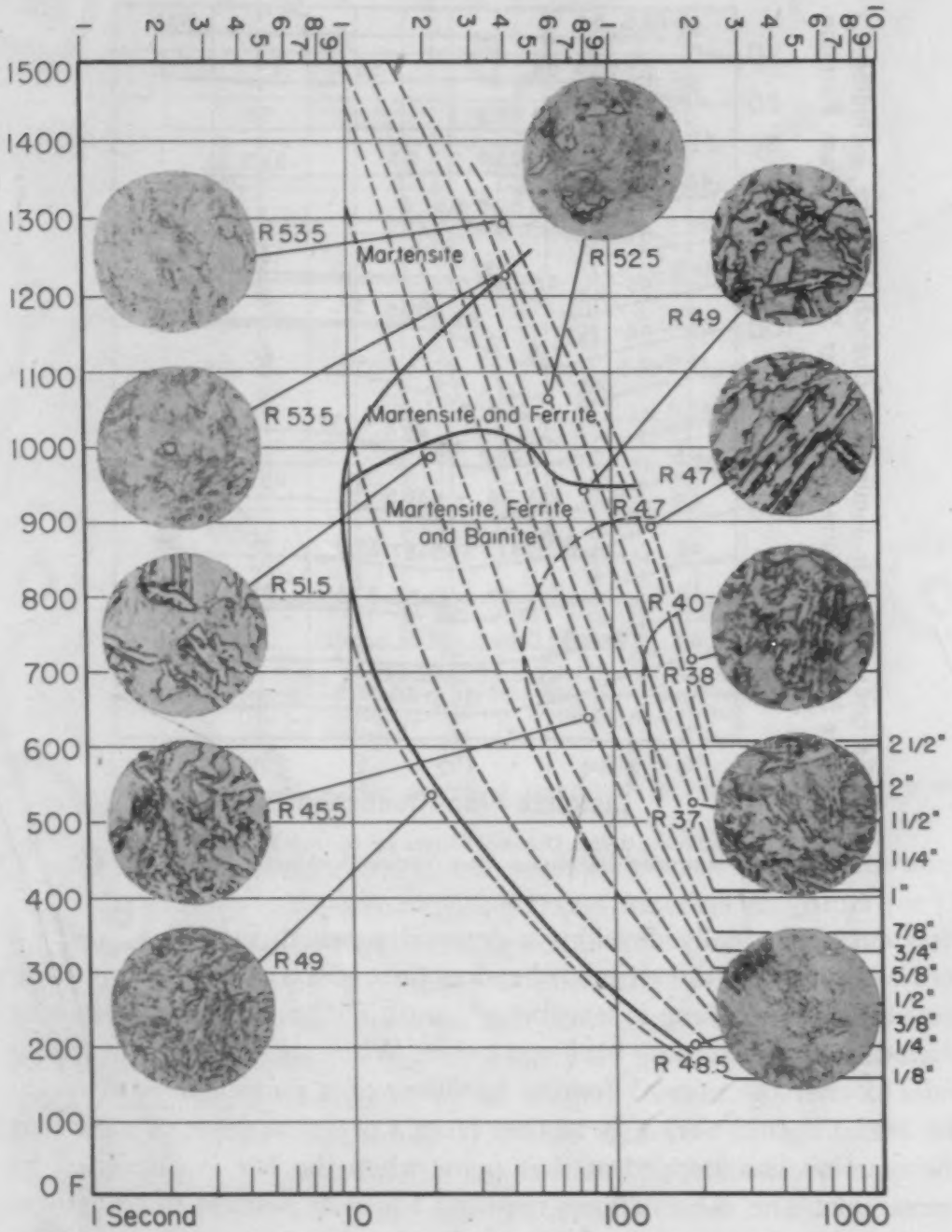


Fig. 1—Continuous Cooling Transformation Diagram for SAE 4330 Steel of Heat No. 3801.

Fig. 1 is a finished continuous cooling transformation diagram with hardness contours for SAE 4330 steel. Transformation diagrams of the same type have been published also for SAE 6135 (3), NE 8630 (5), SAE 4130 (6), SAE 4315 (7), and another heat of SAE 4330 (4).

Fig. 2 shows the effect of the all-over quenching after the various end-spray periods on the Jominy hardness curves: Note that the hard-

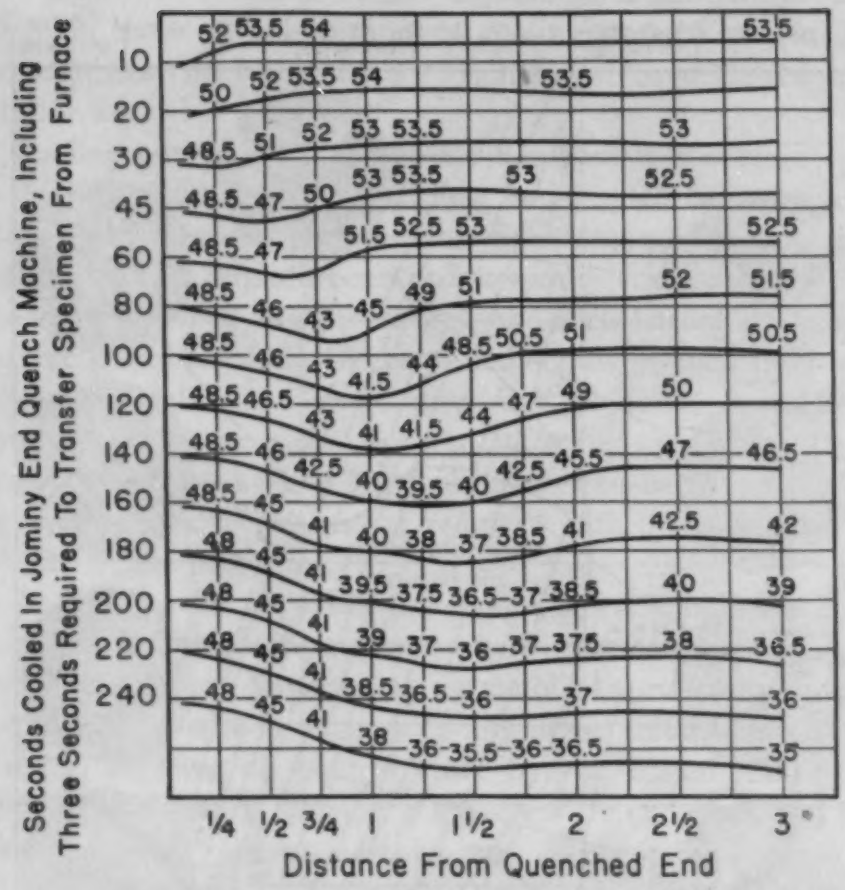


Fig. 2—Hardness Versus Distance Curves for ½-Inch Diameter Jominy Bars Upon Immersion Quenching After Various End-Spray Periods.

ness curve gradually develops a depression which increases in depth and width toward the air-cooled end as the end-spray period preceding the all-over quenching is lengthened, until, finally, the curve coincides with the regular Jominy hardness curve. When the all-over quenching fails to alter the normal Jominy hardness of a particular position on the bar, it should obviously be true from a practical point of view that the reaction has stopped at that point when the bar is quenched by immersion. The various times required for each position to transform to the state indicated by its true Jominy hardness then could be determined approximately from the curves of Fig. 2 if the increment in hardness due to the immersion were plotted against the length of the end-quench period. Fig. 3 shows this way of plotting the hardness increment against the end-quench period for the 1¼-inch distance from the quenched end. It was intended to determine the curve indicating the virtual end of premartensite transformation from such plots, but the number of hardness data available for each position was not

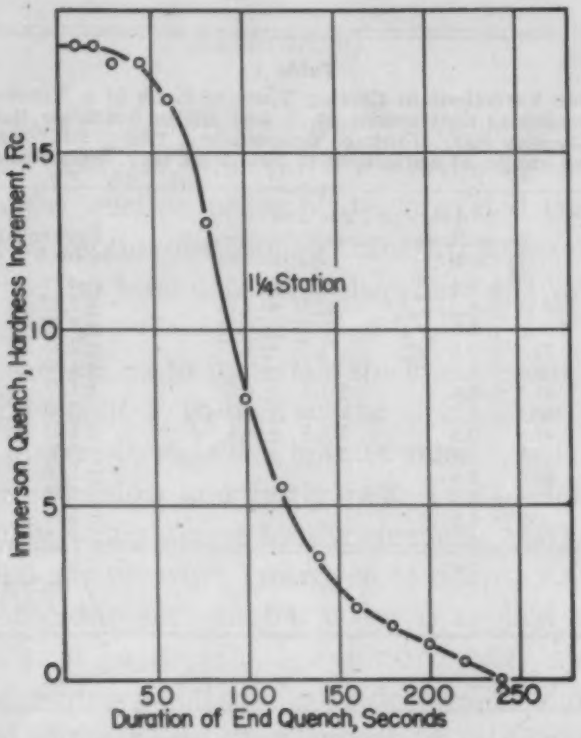


Fig. 3—Hardness Deviation From the Regular Jominy Hardness at 1¼ Inches From the Quenched End, Plotted Against the Duration of the End-Spray Period.

sufficient to determine the average hardness with the necessary extreme precision.

Since the reproducibility of the cooling curves largely determines the value of the continuous cooling transformation diagrams for the prediction and control of metallographic structures, the illustrative data of Table I have been included. These data represent very recent studies on the reproducibility of such cooling curves. With the present technique, the distance of the thermocouple from the quenched end of the Jominy bar is controlled by an accurately made jig which allows the drilling of two individual 1/32-inch diameter by 1/32-inch deep holes, 1/16-inch apart, on the lateral circle at each desired position. The thermocouple wires are inserted and the holes closed by peening them together with a small punch so as not to effect any displacement in the longitudinal direction. By the older method (3), a thermocouple bead was peened into a single 1/16-inch diameter hole.

It is noted from Table I that the cooling times to the various listed temperatures obtained by the latest method for the ½ and 2½-inch distances from four parallel determinations varied by a maximum of about ± 4.2% for the ½-inch distance and ± 5.1% for the 2½-inch

Table I

Absolute and Relative Variations in Cooling Time to Each of a Number of Temperatures Recorded by the Speedomax Instrument at ½ and 2½ Inches from the Quenched End of a ½-Inch Diameter Jominy Bar. Furnace temperature, 1700 ± 5 F. Each computed average and range of variations is based on four determinations.

Temperature, F	Average Time and Range in Seconds		Percentage Variations	
	½ Inch	2½ Inches	½ Inch	2½ Inches
1400	12 ± 0.5	29.5 ± 1.5	±4.17	±5.08
1300	15 ± 0.5	42.75 ± 1.75	±3.33	±4.09
1200	18 ± 0.5	57.75 ± 1.75	±2.78	±3.03
1100	21.5 ± 0.5	75.25 ± 2.25	±2.33	±2.99
1000	26.5 ± 0.5	98.75 ± 2.75	±1.89	±2.78
900	31.5 ± 0.4	141.5 ± 6.5	±1.27	±4.59
800	38.5 ± 0.25	182.75 ± 4.25	±0.65	±2.33
700	47.5 ± 0.5	218.5 ± 4.5	±1.05	±2.06
600	62 ± 1.0	256 ± 3.5	±1.61	±1.37
500	85.5 ± 1.5		±1.76	
400	126 ± 3.5		±2.78	
300	197 ± 6.5		±3.30	

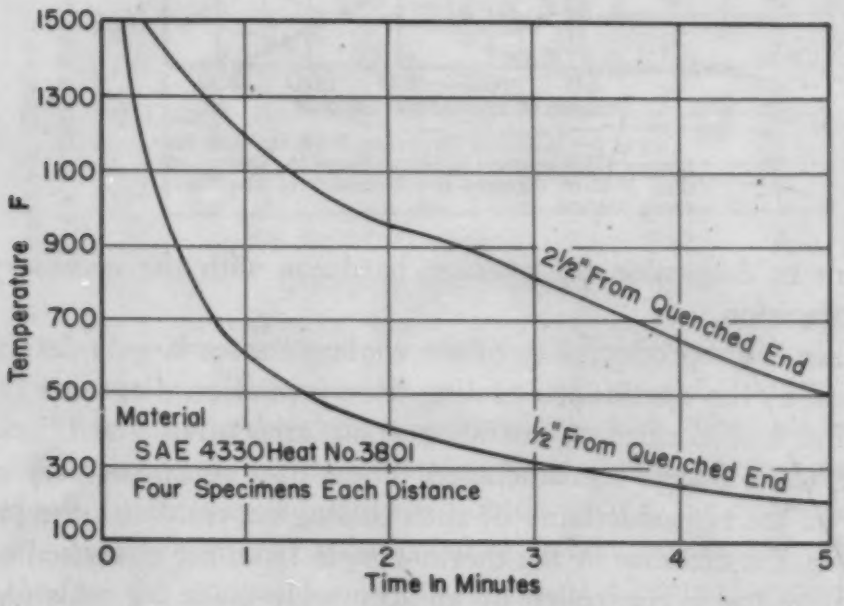


Fig. 4—Quadruple Speedomax Curves for ½ and 2½-Inch Distance From the Quenched End of ½-Inch Jominy Bars, Illustrating the Duplicability of These Cooling Curves.

distance. The maximum percentage variations arose in the former instance from ± 0.5-second errors and in the latter, from ± 1.5-second errors. Note, however, that no corrections have been made for variations in transfer time from furnace to quenching fixture. This time, for a good operator, has been found to be very close to 3 seconds, which observation agrees well with the 2.5 seconds reported by Morse Hill (8). Fig. 4 shows the replotted Speedomax curves.

Applications

Propeller Blade Heat Treatment—The need for a rational but simple method of analyzing the variables involved in the die-water quenching of hollow steel propeller blades provided the incentive for the development of continuous cooling transformation diagrams. This original application has been discussed elsewhere (3), (9), but will be briefly reviewed.

Because of variations in materials thickness from over 1 inch at the shank to only about 1/16-inch at the tip, hollow steel propeller blades, cooling in air, contain an infinite number of cooling cycles varying between very slow and fairly fast. The blades are hardened and simultaneously straightened by die quenching after the application of an internal gas pressure (nitrogen at 825 to 900 psi). The die cooling hardens the thin sections but water is applied externally over the thickest material in the shank outboard over about a 17-inch length. The first requirement of the blade steel is sufficient hardenability to respond to the die or water quench by satisfactory hardening. The size of the blades and the necessity of positioning them carefully in the die imposes an air cooling period, always preceding the quenching operation and varying in length because of the human factor. The problem originally solved by the continuous cooling transformation diagram was to permit the accurate determination of the allowable maximum air cooling period preceding the water quench. This period varies between 15 seconds for SAE 6130 steel to 60 for a new blade material resembling SAE 4320, and 90 seconds for SAE 4330 (a slightly modified composition was used).[2] An approximate method of determining quench delay is merely to perform a series of interrupted end-quench tests such as illustrated in Fig. 2 above. It will be shown presently, however, that more instructive information can be obtained from the continuous cooling transformation diagram.

Rejected Ferrite in Quenched and Drawn Steel—Many reports on failure diagnosis have, without hesitation, charged fatigue cracks to the occurrence of ferrite rejection in the failure area of heat treated parts. Rejected ferrite at least is viewed with suspicion in any part requiring high endurance strength. The actual effect of various per-

[2]The 60-second quench delay employed for the new blade material and the 90-second delay used for the now discontinued SAE 4330 material are long enough to cause ferrite precipitation in heats of low hardenability, but are necessary to minimize quench cracking in heats of relatively high carbon content and high hardenability. The amount of ferrite precipitation is controlled by the requirement that the hardness after draw nowhere must be less than Rockwell C-27. It will be shown that this requirement is an adequate safeguard against any appreciable loss of endurance strength.

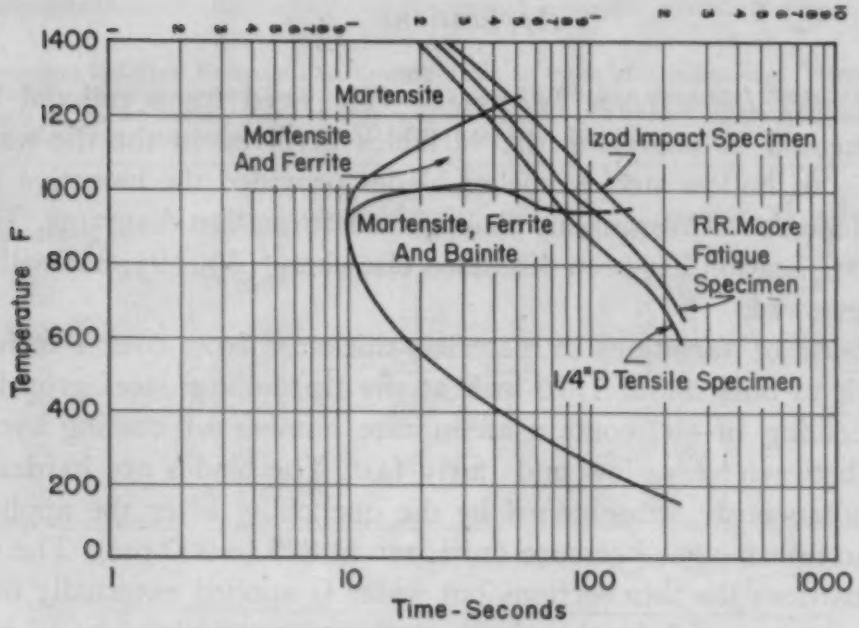


Fig. 5—Cooling Curves for Impact, Fatigue, and Tensile Specimens, Superimposed Upon the Continuous Cooling Transformation Diagram of the Material.

centages of rejected ferrite on the hardness, fatigue, tensile, and impact strengths of SAE 4330 steel hardened and drawn at 1120 F has been determined by the superimposition of the center-section cooling curves for the various test specimens, on the continuous cooling transformation diagram of the heat of steel from which the specimens were machined; see Fig. 5. The analysis of this material (heat No. 3801) was as follows:

Heat No.	% C	% Mn	% Si	% S	% P	% Cr	% Ni	% Mo
3801	0.27	0.73	0.31	0.008	0.006	0.72	1.84	0.31

Different sets of the specimens were quenched after various periods of air cooling, determined from Fig. 5, to allow the following stages of transformation to be reached prior to quenching:

(a) No ferrite precipitation
(b) Trace rejected ferrite
(c) A few per cent
(d) About 10%
(e) About half completed ferrite rejection
(f) Maximum ferrite compatible with the cooling cycle, plus bainite.

Each set of specimens of the same kind and quench delay was air-cooled in a symmetrically loaded holder, whereupon holder and specimens were quenched together. The procedure, of course, required the

air cooling cycle to be determined for each kind of specimen in the properly loaded holding fixture. It was found that the cooling cycle of the ¼-inch diameter shoulder type tensile specimens used in this particular investigation was approximated by the 1⅜-inch Jominy distance, and that of the R. R. Moore fatigue specimens by the 2½-inch distance; whereas, the Izod specimens cooled slower than the 2½-inch Jominy position.

Average results including the metallographic structures of the partly transformed specimens, obtained on duplicate series of transverse fatigue, and triple transverse tensile specimens from ½-inch plate material, have been plotted in Figs. 6, 7, and 8, against quench delay time, and against percentage of ferrite. The latter quantity was determined by the cutting of 8 by 10-inch enlargements of 300-diameter photomicrographs into ferrite and nonferrite areas and weighing the pieces. Fig. 9 shows the percentages of ferrite determined on the tensile specimens, plotted against the various quench delays.

It will be noted that the physical properties, and especially the fatigue strength, were not radically lowered by the ferrite rejection. Even with 51% rejected ferrite and appreciable amounts of bainite, the lowering of the fatigue strength amounted to only about 8% for this material. If one considers that a 60-degree notch with a radius of 0.002 inch lowers the fatigue strength by some 75%, the effect on this property of the partial transformation resulting from overdelayed quenching of this high hardenability material, within the limits studied, appears slight. This observation is important in connection with the establishment of heat treating specifications for propeller blades, and in connection with failure studies.

The maximum lowering of the tensile strength amounted to 14%, the as-quenched hardness fell by a maximum of 16 points Rockwell C, and the hardness after draw, 6 Rockwell C. The average values obtained on groups of six transverse Izod impact tests varied between 61.5 and 67.2 foot-pounds throughout the whole range of investigated structures.

An attempt was made to determine whether or not the results could have been estimated with reasonable accuracy from a knowledge of the tensile strength of the alloyed ferrite and of tempered martensite of various carbon contents. The tensile strength of the ferrite was calculated to be about 64,000 psi, using the method reported by Gensamer (10). The strength of the tempered martensite-bainite fraction was taken from a curve correlating tensile strength and carbon content

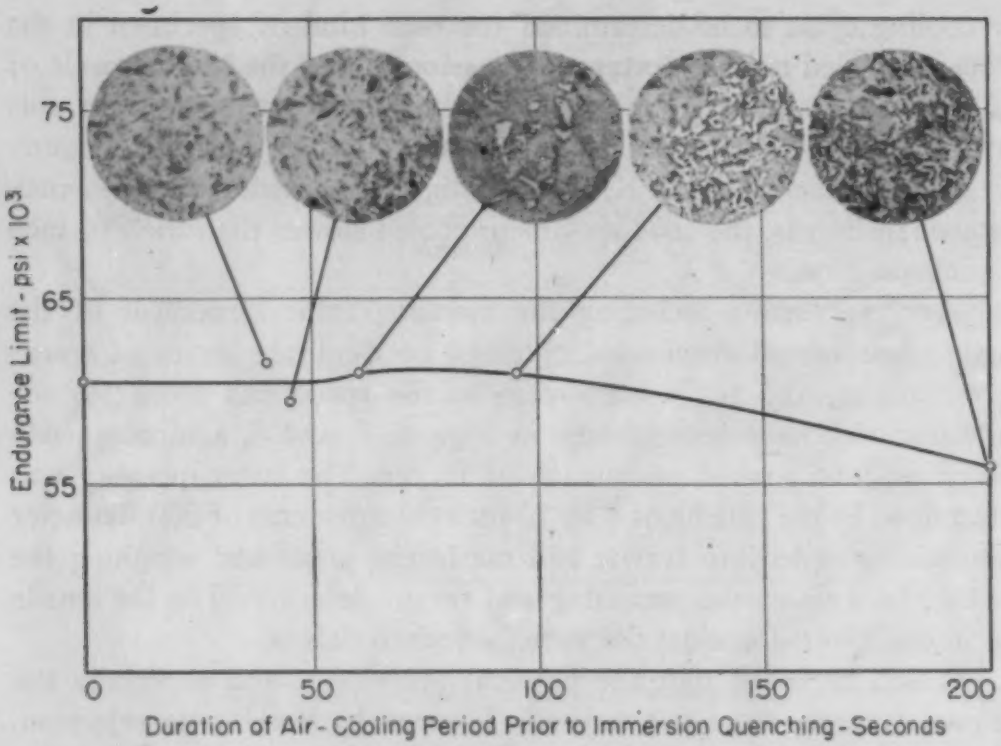


Fig. 6—Transverse Fatigue Strength Versus Quench Delay for Heat No. 3801. Typical Structures Illustrated by Photomicrographs.

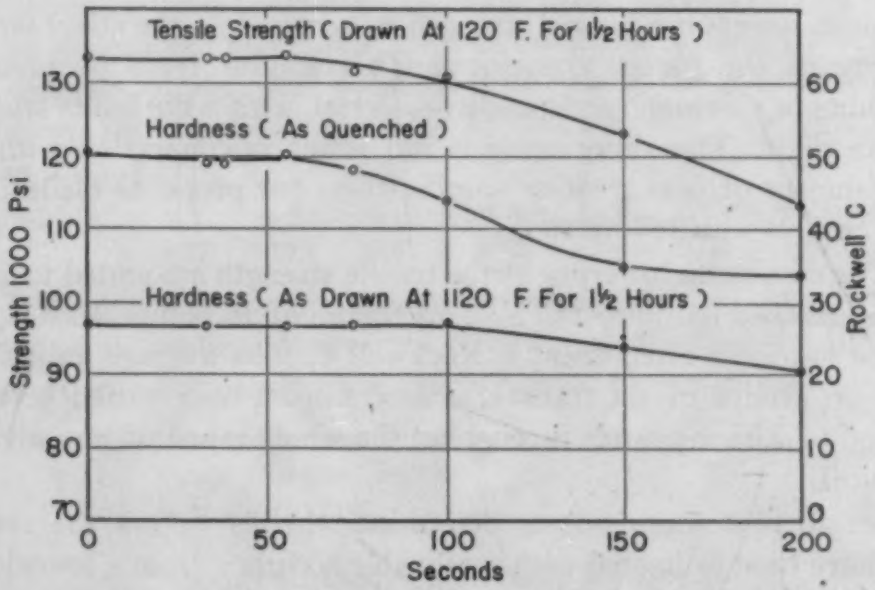


Fig. 7—Tensile Strength and Hardness in the Drawn Condition, and Hardness As-Quenched, Versus Quench Delay for ¼-Inch Diameter Specimens.

for steels in the SAE 4300 series, developed by this laboratory (11) for materials quenched in oil and water and subsequently drawn at 1140 F

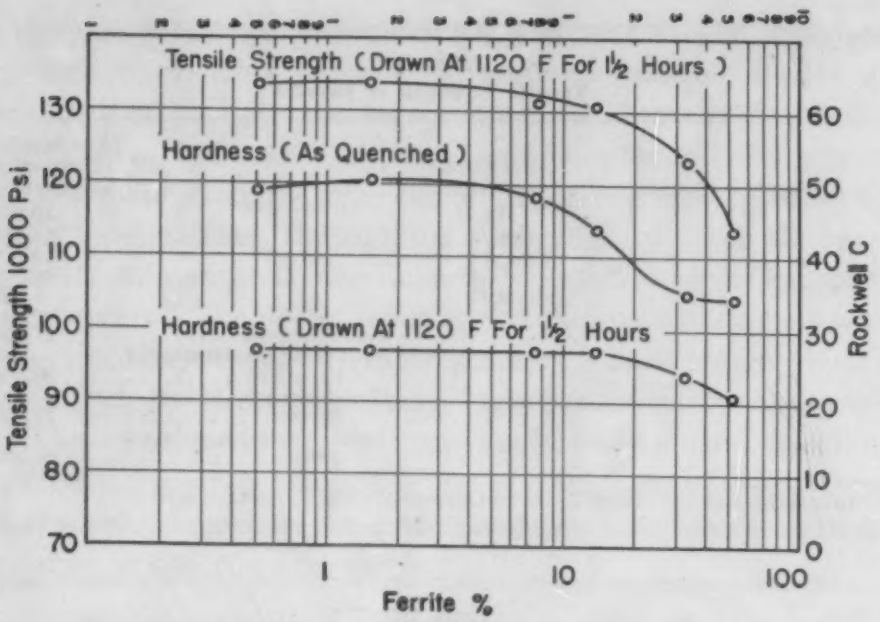


Fig. 8—Tensile Strength and Hardness in the As-Quenched and As-Tempered Conditions Versus Percentage of Rejected Ferrite.

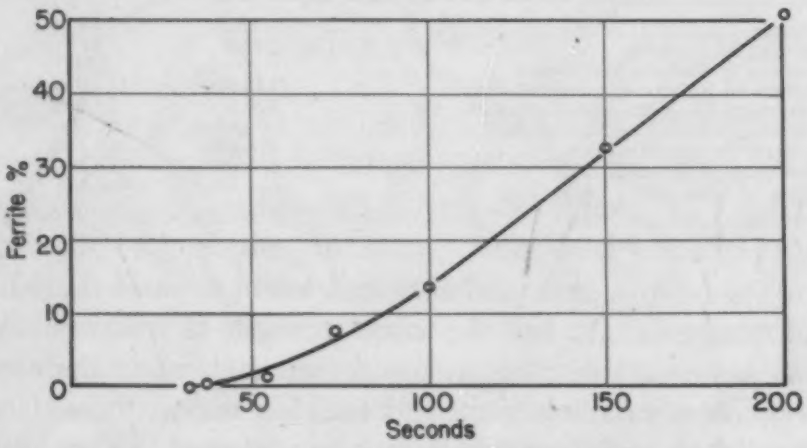


Fig. 9—Quench Delay Versus Percentage of Ferrite for ¼-Inch Diameter Tensile Specimens.

(615 C). Since the data for heat 3801 were obtained on specimens drawn at 1120 F (605 C), the somewhat higher values of the water-hardened and tempered condition were employed. It was assumed that each structural fraction (ferrite and tempered martensite-bainite) contributed strength in proportion to its relative area and inherent tensile strength and that the martensite-bainite fraction contained all the carbon indicated by the analysis. The basic data employed and the results obtained are assembled in Tables IIA and IIB.

Although these estimates were based on the arbitrary assumptions that each microconstituent contributed to the tensile strength in pro-

Table IIA
Tensile Strength of Ferrite

Element	Per Cent by Weight		Flow Strength, Psi Increase Above Unalloyed Ferrite
Mn	0.73		10,000
Si	0.31		13,000
Cr	0.72		3,300
Ni	1.84		16,000
Mo	0.31		5,100
		Total Increase	47,400
		Flow Strength, Unalloyed Ferrite	30,000
		Flow Strength, Alloyed Ferrite	77,400
		Tensile Strength, Alloyed Ferrite	64,000*

*Obtained through the interpolation of Gensamer's Fig. 4, Reference 13.

Table IIB
Fractional Strength from Microconstituents and Total Strength, Calculated and Experimental

Per Cent Ferrite	13.5	33	51
Per Cent Bainite-Martensite	86.5	67	49
Per Cent Carbon in Bainite-Martensite	0.31	0.40	0.55
Tensile Strength of Bainite-Martensite, Psi	138,500	147,000	161,000
Fractional Strength from Bainite-Martensite, Psi	120,000	98,500	79,000
Fractional Strength from Ferrite, Psi	8,650	21,200	32,700
Total Calculated Tensile Strength	128,650	119,700	111,700
Experimental Tensile Strength	131,000	123,500	114,000
Per Cent Error of Calculated Value	—1.9%	—3.4%	—2.0%

portion to its relative area and inherent strength[3] and that the tempered martensite-bainite had the same strength as tempered martensite of the same carbon content, the agreement among the estimated and experimental values is good and for that reason these data were thought to be of sufficient interest to be reported. (The maximum error was 3.4%.)

Material and Process Improvements—The purpose of the preceding review of the present applications of the continuous cooling transformation diagram was not to suggest that any general conclusions can be drawn from the data presented herein on a material of high hardenability and alloy content, regarding the properties of typical microstructures formed during the continuous cooling of various steels. The intention is, however, to substantiate the suggestion that information of this type can be developed rather readily for many other materials by similar methods.

[3]The mean ferrite path could not be determined experimentally for the tempered martensite-bainite and, hence, no attempt was made to base the estimate on Gensamer's correlation between strength and log of mean ferrite path (10).

In the past, it has always been considered necessary to select steels of very high hardenability for die-quenched propeller blades and, therefore, data on cooling transformation of less hardenable steels are not yet available. However, it appears quite possible to build propeller blades of adequate strength, from fairly low-carbon steel of lower than the present hardenability, through the application of these methods to the proper co-ordination of material and processes, and the subsequent production control. The object would be to eliminate numerous manufacturing difficulties, especially those pertaining to welding, which are the bane of steels with excessively high hardenability and carbon content. The envisioned heat treatment could be described metallurgically as a slack quench controlled within specified limits. The first step in work toward this goal is the design and construction of a flat end-quench bar to be described presently.

Flat End-Quench Bar

Procedure and Results

The possibility of slack quenching a material to uniform physical properties through various two-stage cooling cycles (air cooling followed by water or die quenching) obviously requires an experimental procedure which allows the direct and ready determination of tensile and possibly endurance properties, in addition to hardness, for many different air cooling cycles and various delays prior to quenching.

The fully satisfactory procedure should be as free as possible from limitations such as affect the data just presented on the effect of percentage of ferrite on mechanical properties. The various specimens should not be inflexibly associated with an "air cooling" cycle peculiar to the design of the specimens. Rather, it should be possible to obtain tensile or fatigue as well as hardness tests that could be cooled in accordance with any predetermined cooling cycle, so that various properties could be compared on any desired common basis of cooling cycle and quench delay or metallographic structure. Flat end-quench tests provide a reasonably satisfactory answer to these requirements, because they provide a range of cooling cycles which, once determined, can be used to select the desired specimen on the basis of its cooling cycle and, hence, permit a more general correlation among cooling cycle, quench delay, structure, and mechanical properties. They have the drawback, however, that each specimen, even if very small, repre-

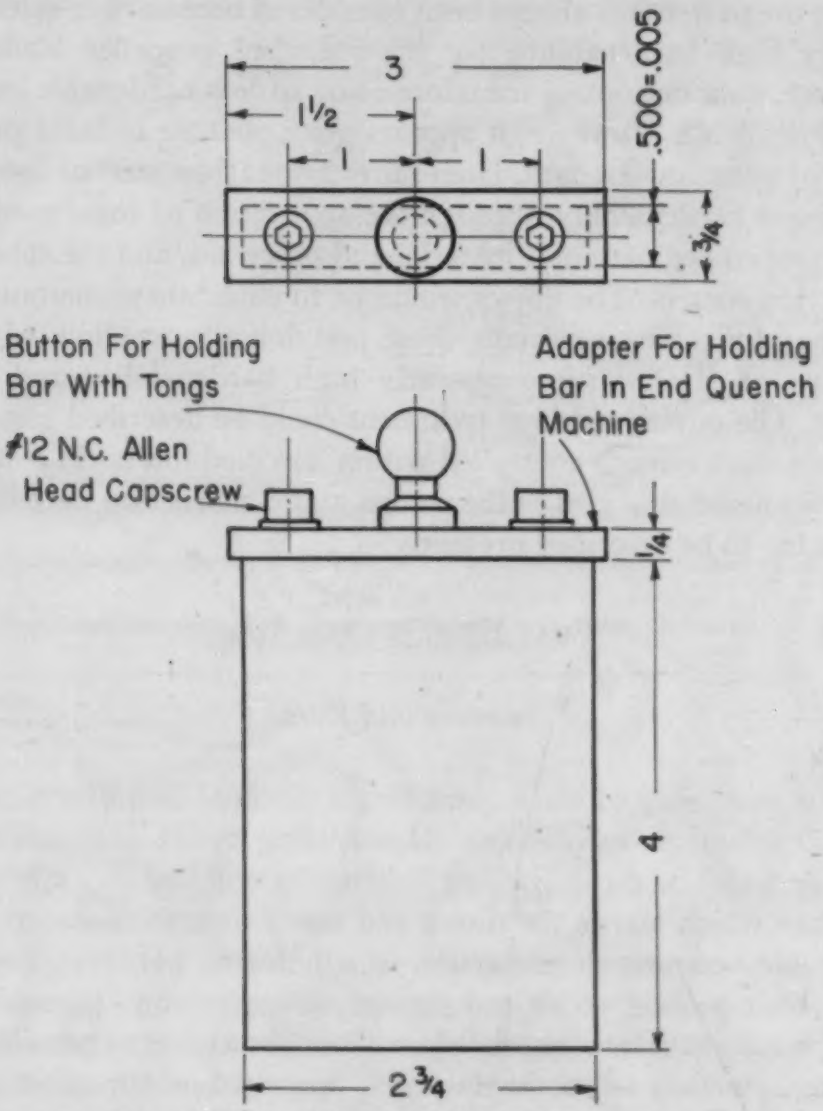


Fig. 10—Design of ½-Inch Thick Flat End-Quench Bar.

sents a range of cooling cycles whose width increases as the distance from the quenched end decreases, rather than a single narrow range of cooling cycles of negligible width. However, through the use of ⅛-inch diameter specimens and properly staggered test positions on duplicate test series, this disadvantage can be partly alleviated.

The procedure used in this work is illustrated by Fig. 10, showing the design of the specimen; Fig. 11, showing the quenching jet; Fig. 12, showing the end quenching of a flat specimen; and Fig. 13, showing how the original bars were sectioned after end quenching in order to study possible hardness variations across the specimens due to the edge-effect. Table III shows a series of hardness results obtained on

Table III
Rockwell C Hardness Survey on Flat End Jominy Bars

Dist. From Quenched End Inches	Outside Hardness							Inside Hardness					Deviation Between Avg. Inside & Avg. Outside
	Bar A	Bar B	Bar C	Bar D	Bar E	Deviation	Average	Bar A	Bar C	Bar E	Deviation	Average	
1/16	50.5	50.0	50.0	50.0	50.0	0.5	50.0	49.0	49.5	49.5	0.5	49.5	0.5
3/16	49.0	49.5	49.5	49.5	50.0	1.0	49.5	50.0	49.5	49.0	1.0	49.5	0.0
5/16	49.5	49.0	49.5	48.5	49.0	1.0	49.0	50.0	49.0	49.0	1.0	49.5	0.5
1/4	49.0	49.0	49.0	48.0	49.0	1.0	49.0	49.5	49.0	49.0	0.5	49.0	0.0
5/16	48.0	48.5	49.0	48.0	48.5	1.0	48.5	49.0	48.5	49.0	0.5	49.0	0.5
3/8	48.0	48.5	48.0	48.0	48.5	0.5	48.0	48.5	48.0	48.5	0.5	48.5	0.5
7/16	48.0	48.0	47.5	47.0	48.0	1.0	47.5	48.0	47.5	48.0	0.5	48.0	0.5
1/2	47.5	47.5	46.5	46.5	46.5	1.0	47.0	47.5	46.5	47.5	1.0	47.0	0.0
9/16	46.5	46.0	45.5	45.5	46.5	1.0	46.0	47.0	45.0	47.0	2.0	46.0	0.0
5/8	46.0	45.0	44.0	44.5	45.0	2.0	45.0	45.5	45.0	45.5	0.5	45.5	0.5
11/16	45.0	44.5	43.5	43.0	43.0	2.0	44.0	45.0	43.0	44.5	2.0	44.0	0.0
3/4	43.0	42.5	43.0	41.5	41.5	1.5	42.5	42.5	42.0	43.0	1.0	42.5	0.0
13/16	42.0	41.0	41.5	40.0	41.0	2.0	41.0	41.5	41.5	41.5	0.0	41.5	0.5
7/8	40.5	39.0	40.5	39.0	40.5	1.5	40.0	40.0	41.0	41.0	1.0	40.5	0.5
15/16	38.5	38.0	39.5	38.0	39.5	1.5	38.5	39.0	40.0	40.5	1.5	40.0	1.5
1	37.0	37.5	39.0	37.5	39.0	2.0	38.0	38.0	38.5	37.5	1.0	38.0	0.0
1¼	36.0	36.5	36.0	35.5	35.5	1.0	36.0	37.0	36.5	36.5	0.5	36.5	0.5
1½	35.5	35.0	34.0	35.0	33.0	2.5	34.5	35.0	35.0	34.5	0.5	35.0	0.5
1¾	34.0	34.0	33.5	33.0	32.5	1.5	33.5	33.0	34.5	33.5	1.5	33.5	0.0
2	34.0	34.0	33.5	33.5	33.0	1.0	33.5	33.5	34.0	33.0	1.0	33.5	0.0
2½	32.5	33.5	33.5	32.5	32.5	1.0	33.0	32.5	33.0	33.5	1.0	33.0	0.0
3	33.0	33.0	33.5	32.5	33.0	1.0	33.0	33.0	32.5	33.5	1.0	33.0	0.0
3½	31.0	33.0	32.0	31.5	32.0	2.0	32.0	32.0	32.0	32.0	0.0	32.0	0.0
4	30.0	30.0	30.5	30.5	30.0	0.5	30.0	30.0	30.0	29.5	0.5	30.0	0.0

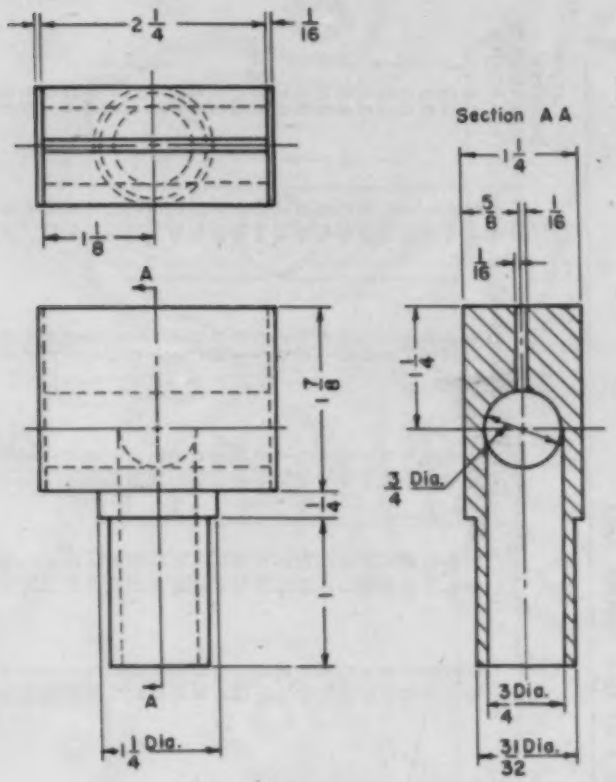


Fig. 11—Quenching Jet for Flat Jominy Bar.

the face of sections A through E of Fig. 13, and on the interior section surfaces, A, C, and E. These data indicate the hardness variations across the specimens to be negligible for the class of materials discussed herein.

The cooling cycles for various distances from the quenched end have been determined for flat bars of SAE 4330 steel and plotted in Fig. 14. In Fig. 15, the half-temperature cooling times obtained in this work have been correlated on the basis of equivalent positions, with the calculated values of Asimow, Craig and Grossmann (12) (whose H-values for the Jominy jet quench and for air cooling were computed from Jominy's experimental cooling curves). Note that the experimental data presented in this paper deviate from Jominy's, giving consistently shorter half-temperature times. Various assumptions regarding the reasons for these deviations have been checked with negative results. It has been thought, for instance, that heat might have been carried away by the 20-gage thermocouple wires, causing faster curves than would be obtained with finer wires. Three determinations using (a) 20-gage (0.032-inch diameter), (b) 22-gage (0.025-inch diameter), (c) 28-gage (0.012-inch diameter) couples at the 1-inch



Fig. 12—End Quenching of Flat Jominy Bar.

station gave very nearly one and the same curve. See Fig. 16, showing the extremely good agreement between the three curves.

Another theory would ascribe these faster cycles to better pro-

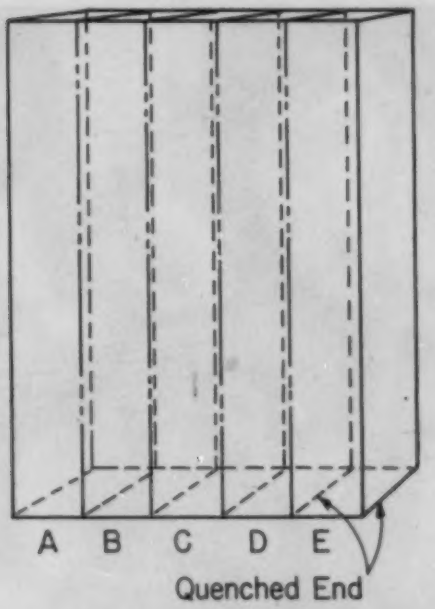


Fig. 13—Sectioning of Flat End-Quenched Bar to Test Hardness Distribution.

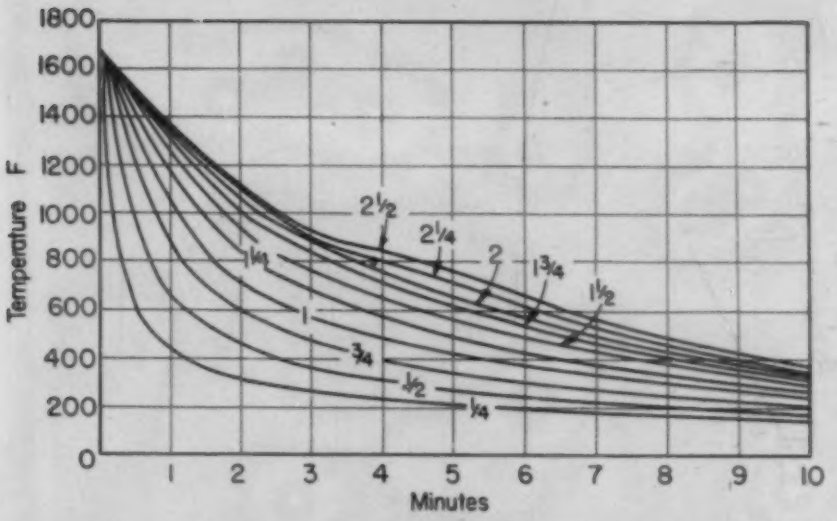


Fig. 14—Cooling Cycles of Various Distances From Quenched End of Flat Jominy Bar.

tection against scaling during the heating period, the present experiments having been performed in a very carefully controlled atmosphere, such as employed for experimental propeller blades (13). But according to Morse Hill (8), slower cooling due to scaling would be noticeable only in the air-cooled end. However, Hill (8) reported that the Materiel Center's cooling curves also were faster than Jominy's. His data show some scatter and his curve seems to favor the points on the high side

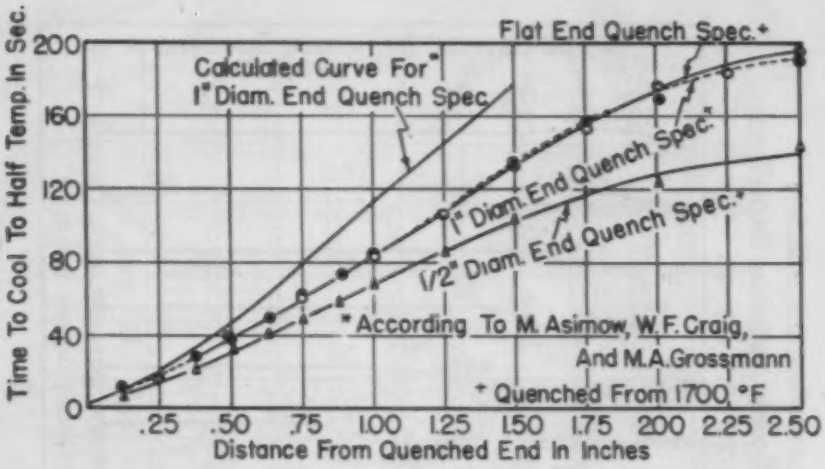


Fig. 15—Half-Temperature Cooling Time for ½-Inch Diameter, 1-Inch Diameter, and Flat End-Quench Bar Plotted With Asimow, Craig and Grossmann's Theoretical Half-Temperature Times, Based on Data by Jominy (12).

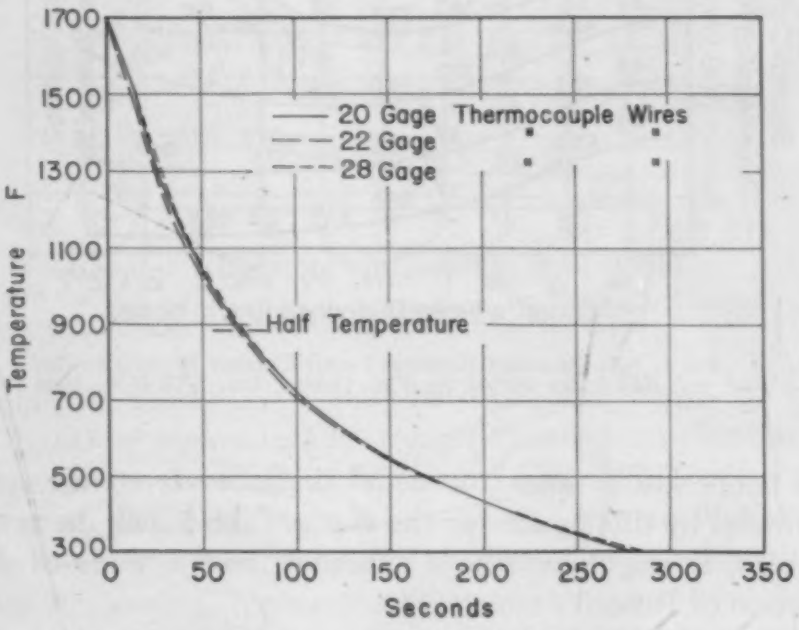


Fig. 16—Cooling Curves at Surface of ½-Inch Diameter Jominy Bar 1 Inch From the Quenched End Using Three Different Gage Thermocouples.

of the scatter band. Although it is rather obvious that the curve should show a tendency to become asymptotic to a finite half-temperature time, both Asimow, Craig and Grossmann's, and Hill's curve show a steep slope toward the far end; Hill's curve in that region goes through the highest experimental point, disregarding several others.

The data contained in this report can be converted to the older cooling curves if desired, or vice versa, by the use of Fig. 15. It is believed important enough to point out the almost exact similarity of

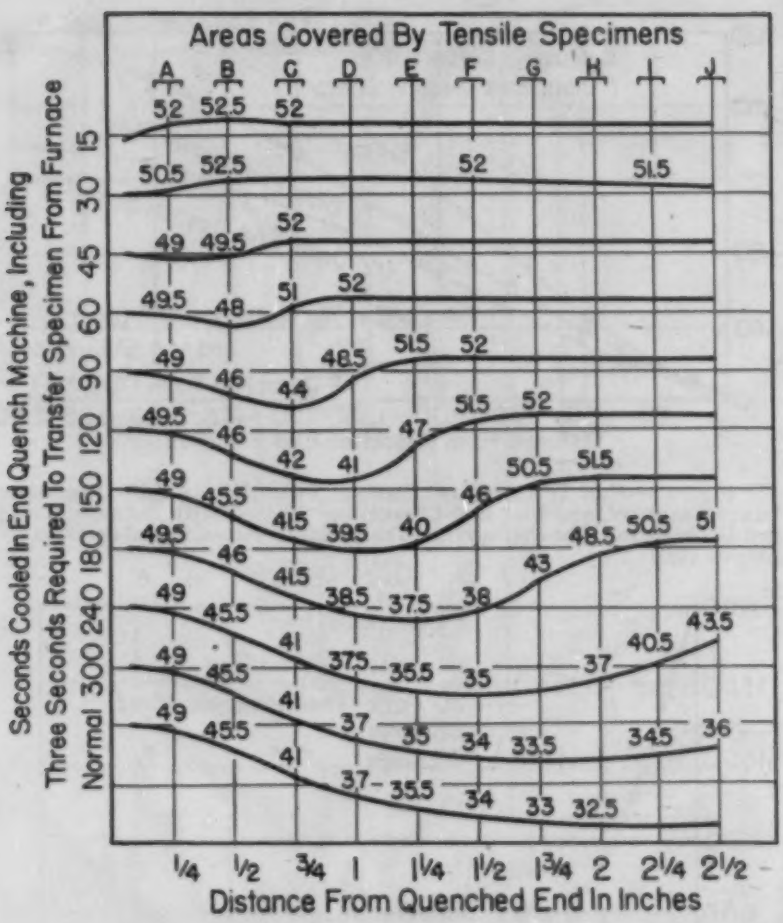


Fig. 17—As-Quenched Hardness Versus Distance From Quenched End and End-Spray Period for Flat Jominy Bar, SAE 4330, Heat No. 3801.

the half-temperature times for equal distances from the quenched end, indicated by this figure for the flat and the 1-inch diameter end-quench bars, as might have been expected from a study of Austin's reproduction of Russell's tables (14).

Discussion

The first experimental results on specific mechanical properties of SAE 4330 steel, obtained from flat end-quench bars, immersion-quenched after various end-spray periods, have been plotted in Figs. 17, 18, 19 and 20. These results have been included to give an idea of the usefulness of this test method. To begin with the "normal" Jominy curves, which for this steel and specimen type are quite similar to the curves resulting from a 300-second end-spray period, the observations taken from Figs. 17 to 20 and listed in Table IV are of interest.

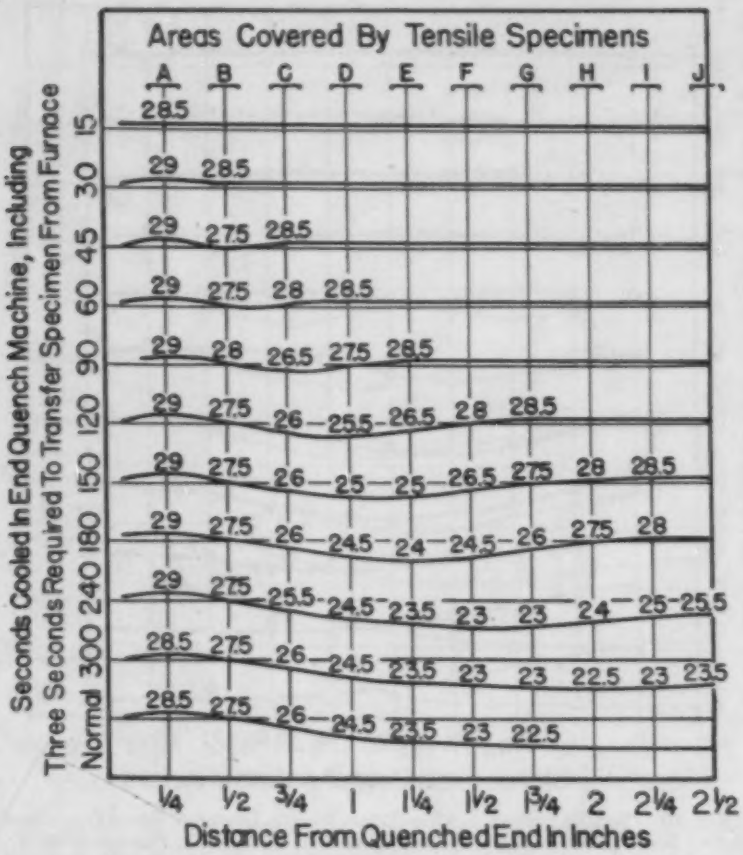


Fig. 18—Hardness After Draw Versus Distance From Quenched End and Spray Period, ¾-Inch Flat Bar, SAE 4330, Heat No. 3801.

Table IV shows that a fully hardened and drawn structure had about 18,000 psi higher tensile strength than a normalized and drawn structure, when the draw temperature was 1120 F (605 C). The tensile strength for both conditions was 11,000 psi higher than the yield strength, and the hardness of the hardened and drawn steel was 6 points Rockwell C higher than that of the normalized and drawn steel. Bear in mind that, in accordance with Fig. 8, the normalized steel contained at least 50% ferrite. For a less highly alloyed steel, the

Table IV

Location Condition	Quenched End Fully Quenched	Air-Cooled End "Slack-Quenched" (1" dia. air-cooled)
Hardness, before draw	Rockwell C-50	C-32.5
after draw	Rockwell C-28.5	C-22.5
Amount of softening in draw	21.5 points Rc	10 points Rc
Tensile after draw (1120° F.)	134,000 psi	116,000 psi
Gain through hardening	18,000 psi	....
Yield after draw*	123,000 psi	105,000 psi
Gain through hardening	18,000 psi	....

*At 0.2% offset.

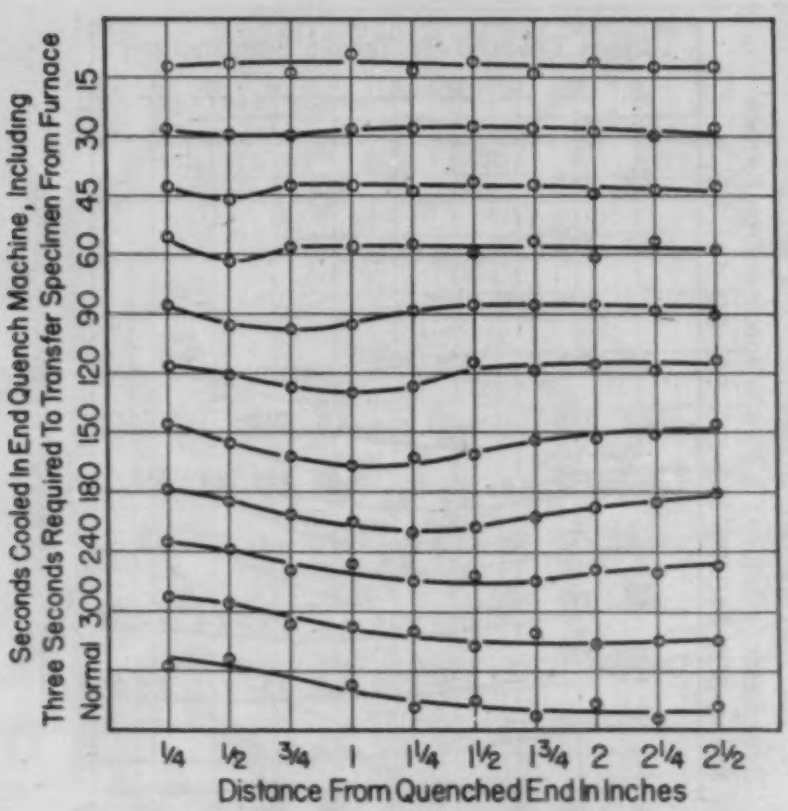


Fig. 19—Tensile Strength After Draw Versus Distance From Quenched End and End-Spray Period (½-Inch Flat Bar, SAE 4330, Heat No. 3801). Abscissas shown in the graphs are at 130,000 psi. Scale: Height of block 20,000 psi.

differences in properties due to variations in the cooling cycle would, of course, have been much greater. Note that heat 3801 had insufficient hardenability and carbon hardness to meet the specified minimum tensile of 130,000 psi after a 1120 F (605 C) draw (the standard draw temperature is 1140 F) when the quench delay exceeded 30 seconds.

From the immersion-quenched bars, it was observed that whereas, the hardness, tensile strength, and yield point varied consistently with the cooling cycle and quench delay or spray period, the reduction of area and per cent elongation appeared independent of these factors within the range studied. All the ductility data, therefore, were thrown together and plotted in the form of histograms shown in Figs. 21 and 22. The means of the distribution were 68.4% for the reduction of area and 20.2% for the per cent elongation, and the standard deviations 1.52 and 1.06, respectively. Hence, it appears that these properties were affected but slightly if at all by the variations in cooling cycles. It should be remembered, however, that the steel had been drawn before testing; had it been tested in the quenched condition, the story might

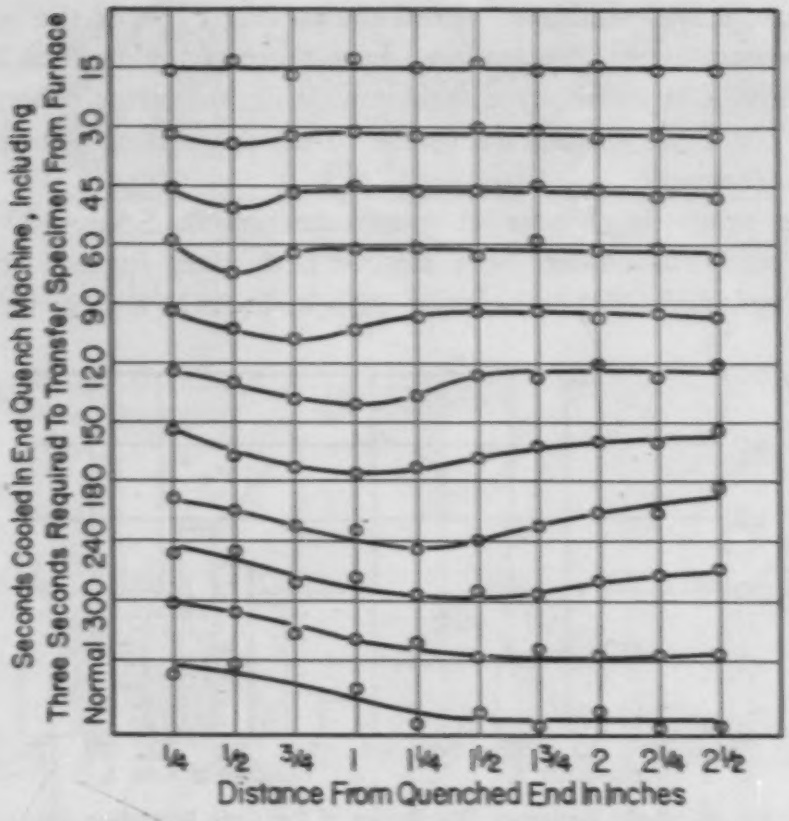


Fig. 20—Yield Point After Draw Versus Distance From Quenched End and Spray Period (¾-Inch Flat Bar, SAE 4320, Heat No. 3801). Abscissas shown in the graphs are at 125,000 psi. Scale: Height of block 20,000 psi.

have been different. The ductility might have shown a minimum for certain cooling cycles, corresponding to that observed by Gensamer in steel which had been reacted isothermally at certain intermediate temperatures (15).

Isothermal Reactions Preceded by Gradual Cooling

Procedure and Results

The observed lack of agreement between the progress of bainite transformation in postheated weldments and isothermally transformed specimens of the same steel (16) suggested the experimental study of isothermal reactions preceded by gradual cooling to the isotherm. The experimental procedure can obviously be varied within wide limits. For instance, small specimens can be austenitized in one furnace and transformed in another, or they can be cooled in one and the same furnace from the austenitizing temperature to the isotherm and then withdrawn and quenched at appropriate time intervals. With the former

procedure, it is desirable to record the cooling cycle of the specimens with a separate recorder operated by a thermocouple which has been peened into a representative specimen. With the latter procedure the furnace chart will contain the record of the approximate cooling cycle to the isotherm.

The progress of pearlite transformation in SAE 4330 steel at various temperatures has been studied both after furnace cooling to the isotherm and after transfer of the specimens to a separate furnace

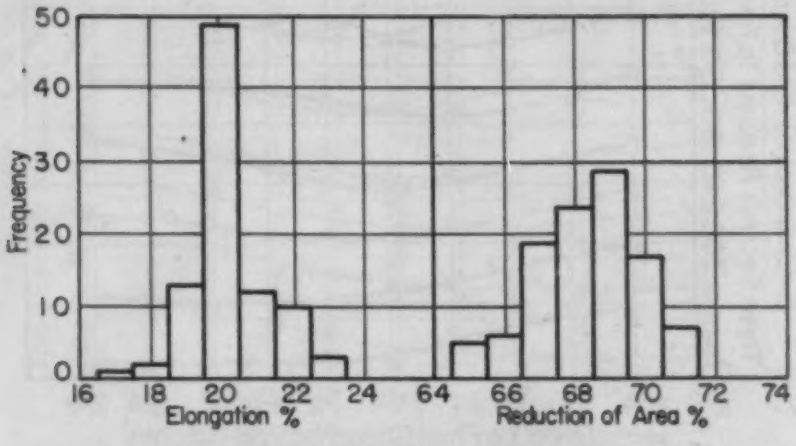


Fig. 21—(Left) Frequency Distribution of Per Cent Elongation Data.
Fig. 22—(Right) Frequency Distribution of Reduction of Area Data.

held at the reaction temperature. At 1200 F (650 C), this steel has been found to react very nearly in the time predicted by the SAE 4340 S-curve, an observation not made fully clear in Reference 16. Therefore, it is considered probable that apparent discrepancies in reaction time observed at other adjacent temperatures have been due to the very rapid change in slope of the end-of-reaction curve above as well as below 1200 F (650 C). As the distance above or below this temperature of minimum reaction time increases, the time to completion becomes increasingly sensitive to temperature deviations and the curve becomes increasingly difficult to locate with a high degree of precision.

In the bainite region, the time to complete reaction has been studied through the transfer of ½-inch cube specimens to a furnace maintained at the transformation temperature. In this region, ferrite rejected during the cooling cycle very effectively retarded the completion of the reaction. This effect is illustrated in Fig. 23, which has been reproduced from an article by Liedholm and Coons (16). This figure shows the end-of-transformation lines for SAE 4340 and 4360, reproduced from U. S. Steel Corporation's "Atlas of Isothermal Trans-

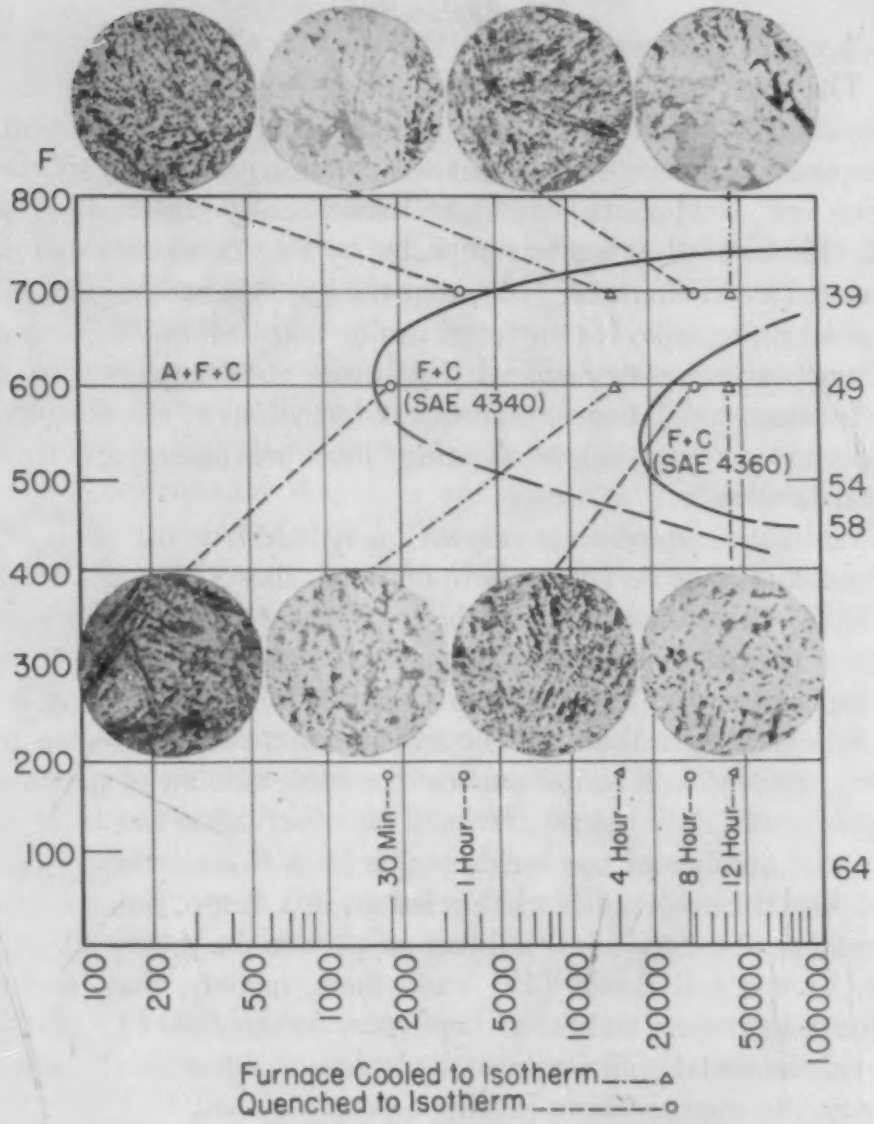


Fig. 23—Effect of Gradual Cooling Versus Quenching Upon the Total Reaction Time In the Bainite Region.

formation Diagrams" with photomicrographs inserted by the author and W. C. Coons. The micrographs of isothermally transformed SAE 4330 specimens which had been quenched to the 700 and 600 F isotherms showed reaction times of about 60 and 30 minutes, respectively, which is well within the limits predicted from the SAE 4340 S-curve. But when the specimens of the same steel were cooled slowly to either isotherm, transformation was still incomplete at both temperatures after 12 hours. At the lower temperature, transformation in that time had progressed further than at the higher, but was still far from completed, even though the time in this instance had been increased by a factor of 24.

Applications

The most direct application of these experimental studies is the postheating of weldments. The results reported above reveal some widespread misconceptions about the metallurgical effect of the postheating of weldments of high hardenability materials such as SAE 4330 or 4340. It has been reported by Pugacz and associates (17), and stated by Williamson (18), that the approximate minimum effective postheating time for any steel can be taken from the S-curve, and that postheating so determined will insure the completion of bainite transformation and, hence, prevent the formation of martensite during cooling after completed postheating, thus preventing the formation of "hard cracks".

While these statements very well may hold true for steels of lower hardenability, they do not apply to materials like SAE 4330. Reference to Fig. 23 shows that it would be impractical and perhaps useless to postheat this steel until completely transformed above M_s, but nevertheless, hard cracks in this material can be eliminated by postheating 3 to 4 times longer than the S-curve reaction time. After such postheating, the steel will contain almost the same amount of martensite as not postheated steel but no cracks. This observation has been verified on a large number of test welds prepared in this laboratory and it is hoped that the evidence can be presented in a future publication. This observation does lend some indirect support to the theory advanced by Hoyt, Simms and Banta (19) and others, namely, that hard cracks are due to hydrogen, and the main purpose accomplished by postheating is to rid the metal sufficiently of hydrogen to allow martensite transformation to occur without causing cracks.

Summary

1. A method for the construction of partial continuous cooling transformation diagrams has been presented and discussed.

2. Various applications of continuous cooling transformation diagrams have been discussed.

3. Data obtained by this method on the effect of rejected ferrite upon the endurance, tensile properties, impact strength, and hardness have been presented for SAE 4330 steel.

4. An attempt to estimate the tensile strength of SAE 4330 steel with various percentages of rejected ferrite, using Gensamer's method

(10) of evaluating the strength of ferrite, has resulted in good agreement with experimental data.

5. A flat end-quench bar with suitable quenching fixture permitting the correlation of cooling cycle with tensile properties as well as hardness has been developed and described.

6. Cooling curves have been obtained and presented for various distances from the quenched end of the flat Jominy bar.

7. Half-temperature cooling times based upon determinations performed in the Engineering Materials Laboratory, Curtiss-Wright Corporation, Propellet Division, have been plotted against older data (12) for the ½-inch diameter by 4-inch long Jominy bar used for the cooling transformation diagrams and also for the standard 1-inch diameter Jominy bar and the new flat end-quench test.

8. Data have been presented on the reproducibility of the cooling curves obtained by this laboratory.

9. Isothermal transformations preceded by slow cooling have been investigated in the pearlite and bainite regions of SAE 4330 steel.

10. It has been found that the pearlite reaction remains practically unaffected by prior slow cooling but the effect of such cooling upon the time to completion in the bainite region is very great. The completion of transformation in this region progresses so slowly when the steel has cooled gradually to the isotherm that it is impractical to prevent martensite formation during the final cooling by transformation just above M_s.

11. The S-curve, hence, has been shown to invite misinterpretation of the time-to-completion of the reaction in the bainite region of steels of high hardenability which have cooled slowly to isotherms located above but fairly near the M_s temperature.

12. Experimental results of the kind presented herein are desirable supplements to S-curves and Jominy tests in that they amplify the information obtained by those methods.

Acknowledgments

The author wishes to thank the following present or past members of the Engineering Materials Laboratory's staff for their important contributions to this work: A. I. Rush and Miss S. E. Lopez who have contributed many original ideas and produced most of the experimental data through faithful and painstaking labor; and W. C. Coons who performed the majority of the metallographic studies.

References

1. W. E. Jominy, "Hardenability Tests," ASM Symposium on Hardenability of Alloy Steels, American Society for Metals, 1938, p. 66-87.
2. E. S. Davenport and Edgar C. Bain, "Transformation of Austenite at Constant Subcritical Temperatures," *Transactions*, American Institute of Mining and Metallurgical Engineers, Iron and Steel Division, Vol. 90, 1930, p. 117-114.
3. C. A. Liedholm, "Continuous Cooling Transformation Diagram from Modified End Quench Method," Metal Progress, Vol. 45, No. 1, January 1944, p. 94-99.
4. C. A. Liedholm, "Transformation of SAE 4330 During Continuous Cooling," Metal Progress, Vol. 45, No. 6, June 1944, p. 1110-B.
5. C. A. Liedholm, A. I. Rush and D. J. Blickwede, "Transformation of NE 8630 During Continuous Cooling," Metal Progress, Vol. 46, No. 3, September 1944, p. 496-B.
6. C. A. Liedholm, S. E. Lopez and W. C. Coons, "Transformation of S. A. E. X-4130 During Continuous Cooling," Metal Progress, Vol. 46, No. 5, November 1944, p. 1096-B.
7. C. A. Liedholm, S. E. Lopez and D. J. Blickwede, "Transformation of S. A. E. 4315 During Continuous Cooling," Metal Progress, Vol. 48, No. 4, October 1945, p. 696-B.
8. Morse Hill, "The End Quench Test Producibility," Transactions, American Society for Metals, Vol. 31, No. 4, December 1943, p. 922-937.
9. C. A. Liedholm, "Diagram of Transformation During Continuous Cooling of Steel (A Necessary Guide for Propeller Heat Treatment)," Metal Progress, Vol. 46, No. 5, November 1944, p. 1097-1101.
10. M. Gensamer, "Strength and Ductility," Metal Progress, Vol. 49, No. 4, April 1946, p. 731-734.
11. C. A. Liedholm and W. S. Bath, "Carbon Content of S. A. E. 4330 Type Steel Versus Weld Crack Sensitivity Represented by Tensile Ductility and Impact Strength of Hardened Specimens," Metallurgical Memorandum Report No. 426, Engineering Materials Laboratory, Curtiss-Wright Corporation, Propeller Division, May 11, 1945. Not published.
12. M. Asimow, W. F. Craig and M. A. Grossmann, "Correlation Between Jominy Test and Quenched Round Bars," *Journal*, Society of Automotive Engineers, Vol. 49, No. 1, p. 283-292.
13. C. A. Liedholm, "Atmosphere Calibration for Heat Treating Airplane Propellers," Metal Progress, Vol. 49, No. 4, April 1946, p. 744-749.
14. J. B. Austin, "The Flow of Heat in Metals," American Society for Metals, 1942, p. 122-138.
15. M. Gensamer, E. B. Pearsall, W. S. Pellini and J. R. Low, Jr., "The Tensile Properties of Pearlite, Bainite, and Spheroidite," Transactions, American Society for Metals, Vol. 30, No. 4, December 1942, p. 983-1019.
16. C. A. Liedholm and W. C. Coons, "Effect of Cooling Transformation Upon Subsequent Isothermal Reactions," Metal Progress, Vol. 46, No. 1, January 1946, p. 104-107.
17. Myron A. Pugacz, Geoffrey J. Siegel and Jay O. Mack, "The Effect of Postheat in Welding Medium Alloy Steels," *The Welding Journal*, Vol. 23, No. 10, October 1944, p. 536-S—544-S.
18. Arthur J. Williamson, "Effect of Recent Research on the Weldability and Control of the Production of Steel Aircraft Tubing," *The Welding Journal*, Vol. 24, No. 10, October 1945, p. 485-S—496-S.
19. S. L. Hoyt, C. W. Sims and H. M. Banta, "Metallurgical Factors of Underbead Cracking," *Metals Technology*, Vol. 12, No. 4, June 1945.

THE INTERRUPTED QUENCH AND ITS PRACTICAL ASPECTS

By Howard E. Boyer

Abstract

The generally recognized advantages of martempering as applied to treatment of low and medium carbon alloy steels may also be obtained with steels of the higher carbon types. Under certain conditions, however, the higher carbon steels exhibit a susceptibility to cracking not found in the other types during martempering nor in the high carbon steels when treated by the more conventional method of direct oil quenching from the austenitizing temperature.

This paper is a treatise on the interrupted quench only and does not in any way deal with isothermal transformation. The author's work on tempering the alloy carburizing steels is briefly reviewed though principal attention is given to the results of development work which has been done on the higher carbon low alloy steels. SAE 52100 ball bearing type steel was selected for study after it was found to give results somewhat adverse to those which might be logically expected from the martempering practice.

Introduction

MARTEMPERING, which is the accepted term applied to the interrupted quenching method of hardening certain types of steels, has been received with increasing popularity since the start of World War II. Most metallurgists and heat treaters are quite familiar with the mechanics of this process which, briefly, consist of quenching rapidly from the austenitizing temperature past the knee of the S-curve to some temperature slightly above the Ms point where the parts, if properly quenched, will still be austenitic. After equalizing at the temperature of the quenching medium, parts are allowed to cool slowly to room temperature. During cooling from Ms to Mf, martensite is formed at a fairly uniform rate throughout the section, since the temperature from outside to center had been equalized just

A paper presented before the Twenty-eighth Annual Convention of the Society held in Atlantic City, November 18 to 22, 1946. The author, Howard E. Boyer, is chief metallurgist, American Bosch Corp., Springfield, Mass. Manuscript received May 8, 1946.

above the Ms point. The practical advantages of this process, which theoretically can be applied to any steels which can be hardened by quenching in oil and even in some cases to steels which normally require a water quench, are well known. It is obvious that less deformation will be encountered by taking advantage of the interrupted quench and certainly, by all logical reasoning, the finished parts should contain less unbalanced residual stresses, so that premature failures should be fewer.

The author's original work with this process dates back about three years. At that time, we were doing a great deal of development work on the carburizing and hardening of high alloy carburizing steels. It was proved conclusively that alloy steels of the carburizing types could be martempered not only with less deformation, less retained austenite and with cleaner surfaces, but also that the process was much cheaper, since a long diffusion cycle after gas carburizing as well as difficult cleaning operations could be eliminated.

After this process worked out to such advantage for the alloy carburizing steels, we began to apply it to the medium carbon alloy types such as SAE 4140 and 6150 with equally desirable results. With entire absence of failures up to this point, it was understandable that we came to regard martempering as a "cure all" and to apply it to other steels of the oil hardening types.

No difficulty was encountered until we attempted to martemper SAE 52100 steel on a mass production basis but after a short time we encountered cracking on a large scale making it necessary to discontinue the process immediately for this particular steel. Investigation showed, surprisingly, that parts made from the same bars and austenitized under the same conditions would not crack when quenched in oil, but would show extremely bad cases of stress-cracking either immediately after the air cool from the salt quench or during the subsequent tempering operation.

Such findings started an investigation which has been carried on over several months. The problem, for practical purposes, has been entirely solved though there is apparently a great deal yet to be learned about applying the interrupted quench to steels of the high carbon types. The author frankly admits that some of the conclusions given in this paper are based on limited development work, so that the door is left open for further research. It is to be hoped that the data given will not only be of practical value to others who use or hope to use martempering but also that they will invite further

efforts to obtain fundamental information on a process which promises to be extremely valuable.

Procedure of Investigation

After it was definitely proved that, at least under certain conditions, SAE 52100 steel was more susceptible to cracking when martempered than when treated by the more conventional method of oil quenching, a rather elaborate program of investigation was immedi-

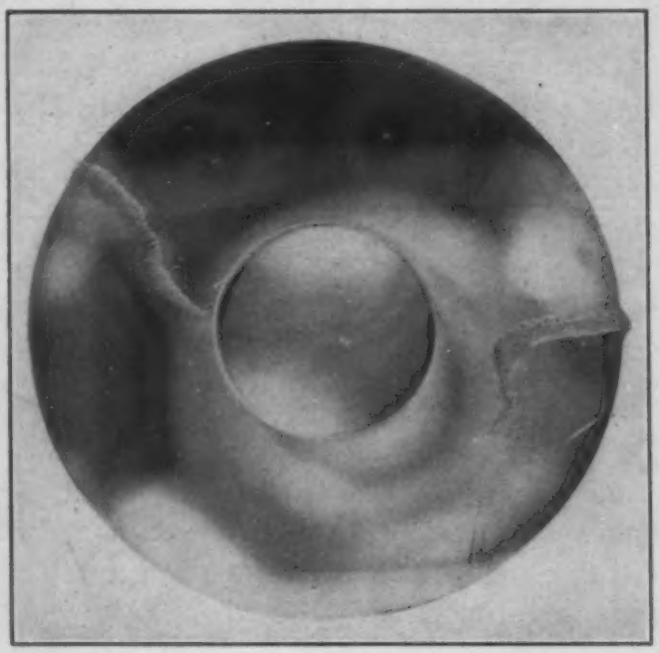


Fig. 1—Photograph of Cylinder Made of SAE 52100 Steel, Cracked in Martempering. Actual size.

ately planned. This project was set up in an attempt to learn what condition or combination of conditions had caused such very unexpected results. In order to make this project quite complete, it was necessary to give consideration to all of the possible variables which normally occur in heat treatment and, in addition, the variables added by this relatively new method of quenching.

Fig. 1 well illustrates the type of cracks which were encountered. This photograph is an end view of a hardened cylinder, approximately actual size. This test piece was austenitized in an atmosphere-controlled furnace at 1550 F (845 C), quenched in an agitated salt bath at 450 F (235 C), held for 7 minutes and cooled in air to room temperature. The cracking occurred a few minutes after the piece

had reached room temperature. The magnaflux indications show the crack-pattern very clearly.

The various factors which were thought to have some possible bearing on the cracking and which were thoroughly investigated singly, as well as in some combinations, are listed as follows:

1—Chemical composition of the steel.
2—Microstructure of the bar steel.
3—Carburizing atmospheres.
4—Decarburizing atmospheres.
5—Overheating.
6—Underheating.
7—Effects of agitation in martempering bath.
8—Chemical composition of salt quenching bath.
9—Ms point location.
10—Hardenability—martempering versus oil quenching.
11—Holding time in the martempering bath.
12—Cooling rate from martempering bath.
13—Percentage of retained austenite—martempering versus oil quenching.

Results which have been obtained upon the investigation of these various factors as listed above are discussed individually in the following paragraphs. Again it should be stated that the results are given exactly as we have found them so far, though further research might possibly cause some of the conclusions given later in this paper to be altered, or at least modified.

Discussion of Investigations and Results

Chemical Composition of the Steel—Since SAE 52100 will usually harden completely through a 1-inch round section after oil quench, it is generally classed as a deep hardening steel. The deeper hardening steels are usually more sensitive and susceptible to cracking from mishandling or changes in chemical composition. It was logical therefore to suspect that either some of the specified elements were outside prescribed limits or that possibly some unsuspected residuals had reached high percentages. Chemical analysis was made on test pieces which had cracked from martempering in comparison to others which were hardened by oil quenching and did not crack. Carbon, chromium and other specified elements were found to be well within the commercial limits. Spectrographic analysis showed

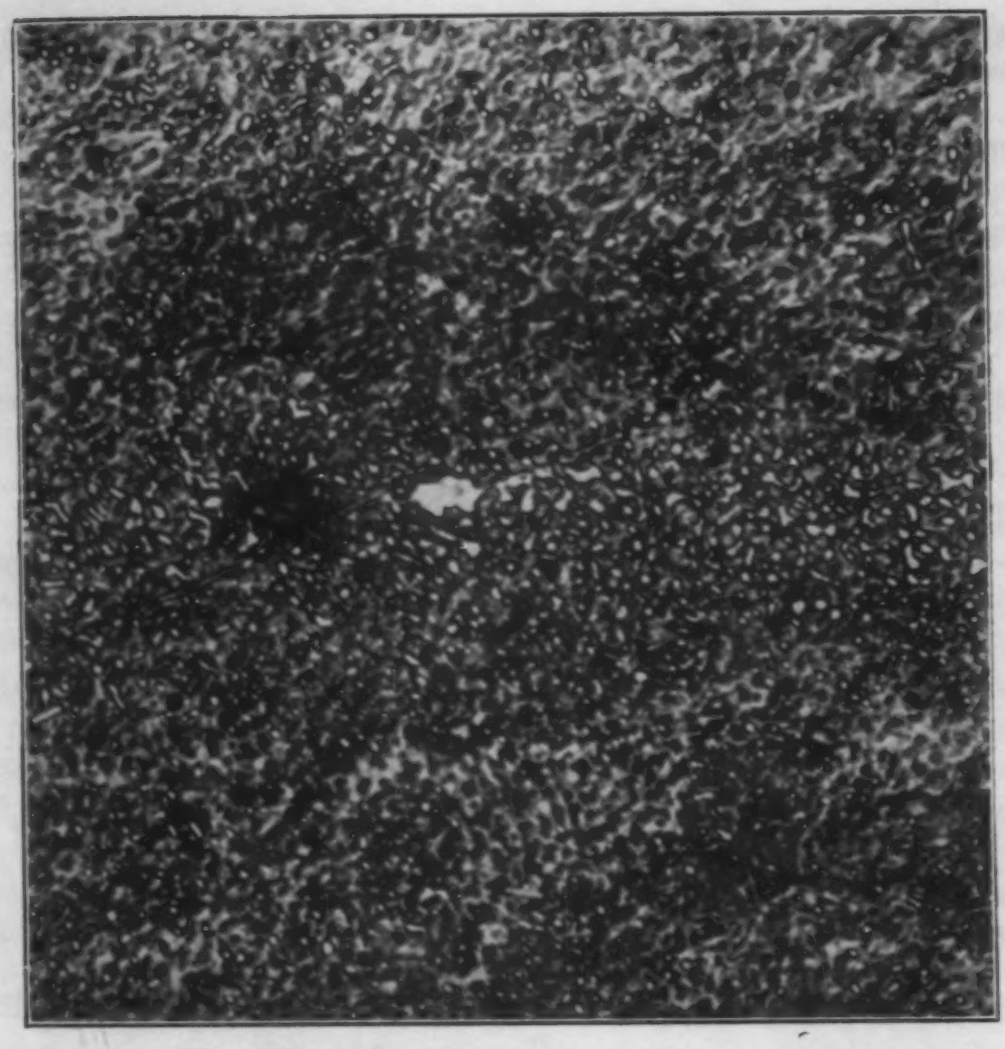


Fig. 2—Carbide Segregation in Hardened SAE 52100 Steel. Vilella's martensitic reagent. × 1000.

only small residuals of molybdenum and copper. The nickel content was found to be less than 0.15% which would not be considered as harmful. After such investigation it seems logical to conclude that the chemical composition indicated no reason for increased tendency to stress cracking by the martempering process.

Microstructure of the Bar Steel—Metallurgists and heat treaters who are accustomed to processing steels of this type are thoroughly acquainted with the dangers involved from heat treating parts made from steels of varying microstructures. Microstructures having carbide banding, lamellar pearlite, or coarse carbides are all far more susceptible to cracking than the more desirable finely spheroidized structures. Many pieces were examined by means of the metallurgical microscope. None was found which could generally be re-

garded as extremely undesirable though some did show more than normal carbide segregation.

Fig. 2 is a photomicrograph of a longitudinal section out from the cracked cylinder pictured in Fig. 1. This specimen was electrolytically polished and etched in Vilella's reagent. Many of the oil-quenched specimens showed conditions equivalent to this, but no cracking, so that no definite conclusions could be drawn as to why cracks should result from one type of quench and not from the other.

Carburizing Atmospheres—In order to determine just what effects a carburized surface might have on conditions after quenching we heated a large group of test pieces in an extremely rich atmosphere of cracked dipentene 1550 F for an abnormally long time. The pieces were carburized quite heavily as was shown by microscopic examinations. The surface showed a grain boundary outline of cementite to a depth of 2 to 3 grains. One half of this group of pieces were quenched in oil while the other half were martempered in the normal manner. No cracks were found from either type of quench. Though, of course, such malpractice would not be recommended, it certainly did indicate that carburizing was not a factor worthy of consideration as a possible answer to the problem.

Decarburizing Atmospheres—Although decarburized parts have usually been thought to be less rather than more susceptible to cracking it was felt that to complete the investigation this possibility should also be thoroughly checked. A group of test pieces was heated in the normal manner except that the prepared atmosphere was shut off entirely, so that the pieces were scaled and showed almost complete decarburization to a depth of 0.010 to 0.015 inch. As in the case of the carburizing experiment, one half were quenched in oil while the others were martempered in the normal manner. No cracks were found by either method of quench, so that no further investigating was done along this line. This merely proved decarburization to be undesirable for the well known reasons, but apparently does not increase the sensitivity to cracking.

Overheating—The practice of holding the higher carbon steels at the austenitizing temperature for extremely long periods of time or at temperatures higher than necessary has long been agreed upon to be detrimental, at least for most practical purposes. It is granted that for certain special purposes it may be quite advantageous to austenitize SAE 52100 at temperatures somewhat higher than 1550 F (845 C) in order to obtain a greater percentage of carbide solution

and subsequently a higher Rockwell hardness after the quench. This higher hardness, however, is gained only at the sacrifice of considerable impact value. For example, it has been the author's experience that SAE 52100 austenitized at 1550 F (845 C) quenched in oil and tempered at 250 F (120 C) will result in a hardness of Rockwell C-65 and an impact value of 12 to 15 ft-lbs (unnotched Izod bars). If, however, the austenitizing temperature for the same steel is increased to 1625 F (885 C), quenched in oil and tempered at 250 F the hardness will be about Rockwell C-67 while the impact value will have dropped to 4 to 6 ft-lbs. These conditions are, of course, caused by growth of the austenitic grain and by the matrix being extremely rich in dissolved carbide.

It was in this part of the series of experiments that the author was first able to duplicate the stress-cracking condition illustrated in Fig. 1. By increasing the austenitizing temperature to 1600 F (870 C) or above it was found that a large percentage of the pieces quenched in the martempering bath were cracked after cooling to room temperature while no signs of cracking were found in those heated at the same time, but quenched in oil. Such findings then led to considerable more research work in order that a logical explanation could be found. Results of further work which did offer such an explanation are given later in this paper.

Underheating—While it is usually agreed that heating for periods of time too short or at temperatures too low merely results in low hardness values and shallower hardening, but with increased toughness, it was deemed desirable to explore this possibility also. Various cycles were tried in atmosphere-controlled furnaces as well as a neutral salt bath. Pieces heated for extremely short lengths of time at temperatures of 1450 to 1500 F (790 to 815 C) showed absolutely no signs of cracking irrespective of the type of quench used. Some of these test pieces showed hardness readings of Rockwell C-40 to 60 which indicated that the degree of carbide solution varied over a wide range. Actually the results from this part of the experiment only eliminated one more possible contributing factor.

Effects of Agitation in the Martempering Bath—It is the tendency of SAE 52100 to transform rapidly from austenite when austenitized in the normal temperature range of about 1550 F (845 C). Therefore, when the martempering practice is employed it is necessary to quench into a highly agitated bath, so that the parts will be cooled through the gate of the S-curve, in 3 seconds or less, and

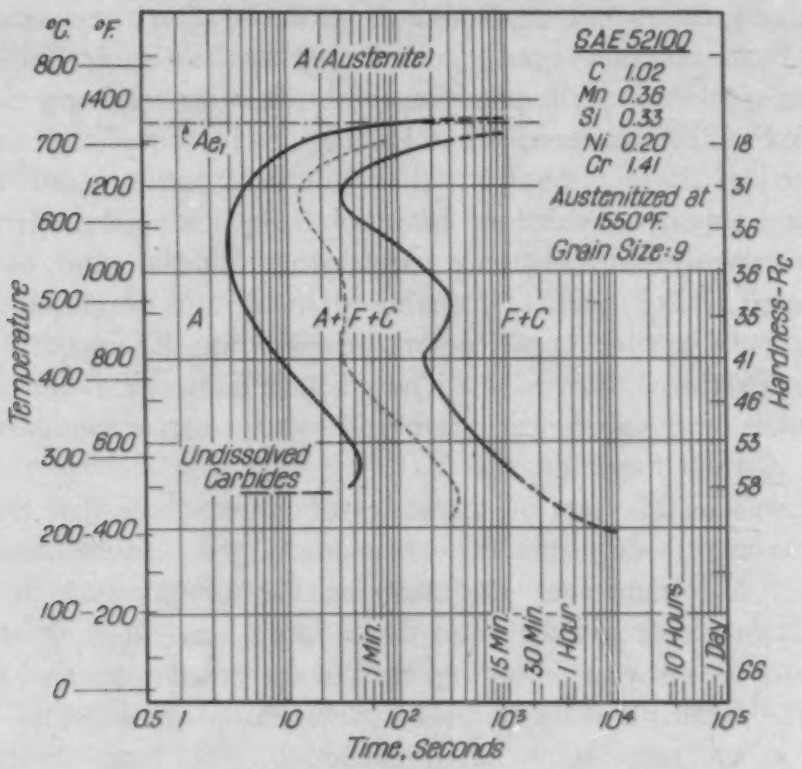


Fig. 3—Isothermal Transformation Diagram for SAE 52100 Steel.*

the formation of pearlite avoided. The S-curve for SAE 52100 austenitized at 1550 F (845 C) is illustrated in Fig. 3 (see footnote*). In order to obtain a cooling rate sufficiently rapid for martempering on a production basis it was necessary to employ vigorous agitation. By using mechanical stirring in combination with dry compressed air, rapid agitation in the vertical as well as the horizontal direction was obtained. It hardly seemed logical that overagitation could be a contributing factor to cracking, since it is, at least theoretically, impossible to cool any steel too fast if the Ms point is not passed. Nevertheless this angle was thoroughly investigated. Results proved conclusively that, all other factors being equal, no greater percentage of cracked specimens could be obtained with vigorous agitation than with mild agitation.

Chemical Composition of Salt Quenching Bath—Since the pattern of cracks obtained on some of the test pieces suggested the possibility of stress corrosion cracking, the condition of the salt in the martempering bath was also thoroughly investigated. Since the bath had been bailed and replenished at regular intervals the possibility

*From Atlas of Isothermal Transformation Diagrams by United States Steel Corp.

of the salt itself being a contributing factor seemed rather remote, but nevertheless worthy of investigation. Analysis of the salt showed it to be slightly on the alkaline side but it was not regarded as being unusual in any respect by the manufacturers of the salt. To prove further that the salt condition was probably not a contributing factor test pieces were quenched into the salt bath at 500 F (260 C) and allowed to remain for periods of time ranging up to 24 hours. Not

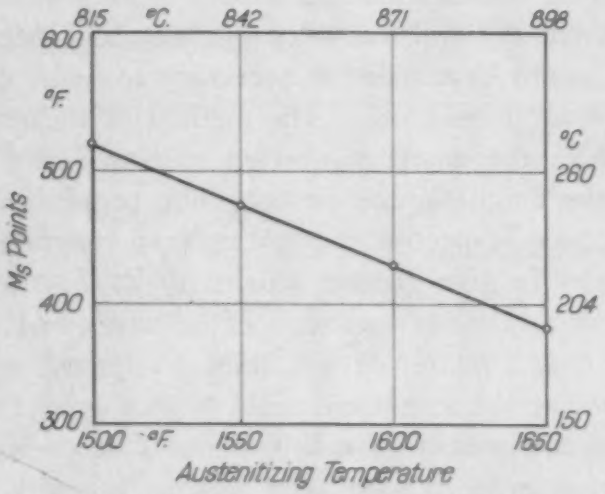


Fig. 4—Effect of Austenitizing Temperature on Ms Point.

in any case did signs of chemical attack appear on the test specimen which might have contributed to cracking.

Ms Point Location—Since the rate of cooling by quenching in salt is extremely rapid it seems logical that cracking might be likely to occur if the temperature of the quenching bath was held below the Ms point. The reasoning in this case is, of course, that if the bath temperature was below the Ms point martensite would start to form before the temperature had become equalized throughout the section and might thus approximate conditions obtained in a direct water or brine quench. After it had been found in previous work that the temperature of the austenite to martensite transformation is very much a function of the austenitizing temperature it seemed necessary to determine the exact Ms point location, as well as to have a clearer conception of the rate of transformation below the Ms point.

Fig. 4 illustrates the result of this investigation. This chart shows Ms point plotted against austenitizing temperature. The author realizes that this line may not be 100% accurate, but should be close enough to meet practical requirements. The Ms points fall

in a straight line for the range of austenitizing temperature 1500 to 1650 F (815 to 900 C). The Ms point for SAE 52100 austenitized at 1500 F (815 C) is shown to be 525 F (275 C) which then decreases to about 375 F (190 C) for an austenitizing temperature of 1650 F (900 C).

The above information was obtained by the use of round test specimens—2 inches long and $\frac{9}{16}$ inch diameter, machined all over and held to close dimensional tolerances. This size was selected merely for convenience and was kept as a standard, because a change in dimensions would have made it necessary to make changes in the equipment used for measuring. The method of measuring the temperature at which the austenite started to transform to martensite was based on the magnetic and nonmagnetic properties of the alpha and gamma phases respectively. A standard magnetic comparator was rebuilt, so as to give greater sensitivity in the measurement of core loss. After adjusting the range of sensitivity of the apparatus it then became only a matter of installing it adjacent to the martempering bath so that the specimen could be removed from the bath, placed in a coil and measured within about 2 seconds. By the use of the specimen described above there was no difficulty in undercooling the test specimens to the temperature of the austenite to martensite transformation thus assuring that they were absolutely austenitic in the martempering bath. One constant austenitizing temperature was selected and the time at this temperature and the time in the martempering bath were kept constant. Specimens were then quenched into the salt bath which was held at a temperature well above the estimated Ms point. This procedure was then repeated except that the martempering bath temperature was lowered in 25 F steps until the temperature was found which showed the specimen to be slightly magnetic when removed from the salt quenching bath. The above procedure was then repeated for each austenitizing temperature in order to obtain the information as shown by Fig. 4. The Ms line in Fig. 4 shows the temperatures above which specimens were found to be absolutely nonmagnetic. It was easily proved by this method that the transformation from austenite to martensite is not abrupt, for even 25 to 50 F below the Ms line specimens were found to have transformed very slightly.

This information does indicate that the temperature of the martempering bath is not extremely critical. Since the transformation is so slow in a specimen quenched somewhat below the Ms point it

hardly appears logical that this practice would be any major contributing cause to cracking.

Hardenability—Martempering Versus Oil Quenching—Since it has long been accepted as a fact that deeper hardening steels are more susceptible to cracking than shallow hardening steels of similar chemical composition, it appeared necessary that the hardenability of SAE 52100 as quenched in oil should be compared with that of the same steel hardened by martempering. Test specimens 1⅜ inch in diameter by 2 inches long were used for securing this information.

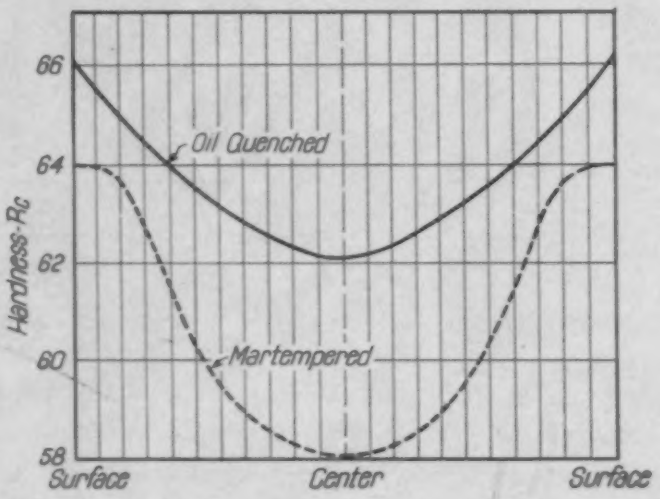


Fig. 5—Hardenability of SAE 52100 Oil-Quenched Compared to Martempered.

The reason in this case for the particular size was to obtain about the minimum size which would not harden throughout the entire section so that an accurate comparison of the hardenability could be made. Fig. 5 illustrates the average results obtained from several tests made by austenitizing the test specimen at 1550 F (845 C) and quenching into an agitated salt bath at 475 F (250 C). As may be observed in Fig. 5 there is not a great deal of difference though the oil-quenched specimens definitely showed a slightly higher surface hardness as well as somewhat greater depth. The oil-quenched specimens showed an average hardness of Rockwell C-66 at the surface and dropped to Rockwell C-62 at the center of the 1⅜-inch diameter. The martempered specimens showed an average surface hardness of Rockwell C-64 which then dropped to Rockwell C-58 in the center of the same size section. As would be expected, both specimens, when examined microscopically, showed fully martensitic structures

near the surface but considerable quantities of the structure commonly known as "quenching pearlite" in the center areas.

Holding Time in Martempering Bath—There have been numerous publications in the past showing the length of time necessary to hold various sizes of parts at the martempering temperature before air cooling. Since, however, such an extensive investigation was carried on, it was found desirable to also check this factor as it may be considered a variable in the martempering process.

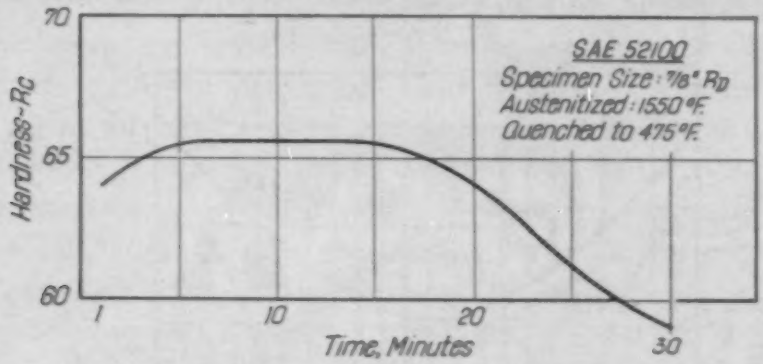


Fig. 6—Effect of Time in Martempering Bath on Hardness.

For this part of the project test specimens 2 inches long by 7/8 inch in diameter were used. The austenitizing temperature of 1550 F (845 C) with, time at the austenitizing temperature and temperature of the martempering bath were held as constants. The varying factor was, of course, the time at 475 F (245 C).

Fig. 6 illustrates the results obtained in holding these specimens for lengths of time varying from 1 to 30 minutes with respect to Rockwell C hardness. It is very apparent from results shown on this chart that the holding time is not critical, at least, with respect to obtaining full hardness. For a 7/8-inch round section it is very apparent that full hardness is possible using any holding time between 5 and 15 minutes. After approximately 15 minutes isothermal transformation begins which, of course, lowers the hardness rather rapidly. There was no indication that variations in the martempering time tended to make any difference in susceptibility to cracking. Of course, if some hardness can be sacrificed, there is no doubt but what parts can be produced which are less susceptible to cracking and much tougher, but this comes from the isothermal transformation to bainite which is not discussed in this paper.

Cooling Rate From Martempering Bath—There is no doubt that parts made of SAE 52100 are extremely sensitive to sudden cooling

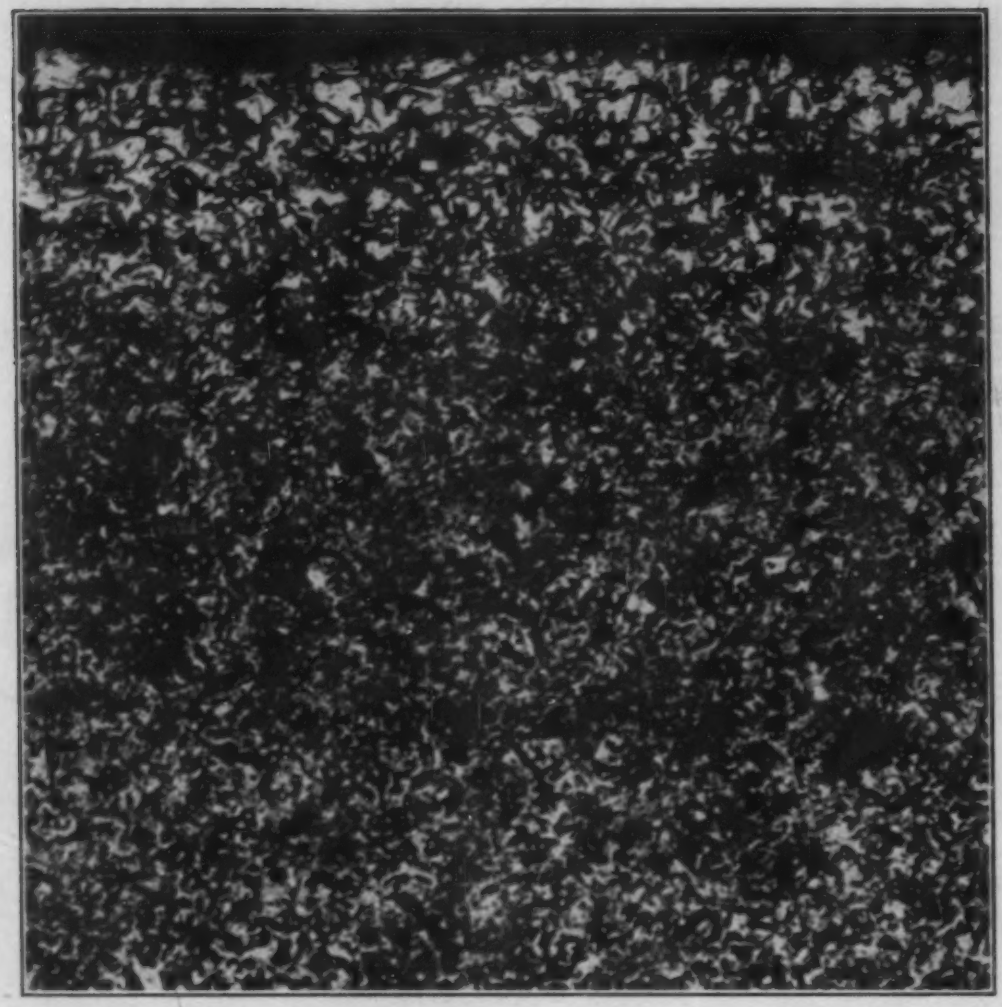


Fig. 7—Carburized Case of E-3316 After Martempering. Vilella's martensitic reagent. × 350.

upon removal from the martempering bath and during the time interval in which martensite is formed. In the martempering of the alloy carburizing steels it has not been an uncommon practice to quench parts into hot water soon after removal from the martempering bath. This is usually done to aid removal of salt. The author has never yet observed the carburizing steels to show any tendency to cracking from this practice. In the case of SAE 52100, however, the situation is entirely changed. It has been found to be extremely dangerous to use any method of cooling which is more rapid than still air. Water quenching from the martempering bath is almost certain to crack parts 100%, while cooling in oil or an air blast also tends to cause cracking. By checking time against transformation it has been found that at least 15 minutes per ½ inch of section is

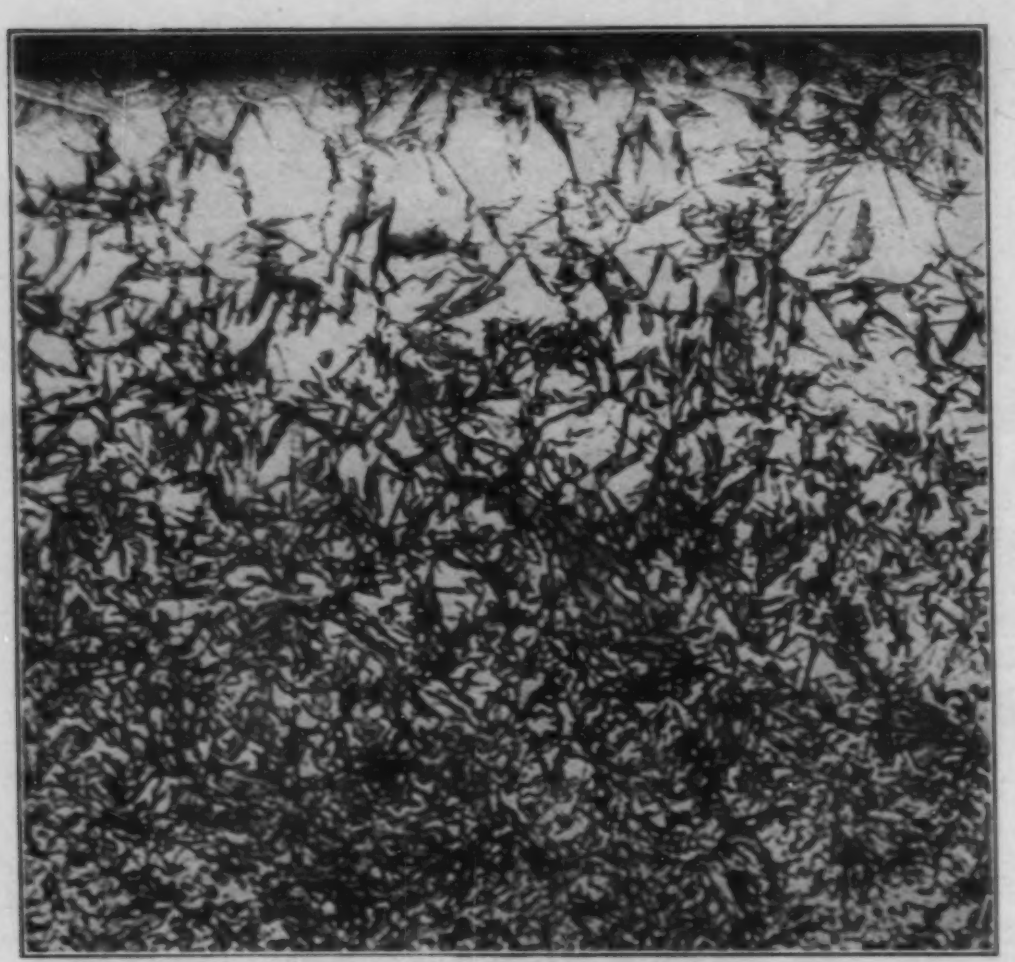


Fig. 8—Same Material and Heat Treatment as Shown in Fig. 7 Except Oil-Quenched. Vilella's martensitic reagent. × 350.

required for transformation to be completed when cooled in still air. When cracking was first encountered, however, the work was being cooled in still air from the martempering bath, so that it hardly seems that cooling too fast through the martensite formation range could have been the entire cause for the difficulty.

Percentage of Retained Austenite—Martempering Versus Oil Quenching—A difference in the amount of austenite retained from the two methods of quenching was suspected earlier in the investigation as being a probable contributing factor to cracking. The basis for this theory came from data collected by martempering carburized SAE 3316 steel. It was found that there was definitely far less tendency to retain austenite in this type of carburizing steel by using the martempering method of quenching as compared to oil quenching.

Figs. 7 and 8 illustrate this condition quite clearly. Fig. 7 is a photomicrograph of the edge of a carburized and hardened case on

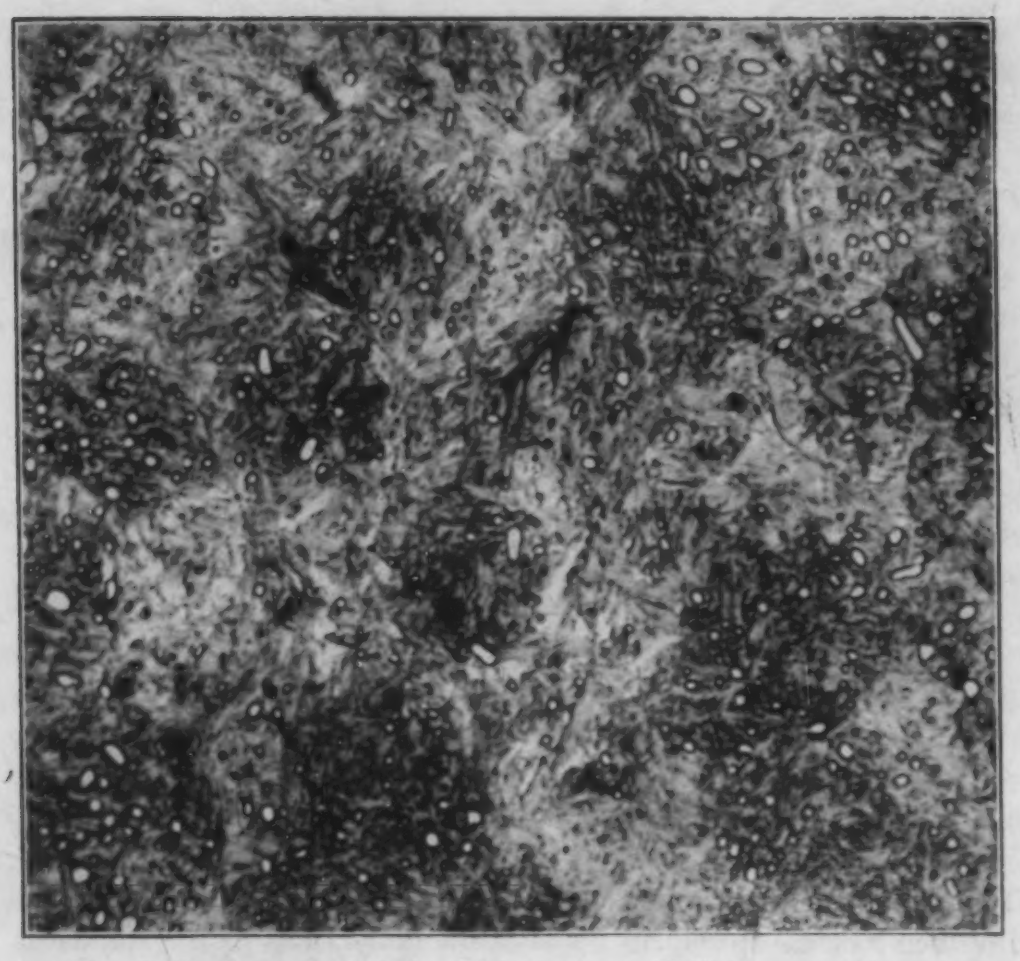


Fig. 9—Specimen Cracked by Martempering. Vilella's martensitic reagent. × 1500.

SAE 3316. This specimen was gas-carburized at 1650 F (900 C), temperature lowered to 1450 F (790 C), quenched into salt bath at 450 F (230 C) and cooled in air from 450 F. The hardness of this specimen is Rockwell C-63. Obviously this specimen contains very little retained austenite.

Fig. 8 shows a specimen of the same steel heat treated in exactly the same manner except that it was quenched in oil. The high percentage of retained austenite is quite obvious in the surface. Hardness of the specimen in Fig. 8 is Rockwell C-58, but with an extremely low superficial hardness. Since it was well proved that one type of steel had far less tendency to retain austenite by martempering it seemed reasonable to believe that other types might react in a similar manner and that possibly a relatively quick and complete transformation of austenite to martensite was not desirable in many cases. During all this investigation many microstructures

were carefully studied though most of them did not seem to reveal any unusual conditions. One of them which was purposely austenitized at 1600 F (870 C) is shown in Fig. 9.

Fig. 9 shows this microstructure at ×1500. There appear to be some martensitic cracks when the magnification is increased to ×3000 though it is difficult to be certain. By employing the same equipment as was used for locating the Ms points the author was able to determine quickly the amount of gamma phase present after the quench.

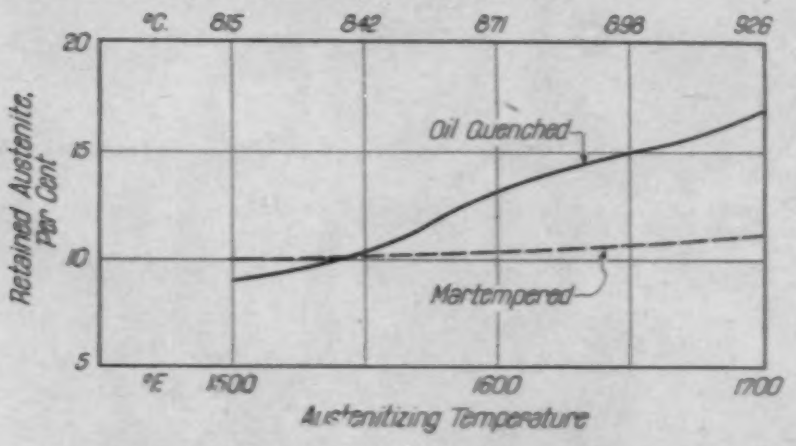


Fig. 10—Per Cent Retained Austenite After Oil Quenching as Compared to Martempering.

To accomplish this, it is merely necessary to use known standards and then have all specimens made to the dimensions of the standards. The standard assumed to be 100% alpha was a specimen of fully annealed SAE 52100 while a piece of 18-8 stainless steel fully annealed and of the same physical dimensions was used for the 100% gamma standard. The data obtained from checking many test specimens against these standards, after quenching, are shown in Fig. 10. This shows the condition which was suspected early in the investigation. As shown on this chart the amount of retained austenite is 10% or less of the total volume using austenitizing temperatures up to 1550 F (845 C), irrespective of the type of quench used. As the austenitizing temperature is increased above 1550 F (845 C) the lines quickly part showing that the oil quench retains considerably more austenite as the austenitizing temperature is increased while the tendency is for the per cent of austenite to remain about the same in case of the martempered specimen. It is the writer's theory that most of the real answer to the cause for cracking is shown on this chart. It is obvious that the percentage of retained austenite in parts after quenching is a major governing factor in the susceptibility

to subsequent cracking caused by residual stresses. This is only logical since retained austenite, due to its plasticity, will have a cushioning effect during the period of time in which martensite is formed. All evidence points to an overheated condition being the cause of the original cracking which was experienced prior to the time of this investigation. It is apparent that the actual furnace temperature was higher than indicated by the control instruments.

Conclusion

It is the author's opinion that the higher carbon low alloy steels such as SAE 52100 can be hardened successfully and advantageously by the martempering method. To accomplish this, however, it is absolutely necessary to have good equipment and careful control. The detrimental effects of malpractices such as overheating are more obvious when the martempering practice is used. Parts austenitized under identical conditions are less likely to crack when oil-quenched due to the higher percentages of retained austenite after quenching.

It is not the policy of the author to recommend any particular equipment. As far as has been found either an atmosphere-controlled furnace or neutral salt bath is quite satisfactory for the austenitizing operation prior to martempering. The author does strongly recommend, however, that if an atmosphere-controlled furnace is used, it should possess good circulation, otherwise there may be portions which will overheat and eventually lead to failure.

The author would also recommend that anyone contemplating the installation of equipment for martempering the higher carbon steels should develop the process carefully in their own plant, in order to avoid failures which might ordinarily be charged to some inherent weakness of martempering.

Acknowledgment

The author wishes to express appreciation to the personnel of The American Bosch Metallurgical Department for their assistance in the preparation of this manuscript.

DISCUSSION

Written Discussion: By F. R. Morral, Metal Trades Laboratory, Technical Service and Development Division, American Cyanamid Co., Stamford, Conn.

The author points out in his interesting paper the necessity of control and the ill effects of overheating. He makes definite recommendations to avoid the latter in atmosphere-controlled furnaces. A brief review of the features of salt baths may be in order here.

1. Ease of control of temperature of the bath in electrode-type furnaces.
2. Uniformity of temperature throughout the bath.
3. The temperature of the surrounding salt automatically determines the maximum temperature attainable by the steel. This makes also for uniform heating between dissimilar sections.
4. Speed of heating in salt. Approximately four to six times faster than in atmosphere furnaces.
5. The adhering salts provide a protective film during transfer to quench bath.
6. Scale-free hardening.
7. Equipment and operation of electrode-type furnaces, where control is paramount, are simple.

Written Discussion: By J. G. Christ, section engineer, Metallurgical Section, Nuttall Works, Westinghouse Electric Corp., Pittsburgh.

Mr. Boyer has done an excellent job of determining the cause of cracking of SAE 52100 steel during martempering. It is practical experimentation of this nature that adds to our working knowledge and that does much to establish the limits as well as the virtues of a given process.

Mr. Boyer makes the statement that decarburized parts are less rather than more susceptible to cracking. I have heard a number of outstanding men in the metallurgical field disagree as to the effect of decarburization on the cracking of steel. Although it is somewhat away from the subject of this paper, I would appreciate Mr. Boyer's elaborating on his statement concerning decarburization.

Mr. Boyer's graph of hardness versus holding time in the martempering bath is very interesting and should be of value to companies doing martempering. It clearly shows that withdrawing the work too soon can be harmful.

Near the latter part of his paper, Mr. Boyer states that hot water quenching from the martempering bath is generally satisfactory for most steels. It should be remembered that even this may result in some undesired distortion and in setting up some stresses.

Written Discussion: By Paul C. Farren, president, Springfield Heat Treating Corp., Springfield, Mass.

It appears that the author has sounded a timely note of warning which may save some of us from the headaches caused by a very human tendency to conclude, too generally, that certain new processes may be applied indiscriminately to the solution of our problems.

No doubt this paper will set the stage for widespread investigation to determine the precautions necessary to avoid trouble in the relatively new process known as "martempering".

The following quotation is from United States Steel "Atlas of Isothermal Transformation Diagrams," p. 13:

"In using the diagrams one should bear in mind that the composition of the steel, as determined by chemical analysis, sets only the general pattern of the

curve; the actual behavior of a given steel is influenced significantly by the grain size and degree of homogeneity of the austenite and by its actual composition which may differ from its nominal composition because of the presence of undissolved carbides or of other phases. For this reason, if a chart is to be used as a guide to the practical heat treatment of a steel of like composition, proper attention must be paid to both temperature and time in the austenitizing part of the schedule, so as to insure a correspondingly homogeneous austenite phase and a grain size differing little from that to which the diagram specifically refers."

The conventional S-curve is constructed with a particular austenitizing temperature and there seems to be no definite agreement as to the relation between this austenitizing temperature and the Ae_3 temperature representing the point above which the austenite becomes stable. The time factor above Ae_3 and its effect upon grain size and actual austenite composition appears to be neglected.

The present paper shows quite clearly the need for further work in this respect and it would seem to me that, for many steels, a complete picture would involve a series of S-curves over a range of austenitizing temperatures and with time at temperature being given due consideration. Such a series of S-curves should help to define the relationship between austenitizing procedure and the location of Ms points as attempted by the author in Fig. 4.

The method of determination of retained austenite appears to offer numerous advantages over the more conventional but time-consuming methods now in general use and the author deserves commendation for this development. It is to be hoped that he may see his way clear to make available to others further details of the equipment used.

In conclusion I should like to ask the author if there were noticeably more service failures among the oil-quenched pieces due to subsequent spontaneous dimensional changes which might be expected in parts with higher amounts of retained austenite.

Written Discussion: By H. G. Johnstin, metallurgical engineer, Vanadium-Alloys Steel Co., Latrobe, Pa.

Upon reviewing Mr. Boyer's paper, I am certain that one is impressed by the many phases of testing employed in attempting to establish the absolute reason for failure by cracking in parts made from SAE 52100 steel.

In referring to the curve presented in Fig. 10, it can be observed that at temperatures in excess of 1550 F (845 C) there is a definite trend for a greater amount of austenite to be retained with oil quenching than is found through using a martempering treatment. The percentage of austenite produced in martempering holds practically constant with change of hardening temperature. However, the amount of austenite after oil quenching at 1600 F (870 C) is only 3% greater and at 1650 F (900 C) 4% greater than after martempering. This scarcely seems sufficient to totally account for the cracking, since the steel when subjected to martempering at these temperatures contains as much as 11% austenite.

Mr. Boyer has pointed out, under the caption of Overheating, that this grade of steel, if austenitized at 1625 F (885 C) and tempered to 250 F (120 C), will have impact values considerably lower than when austenitized at 1550 F

(845 C) and subjected to the same degree of tempering, which he attributes largely to a difference in austenitic grain size. Since SAE 52100 is susceptible to grain coarsening at temperatures above 1550 F (845 C), I would like to ask the author whether any record was made of grain size at the elevated temperatures.

It has been the experience of our Laboratory that in attempting to harden larger sized sections of SAE 52100 to hardnesses of Rockwell C-63 or better by using an oil quench from 1600 to 1650 F (870 to 900 C), failure was often encountered by cracking which could be attributed to the grain of the steel having coarsened. We have found that through slightly adjusting the composition of 52100 by lowering the manganese content and adding a small percentage of vanadium the difficulty could be readily overcome.

Written Discussion: By Harold J. Babcock, research engineer, Ajax Electric Company, Inc., Philadelphia.

According to Fig. 10, at an austenitizing temperature of 1550 F (845 C), there is the same percentage of austenite retained whether an oil or a martempering quench is used. The observations concerning the cushioning effect of retained austenite, during the time in which martensite is formed, would apply only if the steel is overheated during the preparation for hardening. Whatever benefit may have been derived by use of an oil quench would be seriously offset by the accelerated increase in retained austenite when the steel was heated above 1550 F (845 C). The internal stressed condition in such a structure presents a problem of its own which might be concealed by use of an oil quench where conditions of equipment permitted overheating. The martempering quench apparently gave immediate warning by the quench cracking that a local overheating was occurring during austenitization.

The author says he tried various cycles in a neutral salt bath as well as in an atmosphere furnace at temperatures of 1450 to 1500 F (790 to 815 C). I am interested to learn why he did not explore the temperature range above 1500 F (815 C). Time at temperature above 1550 F (845 C) is the prime cause in this problem of surface cracking. The effect of radiant heat in a hearth-type furnace would produce local overheating beyond the control of the furnace thermocouple. In a salt bath, no part of the charge is exposed to a source of heat higher than that of the molten salt in which the steel is immersed. Furthermore, a salt bath will heat metal in approximately one-quarter the time required in a hearth-type furnace.

How did the author solve his problem and obtain control of the austenitizing temperature?

The author is to be complimented on the thorough manner in which he investigated the factors involved in this interesting martempering application.

Written Discussion: By Carl G. Johnson, associate professor, Worcester Polytechnic Institute, Worcester, Mass.

The practical importance of Mr. Boyer's paper, which deals largely with the problem of cracked parts made from SAE 52100 upon martempering, will be obvious to all readers. I believe the author has uncovered the cause of failure by cracking, i.e., more martensite being formed during martempering than during oil quenching of similar sections of 52100 steel. However, I am disappointed in his findings on hardenability, martempering versus oil quenching, as shown by

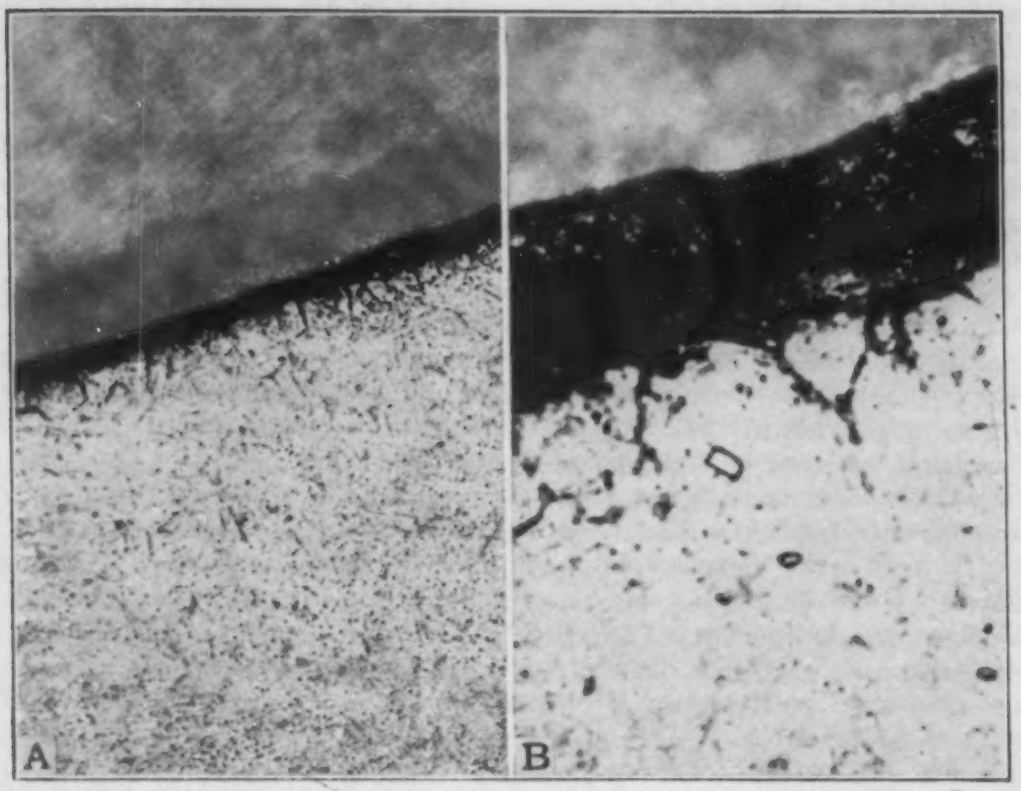


Fig. A—Photomicrograph of SAE 52100 Steel. Cracked part martempered at 450 F, 7 minutes. Etched in 2% nital. × 250.
Fig. B—Photomicrograph of SAE 52100 Steel. Cracked part martempered at 450 F, 7 minutes. Etched in 2% nital. × 1000.

Fig. 5. It would be interesting to know whether or not the sections that cracked during martempering were of such design and section to fully harden and develop a uniform hardness throughout. If these sections hardened less uniformly than the oil-quenched parts I would expect that the author should add this variable to the 13 listed in this paper.

I have experienced cracking of alloy steels that have been subjected to hot salt bath quench (martempering). Cracks have developed in both high speed steels and the oil hardening grades of tool steel. The type of cracks developed would lead the observer to believe the parts have been cracked during a grinding operation when no grinding had been applied to the parts. In the case of the high speed steels the cracks appeared when the surface of the tools had been carburized by the quenching bath. Also, any microscopic examination of steels subjected to a hot salt quenching media will reveal a surface action that I have named "the dark layer". This "dark layer" seems to form a network effect along the surface layers of the steel and, I believe, forms a marked notch-brittle condition that under certain conditions might lead to the type of stress cracks developed by the martempering process. Perhaps this "dark layer" and network condition is due to the action of the molten salt bath containing cyanide salts. This "dark layer" and network is illustrated in Figs. A and B. These photomicrographs were taken of a part made from SAE 52100 which cracked

after heating to 1550 F (845 C) and quenching into a molten salt bath held at 450 F (230 C) for 7 minutes. The author seems to have eliminated the action of the salt bath as a cause of cracking by the 24-hour soak at 500 F (260 C), but this treatment resulted, no doubt, in an isothermal change and would have changed the final results as far as obtaining the maximum hardness and served to reduce the sensitivity to cracking. It would seem to me that in order to avoid or prove that the action of the salt was not a factor another type of quenching media could be used such as a metallic bath.

Written Discussion: By R. V. Grimm, Metallurgical Department, Steel and Tube Division, The Timken Roller Bearing Co., Canton, Ohio.

The author has presented some very practical and useful information concerning the interrupted quench as it applies to constructional alloy steels and especially the SAE 52100 type. There are a few points made in regard to this latter steel that we feel warrant further consideration.

The author mentions that SAE 52100 steel will usually harden completely through in a 1-inch round section after oil quenching.

It is the writer's opinion that 52100 steel is generally accepted as a shallow hardening steel, and is not capable of producing full hardness throughout on sections much larger than ⅝ inch.

Of course, the depth of hardening is to a considerable degree dependent upon the prior structural condition, which feature is not specifically covered by the author.

The information obtained regarding the per cent austenite retained on oil quenching versus martempering is very interesting and undoubtedly merits more investigation regarding the reasons for this phenomenon.

It is the writer's opinion that retained austenite can very readily cause cracking and would also like to point out that austenitizing temperatures in excess of 1550 F (845 C) are not considered good practice for the hardening of 52100 steel.

It was also noted, in the case of martempering carburized parts, that no cracking was obtained where parts were quenched into hot water soon after removal from the martempering bath, while 52100 parts cracked 100%. Inasmuch as the carbon content of carburized parts and 52100 is practically the same, would it not be logical to expect them to behave similarly?

The writer is in agreement with the conclusions reached and believes this paper should be very useful to anyone interested in the martempering process, especially those people in the ball bearing industry, where SAE 52100 steel has its largest application.

Written Discussion: By Harry W. McQuaid, consultant, Cleveland.

A paper of this kind is one which becomes at once of interest to many ASM members because of its real practical value to those directly interested in heat treating. Every encouragement should be given to the writing of papers like this one, because of their value in everyday operations, and because they fulfill, in the most practical way, the principal purpose of the ASM.

Like other important developments, some time will be required to develop the limitations in the application of martempering of which this is an example. There is no doubt but what martempering will become one of the most used

methods of hardening alloy steel, since it offers a method of controlling warpage and achieving valuable properties not possible in any other way.

There is no doubt but what we should be careful in making any general statement that a given quench (usually because it is slower) will result in any less inherent stresses than another. I know that, in the quenching of armor piercing shot, under certain conditions the oil-quenched shot showed a much greater tendency to crack than when the quench was water.

In the case of SAE 52100 steel, we are dealing really with a steel in a state of unstable carbide solution where the actual carbon in solution when quenched depends on the previous degree of spheroidization, the temperature, and time to develop the austenite in the part as quenched. Two curves in Mr. Boyer's paper are of interest in this connection, Figs. 4 and 10, and those depend, I would think, on the size and dispersion of the carbide particles at the time of heating for solution. Probably, the annealing of no other steel has been given so much attention in order to obtain a definite carbide size and dispersion as the SAE 52100 and this is a principal factor in its behavior in heating for quenching.

Because of the time required for solution of the larger spheroids of carbide in a steel containing chromium it is possible by varying the temperature and the time at temperature to vary greatly the carbon in solution in the austenite at the time of quench. Thus, we have what is to all interests a steel whose carbon content, as far as quenching is concerned, is directly related to the melting practice, the annealing cycle and the time and temperature of heating for quenching. It is this variation in carbon due to temperature differences that accounts for the slope of the line in Fig. 4.

Apparently, the martempering differs from the oil quench as far as internal stresses are concerned, principally in the fact that the transformation is depressed below room temperature so that ductile austenite is retained after quenching. The higher the content of carbon in solution, the more retained austenite in the as-quenched piece. This leaves two questions to be answered:

(a) Why does the martempering operation result in such high internal stresses, and (b) how can we eliminate these stresses?

Stresses of this type must be due to nonuniform transformation and especially due to an important difference in time between martensite formation near the surface and in the center of the quenched mass. My opinion would be that the stresses present in the martempered specimens are due to a difference in the degree of spheroidization or rate of carbon solution between the center section and the surface zone of the bars from which the parts tested were made. Thus, I would expect that the carbides were smaller and less spheroidized in the center than nearer the surface so that we would have, at the time of quenching, essentially a duplex steel which is high carbon in the center and lower carbon near the surface. Then we would have, as indicated in Fig. 4, a lower temperature and hence a delayed transformation to full martensite in the center with the resulting introduction of high stresses on full cooling.

The correction would then lie in obtaining a uniform carbide dispersion and spheroidization throughout the bar section.

Spheroidization is an important factor in the machining of this grade of steel and to obtain uniform spheroidization throughout is not a simple problem in bars

of any section, and extremely difficult in bars over 2 inches in diameter. The answer to this problem arrived at by Mr. Boyer seems simple but means that the metallurgist is always faced with the possibility of some slip-up. At present, it seems the logical way out.

As a suggestion, it might be worth trying to requench, by transferring from the martempering bath into boiling water and to hold in the water long enough to insure complete uniformity of temperature. This would be an attempt to equalize the temperature throughout the part at a point where transformation will be proceeding almost to completion in all parts of the mass where now it must be nearly finished near the surface before it has made much progress near the center. This is one way of saying that in a steel combining two carbon ranges, we should be careful to suit the martempering to meet the requirements of the high carbon zones and perhaps the second quench in boiling water will do this in your case. Perhaps a higher temperature than 212 F is necessary. A similar arrangement of two steps in martempering might give some improvement in certain carburized high alloy grades of steel.

Written Discussion: By L. D. Jaffe, metallurgist, Watertown Arsenal, Watertown, Mass.

At first glance, Figs. 7, 8 and 10 of this paper seem most disturbing, for it has long been established that the extent of the transformation of austenite to martensite (at any fixed temperature below the Ms) is greater the faster the cooling rate in the martensite range.[1-4] One would then expect that the per cent of retained austenite would be less in an oil-quenched specimen than in one air-cooled through the martensite range in the martempering process. Figs. 7, 8 and 10, on the contrary, indicate a larger percentage of retained austenite in the oil-quenched specimen.

The explanation of the discrepancy, for Fig. 10, can probably be found in Fig. 3. This figure indicates that holding the SAE 52100 for 7 minutes at 450 or 475 F (230 or 245 C) would cause half the austenite to transform isothermally to bainite. This, clearly, would reduce the per cent of austenite left after subsequent cooling to room temperature. The lower bainite would be difficult to distinguish from martensite under the microscope.

Would the author give the values of the magnetizing force and flux density used in deriving Fig. 10? If these were not high enough to insure magnetic saturation, it is possible that the difference found between the martempered and oil-quenched specimens was due not to retained austenite but simply to more residual stress and strain in the oil-quenched specimen. It is well known that residual strains markedly decrease the magnetic permeability at flux densities below saturation.

The difference between Figs. 7 and 8 also may arise from a greater per cent of isothermally formed lower bainite in the latter. Another explanation is that

---

[1]J. A. Matthews, "Austenite and Austenitic Steels," *Transactions*, American Institute of Mining and Metallurgical Engineers, Vol. 71, 1925, p. 568-596.

[2]H. Hanemann and H. J. Wiester, "Martensite Crystallization in High-Carbon Steels" (in German), *Arch. Eisenhüttenw.*, Vol. 5, 1932, p. 377-382.

[3]S. S. Steinberg and V. I. Zyuzin, "Transformations of Austenite in Plain Carbon Steels and Some Special Steels at Low Temperatures" (in Russian), *Metallurg*, Vol. 11, No. 8, 1939, p. 3-15.

[4]J. H. Hollomon, L. D. Jaffe and D. C. Buffum, "Stabilization in the Austenite-Martensite Reaction." To be published.

martensite, formed while the specimen of Fig. 7 cooled slowly from the martempering temperature, tempered during this cooling, and so etched dark. The martensite of the carburized case in Fig. 8 was cooled rapidly during the oil quenching, may have had no chance to temper, and so may have etched light in Vilella's reagent.

If the percentage of retained austenite was, in fact, less in the martempered specimens of SAE 52100, this may, as the author points out, account for the difference in tendency to quench-crack. An alternative explanation is that the bainite presumably present in these specimens was less resistant to brittle failure than the martensite of the oil-quenched specimens.

Written Discussion: By J. W. Spretnak, Metals Research Laboratory, Carnegie Institute of Technology, Pittsburgh.

The author has presented an interesting observation on the martempering of SAE 52100 steel. This is a treatment that is successful in preventing cracking in steels of medium carbon contents but which failed for a steel containing 1% carbon.

The amount of retained austenite is offered as the chief reason for the success in oil quenching of the SAE 52100 steel. Several investigators have demonstrated previously that the quench cracking tendency is reduced as the amount of retained austenite is increased. If it can be concluded that the amount of retained austenite is definitely greater in the oil quench, then the author's conclusion bears validity. Unfortunately, the determination of the amount of retained austenite has proved to be a difficult and troublesome problem. Much divergence in results occurs when the various methods are used. The most dependable one appears to be the X-ray method, described by Dr. Morris Cohen. It seems advisable to check the results on retained austenite by this method. For instance, a conflict with previous work is evident when the rate of cooling through the martensite range is considered. It has been demonstrated that more austenite is retained the slower the cooling rate through the martensite range. This rate is faster in oil quenching as compared to that in the martempering treatment.

Another factor, perhaps more fundamental than the amount of retained austenite and not considered by the author, is the state of the thermal stresses present in the steel after the equalizing hold above Ms in the martempering of the high carbon steel. Fig. C is a representation of the generation of stresses in the annealing of glass from the work of Adams and Williamson,[5] which is indicative of the formation of stresses in the cooling of steel undergoing no transformation. Above the annealing range, the glass is plastic and below, the glass is elastic.

In case a, a temperature gradient is set up in the glass in the elastic range and temporary tensional stresses at the surface and compressional stresses in the center result. As the gradient is removed, the stresses disappear. Thus no residual stresses can be formed without prior nonuniform plastic deformation.

In case b, a thermal gradient is set up in the plastic region. The resulting thermal stresses are quickly dissipated by plastic deformation. When the thermal

---

[5]L. H. Adams and E. D. Williamson, *Journal*, Franklin Institute, Vol. 190, 1920, p. 597, 835.

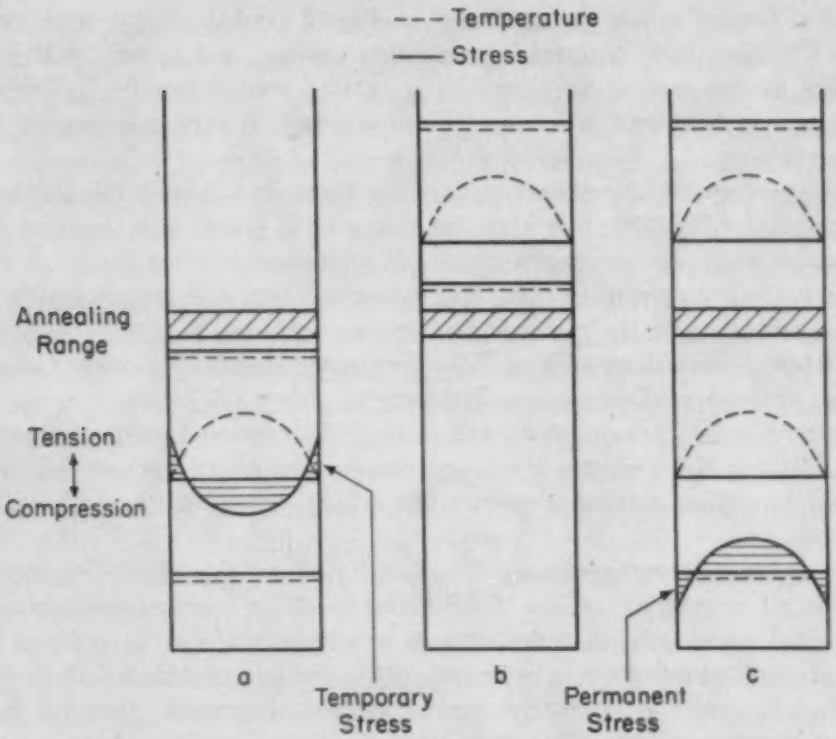


Fig. C—Relation Between Stress and Temperature Distribution in Slabs of Glass Cooling Linearly (After L. H. Adams and E. D. Williamson). The glass is assumed to be plastic above the annealing range and elastic below it.

gradient is removed, no residual stresses result if the glass is kept in the plastic region.

In case c, a thermal gradient is set up in the plastic region and these stresses are removed by plastic deformation. The glass is cooled into the elastic region with its thermal gradient. As the gradient is removed, the center contracts relative to the outside and residual stresses result, compression on the outside and tension on the inside.

Bühler and Scheil[6] have demonstrated that the austenite is effectively plastic before the transformation to martensite begins in steels with relatively high Ms points but becomes effectively elastic before transformation occurs in steels with Ms points close to room temperature. Thus the thermal stresses before the transformation begins in medium carbon steels are given by case b, that is, the thermal stresses are practically zero. In the case of high carbon steels, the thermal stresses after the martemper hold are given by case c, compression on the outside and tension on the inside. As the transformation to martensite begins on the outside, an expansion results which sets up compressional stress on the outside. The residual thermal stress is also in compression and is thus additive. This high resultant compressive stress at the surface changes to a high tensile stress as the final reversal is completed, which is instrumental in promoting cracking.

This difference in thermal stresses in martempering steels with high Ms

[6]H. Bühler and E. Scheil, *Arch. f. Eisenh.*, Vol. 6, 1933, p. 283-288.

points as compared to steels with low Ms points is offered as a possible fundamental reason for the failure of the martempering of the SAE 52100 steel. The importance of retained austenite should not be disregarded, especially if the author's determinations on this variable can be corroborated.

Author's Reply

The volume of pertinent discussion is evidence of the general interest in the martempering process which serves to emphasize how much investigation remains before such a process can be used to obtain maximum benefit and avoid difficulty.

F. R. Morral has pointed out some interesting facts about the advantages of salt bath heating. It has already been stated that the austenitizing operation can be accomplished satisfactorily in either the salt bath or an atmosphere-controlled furnace provided with circulation. It is readily granted that the salt bath has many advantages. The only disadvantage in the use of a salt bath for austenitizing is the tendency of the salt film to insulate the surface, thus requiring more vigorous agitation in the quenching bath in order to avoid the formation of pearlite in the work. Atmosphere-controlled furnaces present less difficulty along this line.

J. G. Christ has stated that the effects of surface decarburization have been a subject of much debate among men in the metallurgical field. It is the author's opinion that decarburization in itself will not contribute to cracking, due to the relatively plastic nature of the decarburized structure. It seems more logical that the malpractices which caused the decarburization are more likely to cause cracking in most cases. In other words, the author feels that decarburization may receive the blame for cracking for which it was not the direct cause. The author has never practiced hot water quenching from the martempering bath except for carburizing steels. There is no advantage in using such a practice except for parts which have numerous holes and recesses, so that removal of the salt is almost impossible if allowed to solidify. It does seem reasonable to expect that more distortion would be encountered by this practice though we have not been able to find any difference in deformation between those hot-water-quenched from the martempering bath as compared to those air-cooled.

The writer is entirely in agreement with Paul C. Farren in that there is a noticeable need for more complete TTT-curves which will establish the relationships between variations in the austenitic grain and the decomposition curve.

A discussion of the apparatus used to determine the per cent of austenite would be much too lengthy to incorporate in this paper. The author would be more than glad, however, to give assistance individually to anyone interested in the construction or use of such apparatus.

The author cannot accurately answer Mr. Farren's question relative to service failures although we do know from our own experiments that two mated parts made of SAE 52100 and overheated in heat treatment will change dimensions noticeably over a period of some months while remaining idle and undisturbed at room temperatures. The only logical explanation for such a

condition seems to be that the retained austenite has isothermally transformed.

H. G. Johnstin has commented that the difference in per cent of retained austenite shown on the curves in Fig. 10 seems hardly enough to totally account for cracking. It probably should have been explained more carefully that the curves in Fig. 10 represent the average results of many tests. In numerous cases the difference in per cent of retained austenite between oil quenching and martempering was found to be as high as 10% at an austenitizing temperature of 1700 F (925 C). In all cases the oil-quenched specimens tended to retain a higher percentage of austenite.

As to the grain size after quenching from the various austenitizing temperatures, it was found that in most cases specimens showed a grain size of Shepherd 9 when austenitized at 1550 F (845 C), while specimens from the same bar austenitized at 1700 F (925 C) had coarsened to No. 6.

Harold J. Babcock has asked a question as to why, in the underheating part of the experiment, the range of 1500 F (815 C) and upward was not explored. The part of the research work which dealt with underheating was done not only to create a condition of nonuniform carbide solution, but also to arrest some portions in the state of the alpha to gamma transformation. It was much easier to accomplish this by using the lower furnace temperatures rather than the shorter time periods. Some work was actually done by using austenitizing temperatures of 1600 to 1700 F (870 to 925 C) for very short time periods. No cracking was experienced in this part of the project, but results tended to be somewhat erratic and fewer specimens actually showed the underheated condition which was desired. It was interesting to note during this part of the project that steel is heated throughout in radiant heat considerably faster than most of us heretofore believed.

Mr. Babcock's question concerning control of the austenitizing temperature is answered in the conclusion of the paper where it is recommended that austenitizing should be done only in salt baths or atmosphere-controlled furnaces which possess good circulation. It seems well proved that there are many advantages to be derived from martempering, but the process will not lend itself to be used in conjunction with certain malpractices without disastrous results.

Relative to Carl G. Johnson's comments on the relative hardenability, the author was also surprised to find a higher hardenability on a 1⅜-inch diameter specimen when quenched in oil than when martempered. If the reverse had been true a logical explanation for the cracking would have been much more evident. The specimens that showed cracks, however, were all between ½ and 1 inch and showed a uniform Rockwell C hardness irrespective of the type of quench used.

The possibility of chemical attack by the salt was given due consideration in the procedure of investigation. It is, of course, possible that some specimens which might have cracked were isothermally transformed to bainite which would be less susceptible to cracking. Considering all other test results, it seems that chemical attack by the salt was not at least the basic cause of cracking. Whether or not it was a contributing factor is a question which could be answered only by further research.

R. V. Grimm stated that he regards SAE 52100 as a shallow hardening

steel. Perhaps the author should have stated that SAE 52100 is generally regarded as a relatively deep hardening steel, though it has been the experience of the author that 52100 having a finely spheroidized structure in the annealed bars will usually harden fully through a 1-inch round. There will be, of course, a considerable amount of fine pearlite in the center portion, but it will be sufficiently martensitic, so that little if any decrease in hardness will be noticed.

The author cannot agree with Mr. Grimm in his belief that the presence of austenite will cause cracking. Austenite is definitely a softer and more plastic constituent. Citing an example of a high alloy steel such as high speed steel which is known to retain a high percentage of austenite when cooled from the austenitizing temperature, cracking rarely occurs in such steels until the tempering operation is performed. The reasoning in this case is that the tempering operation transforms a high percentage of the austenite retained, so that after tempering there is but little left for a cushioning effect and cracking is more likely to occur. It seems that the same reasoning can be applied to the lower alloys.

It does not seem that a carburized steel can, in most cases, be compared to SAE 52100. It is granted that the carbon content in the surface layers may be nearly the same, but the softer cores of the carburized steels have the ability to cushion the effects of the volumetric changes which occur during transformation.

Harry W. McQuaid presented a most interesting discussion on results obtained by martempering 52100 steel. The author has already proved that nonuniform solution of the carbide throughout a section will tend to increase the unbalanced residual stresses. While the author's results as given in this paper show this condition as obtained by overheating, there is probably no doubt that the same degree of nonuniform carbide solution could be obtained by variables in the melting and annealing of the steel.

An attempt to, at least partially, answer L. D. Jaffe's question regarding the magnetizing force and flux density used for deriving the data shown by Fig. 10 is as follows: The value of the magnetizing force and the flux density was the same on all specimens, and since the core loss data were taken with 60-cycle current it seems safe to assume that the duration of the magnetizing cycle at this frequency was not sufficiently long to saturate the core before the flux removal took place. The possibility of variations in residual stresses showing erratic readings by this method of measurement was not entirely overlooked, though the author's work along this line was limited. As a check on the condition, a number of specimens were taken from a bar about twice the diameter required for the specimens. Some of these specimens were turned nearly to size prior to hardening while others were ground to size at a high rate of speed after they were hardened. This was, of course, an attempt to have some specimens which were in a highly stressed condition from grinding to compare with those which had been ground only a small amount. After no variations were found greater than were regarded as being within limits of error, no further attempts were made to establish the effects of residual stresses as being a variable worthy of consideration.

Mr. Jaffe mentions that holding a specimen of 52100 at 475 F for 7 minutes would cause one-half of the austenite to transform to bainite. It must be remem-

bered that this would be true only for a very thin section. The specimen shown in Fig. 1 had a wall thickness of over ¾ inch, so that a much longer time would be required for this specimen to assume the temperature of the quenching medium. It seems very unlikely to the author that any appreciable amount of bainite had been formed for two reasons: (a) the hardness was Rockwell C-65 and (b) the specimen cracked. It is, of course, possible to form some bainite before any marked decrease in hardness is noticed, but certainly any great amount would show some decrease in Rockwell value. Bainite, being a more ductile structure, should show much less tendency to the cracking which was experienced and shown in Fig. 1. By the same token it scarcely seems logical that there could be much lower bainite present in the specimen shown in Fig. 7, due to the fact that the hardness is Rockwell C-63. Even though the hardness of the specimen shown in Fig. 8 is Rockwell C-58, 15N Rockwell readings showed an equivalent of only Rockwell C-45, which proves that the surface was composed of a very soft structure. Magnetic readings on these specimens shown in Figs. 7 and 8 were also considerably different, which further suggested that the oil-quenched specimen was much higher in retained austenite, rather than being composed partially of untempered martensite which was suggested by Mr. Jaffe as a possibility.

J. W. Spretnak has also submitted some very interesting comments on the author's paper in general and the method of phase measurement in particular. It is granted that there is probably some slight inaccuracy in this method of measurement though it seems to be more consistent than most other methods and certainly it is much faster, thus enabling one to make measurements at any given temperature within a time period of about 2 seconds. Some more recent work which the author has done on high speed and other high alloy steels bears out all the more that the core loss method of phase measurement is of considerable industrial value.

The author wishes to take this opportunity to thank those who have submitted these interesting discussions on the foregoing paper.

A PERIODIC CHART FOR METALLURGISTS

By Carl A. Zapffe

Abstract

A periodic chart has been developed of somewhat novel design which includes the common relationships of the Mendelejeff table and in addition has the following characteristics:

1. Schematically a cross section of the electron shells of the heaviest atom, the chart has all the elements so placed that for any one of them the elements of lesser atomic number depict the number of electrons in that atom and their placement in the principal shells and in the s, p, d, and f subshells;

2. Rearrangement of the elements beginning with actinium [89] and including the four newly discovered elements neptunium [93], plutonium [94], americium [95], and curium [96] leads to a new concept of these elements as a second subtransition or rare-earth series;

3. Separate sectors of the chart contain the B-subgroup series, the transition series, and the subtransition series (rare earths);

4. Analogous properties of the elements appear along radii, along diameters, along peripheries (shells), and within the separate sectors.

On the basis of this chart a series of metallurgical alloy systems is presented to show the characteristic patterns that result, to aid in understanding certain principles governing metallurgical phenomena, and possibly to serve as a useful means for predicting the characteristics of new alloy systems.

Introduction

IN the eight decades following Newland's discovery of the Law of Octaves (1864), and Meyer's (1868) and Mendelejeff's (1869) development of the Periodic Table of Elements, many students of atomic theory have found useful and enlightening entertainment in rearranging the elements in two- and three-dimensional patterns to

A paper presented before the Twenty-eighth Annual Convention of the Society held in Atlantic City, November 18 to 22, 1946. The author, Carl A. Zapffe, is a consultant, Baltimore, Maryland. Manuscript received July 12, 1946.

illustrate more effectively the periodic occurrence of analogies among the elements.

All periodic tables have the common feature that they postulate, tacitly or explicitly, the existence of a natural law of uniform atomic plan to which all atoms conform. Essentially this law is that the electronic structural pattern of every atom is a recapitulation of the patterns of all atoms having fewer electrons.

Even at this late date useful information remains to be gained from such studies of the previously known elements; and the recent accomplishment of nuclear fission, along with the four new elements it has already introduced, increases the desirability of re-examining the periodic system.

The purpose of the present paper is to review briefly certain theoretical aspects of the periodic system and to develop a chart which has some theoretical interest, and perhaps some practical usefulness as well. Although of general chemical application, the chart will be applied specifically to portraying certain metallurgical systems in an attempt to improve the understanding of the structure of the elements and the metallurgy of alloying.

Atomic Structure

The Fundamental "Double-Pair" Unit—In its simplest sense, an element can be regarded as a given arithmetical composition of minus charges (electrons) and plus charges (protons) which arrange themselves in two specific manners with respect to one another.

First, there is a collapsed proton-electron pair which is electrically neutral and is therefore referred to as a neutron. Although this neutron is a discrete entity, useful chemically in the reactions of nuclear fission, an element in the accepted sense does not result until a second pair of these charges is added. This second pair is not collapsed. Instead, the proton associates with the other proton-electron pair (neutron), just named, to form together the nucleus of element No. 1 having as a consequence a single plus charge $+e$; and its corresponding electron remains outside this nucleus traversing a spherical (or elliptical) orbit whose location is symmetric with the nucleus and is referred to as the electron orbit or shell. Although the concepts of wave mechanics require expressing the position of this orbit as a probability function only, it is discrete with respect to its state of energy.

Hydrogen is this element No. 1*; and all other elements develop

*More properly, deuterium, for hydrogen is an exception which contains no neutron.

progressively by simple arithmetic addition of one of these "double-pair" units — one collapsed pair (neutron) added to the nucleus, and one dilated pair disposed as described.

Rather frequently an exception occurs to this general rule, in which too many or too few collapsed pairs (neutrons) occur in the nucleus, giving rise to an "isotope". An isotope consequently has a weight which differs from the normal element; but its chemical behavior, which is determined only by the electrons in its surrounding shells, is identical. Some 400 isotopes have now been identified, there being at least one known for every element. It is interesting to note that all principal isotopes (longest-lived) have even numbers of neutrons, with but the several exceptions of Be, N, and possibly Pt (1).[1]

Electron Shells—Following the earlier development of the quantum theory, Bohr, also Stoner and Main-Smith, discovered from a study of optical spectra that the orbital electrons possessed a further arithmetical feature in that a specific structure existed within the electron shell. Stated simply, the electrons in elements of advanced structure methodically occupy principal shell groups which can be identified progressively as shells 1, 2, 3, 4, 5, 6, and 7 in conformity with the so-called principal quantum number. The concept of a quantum state developed from the fact that electrons dropping back from excited states emit radiation conforming to the expression:

$$E_2 - E_1 = h\nu$$

where ν is the frequency and h is a universal constant known as Planck's constant.

Subshells and the Quantum Theory—Next, Pauli called attention to the Exclusion Principle, which follows from the mathematics of wave mechanics and states that no two electrons can occupy the same quantum state. Consequently, each of the major shells derives a detailed subshell structure which is based upon four variables, or degrees of freedom, available to the electron. The first variable is the principal shell, or quantum number, already mentioned. The second and third concern measures of angular momentum; and the fourth allows two electrons to have identical quantum numbers, but opposite spin.

For present purposes the subdivision resulting from the third quantum state will be neglected. The major shells numbering 1 through 7 will be used, as will those *s*, *p*, *d*, and *f* subshells which relate to the second quantum number.

[1]The figures appearing in parentheses pertain to the references appended to this paper.

In keeping with the simple logic of periodicity, the population of these shells and subshells follows a simple arithmetic progression. The *s*, *p*, *d*, and *f* subshells have odd-number 1, 3, 5, and 7 orbital positions, respectively, each position open to two electrons with opposite spin. The principal shells, which comprise these subshells, have in turn a capacity expressed by $2 \cdot n^2$, where n is the shell number, and the factor 2 accounts for the spin doublets.

Electronic Arrangement of the Elements—As a consequence of these laws, the second "double-pair" unit added to element No. 1 fulfills the stipulations both for the subshell *s* and for the principal shell 1. Helium, an inert gas, results.

With the addition of a third unit, the *s*-subshell in the second principal shell consequently begins to fill. Whenever a new shell is begun, the single orbital electron tends toward great chemical activity; in this case the resulting element lithium belongs to the reactive univalent group known as alkali elements. A fourth unit completes the *s*-subshell; but the principal shell now contains in addition a *p*-subshell having orbitals for six electrons. Since the principal shell at this stage is thus only one-fourth occupied, the element beryllium shows chemical activity exceeded only by the alkali, lithium; and it belongs to a group known as alkaline earths.

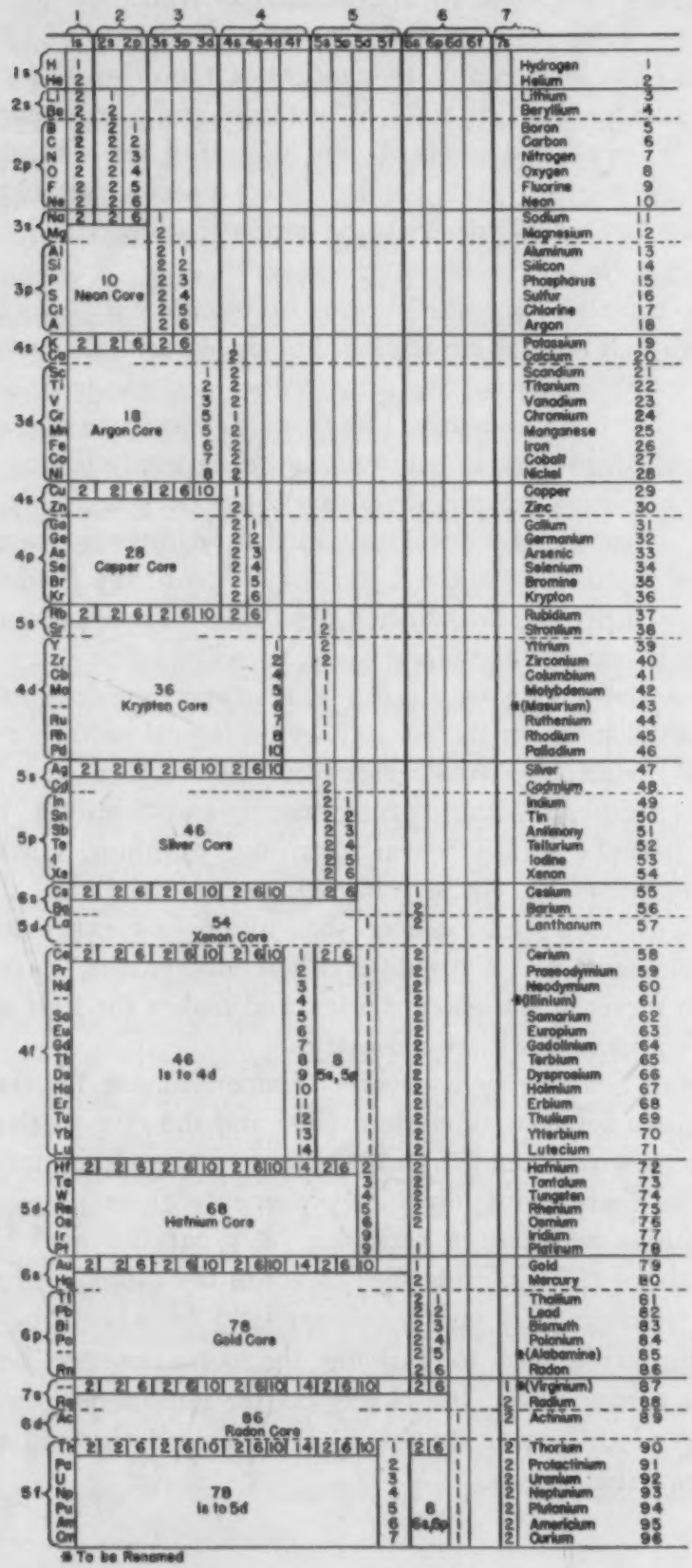
Before proceeding further, we will refer to Table I where all elements are listed according to their electronic division and subdivision from hydrogen through the four new elements neptunium, plutonium, americium, and curium. The fact that each period begins with a univalent alkali metal, following an inert gas of the previous period, involves that each alkali metal contains the stable structures of all the preceding inert gases, and similarly for every other element in the classification. This is indicated in the table, which is a conventional compilation (2), (3), with exceptions to be noted. Since the table is self-explanatory, only a few further remarks need be made in the text.

First, note that the solid horizontal subdivisions mark the completion, at least temporarily, of a principal shell and the dashed divisions a subshell. Shell 1, filled with two electrons, provides helium, as just described; shell 2, filled with eight electrons, provides inert neon; shell 3, filled with eight additional electrons, provides inert argon.

However, 2×3^2 is 18, the capacity of shell 3. Consequently, immediately after the *s*-subshell is filled in shell 4, the additional units resume filling the third shell to bring the 3*d*-subshell up to $2 \times 5 = 10$ electrons before returning to complete the fourth shell. This introduces

Table I

Enumeration of Electron Disposition Within the 96 Known Elements



* To be Renamed

a series known as "transition elements", among which some of mankind's most useful metals are found, notably iron.

With the third shell expanded to its full capacity of 18 electrons, made up in part, incidentally, by capture of the original 4-*s* electrons, the fourth shell proceeds to refill. When its *s*- and *p*-subshells are filled, a temporary stability is attained, but only until the *s*-subshell in the next principal group, shell 5, is filled. Then a second series of "transition elements" develops, wherein the action just described for the 3-*d* subshell is repeated with 4-*d*.

By the time the sixth shell begins filling, not only does the underlying 5*d*-subshell require expanding, but the 4*f*-orbital two shells deep also requires electrons to conform to the total capacity of shell 4: $2 \times 4^2 = 32$. Consequently, after two 6*s* electrons are added, the next electron drops back to begin filling 5*d*, but only begins this process, for succeeding electrons drop two shells deep to fill 4*f*. A "subtransition" series thereby develops which constitutes the rare earths—14 elements conforming to the $2 \times 7 = 14$ law of the *f*-subshell.

With 4*f* filled, the 5*d*-subshell next fills (transition series); and finally there is resumed the filling of 6*p*, then 7*s*.

A New Series of Rare Earths—This recurrent dropping back to fill incompleted inner shells has followed a logical pattern up through radium [88] with its two 7*s* electrons. Heretofore, the remaining elements, actinium, thorium, protactinium, and uranium, have been placed on periodic tables beneath yttrium, hafnium, tantalum, and tungsten, respectively. Such placement interferes with the logical progression of deeper and deeper shell-filling just expressed for the transition elements and the subtransition rare earths, in conformity with known increasing shell capacities, and makes the first set of rare earths more anomalous than necessary.

However, Seaborg, codiscoverer of americium and curium, points to a parallelism between americium [95] and the rare-earth europium [63], and between curium [96] and the rare-earth gadolinium [64] (4). This permits rearranging the heavy elements from previously suggested positions and setting actinium [89] parallel with lanthanum [57]. In Table I lanthanum is seen to act in the established transition manner of yttrium [39] and scandium [21] by adding to the inner *d*-subshell in preference to building the outer valence beyond the *s*-state. But cerium [58], the element after lanthanum, discontinues the building of this inner *d*-subshell and proceeds instead to fill the *f*-subshell two shells deep.

On this basis, then, it is here assumed that analogies remain the rule, and that thorium [90], the element after actinium [89], is an analog of cerium, the element following lanthanum, and proceeds to build the subshell two shells below, establishing parallelism with the first subtransition rare earths.

Uranium [92] then compares with neodymium [60], rather than with tungsten [74]; and a second series of "rare earths" is established which should continue through element 103—if such is ever discovered. Similarly, elements above No. 103, if developed or discovered, should resume building the *6d*-subshell up through No. 110. Numbers 111 and 112 would probably have *7s* electrons customarily beginning again over the foundation of these expanded inner shells; and beyond element No. 113 there might appear a new order of rare earths whose construction would involve filling a subshell *three* shells deep, for the shell capacities are 2, 8, 18, 32, and *50*, the latter conforming with the expression $2n^2 = 2 \times 5 \times 5 = 50$.

Such an arrangement, incidentally, does not preclude uranium having some chemical analogy with tungsten, as previously suggested, for there are also parallelisms among the transition elements and the subtransition elements which are not yet well defined.

Development of a Periodic Chart

Consideration of Electronic Energy Levels—To regain a simple understanding of the periodicity of the elements after this involvement with transition structures, a schematic energy diagram of the principal quantum states is presented in Fig. 1. There the periphery is divided into *s*, *p*, *d*, and *f* states, and the inner circles represent the energy levels of a schematic cross section of the heaviest known atom. Energy is measured along the radius, increasing toward the periphery. The *s*-state is identified with one orbital position (indicated on the diagram) which allows occupancy by 2 electrons of opposite spin, as described before. The *p*-state has three positions indicated, accommodating 6 electrons, the *s*- and *p*-states together contributing the common grouping of eight valence electrons and sharing on a proportionate basis the top semicircle of the diagram. The lower semicircle is reserved for transition and subtransition elements, the *d*-state sector with five positions (10 electrons) containing the transition elements; and the *f*-state with seven positions (14 electrons) the subtransition or rare-earth elements. The heavily inked arc on each of the circles represents occupancy; the remainder of the circle nonoccupancy.

Beginning with the center and proceeding radially outward, any radius intersects the orbitals or quantum states in order of increasing energy. Thus, the state of lowest energy is shell 1, and its arc indicates occupancy only in the *s*-subshell. Next is shell 2, again the *s*-subshell. Next is 2*p*; then 3*s*, 3*p*, and 4*s*. The circle of lowest energy after 4*s*, however, is 3*d*, incepting the first transition series. Similarly, beyond

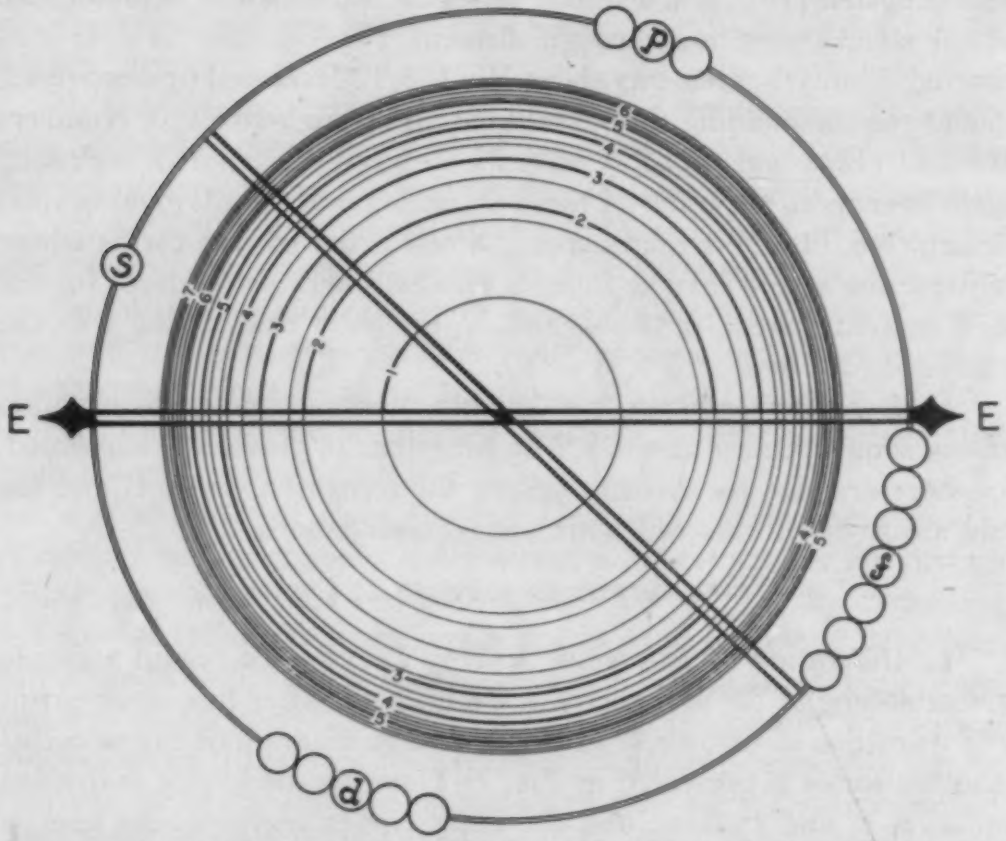


Fig. 1—Schematic Representation of the Electron Energy Levels of the *s*, *p*, *d*, and *f* States for the Seven Principal Quantum Shells. Heavy arc denotes occupancy.

5*s* there is a 4*d* state having lower energy than 5*p* and accounting for the second transition series.

In the *f*-sector, the 4*f* and 5*f* levels have respectively lesser radii than 5*d* and 6*d*, and 6*p* and 7*p*. They therefore account for the fact that the electrons drop into these inner shells instead of filling the outer shells, for the system, of course, always seeks the state of minimum energy.

This diagram has some significance in indicating why the heavier elements tend toward poorly defined valences and generally complicated behavior, for very little difference in energy exists between neighboring states; and positions of the outer electrons are therefore not too

rigorously defined. Also, atoms of transition groups are not restricted to the formation of single covalent bonds, but can form multiple covalent bonds with electron-accepting groups by making use of the electrons and orbitals of the shell or shells underlying the valence shell.

Arranging the Elements—With the diagram in Fig. 1 serving as a general basis for placement of the elements, the periodic chart in Fig. 2 was developed.

This chart, similar to the preceding figure, is divided into an upper semicircle containing those elements which progressively add electrons to the outer valence shell, and a lower semicircle which contains all others, specifically the transition elements. The continuity begins for each new valence shell in the *s*-sector on the left of the upper semicircle and proceeds clockwise as indicated by arrows. In the center the neutron is indicated as element No. 0. The significance of the radius is retained from Fig. 1 in a qualitative sense so that the chart indicates relative states of energy and depicts up to any given element the number of electrons and their quantum position in shell and subshell by regarding all element positions of lesser atomic number.

Beginning nearest the center at the left with hydrogen, the second electron produces inert helium. One of the few discrepancies in the chart stands there in placing helium in the *p*-subshell instead of in the *s*, where it belongs; but it was done for a schematic purpose soon to be disclosed. With the closing of shell 1, the chart proceeds back to the left and begins the clockwise series of lithium through neon, the last an inert gas. Beginning again on the left in shell 3, subshell *s*, the sodium series forms, ending with inert argon.

Next, the 4 shell begins with potassium and calcium in the *s*-state, but promptly bypasses the *p*-state to enter the *d*-transition sector radius III, in the lower semicircle, as described in discussing Fig. 1. The elements then progress through scandium, titanium, vanadium, chromium, manganese, into the triad of iron, cobalt, and nickel. These transition elements are located on shell 4 in this group, because their cross section would show the fourth shell while the third shell is filling.

With the completion of this transition series, the next element, copper, now has an inner construction which is expanded and heavier than its positional predecessor, potassium. Consequently, the ensuing series of copper through inert krypton is offset slightly and is marked with a heavier circle. These elements in the upper semicircle which build *s*- and *p*-valence electrons upon expanded internal shells comprise the so-called "B-subgroup" of the periodic table.

After krypton, the continuity methodically reverts to the left again, where rubidium and strontium begin the fifth shell. The following elements likewise bypass the *p*-subshell and enter the transition sector, radius III, becoming the elements beginning with yttrium and ending with the rubidium-rhodium-palladium triad; and upon that expanded shell is built the B-subgroup elements beginning with silver and ending with inert xenon [54].

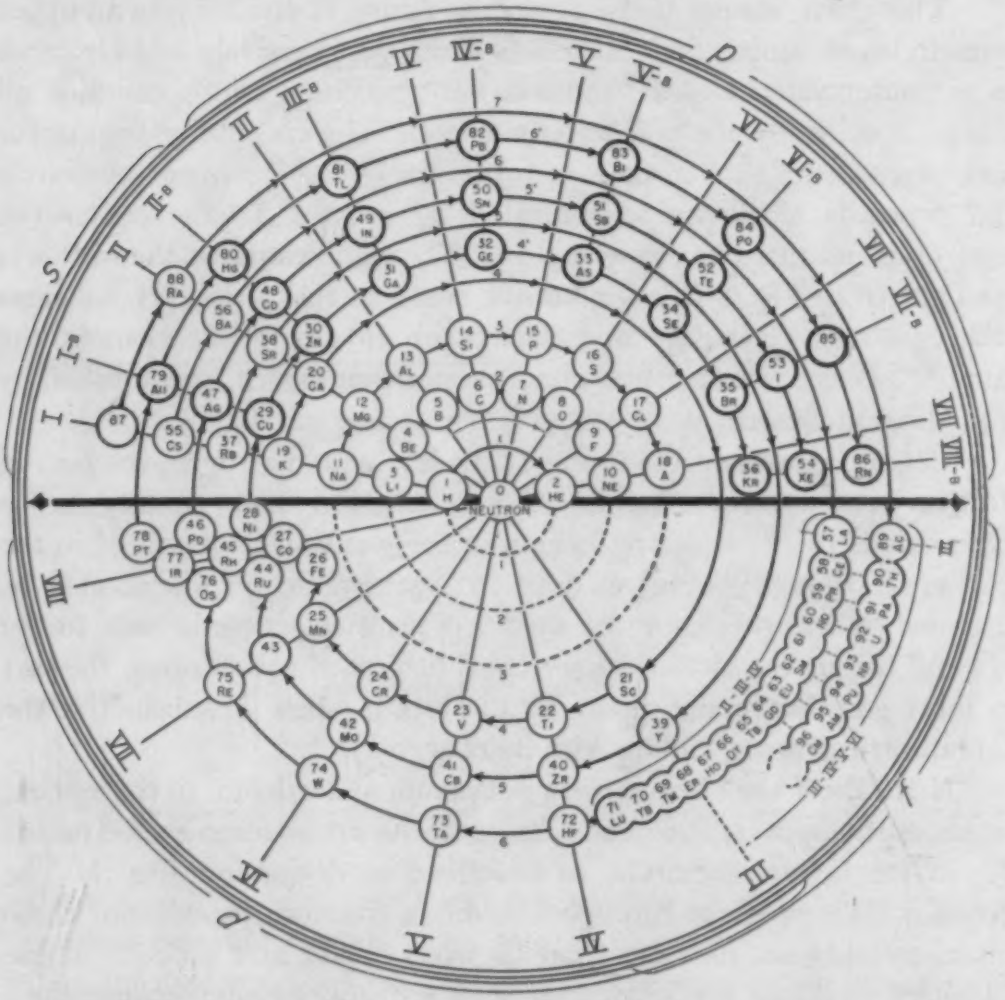


Fig. 2—Periodic Arrangement of the Elements on a Schematic Basis of Their Electronic Configurations.

Again from the left on shell 6, cesium [55] and barium [56] progress to the transition element lanthanum. But this time the progression in turn gives way to an expansion *two* shells deep, providing the rare earths as has already been described. The valence positions of these rare earths conveniently fit in the *f*-sector made vacant by the absence of transition elements in the first two valence periods. The

valences of the rare earths vary among II, III, and IV, and they are best left in their indicated positions until more is known about them. So far Ce and Tb are known to have valences greater than 3; and Sm, Eu, and Lu are known to be bivalent.

With 14 electrons added to the *f*-subshell, the subtransition series graduates into a transition series which continues by customary building in the *d*-subshell and ending again with triads, Os, Ir, and Pt.

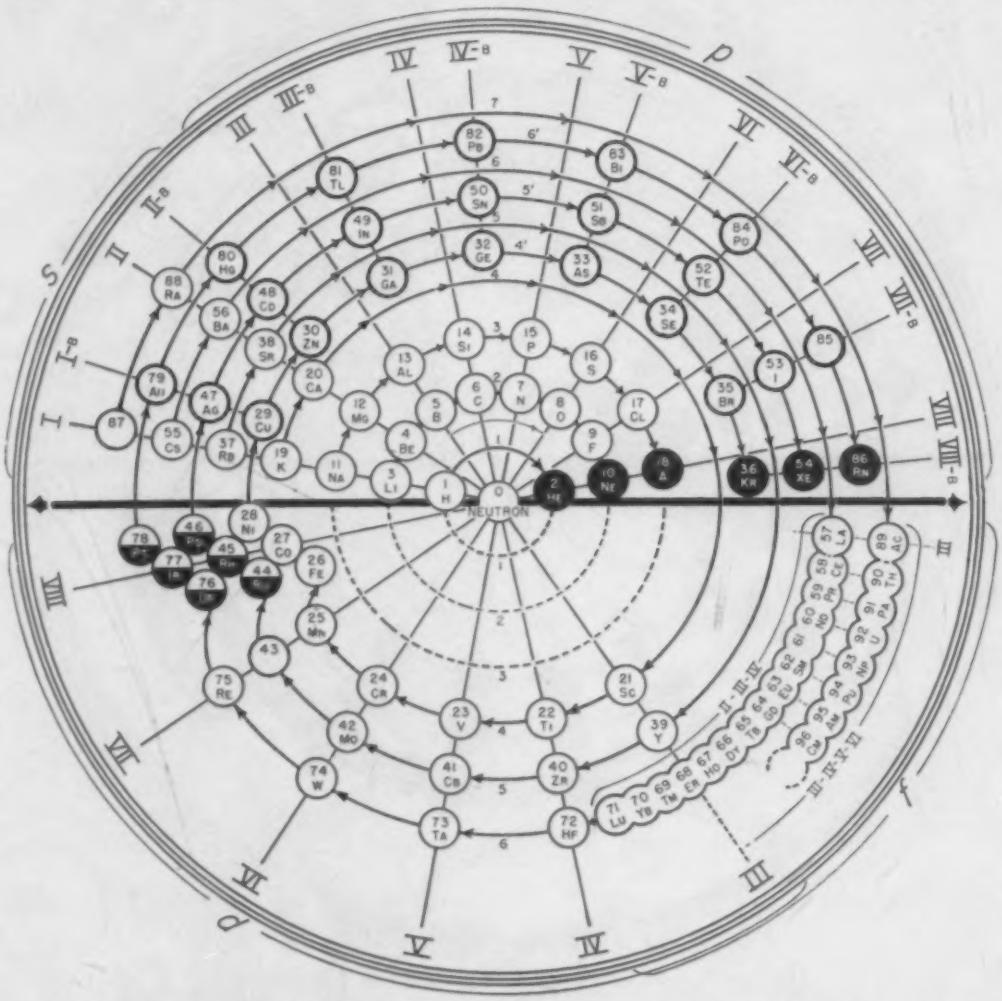


Fig. 3—Pattern of Chemical Inertness on the Periodic Chart.

As for the remaining elements, including the newly discovered neptunium, plutonium, americium, and curium, they are arranged on the chart following exactly the same progression as the rare earths before them, in conformity with the discussion provided earlier.

Characteristics of the Chart—Immediately it will be noted that this arrangement of the elements expresses the commonly denoted relationships of periodic charts and includes more.

First, the radii correspond to periods in the Mendelejeff chart, and the shells to rows. Second, the chart up to any given element schematically depicts the number of electrons and the energy state of each electron in that atom. Third, not only the principal quantum shells, but also the *s*, *p*, *d*, and *f*-subshells are indicated for each element. Fourth, all transition elements are in the lower semicircle. Fifth, all

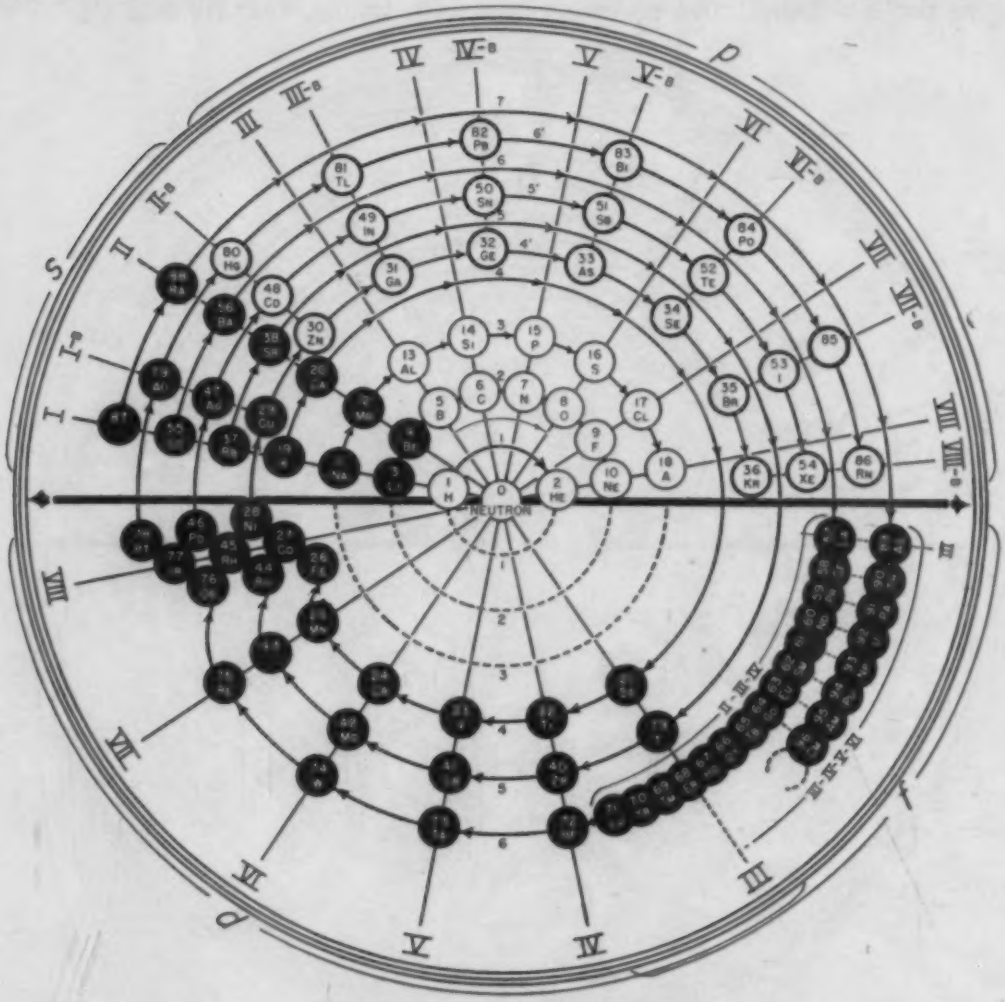


Fig. 4—Pattern of Hume-Rothery's Class I Elements.

rare-earth elements are in the *f*-sector. Sixth, all B-subgroup elements are designated. Seventh, a new series of rare earths is indicated.

Along each radius, valence characteristics are expressed. In the upper semicircle, radius I contains all the alkali elements; radius II all the alkaline earths; radii III, IV, V, and VI the amphoteric elements; radii 7 and 7-B all the halides (except hydrogen); and radii 8 and 8-B all the inert gases. In the lower semicircle, the valence principle similarly applies to the transition elements.

Electronegativity, which is a qualitative property expressing the power of an atom or molecule to attract electrons to itself, decreases clockwise along peripheries and increases toward the center.

In addition to radial relationships, analogies likewise hold along diameters. Thus aluminum and boron in the upper semicircle, radius III, extend directly into the analogous scandium and yttrium on

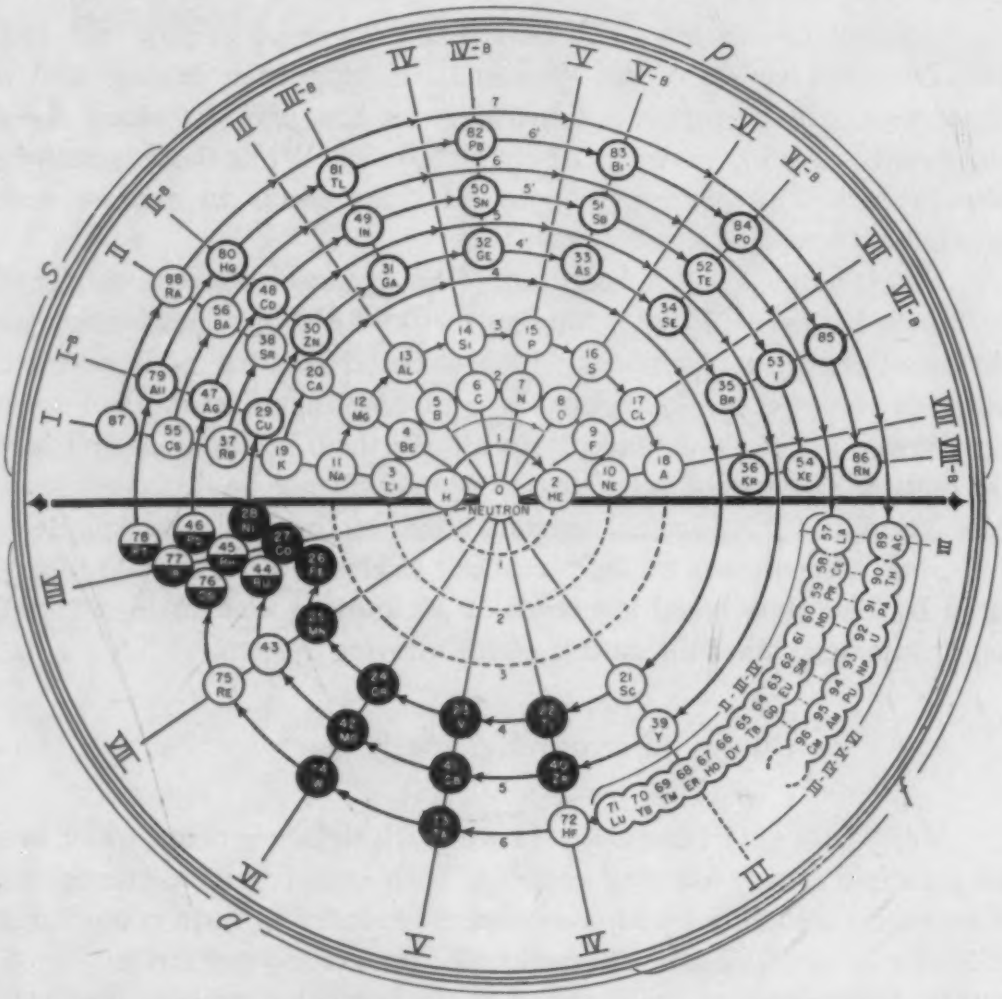


Fig. 5—Pattern of Major Alloying Elements in Ferrous Metallurgy, Having Extended Solubility Ranges.

radius III in the transition semicircle. Similarly, Si and C on radius IV (above) extend to Ti, Zr, and Hf on radius IV (below). Even more interesting is the VIII - VIII-B inert gases which extend into the noble transition metals in the lower semicircle. In Fig. 3 this relationship is indicated by marking the inert gases with full black circles and the passive metals with half-black circles.

Elements 43, 61, 85, and 87, formerly known as masurium, illin-

ium, alabamine, and virginium, respectively, are left unnamed on the chart because they have recently been found to be radioactive and therefore will be renamed by their discoverers (4).

Applications of the Chart

General Chemistry—The remarkable logic underlying the progressive construction of the elements has long been known, and is made especially apparent by marking on the periodic chart those elements having any given set of characteristics. While there is nothing new in such a procedure, the present chart seems to express such relationships with unusual clarity.

For example, Fig. 4 has marked on it those elements cataloged by Hume-Rothery (3) as belonging to Class I. This classification includes all elements crystallizing in face-centered cubic, body-centered cubic, or close-packed hexagonal structure. Manganese and one form of tungsten are the only exceptions among them. Aluminum and lead are omitted because of peculiarities which will not be discussed here. Also, certain of the *f*-sector elements remain to be cataloged definitely.

Such compactness of the blackened circles is significant to metallurgy because the crystal structure of an alloying element is a prime factor in determining the nature of the alloying system.

Ferrous Metallurgy

Major Alloying Elements—If we mark those elements which are the principal binary alloying elements with iron from the standpoint of extensive solubilities with a minimum tendency to form compounds of brittle or semi-metallic character, the interesting pattern in Fig. 5 results. Such elements are confined to the transition groups. Furthermore, those elements on the same periphery with iron form in general the most homogeneous systems, only Ti at the far counterclockwise end forming a compound stable at high temperatures.

In the fifth and sixth shells homogeneity of the alloy systems tends to decrease, reaching a minimum again in Zr at the far end. The six noble elements are marked with half-circles, principally because they are not commonly used in steel.

Minor Alloying Elements—Obviously in a chart of this kind, and in following charts, division of the alloying elements into major and

minor groups will involve boundary elements whose inclusion or exclusion becomes arbitrary.

Nevertheless, if we next consider those elements which alloy with iron, but which either have solid solubility limits or tend strongly toward forming compounds of generally undesirable engineering properties, a secondary group becomes fairly well defined. Fig. 6 shows their pattern.

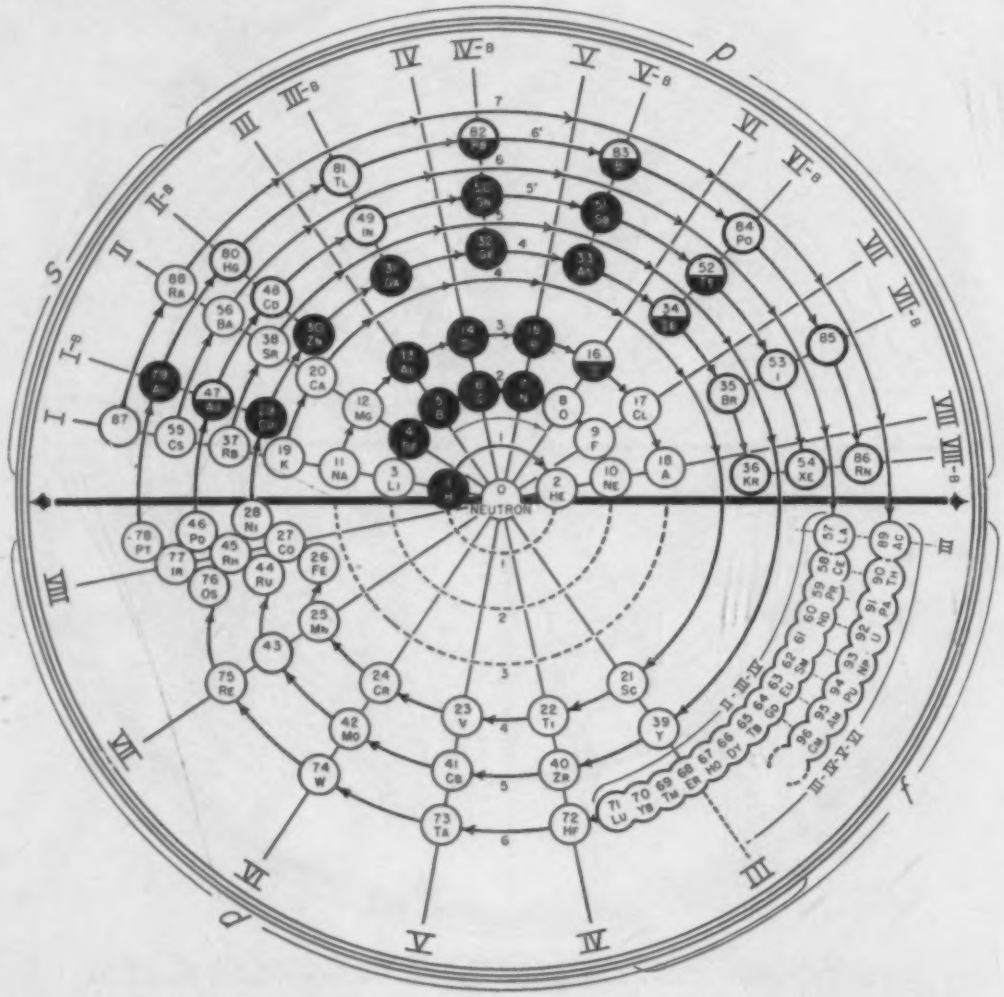


Fig. 6—Pattern of Minor Alloying Elements in Ferrous Metallurgy, Having Restricted Solubilities or Undesirable Compound Formation.

None of the elements on radii I, II, VII and VII-B, and VIII and VIII-B alloys with iron with the exception of Be, and possibly H. As in the previous pattern, a preference appears for elements on the same shell with Fe. In the shell below, Al and Si form extended and useful alloy series with Fe, but marked compound formation intervenes. In shell 2, the three elements beyond Be dissolve interstitially, as does oxygen, which is not marked.

Au, Sn, and Sb are the only other elements having appreciable solubilities in Fe, and they again form marked compounds. Ag, though virtually insoluble, is included as a half-circle because of its position between soluble Cu and Au and because attention has periodically been drawn to its possible usefulness in Fe alloys. Pb, Bi, S, Se, and

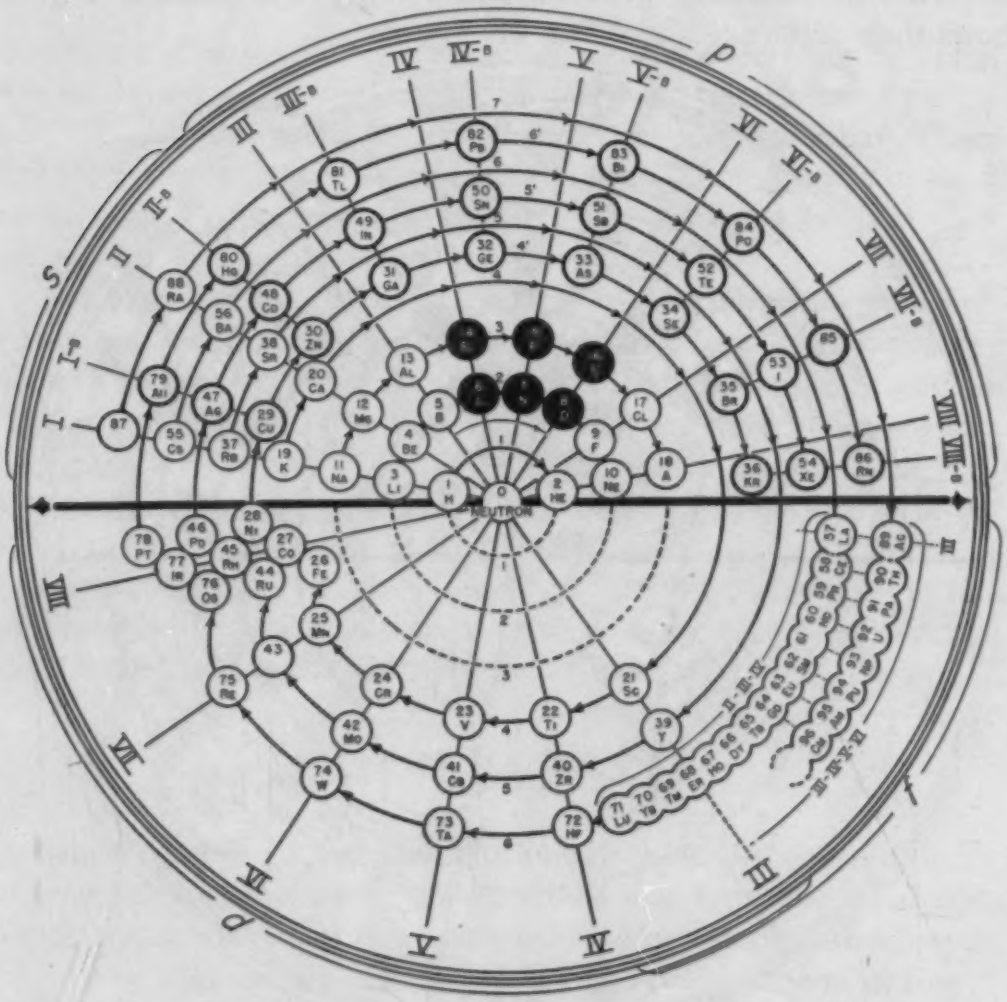


Fig. 7—Pattern of the Characteristic Nonmetallic Impurities in Steel.

Te are similarly included as half-circles because, though virtually insoluble in Fe, they are sometimes added commercially to steel for improving machining. Oxygen is arbitrarily omitted because it has but slight solubility and is not added purposefully to steel.

Nonmetallic Alloying Elements—Although the definition of impurities in steel is also highly arbitrary, it is interesting that all of the common nonmetallic impurities in steel occupy a confined area in a special part of the chart. (See Fig. 7.)

Ferrite-Formers—As for the important effect of crystal structure in alloy metallurgy, Fig. 8 designates those elements which are known to favor the body-centered cubic structure of iron and are generally referred to therefore as "ferrite-formers". Note the prominence of the IV, V, and VI periods in the transition group containing

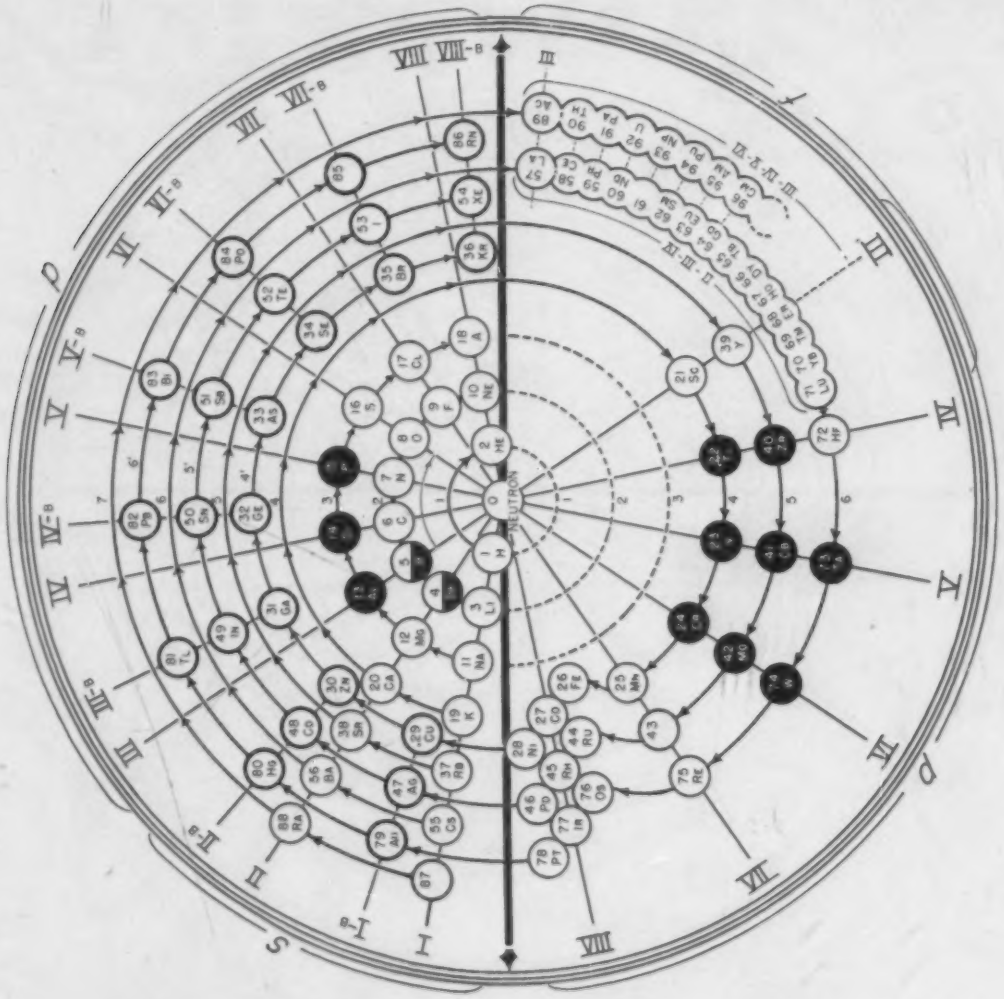


Fig. 8—Pattern of Elements Which Favor the Ferritic Form of Iron.

such well-known ferrite-formers as Cr, V, Ti, Mo, Cb, Zr, W, and Ta. The effect extends no further clockwise, but is untested for elements lying counterclockwise, such as scandium, hafnium, yttrium, and the two series of rare earths.

Also interesting to note are the diametric projections of ferrite-former radii IV and V into ferrite-formers Si and P in the upper semicircle; and conversely the projection of upper radius III makes it likely that scandium and yttrium, also hafnium, are ferrite-formers.

The role of aluminum as a ferrite-former, incidentally, now sheds some light on why that FCC metal is excluded from Hume-Rothery's Class I elements for being anomalous.

Beryllium and boron are arbitrarily marked with half-circles, although Hansen (5) reports that 0.45% Be closes the gamma loop.

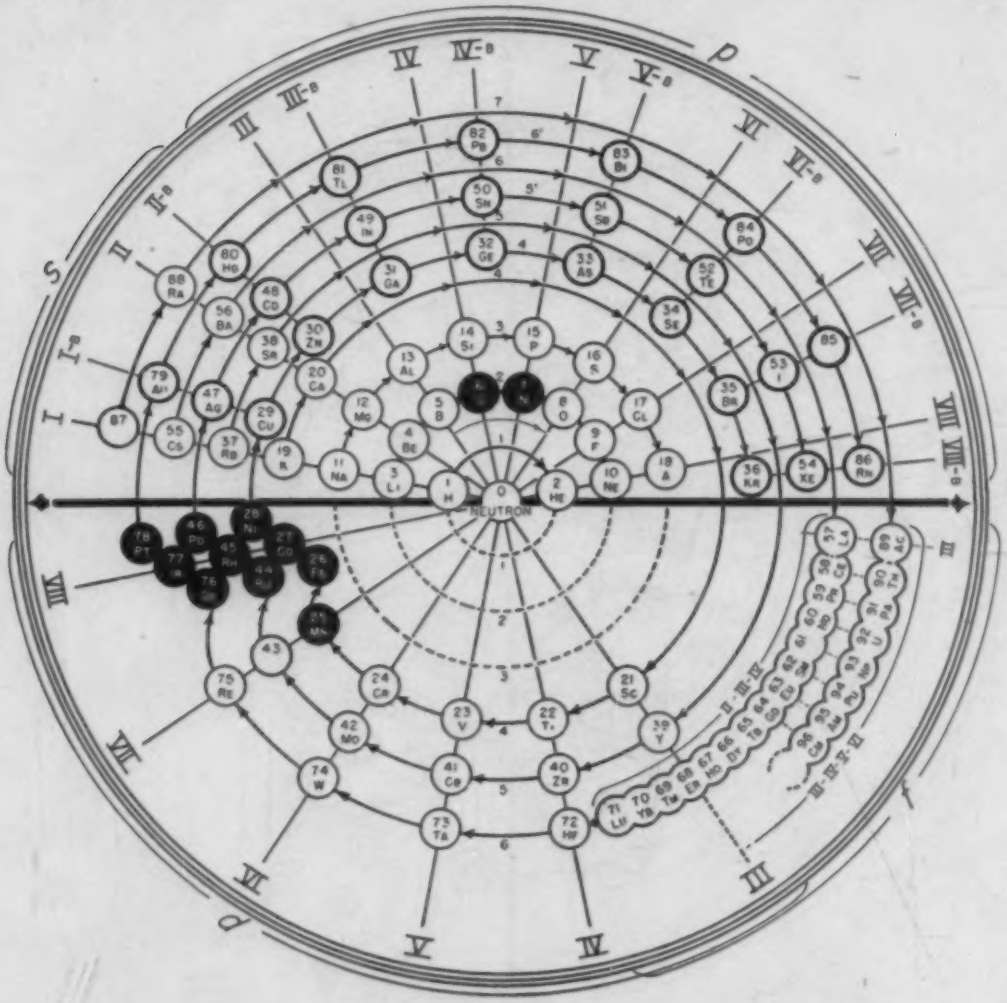


Fig. 9—Pattern of Elements Which Favor the Austenitic Form of Iron.

Boron is known to make a minor contribution, but possibly only because it takes carbon out of solution.

Austenitizers—Similarly, the pattern of alloying elements favoring the face-centered cubic gamma structure of iron has distinguishing characteristics. (See Fig. 9.) Although the noble metals in the triads adjoining iron favor austenite, the important austenitizing elements in steel include only Ni, Co, and Mn immediately adjoining Fe in the lower semicircle, and the two nonmetallic neighbors C and N (both in-

terstitial solutes) in the upper semicircle. Other weakly austenitizing elements, such as Cu, are omitted because of their relative unimportance.

Nonferrous Metallurgy

Aluminum-Base Alloys—For those elements used in the alloying of aluminum, there will be chosen four principals: Mg, Zn, Cu, and Si, which lie in the upper semicircle (full circles in Fig. 10); and six

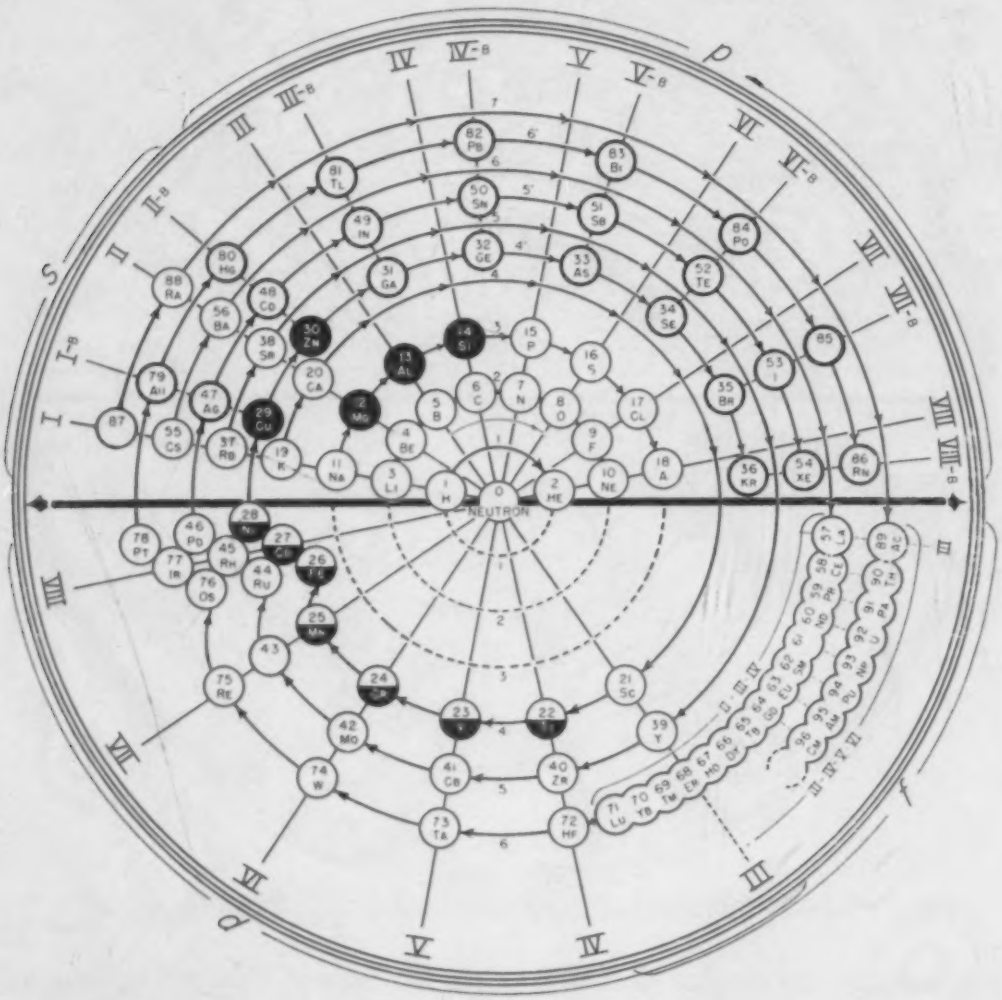


Fig. 10—Pattern of Exemplary Elements Comprising Aluminum-Base Alloys.

subordinates: Ni, Co, Fe, Mn, Cr, V, and Ti, which lie in the 4-shell of the transition sector (half-circles). This disposition in the semicircles is exactly opposite to that for iron (previous Figs. 5 and 6), in keeping with the position of Al in the opposite semicircle.

Obviously, not all elements alloying with Al are included in this selection; but exemplary ones are. Ag, Ga, and Li have appreciable

solubilities, but are uncommon constitutents of Al alloys. The magnesium neighbors, Ca and Be, have very slight solubilities. Ge does not measurably dissolve in solid Al, but as a eutectiferous alloying element it has been proposed to replace its much cheaper analog, Si (6). Pb, Cd and Bi are virtually insoluble in solid Al, but are added to improve

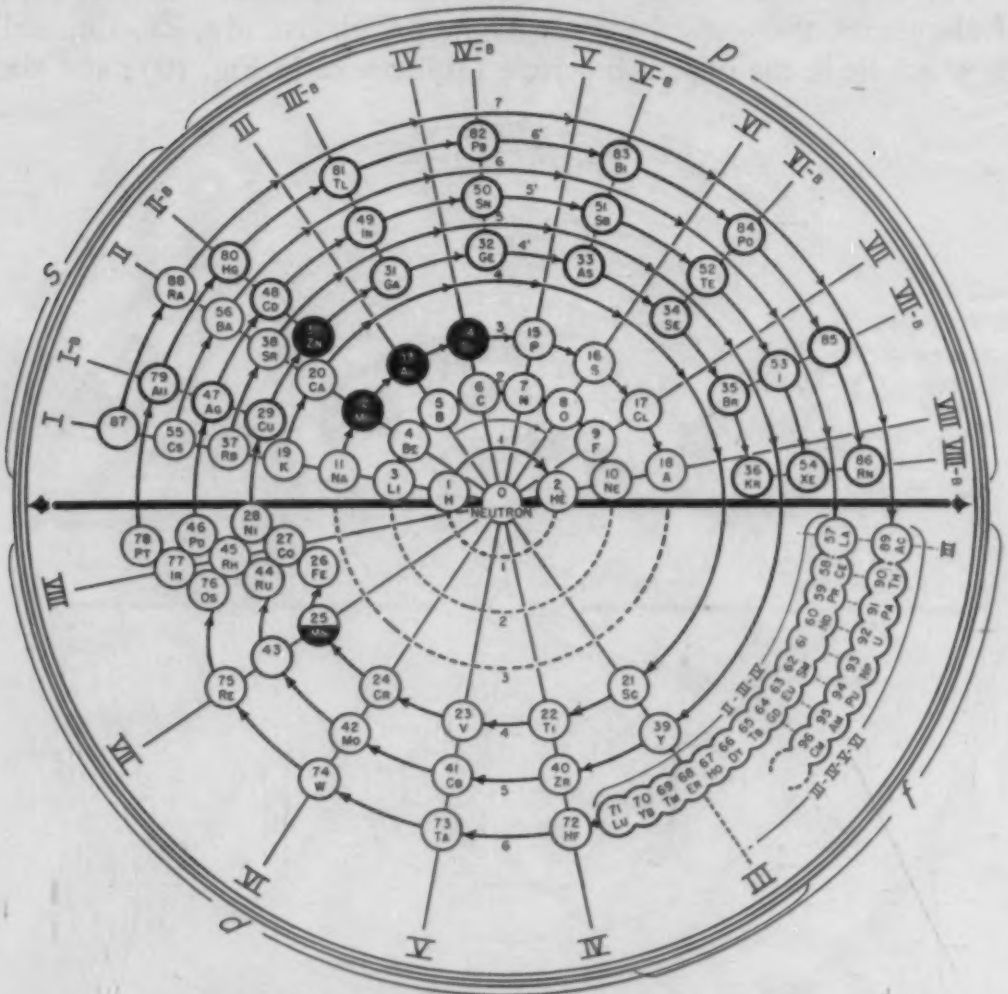


Fig. 11—Pattern of Exemplary Elements Comprising Magnesium-Base Alloys.

machining; and a similar situation exists for Sn and Cd used in bearing alloys. Other elements have also been studied as alloy constituents; but Al is a near-neighbor of the alkaline earths, and its alloys tend strongly toward compound formation and small solid solubilities.

With the chart confined to these exemplary elements, certain structural principles immediately reveal themselves. Thus, as with Fe, a marked preference appears for elements lying on the same shell with the basis element, Al; and next for those on adjacent shells 2 and 4. Mg, lying on the same shell, dissolves extensively in solid Al; Ca

and Be, on the higher and lower adjacent shells, respectively, also dissolve in solid Al, but only in minute amounts. Beyond Ca on that same radius II there is no measurable solid solubility (Sr, Ba, Ra).

Departure from this "shell rule" lies principally in the low-melting

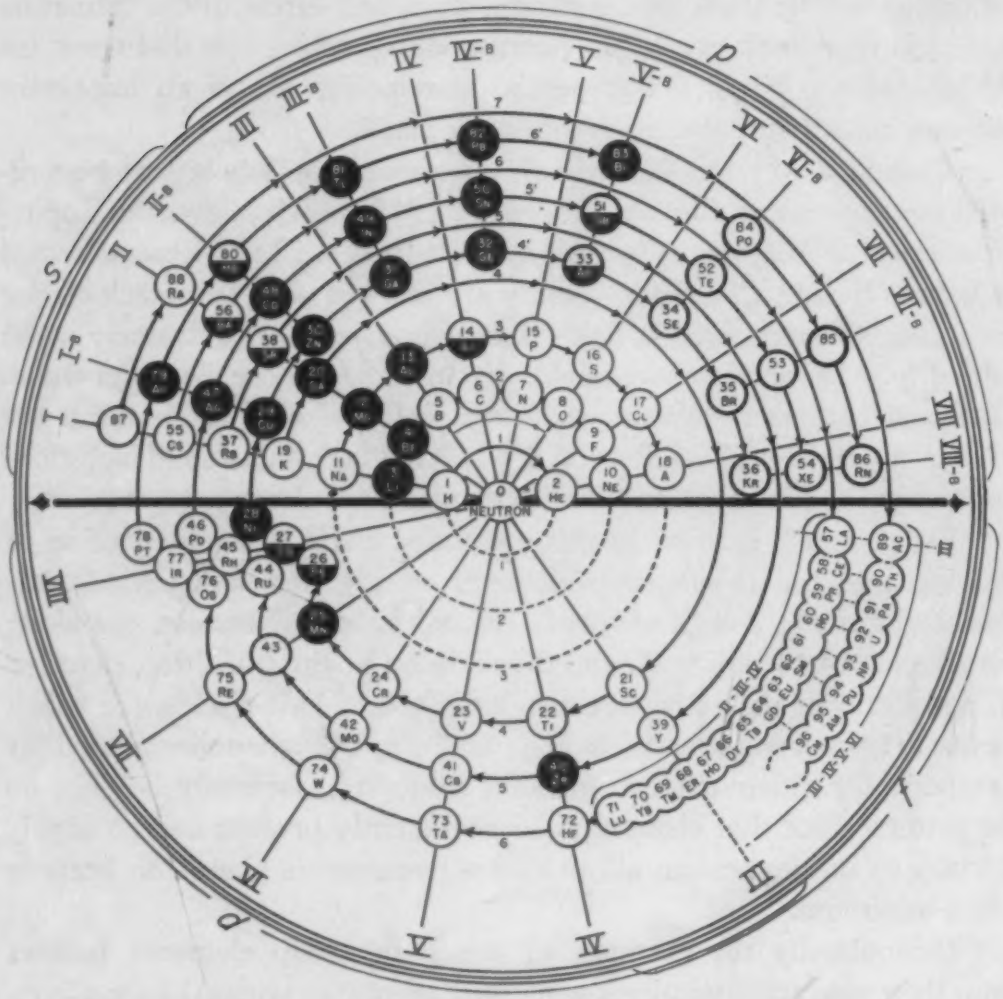


Fig. 12—Expanded Pattern Showing All Known Elements Alloying With Magnesium, as Listed by Carapella.

B-subgroup elements, for the possible reason that they have similar melting temperatures.

Conversely, since the transition elements have characteristically high melting temperatures, those elements in the lower semicircle, marked with half-circles, have very low solubilities in Al and are principally important as hardeners and grain-refiners.

There is no measurable solid solubility for any element clockwise of radius IV in the upper semicircle; nor along radius I, with the single exception of Li.

Magnesium-Base Alloys—If one similarly selects exemplary elements used in magnesium-base alloys, the consistent pattern in Fig. 11 is observed. As with aluminum, the major alloying constituents again lie in the upper semicircle; and they neighbor one another both by radius and by shell. Mn, indicated by a half-circle in the transition group, is representative of the corresponding series just discussed for Al-base alloys. From a commercial standpoint, Mn is an important alloying constituent; but its solubility is small.

Carapella (7) has recently ably reviewed the whole situation regarding magnesium alloys as known in 1945, which allows developing a rather complete pattern for this system. In Fig. 12 all elements which he lists as having a known solubility are marked with full-black circles excepting silicon, which is half-circled because of its extremely small solubility. Also on the chart as half-circles are all those elements which Carapella lists as developing a known eutectic with magnesium, but having no measured solid solubility. While terminal solid solutions must exist for such systems, their extent is not yet known.

Of principal interest in this expanded chart is the projection of alloying into the B-subgroup elements of the first five periods, the reaching into the 2-shell elements Be and Li, the extension out along the alkaline earth radius II, and the addition of the transition elements Ni and Zr. Iron and cobalt are also indicated by half-circles, for cobalt forms a known eutectic with Mg; and Fe, though undesignated by Carapella for either eutectic or solid solubility, obviously belongs on the pattern since that element is so persistently present and so highly deleterious in magnesium alloys that a premium is placed on keeping it to a minimum.

Undoubtedly the entrance of the B-subgroup elements follows from their characteristically low melting points, as with Al-base alloys. Three rare earths, cerium, lanthanum, and praseodymium, have been studied in the metallurgy of magnesium, but are not marked on the chart.

From the isolated position of Zr on the chart, one can predict possible future development of the remaining IV-V-VI-period transition elements, whose ability to alloy will probably be highly restricted, will decrease with increasing shell number, and will be controlled also by the crystal structure and the atomic size factor, discussed by Carapella.

Copper-Base Alloys—An historic art and science, copper metallurgy has pretty well pushed to the far reaches of the periodic table,

with the exception of the subtransition rare earths. Once again a problem presents itself in partitioning among major, minor, and excluded groups; but the pattern in Fig. 13 should be acceptable in most respects. There the boundary between major (full-circles) and minor (half-

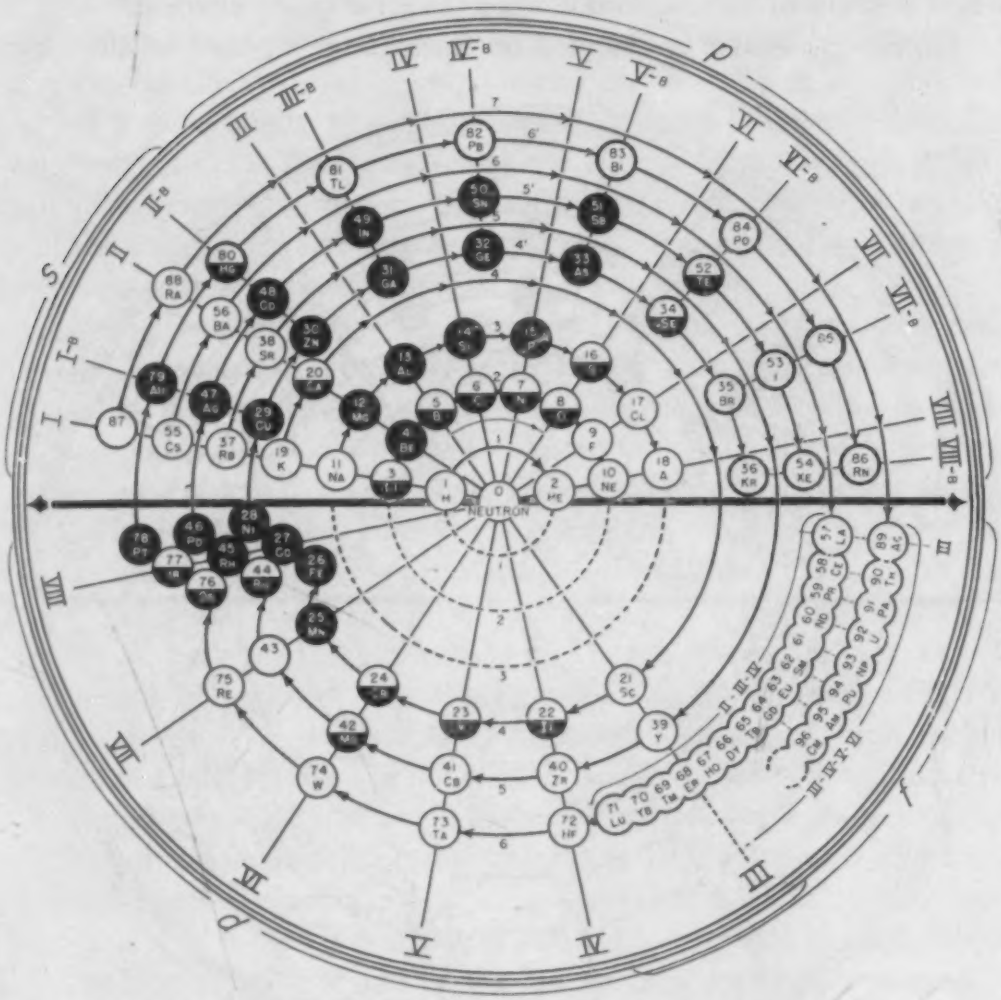


Fig. 13—Pattern of Elements Comprising Copper-Base Alloys.

circles) alloying elements is placed roughly in the neighborhood of 1% alpha solubility.

Immediately the "shell rule" reappears, with the historic principals Zn, Ni, and Sn placed on the same shell, or on the one immediately above. Zinc and nickel are immediate peripheral neighbors of Cu; and Sn, most removed of the three, correspondingly evidences the most restricted solubility (10 to 15%). The "shell rule" is again evident in the low-melting B-subgroup elements, whose solubilities approach zero in the outer shells; and in the transition semicircle a similar effect appears.

As for valence, the solid solubility wanes clockwise and virtually disappears in the VI and VI-B elements; and the 6-shell series Au-Hg-Tl proceeds from complete solubility for Au to virtually zero solubility for Tl. Although Hg and Cu are quite miscible, Hg is half-circled because of its uncommon usage as an alloying element.

Similarly, shell 2 is bounded on the left by Mg and on the right

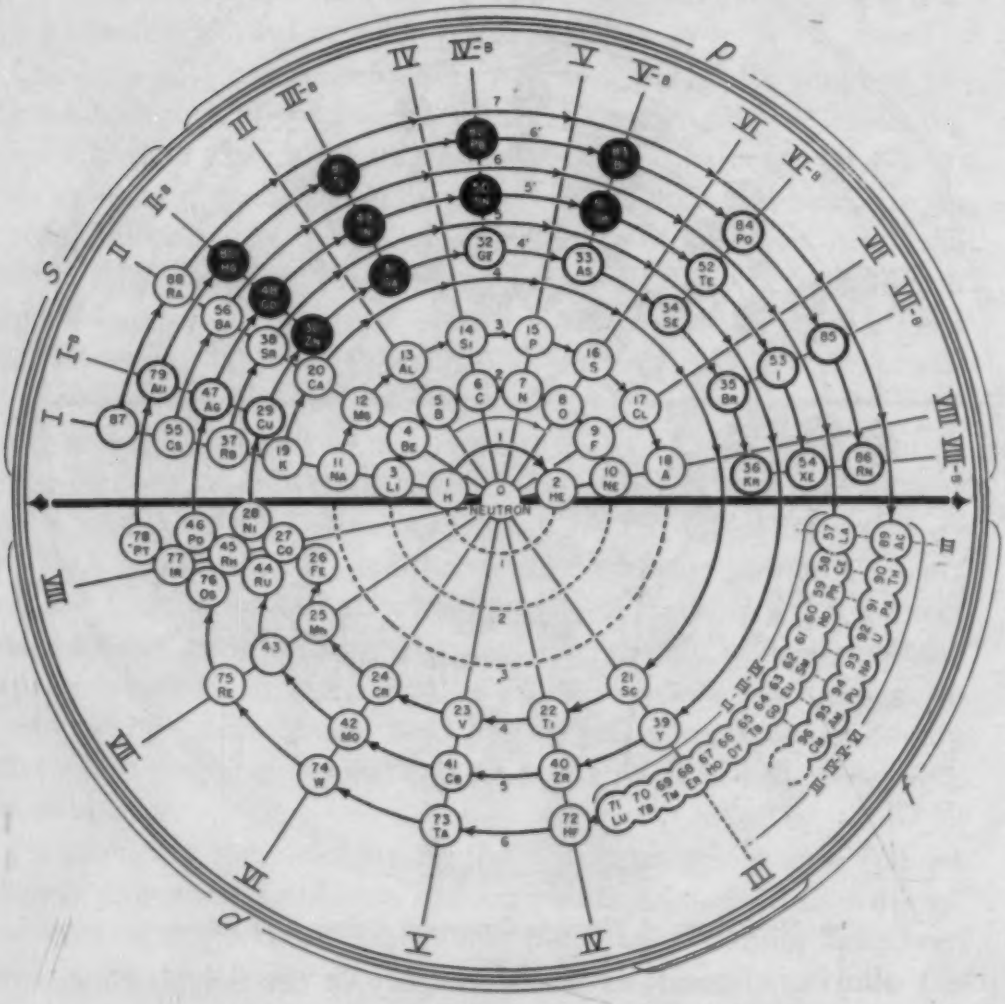


Fig. 14—Pattern for Low-Melting Alloy Systems.

by S; and the only principal alloying element in shell 1, Be, is flanked with highly restricted solubilities clockwise by B, C, N, and O, and counterclockwise by Li. Actually, Li has such a negligible solubility in solid copper that radius I probably should remain blank; but the commercial usage of Li introduced into Cu by Li-Ca alloy as a deoxidizer and purported dehydrogenizer led to its inclusion as a minor alloying element.

Along radius II an interesting relationship appears in that these alkaline earths show a major solubility in the 2-shell, a restricted solubility in the 3-shell, and a virtual disappearance of solubility by the time the Cu 4-shell is reached—an apparent exception to the "shell rule".

In the transition group, major alloying occurs with those elements adjacent to Cu, diminishing regularly at positions removed from Cu both counterclockwise along peripheries and also diagonally out into the noble metal triads, as indicated by half-circled Os, Ru, and Ir. The proximity of Cu to the transition group and its relatively high melting point apparently enlarges its alloyability with these elements, as does the fact that the crystal structures of most of the full-circle elements in the transition group are similar.

Low-Melting Alloys—Solders and low-melting alloys in general are based almost exclusively upon the B-subgroup elements designated in Fig. 14. These elements are metallic and characteristically have low melting points, which allows them to serve as possible alloying elements in nonferrous metallurgy and virtually excludes them from ferrous metallurgy. Also, since the B-subgroup by definition contains expanded internal shells, these low-melting metals are characteristically heavy. Note that the well-defined boundaries of this group exclude on the left all elements short of radius II-B, even though Cu, Ag, and Au are metals belonging to the B-subgroup. Low-melting eutectics may occur between the designated elements and others of high melting point, but such systems are not considered here. Proceeding clockwise, the lowest shell expires with high-melting temperature germanium (960 C) and compound-forming arsenic in the IV-B and V-B periods, respectively. Germanium does form a eutectic of low melting point with gold, and it dissolves in liquid Pb; but is insoluble in solid Pb (6).

In larger shells, 5′ and 6′, the low melting temperatures continue further clockwise to VI-B; and it is possible that in the 6′-shell the alloying continues through polonium in VI-B.

Thus, the melting temperature of these elements seems to drop with increasing shell number. This effect is evident along radius II-B to such an extent that in shell 6′ the element Hg is a liquid at room temperature. Along radius V-B the same effect is pronounced; along IV-B, Sn introduces only a slight exception; but along III-B exactly the opposite occurs, the melting points increasing outward along the radius progressively from gallium (30 C) to indium (161 C) to thallium (303 C).

Other Periodic Patterns—Following this or a similar procedure,

one can elaborate on the analog and periodicity phenomena of the elements virtually without limit. For example, in the acid or cathodic pickling of steel there is a poorly understood phenomenon by which extremely small amounts of certain elements present in the pickling liquor greatly increase the normal proportion of hydrogen which the steel absorbs during pickling. These elements are referred to as

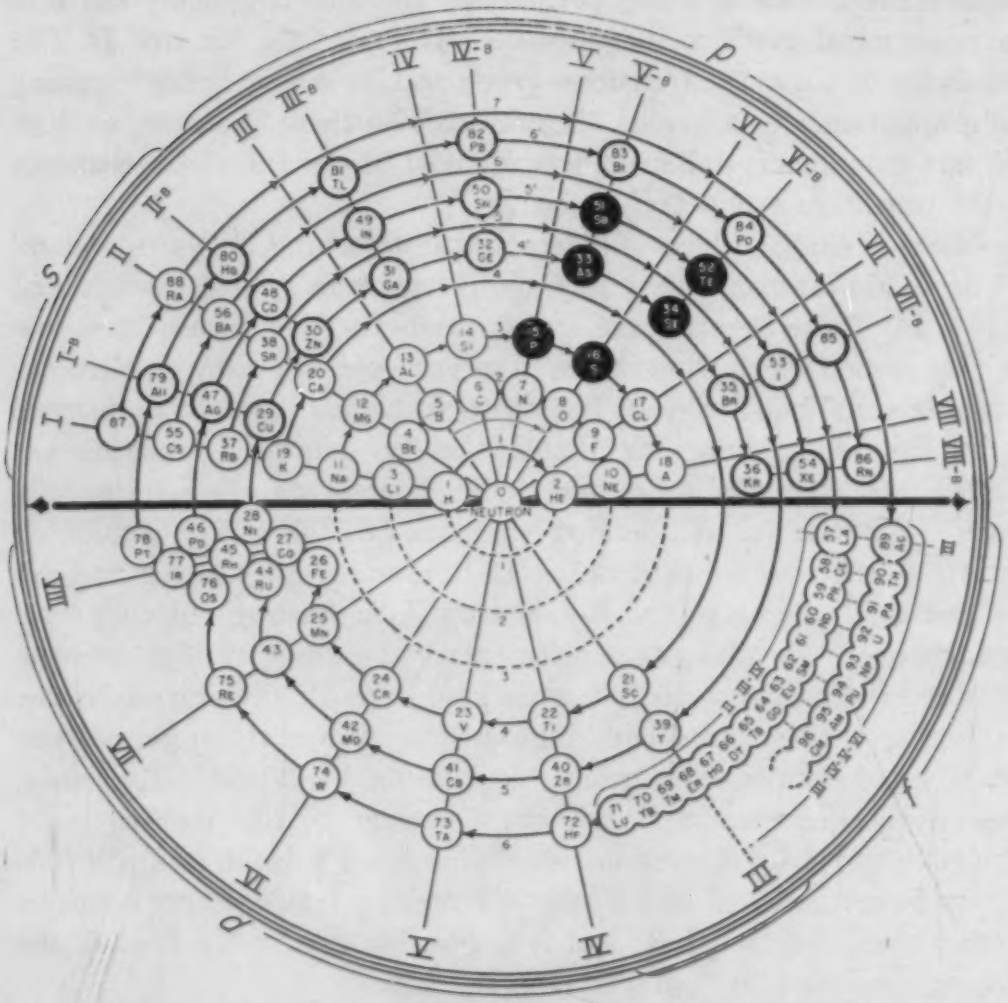


Fig. 15—Pattern of "Promoter" Elements Effective in Hydrogen Absorption by Steel During Acid or Cathodic Pickling.

"promoter" elements (8); and they comprise the narrow range designated on the chart in Fig. 15. The effect dies out quickly either to the right or to the left of the indicated elements, and at either lesser or greater shell positions.

Conclusion

But little claim can be made for originality in working with such

a thoroughly studied subject as the periodic arrangement of the elements. The principal object of this paper has been to renew discussion of the structure of the elements at a time when attention is being focussed on atomic theory, new elements are being discovered, and new things are being discovered about known elements.

Some additional clarity of the periodic laws seems to be provided by the charts that are presented; and the construction of a second series of rare earths on the basis of Seaborg's discoveries is a relatively new concept worthy of attention.

Acknowledgment

The writer wishes to acknowledge the assistance of Miss M. Eleanor Haslem in preparing the periodic charts presented in this paper.

References

1. F. L. Breusch, "Some Regularities in the Series of Stable Principal Isotopes of the Elements," Rev. faculté sci. univ. Istanbul 9A, 1944, p. 115-19.
2. L. Pauling, "The Nature of the Chemical Bond and the Structure of Molecules and Crystals," Cornell University Press, Ithaca, 1939, 429 pages.
3. W. Hume-Rothery, "The Structure of Metals and Alloys," *Institute of Metals* Monograph and Report Series No. 1, 1936, 120 pages.
4. G. T. Seaborg, "The Impact of Nuclear Chemistry," *Chemical and Engineering News,* Vol. 24, No. 9, 1946, p. 1192-98.
5. M. Hansen, "Der Aufbau Der Zweistofflegierungen," J. Springer, Berlin, 1936, 1083 pages.
6. R. I. Jaffee, E. W. McMullen and B. W. Gonser, "Technology of Germanium," *Electrochemical Society,* Preprint 89-19, 1936.
7. L. A. Carapella, "Fundamental Alloying Nature of Magnesium," Metal Progress, Vol. 48, 1945, p. 297-307.
8. C. A. Zapffe and M. Eleanor Haslem, "A Test for Hydrogen Embrittlement and Its Application to 17 Per Cent Chromium, 1 Per Cent Carbon Stainless Steel Wire," *Metals Technology,* Vol. 13, No. 1, T.P. 1954, 1946, 28 pages.

DISCUSSION

Written Discussion: By Hallock C. Campbell, associate director of research and engineering, Arcos Corp., Philadelphia.

Dr. Zapffe's periodic table has several interesting features not found in other arrangements of the elements, such as the revised grouping of the radioactive metals and the inclusion of the transuranic elements. The position of the transition elements in the lower semicircle makes it easy to locate the most likely analogous nonmetal by its diametrically opposite position. However, this introduces an undesirable separation of scandium from calcium (and yttrium from strontium, etc.); for example, in Fig. 13 the open circle for scandium is anomalous, since it interrupts a series of half circles starting with calcium,

but that fact is not obvious in Dr. Zapffe's arrangement of the elements. Also the use of secondary radii in the P-sector is an unhappy compromise, for the concept of B-subgroup elements is very misleading for most of the P-sector groups. In point of fact such a distinction is chemically nonexistent for the halogen and inert gas groups (numbers VII and VIII).

Nevertheless chemists and metallurgists alike, including those who prefer alternate forms of the periodic table, will heartily welcome Dr. Zapffe's compilation of the "patterns" exhibited by the major and minor alloying elements in ferrous and nonferrous metallurgy.

The writer has the following criticism to make of Dr. Zapffe's concept of a "double-pair" unit of atomic structure, and particularly his presentation of the structure of hydrogen. The actual weights of the proton and neutron and the weight of the hydrogen atom are known from independent measurements. Dr. Zapffe's hydrogen atom constructed from double-pair units would have a nucleus twice as heavy as the observed value. In the heavier elements the double-pair theory of construction is a very reasonable concept. However, Dr. Zapffe's description of element No. 1 is a description of deuterium (atomic weight 2), not of hydrogen. In hydrogen (atomic weight 1) the collapsed proton-electron pair is absent.

Written Discussion: By L. S. Darken, United States Steel Corp. Research Laboratory, Kearny, N. J.

It seems quite proper every now and then to recall attention to the periodic chart and point out its bearing on things of everyday interest. It seems particularly fitting in the case of metallurgists because as a group we tend to take it for granted and imagine that we know the relationships between common properties and the periodic chart better than we actually do. Dr. Zapffe's somewhat novel arrangement stimulates interest; it has served a good purpose. I for one had not fully realized, before looking at these charts, how far this sort of thing could be carried—for example that the ferritizing elements are grouped together so neatly as shown by Fig. 8. This suggests several other patterns it would be interesting to see—for example, that formed by the elements with strong tendency to form stable carbides.

In the beginning of this paper, there is definite implication that the neutron is not quite on par with the electron and proton in atomic architecture. The current accepted viewpoint is that there are these three fundamental particles, and that the neutron should not be regarded as a proton-electron pair.

The later work of Hume-Rothery places aluminum in the Class I elements (the metals) rather than in Class II as indicated by the author.

Written Discussion: By Harold Hessing, metallurgist, U. S. Department of Commerce, National Bureau of Standards, Washington, D. C.

The nucleus of the hydrogen atom described by the author on page 240, paragraph 6, of this paper is in reality that of deuterium, the "heavy", comparatively rare isotope of Element No. 1. An atom of the principal isotope of hydrogen has one proton and no neutrons in its nucleus.

The author states on page 256, paragraph 1, that aluminum, a face-centered cubic metal, is excluded from Hume-Rothery's Class I elements. It is of interest to note that this exclusion is no longer made in recent revisions of Hume-Rothery's "Structure of Metals and Alloys" (author's reference No.

3). On page 30 of the 1945 reprint Hume-Rothery states "aluminum should be regarded as belonging to Class I". Furthermore, aluminum is included among Class I elements in the periodic table (Fig. 4) on page 24 of this same reprint. The reference on which this classification was based is W. Hume-Rothery and G. V. Raynor[2].

Is the author's omission of uranium from his list of Class I elements intentional? Hume-Rothery includes uranium in Class I despite its orthorhombic structure.

Written Discussion: By F. R. Morral, Metal Trades Laboratory, Technical Service and Development Division, American Cyanamid Co., Stamford, Conn.

This paper is considered very interesting because of the novel and systematic presentation of the data. It is possible that someone may be able to make a rotary slide rule showing all the patterns in this paper and possibly others.

Dr. Zapffe's article, or the circular slide rule, should prove useful not only in the teaching profession, but particularly to the student and to those working in research and development.

Leverenz[3] has published a chart of the elements condensing considerable physical, chemical and metallurgical data.

In a data sheet on magnesium-rich binary alloys,[4] the eutectic temperature and composition, the solid solubility and the compounds formed with lanthanum, cerium and praseodymium were given in schematic form. The solid solubility was not available for two of them in the literature, while that for cerium in magnesium had been determined.

Written Discussion: By Gerrit DeVries, assistant metallurgist, U. S. Naval Proving Ground, Dahlgren, Va.

The author states that element No. 1 (hydrogen) is formed when a second pair of charges (a proton and an electron) is added to a neutron. This would give hydrogen an atomic weight of two.

Written Discussion: By Laurence S. Foster, Watertown Arsenal, Watertown, Mass.

I should like to make the following comments on this paper by Dr. Carl A. Zapffe. Dr. Zapffe has done metallurgists a service in calling the periodic table to their attention once more in such a well-rounded presentation of the correlations among properties which are revealed by its study. The use of the circular chart is interesting but it is felt that the construction of a "long form" rectangular chart is so much simpler it should be advocated in preference to the circular chart. The striking relationships revealed by the circular charts are nearly all revealed by the rectangular form; the only ones which are not brought out are those on radii passing from the upper half into the lower half of his diagrams, and these relationships are of no importance except to point out the analogous position of the inert gases and the passive noble metals.

---

[2]W. Hume-Rothery and G. V. Raynor, *Proceedings*, Royal Society, Vol. 177, 1940, A, p. 27.

[3]H. W. Leverenz, R.C.A., in Foote Prints, 1939.

[4]F. R. Morral, *Metal Progress*, October 1944, p. 720 B.

Dr. Zapffe does not point out that the reason for many of the similarities exhibited by the transitional elements is due to their comparable radii and the number of electrons in their outermost shells. These important characteristics cannot be read any better from his circular charts than from the long form rectangular chart advocated by this reviewer but are to be gleaned from study of lists like his Table I and from tables of atomic and ionic radii.

There are several other places where there are inconsistencies in Dr. Zapffe's presentation. It does not seem useful to substitute the concept of "a fundamental double-pair unit," "collapsed pairs" corresponding to neutrons, and "dilated pairs" corresponding to protons and extra-nuclear electrons. In his development of the Bohr type of atom the concept is not particularly useful and confuses the issue. In this discussion in which the only important property of the nucleus is its atomic number, or its positive charge, nothing is gained by making it more complicated than necessary. Furthermore, it is not strictly true that a neutron is a "collapsed pair," and until the debate concerning structure of nuclear particles is settled, it would be preferable to consider the neutron as a fundamental entity.

In Table I, the structures of the rare earth elements, Nos. 58-71, are shown with a steady increase in the 4*f* shell which is not in accordance with the facts published by Dr. Meggers of the National Bureau of Standards,[5] in which premature filling of the 4*f* shell is postulated and other irregularities brought out. In Table I, lanthanum is shown with the correct structure, but it is not placed correctly on the circular charts. It should appear not as a rare earth but as a transitional element under III immediately adjacent to Ba-56 (II). The same objection is raised to the placing of Actinium-89, which is also not a rare earth type but a transitional element and should appear above lanthanum, immediately adjacent to Ra-86 (II).

The argument in favor of considering the "Actinides" as a group similar to the rare earths can be made much stronger than Dr. Zapffe has done. Further evidence of the validity of this conclusion has been published recently. C. C. Kiess, C. J. Humphreys and D. D. Laun of the National Bureau of Standards[6] have analyzed the first spectrum of uranium and reached the conclusion, "From the spectroscopic evidence presented in this paper, it is clear that uranium is an element of the rare-earth type; that, in fact, it is a homologue of neodymium, being the third member of a series beginning with thorium. That the seventh period of elements in the periodic system should encompass a second group of rare earths similar to the group in the sixth period was foreseen more than 20 years ago by Bohr,[7]

"Some investigators, notably Villar, have suggested Th[90], others U[92] and still others, including Starke, the transuranium element 93 as the first in which a 5*f* electron appears. In each instance the basis of opinion was evidence derived from chemical behavior, nuclear activity, behavior of ions in crystals and solutions, etc. The testimony of the spectroscope, however, in selecting thorium for this role is unique and decisive, and it is supported by the

---

[5]Dr. Meggers, *Journal*, Optical Society of America, Vol. 31, 1941, p. 157.

[6]C. C. Kiess, C. J. Humphreys and D. D. Laun, *Journal of Research*, National Bureau of Standards, Vol. 37, July 1946, p. 57-72.

[7]Bohr, *Nature*, Vol. 112, 1923, p. 43.

Periodic Classification of the Elements

The Atomic Numbers are Placed Above the Symbols of the Elements; Atomic Weights Below the Symbols

Group	Ia	IIa	IIIa	IVa	Va	VIa	VIIa	VIII		Ib	IIb	IIIb	IVb	Vb	VIb	VIIb	O	
Type	R_2O RH	RO RH_2	R_2O_3	RO_2	R_2O_5	RO_3	R_2O_7	RO_4		R_2O	RO	R_2O_3	RO_2 H_4R	R_2O_5 H_3R	RO_3 H_2R	R_2O_7 HR	Inert Gases	
Period 1 2 Elements	1 H 1.0080																2 He 4.003	2
	3	4										5	6	7	8	9	10	2 8
Period 2 8 Elements	Li 6.940	Be 9.02										B 10.82	C 12.010	N 14.008	O 16.0000	F 19.00	Ne 20.183	
	11	12										13	14	15	16	17	18	2 8 8
Period 3 8 Elements	Na 22.997	Mg 24.32		Transitional Elements								Al 26.97	Si 28.06	P 30.98	S 32.06	Cl 35.457	A 39.944	
	19	20	21	22	23	24	25	26	27	28	29	30	31	32	33	34	35	36	2 8 8 18
Period 4 18 Elements	K 39.096	Ca 40.08	Sc 45.10	Ti 47.90	V 50.95	Cr 52.01	Mn 54.93	Fe 55.85	Co 58.94	Ni 58.69	Cu 63.57	Zn 65.38	Ga 69.72	Ge 72.60	As 74.91	Se 78.96	Br 79.916	Kr 83.7	8
	37	38	39	40	41	42	43	44	45	46	47	48	49	50	51	52	53	54	2 8 18 18
Period 5 18 Elements	Rb 85.48	Sr 87.63	Y 88.92	Zr 91.22	Cb 92.91	Mo 95.95		Ru 101.7	Rh 102.91	Pd 106.7	Ag 107.880	Cd 112.41	In 114.76	Sn 118.70	Sb 121.76	Te 127.61	I 126.92	Xe 131.3	8
	55	56	57 *58–71	72	73	74	75	76	77	78	79	80	81	82	83	84	85	86	2 8 18 18
Period 6 32 Elements	Cs 132.91	Ba 137.36	La 138.92	Hf 178.6	Ta 180.88	W 183.92	Re 186.31	Os 190.2	Ir 193.1	Pt 195.23	Au 197.2	Hg 200.61	Tl 204.39	Pb 207.21	Bi 209.00	Po (210)		Rn (222)	8
	87	88	89	**															2 8 18 18
Period 7		Ra 226.05	Ac	90–96															8

*Rare Earth Elements (Lanthanides) Group IIa	58 Ce 140.13	59 Pr 140.92	60 Nd 144.27	61	62 Sa 150.43	63 Eu 152.0	64 Gd 156.9	65 Tb 159.2	66 Dy 162.46	67 Ho 164.94	68 Er 167.2	69 Tm 169.4	70 Yb 173.04	71 Lu 174.99	
**Actinides Group IIIa	90 Th 232.12	91 Pa 2.31	92 U 238.07	93 Np	94 Pa	95 Am	96 Cm								

recent spatial classifications of the elements by Djownkorsky and Karis[8] and by Talpain,[9] which array thorium, protoactinium and uranium as the chemical homologues of cerium, praseodymium and neodymium."

The use of the word *expanded* (page 247) for the inner construction of copper as compared to potassium is not fortunate. The structure is more *complicated* but *contracted,* copper being a smaller atom than potassium and the copper ion also being smaller than the potassium ion.

In support of my arguments in favor of the rectangular long form of the periodic table, I have enclosed one based on the recommendations of Seaborg which appeared in the December issue of the *Journal of Chemical Education.*

Author's Reply

An apology is required for the obvious error, noted by Drs. Campbell, Hessing, and DeVries, in confusing the structures of hydrogen and deuterium. Drs. Hessing and Darken also bring the author up to date on Hume-Rothery's acceptance of Al as a Class I element. As for Dr. Hessing's question about uranium, it stands in the Class I pattern with the rare-earth elements.

Drs. Campbell, Darken, and Foster question the advisability of the "double-pair" concept. No refuge is taken, for this concept does have fine-scale departures from the rigorous definition. It was adopted only as a means of translating the highly technical language into acceptable lay language without serious loss of verity.

Dr. Morral's suggestion of a rotary sliding chart has strong possibilities, although it seems at first blush that the system is fixed, rather than movable. The discussion of alloys of Mg with certain of the rare earths was deliberately omitted because the pattern is too incomplete. On the other hand, perhaps it would have been better to have included them. As explained in the paper, the selection of elements for these patterns is somewhat arbitrary.

In answer to Dr. Foster, attention is drawn to the small radius "III" drawn through Ac and La at the far right of the rare earths, indicating that they belong on Radius III as a transition element. The text perhaps does not make that clear. While their present position is confusing, one will quickly recognize that an even greater problem follows from placing them on Radius III and adding the rare earths as a subsequent series. Also, by referring to the B-subgroup elements as having "expanded" shells, the writer perhaps thoughtlessly confined it to the sense of population, for those shells have numerically expanded groupings.

These criticisms are all welcomed. The paper presumes to do no more than to stimulate among metallurgists a timely interest in atomic structure.

---

[8]Djownkorsky and Karis, *Journal Phys. Radium,* Vol. 5, 1944, p. 53.
[9]Talpain, *Journal Phys. Radium,* Vol. 6, 1945, p. 176.

THE MEASURED KNOOP HARDNESS OF HARD SUBSTANCES AND FACTORS AFFECTING ITS DETERMINATION

By Newman W. Thibault and Helen L. Nyquist

Abstract

This paper discusses in detail the factors, many hitherto unknown or little realized, which may influence the measured Knoop hardness number, especially of hard, brittle substances. As a result of the study the authors have specified the conditions under which they believe a determination of the Knoop hardness number of such substances should be carried out, and they present in Table II a self-consistent series of Knoop numbers determined in this manner for a variety of materials ranging in hardness from boron carbide down to hardened tool steel, Rockwell C-60.5.

Introduction

FOR some time prior to 1936, Frederick Knoop and his associates at the National Bureau of Standards had been experimenting with different methods for the quantitative determination of the hardness of various crystals and glasses (1).[1] After abandoning scratch methods because of excessive wear of points and edges, and indentation methods of the cone, ball and square-based pyramid types because of excessive fracture of the specimen even under light loads, an instrument was designed to permit indentations to be made with a diamond which was lapped to the form of an elongated four-sided pyramid with obtuse included angles.

The original apparatus, allowing the application of the indenter under loads of 25 to 4000 grams, was entirely mechanical in construction. Because it has been adequately described and illustrated (2), (3), the details will not be repeated here. The instrument offers certain advantages over other common indentation methods. For example, brittle substances may be indented with much less fracturing, and the

[1]The figures appearing in parentheses pertain to the references appended to this paper.

A paper presented before the Twenty-eighth Annual Convention of the Society held in Atlantic City, November 18 to 22, 1946. Of the authors, N. W. Thibault is research crystallographer, and Mrs. H. L. Nyquist was assistant in the Research Laboratories, Norton Company, Worcester, Mass. The junior author's present address is Conneaut, Ohio. Manuscript received July 17, 1946.

hardness of thin films, such as platings, may be determined because of the very shallow depth of penetration of the diamond into the specimen. Futhermore, because of the small size of the indentations which result from the use of low indenting loads, the hardness of microconstituents may be determined, and steep hardness gradients, such as may exist in metals due to case hardening, may be investigated.

Sometime prior to 1940, the Wilson Mechanical Instrument Company was requested to design, manufacture, and market an instrument embodying the principles of the original National Bureau of Standards apparatus, and they were licensed to make the Knoop indenter (4). The Wilson instrument, known as the "Tukon Tester", is fully automatic, being electrically controlled during the complete indenting cycle, and permits indentations to be made under loads of 25 to 3600 grams. Both the original Tukon instrument and the newer model incorporating the solenoid device (5) have also been adequately described and illustrated (6), (7), (8), (9), (10). It is now customary to refer to the diamond indenter described above as the "Knoop" indenter, and the hardness value obtained by its use, the "Knoop" hardness number.

Norton Company purchased one of the first of the original Tukon instruments, and associated optical equipment, and the authors have been actively engaged in Knoop hardness investigations since the spring of 1942.

As with any method of hardness testing, there are two broad methods of approach. The first, the more practical, is to attempt to control the testing conditions only to such an exent that self-consistent data will always be obtained. The second, more critical, is to attempt to obtain hardness values which are not only self-consistent, but which agree rather closely with the results obtained on the very same specimens by other careful, qualified investigators using the same method in other laboratories.

It is obvious that self-consistent, comparative results are more easily achieved than are universally concordant values, because, in the former case, there are fewer variables, and control over them may be exercised by a single person, or a very closely associated group of workers. In the latter case, however, not only is the number of variables much greater, but a large amount of co-operative work may be necessary among a number of different laboratories before concordant results can be obtained.

Believing that the Tukon tester employing the Knoop indenter

was an instrument of high precision capable of yielding hardness values which would be concordant from laboratory to laboratory, we prepared a series of standard samples of different substances varying in hardness from a methacrylate plastic to silicon carbide. These were to serve as our master standards to check the self-consistency of our own results. These samples were submitted to the National Bureau of Standards which indented them under various loads using their original instrument, and measured the indentations by their standard method. Later we did the same, using our own Tukon tester and optical equipment. Subsequently, similar co-operative work was undertaken with the Wilson Mechanical Instrument Company and five other laboratories.

Because of the early lack of agreement between the Knoop number determined by ourselves and others on the very same prepared specimen, and our own occasional inconsistencies, it was decided to investigate, as systematically as possible, the various factors influencing the Knoop number of hard substances.

This study, now complete, has been most fruitful. It has been found that a large number of factors, many of them generally unknown or little realized previously, may greatly affect the Knoop number, especially in the case of hard, brittle substances. These have served to explain in large measure the differences between our own results and those of other laboratories, as well as many of the gross discrepancies to be observed in the literature (see Table I). From a very practical point of view, the study has led to a better control of the variables affecting our own determinations, and has resulted in our ability to produce self-consistent data which are much more precise than they otherwise would have been.

In Table II we present our own Knoop hardness values for a variety of hard substances.

This paper discusses the determination of the Knoop hardness number of hard substances, both nonmetallic and metallic. There are several reasons for devoting a seemingly disproportionate amount of space to nonmetallic substances in an article addressed principally to metallurgists. First, although the study mainly concerned hard nonmetallic materials, most of the factors investigated also affect the determination of the hardness of ductile metals, although often to a lesser degree. Secondly, there is an advantage in studying brittle nonmetallic substances because there is little likelihood of any disturbing effects caused by cold work, either during the preparation of the surface or during the indentation itself, as may occur with metals. Finally,

Table I
Uncertainty of the Knoop Hardness Numbers of Hard Substances as Reported in the Literature

Mohs' Scale	Substance (as Designated in the Literature)	Published by Members of the Staff of the National Bureau of Standards (1) (2) (3)	Brodie (6)	McKenna (12)	Winchell (7) (From His Table II)
10	Diamond	8200, 8200-8500; 5500-6950* 8000-8500	....	....	....
	Tungsten titanium carbide	....	....	2600	....
	Boron carbide	2265; molded: 2230; 2250-2260	....	....	....
	Tantalum carbide	....	>2200	....	....
	Silicon carbide	2000; 2130; green: 2130-2140 black: 2050-2150	....	ca. 2150-2250	green: 2675-2830 black: 2855-3010
9	"Alundum"	Variety not stated: 1635; 1655; "Regular": 1620-1635; "98": 1670-1680	....	....	.... synthetic colorless: 1930-2240
	Corundum	....	....	....	light ruby: 1425-2310 dark ruby: 1750-1955
	Spinel	....	....	....	synthetic blue: 1115-1235
8	Topaz	1250	....	....	985-1230
	Tungsten carbide	....	>2200	WC: ca. 1950	....
	"Carboloy"	1050; 1050-1500	....	....	....
7	Quartz	710-790	....	....	653-902

*Given by Lysaght (10) as the revised values from the National Bureau of Standards.

Table II
Knoop Hardness Numbers Determined at 100-Gram Load (K_{100}) for Various Hard Substances. Random Crystal Orientation

Substance	Knoop Number —100-Gram Load (K_{100})— Average	Range
Primary boron carbide ("Norbide")	2800	2670-2940
Molded boron carbide ("Norbide")	2760	2580-2900
Gray silicon carbide (Regular "Crystolon")	2460	2250-2680
Gray silicon carbide [Regular "Crystolon" (check)]	2550	2320-2760
Green silicon carbide (Green "Crystolon")	2480	2230-2740
Green silicon carbide [Green "Crystolon" (check)]	2480	2130-2620
Titanium carbide	2470	2350-2620
Tungsten titanium carbide	2190	2050-2320
Alpha-aluminum oxide ("38 Alundum")	2050	1860-2200
Alpha-aluminum oxide (synthetic boule)	1950	1680-2100
Primary (unbonded) tungsten carbide (WC)	1880	1570-2140
Cemented carbide ("Kennametal K6")	1800	1700-1940
Cemented carbide ("Kennametal KM")	1500	1390-1600
Cemented carbide ("Kennametal K12")	1410	1280-1500
Garnet (Barton Mines, New York)	1360	1240-1440
Topaz (Thomas Range, Utah)	1340	1240-1500
Synthetic blue spinel (Linde)	1270	1190-1460
Quartz	820	760-880
Hardened tool steel, Rockwell C-60.5	740	730-760

the sections devoted specifically to the brittleness characteristics of the nonmetallics are directly applicable to hardness studies of brittle metals and intermetallic compounds whose hardness it has been impossible to determine with the conventional Vickers or Rockwell instruments.

Review of the Literature

In this section, only those articles concerned largely or entirely with the Knoop method, or which contain original Knoop data on hard substances, will be reviewed. Those who are interested in the application of the method to the solution of specific problems are referred to the recent papers by Lysaght (9), (10).

A preliminary description of the Knoop indenter was given by Peters and Knoop (11) who applied the method to the measurement of the hardness of a series of glasses.

In 1939, Knoop, Peters and Emerson (2) published a detailed description of their original instrument. In addition to discussing the factors which led to the selection of the shape of the indenter for

general use, the recommended indenting procedure, and the dimensional basis for computation of the Knoop hardness number, other factors influencing Knoop results were considered, including the effect of load on the hardness number. The field of application of the indenter was stated, and comparisons made between the Knoop, and Vickers and Brinell numbers for a few metals. Hardness data given by these and other authors for materials as hard as or harder than quartz, omitting values quoted for certain metals whose hardness was not investigated by the present authors, are given in Table I of the present paper.

At about the same time Peters and Knoop (1) briefly described the method and gave the hardness number of a series of glasses and other substances. The values quoted for the harder materials are also included in Table I since they differ slightly from those previously quoted (2).

Later, Peters and Knoop (3) again described the apparatus, and outlined the results of the application of the method to several metallurgical problems.

Mrs. Brodie (6) was the first to discuss and illustrate the original Wilson adaptation of the National Bureau of Standards instrument, her experience being almost exclusively with metals. Various applications of the instrument were described and illustrated, and the hardness of a number of metals was given. In this paper and the accompanying discussion a number of factors affecting the Knoop number were mentioned. These will not be enumerated here, but will be included in the appropriate section later in the present paper.

McKenna (12) published a Knoop value for $WTiC_2$ as compared with those for silicon and tungsten carbides.

Winchell (7) stressed the effect of the crystallographic orientation of the test specimen on the Knoop number, and suggested a method for rigorously defining the orientation relative to the long dimension of the indenter by the use of three independent co-ordinate angles. Knoop numbers were given for a large number of different orientations on 16 different minerals and allied substances which he tested.

Tate (8) showed that, when steel and glass were indented, the Tukon tester equipped with the solenoid device consistently gave increasingly higher Knoop numbers with lower loads, an observation previously made by others (6). Tate gave evidence suggesting that this effect might be due to elastic recovery in the long dimension of the indentation, the amount of recovery being essentially independent of load.

Lysaght (9) described the latest model of the Tukon tester equipped with solenoid device, microscope attached to the instrument, and a mechanical stage which permits very precise movement of selected small areas from the microscope to the indenter. He mentioned a number of metallurgical problems to which the instrument has been advantageously applied, and discussed several factors affecting the Knoop number. Later Lysaght (10) discussed the application of the method to the study of the hardness of nonmetallic substances.

Measured Knoop Hardness Numbers of Various Hard Substances

As a result of our study of the factors affecting the determination of the Knoop hardness number of hard substances, we have found it necessary to establish a rigorous set of conditions governing the determinations. These are fully discussed in the following section, and are recapitulated in the summary. They are recommended to those studying the Knoop hardness of such materials.

Table II gives the average and range of Knoop hardness numbers for 100-gram load and random orientation for a variety of hard materials determined in this manner. It differs from previously published data in that it is self-consistent and is accompanied by the necessary details concerning the conditions of indentation and measurement.

No data for diamond are included in Table II because we had no facilities for making impressions at the extremely slow indentation rate said to be necessary to avoid excessive damage to the indenter (6, discussion). Since all the values quoted for the diamond were based on experiments made at the National Bureau of Standards with a load of 500 grams (10), no direct comparison can be made with our data for hard compounds as given in Table II.

Precision of the Data—It is quite impossible to calculate the precision of the data given in Table II because of the large number of possible variables which might affect the results, but which could not be evaluated mathematically. A better test of the precision is to repeat the determinations by making and measuring another set of indentations on the same specimen.

This procedure was adopted for both gray and green silicon carbide ("Crystolon") with the results given in Table II. A difference of 90 units, such as was obtained with gray SiC, might at first glance appear rather great. This is equivalent to a difference of only 0.4 micron

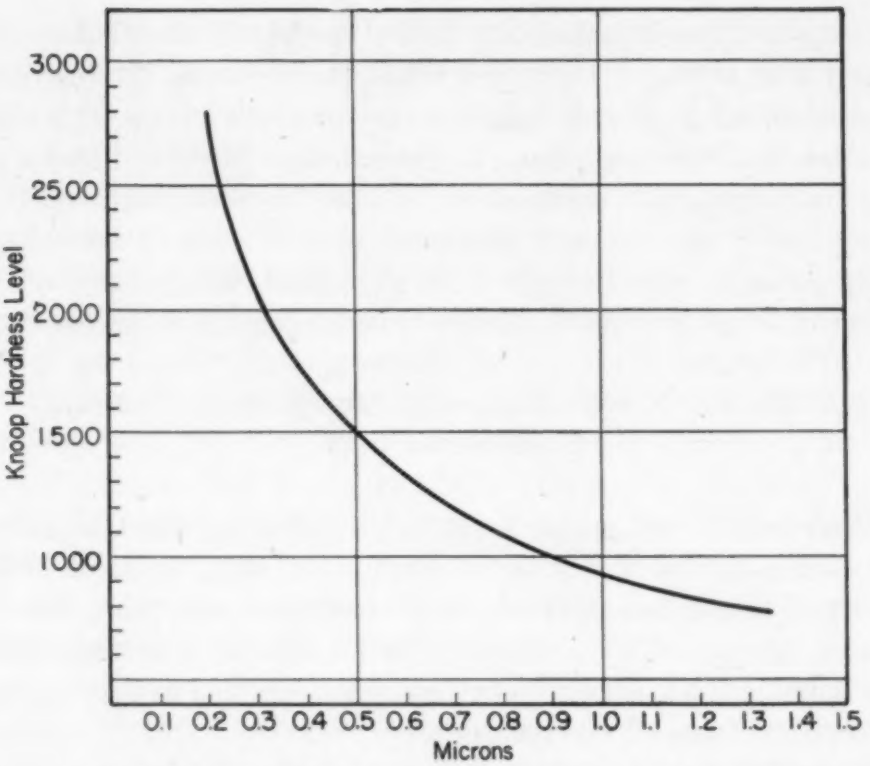


Fig. 1—Number of Microns Equivalent to Plus 50 Knoop Units at Different Knoop Hardness Levels. 100-gram load.

in the average length of the indentations, and considering the many factors which may affect the determinations, it cannot be considered excessive. Fig. 1 shows the number of microns equivalent to plus 50 Knoop units at various Knoop hardness levels for indentations made at 100-gram load, and is presented to indicate how precisely 100-gram indentations in hard substances must be measured to minimize differences in the resulting Knoop number. For example, at a Knoop hardness level of 1000, 50 Knoop units is equivalent to 0.9 micron in length of indentation, whereas at 1500 the same difference is equivalent to 0.5 micron. At 2800 this difference is only 0.2 micron. This figure also indicates that greater precision may be expected with the softer than with the harder substances merely because indentations in the former are longer, and errors are therefore likely to be a smaller percentage of the determined length. Factors, such as the tendency of the sample to crack badly, and poor reflectivity of the polished surface may counteract this trend in specific instances.

No difference is claimed between primary and molded boron carbide, between commercial green and gray silicon carbide ("Crystolon") and titanium carbide, between the alpha alumina in "38

Alundum" and in colorless synthetic sapphire boules, or between the garnet and topaz.

The average values of Table II can be repeated much more closely than the range. Not only is the former an average of a much larger number of indentations, but, when only 25 grains are indented to obtain "random" crystal orientation in the case of coarsely crystalline substances, there is little likelihood that the hardest and softest possible directions are indented during the experiment.

Factors Affecting the Knoop Hardness Number

Preparation of Surface to be Indented

Previously (9) it has been pointed out that one of the serious disadvantages of the Knoop method is the necessity of preparing samples which are plane, highly polished, and free from scratches. This is particularly applicable to the determination of the Knoop number of hard, brittle substances because, while it is of utmost importance to approach perfection in these respects if any degree of precision in the determination of Knoop hardness is to be attained, it is at the same time very difficult to prepare the surfaces properly.

Since, as will be indicated later, the precise measurement of indentations even in ideally prepared specimens of hard materials is very difficult, deep scratches, pits, and irregularities due to imperfect polishing cannot be tolerated. If such defects occur at the extremities of the indentations, greater uncertainty as to the actual ends will exist; or if the surface is irregular, rounded or otherwise departs even minutely from a plane, the effect on the hardness number may be noticeable. This will be particularly evident when it is realized that indentations made with a 25-gram load on boron carbide or silicon carbide are only about one-third of a micron deep when under load.

We therefore feel it necessary to prepare surfaces which are optically flat, highly polished, and which, in the areas indented, show a minimum of minute scratches of low contrast when examined with optical equipment of high resolving power. Figs. 5, 7b, and 9 illustrate surfaces which we believe were properly polished.

Methods of Polishing Hard, Brittle Substances—After considerable experimentation with various possible methods of obtaining the desired results, a sequence of operations has been evolved which, although not at all foolproof, and requiring considerable skill, has given satisfactory results with most nonmetals harder than quartz as

well as with cemented carbides. Because a number of experimenters have shown considerable interest in the method, which has not been published previously, it will be described briefly.

If the specimen to be polished is small enough and contains a relatively flat surface not over about 0.5 inch in diameter, it is mounted in phenol formaldehyde resin ("Bakelite") by the use of molding powder and a standard specimen mount press. The sample is placed as nearly in the center of a 1.25-inch diameter mount as possible.

If the original specimen is too large, one of the proper size and shape must be broken or cut from it. For several reasons we find it advantageous to mount the original irregular specimen on a suitable plate with an adhesive such as DeKhotinsky cement, and cut the small specimen from the larger by the use of a diamond cut-off wheel mounted on a suitable rigid machine. A resinoid-bonded disk as small in diameter and as thin as possible, with the diamond about 100 grit and 100 concentration, is recommended. The cutting should be done wet, preferably using kerosene or light oil. If this operation is properly conducted, the cut surface of the sample will ordinarily be flat with a fine matte finish, requiring a minimum of time in subsequent operations.

All lapping, honing and polishing of the specimen are accomplished on the Graton-Vanderwilt polishing machine (13) using diamond abrasive exclusively.

If the surface of the sample mounted in the resin is irregular, requiring the removal of considerable stock to produce a flat surface, loose diamond powder as coarse as Department of Commerce grade 60 (35 to 85 microns) (14) followed by successively finer sizes may be used on a cast iron lap with kerosene or light oil or a mixture of the two being employed as lubricant. Surfaces prepared by cutting off the specimen with a diamond wheel are usually so flat that no lapping with loose diamond powder is necessary.

We find it distinctly advantageous to follow the loose grain lapping operation by another in which the specimens are honed on a specially prepared lap in which size 500 (Department of Commerce grade 25) diamond is bonded with bronze by powder metallurgy. Using a small amount of light oil as lubricant, a specimen, previously prepared by cutting off or by lapping with loose diamond, should be suitably prepared for the polishing operation in from 1 to 5 minutes' honing time.

Polishing is effected by the use of Department of Commerce grade 14 (8 to 20 micron) diamond on a lead lap, followed by another

lead lap with grade 2 (1 to 3 micron) diamond. Polishing on lead laps is a very critical operation, much more of an art than a foolproof procedure, so the outline given will serve only as a guide; satisfactory results will be obtained only by trial and error.

The lap is wiped with a solvent such as carbon tetrachloride to remove oil and accumulated debris. Then a very small amount of the diamond, made up into a paste with light oil, is daubed onto the lap surface in about a dozen places. A drop or two of oil may be added, and the diamond and oil spread around with the fingers. Under proper operating conditions the surface of the lap has a velvety appearance when the specimens are being polished. The lap must be kept free from excessive oil or accumulated debris since these tend to cause relief polishing and "plucking out" of the softer constituents.

A polish may usually be obtained by use of the grade 14 diamond on the lead lap, but the surface usually is badly scratched. These relatively deep scratches may be removed almost completely by employing grade 2 diamond on another lead lap which is best operated nearly dry. For the final polish the lap is often wiped dry with carbon tetrachloride, and used a very short time in that condition. Care should be exercised not to operate a dry lead lap for long periods, since there is danger that excessive heat may cause galling, which results in an undesirable undulatory lap surface.

The time required for polishing varies considerably, depending upon the material and lap conditions. At times, samples have been polished satisfactorily in 10 minutes, but, on the other hand, several hours may be required to finish a specimen properly.

With molded boron carbide a better polish was obtained by the use of levigated alumina on hardwood, or on a lap made from size 600 "Alundum" bonded with shellac.

Method Used to Polish Steel—The hardened tool steel, data on which are included in this paper, was very carefully polished by Dr. L. P. Tarasov in such a manner as to minimize any cold working and pitting of the surface. After it had been polished on a rotating 3/0 metallographic emery-paper disk, it was repeatedly polished on a series of kerosene-soaked 4/0 disks so that the scratches were alternately removed in one direction, and then at right angles thereto. By finishing with partially used 4/0 disks at very low pressure it was possible to employ only a single stage of wet polishing using levigated alumina. Repeated light etching with nital, followed by repolishing with levigated alumina, completed the process. This method was

selected as being the most suitable from the standpoint of available equipment.

Effect of Polishing Operation on Hardness Number—Several of the hard, brittle substances included in our study occurred in the form of crystals with plane, reflective natural faces relatively free from imperfections. This offered an opportunity to determine whether the polishing method utilizing diamond on a lead lap had any effect on the Knoop number. Crystals of silicon carbide and quartz were mounted in resin in such a manner that specific crystal faces were at the surface of the mount. A series of ten indentations, using 100-gram load, was placed on these faces and the average Knoop number determined. Then a few microns were removed from the surface of each specimen by use of the honing and polishing method outlined, and the Knoop number redetermined on the polished surface with the same load and same orientation of the long dimension of the indentation. The results of the study were as follows:

	Knoop Number at 100-gram Load (K_{100})			
	Crystal Face		Polished Surface	
Substance	Average	Range	Average	Range
Silicon Carbide	2550	2480-2610	2520	2450-2630
Quartz	840	810-860	830	800-860

From this we conclude that polishing hard, brittle substances by the use of diamond on a lead lap has no measurable effect on the Knoop number for loads at least as low as 100 grams.

Indenting Equipment

Effect of the Solenoid—Unlike the National Bureau of Standards instrument in which the indentation was made by slowly lowering the diamond into the specimen being tested, the original Tukon apparatus effected indentation by raising the test sample into the diamond, the entire indenting load being applied by the speed of the elevating screw.

As a result of our early co-operative work with the National Bureau of Standards, certain differences between values determined in the two laboratories were evident; particularly, our Knoop numbers, determined on hard substances such as SiC using a 100-gram load on the original Tukon, were considerably lower than the values reported by the Bureau, using the instrument which they had designed. The Bureau was kind enough to point out that their Tukon instrument was giving similar low values with low loads and attributed it to errors introduced by inertial forces acting at the instant the beam was picked

up. This effect seems to have been quite general with the original Tukon instruments (6, discussion), (8), (9).

To correct this defect inherent in the original Tukon model, D. R. Tate of the National Bureau of Standards developed a solenoid device which prevented full application of the indenting load until after the upward motion of the specimen had been arrested (5). In addition, side-play was practically eliminated by a torque-arm attached to the elevating screw.

Fig. 2 shows a comparison of the Knoop results obtained by indenting the base of our standard sample of SiC before and after

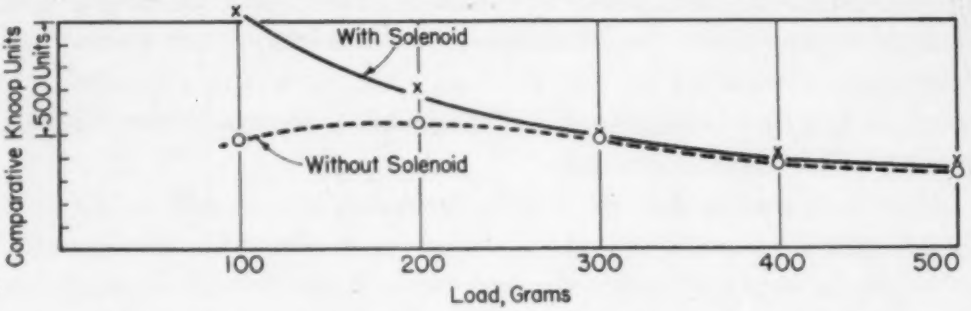


Fig. 2—Effect on Knoop Hardness of Installation of the Solenoid to the Tukon Tester. Comparison made by indenting the same crystal of SiC in the same orientation before and after attachment of the device.

attachment of the solenoid and torque-arm to our Tukon. Although the curves shown in Fig. 2 are directly comparable, the effect of the solenoid and torque-arm being the only variable outside of normal experimental error, the actual Knoop numbers obtained under the conditions are not given in Fig. 2. This is because both curves are affected by other variables of indenter and conditions of measurement, discussed subsequently, which resulted in actual values which are not in accord with those we now accept. There is no doubt, however, that our original Tukon gave hardness numbers which were too low both for 100 and 200-gram loads. In the case of SiC, the original instrument gave Knoop numbers which were nearly 20% too low at 100-gram load. With plate glass, the only other comparison made, the curves were quite similar to Fig. 2 in general appearance, and the value obtained by the original instrument was about 12% too low.

Winchell (7) stated that the solenoid device was installed on his instrument when about half the corundum tests reported had been completed. He felt that such installation had not vitiated his previous results because indentations made on fluorite (a soft mineral with a Knoop hardness of about 150) were about the same before as after installation of the solenoid.

It is quite probable that some of the original Tukon instruments showed less of an error due to inertia of the beam and weights than did ours. However, we do not believe that the attainment of concordant results on a soft substance with Knoop hardness of only 150 before and after installation of the device is sufficient evidence that similarly concordant results would have been obtained on a hard substance with a Knoop number of about 2000 (e.g., aluminum oxide).

Our co-operative work with the National Bureau of Standards also indicated that our indentations made with the original Tukon model were cracked to a greater extent than those made with the National Bureau of Standards instrument at the same indenting load. As would be expected, the attachment of the solenoid and torque-arm to our Tukon resulted in less tendency to crack the specimen, the amount of fracture being about the same as that shown by the National Bureau of Standards apparatus.

It is our opinion that no Knoop hardness investigations, particularly of hard substances at low indenting loads, should be made unless the Tukon is equipped with the solenoid. Even though it might be proven that a particular instrument, unequipped with solenoid, was not giving abnormally low Knoop values nor excessive cracking of brittle substances at low loads, it seems very likely that the effect mentioned would sooner or later appear as the apparatus became slightly worn. The Wilson Mechanical Instrument Company has informed us that all Tukon instruments manufactured since April 1943 have been equipped with the solenoid and torque-arm.[2]

External Vibration—Although it has been stated (6, discussion) that inconsistent results may arise from vibration being transmitted from control box to the Tukon, we were never able to substantiate this contention. Neither could any variations in hardness results be traced to slight vibrations present in the building, although such vibration was often sufficient to cause considerable movement of the image of the indentation when viewed through the microscope attached to the Tukon cowl. It was easily shown, however, that abnormally long indentations would result if the table on which the apparatus was mounted was jarred slightly during the indenting period, especially when very low loads were being employed.

As a precautionary measure, however, the table on which the instrument was mounted was equipped with shear rubber vibration dampers on each leg, and an inch-thick felt pad was placed under the

[2]Personal communication, V. E. Lysaght, May 29, 1946.

control box. Vertical coil suspension springs, similar in design to those used for eliminating vibrations on the Bausch and Lomb metallographs, would probably be even more effective than shear rubber dampers. Great care should be exercised to be certain that the apparatus is not rocking at the time indentations are being made, and that the table is not jarred during the indentation period.

Balance of Beam and Precision of Applied Load—When the apparatus was returned after installation of the solenoid, the balance of the beam and the precision of the load applied from 25 to 500 grams were checked by mounting an equal-arm balance on the Tukon stage. The applied loads were found to be correct to within at least $\pm$ 0.2 gram, the approximate sensitivity of the method which we employed for checking.

Diamond Damage or Wear—The elongated pyramidal diamonds used as the Knoop indenters may be inspected and certified either at the Wilson Mechanical Instrument Co. or the National Bureau of Standards. One of the specifications reads: "The longitudinal edges shall be free from nicks greater in length than 0.5 micron for a distance of 125 microns from the point" (15).

Although this inspection insures that a new or relapped diamond is at least free from all but extremely minute nicks, the user should make certain that his diamond is carefully handled, inspected periodically for the appearance of nicks on the longitudinal edges, and returned for resharpening whenever such a condition becomes evident.

We have selected certain specimens of different hardnesses which serve as master standards not only for the purpose of inspecting indentations for imperfections indicative of the presence of nicks on the diamond edges, but also for the purpose of ascertaining whether the apparatus is giving consistent results at all times. Obviously, inspection of the indentations for evidence of imperfections should be made under conditions of the greatest optical resolving power. Wherever possible we employ the 80X apochromatic oil immersion objective (1.40 N.A.) on the Bausch and Lomb Research Metallograph using bright-field illumination.

Fig. 3a shows the first indentation made with one of our recently purchased diamonds. It was made on the base of a crystal of SiC, using 100-gram load. Although the ends of the indentations gradually faded out in the normal manner, there was a minute nick in the longitudinal edge of the diamond as indicated by the arrow on the photomicrograph; the inspector apparently considered this nick to be less than 0.5 micron

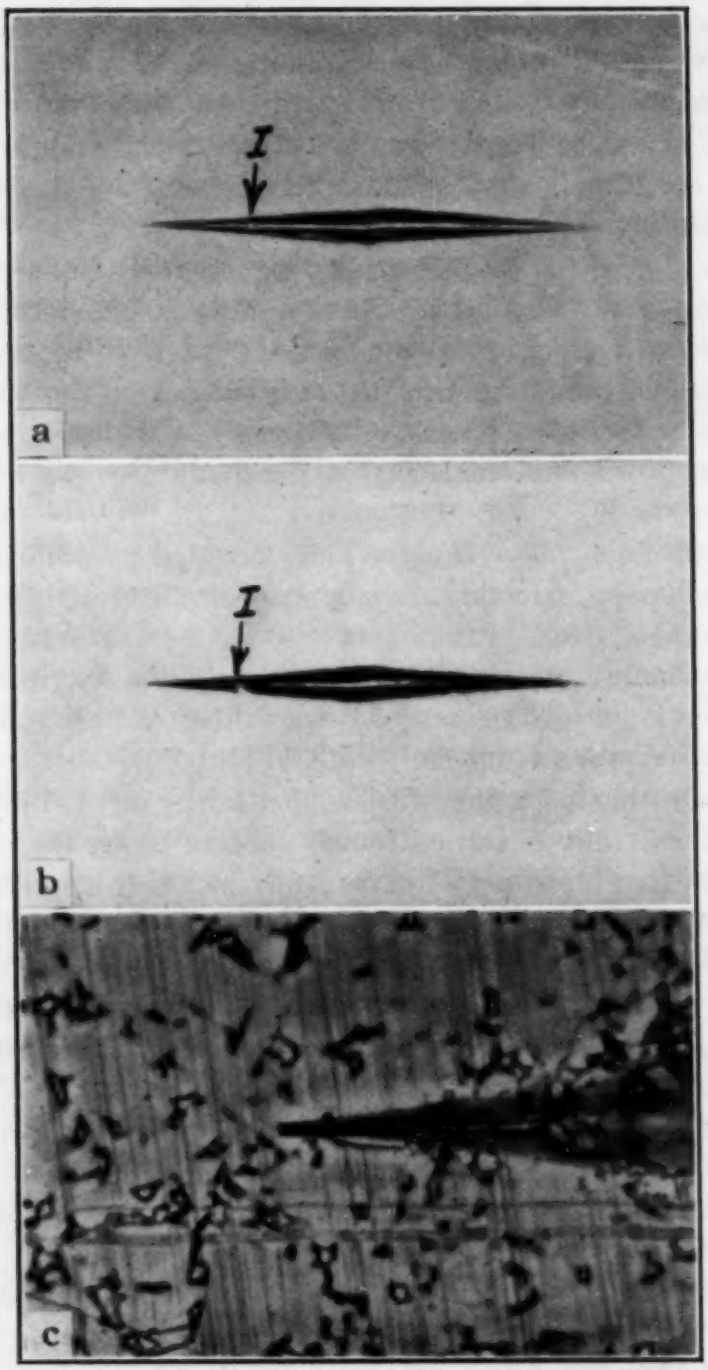


Fig. 3—Imperfections in Knoop Indentations Caused by Nicks in the Longitudinal Edge of the Diamond. Photomicrographs made on the Bausch and Lomb Research Metallograph using 80X oil immersion objective, bright-field illumination. (× 2000). (a) Indentation made in SiC by a new diamond indenter using 100-gram load. Note minute imperfection, I. (b) Same as 3a except indentation made after the diamond had been constantly used for about 6 months, indenting various hard substances. Note enlargement of original nick. (c) Abrupt termination of an indentation caused by a nick occurring precisely at the end of the impression. The indentation, made in a cemented carbide, should be several microns longer.

long, although our measurements would indicate that it slightly exceeded the limit. There is, of course, a slight possibility that the nicking may have occurred during the first indentation made on the silicon carbide.

Periodically, indentations were made on the same specimen under the same conditions. It was found that the original minute imperfection was becoming larger, until, after a period of approximately 6 months during which time the indenter was constantly being used to indent hard substances, the indentation appeared as in Fig. 3b. Not only was there one rather prominent imperfection, but other smaller ones, not evident in the photomicrograph, were developing near the opposite end of the indentation. At this stage the diamond was returned for relapping.

The possible effect of imperfect diamonds on the Knoop number is well illustrated by Fig. 3c. Here it is quite evident that the indentation would have been several microns longer if the nick in the longitudinal edge of the indenter had not occurred precisely at one end of the impression, causing an abrupt termination.

Our co-operative work with other laboratories has indicated that the possible effect on the Knoop number of damage to or wear of the indenter is not fully appreciated, since indentations are being made with badly nicked diamonds. Certainly such imperfection should not be tolerated if precise results are to be expected, especially with hard substances indented under low loads.

In order to prevent possible delays in hardness testing due to the necessity of having diamonds relapped, it is advisable to have an extra indenter on hand.

Weight of Diamond and Holder—The combined weight of the Knoop diamond and its metal mount is not held constant. For this reason it is necessary to rebalance the instrument if a new diamond indenter is employed, or if an old diamond is being returned to the Tukon after having been relapped. Eventually the Wilson Mechanical Instrument Co. hopes to control the combined weight of diamond and holder, and in the meantime has changed the design of the counterweight to allow easier rebalancing of the beam.[3]

Different Certified Diamonds—For approximately three years from the time our Tukon was purchased, we continued to use the original certified diamond indenter 20 supplied with the instrument. Then, while attempting to study the effect of asymmetry of indentation

[3]Personal communication, V. E. Lysaght, May 29, 1946.

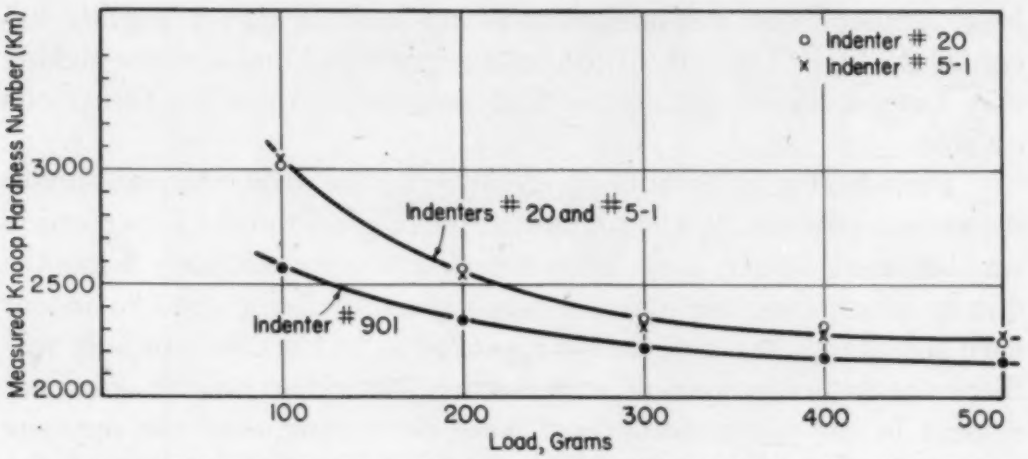


Fig. 4—Differences in Knoop Hardness Numbers Caused by the Use of Different Diamond Indenters.

on the Knoop number, the tip of the indenter was badly fractured by inadvertently drawing it across a crystal of silicon carbide. The indenter was immediately returned for relapping, and a new indenter [901] purchased.

After carefully rebalancing the instrument to compensate for the different weight of the new diamond and holder, a series of indentations was made at various loads in the standard sample of silicon carbide, the same orientation of the long dimension of the indenter relative to the crystal structure being observed. In Fig. 4 the Knoop numbers obtained with indenter 901 are compared with those obtained with indenter 20 a short time before it became damaged. So far as is known, all other factors likely to influence the Knoop number were constant, the two sets of indentations having been measured with the same optical equipment by both of the authors. Within experimental error, the difference in microns obtained at the various loads was a constant, but the Knoop values showed greater differences at 100 grams than at higher loads because of the characteristics of the formula used to convert length in microns to Knoop hardness.

In attempting to explain these differences, indentations made by indenter 20 just prior to the accident were examined very critically on the research metallograph at highest magnifications, but no evidence of nicks in the diamond nor wear of the very tip of the indenter could be found.

Variations recorded in Fig. 4 were due either to some inherent difference between the two diamond indenters, or to an imperceptible dulling of the very tip of indenter 20 during three years of use, or to both possibilities.

Unfortunately it was impossible to resolve the question further for two reasons. First, although we had preserved indentations made with indenter 20 when it was nearly new, they were not comparable to later results because of differences introduced by the installation of the solenoid and torque-arm devices mentioned previously. And secondly, for some reason the present manufacturers of the diamond indenters were never able to relap diamond 20 to meet the National Bureau of Standards specifications with respect to nicks, although many attempts were made to do so.

As a result of this inquiry, the Wilson Mechanical Instrument Company was kind enough to undertake a series of experiments using the same sample of silicon carbide which we employed in the experiments resulting in Fig. 4. They made ten indentations each at loads of from 100 to 500 grams inclusive using six different diamond indenters in stock at the time.

These tests indicated that, while five of the indenters gave results at these loads which agreed with those which we obtained with our new indenter 901, one indenter produced impressions consistently shorter than the others. The indenters giving concordant results were all of recent manufacture and met the present specifications for Knoop indenters (15), while the one giving discordant results [5-1] was prepared sometime previously by another lapidary when cutting techniques had not been as nicely perfected as at present. As indicated in Fig. 4, although the results obtained by the use of indenter 5-1 disagreed with those obtained with indenters of recent manufacture, the agreement with the values from our old indenter 20 is remarkable.

Diamond 5-1 had an offset of 2.5 microns at the tip. This is greater than most indenters of recent manufacture but whether it is the cause of the discrepancies noted is problematical.

D. R. Tate of the National Bureau of Standards reported[4] that indenter 20 was mounted with one crystallographic (cubic) axis of the diamond parallel to the axis of the indenter mount. The longitudinal edges were in a plane bisecting the angle between the other two crystallographic (cubic) axes.

Since the present specifications (15) call for the longitudinal edges to lie in a plane containing one of the other crystallographic axes, it is at least very suggestive that this difference in crystallographic orientation between the diamond indenters may have been the cause of the different Knoop values obtained with indenters 20 and 901, as

[4]Personal communication, June 14, 1946.

illustrated by Fig. 4. The orientation of the diamond in indenter 5-1 is now being checked.

Although we have no definite assurance, it would appear that the results obtained from indenter 901, at least for impressions longer than about 20 microns, are those to be expected from indenters of present manufacture. We have therefore discarded all values obtained with the older diamond.

To make certain that our Knoop numbers are always in agreement with those originally obtained with the use of indenter 901, we have a standard sample of silicon carbide containing impressions made at various loads with this indenter when it was new. By this control we are able to detect any substantial differences which might result from diamond wear, or from a new or relapped indenter.

The Wilson Mechanical Instrument Company has informed us the inspection of a Knoop indenter now involves not only the measurement of the indenter angles, the offset, and the constant relating the length to the projected area, but also that indentations are made at various loads from 25 to 3000 grams in hard steel of approximately Rockwell C-63, and measured in a standardized manner. Inspection indentations are not ordinarily made on hard carbides, but this could be done if the diamond being certified were to be used on such hard, brittle substances.[5]

When it is realized that 100-gram indentations in silicon carbide are less than a micron deep under load, it is surprising that greater differences in Knoop number due to various indenters have not been found. The fact that recently lapped diamonds gave concordant results on silicon carbide is in itself a testimony to the precision with which the facets are lapped to the very edges.

Measurement of Indentations

Tate (8) and Lysaght (9) have pointed out that different Knoop numbers may be obtained from the same indentations by different observers using the same optical equipment, or by a single observer using different optical set-ups, but no details have been published.

With the standard Knoop indenter the length of the indentation under load is approximately seven times the width. Since upon removal of the indenter a larger percentage of elastic recovery may take place in the short than in the long dimension of the indentation, the ratio of length to width may be eight or greater when the impression

[5]Personal communication, V. E. Lysaght, May 29, 1946.

is measured. The result is an elongated diamond-shaped indentation which is very acute in the long dimension, and which, instead of ending abruptly, seems to fade out gradually when examined microscopically at high magnification. Although less apparent with indentations in metals and other substances of high reflectivity, it is particularly evident in the case of impressions made in transparent substances of relatively low index of refraction, such as quartz and topaz.

Because of this indistinctness, the resolving power of the optical system used, and the visual acuity of the observer, may affect the measurement of indentations considerably.

Furthermore, since the length of an indentation enters as the square into the formula for the calculation of the Knoop hardness, the effect on the Knoop number will be much greater, especially with hard materials, where the total length of the indentations is small, not only because of the hardness of the substance itself, but also because of the necessity of indenting with low loads to prevent excessive cracking.

Filar Micrometer—The filar micrometer used during our studies was manufactured by the Spencer Lens Company. It consisted of thirty equally-spaced divisions placed at the focal plane of the eyepiece. There was no independent cross-hair, the entire scale being moved laterally one scale division for each complete rotation of the filar micrometer drum.

The graduations in the eyepiece were rather broad and interfered considerably with measurements when an indentation was placed within the ruled area. Much more satisfactory results were obtained by placing the long dimension of the indentation just outside the ruled area, at right angles to the direction of the rulings. One end of an indentation was placed just at the tip of one of the graduations. The other end was then moved to the tip of the graduation nearest it by means of the micrometer drum and the length of the indentation thus determined.

In order to ascertain whether the eyepiece graduations were equally spaced, the distance between the images of two close, sharply defined cracks in a specimen of SiC was measured using four different parts of the filar micrometer scale and the optical equipment now used to measure most indentations, as discussed below. Later an indentation in SiC was measured several times using various parts of the scale, but no differences caused by inaccuracies of the filar micrometer scale graduation, or by a variable relationship between the drum and the scale, could be detected by either of these tests.

Since a lens system usually shows some distortion, the object to be measured should be located in the same region of the field as was used for calibration of the filar micrometer, preferably the center.

Calibration of Filar Micrometer—Since all measurements of indentations are directly in terms of filar micrometer divisions, it is obviously of utmost importance that the micron equivalent of a filar division be determined as precisely as possible by reference to an exact primary standard.

The stage micrometer employed as our standard consisted of lines ruled on glass by a domestic manufacturer. Although the individual 0.1-millimeter divisions were found to vary as much as 1%, the filar micrometer calibrations resulting from the use of the entire scale were found to agree very closely with values obtained by using a micrometer consisting of lines ruled on a steel plate by the use of the interferometer at the National Bureau of Standards.

Optical Equipment Used for Measurements—No matter what optical equipment is employed for measuring the indentations, certain conditions must be maintained.

In the first place, both ends of the indentations must be in focus at the same time, because of the probability of some lateral shift of the image during change of focus. The depth of focus of lenses of high magnification is very shallow, and some difficulty may be encountered if the axis of the microscope is not precisely perpendicular to the specimen.

Then again, the optical equipment should be rigid and free from vibration; it is most disconcerting to observe considerable motion of the image of the Knoop indentation upon lightly touching the filar micrometer drum, or to note a sudden fuzzing of image due to building vibration. The former difficulty, which gave us considerable inconvenience when the microscope was first mounted on the cowl of the Tukon and the oil immersion lens discussed below was employed, was traced to excessive play in the rack and pinion for coarse focusing of the microscope. The latter condition was easily corrected by the use of vibration dampers on the legs of the instrument table.

The original Tukon model did not provide facilities for attaching a microscope to the instrument, it being necessary to remove the specimen from the Tukon for measurement. Our original optical equipment consisted of a small metallographic microscope manufactured by the Spencer Lens Company and provided with 16, 8 and 4-millimeter achromatic objective lenses.

We were never satisfied with such equipment for the precise measurement of indentations 20 to 25 microns long, and immediately began to experiment with oil immersion objectives and other variations in optical set-up.

Because our early experiments indicated that the measured length of an indentation was greater when optical equipment of higher resolving power was employed, we sought the aid of J. R. Benford of Bausch and Lomb Optical Company, who very kindly examined a series of 100-gram indentations in silicon carbide using various optical set-ups. He recommended a 54X, 1.00 N.A. fluorite oil immersion objective and bright-field illumination, stating that "a comparable dry objective, the 58X, 0.85 N.A., gave a much less crisp and well-defined outline to the diamond indentations."[6]

When our Tukon was rebuilt to include the solenoid device and to provide facilities for attaching a microscope to the cowl of the instrument, we purchased the oil immersion lens recommended and mounted it on a Bausch and Lomb body tube which was attached to the Tukon. Since the objective was designed for a 215-millimeter tube length, it was necessary to insert a single nosepiece between tube and objective to increase the tube length to the proper value.

Later when a Bausch and Lomb Research Metallograph became available we made a series of experiments on the effect of different optical equipment on the measurement of one indentation each in silicon carbide and aluminum oxide (synthetic corundum).

In the case of silicon carbide, four qualified observers, each accustomed to measuring Knoop indentations, measured the impression five times with each of five different optical arrangements, while, with the indentation in aluminum oxide, the authors alone made the measurements. The results of these studies are given in Table III.

Considering the indentations in silicon carbide, it is evident that the use of oil immersion objectives resulted in higher micron values for the indentation than when dry lenses were employed. In spite of its lower numerical aperture the 54X oil immersion lens gave measurements even slightly greater than those obtained with the 80X objective. This appears to be due to the fact that, because of lens design, the 54X objective produces an image of greater contrast than afforded by most other objectives.

With dry lenses, the lower the numerical aperture of the objective used on the Research Metallograph, the shorter the indentations

[6]Personal communication, April 13, 1944.

Table III

Effect of Different Optical Equipment and Different Observers on the Knoop Number. One indentation each in silicon carbide and aluminum oxide. Four observers for SiC; two for Al_2O_3

Optical Equipment	Length of Indentations (Microns) (Avg. of All Observers) SiC	Al_2O_3	Max. Difference Between Observers SiC	Al_2O_3	Knoop Number (Avg. of All Observers) SiC	Al_2O_3	Max. Difference Between Observers SiC	Al_2O_3
80X, 1.40 N.A., oil immersion objective on Research Metallograph	23.73	26.50	0.20	0.13	2525	2030	40	25
54X, 1.00 N.A., oil immersion, on microscope attached to Tukon	23.85	26.74	0.29	0.11	2500	1990	60	20
62X, 0.95 N.A., dry, on Research Metallograph	23.20	26.45	0.27	0.44	2645	2035	60	70
41X, 0.65 N.A., dry, on Research Metallograph	23.14	25.92	0.54	0.07	2660	2115	120	10
45X, 0.85 N.A., dry, on Spencer	22.56	25.85	0.50	0.30	2795	2130	125	50
Maximum Difference in Average	1.29	0.89			295	140		

appeared to be. This is more clearly illustrated in the separate paper by Tarasov and Thibault (16), where a similar experiment with indentations in steel is described. In spite of its higher numerical aperture, the 45X objective on the small Spencer metallographic microscope consistently gave smaller measurements than the 41X lens on the Research Metallograph. Probably this could be explained by objective design, or factors connected with the vertical illuminator or light source.

As indicated in Table III, the maximum difference in micron value due to the different optical systems is over 5%, the corresponding difference in Knoop number is almost 12%.

There can be little doubt concerning the validity of these conclusions. In the first place, each of the four observers agreed on the matter. Secondly, the difference cannot be accounted for by errors in calibration of the filar micrometer, since both of the authors recalibrated the micrometer for each of the five optical arrangements just prior to the experiment. And thirdly, we have nine additional comparisons, involving six observers, in which the same trends are shown.

We believe that the most satisfactory method of measuring indentations in silicon carbide and other substances of equal or higher reflectivity, at least with standard equipment, is by the use of either the

54X, 1.00 N.A. fluorite, or the 80X, 1.40 N.A. apochromatic oil immersion objective on the Bausch and Lomb Research Metallograph or equivalent, using bright-field illumination and decentering the aperture diaphragm slightly to increase contrast without unduly distorting the image. There are certain disadvantages, however, to using such equipment. The necessity of removing the specimen from the Tukon and mounting it on the Metallograph makes the determination of Knoop numbers even more time-consuming since it is often very difficult to locate and to identify positively a particular indentation or set of indentations under consideration.

We have therefore standardized on the 54X fluorite oil immersion lens mounted on the microscope attached to the cowl of the Tukon. For specimens of high reflectivity, such as cemented carbides, the light source attached to the tube of the plate glass type vertical illuminator was found to be satisfactory for illumination. In the case of other less reflective substances such as silicon carbide, this light source was entirely inadequate, since the image of the indentation was dim and lacked contrast. A ribbon filament lamp operating at 6 volts, 18 amperes, and not attached to the microscope was employed for most of our determinations. Best results were obtained by focusing the image of the ribbon filament on the diaphragm of the vertical illuminator, but allowing the light beam to enter the vertical illuminator tube at a slight angle. This increased contrast tremendously without introducing noticeable distortion, and had the same effect as decentering the aperture diaphragm on the Research Metallograph.

Although the use of an oil immersion objective proved to be distinctly advantageous with substances of relatively high reflectivity, it is obvious that it cannot be used to measure indentations in transparent substances of low reflectivity and index of refraction such as quartz. Since the refractive index of the immersion medium is so close to that of the substance, the indentation is either entirely invisible or so lacking in contrast that its length cannot even be approximated.

In such a case the use of a dry lens under conditions of highest possible resolving power would seem to offer the best solution to the problem. Since anti-reflection films on metallographic objectives, as recently described by Benford (17), produce increased image contrast, especially with specimens of low reflectivity, they should increase the contrast of Knoop indentations in low index substances, and result in greater resolving power. This probability is now being investigated.

Dr. Horace Winchell suggested[7] the use of water immersion

[7]Personal communication, May 29, 1946.

objectives of high resolving power. If such lenses, designed for use in vertical illumination, could be obtained, they might possibly prove advantageous.

Between these two types of substances there are those of intermediate index of refraction and reflectivity, for example, aluminum oxide, where it appeared that the greater resolving power of the conventional oil immersion lens could not be realized because of the necessity of restricting and decentering the aperture diaphragm considerably more to gain sufficient contrast than was necessary with compounds of higher index of refraction and reflectivity. In order to clarify this point, the authors used various types of optical equipment to measure one indentation in aluminum oxide, the results of the study being given in Table III.

The data would appear to indicate that with such substances there is no advantage, nor yet any disadvantage, in using an oil immersion lens. As was found in the case of SiC, however, optical arrangements of lower resolving power seem to result in lower micron values of the Knoop indentation.

The effect of the resolving power of the optical equipment on the apparent length of an indentation may be illustrated by the experiment resulting in Fig. 5. We happened to have on hand a polished specimen whose surface contained a large number of minute pits, and also a Knoop indentation so asymmetrical that one side was five times as long as the other. As a result, the long end was much more acute than normal.

First, a photomicrograph was taken of this gradually tapering end at a magnification of 1000. It was purposely made slightly out of focus so that the end of the indentation was hazy, but at the same time the pits in the surface were distinct. Then two positives were made by contact printing. By correlating the photomicrograph with the appearance under the microscope, each of two observers then independently marked on his own photomicrograph the apparent end of the indentation when examined with the following three objective lenses on the Research Metallograph: (1) 41X, 0.65 N.A. dry; (2) 62X, 0.95 N.A. dry; (3) 80X, 1.40 N.A. oil immersion.

There was remarkably good agreement between the two observers, but a substantial difference due to optical equipment used. According to one observer the maximum difference was about 6 microns; according to the other, 7 microns. It is true that the extraordinary acuteness of the indentation accentuated the difficulty in determining the true

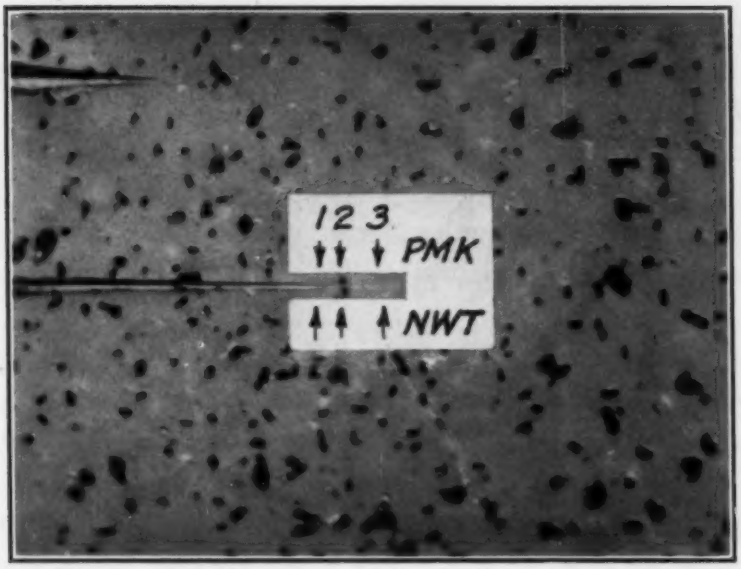


Fig. 5—Effect of Resolving Power of Optical Equipment on the Determination of the End of a Knoop Indentation. (× 1000). Apparent extremity of one end of an unusually acute impression as determined by two observers using the following objectives on the Bausch and Lomb Research Metallograph: (1) 41X, dry; (2) 62X, dry; (3) 80X, oil immersion.

extremity of the indentation, but the same trends are to be found on a reduced scale with normal Knoop impressions.

Personal Factor Affecting Measurements—As might be expected with Knoop indentations which, even under conditions of maximum resolution, seem to fade gradually away instead of ending at any definite place, differences in the visual acuity of different individuals may greatly affect the determined length of impression and hence the Knoop number. So elusive are the ends of the indentations, particularly in transparent, low index substances, we sometimes wonder to what extent imagination enters into the determination. Of this we are certain: The measurement of Knoop indentations, made in hard substances under low loads, is the most exasperating type of microscopy which we have ever experienced. Harassed by the indistinctness of the indentation terminations which actually seem to vacillate while being examined, and the realization that the utmost precision must be obtained, we have never been able to spend more than a very few hours a day measuring Knoop impressions.

Most of the Knoop numbers reported in this study were based on averages determined by the authors independently, or by the senior author and Miss Pauline Krukonis. In order to make the measurements as objective as possible, we found it necessary for the second observer to measure the indentations without knowing the results obtained by

the first. If this procedure were not followed, the second observer would tend to be prejudiced and thus agree with the determinations made by the first observer more closely than otherwise would have been the case. No deceit is involved, merely an unconscious reaction caused by the normal uncertainty as to exact ends of the indentations.

The effect of the personal equation on the measurement of indentations may be either consistent or inconsistent as illustrated by the following experiences.

When, in the early days, we were using the 4-millimeter lens on the Spencer Metallograph for measuring indentations, the senior author had an opportunity to compare his determinations of the lengths of a large number of indentations in silicon carbide with the values obtained under precisely the same conditions by a well-known scientist also accustomed to measuring such impressions. The latter consistently read the lengths of the SiC indentations from 0.7 to 1.7 microns longer than the senior author. The average difference was 1.0 micron. Unfortunately, it is impossible to make the same comparison now using the oil immersion objective later found more suitable for measurement.

No consistent differences between observers were revealed by the measurements of the indentation in SiC and aluminum oxide recorded in Table III. As revealed by the data for SiC, which are more significant because four observers were involved, a better agreement between observers is obtained when optical equipment of high resolution is employed.

Considering the measurements made on the same sample by the two authors, no consistent differences extending over the entire period of the investigation could be found. However, in the case of certain series of measurements small consistent differences did appear to exist. These usually disappeared, however, on remeasurement of the indentations by both observers at a later date. The only explanation which we can offer is that our relative visual acuities varied slightly from time to time for physiological reasons.

Time between Indentation and Measurement—The opinion has been privately expressed that the apparent length of an indentation in hard, brittle materials might decrease with elapsed time between indentation and measurement due to gradual closing of the indentation by recovery of the material indented.

On three separate occasions, the authors attempted to detect such an effect by measuring indentations in boron carbide and silicon carbide with the same optical equipment within about 30 seconds of the time

of indentation, and again several months later. We were, however, unable to obtain any evidence to support the view, and conclude that whatever recovery takes place is completed before the indentation can be measured.

Standard Optical Set-up Needed—This study has certainly shown clearly that, if concordant results in the determination of the measured Knoop number (K_m) of a particular sample of a substance are to be obtained from various laboratories, one of the necessary prerequisites is a standardization of the optical equipment used for measurement.

Because every laboratory equipped with the Tukon microhardness apparatus cannot be expected to have a Bausch and Lomb Research Metallograph or equivalent available for measurements, and because of the great convenience of a microscope attached to the Tukon cowl, we recommend the use of the 54X, 1.00 N.A. fluorite oil immersion objective on this microscope, and an adequate adjustable light source, such as described above, for supplying illumination to the plate glass vertical illuminator equipped with diaphragm. In those cases where an oil immersion objective cannot be used, either because the indentations are so large as to be off the filar micrometer scale, or because of the low index of refraction of the substance being indented, a dry objective of as high resolving power as possible should be employed.

Such a standardization would certainly reduce to a minimum the differences obtained in the measurement of the same indentation by various observers in different laboratories.

The Sample Indented

Identity and Description of Specimens Used—One need hardly mention the necessity of properly identifying and describing the substance whose Knoop hardness is being quoted. The various materials whose Knoop hardness we investigated may be described as follows:

Primary Boron Carbide (B_4C), "Norbide"—Norton Company manufactures boron carbide (B_4C) under the trade name "Norbide" by reducing anhydrous boric oxide glass with carbon in a resistance type electric furnace at about 5000 F (2760 C). The Knoop data of Table II were obtained by preparing a suitable specimen from fine "Norbide" grain and indenting only boron carbide itself, avoiding impurities which may occur in small amounts in the product.

Molded Boron Carbide, "Norbide"—This substance, also manufactured by Norton Company and known as molded "Norbide", is produced by sintering fine primary boron carbide powder by the

simultaneous application of heat and pressure. No cementing agent is added, the compound being self-bonding. The molded "Norbide" was of nearly theoretical density (2.52) and theoretical composition (boron to carbon ratio about 4.0), and the polished surface contained a relatively small number of imperfections, most of which were less than 2 microns in diameter.

Silicon Carbide—All the Knoop data on single crystals, such as the values included in Fig. 11, were obtained from indentations on the upper (0001) plane of transparent, green crystals of α-SiC, Type II (18). The hardness numbers for gray SiC included in Table II were determined by mounting, polishing and indenting fine grains of regular "Crystolon", the silicon carbide manufactured by Norton Company. Similarly, the values given in Table II for green SiC were obtained from indentations on grains of green "Crystolon". The data indicated by "check" in Table II were obtained by indenting other grains in the same polished specimens. X-ray powder photographs of both the gray and green "Crystolon" samples indicated that they were mixtures of a large amount of α-SiC, Type II, and a small amount of Type I.

Titanium Carbide—This was a product made experimentally at Norton Company by the reduction of fused TiO_2 with carbon in an electric furnace. It had the following chemical analysis:

Ti	=	79.66%
C	=	19.73
N	=	0.23
Fe	=	0.04
Total		99.66%

Most of the remainder was probably oxygen. An X-ray powder photograph made with filtered Cu radiation indicated a cubic compound of the NaCl type with $a_0 = 4.31$ Å. This is in good agreement with the value $a_0 = 4.311$ Å quoted in Ref. 19, and with most of the data given for the compound in Ref. 20.

Tungsten Titanium Carbide ($WTiC_2$)—This sample was obtained from Kennametal, Inc., in the form of a powder finer than 200 mesh. Determinations made in our Laboratories indicated a density of 9.85, and a carbon content of 9.03%, check 9.34%, agreeing reasonably well with the data given by McKenna (21). Only a single phase could be detected upon examination of the polished or the etched specimen on the Research Metallograph.

Alpha Aluminum Oxide ("38 Alundum")—Norton Company manufactures a white aluminum oxide abrasive by fusing Bayer-process

alumina in an electric arc furnace. The resulting product, known as "38 Alundum", consists almost entirely of pure alpha aluminum oxide with a small amount of the so-called "beta" alumina (nominally $Na_2O \cdot 11Al_2O_3$) as a separate impurity. The Knoop data for this material as given in Table II were obtained by indenting "38 Alundum" grain, care being taken to indent only the pure alpha alumina phase.

Alpha Aluminum Oxide (Synthetic Boule)—Alpha alumina of the highest purity is obtained by melting fine, extremely pure alumina powder by a modification of the Verneuil process, and allowing the melted drops to build up a pear-shaped mass or boule. The data in Table II were obtained by crushing a boule of colorless alpha alumina, also known as colorless synthetic corundum, manufactured by the Linde Air Products Company. The values in Fig. 11 were determined from indentations on a block of colorless synthetic corundum kindly supplied us by Dr. Horace Winchell, formerly of the Hamilton Watch Company. The orientation given in connection with Fig. 11 was determined by Dr. Winchell.

Cemented Carbide ("Kennametal K6")—A sample of this product was obtained from the manufacturer who characterized it as one of the hardest regular commercial Kennametal grades. It was said to be a "straight tungsten carbide composition with a low cobalt content."[8]

Cemented Carbide ("Kennametal KM")—This item, also obtained from the manufacturer, was said to be a "steel-cutting grade containing tungsten carbide, $WTiC_2$, carbides of tantalum, columbium and titanium with high cobalt content."[8]

Cemented Carbide ("Kennametal K12")—The manufacturer described this product as one of the softest of his regular commercial Kennametal grades, "a straight tungsten carbide composition with a high cobalt content."[8]

Topaz—The specimens used in this study were transparent, colorless crystals from the Thomas Range, Utah. All associated impurities were removed by hand sorting. The identity of the crystals as topaz was confirmed by the determination of the optical properties which agreed with those published by Larsen and Berman (22). Several interfacial angles were measured goniometrically to establish crystal orientation, reference being made to Dana's System (23).

Garnet—This was obtained from the Behr-Manning Corporation of Troy, New York, as representative of the garnet used in sandpaper products. It is of the almandite variety obtained from the Barton Mines,

[8]Personal communication from J. C. Redmond, Kennametal, Inc., September 8, 1945.

North Creek, New York. Care was taken to indent only garnet, the impurities, such as hornblende, being avoided.

Synthetic Blue Spinel—This material, obtained from the Linde Air Products Company, was in the form of a boule. Since its index of refraction was found to be 1.727 for sodium light, it is presumed that the ratio of Al_2O_3 to MgO is greater than the 1 : 1 of normal spinel.

Quartz—The data included in Table II were obtained from indentations made on grains of quartz representative of the "flint" used by Behr-Manning Corporation in the manufacture of sandpaper products. The values for quartz, in Fig. 11, resulted from indentations on a small transparent, flawless, euhedral crystal from Herkimer, New York.

Steel—This was a manganese oil hardening tool steel, hardened and tempered to Rockwell C-60.5.

Variations Within and Between Samples of the Same Designation—We have been careful to define as completely as possible the substances whose Knoop numbers have been determined during the course of the present study. The data refer only to the samples described, and should not be construed as applying equally well to other substances of the same general appellation. For example, garnet refers to a group of minerals known to vary considerably in hardness. Lacking a complete chemical analysis, the variety of garnet and the locality of occurrence should at least be stated.

In connection with the measurements on the steel, hardness variations existed from point to point, necessitating a definite plan in making the indentations. When the data presented in Fig. 11 were being determined, sixteen indentations at a given load were placed in a square lattice, 0.060 inch between centers in each direction, so that there were four rows and four columns of indentations. Corresponding arrays of indentations at other loads were suitably displaced from each other so that the closest distance of approach between the centers of any two indentations was 0.020 inch. Some of the indentations at the lower loads were found to be faulty on account of pits or scratches, so these were replaced by additional indentations in the general vicinity of the faulty ones. When the sixteen visually satisfactory indentations at a given load were measured, it was found that the lengths of most of the indentations fell within a narrow range, but that a few were considerably longer or, in some cases, shorter. These were arbitrarily discarded as being caused by soft or hard spots and the remainder, twelve or more, were used in calculating the average length for that load.

In the case of molded specimens, an additional factor, the porosity, may greatly affect the results. An excellent example is afforded by a recent experience with an experimental series of molded boron carbide ("Norbide") products.

Five "Norbide" pieces of the same shape were molded from the same molding powder, presumably in the same manner. Four of the finished pieces were of nearly theoretical density and a polished cross section showed only a relatively few imperfections, mostly less than 2 microns in diameter. The fifth piece, however, was much lower in apparent density than the inspection limit, and consequently the polished cross section contained many more imperfections per unit area.

Ten Knoop indentations were made in each of the five molded items using 100-gram load, the following hardness numbers being obtained:

	K_{100}	
	Average	Range
High density item 1	2660	2580-2730
High density item 2	2620	2460-2790
High density item 3	2700	2550-2800
High density item 4	2610	2500-2720
Low density item 5	2170	1760-2400

Note that the average Knoop hardness of rejected item 5 was much lower than that of the other pieces, and that there was no overlap in the range of the Knoop numbers obtained from individual indentations.

Undoubtedly this same effect has been observed by other manufacturers of molded products such as cemented carbides.

Crystallographic Orientation—Since it is well known that hardness, however determined, is a vectorial property in single crystals, it is not surprising that variations in Knoop number with crystallographic orientation were reported by the earliest workers with this new method of hardness testing (11).

Recently Winchell (7) has emphasized the effect of orientation on Knoop number, and pointed out that differences in hardness may result not only from differences in the orientation of the surface being indented, but also from variations in the direction of the long dimension of the indentation on that surface.

He proposed that the orientation of the test surface be defined, as in two-circle goniometry, by two co-ordinate angles. Phi (ϕ), the "longitude", is measured clockwise around the fundamental circle of the stereographic projection from the (010) or ($11\bar{2}0$) position, and rho (ρ), the "co-latitude", is the angular distance from the pole or the *c* crystallographic axis. Further, he suggested that the direction of the

long dimension of the indentation on the surface being tested be specified by the angle theta (θ), measured clockwise from the meridian position to the long diagonal of the indentation. When rho is zero, theta must be specially defined, so in this case it is measured around the fundamental circle in the same manner as phi.

This method of defining crystal orientation for Knoop hardness investigations is fundamentally sound, and has been adopted by the authors. The three co-ordinate angles may always be determined by X-ray methods, particularly by the use of projections based upon Laue back-reflection photographs, as described by Winchell (24). Except for the sample of synthetic corundum kindly furnished us by Dr. Winchell, all of the orientations mentioned in our paper were determined by relating the long dimension of the indentations to planes and directions obtained from a study of the crystal morphology. Obviously, this is possible only when the substance being indented exhibits a sufficient number of well-developed crystal faces, or cleavages.

As an example of the effect on the Knoop number of the orientation of the long diagonal of the indentation on the same test surface, the following data for topaz are of interest. The Knoop numbers marked "check" resulted from measurements of additional indentations made on the same sample several weeks later.

Orientation		Observer	Average K_{100}	Range of K_{100} (10 Indentations)
ρ	θ			
0°	0°	N.W.T.	1190	1150-1310
0°	0°	P.M.K.	1200	1120-1300
0°	0°	N.W.T.	1220 (check)	1150-1280
0°	0°	P.M.K.	1200 (check)	1150-1260
0°	45°	N.W.T.	1380	1280-1440
0°	45°	P.M.K.	1400	1320-1460
0°	45°	N.W.T.	1410 (check)	1370-1450
0°	45°	P.M.K.	1430 (check)	1370-1460

There can be no question that a difference of approximately 200 Knoop units, due entirely to differences in orientation of the indentation on the same test surface, actually exists.

Since most of the hard substances in which we were interested were coarsely crystalline, the question arose as to a method of procedure which would yield an average hardness number. After preliminary unsuccessful attempts to derive average values from determinations resulting from indentations made in a few precisely determined orientations, we decided that more satisfactory average results would be obtained with coarsely crystalline products by indenting a large number of randomly oriented surfaces.

To accomplish this, the following procedure was used: If the sample was not already in grain form, the specimen was broken in a mortar and a fine size or mixture of sizes was screened out. Grains about 0.5 millimeter in diameter were used in most of our experiments, although finer sizes down to about 50 microns have also been employed.

If the grains exhibited no particular cleavage, or crystal faces, they were mounted in phenol formaldehyde plastic as described previously. If cleavages or crystal faces were common, however, this method of mounting resulted in preferred orientation because flat crystal planes or cleavages would invariably lie against the bottom platen. To overcome this diffculty, the grains were first bonded with resinoid to form a small cylinder. Then this was either sawed or broken up to form aggregates which were then subsequently bonded with plastic to form the 1.25-inch diameter mounts used. In this manner preferred orientation was largely avoided.

To obtain average Knoop hardness data such as given in Table II, the mount was lapped and polished as previously outlined. Then three to five indentations of the same random orientation were placed on 30 to 35 grains using a 100-gram load. In each of 25 grains, the same two indentations were measured by each of the authors three times, averages being computed for each grain. As previously discussed, some indentations were not measured because of interference by scratches; others were omitted because of excessive cracking. In Table II the range values represent maximum and minimum Knoop numbers obtained from individual grains.

It is quite evident that this method of determining the average Knoop hardness number of coarsely crystalline substances would have been impractical without the Wilson Mechanical Instrument Company's "Microton", or a similar mechanical stage accessory permitting rapid and very precise movement of an object from its position beneath the microscope to beneath the indenter.

Some of the discrepancies in Table I may be due to the factor of crystal orientation. Except Winchell, the early workers made no mention of orientation so it is not known whether the results quoted were based on one set of indentations representing one orientation, or whether they were the average obtained on several orientations.

When Knoop values determined on single crystals are quoted, the orientation should be specified, or a statement made to indicate that the hardness number is an average resulting from a large number of indentations made in random orientation.

If the substance being indented is extremely fine-crystalline so that a relatively large number of grains are affected by a single indentation, crystal orientation may have little meaning. Each indentation should represent more or less of an average condition unless there is a preferred crystal orientation which has developed during crystal growth or recrystallization, or as a result of some forming operation such as wire drawing.

Because molded boron carbide, the commercial cemented carbides, and the hardened tool steel were all very fine-grained, it was not necessary to resort to the crushed grain method outlined above to obtain average Knoop hardness numbers.

Relationship of Indenter to Specimen

Cracking of Specimen by Indenter—One of the advantages claimed for the Knoop method of hardness testing was that indentations could be made in glass and other brittle materials which shattered when tested with the usual ball, cone and square-based pyramidal tools commonly used for metals (2). Although this statement is certainly quite true, the failure of the early workers to mention any cracking of hard compounds when indented with the Knoop instrument gave the unfortunate impression that none occurred.

Later, Hubbard (6, discussion) pointed out that satisfactory Knoop values could not be obtained with chromium plate using loads greater than 100 grams, because the higher loads caused excessive cracking of the specimen, resulting in low and erratic Knoop numbers.

Winchell (7) indicated that a large number of the nonmetallic substances included in his study were fractured by the indenter even at loads as low as 100 grams. In fact, indentations made in one crystallographic orientation in gypsum with 100-gram load were so badly cracked that it was impossible to measure them at all. When a series of indentations made in one crystallographic orientation in a substance resulted in fracturing, Winchell regarded the maximum Knoop number obtained as most representative of the true hardness in this direction. Otherwise the average of a series of indentations was accepted.

Obviously, it would be most desirable to make all Knoop indentations under conditions of elastic and plastic deformation and thus avoid any effect which fracturing might exert on the Knoop number. Unfortunately, however, many substances in various orientations cannot be indented with the Tukon even at 25-gram load without the

development of considerable cracking, so it becomes important to investigate the effect of such fracturing upon Knoop hardness.

In our study of this problem we examined indentations made at various loads in different transparent, hard, brittle substances, and attempted to classify the amount of cracking into six categories or "cracking classes", which are described as follows:

Class 1—There was no fracturing of any nature visible when the indentation was observed on the Bausch and Lomb Research Metallograph using either bright-field illumination or polarized light supplied by the carbon arc. During this examination the aperture diaphragm was decentered and rotated or the lighting was otherwise altered so as to catch reflections from any possible fractures beneath the surface. If the substance being examined was suitable, the 80X oil immersion objective was employed; if the index of refraction of the substance was too low the 62X or 41X dry objective was substituted.

Class 2—Only very slight subsurface cracking was evident. Usually this was so trivial that it could be noticed only in polarized light.

Class 3—In this case there was a large amount of subsurface cracking, usually visible in bright-field illumination as reflections from beneath the surface, but no cracks were visible at the surface, as illustrated by Fig. 6a. Included also in this classification were indentations showing only a small amount of subsurface cracking, and slight surface cracking as well. The latter usually occurred at or near the terminations of the long dimension of the indentations.

Class 4—Here there was a large amount of subsurface cracking accompanied by slight to moderate surface cracking, as in Fig. 6b.

Class 5—In this category were placed indentations, such as illustrated by Fig. 7a, which showed considerable surface and subsurface cracking with or without the loss of small portions of the specimen adjacent to the short diagonal of the indentation.

Class 6—In this case, fracturing was so pronounced that large portions of the specimen were chipped away. In some cases, as in Fig. 7b, one or both ends of the indentation extended beyond the chipped area. In other cases, large scallops in the specimen marked the site of the indentation, but no evidence of the impression itself could be found.

Obviously, these six classes of cracking are entirely arbitrary, all possible gradations being observed. Furthermore, all substances did not exhibit exactly the same type of fracturing, so it was necessary to use

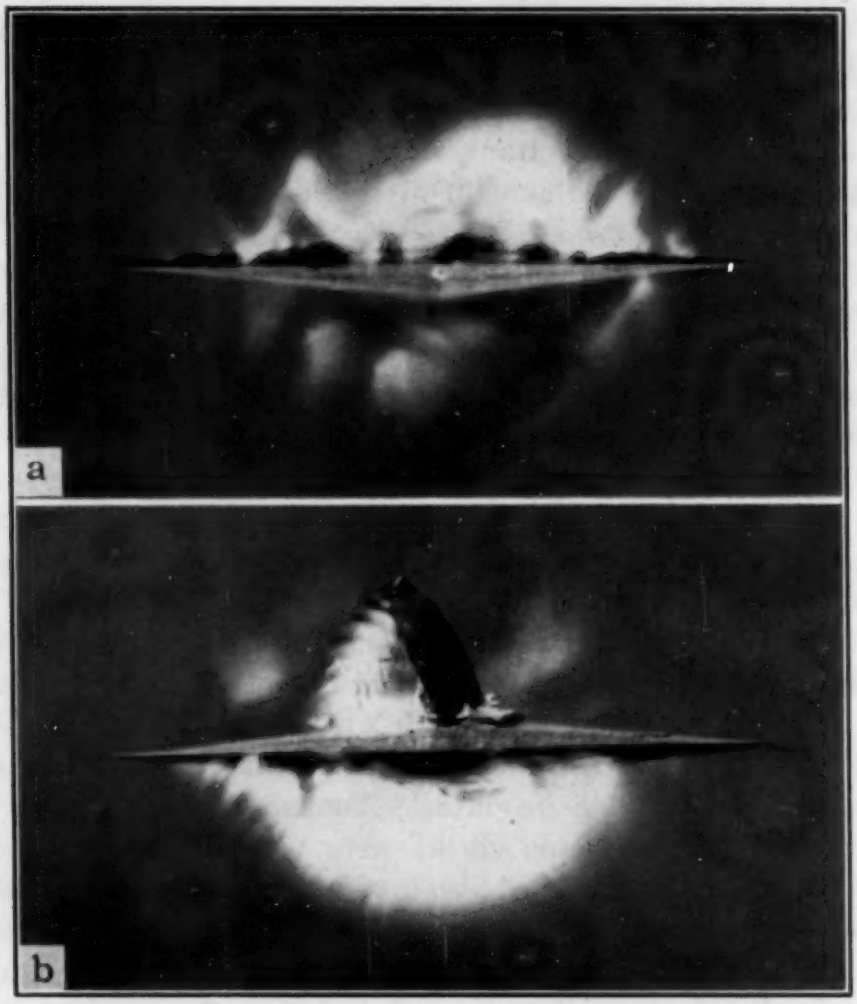


Fig. 6—Moderate Cracking of a Hard, Brittle Substance by the Knoop Indenter. (a) Illustrative of cracking class 3 (see text). 300-gram indentation in transparent green SiC. Reflected light. (× 1500). (b) Illustrative of cracking class 4. 300-gram indentation in green SiC. (× 1500).

judgment in assigning classes. We believe, nevertheless, that the data obtained in such a manner are reliable enough to be considered at least semiquantitative. Different substances showed markedly different *average* susceptibilities to cracking when indented with the same load, an excellent comparison being furnished by the behaviors of green silicon carbide and topaz.

As previously discussed, the Knoop values quoted in Table II were determined by indenting a number of grains in random orientation with a 100-gram load and calculating average Knoop numbers and ranges on this basis. After this had been completed, the samples were examined on the Research Metallograph and all the indentations classified according to amount of fracturing. The data on fracturing of

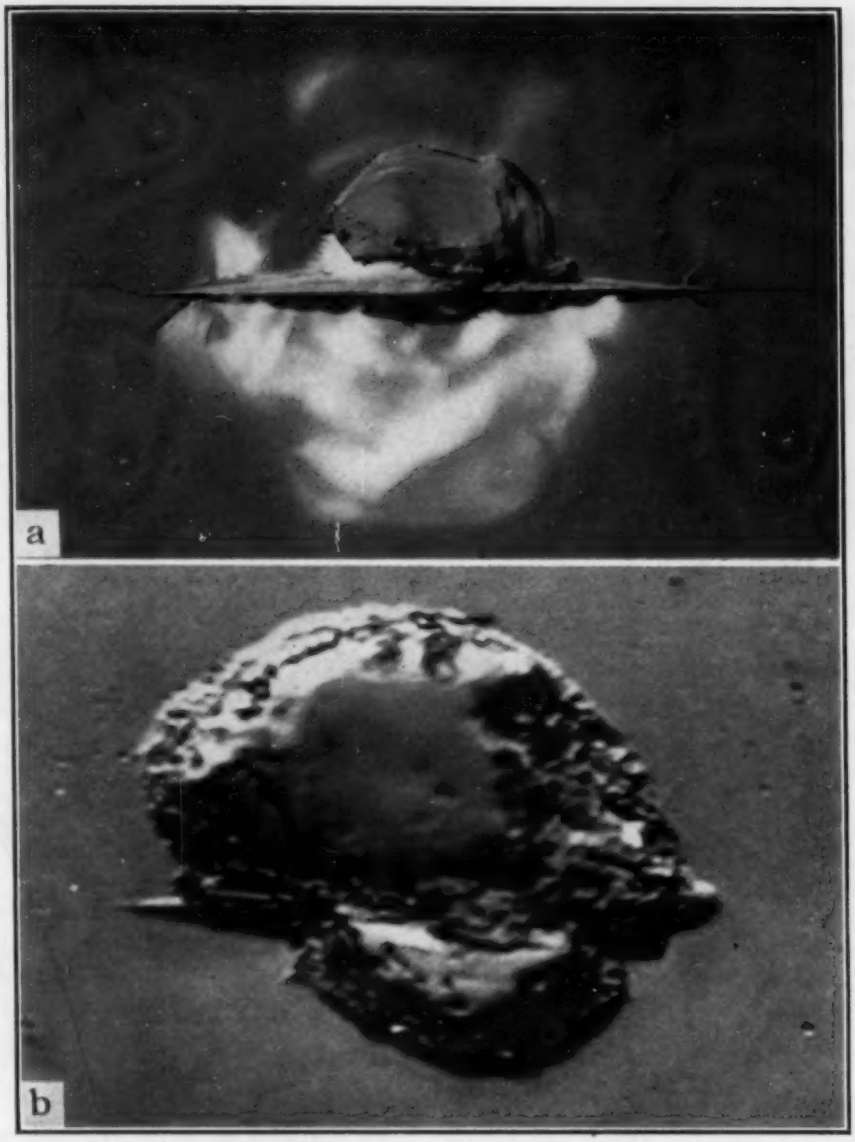


Fig. 7—Excessive Cracking of Hard, Brittle Substances by the Knoop Indenter. (a) Illustrative of cracking class 5. 500-gram indentation in green SiC. (× 1000). (b) Illustrative of cracking class 6. 100-gram indentation in topaz. (× 2000).

SiC were based on 90 indentations in 27 grains at random, while those for topaz resulted from the examination of 152 indentations in 41 grains. The following comparison was afforded:

Class of Cracking	Per Cent of Indentations in Each Class	
	Green SiC	Topaz
1	34	1
2	56	1
3	9	8
4	—	20
5	1	30
6	—	40

Of the 40% of the topaz indentations falling in class 6, about two-thirds were entirely unmeasurable because one or both ends of the indentations were missing.

That the same substance resists fracturing by the indenter to varying degrees depending upon orientation may be illustrated by the following comparison of two series of 15 indentations each made in each of two directions on the (001) plane of topaz ($\rho = 0°$) using a 100-gram load:

	Per Cent of Indentations in Each Class			
	$\theta = 0°$		$\theta = 90°$	
Class of Cracking	1st series	2nd series	1st series	2nd series
3	5	—	—	—
4	90	80	—	—
5	5	20	20	—
6	—	—	80	100

Obviously, the greater the load on the indenter the more a hard, brittle material will be cracked. An example of this trend may be illustrated by the following observations on four series of 10 indentations each made with various loads on SiC, the orientation being: $\rho = 0°$, $\theta = 0°$.

	Per Cent of Indentations in Each Class			
Class of Cracking	25 g.	100 g.	300 g.	500 g.
1	80	80	10	—
2	20	20	—	—
3	—	—	80	50
4	—	—	10	20
5	—	—	—	20
6	—	—	—	10

Undoubtedly if a larger number of indentations had been made at each load, the increased tendency to crack with greater loads would have been more uniform, and a difference between the amount of fracturing at 25 and at 100-gram load would probably have been observed.

Effect on Knoop Number of Degree of Cracking—As previously discussed, most of the Knoop data included in Table II were determined by indenting randomly oriented grains. In making the measurements indentations were omitted if scratches, inclusions, or imperfections interfered, or if an impression was fractured considerably more than others in the same grain. If there was no such reason for omitting an indentation, the first two made in the grain were measured. Occasionally the results on a grain were omitted because scratches, etc., interfered with all, or all but one, of the indentations made in it.

Because topaz fractured so badly, more grains were indented and more indentations discarded than with any other substance. All inden-

tations in cracking class 6 were rejected even though many were measurable, and those in classes 4 and 5 were accepted only when all the indentations in a single grain were of nearly the same length. Because such a large number of indentations were rejected, the data for topaz were based on 39 indentations in 25 grains at random. All indentations in 16 grains were discarded because of excessive cracking, and since fracturing varies with orientation, the data were not obtained on a strictly random basis as was the case with all the other substances included in Table II. We believe that it was better to omit these grains, however, than to base any Knoop values on indentations which were suspected to be too long because of excessive cracking.

Several months after the Knoop data had been determined on green SiC and topaz, the indentations used to determine the Knoop hardness of these substances, as given in Table II, were examined on the Research Metallograph, classified into the class of cracking, and the Knoop number and range was determined for each class. The following results were obtained:

Substance	Class of Cracking	No. of Indentations	K_{100} Average	K_{100} Range
Green SiC	1	25	2490	2230-2760
Green SiC	2	20	2500	2260-2710
Green SiC	3	5	2460	2440-2580
Topaz	1-3 incl.	5	1390	1310-1500
Topaz	4	22	1350	1240-1490
Topaz	5	12	1360	1240-1500

This certainly indicates that cracking had no measurable effect upon the determination of the Knoop hardness of either SiC or topaz when it was carried out as described above.

To ascertain what results would have been obtained with topaz if all measurable indentations in classes 4, 5 and 6 had been used, they were all measured, with the following results:

Class of Cracking	Number of Indentations	K_{100} Average	K_{100} Range
4	29	1340	1200-1500
5	42	1260	1000-1500
6	22	1070	640-1430

From this and other studies, we believe that Knoop numbers based on indentations of classes 1 to 3 inclusive are not affected by the fracturing observed. Indentations of classes 4 and 5 should be avoided if possible, by the use of lower indenting loads but, if unavoidable, only the shorter indentations should be accepted for measurement. In our opinion, it is inadvisable to base any Knoop numbers on indentations of class 6.

Obviously, these remarks apply particularly to transparent substances. Subsurface cracking cannot readily be determined in opaque or very translucent materials, and, therefore, with such substances no distinction can ordinarily be made between our classes 1, 2 and even 3. If any great amount of cracking is evident with opaque samples, the effect of fracturing may be noticeable.

It would be interesting to determine whether the observed cracking occurred largely at and during the time of indentation or at and subsequent to removal of the load from the specimen. While it would be expected that the former would affect the length of the indentation, the latter should not. Occasionally we have noticed a subsurface crack enlarge and reach the surface while the indentation was being measured shortly after being made.

Asymmetry of Indentation—It has been stated (2) that some asymmetry of indentation could be permitted without appreciably affecting the Knoop number. Our co-operative work with other laboratories indicated that Knoop numbers were, in some cases, based on indentations so asymmetrical that one end was from two to seven times as far from the short diagonal of the indentation as the other end.

To ascertain the possible effect of this condition on the Knoop number, several series of indentations were purposely made in varying degrees of asymmetry on molded boron carbide, silicon carbide, and "Kennametal K12". In this work, degree of asymmetry of the long diagonal was defined as the percentage difference between the distance of each end from the short diagonal, the total length of the indentation being unity.

Fig. 8 gives the results of the variation of Knoop number with degree of asymmetry for "Kennametal K12" at 100-gram load. For each of the five different degrees of asymmetry investigated, ten indentations were made, and the average, as well as the maximum and minimum, Knoop numbers obtained are indicated.

Photomicrograph, Fig. 9, shows for molded boron carbide the lengthening of the indentation, and hence the lowering of the Knoop number, with increasing asymmetry of indentation. The Knoop hardness was about 2820 when the indentation was almost perfectly symmetrical. When the asymmetry was about 35%, the Knoop number was about 2390 and with an asymmetry of 75% it was only about 1240.

In all our work the same trend as shown in Fig. 8 was experienced, but, because of the normal experimental error involved in determining Knoop numbers even with perfectly symmetrical indentations, it was

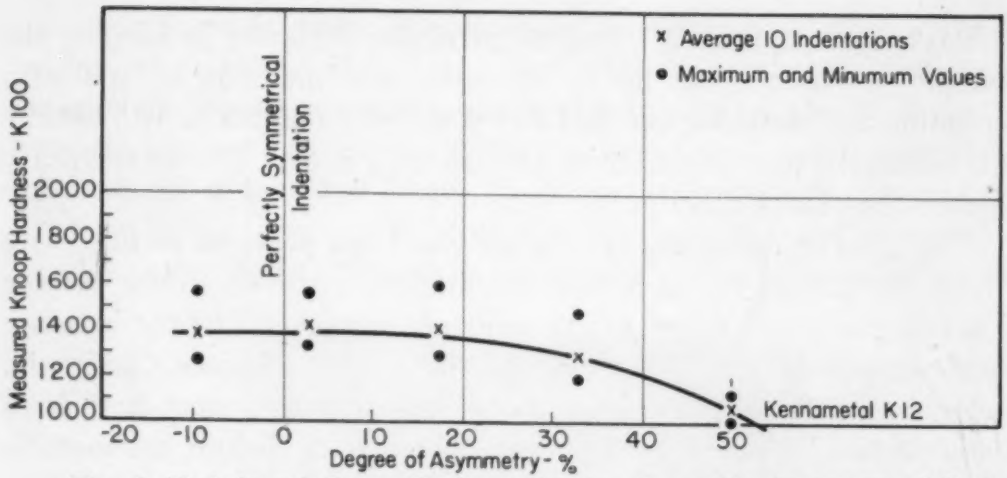


Fig. 8—Variation of Knoop Hardness Number, K_{100}, with Asymmetry of Long Dimension of Indentation in the Case of "Kennametal K12."

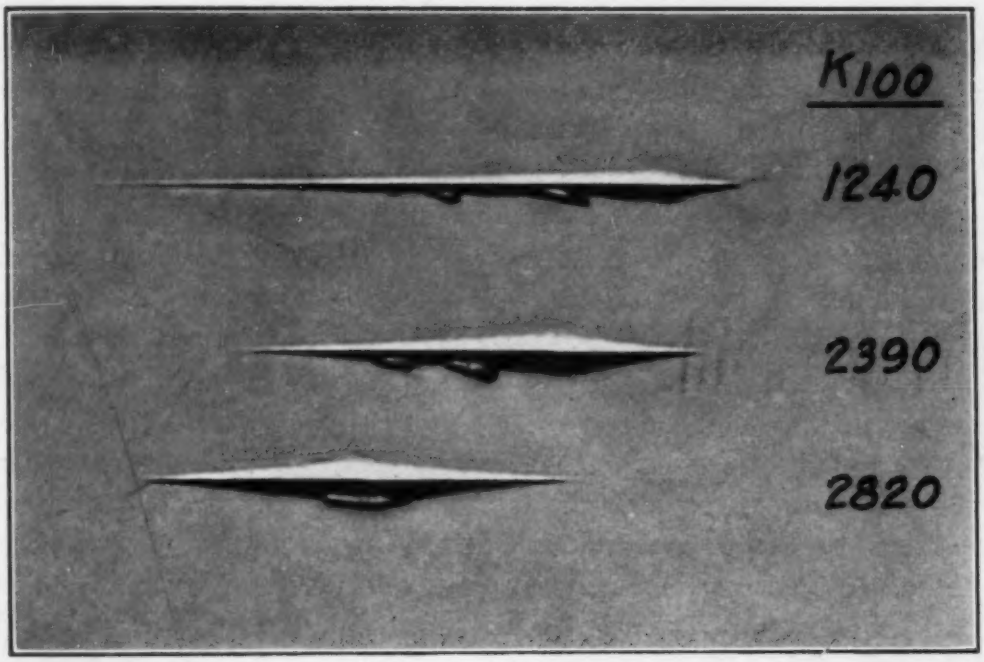


Fig. 9—Effect of Asymmetry of Indentation on the Knoop Hardness Number, K_{100}, for Molded Boron Carbide ("Norbide"). (× 2000).

difficult to determine at just what degree of asymmetry the effect was noticeable. The evidence seems fairly conclusive that a lowering of the Knoop number of hard substances can be detected if the asymmetry, as defined above, exceeds about 20%.

As a precautionary measure, however, we kept the asymmetry of the indentations used to determine Knoop numbers under 10%. To express it in another way, the length of the shorter portion of the long diagonal of an indentation was always at least 80% of the length

of the longer portion. We find no particular difficulty in keeping the symmetry within these limits. By using the methods of specimen mounting and polishing outlined above, all the indentations will usually fall within the prescribed limits. Occasionally it may also be necessary to shim the mount slightly.

Spacing of Indentations—As indicated in a previous section, with a large percentage of the Knoop indentations made on silicon carbide at a 100-gram load, there was no evidence whatever that the indenter had fractured the specimen either at or beneath the surface. Obviously, under such a circumstance, the observed indentation must have been accomplished by plastic flow even in such a hard, brittle, nonmetallic substance as silicon carbide.

To investigate the matter further, several Knoop indentations, made at various loads from 100 to 500 grams, were placed on a basal plate of silicon carbide only about 0.2 millimeter thick. The various indentations were then examined on the Research Metallograph and the class of cracking of each impression noted.

Then the thin plates were transferred to the petrographic microscope, where the same indentations were examined in polarized light at a magnification of about 600. It was observed that the silicon carbide adjacent to every indentation was considerably strained, as indicated by the appearance of anisotropism adjacent to the indentations, the silicon carbide at a distance from the impressions being isotropic in this orientation. The greatest amount of anisotropism was adjacent to the short diagonal of the indentations, and it became progressively smaller with increasing distance from the center of the impression. In all cases, irrespective of the load at which the indentations were made, or whether they were accompanied by fracturing, the affected area seemed to extend out from the center for a distance roughly equal to the length of the indentation. The appearance of one of the 500-gram indentations in transmitted light under crossed nicols is illustrated by Fig. 10, the vibration directions of the nicol prisms being parallel to the diagonals of the indentation. As might be expected, the isogyres of the interference figure pulled apart slightly, although definitely, when the section immediately adjacent to the short diagonal of the indentation was reached on traversing the indentation under the conoscope. Such a biaxial interference figure in a substance normally uniaxial is also evidence of considerable strain in the crystal.

Mrs. Brodie (6), apparently as a result of experiments made on various metals, recommended a minimum spacing of 12 microns for

indentations made with 100-gram load in substances whose Knoop hardnesses exceeded 750. Tate (6, discussion), on the other hand, reported that errors might be introduced in the determination of Knoop numbers of metals if the indentations were spaced closer than about 1.5 times the indentation length, probably due to cold working of the specimen by the indenter for some distance from the indentation itself.

We attempted to determine the effect on Knoop number of the



Fig. 10—Strain Produced in Silicon Carbide by a 500-gram Knoop Indentation. Transmitted light, crossed nicols. (× 600).

distance between indentations by making several series of indentations at different spacings on the base of a crystal of silicon carbide using a 100-gram load. Series were made in which successive indentations were placed progressively closer together; other series were made in which indentations were placed halfway between those previously made. At the load used, the indentations were approximately 24 microns long.

A distinct effect on the amount of cracking of the substance was observed. Examination of the indentations made successively at closer intervals revealed no definite increase in cracking tendency until the indentations were only about 10 microns apart. However, when indentations were placed midway between a series of impressions previous-

ly made, a noticeable effect was apparent when the later indentations were 15 microns from the first series. For example, when 11 indentations were placed successively 30 microns apart, all were of cracking class 1; of 10 indentations, which were later placed halfway between the first, 3 were of class 1, 5 of class 3, and 2 of class 4. Undoubtedly the strain introduced into the silicon carbide specimen by an indentation lowers its tensile strength locally, and renders it more susceptible to cracking by a later indentation made within, or close to, the affected area.

The effect on the Knoop number of the distance between indentations was much more difficult to determine. With a series of indentations made successively at closer intervals, no effect could be noted which was outside the normal variations to be expected under the best possible conditions for the determination of the Knoop number, at least for spacings down to 25 microns. When the spacing was 10 microns, however, a slight increase of Knoop number seemed evident, especially when hardness values obtained from the more severely cracked impressions were omitted.

In the case of the various series of indentations which were placed midway between others, the same tendency toward an increased Knoop number seemed to be observed when the distance was 15 microns, and possibly even 25.

Applying a safety factor because of the inconclusiveness of our data, and considering the evidence of strain as illustrated by Fig. 10, we agree with Tate in recommending a minimum spacing of 1.5 times the indentation length.

Rigidity of Specimen on Tukon Stage—During our early work with the Tukon, some of our difficulties were traced to lack of rigidity of the specimen on the stage, resulting in an apparent sideways movement of the sample at the moment of indentation. This naturally resulted in low and erratic Knoop numbers and abnormal fracture of hard, brittle specimens.

Because of this experience, we prefer, wherever possible, to mount the sample in phenol formaldehyde plastic as described above, and to place the mount in a small specimen holder consisting of a section of brass pipe soldered to a flat plate. The walls of the pipe are about 0.5 inch high, and contain two fixed stops and a thumbscrew, which permit rigid clamping of the mount.

If the specimen is unsuitable for mounting in plastic, it should be carefully ground so that the surface bearing on the stage is flat and

parallel to the surface being indented. Such a specimen may be satisfactorily secured to the stage by the use of small wads of beeswax placed at the side of the specimen.

Indenting Load

Although it was originally believed that the Knoop number was independent of the applied indenting load (2), it was soon found that the hardness value was greater the lower the load used on the Tukon, especially in the range of 25 to 200 grams (6). Tate (8) and others (8, discussion) observed that this effect was considerably greater with hard than with soft materials, and pointed out that every Knoop number should be accompanied by a statement of the load used for its determination.

During our study we determined the variation of Knoop number with indenting loads from 25 to 500 grams for five different nonmetallic substances ranging in hardness from quartz to boron carbide, and for a cemented carbide. Dr. L. P. Tarasov kindly supplied similar data for a hardened tool steel, Rockwell C-60.5. The results are given in Fig. 11. The orientations of the indentations made on the single crystals were:

Silicon carbide	$\phi =$ —;	$\rho = 0°$;	$\theta = 0°$
Aluminum oxide	$\phi = 8°$;	$\rho = 89°$;	$\theta = 135°$
Topaz	$\phi =$ —;	$\rho = 0°$;	$\theta = 0°$
Quartz	$\phi = 30°$;	$\rho = 90°$;	$\theta = 0°$

When rho is zero, phi is indeterminate.

The values for the four hardest substances were obtained from measurements made with the 54X oil immersion objective on the microscope attached to the Tukon. The three softer samples were measured on the Research Metallograph, using the 41X dry lens for the shorter indentations, and the 21X for the longer.

The points plotted in Fig. 11 are those resulting from the measurements as actually carried out. As is indicated in the separate paper by Tarasov and Thibault (16), however, all the indentations made in a given substance at the various loads should be measured with the same optical equipment or some adjustment should be made to compensate for the error introduced by the measurement of some of the indentations with an optical set-up of lower resolving power.

The curve for topaz is undoubtedly the least accurate of those included in Fig. 11 because of the very poor contrast of the indentations and the great tendency for the substance to fracture excessively.

Obviously, unless some method of calulation which will give a

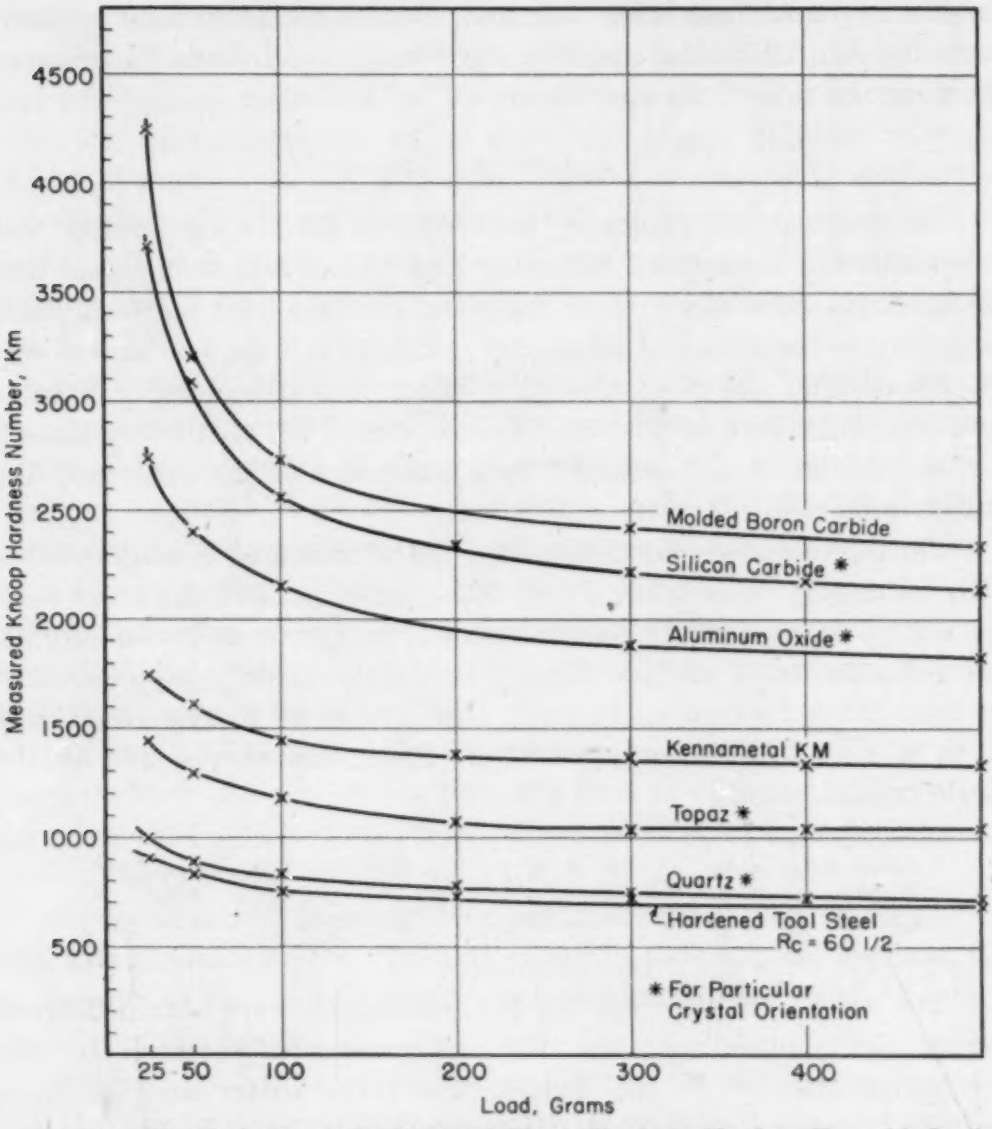


Fig. 11—Variation of the Measured Knoop Hardness Number, K_m, with Load on the Indenter for Several Hard Substances. Curves for silicon carbide, aluminum oxide, topaz and quartz apply only to the special orientations mentioned in the text.

Knoop number independent of load is applied, a statement of the load used must certainly accompany Knoop hardness values.

Since the cause of the variation of the measured Knoop hardness number with indenting load is discussed in detail in the separate paper by Tarasov and Thibault (16), it will not be repeated here.

It is proposed that the Knoop number determined in the usual manner by use of the standard formula be referred to as K_m, since it is based upon measurements of the long dimension. Determinations made at various loads would then be noted by the letter "K" and a subscript denoting the load used, e.g., K_{100}, the subscript "m" being

unnecessary. K_u is reserved for the Knoop hardness number independent of load as described in the separate paper (16).

The failure of all previous investigators, except Winchell, to state the load at which the hardness values given in Table I were based will probably account for a large part of the discrepancies noted within this table, and between this table and our own data as given in Table II.

Most of Winchell's data were derived from indentations made with a load of 100 grams, while comparison of the values quoted by the National Bureau of Standards and those resulting from our own study indicates that the former were probably based on indentations made with a greater load, probably 500 grams. Even Winchell's values for the harder materials are not directly comparable, since the Knoop numbers given for synthetic blue spinel and dark ruby corundum were obtained only with a load of 300 grams while the other substances except for light ruby corundum were indented only with a 100-gram load.

The misconception that tungsten titanium carbide is harder than silicon carbide or boron carbide was brought about by comparing data for $WTiC_2$ based on indentations made at a 25-gram load[9] with values for SiC and B_4C determined from indentations made at higher loads. This misunderstanding was fostered by the tabulation of Knoop hardness numbers published by Twells (25), who, quite naturally, was unaware that the values quoted in the literature were not necessarily directly comparable. As indicated in Table II, the hardness of tungsten titanium carbide actually lies between that of aluminum oxide and silicon carbide.

Summary and Conclusions

The determination of the measured Knoop hardness number of hard substances is not to be entered into inadvisedly or without due consideration of the many factors which might greatly affect the results obtained.

If one is willing to exercise the care, and take the time necessary to control the variables, Knoop numbers of sufficient precision for any practical purpose may be obtained readily. It is estimated that 15 to 20 man-hours were required for each of the Knoop determinations included in Table II, even after the conditions of the experiment had been established. For routine and exploratory work, where the utmost of

[9]Personal communication from J. C. Redmond, Kennametal, Inc., November 3, 1945.

precision is not required, satisfactory results may ordinarily be obtained in 4 to 8 hours, including the time necessary to properly prepare the specimen for the test.

The Knoop numbers quoted in this paper were determined under the conditions summarized below. These are strongly recommended to anyone interested in the determination of the Knoop hardness number of hard substances.

1. All the specimens, except the steel, were lapped and honed with diamond exclusively. Practically all were polished on the Graton-Vanderwilt machine using extremely fine diamond on a lead lap to produce an optically flat surface practically free from scratches. The steel was mechanically polished, first with emery paper and then with levigated alumina on a cloth lap, great care being taken to minimize cold working of the surface.

2. The Tukon equipped with solenoid and torque-arm devices to minimize additional inertial load was used exclusively.

3. External vibration was minimized by installing shear rubber and other vibration-dampening devices.

4. The balance of the beam and the precision of the applied load were checked.

5. Periodically, indentations were made on a standard sample of silicon carbide and examined for evidence of damage to or wear of the diamond indenter, which was returned to the supplier for repolishing as soon as imperfections were noticed.

6. Differences in total weight of diamond and holder were overcome by rebalancing the beam when a new or repolished diamond was used for the first time.

7. All the values quoted in this paper were determined by the use of two different certified diamonds which, under the same operating conditions, gave indentations which were of equal length. Furthermore, the Knoop numbers obtained by the use of these two indenters were practically the same as those resulting from the use of three other recently lapped diamonds in the supplier's stock. It has been demonstrated, however, that differences in Knoop number may result from differences in indenters.

8. The filar micrometer was checked and found to be accurately graduated. It was calibrated with a commercial stage micrometer, which in turn had been checked against a micrometer consisting of lines ruled on steel by the use of the interferometer at the National Bureau of Standards.

9. The optical equipment used for the measurement of the indentations has a marked effect on the Knoop number, the higher the resolving power of the lens system, the longer a given indentation will appear to be. Indentations made in all the substances listed in Table II and Fig. 11, except topaz, quartz and steel, were measured with a 54X fluorite oil immersion objective on the microscope attached to the Tukon cowl. Illumination was supplied either by the small light source attached to the vertical illuminator, or by a ribbon filament lamp operated at 6 volts, 18 amperes, not attached to the microscope. Measurements of the indentations in topaz, quartz and steel were made using the Bausch and Lomb Research Metallograph and the 41X dry objective for the shorter indentations and the 21X for the longer.

10. To reduce to a minimum differences due to the personal factor, or the visual acuity of the observer, all the indentations, except those in steel, were independently measured by each of the authors. The Knoop numbers quoted in Table II are the averages of the two sets of values which usually agreed closely.

11. No differences due to time between indentation and measurement could be found.

12. Since hardness variations may occur within and between samples of the same substance, a complete description of the specimens used is quite necessary.

13. It has been shown that the Knoop hardness of coarsely crystalline substances varies, sometimes very greatly, with the crystallographic orientation of the indentation relative to the crystal structure. If single crystals are indented, the orientation should be specified. To obtain average hardness numbers of such substances as given in Table II, it is preferable to indent a large number of particles in random orientation.

14. The effect of cracking of the specimen by the indenter was minimized by using a 100-gram load, and by measuring those indentations which showed least fracturing.

15. In order to eliminate errors which might result from asymmetry of indentation, the length of the shorter portion of the long diagonal of an indentation was maintained at a minimum of 80% of the length of the longer portion.

16. In practically all cases the spacing of the indentations was about 1.5 times the indentation length. In a few cases, where size of grains available was small, indentations were placed one length apart.

17. All specimens were rigidly attached to the Tukon stage by means of a specially designed holder.

18. Since the measured Knoop number varies considerably with the load on the indenter, it is necessary to indent all substances with the same specified load, if strictly comparable results are to be obtained. Because of the tendency of some of the hard, brittle substances included in Table II to fracture excessively, it was found necessary to use a 100-gram load for these determinations. The separate paper by Tarasov and Thibault (16) discusses the determination of Knoop hardness numbers independent of load.

Acknowledgments

So many individuals have contributed to the success of the study in one detail or another, that only a few can be mentioned.

At Norton Company special thanks are due Miss Pauline Krukonis who has ably assisted the senior author in recent months, and to A. A. Klein and Drs. L. H. Milligan and L. P. Tarasov for counsel and suggestions during the progress of the study.

We are indebted to the following individuals and concerns who supplied samples, criticized the manuscript, and permitted publication of Knoop data on their specimens, or otherwise co-operated with us in our study:

James Benford, Bausch & Lomb Optical Co., Rochester, N. Y.; V. E. Lysaght, Wilson Mechanical Instrument Company, New York, N. Y.; C. G. Peters, National Bureau of Standards, Washington, D. C.; J. C. Redmond, Kennametal, Inc., Latrobe, Pa.; D. R. Tate, National Bureau of Standards, Washington, D. C., and Dr. Horace Winchell, formerly with the Hamilton Watch Company, Lancaster, Pa., now at the Mineralogical Laboratory, Yale University, New Haven, Conn.

References

1. C. G. Peters and Frederick Knoop, "Resistance of Glass to Indentation," *Glass Industry*, Vol. 20, May 1939, p. 174-176.
2. Frederick Knoop, C. G. Peters and W. B. Emerson, "A Sensitive Pyramidal-Diamond Tool for Indentation Measurements," *Journal of Research*, National Bureau of Standards, Vol. 23, July 1939, p. 39-61.
3. C. G. Peters and Frederick Knoop, "Metals in Thin Layers—Their Microhardness," *Metals and Alloys*, Vol. 13, Sept. 1940, p. 292-297.
4. Frederick Knoop, U. S. Patent 2,091,995 (Sept. 7, 1937).
5. D. R. Tate, U. S. Patent 2,357,856 (Sept. 12, 1944).
6. Constance B. Brodie, "The Microhardness Tester as a Metallurgical Tool," TRANSACTIONS, American Society for Metals, Vol. 33, 1944, p. 126-149.
7. Horace Winchell, "The Knoop Microhardness Tester as a Mineralogical Tool," *American Mineralogist*, Vol. 30, 1945, p. 583-595.

8. D. R. Tate, "A Comparison of Microhardness Indentation Tests," TRANSACTIONS, American Society for Metals, Vol. 35, 1945, p. 374-389.
9. V. E. Lysaght, "Microhardness Testing of Materials," *Materials and Methods*, Vol. 22, Oct. 1945, p. 1079-1084.
10. V. E. Lysaght, "The Knoop Indenter as Applied to Testing Nonmetallic Materials Ranging from Plastics to Diamonds," *Bulletin*, American Society for Testing Materials, No. 138, January 1946, p. 39-44.
11. C. G. Peters and Frederick Knoop, "Measurements of the Relative Hardness of Glasses," *Glass Industry*, Vol. 17, May 1936, p. 153-154.
12. P. M. McKenna, "Tungsten-Titanium Carbide Hardness," *Automotive and Aviation Industries*, Vol. 91, Aug. 15, 1944, p. 40, 92.
13. L. C. Graton, "Technique in Mineralography at Harvard," *American Mineralogist*, Vol. 22, May 1937, p. 491-516.
14. "Grading of Diamond Powder," U. S. Department of Commerce Commercial Standard CS123-45, 1945.
15. National Bureau of Standards Specification for Knoop Indenters, Letter Circular, LC819, April 1, 1946.
16. L. P. Tarasov and N. W. Thibault, "Determination of Knoop Hardness Numbers Independent of Load," submitted for publication in TRANSACTIONS, American Society for Metals.
17. J. R. Benford, "Anti-Reflection Films for Metallographic Objectives," TRANSACTIONS, American Society for Metals, Vol. 36, 1946, p. 453.
18. N. W. Thibault, "Morphological and Structural Crystallography and Optical Properties of Silicon Carbide," *American Mineralogist*, Vol. 29, 1944, p. 249-278, 327-362.
19. C. D. Hodgman, "Handbook of Chemistry and Physics," 29th Edition, 1945, p. 2001. Chemical Rubber Publishing Co., Cleveland.
20. P. P. Ewald, C. Hermann and others, "Strukturbericht," Vol. 1-7 inclusive, 1931-1943. Akademische Verlagsgesellschaft M. B. H., and others, Leipzig.
21. P. M. McKenna, U. S. Patent 2,113,353 (April 5, 1938).
22. E. S. Larsen and H. Berman, "The Microscopic Determination of the Nonopaque Minerals," 2nd Edition, *U. S. Geological Survey*, Bulletin 848, 1934, p. 113.
23. E. S. Dana, "System of Mineralogy," 6th Edition, 1914, John Wiley and Sons, Inc., New York, N. Y.
24. Horace Winchell, "Navigation in Crystallography," *Bulletin*, Geological Society of America, Vol. 57, April 1946, p. 295-308.
25. Robert Twells, "Ceramic Gauges of Abrasion-resisting Compositions," *Bulletin*, American Ceramic Society, Vol. 23, Nov. 1944, p. 408-411.

DISCUSSION

Written Discussion: By E. E. Wicker and John C. Redmond, Kennametal, Inc., Latrobe, Pa.

The authors are to be complimented upon this excellent and thorough study of the measurement of Knoop hardness. Their work is very timely in view of the growing doubt concerning the value of Knoop hardness numbers because of the wide variations reported by various workers. This was especially true in the field of hard substances, in which field the Knoop hardness determination is particularly valuable.

It has been our privilege to co-operate with the authors and to determine the closeness of agreement which could be obtained by two independent laboratories. The purpose of this discussion is to report some of these results.

To begin with, before learning of the work which was being done by Dr.

Thibault and Mrs. Nyquist, we had, as a result of our early work, arrived qualitatively at their conclusions with regard to the importance of freedom from vibration of the equipment, of proper optical equipment, illumination, surface preparation and similar factors affecting the determination of Knoop hardness numbers.

In November of 1945, Dr. Thibault supplied us with a mounted specimen of boron carbide which had been polished, indented and the indentations measured at the Norton Company. By means of this specimen we were able to determine the agreement which could be expected between the two laboratories with regard to the measurement of indentations. We also confirmed the desirability of the oil immersion type of objective as compared with the dry objective and have standardized upon a 2.75-mm oil immersion objective used in conjunction with a Gaertner Scientific Company filar micrometer. These optics were used in the microscope mounted on our Tukon tester. Table A shows the results we obtained on the measurement of these indentations in comparison with those obtained by Dr. Thibault and Mrs. Nyquist. The agreement is seen to be excellent and, as might be expected, is somewhat poorer at light loads where resolution of the ends of the indentations is most difficult.

Table A

Load	Knoop Hardness by Kennametal H	Range	Knoop Hardness by Norton Co.
500	2340	2226-2434	2340
300	2421	2339-2470	2420
100	2725	2636-2827	2728
50	3233	3206-3257	3200
25	4306	3726-4890	4240

Further quantitative comparisons may be drawn by consideration of the work done at our laboratory on tungsten titanium and boron carbides. The boron carbide was in the form of primary crystals supplied to us by Dr. Thibault. Samples of these carbides were mounted in Lucite molding powder and polished with diamond dust on lead-tin laps using a technique comparable to that described by the authors. Indentations were made on the randomly oriented crystals and measured by means of the optical equipment described above. Results for these specimens and the comparative values obtained by Dr. Thibault and Mrs. Nyquist are shown in Table B. In connection with our determination of the Knoop number for boron carbide, it should be mentioned that one value of 3127 was obtained. This appeared to be a spurious figure and was not included in the average above.

Table B

Specimen	Load	Knoop Hardness by Kennametal H	Range	Knoop Hardness by Norton Co. H	Range
Tungsten Titanium Carbide	100	2160	1976-2354	2190	2050-2320
Boron Carbide	100	2808	2681-2916	2800	2670-2940

Results on cemented carbide compositions have comprised the largest part of the work at our laboratory. When comparisons are drawn between the work of Dr. Thibault and Mrs. Nyquist and the determinations made by our laboratory, they again show quite satisfactory agreement. It is unfortunate that we were unable to make our determinations on the same specimens used by Norton Company. However, the results as shown may possess greater value in that they illustrate that variations in the method are in accord with the possible variations in the material. Results at both 500 and 100-gram loads are shown in Table C with comparative values reported to us by Dr. Thibault.

Table C

Specimen (Kennametal Grade)	Load	Knoop Hardness by Kennametal H	Range	Knoop Hardness by Norton Co. H	Range
KM	500	1368	1335-1397	1345	.....
KM	100	1487	1392-1594	1500	1390-1660
K6	100	1788	1739-1843	1800	1700-1946

The variation of Knoop numbers with density of the material was mentioned by Dr. Thibault, and we have observed variations in hardness of a single specimen resulting from changes in the nature of the material. We feel that in cemented carbide compositions this is explainable on the basis of segregation of constituents, and low values are attributable to a concentration of the relatively soft matrix metal phase. Inasmuch as the Knoop hardness of such fine-grained materials can only represent an averaging of the grains included in projected area, the presence of large quantities of the soft, less dense binder would be reflected in lower Knoop hardness numbers.

The conclusions derived from the work done on Knoop hardness in this laboratory can indicate only very close agreement with that done by Dr. Thibault and Mrs. Nyquist. Their recommendations with regard to surface preparation, measuring equipment and methods have been investigated and thoroughly substantiated.

The method, when used with all recommended precautions, has shown that precise quantitative hardness measurements of brittle substances can be made, which values can be duplicated by other laboratories. Possibly the greatest value of the method lies in the fact that it permits accurate determinations of the hardness of small crystalline particles and particularly of the various phases existing within a substance, and the value of these determinations will be greatly enhanced by being able to compare values with those reported in the literature.

Written Discussion: By Vincent E. Lysaght, Wilson Mechanical Instrument Co., Inc., New York.

A very clear picture of studies of Knoop hardness testing has been presented by the authors and they are to be congratulated on the care and thoroughness with which they have accumulated and abstracted the data.

There is one feature of this paper which should be called to the attention of the members of the Society.

A considerable portion of the materials which have been investigated is hard nonmetallic substances of more interest to the mineralogist than to the metallurgist. The experience of the majority of users of the Tukon tester and Knoop indenter does not bear out the fact that on metals anything at all like 15 to 20 man-hours are necessary for each Knoop determination where the utmost of precision is required, or anything even approaching 4 to 8 hours where such precision is not necessary. Certainly such slow work has nothing to do with metal testing. The Hamilton Watch Co.[10] has reported over 4600 tests on small precision parts during two months.

Many of the conditions summarized in the conclusion relate to only the earliest tentative model and have been automatically taken care of in 95% of Tukons in use and, of course, in all of the current design of the Tukon testers. Other conditions need only be checked when the machine is set up. As pointed out by the authors, no Tukon testers without solenoid and torque arm have been manufactured since April 1943. Such matters as balancing of beam, changing of indenters, standardizing of the longitudinal edge of the diamond with respect to its crystallographic orientation, etc., have changed by design, standardization and evolution since the early equipment was built.

Even with the care and time necessary to control the variables as specified by the authors, it is gratifying to know that for hard, and oftentimes brittle, substances the determination of the Knoop hardness is possible with such precision. Before this invention, no suitable equipment was available.

Written Discussion: By R. Smoluchowski, Metals Research Laboratory, Carnegie Institute of Technology, Pittsburgh.

The authors should be congratulated on presenting such a perfect example of a careful analysis of various factors affecting the measurement of a physical magnitude. Indeed, there is little which remains to be added. I would like to mention my own experience with measurement of indentations at high magnification. Monochromatic illumination turned out to have a beneficial influence on the accuracy and the reproducibility of measurements. The proper color was different for different observers and varied for different materials. Also, the angle of illumination and the resulting contrast between light reflected from the surface of the sample and the slopes of the indentation proved to be of importance in the quality of measurement. Without making any definite recommendations, I want to draw attention to these two factors hoping they may be useful in high precision work.

Written Discussion: By James R. Benford, Scientific Bureau, Bausch & Lomb Optical Co., Rochester, N. Y.

The work of the Norton Co. investigators is a significant step forward toward more correct measuring technique in Knoop hardness testing. The choice of the optical equipment best suited for the job is, of course, of interest to Bausch & Lomb and we fully agree on the necessity of standardizing conditions of measurement and of recording all pertinent data in the various laboratories.

In line with the authors' recommendation of completely specifying conditions of measurement we believe the mode of illumination should be always specified.

[10] Vincent E. Lysaght, "Microhardness Testing of Materials," *Materials & Methods*, October 1945.

In polarized reflected light, for example, we have obtained definitely larger measurements than in unpolarized light due, we believe, to the reversal of the diffraction pattern where the diamond appears brighter than the background. The same effect seems to be present in Fig. 9 of the authors' work where (probably by the use of oblique illumination) the two halves of the diamond are respectively brighter and darker than the background. The brighter half looks longer than the darker due, we believe, to the diffraction pattern falling within the dark half and outside the light half.

In recording Knoop data we recommend not only the recording of the objective data but also the relative aperture illuminated and the relative offset of aperture when oblique illumination is used.

Written Discussion: By Horace Winchell, professor of mineralogy, Yale University, New Haven, Conn.

The authors of this paper have unquestionably accomplished the most thorough evaluation, to date, of factors affecting Knoop hardness numbers obtained in testing hard substances. Their work stands as an example for future researchers to emulate.

An interesting development that might now be attempted would be a determination of the minimum load which will just produce fractures or cracks consistently—say, for example, at 10% of the indentations. Such a determination might have commercial value as a measure of the brittleness or friability of an abrasive, and therefore as a measure of the rate at which its grains will probably break down to finer sizes in use. Such behavior of abrasives is essential for the success of certain types of finishing operations in the processing of watch parts; lack of uniformity of such behavior is an expensive source of trouble and spoilage, and the ability to identify an abrasive that will break down at a desired rate under certain conditions of use would be valuable. Analogous applications should be possible in other industries.

A detail of great theoretical interest to crystallographers, and probably of some practical importance in metallurgical applications where preferred orientation may affect directional properties, would be an attempt to determine the effect of crystal orientation on hardness readings under the conditions set up by these authors.

The existence of the data leading to the construction of Fig. 4 leads one to suspect that additional research on the effect of diamond orientation in the indenter itself might be profitable. For example, it is possible that a better diamond orientation could be found, which would be less subject to damage or wear in use, or possibly that a better orientation would reduce the elastic yield of the indenter, thus probably reducing the dependence of Knoop number on load.

The suggestion of these additional possibilities will in no way detract from the recognition of the paper under discussion. Such possibilities hardly existed before this paper became available; they could be tested only by careful work of the type and quality demonstrated here. Congratulations for research of this kind.

Written Discussion: By J. E. Burke, assistant professor, Institute for the Study of Metals, University of Chicago, Chicago.

The authors are to be complimented for the exceedingly careful study which they have made of the factors which influence the value of the Knoop hardness

number. The necessity of specifying so many variables emphasizes the fact that this hardness test, as do all others, merely gives a means of empirically comparing several properties of the materials in question, which properties are collectively called hardness.

The difference in hardness number obtained with different diamonds, as summarized in Fig. 4, is quite interesting. The authors give data which strongly indicate that the values obtained from diamonds 20 and 901 differ because the crystallographic orientation of the diamond indenters differs. This is not surprising because diamond is not elastically isotropic; thus the same stress in different crystallographic directions would produce different deformations of the diamond. The fact that other diamonds of the same orientation as 901 give the same hardness values adds weight to this explanation. If the orientations of diamonds 20 and 5-1 prove to be identical, not only will the crystallographic origin of the difference be verified, but it will also be demonstrated that the lack of precision due to other variables can be made small compared to the effect produced by a change in orientation of the diamond. It is to be hoped that the authors will be able to give the orientation of diamond 5-1 in their closure.

Fig. 8 shows the effect of asymmetry of indentation on the measured hardness number. The length of an asymmetrical indentation is much greater than that of a symmetrical indentation, while the precision of measurement of the absolute length is apparently somewhat better. Do the authors consider it feasible to gain precision in the measured hardness number by purposely producing asymmetrical indentations, and calibrating the instrument in terms of such indentations?

Authors' Reply

We are particularly indebted to Messrs. Wicker and Redmond for their data because of the comparisons afforded between Knoop values determined on hard substances independently in two different laboratories. The agreement between us was gratifying since closer concordance could not have been expected had we made duplicate determinations in our own laboratories.

Mr. Lysaght has quite correctly pointed out that precise determinations of the Knoop number of metals may be made in a small fraction of the time which we required for practically all of our determinations. The principal reasons are: First, it is much more difficult and time consuming to prepare, mount, and properly polish hard abrasive substances than to polish most metals; secondly, because of the factors of crystal orientation and tendency for the grains to fracture, it was necessary in the case of most substances to make a total of from 90 to 175 indentations in 30 to 35 grains of random orientation and to relocate these indentations for measurement. With most metals 10 to 25 indentations would probably be sufficient; and thirdly, to obtain checks, the authors measured indentations independently, a precaution which may have been unnecessary.

It is, of course, true that some of the factors which we have discussed are now of more historical than active interest. They have been included, without undue emphasis, to complete the study, and with the feeling that they were worth mentioning inasmuch as some Tukon instruments not equipped with the improved features are still being used.

In answer to Dr. Smoluchowski, we have never experimented with the use of monochromatic illumination of various wave-lengths for the measurement of Knoop indentations. We are certain, however, that the use of practically monochromatic light, afforded by the filters supplied for use with the Bausch & Lomb Research Metallograph, is much more satisfactory than white light on the same instrument.

Both Dr. Smoluchowski and Mr. Benford have mentioned the mode of illumination. As stated in our paper, we favor the use of slightly oblique bright-field illumination, which almost always increases the measured length of an indentation slightly. We believe that this is at least partly due to the fact that oblique illumination increases the contrast between the end of the indentation and the polished surface, the effect being greater with substances of lower reflectivity. Because of the greater contrast, the effective resolution of the end of the indentations appears to be greater.

Through the courtesy of Mr. Benford, we were able to study the effect on Knoop number of anti-reflection films on metallographic objectives by means of paired objectives loaned us for the purpose. We found that when centered bright-field illumination was employed to measure indentations in silicon carbide and boron carbide, the use of coated objectives resulted in length determinations slightly greater than when similar unfilmed objectives were used. However, no difference could be noticed between the paired objectives when slightly oblique illumination was employed. Since we advocate the latter mode of illumination, we feel that coated lenses offer no particular advantages in Knoop hardness determinations.

In reply to Dr. Winchell, we have used the Knoop indenter to compare the friability of different varieties of "alundum", which is an aluminum oxide abrasive. Instead of determining the minimum load which would just produce a fracture, we employed a constant load of 200 grams and classified the resulting indentation into one of the classes of cracking mentioned in our paper. Although there was always the uncertainty as to just what class should be assigned to a given indentation, and although it was found necessary to indent upward of a hundred randomly oriented grains because of the great variation of cracking with crystallographic orientation, we did obtain differences which explained the behavior of the abrasives in certain grinding applications.

In answer to Dr. Burke, unfortunately it has not been possible to determine the orientation of diamond 5-1. The Wilson Mechanical Instrument Company has informed us[11] that they were not able to relocate this particular indenter, and believe that the diamond was demounted and used for another purpose inasmuch as it did not meet the specifications for Knoop indenters because of the presence of nicks in the longitudinal edges (but further from the tip of the indenter than the area involved in the 100-gram indentations in silicon carbide).

We hope that, when time permits, either the Wilson Company or the National Bureau of Standards will prepare Knoop indenters of different crystallographic orientations and determine whether such differences result in indentations of the same or different lengths in hard substances such as silicon carbide or boron carbide. It would be expected that such differences would be maximum when one diamond was mounted with one of its crystallographic axes of fourfold

[11]Personal communication from Mr. V. E. Lysaght, December 23, 1946.

symmetry parallel to the axis of the holder, and the other diamond mounted with a diagonal axis of threefold symmetry in this position.

We believe that the smaller difference between minimum and maximum values for the Knoop hardness of Kennametal K12 resulting from indentations made with an asymmetry of 50% as given in Fig. 8 is entirely fortuitous. There might be some increase in the precision of measurement of a very asymmetrical indentation because of its greater over-all length, but there would be certain disadvantages in adopting the practice of purposely making asymmetrical indentations, among which is the fact that, as indicated by Fig. 8, the Knoop number is affected by slight changes in degree of asymmetry to a greater extent with distinctly asymmetrical than with symmetrical indentations. Considering all the factors, the authors do not believe it advisable to standardize the instrument on the basis of asymmetrical indentations.

A number of readers have privately suggested that data on primary (unbonded) tungsten carbide (WC) might appropriately appear in Table II since this compound is the main constituent of most cemented carbides. Accordingly, a sample of WC was obtained from Kennametal, Inc., and its Knoop hardness was determined under the same conditions as used with the other substances appearing in this table. The chemical analysis of the sample of tungsten carbide was not determined, but an X-ray powder photograph made with filtered copper radiation showed a pattern very similar to that given for WC in the ASTM file of X-ray diffraction data, Card II-2299, but with slightly different cell dimensions. No other substance was indicated.

DETERMINATION OF KNOOP HARDNESS NUMBERS INDEPENDENT OF LOAD

By L. P. Tarasov and N. W. Thibault

Abstract

Previous investigators have shown that the lower the indenting load, the greater is the measured Knoop hardness number. This has been attributed to elastic recovery of the long dimension of the indentation upon removal of the load, the recovery being a larger percentage of the indentation length when the load is low than when it is high.

This paper indicates how a very precise Knoop hardness number independent of load can be computed for a given specimen from the lengths of indentations made at several different loads. A constant length correction is found by trial and error which, when added to the measured indentation lengths, results in essentially the same hardness number for each of the loads. This hardness number, which is shown to be the unrecovered hardness number, is given for molded boron carbide, a cemented carbide, a hardened tool steel, and for single crystals of silicon carbide, aluminum oxide, topaz and quartz.

The length correction is needed to compensate for the elastic recovery of the long dimension of the indentation and for a visibility error. The latter results from the inability of the observer to locate the actual ends of the indentation and depends on the optical equipment used, on the visual acuity of the observer, and on the indentation contrast. The elastic recovery and the visibility error may each amount to several microns. Although the visibility error, and hence the length correction, can be expected to vary from one laboratory to another, the unrecovered hardness number of a given specimen should be the same regardless of where the measurements are made.

Introduction

UNTIL recently, it was generally taken for granted by the users of the Tukon Tester that the length of the Knoop indentation does not decrease appreciably when the load is removed; elastic re-

A paper presented before the Twenty-eighth Annual Convention of the Society held in Atlantic City, November 18 to 22, 1946. The authors, L. P. Tarasov and N. W. Thibault, are associated with the Research Laboratories, Norton Company, Worcester, Mass. Manuscript received July 17, 1946.

covery was believed to take place, for all practical purposes, only in the short dimension, and the measurements were supposed to give the unrecovered hardness directly. These were the original assumptions made by Knoop, Peters and Emerson (1)[1] in developing their hardness test and it is on this basis that the standard table furnished with the Tukon Tester for converting indentation lengths to Knoop hardness numbers has been calculated.

However, it was conclusively demonstrated by Tate (2) that considerable elastic recovery, of the order of 5 microns, may occur in the long dimension. He was able to measure the indentation length in a thin piece of glass while it was under load by focussing the microscope on the indentation through the glass. The indentation became shorter when the load was removed.

Brodie and Smoluchowski (3) described briefly another method for determining the recovery in the long dimension. The diamond indenter was coated with graphite and an indentation was made in the usual manner. Then the projected length of the cleaned-off portion of the diamond was compared with the length of the indentation in the specimen itself, the difference being the amount of elastic recovery. Preliminary results indicated that the elastic recovery of tungsten and copper amounted to several microns.

Turning now to the Knoop hardness numbers as calculated from the recovered indentations, it has been repeatedly observed (2), (3), (4) that as the load is decreased, the hardness number increases, at first gradually and then more rapidly; and that the harder the specimen, the more pronounced is the increase at low loads. By adding the average observed recovery value of 5 microns for glass to the recovered indentations in two steels and in glass, Tate (2) obtained hardness numbers that were roughly the same for all loads, the variation from the average values being not greater than 3%. Applying this same correction to the indentations in several Rockwell steel test blocks, Rustay (3) was able to attain a similar result.

It would obviously be very desirable to be able to determine in a reasonably simple manner a Knoop hardness number which would be independent of the indenting load and which would be at least as precise as the load-dependent hardness numbers determined in the usual manner. Such a number would be useful even if obtained by a strictly empirical treatment of the observed data for a given specimen, but this number would be more satisfactory from a theoretical

[1]The figures appearing in parentheses pertain to the references appended to this paper.

standpoint if it could be shown to be the unrecovered hardness number, which is a measure of the load actually supported per unit area of the indented material. The primary purpose of this paper is to show that it is possible to obtain satisfactory hardness numbers which do not vary with the load and that these numbers do represent the unrecovered hardness.

The significance of the unrecovered hardness number can be illustrated by considering what would happen if a piece of soft rubber, like that in a rubber band, were tested with the Knoop indenter. The area in contact with the indenter would be quite large so that the unrecovered hardness would be low; however, the indentation would disappear as soon as the load was removed and, according to the orthodox method of calculating hardness, soft rubber would be infinitely hard. Thus in this extreme case, the unrecovered hardness has a definite physical significance, even though it would be difficult to make such a measurement, whereas the recovered hardness is meaningless.

Theoretical Considerations

The Knoop hardness test is based upon the premise that the projected unrecovered indentation area, which is the area supporting the load, is proportional to it. This hypothesis, discussed briefly by O'Neill (5), should hold for any pyramidal indentation, the reason being that for a given indenter all indentations are geometrically similar, so that the reaction stresses in equilibrium with the load are presumed to remain the same per unit area regardless of the load. The experimental verification of this hypothesis is to be found in the essential constancy of Vickers hardness numbers for different loads, the errors arising from recovery and other causes being small enough to be neglected. Whether it also holds for the much lower loads and the different shape of the indenter used in Knoop hardness studies remains to be established.

Operationally, we are concerned not with the projected area of a Knoop indentation but with its length. Since the width of an unrecovered indentation is a constant fraction of its length, it follows that the square of the unrecovered length should be proportional to the load provided that the basic premise is justified for Knoop hardness measurements.

As has been pointed out, Knoop hardness numbers as ordinarily

determined are not independent of the load, the reason being that the ratio of the load to the square of the measured indentation length is not constant. This deviation from constancy is caused not only by the elastic recovery of the indentation, but also by the inability of the observer to locate the actual ends of a recovered indentation. The latter is a systematic visibility error and depends mostly on the optics of the microscope used for measuring the indentations but it is also affected by the visual acuity of the observer and by the contrast of the indentation relative to its background.

In considering these factors, it is important to keep in mind that the shape of the end of the indentation is independent of the length of the indentation. In the case of recovery, it is reasonable to assume that the same stress distribution is reached near the end of the unrecovered indentation, no matter what the load. Since the amount of recovery taking place when the load is removed is related to the stress distribution by Young's modulus, the recovery should also be independent of the load. The same must be true of the visibility error, for it obviously depends only on the shape of the end.

We see, therefore, that for a given specimen it is logical to apply a constant correction Δl to the measured indentation length l_m in order to obtain the unrecovered length l_u. If a constant correction can be found that will lead to an essentially constant hardness number for a given specimen, then this must be the true unrecovered hardness number, K_u. On the other hand, if it is impossible to determine a hardness number independent of the load, then either the unrecovered hardness number or the elastic recovery of the long dimension of the indentation must be a function of the load.

The measured hardness number corresponding to the measured indentation length l_m will be designated K_m. Were it not for the presence of the visibility error, l_m would be the true recovered length. Actually, it is only the apparent recovered length. K_m is the measured Knoop hardness number as ordinarily determined and it differs from the true recovered hardness number by a factor depending on the magnitude of the visibility error relative to the measured indentation length.

The visibility correction for a given material will be a constant independent of load only if the same optical equipment is used to measure all the indentations. Thus, if in measuring a series of indentations made at various loads, it is necessary to change from a high-power to a low-power objective to bring the comparatively large

indentations made at high loads into the field of view of the filar micrometer, a correction should be applied for the change in resolving power of the lens system. This can be done easily by measuring an indentation of intermediate length with both objectives. A similar sort of correction for change in visual acuity would be in order if the indentations at different loads were not all measured by the same observer. The potential magnitude of the corrections for resolving power of the lens system of the microscope is discussed later in connection with experimental data on Knoop indentations.

Calculation of Unrecovered Hardness Numbers

The experimental data of Thibault and Nyquist (4) on the variation of Knoop hardness with load for molded boron carbide, silicon carbide, alpha aluminum oxide, a cemented carbide (Kennametal KM), topaz, a hardened tool steel, and quartz[2] served as the starting point for the procedures and results reported here. The conditions under which the indentations were made and measured are given in the above-mentioned paper.

The advantage of using these data is that two of the nonmetallics, silicon carbide and quartz, were shown to give exactly the same hardness whether the indentations were made in the original crystal face or in the same face after it had been polished mechanically. Thus there is little possibility that the hardness numbers found for the nonmetallic substances were influenced by work hardening of the surface during preparation of the specimens. If we find that the two metallic materials, cemented carbide and hardened steel, follow the same type of behavior as the nonmetallics, then we can safely conclude that work hardening of the surface caused by mechanical polishing cannot explain the variation of Knoop hardness with load that is observed with hard metals.

The measured indentation lengths for a given specimen first had to be corrected for any change in the objective used for measuring the indentations made at different loads. This was required only in the case of topaz, steel and quartz.

The necessity of doing so is illustrated in Fig. 1, in which the measured hardness number K_m of the steel is plotted as a function of the load. The broken line passes through the points calculated

[2]Of these, only boron carbide, Kennametal KM and the tool steel were randomly oriented so that the hardness would be the same in all directions. The rest were single crystals indented in particular crystallographic directions as described in (4), and the hardness data apply only for those directions.

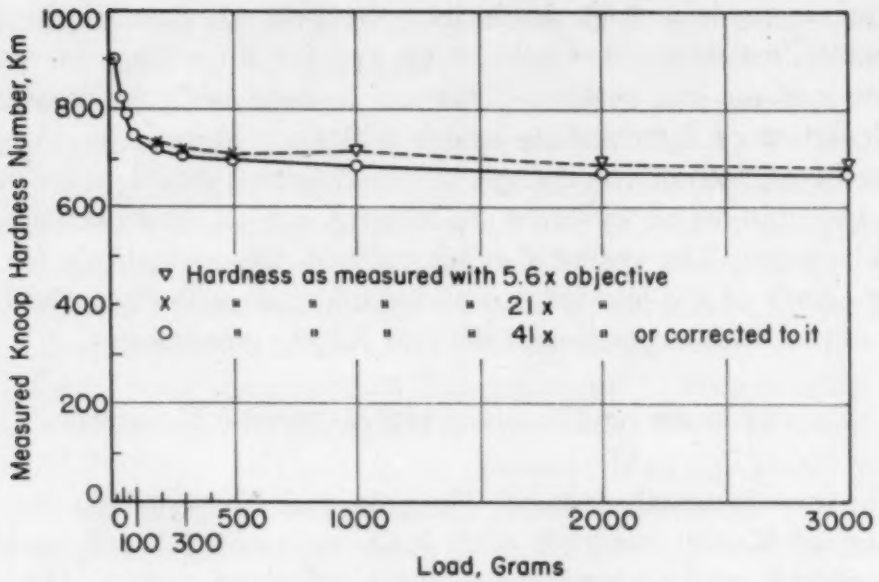


Fig. 1—Variation of Measured Knoop Hardness Number with Indenting Load for a Hardened Tool Steel, Rockwell C-60.5. The four circles at the extreme left and the crosses and triangles were calculated from the indentation lengths as measured with the various objectives. Correction of the lengths to the 41× objective used for the indentations made at the four lowest loads resulted in the points that fall along the solid curve.

directly from the observed indentation lengths, three different objectives on the Bausch and Lomb Research Metallograph having been required to cover the whole range of loads. The irregularities in this curve are evident, especially the slight rise between 500 and 1000 grams. Corrections were then established between objectives by measuring indentations of suitable length with two objectives. When the indentation lengths for all but the lowest loads were suitably corrected to those that would have been observed with the 41× objective used for the smallest indentations, the resulting hardness numbers were found to fall on a smooth curve, which is drawn solid. Indentation lengths corrected in this manner, together with the corresponding loads, comprised the data from which it was found possible to obtain hardness numbers that did not vary appreciably with the load.

The best value of the correction Δl, which was found by trial and error to the nearest tenth of a micron, was simply the one that resulted in the most nearly constant set of hardness numbers for the various loads. This was the set of numbers with the smallest value of the standard deviation σ, which is defined as the square root of the average of the squares of the deviations of the individual values from their average (6). The average of such a set of hardness

numbers is the unrecovered Knoop hardness number that we are seeking.

The advantage of using the standard deviation as the criterion for the best value of Δl is that it gave a more sharply defined answer as to the best value than did either the average deviation or the range (6). It was felt that this advantage outweighed the disadvantage of a slightly greater amount of calculation. For a brief description of methods that can be used for quickly establishing the narrow range in which the best value of Δl is to be found, the reader is referred to the Appendix.

In applying this procedure to the experimental results, it was discovered that by omitting the data for loads less than 100 grams, a best value of Δl could be determined that would lead to a much narrower range of unrecovered hardness values than when all the data were used in obtaining the best value of Δl. In other words, discarding the data for loads less than 100 grams resulted in each instance in considerably smaller values of the standard deviation for K_u. The justification for treating the experimental data in this fashion is that the excluded indentations were apparently influenced by an unknown factor not operating noticeably upon the remainder of the indentations. If such a factor did not exist, then discarding certain indentations would not be expected to improve appreciably and in every instance the consistency of the hardness numbers calculated from the remaining indentations.

The essential constancy of K_u with load when calculated in this manner is shown graphically in Fig. 2 for the seven specimens for which data were available. The corresponding curves for K_m are shown in Fig. 11 of the paper by Thibault and Nyquist. The K_u values for loads of less than 100 grams were obtained by applying the same values of Δl to the original data as were used for the higher loads. It is seen that the points for the lowest loads, connected by broken lines, are erratic and show no recognizable trend as the hardness of the specimen is progressively changed. The points for 100 grams and higher lie quite accurately on horizontal lines, the biggest deviations occurring for topaz, which could not be indented without considerable cracking. The indentations in it were also difficult to measure accurately. The value of K_u for hardened tool steel is based upon the data obtained for loads ranging from 100 to 3000 grams, but for convenience the curve is drawn only as far as 500 grams; were it extended to 3000 grams, the points would

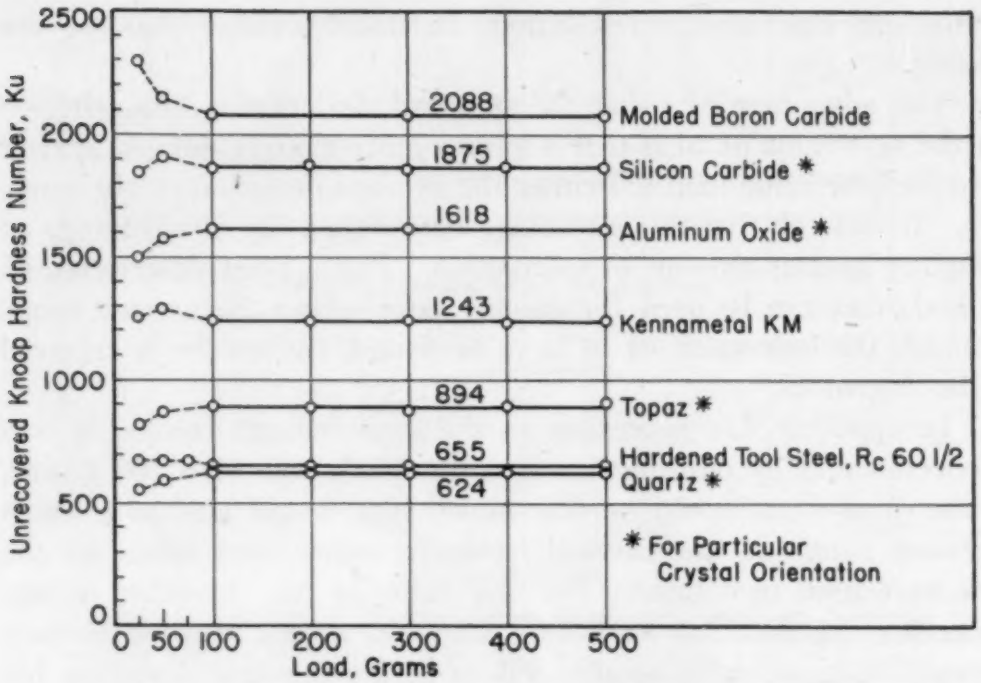


Fig. 2—Unrecovered Knoop Hardness Number as a Function of the Indenting Load.

continue to fall on the horizontal line just as well as they do in the region shown.

Additional numerical data, having to do with the internal accuracy of the results and with the relative magnitudes of Δl and l_m, are presented in Table I. The hardness numbers K_u have been corrected for the slight difference between the actual and nominal indenter angles, the correction amounting to +0.3%. The standard deviation σ is of the order of a few hardness units, hence the justification for expressing K_u to the nearest unit. The next column gives the coeffi-

Table I
Unrecovered Knoop Hardness, K_u

Specimen	K_u Kg/mm²	n	σ Kg/mm²	v %	l_{100} —Microns—	Δl
Molded Boron Carbide	2088	3	1.4	0.07	22.84	3.3
Silicon Carbide	1875	5	6.5	0.35	23.51	4.1
Aluminum Oxide	1618	3	1.3	0.08	25.70	4.0
Kennametal KM	1243	5	4.3	0.35	31.4	2.5
Topaz	894	5	12.3	1.38	34.6	5.2
Hardened Tool Steel, R_c 60.5	655	7	2.3	0.35	43.66	3.1
Quartz	624	5	3.7	0.59	41.3	6.5

K_u = unrecovered Knoop hardness number.
n = number of different loads used in establishing K_u.
σ = standard deviation of K_u.
v = coefficient of variation, equal to $100\sigma/K_u$.
l_{100} = measured indentation length for 100-gram load.
Δl = linear correction giving best agreement in K_u at different loads.

cient of variation, which is simply the standard deviation expressed in terms of K_u on a percentage basis. The only material for which this quantity exceeds 1% is topaz. Three of the materials, silicon carbide, Kennametal KM and hardened steel, fortuitously have exactly the same coefficient of variation, 0.35%.

The importance of such a small coefficient of variation is that it was based in each case on indentations made at either five or seven different loads. It is most unlikely that such concordant results could have been obtained if there were no basis for the Δl correction. The even smaller coefficients of variation for boron carbide and aluminum oxide are further evidence in the same direction. In these two cases, however, the extreme smallness of this coefficient may be of an accidental character since only three experimental hardness values had to be adjusted to constancy by means of Δl. It is possible that had data been available for more loads, the coefficients of variation would have been more nearly like those for silicon carbide and the others. It should be pointed out that the standard deviations or coefficients of variation are measures of the internal accuracy of the data and that there may be a small systematic error in the derived values of K_u caused by an error in the calibration of the filar micrometer, the accuracy of which is discussed by Thibault and Nyquist (4).

Two conclusions can be fairly drawn from these data. One, already mentioned, is that for a given specimen it is proper to apply a constant correction Δl to the measured indentation lengths for different loads, and this means that the elastic recovery in the long dimension must have a constant length for a given material. The other conclusion is that the basic premise of Knoop hardness testing is established within a very small experimental error, this premise being that the projected area under load is proportional to the indenting load. These conclusions are subject to the qualification that they are not yet established for loads of less than 100 grams, as evidenced by the points at the extreme left in the curves of Fig. 2. The possible reasons for this difference in behavior at very low loads will be discussed later.

Returning to Table I, we see that Δl may be an appreciable fraction of the measured indentation length at low loads, such as 100 grams. The values of Δl consist of an elastic recovery, whose magnitude depends on the material, and of a visibility correction, which is constant for a given optical system and a given observer.

The optical system used for measuring indentations in the first four materials was different from that used with the other three (4) and the Δl values for the two groups of materials are thus not strictly comparable in so far as elastic recovery is concerned. This point is discussed in detail in a subsequent section.

About all that can be said at present in regard to elastic recovery is that it depends on both Young's modulus and the yield strength. If two materials have the same yield strength, then the one with the lower modulus would be expected to have the higher recovery, while if two materials have the same modulus, the one with the higher yield strength would be expected to have the higher recovery.

An appreciable difference in Δl for two materials of nearly the same hardness makes it possible for their curves of measured hardness versus load to cross. Thus the sample of quartz listed in Table I had a higher measured hardness than did the steel for loads of 100 or 500 grams and yet the steel was found to have a higher K_u value. Calculation showed that for a load of 900 grams the steel and quartz would both have had a measured hardness number of 683, while for even higher loads the steel would have been found to be the harder. This assumes that the quartz could have been measured at those loads without cracking.

The question will naturally arise as to how many different indenting loads should be used in establishing K_u. When indentations have been made at two loads, a value of Δl can always be found that will make the two calculated unrecovered hardness numbers exactly equal; however, there can be no check on the internal accuracy of the data, which may be in considerable error. Three is the minimum number of loads from which some idea of the internal accuracy can be obtained but even in this case it may be possible to hide a considerable portion of the error by a suitable choice of Δl. It is only when measurements at four or preferably five loads are available that it is possible to get a true picture of the accidental errors that are present.

In many cases, it would be desirable to be able to approximate the unrecovered hardness number from the knowledge of a measured hardness number obtained for a single load. However, a study of the available data for the seven materials discussed in this paper showed that a constant relationship did not exist between K_m for some given load and K_u. The K_m values were first corrected to a constant observational condition, which was the one prevailing when

the 41× objective was used on the Bausch and Lomb Research Metallograph. The ratio K_m/K_u for a 100-gram load was found to vary from 1.14 for hardened tool steel to 1.54 for silicon carbide. Although the harder materials in general had a higher ratio, the relationship between K_m/K_u and hardness was very irregular and unpredictable.

Other Considerations Involved in Knoop Hardness Measurements

Magnitude of Visibility Error—We have seen in Fig. 1 how the measured Knoop hardness number is affected by the optical conditions under which the measurements are made. If the other conditions remain the same, a decrease in numerical aperture as one changes from a high to a low magnification objective results in a shorter observed length of indentation. To simplify the discussion of the visibility error, we shall first assume that this error, Δl_v, is zero for the objective with the highest numerical aperture, this being the 80× oil immersion apochromatic objective.

Careful observations on suitably chosen indentations made in the hardened steel or in silicon carbide showed that the values of Δl_v given in the third column of Table II had to be added to the observed values to bring all the data to a common basis, this being the length that would have been observed with the 80× objective. All the corrections were obtained for steel except for the 62× objective, which was for silicon carbide only. The correction for the 41× objective was for both materials and was exactly the same, the reason

Table II
Visibility Corrections for Steel Specimens, Using Various Objectives in the Bausch and Lomb Research Metallograph

Diameters	Numerical Aperture	Correction Based on 80× Objective Microns	Actual Correction Microns
80	1.40	0.00	1.2
62	0.95	0.53	1.7
41	0.65	1.16	2.4
21	0.40	1.7	2.9
13.5	0.25	2.5	3.7
5.6	0.12	4.0	5.2

being that contrast shown by the indentations is essentially the same for these two materials. These data apply only to the Bausch and Lomb Research Metallograph equipped with unfilmed objectives but

a similar table could be constructed for a different optical system, such as a microscope mounted on the cowl of the Tukon Tester. The corrections may be somewhat different for other observers. The recently introduced filmed objectives may also require a different set of corrections since they may give better contrast and hence an increase in the visible indentation length.

When the relative corrections for visibility are plotted against

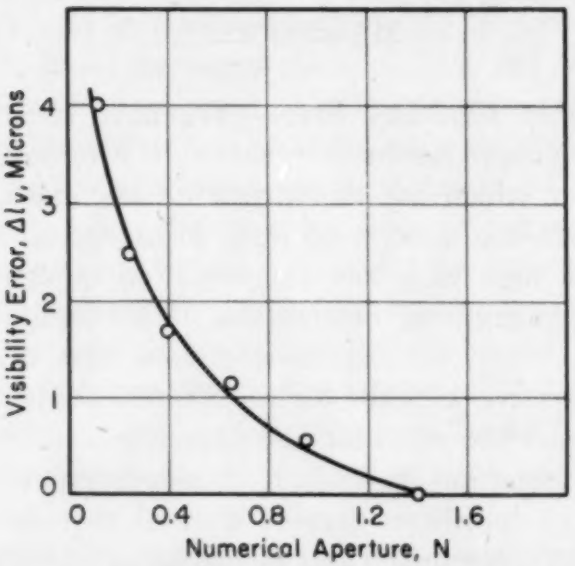


Fig. 3—Relative Visibility Error as Function of Numerical Aperture. Error is assumed to be zero for the 1.40 N. A. objective. The curve is the best hyperbola that can be drawn through the experimental points.

the numerical aperture N, as in Fig. 3, they are seen to lie very close to a rectangular hyperbola, the greatest deviation being only 0.2 micron. The equation of this hyperbola can be shown to be $(\Delta l_v + 1.2)(N + 0.3) = 2.09$. By means of this purely empirical equation it is possible to extrapolate roughly to a hypothetical objective having infinite resolving power and zero visibility error. Graphically, this is done by plotting Δl_v against $1/(N + 0.3)$, which results in an essentially straight line. The value of Δl_v for which $1/(N + 0.3)$ is zero is the correction that should be applied to the 80× objective to take care of the visibility error in the length introduced by its use. This value amounts to 1.2 microns. Of course, the accuracy of this figure depends on the validity of the extrapolation, but the extrapolated correction for the 80× objective certainly appears to be reasonable in view of the large corrections found for the other objectives relative to the 80× objective.

On the same basis, we find that the actual visibility correction for the 41× objective used in measuring hardened steel amounts to about 2.4 microns. Referring to the Δl column in Table I, we see that for steel, with Δl equal to 3.1 microns, most of the error is due to lack of visibility and only 0.7 micron can be attributed to elastic recovery.

The situation is different for silicon carbide. Its Δl value in Table I was obtained from measurements with a 54× oil immersion fluorite objective in a Bausch and Lomb microscope mounted on the Tukon Tester. Thibault and Nyquist (4) have shown that the indentation length measured under these conditions was 0.12 micron *longer* than when it was measured with the 80× objective on the Research Metallograph. This means that the actual visibility correction for the 54× objective was 0.12 micron less than that for the 80× objective, or only 1.1 microns. Subtracting this from the observed Δl value of 4.1 microns, we find that the elastic recovery of silicon carbide was 3.0 microns, as compared to the visibility error of 1.1 microns; both values are, of course, approximate. Here most of the contribution to Δl was made by the elastic recovery, while in the case of the hardened steel it resulted mostly from the visibility error.

Since the indentation contrast in boron carbide and in cemented carbide is about the same as for silicon carbide, the visibility error for the 54× objective used in measuring these substances should also be about 1.1 microns. Subtracting this from the Δl values in Table I, we find that the elastic recovery of boron carbide was 2.2 microns while that of Kennametal KM was 1.4 microns.

To recapitulate, the elastic recoveries were approximately as follows: 3.0 microns for silicon carbide, 2.2 for boron carbide, 1.4 for Kennametal KM, and 0.7 for hardened steel. In these cases, at least, the elastic recoveries of the metals are lower than those of the nonmetallic materials.

The elastic recoveries of aluminum oxide, topaz and quartz, which have poor contrast characteristics so that the ends of the indentations are even more difficult to see, cannot be calculated for lack of data similar to that of Table II for materials of moderately good contrast characteristics. However, the visibility corrections are undoubtedly higher than reported in this table.

It is because of the variations in the elastic recovery for different materials and in the visibility conditions that a generally useful

relationship cannot be established between the measured hardness number at some load and the unrecovered hardness number.

Even though the visibility error is bound to differ with the experimenter and his equipment, the unrecovered hardness number K_u is not affected thereby. If one observer consistently finds a given set of indentations to be one micron shorter than does an observer in a different laboratory, resulting from differences in optical equipment and visual acuity, the Δl value that he determines will be one micron greater but the K_u value will be identical in the two cases. This assumes, of course, that both filar micrometers have been calibrated correctly. Thus the unrecovered hardness as calculated from the same set of indentations in a given specimen should be the same no matter in what laboratory it has been determined although the individual measured hardness numbers may differ from one investigator to another.

Recovery of Indenter—Since all the substances investigated so far have shown some elastic recovery, it is reasonable to expect that the same will be true of diamond when it is indented, and also of the indenting diamond. The elastic behavior of the indenter in the long dimension cannot affect the indentation length because the indenter would stretch along the indentation being formed as the load is applied. Thus any measurement of the length of a graphite-coated indenter that is cleaned off by contact with the specimen would be too short by the amount of the elastic recovery of the indenter. This recovery would not necessarily be the same as the recovery taking place in an indented diamond since the geometry of the contiguous surface, which may affect the recovery, is different in the two cases.

Another effect worth considering briefly is the elastic flattening of the indenter under load, which results in a slightly shallower indentation under load than would be expected from the geometry of the unloaded indenter. This flattening would be of consequence only if the load sustained per unit projected area was affected by the indenter angles. It is not known whether such an effect is measurable for the slight flattening of the indenter that must take place in the Knoop hardness testing of very hard substances.

Significance of Erratic Low-Load Values of K_u—According to Fig. 2, loads of less than 100 grams result in erratic hardness numbers after the same Δl correction has been applied that makes the hardness numbers for all higher loads substantially constant. The solenoid attachment on the Tukon Tester intended to overcome in-

ertia effects of the indenter at low loads and the torque-arm attached to the elevating screw to eliminate side-play have unquestionably taken care of most of the error that formerly existed at the low loads, but there may possibly be a residue of uncorrected error that shows up only when unrecovered hardness numbers are calculated. To test this possibility it would be necessary to make similar investigations on a manually operated indenting instrument, such as the National Bureau of Standards possesses.

These erratic low-load values can hardly be attributed to surface-tension effects. Even though the depth of the indentation in boron carbide under a 25-gram load is only about 0.3 micron, this corresponds to roughly 1000 interatomic spacings and surface-tension effects cannot be expected to extend to more than a very small fraction of such a depth.

It should be stressed that even though indentations made at loads below 100 grams should not be used in the calculation of unrecovered hardness numbers, they are still perfectly satisfactory in the ordinary type of hardness measurement where there is no need of comparing hardness values obtained at various loads, as in hardness gradient studies.

Discussion

There are three essentially different approaches to Knoop hardness testing, each of which has its place. The one that has been most commonly used has been based on the assumption that the indenting load is irrelevant and that the choice of load depends entirely upon the size and depth of indentation considered most desirable in a given instance.

As long as a single load is used throughout an investigation, this approach has its merits. The indentation is made as large as possible for the greatest accuracy consistent with space limitations. Thus in studies of steep hardness gradients as in thin nitrided cases or near grain boundaries, it is necessary to keep the indentations quite small in order to avoid an average hardness number for an area in which the hardness changes rapidly. The use of several different loads in a single investigation, on the other hand, introduces differences in measured hardness numbers resulting from the changes in load and hence must be avoided if the hardness differences are to have any real meaning. Another misuse of this approach has been to compare

Knoop hardness numbers of certain hard substances obtained by various investigators using different loads, mostly unspecified.

The second approach is to standardize on some particular load or loads, just as was done long ago in Brinell testing. For hard, brittle materials, Thibault and Nyquist (4) have found it desirable to use a 100-gram load to minimize the effect of fracturing which may occur. For softer materials, like most metals, it may be desirable to standardize on a higher load, such as 500 or 1000 grams, although there is no reason why 100 grams should not be used. This limitation to a single load permits comparison of results obtained by various investigators but it has the disadvantage that the results are affected to some extent by the optical system used and by the visual acuity of the observer. To get the maximum benefit of this method requires that standard optical equipment be agreed upon by all users of the Tukon Tester, which is probably not practicable at present. It may be possible, however, to correct for visibility error by means of standard test blocks.

The third approach, which is the subject of this paper, is to compute the unrecovered hardness number K_u from measurements at several different loads, preferably at least five. This obviously involves considerably more work but there is the clear-cut advantage that the optical system and visual acuity are no longer factors affecting the hardness determination so that results obtained in different laboratories are directly comparable, assuming that the indentations have been properly made in each laboratory. Of course, this method should be validated for soft metals but there is no reason to believe that it is not applicable in such cases. A further advantage of this method is that it gives a truer picture of the indentation hardness than when a standard load is used in that it tells what load is actually supported per unit area and is not influenced by the elastic recovery of the material nor by visibility errors. In constructing a table of hardness numbers for various substances, this is undoubtedly the most satisfactory approach in spite of the extra work involved.

Conclusions

In determining the unrecovered hardness number of a specimen it is necessary that all the indentations made at various loads be measured under the same observational condition or that they be corrected to a standard condition. Loads of less than 100 grams

should not be used in this calculation unless some method is found of obtaining the same K_u value as is obtained within an extremely small error when higher loads are used. Except for materials that are difficult to indent without excessive fracture or difficult to measure accurately because of poor indentation contrast, the standard deviation of K_u can be expected to be less than 0.5%. The true value of K_u also depends on how accurately the filar micrometer has been calibrated.

By measuring a set of indentations with a series of objectives, an empirical curve was constructed relating the numerical aperture to the correction for visibility error, based on the assumption that one of the objectives had zero error. Extrapolation of the hyperbolic curve indicated that the indentation lengths measured with the 80× objective were actually about 1.2 microns longer than measured. The amount of correction depended on the optical system and on the contrast of the indentation relative to the surrounding material. From an approximate knowledge of the actual visibility error for the materials in which the indentations showed satisfactory contrast, it was possible to show that the elastic recovery was greater for boron carbide and silicon carbide than for the two metals investigated.

Appendix

In determining the internal consistency of a set of measured indentation lengths obtained at different loads, it is advantageous to plot them on log-log paper. If the length l_m is the abscissa and the load L is the ordinate, the points can be expected to fall on a nearly straight line curving to the left at the bottom and having a slope somewhat less than 2. The deviation from an exactly straight line of slope 2 is caused by the elastic recovery and visibility errors. This slope is the theoretical slope when the square of the indentation length is proportional to the load.

When the correct value of Δl is added to the measured indentation length l_m (which should be corrected first to a standard set of observational conditions), the new points fall on a straight line of the proper slope. The erratic behavior of the points for loads of less than 100 grams was first noted when an attempt was made to adjust these points by means of Δl so as to get them on a straight line passing through all the other points with the theoretical slope. Any other erratic points would be similarly noted.

An approximately correct value of Δl can be quickly obtained graphically by the foregoing method without the necessity of any calculation. The l_m values are first plotted, then each one is increased by some arbitrary values of Δl until the originally curved line is straightened. This generally permits finding a Δl value to the nearest micron.

The next step is to calculate K_u values for two or three Δl's in the vicinity of the one just obtained, this being done for each of the loads used. When K_u is plotted against Δl for each load, we have a series of straight lines of different slopes. At too high or too low a value of Δl, the lines are comparatively far apart. The best value of Δl is the one at which the lines are closest together. Sometimes this can be found by inspection but more commonly it is necessary to calculate the sum of the squares of the deviations of K_u for several adjacent values of Δl. In this way the best value of Δl can be narrowed down to 0.1 micron. Of course, it is possible to make the least square calculations from the very start, without any of the graphical preliminaries, but this is likely to take much more time.

References

1. F. Knoop, C. G. Peters and W. B. Emerson, "A Sensitive Pyramidal-Diamond Tool for Indentation Measurements," *Journal of Research,* National Bureau of Standards, Vol. 23, 1939, p. 39-61.
2. D. R. Tate, "A Comparison of Microhardness Indentation Tests," TRANSACTIONS, American Society for Metals, Vol. 35, 1945, p. 374-389.
3. Discussion of (2) by C. B. Brodie and R. Smoluchowski; A. L. Rustay; and E. J. Hubbard.
4. N. W. Thibault and H. L. Nyquist, "The Measured Knoop Hardness Number of Hard Substances and Factors Affecting Its Determination," TRANSACTIONS, American Society for Metals, Vol. 38, 1947, p. 271.
5. H. O'Neill, "The Hardness of Metals and Its Measurement," 1934, p. 40, 53. Chapman and Hall, London.
6. "A.S.T.M. Manual on Presentation of Data," April 1945 reprinting, American Society for Testing Materials, Philadelphia.

DISCUSSION

Written Discussion: By James R. Benford, Scientific Bureau, Bausch & Lomb Optical Co., Rochester, N. Y.

I would like to ask the authors what experience they have had with measuring the diamond indentations by setting on the apparent rounded tip of the image as against setting on the imaginary projected crossing point of the

tapering sides of the indentation. The latter gives a longer apparent length than the former and is, I believe, the accepted technique for measuring.

In Table II, the authors give actual corrections to be added to the observed length to arrive at a constant corrected length. These values are somewhat smaller than one would compute on theoretical grounds particularly for the lower N.A. objectives, e.g., using the theoretical expression: Resolution = $\frac{\lambda}{2\,\text{N.A.}}$, where λ is the wave length of light (0.55 micron), and N.A. is the numerical aperture of the objective, one would compute the resolution of the 0.65 N.A. objective to be 0.427 micron. To get the theoretical length correction one multiplies this value by 7.11, the ratio of the two dimensions of the indentation, giving a computed correction value of 3.03 microns, i.e., somewhat larger than the actual 2.4 microns as determined by the authors.

This difference is less at the higher N.A.'s and greater at the lower N.A.'s but in all cases the theoretical value exceeds the measured value. We believe it is explainable if the authors used the technique of setting on the imaginary projected crossing point of the indentation sides. In other words, the objectives appear to be doing considerably better than one would compute them to be capable of doing, and we wonder whether the authors concur in the idea that this may be due to the measuring technique adopted.

In attempting to determine which objective is best to recommend for metal specimens we have recently tried five objectives ranging from 0.65 to 1.40 N.A. on indentations in hardened steel. All objectives were filmed for anti-reflection. Two observers measured the same indentation 30 times with each of the five objectives. The measurements showed the same trend as described by the authors, the measured lengths increasing with increasing N.A. However, upon adding the theoretical correction factor $\frac{(7.11\lambda)}{2\,\text{N.A.}}$ to each result it was found that three (6mm, 0.65 N.A., 4.3mm, 1.00 N.A. Fluorite, and 2.75mm, 1.25 N.A. Fluorite) of the five objectives gave corrected lengths substantially equal, while the other two (4mm, 0.95 N.A. and 3mm, 1.40 N.A. Apochromats) gave lower and unequal readings.

Thus we are right now of the opinion that any one of the first three objectives may be interchangeably employed on metals as long as one adds the proper theoretical correction factor. For nonmetals, using unfilmed objectives, this simplification cannot be used as the authors' data show. We would appreciate the authors' comments on this method of attack to the problem of standardizing on a recommended objective, for although we are sometimes called upon for advice in this field we feel like anything but experts in it.

Written Discussion: By Vincent E. Lysaght, Wilson Mechanical Instrument Co., Inc., New York.

The paper throws additional light on the original work presented by D. R. Tate[1] in connection with the increase in Knoop numbers with decreasing load. It is hoped that it will cause others to continue this study further.

The Wilson Mechanical Instrument Co. most emphatically urges all users of all hardness testing equipment—not only the Tukon Tester and Knoop

[1]Douglas R. Tate, "A Comparison of Microhardness Indentation Tests," TRANSACTIONS, American Society for Metals, Vol. 35, 1945, p. 374.

Indenter—to follow the second approach as presented under the discussion section. The first approach is likewise satisfactory but oftentimes it is necessary to use different loads for different problems.

The assumption that the indenting load, in any kind of indentation hardness test, is irrelevant is made by the user of hardness testing equipment only in a state of "wishful thinking" rather than being based on scientific fact.

The load should always be specified with the hardness number. Under certain conditions when used with caution, comparisons may be made with results obtained under different conditions, but these cases are rare and should only be used as a last resort.

To know the cause of high Knoop numbers with decreasing loads is a valuable contribution to the art of hardness testing, but it is hoped that such a theory will not lead to the wholesale use of Knoop hardness numbers without specification of load. Even if a mathematical correction is developed and granting geometric similarity, such factors as work hardening and work softening with increasing loads still enter the picture.

Written Discussion: By R. Smoluchowski, Metals Research Laboratory, Carnegie Institute of Technology, Pittsburgh.

Drs. Tarasov and Thibault's results are of great interest and importance. Naturally, the possibility of correcting for the recovery of the tested material and for the visual errors is extremely interesting and of great practical importance. For some time, I have been interested in developing a method to measure the size of indentation before the load is removed. Although the results are not yet ready for publication, I would like to describe briefly the method.

The pyramid of the diamond is covered with a thin layer of Aquadag, which is a fine suspension of graphite. While the diamond penetrates into the metal, a layer of graphite is pushed away from the tip of the diamond. The diamond is subsequently removed from the tester and examined under the microscope. That part of the diamond which was below the surface of the tested material appears clear and stands out sharply against the graphite-covered rest of the indenter.

By comparing the size of the bare part of the diamond with the size of the indentation in the metal, the recovery of the metal can be measured. The method is naturally much too complicated for a practical application; however, it seems to be of great value for checking of various theories of hardness measurement and of various corrections introduced to the observed data. We hope to be able to establish an actual experimental verification of Drs. Tarasov and Thibault's theoretical analysis. First mention of this method was made in the discussion to Tate's paper about two years ago, but the research was interrupted because of the wartime emergency.

Written Discussion: By Horace Winchell, professor of mineralogy, Yale University, New Haven, Conn.

The idea of extrapolating physical test data from those obtained under imperfect conditions to the values that would be obtained under theoretically ideal conditions is not new, but the analysis of data such as Knoop hardness numbers, which involve several initially unknown sources of error, is an especially remarkable achievement for which the authors of this paper are to

be congratulated. It is not surprising that this fundamental contribution comes to us from the laboratory that produced the data presented by Thibault and Nyquist. Only such data as theirs would be worthy of the effort necessary for extrapolating to theoretical results obtained under conditions of infinite load and perfect observation. We recognize the fundamental importance of this contribution. It will almost surely lead to improved methods for making and treating the necessary observations.

Authors' Reply

In reply to Mr. Benford, we have always measured Knoop indentations by setting on their apparent ends, as described in detail on page 291 of the paper by Thibault and Nyquist (4). Whether the ends of a properly made indentation appear slightly rounded or sharp seems to depend on the observer; when the ends are obviously rounded, this shows that the indentation is not satisfactory. Projecting the sides of an indentation to an imaginary crossing point would perhaps give somewhat longer measured lengths, but we had no way of doing so in a reproducible manner. It is our impression that the generally accepted technique for measuring a Knoop indentation involves its apparent ends rather than the projected intersection of its sides. The uncertainty in the second of these methods would appear to be greater.

The reason for the discrepancy between our empirical visibility corrections and those calculated from straightforward optical theory can best be explained by considering the data in the third column of Table II. These values are the visibility corrections relative to that for the objective with the highest numerical aperture and since they have been determined directly by experiment, they are not subject to any error of extrapolation. The difference between the corrections for any two objectives is the relative visibility error of one with respect to the other. The corresponding difference between the visibility corrections predicted by theory should be the same within an experimental error of not more than a few tenths of a micron; otherwise, the theory in its present form is not valid for Knoop indentations.

If we perform the calculations for the 0.65 N.A. and 0.25 N.A. objectives, for instance, we find that the measured relative visibility error is only 1.3 microns as compared to a theoretical value of 4.8 microns. Similar large discrepancies are found for other pairs of objectives. Thus it is clear that the optical theory will have to be modified appreciably before it can be applied successfully to the correction of Knoop indentation lengths. Possibly certain diffraction phenomena associated with contrast, which are neglected in the present simple theory, will have to be taken into consideration.

It may be instructive to compare the equations for the actual visibility correction, i.e., the correction relative to an ideally perfect objective. The equation best fitting our experimental data is $\Delta l_v = 2.09/(N + 0.3)$, while the theoretical equation used by Mr. Benford proves to be $\Delta l_v = 1.96/N$, where N is the numerical aperture. The two equations are quite similar; the marked discrepancy between the results obtained from them is due mostly to the presence of the numerical factor (0.3) in the denominator of the experimental equation. This factor becomes relatively more important as the numeri-

cal aperture diminishes, and this is the mathematical reason for Mr. Benford's observation that the discrepancy is greater for the lower numerical apertures.

In regard to the criterion proposed by Mr. Benford for the selection of the most suitable objectives, the foregoing evidence indicates that the theoretical visibility corrections are much too large; hence the agreement found for three of the objectives, after the theoretical corrections had been applied to the measured indentation lengths, was probably fortuitous. At present, we would hesitate to say that these three objectives were inherently more suitable for Knoop hardness work than the two objectives which did not give the same corrected lengths.

In our opinion, the most suitable objective is the one giving the greatest indentation length in microns, provided the largest indentations to be measured with it fall within that portion of the field of view that is normally used for measuring purposes, and also provided the contrast is satisfactory. For example, the 0.95 N.A. objective gave such poor contrast on steel, compared with the 0.65 N.A. objective, that the latter would certainly be preferable even though the indentations measured with it were 0.7 micron shorter.

The situation with respect to visibility error is admittedly unsatisfactory. One reason is that the existence of such an error was not hitherto recognized. With its existence and importance demonstrated, it is to be hoped that a method will be devised by the optical industry to permit the determination of the actual visibility error without having to depend on an extrapolation of uncertain accuracy and having no theoretical justification. Until this is done, users of the Knoop hardness test who expect others to be able to check their hardness values very closely should specify not only the load but also the optical conditions. The alternative is to make indentations at several loads and thus obtain K_u, since this method does not require a knowledge of the visibility correction.

Mr. Lysaght has stressed the importance of always specifying the load, a matter in which we are essentially in agreement, as just mentioned. It is only when the unrecovered hardness number K_u is obtained that the load has no significance, but most users of the Tukon instrument will have no reason to use K_u in their work. This type of hardness number will be primarily useful in studies designed to increase our understanding of hardness and its measurement.

For instance, Mr. Lysaght mentions that work hardening may enter the picture. Presumably, changes in work hardening with depth of indentation are meant, since some physical change must inevitably occur near the surface of the indentation where the material has been disturbed. A work hardening effect would be contrary to the basic premise of pyramidal hardness testing, but possibly the premise is incorrect. We found no evidence of a work hardening effect in our measurements, which were restricted to hard, brittle materials, but such an effect may conceivably be present in soft, ductile metals. If the amount of work hardening varied with the load, so would K_u, and we would, in general, be unable to find a single value of Δl that would lead to a constant value of K_u for all loads.

Perhaps this situation will be observed in ductile metals when they are investigated in the same manner. In that case, it may still be possible to

obtain Δl from experiment instead of by computation, as we have done. The visibility correction might be determined on a hard material of the same reflectivity but not subject to a work hardening effect, and the recovery correction might be obtained by direct measurement of the cleaned-off area on an indenter previously coated with graphite, as suggested by Dr. Smoluchowski. Correction of the measured indentation lengths for these two experimentally determined quantities would give unrecovered hardness numbers that varied with the load in accordance with the amount of work hardening.

In closing, it is our hope that other experimenters in the field of Knoop hardness testing will try out on a variety of metals the method we have described for obtaining K_u, to determine whether or not it is applicable in all cases. The usefulness of such study would be greatly enhanced by a parallel investigation of Vickers indentations, for these are undoubtedly subject to visibility and recovery errors, just as are Knoop indentations. From data obtained in this manner, it may be possible to get a better insight into the relationship existing between these two types of hardness measurement.

HARDENABILITY OF SHALLOW HARDENING STEELS DETERMINED BY THE P-V TEST

By B. F. Shepherd

Abstract

This paper describes a new test specifically suited for the determination of the hardenability of shallow hardening steels which require cooling rates faster than 80 F per second at 1300 F for the microstructure to retain 50% martensite.

THERE are many applications in machinery manufacturing where a definite knowledge of the hardenability of shallow hardening steels is required so that the metallurgist can insure maximum performance in service. At the present time there is no universal standard, either of hardenability or of hardenability tests. A number of tests have been proposed; one of them (the so-called Jominy test) is now widely used by both producers and consumers of steels to measure the characteristics of the engineering alloy steels of fair to deep hardenability. Others are more adaptable for the shallow hardening steels, and are used by certain steel mills or individual customers, but all of the latter have objectionable features such as insufficient sensitivity, insufficient accuracy, noninterchangeability, high cost of machining specimens, limited latitude of application, expense, and these factors have prevented widespread acceptance and standardization.

For example, the present author, many years ago, devised a useful test for controlling heat treatment of plain high carbon steels used in important parts of rock drills and other battering tools. Perhaps even prior to that certain tool steel mills had put their own tests into use for controlling the quality of trade-named brands. The author's so-called P-F test (for Penetration-Fracture characteristics) was described in a brief paper printed in the Transactions, Vol. 22, December 1934, under the title "The P-F Characteristic of Steel." In this test four specimens 3 inches long cut from ¾-inch rounds

A paper presented before the Twenty-eighth Annual Convention of the Society held in Atlantic City, November 18 to 22, 1946. The author, B. F. Shepherd, is chief metallurgist, Ingersoll-Rand Co., Phillipsburg, N. J. Manuscript received June 20, 1946.

are normalized and oil-quenched, then hardened by heating in an electric furnace to 1450, 1500, 1550 and 1600 F respectively, and quenched in brine. These samples are then notched to $\frac{1}{16}$ inch and fractured by transverse impact. The F or fracture grain size is determined by comparison to fracture standards—carefully prepared tool steel rounds heat treated to a graded series of grain sizes.[1] Hardness penetration on each of the specimens is measured microscopically to the nearest 64th inch on the other half of the fractured samples after etching. Characteristics of the steel are then recorded as eight numbers, the first four representing the hardness penetration in 64ths for each of the four quenching temperatures, and the last four numbers the fracture grain size.

While this test and the Shepherd slab test[1a] have been successfully used by Ingersoll-Rand Co. and its principal steel suppliers for many years, and a great deal learned from it as to the idiosyncrasies of plain high carbon steels, they are obviously not the simplest tests in the world.

The well-known Jominy hardenability test offers a means of determining differences in hardenability between steels having critical cooling rates under 80 to 100 F per second, but is not satisfactory for the faster rates required for carbon steels. A modification, known as the L-type bar, is not satisfactory because much care is required in machining, and it has a tendency to crack when hardened. Greene and Post of Carpenter Steel Co. have prepared (and used to advantage in their own works) a tapered test piece,[2] quenched by complete immersion, but neither has this test been widely adopted.

Shortcomings of Quenched Rounds as a Test—It must be recognized that there is a considerable difference between a hardenability test and the determination of hardenability, although the two terms are used synonymously many times. A hardenability test is a method of producing reproducible cooling rates at various locations in a specimen. The determination of hardenability involves the use of this test to determine the reaction of the steel to known cooling rates when cooled from a known and controlled austenitic structure. Different steels may respond in the same manner when subjected to a hardenability test, or they may not respond in the same way that

[1]For stereoscopic photographs of the Shepherd grain size standards see METAL PROGRESS Data Sheet No. 78 (1946 edition).

[1a]B. F. Shepherd, "Inherent Hardenability Characteristics of Tool Steel," TRANSACTIONS, American Society for Steel Treating, Vol. 17, 1930, p. 90.

[2]O. V. Greene and C. B. Post, "Determination of Specific Hardenability of Shallow Hardening Steels," *SAE Journal (Transactions)*, Vol. 49, July 1941, p. 278.

another heat of closely similar chemical composition does, but a single steel will also react in a different manner dependent upon the conditions of austenitizing.

It might be supposed that the simplest way to make a hardenability test would be to adopt the most commonly used method of quenching a round bar under predetermined conditions, and then ascertain the depth of hardness penetration by fracturing, etching, or hardness measurements. Fully hardened structure at the very surface would be nearly 100% martensite; "depth of hardness" is usually measured down to a hardness or structure corresponding to 50% martensite. As is well known, this structure corresponds closely to the point of inflection of depth-hardness curves, and the change in color upon etching darkened case, lighter core.[3]

However, ample experience proves that the determination of hardenability by such a test is not as simple as it seems. The round bars must be of a size suited to the steel under investigation and this may not be known in advance. Small sized rounds may harden too deeply, and as the gradation zone between case and core widens under these conditions, accurate measurement of depth of hardness will be difficult. Larger sized rounds may give a sharp gradation zone, but the test is then too insensitive, penetration of hardness being often unaffected by considerable changes in the velocity of the quenching medium. Likewise, it is well known that a considerable change in cooling rate of the outside of a round bar may be made without substantially affecting the interior; erroneous impressions of relative hardenability may therefore result; material of unknown hardenability will require a number of sizes of round bars; this obviously increases the expense of the test unduly.

For those not familiar with the vagaries of modern steels marketed as "plain high carbon tool steel"—as far as penetration of hardness after controlled quenching is concerned—Fig. 1 is presented. This shows bars from 12 heats of carbon tool steel quenched from 1450 F in an overflow 10%-brine spray (25 gallons per minute). Sizes are ½ to 1¼-inch round. The prehardening structures in all bars were fully spheroidized, and they were held essentially the same time at hardening temperature. These heats represent approximately the shallowest and the deepest hardening steels to be expected without "alloy additions", although, from the analyses shown

[3]This is the criterion used in this paper, but any user of the test to be described can make changes in this parameter to suit individual requirements without alteration of the test procedure.

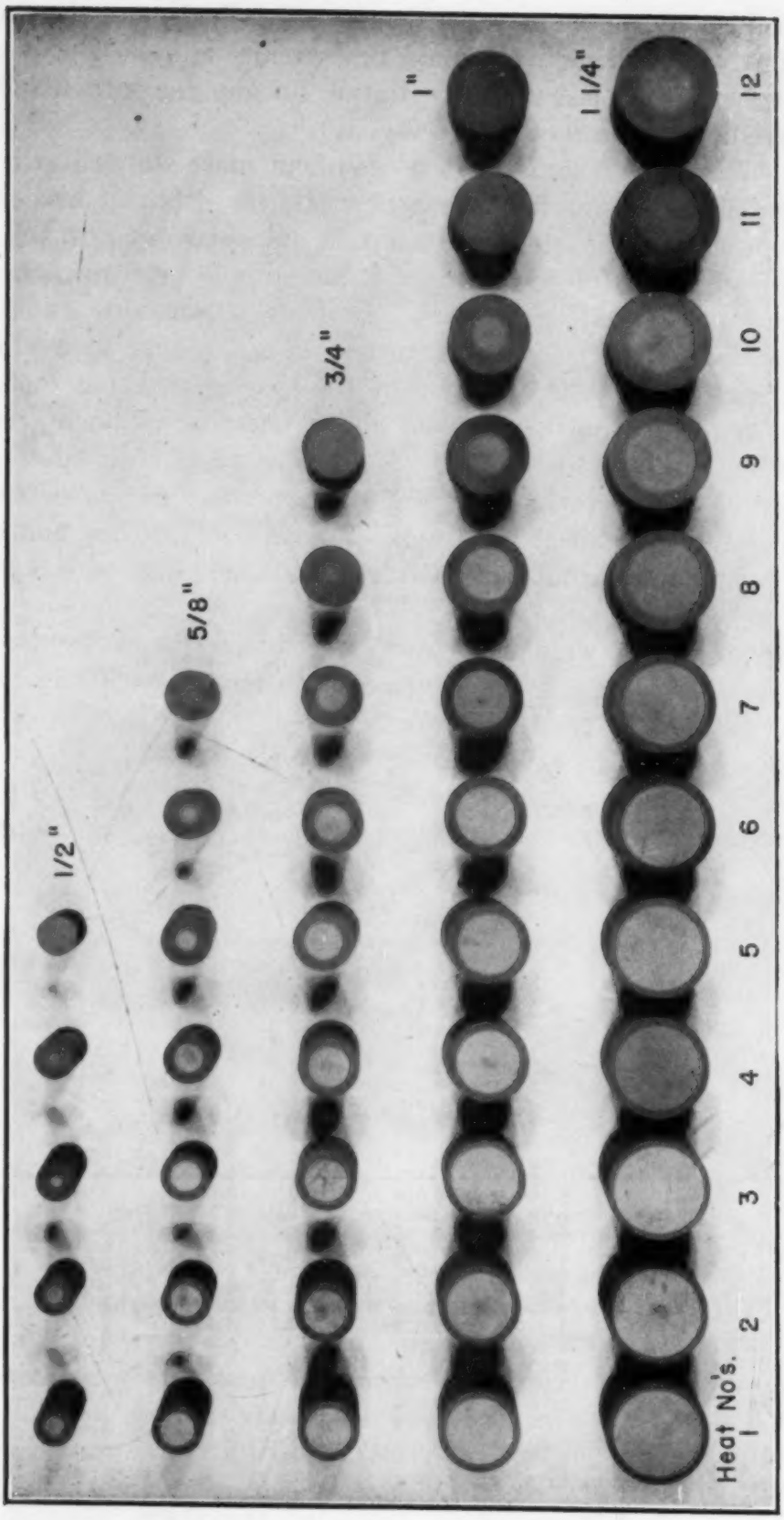


Fig. 1—Variability of Hardness Penetration in Rounds of Various Diameters from 12 Heats of Carbon Tool Steel, Ranging from Shallowest to Deepest Hardening Steels Ordinarily Encountered. All steels were fully spheroidized prior to hardening, and hardening routine was the same for all bars. Quenched bars were sectioned smooth and etched in nital. Reproduction about half size.

in Table I, many of the more hardenable steels had more than what might fairly be called "incidental" or "tramp" alloy. The above-mentioned effect of mass upon penetration for any one particular heat is also readily seen in the bars of Fig. 1.

Test Piece for New P-V Test—Without more words justifying the desirability for searching for a new test for depth of hardening on shallow hardening steels, a test not only accurate, capable of reproducing cooling rates, and cheaply and simply performed in the laboratory on a production basis. Perhaps it was our extensive experience with rock drills that turned our attention to a chisel-shaped test piece. It is a matter of common observation that the depth of hardening on the diagonal of a square bar is much greater than the depth normal to the flat face. This diagonal distance may therefore be looked upon as a magnified measure of the depth of hardening. The width of the transition zone between case and core is also greater, indicating that the cooling rate gradient is less steep at the diagonal.

These features were used as a basis for selecting the wedge-shaped samples (Fig. 2) used in the new P-V test (symbolizing Penetration-Velocity or Penetration-Vee Shape).

The specimen has a 90 ± 1-degree chisel edge and is $1\frac{1}{8} \pm \frac{1}{16}$ inch long over all. In sizes 1¼ to 1¾-inch round they are made directly from the bar. Sizes larger than 1¾-inch round must be

Table I
Chemical Composition of Some of the Steels Tested

Code	Shown in Fig. No.	Chemical Composition C	Mn	P	S	Si	Ni	Cr	Mo	V	Cu
A-67 (No. 1)	1	1.02	0.09	0.011	0.013	0.03	0.02	0.05	0.03	0.03	....
UW (No. 2)	1	1.03	0.28	0.012	0.015	0.15	0.02	0.04	Nil	....	....
TA (No. 3)	1	1.07	0.15	0.012	0.010	0.09	0.10	0.05	Nil	....	....
UP (No. 4)	1	1.07	0.34	0.015	0.015	0.22	0.03	0.10	Nil	....	....
BK (No. 5)	1	1.00	0.24	0.015	0.019	0.17	0.07	0.09	0.01	....	....
SX (No. 6)	1	1.09	0.26	0.014	0.018	0.26	0.20	0.17	Nil	....	....
No. 7	1	1.04	0.29	0.013	0.031	0.16	0.14	0.15	0.03	....	....
No. 8	1	1.00	0.31	0.017	0.027	0.28	0.07	0.13	0.03	....	....
No. 9	1	0.97	0.46	0.020	0.030	0.29	0.05	0.17	Nil	....	....
No. 10	1	0.99	0.36	0.018	0.024	0.31	0.17	0.15	0.03	....	....
No. 11	1	0.98	0.50	0.023	0.026	0.27	0.12	0.23	0.03	....	....
No. 12	1	0.94	0.45	0.020	0.021	0.36	0.16	0.21	Nil	....	....
BH		1.00	0.31	0.009	0.031	0.20	0.26	0.05	0.01	....	....
CC		1.00	0.37	0.018	0.026	0.27	0.32	0.22	0.03	....	....
WN	14	1.12	0.27	0.015	0.035	0.22	0.08	0.06	0.00	....	0.05
PV	14	1.03	0.22	0.010	0.029	0.20	0.10	0.09	0.03	....	0.04
BX	14	1.03	0.38	0.019	0.030	0.23	0.02	0.04	0.01	....	....
UZ	14	1.02	0.43	0.019	0.025	0.28	0.08	0.14	0.02	....	0.05
VY	14	0.90	0.59	0.012	0.030	0.28	0.04	0.06	0.01	....	0.05
UX	14	1.01	0.45	0.020	0.022	0.36	0.09	0.30	0.03	....	0.09
PX	14	0.98	0.55	0.027	0.029	0.37	0.14	0.15	0.01	....	0.06
TI		1.09	0.15	0.010	0.013	0.12	0.06	0.05	Nil	Nil	....
1-R-143		0.80	0.35	.....	.....	0.14	0.14	0.10	0.04	....	0.04
2-R-143		0.75	0.25	.....	.....	0.12	0.10	0.05	0.01	....	0.09

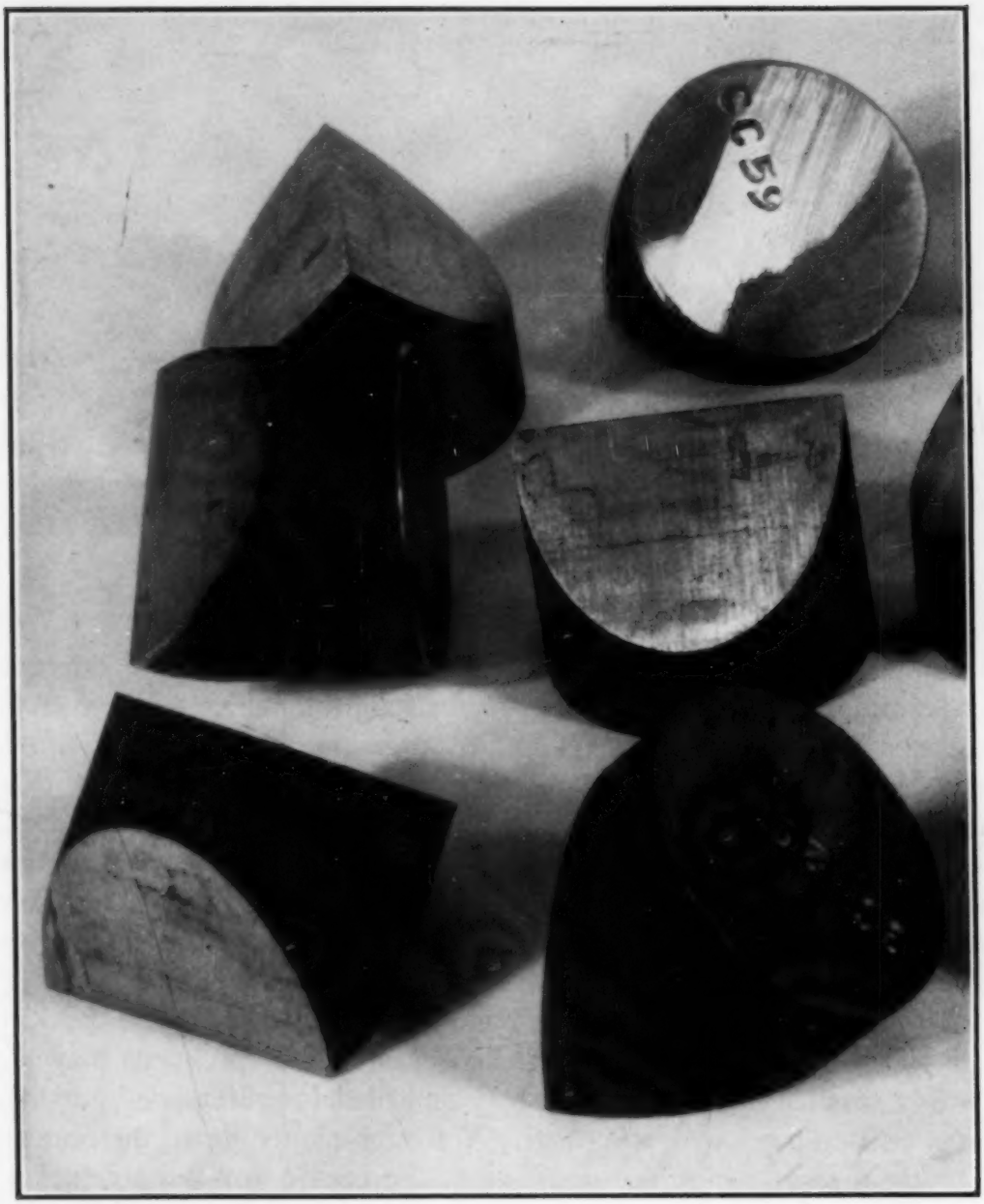


Fig. 2—Several P-V Test Pieces Sawed from Rounds As-Received. Note identification stamp on the base along the diameter perpendicular to the chisel edge.

machined preferably to 1½-inch round. Sizes smaller than 1¼-inch round can be quenched, but require a special spray nozzle in the quenching fixture later to be described.

These specimens may be made simply by a number of methods. Fig. 3 shows a fixture for a power hacksaw. The bar is fastened in the vise or jig and a cut taken at 45 degrees to the longitudinal axis of the bar. The jig is then swung to a position where another cut

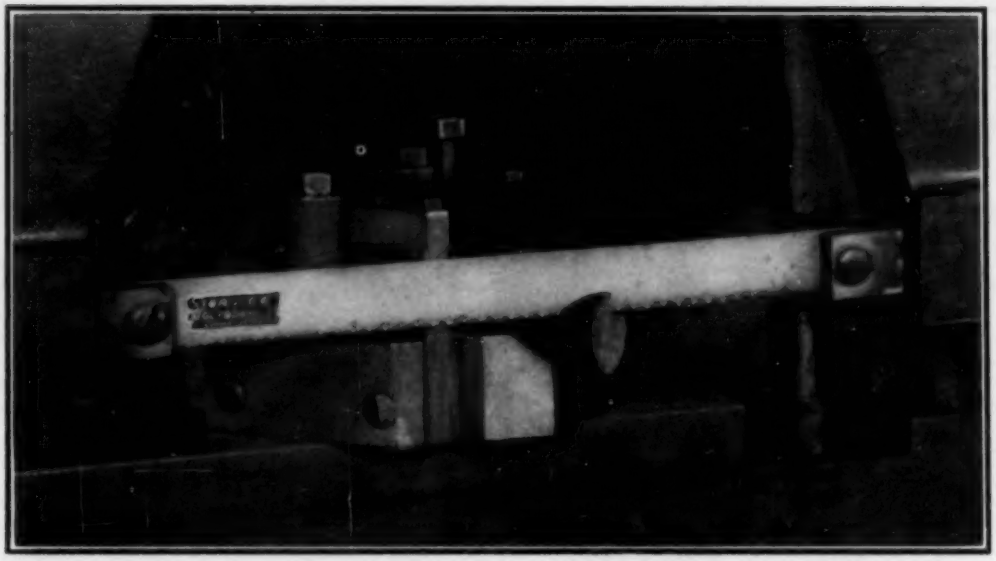


Fig. 3—Swivelling Vise for Holding Tool Steel Rounds in Power Hack-Saw; the First Cut on "V" End is Half Through.

is taken 90 degrees to the first cut. It is again swung 45 degrees back, and a cut made 90 degrees to the longitudinal axis of the bar; this removes the specimen. The "V" edges are then slightly buffed on a power sander. The total time of making specimens by this method including removal from the bar is approximately 3½ minutes.

Specimens may also be made much faster in a cut-off machine such as the DeWalt. They may also be made in a milling machine with two 45-degree cutters at right angles to each other, or by a number of other methods suitable to the laboratory facilities.

Cast bars approximately 1½ inches in diameter can be quickly fabricated into test specimens of this sort. These specimens may be readily handled in shop or laboratory and filed for reference by using long wooden trays with a 90-degree V trough planed down the center.

Passing over, for the time being, the reason for the acceptable heat treatment schedule, other than to say that most of the tests described were completely spheroidized, then heated to 1450 F in electrically heated muffle, 1 hour total furnace time, and quenched in 10% brine at 85 F, let us pass to the design of the fixture for spray quenching the chisel edge of this test piece.

Fig. 4 is a detailed drawing of the quenching fixture, and Fig. 5 is a photograph of it while quenching a P-V test piece. The fixture is screwed to the top of a vertical ½-inch pipe located conveniently in a suitable tank. Quenching fluid, coming up through this pipe, through the fixture, out the slots and onto the hot test piece, is con-

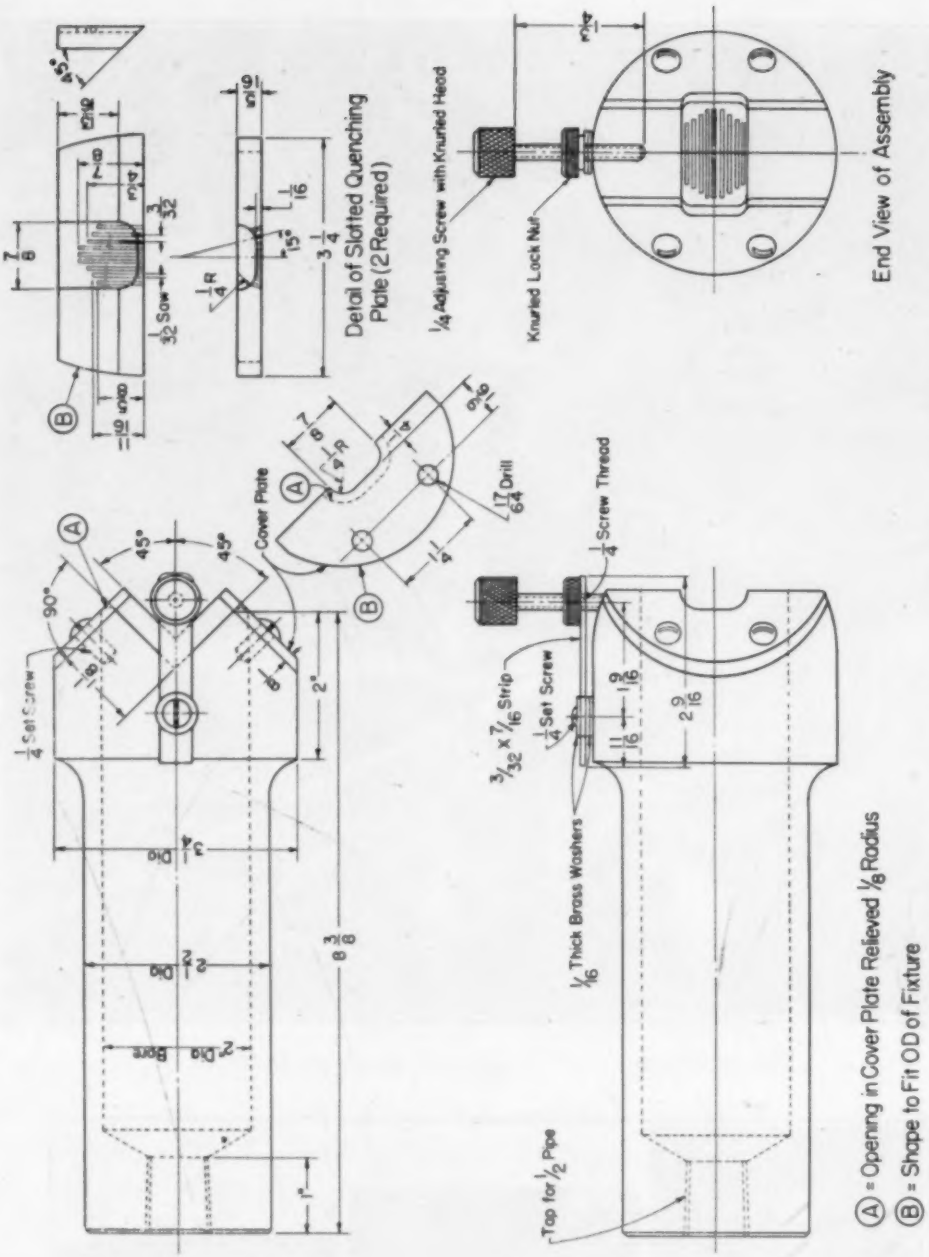


Fig. 4—Detailed Drawing of Quenching Fixture for P-V Test Pieces.

trolled by a quick acting valve whose handle is connected to a foot treadle outside the tank by a brass chain. Pressure is so regulated that the fluid flows at 5½ gallons per minute; if there is no specimen in place the streams flowing through the slots rise 3 inches, measured from bottom of slots. In use, the locating screw is adjusted for the diameter of piece being quenched so the specimen is centrally located, the hot specimen placed on the fixture, the quick acting valve opened, and flow continued until the test piece is cool enough to be removed with bare fingers.

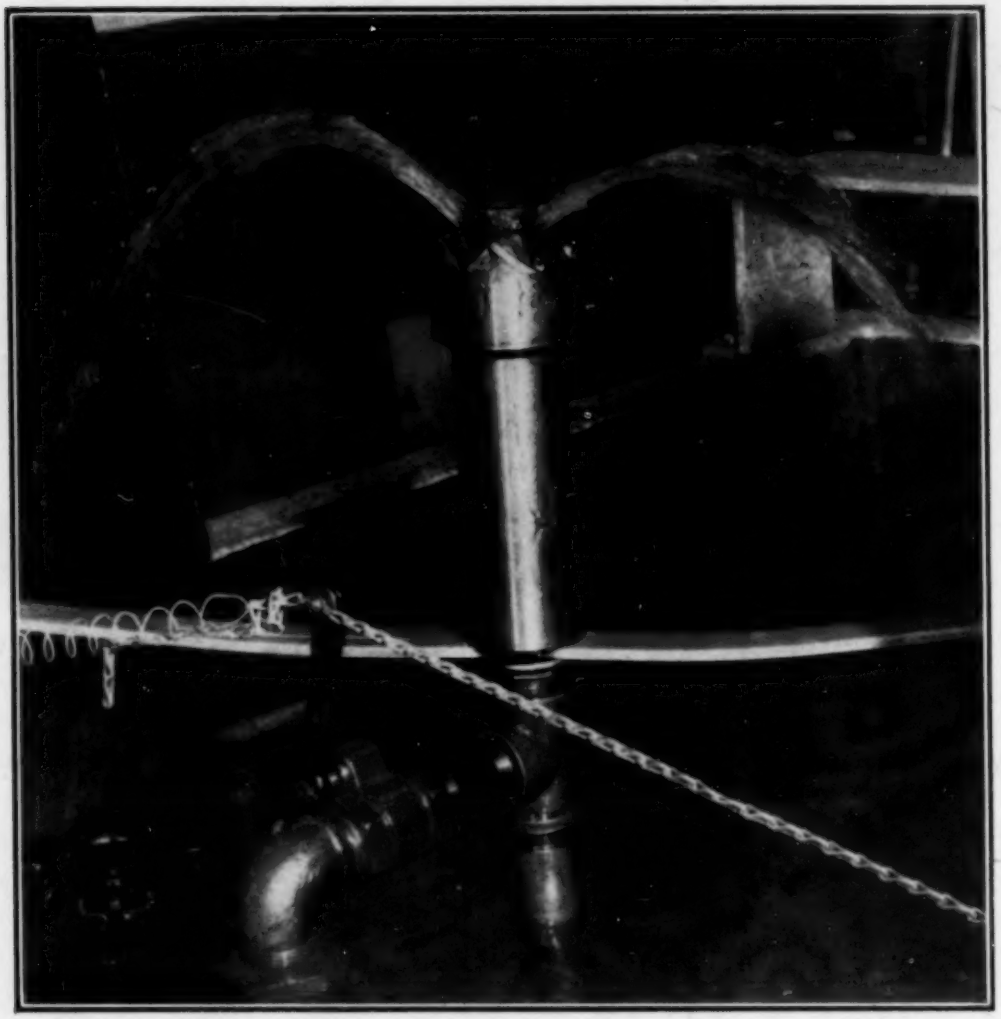


Fig. 5—Photograph of P-V Test Piece Being Quenched.



Fig. 6—Axial Section Through P-V Test Pieces, Etched with Nital, Showing Uniform Depth of Hardening Below Chisel Edge (Upper Edge of Photographs) and Lack of "Edge Effect" at Right and Left—Elements of the Outer Cylindrical Surface of the Original Test Pieces. Full size.

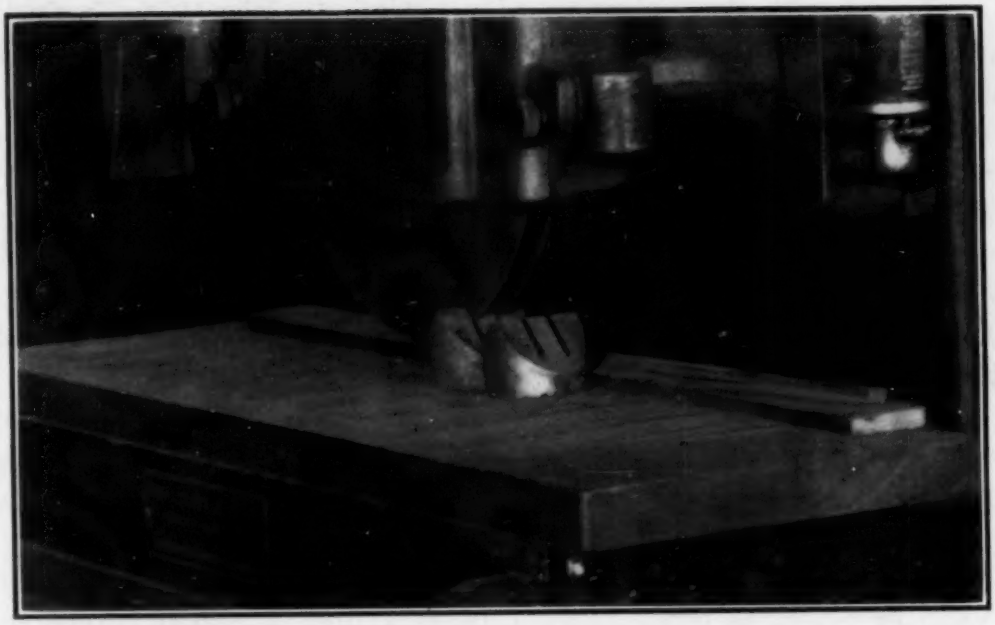


Fig 7—Slabs Being Cut from P-V Wedges with Two Diamond Wheels. Ground sides of these slabs are traversed for hardness-depth data.

We have found that this method produces a quenching speed of such intensity that the heat removal becomes a factor of the heat conductivity of the steel. The shape of the specimen so extends the range over which the critical cooling rates of shallow hardening materials occur that inherent differences in reaction to cooling rates are readily and easily measurable. This has been proved by cutting a number of the specimens of steels ranging through the entire series shown in Fig. 1 longitudinally—that is to say, the plane of section contains the chisel edge—and measuring the hardness gradient from the edge at intervals suitable to the hardness measuring instrument used. Likewise, when these diametral sections are etched with nital the darkened portion representing hardened metal (down to 50% martensite) they show a uniformly hardened pattern whose inner edge parallels the chisel edge clear across the bar (Fig. 6). For equally good results on small sized rounds—1 inch or ¾ inch—a slotted plate with proportionately smaller and fewer slots must be inserted in the quenching spray. As noted, large rounds should be machined to 1½ inches before forming off P-V wedge.

Slabs for Hardness Testing—It should be emphasized that the split specimens mentioned above were cut especially to show uniformity of depth hardness in the axial plane of the chisel edge. This is by no means a routine operation.

For routine determination of penetration, slabs, ⅜ inch thick, are cut from these quenched P-V wedges as shown in Fig. 7, which shows the slabs partially cut from two specimens on the magnetic chuck of a Brown and Sharpe grinder using Norton Alundum grade 60M4L, $\frac{1}{16}$ by 7-inch cutting wheels. Wheel wear and risk of "burning" or tempering the hardened test pieces is reduced by use of wax impregnated wheels 60NAT from F. Bancroft, Dearborn, Mich. Fifteen samples were cut with a pair of these wheels (in lots of three) in an average time of 6 minutes each. The diameter of the wheels was reduced ¼ inch per set of three specimens.

The slabs are then laid flat on the magnetic chuck and ground on both sides with a Norton grade 19A46G wheel. Twelve specimens ground at the same time had 0.010 inch removed from each side in an average time of 5 minutes each.

It should be noted that the stamping that identifies the specimen should be placed as noted in the caption of Fig. 2, and it is obvious that the slab cut as above will be permanently marked.

Another satisfactory method of getting a surface for testing is to take one cut through the specimen not more than $\frac{3}{16}$ inch off center. A small flat is then ground on the outside diameter of the bar parallel to the cut on the far side; this flat properly supports the specimen during hardness testing.

Inasmuch as the pieces are placed on a magnetic chuck the cuts are at right angles to the base instead of to the P-V edge, whereas, as mentioned above, the hardening pattern is parallel to the P-V chisel edge. If the original test wedge was sawed from the bar, there is a possibility that the chisel edge and the base may not be exactly parallel—the fixture shown in Fig. 3 not being one of high accuracy. However, the angularity need not be great, and the error introduced by lack of parallelism is very small. For example, for 5 degrees off parallel—an extreme amount—the theoretical increase in measured depth over the actual (perpendicular) distance is 0.4% —a negligible amount, well within the accuracy of the hardness testing procedure.

Hardness-Depth Survey—Now that the steel is sampled, the V-wedge hardened and a slab cut from it, the next step is to make a series of hardness tests down the line bisecting the wedge's angle and at known distances from the apex, plotting the observed hardnesses against the known distances and interpreting the curve. It is apparent that some handy fixture must be mounted on the anvil

of the Rockwell hardness testing machine so that these tests can be made at accurate and known intervals.

At first these hardness surveys were made by putting the sample in a parallel motion fixture where locations along a straight line were noted by a depth micrometer built into one end of the fixture. Later another device similar to a microscope stage, capable of vernier

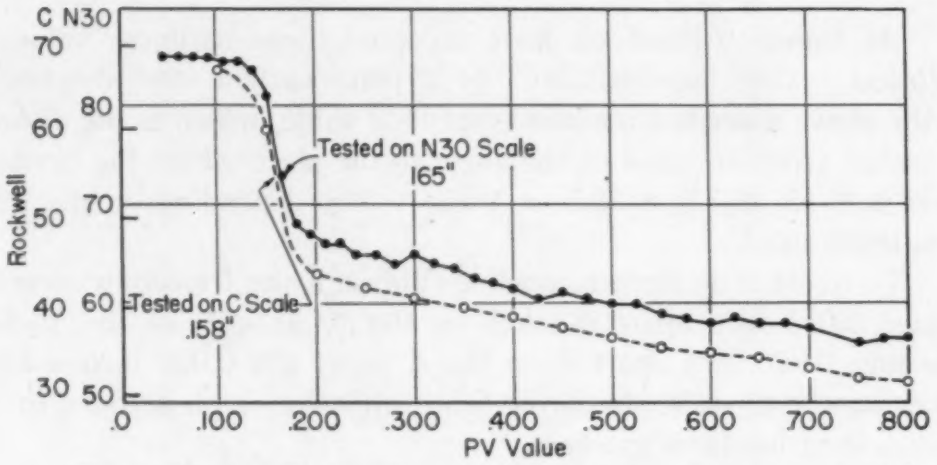


Fig. 8—Complete Hardness-Penetration Curves for a Slab of Steel (Code A-67), One Side Surveyed by Rockwell N-30 Scale, the Other Side Surveyed by Rockwell C Scale.

movements at right angles was built for us by Valley Tool & Precision Co. of Easton, Pa. By its means we can survey an area 2½ by 2 inches in dimension. A feature of our operation is a 10-power magnifying glass permanently fixed to the Rockwell machine and focussed on the very point of the indenter. By this means the zero point of the hardness-depth curve (where the point of the indenter is exactly over the apex of the angle of the test piece) can be readily located.[4]

Two complete plots of such hardness surveys are shown in Fig. 8. One set of tests was made with the Rockwell N-30 scale at 0.015-inch intervals; the other set was made on the other side of the slab with the Rockwell C scale at 0.050-inch intervals. (The relationship between the two scales, shown on the vertical ordinates, is the one shown by the maker's chart No. 38.)

As mentioned already, the criterion of hardenability is a quenched structure containing 50% martensite.[5]

[4]Editor's Note: Mr. Shepherd's original manuscript contained pictures of all these devices, but in the interest of economy they have not been reproduced. Any interested person can examine them in the library of the American Society for Metals, where they will be permanently preserved, or may arrange to have photostats made thereof.

[5]It is understood, of course, that other criteria may be used to suit local needs.

Microscopic examination of a number of such surveyed slabs shows that this condition for plain high carbon steels is very close to the following hardness levels:

Rockwell C-55
Rockwell N-73
Rockwell A-78.5
Vickers (10g.) 598

At Ingersoll-Rand we have accepted these hardness values as identical. The "hardenability" of a plain carbon steel determined in the above described manner is its P-V value, which is the distance in inches from the apex of the angle to the place where the hardness level is C-55, N-73, A-78.5 or Vickers 598, depending on the hardness tester used.

To avoid interference, readings through the transition zone are spaced 0.015 inch apart if taken on the N-30 scale or the Vickers machine, 0.020 inch apart if on the A scale, and 0.050 inch apart if taken on the C scale, the latter being undesirable on account of the steepness of hardness gradient.

For the test shown in Fig. 8 the P-V value of that steel (code A-67) was 0.165 inch when tested on the N-30 scale, and 0.158 inch when tested on the C scale. Obviously, in routine testing, only a few hardness impressions at the transition zone are necessary—hardnesses of the completely martensitic case and of the unhardened core are seldom of interest.

A number of specimens covering a wide range of P-V values (quenched in 10% brine at 85 F, from spheroidized structure, 1 hour total furnace time at 1450 F) were selected from our storage cabinet, carefully reground and tested to establish typical curves for the various hardenabilities. Fig. 9 shows the etched specimens; Fig. 10 the plots whereby the P-V values were determined of some 15 steels of increasing hardenability.[6] Table II gives the P-V rating of each specimen taken from old records; it also contains the retest (N-30 value) as well as a second estimate made on the opposite side of each slab using one of the other hardness scales. It will be observed from the last column that the correlation is very good, and that in all specimens the other hardness scales gave a shallower P-V value then the tests with N-30 scale. Metallographic examinations made on faces tested with N-30 scale checked the P-V value (location of 50% martensite point) very closely.

[6]The original manuscript contained complete hardness-penetration curves of all these tests and retests.

Table II
Retests on Slabs to Establish Correlation of Various Hardness Scales[1]

Heat Code and Specimen No.	P-V Value Av./Spread/No. Tests	Dia. Spec.	P-V Values: Orig. Test (N-30)	Slab Thickness	N-30 Value to N-73	C Value to C-55	A Value to A-78½	Vickers (10g.) to 598	Maximum Deviation[6] %
A-67-1	0.162/0.001/2	1½[2]	0.162	3/16	0.165	0.158	.....	.....	3.4
E-3916-SC	0.202/0.003/2	1½[3]	0.200	11/32	0.200	.....	0.200	.....	...
OK-3	0.227/0.006/3	1½	0.225	3/8	0.231	0.223	.....	.....	2.2
BC-2	0.256/0.013/3	1⅜	0.258	7/16	0.267	.....	0.254	.....	3.2
BC-3	0.256/0.013/3	1⅜	0.248	7/16	0.258	.....	.....	0.248	2.0
BS-3	0.297/0.006/3	1½	0.297	9/16	0.308	0.292	.....	.....	3.3
BR-1	0.342/0.013/3	1⅜	0.348	7/16	0.343	.....	0.333	.....	3.5
BR-2	.....	...	0.344[4]	5/16	.....	.....	0.344[5]	.....	0.3
CB-1	0.366/0.004/3	1½	0.367	¼	0.378	0.369	.....	.....	0.9
MU	0.446/0.005/3	1¾	.....	5/16	0.447	0.436	.....	.....	2.5
PX	0.456/0.006/3	1½	.....	5/16	0.461	.....	0.454	.....	1.5

[1]Spheroidized structure; hardened from 1450 F.
[2]Hardened from 1450 F. lead, previously oil-treated 1600 F, 40 minutes at temperature.
[3]Hardened from 1420 F. lead, previously oil-treated 1600 F, 40 minutes at temperature.
[4]Tests on one side of alternate specimen from Heat BR.
[5]Tests on other side of BR-2.
[6]Average of N-30 tests taken as actual hardenability; largest deviation of depth of hardening by other hardness methods—figured as per cent of actual hardenability. All deviations are minus.

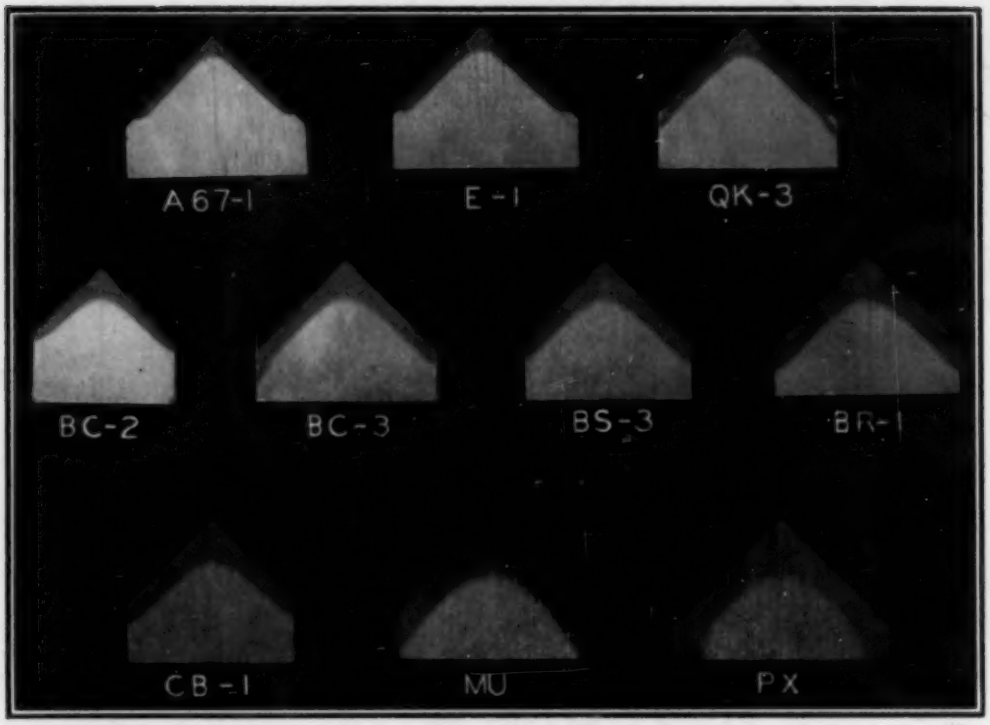


Fig. 9—Photograph of Etched Slabs Whose P-V Hardenabilities are Listed in Table II. Transition zone (by etching) is much sharper in steels of lesser hardenability. Natural size.

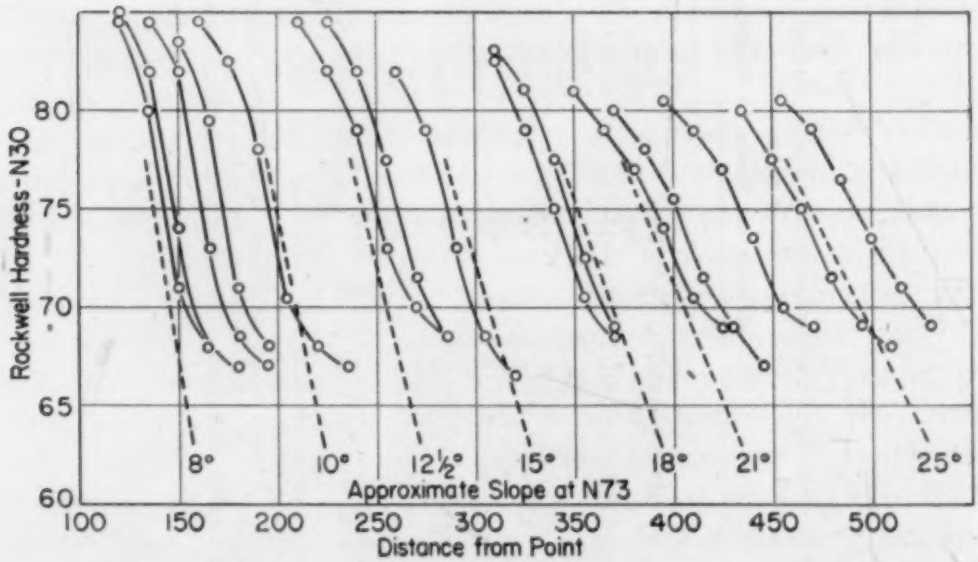


Fig. 10—Typical Hardness-Penetration Curves (Transition Zones Only) of 15 Steels Comprising a Wide Range of Hardenabilities. It will be noted that the slope of the tangent to these curves increases with increasing P-V value, corresponding to the reasonable supposition that the transitional microstructures are the more closely concentrated in steels with the lesser the hardenability.

Table III
Effect of Low Tempering on P-V Determination

Heat Code and Acceptance Test on Heats		Data on Original Specimens			Tempering Temperature	Retest after Tempering
Code	Av./Spread/No. Tests	Spec. No.	Original P-V	Retest after Grinding*	F	
TI50SC	0.151/0.009/2	1	0.147	0.151	200	0.151
TI50SC	.....	2	0.156	0.156	300	0.156
TI50LC	0.170/0.007/2	1	0.166	0.171	400	0.171
TI50LC	.....	2	0.173	0.174	500	0.166
AO	0.308/0.01/3	1	.....	0.314	200	0.310
AO	.....	2	.....	0.318	300	0.316
AI	0.315/0.008/3	1	.....	0.312	400	0.313
AI	.....	2	.....	0.322	500	0.310
MU	0.446/0.005/3	2	.....	0.453	200	0.455
MU	.....	3	.....	0.460	300	0.449
PX	0.447/0.013/3	1	0.448	0.451	400	0.455
PX	.....	11	0.453	0.464	500	0.448

*May or may not be same side of slab.

Effect of Tempering During Sample Preparation (Cutting and Grinding)

The technique of sample preparation should avoid any inaccuracies in the results due to overheating during cutting or polishing. Likewise, Engel[7] has shown that mixtures of martensite and transformation products are less readily tempered than 100% martensite, and any moderate amount of heat would be unlikely to change the location of the transition zone a measurable amount. Our experience confirms this, but it was thought desirable to artificially temper specimens and determine the influence of such tempering temperature upon the P-V value and hardness gradient in order to assess the actual heat effect of grinding.

Samples of low, medium and deep hardening steels were selected from our file cabinets and approximately $\frac{1}{32}$ inch removed from the original tested surface before retesting. They were then tempered in a Lindberg furnace for 1 hour total time at the temperatures indicated in Table III, reground, removing approximately $\frac{1}{32}$ inch and any trace of decarburization, and retested using the N-30 Rockwell scale.

Results shown in Table III[8] indicate that the P-V figure on any of these steels is unaffected (measurably) by temperings up to and including 400 F. It is unlikely that this temperature will be exceeded, in sample preparation, except by gross carelessness.

[7]F. H. Engel, Transactions, American Society for Metals, Vol. 27, 1939, p. 1-15.

[8]The original manuscript contained complete hardness-penetration curves substantiating the figures of Table III.

Intra-Laboratory Checks and Uniformity of Pattern

In order that we might be sure our testing technique could readily be reproduced and give equivalent results by various laboratories, ten P-V slabs about $\frac{5}{16}$ inch thick were sent to the following gentlemen, one after another: W. F. Towne, metallurgical supervisor, Bethlehem Steel Co.; H. J. Stagg, Crucible Steel Co. of America, Halcomb Works, Syracuse, N. Y.; R. L. Stephenson, chief metallurgist, Carnegie-Illinois Steel Corp., Duquesne Works; H. B. Chambers, metallurgical engineer, Atlas Steel Co., Ltd., Welland, Canada; N. H. Barlow, manager, Crucible Steel Co. of America, New York; and A. P. Terrile, Crucible Steel Co. of America, Pittsburgh Crucibile Division, Midland, Pa.

Each laboratory removed 0.030 inch from one surface of each slab and determined the P-V value from a hardness survey as described earlier in this paper, using Rockwell N-30 scale or A scale at discretion. Results are summarized in Table IV, from which it appears that results for shallow to deep hardening steels are readily reproducible at different laboratories, the averages and maximum limits reported being as follows:

Code	Retests			Average for Original Heat
	Max.	Min.	Av.	
BH	0.252	0.244	0.247	0.245
BW	0.317	0.305	0.309	0.309
CF	0.362	0.348	0.356	0.356
XO	0.411	0.394	0.400	0.406
PX	0.464	0.450	0.454	0.456

Table IV
Checks by Various Laboratories on P-V Value

	Heat Evaluation Tests			Retests of Specific Slabs						
Heat No.	Orig. Test of Heat Av./Spread/No. Tests Max. to Min.	Spec. No.	Orig. Insp. Test N-30	Retest I-R N-30	Beth. N-30	Atlas A	Halcomb N-30	Duquesne A	Midland N-30	Retest I-R
BH	0.245/0.003/3	B	0.244	0.246	0.246	0.242	0.244	.....	0.249	.....
1½-In. Rd.		M	0.245	0.252	0.247	0.252	0.251	0.247	.....	.....
BW	0.209/0.10/3	1	*	0.310	0.311	0.310	0.313	.....	0.316	.....
1⅜-In. Rd.		2	*	0.310	0.305	0.300	.....	0.317	.....	.....
CF	0.356/0.015/3	1	*	0.357	0.360	0.356	0.350	.....	0.359	.....
1⅜-In. Rd.		2	*	0.362	0.364	0.352	0.353	0.348	.....	.....
XO	0.405/0.010/4	2	0.411	0.403	0.397	0.395	0.408	.....	.....	.....
1½-In. Rd.		3	0.405	0.398	0.394	0.390	0.400	0.396	.....	.....
PX	0.456/0.006/4	6	0.452	0.453	0.450	0.460	0.450	0.452†	.....	0.452
1½-In. Rd.		10	0.458	0.464	0.454†	0.453	0.452	0.457	.....	.....

*Routine tests are not usually recorded individually.
†Average three tests axial line, 0.030 inch right and 0.030 inch left of axial line.

The averages reported from the six laboratories check almost exactly the gradings originally made for the respective heats by Ingersoll-Rand. It is of course true that this is not a verification of the entire testing method; it is, however, good proof that various laboratories can closely check each other in the necessary survey of hardness penetration, and in the accurate determination of a definite hardness level. Since each laboratory ground deeper and deeper into the specimen, it is also a demonstration that the hardenability

Table V
Tests on Two Heats at Various Laboratories

Quenched at	Quenched in	Tested at	Tested with	Code BH Av./Spread*/No. Tests	Code CC Av./Spread*/No. Tests
Phillipsburg	10% brine	Phillipsburg	N-30	0.257/0.003/3	0.347/0.013/3
Midland	Water	Midland	N-30'	0.245/0.006/3	0.344/0.009/3
		Phillipsburg	N-30	0.253/0.009/3	0.353/0.005/2
Duquesne	Water	Duquesne	A	0.255/0.005/3	0.355/0.014/2
		Phillipsburg	N-30	0.256/0.013/2	0.344/0.006/3
Parks Works	Water	Phillipsburg	N-30	0.252/0.003/2	0.341/0.009/3
Bethlehem	10% brine	Bethlehem	N-30	0.249/0.004/3	0.347/0.009/3
		Phillipsburg	N-30	0.252/0.007/3	0.345/0.004/3

*"Spread" means difference between maximum and minimum P-V reported.

pattern in the test piece is quite constant for a reasonable distance, quite sufficient to provide against errors introduced by cutting the slab considerably off center.

Reproducibility of results is better illustrated by the facts presented in Table V. We took P-V specimens of two different heats of tool steel (Code BH and CC) with full spheroidized, prehardening structure. They were hardened on the quenching fixture (Fig. 4) with standardized procedure for the particular type of steel at the various laboratories. Half of the specimens were tested at the laboratory concerned, the balance at the Phillipsburg laboratories of Ingersoll-Rand Co. with the results given in Table V. The uniformity is apparent. Arithmetically, it may be expressed as follows:

	Code BH	Code CC
Grand average	0.252	0.347
Maximum deviation from grand average	0.007	0.008
Minimum deviation from grand average	0.005	0.006
Maximum difference between any individual averages	0.012	0.014

This uniformity of pattern was verified by some definite experi-

Table VI
Effect of Variation of Tests from Axial Line

	Code QK 1½-In. Rounds	Code AC 1½-In. Rounds	Code MU 1¾-In. Rounds
Specimen No. 1			
0.030 inch right	0.224	0.337	0.447
Center	0.224	0.337	0.452
0.030 inch left	0.225	0.337	0.458
Average	0.224	0.337	0.452
Spread	0.001	0.000	0.011
Specimen No. 2			
0.030 inch right	0.233	0.335	0.445
Center	0.230	0.333	0.452
0.030 inch left	0.234	0.338	0.451
Average	0.232	0.335	0.446
Spread	0.004	0.005	0.007
Specimen No. 3			
0.030 inch right	0.225	0.342	0.438
Center	0.228	0.337	0.443
0.030 inch left	0.224	0.338	0.442
Average	0.226	0.339	0.441
Spread	0.004	0.005	0.005
Average center values and spread	0.227/0.006	0.336/0.004	0.449/0.009
Grand average of P-V values and spread	0.227/0.008	0.337/0.004	0.446/0.011

ments. Two types of investigation were made to determine the effect of any deviation of the hardness-penetration tests from the true axial line. One consisted of supplementing the usual acceptance tests of 17 heats of 1.00% carbon tool steel with a second and a third row of hardness impressions made 0.030 inch to the right and 0.030 inch to the left of the axial line. These heats varied in P-V value from 0.227 inch to 0.446 inch, thus representing a considerable spread in hardenability. Three samples had been prepared from each of the heats, in conformity with our usual practice. Results in three of these steels, widely varying in hardenability, are given in Table VI, and these data are quite indicative of the information from the rest of the 17 heats.[9]

The second investigation to prove uniformity of conditions in the normal test area consisted of surveying the hardness over a considerable area near the transition zone of slabs from two heats of steel, using N-30 and C scale hardness readings, as well as macro-etching.[9]

The steels (Code ZE, 1½-inch round, and PX, 1¾-inch round) had been tested in the usual way and showed an average, determined by three samples tested along the axial line with N-30 Rockwell at 0.015-inch spacing as follows: Heat ZE (average of three tests),

[9]Editor's Note: Complete numerical data, photographs and hardness-penetration curves are on file with the original manuscript in the ASM library.

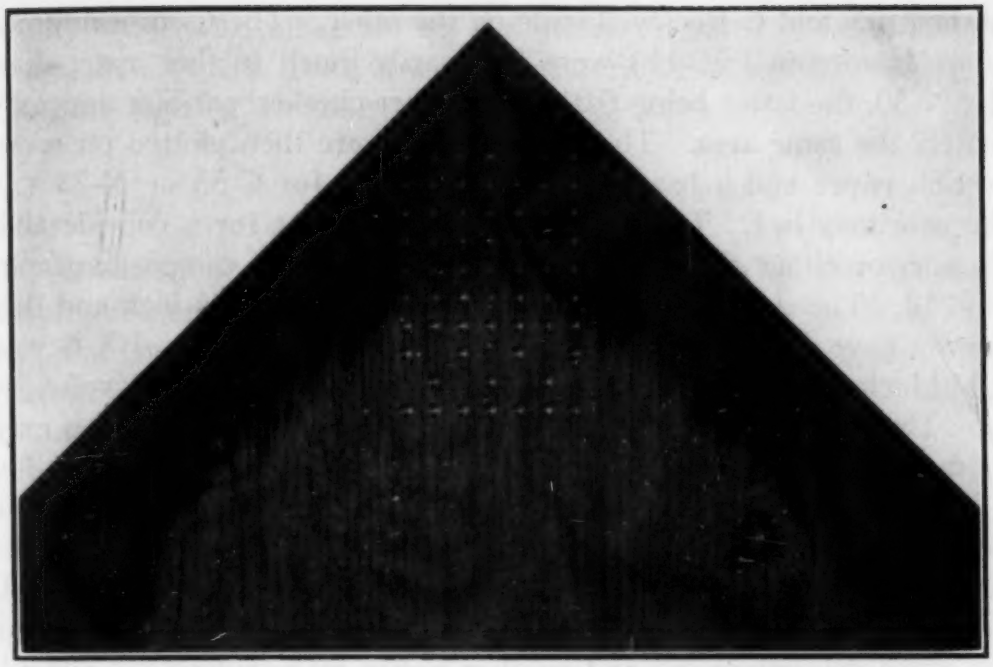


Fig. 11—Photograph of Slab of Steel PX, Specimen 6, Showing Area Surveyed by Rockwell C-Scale Impressions, and Depth of Hardness as Determined by Etching. × 4.

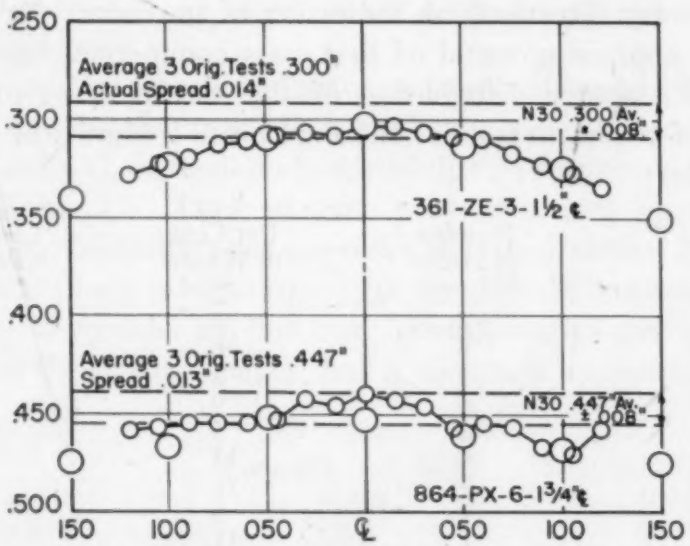


Fig. 12—Summary of Contours Determined by Hardness Surveys on Two Slabs, N-30 Tests on Tops, C-Scale Tests on Bottoms.

P-V = 0.300 inch, spread 0.014 inch. Heat PX (average of three tests), P-V = 0.447 inch, spread 0.013 inch.

Specimen ZE-3 and specimen PX-6 were retested after removing sufficient material to cancel the work hardening effect of the previous tests. Each piece was then surveyed with the N-30 Rockwell scale

on one side and C Rockwell scale on the other. The C-scale impressions (shown in Fig. 11) were necessarily much further apart than the N-30, the latter being 0.015 inch apart checkerboarding approximately the same area. These hardnesses were then plotted on cross section paper and a hardness contour drawn for C-55 or N-73 (as the case may be). These contour lines were flat for a considerable distance on either side of the center, as shown by the composite graph, Fig. 12. The original test of specimen ZE-3 was 0.303 inch and this survey gave 0.303 inch. The original test of specimen PX-6 was 0.440 inch and this survey checked 0.440 inch on N-30 Rockwell.

The summary in Fig. 11 shows that a considerable variation may be made on either side of the axial line without affecting the results.

Another indication of uniformity comes from a study of tests on 64 consecutive heats of carbon tool steel bars received by Ingersoll-Rand. As is our custom, three bars of each of these were sampled, hardened and tested, the P-V value being recorded as an average of the three determinations and another figure representing the spread, high to low. While the figure for spread is designed to give us some idea as to uniformity of the metal, bar to bar, in the heat, still it is (in the contrary direction) an indication of uniformity in the testing method for appraising metal of first class commercial quality.

The satisfactory distribution of the spread from minimum to maximum of triplicate tests of these 64 heats is shown in the following tabulation:

Spread Inch	Number of Heats	Per Cent of Whole	Cumulative Per Cent
0.000	1	2	2
0.001	2	3	5
0.003	4	6	11
0.004	2	3	14
0.005	6	9	23
0.006	3	5	28
0.007	8	13	41
0.008	7	11	52
0.009	4	6	58
0.010	7	11	69
0.011	1	2	70
0.012	3	5	75
0.013	5	8	83
0.014	4	6	89
0.015	5	8	97
0.017	2	3	100

When these individual values for spread are plotted against their respective average P-V values, it is also found that there is no concentration of high or low spreads at any particualr harden-

ability value. In other words, the entire range of spreads can be found in all steels from low hardenability (P-V = 0.250 inch) to those of high hardenability (P-V = 0.450 inch).

Effect of Dimensions of Specimen

Diameter of Specimen—The effect of diameter of specimen was determined on heat PX, 1¾-inch round. Tests were made on each end and from the middle of the bar in the original size, and also after machining to 1½ and to 1¼-inch round. The results are shown below:

	1¼ Inch	1½ Inch	1¾ Inch
End bar	0.453	0.458	0.448
Middle bar	0.468	0.452	0.440
Opposite end	0.462	0.458	0.453
Average	0.461	0.456	0.447
Spread	0.015	0.006	0.013

It might appear from these tests that the same steel gives a higher P-V value if tested as small rounds, but the spread of averages (0.461 − 0.447 = 0.014) is no larger than the spread of duplicate tests in a single size.

Length of Specimen—Influence of length of wedge-shaped specimen (Fig. 2) was determined on triplicate specimens cut from two heats, BH and CC, of medium hardenability. (For chemical compositions, see Table I.) Lack of time prevented tests on material of still higher hardenability, but previous tests had shown that a specimen 1⅛ inches long is satisfactory for the deepest hardening material intended to be covered by this test. Detail curves and photographs are given in the original paper, but a summary of the average is as follows:

	Code BH (1⅛ Inch)	Code CC (1⅜ Inch)
⅝ inch long	0.264	0.375
⅞ inch long	0.262	0.355
1⅛ inches long (standard)	0.257	0.347
1⅜ inches long	0.256	0.351

Obviously, slight changes from the 1⅛-inch recommended length will cause no aberrations in the results.

Angle at Chisel Point—Steeper V angles than 90 degrees increase the depth of penetration but also increase the spread between individual tests and make the test specimens liable to crack in the hardening operation. The relationship between 90, 60, or 45-degree

angle, as determined on heat VY having a P-V value of 0.373 inch on a 90-degree standard specimen, is as follows:

Angle 90°	P-V 0.373
Angle 60°	P-V 0.515
Angle 45°	P-V 0.665

This indicates that of all the dimensional tolerances on the wedge specimen the angle of chisel point is the most critical. However, the jig shown in Fig. 3 can be very easily constructed so as to hold the angle within 1 degree, plus or minus.

Effect of Heat Treatment Variables

Nature of Coolant—Ten per cent brine at 80 to 85 F is used at Phillipsburg for the quenching fixture shown in Fig. 5. Many laboratories use water at other temperatures and it was thought desirable to determine the influence of the temperature of both quenching mediums upon the P-V values over a wide range of hardenability. Five heats which had been previously tested were selected. Triplicate samples from three heats were quenched at 60, 80, and 100 F in brine.

Round bars and standard Jominy tests were also quenched, the round bars being quenched according to our old standard P-F procedure. The Jominy tests were also run according to standard procedure and held 20 minutes at temperature.

Two heats were quenched in fresh water at 55, 80, and 100 F, the water being taken directly from the hot and cold water spigots and mixed in the pipe delivering it to the spray.

All quenching temperatures were 1450 F and all prehardening structures fully spheroidized. The P-V tests were held in the furnace for 1 hour total time.

Spacing on the P-V test was 0.015 inch (N-30 Rockwell tests). Flats were carefully ground on four sides of the Jominy bar, two opposite sides tested with C scale, alternate $\frac{1}{32}$-inch spacing, and two remaining sides tested with N-30 Rockwell, 0.015-inch spacing. The round bars were surveyed along three radii, 120 degrees apart on $\frac{1}{8}$-inch disks cut from the center of the bar. Estimation of 50% martensite was made on all types of bars to C-55 Rockwell or N-73.

The P-V results show excellent checks on the tests as made when the material was originally received, as shown in Table VII.

It is apparent that brine and fresh water, both at 80 F, will give interchangeable results.

Table VII
Comparison of P-V Tests Quenched in Water or Brine

	WF	BF	VX	BI	PX
Size	1½ in.	1⅜ in.	1⅜ in.	1¾ in.	1¾ in.
Original inspection tests					
Coolant			10% Brine at 80 F		
Average	0.289	0.281	0.370	0.412	0.447
Spread	0.011	0.007	0.005	0.005	0.013
Number of tests	4	3	4	3	3
Retest					
Coolant	80° brine	80° water	80° brine	80° water	80° brine
Average	0.284	0.290	0.380	0.416	0.448
Spread	0.007	0.009	0.007	0.002	0.007
Number of tests	3	3	3	3	3

Influence of temperature of brine coolant and correlation between Jominy tests and P-V values is given in Table VIII. The averages of the P-V tests consistently show a very slight change in quenching speed, reducing the penetration of hardening slightly as the temperature of the quenching bath is increased.

The spread between some pairs of results on the Jominy bars show that this test does not produce as uniform a cooling rate over the entire cross section for the quenched end of the bar as is generally supposed. This feature has not been given much attention heretofore as the Jominy test has not been utilized for determining the hardenability of shallow hardening steels. The extreme instance is Code VX quenched in 10% brine at 80 F. Jominy traverses on the four ground surfaces are shown in Fig. 13. For comparison the three corresponding P-V plots are also given.[10]

Duration of Quench—The effect of duration of quench of specimen in spray fixture was checked on two heats, PV and UX. These heats had an average P-V value of 0.254 and 0.452 inch respectively,

Table VIII
Jominy Versus P-V Values

	P-V Value			Jominy Depths			
	Slab 1	Slab 2	Slab 3	To C-55		To N-73	
Steel WF							
Brine at 60 F	0.297	0.292	0.292	0.123	0.122	0.128	0.130
Brine at 80 F	0.284	0.288	0.281	0.121	0.121	0.128	0.128
Brine at 100 F	0.281	0.284	0.278	0.122	0.116	0.109	0.124
Steel VX							
Brine at 60 F	0.390	0.383	0.381	0.160	0.168	0.169	0.166
Brine at 80 F	0.382	0.375	0.362	0.167	0.182	0.193	0.198
Brine at 100 F	0.372	0.368	0.375	0.161	0.161	0.157	0.162
Steel PX							
Brine at 60 F	0.473	0.462	0.460	.....	.....	.....	.....
Brine at 80 F	0.447	0.445	0.452	0.197	0.197	0.203	0.210
Brine at 100 F	0.443	0.440	0.445	0.204	0.202	0.215	0.220

[10]Editor's Note: This selection was made from a set of graphs showing all tests on all samples.

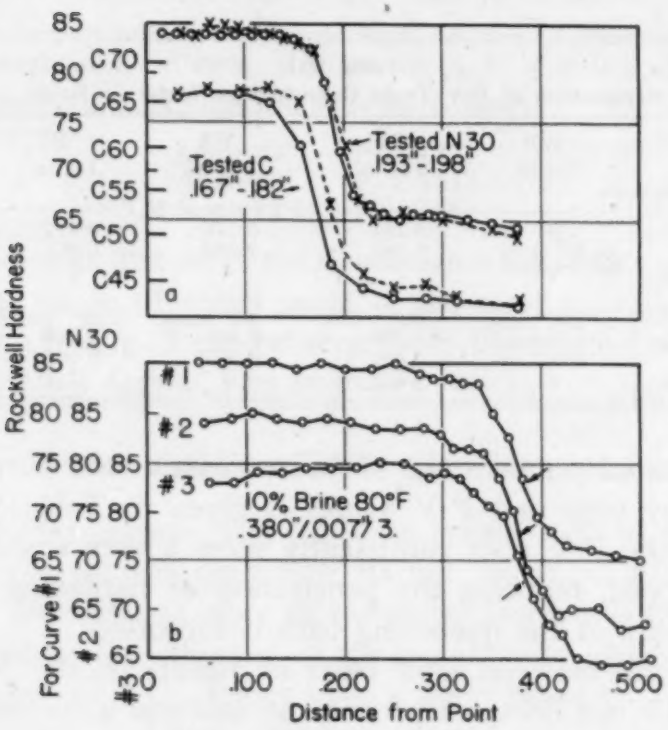


Fig. 13—Hardness Penetration Curves for Jominy Bar (4 Sides) and Three P-V Slabs of Heat VX, Quenched in 10% Brine at 80 F.

when allowed to remain on the spray until cold. When heat P-V was removed after 30 seconds, the back end was above 300 and below 350 F, and the average P-V value of triplicate tests was 0.252 inch (a drop of 0.002 inch, which is within the limit of accuracy of the test). When heat UX was removed after 30 seconds, the temperature was slightly higher—above 400 F and below 450 F—due to its being an ⅛-inch larger specimen. The P-V value was 0.445 inch, a drop of 0.007.

These tests show that there is no effect upon P-V value, provided specimens are left on the spray for 30 seconds as a minimum time.

Transfer Time—The effect of transfer time from furnace to fixture, which normally is 4 to 5 seconds, was checked on the same two heats. When transfer time was increased to 15 seconds (from the time the furnace door was raised until water was turned on) the respective P-V values were 0.259 and 0.466 inch, gains of 0.005 and 0.014 inch. When this time was increased to 30 seconds it was 0.268 and 0.468 inch, gains of 0.014 and 0.016 inch respectively. These figures are the average of triplicate tests and show that P-V value slightly increases, provided an abnormal time is taken for transfer.

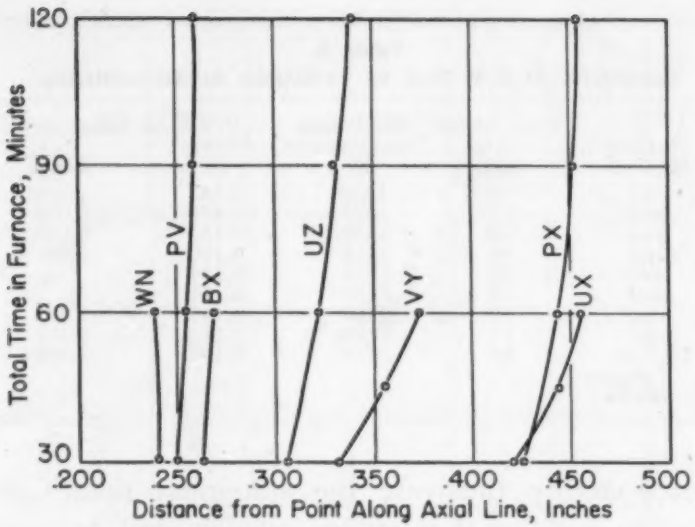


Fig. 14—Influence of Total Time in Furnace on P-V Value of Seven Steels of Low to High Hardenability. Analyses of heats shown in Table I.

It corroborates practical shop experience; the cause of this gain in hardness penetration will be made the subject of a later investigation.

Time in Furnace—Unless otherwise stated, all of the tool steel specimens mentioned in this report were hardened from 1450 F with 1 hour total furnace time. (The furnace is an electric muffle type.) These specimens heat through in 15 to 17 minutes, and the surplus time at temperature is valuable to produce substantially uniform austenite. In these steels grain growth is very slow at 1450 F, nevertheless the effect of total furnace time upon the P-V value was determined on seven heats covering a wide range of hardenability. Results are shown in Fig. 14.

The steels of low hardenability were fairly insensitive to long or short soakings in the furnace; the results on the steels of medium

Table IX
Effect of Furnace Time on P-V Grading and Uniformity of Hardness Pattern on Three Heats of Steel

Code	Time Hr.	Face A	Face B (Opposite)	Face B (Retest After Removing 0.030 In.)
PV	½	0.253	0.254	.....
	1	0.253	0.256	.....
	1½	0.262	0.259	.....
	2	0.262	0.261	.....
UZ	½	0.313	0.320	0.312
	1	0.324	0.328	0.331
	1½	0.332	0.333	0.340
	2	0.338	0.347	0.342
UX	½	0.422	0.418	.....
	1	0.442	0.437	.....
	1½	0.467	0.443	.....
	2	0.452	0.452	.....

Table X
Sensitivity of P-V Test to Variations in Austenitizing

Steel Code	Heating Medium	Time Above Ac Min.	Hardening Temperature F	P-V Determination Average In.	P-V Determination Range	Number of Specimens
TI	lead	10	1420	0.147	.....	1
TI	lead	15	1420	0.152	0.004	2
TI	lead	10	1450	0.151	0.009	2
TI	lead	15	1450	0.170	0.007	2
A67	lead	10	1420	0.144	.....	1
A67	lead	15	1420	0.151	.....	1
A67	lead	10	1450	0.145	0.004	2
A67	lead	15	1450	0.162	0.001	2
A67	Electric Furnace Muffle	45	1450	0.198	0.004	2

and high hardenability illustrate the statement made previously—that austenitizing conditions must be standardized for each type of steel, or a fictitious hardenability comparison may be shown.

In connection with these tests on the effect of total furnace time, a number of the P-V slabs ⅜ inch thick were surveyed on opposite sides, thereby checking the flatness or uniformity of the hardness pattern. Averages of triplicate tests of three heats of low, medium and high hardenability are given in Table IX, where the principal variable is furnace time.

Austenitizing—The sensitivity of the P-V test is illustrated by tests made on a 1% carbon steel under various conditions of austenitizing. It is well known that the time of heating from Ac to the hardening temperature has an influence upon the depth of hardening. To illustrate—this factor was varied on two steels (Codes TI and A-67) of compositions shown in Table I.

P-V test pieces were oil-treated from 1600 F after 40 minutes' soak at temperature, then reheated as indicated in Table X, quenched on standard P-V spray, tested with N-30 Rockwell, and P-V value stated as distance to N-73 hardness.

Hardening Temperature—Tool steels do not necessarily increase in depth of hardness penetration with increase in hardening temperature. For example, two heats of 0.75 to 0.80% carbon steel in 1½-inch round, Codes 1-R-143 and 2-R-143, were heated to 1650 F for 1 hour, cooled in air, and P-V test pieces cut. One set was quenched from 1450 F and the other from 1600 F, 1 hour total furnace time for each. Analyses of these heats are given in Table I.

Steel 1-R-143 from 1450 gave P-V = 0.325-inch average for three tests with 0.006-inch spread; from 1600, P-V = 0.311-inch average and 0.005-inch spread.

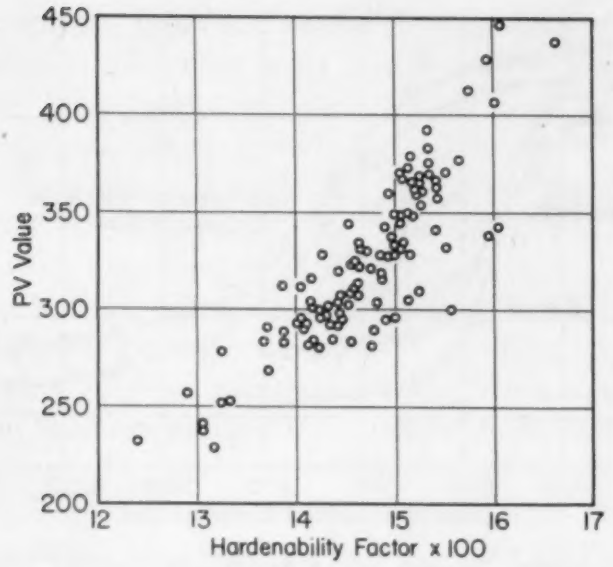


Fig. 15—Hardenability of 108 Heats Calculated from Chemical Composition (Bethlehem Formula) Versus Actual P-V Value.

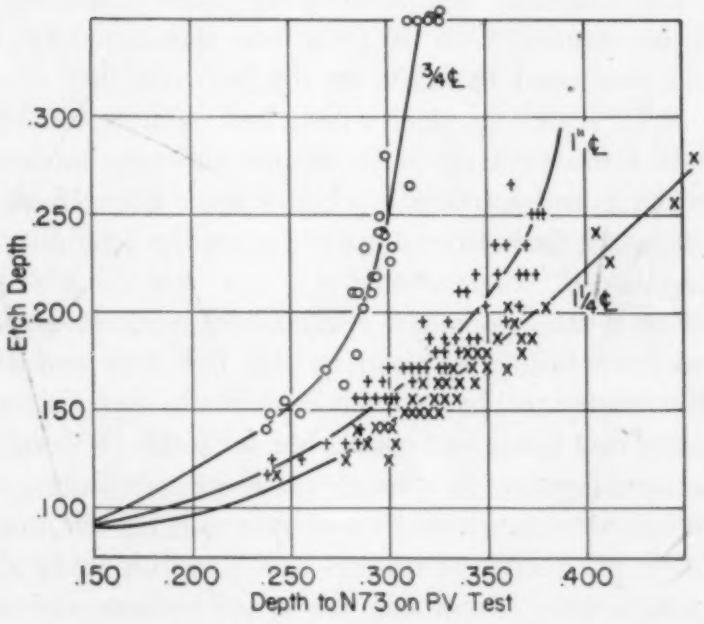


Fig. 16—Correlation Between Penetration of Hardness Into Quenched Rounds (¾, 1 and 1¼-Inch Diameter) with P-V Values of the Same Heats.

Steel 2-R-143 from 1450 gave P-V = 0.247-inch average for three tests with 0.006-inch spread; from 1600, P-V = 0.235-inch average and 0.010-inch spread.

Correlation With Other Tests

Computation of Hardenability—Estimations of hardenability are

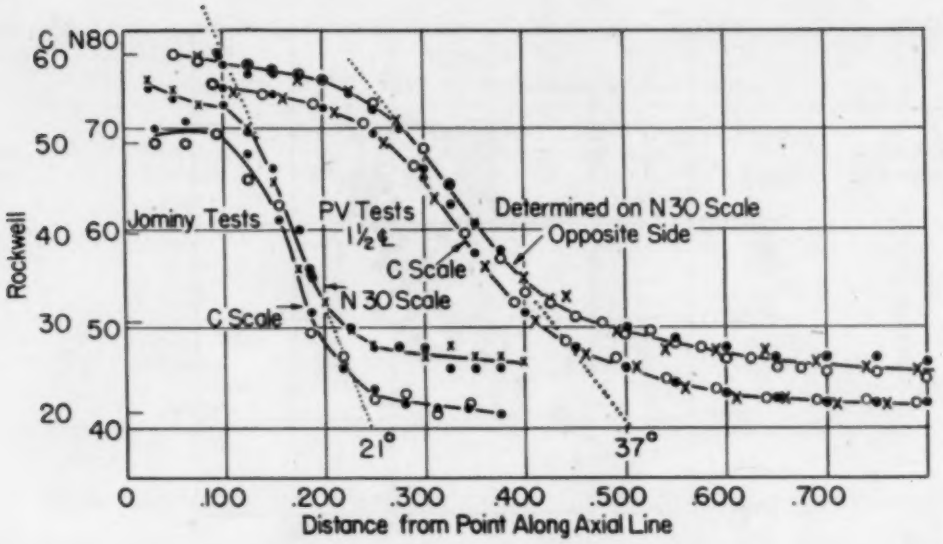


Fig. 17—Correlation Between Jominy End-Quench Test and P-V Test, Both Performed with Both N-30 and C Scales.

made from the chemical composition by many methods, more or less intricate in nature. One of these was developed by Bethlehem Steel Co. and was used to calculate the hardenability of 108 heats of a 0.85 to 1.15% carbon steel which had been tested by the P-V test. All P-V tests were made from the same prehardening structure, austenitizing and hardening conditions. Fig. 15 shows these results and indicates that only an approximate hardenability value can be obtained by use of this formula.

Correlation With Quenched Rounds—A very large number of heats of steel have been appraised by the P-F test and also by the P-V test. We, therefore, have much data on the correlation of hardness penetration in a quenched round bar with the P-V value. In all these comparisons, prior structure, austenite condition, and other important factors were equivalent, and optimum for the tests. Hardness penetration on quenched rounds was determined by cutting the bar across, mid-length, smoothing the cross section, etching it with 50% HCl, and measuring the penetration (depth of darkened case) in 64ths of an inch. Correlation for ¾, 1 and 1¼-inch bars is given in Fig. 16.

Correlation With Jominy End-Quench Test—Some comparisons were made in previous paragraphs, when discussing the effect of the coolant, on the results of Jominy end-quench tests and P-V tests on the same high carbon tool steels. (See Table VIII.) It may be of interest to record a similar comparison made with 0.39% carbon steel, tested in triplicate by the P-V method and in duplicate by the

end-quench method. One side of the P-V specimen was tested on the N-30 Rockwell, the other with C scale. The Jominy specimens were tested on the opposite sides of the bar with standard $\frac{1}{16}$-inch spacing, starting one side at $\frac{1}{32}$ inch to provide closer readings. The P-V tests were quenched from 1550 F and were practically identical with a previous set of triplicate tests quenched from 1450 F. The Jominy tests were quenched from 1500 F.

This steel had the following composition: 0.39% carbon, 0.73% manganese, 0.018% phosphorus, 0.048% sulphur, 0.22% silicon—thus being high enough in manganese to give it a moderate hardenability. It had been normalized from 1650 F to Brinell hardness 170.

Fig. 17 shows the results. In both tests the N-30 readings indicate a slightly higher penetration than the C-scale readings, as has doubtless been noticed in other comparative tests previously described in this paper—an effect of the slight error in equivalence of the two scales shown in Wilson Mfg. Co.'s chart No. 38 (used in our comparisons).

Cooling Rates

Since so much of the practice of hardenability testing and the theory of hardenability is based on the conception of cooling rate through the $Ar_{1,2,3}$ transition, it will be of interest to describe some tests we have made with the P-V specimens. Our automatic recording apparatus[11] was quite similar to that described by Greninger in Transactions, Vol. 30, 1942, p. 8.

In preliminary work with this apparatus, we calibrated it by repeating some work on Jominy bars contained in O.S.R.D. Report No. 3743 by Boegehold and Weiuman. Our results for cooling rates at 1300 F and for cooling time in seconds from 1350 to 900 F checked with O.S.R.D. work quite closely.[12]

The calibration of the P-V tests was made with both $\frac{1}{8}$-inch double-hole insulators and 24-gage thermocouples and $\frac{1}{16}$-inch double-hole insulators and thermocouple wire 0.010-inch diameter for $\frac{1}{2}$-inch length at the hot junction. (See Fig. 18.) A series of seven P-V wedges were drilled centrally from the square end, the depth of the hole being such that the thermocouple junction was at progressively further distances from the chisel edge of the test piece. All test pieces were later sectioned and measured with micrometer

[11]Editor's Note: Photographs and wiring diagram were contained in Mr. Shepherd's original manuscript.

[12]Editor's Note: Complete data submitted, and on file in ASM Library.

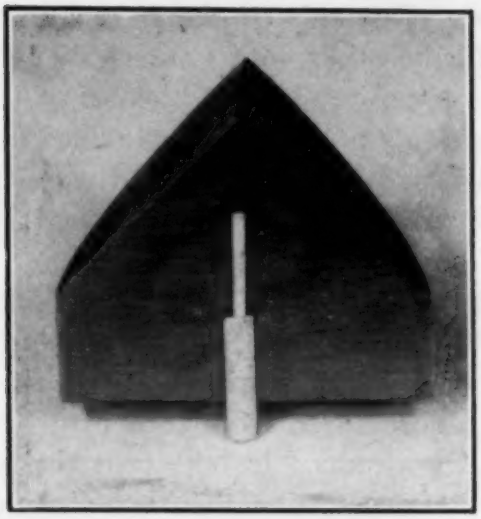


Fig. 18—Sectioned P-V Test Showing Insertion of Thermocouple Insulators.

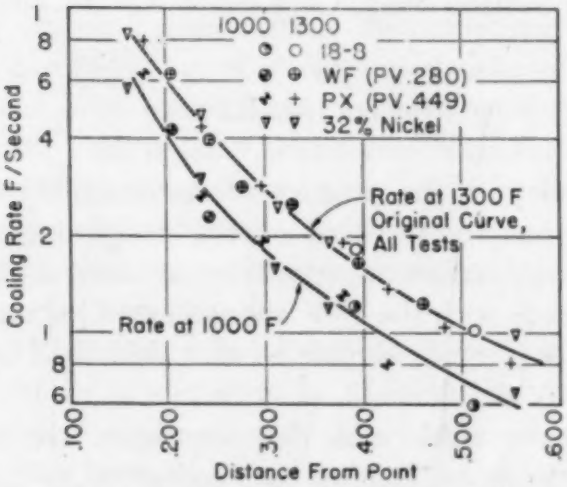


Fig. 19—Cooling Rates at 1300 F at Various Positions in P-V Specimens Below Chisel Edge.

microscope to determine the actual distance of hole-end from the point. The first tests made with the 1/8-inch hole showed that the presence of the insulator did not alter the hardness pattern.

Cooling curves were constructed in this way for a 32% nickel-iron alloy, an 18-8 stainless steel (both of which have no transformations in the temperature range under investigation) and two tool steels of P-V values 0.280 and 0.449 inch respectively. Cooling rates in the quenching fixture, in degrees Fahrenheit per second at 1300 F, are shown in Fig. 19, wherein each plotted point is an average of from two to ten tests. It is seen that the correlation of the results is quite good.

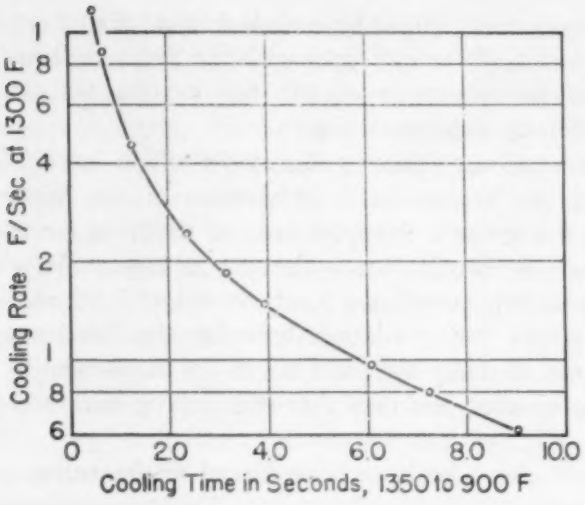


Fig. 20—Relation Between Cooling Rates at 1300 F and Cooling Time Between 1350 and 900 F.

The correlation between cooling rates at 1300 F and cooling time in seconds from 1350 to 900 F was taken from cooling curves of the 32% nickel-iron alloy; each plotted point is the average of from two to ten tests (Fig. 20).

Conclusion

In conclusion I wish to express my appreciation to George Diehl; the Metallurgical Staff of Ingersoll-Rand Co. (particularly F. J. Miller for his patience in making thousands of hardness determinations); Peter Payson of Crucible Steel Co. of America for his stimulating discussions on this subject; to C. B. Post of Carpenter Steel Co. for the 32% nickel-iron used in the calibration tests; R. Sergeson of Rotary Electric Steel Co. for heat A-67, and to E. E. Thum of the ASM staff for his editorial work on the manuscript herewith presented.

DISCUSSION

Written Discussion: By G. A. Roberts and H. G. Johnstin, chief metallurgist and metallurgical engineer respectively, Vanadium-Alloys Steel Co., Latrobe, Pa.

The data presented in Mr. Shepherd's paper clearly reveal the simplicity and reproducibility of the P-V test in determining the hardenability of shallow hardening tool steels. The test has been in use in our laboratory for some time and has proved itself to satisfy the demand for a sensitive end-quench test applicable to those steels with ideal critical diameters under 1 inch. Especially

is it applicable to those steels which have ideal critical diameters between ½ and ¾ inch. The correlation of cooling rates with the distance from the apex of the V permits practical interpretation of the test results on the basis of more complicated commercially important shapes.

It should be pointed out that for the steels which have P-V distances of less than 0.300 inch, an acceptable determination of the hardenability can be made by measuring the distance from the apex of the V to the end of the darkly etched zone and that for routine work the test is applicable without resorting to the somewhat more time-consuming hardness determinations. For the deeper hardening grades where the gradation between the hardened case and the unhardened core is not so sharp the accuracy of the hardenability rating obtained by etching may be somewhat less than that obtained by taking hardness readings along the sample.

For those laboratories who have been forced to determine hardenability on different sized disks or different sized rounds for each and every heat manufactured, the P-V test yielding the same results with only one sample is a welcome addition to our hardenability testing techniques.

Written Discussion: By W. H. McCormick, chief metallurgist, Crucible Steel Company of America, Park Works, Pittsburgh.

Mr. Shepherd is to be complimented on the development of a very practical test for the determination of hardenability in shallow hardening steels. He has demonstrated very clearly that the test he has devised is not only reproducible in his own laboratory but also may be used with accuracy by anyone having a minimum of laboratory equipment. To illustrate its practicability, we would like to describe a test which we have used in our laboratory for a number of years. This test was developed in conjunction with the Crescent Tool Company in co-operation with their metallurgist, J. P. Whalen, and has been used to evaluate hundreds of tons of shallow hardening steel. In describing the requirements for a test for shallow hardening steels, Mr. Shepherd points out that it must have sensitivity, accuracy, interchangeability and must be relatively inexpensive. The test we have employed meets most of these requirements, but certainly does not approach the accuracy of the P-V test.

Our test is a simple chisel-type test which is made by forging a ¾-inch round bar to a chisel shape with a 15-degree taper. This sample is normalized to provide a uniform prior structure, then ground to remove surface bark. It is then heated in a lead pot to a distance of at least 1 inch beyond the taper. It is then quenched, sectioned longitudinally, ground and etched. The samples are rated by measuring the distance from the point to the end of the martensite zone. Mr. Shepherd has pointed out particularly that the variable in his test which will produce the greatest error is the angle of the specimen. It is to be noted, in the simple chisel-type test which we have described, that no unusual precaution is taken to insure that the angle is exactly 15 degrees. Over a period of years, however, we have found that it is entirely possible to rate heats using this method and to set up specifications based on minimum and maximum length of the martensite zone. Obviously, Mr. Shepherd has shown that with his P-V test these shallow hardening steels can now be rated precisely.

It has been our experience that attempts have been made frequently to

utilize the standard P-F test for the determination of the hardenability of shallow hardening steels to a more precise degree than was originally contemplated when this test was developed. The original test was designed to measure the case rather approximately by means of an inclined scale, including as the hardened zone only the depth of the dark-etching constituent. This zone may of course be determined more accurately by polishing, etching and measuring under the microscope from the 50% martensite zone. When this is done it is quite obvious that errors in measurement are quite significant because of the relatively narrow martensite zone. The P-V test, however, magnifies the martensite zone and thus decreases the magnitude of error.

As stated previously, we believe the P-V test is entirely practical and reproducible in the average laboratory. We see no reason why it cannot be used by any laboratory technician, and predict that in a very short while it will become just as popular as the standard Jominy test.

Written Discussion: By D. W. Kaufmann, metallurgist, Halcomb Works, Crucible Steel Company of America, Syracuse, N. Y.

The author of this paper is to be congratulated for providing us once again with a test which no doubt will be as widely adopted as his P-F test. One of the outstanding characteristics of Mr. Shepherd's work is the truly scientific manner in which it is conducted. It is evident from this paper that every phase of the P-V test has been investigated with extreme care in order to eliminate all possibility of error due to mechanical variables. While Howard J. Stagg has maintained most of our contact with this development in the past two years, the writer had the pleasure of discussing the program with the author in his laboratory some time ago and can report that every minute detail had been checked and rechecked many times to insure the accuracy of this method of determining the hardenability of shallow hardening steels.

We naturally were interested in this test, as we are vitally concerned with any method of improving the control of quality in steel, and immediately adopted the P-V test on a trial basis in our laboratory. The standard Jominy end-quench test has been our tool for controlling the deeper hardening steels since the time of its development, and we have used the P-F and the Shepherd slab tests for many years for the shallow hardening steels. However, the latter tests require a highly skilled technician and even at best the results are not sufficiently reproducible when one deals with the grades which are just a little too shallow hardening for accurate Jominy determinations.

As a result of the author's clear instructions, the machining of the P-V quenching fixture from Rezistal 303 in our laboratory machine shop presented no difficulties. While we could have made the special fixture for the Rockwell machine also, we followed the author's advice and purchased it. The preparation of the test samples was a simple matter and we are now conducting P-V tests on carbon tool steel on a routine basis.

While we undoubtedly will continue to determine the fracture grain size of tool steel by the P-F procedure, the indications are that the P-V test will supplement that method for determining the hardenability of the carbon and relatively shallow hardening low alloy tool steels.

As a matter of interest, since the author was careful to correlate the P-V

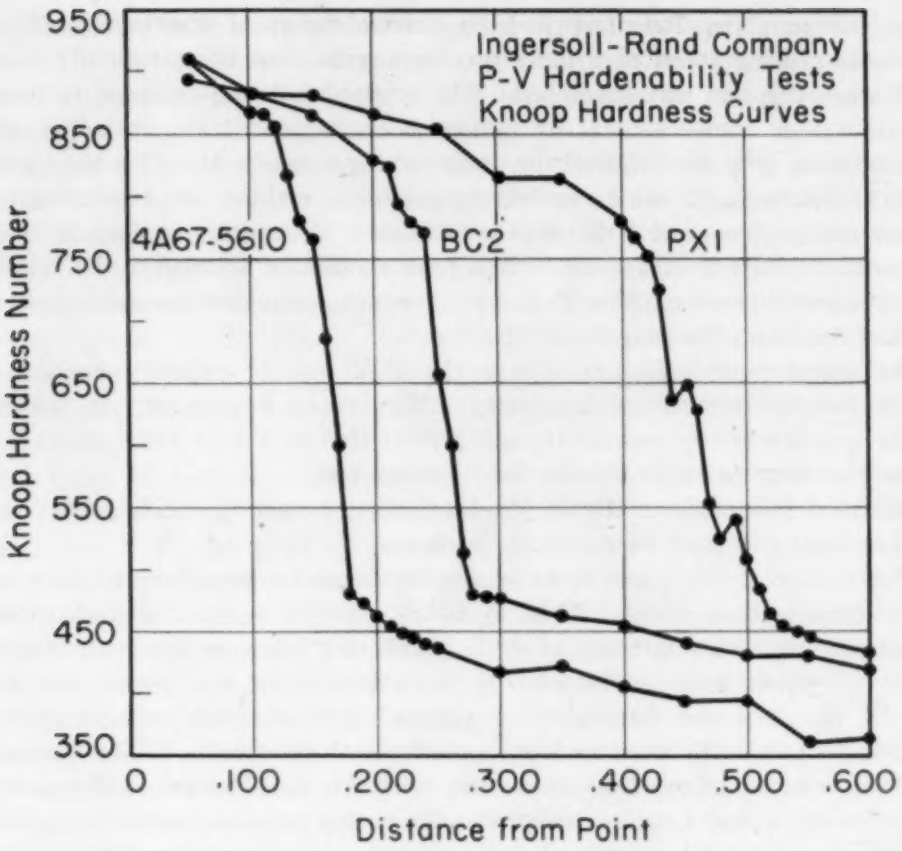


Fig. A—P-V Hardenability Tests. Knoop hardness curves.

values as measured by several of the various methods of hardness testing, we investigated a few samples using the Tukon hardness testing equipment. P-V specimens 4A67-5610, BC-2 and PX-1 were polished for microscopic examination, care being exercised to maintain a flat surface with sharp corners. These were tested with a load of 1000 grams and the impressions measured with a 10.25-millimeter objective lens. Determinations were made every 0.050 inch from the vertex except in the region of the case-core junction where the readings were taken every 0.010 inch. The resulting P-V curves are shown in Fig. A. Converting 650 Knoop to Rockwell C-55, the P-V values of the three samples determined in this manner as compared to the author's results are as follows:

Code	I.R.	Tukon
4A67-5610	0.162	0.163
BC-2	0.256	0.253
PX-1	0.456	0.440

It will be noted that the curve for PX-1 is not smooth. This is due to the more gradual transition from case to core in the deeper hardening heats with the result that the very small Tukon impressions are affected by the mixture of hard and soft areas. If a smooth curve is drawn through the points in the transformation zone for this steel the resulting 0.450 P-V value checks more closely with the author's results.

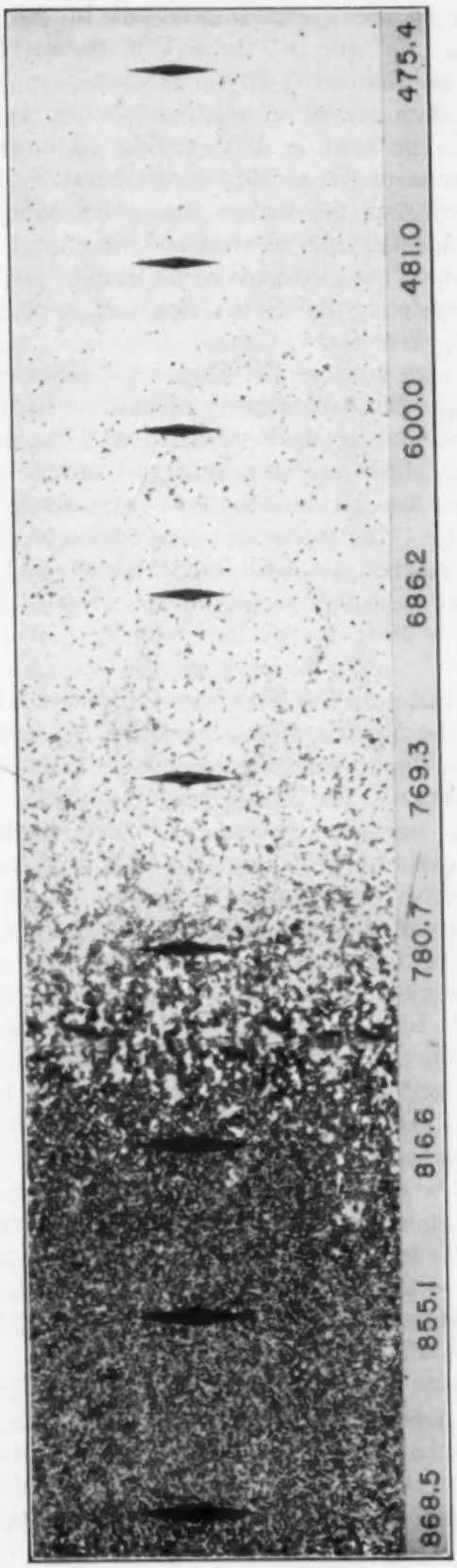


Fig. B—P-V Hardenability Tests. Knoop hardness tests. Etchant 5% nital. Original magnification × 100. Reduced ½ in reproduction.

Fig. B illustrates the Tukon impressions in the first specimen after a metallographic etch. As expected, the P-V distance (650 Knoop) corresponds to the structure of approximately 50% martensite.

The foregoing data are of an academic nature, as the Tukon instrument normally would not be used in P-V testing. However, it adds one more confirmation of results to the already comprehensive coverage of possibilities.

It would appear that the author has added another valuable means of improving the quality standards of steel and we expect that the P-V test will assume its place among the guardians of uniformity for the tool steel industry.

Written Discussion: By S. C. Spalding, metallurgical engineer, The American Brass Co., Waterbury, Conn.

We have read with interest Mr. Shepherd's paper outlining the use of the P-V test to determine the hardenability of shallow hardening steels. We find here described a new tool for the determination of the depth hardening characteristics of steels quenched from an austenitized state. We have other tools for this same purpose but the one described here is relatively simple and inexpensive in preparation and use. The author has gone to considerable length to show the reproducibility and correlation with other hardenability tests and, although it is not claimed that any new properties are revealed by it, it seems to correlate well with other tests and by its simplicity perhaps extend the scope of such testing.

A point of interest was the showing of this test on the effect of delayed quenching. Under the heading "Transfer Time" the author has indicated that delaying the quench by holding the piece after removing from the furnace increases the penetration. The usual recommendations for hardening call for quenching on a rising or stationary heat. This data would indicate that hardenability could be increased by quenching on a falling heat. We believe this point is well worth the further investigation the author indicates will be made.

We are also interested in the indications of the test as shown in Fig. 14, that increased soaking time increases hardenability in most all cases shown. This causes us to wonder about some of the recommendations put out by the trade to quench on a rising heat and particularly not to soak.

In the section on effect of hardening temperature, the test results show that penetration of hardness decreases with increasing hardening temperature. This, we believe, is contrary to general knowledge and deserves some further explanation by the author.

The author is to be congratulated on the development of the new test method and in the very thorough way in which its possibilities and accuracies have been determined. We look forward to further papers from the author on this most interesting subject.

Written Discussion: By Henry Wysor, metallurgical engineer, Bethlehem Steel Co., Bethlehem, Pa.

Mr. Shepherd not only knows how to get around mechanical difficulties but he can elucidate a perplexing subject in a most understandable way. With the exhaustive work that has been done in developing the Jominy test for deep hardening steels, and now with this demonstration before us of a precision method for testing carbon steels, we are pretty well convinced that the end-

quench principle, as exemplified by these two methods of testing, is the best that has thus far been advanced.

After looking at the technique of the P-V test and the tabulations, much of which is here presented, it is difficult to offer anything but commendation for this work. However, believing as I do that the P-V test offers much wider adaptability than it now enjoys and having in mind particularly its use in steels of lower carbon range, I think the test piece should not be cut from the axis of the specimen. In the high carbon steels that Mr. Shepherd is using and in consideration of the manufacturing practice, he gets very little effect from segregation. With steels of lower carbon content, and rolled from large ingots, segregation would undoubtedly be more of a factor and it would be the part of wisdom to follow standard procedure in principle by cutting the test piece from midway between the central axis and the surface.

Written Discussion: By A. P. Terrile, Metallurgical Department, Crucible Steel Company of America, Pittsburgh Crucible Division, Midland, Pa.

Mr. Shepherd is to be congratulated for this excellent contribution to hardenability and hardenability testing.

Many tests have been devised to evaluate the hardenability of shallow hardening steels, but none in our opinion approach the practical utility of the P-V test.

We have been fortunate in having been in contact with the development of the P-V hardenability test, and therefore fully appreciate the painstaking detail with which Mr. Shepherd covered and developed every phase of the P-V test method. Various types of specimens with different sizes and angle tapers were experimented with before it was decided to select the present 1½-inch round, 90-degree taper specimen. Various types of spray design and different size and spacing of holes were tried before the present type of slots and fixture was employed.

This careful research resulted in close reproducibility of hardenability test values. Reproducibility of results is one of the most important factors when considering the use of any laboratory test, particularly when a commercial application of heats is involved.

We have for more than a year been successfully using the P-V test in collaboration with the Ingersoll-Rand laboratory for the application of high carbon heats which must meet Jack Bit hardenability requirements.

The importance of prior structure and its effect on hardenability values is no doubt familiar to most metallurgists.

In order to illustrate the effect of two pronounced differences in prior structure on P-V hardenability, the following experiment was conducted:

Two high carbon shallow hardening steels, one very shallow hardening and one considerably deeper hardening as judged from previous P-V tests, were selected.

Representative forged 1½-inch rounds from each heat were oil-quenched from 1600 F (870 C) for the series covering a fine pearlite-type structure, and another group were annealed in such manner as to develop a thoroughly spheroidized prior structure. P-V hardenability was run from a quenching temperature of 1450 F (790 C). Time at austenitizing temperature was varied

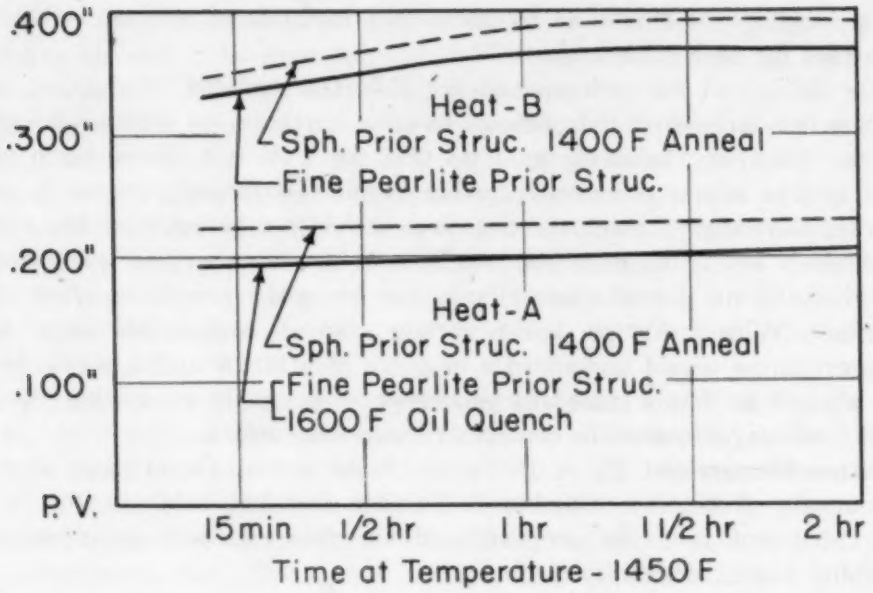


Fig. C—Prior Structure Effect on P-V Values.

from 15 minutes to 2 hours to determine whether or not the prior structure effect would be minimized or possibly eliminated. Table A shows the comparative P-V values obtained on the steels. The prior structure effect is shown clearly by the graphs, Fig. C.

In both steels, a consistently deeper penetration was obtained hardening from the spheroidized prior structure.

The deeper hardening heat showed the increase in penetration more pronounced at the 1½-hour and 2-hour holding times at 1450 F (790 C). The more shallow hardening heat was opposite in this effect, the greater increase in penetration showing uniformly from the 15-minute holding time to 1 hour and then decreasing to the same degree at 1½ to 2 hours.

Table A
P-V Prior Structural Experiment

Prior Structure	P-V Hardenability Quench—1450 F Held at Temperature as Shown Average of 2 Sides of Specimen 15 Min.	30 Min.	1 Hr.	1¼ Hr.	2 Hr.	P-V Increase
Quench in oil 1600 F. Fine pearlite.	0.191	0.193	0.197	0.205	0.205	0.014
Spheroidized—1400 F. Furnace-cooled.	0.222	0.222	0.227	0.226	0.226	0.004
Increased penetration. Spheroidized structure.	0.031	0.029	0.030	0.021	0.021	....

Code	C	Mn	Si	Ni	Cr	Mo
A	1.00	0.21	0.19	0.14	0.07	0.01

Quench in oil 1600 F. Fine pearlite	0.331	0.349	0.364	0.367	0.367	0.036
Spheroidized—1400 F. Furnace-cooled.	0.348	0.367	0.382	0.391	0.391	0.053
Increased penetration. Spheroidized structure.	0.017	0.018	0.018	0.024	0.024	....

Code	C	Mn	Si	Ni	Cr	Mo
B	0.96	0.46	0.39	0.09	0.11	0.01

The fine pearlitic type prior structure of the more shallow hardening steel resulted in 0.014 inch deeper penetration at 2 hours as compared to the 15-minute holding time before quenching.

The spheroidized prior structure of this heat showed only negligible change in penetration as time at temperature was increased.

Time at temperature showed more increased penetration for the deeper hardening heat, the greatest increase occurring with the spheroidized prior structure.

No attempt at this time will be made to explain the differences in hardenability shown.

The experiment serves to show the accuracy and sensitivity of the P-V method in evaluating even slight differences in hardenability and also indicates the reproducibility and consistency of results obtained.

Written Discussion: By G. V. Luerssen, assistant chief metallurgist, The Carpenter Steel Co., Reading, Pa.

The details of the P-V test are so thoroughly and capably covered in this paper that Mr. Shepherd leaves little room for constructive criticism on the test itself.

Mr. Shepherd is to be commended on another of a long list of fine contributions to the technology of hardenability testing of shallow hardening steels. The paper is particularly welcome as it indicates a continuation of the trend away from purely empirical tests toward those yielding specific hardenability values. This is of considerable importance to the tool steel manufacturer, who is confronted with various specifications embodying hardenability. In order to meet these successfully it has become necessary for him to adopt, for the control of his product, a test which yields a specific hardenability value expressed in terms of critical cooling velocity, which value can then be correlated with the various empirical tests.

In our own plant we have used routinely for several years the cone test developed by Greene and Post, and for purposes of comparison it would be extremely interesting to have determinations of specific hardenability made by both the P-V test and the cone test on the same steel.

Written Discussion: By P. Payson, Research Laboratory, Crucible Steel Company of America, Newark, N. J.

It is probable that no testing technique for use in the steel industry was ever introduced with the thoroughness with which Mr. Shepherd presents his P-V test. Throughout his paper it is evident that he constantly had in mind the problems that might be encountered by those who would wish to use the test. He gives in full detail the preparation of the wedge-shaped test piece, the design of the quenching fixture, the procedure for sectioning the test piece after it has been hardened, and the description of the device for making the accurate hardness survey of the sectioned test piece. In all these the practicability of the test is emphasized. But the author has also given thought to all the metallurgical factors that may affect the reproducibility of the results—the dimensions of the test piece; the quenching medium, whether water or brine, or cold or warm; the temperature and time for austenitizing the test piece; the transfer time from furnace to quenching fixture; and the possible effect of tempering during the

sectioning of the test piece on the hardness of the steel at the critical zone. Finally, Mr. Shepherd measured the cooling of different positions of the wedge test piece during the quench so that data would be available for comparison with other methods of quenching steel.

Mr. Shepherd's name has for many years been associated with the most widely accepted tests for establishing the hardenability of shallow hardening steels. If he has seen fit to devise a new procedure which in his opinion is superior to the test methods which he himself developed, it seems safe to conclude that the Shepherd P-V test will rapidly replace the Shepherd P-F test which has been used in the steel industry for over 10 years.

I think it would be helpful if the author presented the cooling curves for the significant positions in the wedge test pieces during the quench. In my opinion the time to cool from about 1200 to 800 F (650 to 425 C) is of more significance in the hardening of shallow hardening steels than the cooling rates at 1300 and 1000 F (705 and 540 C).

Finally, I would like the author to elaborate, if he will, on the two interesting facts which his very sensitive P-V test has disclosed, namely, the increase in hardenability with increased delay between the removal of the test pieces from the furnace and the start of the quench; and the decrease in hardenability with increase in austenitizing temperature from 1450 to 1600 F (790 to 870 C). Both of these, and particularly the latter, seem paradoxical.

Author's Reply

The interest exhibited by the discussions of this paper is much appreciated.

Messrs. Roberts and Johnstin are correct that a measure of hardenability may be made by etching the P-V slab. We find, however, that instead of being "time consuming", determination by hardness tests is quicker than the total time required to heat acid, etch, wash and measure. The etching time variable is eliminated and a more consistent and precise result obtained.

Etching is not very satisfactory on shallow hardening steels which are not tool steels. The P-V test is intended to cover these materials. There is, necessarily, an overlap between the P-V test used for shallow hardening steels and the Jominy test used for medium and deep hardening steels where either test would satisfactorily measure hardenability.

Mr. McCormick has shown a practical utilization of the increase in depth of hardening obtained on a simple chisel test to determine hardenability which has been in use for years.

Present usage of hardenability seems to demand more precise measurements of this characteristic. The P-V test makes no claim to originality of design. The influence of most of the factors influencing such a test has been investigated. The utilization of a spray fixture and hardness surveying stage permits the measure of hardenability to take place under uniform conditions.

The test is also attractive as a means of study of the metallographic structures occurring as a result of different cooling rates, austenitizing conditions, etc., due to the compactness of the specimen.

The additional information provided by Mr. Kaufmann on use of the Tukon tester in determining P-V value is very interesting and valuable. Hardness

tests cover a small area and are necessarily influenced by "segregation" or "fiber". A close look at the case and core junction of a tool steel will show that minute segregation exists even in these high quality materials. If present to an abnormal degree it will result in a jagged P-V curve as shown by Mr. Kaufmann. When such a condition is found, we merely shift the specimen 0.015 to 0.030 inch right and left of the axial line and make two more hardness surveys. This is easily done on the stage. The variation of these readings is used to indicate degree of "fiber" in the steel.

Mr. Spalding's comment that ". . . . its simplicity perhaps extend the scope of such testing" is particularly appreciated.

I do not as yet have complete data to answer the questions regarding transfer time and temperature but offer the following.

First, the general usage of cooling rate at 1300 F (705 C) as a criterion of hardenability is subject to criticism. Cooling rates at 1300 F (705 C) give a general indication of the cooling time in the temperature range where transformation is most likely to occur.

The S-curve shows the tendency to transform at constant temperature but commercial quenches involve continuously changing temperatures.

If carbon tool steels are cooled to 800 F without transformation, they will not transform until the Ms temperature is reached. The cooling time from a temperature at which they are austenitic, i.e., 1300 F (705 C), to a temperature below which transformation products will not form (under commercial quenching conditions), i.e., 800 F (425 C), is a much better criterion of the amount of breakdown of austenite to transformation products or stability of the austenite.

Let us examine the effect of delaying the quench on two P-V specimens of 1% carbon steel having a P-V value of 0.347 inch, maintaining, of course, the same prehardening structure and austenitizing conditions. Thermocouples are inserted in each specimen along the axial line. One specimen, No. 21, is held in air until 3 seconds before quenching.

Specimen	Time Furnace Door Open to Water On sec.	Distance Thermocouple from Point inch	Cooling Rate at 1300 F degrees	Cooling Time 1300 to 800 F sec.
14-B	12.6	0.352	210	4.55
21	29.4	0.349	200	3.60

The lower cooling time in the 1300 to 800 F region gives less time for the austenite to transform and offers a tentative explanation of the increased depth of hardening obtained by a delayed quench.

As long as soaking does not increase the grain size or decarburize the surface what harm can result? Any soaking has tendency to increase the homogeneity of the austenite. Trade recommendations follow the same story year after year and are, of course, governed by general trade conditions.

The statement is often made that quenching temperatures do not affect the cooling rate at 1300 F. The cooling time, 1300 to 800 F, is, however, definitely affected and as shown previously, this time is the real criterion in affecting breakdown of the austenite. Samples of an 0.80% carbon steel were quenched in duplicate from 1450 and 1600 F, one of each pair containing a

thermocouple, same prehardening structure and austenitizing conditions maintained.

Quench Temp. F	Thermocouple Dist. from Point inch	Rate at 1300 F degrees	Time 1300 to 800 F sec.	P-V Value to 73 (N-30) inch
1450	0.296	308	2.35	0.297
1600	0.304	320	2.70	0.279

The greater cooling time of the 1600 F (870 C) quench in the 1300 to 800 F (705 to 425 C) range gives the time necessary for a little more transformation than 1450 F (790 C) quench even though the rate at 1300 F (705 C) is slightly greater at a distance slightly further from the point.

The samples were equally free from residual carbides and had about the same grain size.

Further work is under way and indicates that the cooling time 1300 to 800 F (705 to 425 C) for the same cooling rate varies according to the shape of the piece.

Mr. Wysor raises a point that should be continually borne in mind in any test—tensile, hardness, chemical, etc.—i.e., the test specimen must be representative of the piece. An inspection should be made for segregation by conventional methods and the test specimen located accordingly.

Mr. Terrile has shown the importance of controlling the prehardening structure and austenitizing conditions. These factors must be continually emphasized. His data show the sensitivity and accuracy of the P-V method.

Mr. Luerssen's specialized experience in hardenability testing makes his comments welcome. The cone test has been used in our laboratory since its initiation but is limited to the shallowest hardening steels. It was discarded for routine testing on account of the tremendous amount of grinding required and the fact that duplicate tests require an additional cone, i.e., hardness tests are made only along the center axis.

We hardened a cone specimen from a heat of 1% carbon steel having an average P-V value of 0.347 inch and checked this by means of the hardness tests and the magnetic method of Post.

	Critical Cooling Velocity
Hardenability value—P-V method	0.347 inch or 210°/sec. at 1300 F
Cone Method—Equivalent Cone Tip	0.810 inch or 136°/sec. at 1300 F
Cone Method—Magnetic Determination*	170/175°/sec. at 1300 F

We found that decreasing the angle of the P-V specimen which made it approach the angle of the Carpenter cone test was undesirable. The length of specimen was increased without any gain in sensitivity or accuracy. In fact, the effect of minute segregation present in even high grade steel resulted in a very jagged hardness vs. depth curve.

Mr. Payson's request for cooling curves will be met by incorporating this data in a new paper. This will also prove Mr. Payson's point, i.e., the cooling time is the controlling factor and more significant than rate. This time, however, should be taken from a top point at which the steel is still completely austenitic,

* Made by courtesy of Carpenter Steel Company.

i.e., 1300 F (705 C). Cooling has gained momentum at this point so that it is not affected by the variations in time which occur above this temperature, i.e., removal from furnace, etc. At 1200 F (650 C) transformation may be in progress and will affect the cooling time. On carbon shallow hardening steels 1300 to 800 F (705 to 425 C) is a satisfactory range but on alloy steels some lower temperature will be more satisfactory.

The final questions have been dealt with earlier in this discussion.

THE EFFECT OF MANGANESE ON THE PROPERTIES OF CAST CARBON AND CARBON-MOLYBDENUM STEELS

By N. A. Ziegler, W. L. Meinhart and J. R. Goldsmith

Abstract

The results of an investigation on the effect of manganese on thermal characteristics, microstructures, physical properties and weldability of "plain carbon" and carbon-molybdenum cast steels are presented.

Increasing the manganese content of these steels develops a gradual increase in the thermal sluggishness and hardenability which is less pronounced than that occurring with molybdenum or nickel additions to chromium steels. Complete suppression of the transformations on relatively slow cooling and marked air hardening are not produced until manganese is raised to about 2%. In this regard, manganese has the greatest effect on the "carbon-molybdenum" and "higher" carbon steels.

Raising the manganese content to about 1.5% in "plain carbon" and to about 1.0% in carbon-molybdenum steels increased the tensile strength approximately 20% as compared with similar steels containing about 0.5% manganese. A small decrease in ductility likewise occurred. However, these steels with the above manganese additions developed almost the highest impact resistance of the group tested.

Experiments performed on the welding of these steels indicate that no difficulties should be encountered, provided the manganese content does not exceed about 2%.

Introduction

In one of our previous publications (1)[1] it was pointed out that manganese in amounts of over 1% has some effect on the physical properties, thermal characteristics, hardenability and weldability of cast carbon and carbon-molybdenum steels. The bibliography at the end of this paper is a testimony of considerable work done and informa-

[1]The figures appearing in parentheses pertain to the bibliography appended to this paper.

A paper presented before the Twenty-eighth Annual Convention of the Society held in Atlantic City, November 18 to 22, 1946. Of the authors, N. A. Ziegler is research metallurgist, W. L. Meinhart is assistant research metallurgist, and J. R. Goldsmith is metallurgical engineer in charge of Research Foundry, Crane Company, Chicago. Manuscript received June 20, 1946.

tion accumulated on the effect of manganese on various properties of different types of steels. As is well known, a certain amount of manganese is added to all steels for deoxidizing or general scavenging functions, and for neutralizing the harmful effects of sulphur. There also are several grades of steels known to which manganese is added as an alloying element and which, therefore, are classified as "manganese" steels.

However, it was believed desirable to obtain additional information which would determine more closely the dividing line between "plain carbon" or "carbon-molybdenum" and a so-called "manganese" steel. Likewise, some systematic studies on the variation in different physical properties as a function of manganese content were also wanted. All this was particularly true regarding cast and heat treated steels.

Experimental Procedure

The selected line of approach to this problem was very much the same as that used in studying the effect of copper on the same types of steels, described in one of our previous publications (1).

A series of experimental melts was prepared in a 200-pound, high-frequency induction furnace, using low carbon steel scrap as raw material and conventional melting and deoxidizing technique. Each heat was killed by an addition of about 2 pounds of aluminum per ton, tapped into a 250-pound capacity ladle, and cast into keel coupon blocks, using green sand molds. This series of steels is divided into two groups: (a) "plain carbon" (Table I), and (b) "carbon-0.5% molybdenum" (Table II). Each group is subdivided into three subgroups: (a) steels containing under 0.1% carbon, (b) steels containing about 0.15% carbon, and (c) steels containing about 0.30% carbon. Each subgroup consists of eight or more steels with manganese ranging between about 0.5 and 4.0%.[2]

Each coupon block was sectioned into convenient blanks and heat treated by normalizing from 1700 F (925 C). The normalized blanks from each heat were divided into two groups, one of which was drawn at 1200 F (650 C) and the other at 1250 F (675 C).[3] Blanks thus treated were subjected to tensile,[4] Brinell hardness, and Charpy impact testing.[5] The latter test was performed at (a) room temperature and

[2]Some of these compositions, marked with an asterisk in Tables I and II, were cast in coupon blocks and "welding plates". The latter were used for performing welding experiments.

[3]As may be noted from Tables I and II, some of the compositions were subjected to only one drawing treatment.

[4]Standard 0.505-inch diameter, 2-inch gage test bar.

[5]Standard Charpy test bar with a keyhole notch.

Table I
Carbon-Manganese Steels

Serial No.	Nominal Composition Si	Mn	Mo	C	Chemical Analysis Si	Mn	S	P	C	Mo	Cr	Ni	Dilatometer Data 5 Hr. Cool Run No.	V.P.N.	Air Cool Run No.	V.P.N.	Hard. As Cast B.H.N.
1	0.20—0.45	0.5	0	0.1	0.30	0.29	0.025	0.023	0.07	0.03	0.03	...	1255	105	1256	115	101
*2	0.20—0.45	0.5	0	0.1	0.28	0.46	0.018	0.023	0.07	...	0.03	...	....	...	....	...	...
3	0.20—0.45	0.5	0	0.1	0.32	0.57	0.028	0.023	0.07	0.03	0.03	...	1258	110	1257	120	104
4	0.20—0.45	1.0	0	0.1	0.30	0.96	0.030	0.022	0.06	0.03	0.08	...	1259	111	1260	124	116
5	0.20—0.45	1.5	0	0.1	0.31	1.27	0.025	0.023	0.06	0.03	0.03	...	1262	113	1261	133	109
6	0.20—0.45	2.0	0	0.1	0.32	1.70	0.026	0.024	0.08	0.10§	0.03	...	1263	140	1264	170	159
*7	0.20—0.45	2.0	0	0.1	0.44	2.05	0.015	0.018	0.10	...	...	...	....	...	....	...	...
8	0.20—0.45	3.0	0	0.1	0.33	2.95	0.013	0.023	0.08	...	0.04	...	1348	238	1347	262	...
9	0.20—0.45	4.0	0	0.1	0.51▼	3.94	0.096	0.023	0.12†	0.27§	0.03	...	1297	363	1298	405	331
*10	0.20—0.45	0.5	0	0.15	0.38	0.55	0.028	0.021	0.15	...	...	...	....	...	....	...	...
11	0.20—0.45	0.5	0	0.15	0.33	0.57	0.031	0.021	0.13	0.03	0.18¶	...	1266	110	1265	136	121
12	0.20—0.45	1.0	0	0.15	0.34	0.90	0.030	0.022	0.10	0.03	0.15¶	...	1267	125	1268	160	138
*13	0.20—0.45	1.0	0	0.15	0.45	1.34	0.022	0.019	0.18	...	...	...	....	...	....	...	...
14	0.20—0.45	1.5	0	0.15	0.34	1.72	0.027	0.023	0.13	0.05	0.05	...	1269	137	1270	168	163
15	0.20—0.45	2.0	0	0.15	0.39	2.27	0.020	0.023	0.15	0.05	0.15¶	...	1280	193	1279	225	237
*16	0.20—0.45	2.0	0	0.15	0.57▼	2.31	0.029	0.027	0.20	...	...	...	....	...	....	...	...
17	0.20—0.45	3.0	0	0.15	0.43	3.22	0.021	0.033	0.16	...	0.06	...	1345	363	1346	339	...
*18	0.20—0.45	3.0	0	0.15	0.57▼	3.40	0.030	0.019	0.18	...	...	...	....	...	....	...	...
19	0.20—0.45	4.0	0	0.15	0.42	4.10	0.025	0.021	0.20†	0.05	0.13¶	...	1281	464	1282	473	...
20	0.20—0.45	0.5	0	0.30	0.32	0.60	0.026	0.022	0.28	0.03	0.07	...	1449▲	146	1450▲	160	143
*21	0.20—0.45	0.5	0	0.30	0.49▼	0.83	0.031	0.026	0.30	...	0.03	...	....	...	....	...	...
22	0.20—0.45	1.0	0	0.30	0.52▼	1.20	....	0.023	0.32	0.03	0.03	...	1332	182	1331	191	189
23	0.20—0.45	1.5	0	0.30	0.42	1.56	0.022	0.021	0.21‡	0.03	0.03	...	1289	173	1290	199	197
*24	0.20—0.45	2.0	0	0.30	0.52▼	1.60	0.026	0.018	0.30	...	0.05	...	....	...	....	...	...
25	0.20—0.45	2.0	0	0.30	0.43	1.92	0.024	0.021	0.31	0.03	...	...	1291	196	1292	254	241
26	0.20—0.45	2.0	0	0.30	0.50▼	2.56	0.022	0.021	0.29	0.03	...	...	1293	312	1294	330	293
*27	0.20—0 49	3.0	0	0.30	0.61▼	2.78	0.028	0.025	0.30	...	0.03	...	....	...	....	...	...
28	0.20—0.45	3.0	0	0 30	0.44	3.54	0.014	0.024	0.26	...	0.21¶	...	1344	514	1343	514	...
29	0.20—0.45	4.0	0	0.30	0.54▼	4.08	0.021	0.020	0.28	0.12§	...	...	1296	514	1295	542	...

*Steels used in welding experiments.
†"High" carbon.
‡"Low" carbon.
§"High" molybdenum.
¶"High" chromium.
▼Silicon higher than 0.45%.
▲Dilatometer curves taken on heat containing 0.35% Si, 0.69% Mn, 0.032 % S, 0.019% P, 0.29% C, 0.03% Cr.

Table I—(continued)
Carbon-Manganese Steels

Serial No.	Physical Properties (Norm. 1700 F, Dr. 1200 F)											
	Tensile Properties									Charpy Impact Resistance		Hard. As Cast
	T. S.	Y. P.	P. L.	B. S.	El.	R. A.	M. E. Psi $\times 10^6$	Y. R.	Hard. B.H.N.	Ft-Lbs R. T.	Ft-Lbs —25 F	B.H.N.
	Psi				Per Cent							
1	50,300	23,000	14,000	92,900	44.5	66.5	25.0	0.46	99.2	42.3	37.5	101
*2	.....	.....	.....	.....	....	....	....	....	...	....	....	...
3	50,900	30,300	31,000	106,000	42.5	71.0	28.3	0.60	103	43.8	40.3	104
4	54,700	33,400	36,100	112,700	40.5	70.5	28.4	0.62	108	46.5	42.8	116
5	55,900	34,400	31,900	113,000	39.5	71.5	24.5	0.62	112	52.0	29.3	109
6	66,500	43,500	46,000	135,500	36.5	67.0	29.4	0.66	138	59.3	19.8	159
*7	.....	.....	.....	.....	....	....	....	....	...	....	....	...
8	85,500	66,300	58,000	125,300	32.5	57.5	31.4	0.78	194	2.3	4.8	...
9	46,400	42,600	28,500	46,400	0	0	22.6	0.93	244	30.3	8.5	331
*10	.....	.....	.....	.....	....	....	....	....	...	....	....	...
11	58,000	34,300	36,000	118,500	39.0	67.8	32.0	0.60	115	26.5	18.3	121
12	61,000	36,300	37,000	113,400	37.5	63.0	26.2	0.60	124	44.7	31.5	138
*13	.....	.....	.....	.....	....	....	....	....	...	....	....	...
14	69,500	45,500	45,500	124,800	37.5	59.5	26.7	0.66	140	35.3	18.8	163
15	78,300	49,300	50,000	132,700	29.5	56.0	27.6	0.63	158	27.3	12.3	237
*16	.....	.....	.....	.....	....	....	....	....	...	....	....	...
17	100,300	77,500	64,500	147,800	28.5	46.5	29.7	0.78	224	2.5	2.0	...
*18	.....	.....	.....	.....	....	....	....	....	...	....	....	...
19	26,100	13,700	23,100	26,400	1.0	1.0	18.2	0.53	257	9.6	4.0	...
20	72,000	41,300	40,000	108,600	30.5	48.5	28.9	0.57	134	24.0	16.0	143
*21	.....	.....	.....	.....	....	....	....	....	...	....	....	...
22	86,000	53,900	56,200	136,200	31.0	51.5	30.1	0.63	163	28.8	21.8	189
23	82,300	52,300	50,800	143,000	30.5	57.5	29.2	0.64	161	34.8	18.5	197
*24	.....	.....	.....	.....	....	....	....	....	...	....	....	...
25	94,800	51,000	54,500	155,800	23.5	54.5	28.6	0.54	188	24.5	12.3	241
26	92,500	65,300	64,500	147,200	22.0	47.5	28.7	0.71	200	21.5	10.7	293
*27	.....	.....	.....	.....	....	....	....	....	...	....	....	...
28	72,500	.....	.....	72,500	0	1.0	31.7	....	260	2.5	2.5	...
29	73,000	.....	45,000	73,400	0.5	0.5	27.5	....	293	4.0	1.5	...

*Steels used in welding experiments.

Table I—(continued)
Carbon-Manganese Steels

Serial No.	Physical Properties (Norm. 1700 F, Dr. 1250 F)												Hard. As Cast B.H.N.
	Tensile Properties								Hardness		Charpy Impact Resistance Ft-Lbs		
	T. S.	Y. P.	P. L.	B. S.	El.	R. A.	M. E. Psi $\times 10^6$	Y. R.	B.H.N.	V.P.N.	R. T.	—25 F	
	Psi				Per Cent								
1	50,000	24,000	19,400	83,700	38.0	61.0	33.8	0.48	136	...	...	...	101
*2	53,300	32,000	33,500	101,600	43.5	68.0	30.7	0.60	...	107	42.8	37.3	...
3	51,000	28,500	24,000	110,000	40.0	70.0	37.1	0.56	127	...	...	...	104
4	54,000	31,000	30,000	108,300	39.0	70.0	26.7	0.58	124	...	...	...	116
5	55,300	33,000	34,500	134,000	43.0	75.0	31.5	0.60	123	...	49.3	...	109
6	65,000	41,000	43,000	123,000	37.0	63.0	28.9	0.63	145	...	57.3	...	159
*7	67,400	47,100	49,000	144,800	36.5	71.5	27.9	0.70	...	145	27.8	20.5	...
8	94,500	48,500	33,000	148,000	26.0	49.0	39.0	0.51	195	...	29.6	...	...
9	69,000	61,500	54,000	82,300	6.0	7.0	30.4	0.89	247	...	27.3	...	331
*10	61,800	38,500	39,500	111,600	39.0	63.0	27.7	0.63	...	122	33.8	21.5	...
11	57,500	32,000	30,000	101,400	38.0	63.0	29.4	0.56	130	...	43.5	...	121
12	60,000	34,500	35,000	109,800	35.0	59.0	27.8	0.68	132	...	23.8	...	138
*13	74,000	55,500	51,000	147,600	35.5	63.0	29.1	0.76	...	156	45.8	29.0	...
14	67,700	43,400	45,400	120,200	29.0	56.0	28.9	0.64	149	...	...	...	163
15	75,500	44,500	42,000	130,700	28.0	56.0	28.9	0.59	160	...	22.0	...	237
*16	91,500	65,300	61,300	160,600	28.5	59.5	28.9	0.71	...	195	24.8	10.5	...
17	111,500	73,500	53,000	158,500	22.0	41.0	28.7	0.66	239	...	3.5	...	...
*18	103,800	72,300	62,500	162,600	31.0	46.0	29.4	0.70	...	229	26.8	16.3	...
19	45,500	45,000	36,000	47,700	0.2	0.5	33.2	0.99	276	...	4.0	...	...
20	69,000	37,000	44,000	119,600	34.0	54.0	28.2	0.54	138	...	22.5	...	143
*21	79,500	49,000	50,000	132,300	32.0	52.0	27.7	0.62	...	155	29.0	16.5	...
22	83,200	49,000	52,000	148,800	30.0	57.0	28.2	0.59	167	...	29.0	...	189
23	78,500	48,500	51,000	131,800	37.0	56.0	28.8	0.62	167	...	...	...	197
*24	92,800	61,500	62,500	144,100	25.5	49.5	27.7	0.67	...	194	32.5	18.5	...
25	88,000	52,500	49,000	142,600	30.0	63.0	31.4	0.60	181	...	26.3	...	241
26	97,700	58,200	43,300	135,000	23.0	38.0	30.1	0.60	216	...	17.8	...	293
*27	100,500	76,000	73,500	141,000	25.5	46.0	26.4	0.76	...	216	23.3	10.0	...
28	71,000	63,500	44,000	87,000	2.0	2.0	21.5	0.90	255	...	3.0	...	...
29	92,500	88,000	47,000	93,400	1.0	1.0	28.1	0.95	331	...	4.5	...	...

*Steels used in welding experiments.

Table II
Carbon-Molybdenum-Manganese Steels

Serial No.	Nominal Composition				Chemical Analysis								Dilatometer Data: 5 Hr. Cool		Dilatometer Data: Air Cool		Hard. As Cast
	Si	Mn	Mo	C	Si	Mn	S	P	C	Mo	Cr	Ni	Run No.	V.P.N.	Run No.	V.P.N.	B.H.N.
30	0.20—0.45	0.5	0.5	0.1	0.23	0.39	0.027	0.022	0.04	0.57	0.03	...	1285	108	1286	121	107
*31	0.20—0.45	0.5	0.5	0.1	0.31	0.49	0.046	0.019	0.07	0.50	...	...	....	...	....	...	...
32	0.20—0.45	0.5	0.5	0.1	0.28	0.60	0.029	0.022	0.04	0.56	0.17¶	...	1287	117	1288	133	121
33	0.20—0.45	1.0	0.5	0.1	0.40	0.72	0.027	0.021	0.06	0.53	0.03	...	1323	114	1324	136	121
34	0.20—0.45	1.0	0.5	0.1	0.38	0.94	0.024	0.020	0.05	0.50	0.15¶	...	1326	121	1325	160	143
*35	0.20—0.45	2.0	0.5	0.1	0.35	1.70	0.028	0.017	0.09	0.56	0.03	...	....	...	....	...	...
36	0.20—0.45	2.0	0.5	0.1	0.45	1.90	0.018	0.025	0.14†	0.59	0.03	...	1333	219	1334	251	...
37	0.20—0.45	2.0	0.5	0.1	0.42	2.12	0.028	0.021	0.08	0.56	0.03	...	1327	181	1328	236	...
38	0.20—0.45	3.0	0.5	0.1	0.31	3.04	0.020	0.022	0.10	0.54	...	...	1353	294	1354	322	...
39	0.20—0.45	4.0	0.5	0.1	0.48▼	3.64	0.025	0.021	0.11	0.70	0.03	...	1329	281	1330	394	...
*40	0.20—0.45	0.5	0.5	0.15	0.39	0.55	0.027	0.020	0.14	0.49	0.03	...	....	...	....	...	...
41	0.20—0.45	0.5	0.5	0.15	0.41	0.59	0.028	0.022	0.14	0.50	0.08	0.05	1308	134	1307	172	157
42	0.20—0.45	1.0	0.5	0.15	0.43	0.77	0.024	0.021	0.13	0.53	0.07	0.05	1309	143	1310	179	183
*43	0.20—0.45	1.0	0.5	0.15	0.39	0.95	0.027	0.022	0.13	0.55	0.03	...	....	...	....	...	...
44	0.20—0.45	1.5	0.5	0.15	0.43	1.77	0.023	0.021	0.13	0.57	0.05	1.17§	1311	154	1312	196	231
*45	0.20—0.45	2.0	0.5	0.15	0.30	2.20	0.013	0.020	0.13	0.54	...	...	....	...	....	...	...
46	0.20—0.45	2.0	0.5	0.15	0.47▼	2.24	0.030	0.020	0.16	0.68	0.20¶	...	1313	264	1314	325	275
*47	0.20—0.45	2.0	0.5	0.15	0.55▼	2.63	0.026	0.014	0.17	0.56	0.03	...	....	...	....	...	...
48	0.20—0.45	3.0	0.5	0.15	0.41	3.14	0.025	0.022	0.13	0.62	...	...	1352	357	1351	437	...
*49	0.20—0.45	3.0	0.5	0.15	0.59▼	3.43	0.030	0.021	0.16	0.64	0.03	...	....	...	....	...	...
50	0.20—0.45	4.0	0.5	0.15	0.47▼	4.26	0.032	0.020	0.21†	0.78	0.03	...	1316	401	1315	450	...
51	0.20—0.45	0.5	0.5	0.30	0.46▼	0.47	0.023	0.020	0.25‡	0.60	0.03	...	1317	177	1318	254	225
*52	0.20—0.45	0.5	0.5	0.30	0.41	0.72	0.031	0.017	0.30	0.58	0.03	...	....	...	....	...	...
53	0.20—0.45	1.0	0.5	0.30	0.44	1.25	0.027	0.022	0.32†	0.73	0.03	...	1302	373	1301	542	311
54	0.20—0.45	1.5	0.5	0.30	0.42	1.35	0.025	0.023	0.26‡	0.60	0.10	...	1305	183	1306	274	250
55	0.20—0.45	2.0	0.5	0.30	0.41	1.90	0.026	0.022	0.25‡	0.60	0.10	...	1284	263	1283	370	277
*56	0.20—0.45	2.0	0.5	0.30	0.57▼	2.53	0.026	0.017	0.32†	0.62	0.03	...	....	...	....	...	...
57	0.20—0.45	3.0	0.5	0.30	0.44	3.33	0.026	0.018	0.31	0.58	...	...	1349	566	1350	599	...
58	0.20—0.45	4.0	0.5	0.30	0.46▼	5.76	0.021	0.022	0.32†	0.76	...	...	1299	536	1300	536	...

*Steels used in welding experiments.
†"High" carbon.
‡"Low" carbon.
¶"High" chromium.
§"High" nickel.
▼Silicon higher than 0.45%.

Table II—(continued)
Carbon-Molybdenum-Manganese Steels

Serial No.	Physical Properties (Norm. 1700 F, Dr. 1200 F)								Hard. B.H.N.	Charpy Impact Resistance		Hard. As Cast B.H.N.
	Tensile Properties									Ft-Lbs		
	T. S.	Y. P.	P. L.	B. S.	El.	R. A.	M. E. Psi $\times 10^6$	Y. R.		R. T.	—25 F	
	Psi				Per Cent							
30	51,200	18,500	21,800	86,400	40.0	63.5	25.4	0.36	103	13.3	3.0	107
*31	.....	.....	.....	.....	....	....	....	....	...	....	....	...
32	55,100	26,500	27,000	104,000	39.5	66.5	29.2	0.48	115	46.5	3.5	121
33	56,500	28,200	25,500	100,000	40.0	64.0	28.4	0.50	118	43.5	21.5	121
34	61,400	38,200	38,400	108,000	39.0	64.0	29.2	0.63	127	38.0	21.3	143
*35	.....	.....	.....	.....	....	....	....	....	...	....	....	...
36	93,000	65,000	46,400	141,900	24.0	51.5	29.7	0.70	203	27.0	20.0	...
37	87,500	60,300	41,500	125,400	24.5	44.0	29.7	0.69	186	32.5	10.5	...
38	102,000	77,500	61,000	172,800	25.5	59.0	27.0	0.76	229	23.6	13.5	...
39	120,500	77,300	52,900	144,600	18.0	22.0	27.8	0.64	246	15.0	8.3	...
*40	.....	.....	.....	.....	....	....	....	....	...	....	....	...
41	67,500	41,300	44,500	116,900	37.5	58.5	30.2	0.62	139	30.3	23.5	157
42	70,900	43,200	40,200	115,800	33.0	54.0	27.8	0.61	142	27.3	21.8	183
*43	.....	.....	.....	.....	....	....	....	....	...	....	....	...
44	95,800	67,500	49,500	148,000	23.5	50.0	28.4	0.71	206	25.0	15.3	231
*45	.....	.....	.....	.....	....	....	....	....	...	....	....	...
46	104,300	70,800	48,000	142,800	21.5	45.0	30.2	0.68	225	19.5	18.0	275
*47	.....	.....	.....	.....	....	....	....	....	...	....	....	...
48	117,500	87,800	69,500	183,800	20.5	36.0	25.0	0.75	253	14.3	6.3	...
*49	.....	.....	.....	.....	....	....	....	....	...	....	....	...
50	116,300	94,000	72,000	127,300	7.0	8.0	27.0	0.82	287	16.3	5.3	...
51	79,000	49,100	48,100	118,500	27.5	45.5	30.2	0.62	163	25.0	13.0	225
*52	.....	.....	.....	.....	....	....	....	....	...	....	....	...
53	118,800	84,000	45,500	159,000	18.0	31.5	27.3	0.71	248	25.3	17.5	311
54	100,700	72,800	74,500	142,700	18.5	45.0	30.6	0.73	222	16.5	7.3	250
55	106,300	81,800	66,000	147,800	18.5	42.0	30.1	0.77	228	19.5	8.5	277
*56	.....	.....	.....	.....	....	....	....	....	...	....	....	...
57	143,100	116,400	84,000	154,000	5.1	7.0	31.9	0.82	317	4.0	3.0	...
58	85,000	.....	35,900	85,400	0.4	0.5	25.5	....	318	4.0	4.0	...

*Steels used in welding experiments.

Table II—(continued)
Carbon-Molybdenum-Manganese Steels

Serial No.	Physical Properties (Norm. 1700 F, Dr. 1250 F)												Hard. As Cast B.H.N.
	Tensile Properties								Hardness		Charpy Impact Resistance Ft-Lbs		
	T. S.	Y. P.	P. L.	B. S.	El.	R. A.	M. E. Psi $\times 10^6$	V. R.	B.H.N.	V.P.N.	R. T.	—25 F	
	Psi				Per Cent								
30	50,000	23,500	23,000	82,400	36.0	66.0	30.0	0.47	136	...	...	...	107
*31	56,500	30,000	28,500	102,000	41.0	66.0	28.6	0.53	...	115	51.0	30.3	...
32	54,000	27,000	24,000	109,400	40.0	68.0	29.7	0.50	138	...	32.8	...	121
33	57,000	28,000	22,000	98,700	39.0	62.0	25.8	0.49	141	...	35.5	...	121
34	61,000	35,500	36,000	106,300	37.0	60.0	33.4	0.58	128	...	28.5	...	143
*35	81,500	60,000	56,500	126,300	26.0	51.0	28.5	0.74	...	187	30.0	17.5	...
36	85,500	61,000	52,000	144,000	27.0	58.0	26.7	0.71	183	...	27.0	...	...
37	83,000	56,000	47,000	124,000	27.0	44.0	27.9	0.68	191	...	16.8	...	...
38	107,500	60,500	48,000	191,900	28.0	44.0	27.8	0.56	208	...	28.5	...	...
39	89,500	57,000	36,000	94,200	5.0	5.0	25.3	0.64	275	...	25.3	...	...
*40	68,800	44,300	45,000	121,500	33.0	61.5	28.4	0.64	...	142	37.3	17.8	...
41	67,000	41,000	43,000	114,000	29.0	57.0	28.2	0.61	142	...	28.0	...	157
42	.....	.....	.....	.....	....	....	....	....	...	...	...	...	183
*43	76,300	53,500	54,800	142,500	33.0	60.5	27.2	0.70	...	161	29.5	25.0	...
44	79,500	50,500	53,000	118,800	31.0	52.0	29.8	0.65	166	...	23.3	...	231
*45	82,500	59,500	51,000	136,800	31.0	62.0	27.4	0.72	...	185	27.8	18.0	...
46	93,000	64,000	52,000	145,700	24.0	54.0	29.6	0.69	210	...	23.0	...	275
*47	107,000	75,300	62,000	170,900	23.0	46.0	25.5	0.71	...	246	28.0	19.5	...
48	132,500	87,000	63,000	181,500	23.0	27.0	39.0	0.56	254	...	17.5	...	...
*49	115,000	79,300	65,500	184,300	25.5	44.0	28.3	0.69	...	248	17.3	12.8	...
50	53,500	52,000	36,000	45,500	0	0	22.0	0.97	293	...	24.8	...	...
51	91,000	65,500	60,000	134,700	26.0	51.0	32.5	0.72	203	...	...	...	225
*52	92,000	66,800	69,000	134,100	30.5	45.0	29.5	0.73	...	201	25.3	16.3	...
53	106,000	76,000	61,000	155,500	21.0	45.0	28.9	0.72	232	...	17.0	...	311
54	93,500	69,000	70,000	139,800	22.0	46.0	31.7	0.74	211	...	...	...	250
55	105,000	74,500	70,000	146,200	24.0	47.0	31.5	0.71	220	...	14.8	...	277
*56	117,300	98,800	98,800	154,600	20.5	38.5	29.6	0.85	...	250	25.5	9.0	...
57	72,500	72,500	35,000	72,500	0	0	34.2	....	321	...	....	....	...
58	84,000	79,000	65,000	84,800	1.0	1.0	20.5	0.94	317	...	5.3	....	...

*Steels used in welding experiments.

(b) —25 F (—32 C). Most of the compositions were also subjected to thermal analysis, using a dilatometer. Test data thus accumulated are presented in Table I for "plain carbon", and in Table II for "carbon-molybdenum" steels, together with the chemical analysis of each heat. Figures representing physical data (Tables I and II) were averaged from at least two or more tests.[6]

The contents of silicon, sulphur and phosphorus in Table I, and of the same elements with the addition of molybdenum in Table II, are reasonably uniform in all steels, even though silicon, in some cases, is present in amounts slightly higher than the specified maximum of 0.45%. Chromium, in some instances, is present in amounts as high as about 0.25%. Nickel, in one case (Serial No. 44, Table II), is present in the amount of 1.17%. There also is some nonuniformity in the carbon content, and overlapping from one subgroup to another. Nevertheless, in spite of these incidental interferences, it was felt that the compositional uniformity was sufficient to warrant systematic studies of the effect of manganese which, as has been pointed out, ranged within each subgroup between about 0.5 and 4.0%.

Thermal Analysis and Microexamination

Most of the compositions presented in Tables I and II were subjected to thermal analysis using a self-recording differential dilatometer. In each case, a specimen (50 millimeters long and 4 millimeters in diameter) was heated in vacuum to 1000 C (1830 F) in 2 hours, and then cooled to room temperature (a) in 5 hours (an average rate of 3.2 C per minute, or 5.8 F per minute) and (b) "in air" (an average rate of 50 C per minute or 90 F per minute). Each composition was thus subjected to thermal analysis by cooling two specimens from 1000 C (1830 F), one at a slow and the other at a more rapid rate. The results thus obtained on the two groups of "plain carbon" (Table I) and "carbon-molybdenum" (Table II) steels are presented in Figs. 1, 2, 3 and 4. The chemical analysis and the final Vickers hardness are given adjacent to each curve. Figs. 1 and 2 are reproductions of the dilatometer curves obtained with "plain carbon", and Figs. 3 and 4, those obtained with "carbon-molybdenum" steels. Moreover, Figs. 1 and 3 illustrate the slow cooling rate (3.2 C per minute or 5.8 F per minute), and Figs. 2 and 4, the more rapid cooling (50 C per minute

[6]Variations in test results represented by each average figure (Tables I and II) come within normal limits of experimental error, with the exception of steels containing over 3% manganese, which came out somewhat porous and unsound.

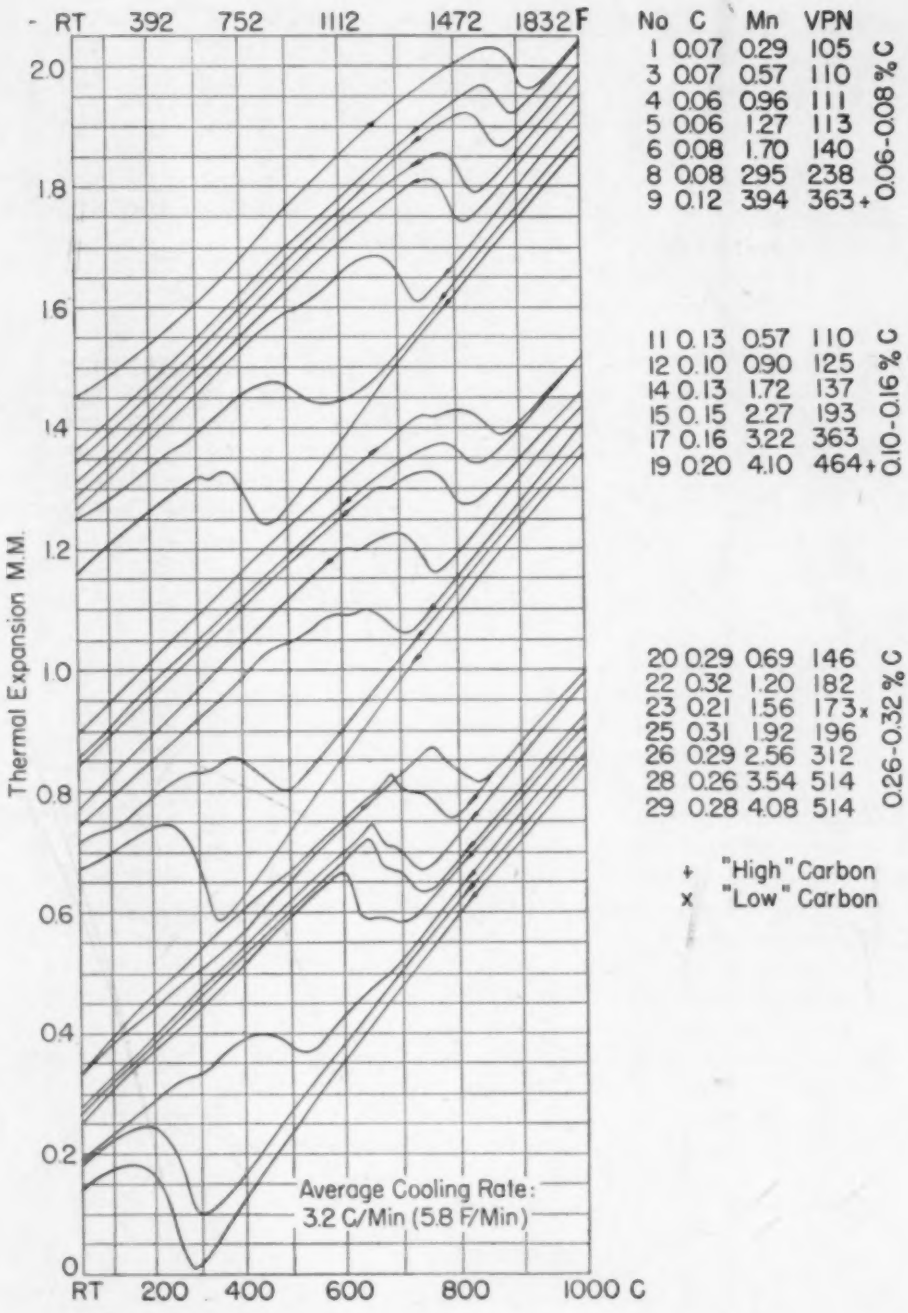


Fig. 1—Thermal Cooling Curves of Carbon-Manganese Steel (Slow Cooling Rate).

or 90 F per minute). In each figure, the curves are arranged into three subgroups: those representing (a) steels containing 0.04 to 0.08% carbon, (b) steels containing 0.10 to 0.16% carbon, and (c) steels containing 0.25 to 0.32% carbon. Within each subgroup, they represent steels with the manganese content progressively increasing from about 0.5 to 4.0%. It may be noted that within each subgroup

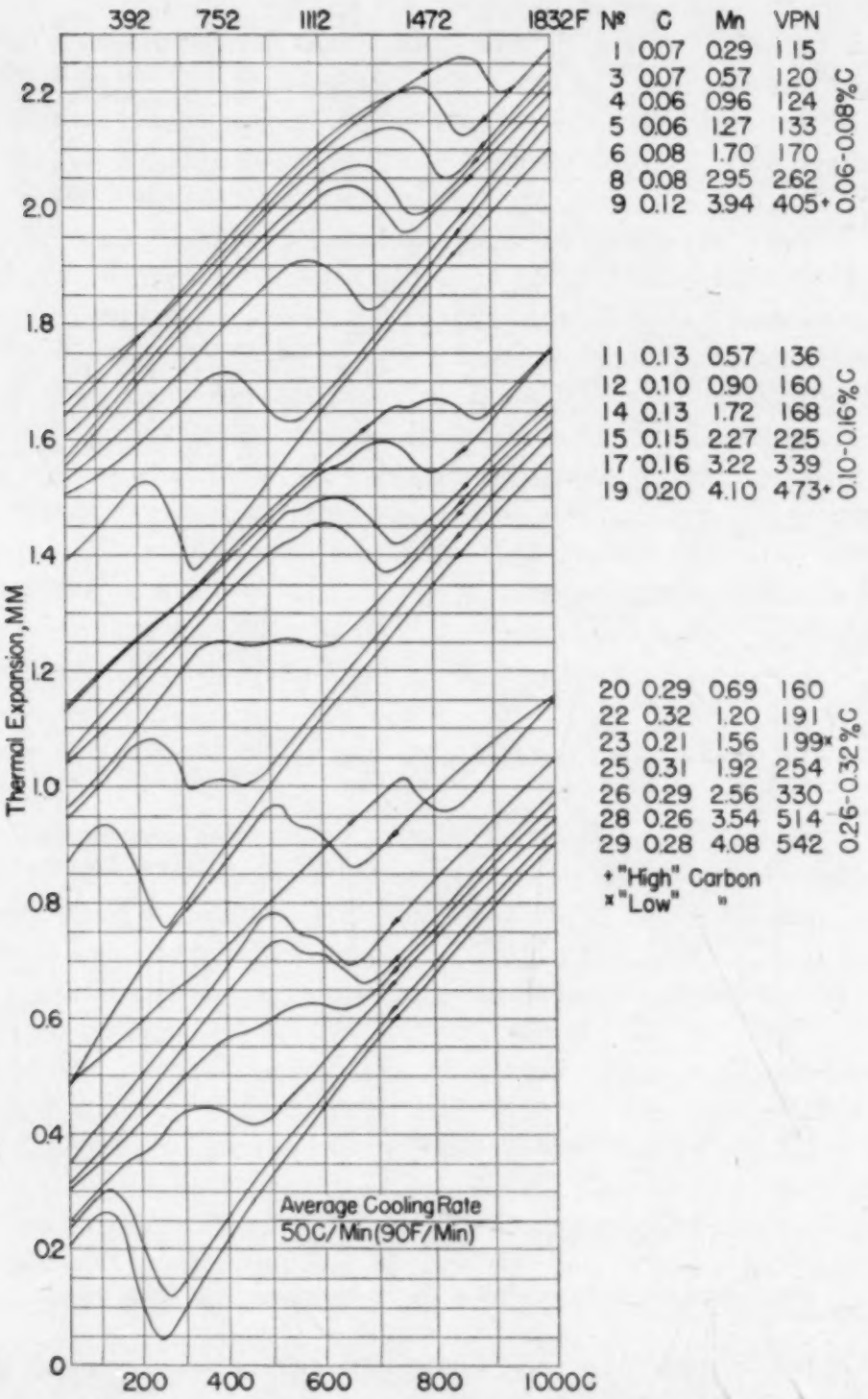


Fig. 2—Thermal Cooling Curves of Carbon-Manganese Steel (Rapid Cooling Rate).

the steel with the lowest manganese is represented by a complete dilatometer curve with heating as well as cooling branches. The re-

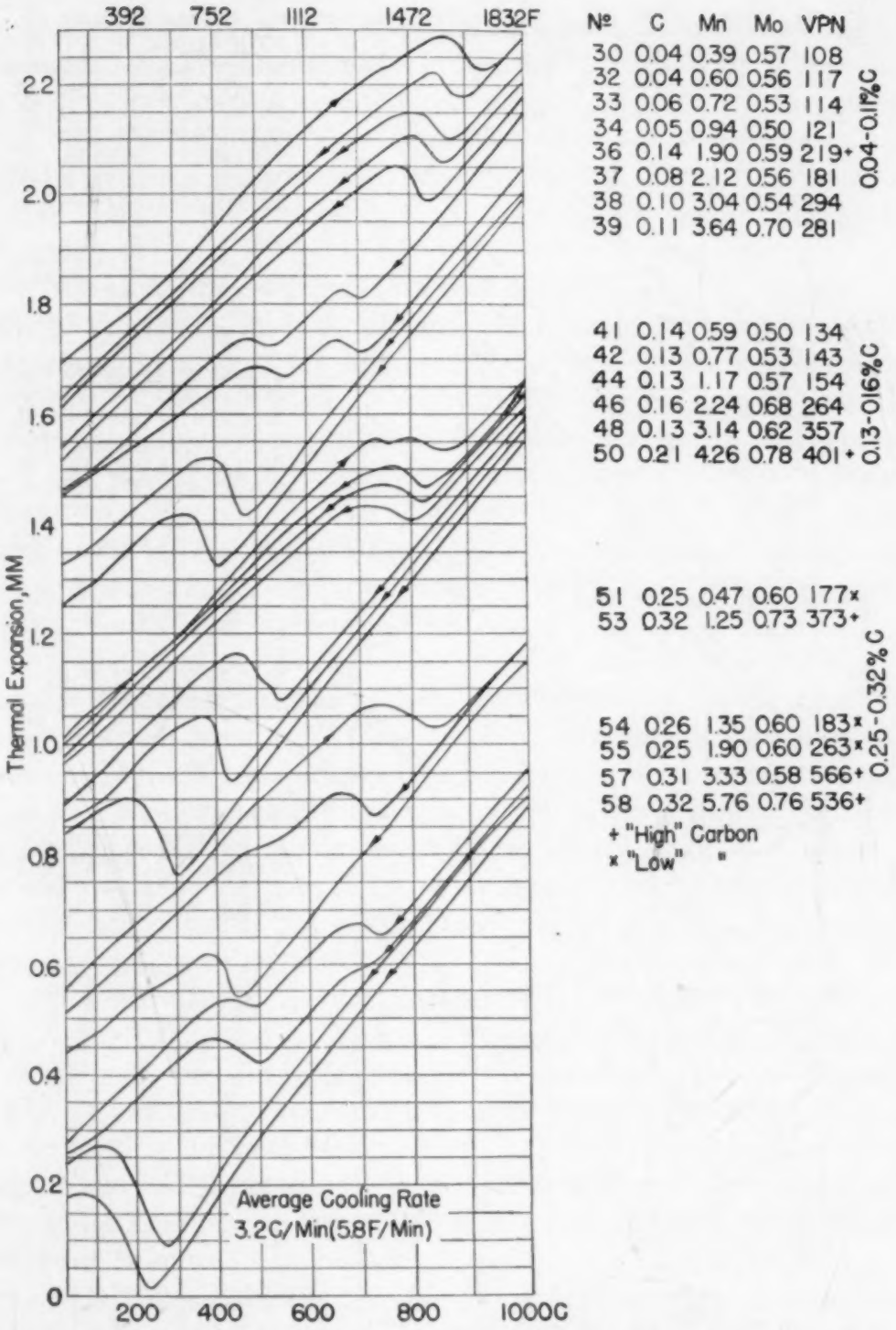


Fig. 3—Thermal Cooling Curves of Carbon-Manganese-Molybdenum Steels (Slow Cooling Rate).

mainder (for the sake of space economy) have only the cooling branches reproduced. It should be mentioned, however, that increasing man-

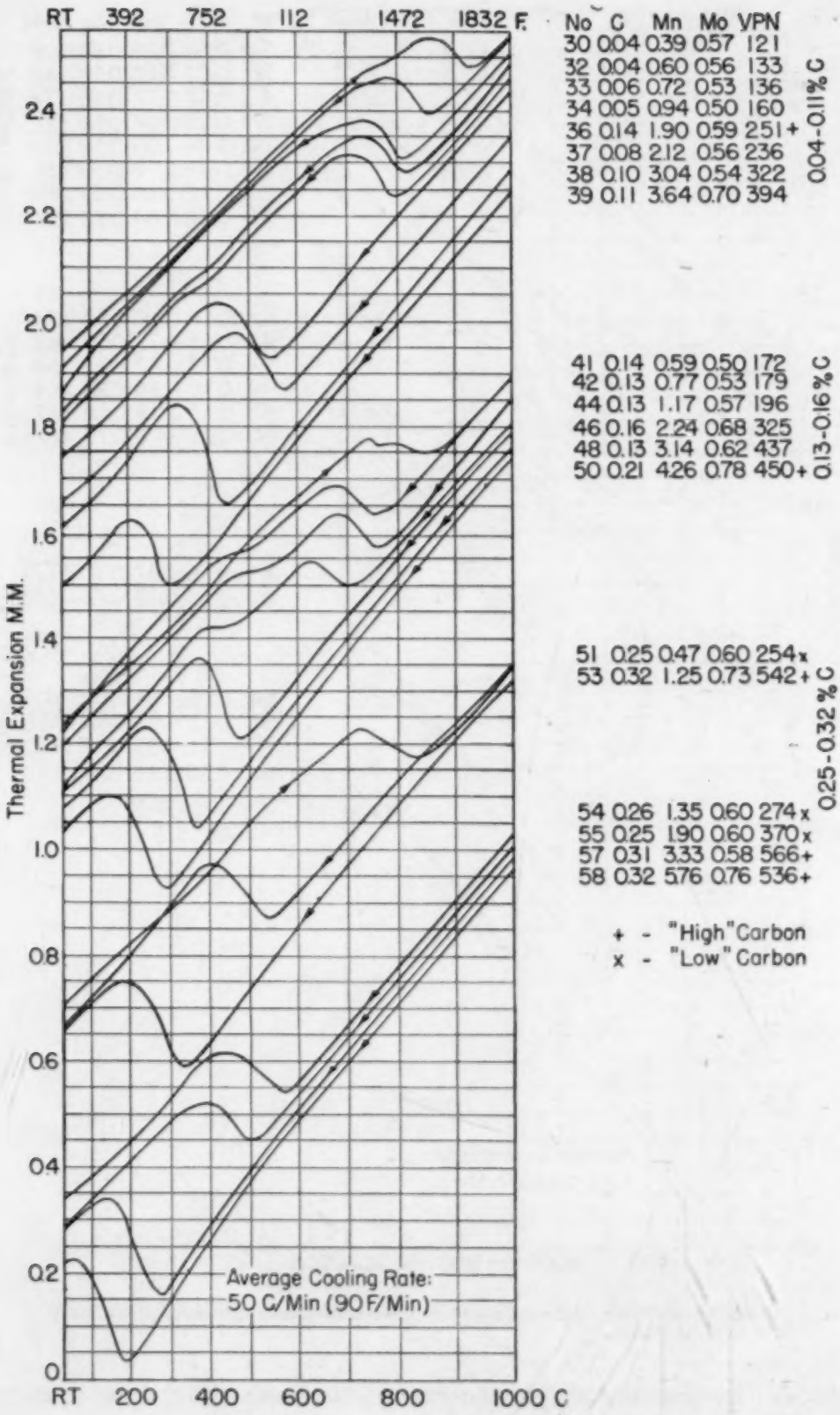


Fig. 4—Thermal Cooling Curves of Carbon-Manganese-Molybdenum Steels (Rapid Cooling Rate).

ganese has a tendency to suppress the transformation on heating to somewhat lower temperatures and to spread it over a wider range. All of these curves are tracings of the original photographically recorded dilatometer curves. Every dilatometer specimen, after the run, was tested for Vickers hardness and microexamined. Some of the photomicrographs of the resultant structures are presented in Figs. 5 to 14, inclusive.

In general, these results check with our previous observations (1), (2), (3); namely, that on uniform cooling from the austenitic state, transformations occur at either relatively high or low temperatures, resulting in ferrito-pearlitic structures for the former, and martensito-bainitic structures for the latter. In the case of chromium-molybdenum (2) and chromium-nickel-molybdenum (3) steels, these two transformation temperature ranges are separated by a "neutral" range from about 450 to 650 C (840 to 1200 F), where transformations are extremely slow. In the present group of steels, there does not appear to be any such "neutral" temperature range.

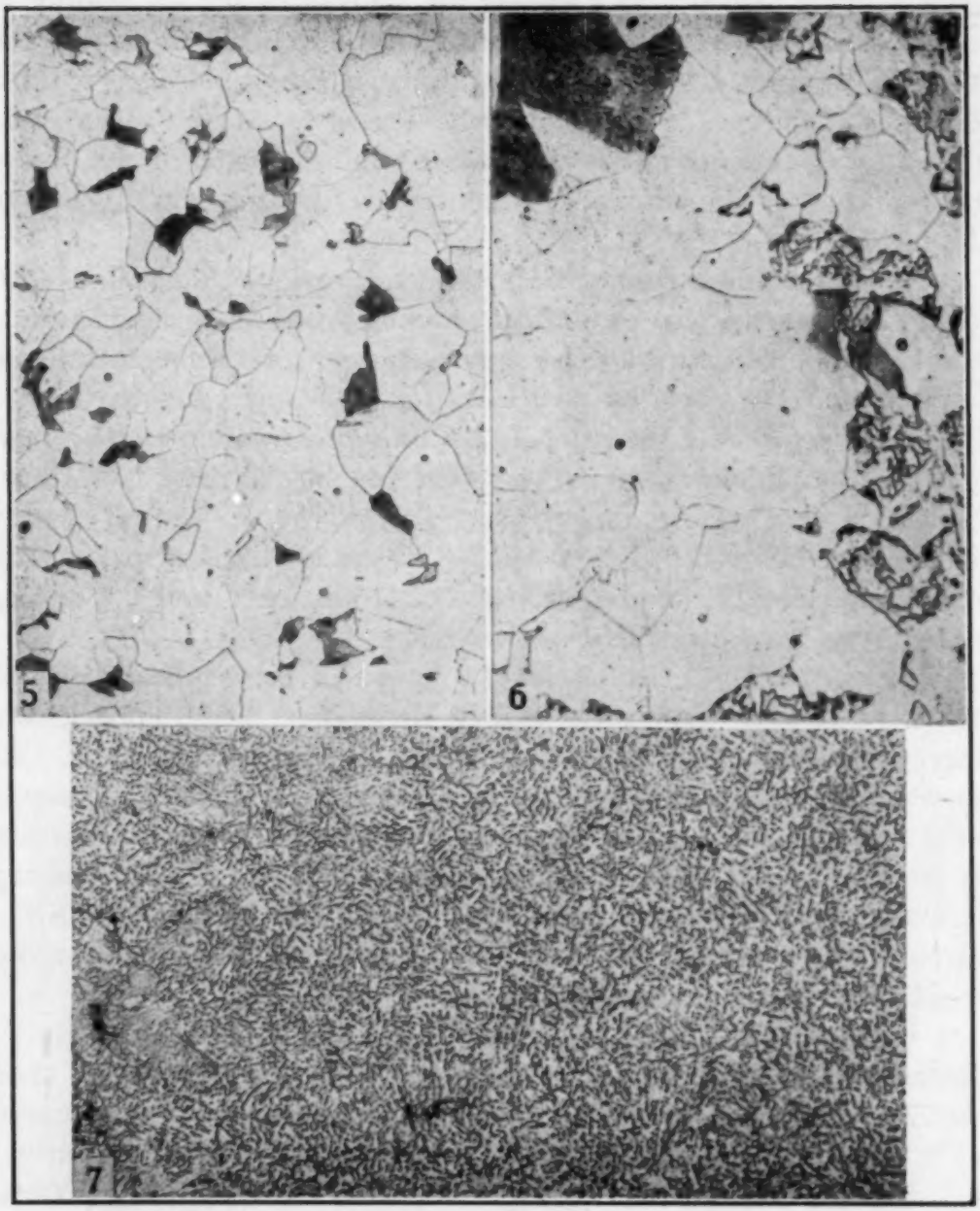
"Plain Carbon" Group—In the "plain carbon" group (Figs. 1 and 2), increasing manganese content above about 1.5% increases the thermal sluggishness. Up to about 2.0% manganese, however, this increase in the thermal sluggishness is quite gradual and still results in at least a partial pearlitic transformation. With still further increase in manganese, the transformation is completely suppressed resulting in martensito-bainitic structures. This seems to be independent of the carbon content and is true for the slow (Fig. 1) as well as for the more rapid (Fig. 2) cooling rates.

For example, Fig. 5 illustrates the structure of steel, Serial No. 5, containing 0.06% carbon and 1.27% manganese, cooled at the slow rate. No suppressed transformations are recorded on the cooling curve (Fig. 1), and the resultant structure is composed of ferrite and pearlite.

Fig. 6 is the microstructure of Serial No. 6, containing 0.08% carbon and 1.70% manganese, cooled at the slow rate. The transformation (Fig. 1) is split and the resultant structure shows a certain amount of upper bainite.

Fig. 7 illustrates the microstructure of Serial No. 8, containing 0.08% carbon and 2.95% manganese, cooled at a rapid rate, when transformation (Fig. 2) is suppressed, and is composed of bainite.

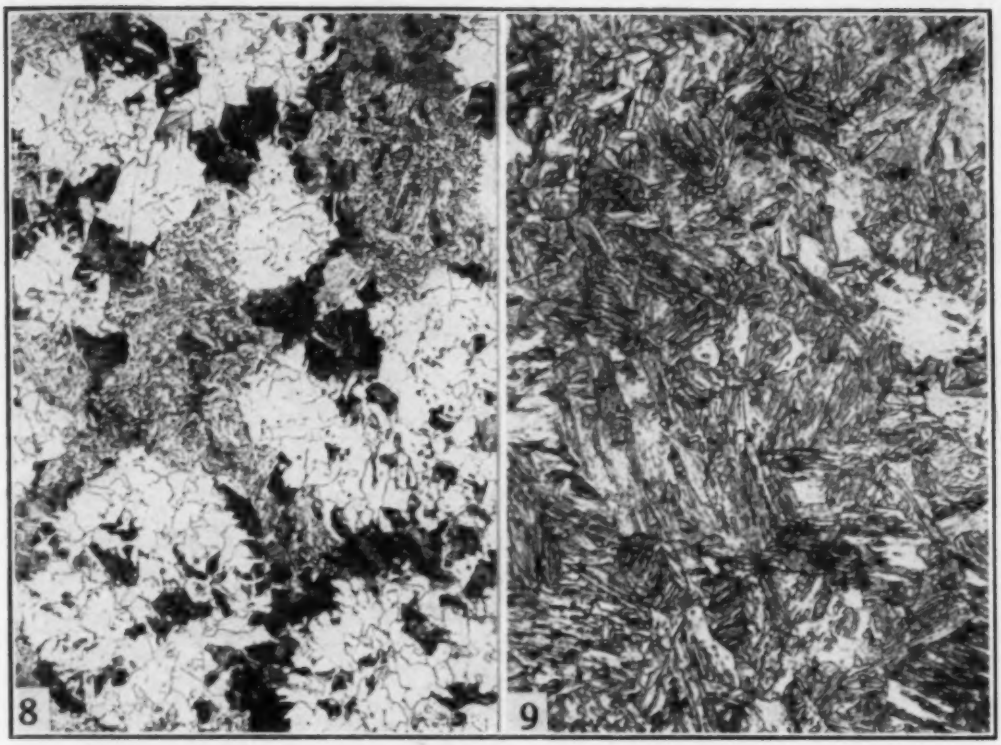
Passing over to the steels with intermediate carbon, Fig. 8 is the microstructure of Serial No. 15, containing 0.15% carbon and 2.27% manganese, cooled at a slow rate. The transformation (Fig. 1) is split



Figs. 5–7—Low Carbon, Molybdenum-Free Subgroup. Fig. 5—Serial No. 5. 0.06% C, 1.27% Mn. 5-hr. cool, 113 Vickers. Etched in Nital. × 150. Fig. 6—Serial No. 6. 0.08% C, 1.70% Mn. 5-hr. cool, 140 Vickers. Etched in Nital. × 500. Fig. 7—Serial No. 8. 0.08% C, 2.95% Mn. Air cool, 262 Vickers. Etched in Nital. × 150.

and the resultant structure is composed of ferrite and pearlite (formed at the beginning of the transformation) and upper bainite (formed at the latter stages of the transformation).

Fig. 9 illustrates the microstructure of Serial No. 17, containing 0.16% carbon and 3.22% manganese, cooled at a rapid rate. Transformation in this case (Fig. 2) is completely suppressed and the result-



Figs. 8–9—Intermediate-Carbon, Molybdenum-Free Subgroup. Fig. 8—Serial No. 15. 0.15% C, 2.27% Mn. 5-hr. cool, 193 Vickers. Etched in Nital. × 150. Fig. 9—Serial No. 17. 0.16% C, 3.22% Mn. Air cool, 339 Vickers. Etched in Nital. × 500.

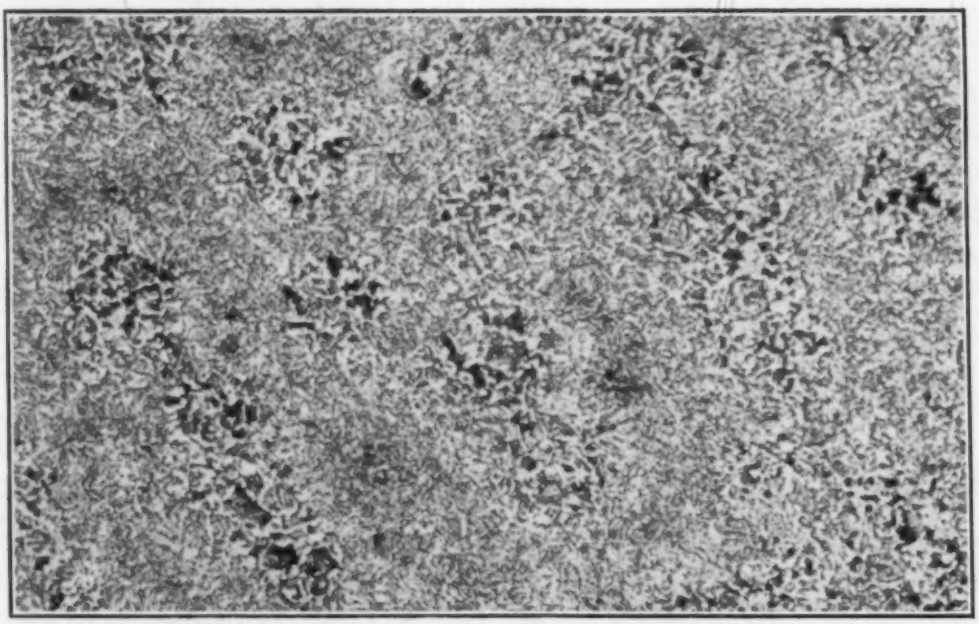
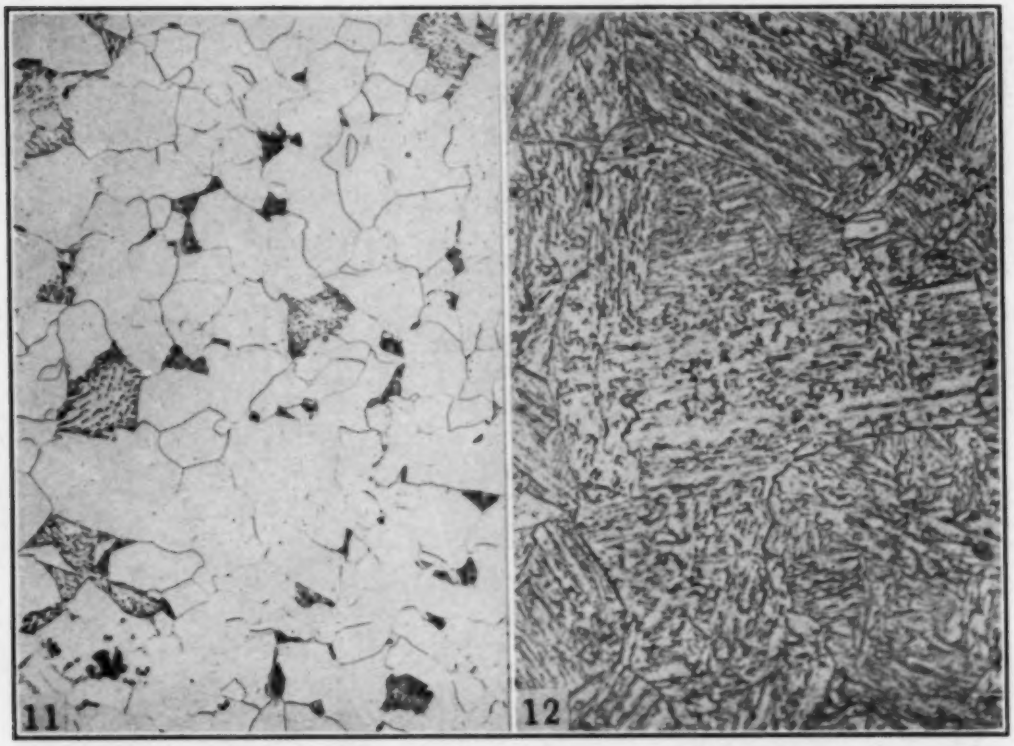


Fig. 10—High Carbon, Molybdenum-Free Subgroup. Serial No. 25. 0.31% C, 1.92% Mn. Air cool, 254 Vickers. Etched in Nital. × 150.



Figs. 11–12—Low Carbon, Molybdenum-Bearing Subgroup. Fig. 11—Serial No. 33. 0.06% C, 0.72% Mn, 0.53% Mo. Air cool, 136 Vickers. Etched in Nital. × 150. Fig. 12—Serial No. 38. 0.10% C, 3.04% Mn, 0.54% Mo. Air cool, 322 Vickers. Etched in Nital. × 500.

ant structure consists of bainite and probably some martensite.

Finally, for "high" carbon steels, Fig. 10 presents the structure of the steel, Serial No. 25, containing 0.31% carbon and 1.92% manganese, cooled at a rapid rate (Fig. 2). The transformation is split and spread over a wide temperature range. The structure consists of small amounts of pearlite and ferrite formed during the initial stages of the transformation and of bainite formed during its latter stages.

With a further suppression of the transformation (as in Serial No. 26, Fig. 2), pearlite practically disappears and is replaced by bainite. When transformations are suppressed to still lower temperatures (as in Serial Nos. 28 and 29, Fig. 2), lower bainite in turn is gradually replaced by the martensitic structure.

Carbon-Molybdenum Steels—In the "carbon-molybdenum" group, the increasing thermal sluggishness produced by raising the manganese content and the sequence of the resultant structures is quite similar to that of "plain carbon" steels, except that the 0.5% molybdenum present in all of them also contributes to the suppression of the transformations. (Compare Fig. 1 with Fig. 3, and Fig. 2 with Fig. 4.)

Fig. 11 represents the structure of rapidly cooled Serial No. 33 (Fig. 4), containing 0.06% carbon and 0.72% manganese. This structure consists of ferrite and small amounts of pearlite as well as upper bainite. The latter is a product of the suppressed transformation, indicated by a slight discontinuity on the cooling curve.

When the transformation is completely suppressed, as in Serial No. 38 (Fig. 4), containing 0.10% carbon and 3.04% manganese, the resultant structure, illustrated in Fig. 12, is composed of upper and lower bainite.

Fig. 13 illustrates the structure of a steel with intermediate carbon, Serial No. 42, containing 0.13% carbon and 0.77% manganese, obtained on rapid cooling (Fig. 4). It is composed of ferrite and some pearlite, formed in the upper transformation temperature range, and of upper bainite formed by the suppressed transformation manifested by a discontinuity on the cooling curve. With further increase in the manganese content, the thermal sluggishness increases, and ferrite-pearlite structures with the same cooling rates are gradually replaced by lower bainite and martensite.

In the "high" carbon subgroup, the carbon content is less uniform than in the other subgroups discussed so far. For this reason (Figs. 3 and 4), it appears that some of the higher manganese steels are less thermally sluggish than those containing lower manganese. Actually, however, this is due to the interference of the carbon content which, in the presence of these alloying elements, has a greater effect in suppressing the transformation than manganese itself.

This subgroup is illustrated by Fig. 14, which is the structure of the slowly cooled Serial No. 53, containing 0.32% carbon and 1.25% manganese (Fig. 3). It is predominantly composed of a mixture of upper and lower bainite, formed at the suppressed transformation range. It also contains some ferrite and a pearlite-like constituent formed at the upper transformation range, manifested by a slight discontinuity in the cooling curve (Fig. 3).

In conclusion, it can be stated that progressively larger percentages of manganese in amounts over 1.5% increase the thermal sluggishness of carbon and carbon-molybdenum steels containing carbon up to about 0.3%, increase their air hardenability and promote formation of structural constituents resulting from suppressed transformations (i.e., lower bainite and martensite). This increase in thermal sluggishness, however, is much more gradual and less abrupt than, for example, in chromium-nickel steels and results in formation of transitory structures not observed in the latter.

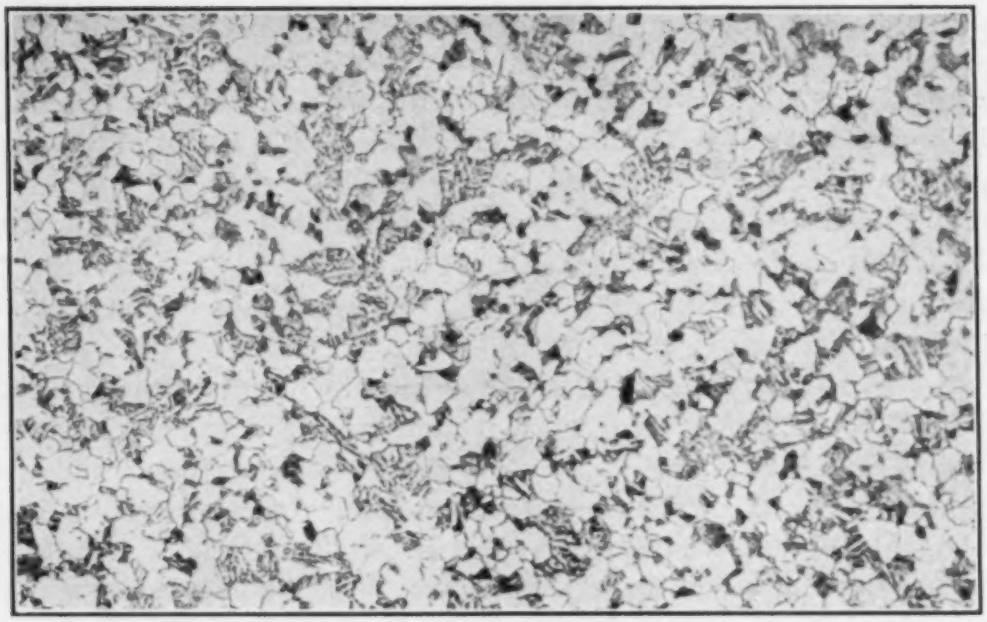


Fig. 13—Intermediate Carbon, Molybdenum-Bearing Subgroup. Serial No. 42. 0.13% C, 0.77% Mn, 0.53% Mo. Air cool, 179 Vickers. Etched in Nital. × 150.



Fig. 14—High Carbon, Molybdenum-Bearing Subgroup. Serial No. 53. 0.32% C, 1.25% Mn, 0.73% Mo. 5-hr. cool, 373 Vickers. Etched in Nital. × 500.

Physical Properties

Figs. 15 and 16 are graphic representations of the test data given in Tables I and II, respectively. Each figure consists of three separate

graphs (A, B, and C), for three different carbon contents. In view of the fact that very little difference was found in the properties of the same steels drawn at 1200 and 1250 F (650 and 675 C), in plotting these curves, average figures were used. In all cases, there was some scattering of the points due to the inevitable experimental error so that the curves represent average values, somewhat on the conservative side. In each figure, the engineering specification requirements for carbon and carbon-molybdenum steels (respectively) are drawn as dotted lines. Since steels with 4% manganese, in all cases, come out somewhat unsound and segregated, the test data obtained from them were not considered as very reliable. In all curves, the portions from 3 to 4% manganese are, therefore, indicated as dotted lines.

The conclusions that may be reached from studying these graphs are that manganese, up to about 3%, to a considerable extent increases the tensile strength, yield point, proportional limit and breaking strength. Elongation and reduction of area decrease somewhat. Up to about 1.5% manganese, however, this decrease is very gradual. In some cases (Figs. 15-A, 15-C, 16-A [Part 2]), there even is a slight increase in ductility with the initial increases in manganese content up to about 1.5%. Of particular interest are the shapes of the impact resistance curves. There is a definite and quite pronounced improvement with the initial increases in manganese. This can be observed in five out of six individual graphs in Figs. 15 and 16 (Part 1).[7] In other words, the impact resistance curves form a peak which, for the plain carbon steels, falls in the vicinity of about 1.5%, and for carbon-molybdenum steels, in the vicinity of about 0.5 to 1.0% manganese. Moreover, this peak is more pronounced in steels with low rather than with the higher carbon, and in "plain carbon" rather than "carbon-molybdenum" steels.

In conclusion, it may be stated that the most efficient manganese content, in the sense of the best combination of strength, ductility and impact resistance, is about 1.5% for plain carbon and about 1% for carbon-molybdenum steels. If, however, it is desired to improve the strength still further at a small sacrifice in ductility and impact resistance, it is quite safe to go as high as 2 to 2.5% manganese. Even at about 3% manganese, ductility and impact resistance are still fair and begin to deteriorate rapidly only at still higher manganese contents while the strength with 3% manganese, at least in some instances, is increased nearly twofold as compared with similar compositions con-

[7] In Fig. 16-B, it is observed in the low-temperature impact resistance curve only, perhaps because the lowest manganese content in this subgroup is higher than in any other.

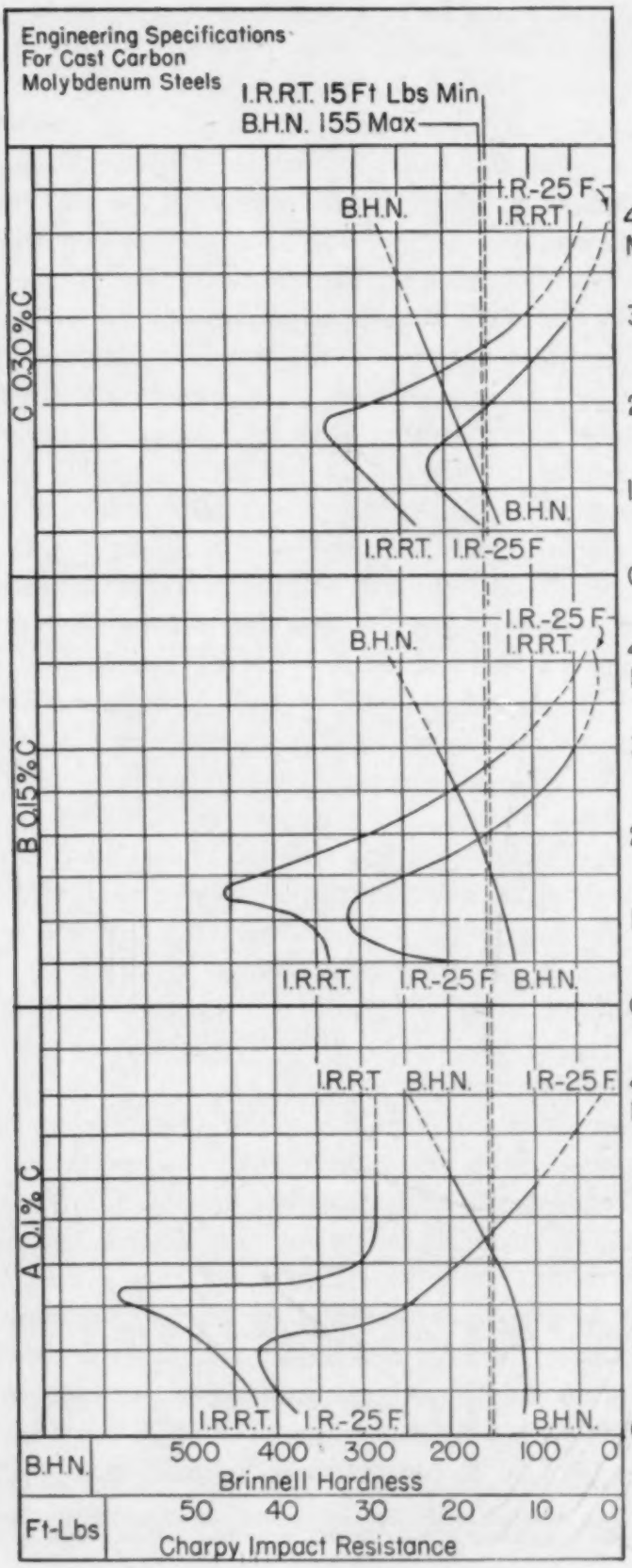


Fig. 15 (Part 1)—Effect of Manganese on Physical Properties of Carbon Steels.

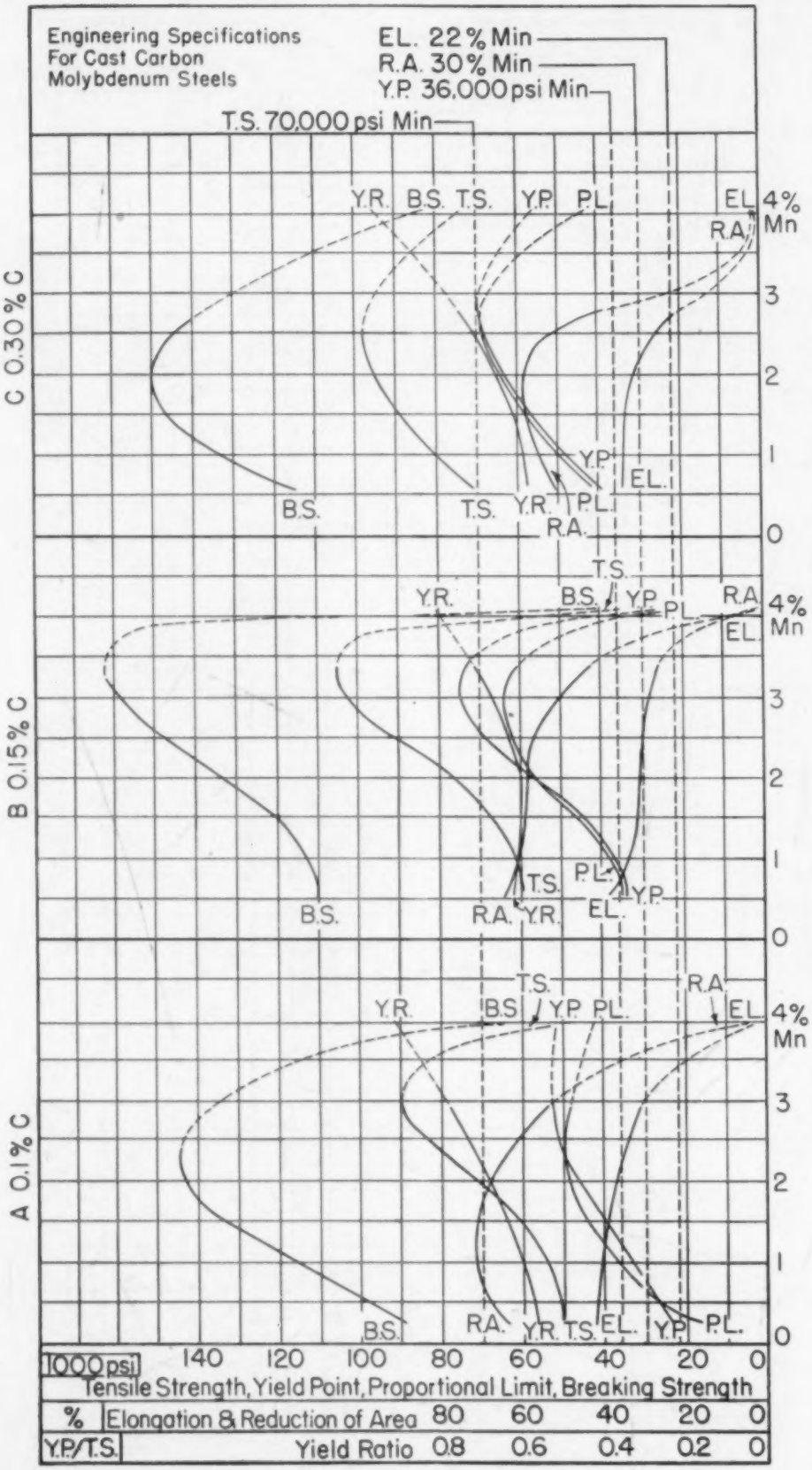


Fig. 15 (Part 2)—Effect of Manganese on Physical Properties of Carbon Steels.

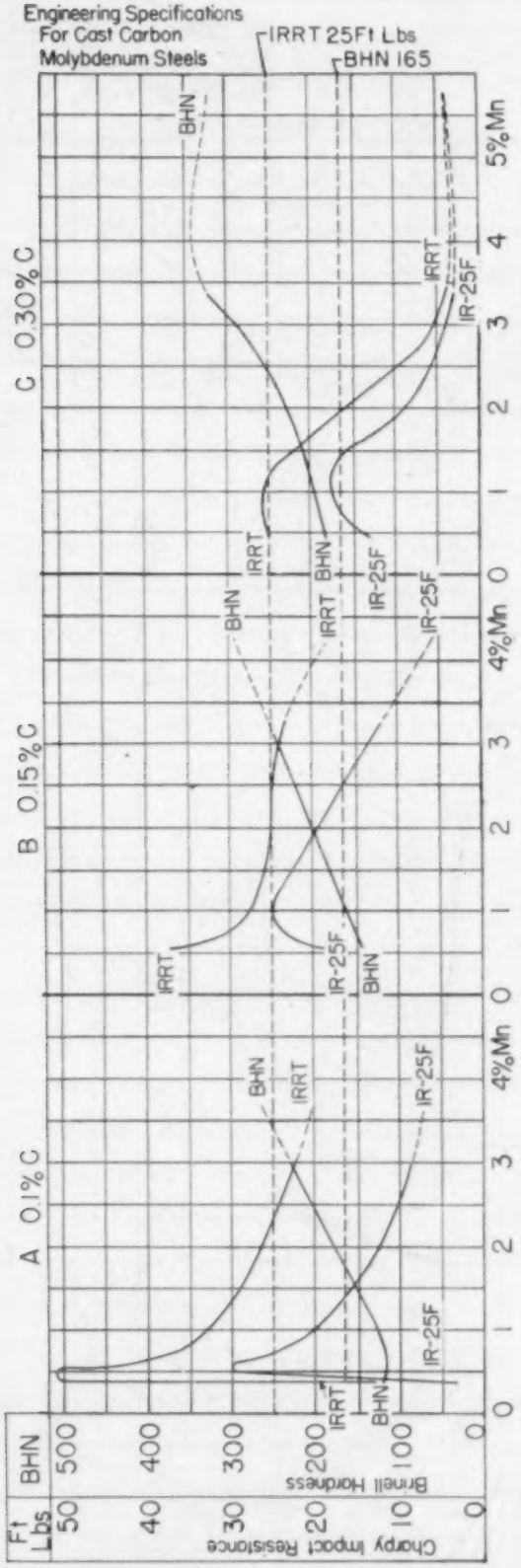


Fig. 16 (Part 1)—Effect of Manganese on Physical Properties of Carbon-Molybdenum Steels.

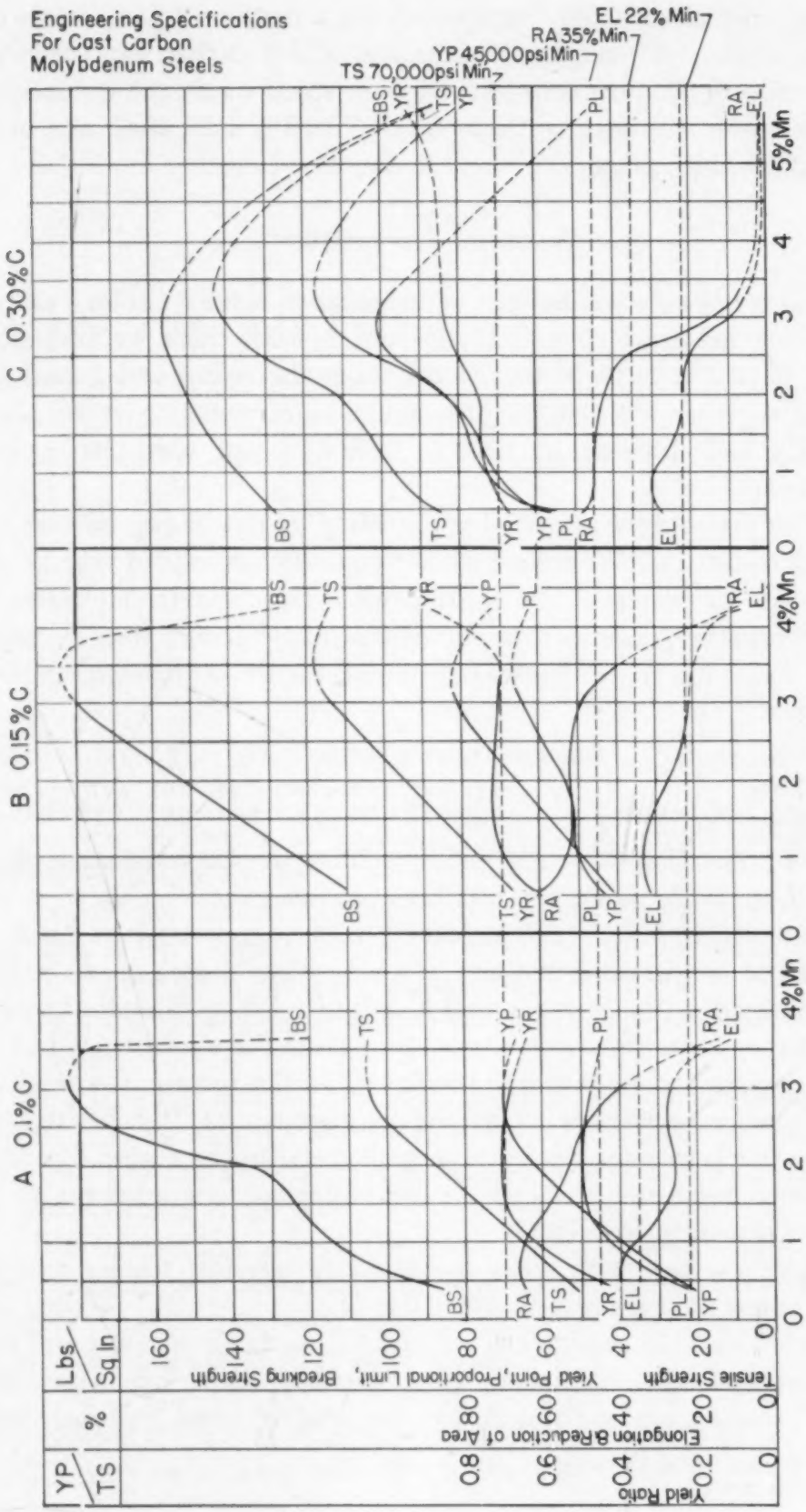


Fig. 16 (Part 2)—Effect of Manganese on Physical Properties of Carbon-Molybdenum Steels.

taining only about 0.5% manganese. As a matter of fact, steels containing about 3% manganese and about 0.15% carbon can easily pass requirements of chromium-molybdenum steels (with the exception of the corrosion resistance of the latter). With 3% manganese and higher carbon contents, physical properties decrease to rather low values.

Welding Experiments

As previously pointed out, representative heats (Tables I and II) were cast into keel coupon blocks and 7/8-inch thick welding plates (Fig. 17). The latter were cut off from the risers and gates; heat treated together with the coupon blocks by normalizing from 1700 F (930 C) and drawing at 1200 F (650 C); and used for welding experiments.

The plates were prepared for welding by machining off one edge of each to form a "V" groove when two plates are placed side by side. Each pair of plates of the same composition was then electric arc welded together, using carbon and carbon-molybdenum steel electrodes of the following approximate composition for the corresponding series of plates:

Electrode	Si	Mn	S	P	C	Mo
Carbon Steel	0.05-0.25	0.30-0.60	0.03	0.03	0.09	—
Carbon-Molybdenum Steel	0.10-0.50	0.30-0.60	0.03	0.03	0.10	0.45-0.65

No preheating was employed in welding carbon-manganese plates, while those made of carbon-molybdenum-manganese steels were preheated to 400 to 500 F (200 to 260 C) with an oxyacetylene flame.

Sound welds were made in seven to eight passes on assemblies 7/8-inch thick with 7-inch running length of welding. Standard tensile[8] and Charpy impact[9] bars were machined from the welds which had not been given any stress relieving treatment. In the former, the weld and the affected zone were left between the gage marks. In the latter, the keyhole notch was cut through the weld metal to the fusion line in an attempt to force the break in the heat-affected zone adjacent to the weld, as shown in Fig. 18.

All these test bars were subjected to physical testing and the resultant test data are recorded in Table III.

From all welds, strips (3/8 by 7/8 by 10 inches) were cut and subjected to bend tests. Each weld was also subjected to "hardness distribution" studies, across the weld and the affected zone. For each weld,

[8] 2-inch gage, 0.505-inch diameter.

[9] Keyhole notch.

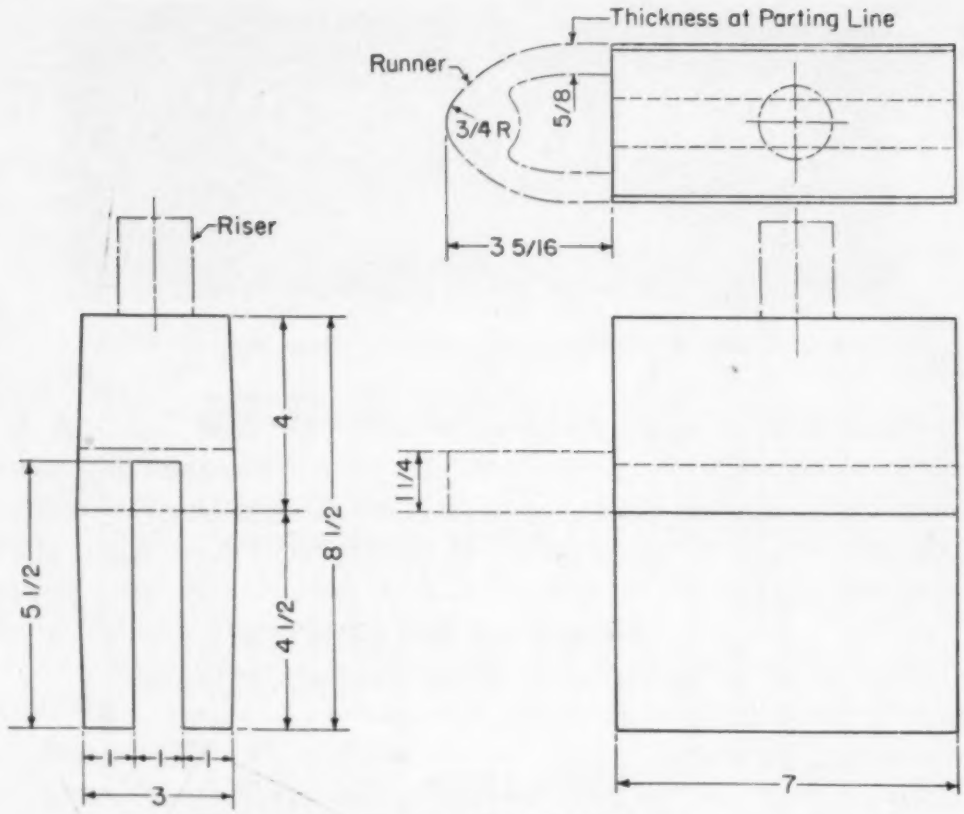


Fig. 17—Welding Test Block Pattern.

this test was performed in "as-welded" condition and also after stress relieving at 1225 F (663 C).

Tensile and Impact Testing of the Welded Assemblies—The results obtained on tensile and impact properties of the welds given in Table III were averaged from duplicate tests. It should be understood that these data represent properties of the welded assemblies and not of the metal.

In most cases, tensile and impact properties of the welds are lower than those of the parent metal and in some (within experimental error) are equal. For this reason, most of the tensile test bars broke through the welds (Table III).

It is interesting to note the relatively high impact resistance in most of these specimens remembering that, in this case, the metal was tested in the most disadvantageous condition, i.e., the zone adjacent to the weld which is most likely to be embrittled.

Bend Tests—Tests were made on plain carbon and carbon-molybdenum steels containing low (about 0.10%), intermediate (about 0.15%), and high (about 0.30%) carbon (all compositions are tabu-

Table III
Physical Properties of Welded Specimens

‡ Serial No.	Nominal Composition				Physical Properties of the Welds ("As Welded")							
					Tensile Properties						Charpy Impact Resistance	
					T. S.	Y. P.	B. S.	El.	R. A.	Y. R.	Ft-Lbs	
	Si	Mn	Mo	C	Psi			Per Cent			R. T.	—25 F
					Carbon Steels							
2	0.20—0.45	0.5	0	0.10	51,000†	35,300	.....	24.5	56.0	0.70	43.3	35.3
7	0.20—0.45	2.0	0	0.10	63,000	42,600	124,700	23.0	62.5	0.68	38 8	29.8
10	0.20—0.45	0.5	0	0.15	60,400†	36,600	.....	21.0	37.0	0.64	41.0	23.0
13	0.20—0.45	1.0	0	0.15	62,000	42,300	125,300	22.0	60.5	0.69	48.0	35.8
16	0.20—0.45	2.0	0	0.15	64,500	44,500	.....	10.5	43.5	0.66	13.0	3.0
18	0.20—0.45	3.0	0	0.15	62,300	44,800	112,500	14.0	47.0	0.72	29.0	3.3
21	0.20—0.45	0.5	0	0.30	62,300	45,000	110,700	19.0	56.5	0.73	31.5	21.8
24	0.20—0.45	2.0	0	0.30	63,000	44,300	109,800	14.5	47.5	0.70	38.8	13.3
27	0.20—0.45	3.0	0	0.30	65,800	49,500	117,300	17.0	58.0	0.76	36.8	13.5
					Carbon-Molybdenum Steels							
31	0.20—0.45	0.5	0.5	0.10	55,500†	35,800	71,800	23.5	50.5	0.65	34.5	32.8
35	0.20—0.45	2.0	0.5	0.10	68,300	44,800	127,400	18.5	59.5	0.66	22.3	18.5
40	0.20—0.45	0.5	0.5	0.15	67,000	45,500	107,200	25.0	56 0	0.68	33.8	34.0
43	0.20—0.45	1.0	0.5	0.15	70,500	48,800	134,000	24.0	61.0	0.69	33.8	18.0
45	0.20—0.45	2.0	0.5	0.15	69,500	57,800	131,600	18.0	59.5	0.83	32.0	17.5
47	0.20—0.45	2.0	0.5	0.15	74,000	41,500	85,000	11.0	41.0	0.56	16.3	9.5
49	0.20—0.45	3.0	0.5	0.15	74,300	42,800	121,000	14.5	42.0	0.58	19.3	10.8
52	0.20—0.45	0.5	0.5	0.30	70,500	47,500	126,100	14.5	43.0	0.67	27.8	17.3
56	0.20—0.45	2.0	0.5	0.30	76,500*	61,300	97,500	6.0	21.5	0.80	18.5	12.8

‡Serial numbers the same as in Tables I and II.
†Samples fractured outside of the weld.
*Sample fractured through the affected zone.



Fig. 18—Keyhole Notch, Charpy Impact Test Piece of the Weld Assembly.

lated in Table III). Longitudinal sections for side bend tests were prepared in accordance with the American Standards Association code requirements and bent at the weld zone around a 1-inch mandrel. All of the strips made from steels containing up to about 2% manganese were bent to 180 degrees without cracking. The higher manganese steels cracked before 180 degrees were reached.

Hardness Distribution Studies—A representative cross section of a weld from each composition was subjected to hardness distribution studies across the weld and the affected zones (using a Vickers pyramid hardness tester with a 30-kilogram load), (a) in "as-welded" condition and (b) stress-relieved at 1225 F (663 C). Fig. 19 illustrates how these tests were performed.

Both sets of these test data are graphically represented in Figs. 20 and 21 for carbon and carbon-molybdenum steels, respectively. In comparing these two figures, it may be observed that in the "as-welded" condition, carbon-molybdenum (Fig. 21) develops higher hardness values than corresponding plain carbon steels (Fig. 20). In both cases, the "low" carbon subgroups do not exhibit hardnesses over about 200 Vickers, even when the manganese content is nearly 2%.

In the intermediate "plain" carbon subgroup (Fig. 20), the hardness exceeds 300 Vickers in the steel containing 2.31% manganese. In a similar carbon-molybdenum steel (Fig. 21), but containing only 2.20% manganese, the maximum hardness is well below 300 Vickers. On the other hand, another steel of the same subgroup, containing 2.63% manganese (Fig. 21), develops a hardness well above 300 Vickers. As has been shown by the dilatometer curves, the thermal sluggishness of plain carbon and carbon-molybdenum steels (containing 0.15 to 0.20% carbon) begins to increase rapidly when manganese contents exceed 2%, thus resulting in rather high hardness values in the affected zone. With still further increase in manganese

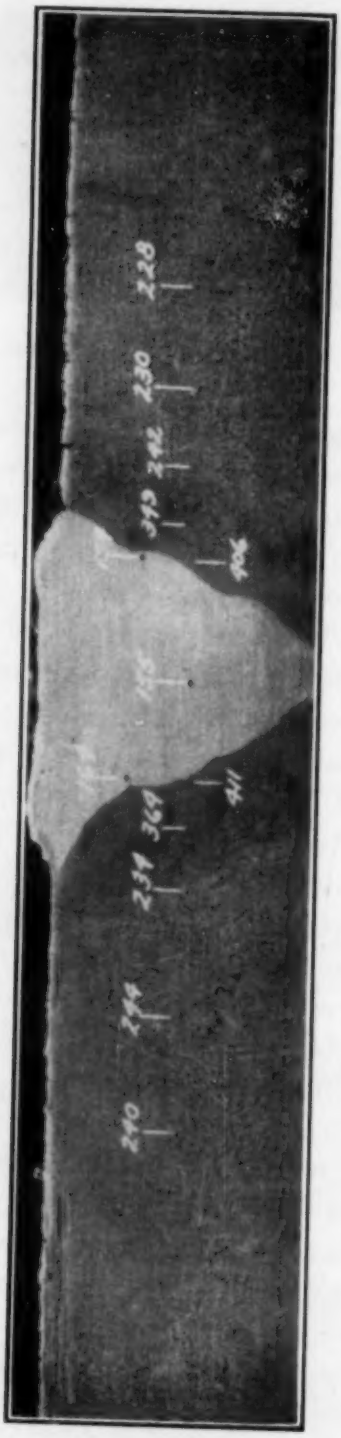
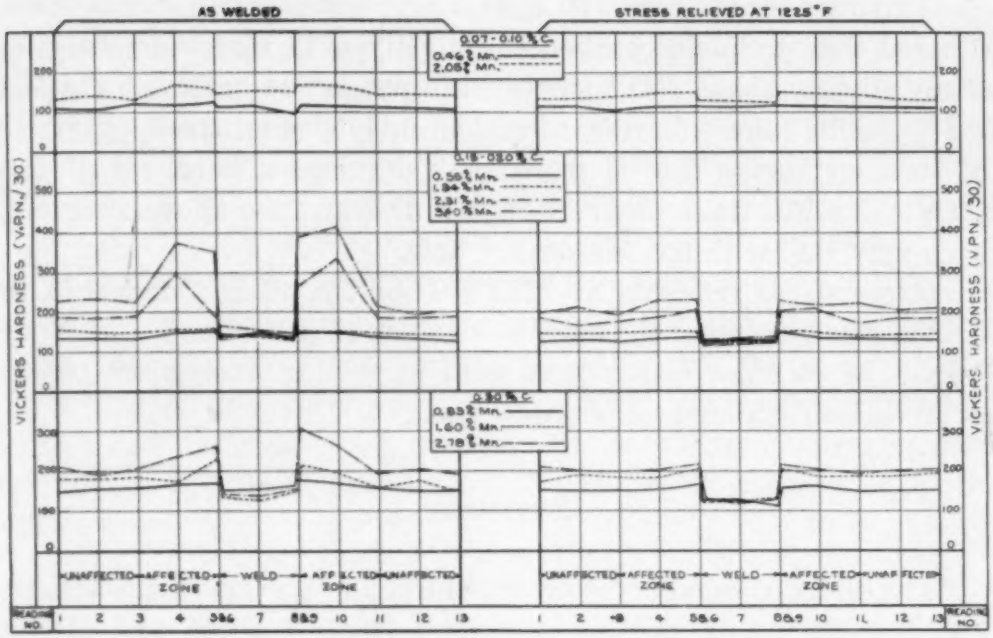


Fig. 19—Serial No. 49, "As-Welded." Hardness distribution across the weld and the affected zones.



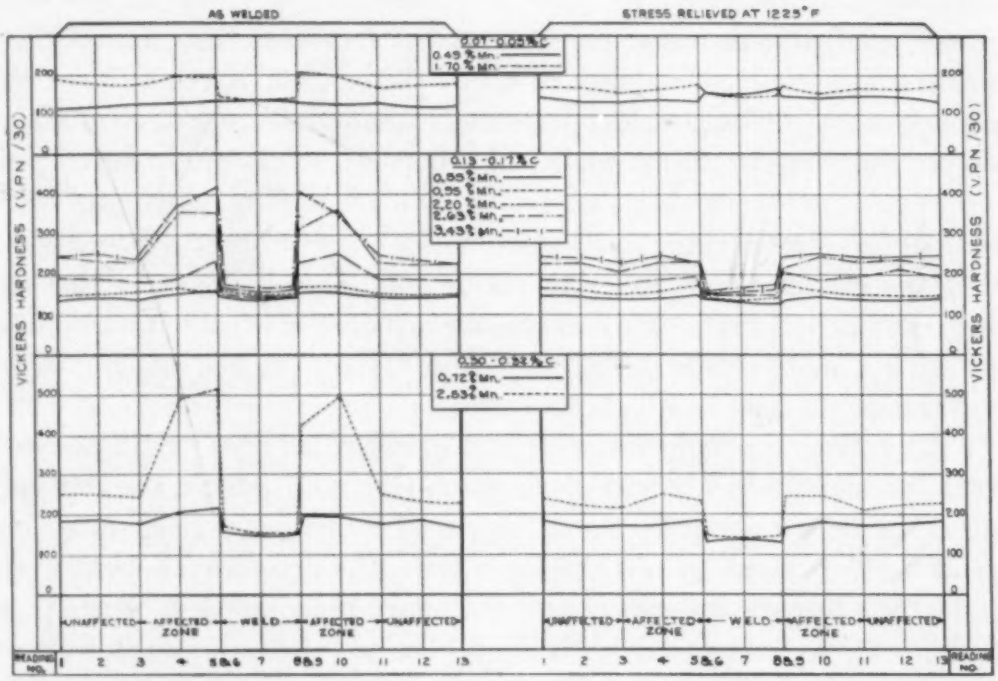


Fig. 20 (Above)—Hardness Distribution Across the Weld and the Affected Zone in Carbon-Manganese Steels.

Fig. 21 (Below)—Hardness Distribution Across the Weld and the Affected Zone in Carbon-Molybdenum-Manganese Steels.

content up and above 3%, the thermal sluggishness increases still further and hardness in the affected zones reaches values over 400 Vickers.

Passing over to "high" (0.30 to 0.32%) carbon subgroups, it may be noted that in "plain" carbon steels (Fig. 20), maximum hardness is only slightly above 300 Vickers with manganese content as high as 2.78%. In the same subgroup of carbon-molybdenum steels (Fig. 21), the steel containing 2.59% manganese develops a hardness of over 500 Vickers. All these observations for this and the above subgroups check very well with the dilatometer data.

After stress relieving at 1225 F (663 C), all hardnesses in the affected zones decrease to rather low values (Figs. 20 and 21). Nonetheless, the increase in hardness with increasing manganese content within each subgroup is quite pronounced.

Summary

The effect of manganese on structural and thermal characteristics as well as on the physical properties of "plain carbon" and carbon-molybdenum cast steels of three different carbon contents has been investigated. It was found that manganese increases the thermal sluggishness and air hardenability of all of them. This increase, however, is much more gradual and less pronounced than in the case of chromium-molybdenum or chromium-nickel-molybdenum steels. Fully developed, suppressed transformations on relatively slow cooling, associated with more or less considerable "air hardenability", can be observed only when manganese content increases to about 2%. This increase in thermal sluggishness as a function of increasing manganese is more pronounced in "carbon-molybdenum" than in "plain carbon" steels, and in "higher" carbon than in "low" carbon steels.

By raising the manganese content to about 1.5% in "plain carbon" and to about 0.75 to 1.0% in "carbon-molybdenum" steels, the strength can be increased about 20%, as compared to similar steels containing about 0.5% manganese. At the same time, the decrease in ductility is slight. The impact resistance with the above manganese contents is at its highest, as compared with that obtained with either lower or higher percentages.

Some welding experiments indicate that there are no welding difficulties encountered within the carbon range used, provided the manganese content is held under 2%. The resultant weld assemblies in steels containing under 2% manganese exhibit considerable ductility and strength. No excessive hardness was developed in the affected zones of these steels.

The present paper has been written with the objective of describing some fundamental technical and engineering data and does not attempt to advocate any definite compositions for specific uses or make any recommendations.

Acknowledgments

The authors wish to express their thanks to Crane Co. for permission to publish these results; to A. F. Lahr and B. F. Grant for their help in melting, preparing and heat treating the steels; to H. A. Peterson for making the dilatometric analyses; to B. E. Jenkins for performing the physical tests; to the Control Laboratory for making chemical analyses; and to R. A. Mueller and P. Hjulin for taking care of the welding tests.

Bibliography

1. N. A. Ziegler and W. L. Meinhart, "The Effect of Copper on the Properties of Cast Carbon-Molybdenum Steels," *Transactions*, American Foundrymen's Association, Vol. 52, No. 4, June 1945, p. 1151.
2. N. A. Ziegler and W. L. Meinhart, "Characteristics and Properties of Some Cast Chromium-Molybdenum Steels," TRANSACTIONS, American Society for Metals, Vol. 34, 1945, p. 589.
3. N. A. Ziegler and W. L. Meinhart, "Effect of Nickel on Physical Properties and Thermal Characteristics of Some Cast Chromium-Molybdenum Steels," TRANSACTIONS, American Society for Metals, Vol. 37, 1946, p. 360.
4. C. H. Herty, Jr., and O. S. True, "The Reaction Between Manganese and Iron Sulphide," *Transactions*, American Institute of Mining and Metallurgical Engineers, Vol. 71, 1925, p. 540.
5. C. H. Herty, Jr., "Chemical Equilibrium of Manganese, Carbon and Phosphorus in the Basic Open Hearth Process," *Transactions*, American Institute of Mining and Metallurgical Engineers, Vol. 73, 1926, p. 1107.
6. J. H. Hall, "Properties of Manganese Steel," *Canada Machinery and Manufacturing News*, Vol. 38, No. 14, Sept. 1, 1927, p. 20.
7. J. A. Jones, "The Effect of Manganese on the Properties of Low Carbon Steels," *The Metallurgist* (London), Oct. 28, 1927, p. 157; Nov. 25, 1927, p. 163.
8. V. N. Krivobok, B. M. Larsen, W. B. Skinkle and W. C. Masters, "Some Characteristics of Low-Carbon Manganese Steel," *Transactions*, American Institute of Mining and Metallurgical Engineers, Vol. 75, 1927, p. 404.
9. J. Strauss, "Low Manganese Steel Gains Favor," *Iron Age*, Vol. 121, No. 13, March 29, 1928, p. 864.
10. J. Strauss, "Medium Carbon Pearlitic Manganese Steel," TRANSACTIONS, American Society for Steel Treating, Vol. 14, No. 1, July 1928, p. 1.
11. A. S. Martin, "Progress in Machining Manganese Steel," *Heat Treating and Forging*, Vol. 14, No. 3, March 1928, p. 282. *Machinery* (London), Vol. 32, No. 827, Aug. 16, 1928, p. 622. *Machinery* (New York), Vol. 34, No. 11, July 1928, p. 862.
12. J. H. Hruska, "Making Electric Manganese Steel," *Iron Age*, Vol. 122, No. 8, Aug. 23, 1928, p. 455.
13. H. P. Evans and A. F. Burtt, "Manufacture and Heat Treatment of Manganese Steel," *Fuels & Furnaces*, Vol. 6, No. 9, Sept. 1928, p. 1203.

14. Anonymous, "Pure Manganese Makes Interesting Alloys," *Iron Age,* Vol. 122, No. 24, Dec. 13, 1928, p. 1499.
15. V. N. Krivobok, "Iron-Manganese Alloys," *Foundry Trade Journal* (London), Vol. 39, No. 634, Dec. 13, 1928, p. 428.
16. M. Hamasumi, "A Study of the Mechanical Properties of Low Manganese Steel," Tohoku Imperial University Technology Reports, Vol. 7, No. 4, 1928, p. 305.
17. C. R. Wohrman, "Heterogeneity of Iron-Manganese Alloys," American Institute of Mining and Metallurgical Engineers, Iron & Steel Division, 1928, p. 197.
18. J. H. Hall, "The Wear Testing of Manganese Steel," *Metal Stampings,* Vol. 2, No. 1, Jan. 1929, p. 16.
19. J. Trantin, Jr., "Explains Manganese Steel Production in Electric Furnace," *Foundry,* Vol. 57, No. 2, Jan. 15, 1929, p. 52; Vol. 57, No. 3, Feb. 1, 1929, p. 128.
20. J. H. Hall, "New Facts About Manganese Steel," *Iron Age,* Vol. 123, No. 9, Feb. 28, 1929, p. 600.
21. E. E. Thum, "Heat Treated Low Manganese Steels," *Iron Age,* Vol. 123, No. 25, June 20, 1929, p. 1691.
22. V. N. Krivobok, "A Study of the Constitution of High Manganese Steels," TRANSACTIONS, American Society for Steel Treating, Vol. 15, No. 6, June 1929, p. 893.
23. E. Maurer, "Maurer Manganese Steel in the Development of Stainless Steel," *Stahl und Eisen* (Düsseldorf), Vol. 49, No. 34, Aug. 22, 1929, p. 1217.
24. Anonymous, "Electric-Furnace High-Content Manganese Steel," *Journal du Four Electrique* (Paris), Vol. 38, No. 8, Aug. 1929, p. 269.
25. V. N. Svetchnikoff, "Hadfield Steel," *Rev. de Metallurgie* (Paris), Vol. 26, No. 8, Aug. 1929, p. 401.
26. J. H. Hall, "Austenite Manganese Steel," TRANSACTIONS, American Society for Steel Treating, Vol. 16, No. 3, Sept. 1929, p. 458.
27. C. B. Bronson, "Medium Manganese Steel Makes Higher Grade Rails," *Railway Age,* Vol. 67, No. 9, Sept. 1929, p. 563.
28. W. Schmidt, "X-ray Investigation of the Iron-Manganese System," *Arch. f. d. Eisenhüttenwesen,* Vol. 3, No. 4, Oct. 1929, p. 83.
29. A. Heinzel, "The Influence of Various Elements on Polymorphism of Iron," *Zeitschr. f. Techn. Phgs.,* Vol. 10, No. 4, 1929, p. 136.
30. J. H. Hall, "Studies of Hadfield's Manganese Steel With the High Power Microscope," *Proceedings,* Iron & Steel Division, American Institute of Mining and Metallurgical Engineers, 1929, p. 382.
31. R. Hadfield, "Manganese Steel and Its Developments," *Proceedings,* World Engineering Congress, Tokyo, 1929. *Mining and Metallurgy,* Vol. 34, Part 2, p. 261.
32. B. M. Larsen, "Effect of Manganese on Distribution of Carbon in Steel," United States Bureau of Mines, Technical Paper No. 466, 1929.
33. H. D. Hibbard, "Manganese in Simple Steels," *Fuels & Furnaces,* Vol. 8, 1930, No. 1, Jan., p. 51; No. 2, Feb., p. 217; No. 3, Mar., p. 391; No. 4, April, p. 541; No. 5, May, p. 673; No. 6, June, p. 815.
34. K. H. Von Scheele, "Manganese Hard Steel," *Giesserei-Zeitung* (Berlin), Vol. 27, No. 4, Feb. 15, 1930, p. 98.
35. E. Decherf, "Semi-Hard Manganese Steel," *Aciers Spéciaux,* Métaux & Alliages (Paris), Vol. 5, No. 54, Feb. 1930, p. 51.
36. A. O. Fulton, "Manganese as an Alloying Element in Pearlitic Steels," TRANSACTIONS, American Society for Steel Treating, Vol. 17, No. 2, Feb. 1930, p. 293.
37. J. H. Hruska, "Study of Pearlitic Manganese Steels," *Blast Furnace & Steel Plant,* Vol. 18, No. 5, May 1930, p. 802. *Heat Treating & Forging,* Vol. 16, No. 4, April 1930, p. 455.

38. A. Osawa, "X-ray Investigation of Iron and Manganese Alloys," *Science Reports,* Tohoku Imperial University, Vol. 19, No. 2, May 1930, p. 247.
39. E. E. Thum, "The New Manganese Alloy Steels," *Transactions,* American Society for Testing Materials, Vol. 30, Part 2, June 23, 1930, p. 215.
40. A. B. Kinzel and W. B. Miller, "Data on Manganese Structural Steels with Chromium Additions," TRANSACTIONS, American Society for Steel Treating, Vol. 18, No. 1, July 1930, p. 55; Vol. 18, July-Dec. 1930, p. 908.
41. H. P. Evans, "Heat Treatment Determines Properties of Manganese Steel," *Foundry,* Vol. 58, No. 17, Sept. 1, 1930, p. 102.
42. M. Grossmann, "Manganese, a Stabilizer for Austenite Structure," *Steel,* Vol. 87, Oct. 9, 1930, p. 68.
43. V. N. Krivobok, "The Alloys of Iron and Manganese," *Heat Treating & Forging,* Vol. 16, No. 12, Dec. 1930, p. 1538.
44. A. Westgren, "Suppressions in Alloys of Manganese," METAL PROGRESS, Vol. 19, No. 2, Feb. 1931, p. 87.
45. V. N. Krivobok, "Diagram of Iron-Manganese Alloys," *Heat Treating & Forging,* Vol. 17, No. 2, Feb. 1931, p. 153.
46. T. Muracami and K. Hatsuta, "The Microstructure and the Hardness of Quenched Manganese Steels," Abstract, *Metals & Alloys,* Vol. 2, No. 3, Sept. 1931, p. 168.
47. G. Guzzoni, "The Hadfield Manganese Steel. Its Structure and Properties," *Giesserei mit Giesserei-Zeitung,* Vol. 18, Nov. 6, 1931, p. 868. *La Metallurgia Italiana,* Vol. 24, March 1932, p. 173.
48. J. H. Hall, "A New Manganese Steel," METAL PROGRESS, Vol. 20, No. 5, Nov. 1931, p. 69.
49. H. Scott, "Tranformational Characteristics of Iron-Manganese Alloys," *Transactions,* Iron & Steel Division, American Institute of Mining and Metallurgical Engineers, 1931, p. 284.
50. Anonymous, "Addition of Vanadium Improves Properties of Medium Manganese Steels," *Vancoram Review,* Vol. 3, No. 2, April 1932, p. 64.
51. F. M. Walters, Jr.; F. M. Walters, Jr., and C. Wells; M. Gensamer, J. F. Eckel and F. M. Walters, Jr.; F. M. Walters, Jr., and M. Gensamer, "Alloys of Iron, Manganese and Carbon," TRANSACTIONS, American Society for Steel Treating, Vol. 19, No. 7, May 1932; Part 1, "Preparation of Alloys," p. 577; Part 2, "Thermal Analysis of Binary Alloys," p. 590; Part 3, "An X-ray Study of the Binary Iron-Manganese Alloys," p. 599; Part 4, "A Dilatometric Study of Iron-Manganese Binary Alloys," p. 608.
52. L. S. Moisseiff, "Medium Manganese Steel," METAL PROGRESS, Vol. 22, No. 2, July 1932, p. 2.
53. W. F. Rowden, "Molybdenum-Manganese Alloy Steels," *Metallurgia* (London), Vol. 7, Nov. 1932, p. 9.
54. J. H. Hall, "Austenitic Manganese Steel Castings," *Proceedings,* American Society for Testing Materials, Vol. 32, Part 2, 1932, p. 238.
55. J. Burns, "The Effect of Molybdenum on Medium Carbon Steels Containing 1 to 2.5% Manganese," *Journal,* British Iron & Steel Institute, Vol. 74, No. 2, 1932, p. 241.
56. E. C. Bain, E. S. Davenport and W. S. N. Waring, "The Equilibrium Diagram of Iron-Manganese-Carbon Alloys of Commercial Purity," *Transactions,* Iron & Steel Division, American Institute of Mining & Metallurgical Engineers, Vol. 100, 1932, p. 228.
57. H. Scott and J. G. Hoop, "The Hardening Transformation in Manganese Steels," TRANSACTIONS, American Society for Steel Treating, Vol. 21, No. 3, March 1933, p. 233.
58. C. R. Austin, "Observations on the Effect of Normalizing Medium Manganese Steels on the Microstructure and Physical Properties," TRANSACTIONS, American Society for Steel Treating, Vol. 21, No. 5, May 1933, p. 435.

59. H. T. Chandler and C. N. Dawe, "Develops Manganese-Chromium-Vanadium Steels for Automotive Forgings," *Steel*, Vol. 93, Sept. 25, 1933, p. 23.
60. V. N. Krivobok and C. Wells; F. M. Walters, Jr.; C. Wells and F. M. Walters, Jr.; J. F. Eckel and V. N. Krivobok, "Alloys of Iron, Manganese and Carbon," TRANSACTIONS, American Society for Steel Treating, Vol. 21, No. 9, Sept. 1933; Part 5, "Microscopic Studies of Binary Iron-Manganese Alloys," p. 807; Part 6, "Factors Affecting Transformations in the Binary Iron-Manganese Alloys," p. 821; Part 7, "Influence of Carbon on 13% Manganese Alloys," p. 830; Part 8, "Influence of Carbon on 10% Manganese Alloys," p. 846.
61. F. M. Walters, Jr.; F. M. Walters, Jr., and J. F. Eckel; F. M. Walters, Jr., and C. Wells; M. Gensamer, "Alloys of Iron and Manganese," TRANSACTIONS, American Society for Steel Treating, Vol. 21, No. 11, Nov. 1933; Part 9, "Transformations and Heterogeneity in the Binary Alloys of Iron and Manganese," p. 1002; Part 10, "Thermomagnetic Analysis of the Binary Alloys of Iron and Manganese," p. 1016; Part 11, "The Variation of Electrical Resistance with Temperature in Binary Alloys of Iron and Manganese," p. 1021; Part 12, "Alloys of Iron and Carbon with 2.5 and 4.5% Manganese," p. 1028.
62. H. W. Hiemke and W. C. Schulte, "Low Temperature Impact Tests of Medium Manganese Steel Plate," *Metals & Alloys*, Vol. 5, No. 2, Feb. 1934, p. 31.
63. Anonymous, "Manganese-Copper Steel Manufactured in Germany with no Deoxidizer Added," *Steel*, Vol. 95. No. 4, July 23, 1934, p. 44.
64. C. H. Herty, Jr., and M. B. Royer, "Solubility of Carbon in Iron-Manganese-Silicon Alloys," Bureau of Mines, Information Circular No. 3230, 1934.
65. V. Zsak, "Manganese Steel Castings with High Strength," *Giesserei*, Vol. 22, April 26, 1935, p. 195.
66. E. Scheit, "Transformations in Irreversible Iron-Manganese Alloys," *Archiv f. d. Eisenhüttenwesen*, Vol. 9, Aug. 1935, p. 115.
67. F. M. Walters, Jr., and C. Wells, "Alloys of Iron and Manganese, Part 13, Constitution of Binary Alloys of Iron and Manganese," TRANSACTIONS, American Society for Metals, Vol. 23, No. 3, Sept. 1935, p. 727.
68. R. Vogel and W. Doering, "System: Iron-Cementite-Manganese Carbide-Manganese," *Archiv f. d. Eisenhüttenwesen*, Vol. 9, Nov. 1935, p. 247.
69. F. M. Walters, Jr., and C. Wells, "Alloys of Iron-Manganese-Carbon, Part 15, The Ternary Diagram and General Summary," TRANSACTIONS, American Society for Metals, Vol. 24, No. 2, June 1936, p. 359.
70. G. F. Comstock, "Titanium Improves Pearlitic Manganese Steel," *Metals & Alloys*, Vol. 8, No. 5, May 1937, p. 148.
71. W. Tofaute and K. Linden, "Transformations in Manganese Steels with Up to 1.2% Carbon and 17% Manganese," *Archiv f. d. Eisenhüttenwesen*, Vol. 10, May 1937, p. 515.
72. F. M. Walters, Jr., "Nature of Iron-Manganese Alloys," METAL PROGRESS, Vol. 32, No. 3, Sept. 1937, p. 254.
73. H. O'Neill, "Alloy and Fine-Grained Steels for Locomotive Coupling Rods," *Journal*, British Iron & Steel Institute, Vol. 135, No. 1, 1937, p. 187.
74. M. L. V. Gayler, "Alloys of Iron Research, Part 12, Note on the βm Transformation in Manganese-Rich Iron-Manganese Alloys," *Journal*, British Iron & Steel Institute, Vol. 135, No. 1937, p. 269.
75. G. F. Comstock, "Effect of Titanium and Vanadium on Forged Pearlitic Manganese Steel," *Iron Age*, Vol. 143, No. 7, Feb. 16, 1939, p. 27.
76. B. Thomas, "Manganese in Carbon Steels," *Metallurgia*, Vol. 21, No. 123, Jan. 1940, p. 73.
77. Anonymous, "Oil Hardened and Tempered Manganese Steels," *The Metallurgist* (London), June 28, 1940, p. 114.
78. Anonymous, "Transformations in Manganese Steels," *The Metallurgist* (London), June 28, 1940, p. 116.

79. Anonymous, "Case Hardening Steels Containing Manganese," *The Metallurgist* (London), June 28, 1940, p. 119.
80. H. Taylor, "Medium Manganese Steels in the Foundry," *Metallurgia,* Vol. 23, No. 133, Nov. 1940, p. 1.
81. M. P. Brown, "Manganese-Silicon Steels for Transmission Gears," METAL PROGRESS (U.S.S.R.), Vol. 39, No. 1, Jan. 1941, p. 73.
82. D. Niconoff, "Quantitative Measurements of Strain Hardness in Austenitic Manganese Steel," TRANSACTIONS, American Society for Metals, Vol. 29, No. 2, June 1941, p. 519.
83. Anonymous, "Manganese in the Steel Industry," *Metallurgia* (London), Vol. 24, No. 141, July 1941, p. 82.
84. Anonymous, "Use of Manganese in Alloy Steels," *The Metallurgist* (London), Aug. 29, 1941, p. 26.
85. D. B. Rice, "Welding Technique for Manganese Steel," *Iron Age,* Vol. 148, No. 11, Sept. 11, 1941, p. 55.
86. V. R. Farlow and L. H. McCreery, "Hadfield Manganese Steel. Another Approach to Its Qualities and Use," *Metals & Alloys,* Vol. 14, No. 5, Nov. 1941, p. 692.
87. R. M. Parke, J. R. Blanchard and A. J. Herzig, "New Data for Evaluating Manganese-Molybdenum Steels," METAL PROGRESS, Vol. 40, No. 6, Dec. 1941, p. 906.
88. J. H. Whiteleg, "Apparent Relations Between Manganese and Segregations in Steel Ingots," *Journal,* British Iron & Steel Institute, Vol. 144, No. 2, 1941, p. 63.
89. C. Wells and R. F. Mehl, "Rate of Diffusion of Manganese in Gamma Iron in Low-Carbon and High-Carbon Manganese Steels," *Transactions,* Iron & Steel Division, American Institute of Mining and Metallurgical Engineers, Vol. 145, 1941, p. 315.
90. C. H. Herty, Jr., "Method for Conserving Ferromanganese Without Seriously Affecting Steel Quality," *Industrial Heating,* Vol. 9, No. 8, Aug. 1942, p. 1047.
91. R. Franks, W. O. Binder and C. M. Brown, "High Manganese Austenitic Steels," *Iron Age,* Vol. 150, No. 14, Oct. 1, 1942, p. 51.
92. F. M. Walters, Jr., I. R. Kramer and B. M. Loring, "Mechanical Properties of Iron-Manganese Alloys," *Transactions,* Iron & Steel Division, American Institute of Mining and Metallurgical Engineers, Vol. 150, 1942, p. 40.
93. B. Thomas, "A Carbon-Manganese Steel for Stamping and Forging," *Heat Treating & Forging,* Vol. 29, No. 3, March 1943, p. 140.
94. D. W. Rudorff, "Development of Austenitic Manganese-Alloyed Steels for Aero-Engine Exhaust Valves," *Metallurgia* (London), Vol. 27, No. 162, April 1943, p. 205.
95. A. R. Troiano and F. T. McGuire, "A Study of the Iron-Rich Iron-Manganese Alloys," TRANSACTIONS, American Society for Metals, Vol. 31, No. 2, June 1943, p. 340.
96. E. G. Wigfield, "Manufacture of Carbon-Manganese Steel in an Open-Hearth Furnace," *Iron & Steel* (London), Vol. 16, No. 13, Aug. 1943, p. 517.
97. L. W. Bolton and J. Hill, "The Continuous Production of Manganese Steel Castings from the Tropenas Converter," *Foundry Trade Journal* (London), Aug. 19, 1943, p. 319; Aug. 26, 1943, p. 347; *Engineering* (London), Vol. 156, Aug. 20, 1943, p. 158; Aug. 27, 1943, p. 177; *Iron & Steel* (London), Vol. 16, No. 14, Sept. 1943, p. 537.
98. J. W. Gardom, "The Mass Production of a Manganese Steel Casting," *Transactions,* American Foundrymen's Association, Vol. 51, No. 1, Sept. 1943, p. 86.
99. D. J. Mack, "High-Manganese Stainless Steels" (A correlated abstract), *Metals & Alloys,* Sept. 1943, p. 507; Nov. 1943, p. 1081.

100. D. Niconoff, "Some Aspects of Strain Hardenability of Austenitic Manganese Steel," TRANSACTIONS, American Society for Metals, Vol. 31, No. 3, Sept. 1943, p. 716.
101. G. F. Comstock, "Comparative Effects of Boron and Manganese on Some Properties of Heat Treated Steels," *Iron Age*, Vol. 152, Sept. 9, 1943, p. 48.
102. G. A. Timmons, "Jominy End-Quench Hardenability Tests on Carbon-Manganese Steels," *Iron & Steel* (London), Vol. 16, No. 5, 6, 7, 1943, p. 209, 241, 275.
103. T. Swinden, "Leaded Manganese-Molybdenum Steel," *Journal*, British Iron & Steel Institute, Vol. 148, No. 2, 1943, p. 441.
104. H. H. Uhlig, "Influence of Hydrogen on Mechanical Properties of Some Low-Carbon Manganese-Iron Alloys and on Hadfield Manganese Steel," *Transactions*, Iron and Steel Division, American Institute of Mining and Metallurgical Engineers, Vol. 158, 1944, p. 183.
105. J. V. Russell and F. T. McGuire, "A Metallographic Study of the Decomposition of Austenite in Manganese Steels," TRANSACTIONS, American Society for Metals, Vol. 33, 1944, p. 103.
106. N. P. Goss, "The Effect of Cold Rolling on the Structure of Hadfield Manganese Steel," TRANSACTIONS, American Society for Metals, Vol. 34, 1945, p. 630.

DISCUSSION

Written Discussion: By Howard S. Avery, research metallurgist, American Brake Shoe Co., Mahwah, N. J.

Steels with manganese content intermediate between the general engineering steels and the 12 or 13% of Hadfield's austenitic manganese steel are occasionally proposed for commercial use as they usually exhibit air hardening tendencies suggestive of value for wear resistance applications. However, the mixtures of austenite and harder transformation products generally exhibit disappointing mechanical properties.

In this paper, a decrease in toughness beyond 3% manganese is apparent. The authors remark that the 4% manganese specimens were somewhat unsound and segregated. Does this fully explain the poorer properties or are they perhaps due to increased amounts of retained austenite?

Written Discussion: By Charles R. Wilks, metallurgist, American Brake Shoe Co., Mahwah, N. J.

It should be noted that the comparisons of mechanical properties with manganese content were made for the same heat treatment rather than at identical hardness and strength levels. That the hardness after normalizing increases generally with manganese content is evident, reflecting the suppression of transformation to lower and lower temperature reaction products until essentially full hardening is achieved; and, when the normalized structures are quite similar, the higher tempered hardnesses indicate the greater resistance to tempering of the more highly alloyed materials.

The initial manganese increments provide improved ductility and toughness despite greater hardness and strength resulting from higher

hardenability; this is as would be expected where the structures developed are progressively sufficiently superior. When the improvement in structure becomes smaller or even negligible within certain increment ranges of manganese, ductility and toughness, which would likely be similar at the same hardness and strength levels, would be expected to decline as tensile strength and hardness are increased. With sufficient alloy content to inhibit the full transformation of the austenite upon normalizing, some deterioration in properties may then occur for the same hardness and strength.

The authors do not indicate the section size or cooling rate of the normalized blanks from which the mechanical test specimens were machined. These are necessary qualifications of their quantitative findings.

The authors have qualified the data for the 4% manganese steels ". . . which came out somewhat porous and unsound", and their inclusion in Figs. 15 and 16 is questionable in view of the hardness strength conversions (e.g., 26,100 psi—257 BHN, 92,500 psi—331 BHN).

Authors' Reply

The authors wish to thank Messrs. Avery and Wilks for their written discussions.

With regard to Mr. Avery's comments on retained austenite in the 4% manganese steels, neither dilatometric nor metallographic examination revealed any evidence of the presence of this phase. There would be less chance of finding any austenite in the tensile or impact test bars than in the air-cooled dilatometer samples, because of the draw treatment given the former. It may be possible that some small local segregations might have high enough manganese contents to produce austenite but our work did not reveal any evidence to substantiate this hypothesis. It is generally known that manufacturing of high manganese steels is an art requiring special techniques. It is quite certain that by refining our experimental foundry technique to meet the peculiarities of high manganese steels, the unsoundness and segregations observed in these 4% manganese compositions could be reduced or even completely eliminated. However, there was not enough interest in the 4% manganese steels to justify continuing these efforts. We agree with Mr. Wilks that the steels with higher manganese contents offer greater resistance to tempering. Moreover, the same general hardness and strength levels for these compositions might be attained by using a different heat treatment for each composition. For example, hardness and strength of those containing less manganese could be increased with certain limitations by water or oil quenching, whereas normalizing followed by higher draw temperatures would produce similar results for the more highly alloyed steels.

This, however, was not the object of the present investigation. Liquid quenching of steel castings, and particularly of the heavy walled ones, for many practical considerations is undesirable. For this reason, in our work heat treatment was restricted to normalizing and drawing. With this restriction in mind, it appears that the most desirable manganese con-

tent is 1.5% for carbon, and 0.75 to 1.0% for carbon-molybdenum steels. But, this does not mean that a production foundry can, without any intermediate experimentation, modify its present manganese contents to these figures, because there may be some complications encountered, which our research does not reveal, but which will have to be overcome before the modified compositions can be successfully manufactured on a production scale.

To answer Mr. Wilks's question regarding the size of our blanks, at the time of their heat treatment they were cut from standard keel coupon blocks to uniform dimensions of 6 inches long by 1 inch wide and by ⅞ inch thick. The cooling from normalizing was performed in still air. It was not measured but should be quite rapid in the high temperature range and progressively decrease with falling temperatures. However, for blanks of uniform size it should be the same, which in our opinion makes the resultant physical properties directly comparable.

The inconsistency of hardness to tensile strength ratio in 4% manganese steels, observed by Mr. Wilks, may partly be attributed to the unsoundness of the castings and partly to the inherent brittleness of this metal.

RELATION OF QUENCHING RATE AND HARDENABILITY TO THE MECHANICAL PROPERTIES OF SEVERAL HEAT TREATED CAST ALLOY STEELS

By Charles R. Wilks, Howard S. Avery and Earnshaw Cook

Abstract

This paper presents the available results of a project to study the effects of quenching rate and of hardenability upon the mechanical properties of several heat treated cast alloy steels. To avoid the handling of unwieldy sections, the double end quench test technique, which has been previously described (1),[1] has been employed to provide quenching rates that correspond closely to those which obtain at the center of plates 2 to 8 inches thick. Tensile and impact properties have been determined, with the latter appearing to be more sensitive to structural differences. It is suggested that, for cast steels, accentuated intercellular segregation militates against increased alloying for heavier sections. Optimum mechanical properties seem to be coincident with the minimum hardenability which will produce maximum hardening for any particular rate of cooling.

While the scheduled testing has been essentially completed, the logical extensions of the research, as originally planned, were abandoned concurrently with the discontinuance of both National Research Council Project NRC-83A and the correlated production of cast tank armor which had motivated the experimental program. The data are presented to make them available to other investigators who are interested in this or related problems.

THE general qualitative effects of quenching rate and hardenability upon the mechanical properties of heat treated alloy steels are well known. Where, for example, the maximum properties of a particular steel in a given hardness range are attained by tempering a martensitic structure, decreasing the quenching rate (e.g., by increasing section size) or reducing the alloy content (i.e., decreasing

[1]The figures appearing in parentheses pertain to the references appended to this paper.

A paper presented before the Twenty-eighth Annual Convention of the Society held in Atlantic City, November 18 to 22, 1946. Of the authors, Charles R. Wilks is metallurgist, Howard S. Avery is research metallurgist, and Earnshaw Cook is consulting metallurgist, American Brake Shoe Company, Mahwah, N. J. Manuscript received July 25, 1946.

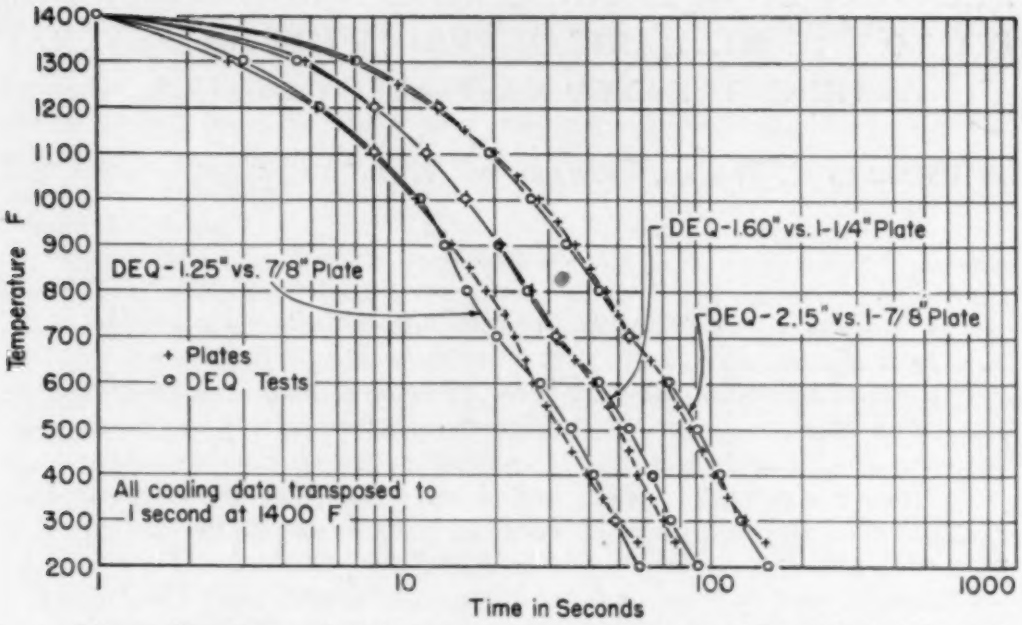


Fig. 1—Comparison of Cooling Curves at the Center of Plates Quenched in Agitated Water with Those of Selected Double End Quench Specimens. Quenched 1650 F.

Chemical Composition	C%	Mn%	Si%	Ni%	Cr%	Mo%
D.E.Q. Tests	0.32	1.62	0.42	....	0.48	0.34
⅞-in. Plate	0.26	1.44	0.59	....	0.44	0.26
1¼-in. Plate	0.27	0.87	0.42	1.75	1.15	0.65
1⅞-in. Plate	0.29	1.60	0.69	....	0.45	0.40

hardenability), to an extent that will allow partial transformation to ferrite or to other high temperature transformation products, will usually result in inferior properties. Impairment may also be encountered if the alloy content is increased to a degree that will inhibit the complete transformation of the austenite during quenching.

Certain alloy steels, particularly those of the Mn-Cr-Mo type, permit the possibility of an additional mode of transformation during continuous cooling. Simple steels that are quenched at a sufficiently rapid rate to avoid the pearlitic reaction above 900 to 1000 F (480 to 540 C) will usually transform to martensite. When large amounts of alloying elements are present, as are necessary for the hardening of heavy sections, prevention of the pearlitic reaction is expected with any reasonably effective quench, but below 900 F (480 C) these steels, under the same cooling conditions, may transform partially or wholly to acicular structures of the bainite type. These reaction products, dependent upon the temperatures at which they are formed, may also exhibit inferior properties after tempering.

Interest in the hardenability requirements for plates of various thicknesses led to the development of the double end quench test (1) which, by selection of a suitable test bar length, provides close match-

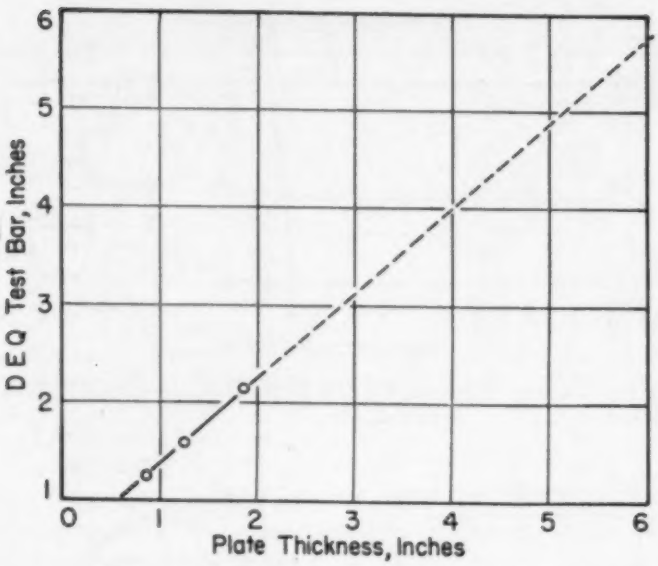


Fig. 2—Correlation, on Basis of Closely Matching Center Cooling Curves, Between Plate Thickness and Double End Quench Test Bar Length for Plates Quenched in Agitated Water. Length diameter ratio of 4:1 must not be exceeded for double end quench test bars.

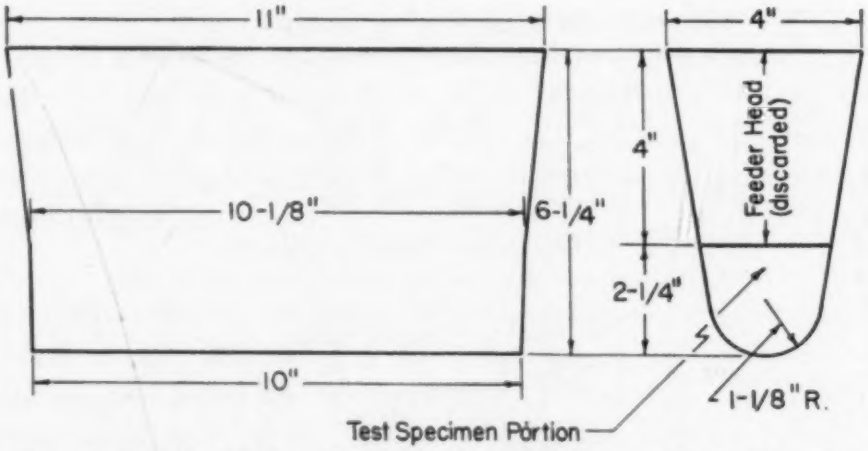


Fig. 3—Casting Practice for 2¼-Inch Diameter by 10-Inch Test Bar.

ing of the thermal history at the center of a given plate (Fig. 1). Correlation of test bar length with plate thickness (Fig. 2) has been previously reported for ⅞, 1¼, and 1⅞-inch plates, quenched in agitated water, and comparison with similar data from other laboratories (not yet published) indicates that this correlation may be extended with confidence for simple as well as for alloy steels.

In this investigation, the depth hardening characteristics and the mechanical properties at selected hardness levels of seven 0.30% carbon Mn-Cr-Mo cast alloy steels have been evaluated at the center of four double end quench bars from 2⅜ to 7⅞ inches long. The

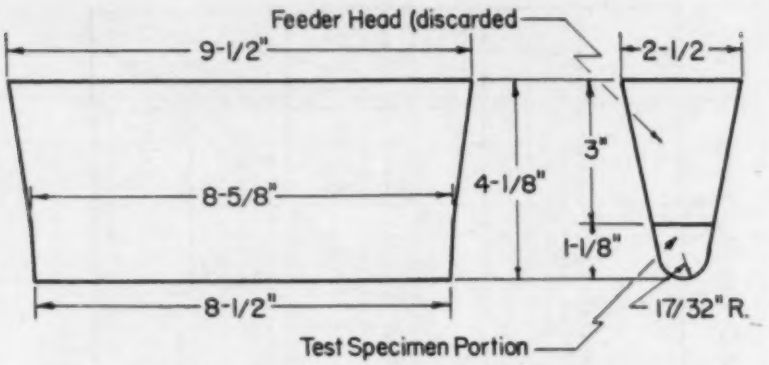
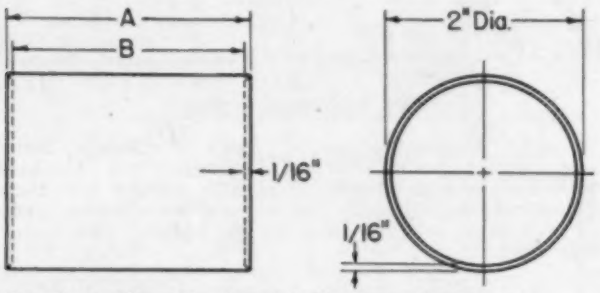


Fig. 4—Casting Practice for $1\frac{1}{16}$-Inch Diameter by 8½-Inch Test Bar.



Specimen Sizes Employed in the Investigation of Mechanical Properties vs. Quenching Rate and Hardenability

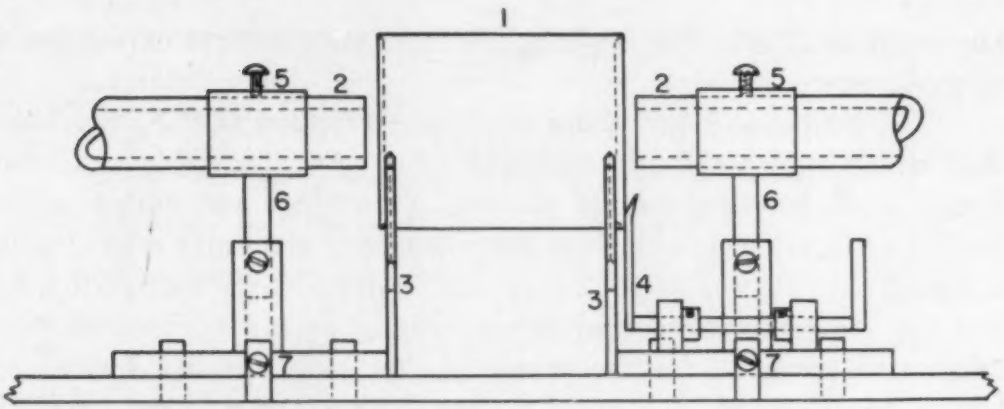
Designation	A	B
DEQ-2-3/8"	2-1/2"	2-3/8"
" -3-7/8"	4"	3-7/8"
" -5-7/8"	6"	5-7/8"
" -7-7/8"	8"	7-7/8"

Fig. 5—Double End Quench Specimens.

center quenching rates correspond to those at the center of water-quenched flat plates approximately 2, 4, 6, and 8 inches thick. It cannot be assumed, however, that identical properties would necessarily obtain in the corresponding plates. It is recognized that the cast test bar, while providing identical cooling rates and chemical composition, does not assure heterogeneity similar to that of heavy sections with different solidification characteristics. It is probable, however, that the separately cast test pieces will reflect maximum properties, within grain size and heterogeneity limitations; the test bar is designed for soundness, while plates or other commercial castings frequently contain at least microscopic shrinkage porosity.

Experimental Procedure

The seven Mn-Cr-Mo steels employed in this study were melted in a basic induction furnace from Armco ingot iron and ferroalloys,



1. Double End Quench Specimen
2. 1/2" Diameter Orifice
3. V-Knife Edge Specimen Support
4. Adjustable End Stop to Locate Specimen Upon Knife Edges Prior to Quenching
5. Horizontal Adjustment of Orifice
6. Vertical Adjustment of Orifice
7. Horizontal Adjustment to Accommodate Specimens of Different Lengths

Fig. 6—Double End Quenching Fixture.

deoxidized in the ladle with 0.07% calcium as calcium silicide, and cast into 2¼-inch diameter by 10-inch and $1\frac{1}{16}$-inch diameter by 8½-inch headed test bars (Figs. 3 and 4). The effects of sulphur upon mechanical properties were minimized by employing this selected melting scrap with a maximum of 0.02% sulphur. Chemical analyses appear in Table I.

Table I
Experimental Compositions

Alloy Steel	Chemical Analysis, %						
	C	Mn	P	S	Si	Cr	Mo
A-1	0.30	0.69	0.014	0.020	0.62	0.02	0.31
A-2	0.29	0.84	0.014	0.012	0.45	0.26	0.36
A-3	0 29	1.31	0.013	0.011	0.52	0.37	0.36
A-4	0.31	1.66	0.018	0.015	0.53	0.55	0.36
A-5	0.31	1.57	0.015	0.013	0.57	1.21	0.35
A-6	0.32	1.61	0.013	0.014	0.58	1.66	0.36
A-7	0.32	1.78	0.015	0.014	0.52	1.76	0.46

After the heads were removed, all cast bars were given a "homogenizing" treatment (air cooling after 8 hours at 1850 F). Three each of the double end quench 2⅜, 3⅞, 5⅞, and 7⅞ by 2-inch diameter specimens which are detailed in Fig. 5 were machined from the 2¼-inch diameter stock of each composition. Identification of the orientation of these specimens with respect to the bottom of the as-cast bars was maintained throughout the investigation with the subsequent testing procedure standardized to minimize

any spurious effects that might result from variations in experimental procedures.

The double end quenching technique was modified slightly from that which was previously reported (1). An adjustable end stop, which could be moved aside prior to quenching, was added to the fixture (Fig. 6) to position the specimen upon the knife edges, while a special set of "five-point" tongs was designed for transferring the test bar from the furnace to the quenching fixture. These changes eliminated the need for the center pin on each test bar which had proved troublesome. To avoid scaling during heating, heat resistant alloy cups, containing a thin graphite disk, were placed over the ends of the specimen as previously described.

One double end quench bar of each length from each heat was used to evaluate the depth hardening characteristics of these alloy steels as well as to pilot the subsequent tempering treatments. These bars were austenitized at 1700 F (925 C) for 2 hours, double end-quenched to 200 F (95 C) (time-quenched), and then air-cooled to room temperature. The quenching periods were as follows:

Double End Quench Specimen	Quenching Time to 200 F
D.E.Q.—2⅜ by 2 inches	230 seconds
D.E.Q.—3⅜ by 2 inches	460 seconds
D.E.Q.—5⅜ by 2 inches	940 seconds
D.E.Q.—7⅜ by 2 inches	1590 seconds

The center cooling curves transposed to 1 second at 1400 F (760 C) for these four test bars are shown in Fig. 7 for one Mn-Cr-Mo composition. While these curves as well as the selected quenching times are strictly applicable only to this particular steel, since composition and other variables will modify the cooling characteristics, the time to cool from 1700 to 200 F (925 to 95 C) for a given test bar was not expected to vary too greatly for the several compositions in Table I.

To determine the depth hardening characteristics of these steels, a longitudinal hardness survey was made on a ground flat on the "top" (feeder head side) of each double end-quenched pilot specimen. A second flat, parallel to the first, was prepared on the opposite side of the specimen to facilitate testing. Following the hardness survey, each bar was cut longitudinally into quarter sections. Two tempering temperatures were selected for each test length on each heat to bracket, where possible, the Brinell 240 to 300 range at the center of each bar, and a quarter section was tempered at each temperature for 6 hours, then air-cooled to room temperature. The

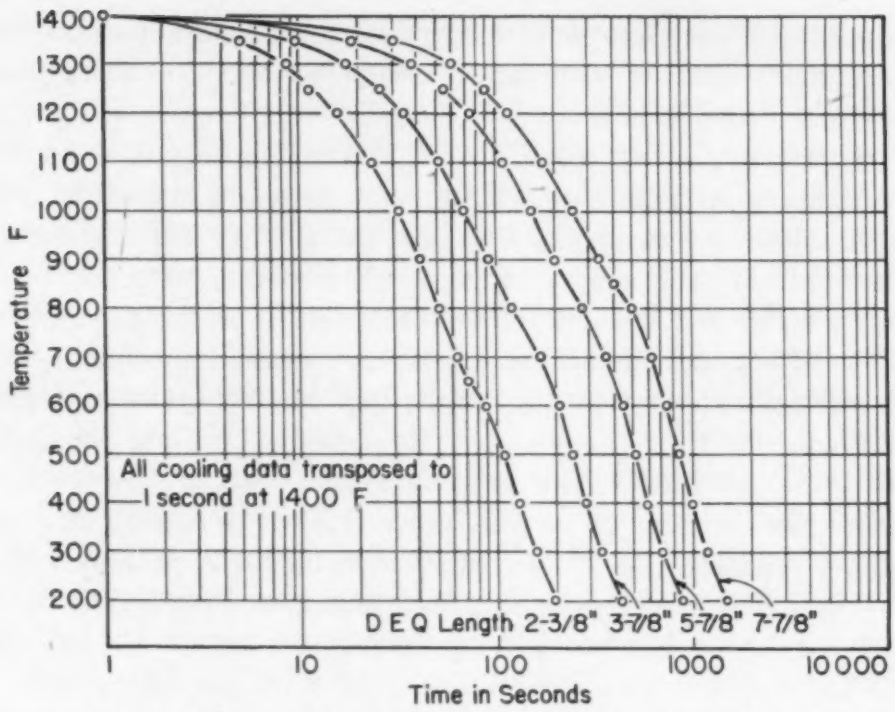


Fig. 7—Center Cooling Curves ($\frac{1}{32}$ Inch Below Surface) for Double End Quench Test Bars of a Mn-Cr-Mo Steel, Quenched from 1650 F. Chemical Composition: 0.32 C, 1.62 Mn, 0.42 Si, 0.48 Cr, 0.34 Mo, 0.134 Al.

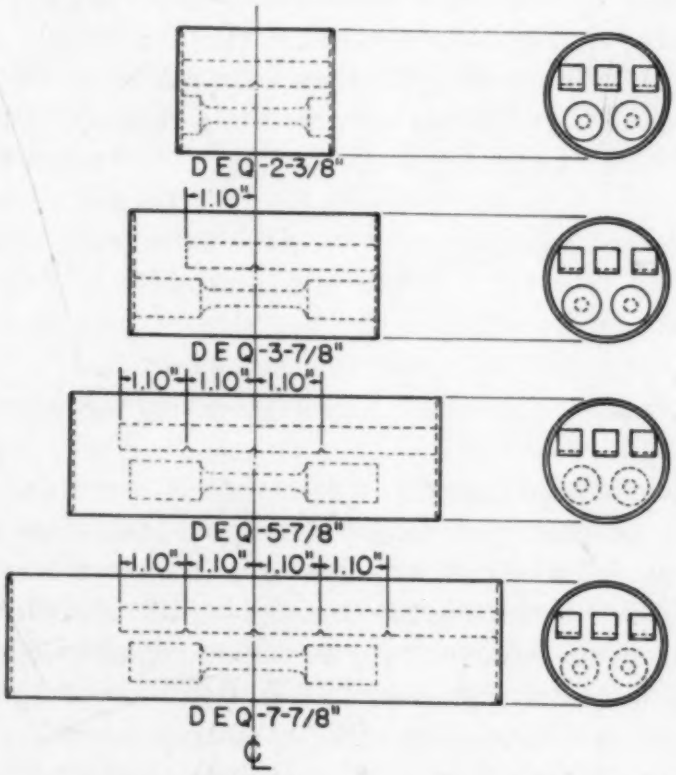


Fig. 8—Location of Mechanical Test Coupons in Quenched and Tempered Double End Quench Specimens.

resulting center hardness was determined and, where possible, the tempering temperatures to obtain Brinell 240 and 300 were interpolated from these data.

The time quench to 200 F (95 C) should result in somewhat lower quenching stresses than would obtain in a full quench to room temperature and was employed to reduce the risk of cracking the test bars during the hardening treatment. While the pilot bars were necessarily air-cooled to room temperature following the time quench to 200 F (95 C), the remaining double end quench specimens were transferred immediately to the tempering furnace at the selected temperature, held for 6 hours, then air-cooled. Original considerations appeared to justify this procedure since the M_f for each of these steels was believed to be well above this temperature (2).

Where possible, one double end quench bar of each length from each heat was tempered to Brinell 240, a second to Brinell 300. When the steels of lower hardenability quenched out below Brinell 240, one test bar was stress-relieved at a temperature consistent with no apparent softening of the as-quenched product, while the companion bar was tested in the as-quenched condition.

To determine the center mechanical properties for correlation with quenching rate and hardenability, two 0.252-inch diameter by 1.0-inch gage length tensile specimens were machined from the "bottom" half of each double end-quenched and tempered bar while the "top" half provided three 0.394-inch square "V" notch Izod impact (cantilever type) tests, as shown in Fig. 8. Tensile test gage length and Izod notches were centered longitudinally with respect to the original D.E.Q. test bar. While it was possible to determine only the center impact properties in the two shortest test bars, additional measurements at 1.10-inch intervals on either side of the center position were obtained for the 5⅞ and 7⅞-inch specimens as illustrated.

The mechanical properties of these steels were also determined at the center of heat treated 1-inch rounds (cut from castings as shown in Fig. 4) where the quenching rate is considerably faster than that which obtains in the shortest double end quench bar. These 1-inch rounds were given a full immersion agitated water quench from the hardening temperature (1700 F), then tempered to the selected hardness levels; tempering temperatures were piloted as before. Although standard 0.505-inch diameter by 2.0-inch gage length tensile coupons were machined and tested, several 0.252-inch

diameter by 1.0-inch gage length tensiles were also included to check the comparability of the two test specimens. While it was doubtful that a quench of this severity could be employed regularly for the steels of higher hardenability when heat treated in 1-inch sections, all were apparently successfully processed except one bar of the most highly alloyed steel A-7, which cracked.

There were not sufficient 1-inch rounds to evaluate the corresponding impact properties. Instead, 1 by 1 by 6-inch bars, which were cut from the 2¼-inch diameter stock, were immersion-quenched and tempered. Multiple Izod impact specimens (0.394 inch square, "V" notched) were machined from the center of most of these bars and tested before work on the project was terminated. Trouble was experienced with cracking of most of these 1 by 1-inch bars from the two highest hardenability heats. While the results are questionable, impact tests were made where specimens could be machined from apparently uncracked portions of these bars.

Specimens for microexamination were cut from the center of the as-quenched pilot double end quench test bars and of the as-quenched 1-inch square specimens. The Izod coupons furnished microsamples from the same locations after quenching and tempering.

Ratings of austenitic grain size prior to quenching, based upon ASTM Standards, were made upon tempered martensitic structures (at the quenched end of double end quench 3⅞ by 2-inch diameter specimens) etched with Vilella's grain size reagent (1% picric acid, 5% hydrochloric acid, in ethyl alcohol).

Experimental Results

Summary of Data—The experimental data have been assembled in several tables for reference. The depth hardening characteristics of the several alloys, as measured by the extent to which they will harden at the center of the four double end quench test bars, are summarized in Table II, together with the mechanical properties which obtain at these locations after tempering to the selected hardness levels. The tensile properties of these steels after heat treatment as 1-inch rounds are shown in Table III, while the expected comparability of the 0.505 and 0.252-inch diameter tensile specimens is evident in Table IV. The available corresponding impact properties for the 1 by 1-inch sections appear in Table V.

Hardenability—The depth hardening characteristics of the sev-

Table II
Summary of Double End Quench Test Bar Data

Alloy Steel	Chemical Composition, % C	Mn	P	S	Si	Cr	Mo	D.E.Q. Test Bar Length Inches	Longitudinal Hardness Surveys Rc Scale As Quenched (a) End	Center	As Tempered (b) Temp. F	End	Center	Double End-Quenched and Tempered Mechanical Properties Tensile Data (c) Center of D.E.Q. Test Bar Yield Strength (e) Psi	Ult. Tens. Strength Psi	% Elong. in 1 in.	% Red. of Area	Izod Impact (d) Strength Ft-Lbs At D.E.Q. Center	1.10 in. from Center	2.20 in. from Center
A-1	0.30	0.69	0.014	0.020	0.62	0.02	0.31	2⅜	49	24	...	49	23	93,000	122,700	26.5	47.4	18.7	...	...
											900	36	21	85,000	114,700	21.0	51.1	17.5	...	...
								3⅜	51	19	...	49	19	82,000	111,200	31.0	51.7	20.2	...	...
		"Hardenability" Number = 2426									900	35	18	80,000	107,500	22.0	51.5	20.7	...	...
		ASTM Grain Size = 5						5⅜	50	17	...	50	18	77,000	105,100	30.0	52.5	17.8	20.4	...
											900	34	15	75,000	103,600	29.0	51.5	18.5	17.5	...
								7⅜	51	13	...	49	17	73,000	101,900	28.0	50.1	15.2	17.3	18.7
											900	33	15	75,000	100,100	25.0	51.5	16.2	16.0	17.5
A-2	0.29	0.84	0.014	0.012	0.45	0.26	0.36	2⅜	48	27	900	35	22	103,000	118,400	19.0	53.5	20.3	...	...
											1050	38	23	110,000	120,700	17.0	55.4	18.2	...	...
								3⅜	48	21	...	48	21	91,000	115,900	24.0	52.5	11.0	...	...
		"Hardenability" Number = 2583									950	34	18	85,500	108,300	22.0	52.5	24.8	...	...
		ASTM Grain Size = 4						5⅜	49	18	...	47	17	81,000	109,700	26.0	50.0	13.0	13.8	...
											950	34	17	82,500	104,350	22.5	55.7	24.8	22.6	...
								7⅜	48	17	...	47	17	83,000	107,700	24.0	49.8	14.3	13.7	14.3
											950	32	17	79,000	102,200	23.3	56.0	24.5	24.8	21.8
A-3	0.29	1.31	0.013	0.011	0.52	0.37	0.36	2⅜	50	42	1060	33	33	134,500	147,950	15.5	47.6	38.5	...	...
											1200	22	21	98,000	118,800	21.0	59.6	60.3	...	...
								3⅜	49	33	950	37	30	122,500	139,600	17.0	41.0	13.2	...	...
		"Hardenability" Number = 2939									1120	31	23	105,000	124,000	20.0	52.6	23.8	...	...
		ASTM Grain Size = 3						5⅜	50	29	950	35	27	110,000	129,800	18.8	47.2	14.3	14.3	...
											1120	32	24	99,000	117,800	19.0	51.4	18.7	20.2	...
								7⅜	50	27	950	36	24	105,000	124,800	19.0	45.0	13.3	13.5	14.3
											1120	29	20	91,000	112,200	21.0	52.7	24.3	22.8	24.0
A-4	0.31	1.66	0.018	0.015	0.53	0.55	0.36	2⅜	51	49	1080	34	32	136,500	153,900	17.0	49.2	38.7	...	...
											1200	23	23	98,800	119,800	22.0	57.9	60.0	...	...
								3⅜	51	48	1080	33	33	137,500	151,350	16.3	50.1	37.2	...	...
		"Hardenability" Number = 3386									1200	25	23	100,000	120,600	22.0	61.7	61.7	...	...
		ASTM Grain Size = 4						5⅜	50	40	1060	35	34	136,500	150,700	15.0	42.8	15.0	17.0	...
											1200	24	21	96,050	118,600	23.3	57.6	51.0	58.5	...
								7⅜	51	36	1060	35	30	121,000	141,750	16.3	43.8	13.3	15.8	17.3
											1200	25	21	92,500	115,400	21.0	53.0	34.5	39.9	57.3

Table II—(continued)
Summary of Double End Quench Test Bar Data

Alloy Steel	Chemical Composition, % C	Mn	P	S	Si	Cr	Mo	D.E.Q. Test Bar Length Inches	Longitudinal Hardness Surveys Rc Scale As Quenched (a) End	Center	As Tempered (b) Temp. F	End	Center	Double End-Quenched and Tempered Mechanical Properties Tensile Data (c) Center of D.E.Q. Test Bar Yield Strength (e) Psi	Ult. Tens. Strength Psi	% Elong. in 1 in.	% Red. of Area	Izod Impact (d) Strength Ft-Lbs At D.E.Q. Center	1.10 in. from Center	2.20 in. from Center
A-5	0.31	1.57	0.015	0.013	0.57	1.21	0.35	2⅜	54	51	1100	33	33	139,500	154,800	16.5	44.2	31.8	...	...
											1230	23	23	99,000	122,100	22.0	55.8	57.5	...	...
								3⅞	54	52	1100	32	32	138,000	151,800	18.0	46.6	31.5	...	...
											1230	23	23	98,000	121,700	24.0	58.1	56.7	...	...
								5⅞	51	45	1100	33	32	134,500	150,750	17.0	47.9	29.7	28.7	...
											1230	23	22	94,000	119,500	26.0	60.2	59.8	60.7	...
								7⅞	53	42	1100	33	31	123,500	142,500	18.0	48.8	22.0	28.3	30.8
											1230	23	20	89,000	114,600	25.0	60.2	58.2	62.3	61.8
A-6	0.32	1.61	0.013	0.014	0.58	1.66	0.36	2⅜	54	51	1150	31	30	126,000	145,250	17.5	46.3	34.8	...	...
											1275	20	20	87,000	112,400	25.0	56.7	57.5	...	...
								3⅞	55	52	1150	30	31	125,000	143,900	18.3	44.7	32.7	...	...
											1275	21	21	91,000	116,100	25.0	55.6	52.0	...	...
								5⅞	51	50	1150	30	30	124,500	143,100	18.3	47.2	37.5	36.8	...
											1275	21	20	88,000	114,500	24.5	54.2	50.7	51.4	...
								7⅞	54	51	1150	31	30	125,000	144,150	18.8	49.4	31.3	30.5	31.8
											1275	20	19	87,000	114,800	26.5	57.0	49.2	50.3	50.2
A-7	0.32	1.78	0.015	0.014	0.52	1.76	0.46	2⅜	53	51	1150	31	32	129,000	147,000	16.8	45.5	31.3	...	...
											1280	23	22	93,000	116,300	22.5	55.1	52.5	...	...
								3⅞	54	51	1150	30	30	122,700	141,850	16.5	45.4	31.5	...	...
											1260	24	21	90,000	114,700	22.5	56.0	47.3	...	...
								5⅞	52	51	1125	32	30	124,500	142,850	17.8	44.9	28.0	28.5	...
											1260	22	21	93,000	116,000	22.5	49.2	48.8	48.4	...
								7⅞	54	51	1125	34	32	129,000	146,450	17.3	44.1	34.8	33.5	32.8
											1260	24	23	98,000	121,600	23.0	54.4	45.5	45.1	47.5

"Hardenability" Number = 3620, ASTM Grain Size = 3

"Hardenability" Number = 3896, ASTM Grain Size = 3

"Hardenability" Number = 4206, ASTM Grain Size = 3

Notes: (a) 1700 F—2 hours—double end quench to 200 F—air cool; preceded by 1850 F—8 hours—air cool.
(b) Tempered at indicated temperature for 6 hours and air-cooled. Preceded by 1850 F—8 hours—air cool; 1700 F—2 hours—D.E.Q. to 200 F.
(c) 0.252-Inch diameter by 1.0-inch gage length tensile specimen.
(d) 0.394-Inch square Izod (cantilever beam) impact specimen ("V" notched).
(e) Drop of beam.

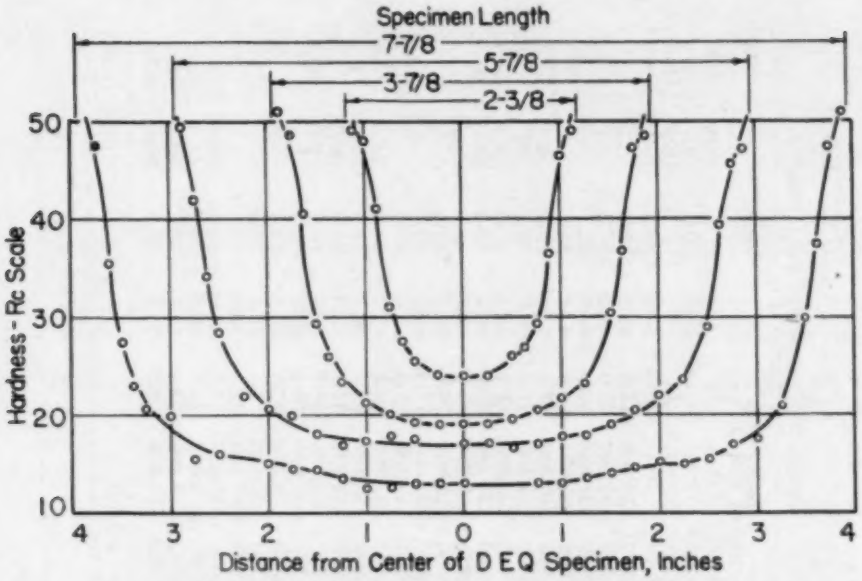


Fig. 9—As-Quenched Hardness Surveys for D.E.Q. 2⅜, 3⅞, 5⅞ and 7⅞ by 2-Inch Diameter Specimens of Alloy Steel A-1.

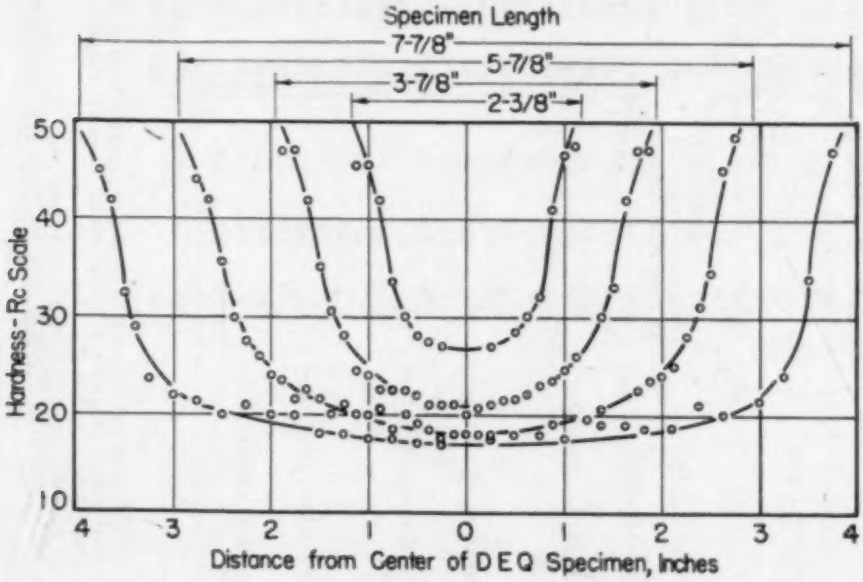


Fig. 10—As-Quenched Hardness Surveys for D.E.Q. 2⅜, 3⅞, 5⅞ and 7⅞ by 2-Inch Diameter Specimens of Alloy Steel A-2.

eral alloys, previously summarized in Table II, are presented graphically in Figs. 9 to 15 inclusive, which show the longitudinal as-quenched hardness surveys of the four double end quench test bars from each heat.

To estimate hardenability from chemical composition an additive system has been employed, the "Hardenability" Number (3), (4), (5)

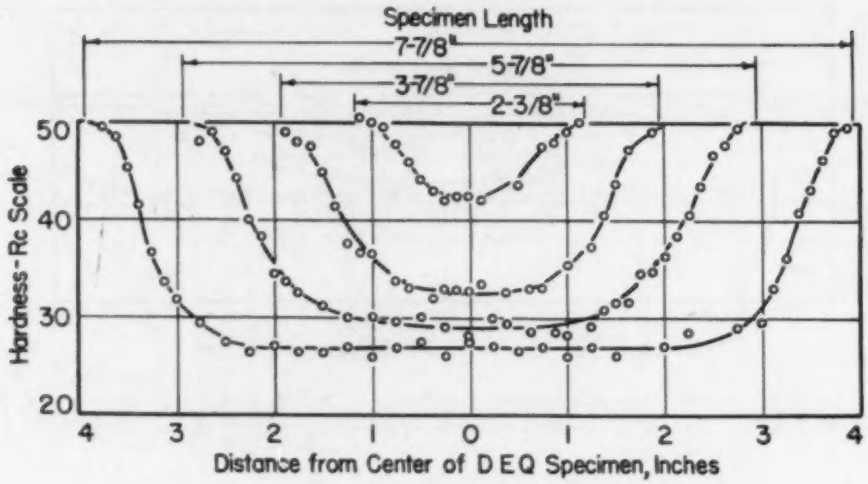


Fig. 11—As-Quenched Hardness Surveys for D.E.Q. 2⅜, 3⅞, 5⅞ and 7⅞ by 2-Inch Diameter Specimens of Alloy Steel A-3.

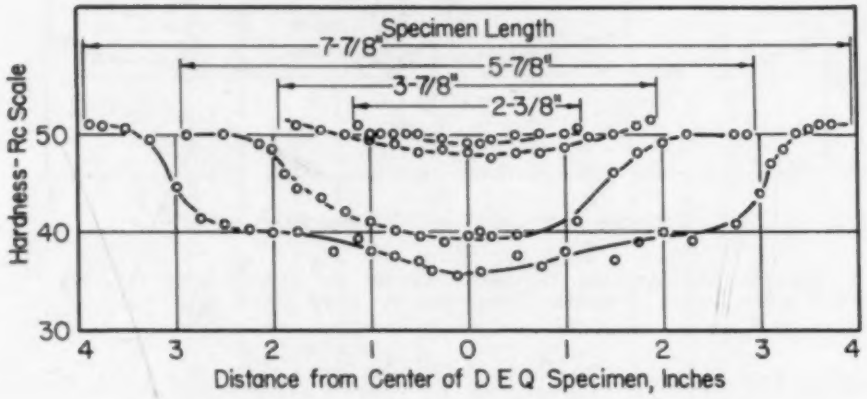


Fig. 12—As-Quenched Hardness Surveys for D.E.Q. 2⅜, 3⅞, 5⅞ and 7⅞ by 2-Inch Diameter Specimens of Alloy Steel A-4.

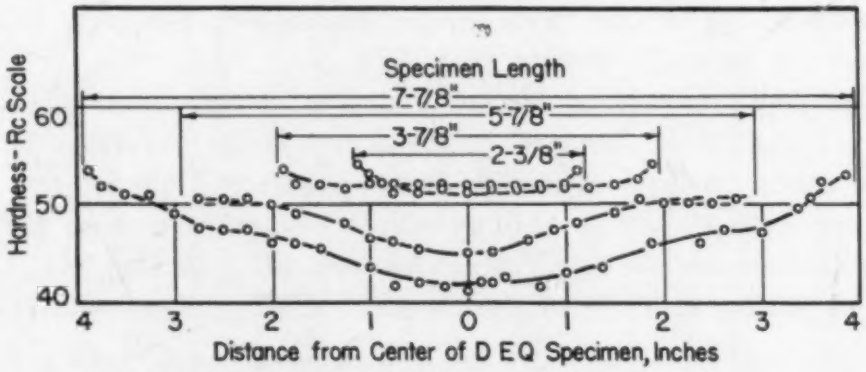


Fig. 13—As-Quenched Hardness Surveys for D.E.Q. 2⅜, 3⅞, 5⅞ and 7⅞ by 2-Inch Diameter Specimens of Alloy Steel A-5.

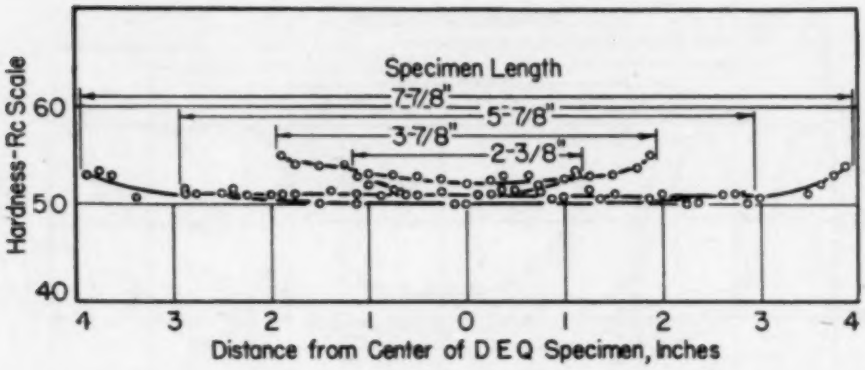


Fig. 14—As-Quenched Hardness Surveys for D.E.Q. 2⅜, 3⅞, 5⅞ and 7⅞ by 2-Inch Diameter Specimens of Alloy Steel A-6.

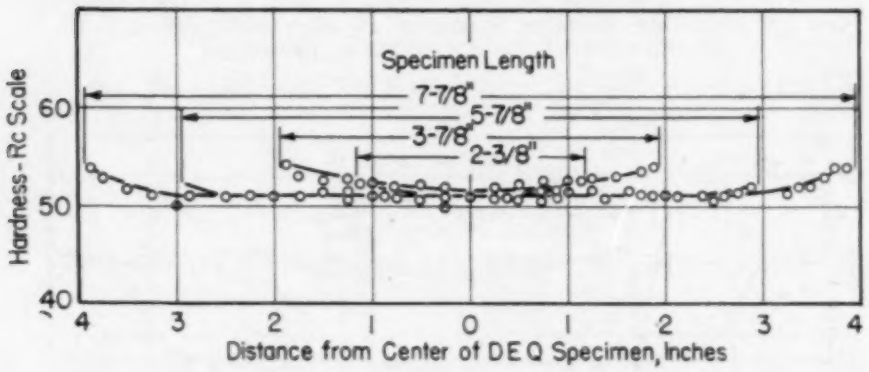


Fig. 15—As-Quenched Hardness Surveys for D.E.Q. 2⅜, 3⅞, 5⅞ and 7⅞ by 2-Inch Diameter Specimens of Alloy Steel A-7.

representing the summation of the weighted values for each element, which are obtained by multiplying the percentage of each alloying element by its proper factor.[2] For comparison, the Grossmann D_1 values (6), (7), (8)[3] have been calculated (Table VI), but the physical significance of these ratings is questionable for the steels of higher hardenability. For the steels under discussion, however, relative rankings are naturally similar (Fig. 16).

The depth hardening characteristics of these seven steels are compared with their chemical hardenability ratings in Figs. 17 and 18; the center hardnesses of the several double end quench test bars have been plotted against "Hardenability" Number in Fig. 17, and against Grossmann's Ideal Critical Diameter (D_1) in Fig. 18. These charts permit an estimate of the chemical hardenability requirements

[2]"Hardenability" Number = % C × 3200 + % Mn × 600 + % Si × 500 + % P × 14000 + % S × 2000 + % Ni × 400 + % Cr × 500 + % Mo × 1600.

[3]Grossmann's original factors for C, P, and S were used in these calculations with the revised factors for Mn, Si, Cr, and Mo as published by Crafts and Lamont (7), (8).

Table III
Summary of Mechanical Properties (a)

0.505-Inch Diameter by 2.0-Inch Gage Length Tensile Tests from Immersion-Quenched and Tempered 1-Inch Rounds

Alloy Steel	Chemical Composition, %							"Harden-ability" Number	Yield Strength (b) Psi	Ult. Tens. Strength Psi	% Elong. in 2 in.	% Red. Area	B.H.N.	Heat Treatment (c) 6 Hrs., A.C.
	C	Mn	P	S	Si	Cr	Mo							
A-1	0.30	0.69	0.014	0.020	0.62	0.02	0.31	2426	79,125	100,750	22.8	59.4	217	1200 F
									128,250	141,375	11.5	33.0	302	950 F
A-2	0.29	0.84	0.014	0.012	0.45	0.26	0.36	2583	92,000	108,500	22.0	58.6	232	1200 F
									134,500	149,875	15.0	50.6	320	1050 F
A-3	0.29	1.31	0.013	0.011	0.52	0.37	0.36	2939	87,750	108,125	24.3	60.1	238	1230 F
									128,000	141,500	17.8	52.8	302	1100 F
A-4	0.31	1.66	0.018	0.015	0.53	0.55	0.36	3386	86,000	107,500	20.5	59.8	228	1250 F (d)
									127,275	144,000	15.5	48.3	302	1115 F
A-5	0.31	1.57	0.015	0.013	0.57	1.21	0.35	3620	86,250	110,750	22.8	59.5	241	1240 F
									122,500	141,875	18.5	47.6	302	1120 F
A-6	0.32	1.61	0.013	0.014	0.58	1.66	0.36	3896	87,250	110,500	23.5	55.6	228	1275 F
									122,225	139,875	18.0	46.5	294	1150 F
A-7	0.32	1.78	0.015	0.014	0.52	1.76	0.46	4206	89,000	112,750	21.0	50.0	241	1270 F (e)
									120,200	140,250	16.3	44.0	293	1150 F

Notes: (a) Average of duplicate tests except as noted.
(b) Drop of beam.
(c) Preceded by: 1850 F—8 hours—air cool; 1700 F—2 hours—water quench.
(d) Single test. No additional stock.
(e) Single test. Second was cracked.

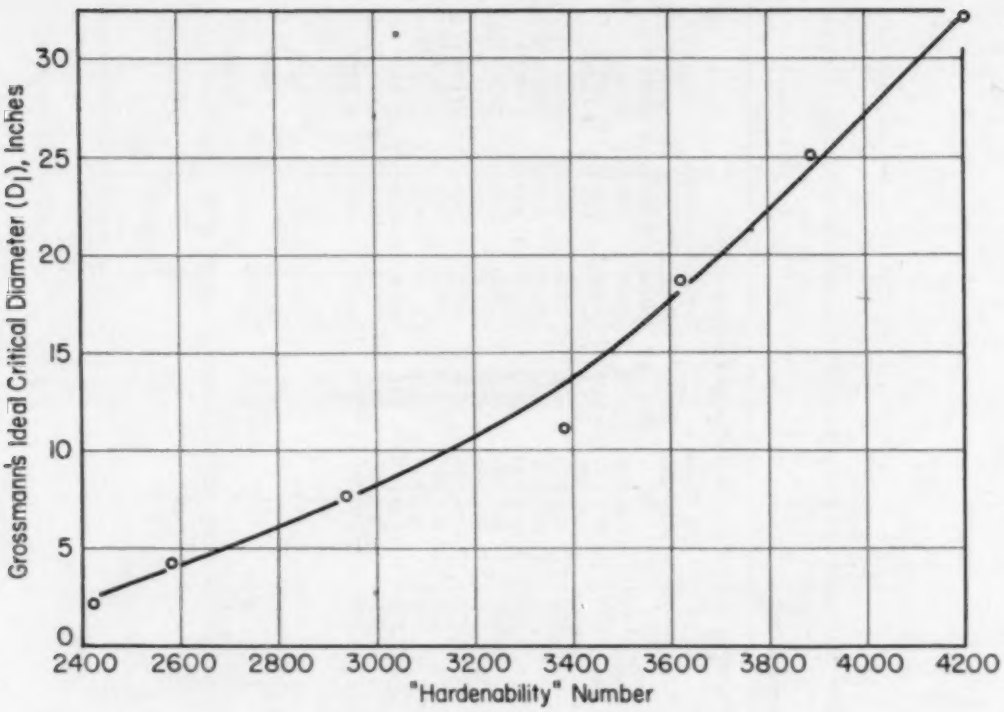


Fig. 16—Comparison of Chemical Hardenability Ratings: Grossmann's Ideal Critical Diameter Versus "Hardenability" Number for 0.30% Carbon Cast Alloy Steels A-1 to A-7 Inclusive.

Table IV
Comparability of 0.252 by 1.0-Inch and 0.505 by 2.0-Inch Tensile Coupons

Alloy Steel	Bar No.	Tensile Coupon Inches	Yield Strength (a) Psi	Ult. Tens. Strength Psi	Elong. %	Red. Area %	B.H.N.	Heat Treatment (b) 6 Hrs., A.C.
A-2	15	0.252 by 1.0	152,000	156,600	11.0	43.7	336	1050 F
		0.505 by 2.0	143,000	161,500	11.5	45.7	336	1050 F
	16	0.252 by 1.0	128,000	139,600	17.0	55.5	302	1050 F
		0.505 by 2.0	126,000	138,250	18.5	55.3	302	1050 F
A-6	14	0.252 by 1.0	126,000	143,800	16.0	34.3	286	1150 F
		0.505 by 2.0	121,500	139,750	18.5	46.8	286	1150 F
	15	0.252 by 1.0	124,000	141,000	17.0	49.0	302	1150 F
		0.505 by 2.0	123,000	140,000	17.5	46.2	302	1150 F

(a) Drop of beam.
(b) Preceded by: 1850 F—8 hours—air cool.
1700 F—2 hours—water quench.

to achieve maximum hardening[4] at the center of the several test bars which, from a correlation of double end quench test bar length with

[4]Maximum hardening should not be confused with full hardening (100% martensite). While the as-quenched hardness increases to a maximum value as hardenability is increased to a suitable level for a given quenching rate, a 100% martensitic structure may be unobtainable either at this or higher hardenabilities because of inability to avoid (a) partial transformation to lower bainitic structures, and/or (b) retained austenite. The lower bainites are difficult to distinguish microscopically from martensite in these steels. Maximum as-quenched hardness, especially when conditions permit essentially full hardening, may not differ appreciably from that characteristic of 100% martensite, and the resultant properties, after tempering, may likewise be similar.

Table V
Summary of Mechanical Properties

0.394-Inch Square Izod Impact Tests ("V" Notched) from Immersion-Quenched and Tempered 1 by 1 by 6-Inch Bars

Alloy Steel	Chemical Composition, %							"Hardenability" Number	Impact Strength—Ft-Lbs						Heat Treatment (a) 6 Hrs., A.C.
	C	Mn	P	S	Si	Cr	Mo		1	2	3	4	Average	Rc	
A-1	0.30	0.69	0.014	0.020	0.62	0.02	0.31	2426	35.5	38.5	36.5	52.5	40.8	26	1110 F
									23.5	24.0	26.0	24.0	24.4	29	950 F
A-2	0.29	0.84	0.014	0.012	0.45	0.26	0.36	2583							1175 F
									53.0	44.5	46.5	48.5	48.1	30	1075 F
A-3	0.29	1.31	0.013	0.011	0.52	0.37	0.36	2939	63.0	63.0	63.0	62.0	62.8	23	1230 F
									53.0	57.0	52.5	53.0	53.9	30	1110 F
A-4	0.31	1.66	0.018	0.015	0.53	0.55	0.36	3386	57.0	59.5	53 5	....	56.7	25	1230 F
									45.0	47.0	47.0	....	46.3	30	1110 F
A-5	0.31	1.57	0.015	0.013	0.57	1.21	0.35	3620	59.0	54.0	56.0	58.0	56.8	26	1230 F
									40.0	37.0	37.0	35.0	37.3	30	1110 F
A-6	0.32	1.61	0.013	0.014	0.58	1.66	0.36	3896							1260 F
									35.0	34.5	34.0	35.5	34.8	31	1125 F
A-7	0.32	1.78	0.015	0.014	0.52	1.76	0.46	4206							1260 F
									38.5	36.5	37.0	36.0	37.0	31	1125 F

Note: (a) Preceded by: 1850 F—8 hours—air cool; 1700 F—2 hours—water quench.

Table VI
Comparison of Chemical Hardenability Ratings

Alloy Steel	Grossmann's Ideal Critical Diameter D_1, Inches	"Hardenability" Number
A-1	2.24	2426
A-2	4.09	2583
A-3	7.64	2939
A-4	11.09	3386
A-5	18.65	3620
A-6	25.00	3896
A-7	32.20	4206

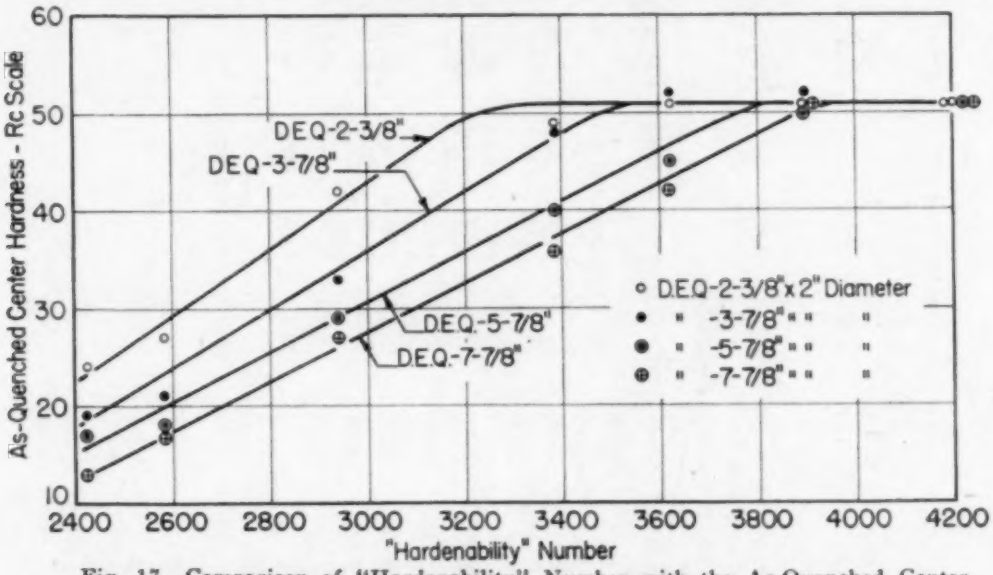


Fig. 17—Comparison of "Hardenability" Number with the As-Quenched Center Hardness of D.E.Q. 2⅜, 3⅞, 5⅞ and 7⅞-Inch Test Bars for 0.30% Carbon Cast Mn-Cr-Mo Steels. Heat Treatment: 1850 F, 8 hours, air cool; 1700 F, 2 hours, D.E.Q. to 200 F, air cool.

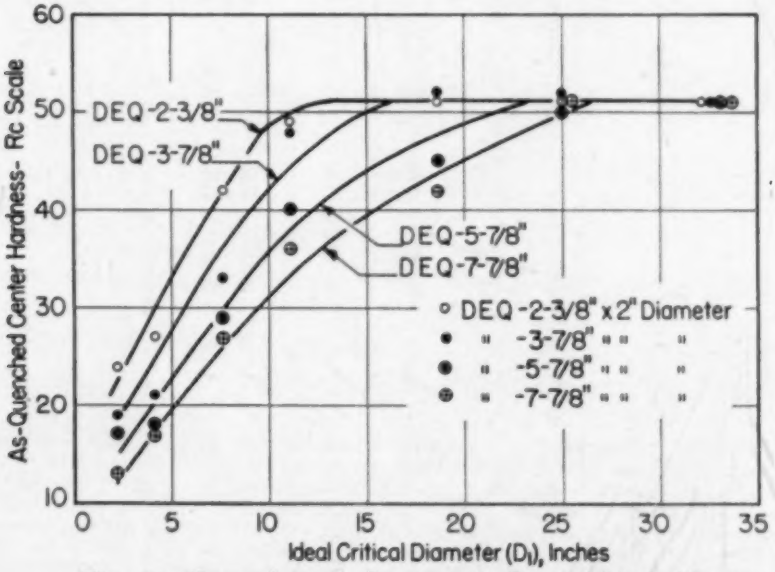


Fig. 18—Comparison of Grossmann's Ideal Critical Diameter (D_1) with the As-Quenched Center Hardness of D.E.Q. 2⅜, 3⅞, 5⅞ and 7⅞-Inch Test Bars for 0.30% Carbon Cast Mn-Cr-Mo Alloys.

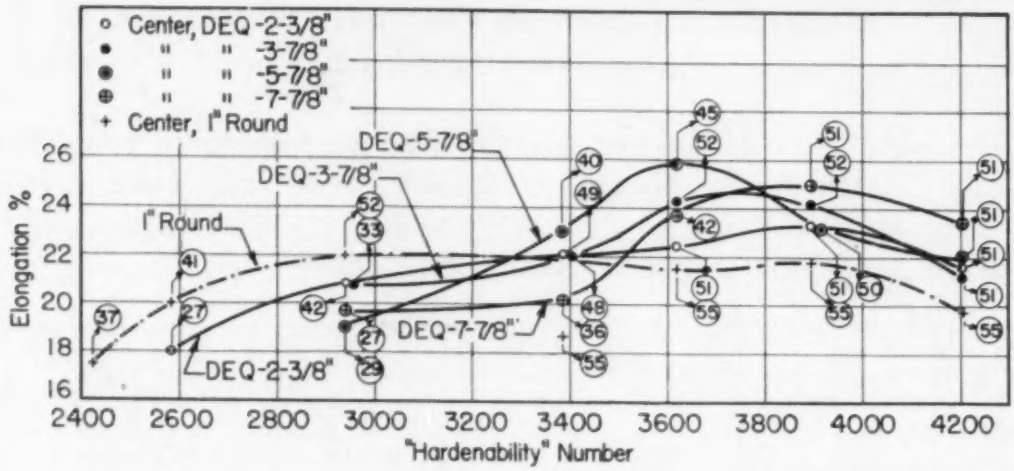


Fig. 19—Comparison of Per Cent Elongation at 120,000 Psi Tensile Strength (Approx. Brinell 240) at the Center of Double End-Quenched and Tempered D.E.Q. 2⅜, 3⅞, 5⅞ and 7⅞ by 2-Inch Diameter Specimens and of Immersion-Quenched and Tempered 1-Inch Rounds with "Hardenability" Number for 0.30% Carbon Cast Mn-Cr-Mo Steels, from Mechanical Test Data in Tables II and III, Interpolated or Extrapolated Where Necessary. Circled figures show as-quenched center hardness Rc scale. 1-inch round values converted from BHN.

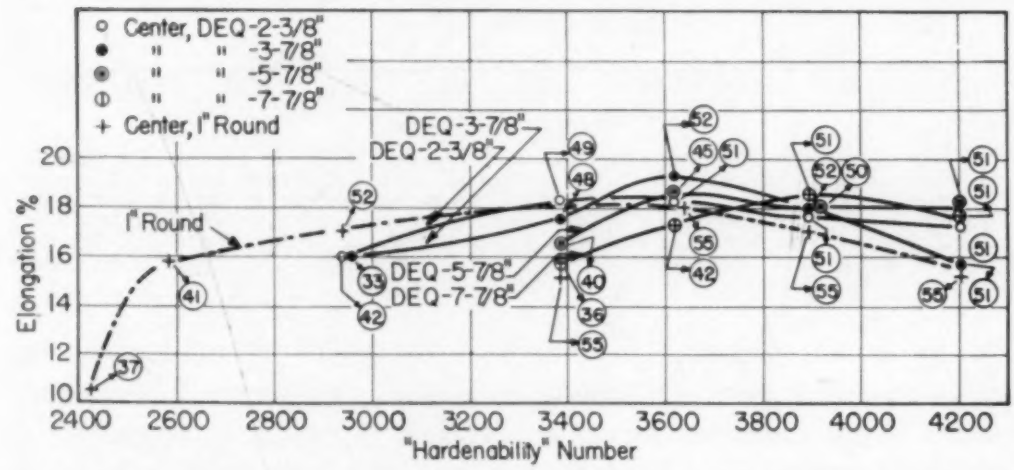


Fig. 20—Comparison of Per Cent Elongation at 145,000 Psi Tensile Strength (Approx. Brinell 300) at the Center of Double End-Quenched and Tempered D.E.Q. 2⅜, 3⅞, 5⅞ and 7⅞ by 2-Inch Diameter Specimens and of Immersion-Quenched and Tempered 1-Inch Rounds with "Hardenability" Number for 0.30% Carbon Cast Mn-Cr-Mo Steels, from Mechanical Test Data in Tables II and III, Interpolated or Extrapolated Where Necessary. Circled figures show as-quenched center hardness Rc scale. 1-inch round values converted from BHN.

plate thickness for given plate quenching conditions, should permit prediction, within heterogeneity and grain size limitations, of the cross-sectional hardnesses of corresponding plates. Fig. 2 shows the correlation for plates quenched in agitated water. Since variations in severity of quench will modify this relationship, it would be desirable, for precise work, to check this for the particular plate practice to be used.

Mechanical Properties Versus Hardenability and Quenching Rate

Figs. 19 to 24 show the variation in the mechanical properties with "Hardenability" Number at Brinell 240 and 300 (interpolated or extrapolated from the data of Tables II and III) at the center of the double end-quenched and tempered D.E.Q. 2⅜, 3⅞, 5⅞, and

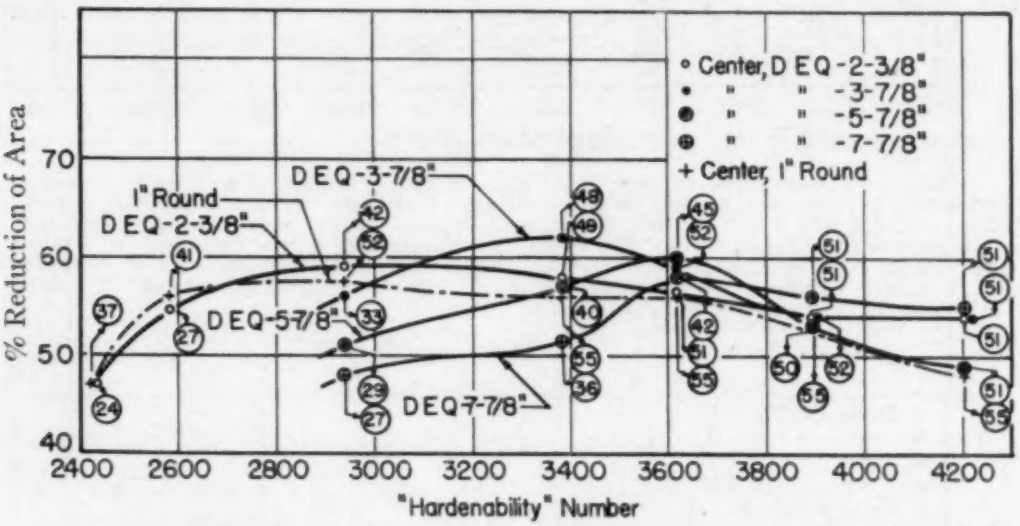


Fig. 21—Comparison of Per Cent Reduction of Area at 120,000 Psi Tensile Strength (Approx. Brinell 240) at the Center of Double End-Quenched and Tempered D.E.Q. 2⅜, 3⅞, 5⅞ and 7⅞ by 2-Inch Diameter Specimens and of Immersion-Quenched and Tempered 1-Inch Rounds with "Hardenability" Number for 0.30% Carbon Cast Mn-Cr-Mo Steels, from Mechanical Test Data in Tables II and III, Interpolated or Extrapolated Where Necessary. Circled figures show as-quenched center hardness Rc scale. 1-inch round values converted from BHN.

7⅞ by 2-inch diameter bars and of the immersion-quenched and tempered 1-inch bars. Similar plots would obtain using Grossmann's Ideal Critical Diameter as the hardenability variable. The effect of quenching rate is evidenced by the greater hardenability that is required to develop optimum properties in the D.E.Q. specimens corresponding to heavier plates.

While the several properties behave similarly, impact strength (Figs. 23 and 24), as expected, exhibits the greatest sensitivity to structural variations brought about by changes in hardenability and quenching rate. The inferior properties resulting from ineffective hardening (i.e., insufficient hardenability for given quenching conditions) are evident. With sufficient hardenability to obtain maximum hardening, optimum properties are achieved, but further increases in hardenability result in a diminution of properties from the optimum values attained. Some discrepancies appear in these interpolated

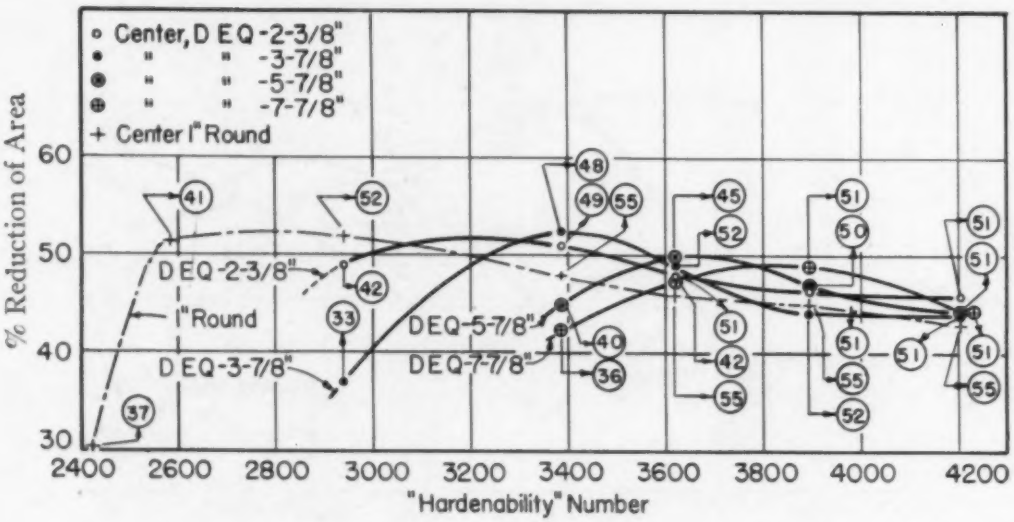


Fig. 22—Comparison of Per Cent Reduction of Area at 145,000 Psi Tensile Strength (Approx. Brinell 300) at the Center of Double End-Quenched and Tempered D.E.Q. 2⅜, 3⅞, 5⅞ and 7⅞ by 2-Inch Diameter Specimens and of Immersion-Quenched and Tempered 1-Inch Rounds with "Hardenability" Number for 0.30% Carbon Cast Mn-Cr-Mo Steels, from Mechanical Test Data in Tables II and III, Interpolated or Extrapolated Where Necessary. Circled figures show as-quenched center hardness Rc scale. 1-inch round values converted from BHN.

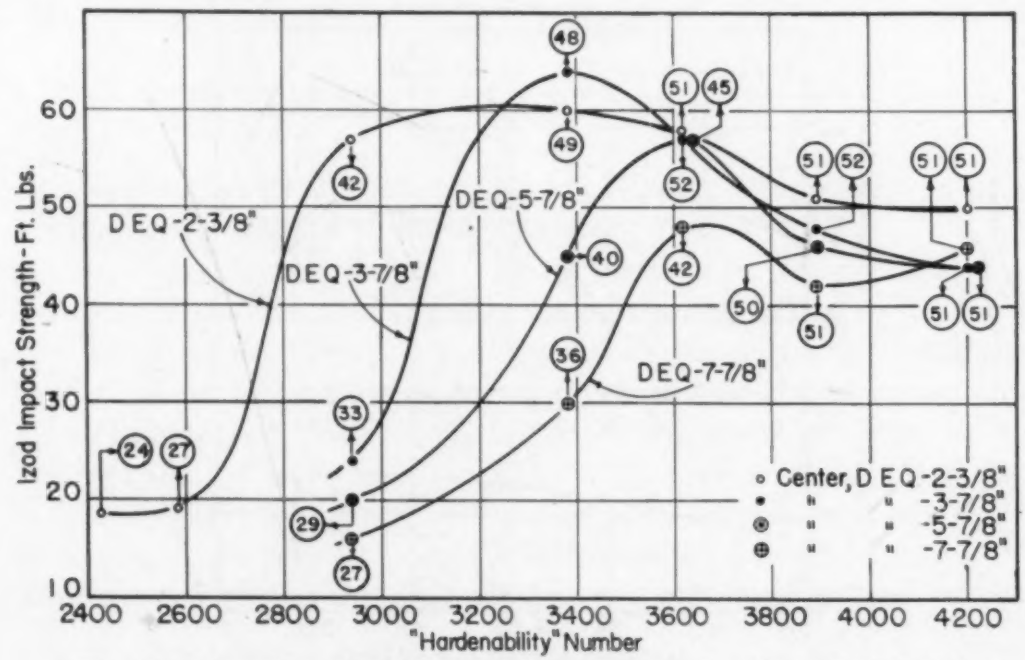


Fig. 23—Comparison of Izod Impact Strength at 23 Rc (Conv. Brinell 240) at the Center of Quenched and Tempered D.E.Q. 2⅜, 3⅞, 5⅞ and 7⅞ by 2-Inch Diameter Specimens with "Hardenability" Number for 0.30% Carbon Cast Mn-Cr-Mo Steels, from Mechanical Test Data in Table II, Interpolated or Extrapolated Where Necessary. Circled figures show as-quenched center hardness Rc scale.

data, partially as a result of inaccuracies in the hardness data because of heterogeneity of the material. In particular, the Rockwell hardness data for the heat treated 1 by 1-inch bars from which impact

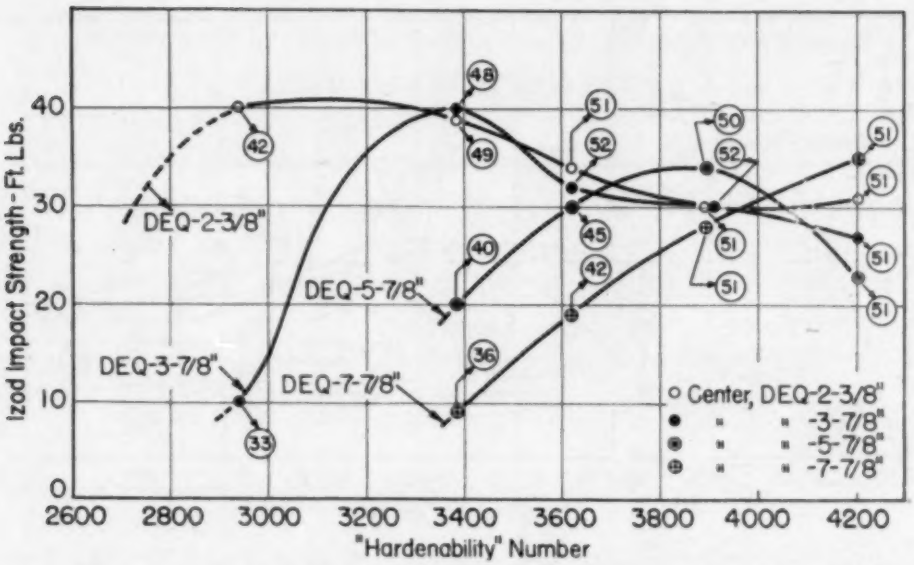


Fig. 24—Comparison of Izod Impact Strength at 32 Rc (Conv. Brinell 300) at the Center of Quenched and Tempered D.E.Q. 2⅜, 3⅞, 5⅞ and 7⅞ by 2-Inch Diameter Specimens with "Hardenability" Number for 0.30% Carbon Cast Mn-Cr-Mo Steels, from Mechanical Test Data in Table II, Interpolated or Extrapolated Where Necessary. Circled figures show as-quenched center hardness Rc scale.

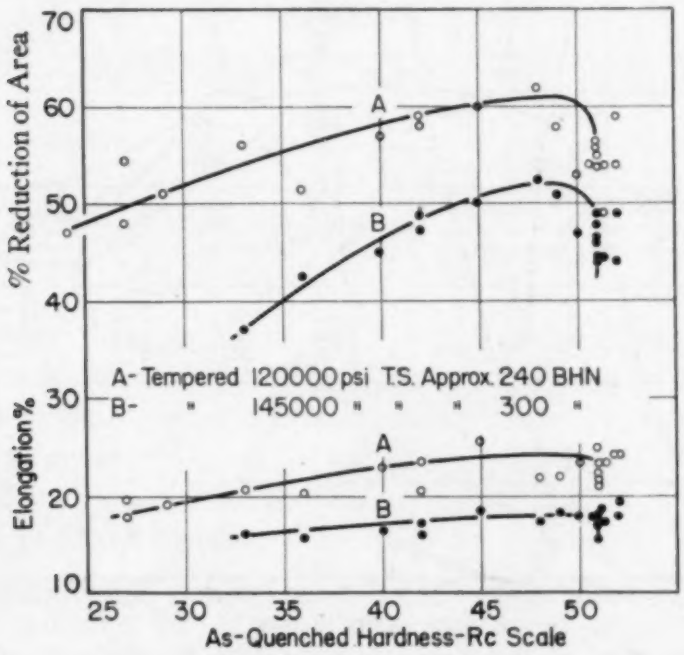


Fig. 25—Comparison of Per Cent Reduction of Area and Per Cent Elongation of Double End-Quenched and Tempered 0.30% Carbon Cast Mn-Cr-Mo Steels with As-Quenched Hardness.

tests were obtained were erratic, with average values generally below those anticipated. Brinell hardnesses were unfortunately not obtained before the bars were machined. Accordingly, these impact

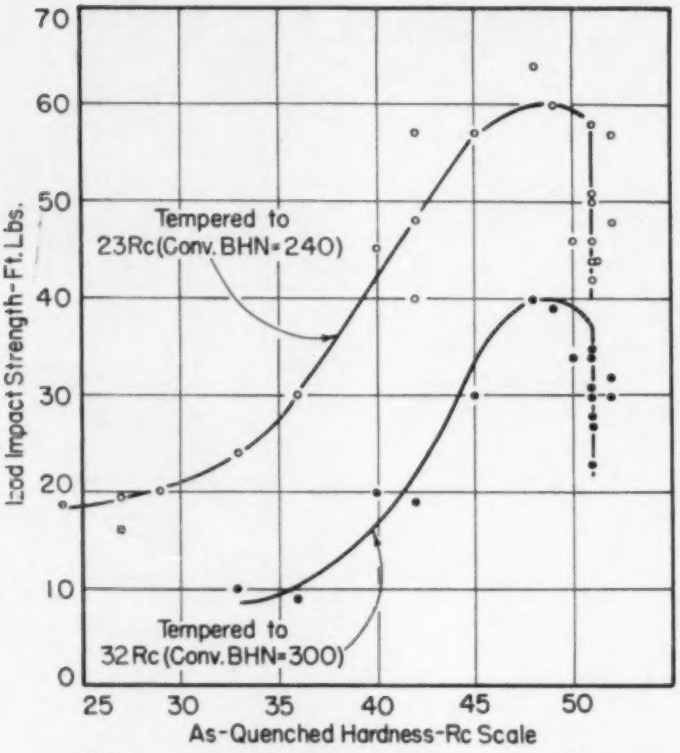


Fig. 26—Comparison of Izod Impact Strength of Double End-Quenched and Tempered 0.30% Carbon Cast Mn-Cr-Mo Steels with As-Quenched Hardness.

data are not plotted in Figs. 23 and 24 since it appeared to be a questionable procedure to interpolate from Table IV.

In Figs. 25 and 26, the three properties are compared at two hardness levels with as-quenched center hardness. While these graphs indicate again the impairment of properties accompanying ineffective hardening, the effect of overalloying can be shown only schematically.

The generally lower level of properties which occurred in the heat treated 1-inch rounds from the higher hardenability heats has not been studied. Possible association with quenching rate, incomplete transformation, or with the solidification characteristics of the 1-inch round versus the 2¼-inch bar are suggested lines of attack.

Microstructure Versus Hardenability, Quenching Rate, and Mechanical Properties

Two series of photomicrographs have been included to illustrate the effects of hardenability and quenching rate upon the microstructure and mechanical properties of these seven 0.30% carbon heat treated, cast alloy steels:

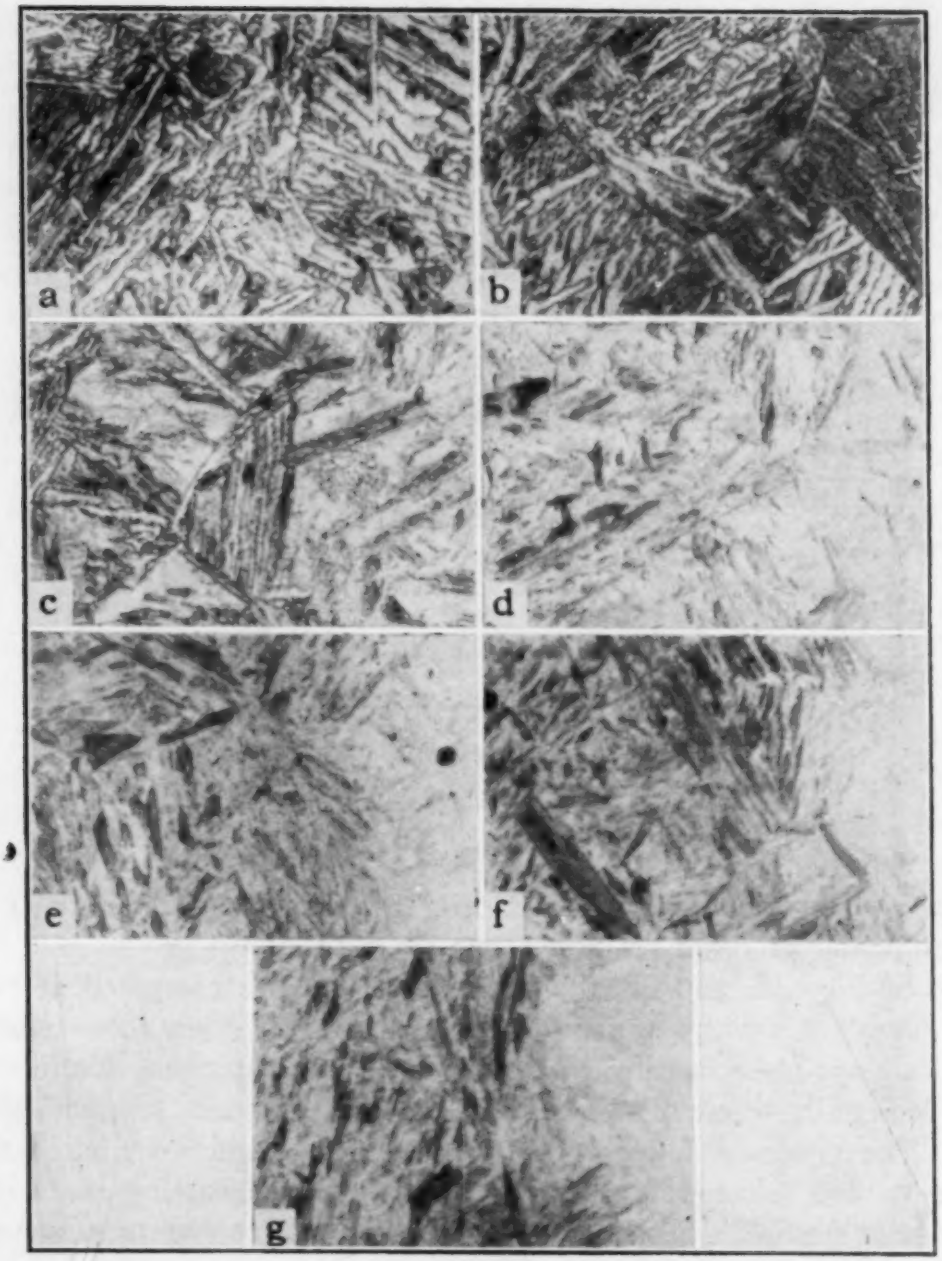


Fig. 27—Change in Microstructure as Hardenability Is Increased, Quenching Rate Remaining Constant, as Obtained at the Center of the As-Quenched D.E.Q. 2⅜ by 2-Inch Diameter Specimen. Effect of segregation upon transformation at each hardenability level is demonstrated, with cell area shown at left, intercell area at extreme right (see Fig. 28). Heat treatment: 1850 F—8 hours—air cool; 1700 F—2 hours—double end quench to 200 F—air cool. Etchant: 3% Nital. × 500.

	Alloy Steel	"Hardenability" No.	As-Quenched Center Hardness D.E.Q. 2⅜ by 2-Inch Diam.
a*	A-1	2426	24 Rc
b	A-2	2583	27 Rc
c	A-3	2939	42 Rc
d	A-4	3386	49 Rc
e	A-5	3620	51 Rc
f	A-6	3896	51 Rc
g	A-7	4206	51 Rc

*Intercell area is at left in this photomicrograph.

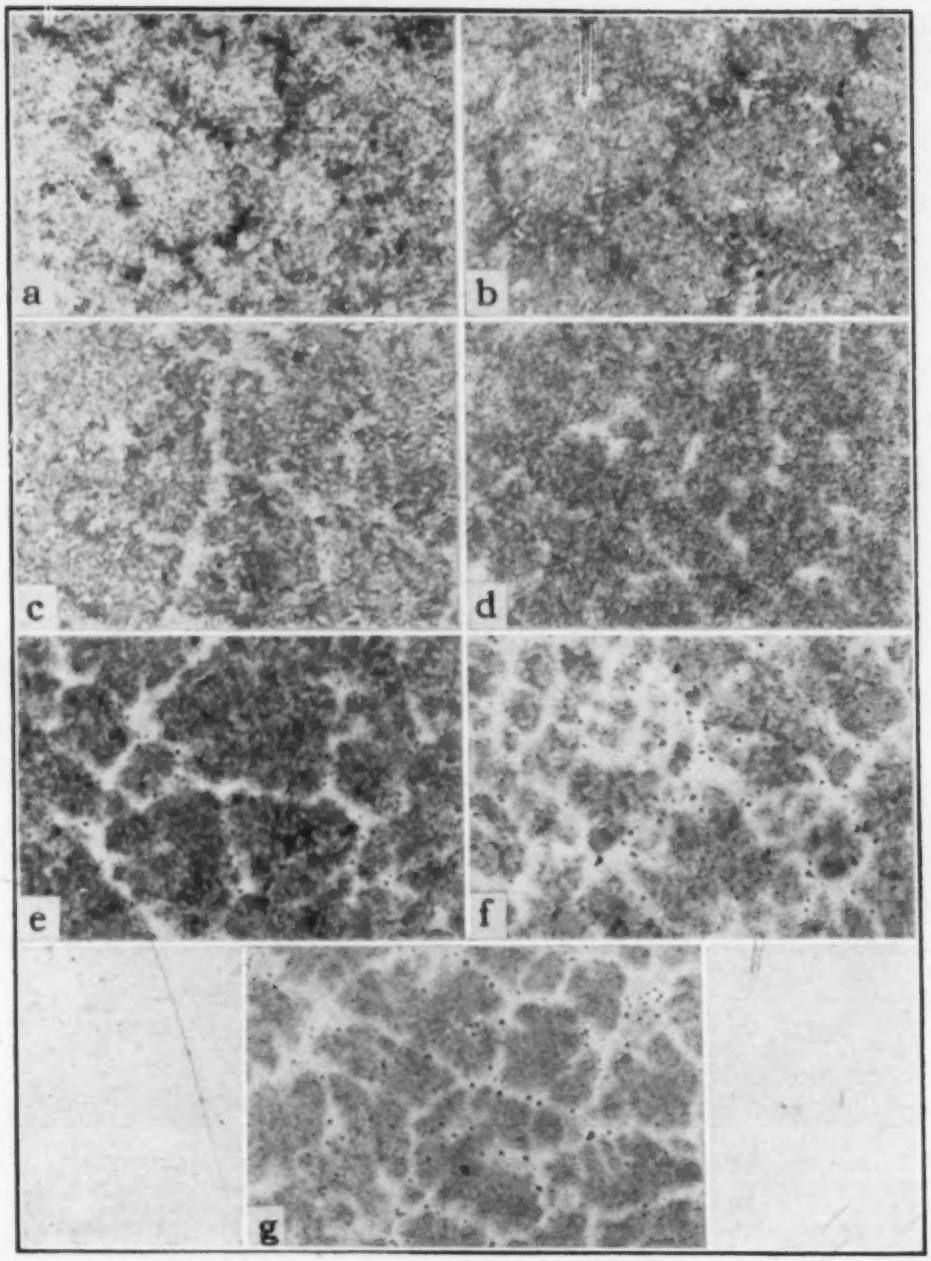


Fig. 28—Macrostructures of Heat Treated Cast Steels, at Same Locations as Shown in Fig. 27, Showing Extensive Segregation Which Is Present. Center of D.E.Q. 2⅜ by 2-inch diameter specimen as-quenched. (Heat treatment: 1850 F—8 hours—air cool; 1700 F—2 hours—double end quench to 200 F—air cool.) Refer to Fig. 27 to observe microstructural details of cell and intercell areas. Etchant: 3% Nital. × 20.

	Alloy Steel	"Hardenability" No.	As-Quenched Center Hardness D.E.Q. 2⅜ by 2-Inch Diam.
a	A-1	2426	24 Rc
b	A-2	2583	27 Rc
c	A-3	2939	42 Rc
d	A-4	3386	49 Rc
e	A-5	3620	51 Rc
f	A-6	3896	51 Rc
g	A-7	4206	51 Rc

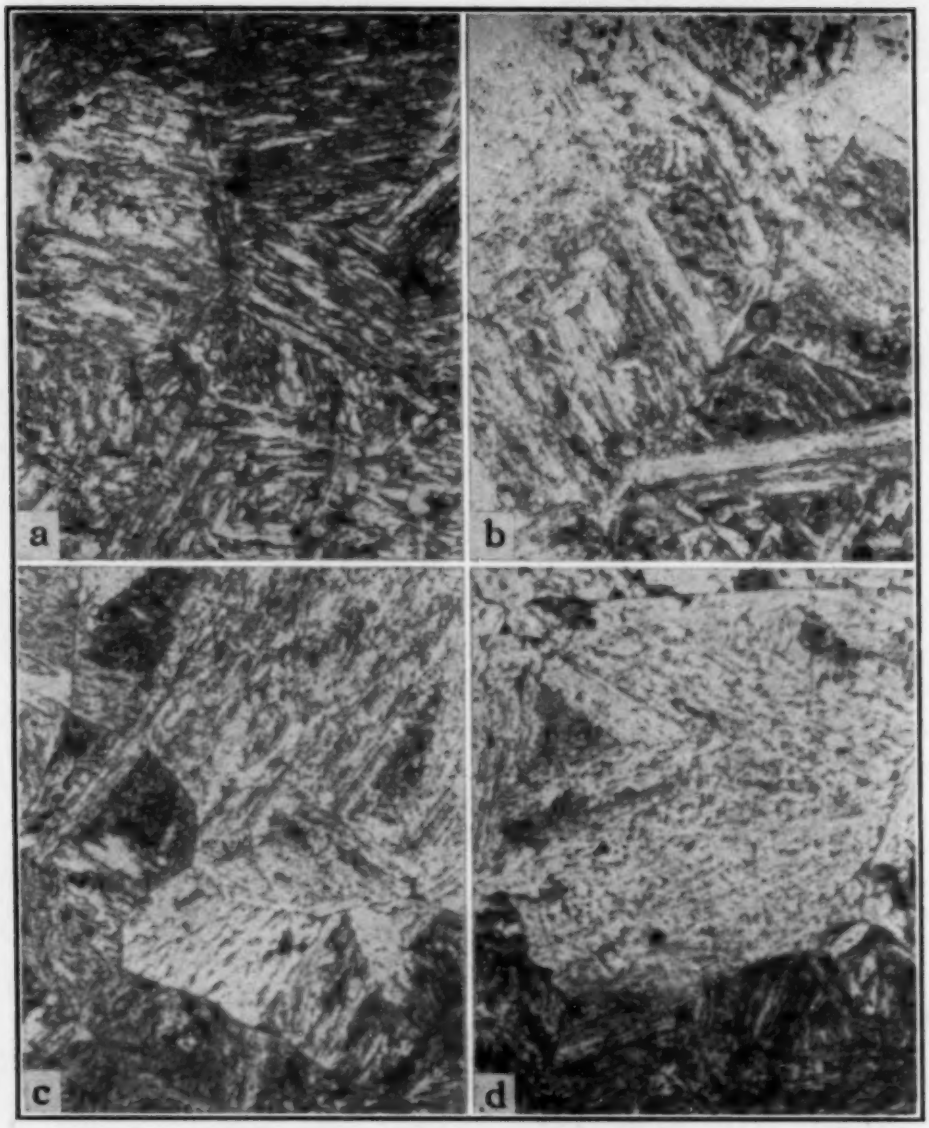


Fig. 29—Microstructure of Quenched and Tempered Alloy Steel A-4 ("Hardenability" No. = 3386; 0.31% C, 1.66% Mn, 0.018% P, 0.015% S, 0.53% Si, 0.55% Cr, 0.36% Mo) Versus Quenching Rate (Decreasing with Increasing D.E.Q. Length) as Obtained at the Center of (a) D.E.Q. 2⅜ by 2-Inch Diameter, (b) D.E.Q. 3⅞ by 2-Inch Diameter, (c) D.E.Q. 5⅞ by 2-Inch Diameter, and (d) D.E.Q. 7⅞ by 2-Inch Diameter Specimens. Heat treatment: 1850 F—8 hours—air cool; 1700 F—2 hours—double end quench to 200 F; (a and b) 1080 F—6 hours—air cool; (c and d) 1060 F—6 hours—air cool. Tempered to 300-325 BHN. Etchant: 3% Nital. × 500.

1. Variable Hardenability — Constant Quenching Rate — The series of photomicrographs in Fig. 27 exhibit the change in the as-homogenized and quenched microstructure with increasing hardenability for a constant quenching rate, as obtained at the center of the D.E.Q. 2⅜ by 2-inch diameter test bars. The marked segregation in these cast steels is illustrated in Fig. 28.

Table VII
Impact Strength Versus Hardenability and Quenching Rate
Variable Hardenability—Constant Quenching Rate

Center—D.E.Q. 2⅜ by 2-Inch Diameter Specimen

Alloy Steel	"Hardenability" No.	As-Quenched Rc	Center Impact Strength—Ft-Lbs Tempered to 240 B.H.N.	Tempered to 300 B.H.N.
A-1	2426	24	18	..
A-2	2583	27	19	..
A-3	2939	42	57	40
A-4	3386	49	60	39
A-5	3620	51	58	34
A-6	3896	51	51	30
A-7	4206	51	50	31

Table VIII
Variable Quenching Rate—Constant Hardenability

Center—D.E.Q. Test Bar of Indicated Length
Alloy Steel A-4

D.E.Q. Length Inches	"Hardenability" No.	As-Quenched Rc	Center Impact Strength—Ft-Lbs Tempered to 240 B.H.N.	Tempered to 300 B.H.N.
2⅜	3386	49	60	39
3⅞	3386	48	64	40
5⅞	3386	40	45	20
7⅞	3386	36	30	9

2. Variable Quenching Rate—Constant Hardenability—In Fig. 29 the change in the as-tempered microstructure with decreasing quenching rate at one hardenability level is demonstrated, as obtained at the center of the four double end quench bars (2⅜ to 7⅞ inches long) from alloy steel A-4.

For comparison, the impact properties at these locations, after tempering of the as-quenched structures where possible to Brinell 240 and 300, are summarized in Tables VII and VIII.

While the investigation had not progressed to the extent of rating quantitatively the occurrence and disposition of the structural constituents in relation to the level of properties which obtain, the general effects of increasing hardenability and/or increasing quenching rate are evident from these photomicrographs. In the as-quenched condition, the marked segregation of these heat treated cast steels is manifested in the lower temperature transformation products in the intercell[5] "areas" (a result of the increased localized hardenability from this segregation) as compared with the cells proper (Figs. 27 and 28).

[5]Cell is considered here to be synonymous with the austenite grain formed upon solidification (i.e., the as-cast austenite grain). The intercell "areas" refer to the contiguous cell surfaces and closely adjacent material where maximum segregation is found.

The predominantly upper bainitic (acicular ferritic) structures shown in Fig. 27 for the two steels of lowest hardenability develop extremely inferior properties after tempering, as expected for such underhardened materials. There is marked improvement in the mechanical properties as hardenability is increased with correspondingly greater hardening during quenching, as evidenced by further lowering of the temperature at which transformation begins and observed microscopically by the increasing presence of the lower temperature products (intermediate bainite, lower bainite, and finally martensite) and the progressive replacement of higher by lower temperature reaction products. As anticipated, optimum properties are developed with sufficient hardenability to permit maximum hardening. With further increases in hardenability, the properties begin to deteriorate.

Microexamination of these higher hardenability heats shows the increasing presence of a lighter etching intercell network which seems to be only partially transformed to martensite. The suspected presence of retained austenite was checked by X-ray diffraction techniques. This work is incomplete, since only the center of the as-quenched D.E.Q. 7⅞ by 2-inch bar from alloy steel A-6 had been investigated, but the "200" and possibly the "111" lines of austenite were observed, together with the expected ferrite pattern. Microscopically, the presence of this austenite could not be verified conclusively. No accurate estimates can be made as to the extent of retained austenite in other sections or compositions, but it is likely that even increased amounts exist after quenching in the more highly alloyed steel "A-7". It is also probable that the amount of retained austenite will be greater in the corresponding tempered bars before tempering, since these were quenched only to 200 F (95 C), while the pilot bars were subsequently cooled to room temperature. While the desirability of cooling to room temperature before tempering to obtain more complete transformation of the austenite is suggested, this is usually not feasible for the higher alloyed steels because of the added hazards of cracking.

While the extent to which retained austenite is present in the several sections and compositions has not yet been determined, the presence of this constituent may well explain the impairment of properties with higher hardenability. The formation of undesirable products with inferior properties may occur by the decomposition of this austenite during heating to the tempering temperature or, if this is avoided, during the tempering treatment proper.

While subject to verification with considerable additional data, the present results (Fig. 24) suggest that, for heavier cast sections, the maximum obtainable properties tend to decrease with increasing section for the heat treatment employed in this investigation. This appears plausible since the hardenability requirements increase with section with a correspondent increase, above an undetermined hardenability level, in the amount of retained austenite after quenching in the "overalloyed" intercell areas.

This would suggest that, for optimum properties, there is an optimum hardenability for each section, lower hardenability reducing the level of properties by the presence of inferior higher temperature transformation products and higher hardenability introducing deteriorating complications by the increased presence of austenite untransformed during quenching but transforming to undesirable structures during the tempering cycle.

For full size sections, retained austenite may have a less detrimental effect upon properties. Such castings, heating more slowly to the tempering temperature because of their mass, will provide greater opportunity for transformation of this austenite to more desirable lower temperature products (as, for example, the lower bainites) which will subsequently be tempered. Dual tempering treatment has been suggested (holding first at some lower temperature before proceeding to the selected tempering temperature) to assure transformation of such austenite to relatively desirable structures.

Several other variables which might influence the observed deterioration of properties at these higher hardenability levels have been proposed, including the possible deleterious effects (a) if secondary hardening occurs during tempering, (b) if temper brittleness is encountered, and (c) if micro cracks develop during quenching. While the first two have not been investigated, no evidence of the latter was observed in the double end quench test bars.

The second series of photomicrographs (Fig. 29) need little comment. These are tempered structures, but the increasing presence of higher and higher temperature transformation products as quenching rate is decreased is clearly evident.

Possible Limitations of the Test Bar Method

While the observed relationships of quenching rate and hardenability to mechanical properties as demonstrated with the double end

quench technique serve to delineate the effects of these several variables, caution must be used in translating these results to predict the behavior of full-scale sections. The main apparent limitation of the present test bar technique has been emphasized, viz., the lack of assurance of heterogeneity similar to that of heavy sections with different solidification characteristics. As heterogeneity (9) is a factor influencing hardenability, this may become an important consideration in testing cast steels although it may be negligible for hot-worked alloys of similar composition. The possible extent of the effect of this variable has not been investigated. Sound double end quench specimens machined from full-size plates might be employed, but this introduces an enormous amount of additional effort to obtain comprehensive surveys such as have been presented here. Furthermore, the securing of microscopically sound material in larger plate sections, while not insurmountable, is difficult of attainment. If properties reflecting all of the variables in actual plates are required, however, double end quench specimens machined from these sections would minimize the handling of unwieldy, heavy pieces.

A second factor that should be considered in an attempt to correlate test bars and plates is the effect that different thermal stresses might have upon the transformation characteristics of a given austenite. Equal cooling rates are no assurance of equal stresses in two different castings.

Finally, the double end quench bar was developed specifically to match the thermal histories at the center of flat plates. The correlation for other sections has not been determined. Considerable discrepancy appears in the respective shapes of the cooling curves for water-quenched rounds and double end quench test bars, but closer matching for oil-quenched rounds is suggested by the available comparisons. The possible modifications in the shape of the test bar and/or of the quenching technique which might permit correlation with these and other types of sections may be such as to limit the broader application of the technique.

Summary and Conclusions

The mechanical properties at selected hardness levels of seven 0.30% carbon heat treated cast alloy steels have been evaluated at the center of four double end quench specimens, whose center quenching rates correspond closely to those which obtain at the cen-

ter of water-quenched flat plates approximately 2, 4, 6, and 8 inches thick. While the several properties behave similarly, impact strength is, as anticipated, the most sensitive of these variables to structural changes brought about by modifications in hardenability and quenching rate. The impaired properties associated with the higher temperature transformation products (in particular, acicular ferrite) resulting from insufficient hardenability for a given quenching rate to attain maximum hardening are demonstrated, together with the optimum properties obtained when hardenability is increased sufficiently to provide maximum hardening. With further increases in hardenability some deterioration in the properties is observed, possibly associated with the increasing presence of austenite, retained upon quenching in the areas of maximum segregation, which is subsequently transformed to undesirable constituents during tempering. The data suggest that, for each particular rate of cooling, as determined by section size, optimum properties are associated with the minimum hardenability necessary to obtain maximum as-quenched hardening.

While a separately cast test bar may provide identical quenching rates and composition it does not assure heterogeneity similar to that of heavy sections with different solidification characteristics. The effect upon hardenability and mechanical properties may become an important consideration in testing cast steels, and it cannot be assumed that the test bar properties will necessarily be attained in the corresponding plate. The extent of the possible deviation has not, however, been investigated.

Further work appears desirable to delineate the relation of the several structural constituents to mechanical properties and to study variations in heat treating techniques to obtain improved properties in the heavier sections. A parallel investigation of heavily forged steels of similar compositions may serve to delineate the deleterious effects of the marked segregation observed in these cast steels and should be examined with respect to the reported conclusion that heavy sections cannot be quenched at sufficient velocities after tempering to suppress low temperature temper brittleness.

Acknowledgments

The authors gratefully acknowledge the helpful suggestions of their associates and, in particular, the assistance of Miss Agnes

Decker, Mrs. Wayne Rule, Mrs. William Appleton, Mr. Clifford Burris, and Mr. Henry Chapin in various phases of this investigation, together with the permission of the American Brake Shoe Company to publish this research.

References

1. C. R. Wilks, E. Cook and H. S. Avery, "Further Developments of the End Quench Hardenability Test," TRANSACTIONS, American Society for Metals, Vol. 35, 1945, p. 1.
2. R. A. Flinn, Earnshaw Cook and J. A. Fellows, "A Quantitative Study of Austenite Transformation," TRANSACTIONS, American Society for Metals, Vol. 31, 1943, p. 41.
3. E. Cook, "Open Hearth Steel Making," published by the American Society for Metals, 1937, p. 142.
4. E. Cook, "Relation of Chemical Composition to Rail Fissures," TRANSACTIONS, American Society for Metals, Vol. 23, 1935, p. 545.
5. "Properties of Frequently Used Carbon and Alloy Steels," Bethlehem Steel Co., 1944, p. 78-87.
6. M. A. Grossmann, "Hardenability Calculated from Chemical Composition," *Transactions*, American Institute of Mining and Metallurgical Engineers, Vol. 150, 1942, p. 227.
7. W. Crafts and J. L. Lamont, "The Effect of Silicon on Hardenability," *Transactions*, American Institute of Mining and Metallurgical Engineers, Vol. 154, 1943, p. 386.
8. W. Crafts and J. L. Lamont, "Effects of Some Elements on Hardenability," *Transactions*, American Institute of Mining and Metallurgical Engineers, Vol. 158, 1944, p. 157.
9. R. M. Parke and A. J. Herzig, "Hardenability of Steel—Dendritic Segregation a Factor," *Metals and Alloys*, February 1942, p. 241.

DISCUSSION

Written Discussion: By Robert M. Parke, Climax Molybdenum Co. of Michigan, Detroit.

Messrs. Wilks, Avery and Cook are to be complimented for obtaining some valuable data on cast steels—data which are difficult to secure under carefully controlled conditions.

The authors have concluded that the optimum mechanical properties are developed in cast steel when the hardenability of the steel is the minimum which produces full hardening for the cooling rate involved. This conclusion is fully substantiated by the authors' data, and is significant.

The underlying cause for the phenomenon is attributed by the authors largely to austenite retained after the quench or to temper brittleness. It is true, as Timmons[6] has shown, that a manganese-molybdenum cast steel (0.28% carbon, 1.62% manganese, 0.37% molybdenum) is susceptible to temper brittleness, and it is also true that the susceptibility to temper brittleness increases with increase in hardenability, as Hollomon[7] has pointed out. Yet, in the present instance it does not appear that temper

[6]G. A. Timmons, "Factors Affecting the Ductility of Cast Steel," *Transactions*, American Foundrymen's Association, Vol. 51, 1943, p. 417.

[7]J. H. Hollomon, "Temper Brittleness," TRANSACTIONS, American Society for Metals, Vol. 36, 1946, p. 473.

brittleness is the major cause of the depreciation in physical properties when the hardenability is in excess of that needed. In general, temper brittleness is not revealed so clearly as a reduction of ductility in the tensile test, as it is in the data of Wilks, Avery and Cook. It seems, therefore, that at least a part of the unknown cause is to be found elsewhere, for example, in the retained austenite, which the authors have shown to be present in the quenched steel.

In any event, a knowledge of the existence of an optimum hardenability can at once be put to good use in castings of invariant cross-sectional area, such as plates. For more complicated castings one should seek to obtain hardenability with elements which, when present in excess, do not adversely affect the physical properties.

Written Discussion: By N. A. Matthews, works metallurgist, Electro-Alloys Division, American Brake Shoe Co., Elyria, Ohio.

The authors have presented a large quantity of valuable data pertaining to the problem of attaining a maximum combination of strength and toughness in heat treated steels of comparatively heavy section. The hardenability "number" concept described appears to be a simple means of relating the relative depth hardening characteristics of steels.

The unmistakable evidence presented that parts may be overalloyed for best results is of great importance. The mechanism for this effect which is presented, namely the incomplete transformation of the austenite upon cooling from the austenitizing temperature, is probably correct and agrees with other experience on comparable analyses. There is evidence that homogenization at higher temperatures may reduce this effect of overalloying, especially in steels comparatively high in chromium content.

The problem of serious temper brittleness developing in overalloyed steels must also be considered but probably was not involved in this investigation because the small sections tempered cooled comparatively rapidly in air from the tempering temperature.

There are many parts made today which, as this paper suggests, are overalloyed for best results. Every now and then one reads that temper brittleness and related maladies are not troublesome in conventional moderately alloyed steels. However, if a complete understanding is obtained of the relationships among these effects, impact properties and service performance, it often develops that such maladies are of paramount importance in many highly stressed parts subjected to shock or fatigue.

Written Discussion: By John G. Kura, research engineer, Battelle Memorial Institute, Columbus, Ohio.

In Table VIII, the 3⅞-inch D.E.Q. test piece produced maximum Izod-impact values upon tempering to 240 and 300 BHN. Although these maximum values are not greatly out of line, they do appear to be significant. Is there an explanation for this?

Authors' Reply

It is gratifying that both Mr. Parke and Mr. Matthews also consider that the underlying cause of the impairment in properties, associated with

further increases in hardenability beyond that necessary to achieve maximum hardening, is at least in part the result of retained austenite after quenching. Their discussions of temper brittleness are appreciated but lead us to believe that our mention of this phenomenon has created the impression that we consider this a possible primary reason for the present impairment of properties. This is not the case, however, it being our opinion that it is only one of several factors which have doubtful significance in this investigation.

In reply to Mr. Kura, several hypotheses (e.g., the possibility of less retained austenite with slower cooling) might be advanced to explain the maximum impact properties at 240 and 300 BHN in the D.E.Q. 3⅞-inch specimen of alloy steel A-4, if the indicated superiority is significant. While 64 ft-lbs. (D.E.Q. 3⅞ inch) vs. 60 ft-lbs. (D.E.Q. 2⅜ inch) might be significant for wrought stock, the marked heterogeneity of cast materials places these variations within experimental error. In particular, these values were obtained by minor interpolation or extrapolation of the data in Table II. The hardness values are averages in each case of several determinations, which varied at least ±1 Rc. Impact strength is the average of three tests; examination of these data indicates that the median variation was 3.5 to 4.0 ft-lbs.

A LABORATORY STUDY OF QUENCH CRACKING IN CAST ALLOY STEELS

By M. C. Udy and M. K. Barnett

Abstract

Alloy steels, when fully quenched, frequently exhibit cracking either during or shortly after the quenching operation. A laboratory test has been developed to demonstrate the effects of chemical composition and heat treatment variables upon the sensitivity of steel to quench cracking.

Composition was the most potent variable studied and, of the individual elements promoting cracking, carbon was the most powerful. Manganese, chromium, and phosphorus appeared to be detrimental, but to a lesser degree than carbon. Sulphur, silicon, nickel, molybdenum, and aluminum, in the ranges studied, showed little, if any, effect. Normal boron additions had no effect on cracking tendency.

High austenitizing temperatures increased the tendency to crack. Prolonged austenitizing periods just before quenching or a prior high-temperature homogenizing treatment lessened somewhat the cracking tendency.

Introduction

WHEN it is necessary to fully harden alloy steel by quenching, particularly massive, irregularly shaped parts, special attention must be paid to the problem of quench-crack elimination. In the production of a particular part, the problem is, to some extent, one of designing the part in such a manner that temperature and stress gradients during cooling will approach that minimum consistent with the utility of the finished product. However, insofar as sensitivity to quench cracking is an inherent function of the steel, which, for a given design of a part, may manifest itself to varying degrees with variations in composition, melting and molding technique, and heat

This paper is based on work done for the Office of Scientific Research and Development under contract OEMsr-450 with Battelle Memorial Institute.

A paper presented before the Twenty-eighth Annual Convention of the Society, held in Atlantic City, November 18 to 22, 1946. The authors, M. C. Udy and M. K. Barnett, are research engineers, Battelle Memorial Institute, Columbus, Ohio. Present connection of M. K. Barnett is assistant professor, Department of Mathematics, University of Dayton, Dayton, Ohio. Manuscript received May 2, 1946.

treating practice, the problem lies in the realm of metallurgy. It is this metallurgical aspect with which the present paper is concerned.

The process of "martempering," which consists of quenching a piece in molten salt or some other suitable medium to some temperature above the martensite transformation point, holding it at that temperature until temperature gradients have been evened out, then air cooling or quenching it to room temperature, has been used as a method of eliminating quench cracks. However, this process has its disadvantages and limitations. It is difficult to install in some plants because of the large size of the necessary equipment. Different steels need different temperatures for the salt quench. For large massive pieces, the process becomes ineffective, because the time necessary to establish a uniform temperature in the piece becomes longer than the time to start transformation at the salt-quenching temperature. Very sluggish austenite, i.e., a highly alloyed and hence expensive steel, is needed in order that the cooling rate of the salt quench will suffice to prevent transformation of austenite at the center of heavy sections. Finally, the cost of such a process is much greater than that of a straight quenching operation. For these reasons, only straight quenching has been considered in the work herein discussed.

Experimental Work

Some 120 steels have been tested. All test material was prepared as 300- to 600-pound heats made in a basic-lined induction furnace from steel scrap (or ingot iron), ferroalloys, nickel, and graphite. Except in those heats devoted to the influence of deoxidation practice, all heats were deoxidized with 2 pounds of aluminum per ton (0.10%). The metal was cast as single-leg keel-block castings. The leg of the block, 1¼ inches square and 15 inches long, was used for test purposes.

The test specimens employed throughout the work were cylinders 2 inches long and 1 inch in diameter. Saw cuts $\frac{1}{16}$ inch wide and of equal depths were cut along the axis in both ends of each cylinder. The two cuts were in the same plane. The depth of cut varied, in increments of ⅛ inch, from ⅛ inch to ⅞ inch. In most cases, specimens with all seven notch depths were tested in duplicate. The ⅛-inch notch was omitted in some cases.

The testing procedure consisted in placing the specimens in cov-

ered graphite crucibles, holding the desired time at the desired temperature, withdrawing the crucible from the furnace, quickly removing the cover, and depositing the specimen in a quenching jig supplied with flowing water. The jig consisted of a 1½-inch diameter vertical pipe, equipped with specimen guides which were topped by

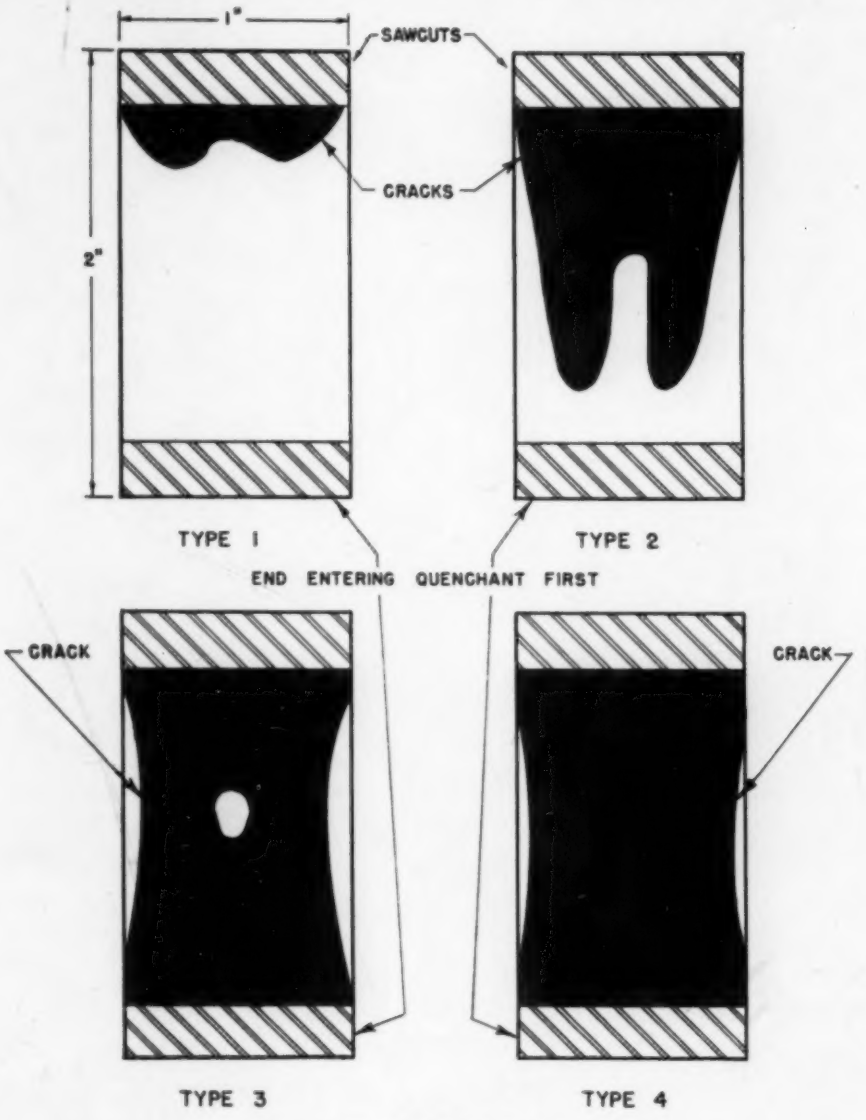


Fig. 1—Typical Crack Patterns.

a sheet metal funnel. The top of the funnel extended 8 inches above the surface of overflowing water. In quenching, the graphite crucible was inverted in contact with the top of the funnel. Thus, the height of fall of the specimen was held constant, and its vertical position was maintained during and subsequent to entry into the quenchant. Specimens remained 30 seconds in the quenching water.

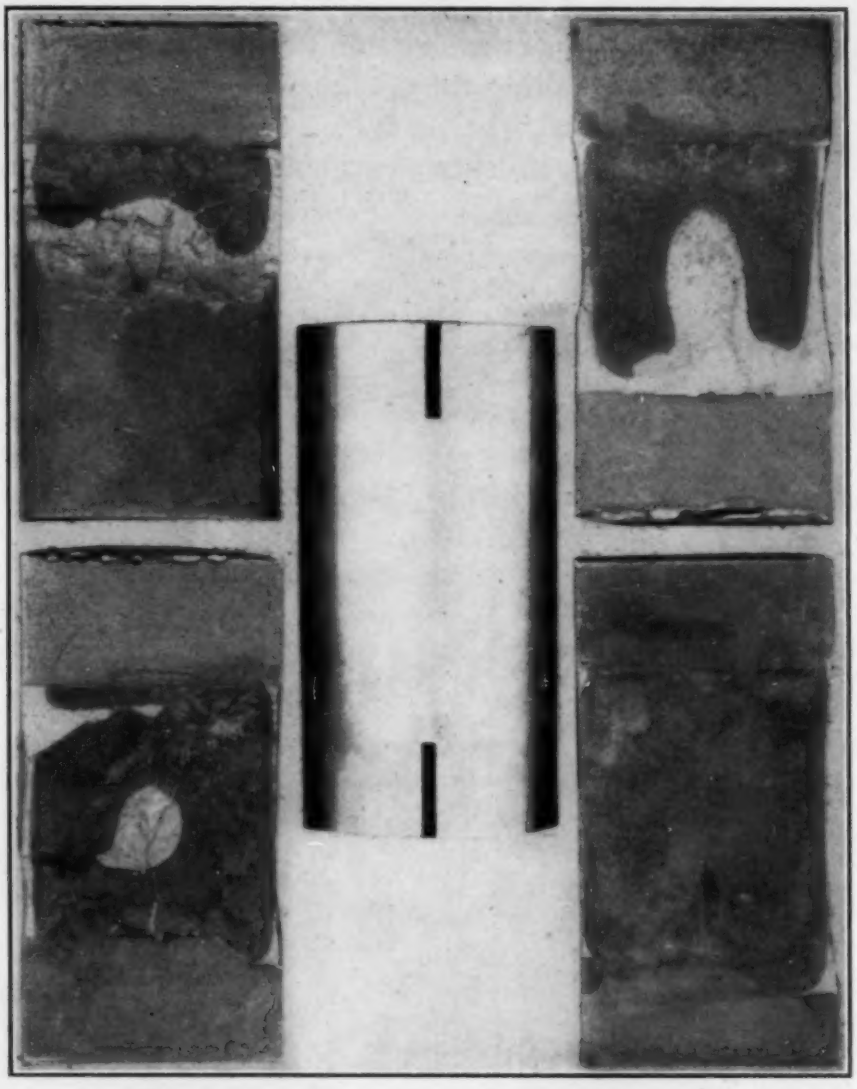


Fig. 2—Typical Crack Patterns.

Specimens were etched within a few hours after quenching. Etching was by 1-hour immersion at 160 to 180 F in a mixture of 50% water, 38% hydrochloric acid, and 12% sulphuric acid. After washing and drying, the specimens were split open by forcing a wedge into the end which entered the quench water last. The cracked zones of the fractures were readily differentiated by their etched appearance.

Typical crack patterns observed in the split specimens are illustrated in Fig. 1. Fig. 2 is a photograph of the same typical cracks. The central specimen is unquenched and unsplit. It shows location of the notches. In every case where the crack failed to extend over

the entire length of the unnotched zone, the crack started at the end which entered the quenchant last. Cracks sometimes lacked the symmetry of those shown in Fig. 1, and extraneous cracks sometimes occurred in the sides of the notch.

The original plan was to take the shallowest depth of notch at which cracking occurred as the indication of cracking sensitivity. However, as the work progressed, it became evident that this index was prone to give too much weight to accidental cracks. An index, consisting of the summation of the lengths of the cracks in all seven specimens (averaged in the case of duplicate specimens) was found to be more reliable. Statistical methods were used to good advantage in the interpretation of the data.

Series of tests were made to study the effects of following variables on quench-crack sensitivity.

1. Carbon content
2. Alloy content (Mn, Si, Mo, Cr, Ni, P, S, B)
3. Deoxidation
4. Heat treatment
   a. Prior treatment
   b. Austenitizing time
   c. Austenitizing temperature

Table I

First Series. Influence of Variations in Carbon Content on Quench Crack Susceptibility

Quench Cracking Index*—I′ = (8 — n) (n = notch depth (1/8 inch) of shallowest notched specimen to exhibit cracking.) I′ = 0 for no cracks.

	Analysis, %							
Heat No.	C	Mn	Si	Cr	Ni	Mo	Others	I′
10404-1	0.23	0.82	0.35	0.52	0.55	0.41	.....	0
-2	0.29	"	"	"	"	"	.....	0
-3	0.34	"	"	"	"	"	.....	0
10405-1	0.23	1.50	0.40	....	....	0.41	.....	0
-2	0.27	"	"	....	....	"	.....	0
-3	0.33	"	"	....	....	"	.....	0
10406-1	0.26	1.00	0.41	0.52	....	0.39	.....	0
-2	0.28	"	"	"	....	"	.....	0
-3	0.32	"	"	"	....	"	.....	3
10407-1	0.23	1.15	0.41	....	....	0.39	0.0025 B	0
-2	0.25	"	"	....	....	"	as	0
-3	0.35	"	"	....	....	"	FeB	0
10973-1	0.24	0.83	0.60	0.51	0.56	0.32	.....	0, 0
-2	0.26	"	"	"	"	"	.....	0, 0
-3	0.28	"	"	"	"	"	.....	0, 0
-4	0.30	"	"	"	"	"	.....	0, 0
-5	0.32	0.82	0.60	"	"	"	.....	3, 3

Ditto marks indicate that actual analysis for the particular element was not made but is assumed to be the same as a prior split of the same heat.

P in Heats 10404 to 10407, inclusive, was about 0.01% and S about 0.025% as judged by analysis of similar heats made with the same melting stock. P and S in Heat 10973 were 0.019% and 0.025%, respectively.

All heats were deoxidized with 0.10% Al.

*This index is not the same as that used in Tables IV, VI, VIII, and IX and is not directly comparable with that index.

Table II

Second Series. Influence of Alloy Variation on Quench Crack Susceptibility (0.30 Carbon Level)†

Quench Cracking Index*—I′ = (8 — n) where n = notch depth of shallowest notched specimen to crack.

	Analysis, %										
Heat No.	C	Mn	Si	P	S	Cr	Ni	Mo	Al Added	Others	I′
10492	0.30	0.82	0.61	0.011	0.026	0.51	0.51	0.40	0.10	0.07 Cu, 0.01 Sn	0
10493-1	0.30	0.55	0.56	0.009	0.022	0.50	0.50	0.41	0.10	....	0
-2	"	1.36	"	"	"	"	"	"	0.10	....	3
-3	"	1.82	"	"	"	"	"	"	0.10	....	3
10494-1	0.28	0.89	0.26	0.008	0.022	0.52	0.51	0.39	0.10	....	0
-2	"	"	0.98	"	"	"	"	"	0.10	....	0
-3	"	"	1.55	"	"	"	"	"	0.10	....	0
10659-1	0.30	0.80	0.61	0.045	0.029	0.48	0.53	0.42	0.10	....	4
-2	"	"	"	0.056	"	"	"	"	0.10	....	4
-3	"	"	"	0.069	"	"	"	"	0.10	....	4
10495-1	0.28	0.87	0.62	0.018	0.026	0.50	0.51	0.41	0.10	....	3
-2	"	"	"	0.144	"	"	"	"	0.10	....	3
-3	"	"	"	0.230	"	"	"	"	0.10	....	3
10496-1	0.30	0.82	0.58	0.010	0.034	0.51	0.50	0.40	0.10	....	0
-2	"	"	"	"	0.042	"	"	"	0.10	....	0
-3	"	"	"	"	0.053	"	"	"	0.10	....	0
10497-1	0.29	0.83	0.52	0.011	0.022	0.08	0.69	0.39	0.10	....	0
-2	"	"	"	"	"	1.11	"	"	0.10	....	0
-3	"	"	"	"	"	1.41	"	"	0.10	....	0
10498-1	0.30	1.81	0.57	0.010	0.024	0.03	0.51	0.40	0.10	....	5
-2	"	"	"	"	"	0.89	"	"	0.10	....	6
-3	"	"	"	"	"	1.56	"	"	0.10	....	5
10499-1	0.29	0.82	0.59	0.010	0.028	0.60	0.04	0.39	0.10	....	0
-2	"	"	"	"	"	"	1.00	"	0.10	....	0
-3	"	"	"	"	"	"	1.48	"	0.10	....	0
10500-1	0.29	0.84	0.60	0.014	0.033	0.50	0.53	0.00	0.10	....	0
-2	"	"	"	"	"	"	"	0.20	0.10	....	0
-3	"	"	"	"	"	"	"	0.60	0.10	....	0
10501-1	0.30	0.83	0.58	0.009	0.027	0.51	0.56	0.39	0	....	0
-2	"	"	"	"	"	"	"	"	0.025	....	0
-3	"	"	"	"	"	"	"	"	0.050	....	0

Ditto marks indicate that actual analysis for the particular element was not made but is assumed to be the same as a prior split of the same heat.

*This index is not the same as that used in Tables IV, VI, VIII, and IX and cannot be directly compared with that index.

†Compare Tables II and III for influence of carbon.

Experimental Results[1]

The range of sensitivity of the test was rather limited. That is, it did not take much change in composition to have the test show no cracks in any specimen as one extreme, or to show cracks in all specimens as the other extreme. No good method was found to extend the range of usefulness of the test.

Table I gives the composition and cracking indices of a series of tests made on steels of similar hardenability and varying the carbon content. These steels were not very susceptible to cracking. But from these results, as well as by comparing Tables II and III, it can

[1]More detailed presentation of the data is given in O.S.R.D. Report No. 4667, Serial No. M-465.

Table III

Third Series. Influence of Alloy Variation on Quench Crack Susceptibility (0.35 Carbon Level)†

Quench Cracking Index*—I′ = (8 − n) where n = notch depth of shallowest notched specimen to crack.

	Analysis, %										
Heat No.	C	Mn	Si	P	S	Cr	Ni	Mo	Al Added	Others	I′
10755‡	0.35	0.90	0.59	0.024	0.035	0.51	0.51	0.41	0.10	....	5
10635-1	0.33	0.54	0.60	0.012	0.023	0.45	0.52	0.42	0.10	....	0
-2	"	1.34	"	"	"	"	"	"	0.10	....	5
-3	"	1.82	"	"	"	"	"	"	0.10	....	5
10636-1	0.34	0.86	0.35	0.013	0.028	0.46	0.53	0.42	0.10	....	5
-2	"	"	1.05	"	"	"	"	"	0.10	....	5
-3	"	"	1.57	"	"	"	"	"	0.10	....	4
10639-1	0.32	0.86	0.57	0.043	0.029	0.45	0.53	0.42	0.10	....	5
-2	"	"	"	0.057	"	"	"	"	0.10	....	5
-3	"	"	"	0.066	"	"	"	"	0.10	....	5
10640-1	0.33	0.84	0.58	0.013	0.035	0.45	0.53	0.42	0.10	....	0
-2	"	"	"	"	0.047	"	"	"	0.10	....	4
-3	"	"	"	"	0.055	"	"	"	0.10	....	4
10641-1	0.35	0.85	0.59	0.013	0.026	0.01	0.50	0.41	0.10	....	0
-2	"	"	"	"	"	1.06	"	"	0.10	....	4
-3	"	"	"	"	"	1.43	"	"	0.10	....	5
10642-1	0.34	1.76	0.56	0.013	0.025	0.01	0.51	0.41	0.10	....	5
-2	"	"	"	"	"	1.05	"	"	0.10	....	5
-3	"	"	"	"	"	1.51	"	"	0.10	....	5
10643-1	0.33	0.86	0.64	0.010	0.029	0.46	0.03	0.41	0.10	....	0
-2	"	"	"	"	"	"	1.04	"	0.10	....	4
-3	"	"	"	"	"	"	1.50	"	0.10	....	5
10648-1	0.34	0.83	0.58	0.012	0.033	0.48	0.53	Nil	0.10	....	0
-2	"	"	"	"	"	"	"	0.22	0.10	....	3
-3	"	"	"	"	"	"	"	0.62	0.10	....	0
10649-1	0.33	0.82	0.61	0.009	0.027	0.45	0.53	0.42	0.0	....	4
-2	"	"	"	"	"	"	"	"	0.025	....	4
-3	"	"	"	"	"	"	"	"	0.05	....	4

Ditto marks indicate that actual analysis for the particular element was not made but is assumed to be the same as a prior split of the same heat.

*This index is not the same as that used in Tables IV, VI, VIII, and IX, and is not directly comparable with that index.

†Compare Tables II and III for influence of carbon.

‡10755 has higher P than other heats in the series where P was not intentionally added.

be seen that carbon is a potent variable in the promotion of cracking.

Tables II and III give the compositions and cracking indices of two series of steels intended to be identical except for the level of carbon content. Within the series, manganese, silicon, sulphur, phosphorus, chromium, nickel, molybdenum, and aluminum contents are varied. No significant effect on cracking could be noted for silicon, sulphur, nickel, or molybdenum in the ranges studied. No differences could be noted between silicon and aluminum deoxidation as practiced. Manganese and chromium increased cracking sensitivity as their contents were increased to 3%. High phosphorus (over 0.02%) also promoted cracking.

Table IV gives the composition and cracking indices of a series of steels made especially to study the effect of phosphorus. The previously noted bad effect of phosphorus was again evident.

Table IV

Fourth Series. Influence of Variations in Phosphorus Content on Quench Crack Susceptibility

(Quench Cracking Index† $I = \Sigma(d)$ denotes sum of crack depths, in sixteenths of an inch, of six specimens of each group.)

Heat and Split No.*	P, %	Crack Depth (1/16 Inch) at Designated Notch Depth, Inches						I (1/16 Inch)
		1/4	3/8	1/2	5/8	3/4	7/8	
163-1A	0.003	0	0	0	0	0	0	0
-1B	"	0	0	0	0	0	0	0
-1C	"	0	0	0	0	0	0	0
163-2A	0.007	0	0	0	0	0	0	0
-2B	"	0	0	0	0	0	0	0
-2C	"	0	0	0	0	0	0	0
163-3A	0.014	0	0	0	0	0	0	0
-3B	"	0	0	0	0	1	0	1
-3C	"	0	0	0	0	0	0	0
163-4A	0.050	0	0	1	1	1	1	4
-4B	"	0	0	0	6	1	1	8
-4C	"	0	0	0	0	1	1	2
163-5A	0.129	0	0	1	1^1	1	1^1	4
-5B	"	0	0	3	2	1^1	1^1	7
-5C	"	0	0	0	2	1^1	1^1	4

(Note: Superscript "1" denotes 3 to 6 extraneous cracks appearing on face of notch.)

Heat and Split No.*	Analysis, %								
	C	Mn	Si	P	S	Cr	Ni	Mo	Added Al
163-1	0.30	0.80	0.46	0.003	0.027	0.52	0.50	0.67	0.10
-2	0.30	"	"	0.007	"	"	"	"	"
-3	0.30	"	"	0.014	"	"	"	"	"
-4	0.30	"	"	0.050	"	"	"	"	"
-5	0.30	"	"	0.129	"	"	"	"	"

Ditto marks indicate that actual analysis for the particular element was not made but is assumed to be the same as a prior split of the same heat.

†This is not the same index as used in Tables I, II, III, and V and is not directly comparable with that index.

Table V contains the compositions and indices of a series of miscellaneous high-alloy steels. The bad effects of carbon and manganese are again evident.

Table VI contains the compositions and indices of a series of steels made primarily to study the effect of boron on cracking susceptibility. No significant effect could be noted.

Table VII gives the composition of a series of steels made primarily to study the effects of variation in heat treatment practice on cracking tendencies. Table VIII gives the heat treatments and the resulting cracking indices for this series. Table IX gives the composition, heat treatment, and cracking indices of some additional steel made for the same purpose.

Substitution of an homogenizing treatment (8 hours at 2300 F) for an ordinary normalizing one (2 hours at 1700 F) decreased quench-crack susceptibility somewhat.

Table V

Fifth Series. Quench-Cracking Characteristics of High-Alloy Steels

Quench-Crack Index*—I′ = (8 — n) where n = notch depth (⅛ inch) of shallowest notched specimen to crack.

Heat No.	Analysis,[1] % C	Mn	Si	P	S	Cr	Ni	Mo	Others	I′	Remarks
10529	0.37	0.71	0.41	0.014	0.025	1.08	1.55	0.46	0.15 V	6	C comparison
10616	0.28	0.63	0.35	0.012	0.023	1.06	1.51	0.47	0.15 V	3	C comparison
10530	0.28	1.51	0.38	0.014	0.033	1.56	....	0.61	....	6	Duplicates
10638	0.28	1.61	0.37	0.017	0.031	1.54	....	0.58	....	5	Duplicates
10531	0.26	1.51	0.45	0.016	0.031	0.85	....	0.47	0.002 B added	4	..
10532[2]	0.30	2.30	0.48	0.018	0.032	....	....	....	....	3[3]	Mn comparison
10637	0.30	2.79	0.47	0.020	0.031	....	....	....	....	6[3]	Mn comparison
10533	0.25	1.04	1.47	0.016	0.034	....	....	....	1.50 Cu	0	
10534	0.28	1.52	0.39	0.014	0.026	2.58	....	0.51	....	5	
10617	0.30	1.54	0.47	0.014	0.025	2.05	0.97	0.45	....	6[3]	Mn comparison
10618	0.29	2.50	0.54	0.024	0.026	1.97	1.01	0.50	....	6[3]	Mn comparison
10619	0.28	3.49	0.53	0.025	0.024	2.07	1.00	0.52	....	7	Mn comparison

[1]Each heat deoxidized with 0.10% Al, except 10533 to which 0.075% Al was added.
[2]Data from quenching jig where quenchant is applied to all portions of specimen simultaneously.
[3]Extraneous cracks on side of notch in addition to crack in unnotched portion.
*This index is not the same as that used in Tables IV, VI, VIII, and IX and is not directly comparable with that index.

Table VI

Sixth Series. Influence of Variations in Boron Content of Quench Cracking

(Quench Cracking Index* = I = Σ(d) denotes sum of crack depths, in sixteenths of an inch, of six specimens of each group.)

Heat No.	Analysis, % (0.10% Al Added to All Heats) C	Mn	Si	P	S	Cr	Ni	Mo	B Added	B Added as	I
168-1	0.35	0.82	0.52	0.015	0.016	0.47	0.54	0.41	.....	.....	44, 0
-2	0.34	"	"	"	"	"	"	"	0.003	Ferroboron	44, 0
169-1	0.36	0.85	0.53	0.014	0.018	0.46	0.54	0.40	.....	.....	60, 16
-2	0.36	"	"	"	"	"	"	"	0.002	Alloy A+	13, 12
170-1	0.35	0.76	0.38	0.014	0.018	0.47	0.51	0.41	.....	.....	20, 8
-2	0.36	"	"	"	"	"	"	"	0.002	Alloy B++	9, 12
171-1	0.40	0.80	0.46	0.011	0.018	0.44	0.54	0.42	.....	.....	44, 52
-2	0.40	"	"	"	"	"	"	"	0.003	Ferroboron	42, 41
172-1	0.39	0.77	0.43	0.015	0.018	0.46	0.54	0.40	.....	.....	40, 44
-2	0.38	"	"	"	"	"	"	"	0.002	Alloy A+	59, 59
173-1	0.37	0.79	0.36	0.014	0.020	0.45	0.54	0.41	.....	.....	47, 41
-2	0.37	"	"	"	"	"	"	"	0.002	Alloy B++	36, 36
220-1	0.30	0.86	0.47	0.014	0.017	0.45	0.55	0.44	.....	.....	0, 0
-2	0.30	"	"	"	"	"	"	"	0.003	Ferroboron	9, 0
222-1	0.31	0.81	0.46	0.014	0.017	0.47	0.57	0.40	.....	.....	12, 0
-2	0.31	"	"	"	"	"	"	"	0.002	Alloy B++	0, 12

*This is not the same index as used in Tables I, II, III, and V, and is not directly comparable with that index.

	C	Mn	Si	Al	Cu	B	Ca	Zr	Ti
+Alloy A, %	0.05	7.5	3.4	13.0	1.7	0.54	...	3.6	19.6
++Alloy B, %	...	..	37.66	7.16	..	1.38	9.76	3.88	9.39

Note: These are analyses of one particular lot of each alloy. Other lots will undoubtedly deviate slightly from the percentages given.

Table VII

Seventh Series. Compositions of Eight Heats Used for Study of Influence of Variations in Heat Treatment on Quench Cracking Susceptibility

	Analysis, %								
Heat No.	C	Mn	Si	P	S	Cr	Ni	Mo	Al Added
10901	0.30	0.89	0.51	0.024	0.019	0.50	0.52	0.45	0.10
10902	0.28	1.75	0.48	0.012	0.021	0.00	0.52	0.45	0.10
10903	0.28	1.73	0.49	0.015	0.022	1.46	0.53	0.43	0.10
10900	0.33	0.84	0.39	0.022	0.023	0.49	0.66	0.47	0.10
10904	0.34	1.85	0.49	0.009	0.020	0.003	0.55	0.42	0.10
10905	0.33	1.77	0.48	0.009	0.020	1.50	0.54	0.40	0.10
10906	0.30	0.79	0.31	0.010	0.021	2.46	0.003	0.51	0.10
10907	0.31	1.69	0.37	0.022	0.028	1.48	0.00	0.53	0.10

Table VIII

Seventh Series. Influence of Variations in Composition, Pretreatment, and Austenitizing Treatment on Quench Cracking

(Values of quench cracking index,* I = Σ(d). Σ(d) denotes sum of crack depths ($\frac{1}{16}$ inch) of six specimens of each group.)

	I				
	Quenching Treatment				
Heat No. and Pretreatment	1900 F 1 Hr.	1675 F 1 Hr.	1450 F 1 Hr.	1675 F 4 Hrs.	Average I
Heat 10900					
2 hrs., 1700 F	55, 56	28, 24	55, 47	12, 0	34.6
8 hrs., 2300 F	29, 20	16, 8	6, 12	0, 0	11.4
Average	40.0	19.0	30.0	3.0	23.6
Heat 10901					
2 hrs., 1700 F	11, 11	9, 10	0, 0	0, 0	5.1
8 hrs., 2300 F	39, 26	5, 0	0, 2	0, 0	9.0
Average	21.7	6.0	0.5	0	7.1
Heat 10902					
2 hrs., 1700 F	16, 20	12, 8	8, 24	0, 0	12.3
8 hrs., 2300 F	29, 21	4, 2	0, 4	0, 0	7.5
Average	21.5	6.5	11.5	0	9.9
Heat 10903					
2 hrs., 1700 F	34, 46	13, 14	9, 8	0, 13	17.1
2 hrs., 2300 F	16, 23	10, 11	7, 3	12, 14	12.0
Average	29.7	12.0	6.7	9.7	14.6
Heat 10904					
2 hrs., 1700 F	33, 31	63, 32	48, 82	0, 16	38.1
8 hrs., 2300 F	37, 32	8, 13	11, 7	0, 2	13.8
Average	33.2	29.0	37.0	4.5	25.9
Heat 10905					
2 hrs., 1700 F	73, 82	72, 84	45, 45	41, 40	60.3
8 hrs., 2300 F	46, 56	59, 54	43, 27	25, 16	40.8
Average	64.2	67.2	40.0	30.5	51.1
Heat 10906					
2 hrs., 1700 F	83, 72	35, 35	14, 0	38, 60	42.1
8 hrs., 2300 F	36, 32	41, 36	0, 0	14, 20	22.4
Average	55.7	36.7	3.5	33.0	32.3
Heat 10907					
2 hrs., 1700 F	58, 58	34, 26	9, 7	10, 2	25.5
8 hrs., 2300 F	39, 49	29, 28	4, 4	11, 5	21.1
Average	51.0	29.2	6.0	7.0	23.3
Average, All Heats					
2 hrs., 1700 F	46.2	31.2	25.7	15.1	29.4
8 hrs., 2300 F	33.1	20.3	8.1	7.4	17.2
Average	39.7	25.7	16.9	11.0	23.3

*This is not the same index as used in Tables I, II, III, and V, and is not directly comparable with that index.

Table IX

Eighth Series. Chemical Analysis of Three Steels and Influence of Variations in Quenching Treatment on Their Quench Cracking

	Chemical Analysis, %								
Heat No.	C	Mn	Si	P	S	Cr	Ni	Mo	Al Added
36	0.32	0.82	0.47	0.007	0.018	0.48	0.63	0.41	0.10
37	0.28	0.82	0.50	0.006	0.022	0.47	0.62	0.39	0.10
38	0.34	1.68	0.54	0.012	0.018	1.51	0.55	0.42	0.10

(Values of quench cracking index,* $I = \Sigma(d)$, i.e., sum of crack depths ($\frac{1}{16}$ inch) observed in six specimens of each series.)

	I Quenching Treatment					
Heat No.	1 Hr. at 1675 F, Water-Quenched	1 Hr. at 1900 F, Water-Quenched	1 Hr. at 1900 F Furnace-Cooled to 1675 F, Held 20 Min., Water-Quenched	4 Hrs. at 1675 F, Water-Quenched	1 Hr. at 1675 F Furnace-Cooled to 1450 F, Held 20 Min., Water-Quenched	1 Hr. at 1675 F, Oil-Quenched
36	0, 0	22, 24	0, 0	0, 0	0, 0	0, 0
37	0, 0	5, 2	0, 0	0, 0	0, 0	0, 0
38	84, 84	73, 82	70, 84	84, 61	78, 82	40, 40

*This index is not the same as that used in Tables I, II, III, and V, and is not directly comparable with that index.

Quench cracking susceptibility decreased as the austenitizing temperature is lowered from 1900 F through 1675 F, and as the austenitizing time at 1675 F was increased from 1 hour to 4 hours. Results with two heats indicated that the high quench-cracking tendency associated with the quench from 1900 F was alleviated by furnace cooling to 1675 F (after holding at 1900 F), prior to the quench.

The change in quench cracking susceptibility caused by variation in the austenitizing temperature was equally evident when either the normalizing or the homogenizing treatment preceded the quench. On the other hand, the decrease in cracking susceptibility attending the increase in austenitizing time at 1675 F was somewhat less pronounced when the quench was preceded by the homogenizing treatment than when it was preceded by the normalizing treatment.

The quench cracking susceptibility of material which has been normalized and then quenched after 4 hours at 1675 F appears to be of the same order of magnitude as that of material which has been first homogenized and then quenched after 1 hour at 1675 F.

The decrease in quench crack susceptibility accompanying the substitution of the homogenizing pretreatment for the normalizing one is more pronounced for heats containing 0.35% carbon than for those containing 0.30% carbon.

The decrease in quench crack susceptibility associated with increasing the holding time at 1675 F from 1 hour to 4 hours is more

Table X

Cracking Tendencies of the Steels As Listed in the Order of Decreasing Martensite Transformation Temperatures (Calculated)

Heat No.	Analysis in Table	Cracking Index I'*	Ms (F)†
10407-1	I	0	714
10407-2	I	0	703
10533	V	0	696
10405-1	I	0	693
10499-1	II	0	692
10404-1	I	0	680
10406-1	I	0	680
10973-1	I	0	678
10497-1	II	0	672
10405-2	I	0	671
10643-1	III	0	669
10406-2	I	0	669
10493-2	II	3	667
10973-2	I	0	667
10499-2	II	0	664
10500-1	II	0	663
10494-1	II	0	662
37	IX	0	660
10495-1	II	3	659
10495-2	II	3	659
10495-3	II	3	659
10500-2	II	0	659
10901	VII	4	655
10973-3	I	0	655
10641-1	III	0	653
10496-1	II	0	651
10496-2	II	0	651
10496-3	II	0	651
10500-3	II	0	651
10635-1	III	0	651
220-1	VI	0	651
220-2	VI	4	651
10492	II	0	650
10499-3	II	0	649
10404-2	I	0	648
10494-2	II	0	648
10501-1	II	0	648
10501-2	II	0	648
10501-3	II	0	648
163-1	IV	0	648
163-2	IV	0	648
163-3	IV	2	648
163-4	IV	4	648
163-5	IV	4	648
222-1	VI	3	648
222-2	VI	3	648
10616	V	3	648
36	IX	0	648
10406-3	I	3	646
10407-3	I	0	646
10973-4	I	0	643
221-1	VI	3	640
221-2	VI	3	640
10639-1	III	5	638
10639-2	III	5	638
10639-3	III	5	638
10643-2	III	4	638
10494-3	II	0	637
10405-3	I	0	636
10640-1	III	0	634
10640-2	III	4	634
10640-3	III	4	634
10649-1	III	4	634

*I' = (8 − n), where n = depth in eighths of an inch of the shallowest notch at which cracking occurs.

†Calculated by method of Payson and Savage (2).

Table X—(Continued)
Cracking Tendencies of the Steels as Listed in the Order of Decreasing Martensite Transformation Temperatures (Calculated)

Heat No.	Analysis in Table	Cracking Index I'*	Ms (F)†
10649-2	III	4	634
10649-3	III	4	634
10648-1	III	0	633
10902	VII	3	631
170-1	VI	3	631
170-2	VI	3	631
10973-5	I	3	631
10636-1	III	5	631
10531	V	4	631
10900	VII	5	630
10648-2	III	3	629
10643-3	III	5	624
168-1	VI	5	623
168-2	VI	4	623
10497-2	II	0	621
10648-3	III	0	621
10404-3	I	0	620
10493-2	II	3	618
173-1	VI	5	618
173-2	VI	5	618
10636-2	III	5	617
10755	III	5	616
169-1	VI	5	616
169-2	VI	3	616
10498-1	II	5	615
10636-3	III	4	608
172-1	VI	5	606
172-2	VI	5	606
10635-2	III	5	603
10641-2	III	4	601
10497-3	II	0	601
10642-1	III	5	596
10534	V	5	593
10493-3	II	3	591
10904	VII	6	590
10906	VII	5	582
10641-3	III	5	581
10530	V	6	580
10638	V	5	578
10529	V	6	576
10635-3	III	5	575
10498-2	II	6	572
10637	V	6	562
10907	VII	6	559
10903	VII	4	558
10498-3	II	5	550
10642-2	III	5	544
10617	V	6	527
38	IX	6	524
10642-3	III	5	521
10905	VII	6	520
171-1	VI	5	516
171-2	VI	5	516
10532	V	3	512
10618	V	6	466
10619	V	7	407

*I' = (8 − n), where n = depth in eighths of an inch of the shallowest notch at which cracking occurs.
†Calculated by method of Payson and Savage (2).

pronounced for heats containing 0.35% carbon than for those containing 0.30% carbon.

It was noted, particularly in the boron series (Table VI), that

increases in hardenability are not necessarily accompanied by increased quench cracking tendencies. If, instead of the simultaneous increase in hardenability which accompanies the additions of most alloys, it is considered that lowering of the martensite transformation temperature by alloy additions promotes quench cracking, then the effect of boron can probably be explained on the basis that while boron is very effective in increasing hardenability, it has practically no effect on the martensite transformation temperature. Table X is a listing of the steels of the eight series in the order of decreasing Ms points (temperature at which the martensite transformation starts) as calculated by the method of Payson and Savage.[2] Cracking tendencies are indicated by the index I′ (I′ = 8 — n where n is the depth in eighths of an inch of the shallowest notch at which cracking occurs). It can be seen that the order of decreasing transformation temperatures is also roughly the order of increasing cracking tendencies.

Conclusions

The known detrimental effects of carbon, manganese, chromium and phosphorus on quench cracking sensitivity have been confirmed by a relatively simple laboratory test.

The same test has also confirmed the known effect on cracking sensitivity of variations in heat treatment practice.

The test has shown that variations in heat treatment practice have a very minor effect on cracking sensitivity as compared to variations in carbon and the other crack-promoting elements.

Boron additions in the amounts desirable for optimum increase in hardenability were shown by the test to have no effect on cracking sensitivity.

High hardenability is not, of itself, responsible for quench-cracking. Rather, it is caused by the lowering of the martensite transformation temperature by most of the elements ordinarily added to improve hardenability.

Acknowledgment

The investigation of quench cracking in cast-alloy steel constituted part of a research program sponsored by the National Defense Research Committee of the Office of Scientific Research and

[2]Payson and Savage, "Martensite Reactions in Alloy Steels," Transactions, American Society for Metals, Vol. 33, 1944, p. 261.

Development as N.D.R.C. Research Project NRC-14. Grateful acknowledgment is made to the Office of Scientific Research and Development for their support and for their permission to publish this work, to the War Metallurgy Division of N.D.R.C. and to the War Metallurgy Committee for supervising and directing the work, and to various members of the Battelle Staff, particularly C. H. Lorig, P. C. Rosenthal, G. K. Manning, and J. G. Kura, for their helpful contributions.

DISCUSSION

Written Discussion: By C. H. Junge, metallurgist, Cleveland Graphite Bronze Co., Cleveland.

It is interesting to know that the test method devised by the authors of this paper correlates well with the observations of heat treating practice. Interesting, too, is the conclusion that quench cracking is not related to hardenability per se, but rather to the lowering of the M_s temperature by the alloying elements. Thus molybdenum and particularly boron become highly desirable hardenability agents from the viewpoint of lessened quench cracking susceptibility.

The extremely potent effect of phosphorus is somewhat surprising to the writer. Even in basic steel for castings it is usual for the phosphorus to exceed the "high" limit of 0.02 referred to by the authors, while in acid practice a value of 0.04 is expected, which apparently causes no particular quench crack trouble. Of course, few steel castings of high hardenability are ever quenched completely cold as was done in the experimental work described in this paper.

In preparing their specimens the authors used a saw cut to notch their specimens. It seems to the writer that this machining practice might easily cause considerable variation in the surface finish in the root of the notch with attendant erratic cracking behavior.

Would the use of a drilled hole with a saw cut into the hole, similar to the Charpy keyhole notch, be an improvement in specimen preparation? It might be instructive to see what effect this type of notch might have on the sensitivity of the test, particularly its effect on the index $I' = (8\text{-}n)$, which was found to be unreliable in some cases.

Written Discussion: By J. W. Spretnak, Metals Research Laboratory, Carnegie Institute of Technology, Pittsburgh.

The authors have presented an interesting and worthwhile contribution to the elusive and complex metallurgical problem of quench cracking of steel. A systematized laboratory study such as the present one is valuable in demonstrating the average effect of such variables as composition and heat treatment which can be studied in the laboratory.

In the study on the effect of the austenitizing temperature, the decrease in cracking susceptibility obtained by austenitizing at 1900 F (1040 C) and lowering the temperature to 1675 F (915 C) before quenching is of interest because it rules out the austenitic grain size as the cause of the increase in

cracking susceptibility brought about by increasing the austenitizing temperature. The effect is due then to the temperature from which the steel is quenched and may be associated with a change in thermal gradients and consequently the state of the thermal stresses at the time the transformation to martensite begins.

Another important observation made in the paper is that for steels which quench out to martensite, the hardenability per se has no direct effect on cracking susceptibility. An increase of hardenability will be accompanied by increased cracking susceptibility only if accompanied by a lowering of the M_s temperature. The temperature range over which the transformation from austenite to martensite transformation occurs is the critical factor. This principle is borne out interestingly by the authors' work on the effect of boron.

Caution should be taken in applying the results of a laboratory test to actual production quenching. The authors have wisely stated in their original report that the results of their studies are based on a given geometry, with a given quench and reported on the basis of an arbitrary index. The cracking susceptibility of a heat as determined in the laboratory will not necessarily correspond to the actual magnitude of losses from cracking in the commercial treatment. This is true because in the laboratory we can study only the variables which affect the steel uniformly, whereas in the field there are variables which affect the heat uniformly and others which are highly localized and occur in some statistical distribution in the heat. It is this statistical nature of the problem in the field which accounts for its complexity.

Written Discussion: By J. G. Christ, section engineer, Metallurgical Section, Westinghouse Electric Corp., Nuttall Works, Pittsburgh.

The authors have presented a very interesting paper on quench cracking of cast alloy steels. The results as indicated by the authors are only true as general statements. The statement, that "High hardenability is not, of itself, responsible for quench cracking," if borne out by further tests offers possibilities to the manufacturers of intricately shaped parts which are drastically quenched to get the high physical properties required.

Quench cracking is an everyday problem in gear heat treatment. The steel must have enough hardenability that the roots of the teeth are properly hardened, for it is at the roots the stresses are highest in gear loading. If, however, the hardenability is too great, the gears may crack during the heat treatment.

Although it has been our experience that the steels with deeper hardenability are more prone to cracking, we have had steels of unusually high hardenability that did not crack and again steels of much less hardenability that cracked when both were manufactured to the same size gears. Possibly the authors' statement quoted above can explain the anomaly cited, although the reference above is to wrought steels.

If the authors are able to continue this quench cracking investigation, maybe a steel will be developed having good hardenability and less tendency to crack than the steels available at the present time.

Written Discussion: By Charles R. Wilks, metallurgist, American Brake Shoe Co., Mahwah, N. J.

Will the authors comment on the reproducibility of duplicate tests?

Authors' Reply

The authors wish to thank Messrs. Junge, Spretnak, Christ, and Wilks for their thoughtful discussions of our paper.

In some of the early preliminary work, notches of various types were investigated as to their effects on the test and its reproducibility. The following notches were tried:

1. Plain $\frac{1}{16}$-inch wide saw cut (as eventually used).
2. Saw cut up to a $\frac{1}{16}$-inch diameter hole.
3. Saw cut up to a $\frac{1}{32}$-inch diameter hole.
4. Milled square-bottom notch.
5. Milled V-bottom notch.

None of these showed any improvement over the plain $\frac{1}{16}$-inch wide saw cut.

At the same time, specimen diameters of ½, ¾, 1, 1½, and 2 inches and specimen lengths of ½, 1, 1½, and 2 inches were tried. Specimens with diameters less than 1 inch cracked in any direction while those with diameters greater than 1 inch were no better than those with a 1-inch diameter. Lengths less than 2 inches were satisfactory but such specimens were more difficult to handle.

We wish to emphasize the statement of Mr. Spretnak that "Caution should be taken in applying the results of a laboratory test to actual production quenching. . . . . The cracking susceptibility of a heat as determined in the laboratory will not necessarily correspond to the actual magnitude of losses from cracking in the commercial treatment." Much more work would be necessary to correlate the results of any such laboratory test, as we have tried to develop, with actual commercial practice.

As regards Mr. Wilks's question on reproducibility, there is much to be desired. The original idea to use the shallowest notch depth at which cracking occurred as an index was discarded because of occasional "accidental" cracks. However, when the summation of crack depths of a whole series of specimens was used as an index and statistical methods were used to compare indices, reproducibility was much better.

STRESS CRACKING OF ELECTROPLATED LOCKWASHERS

By K. B. Valentine

Abstract

This paper presents data from tests made on electroplated lockwashers. It was found that:

a. The lower the hardness, the smaller the percentage of failures encountered.

b. At a hardness of Rockwell C-50 or lower, critical hydrogen embrittlement was eliminated by a thermal aging treatment subsequent to plating.

c. At a hardness of Rockwell C-51 to 56 a subcritical anneal prior to heat treatment and a thermal aging treatment subsequent to plating eliminated the critical hydrogen embrittlement.

d. At a hardness of Rockwell C-48 very little difference was noted between the percentage of failures of lockwashers zinc plated to 0.0005-inch plate thickness and lockwashers having 0.0002-inch plate thickness. In both cases the critical hydrogen embrittlement was eliminated by a thermal aging treatment subsequent to plating.

THE effect of hardness on the failures of electroplated lockwashers has been generally overlooked, and it is the purpose of this report to present data indicating that hardness is definitely related to the percentage of failures encountered. Also, in the hardness range of Rockwell C-43 to 50, a suitable aging treatment subsequent to plating will eliminate the critical hydrogen embrittlement. In the hardness range of Rockwell C-51 to 56 the critical hydrogen embrittlement can be eliminated by a subcritical annealing prior to heat treatment and an aging treatment subsequent to plating. It was likewise observed that plating thickness has little or no bearing on the percentage of failures encountered.

Lockwashers are generally made from SAE 1060 Keystone section wire. They are formed on an automatic coil winding machine

---

A paper presented before the Twenty-eighth Annual Convention of the Society, held in Atlantic City, November 18 to 22, 1946. The author, K. B. Valentine, is project engineer, Metal Treatment and Finishes, Pontiac Motor Division, General Motors Corp., Pontiac, Mich. Manuscript received March 28, 1946.

and then heat treated to a hardness of Rockwell C-47 to 53. When required, cadmium or zinc plating follows.

Two peculiar facts connected with electroplated lockwashers are (a) at the hardnesses used, only a percentage of the lockwashers fail; (b) these failures may occur immediately upon stressing or at some later time. Typical failures are illustrated in Fig. 1.

A test program was started to investigate some of the factors affecting these failures. The lockwashers were tested by placing them between cyanided flat washers on a cyanided bolt and drawing

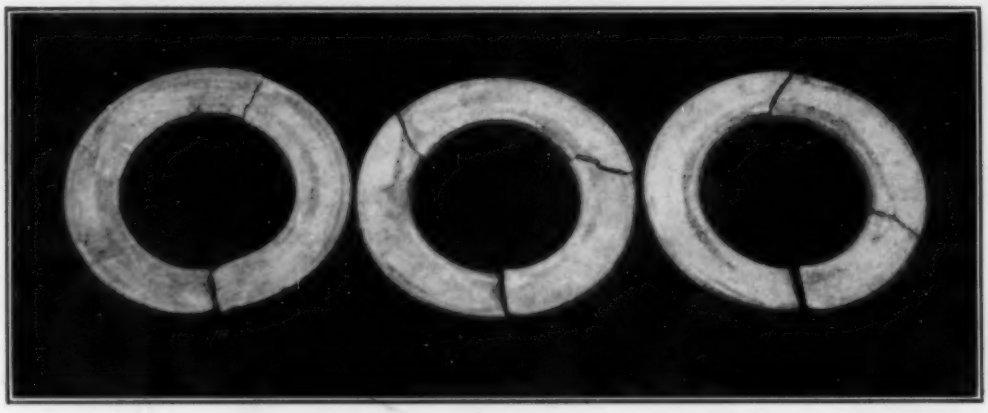


Fig. 1—Typical Failures in Lockwashers.

them down flat with a nut. Fig. 2 illustrates such assemblies. The lockwashers were examined periodically for failures while clamped on the bolts. Lockwashers tested were received from five different sources.

All lockwashers tested were cleaned and zinc plated in a barrel plating system. The acid pickling solution was made up of 18 ounces per gallon of H_2SO_4 and the plating solution made up of 10.5 ounces per gallon of ZnCn, 12 ounces per gallon of NaCn and 14 ounces per gallon of NaOH. A current density of about 20 amperes per square foot was used.

The lockwashers were austenitized in a neutral salt bath, quenched in a conventional mineral oil heated to 140 F, and tempered in a convective air furnace. Low temperature baking following plating was done in a gas oven, and subcritical temperature annealing in a convective air furnace.

The first series of tests was run on five different size lockwashers to determine the effect on failures of a thermal aging treatment following plating.

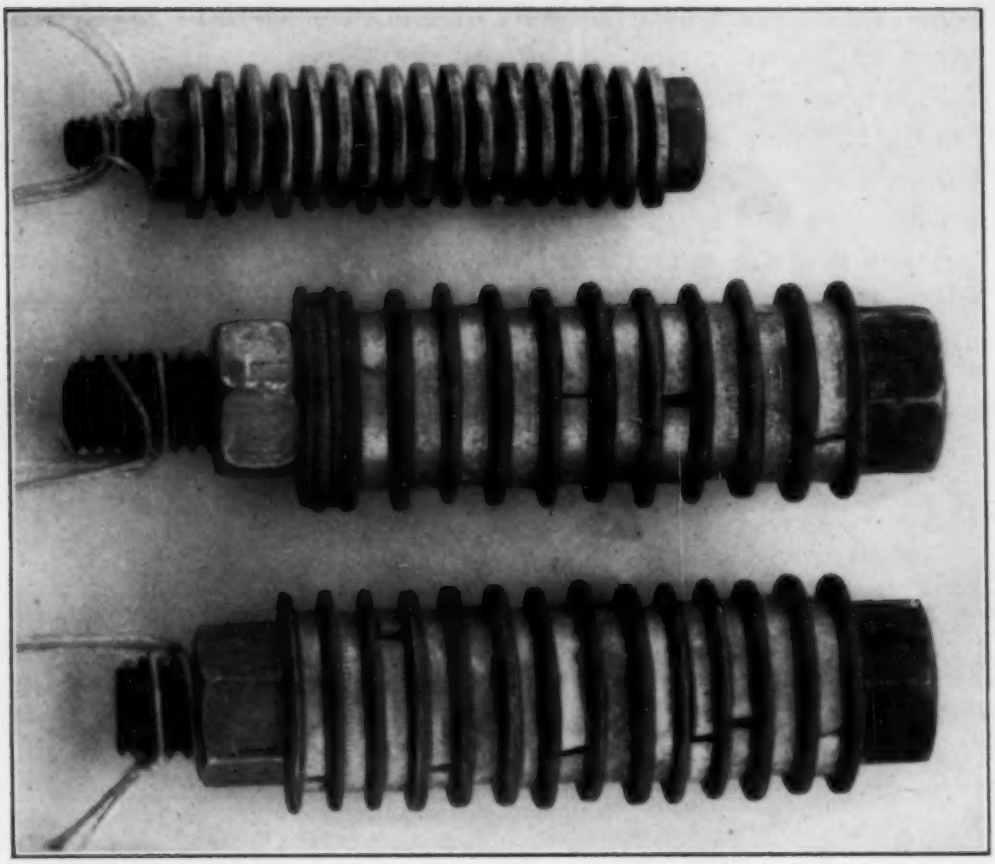


Fig. 2—Photograph of Test Assemblies. Cyanided flat washers are placed between lockwashers on a cyanided bolt.

Moore and Smith (1)[1] have explained that the evolution of hydrogen from iron on heating is a function of temperature. Consequently, it was felt that the higher the temperature used the greater the amount of hydrogen liberated. The highest temperature that could be used without detriment to the plate appeared to be 400 F. Four hours at this temperature was considered to insure practical optimum benefits from this treatment. Results of these tests are listed in Table I. It can be seen from these data that heating subsequent to plating decreased the percentage of failures considerably but results were still far from being commercially acceptable.

The next series of tests was run to determine the effect of hardness on the failures of lockwashers. Inasmuch as 7/16-inch heavy lockwashers were consistently bad actors, they were used for this purpose. Table II lists the results of these tests, showing that hardness is of considerable importance. It also indicates that failures

[1]The figures appearing in parentheses pertain to the references appended to this paper.

Table I
Results of Tests Made at 400 F

0.0002-Inch Zinc Plate Thickness

Treatment After Plating	Lockwasher Size	Rockwell C Hardness	Number Tested	Number Broken After 1 Week	Per Cent Broken
None	¼ Medium	52	23	8	34.8
	⅜ Light	52	17	2	11.8
	⅜ Medium	54	15	8	53.5
	⅜ Heavy	51	13	10	77.0
	7/16 Heavy	51	22	9	41.0
Average			90	37	41.2
Heated at 400 F for 4 hours	¼ Medium	52	22	5	22.7
	⅜ Light	52	16	0	0
	⅜ Medium	54	12	2	16.7
	⅜ Heavy	51	11	1	9.1
	7/16 Heavy	51	12	1	8.3
Average			73	9	12.3

Table II
Results of Tests Made on Heavy Lockwashers

0.0002-Inch Zinc Plate Thickness
7/16-Inch Heavy Lockwashers

Treatment After Plating	Rockwell C Hardness	Number Tested	Number Broken After 1 Week	Per Cent Broken
None	62	200	200	100
None	55	200	184	90
None	50	200	74	37
None	47	200	31	15
None	42	200	0	0
Heated at 400 F for 4 hours	52	200	17	8
Heated at 400 F for 4 hours	50	200	0	0
Heated at 400 F for 4 hours	47	200	0	0
Heated at 400 F for 4 hours	42	200	0	0

can be eliminated if the hardness is at Rockwell C-50 or lower and the lockwashers are aged at 400 F subsequent to plating. (During the past two years a considerable number of zinc-plated lockwashers of various sizes having a hardness of Rockwell C-47 and receiving this aging treatment have been tested and no failures observed.) As previously stated, the cleaning operations, plating operations, and thermal aging operation (when applied) were the same for all lockwashers; and the applied stresses were the same for all lockwashers of a given size. Nevertheless, failures occurred on a percentage of the lockwashers of a hardness of Rockwell C-47 (and harder) with no thermal treatment subsequent to plating; and a percentage of the

Table III
Results of Tests Made on Heavy Lockwashers Heat Treated at 1100 F

		0.0002-Inch Zinc Plate Thickness 7/16-Inch Heavy Lockwashers			
Treatment Before Plating	Treatment After Plating	Rockwell C Hardness	Number Tested	Number Broken After 1 Week	Per Cent Broken
Hardened and tempered	None	51	200	58	30
Hardened and tempered	Heated at 400 F for 4 hours	51	210	13	7
Heated at 1100 F for 2 hours, cooled slowly, hardened and tempered	Heated at 400 F for 4 hours	51	203	0	0
Heated at 1100 F for 2 hours, cooled slowly, hardened and tempered	None	51	208	11	6
Heated at 1100 F for 2 hours, cooled slowly, hardened and tempered	Heated at 400 F for 4 hours	53	200	0	0
Heated at 1100 F for 2 hours, cooled slowly, hardened and tempered	Heated at 400 F for 4 hours	56	187	0	0

lockwashers of Rockwell C-52 heated at 400 F for 4 hours after plating.

Inasmuch as the processing conditions of broken and unbroken lockwashers in each group had been maintained as nearly identical as possible, it was considered that some nonuniformity prior to heat treatment (i.e., hydrogen content or nonuniform structural condition) could be responsible for these failures.

Sieverts' (2) curve of the solubility of hydrogen in iron is reproduced in Fig. 3. It shows a marked decrease in the solubility of hydrogen in iron at and slightly below the critical temperature. C. A. Zapffe and C. E. Sims (3) in explaining some of the factors effecting

Table IV
Results of Tests on Heavy Lockwashers Having Different Zinc Coatings

		7/16-Inch Heavy Lockwashers Used			
Treatment After Plating	Plate Thickness Inch	Rockwell C Hardness	Number Tested	Number Broken After 1 Week	Per Cent Broken
None	0.0002	48	200	73	36
None	0.0005	48	200	76	38
Heated at 400 F for 4 hours	0.0002	48	200	0	0
Heated at 400 F for 4 hours	0.0005	48	200	0	0

flakes in forgings state that hydrogen occurring at cavities is redissolved in steel when heated above the critical temperature. Korber and Ploum (4) found that, upon heating a 0.97% carbon steel, hydrogen was evolved at 752 F.

Accordingly, it was felt that a subcritical homogenizing treatment prior to heat treatment might be beneficial.

In the next series of tests lockwashers that had been heated at

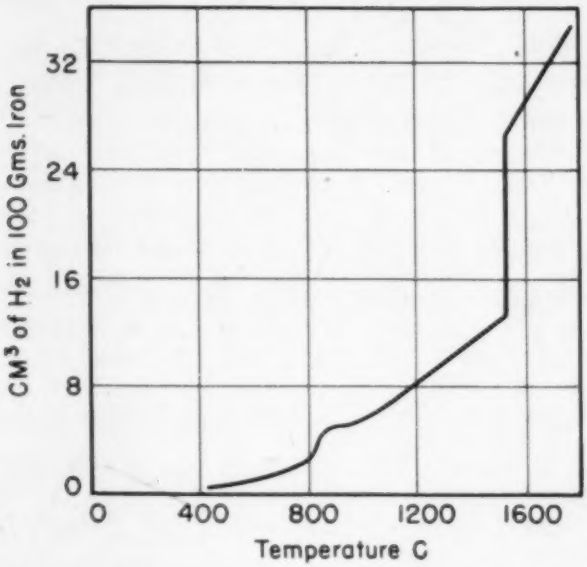


Fig. 3—Solubility of Hydrogen in Iron P_{H_2} 760 MM. (Sieverts).

1100 F for 2 hours and cooled slowly prior to heat treatment were compared with conventionally heat treated lockwashers. Results are listed in Table III.

These data indicate that critical hydrogen embrittlement for these hardnesses can be eliminated by a subcritical annealing prior to heat treatment and a thermal aging treatment subsequent to plating. ¼-inch medium, ⅜-inch light, ⅜-inch medium, and ⅜-inch heavy lockwashers were tested in a like manner with similar results.

Failures of lockwashers having 0.0005-inch zinc plate were compared with lockwashers having 0.0002-inch zinc plate. Results of this series of tests are listed in Table IV. These data indicate that at a hardness of Rockwell C-48 plate thickness has very little, if any, effect upon the per cent of failures.

Conclusions

As a result of this investigation it was found that the lower the

hardness, the smaller the percentage of failures. Likewise at a hardness of Rockwell C-50 or lower, critical hydrogen embrittlement was eliminated by a thermal aging treatment subsequent to plating. At a hardness of Rockwell C-51 to 56 a subcritical anneal prior to heat treatment and a thermal aging treatment subsequent to plating eliminated the critical hydrogen embrittlement. At a hardness of Rockwell C-48 very little difference was noted between the percentage of failures of lockwashers zinc plated to 0.0005-inch plate thickness and lockwashers having 0.0002-inch plate thickness. In both cases the critical hydrogen embrittlement was eliminated by a thermal aging treatment subsequent to plating.

References

1. G. A. Moore and D. P. Smith, "Occlusion and Evolution of Hydrogen by Pure Iron," *Transactions*, American Institute of Mining and Metallurgical Engineers, Vol. 135, 1939, p. 255-292.
2. Curve by Sieverts published in "Metallurgical Aspects of Hydrogen in Electroplating" by C. A. Zapffe and C. L. Faust. American Electroplaters Society, 1940.
3. C. A. Zapffe and C. E. Sims, "Hydrogen, Flakes and Shatter Cracks," *Metals and Alloys*, May 1940.
4. F. Korber and H. Ploum, "Die Aufnahme Von Wasserstoff durch das Eisen Bei seiner Behandlung mit Saure und das Verhalten des Wasserstoff in diessem Metall," *Mitt., Kaiser-Wilhelm Inst. Eisenforsch.*, Vol. 14, 1932, p. 229-248.

DISCUSSION

Written Discussion: By Joseph Gurski, metallurgist, chemical engineering, Ford Motor Co., Dearborn, Mich.

The author is to be congratulated on an able presentation of such a troublesome problem as lockwasher breakage. His treatment of lockwashers with an 1100 F anneal prior to heat treatment certainly appears to have interesting possibilities and the tests made substantiate his conclusions very clearly.

We are in accord with his statement that it is generally believed that thicker plating results in a greater percentage of failures. On the basis of his tests, it would seem that this factor has been overemphasized.

However, we wish to take exception to the statement that the factor of hardness has been generally overlooked. As far back as February 7, 1945, at a joint industry conference in Detroit, definite recommendations were made to the Spring Washer Institute limiting the Rockwell hardness to C-45 to 49. It was generally recognized at this meeting that higher hardnesses were contributing to excessive lockwasher breakage. Mr. Valentine's tests corroborate these assumptions and add another link in the chain of evidence.

We would like to ask Mr. Valentine whether or not he has made any definite tests with respect to the time necessary to hold washers at 400 F in order to eliminate hydrogen embrittlement.

Written Discussion: By R. G. Sartorius, metallurgist, The National Lock Washer Co., Newark, N. J.

Mr. Valentine's paper deals with a problem in which we are not only very much interested, but which we have found to be of great practical importance.

We fully agree with the author's first and main conclusion, but feel that the effect of hardness on the failure of electroplated lockwashers has been recognized by many, and for a long time. For example, Westinghouse Electric Corp. P.D. specification 2052, dated May 28, 1915, calls for a lower hardness range (Rockwell C-44 to 49) just because the spring washers are to be electroplated.

Stress cracking of electroplated spring washers is—to say the least—a very elusive problem, into which enter a great number of variables. Thus, looking at Fig. 2, it is noted that many of the samples appear to have very pronounced knurling on the outer periphery. This is a type of surface imperfection which should be considered in an attempt to evaluate test results. The same holds true for decarburization, and it would be interesting to know whether the author had an opportunity to check his samples for surface imperfections, decarburization, and possibly also prior structure. We are not clear as to whether finished heat treated spring washers were used for the tests or unhardened washers which were then quenched and tempered for the first time.

Acid cleaning is another variable which is difficult to control and, depending on the surface condition (scale) of the various lots tested, could well have affected the test results.

The most startling and interesting conclusion arrived at by the author is that referring to the beneficial effect of a subcritical anneal. We are wondering whether the experiments were carried out on a large enough scale to warrant this conclusion, and whether the test results were not masked by some of the other variables mentioned above.

The same holds true for plate thickness. Our experience has been that the thicker the plate, the more danger there will be of failure due to hydrogen embrittlement.

Written Discussion: By Victor Stefanides, chief metallurgist, Illinois Tool Works, Chicago.

This paper should be studied by all who encounter hydrogen embrittlement, either in acid descaling, electroplating, parkerizing, etc. Unfortunately, statements have been made which cannot be borne out by tests conducted on dome lockwashers, illustrated in Fig. A. These dome lockwashers were fabricated, on a punch press, of SAE 1050, spheroidized anneal strip steel, as illustrated by the photomicrograph at × 400, in Fig. B. After fabricating the washers, part of the lot was subjected to a stress relief anneal at 1100 F (595 C) for 1 hour at heat. Then the annealed and unannealed washers were austenitized in a rotary retort furnace at 1500 F (815 C) and quenched in oil at temperatures from 120 to 130 F. The rotary retort consists of an Archimedes screw which gradually draws the work from cold zone to high temperature zone for 5 minutes.

Tempering was done in rotary retort furnace at 500 F for 1 hour at heat, to obtain Rockwell C-48 to 52, and 700 F for 1 hour at heat to obtain Rockwell C-42 to 44. The work austenitized with and without the subcritical anneal and

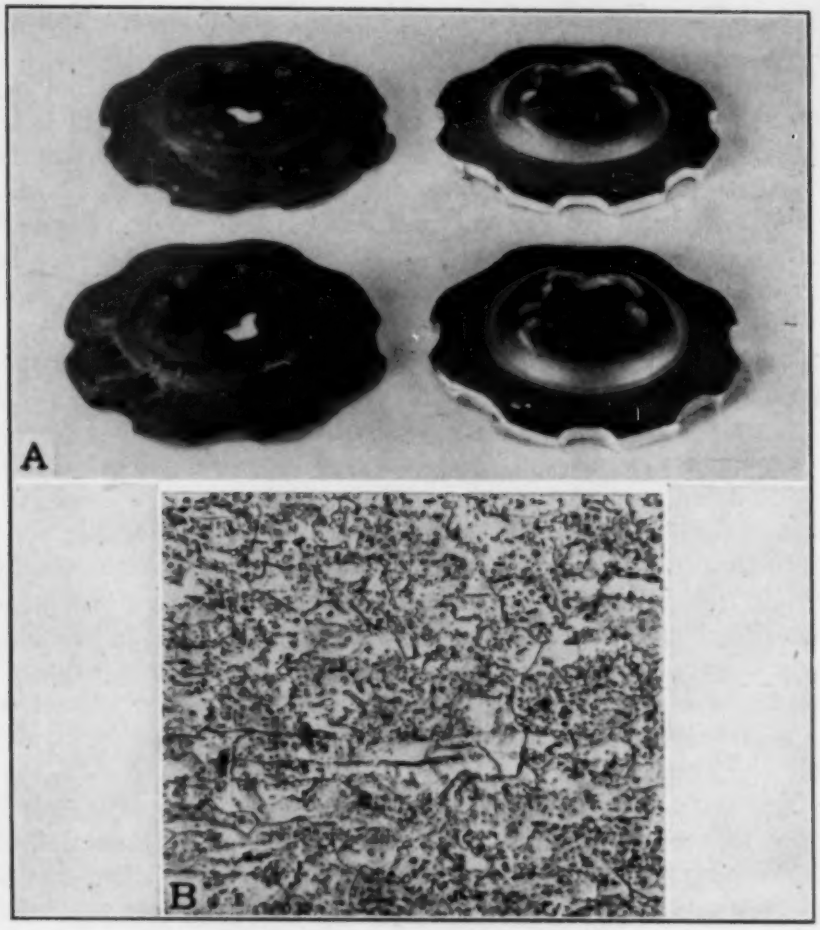


Fig. A—Dome Lockwashers. × ¾.
Fig. B—Spheroidized Anneal. Etched 2% nital. × 400.

tempered to ranges of hardness from C-42 to 44 and C-48 to 52, are illustrated by Figs. C, D, E and F.

Descaling by acid was done, at room temperature, in commercial muriatic acid, to which Turco Products' inhibitor was added at the rate of 2½ cc. per 1½ gallons of muriatic acid. Preliminary pickling experiments proved that it required 8 minutes to completely remove scale, formed in the heat treating operations. Therefore, all the work descaled by acid was pickled for 8 minutes.

Descaling by shot blasting was done in a Pangborn No. 2 Type EN Unit, using No. 70 angular steel grit at 80 pounds air pressure.

Cadmium plating was done in a barrel-type plater in alkaline cyanide solution at a current density of 25 amp./sq. ft.

Baking, to overcome hydrogen embrittlement, was done at 400 F for 4 hours at heat.

The washers are used with ⅜—16 size screw, made of 1010 wire, cold-headed and thread-rolled, with an approximate ultimate tensile strength of 5000 pounds. The screw with the washer, in an assembly, is loaded to 60% of its ultimate strength, or 3000 pounds. At that loading, the washer, pro-

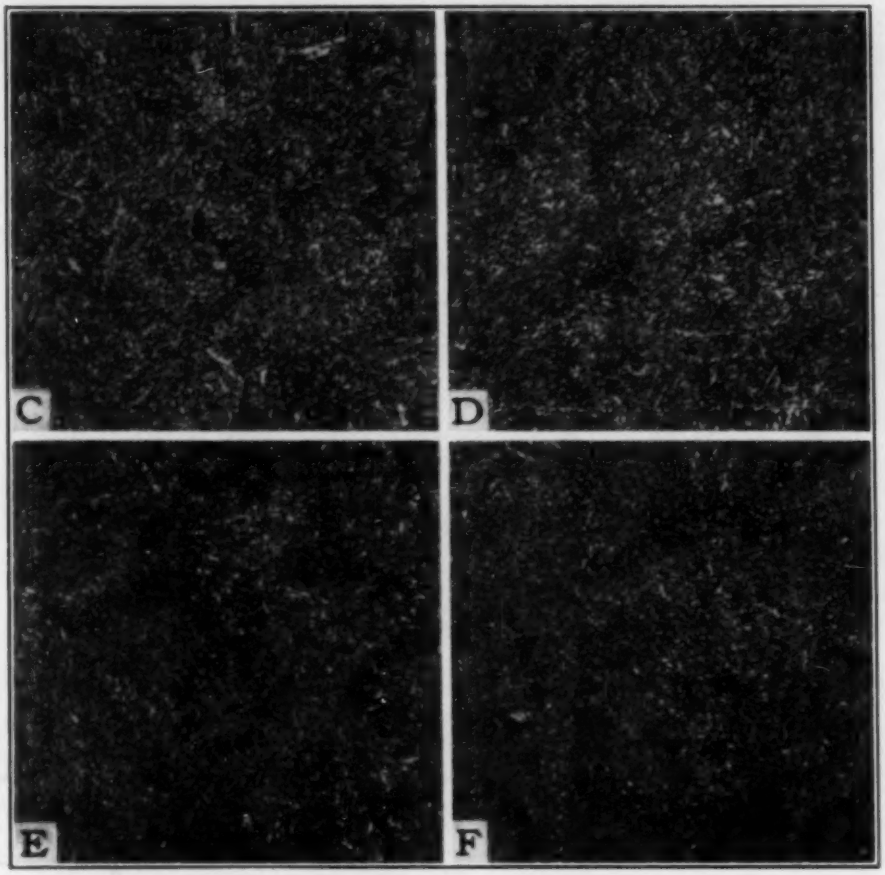


Fig. C—Subcritical Anneal 1100 F. Austenitized 1500 F. Drawn 700 F. 1 hour at heat. Rockwell C-42 to 44. Etched 2% nital. × 400.

Fig. D—Austenitized 1500 F. Drawn 700 F. 1 hour at heat. Rockwell C-42 to 44. Etched 2% nital. × 400.

Fig. E—Subcritical Anneal 1100 F. Austenitized 1500 F. Drawn 500 F. 1 hour at heat. Rockwell C-48 to 52. Etched 2% nital. × 400.

Fig. F—Austenitized 1500 F. Drawn 500 F. 1 hour at heat. Rockwell C-48 to 52. Etched 2% nital. × 400.

viding it is properly heat treated, will support the screw without cracking or collapsing. However, improperly heat treated, too hard, or hydrogen embrittled washer, will crack under such loading. Washers properly heat treated, in proper range of hardness, and free of hydrogen embrittlement, will collapse in excess of 5000-pound loading. Therefore, the screw should fail before the washer collapses, if properly heat treated. The significance of this will be apparent by studying the accompanying Tables A and B.

The work austenitized, with and without the subcritical anneal, was divided into the following groups:

A —Austenitized, without subcritical anneal, tempered to Rockwell C-42 to 44, and not descaled.

A_1 —Same as A, except tempered to Rockwell C-48 to 52.

B —Austenitized, with subcritical anneal, tempered to Rockwell C-42 to 44, and not descaled.

B_1 —Same as B, except tempered to Rockwell C-48 to 52.

C —Austenitized, without subcritical anneal, tempered to Rockwell C-42 to 44, descaled by acid, and cadmium plated to 0.0002 inch.
C_1—Same as C, except tempered to Rockwell C-48 to 52.
C_2—Same as C, except plated to 0.0005 inch.
C_3—Same as C_2, except tempered to Rockwell C-48 to 52.

CC—Austenitized, without subcritical anneal, tempered to Rockwell C-42 to 44, descaled by shot blasting, and cadmium plated to 0.0002 inch.
CC_1—Same as CC, except tempered to Rockwell C-48 to 52.
CC_2—Same as CC, except plated to 0.0005 inch.
CC_3—Same as CC_2, except tempered to Rockwell C-48 to 52.

D —Austenitized, with subcritical anneal, tempered to Rockwell C-42 to 44, descaled by acid, and cadmium plated to 0.0002 inch.
D_1—Same as D, except tempered to Rockwell C-48 to 52.
D_2—Same as D, except plated to 0.0005 inch.
D_3—Same as D_2, except tempered to Rockwell C-48 to 52.

DD—Austenitized, with subcritical anneal, tempered to Rockwell C-42 to 44, descaled by shot blasting, and cadmium plated to 0.0002 inch.
DD_1—Same as DD, except tempered to Rockwell C-48 to 52.
DD_2—Same as DD, except plated to 0.0005 inch.
DD_3—Same as DD_2, except tempered to Rockwell C-48 to 52.

E —Austenitized, without subcritical anneal, tempered to Rockwell C-42 to 44, descaled by acid, cadmium plated to 0.0002 inch, and baked to overcome hydrogen embrittlement.
E_1—Same as E, except tempered to Rockwell C-48 to 52.
E_2—Same as E, except plated to 0.0005 inch.
E_3—Same as E_2, except tempered to Rockwell C-48 to 52.

EE—Austenitized, without subcritical anneal, tempered to Rockwell C-42 to 44, descaled by shot blasting, cadmium plated to 0.0002 inch, and baked to overcome hydrogen embrittlement.
EE_1—Same as EE, except tempered to Rockwell C-48 to 52.
EE_2—Same as EE, except plated to 0.0005 inch.
EE_3—Same as EE_2, except tempered to Rockwell C-48 to 52.

F —Austenitized, with subcritical anneal, tempered to Rockwell C-42 to 44, descaled by acid, cadmium plated to 0.0002 inch, and baked to overcome hydrogen embrittlement.
F_1—Same as F, except tempered to Rockwell C-48 to 52.
F_2—Same as F, except plated to 0.0005 inch.
F_3—Same as F_2, except tempered to Rockwell C-48 to 52.

FF—Austenitized, with subcritical anneal, tempered to Rockwell C-42 to 44, descaled by shot blasting, cadmium plated to 0.0002 inch, and baked to overcome hydrogen embrittlement.
FF_1—Same as FF, except tempered to Rockwell C-48 to 52.
FF_2—Same as FF, except plated to 0.0005 inch.
FF_3—Same as FF_2, except tempered to Rockwell C-48 to 52.

From studying the data recorded in Table A and Table B, it is apparent that the author's allegation No. 1 (author's paper, page 488, par. 1), that "hardness is definitely related to the percentage of failures encountered", is well borne out.

Table A

Austenitized at 1500 F and Tempered to Rockwell C-42 to 44

	Not Descaled		Descaled by Acid—Plated 0.0002 inch			
	A	B	C	D	E	F
		Subcritical Anneal		Subcritical Anneal	Baked	Subcritical Anneal Baked
	6000	6000	6000	6000	6000	6000
	6000	6000	6000	6000	6000	6000
	6000	6000	6000	6000	6000	6000
	6000	6000	3070	6000	6000	4780
	6000	6000	6000	4710	6000	6000
	6000	6000	4540	6000	6000	6000
	6000	6000	6000	6000	6000	6000
	6000	6000	4490	6000	6000	6000
	6000	6000	6000	6000	2840	6000
	5640	6000	6000	4890	6000	6000
Av.	5964	6000	5410	5620	5684	5878

Austenitized at 1500 F and Tempered to Rockwell C-48 to 52

	Not Descaled		Descaled by Acid—Plated 0.0002 inch			
	A_1	B_1	C_1	D_1	E_1	F_1
		Subcritical Anneal		Subcritical Anneal	Baked	Subcritical Anneal Baked
	3140	2880	2520	2000	3160	2600
	3160	2940	3040	2120	2800	2380
	2990	3140	2460	2010	2820	2640
	3220	3260	1880	1870	3160	2920
	3080	3100	2240	1940	2520	2560
	3180	2860	3020	2200	2760	2680
	2990	2900	1920	2090	2600	2680
	3200	3170	1650	2210	2920	2400
	3010	2850	2725	2190	2800	2840
	3170	2220	2015	2040	3120	2680
	3114	2932	2347	2067	2866	2638

Austenitized at 1500 F and Tempered to Rockwell C-42 to 44

	Descaled by Acid—Plated 0.0005 inch			
	C_2	D_2	E_2	F_2
		Subcritical Anneal	Baked	Subcritical Anneal Baked
	4000	2440	6000	3720
	2440	2450	4560	4450
	4620	3630	4920	6000
	2640	4480	6000	4880
	6000	4820	6000	4720
	2680	4760	4840	6000
	2520	4520	6000	3920
	2580	2680	6000	4490
	4760	2450	6000	6000
	2490	2680	4840	6000
Av.	3473	3491	5516	5018

Austenitized at 1500 F and Tempered to Rockwell C-48 to 52

	Descaled by Acid—Plated 0.0005 inch			
	C_3	D_3	E_3	F_3
		Subcritical Anneal	Baked	Subcritical Anneal Baked
	1990	1820	2050	2600
	2100	1740	2040	1920
	2040	2240	2060	2530
	1900	1900	2200	2410
	1960	1690	2330	1700
	2050	2000	2120	2060
	2120	1840	2260	2540
	2160	1960	2230	2140
	1990	2520	2480	2920
	1840	1840	2210	2370
	2015	1955	2198	2319

Table B

Austenitized at 1500 F and Tempered to Rockwell C-42 to 44
Descaled by Shot Blasting—Plated 0.0002 inch

	CC	DD	EE	FF
		Subcritical Anneal		Subcritical Anneal
			Baked	Baked
	6000	6000	6000	6000
	6000	6000	6000	6000
	6000	6000	6000	6000
	6000	6000	6000	6000
	6000	6000	6000	6000
	6000	6000	6000	6000
	6000	6000	6000	6000
	6000	6000	6000	6000
	6000	6000	6000	6000
	6000	4740	6000	6000
Av.	6000	5874	6000	6000

Austenitized at 1500 F and Tempered to Rockwell C-42 to 44
Descaled by Shot Blasting—Plated 0.0005 inch

	CC_2	DD_2	EE_2	FF_2
		Subcritical Anneal		Subcritical Anneal
			Baked	Baked
	6000	6000	6000	5980
	4960	5000	4840	6000
	6000	6000	6000	6000
	4920	6000	4740	6000
	6000	6000	6000	4540
	6000	6000	6000	6000
	6000	6000	6000	6000
	6000	6000	6000	6000
	6000	6000	6000	6000
	6000	6000	6000	6000
Av.	5788	5900	5758	5752

Austenitized at 1500 F and Tempered to Rockwell C-48 to 52
Descaled by Shot Blasting—Plated 0.0002 inch

	CC_1	DD_1	EE_1	FF_1
		Subcritical Anneal		Subcritical Anneal
			Baked	Baked
	2900	2840	2800	2240
	3000	2980	3000	2560
	3000	2240	2660	2380
	2960	2600	3340	2540
	3100	2700	2820	2340
	3060	2560	2760	2640
	3160	2400	2760	2560
	2880	2580	2620	2340
	3010	2440	3120	2260
	3140	2640	3120	2480
	3021	2598	2900	2434

Austenitized at 1500 F and Tempered to Rockwell C-48 to 52
Descaled by Shot Blasting—Plated 0.0005 inch

	CC_3	DD_3	EE_3	FF_3
		Subcritical Anneal		Subcritical Anneal
			Baked	Baked
	2900	2940	3000	2180
	3040	2860	2860	2360
	2960	2480	2960	2540
	3160	2620	2640	2920
	2760	2720	2960	2520
	3080	2880	2860	2810
	3120	2720	3060	2780
	2920	2480	2900	2760
	3120	2700	2760	2600
	2640	2700	2860	2860
	2970	2710	2886	2633

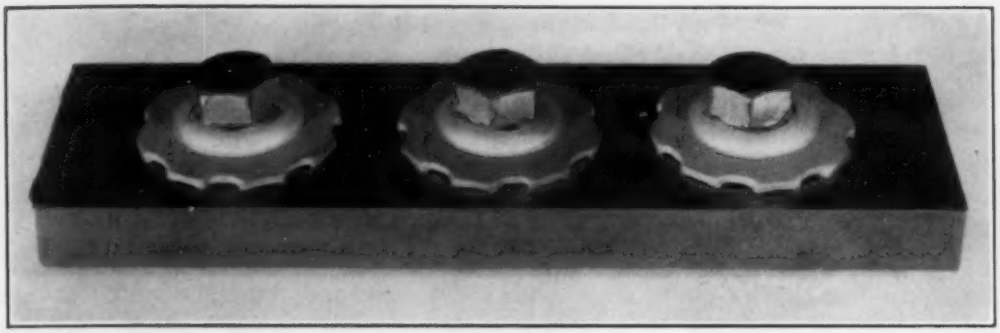


Fig. G—Dome Washers in Assembly. × 1.

Allegation No. 2 (page 488, par. 1), that "in the hardness range of Rockwell C-43 to 50, a suitable aging treatment, subsequent to plating, will eliminate the critical hydrogen embrittlement", the apparent trend is that the baking treatment promotes recovery from the hydrogen embrittlement. This is especially evident when groups C_2 and D_2 are compared with E_2 and F_2. The other groups are either uniformly high or uniformly low, so there is no evidence that baking was very helpful.

Allegation No. 3 (page 488, par. 1), that "In the hardness range Rockwell C-51 to 56, the critical hydrogen embrittlement can be eliminated by subcritical annealing prior to heat treatment and an aging treatment, subsequent to plating",

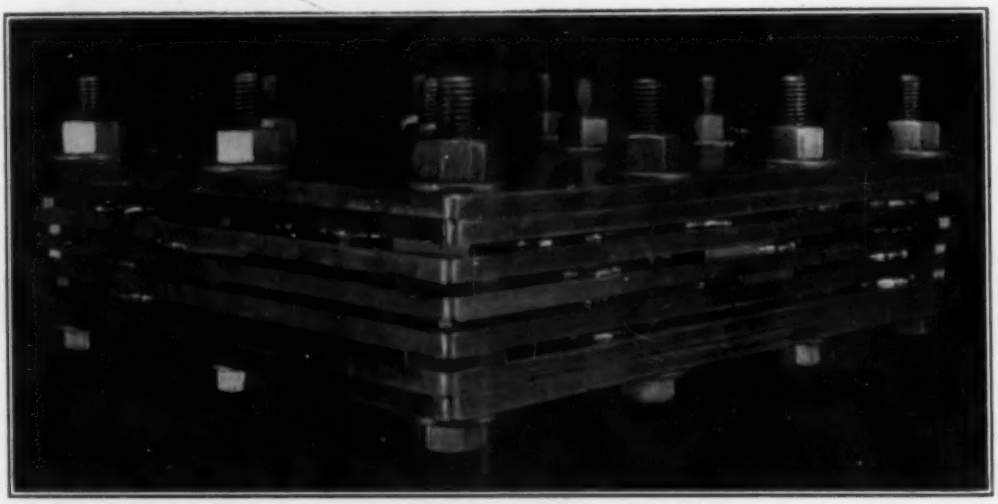


Fig. H—Compressed Dome Washers Between Heat Treated Plates. × ¾.

cannot be substantiated, in any sense of the word, by the data in Tables A and B. The values obtained on the majority of the groups, with the subcritical anneal, are actually lower than those obtained on groups without the subcritical anneal.

The groups in the higher range of hardness, when plated both to 0.0002 and 0.0005 inch depth and baked for hydrogen embrittlement, do not show any recovery either.

Allegation No. 4 (page 488, par. 1), that "Plating thickness has little or no bearing on the percentage of failures encountered", again does not bear out the facts recorded in Tables A and B. The significance of this statement will especially be apparent when cracking of the dome washers, loaded between two hardened plates, is discussed.

In the prior discussion, it has already been pointed out, that in an assembly, as shown in Fig. G, the screw is loaded 60% of its ultimate tensile strength, which is equivalent approximately to 3000 pounds. The 3000-pound loading deflects the Rockwell C-42 to 44 washer 0.135 inch, and the Rockwell C-48 to 52 washer 0.128 inch. The heat treated washers were then placed between hard plates as shown in Fig. H, and compressed until an equivalent deflection of 3000 pounds loading was arrived at. Washers in the loaded position were left for one week. Only the groups of washers which withstood loading of 3000 pounds or more, without cracking, were used in this test. The results so obtained are tabulated hereby:

Group	Number of Washers Loaded	Number of Washers Failed	Group	Number of Washers Loaded	Number of Washers Failed
A	8	0	A_1	8	8
B	8	0	B_1	8	8
C	8	5	C_1	....	....
D	8	8	D_1	....	....
E	8	0	E_1	....	....
F	8	4	F_1	....	....
C_2	8	8	C_3	....	....
D_2	8	8	D_3	....	....
E_2	8	4	E_3	....	....
F_2	8	8	F_3	....	....
CC	8	8	CC_1	8	8
DD	8	7	DD_1	....	....
EE	8	0	EE_1	....	....
FF	8	0	FF_1	....	....
CC_2	8	6	CC_3	8	8
DD_2	8	8	DD_3	....	....
EE_2	8	3	EE_3	....	....
FF_2	8	8	FF_3	....	....

It is significant to note that Groups C, D, F, E_2, F_2, CC, DD, CC_2, DD_2, EE_2, and FF_2, which sustained high loading, failed on compression for one week. In general, all groups in the low hardness range, plated to 0.0005 inch, high hardness range, plated to 0.0002 and 0.0005 inch, failed completely, or to the point where they are not commercially usable. Groups receiving the subcritical anneal prior to austenitizing treatment made poorer showing than groups without the subcritical anneal. Baking treatment is found beneficial, but only in conjunction with low range of hardness, 0.0002 inch of plating, and without the subcritical anneal. Groups not descaled and in low range of hardness stood the compression test without failure, but those in high hardness range failed 100%.

In this discussion, heating to overcome hydrogen embrittlement is referred to as "baking" rather than aging, because aging conveys to a metallurgical mind a meaning pertaining to precipitation hardening. Heating to overcome hydrogen embrittlement is not a precipitation hardening in any sense of the word.

Written Discussion: By R. Vines, The Dentists' Supply Co., York, Pa. Service failures occurring in the widespread wartime use of zinc or cadmium

plated lockwashers necessitated a number of investigations similar to that of Mr. Valentine.

It has been repeatedly demonstrated that cracking of plated lockwashers is avoided at lower hardnesses and by mild heating after plating. However, "safe" hardness levels were invariably below Rockwell C-50. The reported effectiveness of a subcritical anneal in increasing the "safe" hardness level to Rockwell C-51 to 56 is, therefore, very interesting.

Were the washers protected from decarburization during the subcritical anneal and the subsequent heat treatment? Decarburized lockwashers appear to be less susceptible to cracking than nondecarburized lockwashers.

The titles of most prior papers on this subject, including the references cited, employ the terms "hydrogen" or "hydrogen embrittlement" rather than "stress cracking" to indicate the nature of the failure. While these terms may not indicate the true nature of the failure, they do conform to established practice.

Author's Reply

Replying to Mr. Gurski's discussion, the Joint Industry conference on March 19, 1945, recommended a hardness range of Rockwell C-43 to 49 for spring washers. However, on November 28, 1945, the American Standards Sectional Committee B-27 unanimously adopted a hardness range of Rockwell C-45 to 53 and this is the range to which the industry is now working.

The time at 400 F required to overcome brittleness failures of electroplated lock washers probably is a function of internal and applied stresses. As we have pointed out in the paper, 4 hours of 400 F was not sufficient in some instances. Longer heating times were not tried by us. On the other hand we have noted instances where standing at room temperature for a year appeared to be beneficial.

We are glad to know that Mr. Sartorius agrees with us regarding the desired hardness range for electroplated lock washers, and trust that he will prevail upon the spring washer industry to review their decision of November 28, 1945, unanimously adopting the high hardness range of Rockwell C-45 to 53.

It is our understanding that some lock washers are marked by the manufacturer for identification purposes. The knurling mentioned by Mr. Sartorius is one method of marking. No correlation was noted between any of the four different types of surface markings on lock washers tested and the frequency of failures. All of these types of lock washers responded to the subcritical annealing prior to heat treating coupled with the aging treatment subsequent to plating.

Microexaminations were made on a considerable number of broken and unbroken lock washers to determine, if possible, some of the factors contributing to failure. Decarburization did not appear to be a factor influencing cracking. Severely decarburized lock washers might be expected to set and relieve the stresses.

Heat treated lock washers, as received from the manufacturer, re-treated as indicated in the text, were used for these tests.

No work was done by us on dome lockwashers. However, according to the data presented by Mr. Stefanides, they offer some interesting problems;

i.e., when under a constant load, the deflection of the dome lockwashers varies with the hardness.

As stated in the text, subcritical annealing consisted of heating the lockwashers at 1100 F (595 C) for 2 hours, then cooling slowly. A considerably different procedure was employed by Mr. Stefanides.

Replying to Mr. Vine, the subcritical annealing was done in a convective air draw furnace with no atmosphere controls.

HARDNESS TESTING OF METALS AND ALLOYS AT ELEVATED TEMPERATURES

By Frederick P. Bens

Abstract

The principles of the diamond pyramid penetration method of hardness testing have been embodied in an apparatus for determining the hardness of metals at temperatures up to 1700 F (925 C). The apparatus is designed to rest on the stage of a standard Vickers hardness machine and to employ the loading device and optical system thereof. A vacuum chamber protects the test specimen, diamond indenter, and heating element against oxidation at high temperature.

The hardness and strength of some alloys at elevated temperatures are recorded. In stable alloys the hardness at elevated temperatures appears to be a useful index of elevated temperature strength.

Introduction

THE room temperature hardness of metals and alloys is recognized as a good indication of room temperature strength, and very often service performance can be predicted from hardness alone. It is logical to assume that a hardness-strength relationship exists at elevated temperature for those metallic systems which are stable at the testing temperatures.

In research and development work at the laboratory of the Climax Molybdenum Co., the hot hardness test was employed for preliminary selection of high strength alloys for gas turbine blades operating at temperatures up to 1600 F (870 C). Precise hardness measurements at elevated temperatures were required for the work, and this paper describes the apparatus which was constructed to meet that requirement.

Design of the Apparatus

Before the apparatus for hot hardness testing was designed, the characteristics of systems previously developed for measuring hot

A paper presented before the Twenty-eighth Annual Convention of the Society held in Atlantic City, November 18 to 22, 1946. The author, Frederick P. Bens, is research metallurgist, Climax Molybdenum Co. of Michigan, Detroit. Manuscript received May 11, 1946.

hardness were studied. As a result of this study, it was decided that the apparatus should contain the following features:

1. An indentation method commonly used at room temperature was to be employed.
2. The indentations were to be as small as possible, so that a large number of hardness determinations could be made on a small sample. Whenever surveys of metallic systems are desired, valuable time and costly materials can be saved if the data can be secured from small samples.
3. The load was to be accurately determinable and variable at will, to permit both the testing of materials whose hardnesses vary greatly with temperature and the testing of dissimilar materials having widely different hardnesses at the same temperature.
4. The apparatus was to be as simple as possible, durable, and easily serviced.
5. The sample and the penetrator were to be heated to the testing temperature and protected against oxidation, in order to maintain a high degree of accuracy and promote long life of the penetrator.

The Vickers diamond pyramid indentation method satisfactorily supplies the first four features.

The last feature—heating the sample and penetrator to the desired temperature and protecting them from oxidation in a simple manner—was satisfied by the use of a vacuum furnace. A vacuum was deemed preferable to rare gases, because of cost; preferable to nitrogen, because it avoided the possibility of nitriding the sample; and preferable to hydrogen, which might react with the diamond or decarburize the sample. It was expected that it would be unnecessary to attain pressures below 10^{-3} millimeters of mercury. In practice, sufficient protection against oxidation was provided at a pressure of 10^{-2} millimeters of mercury by a small mechanical vacuum pump.

A schematic drawing (Fig. 1) and a photograph (Fig. 2) of the complete apparatus show the essential features of the equipment.

The top plate of the vacuum chamber was designed to hold a cylinder and a piston with the indenter at its lower end. To facilitate making a number of impressions on a single sample, a device was incorporated for moving the specimen under the indenter without destroying the vacuum. Access to the indenter, thermocouple, anvil, and heating element was afforded by the removable lid of the vacuum chamber.

The vacuum chamber is a section of steel pipe, 8 inches in diam-

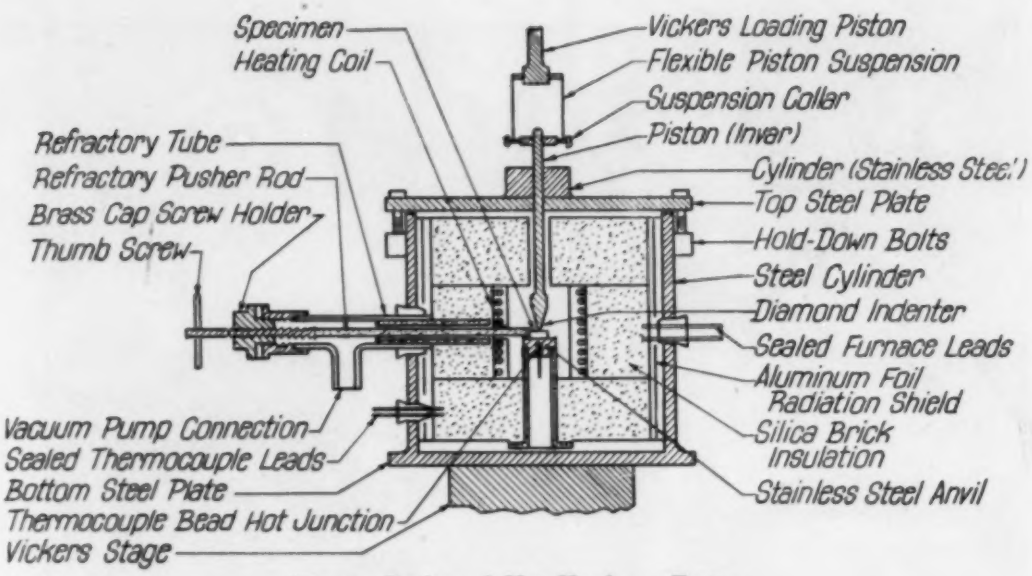


Fig. 1—Design of Hot Hardness Tester.

eter and approximately 8 inches high, with steel plates for top and bottom. The bottom plate is welded to the pipe; the top plate is removable and holds the indenter piston and cylinder. The complete chamber is of such size and weight that one person can easily place it upon, and remove it from, the stage of the Vickers machine.

An 18% chromium, 8% nickel stainless steel cylinder, soldered to the top plate, accommodates a ¼-inch diameter Invar piston, which is lapped to a clearance of 0.0001 inch. By means of lubricating oil having a low vapor pressure, a vacuum seal is produced between the two. Stainless steel and Invar were selected in order to increase clearance with rise in temperature and thus to prevent seizing.

The upper end of the piston is hemispherical, so that only point contact is made with the Vickers loading plunger. This eliminates the necessity for co-axial alignment of the piston and the plunger and insures against eccentric loading of the diamond.

A flexible suspension joins the Vickers plunger and the indenter piston in such a way that by raising the stage of the Vickers machine the specimen is brought in contact with the diamond.

The heating element consists of a $\frac{5}{16}$-inch diameter spiral of a 19-gage Chromel A resistance wire wound on a 2-inch diameter muffle. It is supplied with 110-volt alternating current. A temperature of 1700 F (925 C) is maintained by 600 watts. (This is about half the power required for heating in air. This point should be kept in mind in designing heating elements for use in vacuum.) The turns of the wire are separated around a hole in the side of the muffle

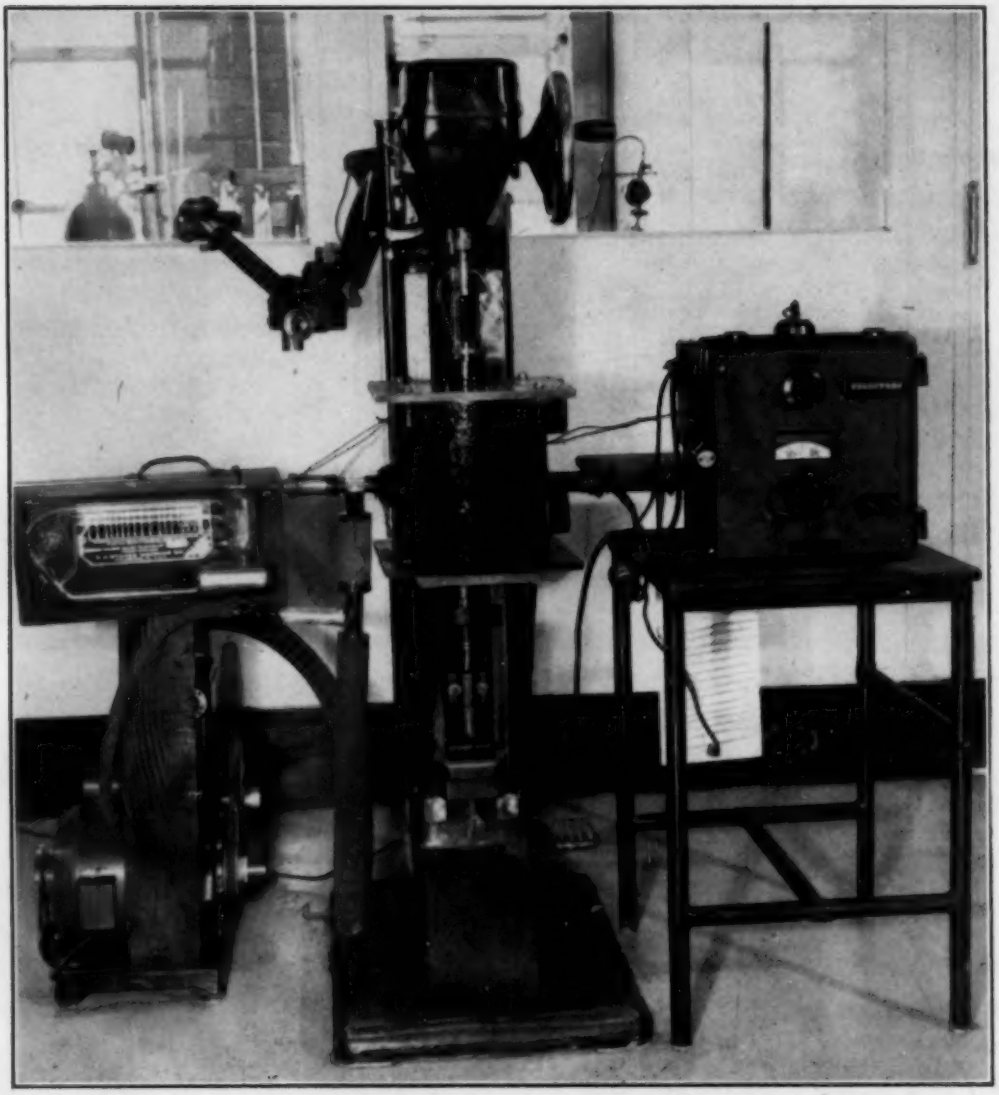


Fig. 2—Hot Hardness Tester.

through which the specimen is slid on the anvil. The muffle and element are held in place by silica bricks which also serve as heat insulators. The electrical leads and thermocouple leads are sealed into the vacuum chamber through rubber stoppers. The thermocouple hot-junction bead is flush with the top of the anvil and filed flat to increase the area of contact with the specimen.

A 1-inch diameter alundum refractory tube provides a path for sliding the samples into the apparatus and houses the refractory pusher rod for moving the sample under the diamond. A glass T-tube is sealed to the vacuum chamber at the outer end of this refractory tube. The vertical arm of the T-tube is connected by

vacuum hose to a mechanical vacuum pump and a vacuum gage. The horizontal arm holds a brass cap and brass thumb screw. The specimen is moved in a horizontal groove, ½ inch wide, cut into the anvil. The refractory pusher rod is placed in line with this groove and against the end of the specimen. A threaded brass rod projects through the brass cap and contacts the outer end of the refractory rod. By turning the thumb screw on the brass rod, motion is translated to the refractory rod and the specimen.

The specimen size most frequently used is 1 inch by ¼ inch by ½ inch. Specimens up to 1½ inches long and ½ inch thick can be accommodated, but the width of the specimen must not be greater than the width of the groove in the anvil. If the specimens are too small to be manipulated easily, they can be mounted in an alloy of suitable melting point, such as Monel metal, and the mounting can be machined to fit the anvil slot.

The hot hardness tester is operated as follows: A sample is slid on the anvil; the brass thumb screw cap and pusher rod are placed in position; the system is evacuated; and the sample is heated to the desired temperature. Then the Vickers stage is slowly raised until the specimen gently touches the diamond. The stage is further raised until the top of the indenter piston is about $\frac{1}{32}$ inch from the bottom of the Vickers plunger. The load is then applied, and when the loading cycle is complete, the stage is lowered until the diamond is suspended above the specimen. The specimen is moved to a new position by rotation of the thumb screw and another impression is made as before, either at the same temperature or at a different temperature, as desired. When the tests are completed the furnace is allowed to cool to room temperature before the chamber is opened and the sample removed. The lengths of the diagonals of the impressions are measured by means of the Vickers optical system.

The Vickers pyramid hardness numbers are obtained from the formula

$$VPN = 1.8544\ (L/d^2)$$

where VPN is the hardness number, L is the load in kilograms, and d is the length of the diagonal in millimeters. The load on the indenter must be corrected for the additional weight of the hot hardness indenter piston and suspension, the force exerted on the piston by air pressure, and the friction between the piston and the cylinder. The friction between the piston and cylinder was measured by sup-

Table I
Hot Hardness of Some Metals and Alloys

	Temperature F	Temperature C	VPN		Temperature F	Temperature C	VPN
Chromium, vacuum melted and cast	80	27	135	Stellite No. 21	80	27	314
	932	500	113		932	500	275
	1112	600	119		1112	600	242
	1292	700	97		1292	700	206
	1600	870	61		1472	800	176
Iron	80	27	77	51% Mo, 49% W Alloy	80	27	298
	932	500	45		900	482	228
	1112	600	21		1100	593	202
	1292	700	16		1200	648	196
					1300	704	196
Molybdenum, sintered and swaged bar	80	27	206		1400	760	190
	932	500	116		1500	815	185
	1112	600	105		1600	870	168
	1292	700	102				
	1600	870	87	18-4-1 High Speed Steel, oil quenched from 2400 F (1315 C)	80	27	870
Tungsten, sintered and swaged bar	80	27	351	and tempered 1 hour at 1050 F	932	500	616
	1000	538	200	(565 C)	1112	600	508
	1100	593	197		1292	700	274
	1200	648	206		1600	870	75
	1300	704	195	6% Mo, 6% W High Speed Steel, oil	80	27	894
	1400	760	194	quenched from 2300 F (1260 C)	932	500	644
	1500	815	184	and tempered 1 hour at 1050 F	1112	600	552
	1600	870	162	(565 C)	1292	700	246
	1700	925	156		1600	870	67

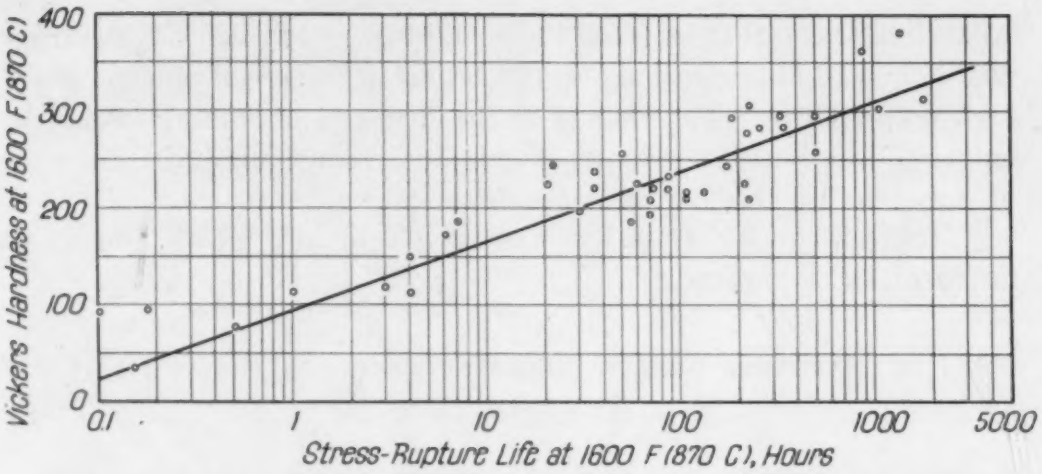


Fig. 3—Vickers Hardness at 1600 F (870 C) of Some Chromium-Base Alloys Versus Their Stress-Rupture Life at 1600 F (870 C) Under a Stress of 20,000 Pounds Per Square Inch.

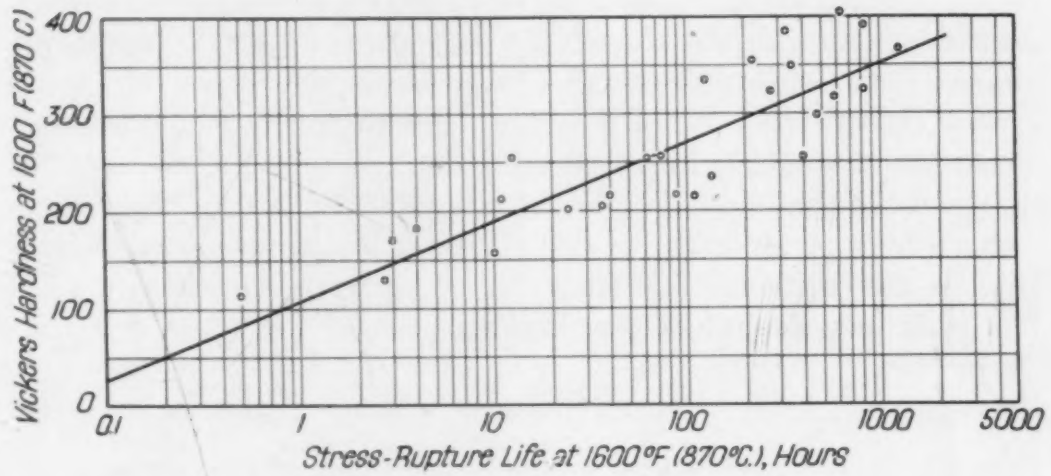


Fig. 4—Vickers Hardness at 1600 F (870 C) of Some Chromium-Base Alloys Versus Their Stress-Rupture Life at 1600 F (870 C) Under a Stress of 24,000 Pounds Per Square Inch.

porting the cylinder and resting one end of the piston on the pan of an analytical balance. The force necessary to move the piston was found to be 2 grams.

The error resulting from making the hardness impression at elevated temperature and subsequently measuring the diagonal at room temperature has been neglected. Even if we consider testing a metal such as copper, having a high coefficient of expansion and low hardness at 1700 F (925 C), the error due to thermal contraction of the diagonal is very small. Assuming a linear coefficient of thermal expansion for the copper specimen as high as 10^{-5} per F (5.55×10^{-6} per C) and a maximum temperature difference of

1600 F (885 C), that is, from 100 to 1700 F (40 to 925 C), the diagonal for a 10-kilogram load would be about 0.540 millimeter at the high temperature. The change in the diagonal on cooling would be only 0.007 millimeter. If neglected, this change produces an error of only two Vickers hardness numbers.

Table I shows the hot hardness of a few pure metals and alloys tested in the apparatus.

Hot Hardness Versus Load Carrying Ability at High Temperatures

Figs. 3 and 4 indicate a relation between the load carrying ability of some alloys at elevated temperatures and their hardness at those temperatures. The Vickers hardness at 1600 F (870 C) versus the stress-rupture life in hours at 1600 F (870 C) of temperature-resistant chromium-base alloys under a tensile stress of 20,000 pounds per square inch and 24,000 pounds per square inch is shown in Figs. 3 and 4, respectively. All of the alloys have chromium as the base element but vary widely in percentage of other alloying elements. The alloys possessing the higher hardness at 1600 F (870 C) are characterized by superior load carrying ability at that temperature, regardless of composition. The scattering of points is surprisingly small for so heterogeneous a collection of samples.

Summary

An apparatus has been constructed for accurately determining the hardness of metals and alloys at high temperature in terms of a well-known hardness scale. It is concluded that with this equipment hardness measurements at temperatures up to 1700 F (925 C) can be made with the same accuracy as at room temperature.

The data obtained with the apparatus indicate that there is a relationship between the hot hardness and the stress-rupture strength of stable alloys.

References

1. J. A. Brinell, "Researches on the Comparative Hardness of Acid and Basic Open-Hearth Steel at Various Temperatures by Means of Ball Testing," *Iron & Steel Magazine*, Vol. 9, 1905, p. 16.
2. A. Kürth, "Investigations on the Effect of Heat on Hardness of Metals," *Zeit. Verein Deut. Ing.*, Vol. 53, 1909, p. 85, 209.

3. Felix Robin, "The Hardness of Steels at High Temperatures," *Revue de Metallurgie,* Vol. 5, 1908, p. 893.
4. Felix Robin, "The Hardness of Metals, Its Measurement at High and Low Temperatures," *Mem. C. r. Trav. Soc. Ing. civils France,* Vol. 62, No. 1, 1909, p. 444.
5. A. H. d'Arcambal, "Hardness of High Speed Steel," *Chemical and Metallurgical Engineering,* Vol. 25, 1921, p. 1168.
6. F. Körber and I. B. Simonsen, "Dynamic Hardness Testing of Steel at High Temperatures," *Mitt. a. d. Kaiser-Wilhelm Inst. f. Eisenforsch.,* Vol. 5, 1923, p. 21.
7. F. Sauerwald, "The Relation Between Hardness and Temperature," *Zeit. f. Metallkunde,* Vol. 16, 1924, p. 315.
8. R. Mouillac, "The Herbert Pendulum for Hardness Tests," *Revue de Metallurgie,* Vol. 22, 1925, p. 230.
9. A. Pomp, "Hardness Testing at High Temperatures," *Apparatebau,* Vol. 39, 1927, p. 245.
10. F. Sauerwald, "The Hot Deformation of Metals, Its Significance and Relation to Cold Deformation," *Metallwirtschaft,* Vol. 71, 1928, p. 1355.
11. W. P. Schischokin and W. Agejewa, "Hardness of Metal Alloys at Different Temperatures," *Zeit. anorg. Chem.,* Vol. 193, 1930, p. 23.
12. I. H. Cowdrey, "Hardness by Mutual Indentation," *Proceedings,* American Society for Testing Materials, Vol. 30, No. II, 1930, p. 559.
13. W. P. Schischokin, "The Hardness and Fluidity of Metals at Different Temperatures," *Zeit. anorg. Chem.,* Vol. 189, 1930, p. 263.
14. E. G. Herbert, "Report on the Hot Hardness Characteristics of Some Modern Tool Steels and Alloys," *Proceedings,* Inst. Mechanical Engineers, 1930, p. 681.
15. A. R. Page, "Some Experiments on the Impact Hardness of High Speed Steel at Elevated Temperatures," *Metallurgia,* Vol. 3, 1930-31, p. 85.
16. P. L. Henderson, "The Herbert Pendulum Hardness Tester," *Commonwealth Engineer,* Vol. 19, 1931-32, p. 291.
17. J. F. Kayser, "Measuring Hardness at High Temperatures," METAL PROGRESS, Vol. 23, No. 3, 1933, p. 50.
18. O. E. Harder and H. A. Grove, "Hot Hardness of High Speed Steels and Related Alloys," *Transactions,* American Institute of Mining and Metallurgical Engineers, Vol. 105, 1933, p. 88.
19. A. M. Borzduika and N. M. Orlov, "Hardness of Metals at High Temperatures," *Zavodskaya Laboratorium,* Vol. 3, 1934, p. 1015.
20. H. O'Neill, "The Hardness of Metals and its Measurement," Chapman and Hall, Ltd., London, 1934, 292 pages.
21. J. Engl and J. Fölmer, "The Relation Between Temperature and Ball Pressure Hardness of Metals. II," *Zeit. f. Physik,* Vol. 98, 1936, p. 702.
22. E. Fetz, "Dynamic Hardness Testing of Metals and Alloys at Elevated Temperatures," TRANSACTIONS, American Society for Metals, Vol. 30, 1942, p. 1419.
23. S. R. Williams, HARDNESS AND HARDNESS MEASUREMENTS, published by American Society for Metals, Cleveland, 1942, 558 pages.
24. E. C. Bishop and M. Cohen, "Hardness Testing of High Speed Steel at High Temperatures," METAL PROGRESS, Vol. 43, No. 3, 1943, p. 413.

DISCUSSION

Written Discussion: By J. D. Nisbet, Research Laboratory, General Electric Co., Schenectady, N. Y.

The author has developed a good tool for rough checking the high temperature properties of metals. The relationship found between hot hardness

and rupture strength is surprisingly good. Relations between these two very different types of testing can be shown only by the most accurate control of the variable involved with each. The rupture tests were performed in oxidizing atmospheres and the hot hardness tests in the absence of atmosphere. The rupture test is done over a period of hours and the hardness test in terms of seconds. Therefore, the effect of corrosion is paramount in rupture testing and nonexistent in vacuum hot hardness testing. This suggests that the relationship between hot hardness and rupture strength might not be so good for alloys that are corrosive. Corrosion is likely to be the most difficult variable to control or evaluate in applying the hot hardness test to alloys which corrode more than chromium-base alloys.

If rupture test data are plotted on linear co-ordination rather than log-log, then the rupture curve falls very fast with high loads and short times and, of course, becomes very flat with low loads and long times. In other words, the curve tends to be vertical in short-time test and tends to be horizontal in long-time test. Therefore, in short-time testing, whether it is hardness or tensile strength, the ability to predict the almost horizontal part of the rupture curve from short-time data which fall on the almost vertical part of the curve is certainly difficult. It can be done only by exercising extreme care in control of time measurements and providing the necessary accommodation coefficients for corrosion which is one major controlling factor in the shape of the curve for prolonged times. I presume that time of loading in the hot hardness tester was quite accurately and automatically controlled. It would be interesting if the author would elaborate on this point.

Metallurgical tools for studying the high temperature properties of materials which reduce the time for test are certainly needed and this high temperature hardness tester developed by Mr. Bens is a valuable contribution.

Written Discussion: By Howard S. Avery, research metallurgist, American Brake Shoe Co., Mahwah, N. J.

This contribution from the Climax laboratories is very welcome. The subject of hot hardness is worthy of extended study in attempts to provide further insight into the relative wear resistance of metals at elevated temperatures.

The relationship between hot hardness and creep behavior is sometimes raised in discussions of hot hardness data.[1] The effect of creep as a variable in testing is also important and should receive consideration. When a fixed load is imposed for a single time interval, and the resulting deformation measured at room temperature, it is difficult to identify or measure the role of creep.

The Rockwell hardness system modified for hot tests as described by Bishop and Cohen[2] permits instantaneous and successive measurements of deformation and has been employed in the American Brake Shoe Metallurgical Laboratory to observe the change in apparent hardness that results from creep. Typical results as obtained on an air hardening weld deposit appear in Fig. A.

---

[1]Discussion of Harder and Grove, "Hot-Hardness of High-Speed Steels and Related Alloys," *Transactions*, American Institute of Mining and Metallurgical Engineers, Vol. 105, 1933, p. 125-132.

[2]E. C. Bishop and Morris Cohen, "Hardness Testing of High-Speed Steel at High Temperatures," METAL PROGRESS, March 1943, p. 413-442.

The data points represent the hardness values after 0,[a] 1, 2, and 3 minutes of load application, while the shaded area indicates the range of apparent hardness that might be encountered if time of loading were a variable within the limits described.

The rapid decrease in apparent hardness, which is greatest during the first minute, suggests that the compressive deformation behavior is similar to the primary stage of elongation in tensile creep and stress-rupture tests. Thus,

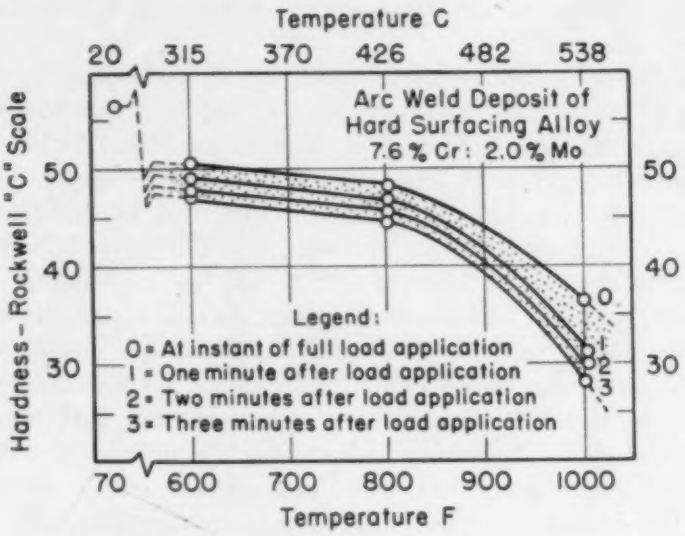


Fig. A—The Effect of Creep, as Controlled by Duration of Load Application, on the Apparent Hot Hardness of an Air Hardening Arc Weld Deposit.

hot hardness may be directly related to certain features of very high load, short-time stress-rupture or tension tests at the same temperature, but the relationship to fracture time probably is somewhat fortuitous.

Because strong alloys have a tendency to be so in both short and long-time tests, and strength generally has the effect of increasing fracture time, the interesting correlations shown by Mr. Bens are understandable and provided a useful preliminary estimate of hot strength. Caution is recommended in the general application of this procedure, however, especially for materials that are more nearly alike in properties. This point is considered pertinent as there is such a definite need for a quick method of determining creep strength and life expectancy, as now derived from long and expensive tests, that there may be a strong temptation to adopt hot hardness as a convenient acceptance test for heat resistant alloys.

Author's Reply

The author thanks Mr. Nisbet and Mr. Avery for their discussions.

Mr. Nisbet's remarks concerning the effect of corrosion on the correlation between hot hardness and rupture strength of alloys serve to emphasize

[a]Nominal. Actually a fraction of a second determined by the reaction time of the operator.

the statement made in the summary of the paper that the relationship is believed most valid when applied to stable alloys. Stability of metals and alloys at elevated temperatures is dependent on many properties and oxidation resistance is certainly one of the most significant. The chromium-base alloys mentioned in the paper were sufficiently high in chromium to possess high resistance to oxidation at 1600 F (870 C) and the low diffusion rates of the elements within the alloys also aided in their high temperature stability.

The time of loading in the hot hardness tester was 15 seconds throughout all of the tests, accurately and automatically controlled by the loading device on the Vickers machine.

Mr. Avery's discussion presents interesting data obtained by Rockwell hot hardness tests to show the change in apparent hardness that results from time of loading, suggesting that compressive deformation behavior is similar to the primary stage of elongation in tensile creep and stress-rupture tests. He recommends caution, however, in the general application of hot hardness results to the prediction of creep strengths and with this the author completely agrees.

It may be well to again emphasize that the hot hardness tester described in the paper was designed and constructed to facilitate the preliminary selection of the most promising refractory alloys for gas turbine service. The results obtained in the apparatus on chromium-base alloys saved considerable time in their development as the hot hardness vs. stress-rupture data indicate, but we must indeed be wary in attempting to apply such a short-time test relationship to all classes of alloys under long-time loads at any or all elevated temperatures. The time factor becomes increasingly more significant in nullifying simple relationships at elevated temperatures as less stable alloys are tested. Oxidation and diffusion rates influence phase changes which definitely complicate the correlation of short and long-time test results.

We may hope, however, that in the future, some of the time-dependent variables can be more accurately evaluated and when combined with hardness testing will serve to predict the elevated temperature properties of metals and alloys.

NONDESTRUCTIVE INSPECTION OF MINE HOIST CABLE

By P. E. Cavanagh and R. S. Segsworth

Abstract

An account of the development of a practical nondestructive method for inspection of wire rope while in service is presented in this paper. Preliminary experiments are described which established fundamental relationships between the magnetic and electrical properties and increases in stress in wire ropes. Proper choices of coil design and test frequencies are important to provide satisfactory meter indications of changes in properties through use of available commercial test instruments. Further tests were carried out under normal operating conditions to determine whether the fundamental relationships between stresses in wire rope and instrument readings still held at high hoisting speeds. It was found that the test procedure did not interfere seriously with normal operation of a mine hoist.

Tests were continued on a small experimental hoist to insure that all possible types of defects could be detected under operating conditions. All type of defects are identified as regions where the remaining load-carrying wires are subjected to a higher unit stress than the unit stress in wires in the rest of the rope.

MANY attempts have been made to devise some nondestructive means of inspecting wire rope while in service, in order to locate defects and possible sources of failure. Although no method has appeared which provided a practical means of achieving this end, considerable work is still going on in several countries in this field.

It had been shown in a brief investigation carried out in 1944 that the Du Mont Cyclograph was capable of locating several types of defects in aircraft control cable (1).[1]

Immediately after the Paymaster Mine Disaster in February,

[1]The figures appearing in parentheses pertain to the references appended to this paper.

A paper presented before the Twenty-eighth Annual Convention of the Society held in Atlantic City, November 18 to 22, 1946. Of the authors, P. E. Cavanagh is research fellow, Ontario Research Foundation, and consulting metallurgist, Allen B. Du Mont Laboratories, Inc., and R. S. Segsworth is research engineer, The General Engineering Company, Ltd., Toronto, Ontario. Manuscript received July 9, 1946.

1945, where sixteen men were killed as a result of the failure of a hoisting rope, The General Engineering Company of Toronto, Canada, began a series of tests to ascertain whether the Cyclograph could be used to detect dangerous faults in wire ropes. Early tests gave encouraging results. Since then, test and development work has been carried on continuously in co-operation with the Allen B. Du Mont Laboratories, Inc., Passaic, New Jersey, and the Ontario Research Foundation, Toronto, Canada.

The Du Mont Cyclograph has been described in current literature (2), (3).

By varying one factor at a time in otherwise identical samples, it may be shown that the Cyclograph will indicate differences in such metallurgical properties as hardness, structure, carbon, alloy content, etc. It will also show differences in stress. It is not particularly sensitive to small changes in volume of the sample. A great deal of experimental work has been performed to establish the fundamental relationships between the changes in stress conditions and the accompanying changes in magnetic and electrical properties of metals, as indicated by the Cyclograph (4), (5).

Preliminary Experiments to Establish Fundamental Relationships

The first laboratory series of tests on wire ropes was limited to ropes of ¼ inch diameter. Fig. 1 shows the apparatus as set up for these tests. Load was applied to the rope by means of an arbor press shown on the right and measured by means of a hydraulic cylinder and pressure gage shown at the other end of the test piece. Coils were wound on suitable forms and moved along the rope during tests.

Good correlation was obtained bewteen Cyclograph readings and load on the rope. Faults, such as those created by breaking a number of wires at a point, could be located by moving the test coil along the rope and noting a change in Cyclograph reading where the coil passed over a fault. This was only possible, however, when the rope was loaded. With the proper test frequency, the change in reading at a fault was in the same sense as that obtained by increasing the load on the rope. Thus the Cyclograph was responsive to stress in the rope and a fault was located as a region of abnormal stresses.

Ultimately it was found possible to select an arbitrary limit and

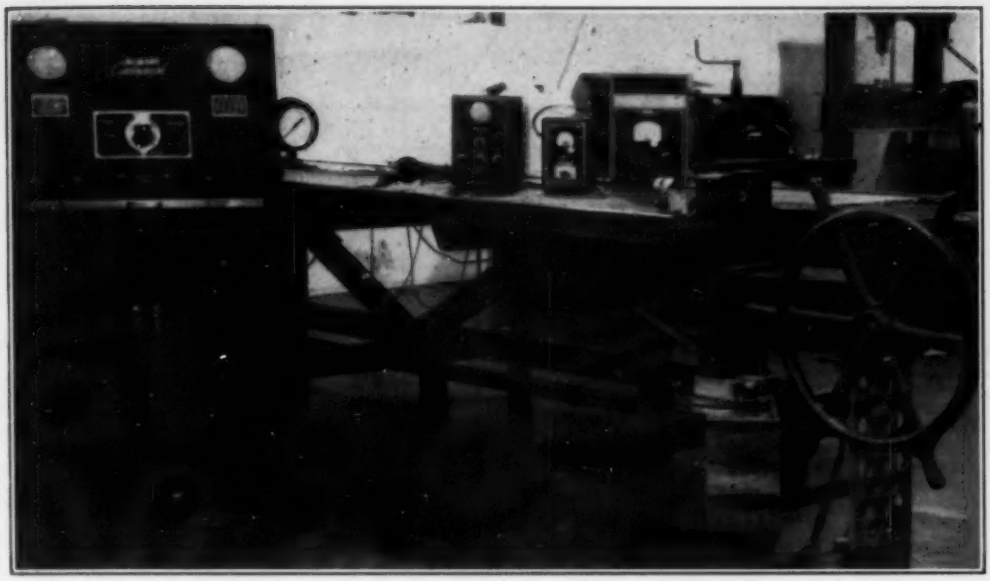


Fig. 1—Apparatus Set Up for Tests of ¼-Inch Rope.

to set the relay circuit in the Cyclograph so that if the stress in the rope exceeded this pre-selected limit, the relay would close, making power available to operate a signal light or other warning device.

The warning would operate if the coil were moved over a fault while the load on the rope was held below the selected limit because unit stress in the remaining load-carrying wires at the fault was higher than in the rest of the rope.

Arrangements were made in co-operation with the technical Committee on the Paymaster Disaster (7) to conduct a series of tests on larger ropes.

Load was applied by the Riehle 400,000-pound testing machine in the General Testing Laboratory in the Electrical Building at the University of Toronto. Babbitt sockets were attached to the ropes by the Rope Testing Branch, Department of Mines, to fit special grips. The initial experiments involved variations in rope diameter, coil diameter, and test frequency of the Cyclograph.

Curves shown in Fig. 2 give the relation between coil diameter and Cyclograph response as the load on the rope was varied. It may be noted that coil S-1 (1-inch diameter hole) gave a response roughly ten times that obtained with coil A-1 (3-inch diameter hole), but it is entirely feasible in practice to obtain satisfactory results with a coil of the larger diameter. It was also found that if the rope was held in an area approximately 2 inches in diameter about the center of the coil A-1, the Cyclograph reading did not change signifi-

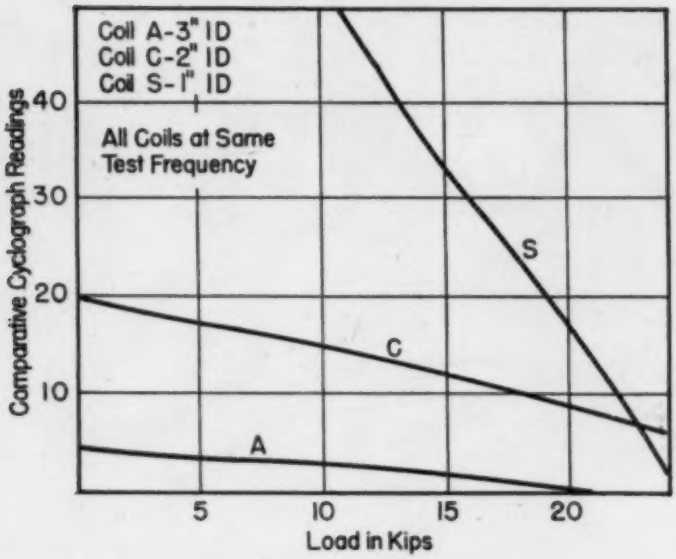


Fig. 2—Test With Varying Coil Diameters—¾ Inch Lang-Lay 6:19 Wire Rope.



Fig. 3—Typical Cyclograph Coils Used for Wire Rope Testing.

cantly with eccentricity of the rope relative to the coil. With coil C-1 (2-inch diameter hole), eccentricity of the rope relative to the coil made no significant change in the Cyclograph reading. Typical coils are shown in Fig. 3.

These results indicated that normal slap and movement of the hoisting rope in the shaft would have no significant effect on the results obtained, if tests were carried out under normal operating

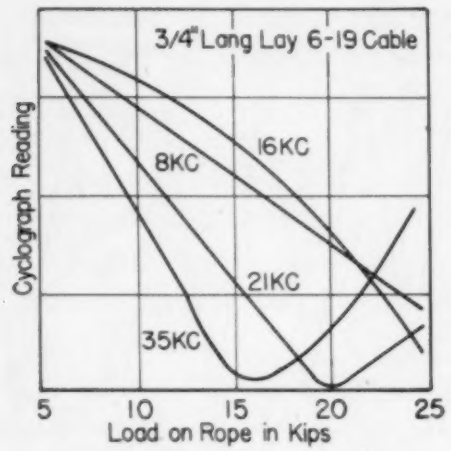


Fig. 4—Effect of Test Frequency on Correlation with Stress in Cable.

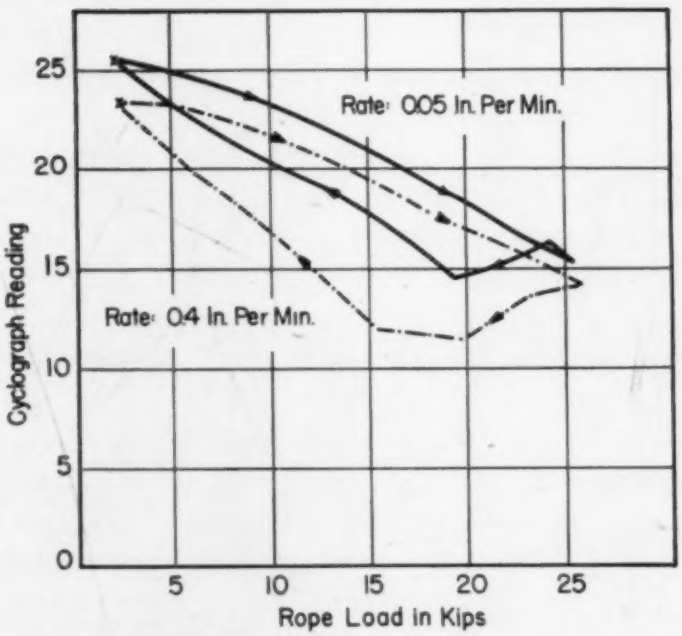


Fig. 5—Hysteresis Effect with Rapid Change of Load on ¼-Inch Lang-Lay 6:19 Rope—Head on Tensile Testing Machine Moved at Rates Shown to Obtain Different Loading Speeds.

conditions (6). A 3-inch coil would provide for 2-inch movement of the rope with no significant change in reading. Larger coils could be used to accommodate greater movement of the rope in the coil.

In practical application of such an inspection method the wire rope will be wet, greasy, and dirty. While these conditions theoretically should have no effect whatever on the instrument reading, a series of experiments was carried out to make sure of this fact. No influence at all was produced by the most extreme conditions of

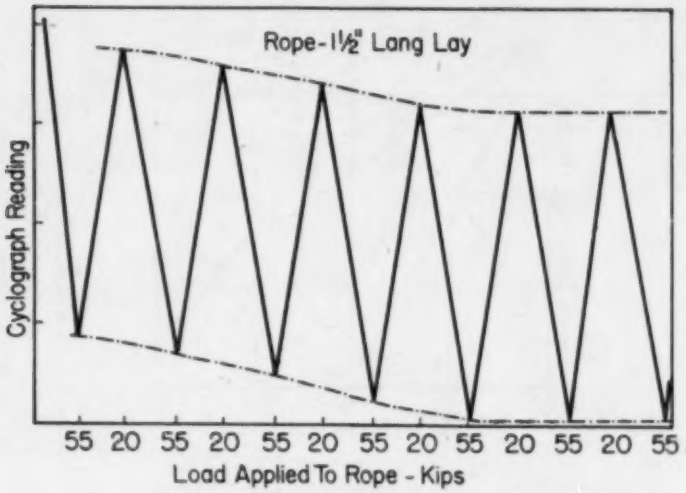


Fig. 6—Showing Change in Cyclograph Reading When Load on a New Rope Was Repeatedly Varied Between 20,000 and 50,000 Pounds.

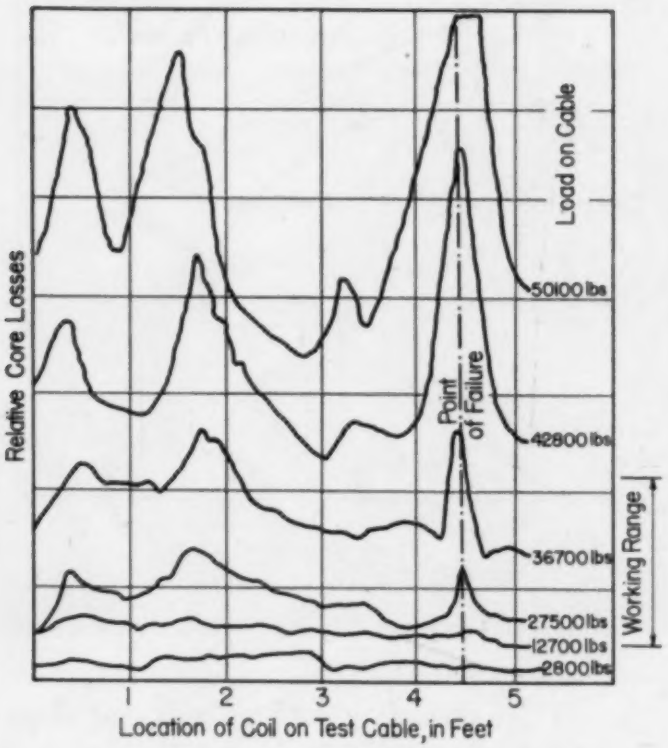


Fig. 7—Prediction of Point of Failure Under Load—Test Frequency of 4 Kc.—Cable 1½-Inch Lang Lay.

moisture, grease, and dirt in the laboratory or in later field tests.

Curves in Fig. 4 show the effect of varying the test frequency. It is anticipated that frequencies between 1500 and 5000 cycles may be employed in testing normal hoisting ropes. The choice of

test frequency is important in obtaining satisfactory results. It is necessary to have all types of defect give an increase in total core losses, and a corresponding decrease in Cyclograph reading, in order to obtain satisfactory operation of the testing instrument. In preliminary experiments, it was found that a certain range of test frequencies would give the desired results for a certain diameter of rope but that a higher or lower test frequency might give an indication in one sense for broken wire and an indication in the other sense for corroded wires.

Curves in Fig. 5 show results obtained at comparatively high frequencies with hysteresis loops in the Cyclograph response decreasing in area with decrease in the rate of loading. This experiment was carried out to determine whether circuit inertia and the hysteresis effect in stress changes would prevent the detection of extremely rapid changes in stress in the rope, which might give rise to failure. This factor did not prove important in practical tests.

The curves in Fig. 6 show results obtained when load on a new rope was repeatedly varied between 20,000 and 55,000 pounds. The maximum Cyclograph reading decreases asymptotically to a steady value. It is a well-known fact that a stretching or "aging" effect takes place when a wire rope is first put in service. The normal stretching of a new rope is accompanied by a permanent change in magnetic properties from their initial value to some new level at any given load.

Fig. 7 shows readings obtained over the whole length of a sample at various loads. It appears that there are sensible initial variations in the properties of the material of any rope along its length which remain even after repeated variations of load. These variations in magnetic properties are associated with unimportant changes in analysis and slight differences in the amount of cold work in the wire.

Detection of Various Defects

A further series of tests was undertaken to determine typical Cyclograph response to faults created in test pieces under load.

In this series of tests, a recording milliammeter was connected to the Cyclograph circuit. The paper drive was connected through a cord and suitable pulleys to the coil so that movement of the paper was proportional to movement of the coil along the sample in the



Fig. 8—Apparatus Set Up on the 400,000-Pound Riehle Testing Machine in the General Testing Laboratory of the University of Toronto.

testing machine. This arrangement gave good permanent records of the Cyclograph response, and greatly reduced the labor involved in making extensive series of comparative tests.

Fig. 8 shows the apparatus as set up with a sample of rope in



Fig. 9—Closeup of a Specimen of Rope and a Stress-Strain Recorder in the Testing Machine.

the machine and the Cyclograph, recording milliammeter, coil and paper drive mechanism in place. A closer view of a sample with test coils and a stress-strain recorder is shown in Fig. 9 and a typical sample with coils and babbitt sockets in place ready to be mounted in the test machine is shown in Fig. 10.

These tests were exploratory rather than exhaustive, since the aim was to establish the scope of useful application rather than to set up accurate calibration. Records of Cyclograph indications were made with stranded steel wire ropes with diameters ¼, ⅝, ¾, 1, 1¼ and



Fig. 10—Sample of 1½-Inch Rope with Babbitt Sockets and Coils in Place.

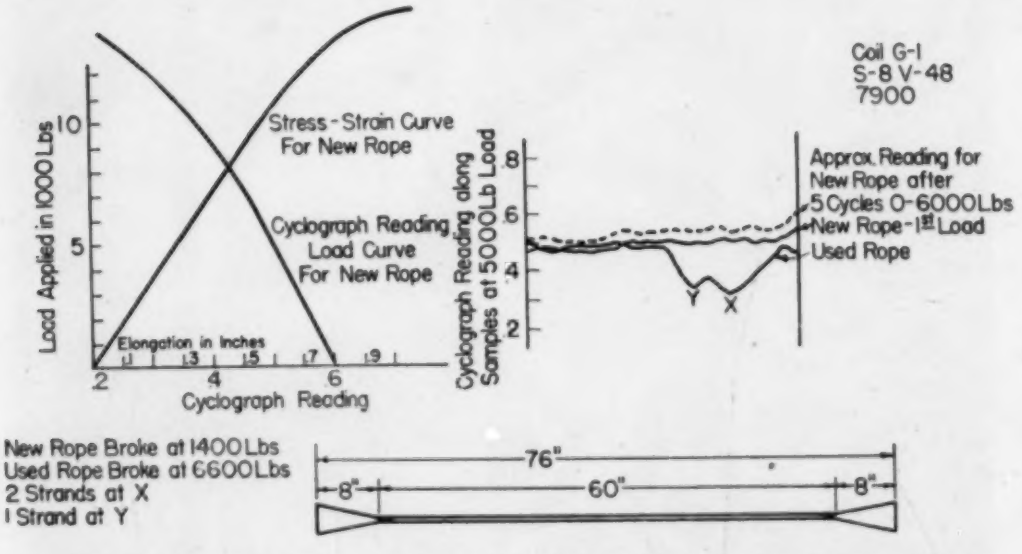


Fig. 11—Comparative Tests Over a Length of New ⅛-Inch Rope and a Similar Length Taken from a Rope Manufactured to the Same Specifications Which Failed in Service.

1½ inch, showing the differences between readings for sound cable and cable with the following artificially prepared faults:

1. Corrosion
2. Abrasion
3. Kinking
4. Bruising
5. Broken Wires

The range of loading was from zero to the breaking point.

As stated previously, the best correlation between change in Cyclograph reading and faults in the rope was obtained with a technique which made the Cyclograph primarily responsive to stress in the rope. With this approach, faults in a loaded rope are disclosed by the Cyclograph as areas with higher than normal stress.

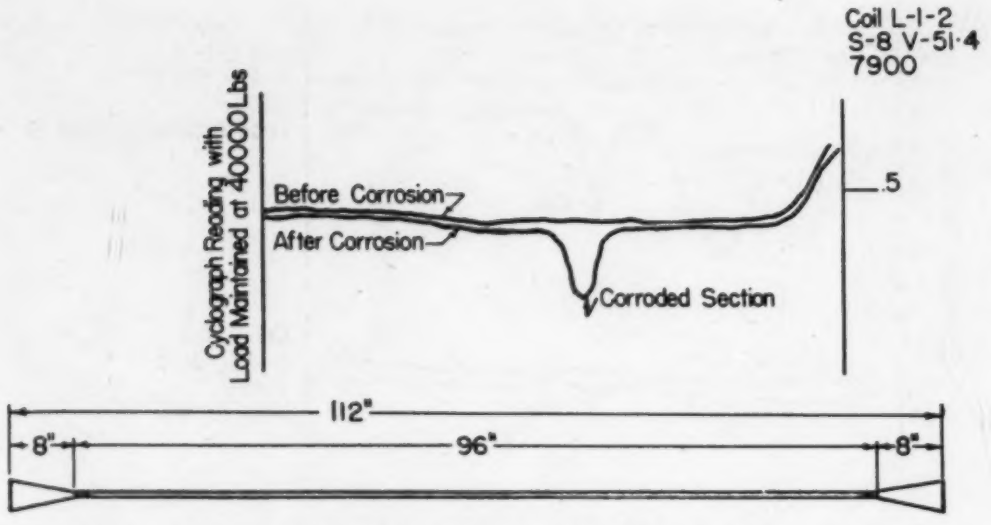


Fig. 12—Cyclograph Readings Along a Sample of 1-Inch 6:19 Lang-Lay Rope Corroded at One Point by Applying Drops of a Mixture of Strong HCl and HNO_3.

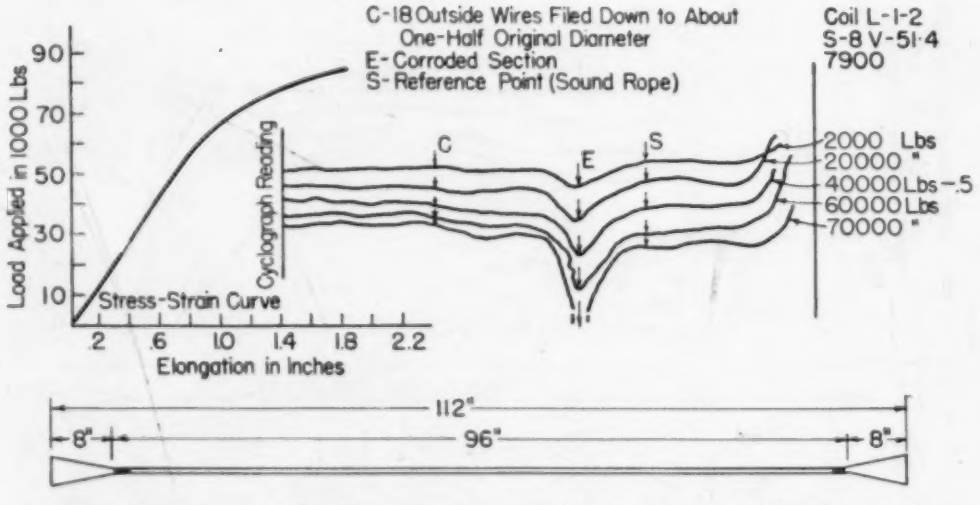


Fig. 13—Cyclograph Readings Along a Sample of 1-Inch 6:19 Lang-Lay Rope Corroded at One Point by Applying Drops of a Mixture of Strong HCl and HNO_3.

Fig. 11 shows comparative tests over a length of new 5/8-inch rope and a similar length taken from a rope manufactured to the same specifications which failed in service. The Cyclograph indicated the weak spots decisively and gave a rough measure of the decrease in strength at these points. It is noteworthy that the external appearance of the sample of rope tested was considerably better in the neighborhood of the rupture than it was in other parts where misplaced and broken wires were visible.

Figs. 12 and 13 show Cyclograph readings along a sample of 1-inch 6:19 lang-lay rope corroded at one point by applying

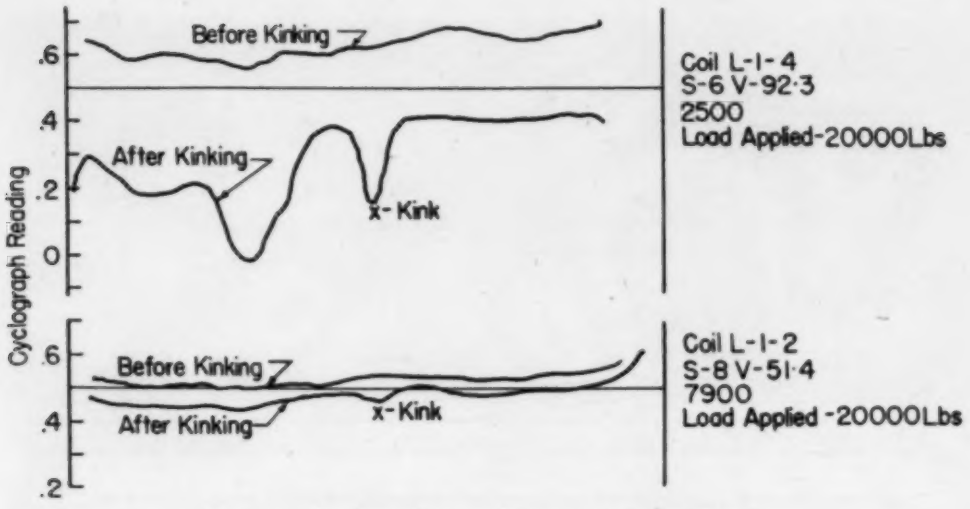


Fig. 14—Cyclograph Response to Kinks in Rope.

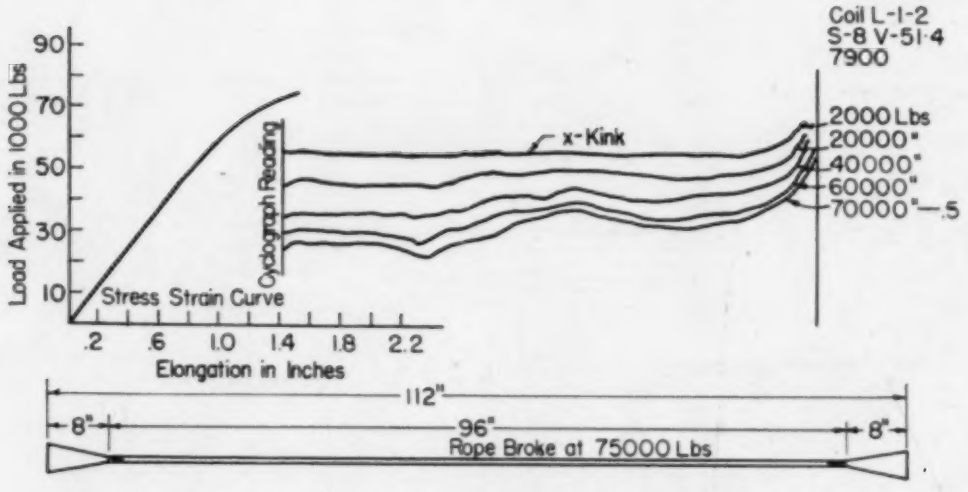


Fig. 15—Cyclograph Response to Kinks in Rope.

drops of a mixture of strong hydrochloric and nitric acids which penetrated the core of the rope. The Cyclograph gave clear deviations in the readings before the corrosion had reduced the strength of the rope by 5%.

In the first test, the load was maintained at 40,000 pounds and Cyclograph readings taken before and after the rope had been corroded at the point marked "E". Under these conditions, the recorded Cyclograph output gave a distinct indication or "dip" at the corroded point. This indication practically disappeared after the load had first been maintained for 16 hours and then dropped to zero and taken to 60,000 pounds. Later, however, when additional acid had reduced the strength of the rope by an estimated 5%, the "dip"

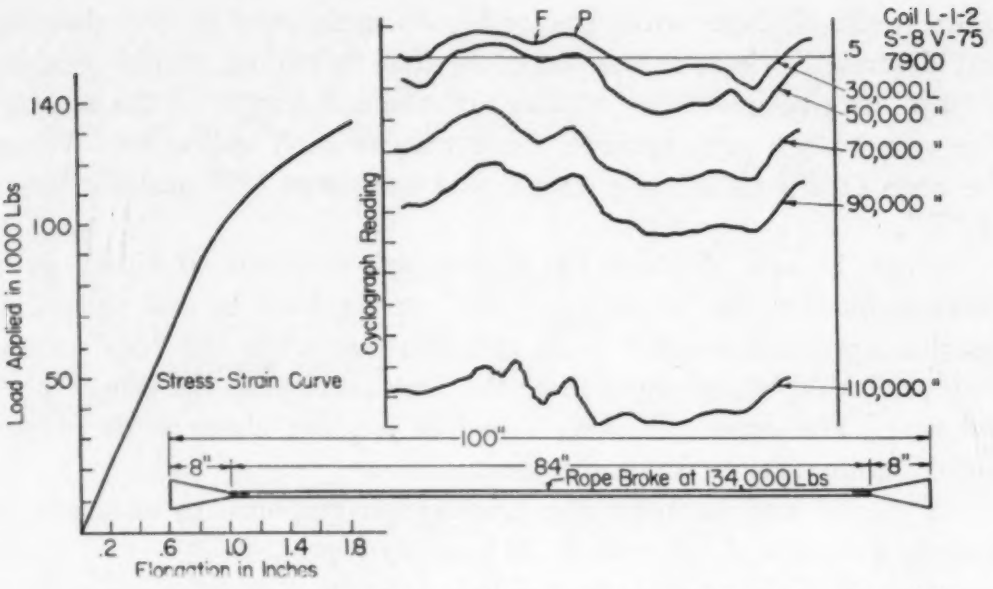


Fig. 16—Cyclograph Response to Abrasion Test in 1¼-Inch Lang-Lay C.W. and C 6:19 Wire Rope (New).

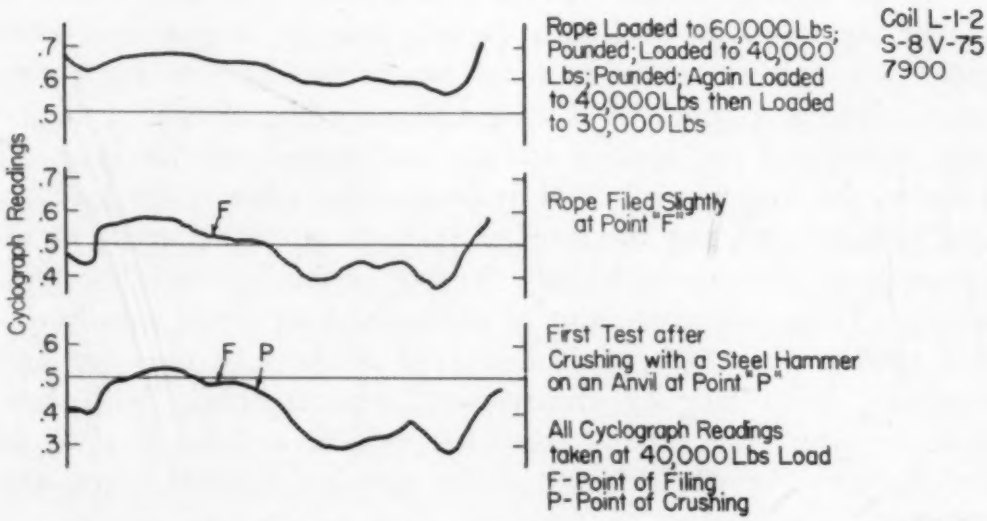


Fig. 17—Cyclograph Response to Abrasion Test in 1¼-Inch Lang-Lay C.W. and C 6:19 Wire Rope (New).

became more pronounced each time the load was applied. Apparently plastic deformation was now taking place in the rope, and each repeated load increased the distortion of the crystal lattice in the metal and thus permanently changed the magnetic and electrical properties.

Before this sample was finally broken, eighteen of the outside wires (at point "C") were filed down to approximately half of their original thickness. Subsequently, at a load of about 60,000 pounds

some seven of these wires snapped. As mentioned in the abrasion test described below, it was expected that this filing would produce a "dip" or else lower the reading for the full length of the sample. For reasons not yet apparent, there was no such indication. When the rope finally failed, one strand was broken at "C" and six wires at "E".

Figs. 14 and 15 show the Cyclograph response to kink. It is noteworthy that the maximum "dip" at the kink is less than that which occurred at another point and also that while the "dip" at the kink practically disappeared after the first load cycle, the other "dip" did not. The rope ultimately failed at a point close to the upper socket, quite remote from the kink.

Figs. 16 and 17 show the Cyclograph response to abrasion in tests on a sample of 1¼-inch 6:19 lang-lay rope.

Discussion

In the limited number of tests conducted, it was noted that with regular lay ropes up to 1 inch (which was the largest size tested under these conditions), when a fault was created by breaking a number of wires at a point, the Cyclograph recording showed a distinct "dip" when load was applied and the coil moved over the spot. If, however, the rope was vibrated by hammering while under load, the "dip" disappeared, but the level of readings over the length of the sample dropped to approximately the level of the bottom of the original dip. The gentle application of additional load would usually produce another dip which would disappear as above, if the rope were vibrated. With lang-lay construction, and especially with large sizes, the "dip" was usually much less evident and the level of the readings over the whole length of the sample fell when wires were broken.

As a possible explanation, it is suggested that the broken wires pick up their share of the load by friction in the regular lay construction within a short distance of the break so that there is a distinct increase in stress in the remaining wires only in the immediate region of the fault. When the rope is vibrated, however, the broken wires slip and release their proportion of the load which is distributed to the others throughout the length of the sample. With lang-lay construction, there is perhaps less locking between wires so that the broken wires do not pick up any significant proportion of the load in the length of the sample.

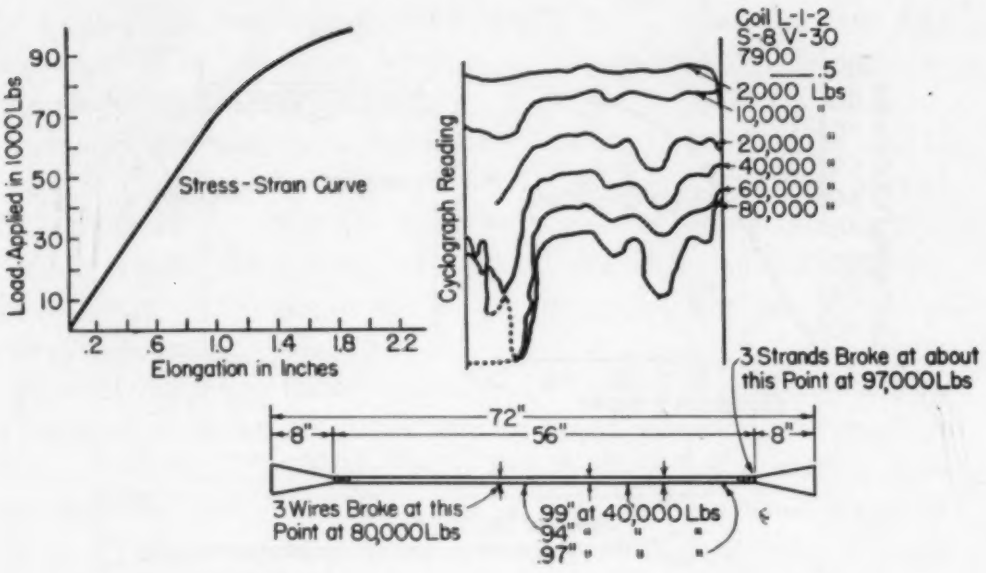


Fig. 18—Cyclograph Response in Test of Three Samples of 1-Inch Flattened Strand Rope Removed from the Skip Compartment of the Paymaster Mines.
Sample 24

Tests on Ropes Which Failed in Service

Figs. 18, 19 and 20 show Cyclograph response in test of three samples of 1-inch flattened strand rope removed from the Skip Compartment of the Paymaster Mines.

Unfortunately, the readings for Sample 24 are not directly comparable with those for Samples 12 and 25, since coil L-1-2 was destroyed when Sample 24 broke and other coils had to be used for the other two samples. It is significant, however, that in Sample 24, the Cyclograph clearly indicated the weakest parts in the section covered, as confirmed by measurements of diameter and the fact that wires started to break at the point shown.

Sample 25 showed little variation over its length and comparatively little change with load, indicating a sound rope, as was confirmed by the high breaking load.

A distinct and rapid change occurred in the readings taken on Sample 12 between the loads of 50,000 and 60,000 pounds. This apparently more or less corresponds to the "break" in the stress-strain curve.

The whole section of rope was badly damaged and in poor condition over its entire length, as indicated by the low breaking load of 78,000 pounds.

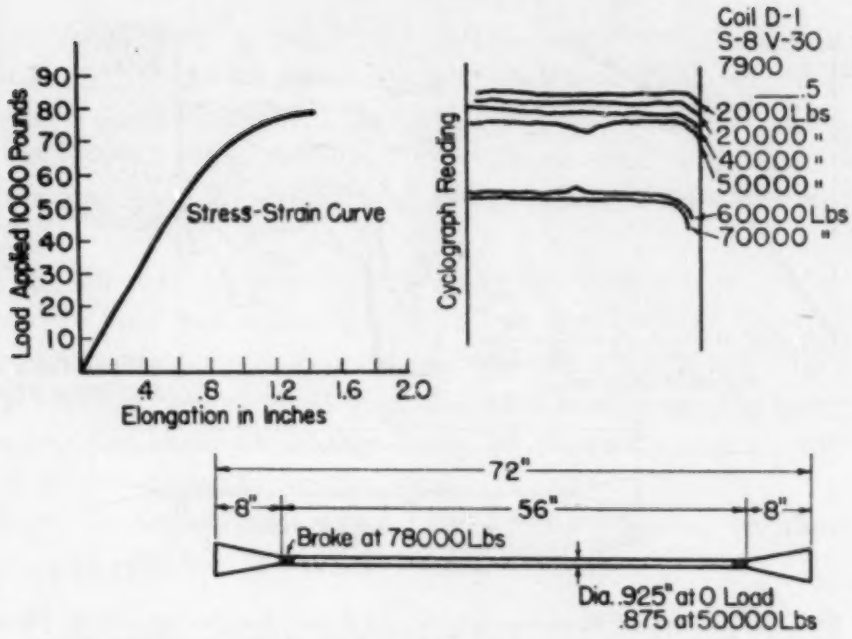


Fig. 19—Cyclograph Response in Test of Three Samples of 1-Inch Flattened Strand Rope Removed from the Skip Compartment of the Paymaster Mines.

Sample 12

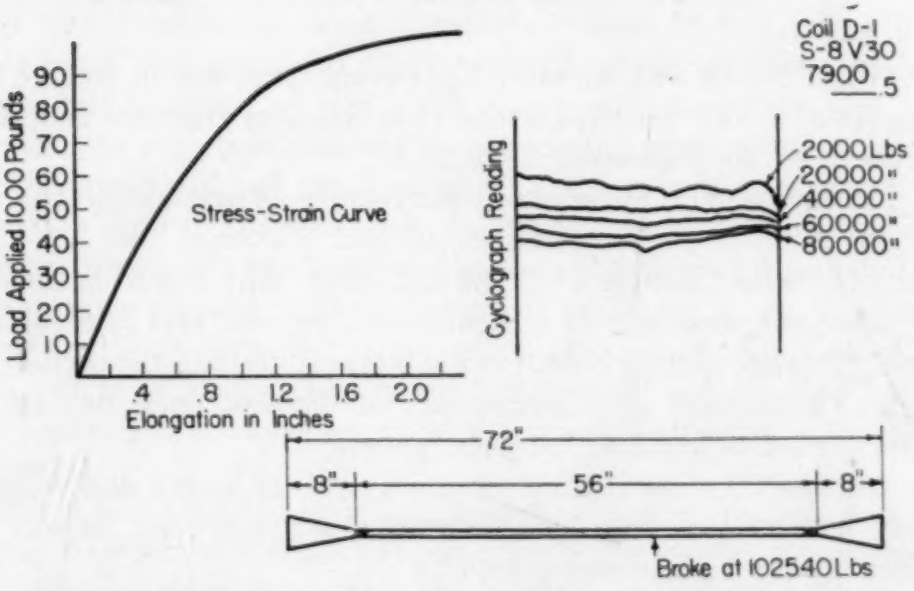


Fig. 20—Cyclograph Response in Test of Three Samples of 1-Inch Flattened Strand Rope Removed from the Skip Compartment of the Paymaster Mines.

Sample 25

Field Tests to Determine Whether Tests Could Be Carried Out Under Operating Conditions

It was not possible to duplicate operating conditions in the laboratory so a series of tests was undertaken to determine the effect

on the Cyclograph readings of rope speed, twist, vibration, etc., and to determine if it would be possible to obtain reliable readings on ropes under operating conditions.

It was found that quite satisfactory charts could be obtained at the usual hoisting speeds and without seriously interrupting normal hoisting operations. Once the apparatus was calibrated, it was possible to determine the suspended load on the rope from the Cyclograph readings. Changes in stress due to acceleration and deceleration were also noted.

None of the ropes tested proved to be faulty. Tensile tests were made on sections taken from portions of ropes where the Cyclograph readings departed appreciably from the average. The tensile tests showed that the ultimate strength of the rope had not been impaired.

In more recent laboratory work similar variations in Cyclograph readings have been produced artificially by straining some wires in the rope a little beyond their yield point (5). The cold working so produced alters the structure and changes the Cyclograph response, but may actually increase the ultimate strength, and sometimes the fatigue life. The important fact is that a stress concentration is causing some lattice distortion at such a point. Further distortion at this point will ultimately result in significant damage to the rope.

The Ontario Department of Mines kindly arranged with Dome and Hollinger Mines for the tests which were conducted on their ropes between September 25 and October 5, 1945. The first work was done at the Dome No. 6 shaft at Timmins, Ontario, Canada, under very favorable conditions, thanks to the generous co-operation of the mine staff.

The Cyclograph was set up on a platform in the headframe and using suitable split coil forms and a simple winding jig, coils were wound in place without disturbing the hoisting rope. An Esterline-Angus recording milliammeter was connected to the Cyclograph to permit making a permanent record. After some preliminary tests the recorder was set up in the hoist room and the paper driving mechanism connected to the hoist through an appropriate drive, so that movement of the paper in the recorder was proportional to movement of the hoisting rope. The hoist was operated at various speeds up to the maximum of approximately 1200 feet per minute and with various loads.

Data from typical charts produced by this means are shown in Fig. 21. It will be noted that except for about 100 feet of rope

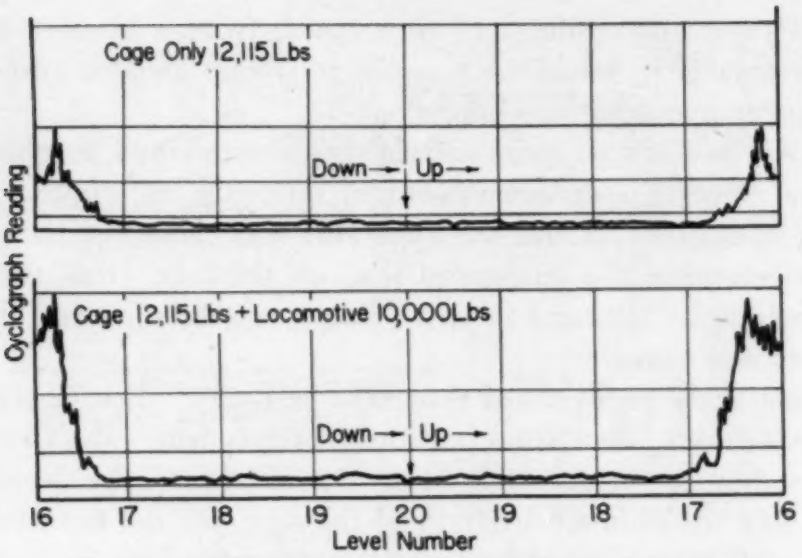


Fig. 21—Cyclograph Charts Made on Platform in the Headframe of Dome Mine Number 6 Shaft.

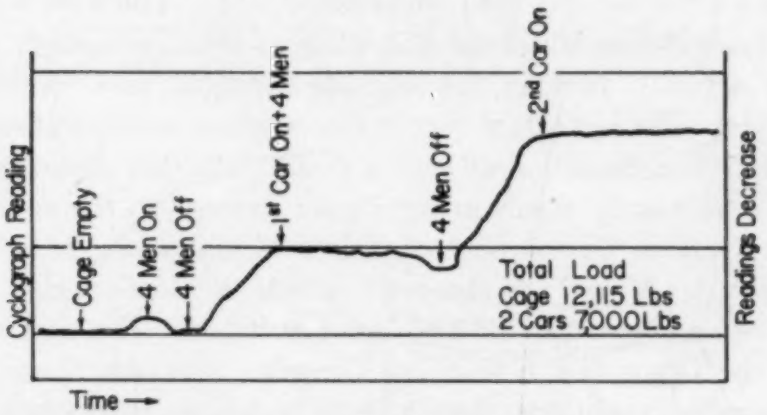


Fig. 22—Cyclograph Charts Made on Platform in the Headframe of Dome Mine Number 6 Shaft.

adjacent to the skip the record is quite uniform. It will also be noted that the addition of 10,000 pounds to the suspended load caused the recorded line to shift but did not change the general characteristics.

The chart shown in Fig. 22 was produced using a comparatively high sensitivity on the Cyclograph and by changing the load without moving the rope. It will be noted that it was possible to record a change of only a few hundred pounds in the suspended load.

Tests were also made on the two skip ropes. Here again the record as shown in Fig. 23 is remarkably uniform except for a short section adjacent to the clamps.

It was found that "bumps" could be produced in the chart by applying the brakes rather suddenly when the hoist was in motion.

Except for this and the fact that at very high speeds friction between the pen and paper in the recorder and circuit inertia tended to prevent recording extremely sharp changes, speed variations did not appear to make any appreciable differences in the charts.

The No. 10 rope on the skip at the No. 1 shaft of the Hollinger Consolidated Ross Mine was about due for replacement at the time of the tests and so arrangements were made to test this rope before it was removed.

In this case the Cyclograph was set up in the hoist house and

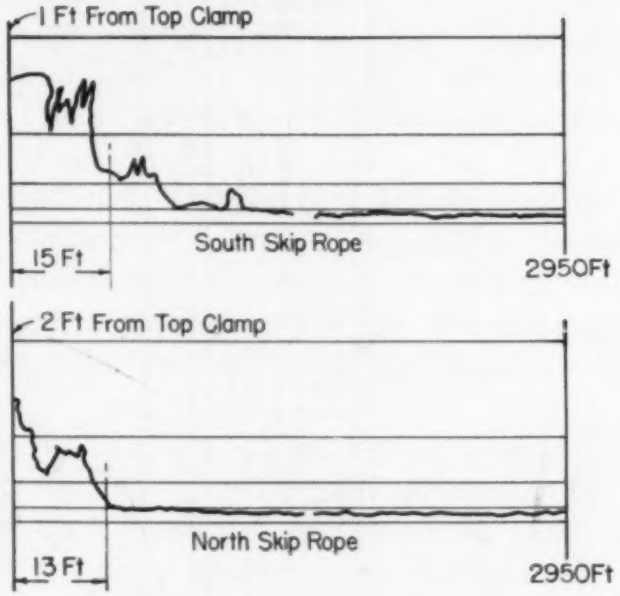


Fig. 23—Cyclograph Charts Made on Platform in the Headframe of Dome Mine Number 6 Shaft.

the coil, wound in place on the rope, was suspended on two wires strung one above and one below the rope slot in the hoist house wall. This permitted the coil to move with the rope as it wound on or off across the face of the drum. Hoisting operations were held up only half an hour while the equipment was being set up and it is felt that this time could be reduced considerably. The paper drive on the recorder was again connected to the hoist and quite satisfactory records were secured at the normal hoisting speed of 1125 feet per minute.

It was anticipated that some trouble would be experienced in locating defects which might occur in only ½ or 1-inch of rope length. Since the test coil only examines about ½ inch of rope length at a time, the speed of response of the instrument circuits would have

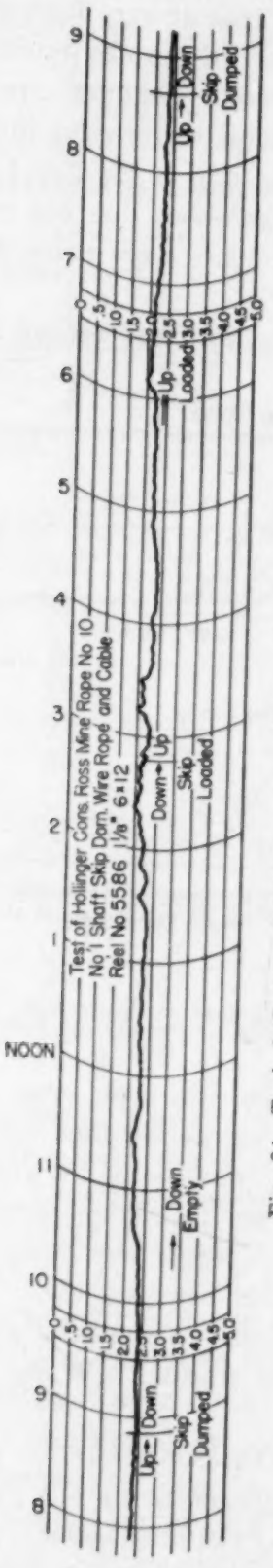


Fig. 24—Typical Cyclograph Charts Taken During Normal Hoisting Operations.

to be very rapid to receive a signal of this type and duration at a hoisting speed of 1000 feet per minute rope travel. Fortunately, due to the efficiency of wire rope in distributing an increased load, the problem is simplified since the increase in unit stress caused by a defect is extended over a considerable length on either side of the defect and allows adequate time for the instrument circuits to respond to any change in properties at maximum hoisting speeds.

Typical charts taken during normal hoisting operations are shown in Fig. 24. Samples were cut from this rope and subjected to tensile tests.

Samples were also cut from the end of the Dome cage rope starting at 7⅜ inches, 6 feet 7 inches, 12 feet 7 inches and 16 feet 7 inches from the top clamp. These have been given tensile tests and have proved to be sound as far as straight tensile tests could determine.

As stated before, it is considered that some of the first variations found in Cyclograph recordings are due to the effect of cold working which can increase the ultimate strength of the rope under some conditions. It is always necessary to determine the amount of change in reading which indicates that significant damage has been done to the rope.

The method indicated for using this test would be to take periodical recordings and set a limit for allowable variation of any portion of the rope from its normal reading under a certain load. By this means, any change in properties which would alter the Cyclograph response could only be due to a change in the unit stress in the rope or the beginning of plastic deformation which would ultimately lead to failure.

Development of Specail Portable Test Equipment

With data and experience gained in these laboratory and field tests, new portable apparatus has been developed primarily for rope testing work. In this apparatus features of the standard Cyclograph not required for rope testing have been eliminated and the circuits especially designed for the particular conditions encountered in the rope tests. This new apparatus is shown in Fig. 25.

The test coil connected by a short length of cable to the smaller unit is mounted in any convenient position such as in a headframe immediately below the sheave. A special cable in 100-foot lengths



Fig. 25—Du Mont Cable Tester.

is provided to connect this smaller unit to the main apparatus which may preferably be located in the hoist house. It is usually easy to arrange a drive from the hoist to the paper drive in the recorder so that movement of the paper will be proportional to movement of the hoist rope.

A block diagram of the instrument is shown in Fig. 26. Provision has been made for adjusting the instrument sensitivity either in the remote headframe unit or the main hoist room unit. Frequency response of the circuits has been adjusted to give optimum performance at the test frequencies used in the inspection of wire ropes. The d.c. output is provided from a circuit designed to operate an Esterline-Angus 1 mil. recording milliammeter. The meter reading increases as total core losses increase. By proper choice of test frequency and adjustment of instrument circuits, the meter response can be made linear with respect to increases in stress in the wire rope over a limited range. A 110-volt relay is also provided, which can be set to operate at any desired level. The operator can take periodic recordings over the length of the rope to determine whether or not any point on the rope has departed from its normal reading at a standard load and hoisting speed. The relay

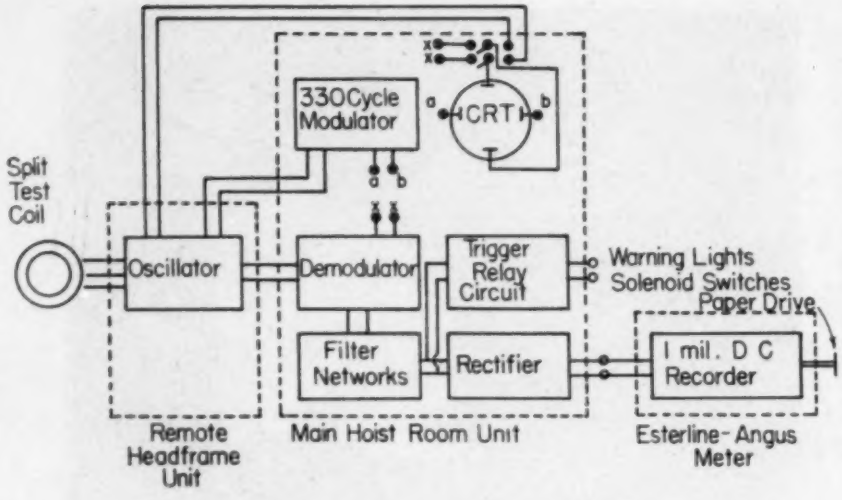


Fig. 26—Du Mont Wire Rope Tester.

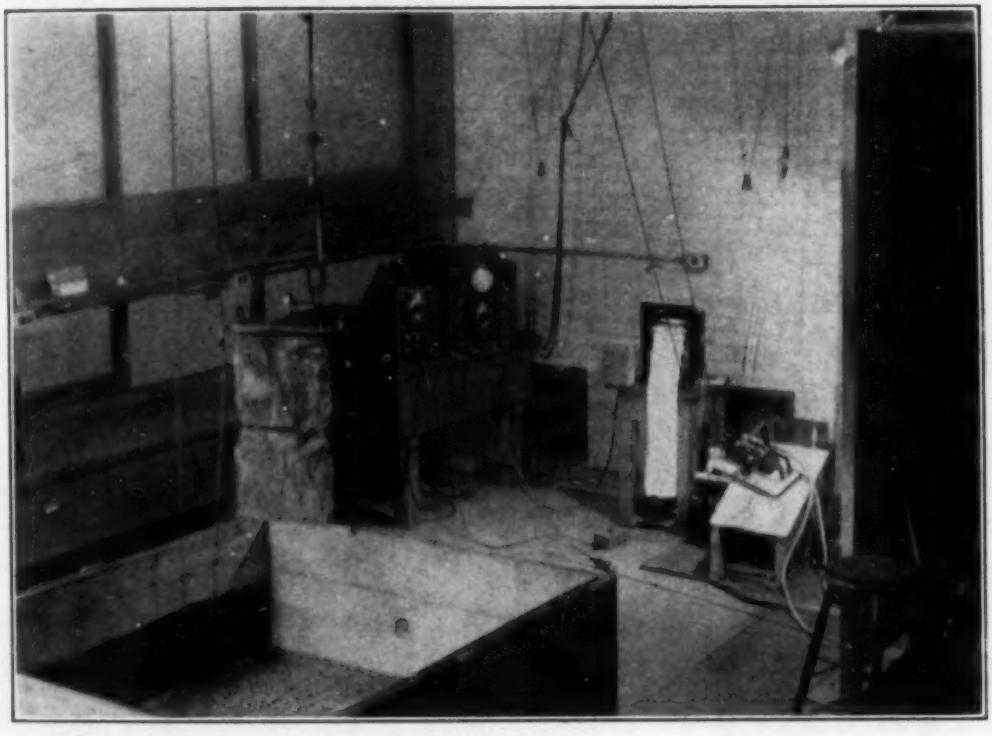


Fig. 27—Experimental Hoist and Cable Tester.

can be set at some specified limit so that if the properties of the rope change more than an allowable amount at any point at any time during normal operation, a warning light will operate. The same signal from the relay can also be used to start the recorder operating and take a continuous record as soon as some unusual condition arises.

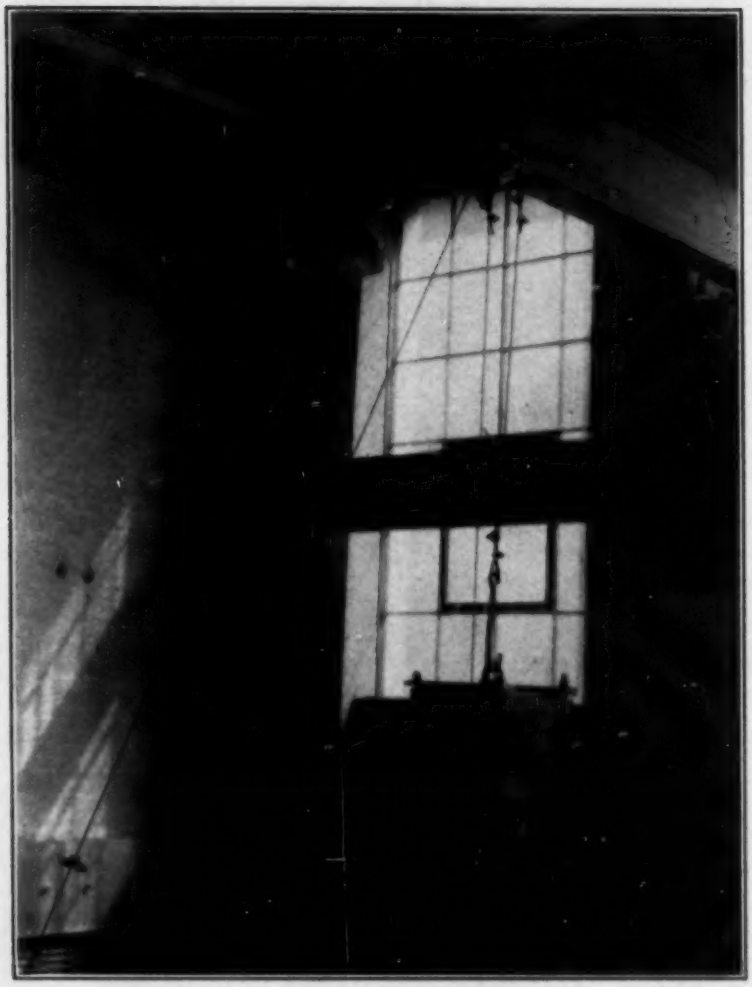


Fig. 28—Experimental Hoist Showing Overhead Sheaves and One 1000-Pound Weight.

Laboratory Tests on an Experimental Hoist

A series of tests has been undertaken in the laboratory of the Ontario Research Foundation where a model hoist has been set up. One-quarter-inch diameter ropes have been used. The general arrangement of the small hoist can be seen in Figs. 27 and 28. The hoist was deliberately designed so as to abuse the rope severely. The overhead sheaves are about one-quarter the proper diameter and the drum which drives the rope is much too small for proper operation. These features provide severe bending of the wire rope. The load applied to the rope is higher than the normal working load so that failure of the wire rope in this hoist is greatly accelerated.

In the first tests the rope was driven by means of a simple cap-

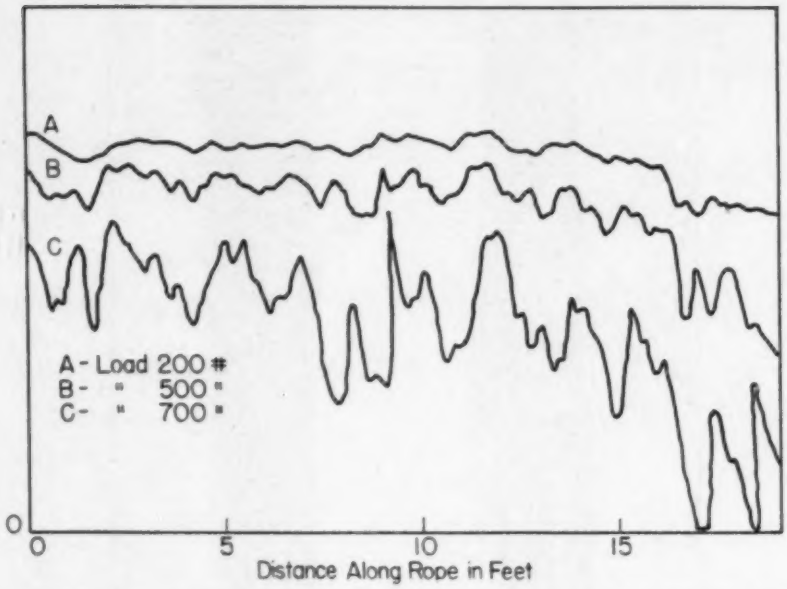


Fig. 29—Cyclograph Recordings Taken at Various Loads—Cable No. 1, Canada Wire and Cable Co. ¼-Inch Wire Rope.

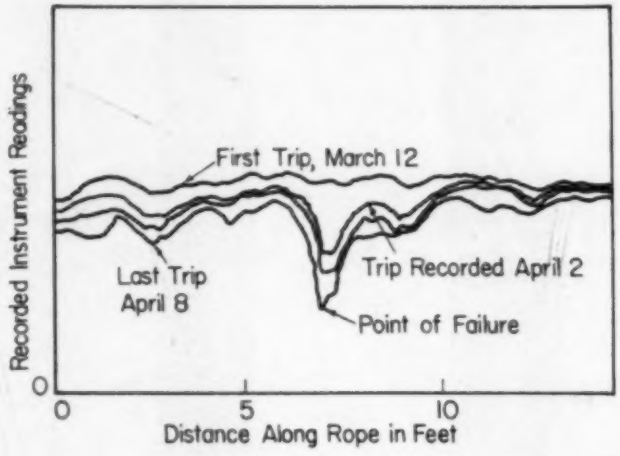


Fig. 30—Cyclograph Recordings Showing Progressive Failure in Rope of Fig. 29.

stan connected through suitable gearing and V belts to a 5 hp. motor. Limit switches were arranged to reverse the motor automatically at the end of each trip and a counter recorded the number of trips completed. A small chain and gear arrangement drove the recorder paper from the hoist drum.

It was discovered that torque introduced into the rope as it slipped over the capstan while winding on and off introduced complicated stresses which sometimes masked conditions it was desired to observe. In more recent work, the capstan has been replaced by a grooved drum which more nearly duplicates conditions encountered

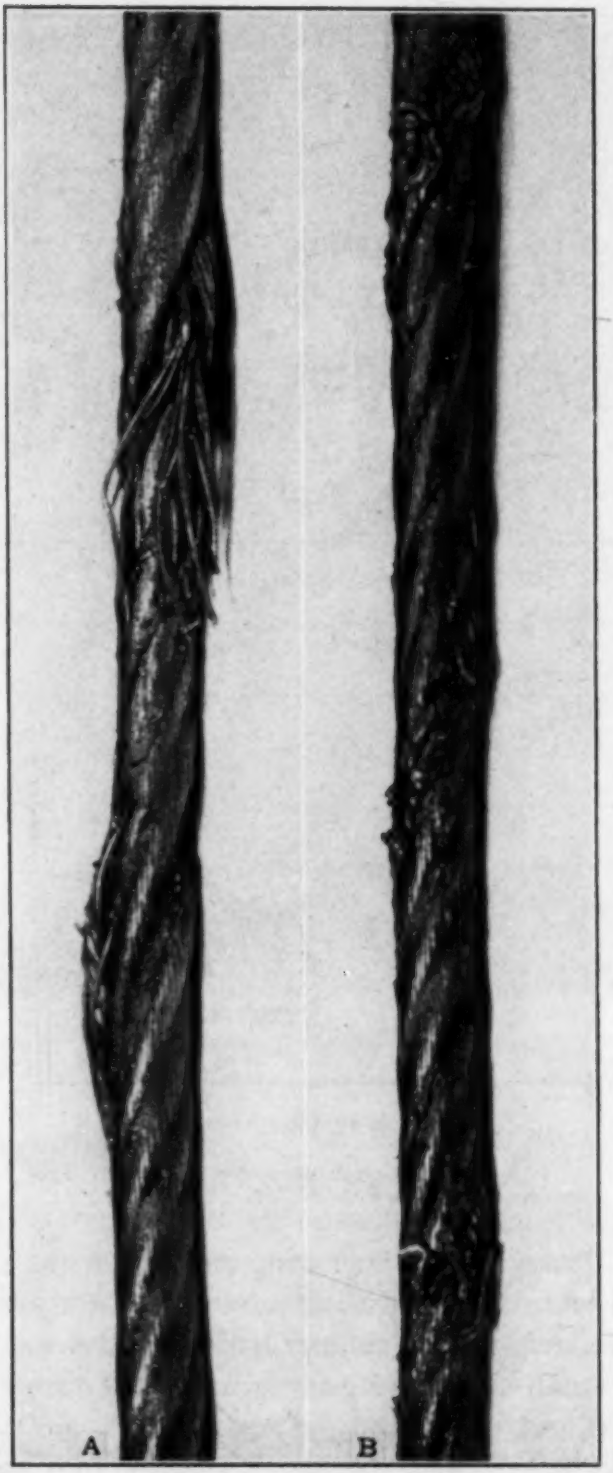


Fig. 31A—Failure Which Occurred at Point Indicated as Defective by Instrument—Cable No. 1—Canada Wire and Cable Co. ¼-Inch Wire Rope.

Fig. 31B—Typical Defect Which Developed at Several Points in Rope—Cable No. 2—Canada Wire and Cable Co. ¼-Inch Wire Rope.

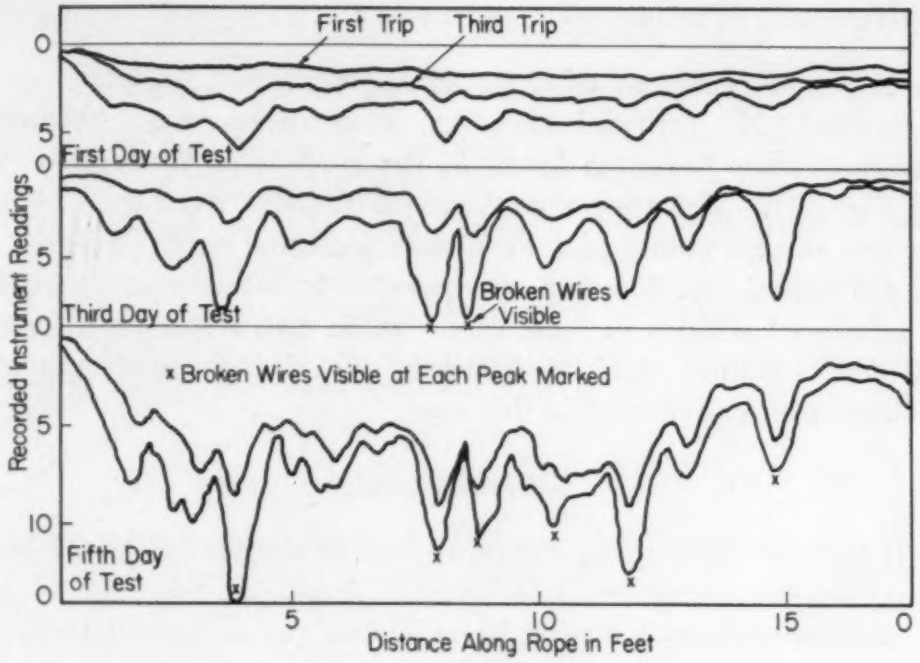


Fig. 32—Cyclograph Recordings of Cable No. 2 Carried to Destruction.

in normal wire rope service. Work with this equipment is continuing and will include further investigations of all normal rope faults as well as providing data on normal changes occurring in a rope throughout its working life.

Several ¼-inch wire ropes have been run to destruction in this experimental hoist and recordings taken as failure progressed.

Cable No. 1 (Canada Wire and Cable Co. ¼-Inch Wire Rope)

This rope was run at gradually increasing loads up to a maximum of 1000 pounds on each end. Typical recordings are shown in Fig. 29. An idea of the sensitivity of the instrument in terms of load in pounds per square inch may be obtained from this series of tests.

One point on the rope was next filed carefully with a flat file until about one-fifth of the diameter of the outer wires of the rope had been removed. The rope was then run to destruction. Failure occurred at the point which had been abraded by the file. Fig. 30 shows the record of the progression of failure in this rope. The photograph, Fig. 31A, shows the manner in which one strand parted at the point of failure.

Cable No. 2 (Canada Wire and Cable Co. ¼-Inch Wire Rope)

This rope was run with the 1000-pound load on each end to destruction. No artificial abrasion or corrosion was performed. Individual wires began to break in the rope after three days' test (see Fig. 32). The rope was examined visually from time to time after this as new points of failure were indicated on the graph. As each sharp peak developed, it was possible to locate visually broken and misplaced strands in most cases but in two instances no visual indication of failure could be observed. Fig. 31B illustrates the type of failure which developed in this rope.

Conclusions

It has been shown that it is now possible, without seriously interrupting normal operations and without damaging the rope in any way, to obtain charts with the Rope Tester (as developed from the Cyclograph) which will give a measure of the stress in a rope. It is considered that it may ultimately be possible to determine the condition of a rope at all points throughout most of its length from a study of such charts, taken over a period of time while the rope is in normal use.

The course now being followed involves continuation of the laboratory tests now in hand and also extensive regular field tests. The latter consist of taking charts of a number of ropes in regular service in mine shafts at periods of not more than a month as well as daily or even hourly charts on one or two selected ropes. Such a program will make it possible to build up data and develop technique to obtain the maximum possible benefit from the very promising possibilities which seem to be offered by this apparatus (7).

Acknowledgment

The authors wish to acknowledge the assistance given this investigation by the Minister of Mines for Ontario, the Committee for the Paymaster Mines Disaster, and the staffs of the gold mines in the Timmins and Porcupine area of Ontario.

References

1. Curtiss-Wright Corporation, "A Study for the Improvement of Fabricating and Handling Aircraft Control Cable," Report No. V-258 D4, February 1945, p. 40.

2. P. E. Cavanagh, "High Frequency Devices for Establishing Identity," METAL PROGRESS, American Society for Metals, Vol. 48, No. 4, October 1945, p. 1000.
3. "The Cyclograph," *Electronic Industries,* November 1943, p. 86, 87, 238 and 240.
4. P. E. Cavanagh, "Stress Comparisons by Correlation with High Frequency Magnetic and Eddy Current Losses," TRANSACTIONS, American Society for Metals, Vol. 36, 1946, p. 137-164.
5. P. E. Cavanagh, "A Method for Predicting Failure of Metals," *Proceedings,* American Society for Testing Materials, Vol. 46, 1946.
6. R. S. Segsworth, "Examination of Wire Rope With the Cyclograph, Report of Field Tests," General Engineering Co. (Canada), Ltd., report of January 29, 1946.
7. Report of the Committee on the Paymaster Mines Disaster, Province of Ontario Dept. of Mines.

DISCUSSION

Written Discussion: By T. W. Wlodek, metallurgist, Physical Metallurgy Research Laboratories, Canada Department of Mines and Resources, Ottawa, Ontario, Canada.

From the results presented in this research paper by P. E. Cavanagh and R. S. Segsworth we have learned that the Cavanagh high-frequency magnetic method for the inspection of mining hoist ropes is quite ready to leave the laboratory stage and to undergo actual field tests for the benefit of the safety of miners.

Especially at present, because of the development of improved working conditions aiming to increase the safety of the miners, this method will be welcomed both by companies and the working community.

As we have seen, Cavanagh's method may be used for the following two purposes amongst others:

1. To detect corrosion, broken wires, etc., indirectly, by revealing the stress concentrations caused along the cable by these defects.
2. To detect the progress of plastic deformation in working cable and determine the places showing stress concentration caused by excessive plastic deformation.

A variety of magnetic methods and instruments are at present in use for periodic inspection of members whose safety is important, e.g., railway tracks, and steel cables used in the mining industry or in transportation. These methods are based mainly on measurements of magnetic stray fields, using AC and DC.

As described by the authors, the application of the high-frequency method to the inspection of wire rope is a considerable step forward in the development of a magnetic method suitable for nondestructive examination of metals and for constant inspection of important elements.

In the United States and Canada the interest of engineers is directed increasingly toward the magnetic analysis of metals. Particularly now, when the fundamental physical basis of ferromagnetism has been greatly advanced, metallurgical engineers are more encouraged to take full advantage of this tool, which is sponsored by DuMont and the Ontario Research Foundation.

This nondestructive method for the inspection of wire rope in service is very promising. Have the authors collected some observations on the stability of the cyclograph reading obtained when using wire rope that has been purposely stabilized magnetically, for example, by (a) magnetization in strong or weak fields directed longitudinally or transversely to rope, or (b) magnetization to a chosen value of saturation and placing the rope in such a direction in the magnetic field that the remanent magnetism will be directed in accordance with the corresponding component of the earth's field, or (c) demagnetization along the whole length?

It is known that the magnitude and sign of the magnetostriction are influenced also by the magnitude of the remanent magnetization, and it might be advisable, in examining a long wire rope in a mine shaft, to check the magnetic state. This state may have some influence on the high-frequency magnetic method.

Also, in view of the fact that the electrical resistance increases with the longitudinal tension for positive magnetostriction and decreases for negative magnetostriction, and, on the other hand, the magnitude and sign of the magnetostriction of steel depend on the tension applied and on the distribution of vectors of spontaneous magnetization of domains, I feel that the equalization of the magnetic state of the whole cable might have an effect on the cyclograph reading. What, at present, is the opinion of the authors upon this point?

It would be very interesting to know if the Cavanagh method would allow one to measure, in addition to the measurements described by the authors, the difference in core losses at two points on the wire rope. This differential high-frequency magnetic method might allow one to increase the sensitivity of reading and will show directly the differences in cyclograph readings at two points on the rope. The differential readings will not show the progress of changes in cyclograph characteristics with the time of use, but only the differences between two points.

It might also be easier to set up the relay for an arbitrary limit of allowed maximum difference of cyclograph readings measured at two points on the rope.

Written Discussion: By O. W. Ellis, director, Department of Engineering and Metallurgy, Ontario Research Foundation, Toronto, Canada.

The authors are to be congratulated on the excellent report of their work on this important problem. Their paper covers the subject so completely that one is rather at a loss to find matter for discussion. There are one or two points, however, on which the speaker would ask for enlightenment.

The authors remark that "In preliminary experiments, it was found that a certain range of test frequencies would give the desired results for a certain diameter of rope but that a higher or lower frequency might give an indication in one sense for broken wire and an indication in the other sense for corroded wires". In view of what seems at first glance to be the likelihood that both the rupture and the corrosion of wires in a rope would lead to an increase in stress in the undamaged wires, why should these two factors lead to what appear to be opposite effects?

In commenting on Fig. 6 which shows the change in the cyclograph reading when the load on a new rope is repeatedly varied between 20,000 and

50,000 pounds, the authors state that "The normal stretching of a new rope is accompanied by a permanent change in magnetic properties from their initial value to some new level at any given load". Is this permanent change in magnetic properties due to permanent changes in the physical state of the individual wires in the rope or is it occasioned by realignment of the wires within the rope due to stretching? Presumably the change is due to a change in the physical state of the individual wires, if one is to accept the statement made earlier in the paper that the cyclograph "is not particularly sensitive to small changes in volume of the sample." Could the authors elaborate on this point? Did they make any observations of changes in the mean diameters of the ropes when the same were under load in these particular tests?

Would the authors comment on their statement to the effect that "the increase in unit stress caused by a defect is extended over a considerable length on either side of the defect and allows adequate time for the instrument circuits to respond to any change in properties at maximum hoisting speeds"? By what mechanism is the increase in unit stress extended over the length of the wire in the vicinity of a defect?

Lastly, in what way do the overhead sheaves in the experimental hoist affect the behavior of the rope undergoing test, in view of the fact that that portion of the rope undergoing test at no time passes over these sheaves?

Once again, the speaker wishes to reiterate his belief that this work is of fundamental importance. Any method of nondestructive testing of wire rope which can predict failure is worthy of investigation, particularly when such investigations at the same time reveal something of the physical nature of the materials under test.

Written Discussion: By R. E. Dye, general manager, Dome Mines Limited, South Porcupine, Ontario, Canada.

The investigations reported in this paper are unquestionably of the greatest interest to the mining industry. Development of a reliable nondestructive method for the accurate determination of the condition of a wire rope throughout its length while the rope is in use has been attempted by many. The attainment of success in this would add materially to the service which could be obtained with safety from wire hoisting ropes. Of far greater importance than any monetary advantage which might emerge is the fact that with such a method available the industry could introduce safety features surpassing those now prevailing.

Investigations by the authors of the paper presented appear to have established the fact that it is possible to make observations by the use of the cyclograph (or a modification of it) which is definitely related to the stress in a rope subjected to test, or in the wires of which the rope is constructed.

The authors of the paper admit, indeed stress, the fact that the accurate interpretation of readings will require further study, as well as the building up of a background of experience through field observations during the life of ropes in service.

A study of the graphs in Fig. 30 showing the progressive development of the failure point at the point at which the outer wires of the rope were filed (not initial "dip" but a rapid development of a "dip" as the test pro-

gressed), coupled with a consideration of the graphs in Fig. 32 where observable broken wires mark the position of successive "dips" in the graphs, leads to the thought that perhaps a residual condition in a wire already broken, or the condition of a single wire which is on the point of breaking, may be the dominating influence in obtaining some of the high curve deflections which are not now readily explained.

To investigate this possibility, if it has not already been eliminated by work done but not recorded in the paper, I believe that it would be worth while to make observations with the rope tester on a single group of say 114 straight wire rope wires which were arranged so that the load on the greater part of the group could be held at a constant figure while the load on each of two or three of the individual wires making up the group could be increased separately up to the breaking point. An experiment or series of tests designed along some such line would highlight the influence on readings exerted by excessive punishment suffered by a single wire which, in the case of a 6 by 19 cable, would be less than 5% of the cross section of the cable.

Having made these few comments with regard to the paper presented, I take this occasion to congratulate the authors—not only upon the timely nature of their contribution, but upon the skill and clarity with which they deal with the subject.

Authors' Reply

As Mr. Wlodek says, a known state of magnetization is necessary for successful use of the high frequency core loss method on wire rope in service. After considerable experiment, the stable state of magnetization reached in the earth's field after initial magnetic "aging" at service loads has been chosen as the reference state. The initial random orientation of domains has been somewhat altered, but under service conditions of vibration, no further permanent change will take place unless lattice distortion or plastic deformation occurs.

Experiments were conducted to determine the effect of permanently magnetizing a rope locally, both longitudinally and transversely. As would be expected, no significant difference in the stress-core loss relationship was produced until fields near saturation were used.

Even where high values of remanent magnetism were produced, the effect on core losses could be ignored. Where a wire rope had been strongly magnetized, a local increase in core losses would be produced. This portion of the recording would stay constant as would any other portion, unless lattice distortion occurred.

To summarize our conclusions on this question, the natural magnetized state encountered in normal service seems the most satisfactory standard state of magnetization, since service vibration is sufficient to prevent spurious results from temporary changes in distribution of magnetization vectors. The advantages which might be gained from complete demagnetization or saturation do not seem worth the trouble. While variations in state of magnetization do occur in the length of a rope in service, they do not interfere with this type of test.

The differential test method suggested would be quite feasible and would have the considerable advantages described by Mr. Wlodek. However, interpretation of results would be very different. This method may come into use later as a supplement to the present development. The readings obtained would indicate differences in analysis, cold working history, internal stresses and strain in the rope. The task of interpreting the indications which would be obtained seems almost impossible at present. It may be that some of the work Mr. Wlodek is doing on magnetostriction will give some useful practical information which will help in direct practical interpretation of magnetic changes in wire.

The present method of test carefully avoids direct interpretation of magnetic changes and provides practical results by watching continuing change only. When the understanding and interpretation of variations in magnetic properties have advanced sufficiently, it may be possible and would be desirable to develop a differential method, as suggested, to provide supplementary detailed information on the state of a wire rope. It is not possible with the cable tester to examine a rope which has never been tested before and obtain a complete picture of its present condition. A differential method might possibly be of some use in such a case.

In regard to the first question by Dr. O. W. Ellis, with respect to the direction of change in core loss for different types of defects at certain frequencies, no detailed satisfactory answer can be given at present. At higher frequencies we believe this effect is not entirely due to the well-known Villari reversal. At low test frequencies magnetic effects predominate, and the reversal in sign of magnetization changes at higher values of stress in steel does cause an increase in some magnetic properties for some defects and a decrease in the same properties for other defects.

One possible explanation for higher frequency behavior is that the total high frequency core losses affecting this instrument depend upon the properties of the material and also upon total flux penetration, which determines the volume of material included in the test field. Changes in electrical resistance do follow the behavior of magnetostriction at the Villari reversal. In addition, at higher test frequencies, flux penetration is affected greatly by changes in resistivity and permeability of the material. It is conceivable that breaking wires in a rope will change load distribution, and therefore flux penetration, sufficiently so that conditions are not comparable to an instance where corrosion produces the same decrease in rope strength. The method of distribution of the additional load on the remaining material may be different for corrosion and broken strands. When the rope is corroded, there is ample time for the load to be evenly distributed. The difference in stress distribution may have sufficient effect on permeability and flux distribution to give rise to the observed differences.

The differences in sign of indication noted (at higher frequencies) between bruised or kinked ropes and other types of defects are more easily understood, since plastic deformation will definitely change flux penetration considerably at high test frequencies and will lead to unpredictable changes in core losses with increasing stress.

With regard to the "magnetic aging" of a new rope, this is due to changes in the magnetic state of the individual wires. The same phenomena can be observed on a solid bar. No doubt some proportion of the change is also due to minor adjustments of the wires within the rope. No observations on rope diameters were made during these aging tests. The cyclograph was originally designed to be relatively insensitive to volume changes. A variation of less than 10% of the volume in samples under normal test conditions does not produce a significant change in reading.

From the viewpoint of this test method, the ability of a wire rope to distribute an increase in unit stress over a considerable length is a very pleasing property. As noted during work under static tension, binding and friction between wires can apparently transmit to broken wires a large proportion of their original load in a very short distance from the break. Vibrating the rope or reducing the load allows the broken wires to slip and forces the remaining wires to bear the full load for a greater distance from the break.

A similar mechanism will bring about a gradual change from the new high unit stress at the location of any weak spot, where one or more wires are not carrying their share of the load, to the original unit stress in the sound cable at a distance from this point.

The experimental hoist in use at present represents an attempt to approximate severe mine hoisting conditions. No matter where a single test coil is located, there will be a portion of the rope which is not inspected. In the tests reported to date, the overhead sheaves had no effect on results. A series of tests is contemplated in which all portions of the rope will be examined by multiple coils. In these experiments, the influence of the sheaves will be determined.

The comment by R. E. Dye, regarding the disproportionate influence of a single wire which has been plastically deformed, is very interesting. We know that the rate of change in magnetic properties with increasing stress increases sharply as plastic deformation starts. It is undoubtedly the case that a few plastically deformed wires in a rope will produce a disproportionately large increase in core losses with increasing stress. This means that the linear relationship at first established between stress and core losses for a sound rope in the elastic range will no longer hold true. In a rope with one or more plastically deformed strands, the core losses will increase much more rapidly with increasing stress than is the case with the original sound rope. This fact explains the reason for the great sensitivity of the core loss method to cold working damage produced by kinking or bruising. The core loss method can reasonably be expected to indicate easily a decrease in rope strength of the order of 5% due to corrosion or abrasion, or even less if local cold working is involved.

It is fortunate that we do not have to interpret the magnitude of all changes in core loss in terms of per cent damage. The conception that only a continuing change can result in failure greatly simplifies the problem. It is possible to set a maximum value beyond which continuing change becomes dangerous, but it is not necessary—or indeed possible at present—to interpret all core loss changes in terms of rope strength.

INFLUENCE OF THE STRAIN RATE AND THE STRESS SYSTEM ON THE MECHANICAL PROPERTIES OF COPPER

By D. J. McAdam, Jr., G. W. Geil and D. H. Woodard

Abstract

By means of slow tension tests of differently notched specimens a study has been made of the influence of the notch angle on the flow stress, ultimate stress, and breaking stress of cold-rolled oxygen-free copper. The results show the influence of the ratio of transverse to longitudinal tensile stress on the flow stress and technical cohesion limit. Comparison of these results with previously obtained results of ordinary tension tests shows the influence of the difference in strain rate on the technical cohesive strength. Diagrams are presented to show the combined influences of strain rate and stress system on the technical cohesion limit. Consideration is also given to the equivalents of increase in temperature and decrease in strain rate in their effects on cohesive strength and ductility.

Introduction

IN a series of papers (2) to (11),[1] it has been shown that the resistance of a metal to fracture, its technical cohesive strength, depends on all three principal stresses.[2] The technical cohesive strength thus comprises an infinite number of technical cohesion limits, each corresponding to a specific combination of the principal stresses. It has been shown also that the technical cohesive strength varies with the stress system (2) to (11), plastic deformation (2) to (11), temperature (6), (7), (9), (10), (12), and the strain rate (12),

[1]The figures appearing in parentheses pertain to the references appended to this paper.

[2]Any stress system may be resolved into three principal stresses normal to three mutually perpendicular planes, known as the principal planes, on which there is no shearing stress. Tensile stresses are viewed as positive, and compressive stresses as negative. In this paper as in previous papers, the algebraically greatest principal stress will be designated S_1, the least principal stress will be designated S_3, and the intermediate principal stress will be designated S_2.

A paper presented before the Twenty-eighth Annual Convention of the Society held in Atlantic City November 18 to 22, 1946. The authors are associated with the National Bureau of Standards, Washington, D. C. Manuscript received July 22, 1946.

and that these variations are qualitatively the same as the corresponding variations of the flow stress.[3]

The most recent of the papers (12) shows the influence of the strain rate and temperature on resistance to fracture, flow stress, and ductility of monel metal and copper. That paper, however, is based primarily on results of creep tests of unnotched specimens. Attention, therefore, is confined to the influence of strain rate and temperature when the stress system is unidirectional tension ($S_2 = S_3 = 0$). The present paper presents results of an investigation of the influence of the stress system and the strain rate on the flow stress, technical cohesion limit, and ductility of copper. The paper is based on results of very slow tension tests at 110 F with variously notched specimens. These results are compared with results of creep tests of unnotched specimens and ordinary tension tests.

In many conditions of temperature and creep rate, the third stage[4] of creep of an unnotched specimen under a constant load begins when the rate of work hardening decreases below a certain value. As shown in a previous paper (12), however, the third stage sometimes is initiated by the formation and growth of microscopic cracks. The "true" stress at the beginning of this progressive disintegration is the technical cohesion limit corresponding to that combination of the stress system, amount of prior plastic deformation, temperature, and strain rate. Moreover, the "true ductility" is measured by the amount of plastic deformation at the beginning of the progressive disintegration, not at complete fracture (rupture). As shown in the previous paper (12), the technical cohesion limit, flow stress, and ductility for unidirectional tension increases with increase in the strain rate and with decrease in temperature. In the present paper, attention is given to the variation of the same properties with the strain rate and the stress system.

Method of Investigation, Specimens, Material and Apparatus

In this paper as in most of the previous papers (5) to (10), attention is confined to stress combinations with two of the principal stresses equal ($S_2 = S_3$). Such stress combinations would be produced by subjecting a cylinder to combinations of uniform axial and

[3] Flow stress is here used in its generally accepted significance to designate the greatest principal stress during flow.

[4] In the first stage of creep, under a constant load, the strain rate decreases; in the second stage, the rate is nearly constant; in the third stage, it increases. The relative duration of the second stage varies considerably with the temperature and the strain rate.

transverse radial stresses. The uniform radial stress may be resolved into two equal principal stresses, with the mutually perpendicular directions rotatable around the axis of the cylinder. Uniform radial tensile stress, however, cannot readily be produced in combination with uniform axial tensile stress. When a notched cylindrical specimen is subjected to longitudinal tension, the minimum section is under transverse radial tension. The mean radial stress tends to increase with the depth and sharpness of the notch, but is always less than the longitudinal stress. The transverse radial stress, however, is not uniform, and is always zero at the periphery of the minimum section. The longitudinal stress, moreover, is initially highest at the periphery. Even slight plastic deformation, however, greatly diminishes the concentration of longitudinal stress. The tangential and radial stresses after plastic deformation are nearly equal at any point in the minimum section except possibly at the periphery, where the radial stress remains zero. By the use of suitably designed notched specimens, the influence of the stress concentration is minimized, and the influence of the radial stress ratio (S_3/S_1) is revealed (5).

In the present investigation this purpose is attained by the use of deeply notched specimens (5). Nearly all the notches were of about the same depth ($k = \text{about } 0.16$),[5] but the notch angle (ω) varied greatly. The root radius (r) for the specimens tested at the slow rates, and for most of the specimens used in the ordinary tension tests, was 0.01 inch. For some of the specimens used in the ordinary tension tests the root radius was 0.004 or 0.001 inch. Most of the notched specimens were about 5½ inches long; those having large notch angles were necessarily somewhat longer. The ends of the specimens were threaded to ¾ inch in diameter. Between the threaded ends, each specimen was ⅞ inch in diameter. A circumferential V-notch of selected angle was machined at the mid-section; the notch radius was carefully machined so that the conical sides of the notch were tangent to the arc at the root. Care was taken also to avoid significant heating, bending, or appreciable cold working during machining.

The specimens were taken from the same cylindrical bar of oxygen-free copper that was used for the creep tests of unnotched specimens (12) and for the ordinary tension tests (5), (6). The bar had been cold-rolled by the manufacturers to 75% reduction of

[5]Notch depth is expressed in terms of the relative area ($k = b^2/B^2$) of the minimum cross section, when b and B are the minimum and maximum diameters of the specimen (see insert sketch of Fig. 2). Thus, the greater the notch depth, the smaller is the value of k.

cross section. It was supplied by the Scomet Engineering Co. through the co-operation of Mr. Sidney Rolle, assistant manager.

The apparatus used for the slow tension tests of notched specimens was the same that was used in the creep tests of unnotched specimens. A description of this apparatus is given in a paper by

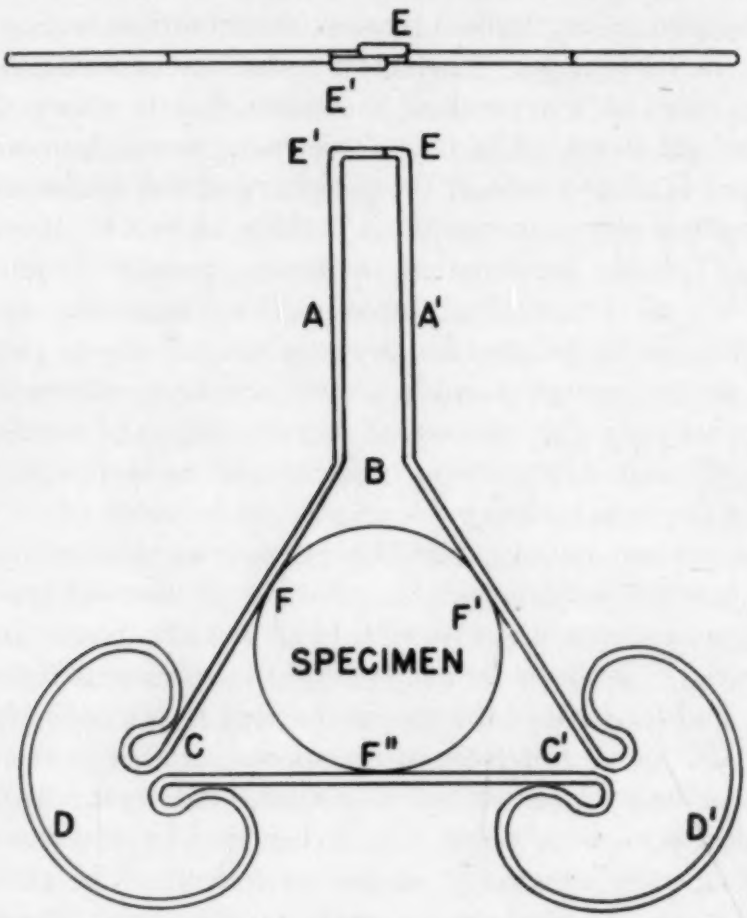


Fig. 1—Reductometer.

Bennett and McAdam (1). A description of the apparatus and methods used in the ordinary tension tests is given in a paper by McAdam and Mebs (5).

During the test of each of the specimens the extension was repeatedly measured by means of an optical extensometer (1). For a notched specimen, such measurements give merely qualitative indication of the strain rate in the minimum section. For quantitative determination of the strain rate, an apparatus was devised for measuring the variation of the diameter of the minimum section.[6] This "reductometer" consists of a single piece of spring steel wire of the

[6]This apparatus was designed by Dr. R. W. Mebs of the National Bureau of Standards.

form illustrated in Fig. 1. The large co-planar loops D and D′ permit enough movement at the corners C and C′ so that the reductometer makes contact with the specimen at three points (F, F′, and F″) nearly 120 degrees apart, and that the distance between the nearly parallel portions A and A′ varies as the diameter of the minimum section of the specimen changes during a tension test. Near the three points of contact, the wire has been ground to sharp edges so as to permit contact at the root of the V-notch in the specimen. Platinum strips with fine gage marks have been welded on the extended ends E and E′. The relative motion of these strips gives a magnified indication of the change in diameter of the specimen. This motion can be measured by means of the optical extensometer. The reductometer was calibrated by making measurements on a ductile unnotched specimen during an ordinary tension test.

As the temperature in the tests of notched specimens was only 110 F, ordinary spring steel wire proved satisfactory for the reductometer. For use at much higher temperatures, more heat resistant metal would be needed.

The Relation Between Stress, Time, and Plastic Deformation in the Slow Tension Tests

For a study of the variation of plastic deformation with stress and time it is necessary to correlate diagrams of two types. One of these types, illustrated by Fig. 2, shows the variation of plastic deformation with time; the other type, illustrated by Figs. 3 and 4, shows the relation between stress and plastic deformation.

In order to study the relation between extension and lateral contraction during the flow of metal in the vicinity of the notch, both these deformations have been expressed in terms of the initial diameter (b_o) of the minimum section. For small deformations of an unnotched specimen $\triangle L/L_o = 2\triangle b/b_o$, where L_o and L represent the initial and current lengths and b_o and b represent the initial and current diameters respectively. The same equation would apply to the plastic deformation of a notched specimen, if L_o be used to represent the length of an unnotched specimen that would give the same relation between longitudinal extension and lateral contraction. This relationship has been utilized in representing the deformations in Figs. 2, 3, and 4. For dimensionless representation, the longitudinal extensions have been represented in terms of $\triangle L/b_o$, and the trans-

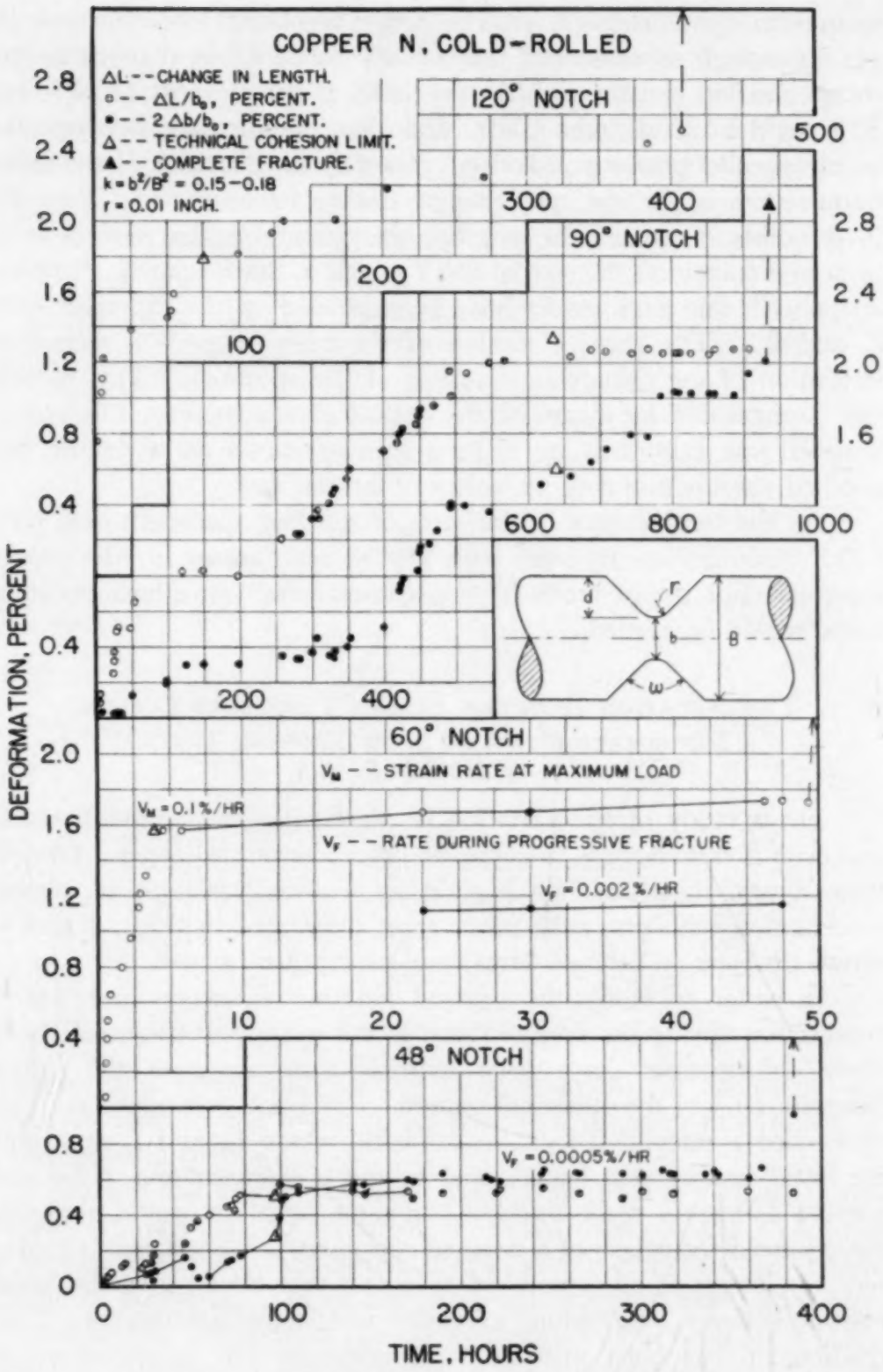


Fig. 2—Variation of Plastic Deformation With Time.

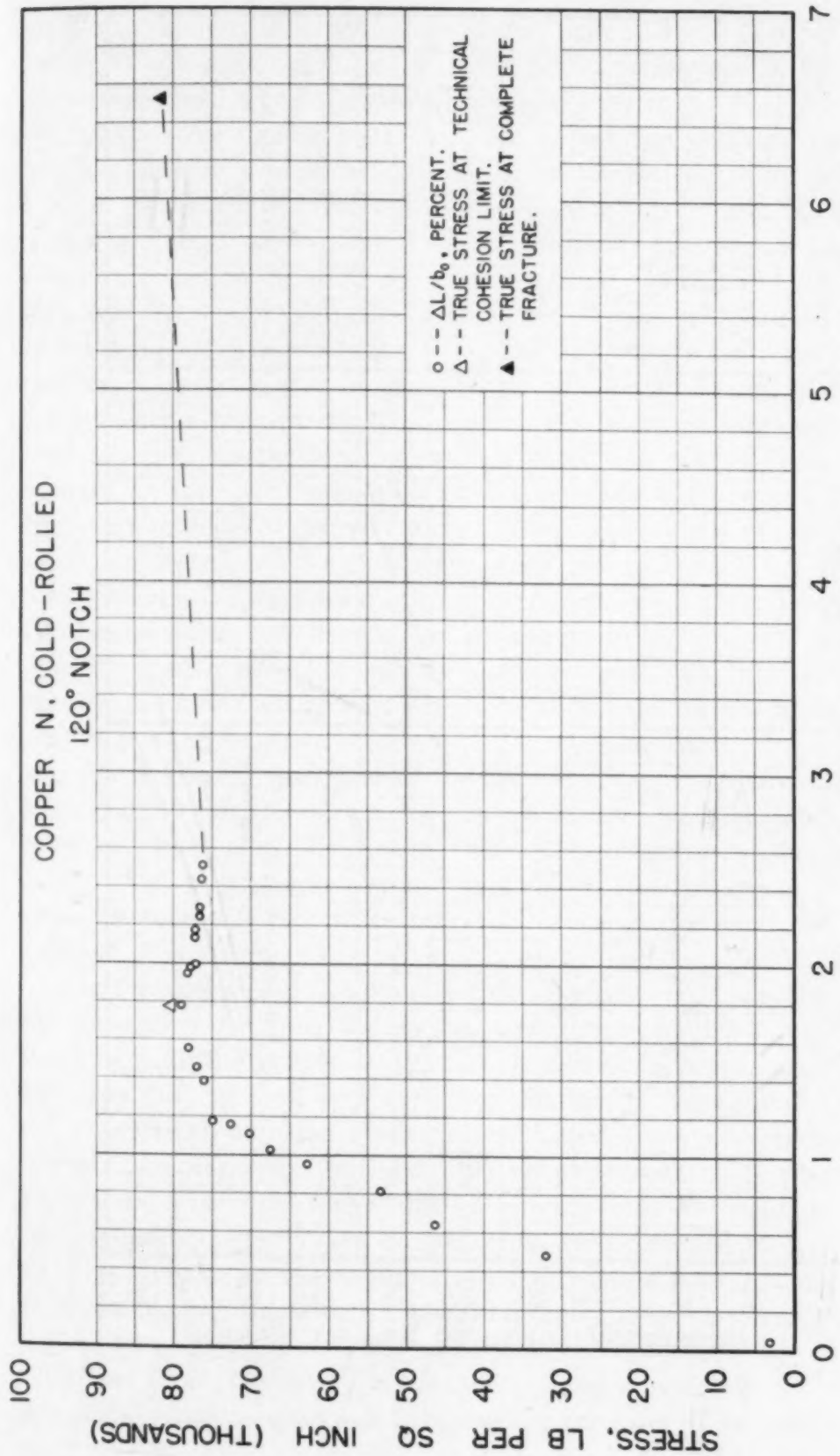


Fig. 3—Relation Between Stress and Plastic Deformation During Slow Tension Test of Notched Specimen.

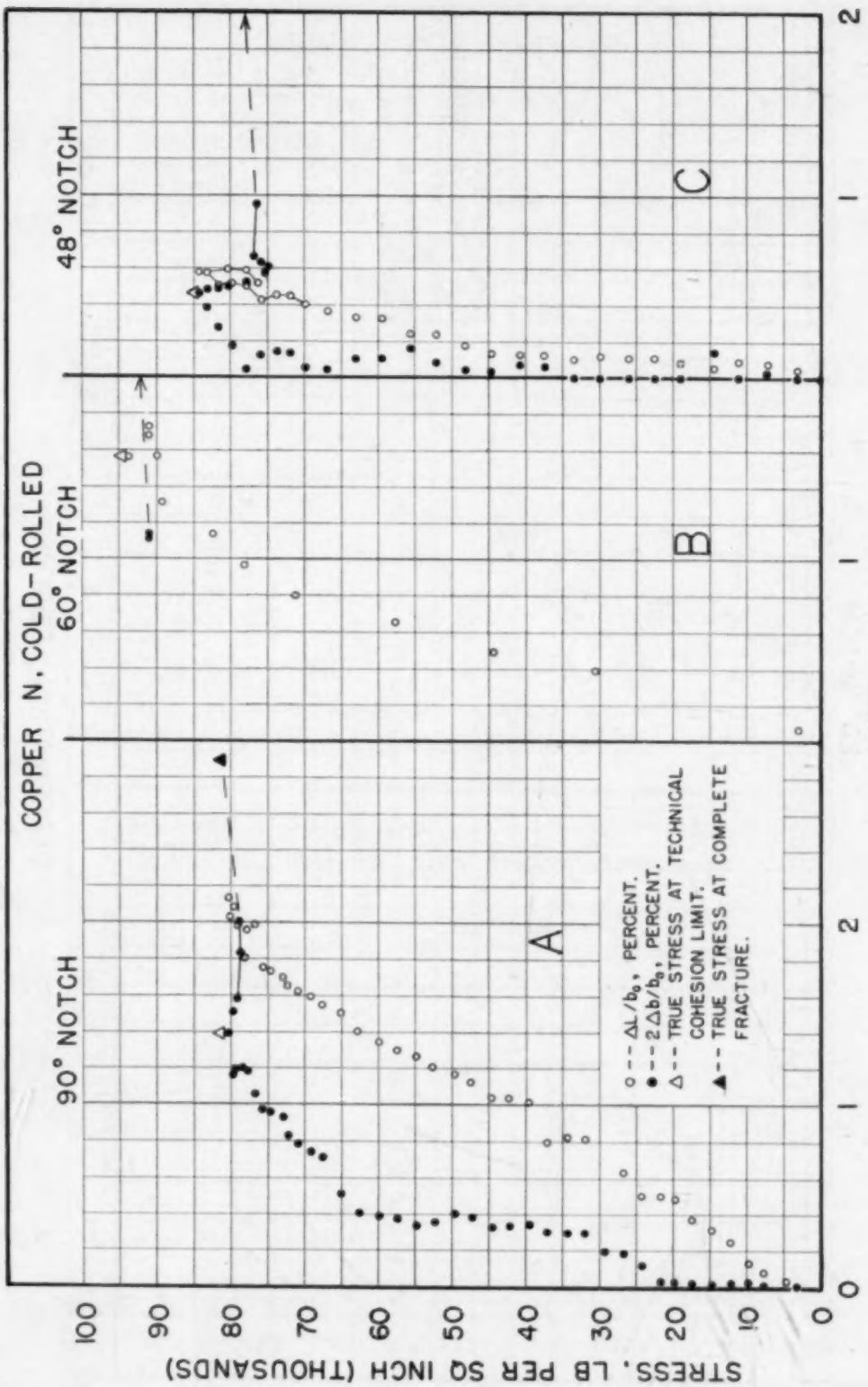


Fig. 4—Relation Between Stress and Plastic Deformation During Slow Tension Tests of Notched Specimens.

verse contractions have been represented in terms of $2 \triangle b/b_o$. The ratio of corresponding values of these two deformations is the ratio of the equivalent length L_o to the initial diameter b_o.

In the slow tension tests, as in an ordinary tension test, the load was increased gradually by repeated weight additions so as to cause a slow predetermined rate of deformation (Figs. 3 and 4). The weight additions were stopped when the strain rate began to accelerate, as it does in the third stage of an ordinary creep test. The load then was decreased gradually by repeated weight removals in order to maintain a fairly constant strain rate. In these experiments with notched specimens, the controlled rate was generally less than the average strain rate during the approach to the maximum load. The time required for the load to reach a maximum ranged from about 4 hours for the specimen with a 60-degree notch to 630 hours for the specimen with a 90-degree notch. A specimen with a 150-degree notch was tested, but the curves are not shown in Figs. 3 and 4. The time required for the load on this specimen to reach a maximum was 410 hours. The rate beyond the maximum load, however, was not properly controlled. Between two observations, the rate increased rapidly and the specimen broke. The final rate, in the absence of load control, must have been very high. Consequently, the ductility was much greater than that of any of the specimens represented in Figs. 3 and 4, and the stress at complete fracture was about twice the stress at maximum load. For the other specimens, the plastic deformation at complete fracture was slight, and the stress at complete fracture differed little from the stress at the maximum load (Figs. 3, 4, and 6).

In the first of the slow tension tests, the test of the specimen with the 120-degree notch, no transverse strain gage was available. Only the longitudinal extensions ($\triangle L/b_o$), therefore, were determined, and only one curve of each type was obtained (Figs. 2 and 3). In the experiment with the 60-degree specimen, the reductometer was not used successfully until late in the experiment. In the other experiments, both the longitudinal and transverse deformations were determined and two curves of each type were obtained (Figs. 2 and 4). As the elastic deformations could not be determined, and were small in comparison with the plastic deformations, no correction for the elastic component of deformation has been made.

The small triangles in Figs. 2, 3, and 4 indicate the "true" stresses at maximum load and at complete fracture. The small circles

indicate stresses and strains immediately before changes in the load. The stresses thus indicated are nominal stresses, obtained by dividing the load by the initial area of cross section. Other measurements were made between weight changes, but results have not been plotted.

During the slow extension of a notched specimen, the relation between the transverse and longitudinal deformations evidently varies greatly (Figs. 2, 3, and 4). Plastic extension began at very low mean stress, probably because of the high initial stress concentration at the root of the notch. The immediate increase in the rate of extension due to an increase of the load was followed by a decrease, which became less prominent with increase in the load. The mean rate of extension was kept at approximately the desired value by suitable increases of the load. The lateral contraction of the specimen, however, was not continuous, and the rate of net contraction was far from uniform. After each addition to the load, there was an immediate lateral contraction, but this was frequently followed by a lateral expansion, which often cancelled the initial contraction and left the diameter practically unchanged. The 90-degree specimen (Fig. 4A) showed practically no net change in the minimum diameter until the stress exceeded 20,000 psi. Moreover, the diameter changed little with increase of the stress from 30,000 to 63,000 psi, although the specimen was extending at a nearly uniform mean rate. The 48-degree specimen (Fig. 4C) showed practically no net change in diameter until the stress exceeded about 33,000. With further increases in stress, there were slight temporary decreases in diameter followed by cancellation of these decreases, but the diameter was about the same at a stress of 78,000 psi as at zero stress. After the load on a specimen reached a maximum, each decrease of the load caused an immediate decrease in length and increase in the diameter; the specimen then generally increased slowly in length and contracted laterally. Sometimes, however, both the length and diameter increased between observations.

The ratio of the equivalent length (L_o) to the initial minimum diameter (b_o) at any instant during the plastic deformation of a notched specimen is the ratio of the corresponding abscissas of the curves of longitudinal and lateral deformations. In the early stage of plastic deformation (Fig. 4), the equivalent length (L_o) was many times the initial minimum diameter (b_o). As the load approached the maximum, however, the equivalent length decreased rapidly until it was nearly equal to the minimum diameter.

The course of a curve of variation of the lateral deformation evidently is greatly influenced by the stress concentration and the transverse radial tension induced by the notch. Each increase in the load induces a temporary increase in the concentration of longitudinal stress at the root of the notch. Evidently the metal near the root of the notch on both sides of the minimum section then flows under the influence of the stress concentration and the transverse radial tension. This localized flow causes the observed expansion after an increase in the load, and thus delays the beginning of continuous lateral contraction. Eventually the localized flow relieves most of the stress concentration and the minimum section begins to contract rapidly with increase in the longitudinal stress.

The Technical Cohesion Limit

The course of the curves beyond the point representing the maximum load in Figs. 3 and 4 indicates that not only the nominal stress but also the true stress decreased as long as the strain rate was properly controlled. The rise of the curves between the point representing the last strain gage reading and the point representing complete fracture must be attributed to an increase in the strain rate (see also Fig. 6B, to be discussed later). The decrease in the true stress beyond the maximum load indicates that progressive fracture began approximately at the maximum load and continued until the specimen failed by complete fracture. Because of the progressive disintegration, the deformation at complete fracture was generally small, and the stress at complete fracture generally differed little from the stress at the maximum load. The only exception is the 150-degree specimen, which extended at rapidly increasing rate after the load reached a maximum (Fig. 6B). In these slow tension tests of notched specimens, therefore, the technical cohesion limit was the true stress at the maximum load, not the stress at complete fracture. The technical cohesion limit for a notched specimen must generally be expressed in terms of the longitudinal stress (S_1) alone, because the transverse radial stress (S_3) is not known. The qualitative influence of the transverse radial stress, however, can be studied by comparing the cohesion limits obtained with variously notched specimens.

In the usual tension tests of notched or unnotched specimens disintegration generally does not begin when the load reaches a maximum. The maximum load then is reached approximately when

the rate of work hardening decreases below a certain value, and the technical cohesion limit is the true stress at eventual abrupt fracture.[7]

Influence of the Notch Angle and the Strain Rate on the Ultimate Stress and Breaking Stress

The upper four curves in Fig. 5 show results of ordinary tension tests, which have been discussed in previous papers (5), (6). Results of the slow tension tests are represented by the symbols $\times$ and $+$, and by curve R′. All the results represented in Fig. 5 were obtained with deeply notched specimens ($k = 0.09$ to 0.18).

In the ordinary tension tests, represented by curves U and R, the strain rate at the maximum load was about 100% per hour. During the local contraction to fracture, the true strain rate probably increased considerably, even though the rate of extension was decreased. At fracture, the true strain rate may have been as high as 1500% per hour in these tests of copper. The curves of ultimate stress (U) rise continuously with decrease in the notch angle (ω). The rise is due to the dominant influence of the continuous increase in the radial stress ratio (S_3/S_1) with decrease in the notch angle. As the initial stress concentration also increases with decrease in the notch angle, the rise of the curves of ultimate stress is opposed by any stress concentration remaining when the load reaches a maximum.[8] The curves of breaking stress (R), however, do not rise continuously with decrease in the notch angle. The course of these curves is influenced not only by the varying radial stress ratio and stress concentration, but also by the varying ductility. In the absence of important stress concentration, the course of a curve of breaking stresses is the resultant of the continuously increasing radial stress ratio and the continuously decreasing ductility. Because plastic deformation causes continuous increase in technical cohesive strength, the continuously decreasing ductility tends to cause a continuous decrease in the breaking stress, and thus opposes the influence of the increase in the radial stress ratio with decrease in the notch angle. In curves R of Fig. 5, the influence of the decrease in ductility eventually becomes dominant, and the curves turn downward.

---

[7]Even at ordinary strain rates, fracture of very ductile metals may extend gradually from the axis to the periphery of the minimum section (5).

[8]Under some conditions, this influence becomes dominant and causes the curves of ultimate stress to turn downward with decrease of the notch angle below a certain value (5), (7), (9).

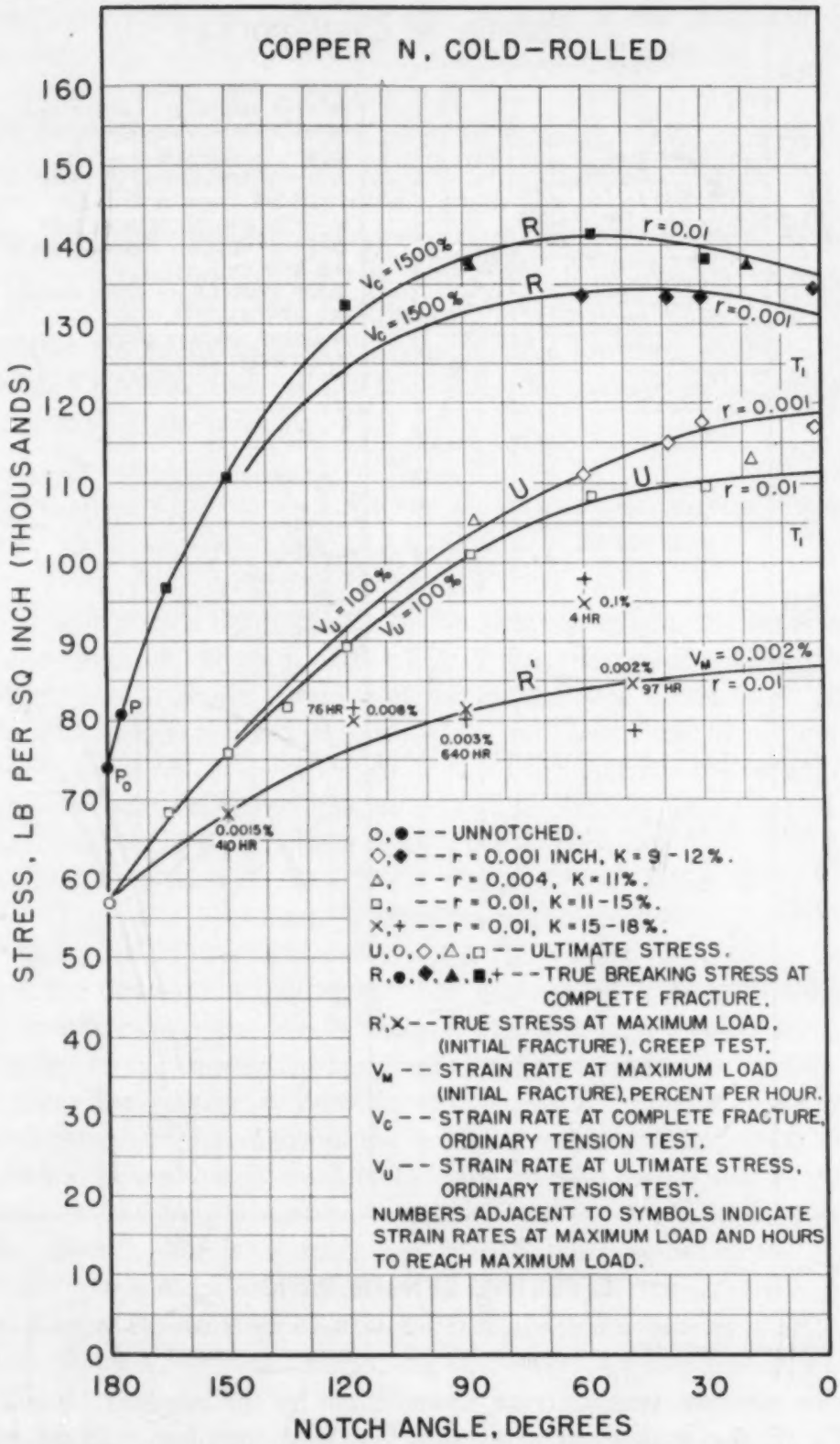


Fig. 5—Influence of the Notch Characteristics and the Strain Rate on the Ultimate Stress and Breaking Stress.

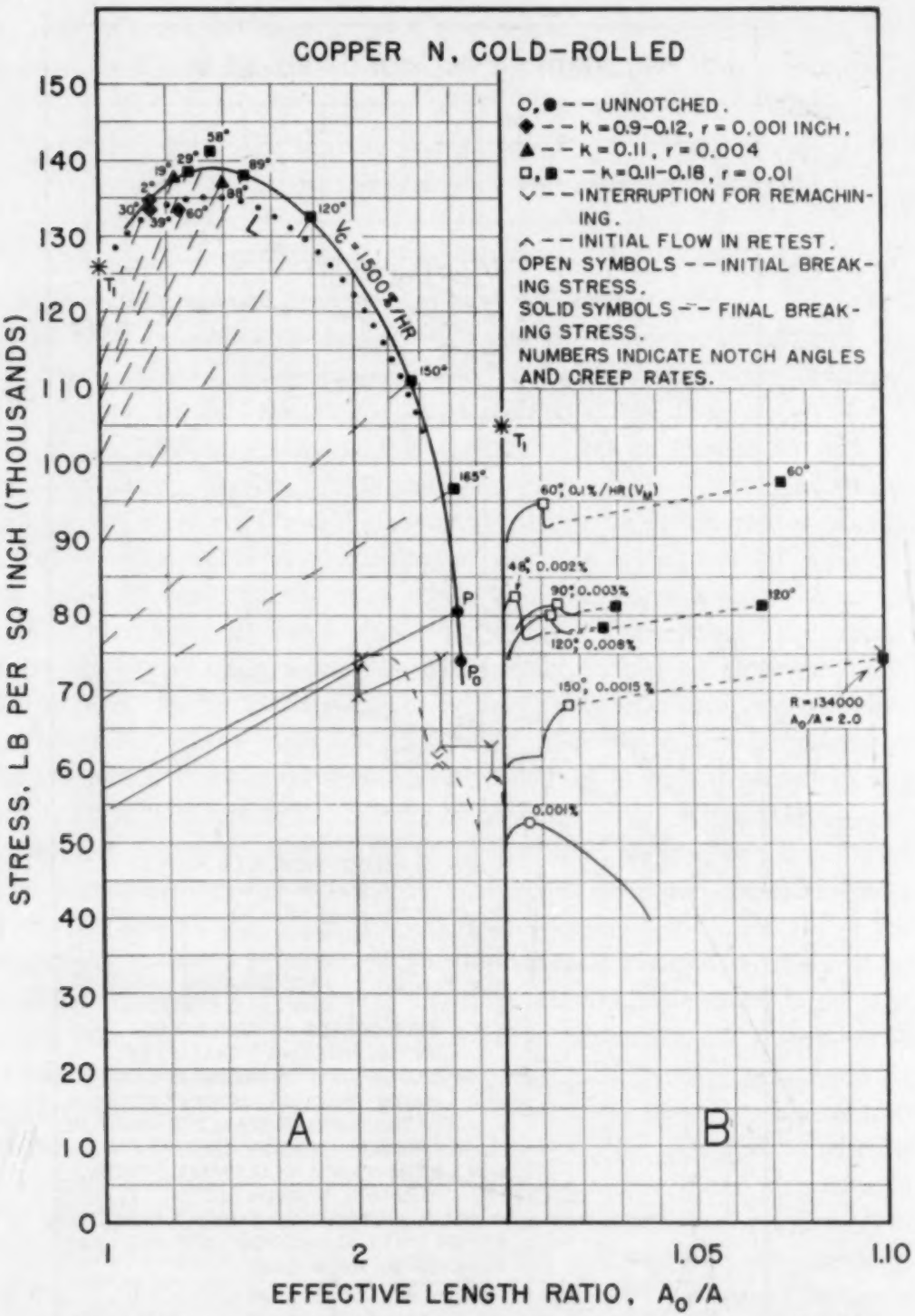


Fig. 6—Influence of the Strain Rate and the Notch Characteristics on Breaking Stress and Ductility.

In the slow tension tests, as indicated by the symbols × and + in Fig. 5, the stresses at maximum load and complete fracture were far below the corresponding values obtained in the ordinary tension

tests (curves U and R). The true stresses at the maximum load (symbols ×), as previously shown, are technical cohesion limits for the corresponding stress systems and strain rates. Curve R′ shows approximately the influence of the notch angle on the technical cohesion limit for a strain rate of 0.002% per hour. The rise of this curve with decrease in the notch angle shows qualitatively the influence of increasing radial stress ratio on the technical cohesion limit. Comparison of curves R with curve R′ shows the effect of a decrease in the strain rate from about 1500 to 0.002% per hour. As shown in the following section, however, the lowering of the curve is due partly to decrease in the technical cohesive strength and partly to decrease in the ductility.

The Influence of the Strain Rate and the Notch Angle on the Breaking Stress and Ductility

Fig. 6 shows the influence of the strain rate and the notch angle on the curve of variation of the flow stress with plastic deformation, and on the breaking stress and ductility. The amount of plastic deformation is expressed in terms of A_o and A, the initial and current areas of cross section. As values of A_o/A are plotted on a logarithmic scale, abscissas represent true strains (5). In Fig. 6B, however, the scale of abscissas differs little from a cartesian scale.

The flow-stress curves for a strain rate of about 0.002% per hour (Fig. 6B) are much lower than the corresponding curves for the faster strain rate of the ordinary tension tests (Fig. 6A). Moreover, the decrease in the strain rate has caused a great decrease in the ductility. At the strain rate for the ordinary tension tests, the ductility of the unnotched specimens of this oxygen-free copper was so great that a special procedure was required to obtain even approximately correct values of the breaking stress and ductility. When ordinary procedure is used, with very ductile metal, the calculated values of breaking stress and ductility are too high because of the "rim effect", that is, a continued plastic deformation of the rim of the minimum cross section after fracture has started near the center (5) (Figs. 18 and 20 of reference 10). Even less ductile metals under some conditions exhibit the rim effect (discussion of Figs. 2 and 5 of reference 7). In the slow tension tests, however, the ductility was slight when the rate was properly controlled during the progressive disintegration. Even for complete fracture, the plastic

deformation was only a few per cent. The true ductility, the plastic deformation at the beginning of progressive fracture, was still less. For the unnotched specimens (Fig. 6B), the true ductility was about 0.7%; for the notched specimens, the true ductility ranged from about 0.3 to 1.4%.[9]

If the metal had been less severely cold-worked prior to the experiments, the ductility would have been greater, but the effect of the strain rate on the ductility would have been qualitatively the same.

In the ordinary tension tests (Fig. 6A), the ductility decreased with decrease in the notch angle. The decrease in ductility is due chiefly to the increase in the radial stress ratio (S_3/S_1). In the slow tension tests, the effect of the notch angle on the ductility was slight (Fig. 6B). This relationship is in accord with the evidence, presented in previous papers, that the effect of the radial stress ratio on the ductility is generally great when the ductility is great, but tends to decrease as the ductility decreases (5) to (11).

As the variation of the ductility with the notch angle in the slow tension tests was so slight (Fig. 6B), little allowance for this variation is required in evaluating the influence of the notch angle on the technical cohesion limit (initial breaking stress). Some allowance, however, must be made for the faster strain rate of the 60-degree specimen. Comparison of the results obtained at strain rates of 0.001 to 0.002% per hour shows that the technical cohesion limit was about 57% greater for the 48-degree specimen than for the unnotched specimen. If the ductility of the 48-degree specimen were the same as that of the other specimens, the difference in cohesion limits would be even greater. As the unnotched specimen failed without local contraction, the true stress at incipient fracture was the cohesion limit for unidirectional tension ($S_3/S_1 = 0$). The cohesion limits obtained with the notched specimens are higher because of the greater radial stress ratios. (Any concentration of longitudinal stress in these specimens would tend to lower the mean stress at fracture.) Even with the 48-degree specimen, however, the radial stress ratio was much less than 1.0. Under polarsymmetric tension ($S_1 = S_2 = S_3$) the cohesion limit probably would be at least twice the cohesion limit for unidirectional tension (5) to (11). In locating point T_1 in Fig. 6B, it has been assumed that the disruptive stress ($S_1 = S_2 = S_3$) is twice the severing stress ($S_3/S_1 = 0$). The same assumption has been made in locating point T_1 in the derived Figs. 7 and 8.

[9] The indicated true ductility for the 150-degree specimen probably is too great; the offset in the curve probably must be attributed to a slip in the reductometer.

Influence of the Radial Stress Ratio and the Strain Rate on Mechanical Properties

From the diagrams in Figs. 5 and 6, other diagrams may be derived to represent the influence of the radial stress ratio (S_3/S_1) on the flow stress, ultimate stress, technical cohesion limit, and ductility. Derived diagrams of two types are shown in Figs. 7 and 8. Fig. 7 shows qualitatively the influence of the radial stress ratio on the yield stress, ultimate stress, and breaking stress. Fig. 8 shows the influence of the radial stress ratio on breaking stress and ductility. Attention will be given first to Fig. 7.

The technical cohesive strength and resistance to plastic deformation generally must be represented by surfaces in a diagram with the three principal stresses as co-ordinates. When two of the principal stresses are kept equal, however, the strength of a metal may be represented by a two-dimensional diagram. From the results of tension tests of notched specimens it is possible to develop a diagram to represent stress combinations with S_2 equal to S_3 (5) to (10). Two diagrams of this type are shown in Fig. 7. Ordinates in this figure represent axial stresses and abscissas represent transverse radial stresses in a cylinder. The values of S_3 and of S_3/S_1 used in constructing these diagrams cannot be obtained directly from the results of tests of notched specimens. They are based on an empirical assumption as to the variation of S_3/S_1 with the ultimate stress (5), (6). The diagrams are assumed to be free from the distorting influence of stress concentration. They are qualitative representations of the strength of the metal in terms of uniform axial and radial stresses.

Each of the radiating broken lines in Fig. 7 is the locus of points representing the indicated constant value of the radial stress ratio. Line H is the locus of points representing polarsymmetric stress ($S_1 = S_2 = S_3$). The field below line H represents stress systems with S_1 in the radial direction and with S_3 in the axial direction; the field above line H represents stress systems with S_1 in the axial direction and S_3 in the radial direction. Diagrams based entirely on tension tests of notched specimens would be confined to the field above line H and to the right of the axis of ordinates.

The two diagrams in Fig. 7A represent the strength of annealed oxygen-free copper N-8 and of the cold-rolled copper N at the usual strain rate for a tension test. The solid curves represent the strength

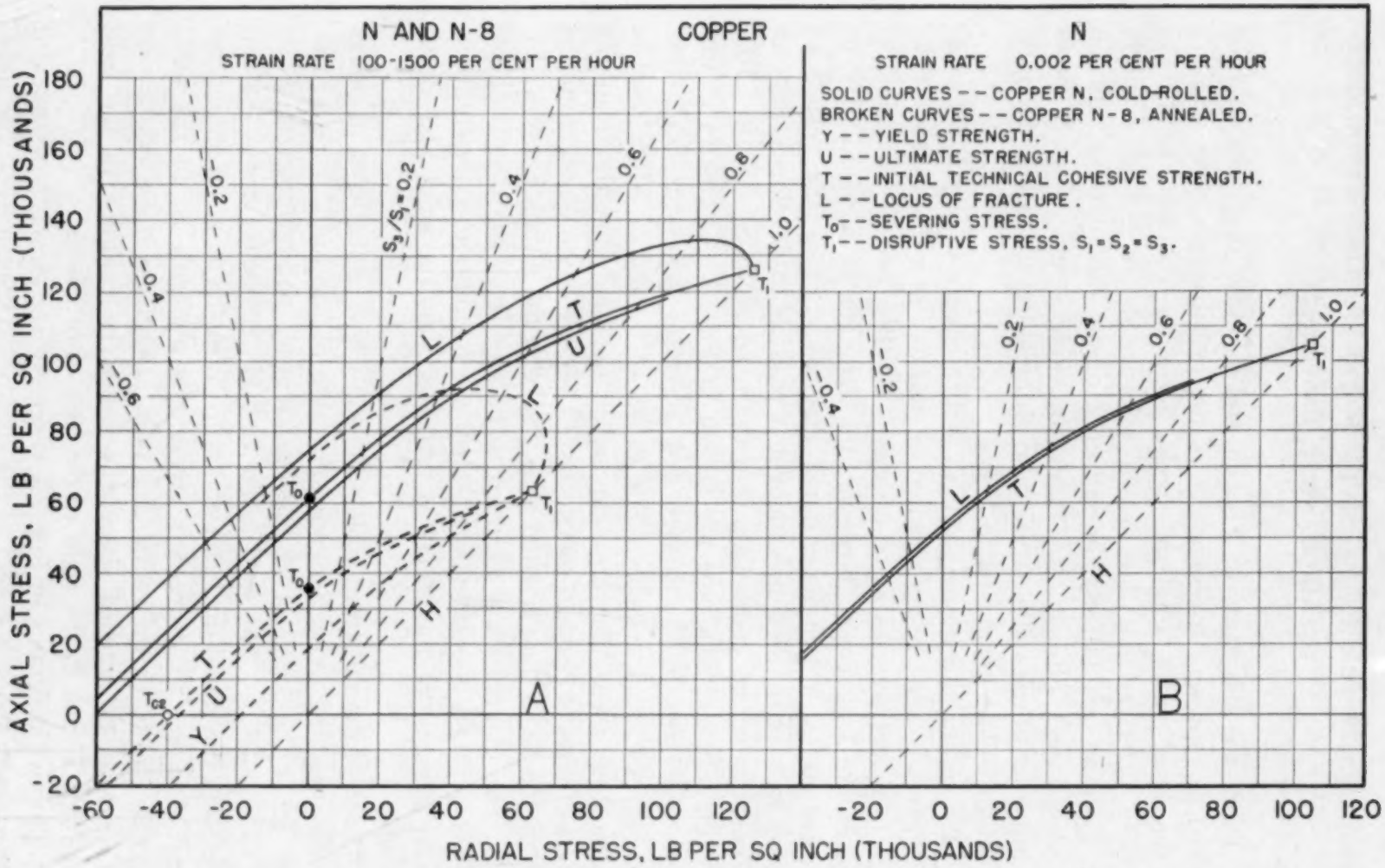


Fig. 7—Influence of the Stress System and the Strain Rate on Resistance to Plastic Deformation and Resistance to Fracture.

of the cold-rolled copper N; the broken curves represent the strength of the annealed copper N-8. The diagram in Fig. 7B represents the strength of the cold-rolled copper at the strain rate for the slow tension tests. Curve L in each diagram represents the variation of the breaking stress with the radial stress. The course of this locus of fractures, however, is affected by the variation of ductility with the radial stress ratio.[10]

Curve T represents approximately the initial technical cohesive strength, the strength prior to the plastic deformation represented in Fig. 8, to be discussed later. Curve T must be between the curve of yield strength (Y) and the locus of fractures (L). When the ductility is great, curves Y and L are far apart and the position of curve T cannot be exactly determined. As shown in previous papers (5) to (10), however, curve T generally should be placed not far from curve U, as in Fig. 7A. When the ductility is slight, the curve of yield strength and the locus of fractures are close together, and the curve of initial technical cohesive strength (T) almost coincides with the locus of fractures (Fig. 7B).

In diagrams of the type shown in Fig. 7, the influence of plastic deformation affects the curves for the indices of strength, but plastic deformation is not represented directly. In the diagrams now to be considered (Fig. 8), abscissas represent plastic deformations and ordinates represent breaking stresses. The co-ordinate scales are the same as in the basic diagrams (Fig. 6). In Fig. 8A (ordinary tension test), the locus of fractures (L) is identical with the locus of fractures in Fig. 6A. In Fig. 8B, curve L has been drawn in accordance with the experimentally determined cohesion limits represented in Fig. 6B. Each locus of fractures is assumed to be free from the distorting influence of stress concentration and deformation gradient, and is assumed to be the locus of cohesion limits determined with radial stress ratios held constant during plastic deformation.

As any point on a locus of fractures represents a cohesion limit corresponding to a specific value of S_3/S_1, it may be made the intersection of a curve of flow stress and a curve of cohesion limits corresponding to that value of S_3/S_1. A series of such curves is shown in Fig. 8A. The left ends of the curves of cohesion limits are in proper correlation with points on curve T in the diagram for cold-rolled copper in Fig. 7A. The ductility of the metal for a specific stress

[10]In the field of negative values of S_3, the course of curve L for a ductile metal is not well established, because the ductility increases rapidly with decrease in the volume stress ($S_1 + S_2 + S_3$). This portion of the curve for some ductile metals possibly turns upward as it extends to the left.

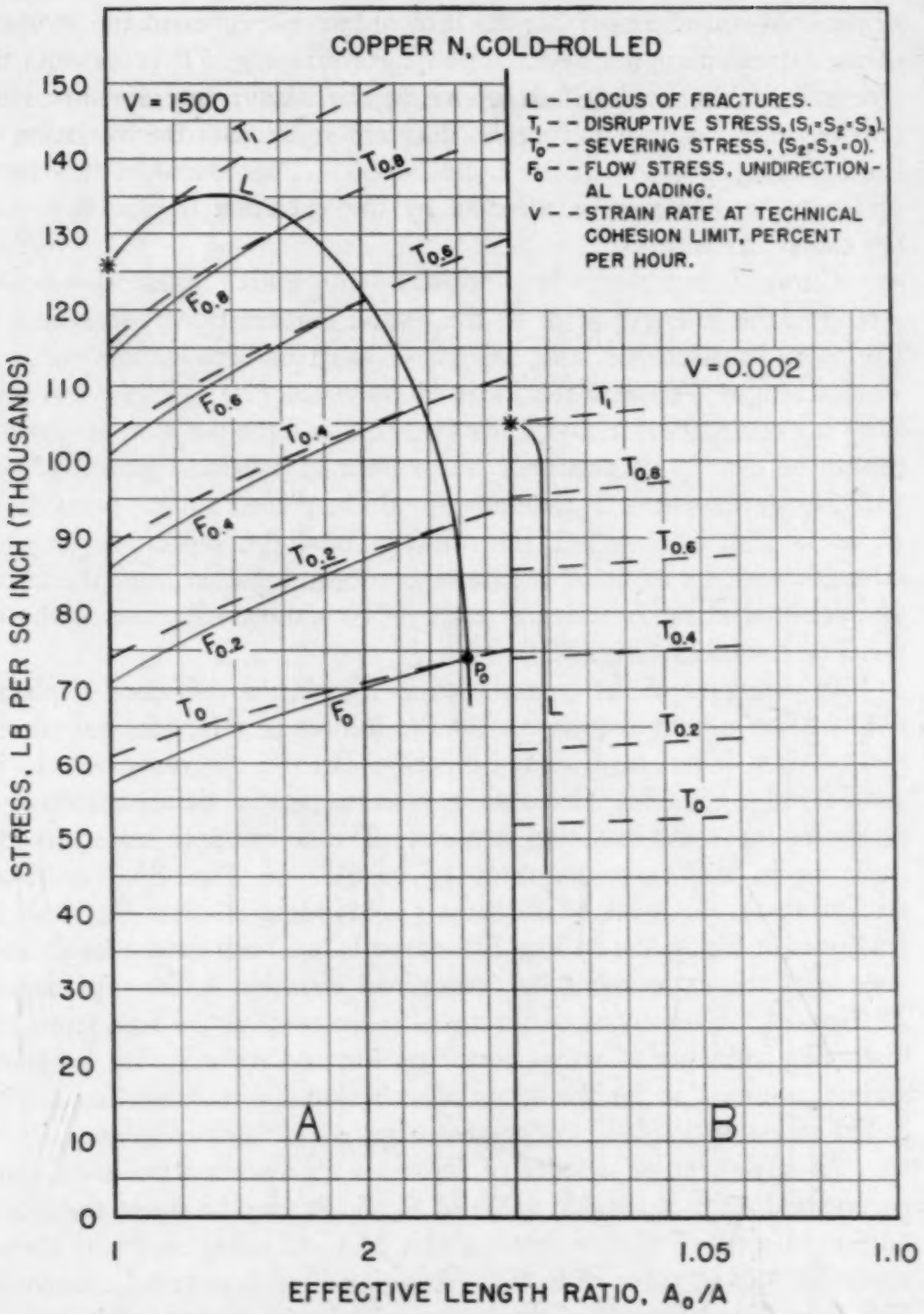


Fig. 8—Influence of the Radial Stress Ratio (S_2/S_1) and the Strain Rate on Flow Stress, Technical Cohesion Limit, and Ductility.

system depends on the difference between the initial flow stress and the initial technical cohesion limit for that system. The ductility thus depends on the vertical distance between the curve of cohesion and

the curve of flow stress at the origin. When the strain rate is very slow, a curve of flow stress for severely cold-rolled copper is only slightly below the curve of cohesion limits, and the ductility is slight. In Fig. 8B curves of flow stress would almost coincide with the curves of cohesion limits.

To the right of the locus of fractures (L), the course of a curve of cohesion limits (Fig. 8) indicates qualitatively the variation of the cohesion limit, for that stress system, with prior plastic deformation under a stress system that permits greater ductility (5), (6).

As indicated by comparison of diagrams A and B of Fig. 8, an increase in the strain rate causes an increase of the technical cohesion limit for any stress system, and also causes an increase of the ductility for any stress system except polarsymmetric tension ($S_1 = S_2 = S_3$). Under polarsymmetric tension there is no true ductility. The disruptive stress, however, probably increases with increase in the rate of elastic strain, at least up to a limiting rate. This conclusion is supported by evidence presented in previous papers that the effect of a decrease in temperature on the cohesive strength is qualitatively similar to the effect of an increase in the strain rate (12), and that the disruptive stress increases with decrease in temperature (6) to (10).

The course of curves T in diagrams of the type shown in Fig. 7 suggests that resistance to fracture, like resistance to flow, is determined by a critical value of the shearing stress, which decreases with increase in the volume stress ($S_1 + S_2 + S_3/3$). This subject is discussed in a previous paper (11). When S_2 equals S_3, resistance to fracture and resistance to flow are similar functions of the radial stress ratio. If the critical shearing stress for fracture is the octahedral shearing stress, the technical cohesion limit and the flow stress vary similarly with the stress system (11).

The Qualitative Equivalence of Increase in Temperature and Decrease in the Strain Rate in Their Effects on Mechanical Properties

Both the flow stress and the technical cohesive strength are decreased by either a decrease in the strain rate or an increase in temperature (12). This relationship is illustrated by Fig. 9, which is derived from data presented in previous papers (6), (12). This figure shows the influence of temperature on the technical cohesive strength of cold-rolled copper. The temperature scale is the same

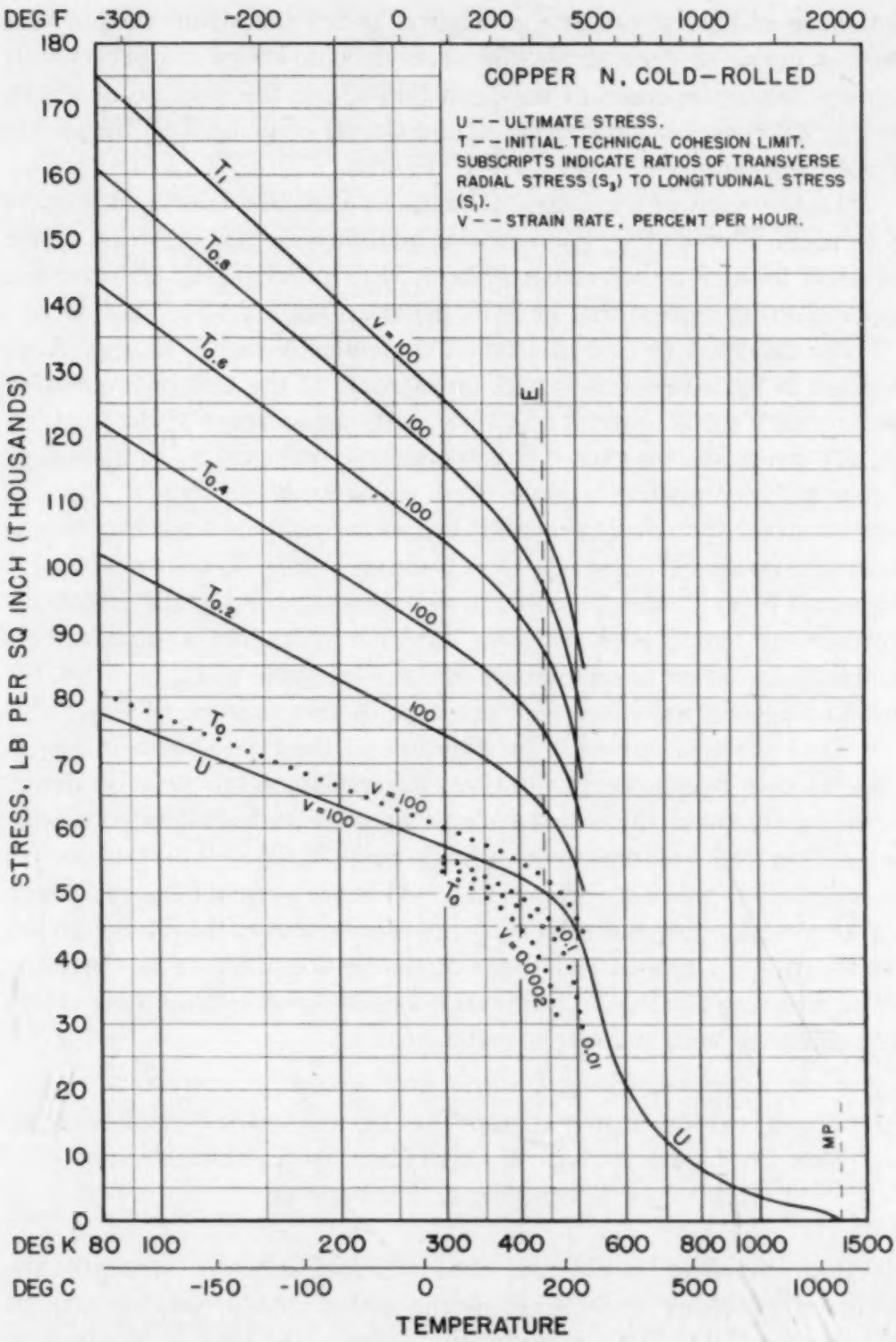


Fig. 9—The Qualitative Equivalence of Decrease in Strain Rate and Increase in Temperature in Their Effect on the Strength of Copper.

that has been used in previous papers (6) to (10). As temperatures in degrees K are plotted on a logarithmic scale, abscissas are proportional to the logarithm of the degrees K, and the scale is the same in principle as Kelvin's original thermodynamic scale. This scale has been used because it gives a linear relationship between temperature and the strength indices for various metals, except when structural changes occur in part of the temperature range (6). With either annealed or cold-worked copper, the yield stress, ultimate stress, and breaking stress vary linearly with temperature (on this scale), at least between −188 C and +100 C; the linear variation is obtained with either notched or unnotched specimens. Moreover, the ductility of this metal and of many other face-centered cubic metals, in ordinary tension tests, varies little throughout this temperature range (6), (10).

Curve U in Fig. 9 shows the influence of temperature on the ultimate stress of the cold-rolled copper. With the use of data obtained by Price with moderately cold-worked copper (13), curve U has been extended to the melting point. Curve T_o above curve U represents the variation of the severing stress (cohesion limit for unidirectional tension) when the strain rate is about 100% per hour, a rate somewhat less than that in an ordinary tension test. For previously cold-worked metal, curve T_o should be a little above curve U; for annealed, very ductile metal, curve T_o probably would be a little below curve U. The T_o curves below curve U in Fig. 9 represent cohesion limits for strain rates of 0.0002, 0.01, and 0.1% per hour (12). Fig. 9 also contains a series of curves (T_o to T_1) corresponding to various radial stress ratios (S_3/S_1) between zero and 1.0, for a strain rate of 100% per hour. These curves are approximate representations derived by an empirical method from results of tension tests of notched specimens (5), (6). As previously shown, the disruptive stress ($S_1 = S_2 = S_3$) is about twice the severing stress (Fig. 7A). At room temperature (about 300 K) the positions of the curves are in accordance with the intersections of curve T in Fig. 7A with the radiating lines representing various radial stress ratios between zero and 1.0.

For a strain rate of about 100% per hour, therefore, the technical cohesive strength at room temperature is represented by the corresponding ordinates of the series of curves T_o to T_1. For a strain rate of about 0.002% per hour, however, the technical cohesive strength at room temperature is equivalent to the technical cohesive

strength for a strain rate of 100% per hour, but at a higher temperature. As illustrated by line E, which is derived by comparison of Fig. 9 with Fig. 7B, this higher temperature is about 440 K (about 300 F). A decrease in the strain rate from 100 to 0.002% per hour is equivalent in effect to an increase of the temperature from 300 to 440 K.

Decrease in temperature or increase in the strain rate causes an increase in both the cohesive strength and the ductility (Figs. 6 and 9). The increase in the ductility, however, is at a decreasing rate. The ductility of many face-centered cubic metals, in ordinary tension tests of notched and unnotched specimens, changes little between room temperature and —188 C (6), (10). Even at the temperature of liquid hydrogen (—252.7 C) unnotched specimens of these metals, including completely austenitic steels, show practically no decrease in ductility (discussion of reference 9).[11] Moreover, impact tests of these metals at room temperature and at —188 C reveal practically no difference in absorbed energy. Curves of ultimate stress and breaking stress, however, rise nearly linearly with decrease in temperature throughout this range, as do the curves in Fig. 9. Moreover, this linear relationship is obtained whether the tension test specimens are notched or unnotched. The evidence thus indicates that relief of stress concentration by plastic deformation of notched specimens of these metals is not decreased appreciably either by decrease of temperature or by enormous increase in the strain rate.

The effects of temperature and the strain rate on ferritic steels are very complicated. The ductility of these steels and their ability to relieve stress concentration generally decrease with decrease in temperature. Curves of ultimate stress and breaking stress of notched or unnotched specimens rise with decrease in temperature throughout a certain range. However, with decrease below a certain temperature, which depends on the composition, heat treatment, notch characteristics and strain rate, the breaking stress of notched specimens decreases abruptly, owing to an abrupt decrease in ductility and in ability to relieve stress concentration (Figs. 12 and 13 of reference 9). At room temperature the ductility of unnotched low carbon steel specimens tends to increase at a decreasing rate with increase in the strain rate. It seems probable that, throughout a range of slow strain rates, and within a certain temperature range, the ductility of notched

[11] On the logarithmic scale a decrease in temperature from —188 C to —252.7 C is about equivalent to a decrease from room temperature to —188 C.

specimens of pearlitic steels increases with increase in the strain rate. Within these ranges of strain rate and temperature, the pearlitic steels would thus behave like the face-centered cubic metals. Above this range of strain rates and below this range of temperature, however, the ductility of the pearlitic steels decreases with increase in the strain rate or with decrease in temperature.

Acknowledgment is due to W. D. Jenkins for assistance in this investigation, and to Miss Frances J. Cromwell for assistance in preparing the illustrations.

References

1. J. A. Bennett and D. J. McAdam, Jr., "Creep Rates of Cold-Drawn Nickel-Copper Alloy (Monel Metal)," *Journal of Research,* National Bureau of Standards, Vol. 28, No. 4, April 1942, p. 417-437.
2. D. J. McAdam, Jr., "The Technical Cohesive Strength of Metals," *Journal of Applied Mechanics,* Vol. 3, December 1941, p. A156-165 in *Transactions,* American Society of Mechanical Engineers, Vol. 63, 1941.
3. D. J. McAdam, Jr., "The Technical Cohesive Strength and Yield Strength of Metals," *Transactions,* American Institute of Mining and Metallurgical Engineers, Vol. 150, 1942, p. 311-357.
4. D. J. McAdam, Jr., "The Influence of the Combination of Principal Stresses on Fatigue of Metals," *Proceedings,* American Society for Testing Materials, Vol. 42, 1942, p. 576-592.
5. D. J. McAdam, Jr., and R. W. Mebs, "An Investigation of the Technical Cohesive Strength of Metals," American Institute of Mining and Metallurgical Engineers, Technical Publication No. 1615; *Metals Technology,* August 1943; *Transactions,* American Institute of Mining and Metallurgical Engineers, Vol. 162, 1945, p. 474-536.
6. D. J. McAdam, Jr., and R. W. Mebs, "The Technical Cohesive Strength and Other Mechanical Properties of Metals at Low Temperatures," *Proceedings,* American Society for Testing Materials, Vol. 43, 1943, p. 661-703.
7. D. J. McAdam, Jr., R. W. Mebs and G. W. Geil, "The Technical Cohesive Strength of Some Steels and Light Alloys at Low Temperatures," *Proceedings,* American Society for Testing Materials, Vol. 44, 1944, p. 593-623.
8. D. J. McAdam, Jr., "The Technical Cohesive Strength of Metals in Terms of the Principal Stresses," American Institute of Mining and Metallurgical Engineers, Technical Publication No. 1782, part of Symposium on Cohesion; *Metals Technology,* December 1944, p. 5-31; *Transactions,* American Institute of Mining and Metallurgical Engineers, Vol. 162, 1945, p. 542-568.
9. D. J. McAdam, Jr., G. W. Geil and R. W. Mebs, "The Effect of Combined Stresses on the Mechanical Properties of Steels between Room Temperature and —188 Degrees Cent.," *Proceedings,* American Society for Testing Materials, Vol. 45, 1945, p. 448-481.
10. D. J. McAdam, Jr., G. W. Geil and R. W. Mebs, "Effects of Combined Stresses and Low Temperatures on the Mechanical Properties of Some Nonferrous Metals," TRANSACTIONS, American Society for Metals, Vol. 37, 1946, p. 497-537.
11. D. J. McAdam, Jr., "Fracture of Metals Under Combined Stresses," TRANSACTIONS, American Society for Metals, Vol. 37, 1946, p. 538-566.

12. D. J. McAdam, Jr., G. W. Geil and D. H. Woodard, "Influence of Strain Rate and Temperature on the Mechanical Properties of Monel Metal and Copper," Preprint No. 54, American Society for Testing Materials, 1946.
13. W. B. Price, "Properties of Copper and Some of Its Important Industrial Alloys at Elevated Temperatures," Symposium on Effect of Temperature on the Properties of Metals, published jointly by American Society of Mechanical Engineers and American Society for Testing Materials, 1931, p. 340-350.

COPPER-MANGANESE ALLOYS

The Properties of Cold-Worked and Annealed Alloys Containing 2 to 20% Manganese

By R. S. Dean, J. R. Long, T. R. Graham and D. P. Sugden

Abstract

The physical properties of copper-manganese alloys containing 2 to 20% manganese, as influenced by cold working and subsequent annealing of 60% cold-worked material, have been determined. In the annealed or zero % cold-worked state there is an increase in tensile strength, yield strength, and hardness with the elongation remaining substantially the same for all alloys of 2 and 20% manganese. The properties of cold-worked alloys show all compositions double the tensile strength of the annealed condition by 80% cold reduction. The elongation shows a rapid decrease with initial stages of cold reduction of 4 to 5% elongation after 40% cold working and remains at this value with additional reductions up to 80%. The variation in properties of 60% cold-reduced stock with annealing temperature follows the normal trends expected with single-phase alloys, that is, as regards stress relief, recrystallization, and grain growth. The addition of manganese raises the recrystallization temperature from 500 to 600 F for copper to 700 to 800 F for the 2% manganese alloy. Higher proportions of manganese up to 20% do not further increase the recrystallization temperatures.

RECENT work on alloys of copper and manganese has been centered largely on the determination of the constitution diagram and on some of the properties of alloys with high manganese content. The Bureau of Mines laboratories have reported the results of X-ray

Published by permission of the Director, Bureau of Mines, U. S. Department of the Interior.

A paper presented before the Twenty-eighth Annual Convention of the Society held in Atlantic City, November 18 to 22, 1946. Of the authors, R. S. Dean was formerly assistant director, Bureau of Mines, U. S. Department of the Interior, Washington, D. C., and is now consultant; J. R. Long and T. R. Graham are senior metallurgists and D. P. Sugden is assistant technologist, Bureau of Mines, Intermountain Experiment Station, Salt Lake City, Utah. Manuscript received June 3, 1946.

and metallographic studies of the system (1), (2).[1] They verified the formation of a continuous series of solid solutions at elevated temperatures and determined the decrease of solubility of manganese in copper with decreasing temperatures. The hardening produced by precipitation of manganese under extended treatments at temperatures below the solubility limit (3), the resistivity (4), thermal coefficient of resistivity, and vibration damping capacity (5) have also been reported. These studies, however, involved alloys usually ranging from 40 to 90% manganese, but little information, especially relative to mechanical properties, is available on alloys containing less manganese. Hesse and Myskowski (6) have presented the most complete data on mechanical properties but were primarily concerned with alloys containing 40% or more manganese. These alloys are quite sluggish with respect to precipitation of manganese; while they are hardened and strengthened by extended treatments at temperatures below 600 F, the nature of the precipitate causes considerable loss in ductility. The few results given for low-manganese alloys indicate that manganese increases the tensile strength considerably without excessive loss of ductility. According to the constitution diagram, alloys containing up to 20% manganese are single phase, and the increase in strength in this composition range is due to the solution of manganese in the copper lattice. The ductility that these workers note is much higher than that indicated by earlier reports in the literature dealing with alloys prepared with impure manganese, but it agrees closely with the results these laboratories have reported on other high-copper alloys prepared with electrolytic manganese (7, 8, 9, 10). It was therefore desirable to examine these solid-solution alloys in more detail and to determine their mechanical properties in the annealed and cold-worked states. This paper presents the data obtained on alloys containing up to 20% manganese in the form of cold-rolled and cold-rolled, annealed sheet.

Preparation of Alloys

The alloys were prepared in 35-pound heats by melting grade A wire-bar copper in a basic-lined, high-frequency induction furnace, adding the required amounts of electrolytic manganese, and deoxidizing with small amounts of aluminum. They were cast into slab molds and processed into sheet by hot rolling at 1400 F (760 C), to 50% reduction in thickness, conditioning the surfaces, and then cold

[1]The figures appearing in parentheses pertain to the references appended to this paper.

rolling with intermediate annealing at 1200 F (650 C) to the $\frac{1}{16}$-inch finished sheet. The cold rolling schedule was arranged to finish the major portion of each alloy at 60% reduction by cold rolling; of the remaining material, portions were finished at 20, 40, and 80% reduction. This permitted testing the alloy in the cold-worked state with various degrees of working. The zero cold-worked state was obtained by annealing (1 hour at 1200 F) material finished at 60% reduction. Other portions of the sheet reduced 60% were annealed at temperatures ranging from 300 to 1500 F (150 to 815 C) to

Table I
Chemical Composition of Alloys Studied

Alloy No.	Per Cent				
	Manganese	Copper	Iron	Aluminum	Silicon
B-42	2.00	98.00	0.0073	0.01	<0.005
B-43	4.70	95.20	0.010	0.02	<0.005
B-44	7.00	93.00	0.011	0.016	<0.005
B-45	8.70	91.20	0.0083	0.026	<0.005
B-46	10.00	90.00	0.0094	0.037	<0.005
B-47	11.40	88.50	0.0095	0.042	<0.005
B-48	14.20	85.70	0.0073	0.047	<0.005
B-49	16.0	84.0	0.010	0.037	<0.005
B-50	17.9	82.0	0.013	0.035	<0.005
B-51	20.0	80.0	0.013	0.039	<0.005

follow the change in properties with annealing temperature. Sheets annealed at temperatures of 300 to 1000 F (150 to 540 C) were heated in air; those treated above 1000 F (540 C) were heated in an atmosphere of helium to minimize oxidation.

All tests were made on a ½-inch sheet tensile specimen with a parallel section 4 inches long and extensions determined on a 2-inch gage length. Property values given in the tables are averages of results on five tensile specimens tested for each condition.

The chemical compositions of the alloys given in Table I show low residual aluminum, low iron, and negligible silicon. The iron contents are well below the amount that produces significant effects in copper-manganese-zinc alloys (11), and since the copper-manganese alloys are also single phase it is believed that aluminum contents less than 0.05 likewise would have no significant effects.

Annealed Properties

The tensile properties of the alloys, after being reduced 60% in thickness and annealed for 1 hour at 1200 F, are given in Table II in the zero cold-worked state. The tensile strength, yield strength,

elongation, and hardness are also graphically presented in Fig. 1 as a function of manganese content. Since the properties of pure copper are well established, this material was not tested along with the alloys, and accordingly the respective property curves have been extrapolated to zero manganese content so as to correspond to the properties given by Wilkins and Bunn (12) for similarly processed, high-conductivity, oxygen-free copper sheet 0.040 inch thick.

The tensile strength, yield strength, and hardness curves emphasize the increase in strength and hardness produced by the first 6 or 7% manganese as compared with that produced by succeeding man-

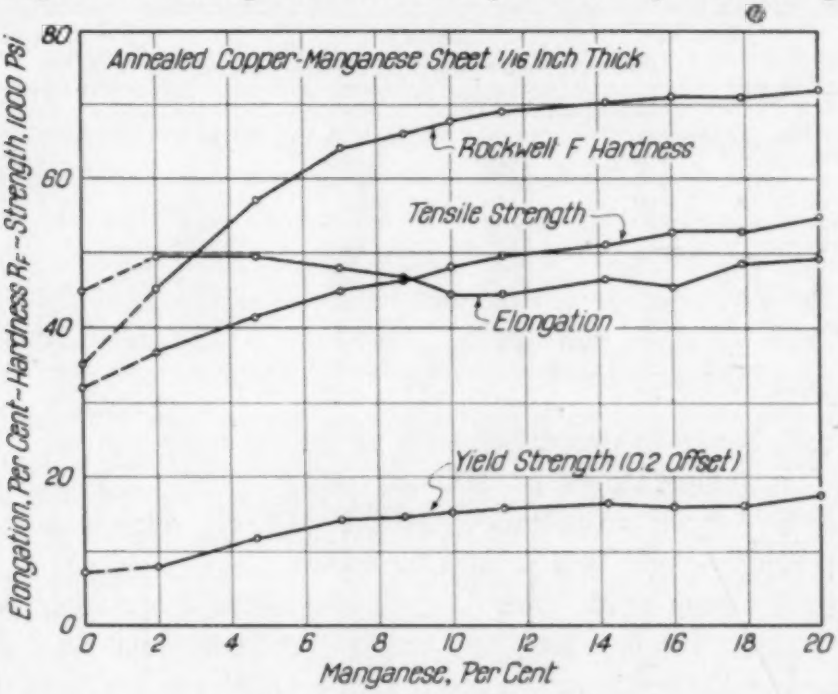


Fig. 1—The Physical Properties of Copper-Manganese Alloys Annealed for 1 Hour at 1200 F (650 C).

ganese increments, that is, the tensile strength increases from 32,000 to 44,000 psi with 6% manganese, or approximately 2000 psi for each per cent manganese. Further increase in manganese content raises the tensile strength at the approximate rate of 800 psi for each per cent manganese until it reaches 55,000 psi at 20% manganese. The yield strength shows a similar trend, rising from 7000 to 13,000, or at the rate of 1000 psi for each per cent manganese up to 6 and thereafter at a rate of about 300 psi for each per cent manganese, reaching 17,500 psi at 20% manganese. Similarly, the hardness rises most rapidly from R_F 35 to R_F 61 with the first 6% manganese and then more slowly to R_F 72 at 20% manganese.

Table II
Variation in Physical Properties with Cold Rolling

Percentage of Mn in Alloy	Cold Reduction %	Ultimate Strength psi	Yield Strength psi 0.2 Offset	Proportional Limit psi 0.01 Offset	Elongation % in 2 In.	Hardness Rockwell F	Hardness Rockwell B
	0	36,600	8,000	5,200	49.4	45	..
	20	46,600	45,400	32,800	12.8	91	..
2.0	40	56,600	55,000	40,200	5.5	97.5	68
	60	63,200	61,400	42,100	4.6	..	74
	80	69,100	68,000	50,600	4.7	..	79
	0	41,400	11,800	7,500	49.3	57	..
	20	51,600	49,600	37,300	13.6	96	64
4.7	40	64,200	62,600	44,700	5.8	..	76
	60	71,600	70,100	50,100	5.0	..	83
	80	80,000	77,600	55,600	4.5	..	88
	0	44,700	14,300	7,700	48.0	64	..
	20	56,900	54,600	41,400	12.0	98	71
7.0	40	68,800	66,100	48,400	5.8	..	81
	60	76,700	75,100	52,300	4.8	..	86.5
	80	88,000	85,500	58,100	4.6	..	92
	0	46,100	14,300	8,400	46.6	66	..
	20	59,100	56,600	43,200	11.3	99	73
8.7	40	71,300	68,000	47,200	5.8	..	83
	60	80,000	78,100	53,000	4.3	..	90
	80	91,500	89,100	62,300	4.2	..	94
	0	48,000	15,200	9,000	44.4	67.5	..
	20	59,300	55,300	42,000	13.3	..	74
10.0	40	74,500	74,100	55,000	5.2	..	84.5
	60	82,700	80,100	58,400	4.2	..	91
	80	92,900	89,500	62,100	4.4	..	95
	0	49,600	15,900	9,700	44.3	69	..
	20	62,400	58,200	42,800	13.2	..	76
11.4	40	77,800	76,000	56,000	4.6	..	87
	60	87,100	84,400	59,500	4.1	..	92
	80	96,900	94,900	67,600	4.2	..	96
	0	51,200	16,300	10,400	46.5	70	..
	20	64,500	58,300	42,000	15.1	..	78
14.2	40	80,200	78,200	55,200	4.9	..	88
	60	91,400	87,100	64,300	4.2	..	94
	80	100,100	98,200	68,000	4.0	..	97
	0	52,800	16,000	10,200	45.3	71	..
	20	66,600	57,800	43,700	16.3	..	79
16.0	40	84,700	80,000	57,000	4.9	..	89
	60	92,800	89,200	67,200	4.0	..	95
	80	103,100	99,900	75,200	3.9	..	98
	0	53,000	16,100	9,400	48.5	71	..
	20	67,300	56,600	42,100	19.7	..	79
17.9	40	86,200	83,500	61,500	4.5	..	90
	60	95,200	90,000	68,100	4.3	..	96
	80	108,900	100,000	72,400	4.0	..	99
	0	54,900	17,100	9,400	49.2	72	..
	20	69,700	58,100	42,300	18.8	..	81
20.0	40	87,000	82,800	58,100	4.8	..	91.5
	60	96,800	92,300	69,800	4.0	..	97
	80	105,700	102,900	72,800	3.9	..	99

The elongation, however, shows relatively little change with increasing manganese content. The 2 and 4% manganese alloys have an elongation 4 to 5% above that indicated for oxygen-free copper annealed at the same temperature, as do the 18 and 20% alloys; although a perceptible minimum occurs in the curve at about 10% manganese, this minimum elongation is still equal to that of the copper. While these small variations are not significant in themselves, the

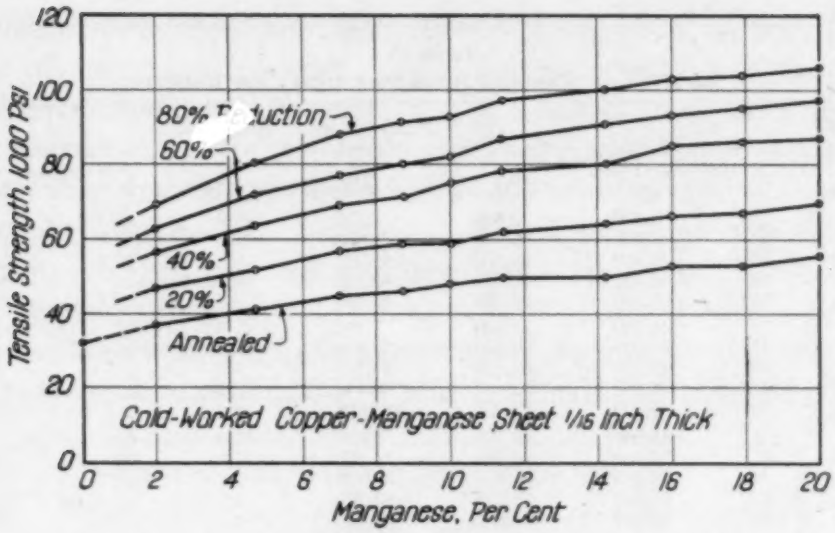


Fig. 2—The Tensile Strength of Cold-Rolled Copper-Manganese Alloys as a Function of the Manganese Content.

fact that the elongation is not decreased by increasing manganese at least up to 20% is significant.

No particular data were obtained regarding the effect of grain size on the properties of these alloys, but metallographic examination of material annealed for 1 hour at 1200 F indicates that manganese has little effect on the grain size. The grain size of alloys containing 2 to 7% manganese was 0.045 mm, and that of alloys containing 7 to 20%, was 0.065 mm. This variation is quite small and doubtless has little effect on the properties as shown in Fig. 1.

Cold-Worked Properties

The properties of material cold-rolled to 20, 40, 60, and 80% reduction in thickness are also given in Table II. It should be pointed out that these specimens were given three to five cold reductions of about 50% each with intermediate annealing for 1 hour at 1200 F before final rolling to the desired reduction and sheet thickness of $\frac{1}{16}$ inch. They are therefore thoroughly representative of material annealed at 1200 F (650 C) and cold-reduced to the extent indicated.

For greater clarity of presentation the tensile strength and yield strength are plotted against manganese content in separate graphs (Figs. 2 and 3), and the hardness and elongation are plotted in Fig. 4.

The properties of this series of alloys show normal changes with

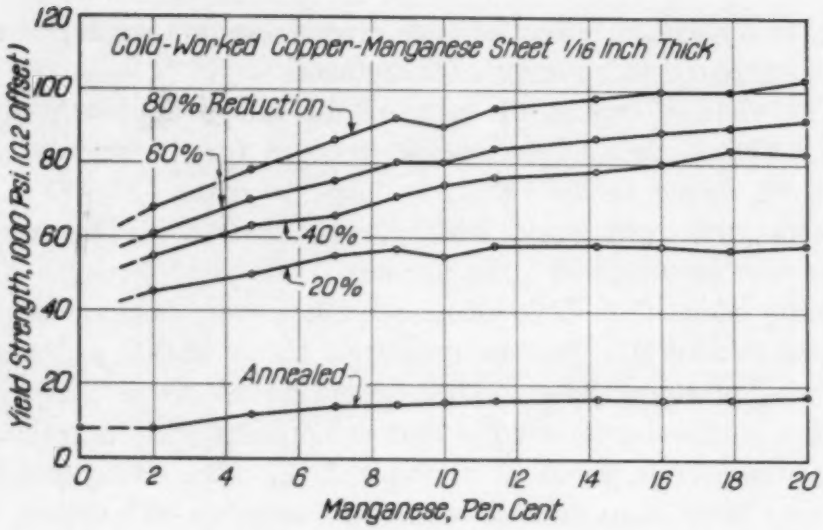


Fig. 3—The Yield Strength of Cold-Rolled Copper-Manganese Alloys as a Function of the Manganese Content.

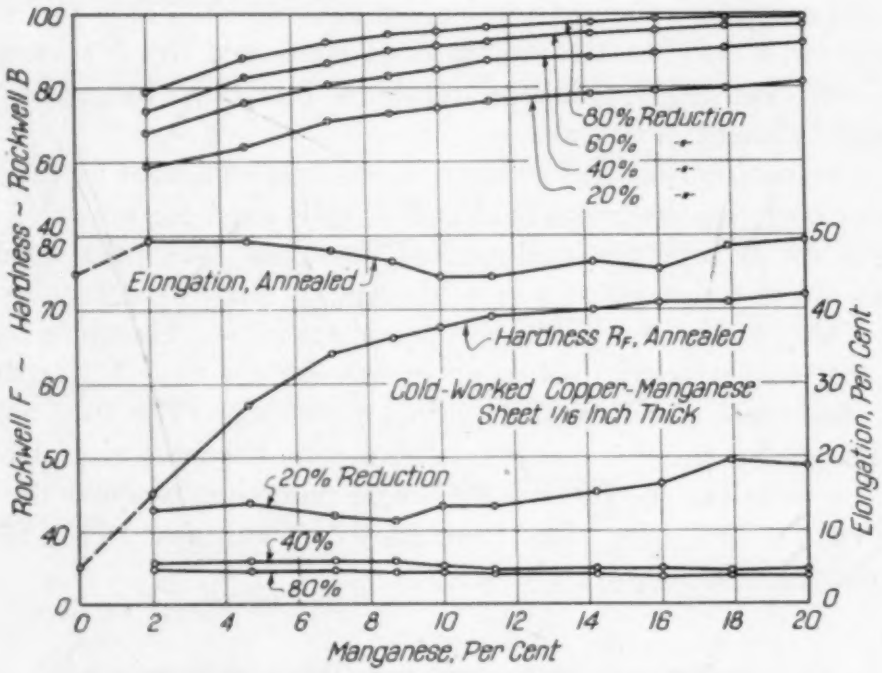


Fig. 4—The Hardness and Elongation of Cold-Rolled Copper-Manganese Alloys as a Function of the Manganese Content.

increasing cold work. The tensile strength of each of the alloys is increased by approximately 10,000 psi for each 20% reduction, roughly doubling the tensile strength of annealed (1200 F) material by 80% cold work. The curves for each reduction are approximately parallel and reflect the same general trend as the annealed data with

respect to the greater effect of each manganese increment for the first 6% as compared to subsequent increments.

The yield strengths of each of the alloys approach to within 2000 to 5000 pounds of the tensile strength for the same amount of cold work, owing to the relatively large increase (35,000 to 40,000 psi) with 20% cold work, which is emphasized by the method of plotting but nevertheless quite normal. The yield strength of alloys containing more than 8% manganese, however, is unusual at 20% reduction in that it remains constant at about 58,000 psi, regardless of increasing manganese. The elongation of these alloys at this reduction is likewise unusual in that it increases with increasing manganese, rising from about 11 to about 20%. The rising trend of the elongation here is in accord with the "as-annealed" values, but no explanation of either anomaly can be offered on the basis of available data.

The elongations of alloys cold-rolled to 40 and 80% reduction are not sensitive to increasing manganese content. This fact is consistent with the data for the annealed state, and the 4% elongation retained after 80% reduction indicates further deformation to be possible without overwork.

Presentation of the hardness values is complicated by the necessity of changing from the Rockwell F scale used for annealed material to the B scale for cold-worked material. The relationship between these scales (90 R_F is equivalent to 60B) is not quite accurate within one or two points of the correct value. Hardness behaves like the yield strength, increasing greatly for the first 20% reduction and then more slowly with additional working. The total increase is greatest for the 2% manganese alloy; the hardness rises from R_F 45 as annealed to R_B 79 after 80% cold reduction, whereas the hardness of the 20% alloy rises from R_F 72 as annealed to R_B 99 with the maximum cold work given.

Effect of Annealing Temperature

Properties obtained by annealing the 60% cold-worked alloys for 1 hour at temperatures ranging from 300 to 1500 F (150 to 815 C) are given in Table III. The tensile strength, yield strength, and hardness at the various annealing temperatures are plotted against composition in Figs. 5, 6, and 7. The curves for some temperatures are omitted from the graphs to avoid the confusion that the close

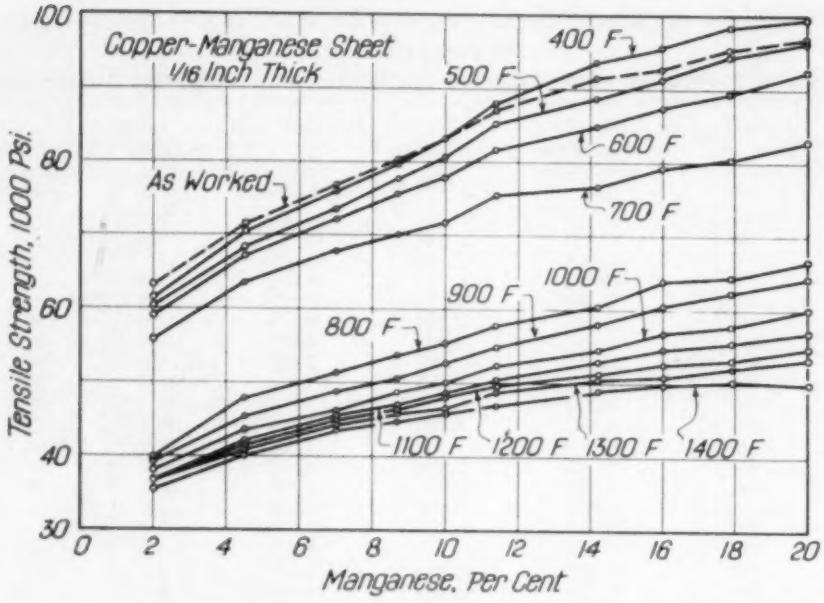


Fig. 5—The Effect of Annealing Temperature on the Tensile Strength of 60% Cold-Worked Copper-Manganese Alloys Heated for 1 Hour at Temperatures Indicated.

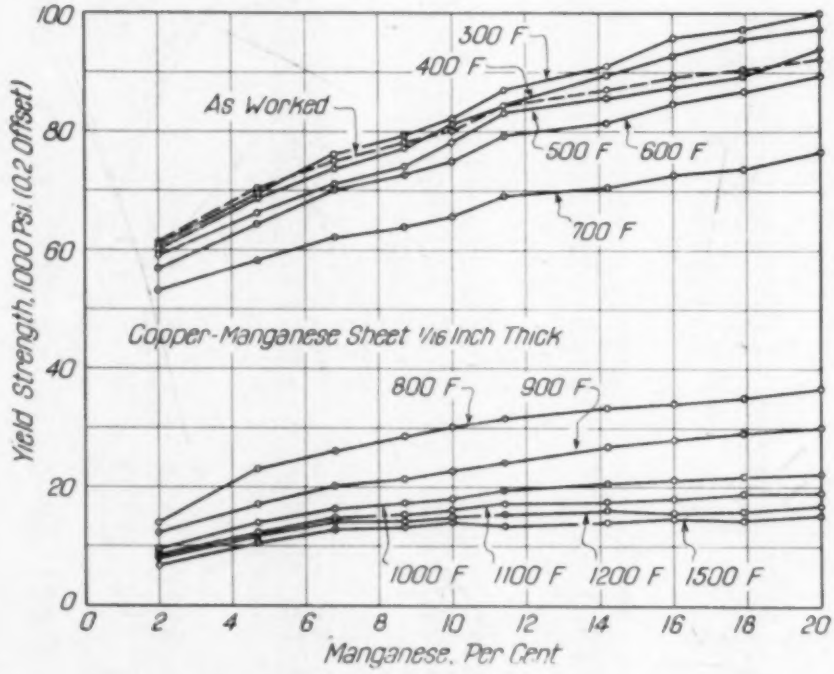


Fig. 6—The Effect of Annealing Temperature on the Yield Strength of 60% Cold-Worked Copper-Manganese Alloys Heated for 1 Hour at Temperatures Indicated.

approach of the data to the next higher or lower temperatures would produce. The maximum and minimum elongations for the alloys as a group are plotted as a function of annealing temperature in Fig.

Table III

Variation of Properties of the Cold-Worked Alloys with Annealing Temperature

Percentage of Mn in Alloy	Annealing Temperature F	Ultimate Strength psi	Yield Strength psi 0.2 Offset	Proportional Limit psi 0.01 Offset	Elongation %	Hardness Rockwell F	Hardness Rockwell B
2.0	As-rolled	63,200	61,400	42,100	4.6	..	74
	300	62,000	61,100	45,700	5.0	..	75
	400	61,200	60,300	45,600	5.8	..	74
	500	60,100	59,100	43,800	6.5	..	73
	600	59,000	57,000	43,900	6.8	..	72
	700	55,800	53,100	40,500	11.0	96	67.5
	800	39,800	13,700	8,000	46.9	61	..
	900	39,300	12,000	7,000	46.8	56	..
	1000	38,000	9,800	5,300	48.9	50	..
	1100	36,800	8,200	5,500	50.2	46	..
	1200	36,600	8,000	5,200	49.4	45	..
	1300	36,800	7,000	5,000	50.0	44	..
	1400	35,300	7,200	4,100	48.8	41	..
	1500	35,300	6,900	4,100	48.2	39	..
4.7	As-rolled	71,600	70,100	50,100	5.0	..	83
	300	71,700	69,800	47,600	5.0	..	82
	400	70,400	69,100	51,900	5.6	..	82
	500	68,200	66,400	50,500	7.1	..	81
	600	67,000	64,600	50 600	8.3	..	80
	700	63,500	58,500	47,600	11.2	..	77
	800	47,900	23,200	14,700	38.7	80	..
	900	45,200	17,000	11,800	46.2	69	..
	1000	43,500	14,000	9,400	46.9	62	..
	1100	42,000	12,100	8,000	48.1	59	..
	1200	41,400	11,800	7,500	49.3	57	..
	1300	41,000	11,100	6,300	49.0	56	..
	1400	40,000	10,500	6,600	46.6	55	..
	1500	40,300	10,900	7,200	46.3	53	..
7.0	As-rolled	76,700	75,100	52,300	4.8	..	86.5
	300	77,800	76,300	56,700	4.6	..	87
	400	75,800	74,000	57,700	5.4	..	86
	500	73,100	71,400	56,800	7.1	..	85.5
	600	72,000	70,200	54,600	7.9	..	84
	700	67,700	62,200	48,400	12.1	..	81
	800	51,200	26,300	17,300	36.8	83	46
	900	48,700	20,200	15,100	45.1	74	..
	1000	46,100	16,500	11,700	45.3	67	..
	1100	45,300	14,900	9,500	47.0	66	..
	1200	44,700	14,300	7,700	48.0	64	..
	1300	44,300	13,600	7,600	46.2	63	..
	1400	43,300	13,100	7,300	45.1	62	..
	1500	43,900	13,100	8,100	46.3	60	..
8.7	As-rolled	80,000	78,100	53,000	4.3	..	90
	300	81,600	79,500	57,700	4.3	..	89
	400	79,900	77,400	58,400	4.8	..	89
	500	77,600	74,300	57,700	5.8	..	88
	600	75,600	72,900	55,200	7.3	..	87
	700	69,900	64,100	51,200	11.5	..	83
	800	53,600	28,700	20 000	38.8	86	52
	900	50,500	21,700	16,400	43.5	77	..
	1000	48,400	17,500	12,400	44.8	71	..
	1100	46,900	15,600	10,800	45.6	68	..
	1200	46,100	14,300	8,400	46.6	66	..
	1300	45,900	14,100	7,700	46.6	64	..
	1400	44,600	14,000	8,500	44.6	64	..
	1500	45,200	13,800	8,700	47.3	63	..
10.0	As-rolled	82,700	80,100	58,400	4.2	..	91
	300	84,500	82,500	63,300	3.9	..	91
	400	83,000	81,100	61,900	4.5	..	90.5
	500	80,200	78,200	62,200	5.7	..	89
	600	77,700	75,100	56,800	7.3	..	88
	700	71,500	65,800	52,900	11.7	..	84
	800	55,300	30,200	21,700	35.6	88	54
	900	52,400	23,000	17,600	42.4	79	..
	1000	50,000	18,100	12,800	46.2	73	..
	1100	48,300	16,400	10,200	45.5	69	..
	1200	48,000	15,200	9,000	44.4	67.5	..
	1300	46,400	14,700	8,200	44.4	66	..
	1400	45,900	14,600	8,600	45.1	66	..
	1500	46,000	14,300	8,700	44.9	64	..

Table III—(Continued)
Variation of Properties of the Cold-Worked Alloys with Annealing Temperature

Percentage of Mn in Alloy	Annealing Temperature F	Ultimate Strength psi	Yield Strength psi 0.2 Offset	Proportional Limit psi 0.01 Offset	Elongation %	Hardness Rockwell F	Hardness Rockwell B
11.4	As-rolled	87,100	84,400	59,500	4.1	..	92
	300	89,500	87,100	62,900	3.8	..	93
	400	88,000	84,600	66,400	3.9	..	93
	500	85,100	83,100	62,200	5.0	..	92
	600	81,600	79,200	59,800	6.3	..	90.5
	700	75,400	69,400	53,700	11.0	..	87
	800	57,900	32,000	24,000	34.6	90	57.5
	900	54,900	24,400	19,900	42.6	82	43
	1000	52,200	19,800	13,800	43.4	76	..
	1100	50,300	17,500	11,000	45.3	72	..
	1200	49,600	15,900	9,700	44.3	69	..
	1300	48,400	15,400	8,800	45.2	67	..
	1400	46,800	14,500	8,600	43.7	65	..
	1500	45,500	13,700	8,000	42.3	62	..
14.2	As-rolled	91,400	87,100	64,300	4.2	..	94
	300	94,100	91,300	69,200	3.9	..	95
	400	93,600	89,700	71,500	3.8	..	95
	500	88,700	85,700	65,700	4.7	..	94
	600	84,900	81,900	61,900	5.9	..	92
	700	76,600	70,800	54,500	11.1	..	88.5
	800	60,500	33,800	26,900	38.6	91.5	60
	900	58,000	27,200	22,000	41.2	85	50
	1000	54,400	20,900	15,500	42.7	77	..
	1100	52,900	17,800	10,200	46.2	73	..
	1200	51,200	16,300	10,400	46.5	70	..
	1300	50,200	15,800	9,100	46.1	68	..
	1400	49,000	15,600	9,800	47.2	67	..
	1500	47,400	14,500	8,300	45.3	65	..
16.0	As-rolled	92,800	89,200	67,200	4.0	..	95
	300	96,800	96,000	74,400	3.8	..	95
	400	95,500	92,900	71,700	3.9	..	95.5
	500	91,200	87,500	68,600	4.6	..	94.5
	600	87,300	84,700	64,100	6.0	..	93.5
	700	79,000	72,900	56,700	11.0	..	89.5
	800	64,000	34,900	28,000	34.0	93	63
	900	60,400	28,300	23,000	39.2	86	53
	1000	56,800	21,500	15,300	41.9	79	..
	1100	54,700	18,500	11,500	44.5	74	..
	1200	52,800	16,000	10,200	45.3	71	..
	1300	50,900	15,200	8,200	48.5	67	..
	1400	49,600	15,300	8,400	47.0	67	..
	1500	48,600	15,100	8,200	46.4	64	..
17.9	As-rolled	95,200	90,000	68,100	4.3	..	96
	300	99,000	97,100	73,900	3.9	..	96
	400	98,400	95,700	72,500	3.8	..	97
	500	94,400	89,400	70,500	4.5	..	96
	600	89,300	86,900	67,300	5.9	..	94
	700	80,200	73,900	59,100	11.4	..	90
	800	64,200	35,200	29,000	37.0	93	63.5
	900	62,400	29,400	23,600	40.0	88	55
	1000	57,800	22,100	15,900	43.5	79	..
	1100	55,500	19,200	13,700	46.4	75	..
	1200	53,000	16,100	9,400	48.5	71	..
	1300	52,100	15,800	8,900	49.7	68	..
	1400	50,100	15,700	9,100	49.8	69	..
	1500	47,800	14,600	7,500	48.7	64	..
20.0	As-rolled	96,800	92,300	69,800	4.0	..	97
	300	102,700	100,100	77,200	3.8	..	97
	400	99,800	97,200	75,100	3.9	..	98
	500	96,400	94,000	73,100	4.2	..	97
	600	92,200	89,500	69,200	6.1	..	95
	700	82,800	76,800	59,000	10.9	..	92
	800	66,700	37,000	31,100	36.3	94.5	66
	900	64,100	30,200	23,700	40.0	89	57
	1000	60,000	22,500	16,000	43.4	81	..
	1100	56,900	19,300	12,500	47.3	76	..
	1200	54,900	17,100	9,400	49.2	72	..
	1300	53,200	16,300	9,200	51.6	69	..
	1400	49,900	15,600	9,500	51.1	69	..
	1500	48,600	15,500	8,100	50.3	64	..

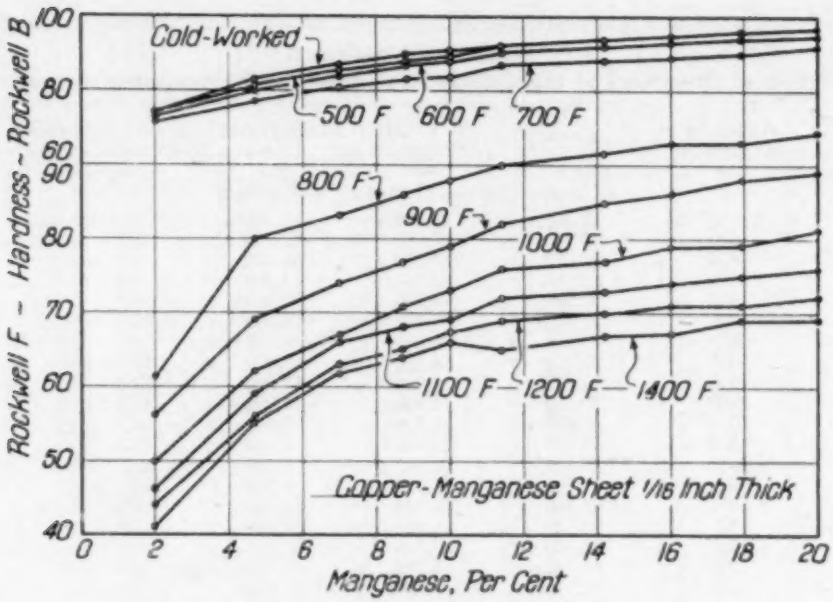


Fig. 7—The Effect of Annealing Temperature on the Hardness of 60% Cold-Worked Copper-Manganese Alloys.

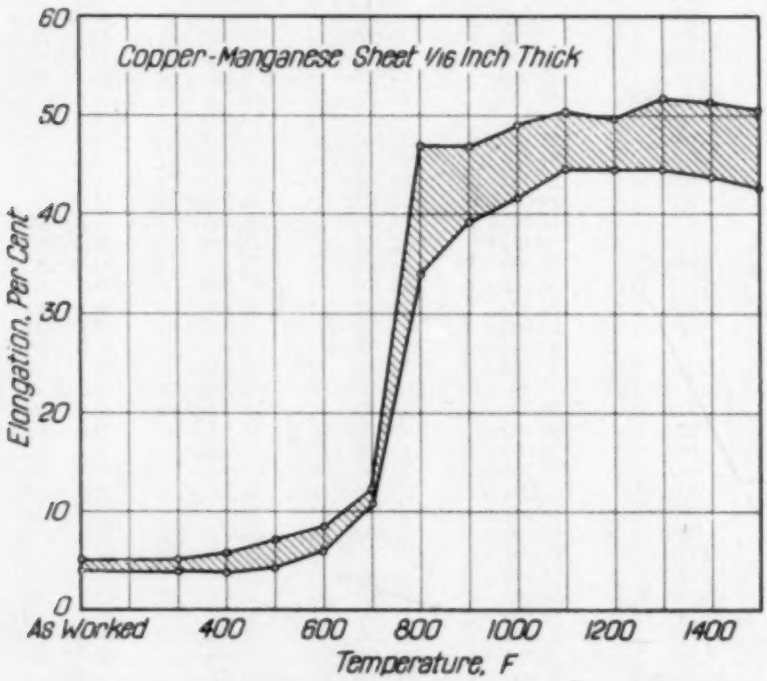


Fig. 8—The Maximum and Minimum Elongation of 2 to 20% Manganese Alloys Versus Annealing Temperature.

8, since the relatively small variations from one composition to another do not lend themselves to the type of graph used for other properties.

The tensile and yield-strength curves show a larger spread of

properties for the higher-manganese alloys by cold working and annealing. It will also be noted that the tensile and yield strengths show a slight aging effect for all compositions greater than 6% manganese and is best illustrated by the yield-strength curves of Fig. 6. The increase in strength values over those for the cold-worked condition occurs on treatment of cold-worked material in the 300 to 400 F temperature range and is not apparent in the lower-manganese alloys. In general, the greater the manganese content above 6% (up to the limit studied) the greater the increase in strength. This gives rise to the speculation that factors incident with the precipitation of alpha manganese are responsible for this effect; that is, the solubility of manganese in copper may continue to decrease below 20% manganese with decreasing temperature. Extrapolation of the solubility curve of the manganese in copper from the equilibrium diagram to these low temperatures suggests that precipitation could occur. Metallographic studies in this region, however, are difficult, owing to existing cold-worked structures, and X-ray data, at the moment, have not confirmed this speculation.

As the annealing temperature is increased, the strength and hardness decrease, the major change corresponding to recrystallization taking place between 700 and 800 F. The elongation rises most rapidly in this same temperature range. Apparently, the first 2% manganese increases the recrystallization range of copper to these temperatures, but further additions of manganese have little effect on it. Higher annealing temperatures cause a further decrease in hardness and strength and some change in elongation because of grain growth. That is, these alloys behave in the normal way, showing the usual strain relief, recrystallization, and softening with grain growth.

The data also show that an annealing temperature of 800 F produces the highest strength and hardness consistent with good elongation in all of the alloys.

Summary

The tensile strength of copper-manganese alloys annealed for 1 hour at 1200 F (650 C) increases from 36,000 psi for the 2% manganese alloy to 54,900 psi for the 20% alloy. For the first 6% manganese the strength increases at a rate of 2000 psi for each per cent manganese. Above 6% the increase is approximately 800

psi for each per cent manganese. The yield strength and hardness behave in a similar manner. Elongation shows little variation with increasing manganese, ranging from 45 to 49% for all compositions. It is significant that increasing manganese content strengthens copper without loss of ductility.

The alloys may be hot and cold-rolled readily and can stand more than 80% reduction by cold rolling. Tensile strength increases about 10,000 psi for each 20% reduction by cold rolling and is roughly doubled by 80% reduction. The changes in yield strength, hardness, and elongation are greatest for the first 20% reduction and continue at a decreasing rate for additional reductions.

Some aging takes place upon heating cold-worked alloys containing more than 6% manganese in the temperature range of 300 to 400 F. The increase in strength is not large but it rises with increasing manganese and amounts to 6000 pounds in the tensile strength and 7800 pounds in the yield strength at 20% manganese. The hardness and elongation do not change significantly with aging. Recrystallization takes place on annealing at 700 to 800 F and is unaffected by composition. Maximum strength of fully recrystallized material is obtained by annealing for 1 hour at 800 F (425 C). Higher annealing temperatures lower the strength and hardness by permitting grain growth but do not increase elongation appreciably.

Acknowledgments

This paper is one of many covering various aspects of the Bureau of Mines program directed toward the more effective utilization of our mineral resources.

Investigations of our mineral resources are carried out by the Mining Branch, under the direction of L. B. Moon, and the Metallurgical Branch, under the direction of R. G. Knickerbocker. Both branches are supervised by R. S. Dean, assistant director.

The scope of this paper falls in the province of the Metallurgical Branch whose activities embrace the separation of difficultly beneficiated ores, the production of pure metals from domestic deposits, the exploitation of marginal ore reserves, the recovery of secondary metals, and the improvement of present industrial metallurgical practice.

References

1. R. S. Dean, J. R. Long, T. R. Graham, E. V. Potter and E. T. Hayes, "The Copper-Manganese Equilibrium System," Transactions, American Society for Metals, Vol. 34, 1945, p. 443.

2. R. S. Dean, E. V. Potter, J. R. Long and R. H. Huber, "Properties of Transitional Structures in Copper-Manganese Alloys," TRANSACTIONS, American Society for Metals, Vol. 34, 1945, p. 465.
3. R. S. Dean and C. T. Anderson, "The Alloys of Manganese and Copper—Hardening by Cold Work and Heat Treatment," TRANSACTIONS, American Society for Metals, Vol. 29, 1941, p. 802.
4. R. S. Dean and C. T. Anderson, "The Alloys of Manganese and Copper—Electrical Resistance," TRANSACTIONS, American Society for Metals, Vol. 29, 1941, p. 788.
5. R. S. Dean, C. T. Anderson and E. V. Potter, "The Alloys of Manganese and Copper—Vibration Damping Capacity," TRANSACTIONS, American Society for Metals, Vol. 29, 1941, p. 402.
6. A. H. Hesse and E. T. Myskowski, "Some Mechanical Properties of Manganese-Copper Alloys," *Transactions,* American Institute of Mining and Metallurgical Engineers, Vol. 147, 1942, p. 243.
7. J. R. Long and T. R. Graham, "Physical Properties of a 65 Cu, 10 Mn, 25 Zn Alloy," *Transactions,* American Institute of Mining and Metallurgical Engineers, Vol. 156, 1944, p. 222.
8. R. S. Dean, J. R. Long, T. R. Graham and C. W. Matthews, "A White High-Manganese Brass," *Transactions,* American Institute of Mining and Metallurgical Engineers, Vol. 161, 1945, p. 244.
9. R. S. Dean, "The Present Status of Electrolytic Manganese and Its Alloys," *Transactions,* American Institute of Mining and Metallurgical Engineers, Vol. 156, 1944, p. 301.
10. R. S. Dean, J. R. Long, T. R. Graham and R. G. Feustel, "Physical Properties of Copper-Manganese-Zinc Alloys Containing 60 Per Cent Copper and 5 to 25 Per Cent Manganese," *Metals Technology,* American Institute of Mining and Metallurgical Engineers, Jan. 1946, T. P. 1956.
11. Unpublished results of U. S. Bureau of Mines.
12. R. A. Wilkins and E. S. Bunn, "Copper and Copper-Base Alloys," McGraw-Hill Book Company, New York City, 1943.

DISCUSSION

Written Discussion: By Floyd C. Kelley, Research Laboratory, General Electric Co., Schenectady, N. Y.

Dr. Dean and his associates are to be congratulated on another of many papers dealing with elements which demand considerable care in processing.

Manganese is a very active element toward oxygen and when melted under ordinary conditions grabs quantities of oxygen from the atmosphere. Manganese-copper alloys melted in air, drawn into wire and used for brazing in a pure dry hydrogen atmosphere, with a dew point of —105 F or lower, have an oxidized shell which is not reduced at 2100 F (1150 C) during the brazing cycle. This oxidized shell is a bright green and holds the molten alloy within so that it cannot break through and wet the metal to be brazed.

Manganese-copper alloys melted under pure dry argon or argon containing 12% nitrogen give a wire which when used for brazing in pure dry hydrogen shows no oxidized shell, wets the metal to be brazed nicely and runs about like copper. The 20% nickel-manganese alloy, used for brazing stainless steels in pure dry hydrogen, when melted in air gives the same oxidized shell described above, but when melted under argon + 12% nitrogen and used for brazing in pure dry hydrogen wets the steel nicely and results in bright shiny joints with nice fillets.

I should like to ask the authors why they did not use argon or helium

as an atmosphere for melting their alloys and avoid the use of aluminum as a deoxidizing agent. It may be that aluminum has little effect on this alloy system as the authors state, and its use may be the most practical way of producing the alloy in quantity, but for a nice fundamental investigation of an alloy system the use of an inert atmosphere for melting would eliminate any question of the effects of aluminum or its resulting oxide.

Written Discussion: By Paul A. Beck, associate professor, University of Notre Dame, Notre Dame, Ind.

Could the authors give us some information concerning the grain growth behavior of these alloys? It would be interesting to know what effect, if any, manganese in solid solution has on the grain size vs. temperature curves after a certain period of anneal. Also, I am particularly interested in knowing whether or not grain coarsening, of the type associated with a duplex structure (mixed large and small grains), has been observed by the authors in these alloys.

Authors' Reply

In answer to Mr. Kelley's discussion, our experience with the melting of manganese alloy wire or rods in nearly inert atmospheres coincides with that of Mr. Kelley. At an early date in our work on manganese alloys we annealed them in ordinary helium; on several occasions the temperature accidentally went above the melting point and the molten metal was held so tightly by the green scale that the only evidence of melting was in the microstructure. Using really pure helium, this does not happen. We wonder if Mr. Kelley means to blame the formation of the coating on the melting technique rather than the annealing.

If the melt is properly deoxidized with aluminum, it is doubtful if a wire made from it would scale any more readily than a wire made from a vacuum melt. The important item would seem to be to avoid scaling during the anneal either by the use of very pure helium as atmosphere or by a rigorous pickling after each anneal. An ammonium sulphate solution has been found to be an effective pickling agent for high manganese alloys.

We agree with Mr. Kelley on the advantages of melting in an inert atmosphere and hope to check the properties of the alloys in this system when melted under pure helium. Our idea in using the procedure of melting in air and deoxidizing was that these alloys have no special properties likely to be greatly affected by vacuum melting and the only outlook for their commercial use would be in the general brass and bronze field, hence their properties when made by what is still the usual technique in this field appeared to have the most general interest.

In answer to Professor Beck's questions, our data, while not bearing directly on the points raised, indicate that the grain growth behavior of these copper-manganese alloys is not greatly different from similar solid solution copper alloys. That is, the grain growth curves would be essentially normal curves showing a slow rate of growth at temperatures near the recrystallization range and rapid growth at higher temperatures. No particular tendency to form "duplex grain structures" — mixed large and small sizes — has been encountered.

AGE HARDENING COPPER-COBALT-MANGANESE ALLOYS

By Jay W. Fredrickson

Abstract

Copper-cobalt-manganese alloys containing 2 to 4% cobalt and up to 15% manganese are shown to have hardenable characteristics and the ability to harden from Rockwell F-67 to Rockwell B-81 from an annealed condition. The optimum treatment consists of aging at 900, 1000 and 1100 F (480, 540 and 595 C). Hardness may be controlled by regulation of aging time and temperature. Material aged from the cold-worked condition does not harden significantly above the original cold-worked hardness. Maximum hardness obtained in cold-worked condition is Rockwell B-97.

RECENT development and expansion of electrolytic cobalt and manganese production have opened up fields of alloy research employing these metals. One field of interest concerns the influence of high-purity manganese on hardenable copper-cobalt alloys. References in the literature on copper-base alloys containing cobalt and manganese are very limited. Köster and Wagner (1)[1] reported the equilibrium conditions of the copper-cobalt-manganese system up to 40% manganese; also that no homogeneously solidifying, hardenable, ferromagnetic alloys are formed in this system. In the copper-cobalt system Tammann and Oelsen (2) determined the solubility of cobalt in copper by measuring the specific magnetization of a series of alloys, this solubility being approximately 5% at 2025 F (1108 C). M. G. Corson (3) studied the hardness and electrical resistance changes in some copper-cobalt alloys, and the range of solid solubility of cobalt in copper. This range is from 3.4% cobalt at 1830 F (1000 C) to 0.35% at room temperature. He also reported that 2.5%

[1]The figures appearing in parentheses pertain to the references appended to this paper.

This paper is based on a thesis to be submitted to the faculty of the University of Utah by the author in partial fulfillment of the requirements for the degree of Bachelor of Science in Metallurgical Engineering.

A paper presented before the Twenty-eighth Annual Convention of the Society, held in Atlantic City, November 18 to 22, 1946. The author, Jay W. Fredrickson, is attending the University of Utah, Salt Lake City, Utah. Manuscript received June 28, 1946.

cobalt is required to obtain a maximum hardening effect of 105 Brinell.

C. S. Smith (4) reported the unusual hardening obtained by air cooling a 3.58% cobalt alloy from 1650 F (900 C), giving a maximum hardness of Rockwell B-60. Gordon and Cohen (5) determined changes in hardness, electrical resistance, magnetic susceptibility, remanence, and microstructure of a 3.2% cobalt alloy. Maximum hardness of Rockwell F-81 was found to occur when the alloy was aged over 100 hours at 1020 F (550 C).

Dean, Long, Graham, Potter and Hayes (6) examined a series of copper-manganese alloys by thermal analysis, X-ray diffraction and metallographic methods, establishing the copper-manganese equilibrium diagram. Copper is shown to be soluble in gamma manganese, with a continuous solid solution field across the diagram at the higher temperatures. This solution breaks down at lower temperatures when the manganese content exceeds 25%. In the cobalt-manganese system Hiege (7) determined the temperature of the initial solidification and the approximate temperature at the end of solidification of cobalt-manganese melts. The shape of the cooling curve found by Hiege suggests a continuous series of solid solutions. Hashimoto (8) later determined that a series of solid solutions of beta cobalt was formed from alloys with up to 51% manganese.

In selecting the compositions for investigation, equilibrium diagrams for the various alloys were studied. The maximum solubility of cobalt in copper was reported to be 5.0% (2). Manganese was reported to be soluble in copper, up to 25%, at low temperatures (6) and in cobalt, up to 51% (7), (8). These reports indicate that a maximum of 4% cobalt and 15% manganese would be completely soluble in copper at some elevated temperature.

The hardening properties of copper-cobalt alloys (3), (4), (5) are known to be rather low, and this investigation was conducted to determine the changes in hardening with the addition of manganese. It was hoped that the addition of manganese would improve the hardening properties. With this purpose in mind a series of alloys containing 2, 3 and 4% cobalt and 0, 1, 3, 5, 10 and 15% manganese was investigated.

Preparation of Alloys

The alloys were prepared in heats of 35 pounds each from wire bar grade copper, electrolytic cobalt and electrolytic manganese. The

Table I
Chemical Analysis of Metals Used, in %

Copper		Cobalt		Manganese	
Fe	0.008	Fe	0.2 → 0.006	Fe	0.01
S	0.01	S	0.01	S	0.02
Ni	0.01	Ni	1.03	Si	Nil
As	Nil	As	0.0001	Al	Nil
Sb	Nil	Pb	0.008	Pb	0.02
Sn	Nil	Mn	0.0016		
Pb	Nil	Cu	Trace		

high purity of the metals used is evident in Table I. The purity of manganese and cobalt is noteworthy. With iron content less than 0.2% and sulphur less than 0.02%, impurities are kept to a minimum. The seemingly high nickel content of 1.03% in the cobalt metal is really inconsequential in view of the fact that a maximum of 4% cobalt is used.

A high-frequency induction furnace was used for melting and alloying. The alloying method consisted of melting the copper down and gradually adding manganese after the bath was molten. The cobalt was added slowly after the manganese had been completely dissolved. When the cobalt was entirely taken up by the melt, the metal was deoxidized with about 0.05% pure aluminum and cast into 3 by 1¾ by 18-inch flat ingots. The ingots were hot-stripped and air-cooled.

Chemical analyses of the heats are given in Table II. The high purity of the alloys is quite evident. Iron content is no greater than 0.014% in all cases and the silicon content is less than 0.005%.

Table II
Chemical Analysis of Alloys, in %

Alloy Designation	Copper	Cobalt	Manganese	Aluminum	Iron	Silicon
2- 0	98.0	1.87	Tr	0.01	0.010	<0.005
2- 1	97.3	1.88	0.73	0.01	0.011	<0.005
2- 3	95.5	2.00	2.50	0.03	0.012	<0.005
2- 5	93.5	1.97	4.70	0.03	0.011	<0.005
2-10	88.5	2.02	9.46	0.03	0.013	<0.005
2-15	83.7	1.97	14.50	0.03	0.012	<0.005
3- 0	97.3	2.45	Tr	0.04	0.013	<0.005
3- 1	96.3	2.76	0.57	0.04	0.014	<0.005
3- 3	94.5	2.82	2.80	0.03	0.013	<0.005
3- 5	92.2	2.95	4.86	0.03	0.011	<0.005
3-10	87.2	3.20	9.50	0.03	0.012	<0.005
3-15	82.2	3.10	14.70	0.03	0.012	<0.005
4- 0	96.3	3.20	Tr	0.01	0.010	<0.005
4- 1	95.5	3.76	0.65	0.04	0.013	<0.005
4- 3	92.5	4.00	3.20	0.04	0.013	<0.005
4- 5	91.0	4.02	4.96	0.03	0.011	<0.005
4-10	86.2	3.75	9.83	0.04	0.013	<0.005
4-15	81.0	4.00	14.83	0.03	0.013	<0.005

Residual aluminum averages approximately 0.03%. The loss of cobalt and manganese during the melting and alloying was negligible in most cases. Since the nominal and chemical analyses are practically the same the alloys are referred to by their nominal analysis.

A portion of the ingots was cut off and heated 1½ hours at 1500 F (815 C), forged to break up the as-cast condition, and returned to the furnace in preparation for hot rolling. The remainder was left in an as-cast condition to be used for further investigation. All heats were heated to 1600 F (870 C), hot-rolled into 0.316-inch plate, annealed by heating to 1600 F (870 C), quenched, cold-rolled to 0.156-inch thickness, annealed again, and cold-rolled further to 0.0625 inch (60% reduction in thickness). Typical solution-treated and cold-worked structures are illustrated in Figs. 1 and 2.

Preliminary Heat Treatment

To obtain the temperature giving minimum hardness, which was taken as the criterion of complete solution, a series of cold-worked samples of each alloy was solution-treated for ½ hour at temperatures varying from 1200 to 1800 F (650 to 980 C). Hardness values determined on these specimens indicated that complete solution was obtained in most cases at 1600 F (870 C). However, the alloys containing 3 and 4% cobalt with 1% manganese, and 3% cobalt with 3% manganese, required a temperature of 1700 F (925 C) for complete solution. As illustrated in Figs. 3a and 3b, the alloy

Table III
Solution Temperatures Giving Minimum Hardness and Grain Size at These Temperatures

Alloy	Temperature F	Temperature C	Grain Size Mm. Av. Dia.
2- 0	1600	870	0.120
2- 1	1600	870	0.150
2- 3	1600	870	+0.200
2- 5	1600	870	+0.200
2-10	1600	870	+0.200
2-15	1600	870	+0.200
3- 0	1600	870	0.150
3- 1	1700	925	0.200
3- 3	1700	925	+0.200
3- 5	1600	870	+0.200
3-10	1600	870	+0.200
3-15	1600	870	+0.200
4- 0	1600	870	0.015
4- 1	1700	925	0.045
4- 3	1600	870	0.035
4- 5	1600	870	0.200
4-10	1600	870	+0.200
4-15	1600	870	+0.200

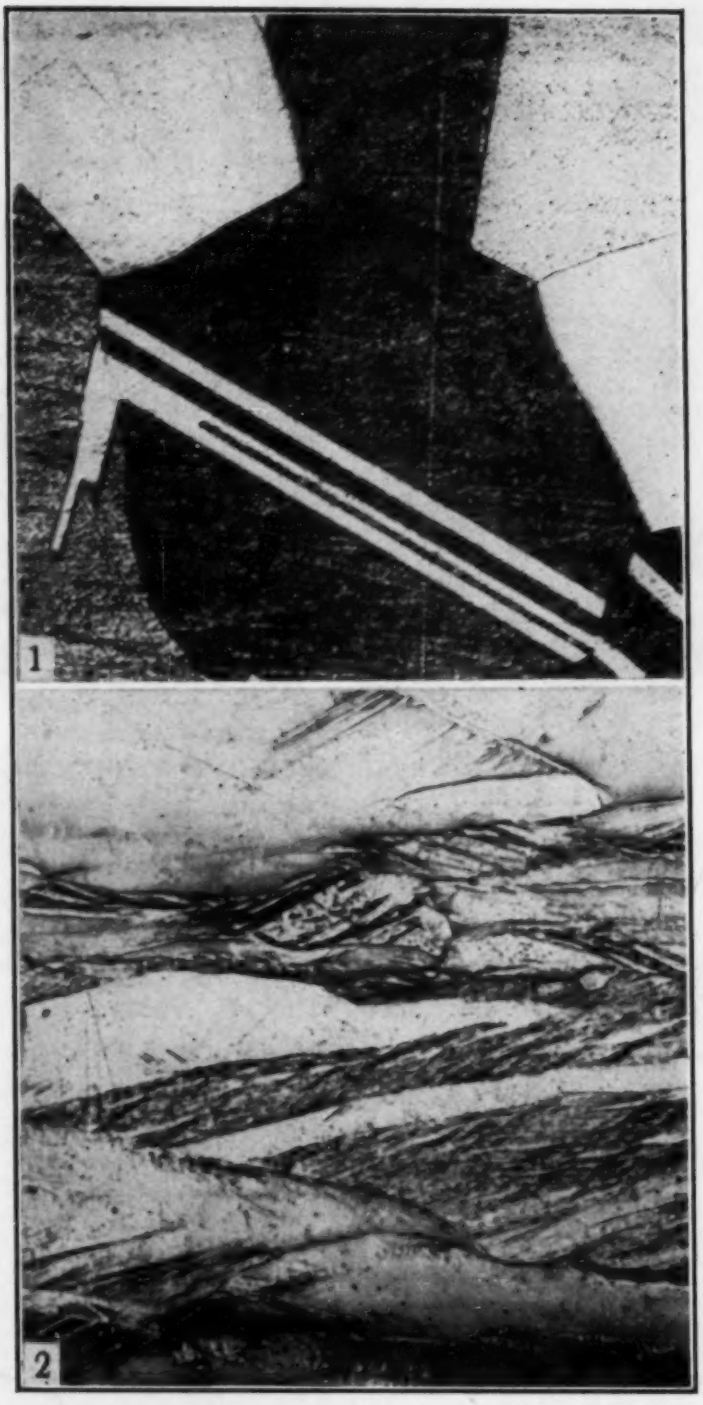


Fig. 1—Alloy 3-15. Solution-treated ½ hour at 1600 F (870 C). × 100.

Fig. 2—Alloy 3-10. 60% cold-reduced. × 250.

is not in complete solution at 1600 F (870 C) but is composed of alpha solid solution and a finely divided precipitate within the solid solution matrix. At 1700 F (925 C) (Fig. 3c) this precipitate prac-

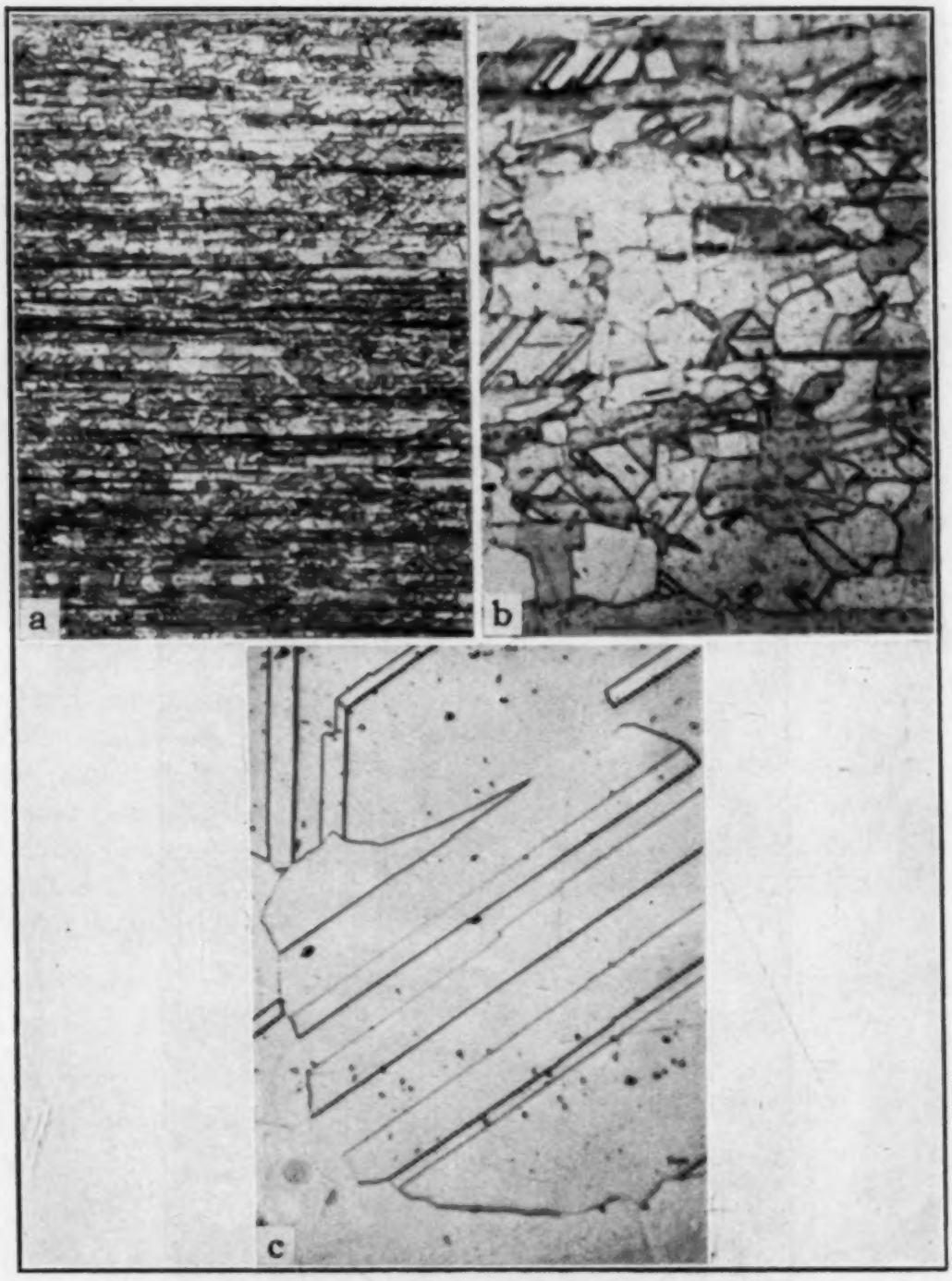


Fig. 3—Alloy 4-1. a. Solution-treated ½ hour at 1600 F (870 C). × 100. b. Solution-treated ½ hour at 1600 F (870 C). × 500. c. Solution-treated ½ hour at 1700 F (925 C). × 500.

tically disappears and the material is at its minimum hardness. Solution-treated material will hereafter be discussed as annealed.

The temperature at which minimum hardness was obtained, and

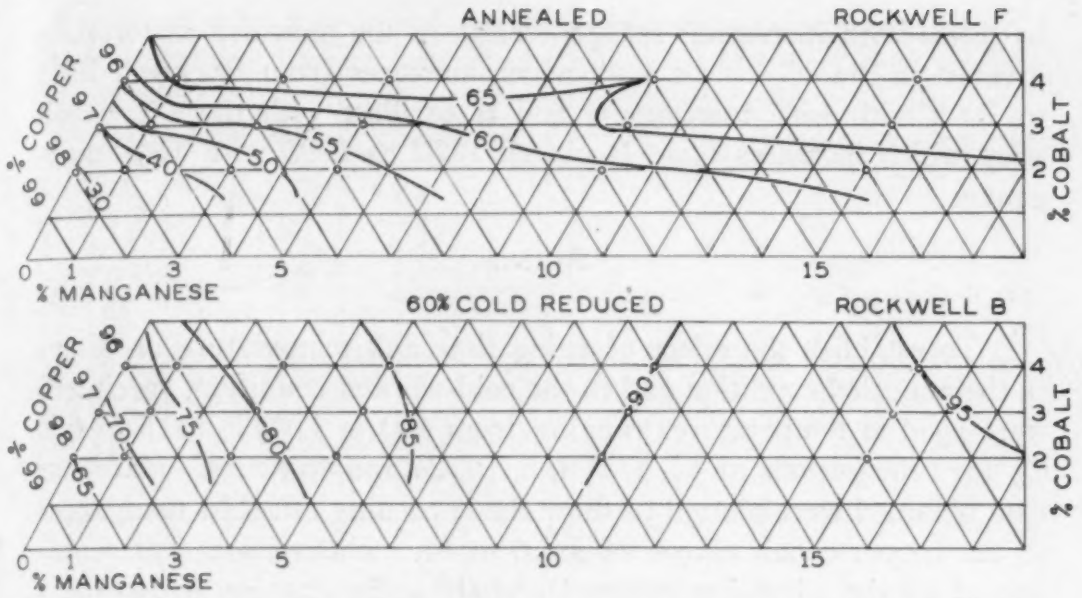


Fig. 4 (Upper)—Ternary Plot in the Copper-Rich Corner Showing Annealed Hardness. Rockwell F.

Fig. 5 (Lower)—Ternary Plot in the Copper-Rich Corner Showing Cold-Worked Hardness. Rockwell B.

the grain size at this temperature, are shown in Table III. As can be seen, the grain size is unusually large in most cases. In fact, this grain size is undoubtedly too large and a smaller grain size in the annealed condition should give greater hardness values upon aging. It is interesting to note the change in grain size with composition. Grain size increases with manganese content and tends to decrease with increasing cobalt content, with the exception of the 3% cobalt compositions whose grain sizes are generally larger.

The effect of manganese on the hardness of binary copper-cobalt alloys in the annealed and cold-worked condition is well illustrated in Figs. 4 and 5. In the annealed material (Fig. 4) manganese has a decided influence on the hardness of the 2% cobalt alloy. This influence decreases with increasing cobalt. The hardness of the 2 and 3% alloys is increased from Rockwell F-30 to F-62 and Rockwell F-40 to F-68, respectively, by the addition of 15% manganese. The hardness of the 4% cobalt alloy is increased from Rockwell F-60 to F-71 by the addition of 5% manganese, but increasing the manganese to 15% decreases the hardness to F-67. This decrease in hardness may be due to some extent to the large grain size.

In the cold-worked material (Fig. 5) hardness increases directly with increasing manganese in all alloys and reaches a maximum in the 4% cobalt alloy at 15% manganese. The change in

hardness with increasing manganese, as in the annealed material, is greatest in the 2% cobalt alloy which increases from Rockwell B-65 to B-93 with 15% manganese, and is smallest with the 4% cobalt alloy which increases from Rockwell B-72 to B-95 with 15% manganese.

Aging

To establish the effect of aging time and temperature on alloys in the annealed condition and in the cold-worked condition, specimens were aged at temperatures ranging from 600 to 1200 F (315 to 650 C) for time periods of ½, 1, 2, 4, 8, 16, 24 and 48 hours. Hardness data obtained were plotted to show the hardening effect of manganese on the copper-cobalt alloys. Figs. 6 to 14, inclusive, are representative of all the alloys investigated and show the changes in hardness

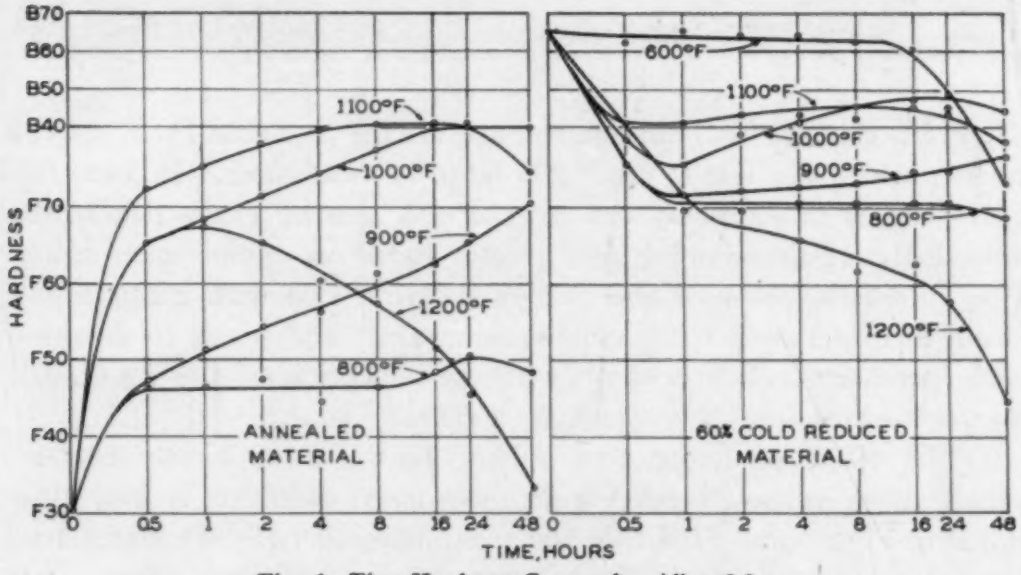


Fig. 6—Time-Hardness Curves for Alloy 2-0.

of a 2, 3 and 4% copper-cobalt alloy with the addition of 1 and 10% manganese. Curves for alloys containing 3, 5 and 15% manganese are omitted since the curves shown are representative. The graphs are arranged so that direct comparison can be made between material aged from the annealed condition and material aged from the cold-worked condition.

Figs. 6 to 8 illustrate the effect of manganese on a 2% cobalt alloy. The addition of manganese increases the initial annealed hardness and the general hardness levels at each aging temperature except

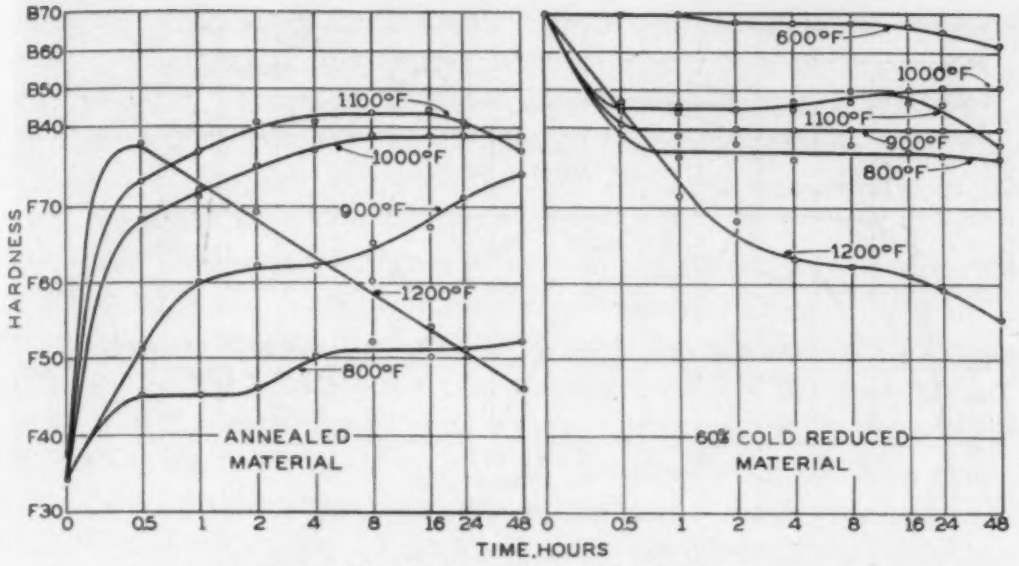


Fig. 7—Time-Hardness Curves for Alloy 2-1.

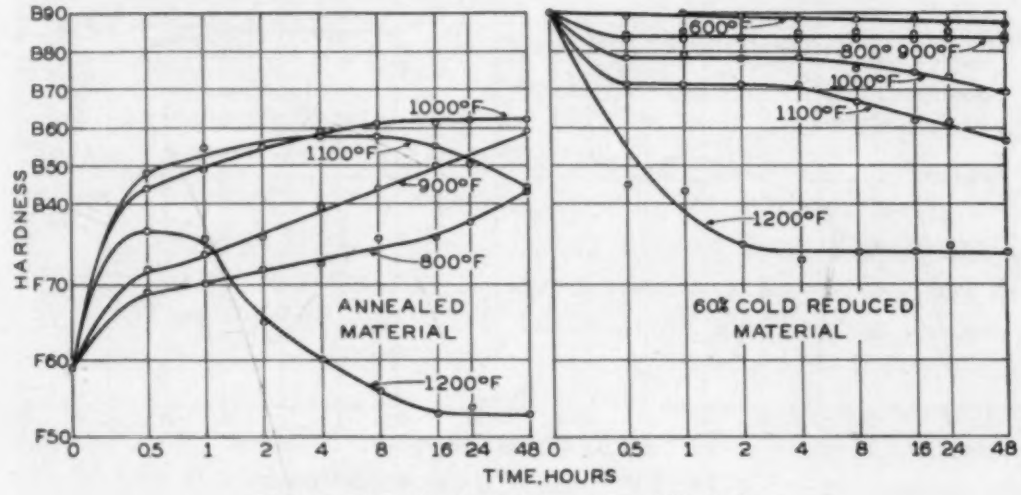


Fig. 8—Time-Hardness Curves for Alloy 2-10.

1000 F (540 C) at which temperature alloy 2-0 has a higher hardness than alloy 2-1. An increase in aging temperature from 800 F (425 C) to, and including, 1000 F (540 C) produces an increase in hardness. At 1000 F (540 C) alloy 2-10 reaches its maximum hardness of Rockwell B-62 at the end of 24 hours' aging and does not overage. Alloys 2-0 and 2-1 do not overage at 1000 F (540 C). Aging at 1100 F (595 C) produces maximum hardness of Rockwell B-40 and B-44 in alloys 2-0 and 2-1. Overaging occurs at this temperature in all three alloys. The time at which overaging occurs decreases with increasing manganese. At 1200 F (650 C) a maximum hardness is obtained in ½ to 1 hour's aging and the alloys over-

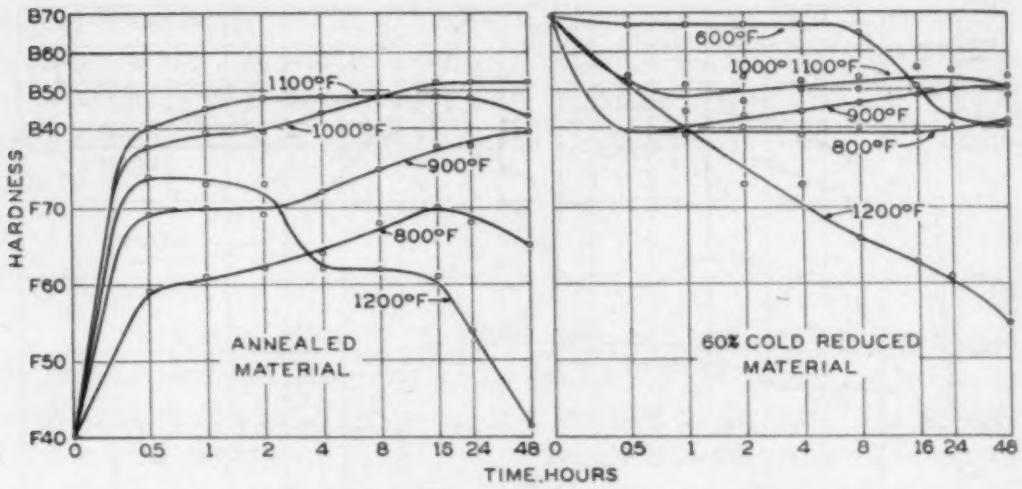


Fig. 9—Time-Hardness Curves for Alloy 3-0.

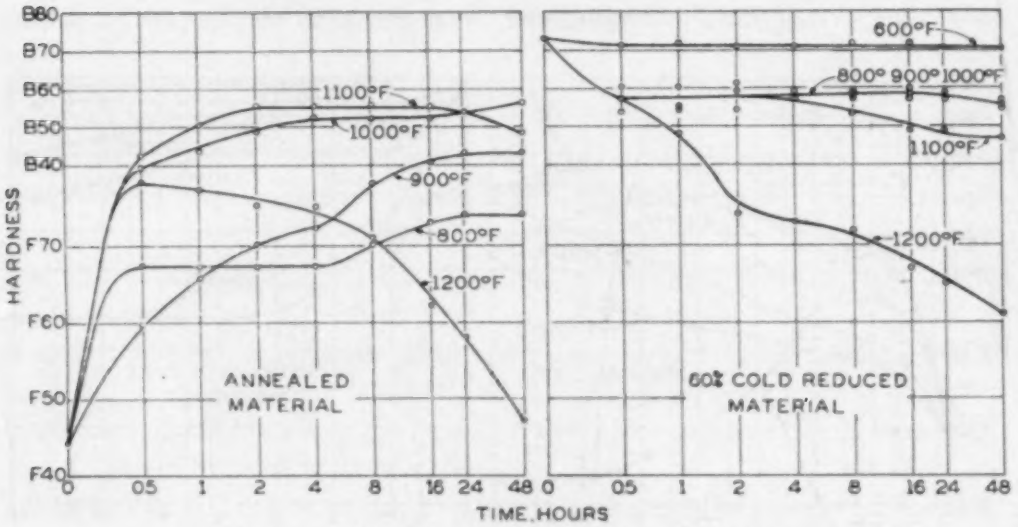


Fig. 10—Time-Hardness Curves for Alloy 3-1.

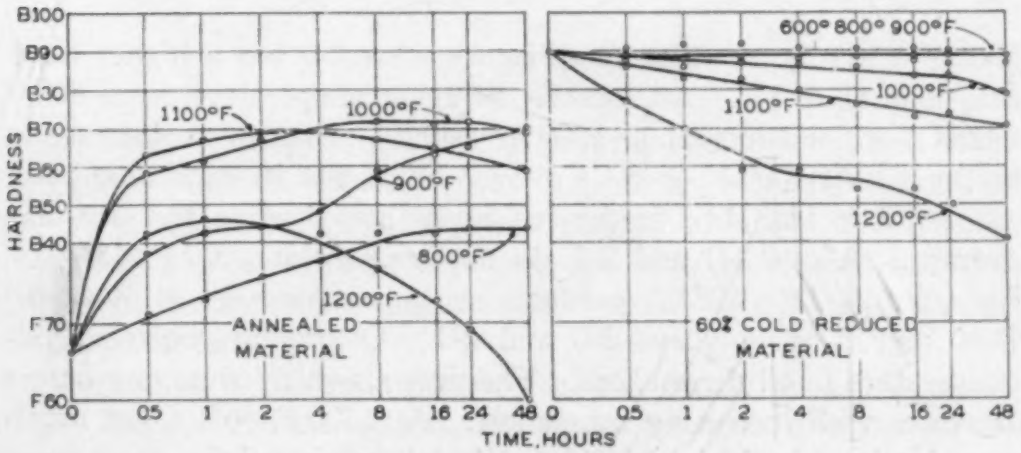


Fig. 11—Time-Hardness Curves for Alloy 3-10.

age in 1 to 2 hours in all cases. Maximum hardness of Rockwell F-78 is obtained at this temperature in alloy 2-1, with the hardness of the other alloys falling below this. Final hardness obtained at 1200 F (650 C) was generally at, or near, the annealed hardness except for alloy 2-1, in which the final hardness was slightly higher than the annealed.

The addition of manganese increases the hardness of the cold-worked material. This hardness increases from Rockwell B-64 in the copper-cobalt alloy to Rockwell B-90 with the addition of 10% manganese. When aged from a cold-worked condition the general hardness level for each aging temperature is increased with the addition of manganese. Aging at 600 F (315 C) produces very little change in original cold-worked hardness until aged 8 hours for alloy 2-0, and 16 hours for alloy 2-1, at which times the material softens, obtaining a minimum hardness of Rockwell F-78 for alloy 2-0 and Rockwell B-61 for alloy 2-1 in 48 hours. Alloy 2-10 decreases in hardness very slightly from its original hardness of Rockwell B-90 during the aging period. When aged at 800 F (425 C) the alloys decrease in hardness during the first ½ to 1 hour and then maintain this hardness generally throughout the aging period. Alloy 2-0 drops to Rockwell F-68, whereas the alloys containing manganese maintain a higher level. Alloy 2-10 has a minor drop from Rockwell B-90 to B-84. A secondary softening occurs in alloys 2-0 and 2-1 after 24 hours' aging. At 900 F (480 C) the alloys age in much the same manner as at 800 F (425 C) except that alloys 2-0 and 2-1 increase their hardness levels with the increase in temperature and the hardness level of alloy 2-10 decreases very slightly, retaining practically the same value as at 800 F (425 C). Aging alloy 2-0 at 900 F (480 C) produces an increase in hardness with time after 1 hour. This effect does not take place in the alloys containing manganese. Aging at 1000 F (540 C) produces higher hardness levels in alloys 2-0 and 2-1, but again a lower hardness level in 2-10 than those produced at 800 and 900 F (425 and 480 C). Both alloys 2-0 and 2-1 age harden after 1 and 2 hours, respectively, at this temperature, obtaining a maximum hardness at 16 hours' aging time. Secondary softening occurs in alloy 2-10 after 4 hours. At 1100 F (595 C) the alloys age in the same manner as at 1000 F (540 C), overaging occurring in alloy 2-0 after 16 hours and in alloy 2-1 after 8 hours, with secondary softening occurring in alloy 2-10 at 4 hours. At 1200 F (650 C) all alloys soften materially from the cold-worked

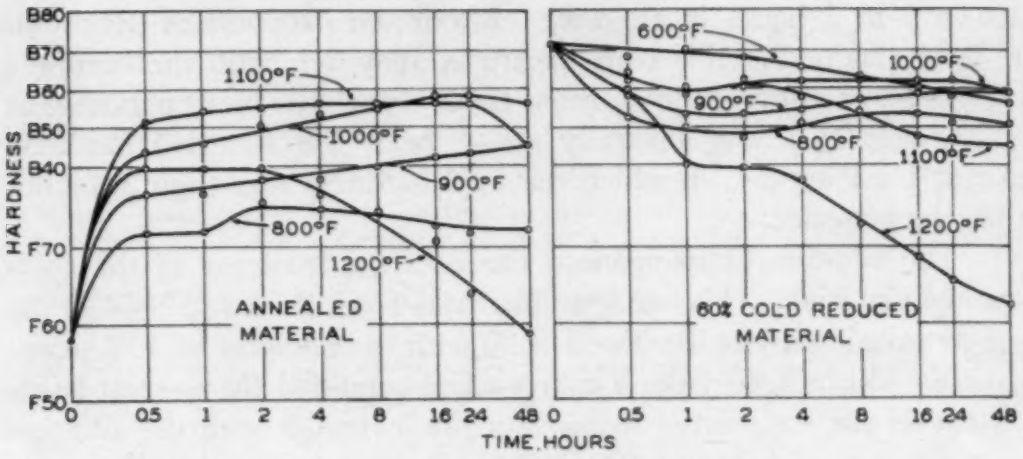


Fig. 12—Time-Hardness Curves for Alloy 4-0.

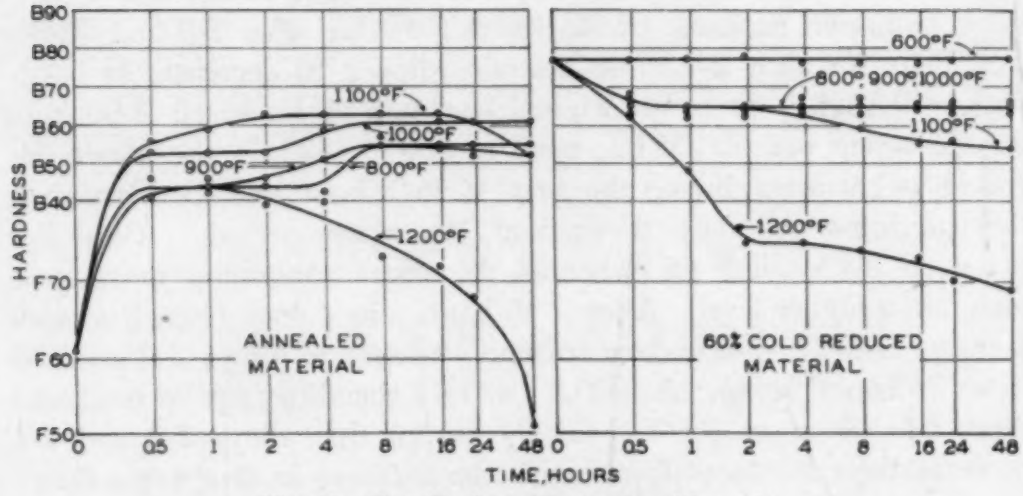


Fig. 13—Time-Hardness Curves for Alloy 4-1.

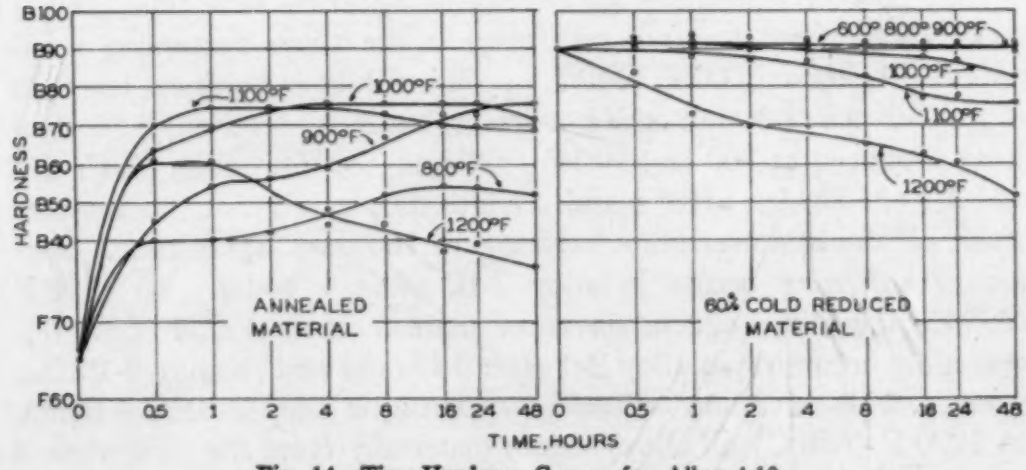


Fig. 14—Time-Hardness Curves for Alloy 4-10.

hardness. The addition of manganese decreases the rate of softening, and in alloy 2-10 minimum hardness is obtained at 4 hours. Hardness values at 1200 F (650 C) are lower than for any previous temperature, but do not decrease sufficiently during the aging time to equal the annealed hardness.

Figs. 9 to 11 show the change in hardness of a 3% cobalt alloy with the addition of manganese. Manganese again increases the initial annealed hardness and the hardness levels at the various aging temperatures. The hardening characteristics are much the same as the 2% cobalt alloys, except the hardness levels are higher in all cases. In the annealed material an increase of aging temperature above 800 F (425 C) and up to 1000 F (540 C) produces an increase in hardness. Aging at 1000 F (540 C) produces maximum hardness in all cases. Maximum hardness values obtained were Rockwell B-52, B-56 and B-72 for alloys 3-0, 3-1 and 3-10, respectively. Overaging occurs in alloy 3-10 at 1000 F (540 C) after 24 hours and does not occur in the others. At 1100 F (595 C) all alloys reach a maximum hardness in 2 hours and then overage, the time for overaging decreasing as manganese content is increased. Aging at 1200 F (650 C) produces the same characteristic results as those obtained in the 2% cobalt alloys with the maximum hardness of Rockwell B-46 being obtained in the 10% manganese alloy.

Aging from the cold-worked condition produces somewhat similar characteristics to those of the 2% cobalt alloys. Aging at 600 F (315 C) produces no change in hardness from the original cold-worked hardness, except the copper-cobalt alloy decreases in hardness after aging 4 hours, reaching a minimum of Rockwell B-41 from B-69. Aging at 800, 900 and 1000 F (425, 480 and 540 C) produces the same effect with the 3% cobalt alloys as with the 2% cobalt alloys, except for a tendency to harden and overage. At 800 F (425 C) alloy 3-0 began to harden at 16 hours, and at 900 F (480 C) at 1 hour, with no indication of overaging. Alloy 3-1 began to harden in 4 hours at 800 and 900 F (425 and 480 C) with a tendency to overage after 16 hours at 900 F (480 C). At 800 and 900 F (425 and 480 C) alloy 3-10 retains the original cold-worked hardness with a slight softening at 1 hour compensated by a gain in hardness at 4 hours. At 1000 F (540 C) overaging occurs in all alloys. Hardness levels are higher in alloys 3-0 and 3-1, and lower in alloy 3-10, than at 800 and 900 F (425 and 480 C). At 1100 F (595 C) none of the alloys show a tendency to harden. Alloys 3-0 and 3-1 show

secondary softening after 2 hours. At 1200 F (650 C) all alloys soften continuously.

The effect of manganese on the hardening properties of a 4% cobalt alloy is shown in Figs. 12 to 14. Manganese again increases the initial annealed hardness and the hardness levels of the various aging temperatures of the copper-cobalt alloy. An increase in aging temperature from 800 F (425 C) to 1000 F (540 C) produces an increase in hardness in the annealed material. At 1000 F (540 C) maximum hardness of Rockwell B-59 and B-56 is obtained in 16 and 4 hours for alloys 4-0 and 4-10, with overaging occurring at 24 and 48 hours, respectively. Maximum hardness of Rockwell B-63 is obtained in 2 hours at 1100 F (595 C) for alloy 4-1. All alloys overage at 1100 F (595 C) and overaging time again decreases with the increasing manganese. At 1200 F (650 C) all alloys reach a maximum in ½ to 1 hour and overage in 1 to 2 hours. At this temperature maximum hardness of Rockwell B-41 occurs in alloy 4-10.

Material in the cold-worked state ages, in general, the same as the other cold-worked alloys. At 600 F (315 C) all alloys, except 4-0, maintain their original hardness. Alloy 4-0 softens after 1 hour, reaching a minimum of Rockwell B-57 in 48 hours. At 800, 900 and 1000 F (425, 480 and 540 C) alloy 4-0 decrease in hardness, then hardens again, with overaging occurring at 800 and 1000 F (425 and 540 C). Alloy 4-1 decreases in hardness to constant values and alloy 4-10 retains its initial hardness, except after 2 hours at 1000 F (540 C). In alloys 4-0 and 4-1, 900 F (480 C) produces higher hardness values than 800 F (425 C), while in alloy 4-10 the values are very nearly the same. Aging at 1000 F (540 C) produces higher hardness values than aging at 800 and 900 F (425 and 480 C) for alloys 4-0 and 4-1, and lower values for alloy 4-10. Overaging occurs in the copper-cobalt alloy after a slight amount of hardening, does not occur in alloy 4-1, and occurs in alloy 4-10 without any evidence of hardening. In all cases aging at 1100 and 1200 F (595 and 650 C) produces no hardening, but continuous overaging.

In general, it can be seen that the addition of manganese increases the hardness of the copper-cobalt alloys in all cases. Greater hardness values are obtained also in the higher cobalt alloys. When aged from an annealed condition the hardness of all alloys is increased with the increase of aging temperature from 800 to 1000 F (425 to 540 C). Copper-cobalt alloys containing 10% manganese

obtain maximum hardness when aged at 1000 F (540 C) from the annealed condition. When aged 48 hours at 900 F (480 C) the 15% manganese alloys attain maximum hardness values of Rockwell B-57, B-73 and B-81 for the 2, 3 and 4% cobalt alloys. Neglecting the appearance of overaging in alloy 4-0 at 1000 F (540 C), overaging occurs only in alloys 3-10 and 4-10 and then at 48 hours. At 1100 F (595 C) overaging occurs in all alloys, the time for overaging decreasing with increasing manganese. With the exception of alloys 3-0, 3-1 and 4-0, maximum hardness is obtained in alloys containing less than 10% manganese when aged at 1100 F (595 C) from the annealed condition. Aging at 1200 F (650 C) produces rapid overaging in all alloys.

When aged from a cold-worked condition at 600 F (315 C) all alloys retain their original cold-worked hardness, except the binary copper-cobalt alloys and the 2% cobalt alloy containing 1% manganese. The copper-cobalt alloys decrease in hardness at 600 F (315 C) after aging, the time of aging decreasing with increasing cobalt content. Alloy 2-1 loses some hardness at 2 hours and again at 16 hours; however, the total decrease in hardness is not great. Alloys containing 15% manganese increase in hardness slightly above their original cold-worked hardness when aged 1 hour at 600 F (315 C). Binary copper-cobalt alloys and alloy 2-1 aged at 800, 900 and 1000 F (425, 480 and 540 C) decrease in hardness with the lowest temperature producing the least hardness. When aged from a cold-worked condition at 800 and 900 F (425 and 480 C) all alloys, except the 2% cobalt and the 3 and 4% cobalt containing 1% manganese, retain very nearly their original cold-worked hardness. Alloys containing 2% cobalt with more than 1% manganese, and alloys 3-1 and 4-1, decrease in hardness slightly after ½ hour's aging at 800 and 900 F (425 and 480 C) and then retain constant values, except that alloy 3-1 hardens slightly at these temperatures. All alloys, with the exception of the 2% cobalt alloys and those containing 1% manganese, decrease in hardness with aging at 1000, 1100 and 1200 F (540, 595 and 650 C) with little tendency to harden. The 2% cobalt alloys containing more than 1% manganese decrease in hardness in ½ hour at 1000 and 1100 F (540 and 595 C) with a secondary softening occurring after 4 hours.

By examination of the final hardness values in the cold-worked material, it can be seen that a definite relationship exists between composition and temperature. The binary copper-cobalt alloys de-

crease in hardness when aged at 600 F (315 C), further decrease when aged at 800 F (425 C), increase considerably above the hardness at 600 F (315 C) when aged at 1000 F (540 C), then decrease progressively with increasing temperature to 1200 F (650 C). Alloy 2-1 behaves in a like manner, except that the hardness at 600 F (315 C) is the highest. All other alloys decrease in hardness from 600 to 1200 F (315 to 650 C) more progressively with increasing temperature, except that temperatures 800, 900 and 1000 F (425, 480 and 540 C) produce approximately the same hardness in the 1% manganese alloys, 800 and 900 F (425 and 480 C) produce the same hardness in the 2% cobalt alloys above 1% manganese, and 600, 800 and 900 F (315, 425 and 480 C) produce approximately the same hardness in the 3 and 4% cobalt alloys containing more than 1% manganese.

Recrystallization temperature was determined to be approximately 600 F (315 C) for the binary copper-cobalt alloys, thus accounting for the softening occurring at this temperature when aged from the cold-worked condition, as well as the greater decrease in hardness at the other temperatures. Alloys containing 2% cobalt with 1 to 15% manganese and alloys 3-1 and 4-1 began recrystallization at approximately 800 F (425 C) and the hardness data substantiate this. The temperature for recrystallization of the 3 and 4% cobalt alloys containing from 3 to 15% manganese was approximately 1000 F (540 C). For this reason these alloys retained their original cold-worked hardness when aged at temperatures not exceeding 900 F (480 C).

The lack of significant increase in hardness in the cold-worked material above the initial hardness is tentatively attributed to the fact that cold working is assumed to produce aging with a submicroscopic precipitate. When further aged above the recrystallization temperature of the alloy, this precipitate grows rapidly producing a softened material due to the coagulation of the precipitate beyond the optimum size. Aging below the recrystallization temperature produces very little change in the initial hardness.

Aging temperatures of 950, 1050 and 1150 F (510, 565 and 620 C) were also investigated. Since these temperatures produced the same hardness characteristics, and for reasons of simplicity, they are not plotted on the graphs.

Table IV shows the maximum hardness obtained in the alloys when aged from the annealed condition at the various temperatures,

Table IV

Maximum Hardness Values, Optimum Aging Time and Overaging Time for Annealed Material at Various Aging Temperatures

Alloy	Hardness C. W.	Hardness An'd	800 F			900 F			1000 F			1100 F			1200 F		
			a*	b*	c*	a	b	c	a	b	c	a	b	c	a	b	c
2- 0	B-65	F-30	F-50	24	..	F-70	48	..	F-80	16	..	*B-40*	8	48	F-67	1	2
2- 1	B-69	F-34	F-52	48	..	F-74	48	..	F-79	8	..	*B-44*	16	24	F-78	½	1
2- 3	B-77	F-47	F-54	48	..	F-75	48	..	B-48	48	..	*B-49*	16	24	F-75	½	1
2- 5	B-83	F-54	F-69	48	..	F-80	48	..	*B-48*	48	..	B-47	8	48	F-64	½	1
2-10	B-90	F-59	B-43	48	..	B-59	48	..	*B-62*	24	..	B-58	4	16	F-77	½	1
2-15	B-93	F-62	F-76	8	..	*B-57*	48	..	B-48	8	..	F-79	2	4	F-63	½	1
3- 0	B-69	F-40	F-70	16	..	F-80	48	..	*B-52*	16	..	B-48	2	48	F-74	½	1
3- 1	B-73	F-44	F-74	24	..	B-42	24	..	*B-56*	48	..	B-55	2	24	F-78	½	1
3- 3	B-80	F-53	F-70	48	..	B-46	48	..	*B-59*	16	..	B-59	4	8	F-80	½	1
3- 5	B-84	F-57	F-76	8	..	B-51	48	..	*B-61*	48	..	B-61	4	8	F-79	1	2
3-10	B-90	F-66	B-44	24	..	B-70	48	..	*B-72*	8	48	B-69	2	8	B-46	1	2
3-15	B-94	F-68	B-51	48	..	*B-73*	16	..	B-70	4	..	B-67	2	8	F-73	4	8
4- 0	B-72	F-58	F-76	2	..	B-46	48	..	*B-59*	16	..	B-57	4	48	B-40	½	4
4- 1	B-77	F-61	B-55	8	..	B-55	8	..	B-61	16	..	*B-63*	2	24	B-46	1	2
4- 3	B-84	F-69	B-40	48	..	B-59	48	..	*B-63*	8	..	B-63	2	8	B-44	½	1
4- 5	B-85	F-71	B-54	48	..	B-64	48	..	B-65	8	..	*B-67*	4	8	B-59	½	1
4-10	B-90	F-65	B-54	16	..	B-76	48	..	*B 76*	4	48	B-75	1	8	B-61	½	2
4-15	B-95	F-67	B-61	48	..	*B-81*	48	..	B-78	2	..	B-76	1	8	B-59	½	2

*a. Maximum hardness. *b. Optimum aging time (hrs.). *c. Overaging time (hrs.).

aging time for this hardness and the time when overaging occurs. Maximum hardness values are *italicized*. As can be seen, an aging temperature of 1000 F (540 C) produces maximum hardness in most alloys with overaging occurring in only two cases. Generally speaking, the 2 and 4% cobalt alloys with low manganese (5% and below) produce maximum hardness values when aged at 1100 F (595 C).

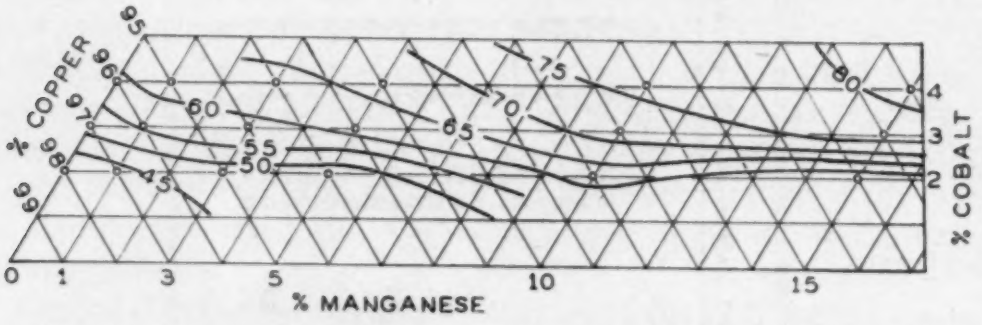


Fig. 15—Ternary Plot in the Copper-Rich Corner Showing Maximum Hardness When Aged from the Annealed Condition.

In some cases both 1000 and 1100 F (540 and 595 C) produce equal hardness, but the lower temperature was selected to avoid overaging. Alloys containing 15% manganese show maximum hardness at 900 F (480 C) when aged for 48 hours. Maximum hardness and overaging are obtained in less aging time with the higher manganese alloys.

A ternary plot in the copper-rich corner giving maximum hardness values obtained when aged from the annealed condition is shown in Fig. 15. The effect of manganese on the hardness of copper-cobalt alloys is well illustrated. The addition of 10% manganese increases the hardness of a 2% cobalt alloy from Rockwell B-40 to B-62 and the further addition of 5% manganese decreases the hardness to Rockwell B-57. The hardness of a 3% cobalt alloy is increased from Rockwell B-52 to B-73 with the addition of 15% manganese, and the hardness of a 4% cobalt alloy is increased from Rockwell B-59 to B-81. The total increase in hardness by the addition of manganese is the same for each alloy, except that maximum hardness is obtained at 10% manganese for a 2% cobalt alloy and at 15% manganese for 3 and 4% cobalt alloys.

Microscopic Examination

Microscopic examination of the aged alloys shows two different types of structures developed in the annealed material, depending upon aging temperature. When aged at temperatures giving maxi-

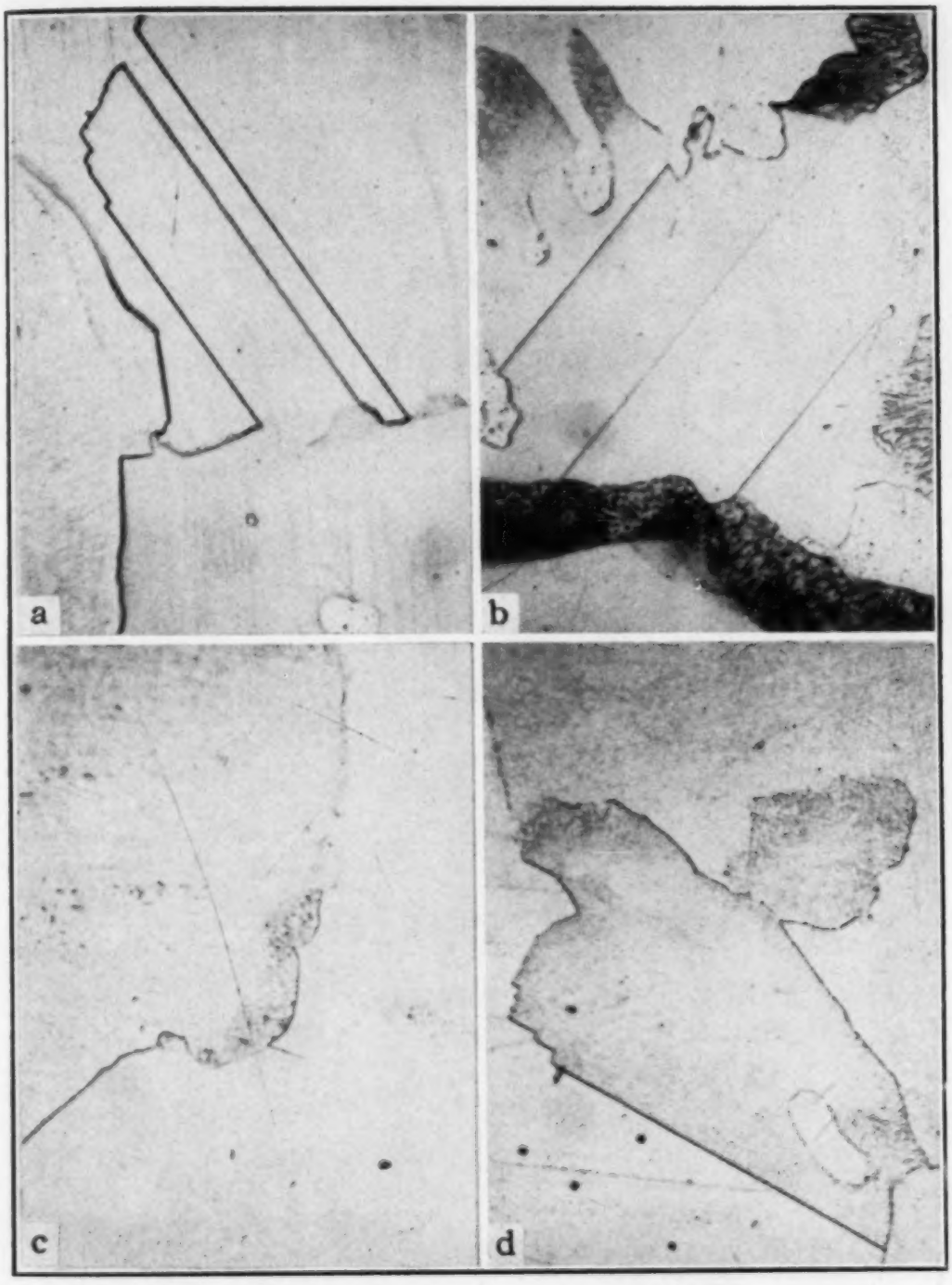


Fig. 16—Alloy 3-3 Solution-Treated ½ Hour at 1700 F (925 C). × 500. a. Aged ½ hour at 1100 F (595 C). b. Aged 48 hours at 1100 F (595 C). c. Aged ½ hour at 1200 F (650 C). d. Aged 48 hours at 1200 F (650 C).

mum hardness, a finely divided precipitate appears in the grain boundary areas at ½ hour (Figs. 16a and 17a) with a slight tendency to spread through the grains themselves (Figs. 16b and 17b).

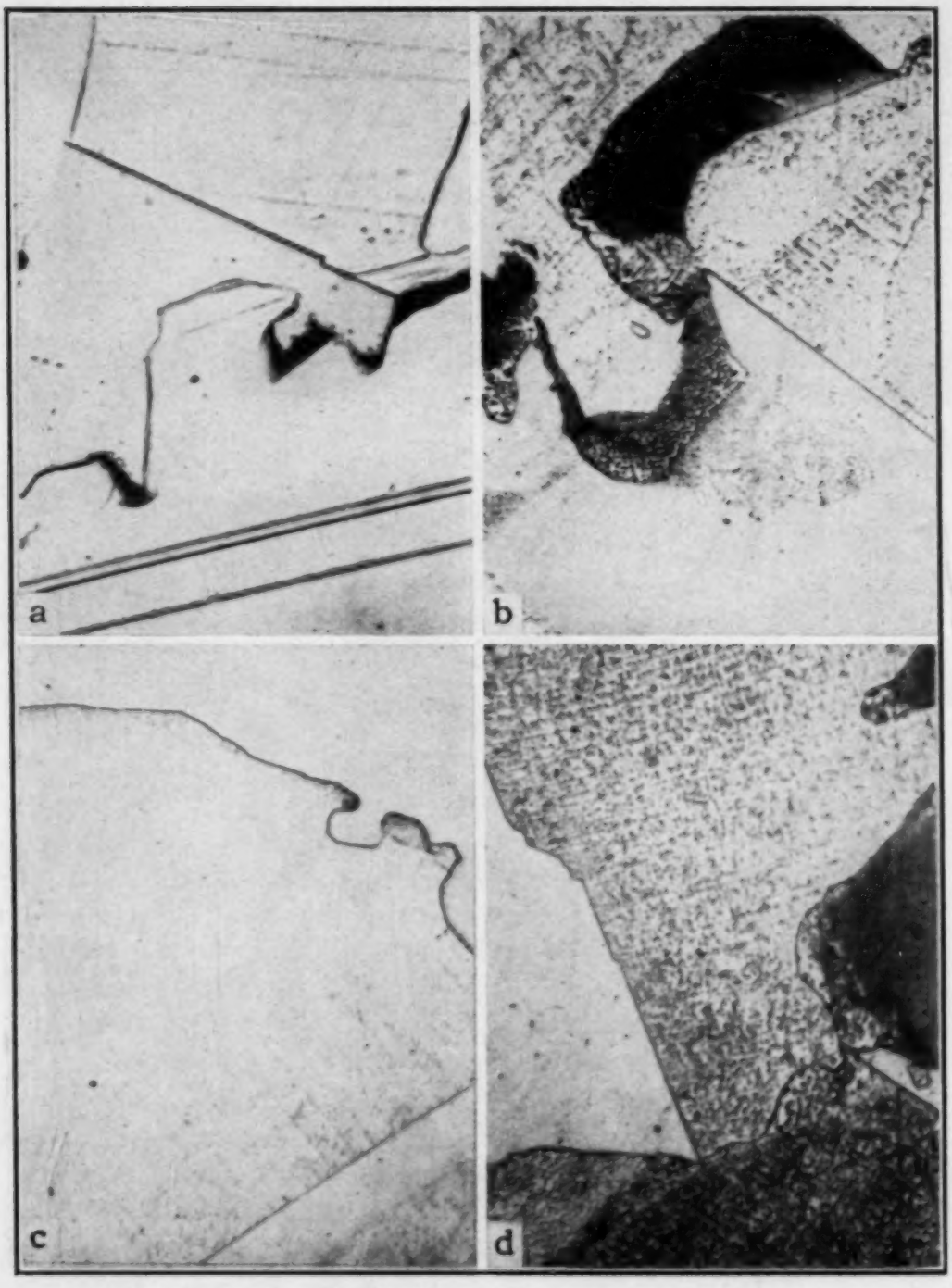


Fig. 17—Alloy 3-5 Solution-Treated ½ Hour at 1600 F (870 C). × 500. a. Aged ½ hour at 1100 F (595 C). b. Aged 48 hours at 1100 F (595 C). c. Aged ½ hour at 1200 F (650 C). d. Aged 48 hours at 1200 F (650 C).

Attention is called to the fact that inasmuch as the precipitate at 48 hours is the same as that at the optimum aging time, and is more distinct, illustrations at 48 hours were chosen. Aging at 1200 F

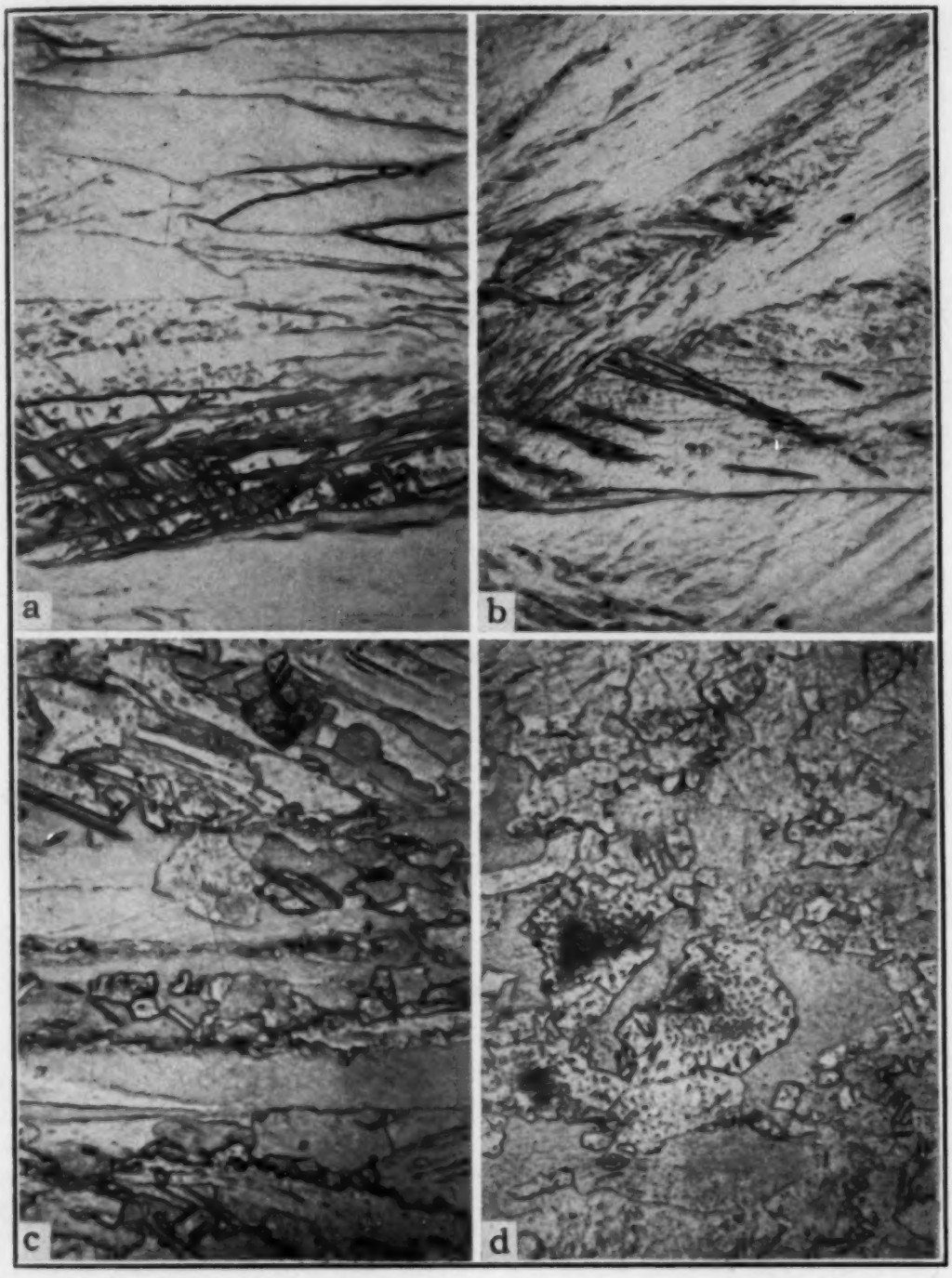


Fig. 18—Alloy 3-5 Cold-Reduced. × 500. a. Aged ½ hour at 600 F (315 C). b. Aged 48 hours at 600 F (315 C). c. Aged ½ hour at 1200 F (650 C). d. Aged 48 hours at 1200 F (650 C).

(750 C) produces a finely divided precipitate in the grain boundaries in ½ hour (Figs. 16c and 17c) and this spreads throughout the grains (Figs. 16d and 17d).

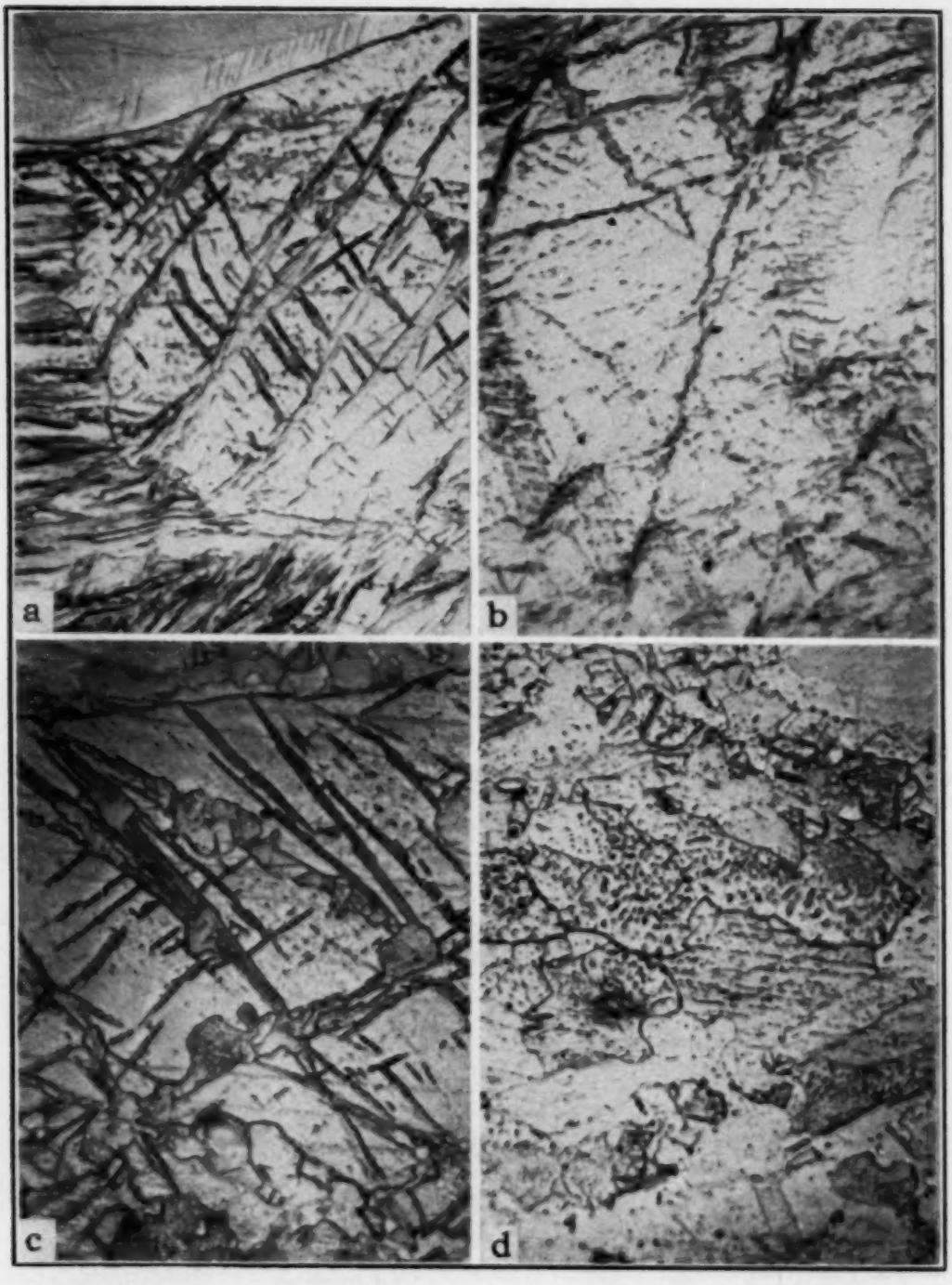


Fig. 19—Alloy 3-10 Cold-Reduced. × 500. a. Aged ½ hour at 600 F (315 C). b. Aged 48 hours at 600 F (315 C). c. Aged ½ hour at 1200 F (650 C). d. Aged 48 hours at 1200 F (650 C).

The effect of aging time and temperature in cold-worked material is shown in Figs. 18 and 19. At 600 F (315 C) the cold-worked structure and the effect of partial recrystallization tend to mask any

precipitate formed. Plate b in Figs. 18 and 19 indicates the degree of recrystallization of the alloys at 600 F (315 C) after aging 48 hours. Aging at 1200 F (650 C) from the cold-worked condition produces no visible grain boundary precipitate, but a general coagulation of the precipitate within the grains themselves (Figs. 18d and 19d). When aged at 1200 F (650 C) recrystallization is well advanced at ½ hour and practically complete in all cases after 48 hours.

Summary

Copper-cobalt-manganese alloys containing from 2 to 4% cobalt and up to 15% manganese respond to age hardening treatment from the annealed condition. Annealing temperatures for complete solution and minimum hardness vary from 1600 to 1700 F (870 to 925 C) depending upon composition. Recrystallization occurs at temperatures ranging from 600 to 1000 F (315 to 540 C), again depending upon composition; the higher manganese and cobalt alloys require higher temperatures for recrystallization. Aging at 900, 1000 and 1100 F (480, 540 and 595 C) from an annealed condition for periods up to 48 hours produces maximum hardness, the optimum aging time at any temperature decreasing with increasing manganese. Hardness properties obtained are reproducible within reasonable limits and the rate of hardening is such as to permit control of aging time.

These alloys do not harden significantly above the cold-worked hardness when aged at any temperature from a cold-worked condition; however, at any temperature less than 1100 F (595 C) the aged hardness in the cold-worked material is higher than the corresponding maximum hardness in the annealed material. Maximum hardness values obtainable are Rockwell B-81 for annealed material and Rockwell B-97 for cold-worked material. Manganese influences the hardening characteristics of the binary copper-cobalt alloys, producing increased hardness values with the addition of manganese up to 10% for the 2% cobalt alloys and 15% for the 3 and 4% cobalt alloys.

Acknowledgments

The author takes pleasure in acknowledging the assistance of the following: Dr. John R. Lewis, Head, Metallurgical Department, University of Utah, who suggested the investigation and under whose

guidance this work was conducted; J. R. Long, T. R. Graham and A. H. Roberson, Metallurgists, U. S. Bureau of Mines, Intermountain Experiment Station, Salt Lake City, Utah, who helped in the preparation of the alloys, and whose valuable suggestions and advice made this investigation possible; and members of the staff, Alloys Department, U. S. Bureau of Mines, Intermountain Experiment Station, Salt Lake City, Utah, who contributed greatly to the investigation.

References

1. W. Köster and E. Wagner, "The Ternary Alloys of Cobalt-Manganese-Copper," *Z. Metallk.*, Vol. 30, 1938, p. 352.
2. G. Tammann and W. Oelsen, "Die Abhangigkeit der Konzentration gesattigter Mischkristalle von der Temperatur," *Z. anorg. Chem.*, Vol. 186, 1930, p. 257, 264.
3. M. G. Corson, "Systeme d'alliages de cuivre avec phase alpha et a limites variables et leur emploi pour le durcissement du cuivre," *Revue de Metallurgie*, Vol. 27, 1930, p. 83.
4. C. S. Smith, "An Air-Hardening Copper-Cobalt Alloy," *Mining and Metallurgy*, Vol. 11, 1930, p. 213.
5. R. B. Gordon and Morris Cohen, "Age Hardening of a Copper-Cobalt and a Copper-Iron Alloy," AGE HARDENING OF METALS, American Society for Metals, 1939, p. 161.
6. R. S. Dean, J. R. Long, T. R. Graham, E. V. Potter and E. T. Hayes, "The Copper-Manganese Equilibrium System," TRANSACTIONS, American Society for Metals, Vol. 34, 1945, p. 443.
7. K. Hiege, "Die Legierungen des Mangans mit Kobalt," *Z. anorg. Chem.*, Vol. 83, 1913, p. 253.
8. U. Hashimoto, "Equilibrium Diagrams of Some Alloys Rich in Cobalt, by Using a New Method of Thermal Analysis," *Kinzoku No Kenkyu*, Vol. 9, No. 2, 1932, p. 57-73.

DISCUSSION

Written Discussion: By J. R. Long, senior metallurgist, U. S. Department of the Interior, Bureau of Mines, Salt Lake City Division, Metallurgical Branch, Salt Lake City, Utah.

I would like to call attention to the fact that Mr. Fredrickson carried out this work as an undergraduate student at the University of Utah and the paper as presented represents part of the work performed as a Bachelor's thesis project. As such, I believe it is an outstanding contribution and congratulate Mr. Frederickson on having performed such an excellent piece of work and presenting it so ably.

We at the Bureau of Mines were able to be of some slight assistance to him in the preparation of the alloys on which he obtained the hardenability data, and from time to time were able to make a few helpful suggestions. One of those suggestions was the aging of the material in the 60% cold-worked

condition. This was intended to permit a comparison of the aging rates in the annealed and cold-worked conditions. Most hardenable alloys age more rapidly from the cold-worked condition than from the annealed condition. It is now evident that a lesser degree of cold work might have permitted some hardening at the low aging temperatures. It is obvious that precipitation has taken place during the cold working and hence none of the alloys on aging exceeded the cold-worked hardness.

Author's Reply

I wish to express my appreciation of the comments and discussion made by Mr. Long. I have nothing to add to his remarks since I am in complete agreement with him regarding the precipitation taking place during cold work.

FORMATION AND TRANSFORMATION STUDIES OF IRON-CARBON POWDER ALLOYS

By John F. Kahles

Abstract

The results presented in this study show that very pure steels may be prepared by pack carburizing compressed carbonyl-L iron powder and that the austenite transformation characteristics of these powder products do not differ markedly from steels made from the liquid state. A TTT-diagram for a "powder" steel is shown for a composition of 0.87% carbon. In addition some interesting trends are presented for the carburization of compressed powdered iron.

Introduction

IN considering the problem of the study of reactions in iron-carbon powder alloys one of the prime interests was to determine whether some of the reactions which occur in the solid state in ordinary steels are similar to those in the powder alloys. W. D. Jones (1)[1] has pointed out that the powder approach to the solution of many intricate problems confronting metallurgists constituted a powerful tool. He states, "By the sintering method it is possible to vary the intercrystalline phase at will." Problems of grain growth, austenite decomposition, intergranular corrosion of stainless steels, season cracking in copper-base alloys, carburization of iron, and graphitization of iron-carbon alloys are but a few of the many problems that may be approached from the powder state. By its methods one often has a better opportunity to incorporate constituents in a controlled fashion in solid solution and in additional phases that may lead to the analysis of a given problem. Of particular interest is the fundamental problem before metallurgists continually—namely, the nature of the grain boundary. Following are listed the objectives sought in this study.

[1]The figures appearing in parentheses pertain to the references appended to this paper.

This paper is a portion of a thesis submitted by John F. Kahles to the Graduate School of the University of Cincinnati in June, 1946, in partial fulfillment of the requirements for the degree of Doctor of Philosophy.

A paper presented before the Twenty-eighth Annual Convention of the Society held in Atlantic City, November 18 to 22, 1946. The author, John F. Kahles, is associate professor of metallurgical engineering, University of Cincinnati, Cincinnati, Ohio. Manuscript received June 29, 1946.

a. How can steels be formed from the powder state and what factors are of particular import?
b. How is the isothermal decomposition of austenite influenced when the steel is formed from the powder state?
c. What are the carburizing characteristics of iron powder?

Some of the questions proposed are answered with a degree of satisfaction in this paper. The results, however, constitute but a small beginning toward thorough understanding of the objectives sought. One may say that new horizons are at least brought into view.

In the following discussion no time is spent in consideration of the general field of powder metallurgy. However, references (1) to (11) inclusive are particularly valuable as sources of both general and specific information relating to problems in powder metallurgy.

The Powder Metallurgy of Steel

In recent years considerable interest has been shown in the field where powder metallurgy is competitive with other fabrication procedures. F. P. Peters (12) and A. J. Langhammer (13) in recent papers have discussed some of the questions relating to this general problem. Peters pointed out that from considerations of design, powder metallurgy may be competitive with sand casting, die casting, permanent mold casting, precision investment casting, machined bar stock, screw machine parts, cold heading, drop forging, stamping, and drawing. Langhammer discussed in a general way the advantages and limitations of powder metallurgy as applied to machine parts. In this field, from a material standpoint, much emphasis has been placed upon the use of iron and iron-base alloys.

Before and during World War II important applications were made of steels developed by powder methods, but it may be said that there is, as yet, not enough work of a fundamental nature in the literature. Some of the more interesting developments are summarized in paragraphs that follow.

W. D. Jones (1) has summarized the work of German investigators, particularly E. K. Offermann, H. Buchholtz, and E. H. Schulz. These men produced steels by sintering carbonyl iron powders of varying carbon and oxygen contents. To these powders they added graphite, ferromanganese, and other agents as desired. After sintering, the ingots were forged into billets. Properties of these steels, including tensile strength, electrical resistance, magnetic properties, hardness, microstructural characteristics, heat treating properties, weldability,

and others, were then studied and compared with steels produced from the molten condition. The results are quite detailed but one gets a very definite impression that the same condition of composition and grain structure in a steel may be achieved either from the liquid or solid state without too much difficulty. When one considers the subtleties possible in the condition of the grain boundary, this is a rather sweeping statement to make. Lest there be a misunderstanding it might be added that the equivalency referred to has not as yet been established but there is a distinct trend toward it.

C. W. Balke (14) has reported some of his studies on the effect of pressure on the properties of powder compacts. He made steels with electrolytic iron as a base and included carbon and other alloying elements necessary to approach steels designated ordinarily as SAE 1000 series, SAE 4560 and SAE 3140. In the case of a certain manganese-molybdenum steel he found in certain respects the powder steel to be superior. Not enough information is given, however, to draw definite conclusions regarding equivalency.

J. Wulff (15) has reported on the production of a steel from powders which approached closely the composition of SAE 4340. He too finds the properties of this material similar to those of the ordinary bar stock.

In addition to these attempts at producing powder alloys resembling the cast and wrought steels, there have been a number of interesting developments where physical properties, though not approaching wrought steels, are more than adequate. F. V. Lenel (16) reported that a number of iron parts have been made and that some of these were used in quantities of a million or more. In particular he has interesting remarks to make concerning production of an oil-pump gear used in automotive work. The microstructure developed might be considered more nearly that of cast iron than of steel. The materials required for the production of the part are reduced iron and graphite, and the resultant structure after sintering is graphite in a matrix of alpha ferrite and cementite. A large amount of the alpha ferrite and cementite is present as pearlite. Some of the advantages gained include: less raw material waste, more accurate contour resulting in better performance, porosity for oil impregnation, lower labor costs, and strengths equivalent to that of the cast iron gears formerly used. Some of the savings made in the production of powder machine parts have been astounding. In some British manufacturing procedures on gun parts 1,250,000 pounds of critical materials and 5,000,000 man-hours

were saved over a 12-month period during the recent war. According to Langhammer (13), even such parts as micrometer frames and V-blocks have been produced. The above publications along with many patents in all countries have dealt with the problem of steel powder and parts production.

In reviewing the literature on steel parts from powders several general methods are prominent. Very frequently carbon in the form of graphite or carbon black has been introduced into the powder mix with hydrogen-reduced or electrolytic iron. In some instances brittle alloys such as white cast iron have been pulverized and mixed in appropriate quantities into iron powders. In both methods satisfactory pressing and homogenization have been attained. One of the prime difficulties encountered in pressing steel powders into compact form is the poor plasticity which gives rise to poor green strength, but the presence of an adequate quantity of the plastic iron powder obviates trouble to a marked degree. In some applications it has been sufficient to provide a soft layer on the surface of alloy powders. This may be achieved by a partial decarburization of the powder particles under conditions where no oxidation occurs. Alloying elements such as manganese, nickel, chromium and others have been introduced in the same way as carbon, i.e., by incorporating them in the powder mix. P. R. Kalischer in a discussion of work by Balke (14) states that by use of controlled atmospheres they have been able to maintain carbon contents in compacts to within 0.02 to 0.03%. This is remarkable.

Another method to which there has been but brief reference in the literature is one involving carburization of a compact already formed. Carburizing and sintering may take place simultaneously—it might be termed carbasintering. Some work has been reported very recently by A. S. Margolies (17).

In reviewing the literature on production of steels from powders it is clearly evident that one of the important factors to consider is oxygen content of the metal powders. In order to provide uniformity in the finished product negligible oxygen or at least uniform oxygen content is essential in powder production. Any number of so-called steel parts that have been examined microscopically are no more than iron-base parts with iron oxide particles distributed in the matrix with little or no carbon present. An examination of some iron powders sold commercially reveals large quantities of iron oxide with no recognition made of quantities of oxide present.

In concluding one may say that the economy of lower strength

iron-base alloys, such as the oil-pump gear referred to earlier, is well established. There is, however, a trend toward the development of higher strength parts made of steel. These have every chance of meeting competition offered by other methods. At the same time the need for fundamental data on their formation, reactions, and performance is clearly manifest.

Production of Steel Compacts by Carburizing

With the revealed interest in the development of high strength steels from powder, a logical study to make is one dealing with the heat treating characteristics of such steels. More specifically it would be valuable to have information concerning the austenite transformation characteristics of steel powder compacts so that they might be compared with the conventional materials. In starting this program it was decided to prepare as pure an iron-carbon alloy as feasible in order to maintain better control of the pertinent variables during the transformation of austenite, and to prepare a foundation for more comprehensive studies later.

The very first attempts at producing an iron-carbon alloy to be used in this study were made by adding graphite to hydrogen-reduced iron of relatively high purity. With the first experiments run, difficulty was encountered in getting carbon into the iron when the material was heated into the austenite field. Later it was found that this was caused by the high oxygen content of the iron powders and much more carbon than required for the alloy should have been added to compensate for the loss due to reduction of iron oxide. Meanwhile, thought was given to the possibility of carburizing pure iron compacts. Listed below are some of the typical analyses from which a selection was made.

Electrolytic Iron Powder—Annealed	
Total Iron	99.50%
Copper	0.01
Silica	0.02
Manganese	0.027
Zinc	0.090
Nickel	None
Sulphur	0.001
Phosphorus	0.002
Free Carbon	0.005
Oxygen	—

Electrolytic Iron Powder	
Metallic Iron	97.2%
Total Iron	98.0
Total Carbon	0.07
SiO_2	0.017

Hydrogen-Reduced Iron Powder

Total Iron	99.0%
Carbon	0.04
Manganese	0.18

Carbonyl Irons

Grade	% Carbon	% Oxygen	% Nitrogen
L	0.005-0.03	0.1 -0.2	0.005-0.05
C	0.03 -0.12	0.1 -0.3	0.01 -0.1
E	0.65 -0.80	0.45 -0.60	0.6 -0.7
TH	0.5 -0.6	0.5 -0.7	0.5 -0.6
SF	0.5 -0.6	0.7 -0.8	0.5 -0.6

The statement carried along with the above analyses of carbonyl irons is "With reference to the chemical analysis shown above it should be noted that spectroscopic analysis shows the rest to be iron with other elements present in traces only."

Inasmuch as chemical purity was an important requirement for this study, it was very easy to make a choice of material. The logical choice was carbonyl-L. By carburizing this iron in compact form it was possible to produce uniform composition samples that could be used for austenite transformation studies. In a very general way the following procedure was adopted.

Step 1. The carbonyl iron "L" as received from the manufacturer was subjected to a hydrogen drying treatment at low temperatures.

Step 2. The iron as prepared in step 1 was pressed into compact form in a steel die.

Step 3. These samples were then weighed on an assay balance to 0.01 of a milligram.

Step 4. The weighed samples were then packed in hardwood charcoal. The carburizing time and temperature were controlled to obtain the desired carbon analysis in the specimens.

Step 5. The specimens were weighed in order to determine the weight increase.

Step 6. The specimens were homogenized in a nitrogen atmosphere at elevated temperatures and reweighed after this treatment.

Step 7. While carbon contents were determined by the weight increase, actual chemical analyses were made by several laboratories to compare the methods so that a correlation could be made.

The samples as prepared above were then cut into smaller pieces for the studies reported in the following section of this paper. Before developing this phase of the work, consideration is to be given to some of the details of the steps just mentioned and to some of the results achieved.

Step 1. The carbonyl iron "L" was treated with dry hydrogen at a temperature of 260 C (500 F) for 24 hours. The hydrogen was bubbled through a mass of powder kept in a vertical position. The gas seemed to make good contact with the powder particles. After treatment there was a noticeable improvement in the color and chemical activity of the powder. One might consider that the treatment given would lead to a highly reactive surface that might pick up even larger amounts of oxygen. As will be shown later this is not the case, for the chemical analyses compared with the weight changes in carburizing indicate a lower oxygen content than the 0.1 to 0.2% reported for this powder.

The temperature of 260 C (500 F) was chosen because it was possible to keep the powder from going into lumps at this temperature. If lumps formed they could be disintegrated by shaking the tube in which the powder was treated. At temperatures around 285 C (545 F) considerable lumping occurs—in fact, in some runs all of the powder was in a fairly hard mass. The only information available from the manufacturer is that sintering occurs below 500 C (930 F). From work on carbonyl "L" and "C" it would seem to occur around 285 C (545 F) in a hydrogen atmosphere. Some work on carbonyl "C" showed that there was no color improvement, i.e., brightening of the powder, when it was treated as above for 18 hours at 150 C (300 F).

When the reduced powder was tested with concentrated nitric acid it was very reactive. With many fine iron powders it is possible to add the nitric acid without having any reaction apparent. In some cases a very slow addition, a drop running down the side of a test tube, will give rise to a vigorous reaction. In the freshly prepared irons above it was impossible to add the nitric acid fast enough to prevent reaction; it was almost explosive in character.

Some passivity tests were also run on the powder using a copper nitrate solution. Directly after reduction with hydrogen the reaction as noted by a color shift in the solution from blue to green takes place rapidly. In one test with freshly reduced powder it took but 2 minutes to show a shift while 40 minutes after drying it took 6.5 minutes. Four days later it took 20 minutes. The carbonyl "L" without hydrogen treatment showed a time of approximately 20 minutes also. If the test is carried to a point where the solution is quite definitely green, the reduced powders generally take more time. Not enough tests were run to gain knowledge of any appreciable significance.

By drying the powder and eliminating some of the oxygen it was

possible to obtain a powder suitable for making carbon analyses by weight changes.

Step 2. The compacts used were pressed in a small heat treated high carbon, high chromium steel die. Care was taken in the design of the die to provide uniform loading. Press capacity was limited so a Brinell hardness tester was used to supply the load. The dimensions of the compacts were ¼ inch in diameter, and thickness of the order of 0.035 inch. They were kept small, of the order of 0.2 gram to minimize density variations through the compact. The load used for the samples was 3000 kg. Considering the exact dimensions of the sample the pressing pressure used was 138,000 psi. This was sufficient to give dense enough samples so that no difficulty was encountered in preparation and subsequent microscopic examination.

Step 3. After careful brushing of the samples they were weighed on the assay balance as indicated previously. The compacts were always handled with tweezers used ordinarily for analytical weights.

Step 4. Forty specimens as prepared above were then transferred to a ¾-inch capped short pipe nipple. The nipple was filled with a 200 through 150-mesh hardwood charcoal surrounding the samples. This capped nipple was then placed inside a similar but larger nipple, a 1½-inch size. Similar charcoal was also placed in the larger nipple. This tube-within-a-tube combination circumvents any difficulty of samples staining by drawing air in upon them during cooling. More consistent carbon pick-up was also obtained by this practice as compared with single tube practice. These samples were carburized for 15 hours at 870 C (1600 F) under carefully controlled temperature conditions. The sample weights in the lot of forty varied from 0.13721 to 0.22694 gram. This, combined with packing variations and the fact that the nipple was "over-crowded", gave rise to more than usual variation in the weight gains. The variation was from 0.85 to 0.91%. There were enough samples of the same content to carry out the tests. Twelve of them were in the range 0.85 to 0.86%, fourteen in the range 0.87 to 0.88% and nine in the range 0.90 to 0.91%.

Whenever tests were run with fewer samples, after the technique was acquired, much better results were secured. Typical are the following, not necessarily carburized at the temperatures and times used for the larger batch.

a.	5 samples	0.88-0.89% weight increase
b.	5 samples	0.71-0.72% weight increase
c.	5 samples	0.61-0.64% weight increase
d.	6 samples	0.84-0.85% weight increase

e. 4 samples 0.97-0.99% weight increase
f. 2 samples 0.72% weight increase
g. 2 samples 0.78-0.79% weight increase
h. 2 samples 0.52% weight increase

These results show that check results are attained, and without too much difficulty, it might be added.

Step 5. In order to make the weight analyses indicated previously, the samples were carefully removed from the carburizing pack and then brushed to remove any of the carbon dust that might have adhered to them. The samples as carburized are perfectly bright.

Step 6. After weighing, the samples used for further work were homogenized in a nitrogen atmosphere for 3 hours at a temperature of 1105 C (2020 F). After removal from this atmosphere the samples were reweighed. Tests with samples of wrought steels in the nitrogen atmosphere used show extremely small changes in weight. Typical would be a loss of 0.00001 gram in a sample weighing 0.36519 gram in a period of 12 hours at 1095 C (2000 F). The same sample showed no change in weight in 2.5 hours at 1040 C (1905 F). The sample was carefully handled, for the tests and weights used were left undisturbed on the balance pan.

The train developed mainly by E. E. Stansbury (18) is described in detail by him. It consists of the following items through which tank nitrogen of high purity is passed.

a. A tower of soda-lime
b. Two bubble towers of concentrated sulphuric acid
c. Tube of freshly reduced copper maintained at about 300 C.
d. A long tube of magnesium perchlorate at room temperature
e. Steel wool just ahead of the sample in the silica tube in which the homogenization is accomplished.

The silica tube is equipped with a solenoid so that samples may be flushed by the furnace atmosphere and may also be allowed to cool in the colder portion of the tube in the same nitrogen atmosphere. The train is regenerated as required with tank hydrogen.

Step 7. For one set of tests on carburization several larger compacts weighing between 2 and 3 grams were prepared in a ⅜-inch diameter die. These samples were carburized and the weight gains noted. They were then run for carbon by the usual combustion method. Results were:

Weight, % gain	Chemical Analysis, % Carbon
1.17	1.21
1.13	1.20
1.13	1.17
0.76	0.83

In addition a set of six of the forty compacts averaging 0.88% weight pick-up showed a value of 0.95% carbon. Another set of six samples of the same group were checked after being homogenized at 1105 C (2020 F). The weight percentage was 0.91% (based upon weight after carburizing) while the carbon determination gave 0.93% carbon. Other results on single samples weighing about 0.2 gram and after homogenization show comparisons that are consistent.

Weight, %	Carbon, %
0.72	0.74
0.89	0.93

During homogenization there is always a weight loss on the compacts. This is because oxygen that is present after the carburizing cycle combines with carbon to go off in the form (CO-CO_2). The train was always checked carefully to see that it was not the N_2 atmosphere causing this loss. Some conception of the loss may be gained from the following tabulation:

	Original Weight as Pressed (g)	Weight after Carburization (g)	Weight after Homogenization (g)
a.	0.18740	0.18902	0.18894
b.	0.20071	0.20242	0.20234
c.	0.20387	0.20564	0.20554
d.	0.20788	0.20973	0.20964
e.	0.17659	0.17811	0.17802

It would appear that by making the appropriate correction the carbon analysis of any sample could be ascertained from a carefully made weight gain check.

Spectrographic estimates were conducted on samples in various stages of processing.

a. Carbonyl iron "L" as received
   The following elements were checked but not found: copper, silicon, sodium, manganese, nickel, chromium, cobalt, molybdenum, vanadium, tungsten, lead, tin, antimony, aluminum, titanium, zinc, calcium, barium, and strontium.
b. Carbonyl iron "L" after the hydrogen treatment and pressing only
   Same as in "a".
c. Carbonyl iron "L" after carburization
   Same as in "a" but two out of three samples showed an estimated quantity of copper equal to 0.0001 to 0.0009%.
d. Carbonyl iron "L" after carburization and then with homogenization at 1105 C (2020 F)
   In addition to 0.0001 to 0.0009% copper it revealed an

estimated 0.0001 to 0.0009% of silicon. Otherwise the sample was like "a".

Spot tests were made for sulphur and phosphorus. Quantitative estimates showed that both sulphur and phosphorus were present in quantities less than 0.001%. Sulphur estimates were obtained by using sodium azide in an iodine solution in contact with the sample. The presence of sulphides is shown by the nitrogen evolved. Strong positive tests are given by 0.05 to 0.12 microgram of sulphur in this test. Phosphorus determinations were made by using the phospho-molybdate print technique.

The compacts thus prepared can logically be considered to be relatively high purity iron-carbon alloys of known carbon content. Those selected for transformation studies had an actual carbon content computed to range from 0.87 to 0.89% carbon and a density after homogenization of 7.2 g/cc.

Austenite Decomposition Studies on Iron-Carbon Powder Compacts

The steels made from powdered iron by carburization were studied further to determine their austenite transformation characteristics. As indicated previously, the carbon content of the steel selected for this work was 0.87 to 0.89% carbon. The TTT- (time-temperature-transformation) diagram or "S" curve for this steel is shown in Fig. 1 and the data from which the curve is plotted are listed in Table I. The conditions under which the data were obtained are as follows:

1. Austenitizing was accomplished at a temperature of 1000 C (1830 F) for 20 minutes in the same nitrogen atmosphere used for homogenization of the samples after they had been carburized.
2. Small notched samples (dimensions approximately 0.035 inch square and ⅛ inch long) were suspended in the atmosphere by a small stainless steel wire (0.003 inch) attached to a nickel wire (0.066 inch). The small samples were made by cutting the ¼-inch diameter compacts into seven or eight pieces with a jeweler's saw. The structure at 1000 diameters is shown in Fig. 3.
3. The samples were held in the nitrogen atmosphere in the cold portion of the tube for flushing. They were then advanced into the hot zone of the furnace. In order to support the nickel wire the end was inserted into the rubber stopper which was used to close the silica tube. After holding for 20 minutes at 1000 C (1830 F), the samples were quickly transferred to the metal baths.

4. Lead was used as a quenching medium in the upper temperature ranges and the quaternary eutectic (Bi 50%, Cd 10%, Pb 27%, Sn 13%) was used for work at lower temperatures. For determination of transformation characteristics to pearlite or bainite the samples were quenched in a dilute NaOH solution directly from the metal baths. When martensite studies were conducted, the samples were tempered at 280 C (535 F) for 10 seconds prior to quenching in the dilute NaOH solution.
5. The analyses of the transformation products were all made by microscopic examination. Figs. 4 to 22 show the typical structures that were obtained in developing the TTT-diagram (Fig. 1).

Table I
Data for TTT-Diagram in Fig. 1

Sample No.	Temperature (C)	Temperature (F)	Time (Seconds) Beginning	Time (Seconds) Ending
		Pearlite Formation		
I98	714	1317	660	
I100	713	1315	..	>3000
I34	704	1299	60	..
I36	704	1299	..	630
I83	688	1270	12	..
I84	688	1270	..	80
I9	676	1249	1	..
I5	676	1249	..	20
..	639	1182	?	..
I63	639	1182	..	2
		Bainite Formation		
..	546	1015	?	..
I62	546	1015	..	1 or less
I59	500	932	1	..
I60	500	932	..	5
I57	455	851	2	..
I68	450	842	..	18
I46	404	759	10	..
I53	404	759	..	60
I65	353	667	30	..
I70	353	667	..	225
I61	308	586	75	..
I64	308	586	..	600
I77	244	471	300	..
I78	244	471	..	3000
		Martensite Formation		
		M_s Point 242 C, 468 F		
		M_f Point 96 C, 205 F		

There are a number of comments of interest that may be made with respect to this diagram. First, it may be stated that it is subject to the limitations of the metallographic method of analysis. It is very difficult to decide when a product first appears and when transformation to it has been completed. This is to be expected when one considers the kinetics of austenite decomposition. In the diagram shown this work was done carefully but not scrupulously. In the opinion of the author the diagram represents an excellent estimate of the transforma-

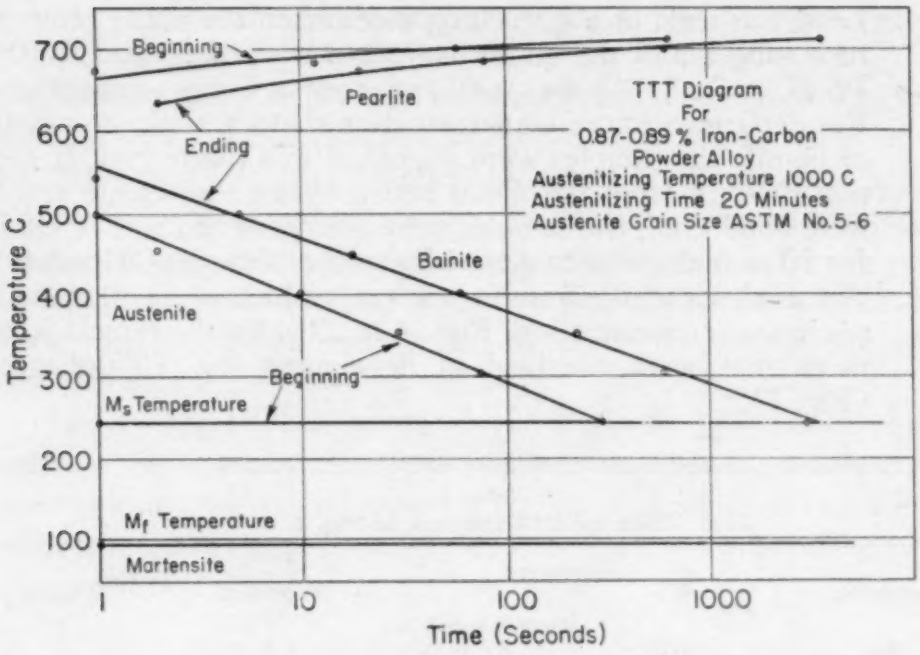


Fig. 1—TTT-Diagram for 0.87 to 0.89% Iron-Carbon Powder Alloy. Austenitizing temperature 1000 C, austenitizing time, 20 minutes, austenite grain size ASTM No. 5-6.

tion of austenite. A conservative estimate would be a 10% variation in placing beginning and ending times except at temperatures where very rapid transformation occurs.

It is interesting to note that the reactions do not seem to be different from those shown in TTT-diagrams for wrought steels. A comparison is difficult to make for no one has published, as far as known by the author, a TTT-diagram for a high purity wrought iron alloy. However, one diagram exists for a 0.89% carbon steel with 0.3% manganese (Fig. 2). No other elements have been reported but it is believed that small quantities of silicon, sulphur, and phosphorus at least are present.

The lower region where martensite formation occurs is entirely wrong in Fig. 2. However, it was possible to compare the M_s points for the powder and wrought alloys. A. B. Greninger (19) showed an M_s point for a 0.85% carbon, iron-carbon alloy of about 240 C (465 F). The data in Table I show an M_s point of 242 C (468 F) for the steel considered. It would appear that these are no different from similar points found in wrought pure steels. In other words, the fact that the density of the powder compact is but 7.2 g/cc as compared to 7.80 g/cc for the wrought pure steels makes no difference in the beginning and ending of martensite formation. Whether this is true for a less

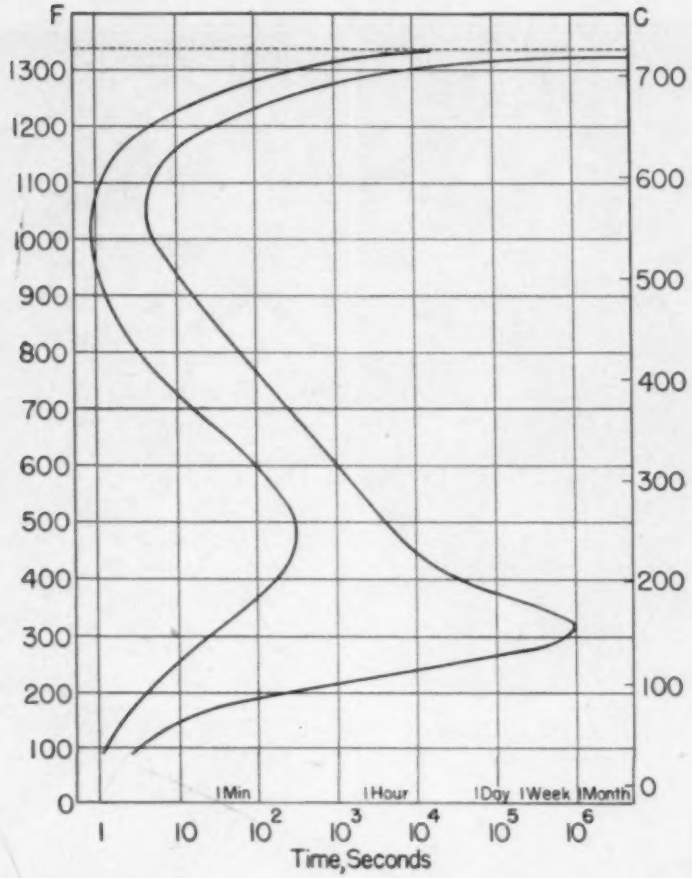


Fig. 2—TTT-Diagram for a 0.89% Carbon Steel With 0.3% Manganese.

dense compact has not been ascertained. Further, it is not known whether the rates of martensite formation with temperature drop are the same. In other words, while the M_s and M_f points are the same, the transformation characteristics could deviate within this range.

It is of interest to note that in the upper part of Fig. 1 there is a large temperature range where very rapid reactions occur. Just what the transformation characteristics are in this range has not been determined. The reactions must certainly be extremely rapid for such high purity alloys as used in these experiments.

Both pearlite and bainite beginning and ending lines seem to be fairly straight when plotted on semilog paper. An examination of the curve as drawn would lead one to believe that the most rapid rate of transformation is somewhere between 600 C (1110 F) and 650 C (1200 F) instead of around 550 C (1020 F) as shown in the diagrams of eutectoid plain carbon steels published previously by other investigators. Some theoretical deductions by C. Zener (20) indicate that the nose of the TTT-diagram should be higher than 550 C (1020 F).

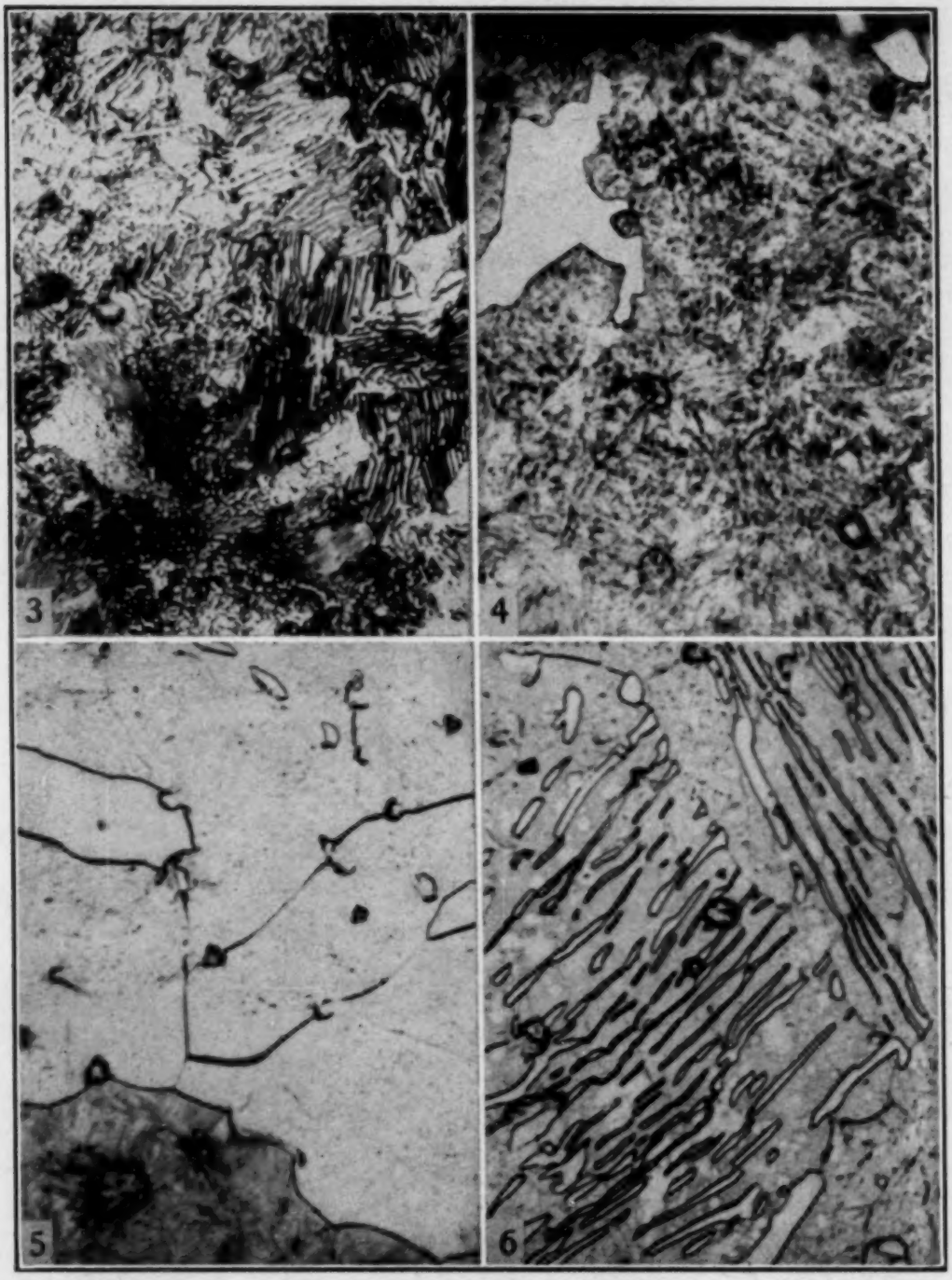


Fig. 3—Sample No. 138. Fine pearlite, the structure of the 0.87 to 0.89% C steel following homogenization. In this form it was used for the isothermal transformation studies.

Fig. 4—Sample No. 1103. Isothermal transformation temperature 720 C (1328 F), Time 60 minutes. Cementite and martensite. Cementite is beginning to form near the edge of the sample. No transformation was shown in the center of the specimen. In this and in all other photographs of isothermal transformations the martensite is equivalent to austenite untransformed at the isothermal transformation temperature.

Fig. 5—Isothermal transformation temperature 720 C (1328 F), Time 15½ hours. Alpha ferrite, cementite, and martensite. Large crystals of cementite are shown. This sample was not used in plotting data for Fig. 1. The austenitizing temperature was 1050 C (1922 F).

Fig. 6—Sample No. 1100. Isothermal transformation temperature 713 C (1315 F), Time 51 minutes. Alpha ferrite and cementite with some present as pearlite.

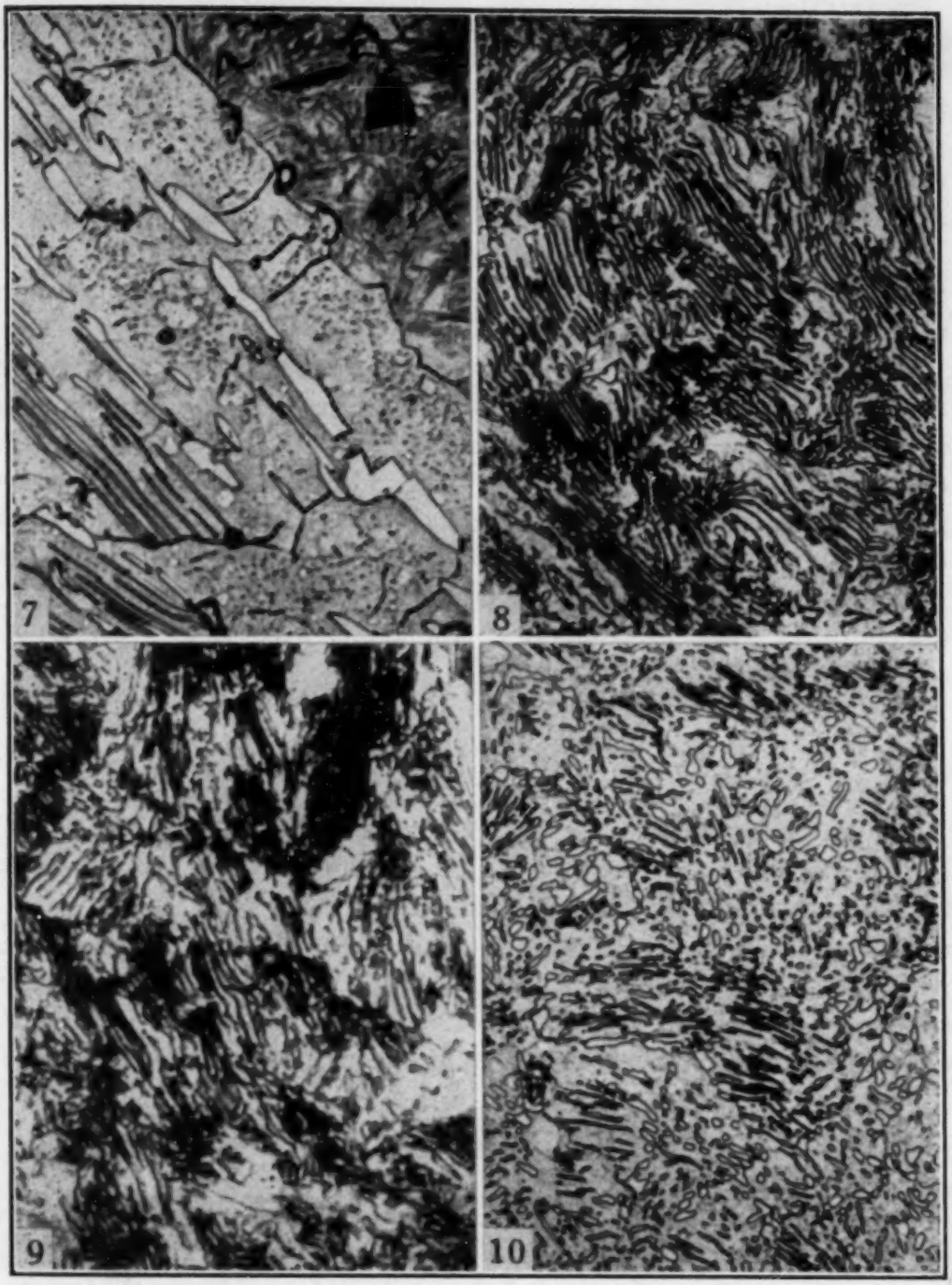


Fig. 7—Sample No. I100. Isothermal transformation temperature 713 C (1315 F), Time 51 minutes. Same as Fig. 6 but a different portion of the specimen. A few sections, as illustrated here, revealed some austenite untransformed. This, as usual, is revealed by the martensite present.

Fig. 8—Sample No. I81. Isothermal transformation temperature 688 C (1270 F), Time 90 seconds. Pearlite.

Fig. 9—Sample No. I82. Isothermal transformation temperature 688 C (1270 F), Time 15 minutes. Pearlite.

Fig. 10—Sample No. I85. Isothermal transformation temperature 688°C (1270 F), Time 55 minutes. Alpha ferrite, spheroidized cementite, and pearlite.

A remaining item of particular interest (not shown in Fig. 1 but for which microstructures are shown, Figs. 9, 10, 11) is the rapid rate at which spheroidization occurs. This is no doubt a function of the purity of the alloy rather than the fact that the material is a powder compact. For example at 690 C (1270 F) spheroidization was noticeable in 15 minutes and almost complete in 93 minutes. In controlling physical properties in relatively high purity alloys in isothermal transformations it would be essential to know when spheroidization occurs after formation of the pearlite.

In addition to the TTT-diagram determined, some points were compared with a variation in the austenitizing temperature. Scattered studies were made with austenitizing temperatures varying from 875 C (1605 F) to 1100 C (2010 F) and with transformations to pearlite, bainite, and martensite. There was little variation if any from the results shown at 1000 C (1830 F). This may be attributed to the fact that there were no marked changes in grain size for the times and temperatures used. More detailed studies are necessary to be certain of the results.

Photomicrographs

Figs. 4 to 22 inclusive are photomicrographs taken of typical transformation products of austenite decomposition for the 0.87 to 0.89% carbon "powder" steel. They were all taken at 1000 diameters magnification with a 54X oil immersion objective. Etching was done with a solution containing 100 cc absolute alcohol, 2 cc of fuming nitric acid and 0.5 g of urea. Other photomicrographs in this paper were also etched in a similar manner and photographed at 1000 diameters.

Pack Carburizing Studies of Iron Powder Compacts

Earlier in this presentation comments were made pertaining to the method used for preparation of iron-carbon alloys by carburizing pure iron compacts in hardwood charcoal. Before this procedure was decided upon, other experiments had been performed which yielded interesting results. The author is aware of the fact that much more data would be desirable. However, some of the results appear to be of enough interest and consequently may serve in precipitating some good discussion.

Carburizing with Energized Charcoal—The samples that were

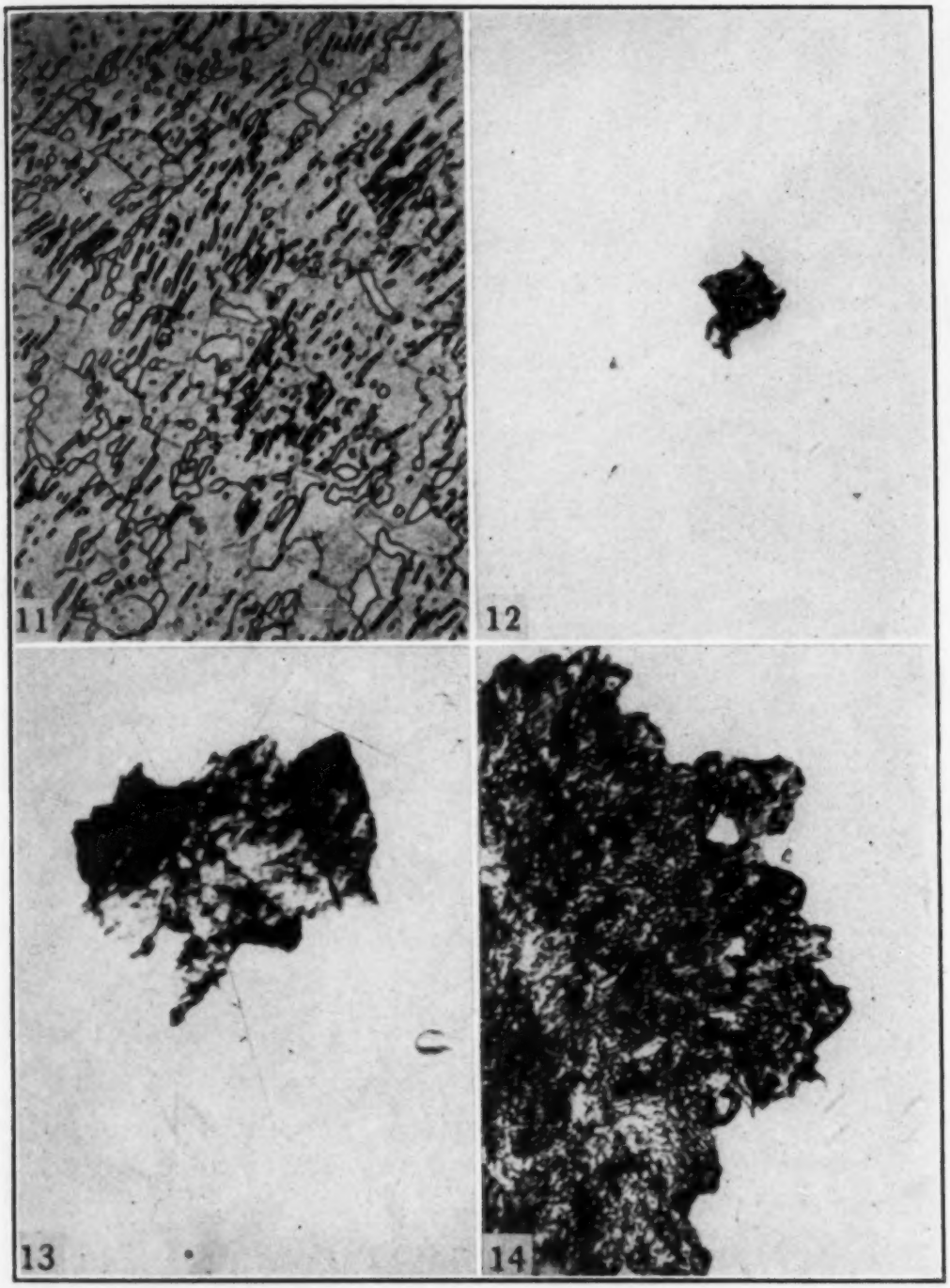


Fig. 11—Sample No. I88. Isothermal transformation temperature 688 C (1270 F), Time 93 minutes. Alpha ferrite, spheroidized cementite, and pearlite.

Fig. 12—Sample No. I9. Isothermal transformation temperature 676 C (1250 F), Time 1 second. Pearlite and martensite.

Fig. 13—Sample No. I10. Isothermal transformation temperature 676 C (1250 F), Time 3 seconds. Pearlite and martensite.

Fig. 14—Sample No. I11. Isothermal transformation temperature 676 C (1250 F) Time 6 seconds. Pearlite and martensite.

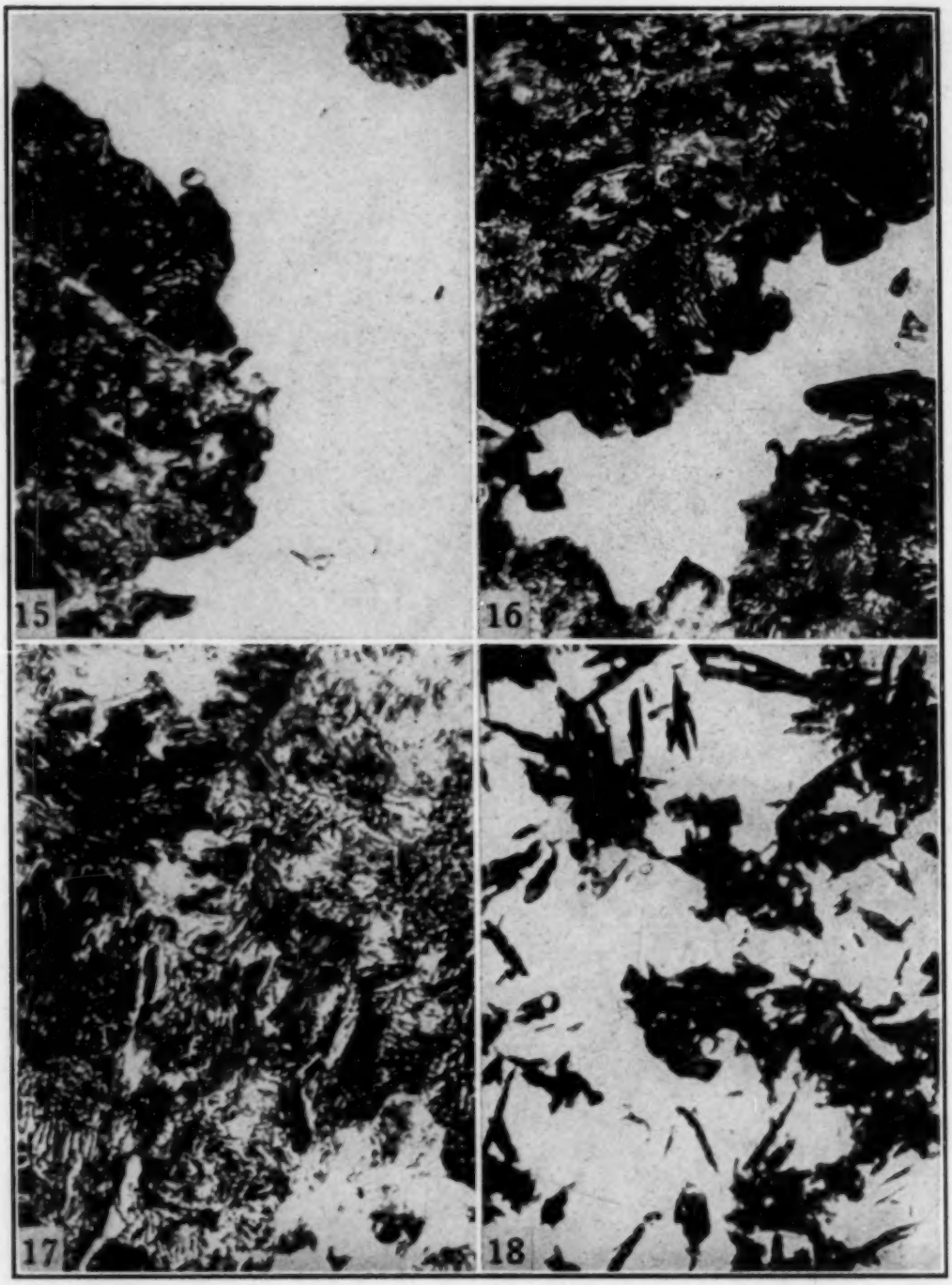


Fig. 15—Sample No. I12. Isothermal transformation temperature 676 C (1250 F), Time 8 seconds. Pearlite and martensite.

Fig. 16—Sample No. I13. Isothermal transformation temperature 676 C (1250 F), Time 10 seconds. Pearlite and martensite.

Fig. 17—Sample No. I5. Isothermal transformation temperature 676 C (1250 F), Time 20 seconds. Pearlite.

Fig. 18—Sample No. I66. Isothermal transformation temperature 353 C (670 F), Time 130 seconds. Bainite and martensite.

prepared for isothermal transformation studies of austenite decomposition were all carburized in ordinary hardwood charcoal. Samples carburized in this manner tend to reach what one might easily consider a maximum carbon content. For example, at 925 C (1700 F) a 0.15-gram sample of carbonyl iron "L" pressed at 25,000 psi will reach an average carbon content of 1.25% carbon after 50 hours' carburizing time. The rate of carbon pick-up is slow after about an hour at temperature. On the other hand, the carbon absorption is very rapid and reaches high values when energized charcoal is used.

In these experiments sodium carbonate was used as an energizer. The energized charcoal was prepared by first dissolving Na_2CO_3 in an amount of water just sufficient to dampen thoroughly the quantity of charcoal used. The amount of energizer added was equal to 10% of the weight of the charcoal. The moistened charcoal after thorough mixing was dried at 150 C (300 F). After drying it was used in a double carburizing tube exactly as in previous studies with ordinary hardwood charcoal.

It was found that with energized charcoal carburizing proceeds very rapidly to extremely high carbon contents and that carbon absorption in appreciable amounts may occur at low temperatures.

Carbon absorption was followed primarily by weight changes and supplemented with microscopic examination and chemical analysis. Table II shows some of the results of energized charcoal studies on carbonyl iron "L", electrolytic iron (as plated), ingot iron, tungsten powder compacts, and titanium powder compacts. The carbonyl iron "L" compacts weighed on the order of 0.2 gram and were ¼ inch in diameter. The specimens of electrolytic iron varied in thickness and in shape and as a result there is a fair variation in average percentage weight increase. The tungsten and titanium powders were pressed as received from the manufacturers. They were not checked for oxygen or moisture contents. It is very likely, therefore, that the actual carbon contents are higher than the values listed as percentage weight increases.

In order to gain a clearer picture of the significance of the percentage weight increase, it may be stated that for short carburizing times and in cases where the temperature is low this percentage value may be at variance with the actual carbon content. For example, samples Nos. 3 and 4 of Table II showed an actual carbon analysis of 5.5% carbon. Further, sample No. 27 after pressing weighed 0.19525 gram and after carburizing weighed 0.19659 gram. This sample was then heated to 1065 C (1950 F) for 10 minutes in the neutral nitrogen

atmosphere referred to earlier. The final weight was 0.19638 gram. If it is assumed that the oxygen leaves as carbon monoxide, then the final carbon content of the compact is about 0.58% and the carbon picked up in carburizing is 0.62%. These values are based on the assumption that there is no oxygen present in the original powder. Both values should probably be about 0.07% higher. In another experiment the following data were obtained when carbonyl iron "L" was carburized with energizer at 650 C (1200 F) for 2 hours:

Sample No.	Weight after Pressing at 3000 kg.	Weight after Carburizing	Weight after N_2 Atmosphere Heating at 1010 C (1850 F) for ½ Hour
a.	0.80732	0.80885	0.80732
b.	0.17165	0.17208	0.17191
c.	0.16547	0.16593	0.16578

	Percentage Weight Increase after Carburizing	Percentage Weight Increase after Homogenization	Estimated Percentage Carbon
a.	0.17	0	0.07
b.	0.25	0.15	0.26
c.	0.27	0.19	0.29

It may be noted that the larger compact, more loosely pressed because of lack of hydrostatic conditions in the powder mass, showed little permanent gain in carbon because of the greater quantities of oxygen absorbed along with the carbon. Samples 28 and 29 of Table II also showed no permanent weight gains. Yet after carburizing, the presence of carbide was ascertained by microscopic examination.

In contrast with shorter times and lower temperatures are the results at somewhat higher temperatures and especially at longer times. Sample No. 19 of Table II when heated at 1040 C (1905 F) showed no greater weight loss than experienced with the samples homogenized for isothermal transformation studies and also gave a microstructure of cementite and pearlite.

In Table II a number of values are shown of carbon contents in a range of 5 to 15%. It appears that the carbon is first picked up in solution in the gamma ferrite at higher temperatures, then precipitated as Fe_3C which then decomposes to give graphite. At lower temperatures, say 650 C (1200 F), the carbide appears to be stable even in contents of 6.35% carbon. Incidentally this material, as one would expect, is very hard and cuts glass readily.

At this time it might be of interest to show what happens, using energized charcoal, below the temperatures listed in Table II. The following data listed in Table III were obtained:

Table II

Sample No.	Pressing Pressure (Psi)	Carburizing Temperature C	Carburizing Temperature F	Time (Hours)	Percentage Weight Increase
		Carbonyl Iron "L"			
1	23,000	925	1697	0.34	5.55
2	23,000	925	1697	0.34	5.82
3	23,000	925	1697	0.50	6.20
4	23,000	925	1697	0.50	6.45
5	9,000	925	1697	0.50	7.50
6	138,000	925	1697	22.5	3.00
7	138,000	925	1697	22.5	3.18
8	23,000	925	1697	22.5	10.4
9	23,000	925	1697	22.5	12.0
10	9,000	925	1697	22.5	15.3
11	9,000	925	1697	22.5	14.6
12	138,000	850	1562	23.0	2.07
13	138,000	850	1562	23.0	2.40
14	138,000	850	1562	23.0	2.30
15	138,000	850	1562	23.0	2.80
16	69,000	850	1562	23.0	3.80
17	69,000	850	1562	23.0	3.62
18	138,000	660	1220	25.8	2.70
19	138,000	660	1220	25.8	2.71
20	46,000	660	1220	25.8	6.12
21	46,000	660	1220	25.8	6.12
22	138,000	650	1202	35.8	3.19
23	138,000	650	1202	35.8	3.28
24	46,000	650	1202	35.8	6.36
25	46,000	650	1202	35.8	6.34
26	138,000	595	1103	41.0	0.69
27	138,000	595	1103	41.0	0.68
28	138,000	585	1085	16	0.10
29	138,000	585	1085	16	0.07
		Electrolytic Iron (As Plated—Thin Sheet) Analysis (C 0.006%, Mn <0.001%, S 0.005%, Si 0.002%, P <0.002%)			
30	.....	925	1697	22.5	3.56
31	.....	925	1697	22.5	3.14
32	.....	925	1697	22.5	3.40
33	.....	925	1697	22.5	2.36
		Ingot Iron (Thin Piece) Analysis (C 0.010%, Mn 0.013%, S 0.022%, Si 0.001%, P 0.005%)			
34	.....	925	1697	22.5	4.80
		Tungsten Powder			
35	46,000	995	1823	21.0	4.07
36	46,000	995	1823	21.0	4.19
		Titanium Powder			
37	46,000	995	1823	21.0	23.0
38	46,000	995	1823	21.0	22.3

Table III

Sample No.	Pressing Pressure (Psi)	Carburizing Temperature C	Carburizing Temperature F	Time (Hours)	Percentage Weight Increase
		Carbonyl Iron "L"			
1	138,000	540	1004	60	1.43
2	138,000	540	1004	60	1.43
3	138,000	540	1004	60	1.35
4	138,000	540	1004	60	1.53
5	46,000	540	1004	60	7.03
6	46,000	540	1004	60	7.05
7	46,000	540	1004	60	6.75
8	46,000	540	1004	60	6.85
9	23,000	540	1004	60	10.27
10	23,000	540	1004	60	10.37

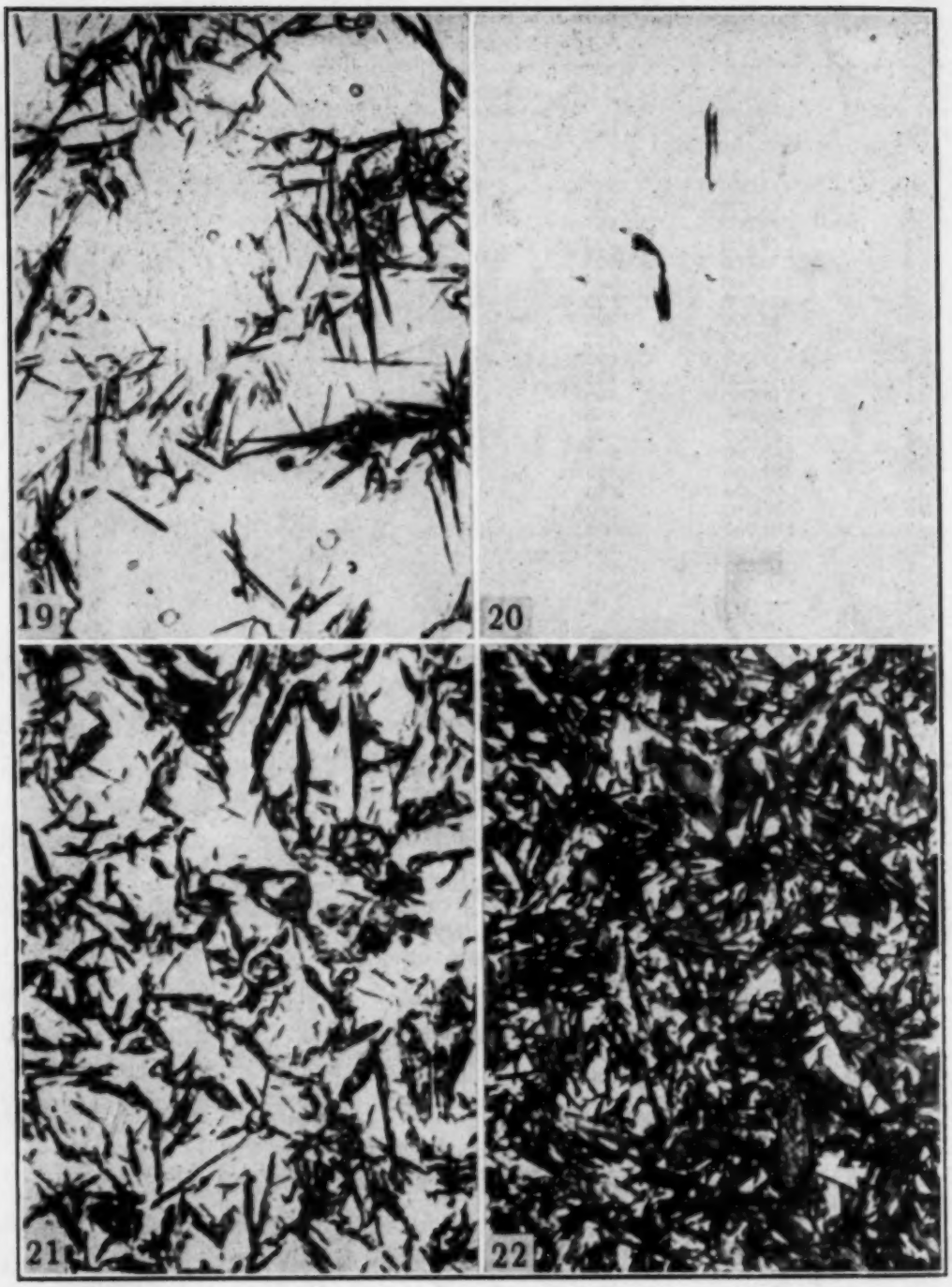


Fig. 19—Sample No. I79. Isothermal transformation temperature 244 C (470 F), Time 15 minutes. Bainite and martensite.

Fig. 20—Sample No. I1. Quenching temperature 242 C (468 F), Time 13 seconds. Tempering temperature 270 C (518 F), Time 10 seconds. Tempered and untempered martensite.

Fig. 21—Sample No. I45. Quenching temperature 175 C (347 F), Time 10 seconds. Tempering temperature 283 C (541 F), Time 5 seconds. Tempered and untempered martensite.

Fig. 22—Sample No. I47. Quenching temperature 126 C (260 F), Time 10 seconds. Tempering temperature 282 C (540 F), Time 5 seconds. Tempered and untempered martensite.

Samples 2, 3, 5 and 6 were analyzed for carbon chemically and showed none. Further, sample No. 4 after being heated at 1040 C (1905 F) for 1.5 hours showed a weight loss of but 0.00008 gram. Microscopic examination revealed no carbon, but instead showed iron oxide dispersed in a matrix of alpha ferrite. It is quite obvious that oxidation has taken place preferentially. From experiments performed

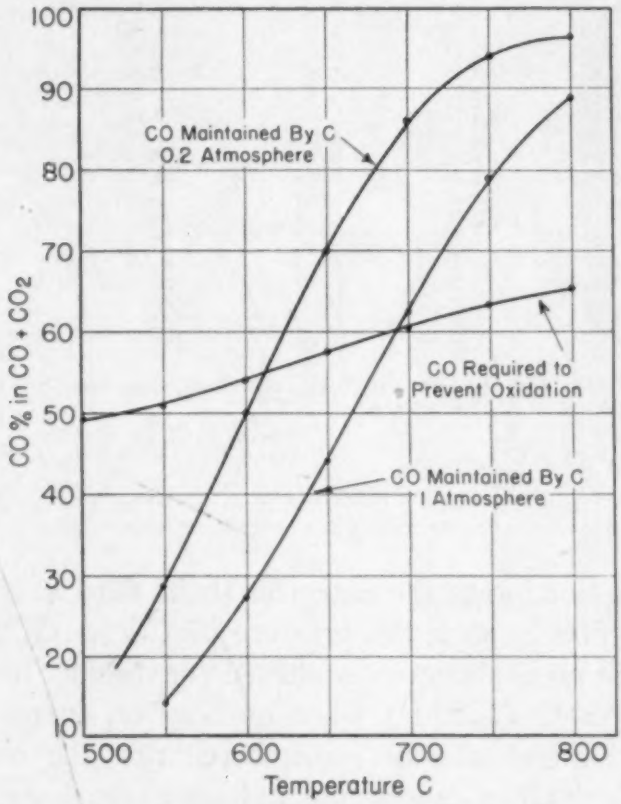


Fig. 23—Plot of Data for Reactions [2] and [4] From Table IV.

it appears that oxidation occurs definitely under the pack carburizing conditions maintained when the temperature is 565 C (1050 F) and carburization occurs definitely at 585 C (1085 F). These values hold when Na_2CO_3 energizer is used. When ordinary hardwood charcoal (on 200 through 150 mesh) without energizer intentionally added is used, then even at 650 C (1200 F) there is no carburization but instead oxidation occurs.

In Table IV are summarized the equilibrium constants for a series of reactions and in Fig. 23 is a plot of data for reactions 2 and 4. Data for 4 is given at 0.2 and 1 atmosphere pressure. From this data one might well expect results such as have been obtained. It shows that a temperature would be expected at which oxidation occurs preferentially. Not enough information, unfortunately, exists to ascertain

Table IV
Equilibrium Constants for Reactions 1 to 5[a]

t °C	t °F	$K_1 = \frac{P_{H_2}}{P_{H_2O}}$	$K_2 = \frac{P_{CO}}{P_{CO_2}}$	$K_3 = \frac{P_{H_2} \times P_{CO_2}}{P_{H_2O} \times P_{CO}}$	$K_4 = \frac{P^2_{CO}}{P_{CO_2}}$	$K_5 = \frac{P^2_{H_2}}{P_{CH_4}}$
400	752	9.12*	0.74*	12.3	9×10^{-5}	5.66×10^{-2}
450	842	6.38*	0.86*	7.38	7.3×10^{-4}	0.164
500	932	4.68*	0.96*	4.88	4.7×10^{-3}	0.422
550	1022	3.53*	1.03*	3.45	0.023	0.977
600	1112	2.99	1.17	2.55	0.096	2.09
650	1202	2.65	1.35	1.96	0.343	3.92
700	1292	2.38	1.53	1.56	1.06	7.16
750	1382	2.17	1.72	1.27	2.96	12.3
800	1472	2.00	1.90	1.05	7.48	20.1
850	1562	1.84	2.07	0.891	17.46	31.8
900	1652	1.72	2.24	0.765	37.76	48.3
950	1742	1.61	2.41	0.668	76.70	71.0
1000	1832	1.51	2.57	0.589	146.5	102.4
1050	1922	1.44	2.72	0.527	264.0	141.2
1100	2012	1.37	2.88	0.474	463.4	192.0
1150	2102	1.31	3.03	0.433	767.4	256.0
1200	2192	1.26	3.21	0.395	1244	335.0
1250	2282	1.22	3.36	0.363	1945	431.5
1300	2372	1.18	3.49	0.339	2951	547.0

*Stable oxide at this temperature is Fe_3O_4, not FeO; the equilibrium constants so marked are not so accurate as the others.

[a] [1] $Fe + H_2O = FeO + H_2$
[2] $Fe + CO_2 = FeO + CO$
[3] $CO + H_2O = CO_2 + H_2$
[4] $C + CO_2 = 2\,CO$
[5] $CH_4 = C + 2\,H_2$

See Reference 21.

whether the introduction of the energizer shifts the CO concentration or whether it serves to shift the pressure of $CO + CO_2$ to a lower value. As a result no explanation is offered for the fact that oxidation occurs even at 650 C (1200 F) when no Na_2CO_3 energizer is used. See Fig. 27. It might also be remembered that the constants for equation 4 are for carbon as graphite and not amorphous carbon.

One experiment conducted on carbonyl iron "L" showed that in 16 hours at 925 C (1700 F) a carbon content of 1.20% was reached in ordinary hardwood charcoal while under the same conditions of time and temperature but 0.69% carbon resulted in using pure finely divided graphite. This too may be a condition of rate of absorption rather than CO concentration maintained. Along these same lines differences were apparent in using charcoal of varying mesh. For example, carbonyl iron "L" was carburized 51 hours at 925 C (1700 F) in 5 to 8-mesh charcoal (no energizer) and another set of samples were carburized in 200-mesh charcoal (no energizer other than the ash of the charcoal). The coarse charcoal run yielded samples of 0.95% carbon, while the fine material gave 1.20% carbon. Again it is difficult to draw conclusions.

Microscopic studies revealed a number of interesting structures

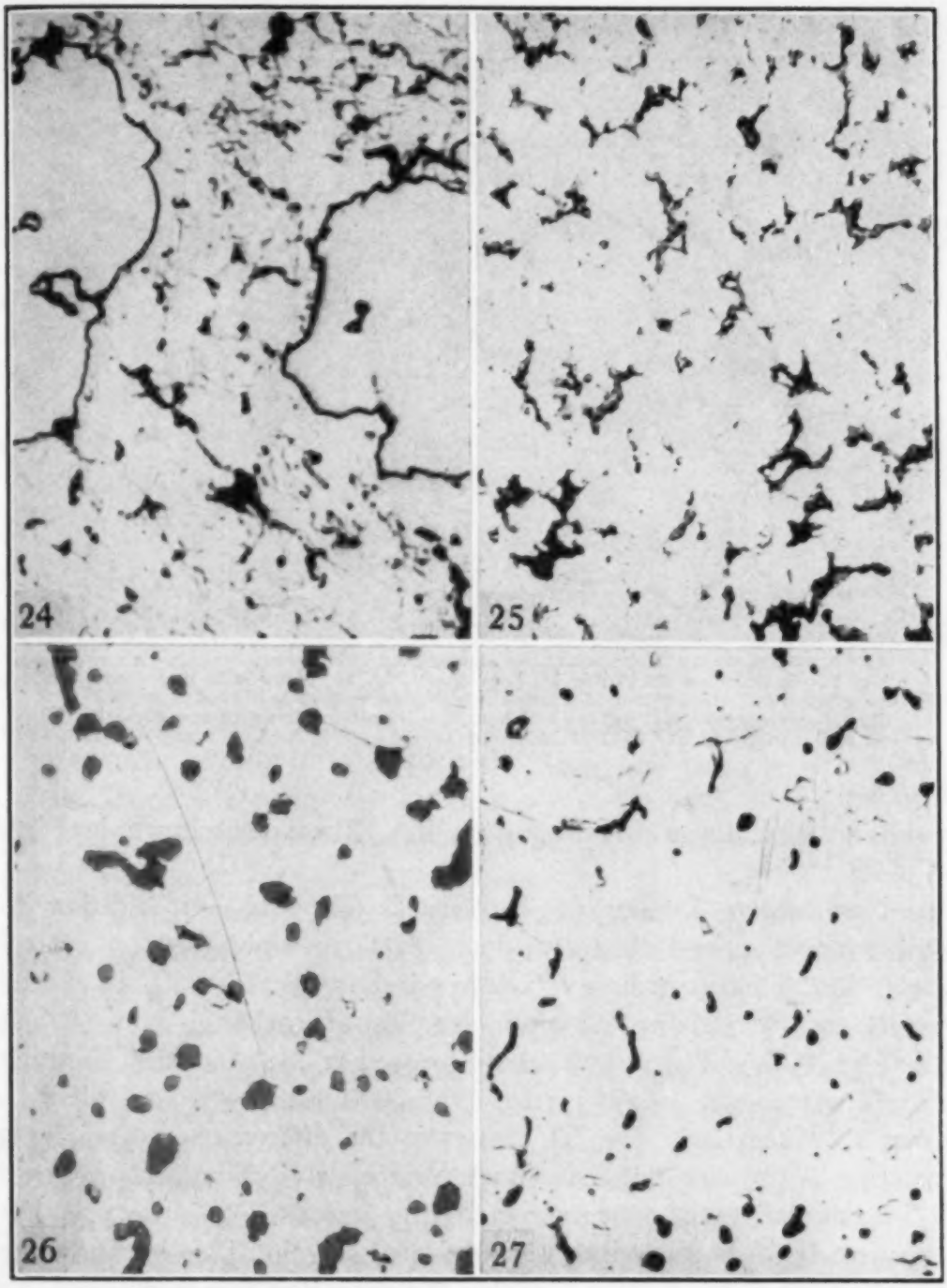


Fig 24—Sample No. 26, Table II, Laboratory No. 25. Alpha ferrite and cementite. Carburized at 595 C (1105 F) for 41 hours in Na_2CO_3 energized hardwood charcoal.

Fig. 25—Sample No. 1, Table III, Laboratory No. 31a. Iron oxide and alpha ferrite. "Carburized" at 540 C (1005 F) for 60 hours in Na_2CO_3 energized hardwood charcoal.

Fig. 26—Sample No. 4, Table III, Laboratory Sample No. 43. Iron oxide and alpha ferrite. "Carburized" at 540 C (1005 F) for 60 hours in Na_2CO_3 energized hardwood charcoal, then heated to 1040 C (1904 F) for 1½ hours in nitrogen atmosphere.

Fig. 27—Laboratory No. 23. Iron oxide and alpha ferrite. "Carburized" at 650 C (1200 F) for 16 hours in hardwood charcoal without Na_2CO_3 energizer added, then the sample was heated to 1000 C (1830 F) for 30 minutes in the nitrogen atmosphere.

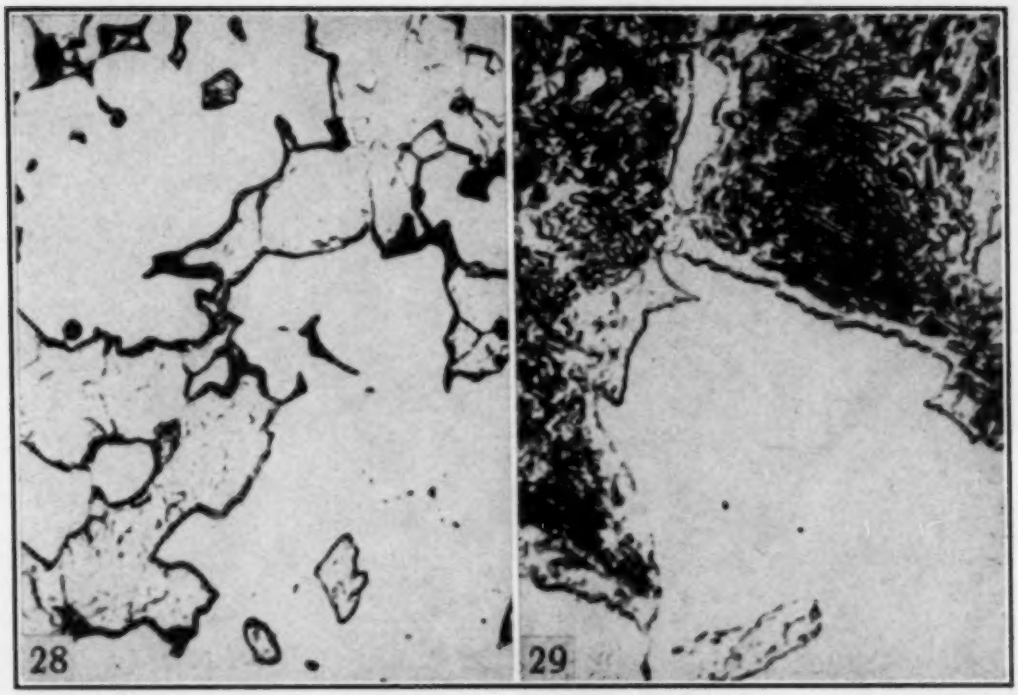


Fig. 28—Sample No. 22, Table II, Laboratory No. 18. Cementite and alpha ferrite. Carburized at 650 C (1200 F) for 35.8 hours in Na_2CO_3 energized hardwood charcoal.
Fig. 29—Sample No. 31, Table II, Laboratory No. 76. Cementite and pearlite. Electrolytic iron carburized at 925 C (1700 F) for 22½ hours in Na_2CO_3 energized hardwood charcoal.

resulting from these carburizing studies. These are shown in Figs. 24 to 29.

Carburizing Studies in Hardwood Charcoal—In addition to studies on energized choarcoal some data were obtained on carbon absorption rates in ordinary hardwood charcoal. Fig. 30 shows the results for carburizing 0.2-gram samples of carbonyl iron "L" at 925 C (1700 F). The samples were pressed at 138,000 psi. The value of 1.22 percentage weight increase for 3000 minutes is equivalent to about 1.29% carbon. Fig. 31 illustrates the differences caused by a variation in pressing pressures used for compacting the carbonyl iron "L" over relatively short-time carburizing periods. For lower pressing pressures there is a much more rapid weight gain. This is caused by oxidation combined with subsequent carburization and as a result the curve goes through a maximum. At the higher pressing pressures no maximum is evident because the oxidation rate is decreased by the more compact powder. Because of the oxidation possible in pack carburizing as the mass is being heated, it would seem much more practicable normally to use gas carburizing procedures where the compressed powder samples are introduced into the hot zone without

a great temperature lag. If long-time carburizing is not objectionable, as was the case in samples prepared for the austenite decomposition studies, the pack carburizing procedure is excellent for preparation of pure steel of controlled carbon content. It was easier with limited facilities to prepare pure steels of controlled carbon content by this

Table V

Pressing Pressure (Psi)	Percentage Weight Increase
23,000	1.61
46,000	1.38
69,000	1.27
92,000	1.15
115,000	0.96
138,000	0.80

Time at 925 C (1700 F) was 20 Minutes

Pressing Pressure (Psi)	Percentage Weight Increase
23,000	1.05
46,000	1.06
69,000	1.02
92,000	1.03
115,000	1.01
138,000	0.96

Time at 925 C (1700 F) was 140 Minutes

method than by gas carburizing or by mixing graphite and iron followed by subsequent heating to form austenite.

In 20 and 140 minutes at temperature under conditions shown in Fig. 31 the percentage weight increase varied with pressing pressure as shown in Table V.

In comparing Figs. 30 and 31 one may at first thought believe that they are in conflict. In 30 minutes at temperature the weight increase shown in Fig. 30 is 0.52% while in Fig. 31 it is given as 0.84%. These values are not in conflict when one considers that in the coarser charcoal the 0.84% weight increase is actually due to a greater quantity of oxide whereas the 0.52% weight change is more nearly the actual carbon content.

Maximum Carbon Content of Carburized Cases—Some investigators believe that the maximum carbon content of carburized cases is limited by the Ac_{cm} temperature in the iron-iron carbide constitutional diagram when the carbon monoxide content is sufficient to permit going to that high a carbon content. Recently consideration has been given to this problem by Floyd E. Harris (22) and Sidney Breitbart (23).

Most certainly this is not the case when Na_2CO_3 energizer is used, as has been shown, but when it is not intentionally used there might be some question. Many samples carburized at 925 C (1700 F)

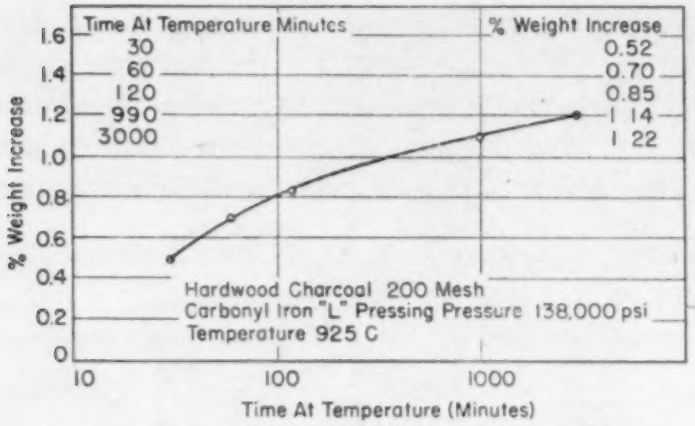


Fig. 30—Graph Showing the Results for Carburizing 0.2-Gram Samples of Carbonyl Iron "L" at 925 C (1700 F).

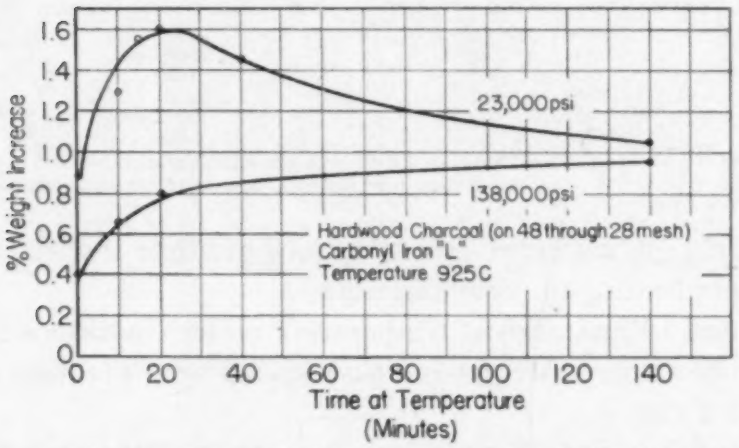


Fig. 31—Graph Showing the Results for Carburizing 0.2-Gram Samples of Carbonyl Iron "L" at 925 C (1700 F).

in hardwood charcoal show that after long times (60 hours) on lightly pressed samples the carbon content is 1.3% at most. The value usually given for the Ac_{cm} at 925 C (1700 F) is about 0.1% less. At 1065 C (1950 F) values as high as 2.3% were obtained after 40 hours at the carburizing temperature. The Ac_{cm} given at 1065 C (1950 F) is close to 1.55% carbon. At 800 C (1470 F) in hardwood charcoal (on 200 through 150 mesh) the following carbon contents were reached:

Pressing Pressure (psi)	Percentage Carbon
138,000	0.90
138,000	0.91
46,000	0.90
46,000	0.90
23,000	0.90
23,000	0.91

At 800 C (1470 F) equilibrium data show that the Ac_{cm} value would

not be reached. The carbon content would be limited to about 0.65% carbon. The data at 800 C (1470 F) show that the less dense compacts do not reach unusually high carbon contents.

Perhaps not enough data are available, but there seems to be no definite theoretical reason why the carbon content should be limited to the Ac_{cm} temperature. It would seem more logical to expect precipitation of Fe_3C as a second phase.

Carburizing of Electrolytic and Hydrogen-Reduced Iron Powders—Electrolytic iron powder and hydrogen-reduced iron powder of the following analyses were given a hydrogen treatment at 260 C (500 F) for 24 hours. This treatment was similar to the one given the carbonyl iron "L" used for all other studies.

Electrolytic Iron (annealed)	
Total Iron	99.50%
Copper	0.01
Silica	0.02
Manganese	0.027
Zinc	0.090
Nickel	None
Sulphur	0.001
Phosphorus	0.002
Free Carbon	0.005
Oxygen	—

Hydrogen-Reduced Iron Powder		
Total Iron	99%	minimum
Carbon	0.04	
Manganese	0.18	

After the hydrogen treatment these powders were pressed and carburized along with carbonyl iron "L". Weight changes were:

Pressing Pressure	138,000 psi
Carburizing Temperature	816 C (1500 F)
Time	22 hours
Carburizing Medium	Hardwood Charcoal
	Percentage Weight Change
Carbonyl Iron "L"	0.77%
Electrolytic Iron	0.52%
Hydrogen-Reduced Iron	0.93% Loss

It was quite evident that the loss in weight encountered was with the hydrogen-reduced iron caused by the presence of the oxide in the powder. Microstructures prepared of all of them showed an estimate of eutectoid carbon content. A fair guess is that all were about 0.85% carbon. In an endeavor to gain some concept of the oxygen contents of these various powders they were run "as-received" in compressed form (46,000 psi) at 1095 C (2000 F). The loss in hydrogen (not necessarily all oxygen) after 25 hours was:

Carbonyl Iron "L"	0.04%
Electrolytic Iron	0.70%
Hydrogen-Reduced Iron	1.92%

The time of 25 hours was split into three periods to determine that a constant weight had been reached. The percentage losses varied with time as follows:

	Hydrogen Loss		
	After 11.5 hours	After 15 hours	After 25 hours
Carbonyl Iron "L"	0.04	0.04	0.04
Electrolytic Iron	0.56	0.70	0.70
Hydrogen-Reduced Iron	1.88	1.92	1.92

This indicates that under these conditions the oxygen removal is slower with the electrolytic iron than with the hydrogen-reduced iron, which has a greater oxygen content. This is also evident when one compares the losses in hydrogen and the percentage weight changes. By adding these values algebraically and considering that the 0.04% carbon in the hydrogen-reduced iron is lost during the hydrogen treatment and present in the original powder, the percentage weight changes in the previous carburizing experiment should have been:

Carbonyl Iron "L"	+ 0.81%
Electrolytic Iron	+ 0.15%
Hydrogen-Reduced Iron	— 1.07%

instead of

Carbonyl Iron "L"	+ 0.77%
Electrolytic Iron	+ 0.52%
Hydrogen-Reduced Iron	— 0.93%

The above calculations are made assuming the actual carbon content of the compact to be 0.85%. The significant point is that 0.37% oxygen remains in the electrolytic iron powder compacts as compared to 0.14% in the hydrogen-reduced powder compacts.

Another set of all three type irons were carburized for 36 hours at 815 C (1500 F) in hardwood charcoal (on 150 through 100 mesh). The samples were pressed at 138,000 psi. After carburizing, the compacts were homogenized at 1100 C (2010 F) for 55 minutes in the nitrogen atmosphere. Results were as follows:

	Weight Percentage Gain As Carburized	Weight Percentage Loss in Homogenization
Carbonyl Iron "L"	0.75	0.06
Electrolytic Iron	0.32	0.39
Hydrogen-Reduced Iron	— 1.05	0.23

These results confirm what has been stated previously; namely, that in spite of higher oxygen content initially present in the hydrogen-reduced powder, more of the oxide is reduced in carburizing. This is true for the conditions under which these experiments were performed, and may not be general. This fact, if generally true, would be of marked importance in any steels made by carburizing methods because if they

were to be heat treated they would decarburize when austenitized. This, of course, would result in poor control of the properties of the product.

When samples of all three type powders were compacted at 46,000 psi, reduced in hydrogen for 25 hours at 1100 C (2010 F), then carburized at 815 C (1500 F) for 36 hours in hardwood charcoal (on 150 through 100 mesh), they gave weight percentage increases of

Carbonyl Iron "L"	0.76%
Electrolytic Iron	0.78
Hydrogen-Reduced Iron	0.78

These might be considered essentially the same. This is but a limited amount of work along these lines but nevertheless again indicates a definite trend.

Conclusions

The more important conclusions reached in making this study are that:

1. Very pure steels may be prepared by pack carburizing a high purity iron such as carbonyl iron "L".

2. Pure steels made from powder without going into the liquid state have austenite transformation characteristics which do not differ markedly from those found in comparable steels made by utilization of the liquid phase. This is considered by the author a significant contribution toward establishing the thesis that by either method products may be produced, without too much difficulty, that are equivalent with respect to composition and grain structure.

3. Sodium carbonate used as an energizer alters markedly the quantity of carbon absorbed in carburizing carbonyl iron "L" compacts.

4. Carbon absorption may take place with sodium carbonate energized hardwood charcoal at temperatures as low as 585 C (1085 F).

5. The oxide content of iron powders is an important factor to consider in the preparation of steels by carburization, particularly those which may be subjected to heat treatment to gain high strengths.

Since it was possible to produce a high grade steel it would seem relatively simple, in further work, to study the influence of the introduction of even small quantities of other elements and compounds into the powder compacts. With a high purity product it may be possible to show, for example, whether cobalt actually does increase the rate of austenite decomposition in steels and what the mechanism may be.

To illustrate further, a more careful grain growth study could be conducted on steels to show more precisely the influence of various compounds such as aluminum oxide on grain growth phenomena. An opportunity exists immediately for securing data to learn how energizers function in carburizing iron and steel. This study might well begin by employing other compounds as energizers. Uncovering some of the secrets in nature is always difficult but it is sincerely believed that with respect to the metallic state the job may be made much easier through the use of metal powders.

Acknowledgments

The author is grateful for the interest and help of Professor R. S. Tour, Head of the Department of Chemical Engineering and Metallurgical Engineering of the University of Cincinnati, and Professors R. O. McDuffie and E. E. Stansbury of the same department. In addition the author is appreciative of aid given so generously by R. H. Bell, Lucius Pitkin, Inc.; J. H. Caine, Sawbrook Steel Castings Company; Dr. Anson Hayes, American Rolling Mill Co.; and Miss Dorothy Leinen, secretary in the Department of Chemical Engineering and Metallurgical Engineering, University of Cincinnati.

References

1. W. D. Jones, "Principles of Powder Metallurgy," Edward Arnold and Company, London, England, 1939, p. 77.
2. John Wulff, "Powder Metallurgy," American Society for Metals, Cleveland, 1942.
3. W. J. Baeza, "A Course in Powder Metallurgy," Reinhold Publishing Corporation, New York, 1943.
4. Franz Skaupy, "Principles of Powder Metallurgy," Philosophical Library, New York, 1944.
5. ASTM "Symposium on Powder Metallurgy," American Society for Testing Materials, Philadelphia, 1943.
6. AIME "Conference on Production and Design Limitations and Possibilities for Powder Metallurgy Parts," American Institute of Mining and Metallurgical Engineers, Institute of Metals Division, Vol. 161, 1945, p. 524-634.
7. N. B. McDonald, "Powdered Metals—A Bibliography," The Library of Congress, Division of Bibliographies No. 2, Washington, D. C., 1943.
8. Clark B. Carpenter, "Powder Metallurgy—A Review of its Literature," Colorado School of Mines Quarterly, Vol. 36, No. 4, 1941.
9. Institute of Metals, "Metallurgical Abstracts," Powder Metallurgy Sections, Vols. VI-XI (1939-1944), Institute of Metals, London, England.
10. ASM "Review of Metal Literature," Powder Metallurgy Sections, Vols. I and II (1944 and 1945), American Society for Metals, Cleveland.
11. E. E. Schumacher and A. G. Souden, "Powder Metallurgy," *Metals and Alloys*, Vol. 20, 1944, p. 1327-1339.

12. F. P. Peters, "Design Factors for the Metal Forms with Which Powder Metallurgy May Compete," *Transactions,* American Institute of Mining and Metallurgical Engineers, Vol. 161, 1945, p. 527-530.
13. A. J. Langhammer, "Powder Metallurgy as Applied to Machine Parts," *Transactions,* American Institute of Mining and Metallurgical Engineers, Vol. 161, 1945, p. 531-535.
14. C. W. Balke, "The Effect of Pressure on the Properties of Compacts," Symposium on Powder Metallurgy, American Society for Testing Materials, Philadelphia.
15. John Wulff, "Alloy Steels from Powders," Powder Metallurgy, American Society for Metals, Cleveland, 1942.
16. F. V. Lenel, "Oil Pump Gears," Powder Metallurgy, American Society for Metals, Cleveland, 1942.
17. A. S. Margolies, "Carbursintering of Iron Powders," *The Iron Age,* Vol. 157, No. 9, 1946, p. 60-63.
18. E. E. Stansbury, "A Study of Several Variables Affecting the Rate of Martensite Formation," University of Cincinnati Thesis, 1946.
19. A. B. Greninger, "The Martensite Thermal Arrest in Iron-Carbon Alloys and Plain Carbon Steels," TRANSACTIONS, American Society for Metals, Vol. XXX, 1942, p. 1-26.
20. C. Zener, "Kinetics of the Decomposition of Austenite," *Metals Technology,* Vol. 13, No. 1, T.P. 1925, January 1946.
21. J. B. Austin and M. J. Day, "Chemical Equilibrium as a Guide in the Control of Furnace Atmospheres—A Review of Equilibrium Data," Controlled Atmospheres, American Society for Metals, Cleveland, 1942.
22. Floyd E. Harris, "Maximum Carbon in Carburized Cases," METAL PROGRESS, Vol. 45, 1944, p. 683-686.
23. Sidney Breitbart, "Maximum Carbon in Carburized Cases," METAL PROGRESS, Vol. 47, 1945, p. 1121-1127.

DISCUSSION

Written Discussion: By F. V. Lenel, Moraine Products Division, General Motors Corp., Dayton, Ohio.

Dr. Kahles' paper is a welcome addition to the literature on iron and steel powder metallurgy. Most investigations in this field have been concerned with practical aspects of making parts from powder rather than the scientific basis of the new art. Any paper which treats the fundamentals of powder metallurgy must, therefore, be hailed as a pioneering effort in the hope that it will stimulate further work in the field. The technique of isothermal transformation has been of great value in shedding light on the theory of the heat treatment of steel and it is gratifying to see the author apply it to a steel made from powder. His results are represented in the form of the time-temperature-transformation diagram of an 0.87% carbon steel made by carburizing carbonyl iron.

Unfortunately no data, which are directly comparable with those presented in this paper, on the transformation characteristics of high purity iron-carbon alloys made by melting have been published, and none have been supplied in this paper. It is, therefore, not possible to decide, on the basis of this study, whether small differences exist, which may be due to difference in grain boundary conditions, in the transformation behavior of steels from powder and conventional steels.

The author's generalized conclusion that the two types of steel do not

differ markedly in their transformation characteristics cannot be considered as particularly new, since the equivalency of steels made from powder has been rather conclusively proven by the work of Offermann, Buchholtz and Schulz.[2]

The additional data on the carburizing of iron powder compacts are of interest, but it is felt that their value could have been greatly increased by a more systematic presentation and evaluation of the data with respect to the various factors which determine the carbon absorption of the compacts.

With regard to the individual sections of Dr. Kahles' paper, the following comments are offered:

In the section on "The Powder Metallurgy of Steel", Dr. Kahles discusses the various methods for producing steel from powders. There seem to exist two fundamentally different methods of introducing the desired amount of carbon into the steel. One method would be to make compacts of straight iron powder and introduce the carbon during sintering; in other words, sinter and carburize simultaneously. Kalischer[3] has discussed the advantages and disadvantages of the method with respect to gas carburizing. He points out that it is much easier to prepare material with a high carbon case and a low carbon core, than to prepare material with a homogeneous carbon content throughout by this method of simultaneous sintering and gas carburizing. For the latter purpose Kalischer advocates[4] using a carefully balanced gas atmosphere of hydrogen, nitrogen, carbon monoxide and small amounts of methane and water vapor which would be in exact equilibrium with a steel of the desired carbon content at the sintering temperature. This is a very intriguing possibility, but whether the necessary exacting process control would be commercially feasible remains doubtful. Dr. Kahles' method of making homogeneous iron-carbon alloys by simultaneous sintering and carburizing in hardwood charcoal is, of course, applicable only to very small pieces, such as his samples which are approximately $\frac{1}{32}$ inch thick. Larger pieces which are sintered in solid carburizing compounds would have a case and core structure such as Margolies[5] showed and homogenization would be virtually impossible, at least under commercial conditions.

The other method would be to introduce the carbon into the powder mixture before compacting. This may be done by mixing with the iron powder elemental carbon in the form of graphite, carbon black, etc., or iron carbides in the form of cast iron powder or high carbon ferro-alloy powder, or it may be done by compacting an iron-carbon alloy powder, in other words, a steel powder. Most commercial sintered iron-carbon alloys are made by mixing graphite with the iron powder.

Dr. Kahles emphasizes that iron powders which are used for such alloys should have negligible oxygen or at least uniform oxygen content. The importance of the oxide content of iron powders has long been recognized by iron powder producers and consumers. The so-called hydrogen loss, i.e., loss in weight of the iron powder when heated in hydrogen under certain standard

[2]E. K. Offermann, H. Buchholtz and E. H. Schulz, *Stahl und Eisen*, Vol. 56, September 1936, p. 1132-1138.

[3]P. R. Kalischer, *Iron Age*, February 5 and February 13, 1942.

[4]U. S. Patent 2,333,573, November 2, 1943.

[5]A. S. Margolies, *Iron Age*, February 28, 1946.

conditions,[6] is an important item in most iron powder specifications. By proper control of hydrogen loss and graphite additions, it is possible to hold the carbon content of eutectoid iron-carbon powder alloys made of reduced iron powder and graphite fairly constant in large-scale production.

At the end of the section on "Production of Steel Compacts by Carburizing", Dr. Kahles discusses the purity of his alloys; no figures are shown for either oxygen or nitrogen. Some doubt remains whether all the oxygen, which was doubtlessly introduced in the alloys during the carburizing treatment in charcoal, was removed during the homogenizing treatment in nitrogen.

In his TTT-diagram, Dr. Kahles showed that in the temperature range near 600 C (1110 F) very rapid reaction from austenite to the transformation product occurs which confirms the results of Digges[7] on the hardenability of high purity iron-carbon alloys. The hardenability of steels made from powders is of considerable practical interest. In this connection it should be remembered that there is another factor besides the time-temperature-transformation characteristics of these steels, which has a bearing on their hardenability. This is the fact that steels which are made from powder and are porous have a lower heat-conductivity than solid steels—the more porous they are, the lower will be their conductivity. Therefore, the cooling rates in such steels at a distance from the quenched surface are slower than for solid steels. This would make a low density steel from powder even shallower hardening than a solid steel having the same time-temperature-transformation characteristics. Data on actual hardenability tests, such as the end-quench test of steels made from powder, would therefore be of interest.

A possible explanation is offered to Dr. Kahles' data on the carburization and the hydrogen-reduced iron powder compacts. Both types of compacts were pressed with the same pressure—138,000 psi in the carburizing experiments, 46,000 psi in the reducing experiments. Most grades of electrolytic iron powder are more compressible than grades of hydrogen-reduced powder. In other words, electrolytic iron powder compacts compressed under a given pressure will have a higher density than reduced iron powder compacts compressed under the same pressure. This higher density may be the reason why the electrolytic iron powder compacts are more slowly reduced than the hydrogen-reduced iron powder compacts in spite of their lower initial oxygen content. It may also be the reason why, under a given carburizing treatment, more oxygen is retained in the electrolytic iron powder than in the hydrogen-reduced iron powder compacts.

Written Discussion: By George Stern, metallurgist, American Electro Metal Corporation, Yonkers, N. Y.

The author has presented an interesting theoretical paper but certain statements are made and impressions created by inference that require clarification.

For one, on page 621, the author says, "Any number of so-called steel parts that have been examined microscopically are no more than iron-base parts with iron oxide particles distributed in the matrix with little or no carbon present". I should like to call the author's attention to the many thousands

[6] Tentative Method for Determination of Hydrogen Loss of Iron Powder, Metal Powder Association Standard 2-45T.

[7] T. G. Digges, TRANSACTIONS, American Society for Metals, Vol. 27, 1938, p. 408-421.

of powder metal steel parts made commercially which have structures very similar to normal SAE steels with the one exception of some residual porosity. Furthermore, many steel parts are made from electrolytic iron powder and do not exhibit any iron oxide inclusions (Reference: "A Study of the Physical Properties and Microstructure of Sintered Steel"—George Stern) and exhibit a normal steel structure. If the author's statement were true, powder metal steel parts could not be made and heat treated to give tensile strengths approaching 150,000 psi, since the material he describes would hardly respond to heat treatment.

In the conclusion the author speaks of future work where "it would seem relatively simple to study the influence of the introduction of even small quantities of other elements and compounds into the powder compacts". With the exception of such elements as carbon and copper, it is difficult to get elements such as cobalt, nickel, chromium, tungsten, manganese, etc., to diffuse into iron, especially at temperatures in the order of 870 C (1600 F) (the carburizing temperature used), or even the higher temperature used for homogenization, 1105 C (2020 F). If work is to be done with these elements in sintered steel, temperatures in the order of 1300 C (2370 F) will be required and the atmosphere problem encountered at this temperature is far from simple.

Although the method of pack carburizing followed by homogenization in a nitrogen atmosphere lends itself very nicely to a theoretical study, I should like to point out that it is hardly a commercial process. In fairness to the author it is not described as such, but some readers of the paper might infer it can be used. The method, however, is impractical commercially due to the long time required for uniform carburization (15 hours), the variation from piece to piece that would be obtained in a large pack, and the problem of homogenizing in a neutral atmosphere. Furthermore, pressures of 138,000 psi are not commercially feasible and it is simpler to combine iron powder with graphite, press, sinter, and coin to make sintered steel parts.

Written Discussion: By F. E. Harris, furnace engineer, Buick Motor Division, General Motors Corp., Flint, Mich.

Dr. Kahles has presented an interesting paper dealing with iron-carbon powder alloys. In the sintering process, various carburizing compounds are used and carbon is added simultaneously to the pressed compacts. When sodium carbonate is added to the compound, the high carbon content found in the compact leads the author to doubt that the A_{cm} line has any practical significance in the problem of carbon addition.

The A_{cm} line may not only be theoretically significant, but it also has a definite significance in the transfer and flow of carbon. This can be demonstrated by a simple experiment.

Four machined white iron samples of approximately 3.5% carbon are used in an atmosphere test at 925 C (1700 F). A decarburizing atmosphere is maintained for 2 hours on all four samples. A carburizing atmosphere is then supplied and the samples are removed at the following intervals: No. 1 after 2 hours, No. 2 after 4 hours, No. 3 after 6 hours, while No. 4 is exposed to the carburizing atmosphere for 22 hours.

Photomicrographs are shown in Fig. A for samples 1 and 4. Two conclusions may be derived from this evidence:

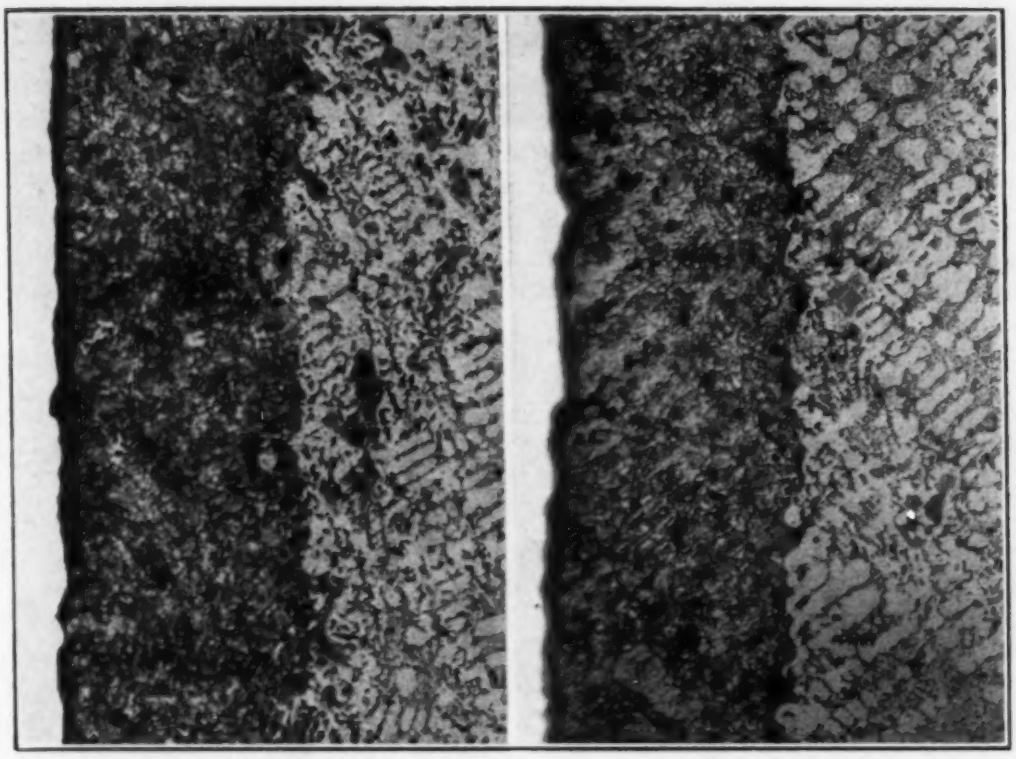


Fig. A—Hypereutectoid Case in Equilibrium with 3.5% Carbon. 5% nital etch. × 100. Sample 1 (left)—Decarburized for 2 hours then carburized for 2 hours. Sample 4 (right)—Decarburized for 2 hours then carburized for 22 hours.

1. A hypereutectoid composition, with a carbon content represented by the A_{cm} line is in equilibrium with an austenite-cementite mixture at 925 C (1700 F).
2. The interface between the two phases does not appreciably change, in relation to the distance from the steel surface, with time.

Perhaps we may consider this interface (or surface) as similar in many respects to the outside surface which has been exposed in turn to a decarburizing, and then a carburizing atmosphere. No appreciable flow of carbon is evidenced from the original 3.5% carbon core to the 1.35% carbon concentration, although these widely different concentrations are in direct contact, inside the solid body, for a time period of 20 hours, and at a temperature of 925 C (1700 F). Why should we consider this interface as differing from that of the outside surface of the specimen?

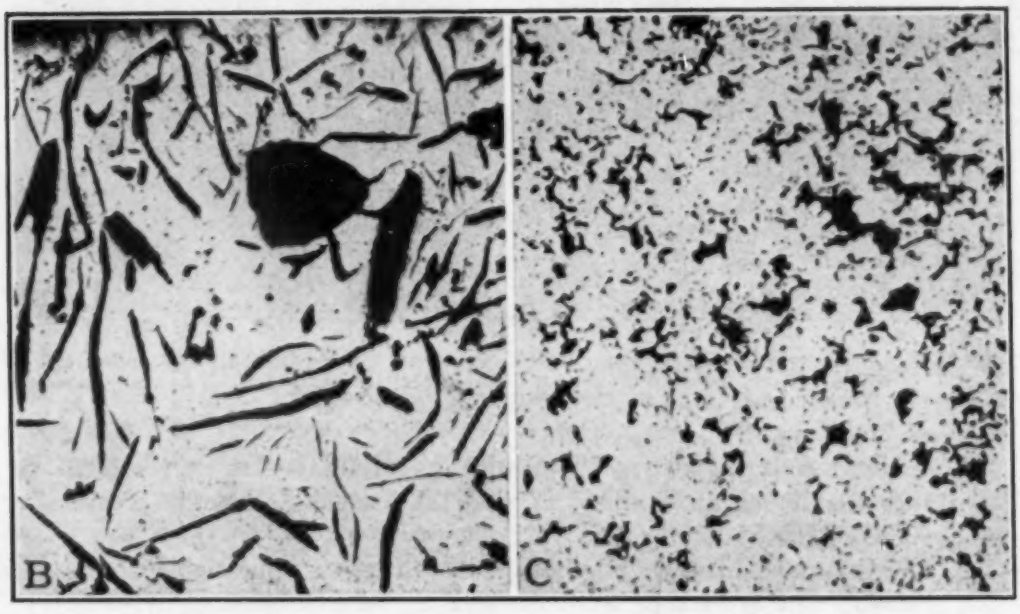
When atmospheres are employed at steel surfaces which allow no reactions other than those of carbon supply, then we may expect that surface concentrations of carbon will not exceed those signified by the saturated austenite line. A timely paper is presented at this meeting under the title, "Carbon Concentration Control".[8] While it may not be exactly true that perfect commercial gas atmospheres are now available, at least it is clear that the equilibrium between such mixtures and carbon concentrations at steel surfaces may be shown in a practical manner. In this connection, as is to be expected, the iron-carbon equilibrium diagram plays an important role.

[8] E. G. de Coriolis, O. E. Cullen and Jack Huebler, "Carbon Concentration Control," TRANSACTIONS, American Society for Metals, Vol. 38, 1947, p. 659.

Written Discussion: By Gerard H. Boss, Naval Air Experimental Station, Philadelphia Naval Base, Philadelphia.

This paper presents some interesting quantitative data on the sintering of iron powders in carburizing atmospheres. In a recent article,[9] the writer reported some of the results of similar work done under Dr. Schneidewind at the University of Michigan. Most of the results of that work, as far as it went, are in agreement with the data quoted in the present paper. Not mentioned, in the paper referred to, were some results which at the time seemed hard to believe, but which take on some significance after reading the present paper.

The carburizing was done on powder compacts placed in a porcelain muffle through which Ann Arbor city gas was passed. The temperatures used



Figs. B and C—Photomicrographs Showing the Modes of Occurrence of the Uncombined Carbon.

were 1120 and 1205 C (2050 and 2200 F). Due to the rapidity with which the compacted powder sintered into nonporous metal at 1205 C (2200 F), the only results quoted are those which were obtained at 1120 C (2050 F). Holding times at temperatures were 1, 2 and 3 hours.

Large amounts of carbon were picked up during the sintering operation. In some pieces it occurred as iron carbide and the compact shrank in volume. These were the pieces whose photomicrographs were used by the present writer.[9] However, in others the carbon occurred uncombined, presumably as graphite. In some pieces both combined and uncombined carbon occurred together. Figs. B and C show the modes of occurrence of the uncombined carbon. The plate-shaped masses tended to occur near the surface while the irregular-shaped masses occurred in the center. Some of the pieces held at 1120 C (2050 F) for 3 hours contained so much uncombined carbon that their volume

[9]Gerard H. Boss, "Maximum Carbon in Gas Carburizing," METAL PROGRESS, Vol. 50, October 1946, p. 657.

was increased as much as × 15. Such pieces no longer possessed metallic properties. They were so friable that they could be crushed between the fingers and would mark paper in the same manner as charcoal.

When trying to determine what caused graphite to occur instead of carbide it seems necessary to consider the source of the carburizing gas. The gas used was natural gas, methane, stored over water in the usual city gas tanks. Thus water was introduced into the gas and carried over into the mains. It follows that variations in the temperature would cause the moisture content of the gas to vary.

Now one assumption of the mechanism of the reactions is that the carbon first enters the compact by combining with the iron to form carbide. Then graphite is formed whenever the moisture content is in a certain range, where its oxygen, and perhaps hydrogen, are able to catalyze the decomposition of the carbide. The difficulty with this theory is that in some of the highly swollen pieces it would be necessary for carbide to be forming and decomposing at the same time.

Another mechanism which might account for the uncombined carbon is that it is deposited directly from the gas. This would occur whenever the moisture content is in a certain range, otherwise it is deposited as carbide. This last assumption does not exclude decomposition of carbide but relegates it to a secondary position as a cause of the occurrence of the uncombined carbon.

Either one of these assumed mechanisms is in accord with Dr. Kahles' results as he obtained uncombined carbon in the presence of energizers which like the moisture in the gas introduce oxygen into the system.

Author's Reply

F. V. Lenel in his discussion refers to the author's generalized conclusion that the two types of steel do not differ markedly in their transformation characteristics. The author was referring specifically to the isothermal austenite transformation characteristics; these were not established by Offermann, Buchholtz and Schulz. As Dr. Lenel has inferred in his second paragraph the word, markedly, covers a multitude of sins, because no data are available on the isothermal transformation of high purity iron-carbon alloys made by melting. These data on carburizing definitely require expansion: It was offered at this time for the purpose of gaining further the views and data of others who may have had similar experiences. The author's experience has shown that not all iron powder producers and consumers are sufficiently aware of oxide control in powders in spite of the Metal Powder Association Standard 2-45T. The author believes that the oxygen content in the specimens used is as low as in steels made by melting because the carbon reacts very rapidly with oxide present in the samples and has a good opportunity to reach an equilibrium condition. It is believed that the nitrogen content is also as low as in the original iron powder because no treatments were given that would introduce it. These are opinions and should be checked by oxygen and nitrogen analyses. It was substantiated by weight change, as indicated in the paper, that no measurable pick-up of nitrogen is experienced in the N_2 atmosphere used. The author doubts whether the work of T. G. Digges

establishes the fact that the most rapid rate of transformation is between 600 and 650 C (1110 and 1200 F). Mr. Digges selected as the critical cooling rate the average cooling rate between 600 and 500 C (1110 and 930 F). These were studies on continuous cooling in contrast to those conducted isothermally. The author believes that variations in density may account for variations in reduction rates of electrolytic and hydrogen-reduced iron powder compacts as suggested by Dr. Lenel. This view in the opinion of the author, however, requires experimental confirmation.

The author is sorry that he gave Mr. Stern the impression that no steel parts are made and that all iron powders reveal large quantities of oxide inclusions. Certainly this is not so, but the fact still remains that the point of oxygen control requires more attention by some. Further remarks of Mr. Stern are well taken when one considers commercial aspects of powder part production but this was not the primary intent of this presentation. It is wise, however, to call attention to this as Mr. Lenel and Mr. Stern both have done, lest there be confusion.

The interesting and valuable discussions of F. E. Harris and G. H. Boss pertain particularly to the questions of carburizing and show along with the author's data the need for further fundamental work on carburizing. At University of Cincinnati metallurgical laboratories further studies are being conducted in an effort to explain more precisely what happens during carburizing.

The author is sincerely grateful for the interest shown by the men who discussed this paper and appreciates the aid they have given toward planning of future work.

CARBON CONCENTRATION CONTROL

By E. G. de Coriolis, O. E. Cullen and Jack Huebler

Abstract

The phase rule is applied to all the possible gas compositions which might be used in gas carburizing, and from the results so obtained the most suitable compositions and variations thereof for commercial purposes are determined. The effects of these compositions on the steel are then developed using the conventional iron-carbon diagram as a basis. The necessary carbon potential, its effect upon steel of varying initial carbon content, its limitations as to range of action, and other interrelationships between the gas and metal are then brought out. Empirical information thus gives way to a straightforward method, flowing from theory to practice with definite and conclusive results.

CEMENTATION of steel is an old art carried out through the centuries by packing mild steel articles in solid carbonaceous material. These solids at operating temperatures gave off gases which became the vehicle for transferring carbon into the metal surface. Control of the process was largely by empirical means developed in the course of time by various practitioners of the art. The process is still in existence on a diminishing scale. Control of its operation still remains largely empirical.

Early in this century attempts were made to divorce the operation from the heretofore necessary packing material and to carry on the cementation wholly by means of carbonaceous gases. This method has met with a fair degree of success largely because of the apparatus used for the purpose. Reference, of course, is to the rotary gas carburizer which received acceptance because it incorporated a mechanical feature of distinct advantage. It was well known that in heating a carbonaceous gas within a retort packed with work there would result a heavy deposit of soot. By rotating the retort this soot was constantly scoured away from the surface of the work, thus exposing it to the cementing action of fresh gas. Since this was a

A paper presented before the Twenty-eighth Annual Convention of the Society held in Atlantic City, November 18 to 22, 1946. Of the authors, E. G. de Coriolis is director, O. E. Cullen is metallurgist and Jack Huebler is engineer, Research Department, Surface Combustion Corp., Toledo, Ohio. Manuscript received July 13, 1946.

batch operation, it was a comparatively easy matter to remove the soot each time the retort was discharged, thereby eliminating any large accumulation. This heavy soot deposit precluded adapting the process to continuous production.

When in the early thirties the first continuous gas carburizer was placed on the production line, the process was modified to incorporate an active vehicle gas as well as the carbonaceous gas. Recognizing that the deposit of soot would have to be removed by chemical instead of mechanical means, the vehicle gas was made slightly oxidizing to convert the deposited carbon to carbon monoxide which in turn would act as a carburizing gas. For the first time there was introduced the independent or extraneous generator which could produce a vehicle gas of known and constant composition. A measure of control was thus introduced into this operation which resulted in its adoption by a number of manufacturing plants. It was still, however, short of the goal in that a rather close balance existed between the condition wherein the vehicle gas was sufficiently oxidizing to the deposited soot and that where this gas encountering work surfaces already carburized would cause some decarburization. This necessitated operating on the sooty side which, although greatly minimizing soot deposition, would still leave an appreciable accumulation of soot within the furnace retort.

The next important step came with the adoption of the refractory-lined furnace heated by radiant tubes. The heavy rates of production required by industry made it uneconomical to continue the use of retort furnaces which had to be discarded in favor of the larger and more economical radiant tube furnaces. There then arose the problem of greatly reducing or completely eliminating the deposition of soot within the laboratory of the furnace. This necessity arose largely from the fact that heat resisting alloy parts when exposed at operating temperature to heavy deposits of soot underwent disintegration by what came to be known as "carbon corrosion". It was imperative to find some means or method of so controlling the process as to make possible operation without the deposition of soot.

It became evident that if this were to be accomplished a far better understanding of the reactions taking place would have to be acquired so that the necessary steps could be taken to mitigate this evil. The chemistry of gas carburizing was well known and had been publicized in numerous writings. Something, however, was lacking in its interpretation. As the study progressed, it became evident

that many factors heretofore completely ignored were actually of prime importance and that if close controls of these factors could be established the desired results might be expected. The groundwork was then laid for experimentation which confirmed the premises previously established theoretically. As a result it is now possible, not only in the laboratory but in the field, to accurately control carbon concentration. Furthermore, with the equipment now available it is possible to carry on these operations with practical absence of carbon deposition.

Application and Value of the Phase Rule

The large number of possible reactions in gas carburizing between many compounds, together with the changing conditions due to the various phase relations of iron and iron carbide, introduce a large number of variables. The controlling factors among these variables may be reduced to an understandable basis by the application of the classical phase rule. The phase rule is valuable because it can be used to show which of these variables need be considered and the general relationships which exist between them. An examination of gas carburizing from the phase rule standpoint will clearly demonstrate the controlling factors in the process.

The phase rule applies only when a chemical system has attained equilibrium and will be freely applied when this condition prevails. Homogeneous steel of a given carbon content throughout will be in equilibrium with a given combination of gases. Having established the equilibrium conditions it will be evident that a change in gas composition will serve to increase or decrease the carbon concentration of the steel. It might be well to observe that the term carburizing as used in this paper does not necessarily refer to the actual addition of carbon to a low carbon steel, but rather to the general relations between iron, iron carbide, and a carbon-bearing atmosphere which indicates a tendency or potential to carry out such an addition.

The Phase Rule

The phase rule is the application to certain chemical and physical problems of the rule of algebra that the number of independent equations in a set of simultaneous equations must be equal to the number of variables involved in order that the value of each variable shall

be fixed. However, when the number of equations is less than the number of variables, the values of some of the variables will not be fixed. An evaluation of the number of unfixed variables will greatly facilitate understanding of the complexities of gas carburizing as will appear later. The phase rule predicts that in an equilibrium system the number of such unfixed or independent variables is two greater than the number of components minus the number of phases. Three of the foregoing terms may require classification and definition.

1. A phase is any homogeneous portion of matter; such as a pure substance, a solution, or a gas. A phase is not necessarily contained in a single portion but may be dispersed throughout the system.

2. The number of components in a system under consideration is given by the difference between the number of substances composing the system and the number of independent chemical equations expressing their chemical interaction. A correct evaluation of the number of components for use in the phase rule is often difficult to make.

3. Since any attempt to give a simple definition of an independent variable would prove unsatisfactory, an example will be used to illustrate a three-variable system containing two independent variables. Suppose that A, B, and C are variables, which uniquely describe a system, and it is known that two of them are independent. Then, if A and B are chosen as the independent variables, C will be a dependent variable. Under these conditions either A or B may be varied at will, the values for A not affecting the values for B. The values for C, however, will depend upon the values picked for A and B. The choice of A and B as the independent variables is arbitrary.

Application to Gas Carburizing

Gas carburizing may be carried out using a simple mixture of CO and CO_2. However, this atmosphere is inconvenient to produce and control industrially and as a result the usual carburizing gas is far more complex, ordinarily containing CO, CO_2, H_2, H_2O, CH_4, and N_2. The analysis and understanding of the controlling factors of this process, therefore, involve the consideration of the equilibrium of a complex, multicomponent system. The many factors involved, therefore, make it difficult to obtain a clear mental picture of the con-

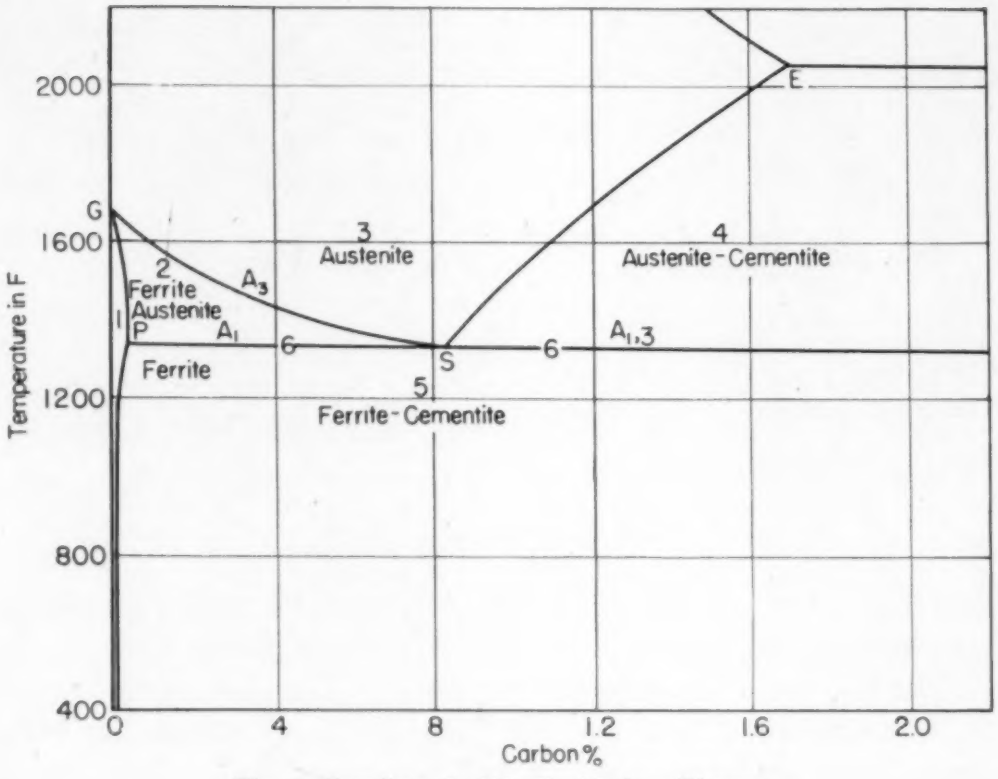


Fig. 1—Iron-Iron Carbide Equilibrium Diagram.

trolling chemical interactions without the guidance of the phase rule. To facilitate the understanding of the phase rule method of attack, application will first be made to the simple carburizing atmosphere consisting of CO and CO_2 alone, and then followed by application to the more complex system actually in use.

Reference to the iron-iron carbide diagram, Fig. 1, indicates that when gas carburizing is carried out *without carbon deposition* there is a total of four phases which must exist in definite combinations. (If carbon deposition occurs, a fifth phase is added and another set of conditions must be considered.) The four phases are:

1. The gas
2. Ferrite
3. Austenite
4. Cementite

Pearlite and ledeburite are mixtures of the phases listed above. The possible combinations of these phases are: (The numbers below correspond to the numbers shown on the iron-iron carbide diagram, Fig. 1.)

1. Gas and ferrite
2. Gas, ferrite, and austenite
3. Gas and austenite

4. Gas, austenite, and cementite
5. Gas, ferrite, and cementite
6. Gas, ferrite, austenite and cementite

All these combinations, it will be noted, are obtained in practice by changing the carbon content and the temperature of any given piece of steel.

The areas represented by numbers 1 and 3 are two-phase systems; areas 2, 4, and 5 are three-phase systems, and the line labeled 6 represents the conditions which constitute a four-phase system.

In all of the cases above there are only four chemical substances: Fe, Fe_3C, CO, and CO_2. These constituents will react chemically according to the equation,

$$1.\quad 3Fe + 2CO = Fe_3C + CO_2$$

Accordingly, to apply the phase rule, there will be three components since there are four compounds and one interconnecting equation.

The number of independent variables (V) as given by the phase rule is, therefore, two more than the number of components (3) minus the number of phases (P). Or,

$$V = 2 + 3 - P = 5 - P$$

When the number of phases is two, there are three independent variables (e.g., $V = 3$); when there are three phases $V = 2$, and when there are four phases there is only one possible independent variable.

The total number of variables or the factors necessary to uniquely describe the state of the system under consideration are:

1. The Fe_3C : Fe ratio in ferrite
2. The Fe_3C : Fe ratio in austenite
3. The CO : CO_2 ratio in the gas
4. The temperature of the system
5. The total pressure of the system

Attention is directed to the fact that only the ratios of the constituents appearing in a single phase are variables, although it might be supposed that the amount of each substance is a variable. This is evident because the total amount of any phase will not alter the equilibrium conditions and, therefore, the only information required to duplicate or describe a phase is the proportion of the constituents of which it is composed.

In addition, the Fe_3C: Fe ratios in ferrite and austenite are actually dependent upon one another. When ferrite and austenite exist simultaneously, reference to the iron-iron carbide diagram indicates that if the Fe_3C: Fe ratio for either phase is specified, the Fe_3C: Fe ratio in the remaining phase is automatically fixed. This is evident because both of the phases must exist at the same temperature and pressure, and the temperature and pressure alone determine these ratios. It follows, therefore, that there are only four variables required to describe the system uniquely in all cases.

Combining the foregoing conclusions with the number of independent variables as given above by the phase rule, the following results are obtained:

Number of Phases	Number of Independent Variables	Number of Dependent Variables
2	3	1
3	2	2
4	1	3

Before proceeding with the application of the above, one important fundamental should be emphasized. The total mass of each of the phases has no bearing upon the equilibrium state. Or, in other words, if a gas and a solid phase are in equilibrium, changing the number of volumes of gas or the pounds of solid will not alter the equilibrium state. Likewise, in certain areas (three and four-phase areas) of the iron-iron carbide diagram variations of the carbon concentration will serve only to vary the relative quantities of the phases present. Accordingly, there will be no change in the chemical composition of any phase, and consequently no change will result in the equilibrium state.

The Simple Carburizing Gas Applied to the Two-Phase Case

As previously stated there are two two-phase cases: the gas-ferrite and gas-austenite systems. The latter is of practical importance. In these two areas (1 and 3 in Fig. 1), three of the four variables have been shown to be independent leaving only one de-

pendent variable. It follows, therefore, that the temperature, pressure, and the Fe_3C: Fe ratio in austenite or in ferrite may be fixed, thus allowing the existence of one, and only one, CO: CO_2 ratio of the atmosphere at equilibrium. It should now also be clear that the temperature and pressure may be held constant and the Fe_3C: Fe ratio changed at will, each new value giving a new CO: CO_2 ratio. Furthermore, the total percentage of carbon in the steel in these cases will be determined by the Fe_3C: Fe ratio, thus making total carbon a function of the gas composition for a given temperature and pressure. In other words, there exists a one-to-one correspondence between the gas composition and the steel composition. That is, each gas composition will be in equilibrium with a distinct steel composition at a specified temperature and total gas pressure. Furthermore, variation of temperature or pressure will also vary the CO: CO_2 ratio required for equilibrium with a given steel composition.

As a practical example of the above principles, consider the case where steel is to be carburized to exactly 0.50% carbon at 1700 F (925 C) and one atmosphere pressure. It follows that there will be one CO: CO_2 mixture which will carburize the steel to the desired uniform composition of 0.50% carbon, regardless of the length of time the steel and gas are held in contact with one another, provided sufficient time at 1700 F (925 C) is allowed to attain equilibrium. This result is independent of the initial carbon content of the steel.

Such a process as this may be termed an equilibrium process to differentiate it from a time-rate process. A time-rate process would be dependent upon the initial steel composition, the carburizing potential or balance of the gas mixture, and the exact time interval of treatment as well as the temperature and pressure.

The phase rule, then, indicates that a given carbon concentration in the austenite phase or in the ferrite phase can be obtained through an equilibrium process by proper adjustment of the gas composition for a given temperature and pressure. The actual numerical relationships connecting the variables are not predicted by the phase rule but may be calculated from existing physical data.

The Simple Carburizing Gas Applied to the Three-Phase Cases

There are three three-phase cases to be considered, two of which are very similar. The similar cases are the gas-austenite-cementite

system (area 4 in Fig. 1) and the gas-ferrite-cementite system (area 5 in Fig. 1). In each of these systems it has been shown that there are two independent and two dependent variables. As a result, if the temperature and pressure are specified, the compositions of the gas and of the austenite or ferrite (in their respective areas) must have singular values. That is, there is only one possible $CO : CO_2$ ratio and only one possible $Fe_3C : Fe$ ratio in austenite or in ferrite at a given temperature and pressure. In these cases, then, there is a one-to-many correspondence between the gas composition and the overall steel composition. That is, one gas mixture may be in equilibrium with many steel compositions. This results from the fact that $Fe_3C : Fe$ ratio in austenite or ferrite in these ranges is not altered by the total carbon. Here carbon content merely determines the relative amounts of austenite and cementite, or ferrite and cementite. Since the equilibrium does not depend upon the amounts of the phases but only upon their composition, the $CO : CO_2$ ratio is independent of carbon concentration. In other words, at a given temperature and pressure the one $CO : CO_2$ ratio is in equilibrium with all carbon concentrations throughout these two ranges. It, therefore, follows that the equilibrium $CO : CO_2$ ratio will neither carburize nor decarburize the steel, whereas any other ratio will either carburize to pure cementite or decarburize to austenite or ferrite. The equilibrium gas compositions for these two ranges have been determined experimentally and are to be found in the literature pertaining to this subject.

The remaining three-phase case, which is the gas-ferrite-austenite equilibrium, has been more or less neglected. Here, as before, the phase rule predicts that if the temperature and pressure are specified, only one $CO : CO_2$ ratio may be used, and only one $Fe_3C : Fe$ ratio exists in ferrite and one in austenite. In this case, a variation of total carbon serves only to change the proportions between ferrite and austenite and does not, therefore, influence the $CO : CO_2$ ratio. Therefore, for this case also there is only one equilibrium gas composition for each temperature and pressure.

Usually it is assumed that the equilibrium constants which apply for the gas-austenite-cementite range also apply to the gas-austenite-ferrite range at equal temperatures. However, if this is true, a discontinuity must necessarily exist between the three-phase ranges and the intermediate two-phase gas-austenite range. Such a discontinuity is not probable. The equilibrium constants which apply in these two ranges are different as will be demonstrated.

The Simple Carburizing Gas Applied to the Four-Phase Case

The line A_1-$A_{1,3}$ is of interest because it represents four co-existent phases; however, it is not of practical importance. As demonstrated above, this four-phase system requires the existence of one independent variable and three dependent variables. Since pressure practically becomes the independent variable, the temperature must become invariant. Therefore, the A_1-$A_{1,3}$ line is a horizontal, or constant temperature line, along which there can be only a single $CO:CO_2$ ratio, a single Fe_3C: Fe ratio for austenite and a single Fe_3C: Fe ratio for ferrite, all of these ratios being independent of total carbon.

The More Complex Gas System

As generally used, the gas for carburizing contains CH_4, H_2, H_2O, and N_2 as well as CO_2 and CO. The addition of these four gases to the equilibrium systems considered above will increase the number of constituents by four. The addition will also introduce many new possible chemical reactions. However, it can be shown that only two new *independent* reactions are introduced, making three reactions in all. Any three independent reactions may be chosen from the many possible ones for the purpose of this analysis. The following three fulfill the requirements:

1. $3Fe + 2CO = Fe_3C + CO_2$
2. $Fe_3C + 2H_2 = 3Fe + CH_4$
3. $3Fe + CO + H_2 = Fe_3C + H_2O$

From the previous discussions it is evident that although four constituents have been added, no new phases have been introduced, but two additional chemical equations appear. Therefore, the number of independent variables will be increased by two in each of the areas previously discussed with the simple carburizing gas. Since there are more than two gases present, the percentage composition of each of the gases will be used as the variables describing the gas phase of the system. Obviously, therefore, there are four more variables required to describe this complex system than were required in the simple system previously discussed. The percentages of H_2, H_2O, CH_4, CO, and CO_2, five in all, will now describe the gas phase whereas the $CO:CO_2$ ratio was sufficient in the simple case. The

percentage of the sixth gas N_2, which is an inert diluent, is determined by the other percentages and is, therefore, not a variable. Accordingly, the relationships which hold for the complex gas system are:

Number of Phases	Number of Independent Variables	Number of Dependent Variables
2	5	3
3	4	4
4	3	5

Remembering that neither the number of phases nor the phase areas previously discussed have been altered by changing from a simple gas to a complex gas, the various areas will again be discussed under the new conditions.

The Complex Gas Applied to the Two-Phase Cases

In the two-phase cases there are five independent variables and three dependent variables. Temperature, pressure, H_2%, CO%, and the Fe_3C: Fe ratio in austenite or ferrite will be chosen as the independent variables. Therefore, the values of the dependent variables (CO_2%, CH_4%, and H_2O%) will be fixed as soon as the values of the independent variables have been assigned.

Because of the large number of variables involved in this system, it is convenient and practical to simplify the system by thinking in terms of a "basic atmosphere", that is, an atmosphere which always contains constant percentages of CO and H_2. The basic atmosphere, since it specifies the CO and H_2 content, actually fixes the value of two of the independent variables. Therefore, for a given basic atmosphere at a given temperature and pressure, there will be a one-to-one correspondence between the values of the dependent variables (CO_2%, CH_4%, and H_2O%) and the steel composition. Furthermore, since each value of H_2O% (or the dew point of the gas) may represent the value of the other dependent variables (CO_2% and CH_4%) at equilibrium, it follows that for a given basic atmosphere there will be only one steel composition in equilibrium with a basic atmosphere having a given dew point.

While the artifice of a basic atmosphere is introduced here for the sake of simplicity, it is nevertheless a very practical concept as will later become apparent. On the basis of adopting a basic atmosphere containing constant percentages of CO and H_2, it follows that

any carbon concentration in the two-phase ranges may be attained by an equilibrium process by proper adjustment of the dew point of the gas mixture. It is evident, of course, that the increased number of gaseous constituents makes the determination of the dew point values required more complex, but the results are easy to apply.

The Complex Gas Applied to the Three-Phase Cases

In the three-phase cases there are four independent and four dependent variables. Before these cases are analyzed, a point previously made should be emphasized; that is, only the temperature and pressure determine the Fe_3C: Fe ratios in the three-phase systems. Accordingly, if the temperature and pressure are chosen as independent variables, the Fe_3C: Fe ratio for the austenite or ferrite must be a dependent variable even though the phase rule allows the choice of two additional independent variables. This restriction upon the choice of the independent variables is a result of the peculiarity of the system. As another example of the latter type of restriction it is obvious that equation 1, above, allows the choice of either the CO% or the CO_2% as an independent variable but not both of them. The general results of the phase rule, however, are unaffected by such restrictions, since the phase rule only restricts the *number* of independent variables which exist.

In accordance with the above, the independent variables chosen are temperature, pressure, CO%, and H_2%. The Fe_3C: Fe ratio, CO_2%, CH_4%, and H_2O%, therefore, become dependent variables. From this it follows, as before, that if a basic atmosphere containing constant percentages of CO and H_2 is assumed there is a one-to-many correspondence between the gas composition and the steel composition. A given gas mixture will be in equilibrium with a steel of any carbon content in these ranges at a given temperature and pressure. In addition, if a particular gas mixture is not in equilibrium with the steel, it will either carburize to pure cementite, or decarburize to ferrite or austenite.

The Complex Gas Applied to the Four-Phase Case

In the four-phase case there are three independent variables and five dependent variables. Again, a restriction occurs in the choice of independent variables. The temperature at which the four phases may co-exist is determined by the pressure. Therefore, the independ-

ent variables are chosen as pressure, CO% and H_2%, leaving the temperature, Fe_3C: Fe ratio, CO_2%, CH_4%, and H_2O% as dependent variables. Assuming a basic atmosphere all the results of the foregoing case apply with the additional temperature restriction.

Summarizing, it has been shown that in the austenite and in the ferrite ranges any desired carbon concentration may be obtained by heating the steel in an appropriate atmosphere for sufficient time. In these ranges there is a one-to-one correspondence between the gas composition and the steel composition. The control of carbon concentration is possible in these areas, and the control may be obtained by an equilibrium process.

In the three and four-phase areas a gas mixture may be in equilibrium with the steel, but the gas composition is independent of the carbon concentration of the steel. Here there is a one-to-many correspondence between the gas composition and the steel composition. If the gas composition is not such that equilibrium will occur, the steel will either be carburized to pure cementite or decarburized into a two-phase area. It follows, then, that a change from one concentration to another in these ranges can only be carried out by a non-equilibrium gas mixture utilizing a time-rate process, that is, by carburizing or decarburizing at a definite rate for a definite time interval, and then allowing diffusion to occur under equilibrium conditions or nonreactive conditions for a predetermined length of time. This method may also be applied in the two-phase areas, but with rather obvious loss of process control and introduction of numerous difficulties. In this connection it may also be remarked that the rate at which carburization or decarburization will occur is a direct function of the departure of the gas composition from the equilibrium gas composition.

The foregoing part of this paper has established the possibility of accurate control of carbon concentration in austenite. The remainder will deal with the actual method of carrying out this control.

Carbon Concentration Control in Austenite

The general theory of carbon control in austenite has been known for some time but has not been put into a practical working form. It is the purpose of this section to review the theory briefly and to expand it by giving the exact details of the elements comprising such control.

For this purpose the gas will again be considered to be composed of CO, CO_2, CH_4, H_2, H_2O, and N_2. As demonstrated in the previous section, the two-phase gas-austenite system is chemically described in the state of equilibrium by the following reactions:

1. $3Fe + 2CO = Fe_3C + CO_2$
2. $Fe_3C + 2H_2 = 3Fe + CH_4$
3. $3Fe + CO + H_2 = Fe_3C + H_2O$

Of the eight variables, five have been demonstrated to be independent and three dependent. The five independent variables will be chosen as temperature, pressure, $Fe_3C\%$ in austenite, CO%, and $H_2\%$. Any five appropriate variables describing the system could be arbitrarily chosen; however, these have been chosen with some forethought. The $H_2\%$ and CO% were selected in accordance with the conception of a basic atmosphere and because they will ordinarily be present in comparatively large amounts. Therefore, values may be assigned to them which will suffer only minor variations from day to day as the atmosphere is used. The pressure, temperature and $Fe_3C\%$ have been selected because they affect all of the primary reactions directly, whereas the $CO_2\%$, $H_2O\%$ and $CH_4\%$ each affect but one. Finally, it is much easier to assign possible practical values to the selected independent variables to arrive at a practical and possible solution.

It is evident that to establish values for the three dependent variables it will be necessary to establish three relationships between them and the independent variables. The necessary relationships are the equilibrium constants of the above reactions.

The Equilibrium Constant

The presentation of the numerical details of carbon control in austenite is preceded by sufficient review of the theory to illustrate and explain the methods used in reaching the end results. Fortunately there are two possible modes of procedure. One is the technical derivation which involves the highly technical concepts of free energies, activities, and related subject matter. This method, while technically most desirable, involves too many abstractions familiar only to those who deal with physical chemistry. The development consequently will be presented on the basis of a more intuitive argument in language more familiar to all. Attention is directed to the

fact that the method of presentation is not intended to argue any mechanism of carburization, but is only intended to provide a basis for understanding the conditions which must exist when equilibrium is attained.

It is a familiar fact that when two gases A and B react according to the equation,

$$4.\ A + B = C + D$$

to form the gases C and D, the reaction will stop when the reactants reach definite proportions. At this time all of the gases will still exist and will have attained partial pressure values (P) such that the expression

$$(a)\ \frac{P_C \times P_D}{P_A \times P_B}$$

becomes a constant K. This constant K is the well known equilibrium constant and has a definite value for a given reaction at each temperature.

When the chemical reaction is a heterogeneous one (that is, when the reactants are not all in the same physical state) a simplification may usually be made. For example, if substances A and C in the reaction above are solids rather than gases, while B and D are gases, it is then often valid to omit P_A and P_C from the equilibrium expression, obtaining the equation:

$$(b)\ K' = \frac{P_D}{P_B}$$

In fact, the expression is so commonly written in this form that the reason P_A and P_C may be omitted has become obscure. P_A and P_C may usually be omitted because the partial pressure of a solid is constant at a given temperature when the solid is pure or of unchanging composition. In other words, when A and C are pure solids their partial pressures remain constant during a reaction even though the relative amounts of the two may change. This allows P_A and P_C to be included in the equilibrium constant K, giving the effective constant K′ above.

Ordinarily the partial pressures of the solids are immeasurably small, thus making the determination of the true equilibrium constant virtually impossible. However, the effective equilibrium constant

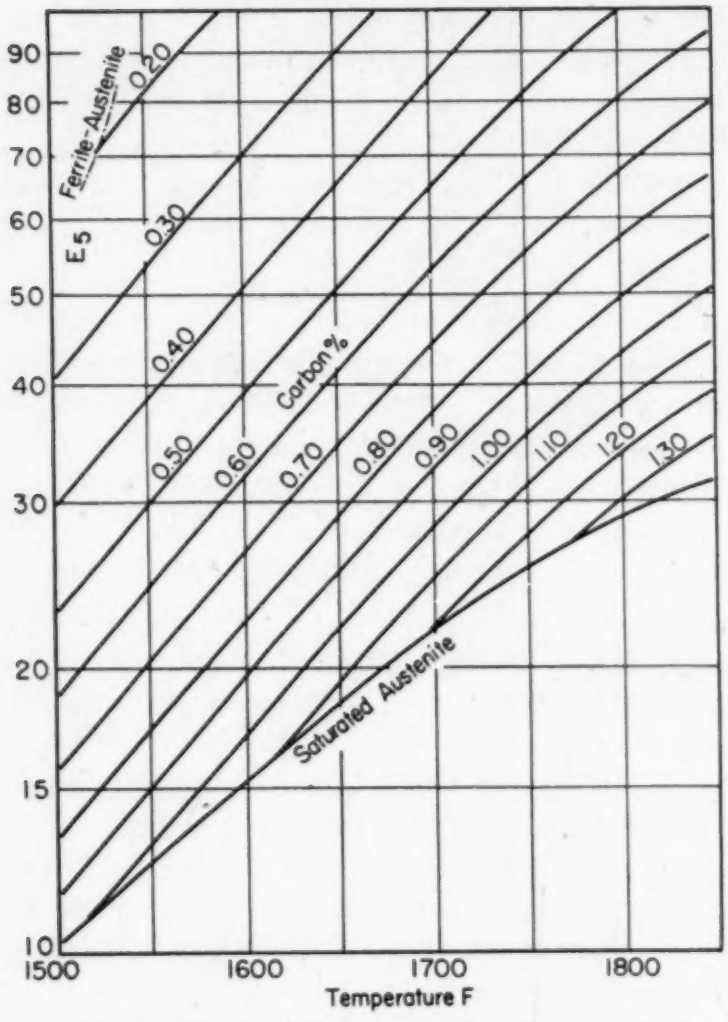


Fig. 2—The Equivalent Equilibrium Constant E_5 for the Reaction $3Fe + CH_4 = Fe_3C + 2H_2$.

is easily determined by measuring the partial pressures of the gases when the equilibrium state has been attained.

All of the above has been devoted to the conditions when the partial pressures of the solids are constants. However, in the two-phase carburizing system under consideration this is not the case. It is well known that when one liquid is dissolved in another, each liquid has a vapor pressure which is a fraction of what it would be if each liquid were in a pure state. This rule holds equally true for solid solutions, and in the cases in question Fe_3C is in solid solution in the iron to form austenite. Therefore, the partial pressures of the solid constituents are *not* constant and must, therefore, be included in the expression for the equilibrium constant.

Furthermore, no great error is ordinarily introduced by assum-

ing that the partial vapor pressure of each constituent is directly proportional to the molar concentration of that constituent in the solution. This idealizing assumption is based on the consideration that the rate of escape of molecules of one of the constituents from the surface of the solution should be proportional to the number of such molecules present at that surface. Since the rate of escape of molecules from the solution determines the vapor pressure, it follows that the partial vapor pressure of each constituent is proportional to its mol fraction. Saying the same thing in an equation gives

$$(c)\quad P_A = \frac{N_A}{N_0} \times P_A^\circ$$

where P_A is the vapor pressure of A over a solution,
P_A° is the vapor pressure of A as a separate phase,
N_A is the number of molecules of A in solution,
N_0 is the total number of molecules in the solution,

This equation relates to a solution in which A is infinitely soluble. It is, therefore, not the desired form, because Fe_3C is only partially soluble in iron. It is apparent, however, that if the mol fraction of the substance A is increased until the solubility limit is reached, any further increase in the amount of substance A will result only in the precipitation of A in the free state. Thus, the partial pressure of substance A will increase uniformly until it reaches the free state value at the limit of solubility. This means that P_A° is realized when N_A reaches the saturation concentration N_A'. Thus, equation (c) must be revised to (d)

$$(d)\quad P_A = \frac{\left(\frac{N_A}{N_0}\right)}{\left(\frac{N_A'}{N_0}\right)} \times P_A^\circ$$

for a solution in which a limited solubility exists. This equation states that the vapor pressure of a constituent in solution is equal to the vapor pressure of that constituent in the free phase, multiplied by the ratio of the mol per cent in solution to the mol per cent possible in solution.

Therefore, in the case of the iron-iron carbide system under consideration, the vapor pressure of Fe_3C is not constant but varies according to the equation (d) when its concentration varies below the solubility limit. The vapor pressure of the iron also varies with its concentration in accordance with the same equation.

The above theory demonstrates that the partial pressures of

Fe_3C and Fe must vary with carbon concentration in the austenite range. Since these partial pressures appear in the equilibrium expression along with the partial pressures of the gaseous constituents, it follows that variations of carbon concentration will also cause changes in the gas composition required to attain the equilibrium state. *Therefore, the gas composition is a function of the steel composition,* a result which was previously predicted by the phase rule. The equation (d) just derived may now be used to calculate the numerical relationships between carbon concentration and the gas composition required at equilibrium.

As an example of such a calculation, equation 2 will be rewritten to

$$5.\quad 3Fe + CH_4 = Fe_3C + 2H_2$$

and the calculation carried through for that reaction.

The equilibrium constant for reaction 5 is given by the expression:

$$(e)\quad K_5 = \frac{P_{Fe_3C} \times P_{H_2}^{\,2}}{P_{Fe}^{3} \times P_{CH_4}}$$

or with arrangement

$$(f)\quad \frac{P_{Fe}^{3}}{P_{Fe_3C}} \times K_5 = \frac{P_{H_2}^{\,2}}{P_{CH_4}}$$

Taking N_A to represent the value of the mol fraction of Fe_3C, and N_A' as representing the mol fraction of Fe_3C at saturation, then the corresponding mol fractions of Fe will be $(1\text{-}N_A)$ and $(1\text{-}N_A')$. Introducing equation (d) into equation (e) with this notation, equation (g) follows:

$$(g)\quad \frac{(1\text{-}N_A)^3 N_A'}{(1\text{-}N_A')^3 N_A} \times \frac{(P_{Fe}^{\circ})^3}{P^{\circ}_{Fe_3C}} \times K_5 = \frac{P_{H_2}^{\,2}}{P_{CH_4}}$$

The expression

$$(h)\quad \frac{P_{Fe}^{\circ\,3}}{P_{Fe_3^{\circ}C}} \times K_5$$

will be recognized, however, as the effective equilibrium constant K'_5, as obtained by experiment under conditions of saturated austenite by measuring the partial pressure of the gases at equilibrium.

Introducing the effective equilibrium constant K'_5, the expression becomes:

$$\text{(i)}\quad \frac{(1-N_A)^3 N'_A}{(1-N'_A)^3 N_A} \times K'_5 = \frac{P_{H_2}^2}{P_{CH_4}} = E_5$$

where E_5 may be called the equivalent equilibrium constant. If reactions 1 and 3 are rewritten as

6. $Fe_3C + CO_2 = 3Fe + 2CO$
7. $Fe_3C + H_2O = 3Fe + CO + H_2$

similar expressions are obtained and are as follows:

$$\text{(j)}\quad \frac{(1-N'_A)^3 N_A}{(1-N_A)^3 N'_A} \times K'_6 = \frac{P_{CO}^2}{P_{CO_2}} = E_6$$

$$\text{(k)}\quad \frac{(1-N'_A)^3 N_A}{(1-N_A)^3 N'_A} \times K'_7 = \frac{P_{H_2} \times P_{CO}}{P_{H_2O}} = E_7$$

It is now evident that the equivalent equilibrium constants E may be calculated from published data on gas equilibrium. The effective constants K′ as mentioned before are given as a function of temperature by many experimenters or may be calculated from basic physical data. The mol fraction of Fe_3C in saturated austenite (N'_A) may be calculated readily from the iron-iron carbide equilibrium diagram for any desired temperature. The various mol fractions of Fe_3C in austenite (N_A) may be calculated by assuming any desired carbon concentration. These calculations have been made for the three reactions and the equivalent equilibrium constants have been plotted in Figs. 2, 3, and 4.

It is now evident that if a basic atmosphere is assumed the proportions of the remaining constituents of that atmosphere which must exist at equilibrium may be computed quite accurately for any desired carbon concentration, temperature, and pressure. Although there are a great number of atmospheres which might be used to carry out this process, an atmosphere containing 40% H_2 and 20% CO will be chosen. This particular atmosphere has the advantage, as can be shown, of placing the major control factor, the dew point, into its most easily measured and controlled range.

Inserting these percentages of CO and H_2 into the equivalent

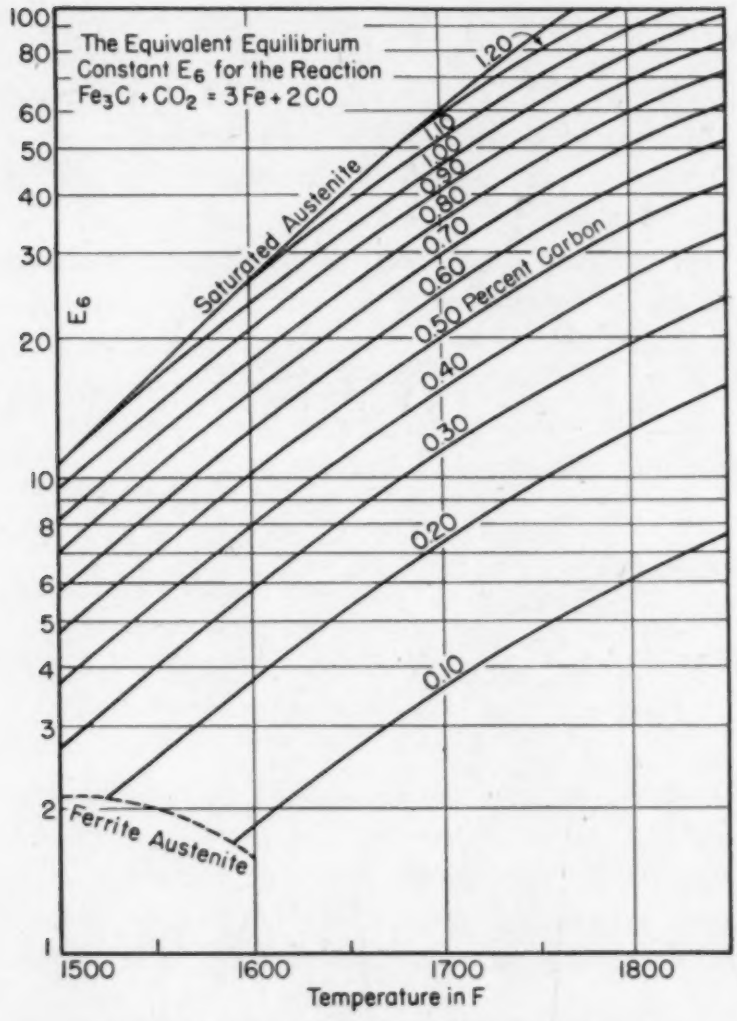


Fig. 3—The Equivalent Equilibrium Constant E_6 for the Reaction $Fe_3C + CO_2 = 3Fe + 2CO$.

equilibrium constant equations and assuming the total pressure to be one atmosphere, the following expressions are derived:

$$\text{(l)} \quad \% \ CH_4 = \frac{16}{E_5}$$

$$\text{(m)} \quad \% \ CO_2 = \frac{4}{E_6}$$

$$\text{(n)} \quad \% \ H_2O = \frac{8}{E_7}$$

$$\text{and} \quad \% \ N_2 = \text{Balance of atmosphere}$$

Using these formulas together with the desired value of E from Figs. 2, 3, and 4, the percentages of CH_4, CO_2, and H_2O (or dew point) may be calculated. The employment of an atmosphere con-

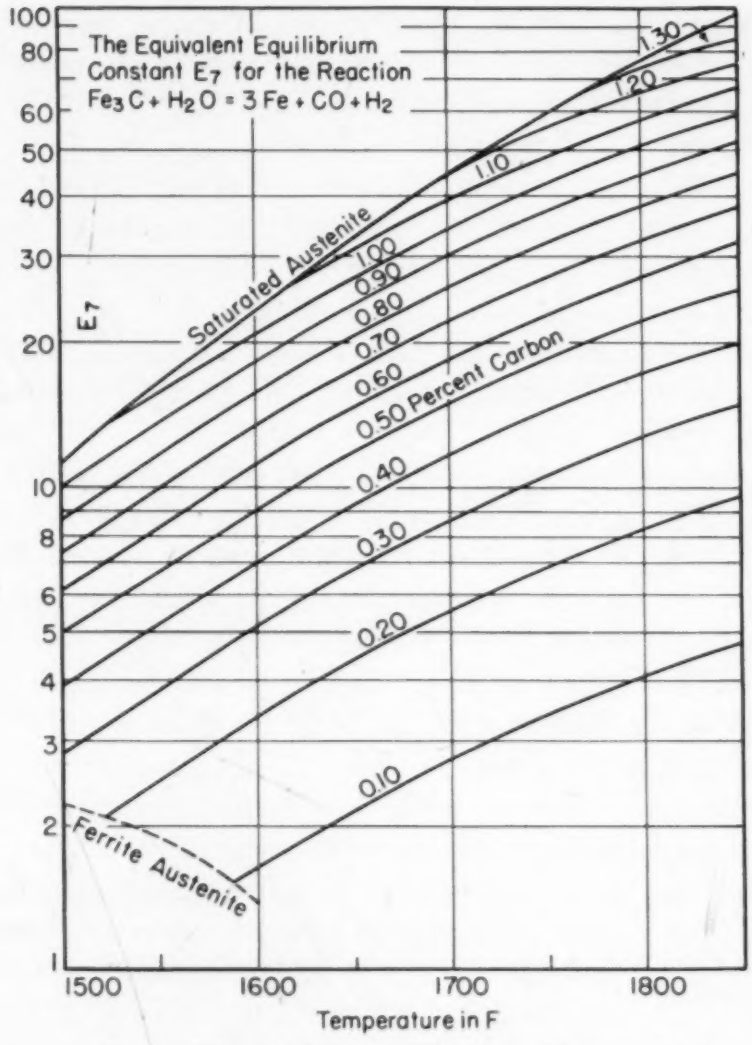


Fig. 4—The Equivalent Equilibrium Constant E_7 for the Reaction $Fe_3C + H_2O = 3Fe + CO + H_2$.

taining the percentages of gases as calculated from these formulas will give any desired carbon concentration in the austenite range.

The Austenite-Ferrite Equilibrium Constants

It was indicated above that the same equilibrium constants which hold for the austenite-cementite area are often falsely assumed to hold also for the ferrite-austenite area. It has now been shown that the equivalent equilibrium constants in the austenite area vary in a continuous manner with the carbon concentration and have either a uniformly increasing or decreasing trend. In addition, it was demonstrated that the constant which holds for the austenite-cementite range holds at the austenite and austenite-cementite boundary. One

of two conclusions must follow from this fact. First, the constant which applies to the austenite-ferrite area may be the same constant which applies to the austenite-cementite area (at the same temperature, of course), in which event there must be a sharp discontinuity in the equilibrium constant values at the austenite and austenite-ferrite boundary. Second, the constant which applies to the austenite-ferrite area may be the constant which applies to the austenite area at the austenite and austenite-ferrite boundary, in which case the equilibrium constants for the two three-phase areas would differ except at the lower critical temperature. The second conclusion is the only possibility.

As an example, consider a group of steel samples all of different carbon contents which range from zero to 1.60% and all heated to 1500 F (815 C). It will now be necessary to find the equivalent equilibrium constant for reaction 7 which applies to each different piece of steel at 1500 F (815 C). Referring to Figs. 1 and 4 it may be seen that any of the steels in the three-phase austenite-cementite area require an equivalent constant of 11.2. This includes all steels which contain 0.98% carbon or over. The invariant value of the equilibrium constant is in accordance with the principle that for the three-phase areas the equilibrium is independent of carbon concentration. Each of the steels which have carbon concentrations between 0.24% and 0.98%, thus placing them in the two-phase austenite area, will require single-valued equivalent constants. For example, the 0.80% carbon steel will require an equivalent constant of 8.7; 0.60% carbon will require 6.2, and 0.40% carbon will require 3.9. In the same manner, the steel which contains 0.24% carbon, thus placing it at the austenite and austenite-ferrite boundary, will require the still lower equivalent equilibrium constant 2.2 For continuity, then, each of the steels which have carbon contents between 0.03% and 0.24%, thus placing them in the three-phase austenite-ferrite area, must require an equivalent equilibrium constant of 2.2 and not the 11.2 value which holds for the austenite-cementite area. Any steels which have carbon concentrations of less than 0.03% will require values of the equilibrium constant which are lower than 2.2. The steel containing zero carbon (pure iron) will require a constant of zero, which is equivalent to restricting the atmosphere to zero CO and CH_4.

In closing, a word should be said about the choice of equilibrium data used. The iron-iron carbide diagram is adopted from "Alloys

of Iron and Carbon", Vol. 1, by Samuel Epstein. The equilibrium constants are not precisely those of any one author as far as it is known but represent, rather, average values which experience has dictated. Considerable attention was paid to free energy values for the constants for reactions 6 and 7, but the values for reaction 5 which involves CH_4 clearly represent practical working values, rather than true equilibrium.

Conclusion

The basic phenomena involved in the process of carbon control in gas carburizing have been covered in detail. First the factors affecting this control, then the effects of these factors in determining the equilibrium between gas and steel, and finally the effects of changes in both have been analyzed and explained. Despite numerous complexities in gas compositions and in steel analyses, it has been shown that when these are known and properly controlled any desired carbon balance can be obtained. That the gas composition is a function of the steel composition has been demonstrated conclusively.

DISCUSSION

Written Discussion: By F. E. Harris, furnace engineer, Buick Motor Division, General Motors Corp., Flint, Mich.

The authors are to be complimented on this paper concerning the equilibrium between gaseous mixtures and steel compositions. It is hoped that a supplementary paper may be written, correlating this data with commercial processes.

The treatment of the three-phase systems may be simplified if the factors affecting the diffusion of carbon in steel are considered simultaneously with gas-metal equilibria. A discussion concerning the gas-austenite-cementite system is given for Dr. Kahles' paper on sintered iron-carbon alloys.

The expression "Fe-Fe_3C ratio" becomes rather confusing when considering carbon gradients in steel. The concept of Fe_3C as the solute in ferrite and austenite may satisfy gas-solid equilibria. However, when studying the diffusion mechanism in the solid state, it seems necessary to accept carbon, not iron carbide, as the solute.

The supply factors for gaseous media are quite dependent upon the rate at which carbon may flow inward from the steel surface at a given time. For this reason, it is desirable to correlate equilibria in steel, and the mechanism of carbon flow in steel, with the gas-solid reactions.

Written Discussion: By T. A. Frischman, chief metallurgist, Eaton Manufacturing Company, Axle Division, Cleveland.

The authors are to be congratulated for undertaking the task of further

exploring gas carburizing reactions which continue to be of interest to those of us carrying on carburizing and controlled atmosphere heat treating operations. The application of the phase rule by the authors to obtain a more complete understanding of the controlling factors among the many variables encountered in gas carburizing reactions is indeed a unique approach to the subject.

My discussion will not embrace the physical chemistry nor the mathematical aspects of the paper as this can best be done by those more familiar with those branches of gas studies, but rather to express some thoughts more concerned with the practical application of these findings. A good many of us remember, in former years, when the purchase of a controlled atmosphere furnace was under consideration, it was often necessary to send samples of the steels to be treated to the furnace builder's laboratory. Here an extended series of tests with different gas atmospheres was made to learn the most suitable to use. With these new findings, furnace equipment can immediately be selected so that when the furnace is later built and ready to start, only slight adjustments in the composition of the atmosphere gas need be made.

The authors state that the gas composition is a function of the steel composition. They appear to refer to the steel composition from a carbon content standpoint only, and if this is the correct interpretation, I would like to ask how they explain the retarding carburizing effect of nickel and the accelerating effect of chromium and vanadium, or, whether these or other elements are to be reckoned with to any extent when applying the phase rule to gas carburizing reactions. It is known that when A-2515 steel and A-6120 steel are carburized simultaneously under identical conditions to the same case depth in the range of 0.055 to 0.065, the carbon concentration of the first 0.002 of case from the surface can approach a value of almost double for the A-6120 steel.

Written Discussion: By N. C. Fick, Battelle Memorial Institute, Columbus, Ohio.

This paper has been very interesting and thought-provoking. The authors mention, but fail to emphasize, the fact that the phase rule applies only when a chemical system has come to equilibrium. The element of time is a factor of great concern to the person who wishes to put carbon in through the surface of a piece of steel. Diffusion rates are slow. A true state of equilibrium can exist only when sufficient diffusion has taken place to give the piece a uniform carbon content throughout and this carbon content is balanced with the atmosphere in the furnace. This condition very rarely exists in the normal commercial carburizing cycle. I would like the authors to elaborate on the statement that the rate at which carburization or decarburization will occur is a direct function of the departure of the gas composition from the equilibrium gas composition. What are the limitations?

Written Discussion: By Lee O. Case, University of Michigan, Department of Chemistry, Ann Arbor, Mich.

This interesting paper illustrates nicely the way in which the long-familiar phase rule condenses in rather brief compass a considerable amount of information concerning equilibrium gathered from diverse sources, both theoretical and practical. While I may thereby add little to the practical

ends served by the authors' clear presentation, I might offer the following comments in connection mainly with the phase rule interpretation:

(a) As briefly mentioned by the authors some of the interesting properties of the systems considered result from what might be described as a degeneracy, in that some of the components are missing from some of the phases. In the case of the "simple" carburizing gas, the three-component system iron, carbon, oxygen is involved, of which the gas phase contains only the latter two, the solid phases, reasonably neglecting the small gas solubility, only the first two. The complex case concerns a system of five components of which the gas phase contains four only, the solid phases as before containing only iron and carbon. There is a consequent limitation in the choice of independent variables.

(b) To demonstrate the point just mentioned—that the complex mixture contains only four components—it may be well to point out that the establishment of the three equilibria listed on page 668 (clearly designated by the authors as the only *independent* ones) also imply, by elimination of Fe and Fe_3C among the equations, the existence of the equilibria:

$$CO + H_2O = CO_2 + H_2$$
$$CO + 3H_2 = CH_4 + H_2O$$

Thus since the six constituents of the gas phase are connected by two equations, four components are sufficient for its description. As the four components there might be chosen: C, O_2, H_2, N_2, or, say, CO, H_2, H_2O and N_2. This means that in making up such a mixture the results of analysis need be stated in terms of only three of these four, not five of the original six. For example, a mixture of 10 mols CH_4, 40 CO, 20 H_2, 15 H_2O, 10 CO_2, 5 N_2 will be duplicated in its behavior as to the final equilibrium state by a mixture of 50% CO, 33.3% H_2, 12.5% H_2O and (by difference) 4.2% N_2.

(c) In connection with the discussion of the Equilibrium Constant, page 672, it seems unnecessary to assume either Raoult's Law (Equation c), or the empirical solubility law (Equation d). For such a reaction as:

$3Fe$(s.s., mol fr. $1 - N_A$) + CH_4 (g) = Fe_3C(s.s., mol fr. N_A) + $2H_2$,

one may immediately write the very useful, hybrid equilibrium constant:

$$K = \frac{P_{H_2}^2}{P_{CH_4}} \times \frac{N_A}{(1 - N_A)^3},$$

with apologies only for the substitution of partial pressures for fugacities and of mol fraction concentrations for activities.

Written Discussion: By J. J. Turin, professor of physics, University of Toledo, Toledo, Ohio.

This important and exhaustive paper presents a careful and highly commendable analysis of a difficult problem. It presents in an understandable way a complete correlation of the fundamental carburizing reactions and what may be expected from them both theoretically and practically regardless of the range of steel composition.

Although the language of the paper is highly technical, the import which it carries is practical and simple. The simple facts bear emphasis and should be closely scrutinized by all practical metallurgists:

First, surface carbon concentration control in the *austenitic* range can be

accomplished by adjusting the composition of the atmosphere surrounding the steel, and the surface carbon content maintained regardless of the time. (This is a rigorously demonstrable fact providing the carbon gradient inward is not too extreme.)

Second, the carbon content may be accurately predicted and maintained by simply controlling the dew point. This is a startling result and can be counted upon eventually to eliminate operating difficulties for many metallurgists and practical heat treating men. The result itself comes about fundamentally from a detailed consideration of the equilibrium constant as a function of the composition of the solids in contact with the gas mixture, a fact usually neglected as unimportant by many working in the field.

Third, carbon concentration control (by gas equilibrium as distinguished from time-rate processes) can only be possible for steels in the austenitic range, *and no others* (practically the ferritic range is unimportant). This is conclusively demonstrated by considering the relationship of all possible variables according to phase rule analysis.

The authors are to be congratulated for an important contribution to the metallurgical field.

Authors' Reply

The fine discussions which have been offered are most gratifying since they indicate a widespread and stimulating interest in the theory of gas carburizing. These discussions also serve to show where additional work of this type could profitably be directed.

Mr. Harris' comments point out that a correlation of the gas-metal equilibria with carbon supply factors and diffusion rates would be of value in simplifying the three-phase cases. We must reassert in this connection that the findings outlined in the paper are rigorous only for the state of equilibrium. The problems he considers deal with nonequilibrium conditions. As was pointed out, in the three-phase cases an atmosphere is either fully carburizing, decarburizing, or in equilibrium independently of the carbon concentration. Therefore, if the atmosphere is made to be of nonequilibrium composition in the carburizing direction, carburization will occur regardless of the amount by which the gas composition differs from the equilibrium condition. This is an important generalization to be drawn from the paper. How highly carburizing the atmosphere should be made as a practical matter depends upon, as Mr. Harris intimates, supply factors, diffusion rates, the type and quality of the furnace. In general, the atmosphere should be held as near equilibrium composition as is consistent with the safety of the work load so as to hold sooting to a minimum. We might also point out that active carburization can be accomplished totally within the austenite range. That is, if a 0.20% carbon steel is surrounded by an atmosphere in equilibrium with 1.00% carbon, the steel will be carburized and the skin carbon will approximate 1.00% carbon after a reasonable carburizing time. One thing the operator may be certain of is that the skin carbon will never be greater than 1.00% carbon.

Mr. Harris' objection to the use of Fe_3C in solution rather than carbon is understandable from a theoretical standpoint. We are not certain of the quantitative division of carbon into Fe_3C and C in the solution. We are sure,

however, that there is some such division, thus making the use of either concept inaccurate. Fortunately, calculations prove that it makes very little difference in the equilibrium curves.

Mr. Frischman points out a nonequilibrium situation which is also beyond the scope of this paper. The effects of chromium and nickel on active carburizing may be summed up as follows:

Chromium, unlike iron, forms a stable carbide and thereby causes high carbon concentrations to result in the surface layers. Nickel lowers the solubility of carbon in iron and does not form a stable carbide. Consequently, nickel tends to lower the surface carbon concentration. While the results of this paper are intended to hold only for a steel consisting of iron and carbon, it may be said that the addition of each extra alloying element will increase the number of components by one while also increasing the number of independent chemical relationships by one. Thus, the general relationships derived in the paper will be unchanged. However, these alloying elements alter the physical data to some extent, thereby changing the numerical relationships of the curves. It is found in the laboratory, however, that no significant changes in the data need be made for mildly alloyed steels.

Mr. Fick emphasizes that this paper deals only with the condition of equilibrium, and he points out that the equilibrium state is rarely encountered in normal carburizing practice. This was very true until the past year or two. Recently, however, there has been a rapidly increasing demand for equilibrium carburizing, particularly in connection with recarburizing or "skin recovery". Other examples are the attainment of a definite surface carbon concentration during ordinary carburizing and the prevention of carburizing or decarburizing during a heating operation.

An elaboration of the statement, "The rate at which carburization or decarburization will occur is a direct function of the departure of the gas composition from the equilibrium composition", could well be the subject of a separate article. The only meaning given to this statement in this paper is that for a given condition of the steel the rate at which carbon will be added or removed depends directly upon the gas composition. In this light the statement has no limitations.

Both Dr. Case and Dr. Turin's remarks point out the most important conclusion of the paper. That is, that the highly complex gas carburizing equilibrium system may be controlled by means of *one* gaseous constituent under the proper conditions. If we employ a suitable atmosphere generator which gives substantially constant percentages of CO and H_2, then any one of the gases H_2O, CO_2 or CH_4 may be used to completely describe the atmosphere potential. Since H_2O is the only one of these three which is easily measured with accuracy, we logically choose dew point as the *single* control factor. Dr. Turin also emphasizes that in the austenitic range any carbon concentration may be obtained by dew point control, whereas in the other practical ranges equilibrium may be established from an appropriate dew point but here the dew point is not influenced by the carbon percentage. These generalizations are found by application of the phase rule. The numerical details are developed by considering the effect of the steel composition, a factor usually neglected, upon the gas composition.

SOME SPECIAL METALLOGRAPHIC TECHNIQUES FOR MAGNESIUM ALLOYS

By P. F. George

Abstract

Some new metallographic techniques for magnesium and its alloys are given. These include methods for analyzing solid solutions within a single grain; for showing diffusion in magnesium alloys; for distinguishing microshrinkage from fusion voids in solution heat treated metal; for distinguishing the $Mg_{17}Al_{12}$ compound from the $Mg_3Al_2Zn_3$ compound; for distinguishing Dowmetal C (Mg, 9Al, 2Zn, 0.1Mn) alloy from Dowmetal H (Mg, 6Al, 3Zn, 0.2Mn) alloy in the as-cast or heat treated condition; for determining the orientation of individual grains; for showing the results of cold working to a remarkable extent; for revealing hard-to-etch grain boundaries such as exist in as-cast metal; for producing good contrast between types of precipitates; and for determining the temperature of aging.

METALLOGRAPHIC techniques for the magnesium alloys have been discussed at various times (1-11),[1] but these have been limited to the methods to delineate general structure in the routine examination of these alloys. It is the purpose of this paper to describe some specialized techniques that have become very useful in magnesium metallography.

Analyzing Solid Solutions

A method for analyzing various parts of a solid solution in a single grain is possible with magnesium alloys. The method requires the use of one of the following etchants:

	Etchant No. 1	Etchant No. 2
5% picral[2]	50 ml	50 ml
Distilled water	20 ml	20 ml
Glacial acetic acid	20 ml	16 ml

The freshly polished specimen is placed in the etchant face up

[1]The figures appearing in parentheses pertain to the references appended to this paper.
[2]5% picral contains 5g picric acid dissolved in ethanol to make 100 ml.

A paper presented before the Twenty-eighth Annual Convention of the Society held in Atlantic City, November 18 to 22, 1946. The author, P. F. George, is metallurgist, Metallurgical Department, The Dow Chemical Company, Midland, Mich. Manuscript received May 13, 1946.

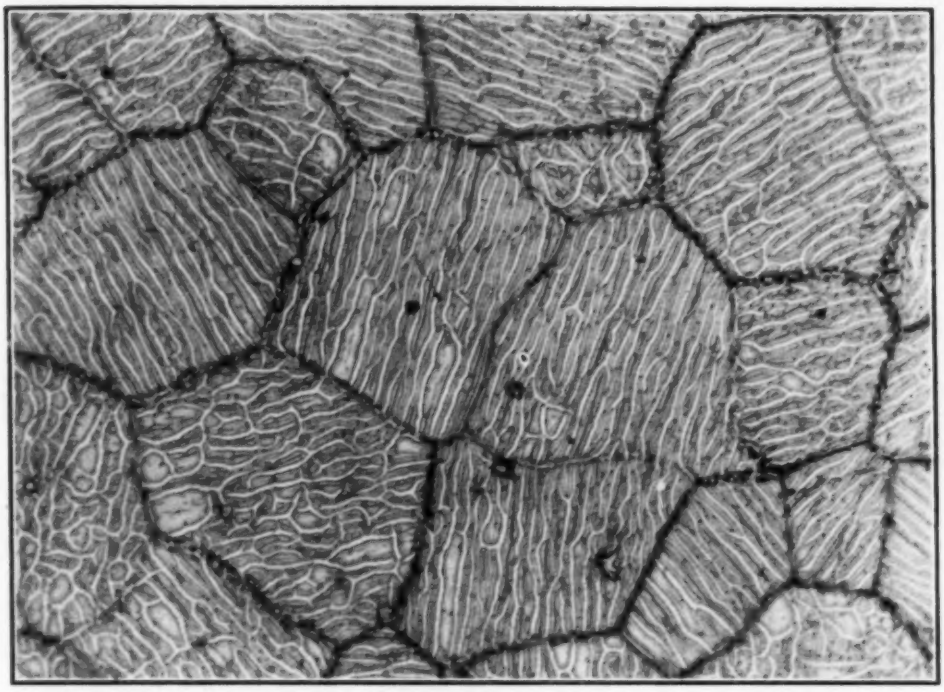


Fig. 1—Cracked Film on Heat Treated Dowmetal C (9Al, 2Zn, 0.1Mn) Alloy. Etchant No. 1. × 250.

for exactly 15 seconds, removed, washed in running 95% ethanol and dried in a gentle stream of air. The etchant forms an amorphous film on the polished surface which, when dried, cracks parallel to the trace of the basal plane in each grain. Fig. 1 shows the cracked film on Dowmetal C alloy when etched in etchant No. 1. It is possible to observe this cracking under the microscope by leaving the specimen wet with the alcohol and letting it dry in place on the microscope stage.

The cracking of the film is sensitive to the composition of the underlying solid solution. Etchant No. 1 forms a cracked film or line structure on magnesium solid solutions with the composition found above curve No. 1 shown in the magnesium corner of the ternary Mg-Al-Zn diagram, Fig. 2. Etchant No. 2 forms a cracked film on compositions within both curve No. 1 and curve No. 2 in Fig. 2. In alloys that have heterogeneous solid solutions, such as the partially heat treated Dowmetal C alloy in Fig. 3, the boundary between the cracked film and the continuous film has the composition of the intersection of a line, drawn between the magnesium corner and the average composition of the alloy and curve No. 1 in Fig. 2.

The appearance of the cracking varies somewhat with small dif-

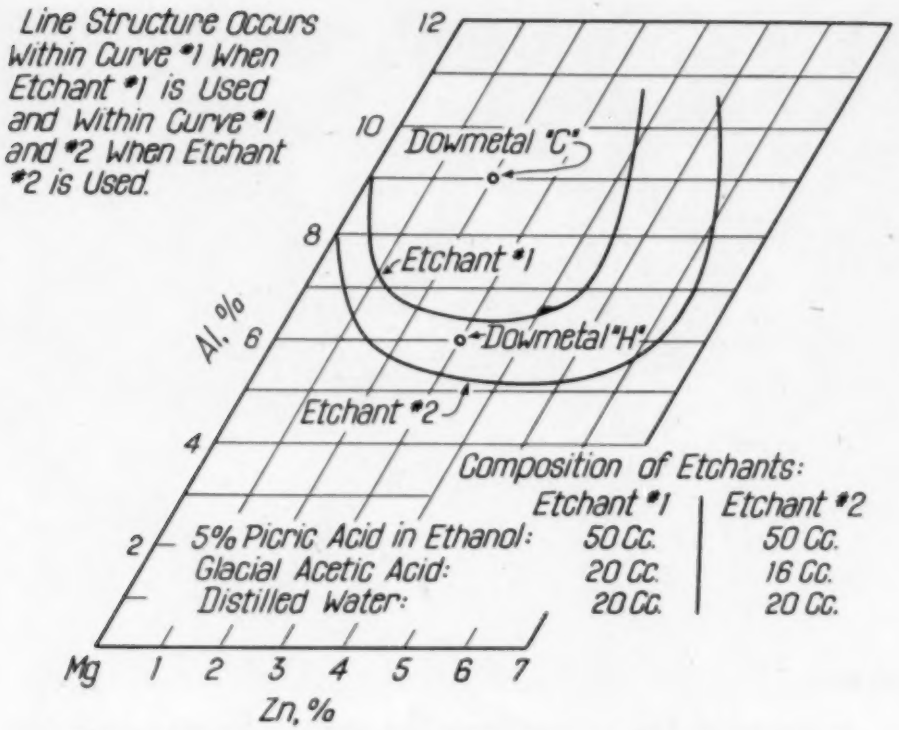


Fig. 2—Magnesium Corner of Mg-Al-Zn Ternary Diagram Showing Compositions of Solid Solutions that Produce the Cracked Film.

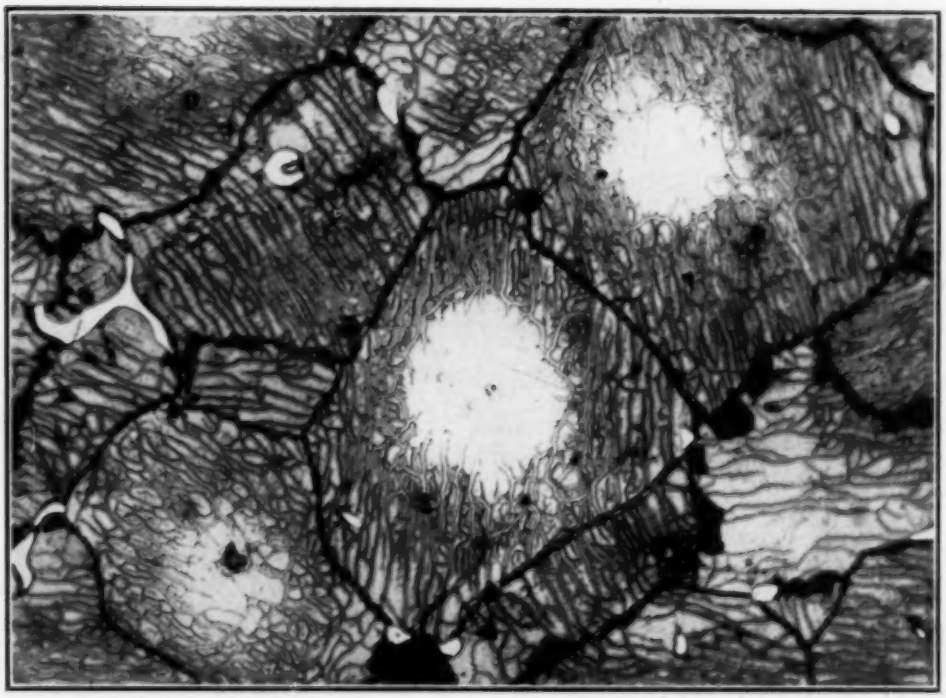


Fig. 3—Partially Heat Treated Dowmetal C Alloy Showing the Low and High Composition Areas in the Solid Solution. Etchant No. 1. × 250.

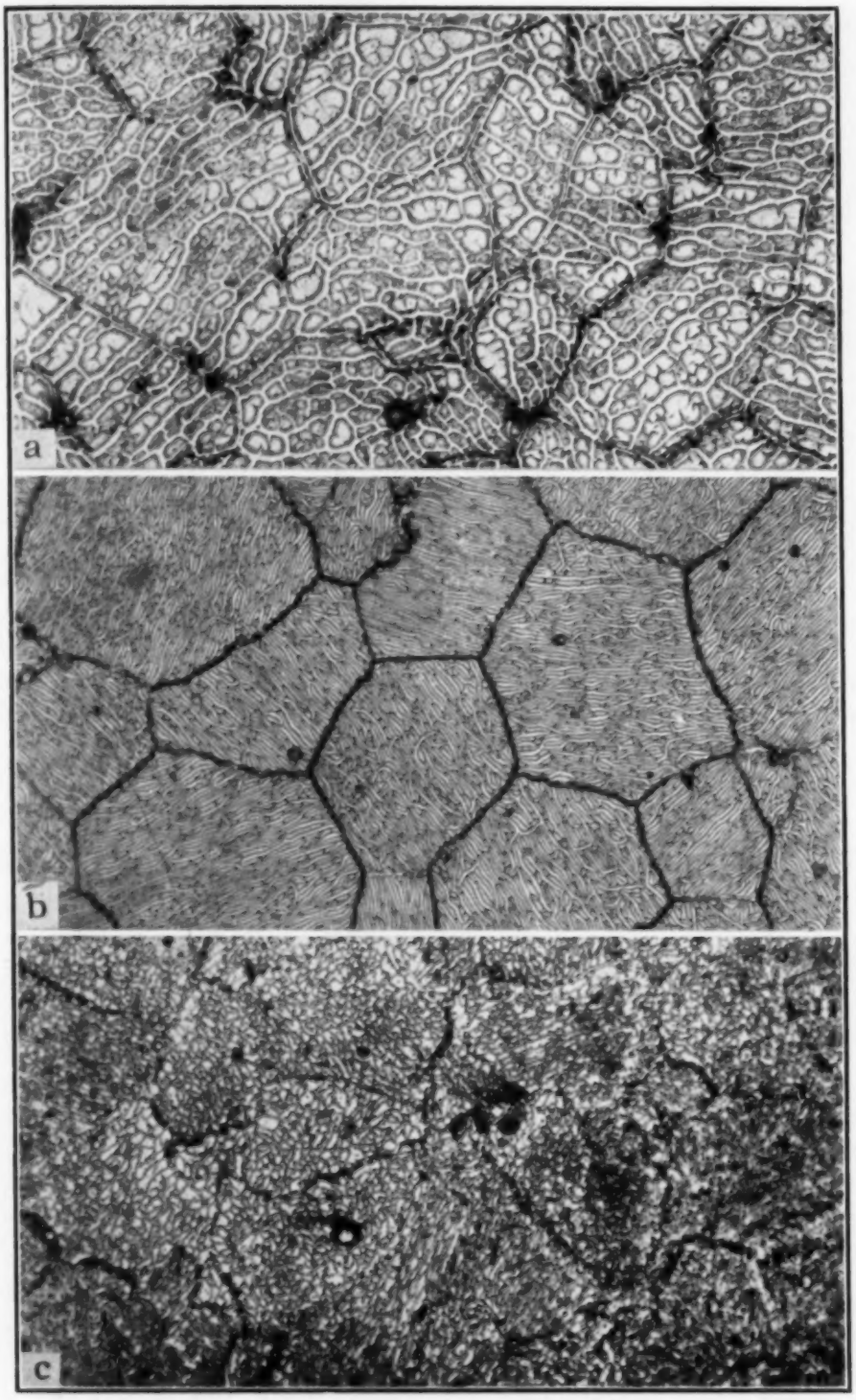


Fig. 4—Heat Treated Dowmetal C Alloy with Slightly Different Compositions. The width of the cracks in the film varies with slight composition differences. Etchant No. 1. × 250. (a) 8.5% Al, 1.7% Zn. (b) 9% Al, 2% Zn. (c) 9.7% Al, 2.3% Zn.

ferences in composition; for example, Fig. 4 shows three alloys, all with a slightly different composition but within the Dowmetal C alloy composition range. The specimens were all etched at one time in etchant No. 1. The difference in the type of cracking is apparent. The higher alloy composition ranges have finer cracks in the film, while the low alloy compositions tend to have coarser cracks. The appearance of the cracking also varies with etching time. For this reason the etching time must be held constant.

Showing Diffusion

Since the etchants just described are sensitive to composition it is possible to show the diffusion, during heat treatment, of the aluminum and zinc from the massive compound in the as-cast magnesium alloys to the α-magnesium solid solution. The etching procedure is the same as described under "Analyzing Solid Solutions." Etchant No. 1 is used for Dowmetal C alloy, and etchant No. 2 is used for Dowmetal H alloy. Fig. 5 shows the diffusion of the aluminum and zinc into the α magnesium crystals in Dowmetal C alloy heat treated for various lengths of time. The composition of the boundary between the cracked and continuous film can be estimated from curve No. 1 in Fig. 2.

The aluminum diffusion from an aluminum-containing base metal to a manganese-containing clad material can be shown especially well by the use of the following etchant:

5% picral	100 ml
Glacial acetic acid	5 ml
Conc. nitric acid	3 ml

The freshly polished specimen is placed face-up in the etchant for 20 seconds, washed in running water, then in alcohol and dried in a stream of air.

The aluminum from the base metal will precipitate manganese from the clad metal as diffusion takes place. The band of precipitated manganese is clearly shown in Fig. 6. The depletion of aluminum in the base metal and the hardness increase due to the manganese precipitate can be shown by microhardness. Fig. 7 shows the Knoop hardness numbers taken across the clad and into the base metal.

Distinguishing Microshrinkage From Fusion Voids

Distinguishing microshrinkage, which occurs during solidifica-

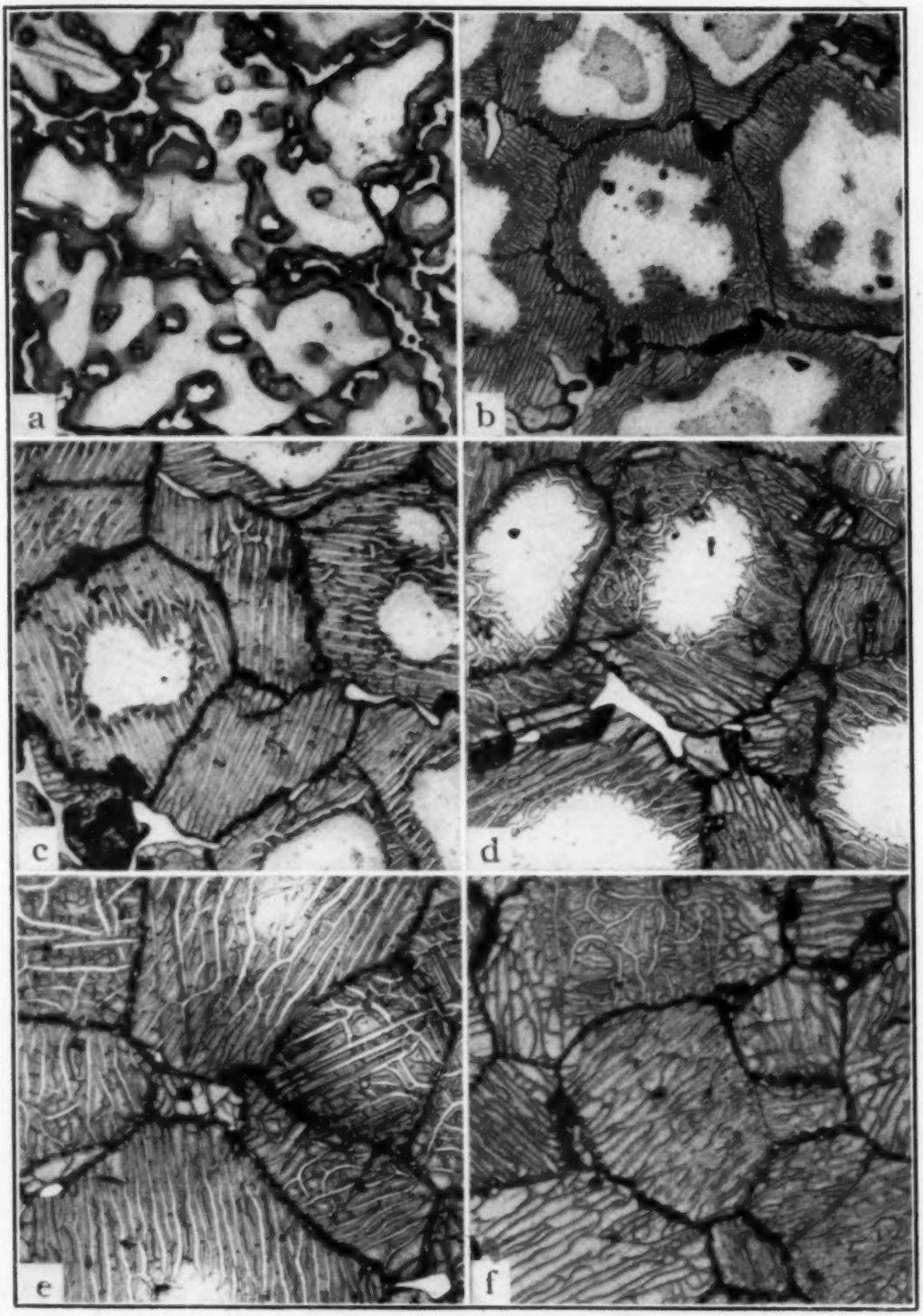


Fig. 5—Diffusion of Aluminum and Zinc During Heat Treatment of Dowmetal C Alloy. Etchant No. 1. × 250. (a) As-cast. (b) As-cast, preheated. (c) 1.2 hrs. at 770 F. (d) 2.4 hrs. at 770 F. (e) 5.5 hrs. at 770 F. (f) 6.8 hrs. at 770 F.

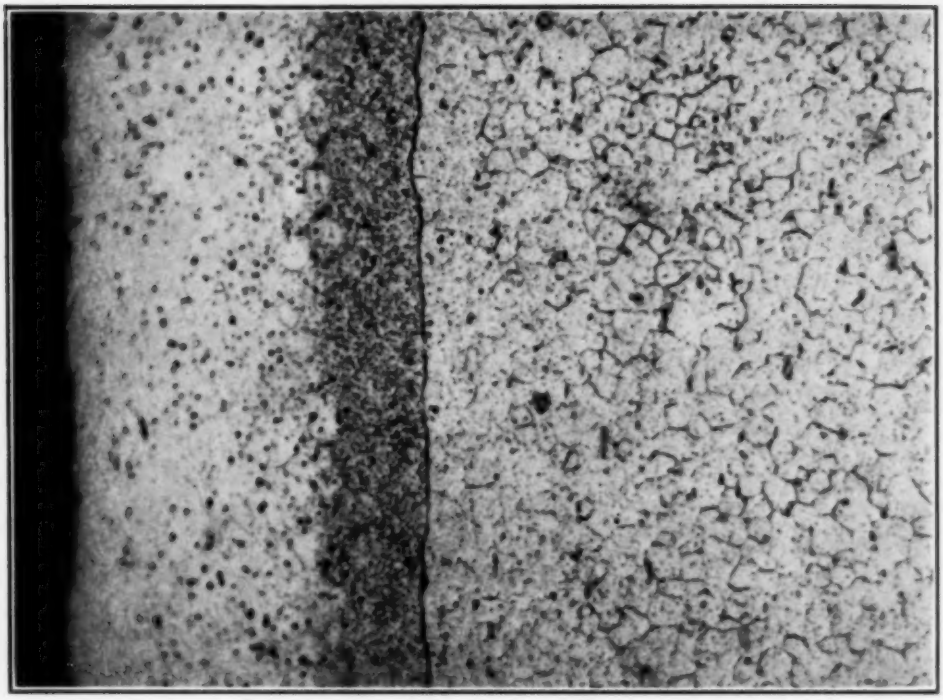


Fig. 6—Diffusion of Aluminum from the Aluminum-Containing Base Metal (right) into the Manganese-Containing Clad Metal (left). Etched in 100 picral, 5 acetic acid, 3 nitric acid etchant. × 200.

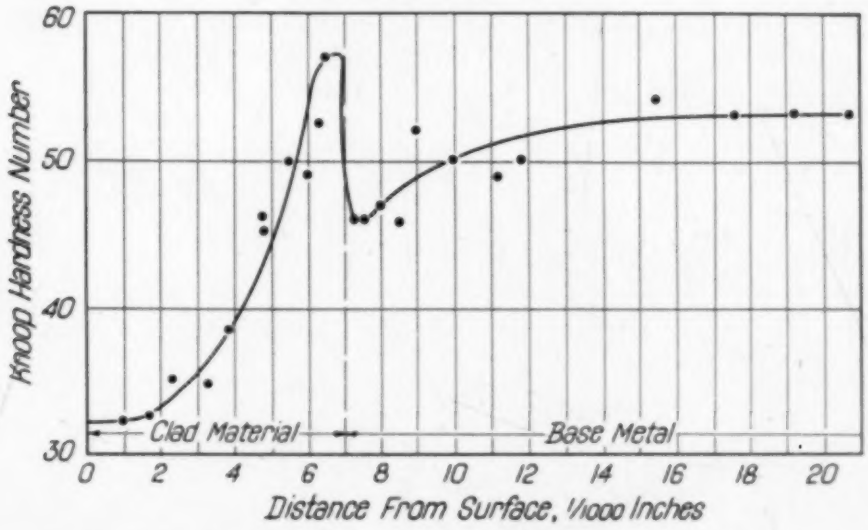


Fig. 7—Microhardness Taken Across the Clad Material Shown in Fig. 6.

tion, from fusion voids, produced by improper heat treatment, of the magnesium alloy castings has been difficult. The methods formerly used for showing this difference have been to reveal the shape of the holes, and compare the amount of precipitated compound that appeared in the vicinity of the holes with that in nonporous regions

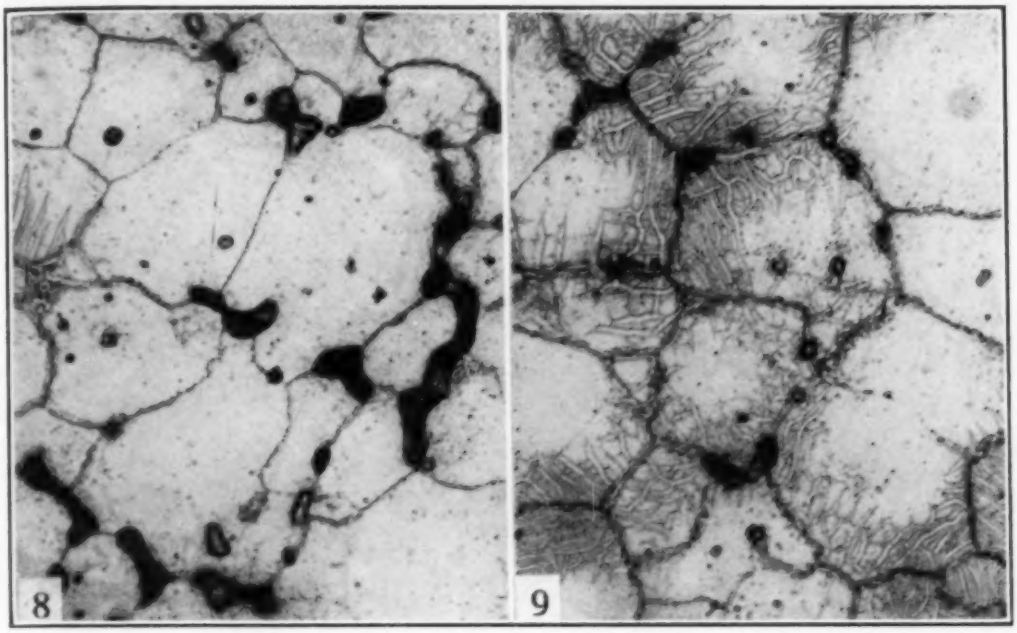


Fig. 8—Microshrinkage in Dowmetal H Alloy Etched with Etchant No. 1. The cracked film is not produced in the area of the voids. × 100.
Fig. 9—Fusion Voids in Dowmetal H Alloy. Etched with Etchant No. 1. The cracked film is produced in the area of the fusion voids. × 100.

(8). Very careful polishing was required to reveal the shape of the holes well enough to distinguish the two, and the latter method required the precipitated compound to be present which was often lacking in heat treated Dowmetal H alloy.

A method that can be used on heat treated Dowmetal H alloy that contains no precipitated compound makes use of etchant No. 1 because of its sensitivity to the composition of the solid solution. The freshly polished specimen of Dowmetal H alloy containing voids is immersed face-up in etchant No. 1 for 15 seconds, washed in running 95% ethanol and dried in a gentle stream of air. This produces a cracked film around the voids if they are caused by improper heat treatment because this area will be of an alloy content greater than the average composition of this alloy and above curve No. 1 in Fig. 2. The film will not crack around the voids if they are due to microshrinkage as the alloy content in the region of such voids is below the average composition of Dowmetal H alloy and far below the composition shown by curve No. 1 in Fig. 2. Microshrinkage and fusion voids in Dowmetal H alloy are shown in Figs. 8 and 9. The cracked film is produced around the fusion voids but none appears around the microshrinkage.

Distinguishing Phases

A large difference of color between the Mg_2Si compound and the manganese constituent can be obtained by using the following etchant:

5% picral	50 ml
Distilled water	50 ml

The freshly polished specimen is immersed face-up in the etchant for 30 seconds, washed in alcohol and dried in a stream of air. The Mg_2Si becomes a brilliant blue, while the manganese retains its usual gray color.

Distinguishing between the intermetallic compounds $Mg_{17}Al_{12}$ and $Mg_3Al_2Zn_3$ is possible with the following etchant:

Hydrofluoric acid 48%	10 ml
Distilled water	90 ml

The freshly polished specimen is immersed face-up in the etchant for 1 second, washed in running water, then in alcohol and dried in a stream of air. The $Mg_{17}Al_{12}$ is darkened, while the ternary compound remains white.

To give more contrast between the white ternary compound and the matrix, the specimen, after receiving the hydrofluoric acid etch, can be immersed in:

5% picral	10 ml
Distilled water	90 ml

for 10 to 15 seconds. This stains the matrix a golden color, giving good contrast between all phases present. Fig. 10 shows a Dowmetal H alloy etched in these two etchants. The $Mg_{17}Al_{12}$ is darkened by the hydrofluoric acid etchant leaving the $Mg_3Al_2Zn_3$ compound white. The matrix is stained to give better contrast. Fig. 11 shows the same area repolished and etched with the "glycol etchant." No difference can be seen between the two compounds. The binary magnesium zinc compound also remains white when etched in the hydrofluoric acid etchant.

Distinguishing Between Alloys

Dowmetal C alloy and Dowmetal H alloy in the as-cast condition can be distinguished from each other by etching in the hydrofluoric acid etchant. The ternary compound $Mg_3Al_2Zn_3$ is found in

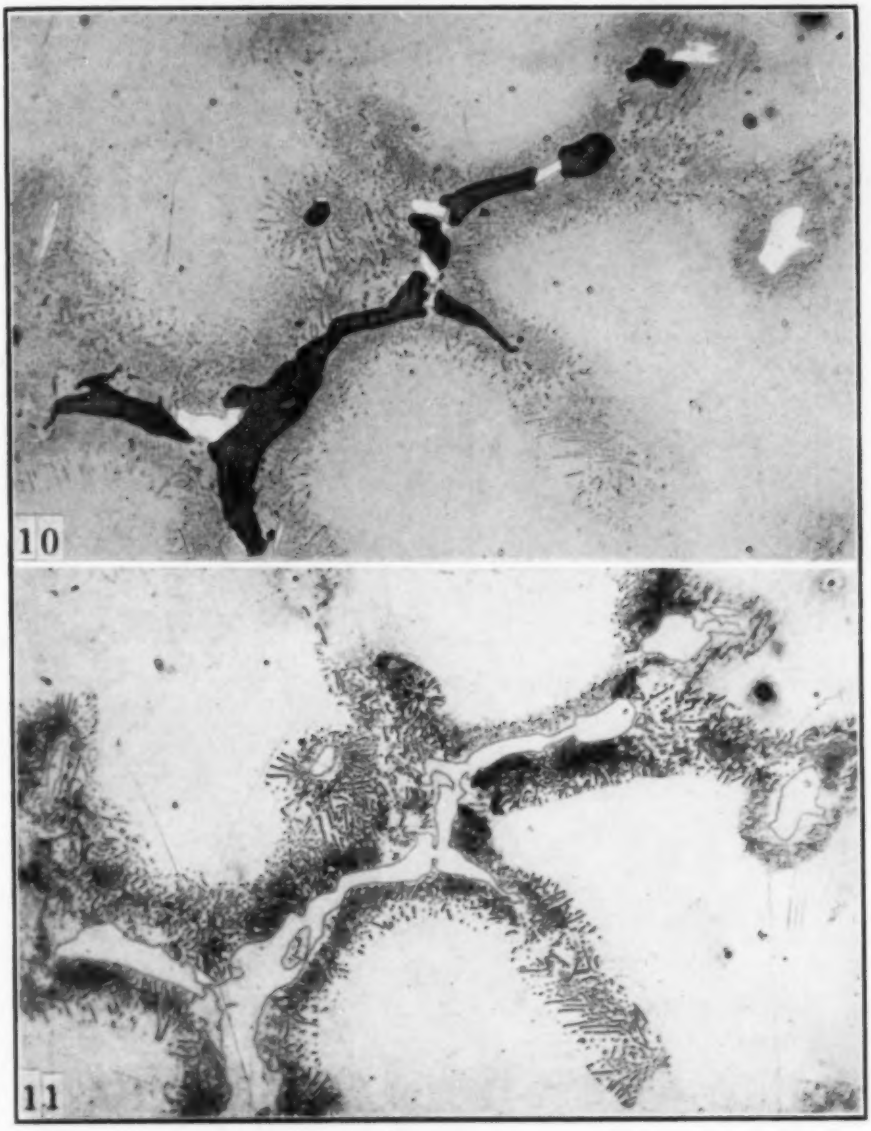


Fig. 10—Dowmetal H Alloy Showing the Darkened $Mg_{17}Al_{12}$ and the White $Mg_3Al_2Zn_3$. HF etchant followed by 10 picral, 90 water etchant. × 200.

Fig. 11—Same Area as Shown in Fig. 10. Etched in the glycol etchant. × 200.

Dowmetal H alloy as shown in Fig. 10, while Dowmetal C alloy contains only the $Mg_{17}Al_{12}$ compound. The 10 picral, 90 water etchant should be used after the hydrofluoric acid etchant each time to make certain that the ternary compound is not overlooked because of the lack of contrast with the matrix.

The ternary compound or one of the magnesium zinc compounds is found in all alloys when the composition is to the right of the line drawn on the Mg-Al-Zn diagram shown in Fig. 12, while

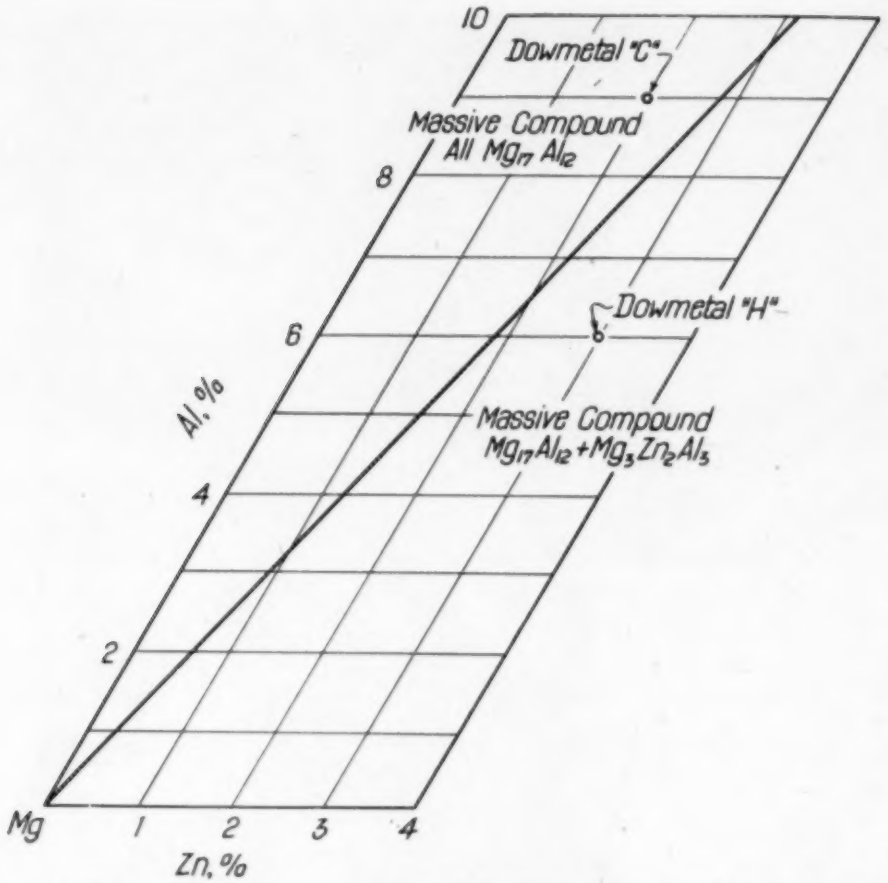


Fig. 12—Line Drawn on the Mg-Al-Zn Diagram to Divide the Compositions which Contain All $Mg_{17}Al_{12}$ Massive Compound from the Compositions that Contain Some $Mg_3Zn_2Al_3$ Ternary Compound in the As-Cast State.

only the $Mg_{17}Al_{12}$ compound is found in alloys with the composition to the left of the line. The Dowmetal C alloy has a composition to the left of the line while Dowmetal H alloy has a composition to the right of the line.

When the Dowmetal H and C alloys are in the heat treated condition and contain little massive compound, they can be distinguished from one another by the use of etchant No. 1. This etchant produces the cracked film on the heat treated Dowmetal C alloy and not on the heat treated Dowmetal H alloy. The composition of the Dowmetal C alloy lies within curve No. 1, Fig. 2, while Dowmetal H alloy lies outside of curve No. 1. Fig. 13 shows the absence of the cracked film on Dowmetal H alloy while Fig. 14 shows the cracked film on Dowmetal C alloy, both etched with etchant No. 1.

Determining Orientation

The magnesium alloys do not lend themselves to the methods

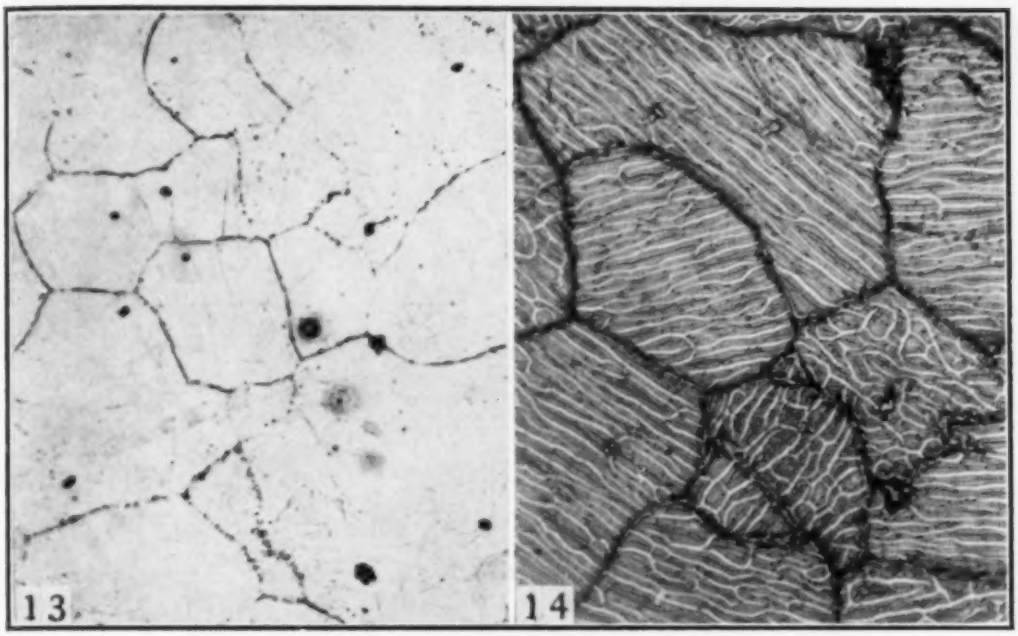


Fig. 13—Heat Treated Dowmetal H (Mg-6Al, 3Zn, 0.2Mn) Alloy. Etchant No. 1. No cracked film is produced with this composition. × 250.
Fig. 14—Heat Treated Dowmetal C (Mg-9Al, 2Zn, 0.1Mn) Alloy. Etchant No. 1. Cracked film is produced with this composition. × 250.

of determining orientation by means of etch pits as do some of the other metals shown by Barrett and Levenson (12).

The trace of the basal plane in each crystal can be determined by the use of the etchants Nos. 1 and 2 since the film formed on the specimen by these etchants, when dried, has been shown by X-ray methods to crack parallel to the trace of the basal plane in each grain. If the grains are distorted or if the basal plane is parallel to the polished surface, the cracks in the film do not follow definite directions. This is shown in many of the grains in the photomicrographs in Fig. 4.

The slope of the basal plane can be determined by the following method: The freshly polished specimen is immersed face-up in

5% picral	100 ml
Distilled water	10 ml
Glacial acetic acid	5 ml

for 10 to 20 seconds, washed in running 95% ethanol and dried in a stream of air. It is then placed on a revolving mechanical stage of a metallurgical microscope and revolved under polarized light. The grains with the basal planes parallel to the polished surface remain unchanged and dark as the stage is revolved, while grains

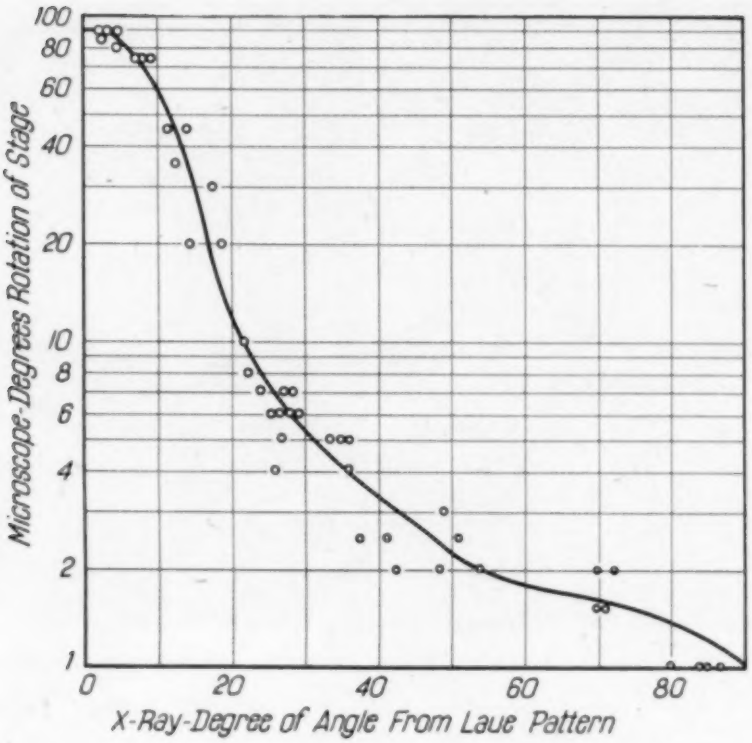


Fig. 15—Degrees of Rotation of the Revolving Mechanical Stage Under Polarized Light, Compared with the Angle Between the Etched Surface and the Basal Plane Calculated by the Laue Method.

with the basal planes at an angle with the polished surface change from light to dark. The maximum number of degrees of rotation of the stage through which the darkened grains remain dark is measured. Then from the curve in Fig. 15 the angle between the polished surface and the basal plane is easily estimated.

The data for the curve in Fig. 15 were obtained from a specimen of magnesium which was annealed to remove all distortion, polished chemically using a 15% nital solution and etched 15 seconds in the above etchant. A photomacrograph was taken of the specimen as shown in Fig. 16 and 44 grains were numbered on the negative to identify each grain. Laue back-reflection patterns were taken from each of the 44 grains and the angle between the etched surface and the basal plane was calculated for each grain. The specimen was then placed on the revolving stage of a metallurgical microscope and the maximum degree of rotation of the stage during which each grain remained dark under polarized light was measured. These measurements, plotted against the calculated angles from the Laue patterns, are shown in Fig. 15. The same specimen was repolished in 15% nital and this time etched for 30 seconds in the

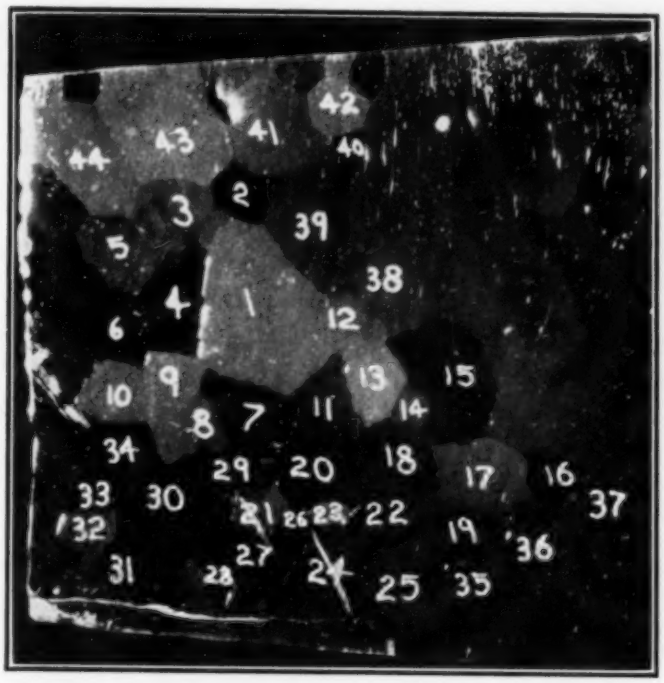


Fig. 16—Macrograph of Magnesium Grains on Which Orientation was Studied. × 3.

above etchant and again the rotations of the specimen under polarized light were measured and found to give approximately the same results.

Existence of preferred orientation can be seen readily under the microscope. If most of the grains turn dark and light at one time on revolving the specimen under polarized light, the basal planes will all have approximately the same slope and the slope will be in the same direction. When viewed under the bright field of a microscope the grains that appear light have their basal planes nearly parallel to the etched surface, while the grains that appear dark have basal planes nearly perpendicular to the surface. This makes it possible to see the existence of preferred orientation under the bright field of a microscope. Fig. 17 shows the preferred orientation as it exists on the surface of an extruded Dowmetal FS-1 alloy etched with the above etchant and photographed under ordinary light.

It was found that microhardness values were sensitive to the orientation of the grains to a remarkable extent in magnesium alloys. Best reproducibility of the microhardness values was obtained by selecting grains with the basal planes nearly parallel to the polished

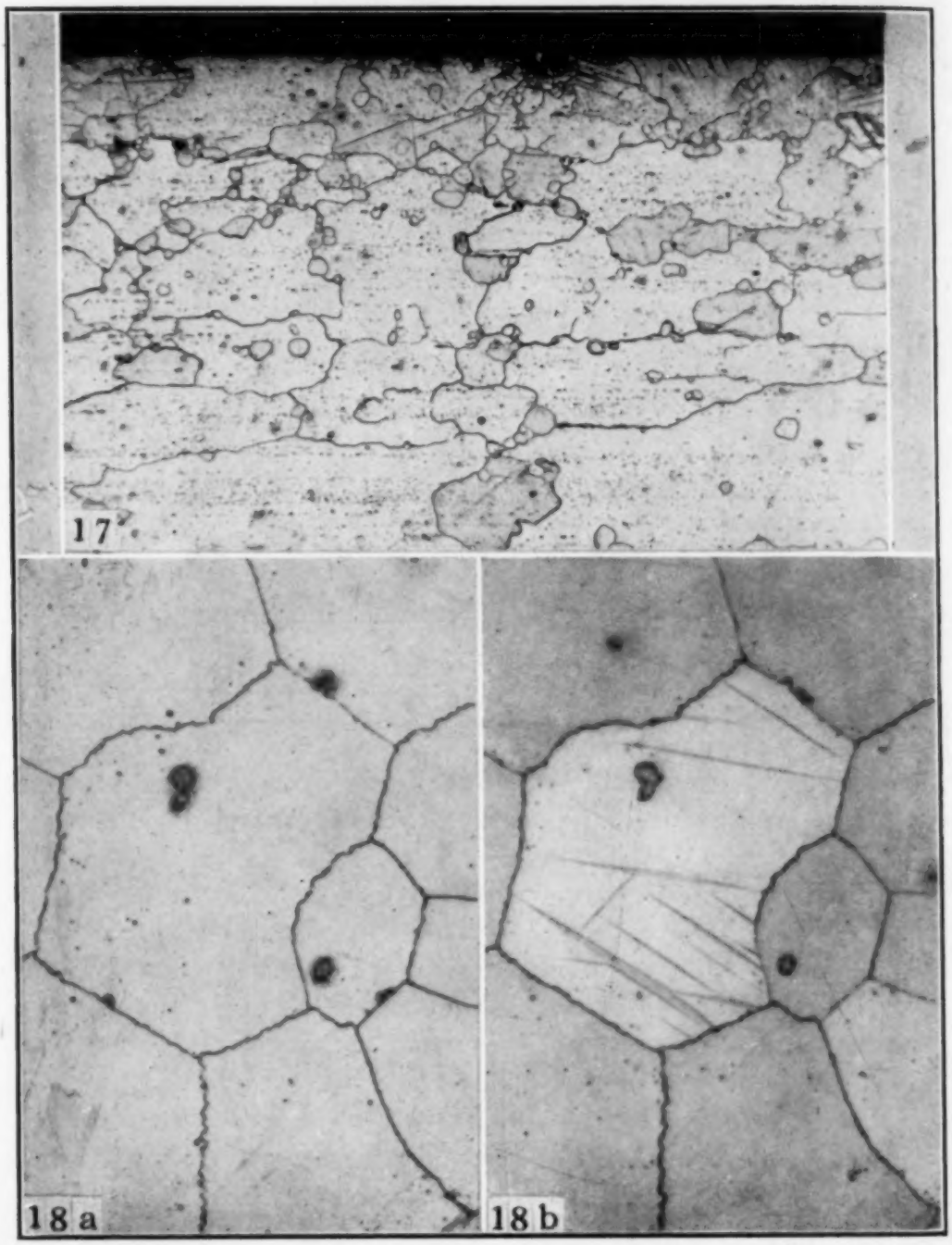


Fig. 17—Extruded Dowmetal FS-1 Etched with 100 Picral, 10 Water, 5 Acetic Acid Etchant. The surface grains are all of the same color, indicating the same orientation and a different orientation from the substructure. × 100.

Fig. 18—Heat Treated Dowmetal C Alloy Etched in the Acetic Glycol Etchant (a) and in the 100 Picral, 10 Water, 5 Acetic Acid Etchant (b). × 400. Note the appearance of the twins in the center grain of right-hand picture.

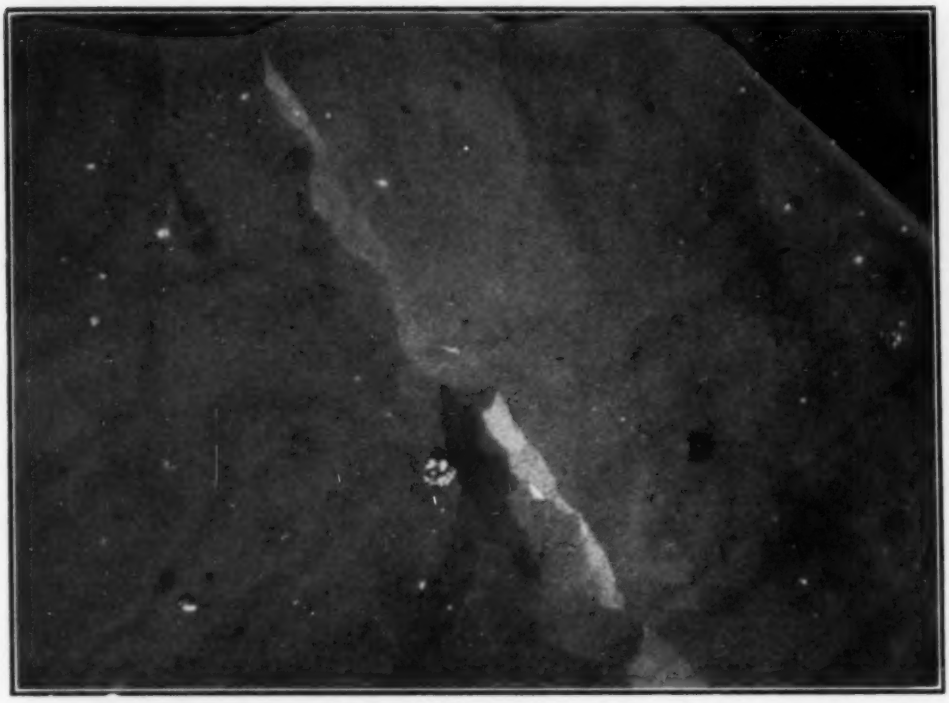


Fig. 19—Slightly Distorted Crystal of Magnesium Etched in 100 Picral, 10 Water, 5 Acetic Acid Etchant. Taken under polarized light. × 50.

and etched surface. The above method was found to be very useful for selecting these grains.

Showing Results of Cold Work

Twinning and distortion in the magnesium alloys can be shown to a remarkable extent by the use of the 100 picral, 10 water, 5 acetic acid etchant described under "Determining Orientation." The etching procedure is the same as previously described. Twins that are not revealed by other etchants are readily detected by this etchant. Fig. 18 shows the same area on Dowmetal C alloy, etched with the acetic glycol and with this picral, water, acetic acid etchant. The twins are hidden when etched with the acetic glycol but are clearly shown with this etchant. The etchant both sharply outlines the twins and colors them a different color than the matrix because of their different orientations.

Very slight distortion in crystals that show no twinning can be detected. The etched specimen is revolved under polarized light and any change in color or darkness from one area of the crystal to other areas on the crystal is noted. If the grains are of a size to

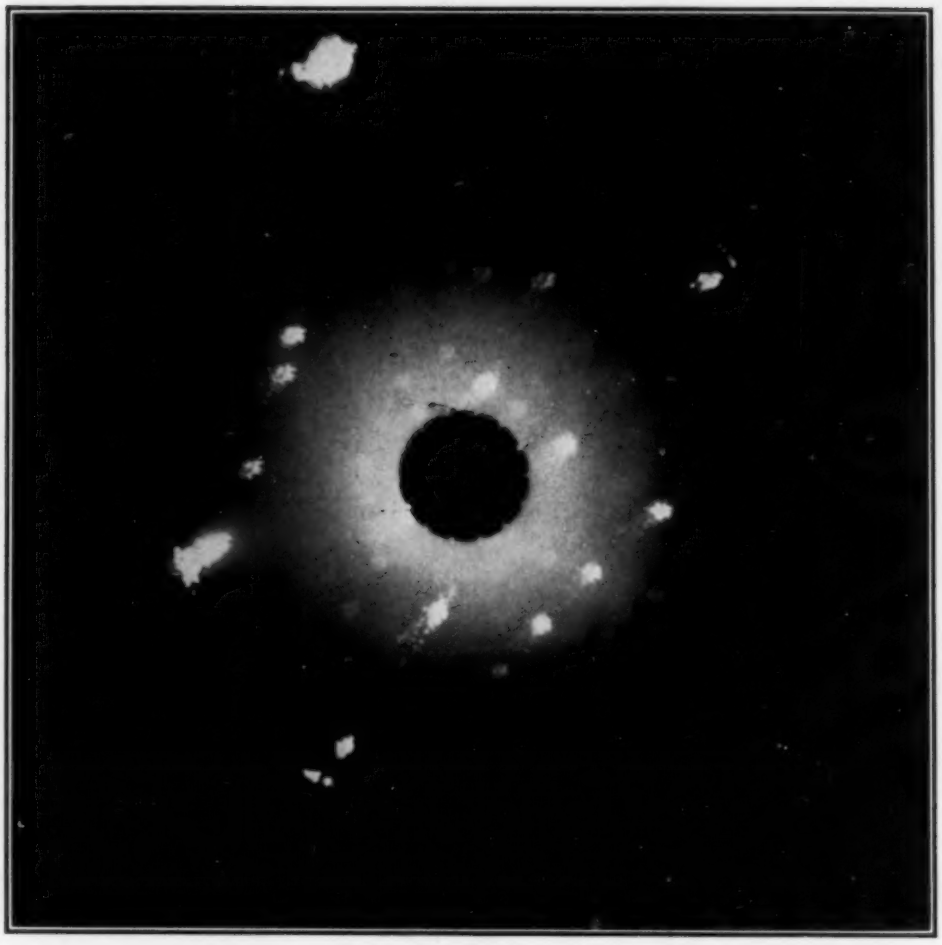


Fig. 20—Laue Diffraction Pattern of the Same Magnesium Crystal Shown in Fig. 19.

permit low magnification (× 50) this method of revealing distortion becomes extremely sensitive. Fig. 19 shows the difference in darkness on a magnesium crystal photographed under polarized light. Another crystal is visible at the top of the photomicrograph. Fig. 20 shows a Laue pattern of the same crystal shown in Fig. 19. The small amount of distortion that can be detected is apparent.

Revealing Grain Boundaries

Grain size measurements on magnesium alloys in the as-cast condition have been difficult. The 100 picral, 10 water, 5 acetic acid etchant previously described reveals the grains in the as-cast metal.

The freshly polished specimen is held face-up in the etchant and gently agitated for 5 seconds. It is removed, washed in running alcohol, and dried in a stream of air. This etchant has three

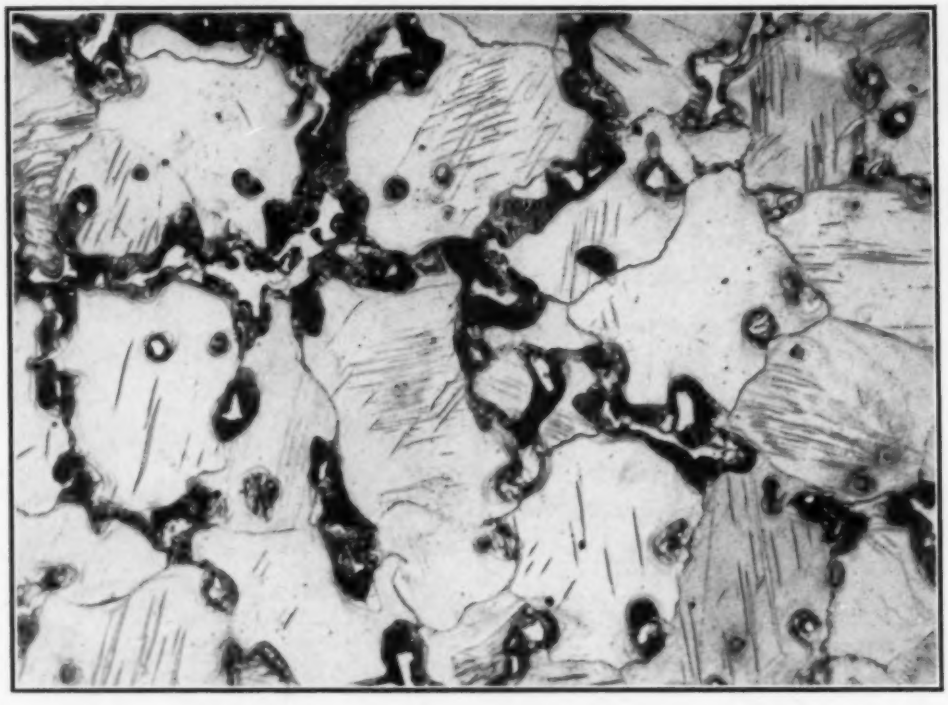


Fig. 21—Grain Boundaries in As-Cast Dowmetal C Alloy. Twinning was intentionally left in specimen to help reveal the grains. Etched in 100 picral, 10 water, 5 acetic acid etchant. × 200.

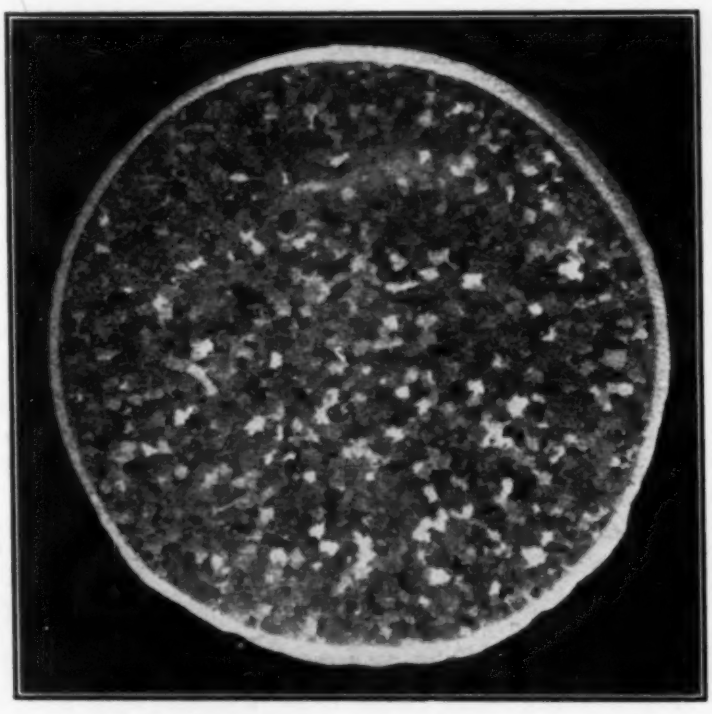


Fig. 22—Macro-Grain Structure in As-Cast Dowmetal C. Etched in 100 picral, 10 water, 5 acetic acid etchant. × 3.

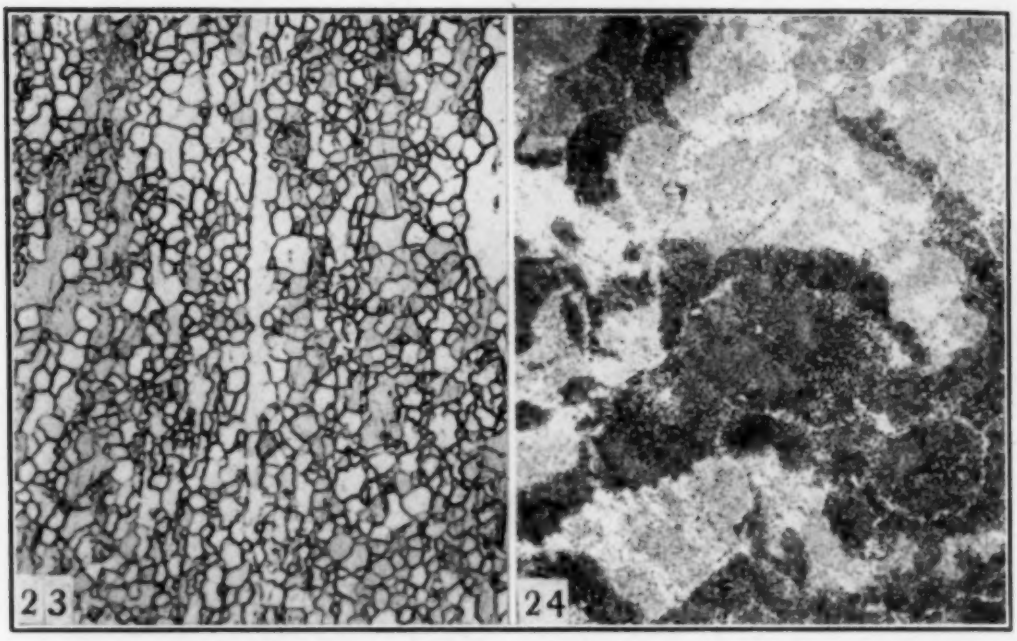


Fig. 23—Extruded Dowmetal FS-1 Alloy Showing the Grain Boundaries Clearly Revealed by the 100 Picral, 10 Water, 5 Acetic Acid Etchant. × 250.
Fig. 24—Aged Dowmetal C Alloy Showing Contrast Between the Two Types of Precipitate as Produced by the 100 Picral, 10 Water Etchant. × 250.

characteristics that enter into its ability to reveal the grains in as-cast magnesium alloys:

1. The grain boundaries are revealed between the massive compound particles.

2. Contrast is shown between one grain and another because of the etchants' ability to stain grains differently, depending on their orientation.

3. Twins are revealed that run in given directions in each grain, which produces still more contrast between grains. Fig. 21 shows the grains in as-cast Dowmetal C alloy as revealed by this etchant.

In obtaining grain sizes on as-cast magnesium alloys, it is advantageous to leave some of the twinned metal, produced by sawing, on the specimen. This is usually easy to do; in fact, much careful grinding and polishing is required to remove the cold-worked layer.

The same etchant is excellent for macro-grain size determinations in all the alloys in the as-cast or heat treated condition. Fig. 22 shows the macro-grain structure in an abnormally large grained as-cast Dowmetal C alloy at × 3.

The etchant is also excellent for revealing the grains in hard-to-etch wrought alloys. Fig. 23 shows the grain boundaries clearly revealed in extruded Dowmetal FS-1 alloy.

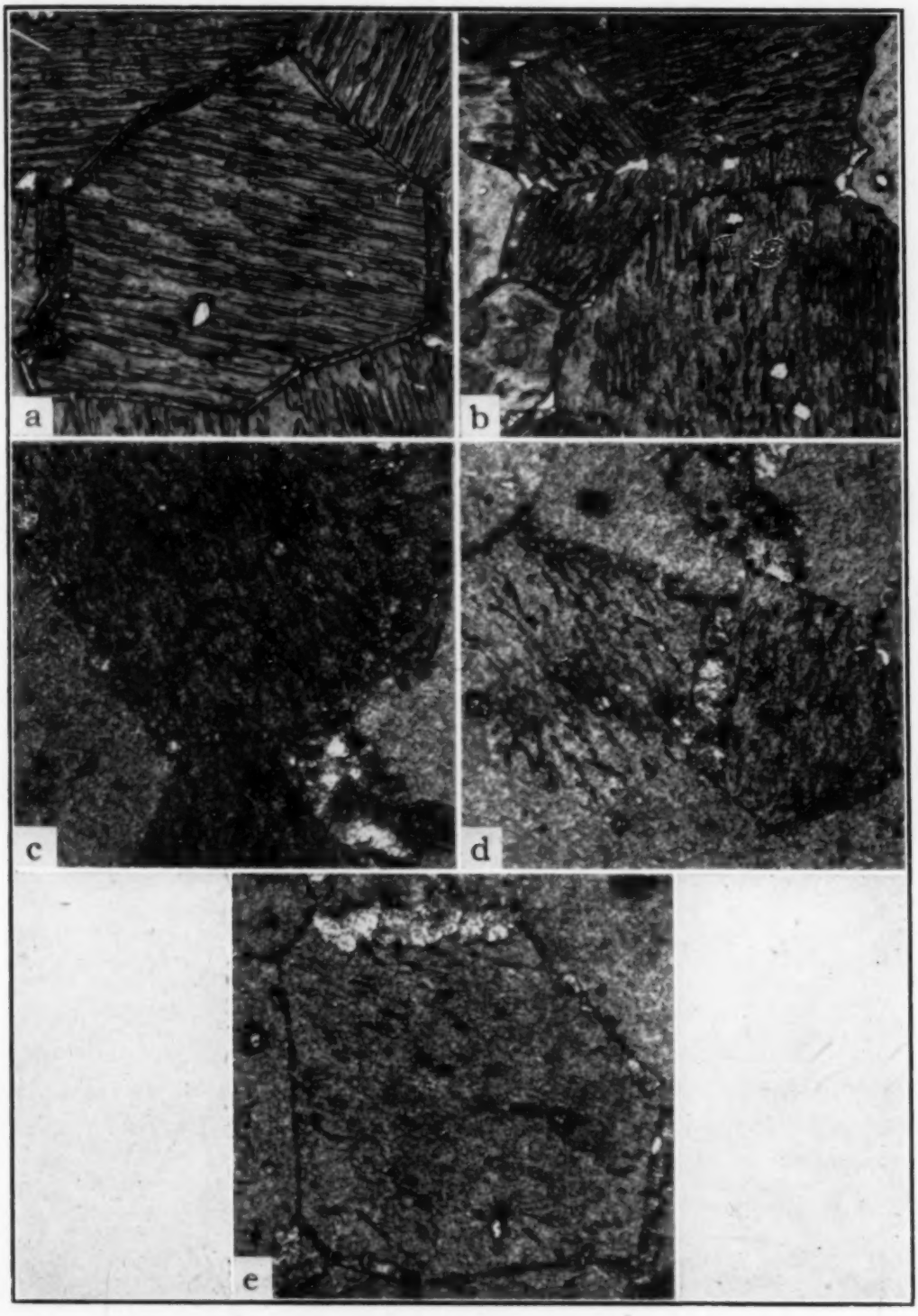


Fig. 25—Dowmetal C Alloy Aged at Various Temperatures for 15 Hrs. Cracked film becomes less as temperature of aging is increased. Etchant No. 1. × 250. (a) 300 F. (b) 325 F. (c) 350 F. (d) 375 F. (e) 400 F.

Table I
Summary of Special Etchants

Composition		Etching Procedure	Characteristic
5% picral Distilled water Glacial acetic acid	50 ml 20 ml 20 ml	Specimen face-up with gentle agitation. Exactly 15 seconds. Wash in running alcohol and dry in gentle stream of air.	1. Shows trace of basal plane. 2. Sensitive to solid solution composition. 3. Distinguishes between microshrinkage and fusion voids. 4. Reveals temperature of aging.
5% picral Distilled water Glacial acetic acid	50 ml 20 ml 16 ml	Same as above.	Same as above except different range of solid solution composition as shown by the curves in Fig. 2.
5% picral Distilled water Glacial acetic acid	100 ml 10 ml 5 ml	Same as above, except time of etching not critical.	1. Reveals hard-to-etch grain boundaries in wrought and as-cast structures. 2. Stains grains of various orientations differently. 3. Very sensitive in revealing distortion.
5% picral Distilled water	50 ml 50 ml	Specimen face-up for 30 seconds, washed in running alcohol and dried in stream of air.	Greater contrast between Mg_2Si compound and Mn constituent. Mg_2Si brilliant blue, Mn dull gray.
5% picral Glacial acetic acid Conc. nitric acid	100 ml 5 ml 3 ml	Specimen face-up for 20 seconds, washed in water, then alcohol and dried.	Shows diffusion of aluminum from the Al-containing base metal into the Mn-containing clad metal.
Hydrofluoric acid (48%) Distilled water	10 ml 90 ml	Specimen face-up for 1 to 2 seconds, washed in water, then alcohol and dried.	Darkens $Mg_{17}Al_{12}$ compound and leaves the $Mg_3Al_2Zn_3$ ternary compound unetched and white.
5% picral Distilled water	10 ml 90 ml	Specimen face-up for 15 to 30 seconds, washed in alcohol and dried.	Used after above HF etchant to darken matrix to give better contrast between matrix and white ternary compound.
5% picral Distilled water	100 ml 10 ml	Specimen face-up for 15 to 30 seconds, washed in alcohol and dried.	Gives good contrast between types of precipitate.

Producing Contrast in Precipitates

At times it is difficult to obtain good contrast between the two types of precipitate found in the magnesium-aluminum and magnesium-aluminum-zinc alloys. An etchant with the following composition:

5% picral	100 ml
Distilled water	10 ml

gives good contrast between the "Pearlitic" type and the fine Widmanstätten type of precipitate (8). Fig. 24 shows an aged Dowmetal C alloy etched for 20 seconds in this etchant. The areas of the two types of precipitate are clearly distinguished.

Determining Aging Temperature

It is possible to show, roughly, the temperature of aging for some of the magnesium alloys. Etchant No. 1 is used as previously described. The aging temperature is determined by the amount of film cracking produced by this etchant. Fig. 25 shows etchant No. 1 used on Dowmetal C alloy aged 15 hours at 300, 325, 350, 375 and 400 F (150, 165, 175, 190 and 205 C). The amount of the cracked film decreases as the temperature of aging increases and entirely disappears above 400 F. The amount of film cracking has been investigated for aging times between 5 and 25 hours at the above temperatures and it has been found that these times of aging do not change the amount of film cracking for any given temperature.

Summary

Table I summarizes the etchants, with their compositions, etching technique and use for the special metallographic techniques described in this paper. The picric acid etchants change their etching characteristics in a few hours, and therefore cannot be made up in advance. However, the 5% picral solution can be made in advance and used as a stock solution in all the etchants containing picral listed in Table I.

References

1. H. Vosskuhler, "The Technology of Magnesium and Its Alloys," F. A. Hughes and Co., Abby House, London, N.W.1, 1940, p. 37.
2. W. Bulian and E. Fahrenhorst, "Metallography of Magnesium and Its Alloys," F. A. Hughes and Co., Abby House, London, N.W.1, 1944.
3. R. Mechel, "An Electrolytic Etching Method for Magnesium Wrought Alloys," *Zeit. f. Metallkunde*, Vol. 33, 1941, p. 34-36.
4. F. A. Fox and H. T. Hall, "Metallographic Technique for Magnesium Alloys," *Magnesium Review and Abstracts*, Vol. 3, No. 3, p. 70-76.
5. W. H. Dearden, "Macro-Etching of Magnesium Alloy Forgings," *Journal*, Institute of Metals, Vol. 66, 1940, p. 85.
6. ASTM, "Tentative Method of Preparation of Metallographic Specimens" (E3-44T), book of ASTM Standards, 1944, p. 1913.
7. J. B. Hess and P. F. George, "The Metallography of Commercial Magnesium Alloys," Transactions, American Society for Metals, Vol. 31, No. 2, 1943, p. 423.
8. P. F. George, "A Numerical Rating Method for the Routine Metallographic Examination of Commercial Magnesium Alloys," *Bulletin*, American Society for Testing Materials, Aug. 1944, p. 35.
9. H. B. Pulsifer, "Magnesium—Its Etching and Structure," *Transactions*, American Institute of Mining and Metallurgical Engineers, Vol. 78, 1928, p. 461.
10. J. A. Gann, "Treatment and Structure of Magnesium Alloys," *Transactions*, American Institute of Mining and Metallurgical Engineers, Vol. 83, 1929, p. 309.

11. R. W. James, METALS HANDBOOK, 1939 edition, p. 1589, published by the American Society for Metals.
12. Charles S. Barrett and L. H. Levenson, "Determination of Orientations by Etch Pits," *Transactions*, American Institute of Mining and Metallurgical Engineers, Vol. 137, 1940, p. 76.

DISCUSSION

Written Discussion: By Alfred Bornemann, associate professor of engineering chemistry, Stevens Institute of Technology, Hoboken, N. J.

Before asking for information, I would like to compliment Mr. George on his excellent metallographic technique. My question deals with the method of preparing magnesium specimens for metallographic examination. Would Mr. George be kind enough to disclose his polishing techniques?

Author's Reply

Answering Dr. Bornemann's question, the polishing technique used for the preparation of the magnesium specimens can be described briefly as follows:

The specimen is ground on Aloxite cloths Nos. 50, 150, 320, and on emery paper No. 0. The Aloxite cloths and emery paper are mounted on rotating disks.

The polishing is carried out on two wet laps both covered with "Vel-Chamee" cloth. A suspension of 600 alundum is used on the first wheel, while a suspension of relevigated alumina and soap solution is used on the final wheel.

The specimen is rinsed well in running water, then in alcohol and dried in a blast of air.

A more detailed description of the polishing technique has been described by Hess and George in previous papers (7), (8).

CALCULATION OF PRESS FORGING PRESSURES AND APPLICATION TO MAGNESIUM FORGINGS

By R. L. Dietrich and G. Ansel

Abstract

The pressures required for forging are a function of size, shape, friction and deformation resistance of the metal. Equations are derived for calculating the forging pressures in simple sections as a function of these variables. From a few simple tests, basic data on deformation resistance and friction may be obtained for a given metal and conditions of press speed, lubrication and temperature. Such data can then be used to calculate, with reasonable accuracy, the loads required for upsetting or for fairly simple die forgings. Some data are given for two commercial magnesium forging alloys (Mg + 8.5 Al + 0.5 Zn and Mg + 6.5 Al + 1.0 Zn), and the comparison between calculated and experimental forging loads is shown for a few magnesium die forgings. Data are also presented on the effect of flash dimensions to illustrate the way in which the derived equations may be used to predict the effects of changes in die design upon the forging load for a particular part.

ONE of the primary considerations in press forging any given part is the force which will be required; for its magnitude is one of the factors which determines the choice of press, die life, and perhaps even the ability or desire of a given plant to produce the forging. The force required for a forging is dependent upon the factors of material, forging conditions, friction and geometry.

Some work of an empirical nature has previously been done on forging pressures to compare the effects of alloy, temperature, press speed, etc. Beck (1)[1] gives data showing the effect of press speed, temperature, and per cent deformation on the specific pressure required for upsetting magnesium alloy extrusions 1 inch in diameter by 1 inch high; Zeerleeder and Irnmann (2) studied the effect of tem-

[1]The figures appearing in parentheses pertain to the references appended to this paper.

A paper presented before the Twenty-eighth Annual Convention of the Society held in Atlantic City, November 18 to 22, 1946. Of the authors, R. L. Dietrich is metallurgist, and G. Ansel is director, Process Development Division, Magnesium Laboratories, Dow Chemical Co., Midland, Michigan. Manuscript received July 22, 1946.

perature and alloy upon the power required to upset 20-mm diameter by 20-mm high aluminum test pieces 50%; Crane (3) gives a graphical computation of the approximate force required for forging steel and brass, which is based upon the projected area of the material to be used; Lucas (4) has compiled examples of many different forgings and the force used on them, to assist those who may have a similar part to forge; Naujoks (5) states that the experienced forger unconsciously takes into account the geometrical factors in a given forging, and can accurately estimate the force required, although he cannot tell how he does it.

A great deal of work on plastic forming of metals was done in Germany at the Kaiser-Wilhelm Institut für Eisenforschung during the late 1920's. Most of this work was done on drawing, extrusion, deep drawing, and rolling; and has been summarized by Siebel (6). Some theoretical work on forging is presented which is further discussed in a later section.

In none of these references have the authors of this paper found a method of calculating the force required to produce a forging. The method outlined in this paper is intended to permit the calculation of such force for a given forging on the basis of its dimensions, its geometry, friction and the flow stress of the metal. Although the method appears rather cumbersome at first, it is fairly easy to use once the principles are understood; and a limited number of checks on actual forgings have indicated reasonable accuracy.

General Requirements for Metal Flow in Forging

The forces required for forging are dependent upon the deformation resistance of the material and the friction of the metal against the press plates. For ideal frictionless compression the force required would simply be equal to the deformation resistance, K_f, times the projected area. To find the forces necessary to overcome friction we must assume that these forces are distributed evenly over the height of the forging. According to Siebel (6) this assumption is the more justifiable the less the height of the forging in comparison to its width.

Assuming unidirectional flow we may derive[2] the equation for the specific pressure on a small element dx wide at a distance x from the nearest free surface, Fig. 1.

[2]The complete derivation for this and other equations is given in the appendix.

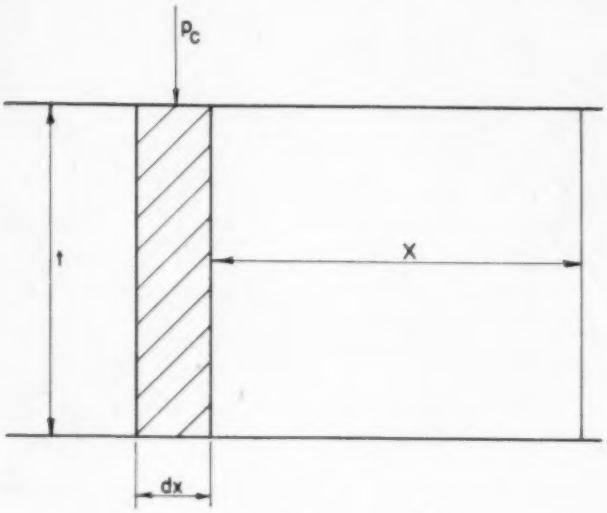


Fig. 1—Element of Specimen Compressed Between Flat Plates.

$$P_e = K_f e^{2\mu x/t} \qquad \text{Equation 1}^3$$

where: P_e = Specific forging pressure at a distance x from the nearest free surface
K_f = Deformation resistance of the metal
e = Napierian base (2.718+)
μ = Coefficient of friction between metal and press plates
x = Distance of point from nearest free surface
t = Distance between the press plates

Starting with this general equation we may derive equations for the various special conditions encountered in forging.

Upsetting a Cylindrical Billet

Upsetting a cylindrical billet between flat plates is the simplest type of forging and therefore the expression for the pressure required in this type of operation will be discussed first; in addition, such upsetting offers a relatively simple way to obtain the values K_f and μ for any given metal under a given set of conditions.

Equation 1 is apparently valid for the condition of rotational symmetry, and applying it to a cylindrical billet of height, t, and radius, r, where t is small compared to r we may derive the equations for the average specific forging pressure, P, or the forging force, F.

[3]Nadai (7) gives a derivation for Equation 1 and also the theoretical evaluation, $\sigma = 1.155$ where σ is the tensile yield strength of metal at the forging temperature.

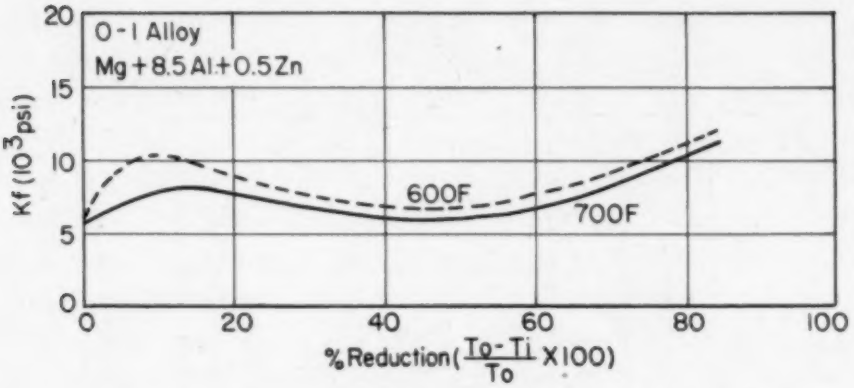


Fig. 2—Deformation Resistance, K_f, Versus Per Cent Reduction—At Press Speed of 35 Inch/Min.

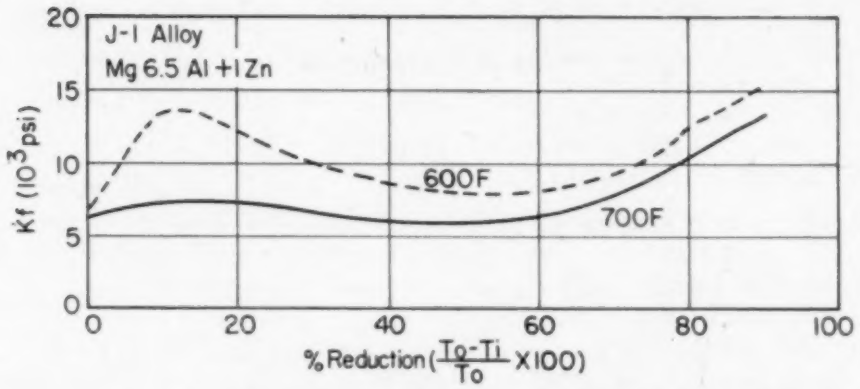


Fig. 3—Deformation Resistance, K_f, Versus Per Cent Reduction—At Press Speed of 35 Inch/Min.

$$P = 2K_fC[C(e^{1/c} - 1) - 1] \qquad \text{Equation 2}$$

or $$F = 2AK_fC[C(e^{1/c} - 1) - 1] \qquad \text{Equation 3}$$

where $C = \frac{t}{2\mu r}$

A = projected area of the billet

Equation 2 derived in Appendix offers a fairly simple method of obtaining the deformation resistance K_f, and the coefficient of friction, μ, for a given metal and alloy under a given set of conditions of temperature, per cent reduction, pressing speed and lubrication, which values are necessary to enable computation of the forces required for die forging. If two billets of different sizes are upset under the same conditions, the values of specific forging pressure, final height, and final radius may be substituted in Equation 2 for each of the billets. If the resulting equations are solved simultaneously, the values of K_f and μ can be obtained. For a nonwork hardening material (isotropic metal worked hot) this is all that is

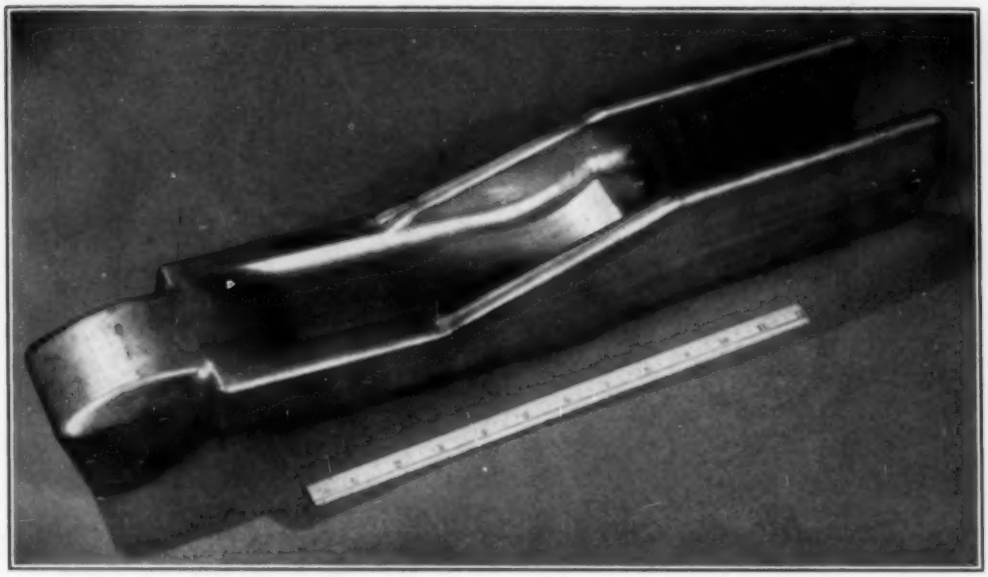


Fig. 4—A Bracket Forging. The geometrical approximation used to calculate the force for this forging is shown in Fig. 5.

necessary; but if it is a function of the per cent reduction, then the value of μ obtained in this way may be used, together with Equation 2 to convert a pressure-stroke curve to a curve of deformation resistance versus per cent reduction. Such curves have been obtained for Dowmetal J-1 and O-1, magnesium forging alloys, and are shown in Figs. 2 and 3.

It is interesting to note the drop in deformation resistance in these alloys from 10 to 50% reduction. Part of this drop is due to developed heat, but not all of it. The rise in deformation resistance after considerable deformation is believed to be due to a combination of work hardening and developing orientation.

Forces Required for Die Forging

In order to calculate in a practical way the forces required for die forging, it is necessary to make several simplifying assumptions:

1. That the flow at any point is unidirectional toward the point of least pressure.

2. That the forging in question, including the flash, can be divided into several sections of simple geometric shape and of constant thickness. In this operation small projections and bosses are neglected since their effect on the total force required is relatively small. The division of the sample forging pictured in Fig. 4 is shown in Fig. 5.

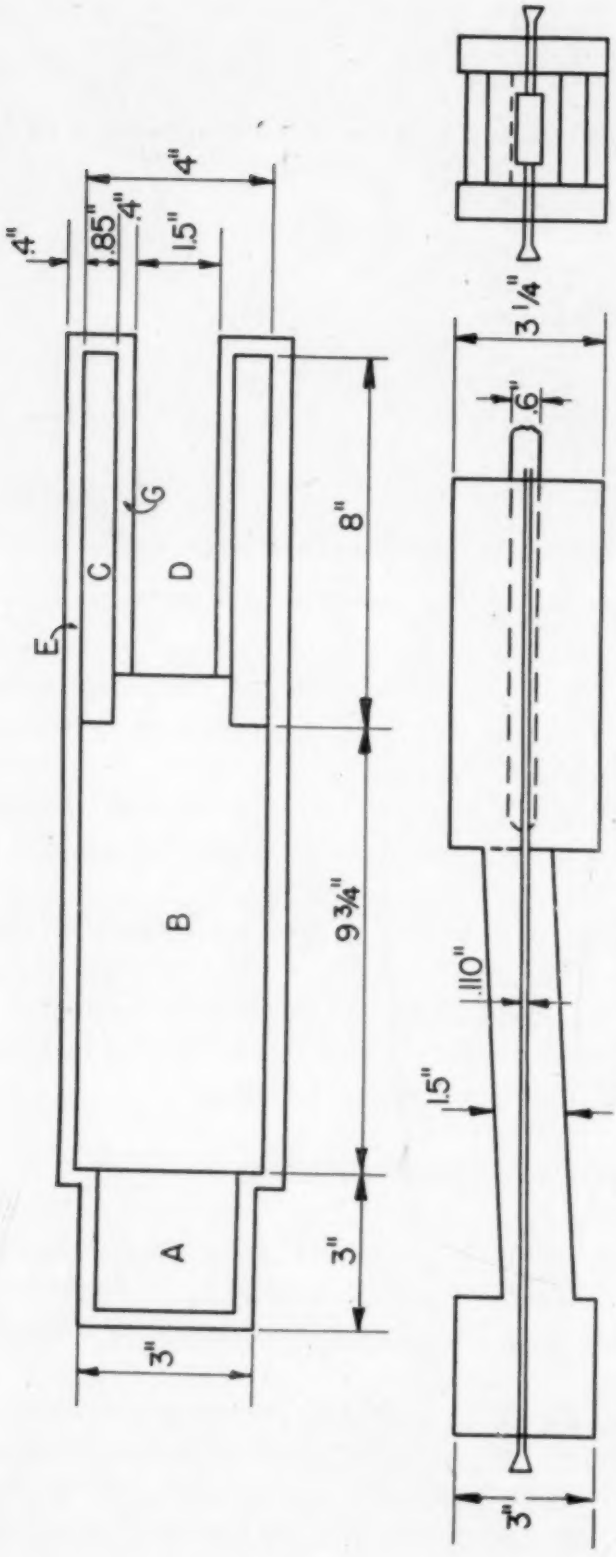


Fig. 5—Division of Forging Shown in Fig. 4 in Simple Geometric Shapes.

3. That the friction over the die area is uniform and that the deformation resistance of the metal is either uniform or a function only of the reduction.

The validity of these assumptions is shown by the reasonable correlation of calculated forces required with the experimental data available.

To calculate the force required for forging a given part, the part is divided into a number of sections of simple geometric shape and the vertical force required for each section calculated. The total force is then simply the sum of the forces upon each of the individual sections.

The force required for a given section of a forging will be the sum of the following forces:

(a) The force required to overcome the deformation resistance of the metal and the friction in this section.

(b) The force required to overcome the back pressure from the adjoining section of lower pressure toward which the metal flows.

(c) In the case where the metal flows from the section in question to a thinner adjoining section, an additional force will be required to accomplish the large amount of additional deformation necessary to extrude the metal into this thinner section.

The forging force for any given section may be calculated from the following equation:

$$F = A\,(K_f + P_b)\,C\,(e^{y/c} - 1) \qquad \text{Equation 4}$$

Where: $C = \dfrac{t}{2\mu y}$

F = vertical force upon the section
P_b = back pressure exerted by the adjoining section of lower pressure
t = thickness of the section
y = minimum horizontal distance from point of maximum pressure in section to edge of section

In Equation 4 the back pressure P_b is considered as the sum of the forces P_b' and P_b'' where P_b' is the back pressure due to friction in the adjoining section of lower pressure and P_b'' is the force of extrusion where the metal is flowing from a thick section into a thinner one.

If the metal flows from Section 1 to Section 2, the back pressure on Section 1 may be calculated from one of the following equations:

When $t_1 > t_2$

$$P_b = P_{b_2} e^{1/c_2} + K_f'' (e^{1/c_2} - 1) + (K_f' + K_f'') \operatorname{Log}_e \frac{t_1}{t_2}$$

Equation 5

When $t_1 \leq t_2$

$$P_b = P_{b_2} e^{1/c_2} + K_f'' (e^{1/c_2} - 1)$$

Equation 6

Where $C_2 = \dfrac{t_2}{2\mu y_2}$

P_b = back pressure on Section 1
P_{b_2} = back pressure on Section 2 if Section 2 doesn't open into free surface
K_f' = deformation resistance in Section 1
K_f'' = deformation resistance in Section 2
t_1 = thickness of Section 1
t_2 = thickness of Section 2
y_2 = width of Section 2
μ = coefficient of friction

Using Equations 4, 5, and 6 the forging force on any section of the forging may be calculated and, therefore, the total force required for a given die.

The Special Case Where C > 10:

In a section of a forging where the ratio of thickness to width is large so that C becomes greater than 10, the Equations 4, 5, and 6 may be simplified, for it can be shown that:

$$\lim_{C \to \infty} C (e^{1/c} - 1) \to 1$$

and Equation 4 then becomes

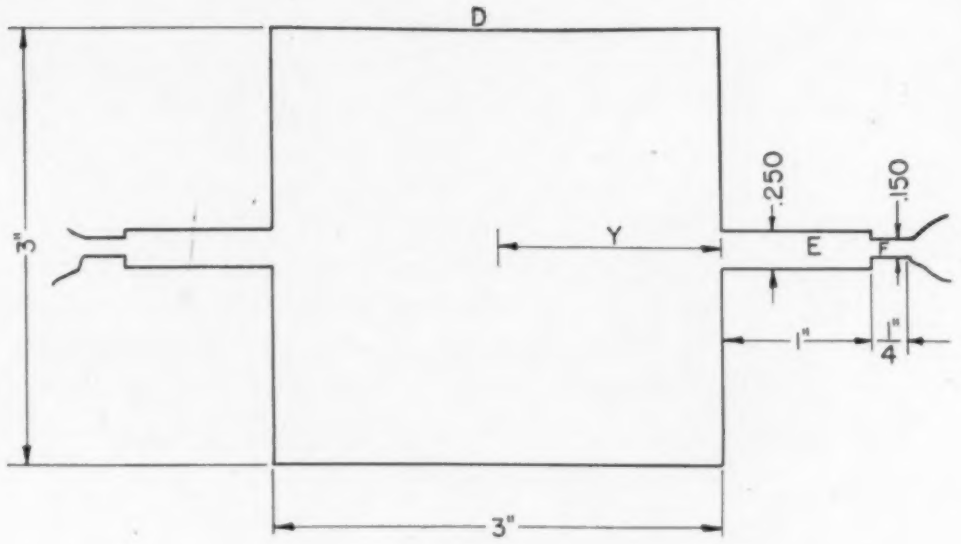
$$F = A (K_f + P_b)$$

Equation 7

Trial shows that if $C \geqq 10$ the error in assuming that $C(e^{1/c} - 1) = 1$ is less than 5%.

Sample Calculation

To show the application of the method, the force required for forging a hypothetical part of the cross section shown in Fig. 6 is calculated. The length is large compared to the width, so flow would



Length = 24"
K_{f_F} = 15,000 psi
K_{f_E} = 13,000 "
K_{f_D} = 10,000 "
μ = 0.09

Fig. 6—Cross Section of Hypothetical Forging for Calculation of Pressure.

be essentially lateral. The values for K_f and μ must be known for the metal and the conditions used. The values given are reasonable for Dowmetal J-1 alloy at 700 F on a fast hydraulic press.

The section of lowest pressure is the flash since this opens on a free edge and the calculations start with this section.

The vertical force is calculated from Equation 4.

$$F_F = A\,(K_f + P_b)\,C\,(e^{1/c} - 1)$$

$$C = \frac{t}{2\mu y} = \frac{0.150}{2 \times 0.09 \times 0.25} = 3.34$$

$P_b = 0$
$K_f = 15{,}000$ psi
$A = 14.75$ in^2
$F_F = 14.75\ (15{,}000)\ 3.34\ (e^{1/3.34} - 1)$
$F_F = 258{,}000$ lbs.

The back pressure on section E is next calculated from Equation 5 as follows:

$$P_b = P_{b_2}\, e^{1/c_2} + K_f''\,(e^{1/c_2} - 1) + (K_f' + K_f'')\,\text{Log}_e \frac{t_1}{t_2}$$

$P_{b_2} = 0$
$K_f' = 13{,}000$ psi
$K_f'' = 15{,}000$ psi

$$C_2 = \frac{t_2}{2\mu y_2} = 3.34$$

$t_1 = 0.25$ inch
$t_2 = 0.150$ inch

$$P_{b_E} = 15{,}000\ (e^{1/3.34} - 1) + (15{,}000 + 13{,}000)\ \text{Log}_e \frac{0.25}{0.15}$$

$$= 19{,}540 \text{ psi}$$

The vertical force for section E is calculated from Equation 4

$$C = \frac{0.25}{2 \times 0.09 \times 1} = 1.39$$

$$F_E = 48\ (13{,}000 + 19{,}500)\ 1.39\ (e^{1/1.39} - 1)$$
$$= 2{,}280{,}000 \text{ lbs.}$$

The back pressure on section D from Equation 5

$$P_{b_D} = 110{,}000 \text{ psi}$$

In section D, $C = \frac{3}{2 \times 0.09 \times 1.5} = 11.1$ which is greater than 10 and therefore Equation 7 may be used:

$$F_D = 72\ (110{,}000 + 10{,}000)$$
$$= 8{,}650{,}000 \text{ lb.}$$

The total force required to forge this part is then:

$$F = F_F + F_E + F_D$$
$$= 258{,}000 + 2{,}280{,}000 + 8{,}650{,}000$$
$$= 11{,}198{,}000 \text{ lbs.}$$
$$= 5600 \text{ tons}$$

Accuracy of Calculated Force

There are several assumptions in the method outlined which contribute to error in the calculated force. The principal sources of error are believed to be:

1. The assumption of simple type of flow in the metal, where the friction is uniformly distributed between the press plates.

2. The error from inability to accurately evaluate the coefficient of friction that is so often found when friction is one of many factors.

3. The assumption of unilateral flow.

4. The disregard of small projections and bosses on the forging and the division into simple geometric shapes in order to simplify the calculations.

5. The uncertainty of the true values for K_f.

Because of these and other sources of error the accuracy of the calculated force in the cases where comparison was made with experimental data was found to be about $\pm$ 20% with few exceptions. For calculations of this type this is a reasonable error and should not seriously impair the usefulness of the method.

Usefulness of Calculations

The estimation of forging pressures has always been an art requiring a great deal of experience. The above method of calculating the force required is an attempt to substitute calculation for the estimate based upon experience. It is given by the authors as another step in the direction of advancing the art of forging to the science of forging.

The authors realize that the method is somewhat laborious and complicated, and that the accuracy of the results is only fair. The method should, however, provide an approximation of the forging pressure of sufficient accuracy to be useful in the selection of the proper press and to be of assistance in die design.

In addition to the calculation of force required, the calculations have indicated that large pressure reductions may be accomplished in closed die forging by comparatively minor changes in die design, particularly in the flash dimensions.

To check experimentally the effect on pressure of changes in flash dimensions, the part shown in Fig. 12 was forged in Mg + 6.5 Al + 0.5 Zn alloy on a hydraulic press. The effect on the forging load of alterations in the flash land of the die is shown in Table I.

Table I
Effect on Forging Load of Alterations in Flash Land of Die

Forging No.	Flash		Part Thickness (Web)	Experimental Load Tons	Calculated Load Tons
	Width	Thickness			
1	0.28″	0.025″	0.156″	...	820
2	0.20″	0.025″	0.156″	550	570
3	0.10″	0.025″	0.156″	385	400
4	0.15″	0.046″	0.156″	300	350

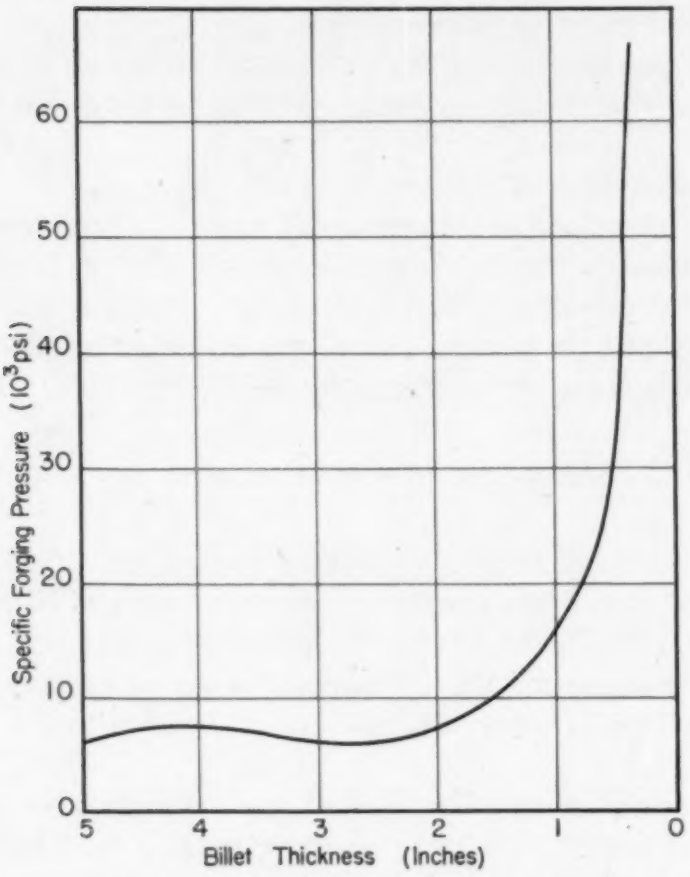


Fig. 7—Specific Forging Pressure Versus Thickness for J-1 Alloy (Mg + 6Al + 1Zn) at 700 F with Press Speed of 35 In./Min. 3⅞-inch diameter by 5-inch high billet.

Application to Magnesium Forgings

By upsetting extruded rounds of the various magnesium forging alloys, pressure stroke curves were obtained and from these graphs of K_f versus per cent reduction were calculated by means of Equation 2. Fig. 7 is a pressure stroke curve for upsetting a 3⅞-inch diameter by 5-inch high cylindrical billet of Dowmetal J-1 magnesium alloy at 700 F with a press speed of 35 in./min. and colloidal graphite lubrication. The K_f values for the same conditions were previously shown in Fig. 3.

The forging force was calculated for the aircraft links shown in Fig. 8 forged to various thicknesses and was compared with experimental data. The comparison of data is shown in Table II.

It may be seen that the agreement between theoretical and calculated values is quite good.



Fig. 8—Aircraft Links. The comparison of calculated and experimental forging forces for this part is given in Table II.

Table II
Comparison of Actual and Calculated Forging Force for Part Shown in Fig. 8

No.	Calculated Force Tons	Actual Force Tons
2	200	200
3	300	312
4	400	470
5	500	518

Appendix

Derivation of Equations for Forging Force

For frictionless compression the force would simply be equal to the deformation resistance, K_f, times the projected area. In thin sections, however, the force required is greatly increased by the friction of the metal against the press plates.

In compressing a plastic mass between flat plates, where the

length is large in relation to the width so that flow is unidirectional, the force will be distributed across the press plates as shown graphically in Fig. 9. If we take a small element dx wide at a distance x from a free surface, shown in Fig. 10a, and make a free body sketch

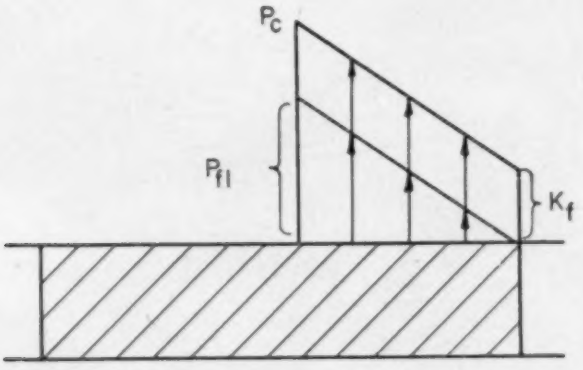


Fig. 9—Distribution of Stress in Pressing Between Flat Plates.

of this element as shown in Fig. 10b, we have, equating the sum of the horizontal forces to zero:

$$2\mu P_e dx + P_{f1}t - (P_{f1} + dP_{f1})\,t = 0$$

Where: P_e = compression force on the press plates
P_{f1} = pressure required for horizontal flow
dP_{f1} = the small increment of P_{f1}

$$\text{or} \quad 2\mu P_e dx = dP_{f1}t$$

But P_e exceeds P_{f1} by the deformation resistance, K_f

$$\text{or} \quad P_e = P_{f1} + K_f$$
$$2\mu(P_{f1} + K_f)dx = dP_{f1}t$$

$$\text{or} \quad \frac{2\mu}{t}dx = \frac{dP_{f1}}{P_{f1} + K_f} \qquad \text{Equation 1a}$$

Integrating both sides of 1a we obtain

$$P_{f1} = Ce^{2\mu x/t} - K_f \qquad \text{Equation 2a}$$

which is the general solution of 1a.

In the case where surface A is a free surface, for the boundary condition, $x = 0$, $P_{f1} = 0$

$$0 = Ce^{0} - K_f$$
$$C = K_f$$

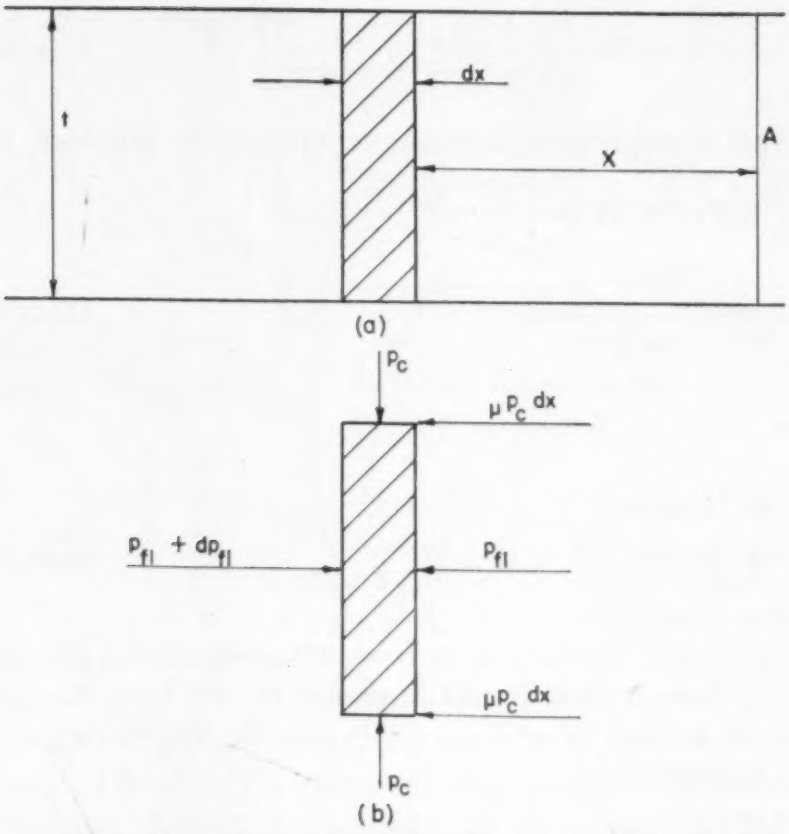


Fig. 10—Forces on Element of Forging. (a) Location of element with respect to free edge A. (b) Free body sketch of element showing forces.

and equation 2a becomes

$$P_{fl} = K_f\,(e^{2\mu x/t} - 1) \qquad \text{Equation 3a}$$

At any point, however,

$$P_e = K_f + P_{fl}$$

and substitution in Equation 3a gives

$$P_e = K_f e^{2\mu x/t} \qquad \text{Equation 4a}$$

Equation 4a is given as equation 1 in the text.

Cylindrical Billet:

Equation 4a is apparently valid for the condition of rotational symmetry, therefore the force, F, on the press plates for upsetting a cylinder of radius, r, and thickness, t

$$F = \int_0^r 2\pi\,(r - x)\,dx P_e$$

$$= \int_0^r 2\pi\,(r - x)\,dx K_f e^{2\mu x/t}$$

$$F = \pi K_f \frac{t}{\mu}\left[\frac{t}{2\mu}(e^{2\mu r/t} - 1) - r\right] \qquad \text{Equation 5a}$$

To find an expression for the average specific pressure, P

$$F = P\pi r^2 = \pi K_f \frac{t}{\mu}\left[\frac{t}{2\mu}(e^{2\mu r/t} - 1) - r\right]$$

$$P = K_f \frac{t}{r\mu}\left[\frac{t}{2\mu r}(e^{2\mu r/t} - 1) - 1\right] \qquad \text{Equation 6a}$$

If we set $C = \dfrac{t}{2\mu r}$

Equation 6a becomes

$$P = 2K_f C[C\,(e^{1/c} - 1) - 1] \qquad \text{Equation 7a}$$

Die Forging Pressure:

In Fig. 11 surface A is not a free surface but is subject to a back pressure P_b from section F and Equation 2a will have the boundary conditions at surface A of $x = O$, $P_{f1} = P_b$ and solving for these boundary conditions

$$P_{f1} = K_f\,(e^{2\mu x/t} - 1) + P_b e^{2\mu x/t} \qquad \text{Equation 8a}$$

but $P = K_f + P_{f1}$

and the pressure at any point in section D, x distance from surface A, will be:

$$P = (K_f + P_b)\, e^{2\mu x/t} \qquad \text{Equation 9a}$$

The sum of the forces acting on section D over a unit distance l will then be:

$$F = 2\int_0^y P\, dA \qquad \text{Equation 10a}$$

where y is the distance from the point of maximum pressure to surface A.

Substituting:

$$F = 2\int_0^y (K_f + P_b)\, e^{2\mu x/t}\, l\, dx$$

$$= l\frac{t}{\mu}(K_f + P_b)\,(e^{2\mu y/t} - 1)$$

but the area is equal to 2yl, therefore

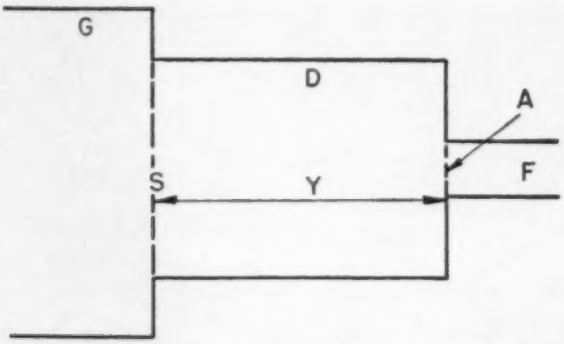


Fig. 11—Section Through Intermediate Section of Forging.

$$F = A \frac{t}{2\mu y} (K_f + P_b) \ (e^{2\mu y/t} - 1)$$

or

$$F = A \ (K_f + P_b) \ C \ (e^{1/c} - 1) \qquad \text{Equation 11a}$$

Where $C = \dfrac{t}{2\mu y}$

Equation 11a is given as Equation 4 in the text.

To use Equation 11a it is necessary to know the back pressure P_b. The back pressure is considered as the sum of the pressure P_b' produced by friction in the adjoining section of lower pressure and the pressure, P_b'', necessary to extrude from a thicker section into a thinner section.

The back pressure acting on section G in Fig. 11 due to friction in section D is simply P_{f1} at surface S or from Equation 8a.

$$P_b' = K_f'' \ (e^{2\mu y 2/t 2} - 1) + P_{b_2} e^{2\mu y 2/t 2}$$

or

$$P_b' = K_f'' \ (e^{1/c 2} - 1) + P_{b_2} e^{1/c 2} \qquad \text{Equation 12a}$$

Back pressure P_b'' is the pressure required for extrusion. Siebel (6) gives the equation for frictionless extrusion.

$$P_e = K_{f_e} \quad \text{Log.}_e \frac{A_o}{A_1} \qquad \text{Equation 13a}$$

Where: P_e = specific pressure in container
A_o = original cross sectional area
A_1 = final cross sectional area
K_{f_e} = average deformation resistance

Sachs (8), however, says that K_{fe} is larger than for other deformation processes by a factor of approximately 2 (determined on extrusion of brass). He attributes this to the very nonuniform

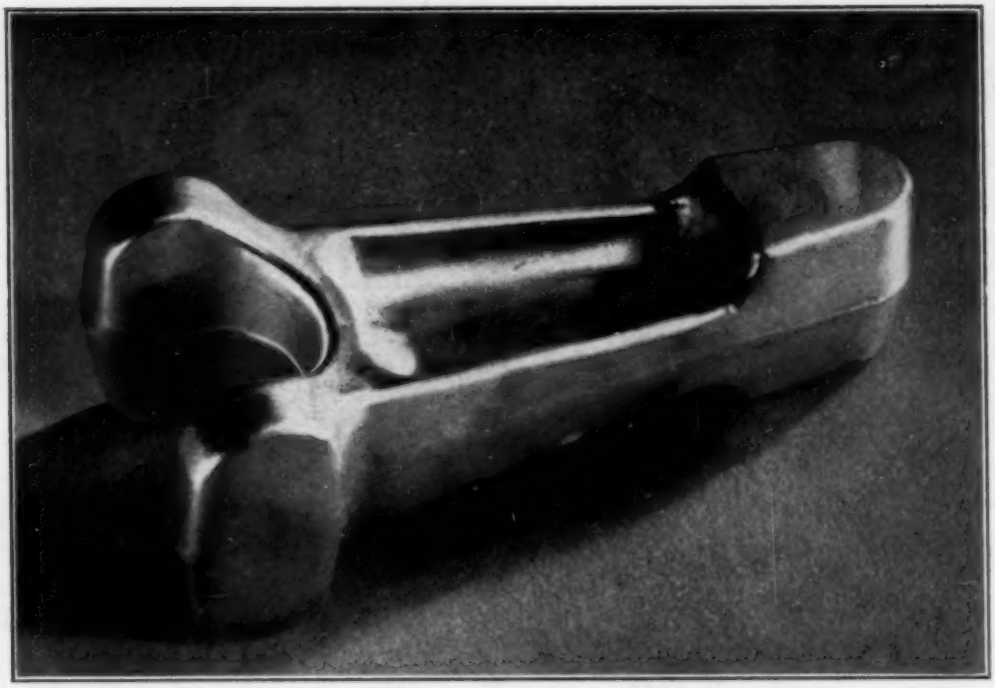


Fig. 12—Part Used for Studying the Effect of Flash Dimensions.

deformation obtained in extrusion. Adding this factor to Equation 13a and substituting terms:

$$P_b'' = 2\left(\frac{K_f' + K_f''}{2}\right) \text{Log}_e \frac{t_1 l}{t_2 l}$$

or

$$P_b'' = (K_f' + K_f'') \text{Log}_e \frac{t_1}{t_2} \qquad \text{Equation 14a}$$

Adding Equations 12a and 14a

$$P_b = P_{b_2} e^{l/c_2} + K_f'' (e^{l/c_2} - 1) + (K_f' + K_f'') \text{Log}_e \frac{t_1}{t_2} \qquad \text{Equation 15a}$$

Equation 15a is given as Equation 5 in the text. In the case where $t_2 \geqq t_1$ there is no pressure required for extrusion and the last expression of Equation 15a drops out giving Equation 6 of the text.

Nomenclature

A = projected area

C = $\frac{t}{2\mu y}$ or $\frac{t}{2\mu r}$

e = Napierian base (2.718 . . . .)
F = forging force
K_f = deformation resistance of the metal
K_f' = deformation resistance in Section 1 of higher pressure
K_f'' = deformation resistance in Section 2 of lower pressure
K_{fe} = average deformation resistance in extrusion
P_c = pressure on compression plates
P_{fl} = pressure required for flow, parallel to the plates
P_b = back pressure from adjoining section
r = radius of cylindrical billet
t = thickness, or distance between press plates
y = distance of metal flow from point of maximum pressure to edge of section
μ = coefficient of friction
1, 2, D, E, F, etc., when used as subscripts refer to a particular section of the forging

References

1. A. Beck, "The Technology of Magnesium and Its Alloys," F. A. Hughes and Co., Ltd. (London), 1940.
2. A. Zeerleeder and R. Irmann, "Power Consumption in Forging and Pressing Aluminum Alloys," *Light Metals Research*, Vol. 4, 1935, p. 3. Translated from *Z. Metallkunde*, July 1935.
3. E. V. Crane, "Plastic Working of Metals," John Wiley and Sons (New York), 1932.
4. C. W. Lucas, "Press Work Pressures," McGraw-Hill Book Co. (New York), 1935.
5. W. Naujoks, "Forging Handbook," American Society for Metals (Cleveland), 1939.
6. E. Siebel, "The Plastic Forming of Metals," *Steel*, Oct. 16, 1933, to May 7, 1934.
7. A. Nadai, "The Forces Required for Rolling Steel Strip Under Tension," *Transactions*, American Society of Mechanical Engineers, Vol. 6 (2), (1939), p. A-54.
8. G. Sachs and K. Van Horn, "Practical Metallurgy," American Society for Metals (Cleveland), 1940.

DISCUSSION

Written Discussion: By John Alico, Briarcliff Manor, N. Y.

Apparently the authors of this paper assume that the temperature throughout the forging operations, as described by them, is constant. Temperature in any metal deformation process is an important factor and should be considered. In press forging operations, the exposure of large surface areas such as die faces and the exterior of the forging stock would indicate a rapid loss of heat between the time the forging stock is placed in the press and the time when forging begins. Consideration of this loss of heat as a variable may tend to reduce the $\pm$ 20% error in the accuracy of the calculated force as outlined by them.

The authors note the drop in deformation resistance from 10 to 50% reduction for the J-1 and O-1 alloys and state that this is due in part to developed heat. It would be interesting to plot a graph showing the relationship between the drop in the resistance to deformation and rise in temperature. Of course, there is a limit to how high this temperature can be, particularly in the case of magnesium alloys because of their tendency to hot-shortness.

The authors should be complimented for their analysis of the problem and the simplicity with which they presented this analysis.

Authors' Reply

Certainly, as shown by Figs. 2 and 3 of the paper, temperature has a very important effect on the deformation resistance of metal and consequently on the forging pressure. Since the die and metal temperatures can be taken into account when the deformation resistance is determined, the usefulness of the calculations is not impaired. Figs. 2 and 3 were obtained with the same die and metal temperatures.

Upsetting a billet of magnesium + 8.5% aluminum + 0.5% zinc, 50% at 600 F results in a theoretical temperature rise of only 30 to 40 F even if there were no heat loss whatsoever. Examination of Fig. 2 will show that this rise is insufficient to account for the drop in deformation resistance which occurs between 10 and 50% reduction.

PLASTIC DEFORMATIONAL ANALYSES ON PURE MAGNESIUM

By Louis A. Carapella and William E. Shaw

Abstract

Plastic deformational effects on pure polycrystalline magnesium metal were investigated according to the ball indentation methods proposed by Meyer and Hargreaves. Empirical indices defining both work hardening and plastic flow properties have been evaluated under several conditions.

Unlike most metals, the results from tests on magnesium rod showed a definite departure from the Meyer law at high loads. Even the Hargreaves plastic flow coefficient exhibited an anomalous behavior within this range. Tri-dimensional stress components induced by the ball indenter at high loads on a polycrystalline system having a large degree of preferred orientation is the proposed explanation.

That plastic flow of magnesium metal can be augmented through the action of a supplemental flow mechanism has been disclosed. Effects from this and other sources on the technical hardness values of magnesium metal under the Brinell and Meyer tests have also been considered.

Introduction

WHILE the fundamental behaviors of magnesium single crystals to deformational stresses have been relatively well established from the outstanding experiments of Schmid and collaborators (1),[1] and of Bakarian and Mathewson (2), there is, however, a scarcity of recorded information concerning the nature of polycrystalline magnesium metals subjected to similar stresses. The present investigation was therefore undertaken to augment the existing knowledge on the deformational characteristics of wrought magnesium metal and to

[1] The figures appearing in parentheses pertain to the references appended to this paper.

A paper presented before the Twenty-eighth Annual Convention of the Society, held in Atlantic City, November 18 to 22, 1946. The authors are Senior and Junior Fellow, respectively, on the Multiple Fellowship on Magnesium at Mellon Institute of Industrial Research, Pittsburgh. Manuscript received June 29, 1946.

establish some empirical indices by which to define polycrystalline behaviors under specified conditions of stress.

Of the many possible approaches to plastic deformational studies of metals, the methods proposed by Meyer (3) and Hargreaves (4) were selected for reasons of accuracy and simplicity. It was possible to evaluate the index of work hardening by the former method and the index of plastic flow by the latter method of analysis. Such variables as magnitude of load, mode of loading, time, and grain size have been systematically analyzed. From this research certain indices and other relationships have been established by which the plastic deformational nature of magnesium may be defined.

Experimental Details

The original Meyer analysis involved the application of a load onto a ball penetrator for a specified time interval followed by the measurement of the diameter of the recovered impression. Next the ball was placed concentrically in the previous impression whereupon a larger load was applied for the same time and again, upon the removal of the load, the size of the impression was measured. This procedure was continued within the limits, $0.1 < d/D < 1$, where d is the recovered diameter of the impression and D the diameter of the ball penetrator. Inasmuch as an integrated effect was accomplished by this method, a single specimen was required for a complete test involving constant time of loading.[2]

In order to isolate any integrated effects, a modified procedure was followed in the present work in which a single unstrained specimen was employed for each load-time test.[3] Apart from this modification, the data were subjected to a similar analysis.

For the Hargreaves analysis dealing with the effect of the load duration on the recovered diameter, two different procedures were employed, one involving the use of an unstrained specimen for each time-load test, and the other the same specimen for each load test with variation in time.

A Brinell hardness testing machine calibrated by the Pittsburgh Testing Laboratory and a 10-mm tungsten carbide ball penetrator[4] were used throughout this work. A total of eight different loads, varying from 250 to 3000 kg, and five load durations of 15, 30, 60,

[2] This procedure is designated as integrated load-time test throughout this paper.

[3] For this modification, the term direct load-time test is used.

[4] The average of five measurements made at different positions on the ball was 0.39368 $\pm$0.00003 inch (or 9.9995$\pm$0.0008 mm).

120, and 180 seconds were employed. All recovered diameters were measured with a traveling microscope accurate to ± 0.002 mm. The average of four measurements made at 45-degree intervals along the diameter of an impression was selected as the final value.

Specimens from extruded magnesium rods around 1.8 inches in diameter were employed. The composition of the material was as follows:

	Per Cent
Aluminum	0.002
Copper	0.007
Iron	0.03
Manganese	0.04
Nickel	0.001
Silicon	0.001
Magnesium	Balance

Other Factors Affecting the Analyses

The factors which might affect the analyses under consideration have been critically reviewed by O'Neill (5). Of utmost importance to this particular investigation are the following variables:

(a) Composition
(b) Residual stresses
(c) Crystal orientation
(d) Grain size
(e) Testing temperature
(f) Specimen dimensions
(g) Deformation of ball penetrator
(h) Rate of loading
(i) Normality of test surface to load axis, and
(j) Duration of load.

The variable of composition was fixed by selecting pure magnesium. All specimens were subjected to a stress-anneal treatment after polishing and etching the testing surface by heating at 200 C for 1 hour; they were therefore rendered stress-free.

Owing to the fact that, according to Morell and Hanawalt (6), a strong tendency for directionality of crystal orientations exists in extruded magnesium bars,[5] all tests were conducted on surfaces normal to the extrusion axis. Consequently the mechanism of plastic deformation was somewhat fixed in all tests. The grain size was kept constant in all cases except where its effect was directly investi-

[5] They observed that in extruded magnesium bars the basal planes of hexagonal crystals tended to orient themselves parallel to the direction of extrusion, while other crystallographic planes had a more or less random distribution about the main axis.

gated.[6] For this study a number of fine grain specimens were coarsened by heat treatment to give a wide range of grain sizes.

The remaining variables deal essentially with testing conditions. All tests were conducted at around 25 C. This factor was maintained constant, for temperature is known to have a profound influence on the plastic nature of metals, especially within the recrystallization range. Specimen size is also very important in attaining true plastic behaviors. The dimensions should be such that neither bulging on the sides nor "mark-through" at the bottom is experienced in the test specimen. The size factor has received considerable attention, notably by Moore (8), by Petrenko and coworkers (9), and by Rajakowicz and Maier (10). They have generally agreed that errors from this source may be avoided under these conditions:

(a) Specimen thickness should be at least 7 times the depth of the ball impression;
(b) Distance between the impression and the edge of specimen should be at least 2 times the diameter, and
(c) Distance between impressions should be at least 4 times the diameter.

Throughout this work specimens with about 1.8 inches in diameter and 1.5 inches in length were employed. No evidences of bulging or extrusion effects were noted on any specimen after testing.

To avoid any incongruent effects on impression diameters resulting from unduly great distortion of the ball penetrator, especially at very high loads, a tungsten carbide ball was installed on a testing machine. Considering that the tungsten carbide has a Young's modulus $E = 79 \times 10^6$ psi compared to $E = 6.4 \times 10^6$ psi for magnesium, errors from this source may be regarded as insignificant.

The effect of load-rate was examined by Petrenko and associates (9) and found to be immeasurable for loading rates up to 500 kg per sec. on most metals. Special care was taken in this work to conform with that limitation.

Errors due to the lack of normality between the load axis and test surface of a specimen were also investigated by Petrenko and associates (9). The disparity of this factor was considered small, provided the angle between the load axis and the normal to the test

[6] In all tests, except where specified, specimens having an average grain size diameter of 0.0010 inch were employed. The grain sizes reported herein were determined from representative photomicrographs according to the following formula suggested by Jeffries (7): $d = \sqrt{A/M^2G}$, where d is the average grain diameter, and G the number of grains in area A at a linear magnification of M.

surface did not exceed 2%. In this research all specimens were carefully machined with test surfaces normal to the load axis.[7]

The factor of load duration depends on the magnitude of the load and the nature of the material under test. As already mentioned, this effect will be considered under the Hargreaves analysis.

Analysis of Experimental Data

Meyer Analysis—The Meyer analysis of the data derived from the procedures described involved the use of this relationship:

$$L = a\,d^n \qquad \text{Equation 1}$$

or

$$\log L = n \log d + \log a \qquad \text{Equation 2}$$

where

L = applied load
d = recovered impression-diameter
n = constant (or index of work hardening), and
a = constant (experimental).

The most probable values of the Meyer constants, n and a, were obtained analytically by the method of least squares (12), which was applied to data obtained from both the integrated and direct load-time tests.

In considering the over-all data, the present results showed the residuals[8] in every case to vary according to a regular curve instead of the usual random fashion. The maximum variation was about 4% and it occurred at around 1350 kg.[9] Inasmuch as this disparity is far in excess of any experimental error, it can only indicate that the over-all data conform none too well with the Meyer equation (see Equation 1). This departure is also apparent in the graph depicted by Fig. 1.

Further study of our results revealed the Meyer equation to hold within 0.5% in every case between two load-ranges, one from 250 to 1500 kg and the other from 1500 to 3000 kg. The Meyer constants differed, naturally, for both ranges. All data, therefore, were analyzed within the two ranges already discussed and in the over-all condition for a specified time test. The results from the integrated load-time tests are set forth in Table I and from the direct load-time tests in Table II.

Grain Size Effects—The influence of grain size on the Meyer

[7] As a point of interest it can be mentioned that Templin (11) in his work with light metals was unable to detect any effect from lubricants present on test surfaces under the Brinell tests.

[8] Residuals imply the differences between calculated and observed impression-diameters.

[9] This deduction was made from a graphical plot of the residuals against the testing loads. The actual curve was approximately parabolic.

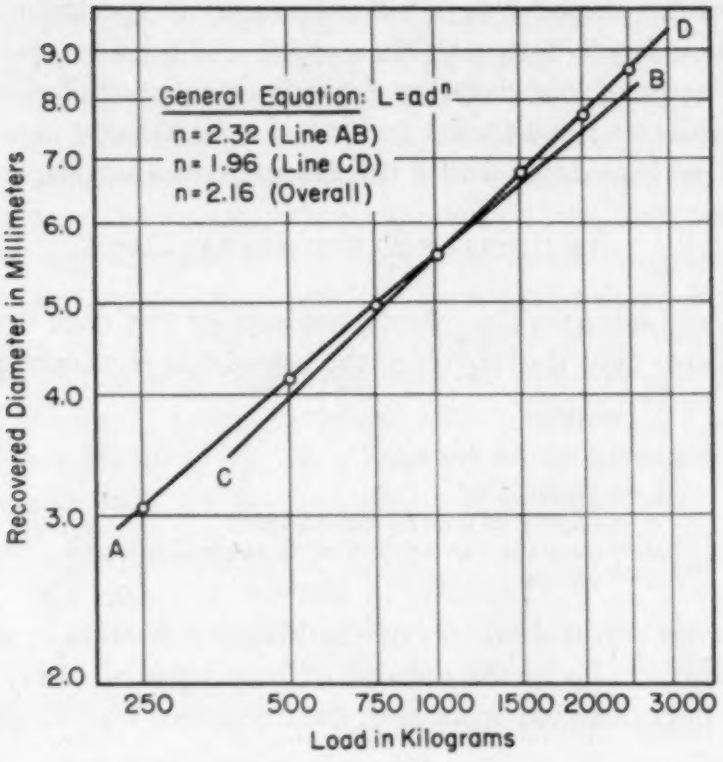


Fig. 1—Departure from the General Meyer Law under the Integrated Load-Time Tests for a 180-sec. Increment on Annealed Extruded Magnesium Rod. (Average grain size diameter = 0.0010 inch.)

constants was also studied over a relatively wide range of grain diameters. For this work the integrated load-time testing with a 180-second time increment was employed. These data were likewise fitted analytically to the Meyer equation under the three conditions already discussed by the method of least squares. The results are presented in Figs. 2 and 3.

Hargreaves Analysis—The Hargreaves analysis, on the other hand, considers the relationship between diameter and duration of

Table I
Meyer Constants, a and n, for Annealed Magnesium Rod Under Integrated Load-Time Tests for Various Time Increments

(Average Grain Size Diameter = 0.0010 Inch)

Time Increment (sec.)	Load Ranges in Kg: 250 to 1500		1500 to 3000		250 to 3000	
	a_{10}	n	a_{10}	n	a_{10}	n
15	20.0	2.30	36.3	1.98	24.4	2.17
30	19.6	2.30	33.8	2.00	24.7	2.15
60	19.2	2.30	37.8	1.94	24.1	2.15
120	17.8	2.32	33.7	1.98	22.8	2.17
180	17.7	2.32	34.7	1.96	22.9	2.16

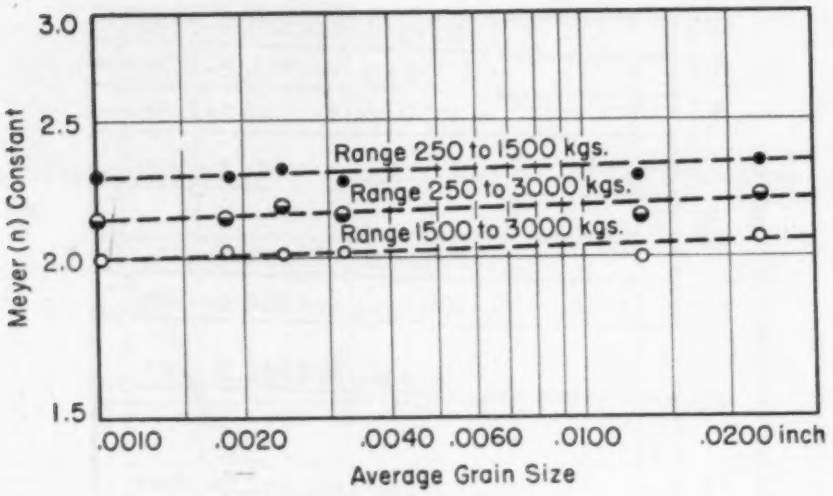


Fig. 2—Effect of Grain Size on the Meyer Constant, n, under the Integrated Load-Time Tests for a 180-sec. Increment on Annealed Extruded Magnesium Rod.

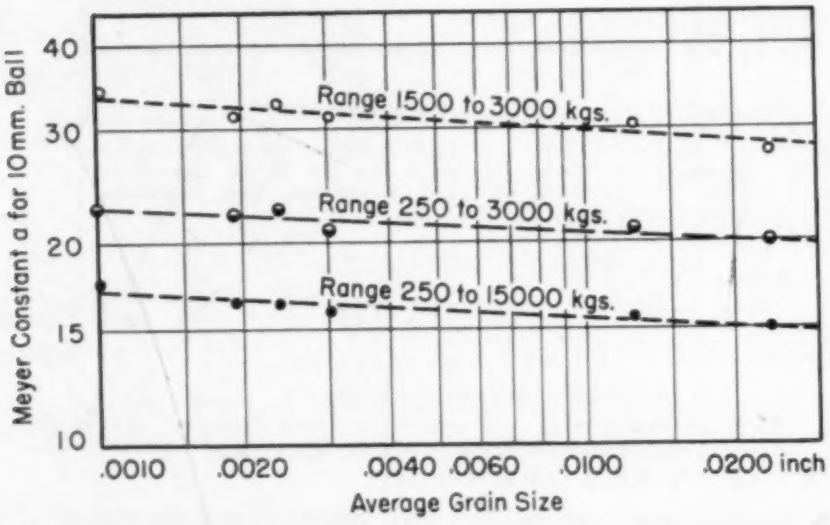


Fig. 3—Effect of Grain Size on the Meyer Experiment Constant, a, under the Integrated Load-Time Tests for a 180-sec. Increment on Annealed Extruded Magnesium Rod.

Table II
Meyer Constants, a and n, for Annealed Magnesium Rod Under Direct Load-Time Tests for Various (Total) Times

(Average Grain Size Diameter = 0.0010 Inch)

Total Time (sec.)	Load Ranges in Kg: 250 to 1500		1500 to 3000		250 to 3000	
	a_{10}	n	a_{10}	n	a_{10}	n
15	20.5	2.29	28.6	2.11	23.1	2.22
30	21.2	2.26	27.4	2.12	22.6	2.22
60	19.9	2.30	36.4	1.99	23.0	2.21
120	18.5	2.33	34.9	2.00	22.2	2.22
180	19.1	2.30	30.4	2.05	22.6	2.19

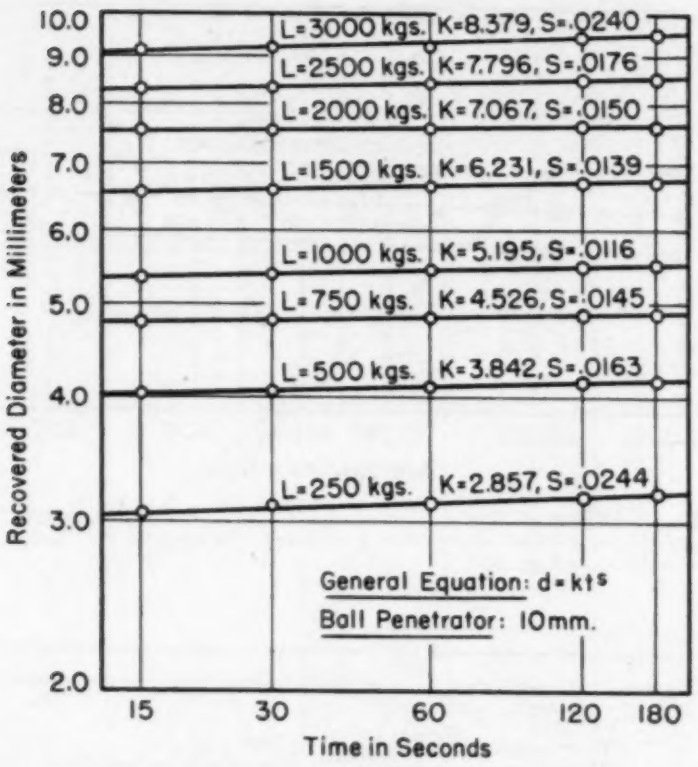


Fig. 4.—Influence of Load-Duration on the Recovered Diameter for Various Loads under the Direct Load-Time Tests on Annealed Extruded Magnesium Rod. (Average grain size diameter = 0.0010 inch.)

loading. Accordingly,

$$d = kt^S \qquad \text{Equation 3}$$

or $$\log d = S \log t + \log k \qquad \text{Equation 4}$$

where d = recovered impression-diameter
t = time
S = constant (or index of plastic flow), and
k = constant (experimental).

This logarithmic expression has been found to hold in many instances within the range from 5 to 1200 seconds of loading time. For much longer times the equation, according to O'Neill (5), is not always valid. In order to obtain the most probable values of the Hargreaves constants, S and k, the data were all fitted analytically to the above equation by the method of least squares. The constants for various loads along with a plot of the experimental data are given in Fig. 4. They are also illustrated in Fig. 5 for the various loads. The experimental constant, k, was found to vary with load according to this equation:

$$L = 21.65\, k^{2.89}. \qquad \text{Equation 5}$$

This expression is similar to the Meyer equation, which should

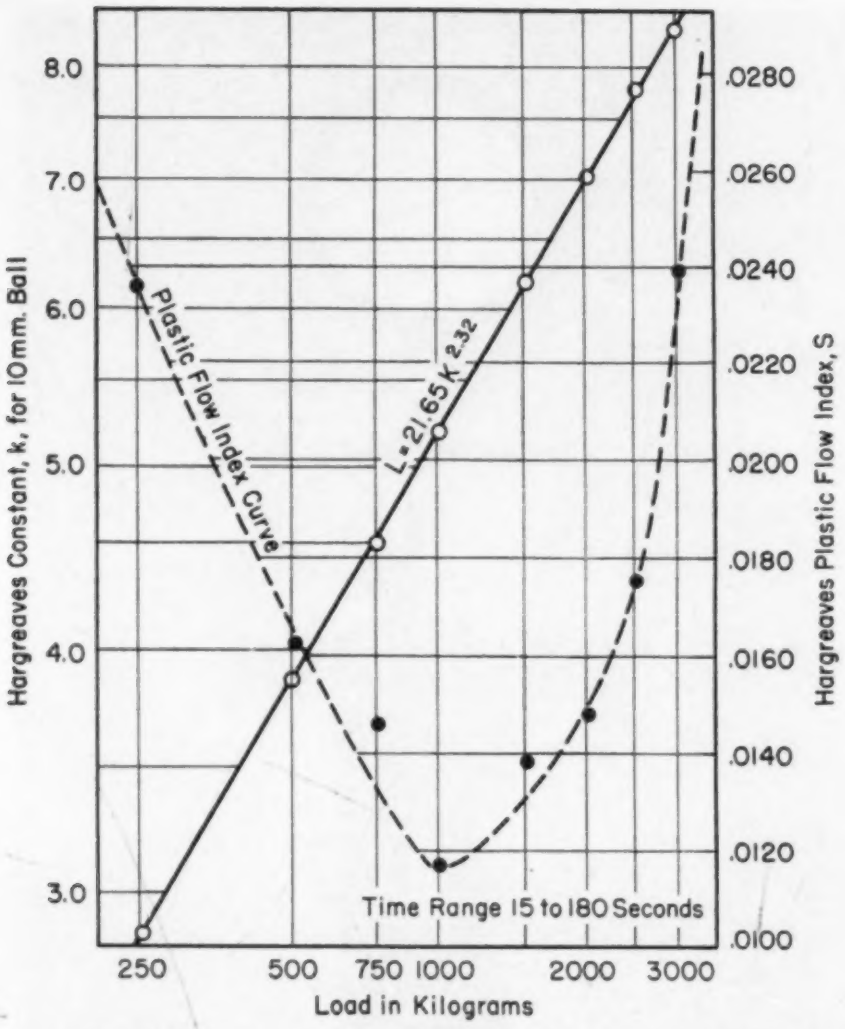


Fig. 5—Influence of Test-Loads on the Hargreaves Constants, S and k, for Annealed Extruded Magnesium Rod under the Direct Load-Time Tests. (Average grain size diameter = 0.0010 inch.)

not be at all surprising, inasmuch as k may be regarded under these conditions as the value of the diameter of an impression produced by a load acting for 1 second on a 10-mm ball. No simple relationship could, however, be established for the plastic flow index curve.

Loading Effects—To study the effect of the mode of loading on the Hargreaves constant S (plastic flow index), three different procedures were followed, all involving a 1000-kg load. The first employed a single specimen for each time of loading (direct load-time test). In another, a single specimen was used for the entire run and the diameters were measured at different times under load with an Ames depth measuring gage,[10] as shown in the set-up illustrated in

[10]The diameter was computed from the equation $d = 2\sqrt{h(D - h)}$, where D = diameter of the ball penetrator and h the depth of the impression.

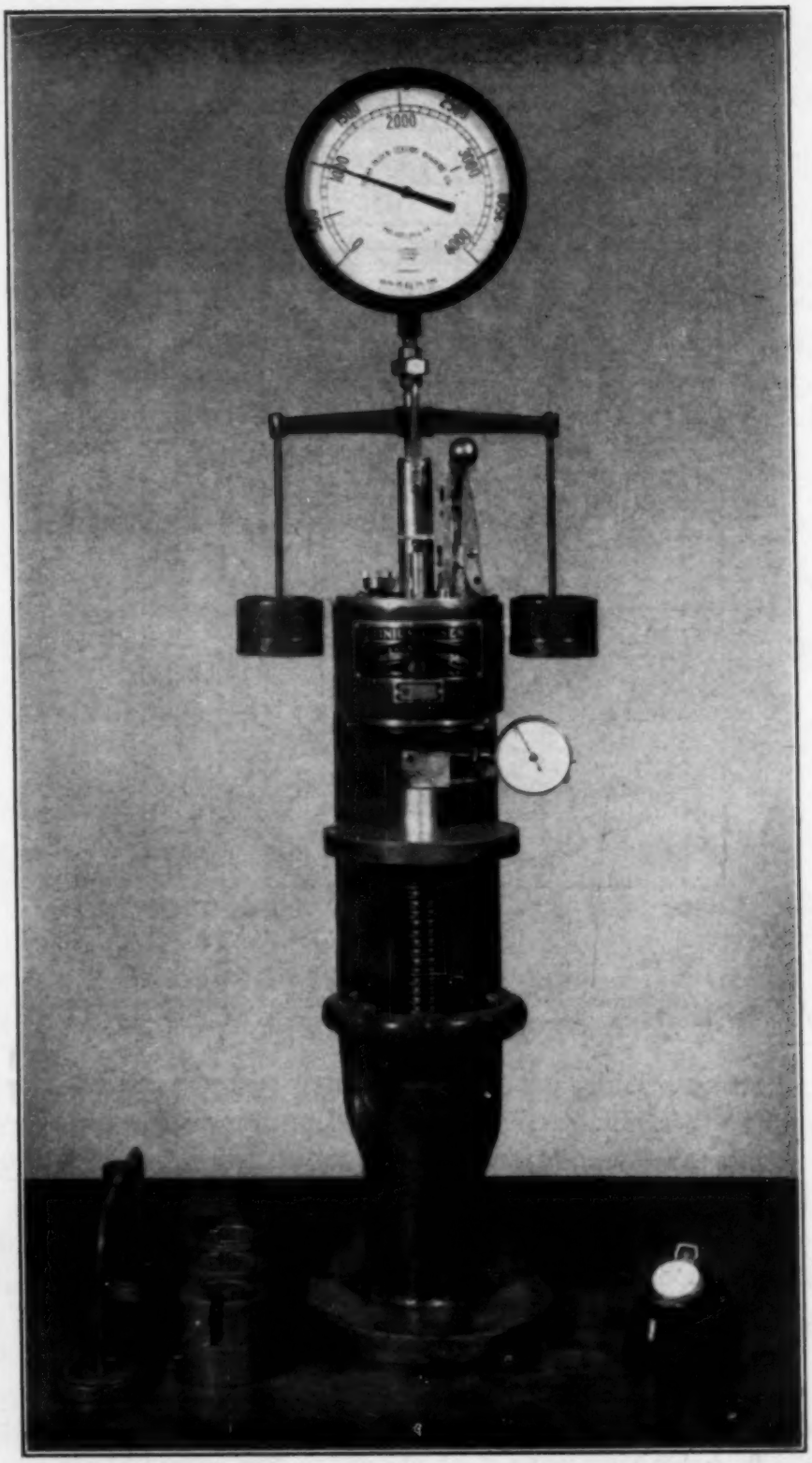


Fig. 6—Set-Up Illustrating the Test Confirming the Hargreaves Law on Annealed Extruded Magnesium Rod with a 1000-kg Test Load and an Ames Depth Measuring Gage.

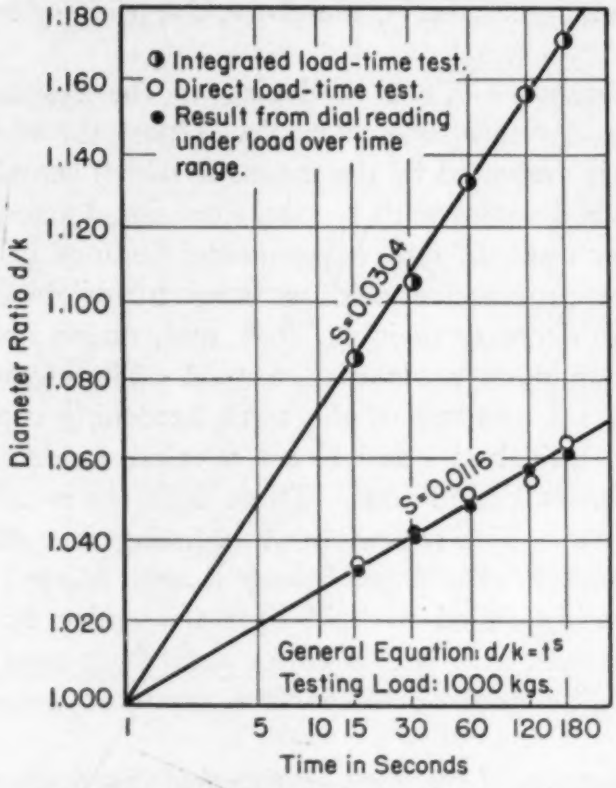


Fig. 7—Influence of the Mode of Loading on Hargreaves Plastic Flow Constant, S, for Annealed Extruded Magnesium Rod. (Average grain size diameter = 0.0010 inch.)

Fig. 6. For the third procedure the integrated load-time method was adopted in which the same specimen was used and the loading time was considered additive after each measurement of diameter. The results from the three different tests are presented in Fig. 7.

Discussion of Results

Wherever magnesium crystals are subjected to deformational stress they undergo plastic flow which proceeds by two fundamental mechanisms, i.e., slip and twinning (1), (2). Slip or gliding takes place at atmospheric temperatures[11] along the basal plane (0001) and in the direction of closest packing of atoms [11$\bar{2}$0] (digonal axis I). Twinning, on the other hand, occurs along the pyramidal plane (10$\bar{1}$2) and about a possible [10$\bar{1}$2] twinning axis with rapidity by well-defined shearing movements of adjacent atomic planes. Mechanical twinning is regarded as a supplemental operation, for by its action slip planes are brought into favorable orientations for

[11] At higher temperatures other slip planes within the magnesium lattice become operative (see particularly references 2 and 6).

further deformation. Slip is, therefore, the primary mechanism for plastic flow.

Meyer Analysis—Work hardening is the resistance which a metallic system develops to further slip. Under the Meyer analysis[12] the resistance is evaluated by the index, n, which actually defines the rate with which d varies with L (see Equation 1) and is unique of the metal under test. In fact, experimental findings (5) conclusively show that the progressive cold working of originally unstrained metals tends to decrease their n-values, and, under severe deformations, the Meyer index becomes equal to 2. Therefore (n—2) may be considered as a measure of the work hardening capacity.

Contained in Tables I and II are n-values as determined under various experimental conditions. Three different n-values are listed for each test run. The reason for this listing was disclosed in an earlier discussion in this paper where it was pointed out that the Meyer relationship failed to hold over the entire load-range (see Fig. 1), but instead held with a closer agreement over two separate load-ranges. The point of departure occurred generally around 1500 kg.

An examination of our data reveals that magnesium has a larger work hardening capacity in the lower load-range (250 to 1500 kg) than in the higher range (1500 to 3000 kg). Actually the n-values for the higher range are around 2 or less. The over-all treatment of the data gives an intermediate value of the work hardening capacity. For comparison some Meyer constants from other sources are given in Table III.

Table III
Meyer Constants for Pure Magnesium

a_{10}	n	Source
26.2	2.29	Mahin and Foss (13)
21.9	2.18	Krupkowski (14)
18.1	2.35	O'Neill (5)

Of supplemental interest is the fact that a linear relationship results where the Meyer constants from the low, high, and over-all load ranges are plotted as shown in Fig. 8. Only the data for the 180-second load duration are presented in the figure. Similar curves also exist for other data but differ only in the values of the constants, b and c. The relative positions of the corresponding curves for the

[12] The analysis holds only for ball indentors and not for cone or pyramid penetrators.

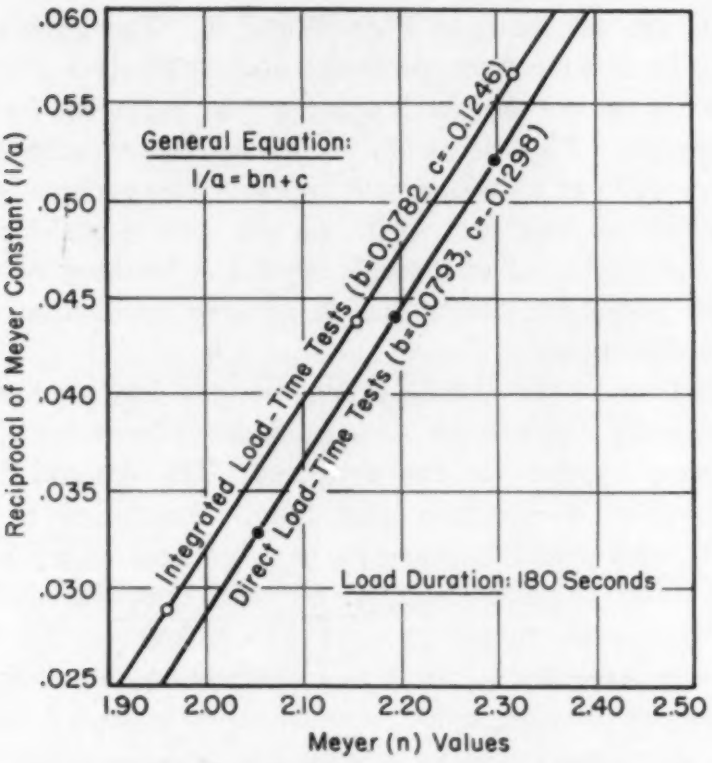


Fig. 8—Relationship Between the Meyer Constants, n and a, for Annealed Extruded Magnesium Rod under Two Modes of Testing. (Average grain size diameter = 0.0010 inch.)

two methods of testing are generally displaced, as shown in Fig. 8. An explanation for this difference may be contained in the postulation advanced by Dorn and Thomsen (15) to account for the anomalous effects on the apparent elastic modulus of magnesium. They assumed that "retwinning" tends to occur as soon as the compressive stresses are relieved. The effect of this factor may be introduced only in the cases of the integrated test procedures for which the same specimen is employed during the entire run.

While the results from the two test procedures show comparatively little or no effect on the n-values in the lower ranges, some differences are evident in the other ranges. These observations suggest that another factor may be introduced in the mode of plastic flow at the higher load-range, which evidently must depend on both the magnitude of load and procedure of loading. More attention to this factor will be given later.

Variations in the Meyer constants can also occur through changes in the grain size of the metal. An attempt was made to evaluate this effect on extruded magnesium rods having a wide range of grain sizes;

the results are set forth in Figs. 2 and 3. The general indication appears to be that the finer grain size aggregate gives a lower n-value and higher a-value than the coarser grain specimen, irrespective of the load-range. This deduction is in agreement with the findings of Norbury (17) in his work with copper. The general behavior may be explained by the fact that, as the polycrystalline metal approaches the conditions of a single crystal, it becomes relatively more plastic, for boundary effects due to adverse orientation of adjacent grains are diminished.

Regardless of the testing procedure, the load maintenance time factor generally introduced no significant effects on n-values but showed some changes in the a-values. The general trend seems for the a-values to decrease with time. According to Kurth and others (5), this trend appears to be a general rule for most soft metals at room temperature. At elevated temperatures, and especially in the plastic range, pronounced changes in the Meyer constants can be expected. For this investigation, however, the effect of temperature was regarded nonoperative inasmuch as all determinations were conducted at around 25 C.

Hargreaves Analysis—Resistance to plastic flow under a constant load was considered in the light of the Hargreaves analysis. Our results along with derived Hargreaves constants are presented in Fig. 4. A further treatment of the data is illustrated by Fig. 5. There are two direct deductions which can be drawn from this study, namely:

(a) The constant, k, is directly related to the applied load, and
(b) The plastic flow index (S) curve is somewhat parabolic in shape, having a minimum at around 1000 kg.

The first deduction is explained on the basis that the k-values may be considered as impression-diameters produced by a load acting for 1 second on a 10-mm ball and therefore they satisfy the Meyer relationship (see Equations 1 and 5). Furthermore, the constants are in the proper relation with those given in Table II. The second, however, shows the rate of plastic flow to decrease sharply and then increase for loads greater than 1000 kg. This condition suggests the operation of a supplementary mode of plastic flow.

The plastic flow rate as measured by the Hargreaves index, S, is also susceptible to the method under which the test is conducted

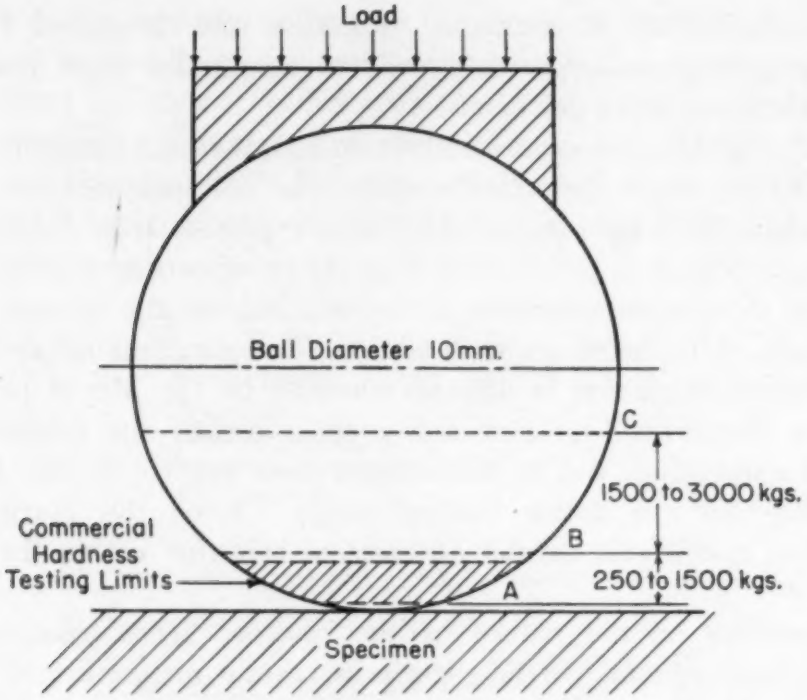


Fig. 9—Illustrating the Zones of the Ball Indentor Employed for Plastic Analysis and for Commercial Hardness Testing.

(see Fig. 7). Three different procedures were employed with a test load of 1000 kg; two gave the same results and the other differed markedly. In the case where a greater rate resulted, a single specimen was used. Normally about 15 minutes elapsed between each application of load, during which time interval, or upon the release of loading, some "retwinning" might have occurred to account for the difference.[13] Owing to the very nature of the other tests, this factor had no influence on their results. The importance of this study is brought out by the fact that a greater plastic flow may be attained in magnesium by the intermittent applications of a given load than by the continuous action of it over the same period of time.

Other Related Evidences

Under the action of the ball penetrator, magnesium metal experiences a "sinking-in" type of impression. From an extensive survey of ball impressions, Norbury and Samuel (17) concluded that "sinking-in" indentations are characterized by metals having considerable ability for strain hardening. Heyer (18) in his work

[13] No measurable changes were noted in the impression-diameters during this interval of time.

with magnesium alloys confirmed this view and developed further that this type of an impression resulted essentially from relatively large underlying shear deformation.[14]

In the light of our experimental findings, it seems that a modified stress pattern might be introduced by the ball indenter for loads greater than 1000 kg (or for d/D values greater than 0.52). By referring to Fig. 9, it can be seen that the tri-dimensional stress pattern must change continuously as the ball indents the specimen (or as the ratio, d/D, increases with load). The resultant behavior for metals under this action is defined normally by the Meyer relationship (see Equation 1). But unlike most metals the response of extruded magnesium rod to this change does not follow the Meyer law throughout the entire loading range. Even the Hargreaves plastic flow coefficients exhibit an unusual behavior within the same range.

Depending on the nature of the resolved stress components, twinning may or may not take place in certain magnesium crystals during plastic flow. Bakarian and Mathewson (2), in their work with single crystals, noted that twinning caused crystals to extend in the direction of the hexagonal axis and to contract in the direction of the basal planes.

Our testing procedures in most instances were somewhat favorable to twin formation, for it has been established that to a large extent the basal planes of crystals within an extruded bar are parallel to the extrusion axis (6). Therefore, axial compression along this axis will introduce similar stresses in the direction of the basal planes. But complexities arise in that pure axial compression is not experienced by the entire system as the ball indents the surface.

In the final analysis of these anomalies, our findings suggest the operation of a complex mechanism which must take into account the fact that changes in tri-dimensional stress patterns or resolved stress components produced by ball indentations cause slip and twinning (and possibly retwinning) to proceed within a polycrystalline aggregate having a large degree of preferred orientation. Moreover, the transition from general behaviors normally occurred around 1000 to 1500 kg (and $d/D \approx 0.6$).

Discussion on Technical Hardness

As hardness measurements derived from ball tests are related to

[14] It should be mentioned here that this fact was concluded from diameter ratios (d/D) up to 0.52. The present work, however, deals with ratios between 0.29 and 0.95, inclusively.

the resistance a metal offers to plastic deformation, the factors already discussed have a direct bearing on such measurements. In this respect we are concerned with the Brinell test, commonly used for measuring the hardness of magnesium and its alloys.

A number of Brinell hardness values were determined for pure magnesium metal from the test data and the following Brinell equation:

$$H = \frac{L}{A} = \frac{2L}{\pi D\,(D - \sqrt{D^2 - d^2})} \qquad \text{Equation 6}$$

wherein: L = applied load
A = contact spherical area
d = recovered impression-diameter, and
D = ball diameter.

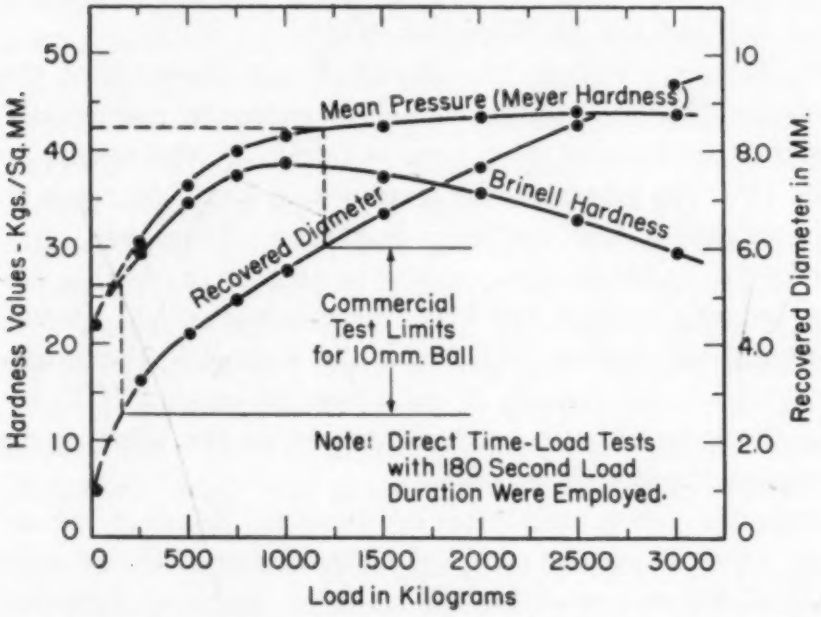


Fig. 10—Variation of Brinell and Meyer Hardness Values with Test-Loads for Annealed Extruded Magnesium Rod. (Average grain size diameter = 0.0010 inch.)

The results for various testing loads are shown in Fig. 10. Two points of technologic importance are clear from this study: (a) the inherent hardness of the metal cannot be determined by this method, as evidenced by the variation in hardness values, and (b) a decrease in hardness values is experienced at higher loads in spite of the drastic work hardening sustained by the metal during the test. This decrease is actually attributable to the geometry of the spherical impression and not necessarily to any softening effects.

Table IV
Brinell Hardness Values of Extruded Magnesium Rod Under Various Test Conditions*

(Average Grain Size Diameter = 0.0010 Inch)

Load Duration (sec.)	Testing Loads in Kg			
	250	500	750	1000
15	33.4	37.8	40.6	40.8
30	32.2	37.0	39.7	40.1
60	31.1	36.1	38.6	39.5
120	30.0	35.2	38.1	38.7
180	29.4	34.8	37.5	38.4

*Direct load-time test procedure was employed for this study. The d/D-values varied between 0.30 and 5.5.

To minimize this difficulty and to attain some standardization of test conditions (5), it has been proposed that for all commercial hardness testing d/D-values be kept between the limits of 0.25 and 0.6. As illustrated in Fig. 9, a very small portion of the indenter is actually required for hardness testing.

The influence of both the magnitude and duration of the testing loads on the Brinell hardness values of extruded magnesium, within the specified limits of d/D-values, is shown by the results contained in Table IV. An increase with testing load and a decrease with time in the hardness values are very apparent. Moreover, the rate of change in the hardness-time curves is greater in the beginning and becomes relatively small for load durations over 120 seconds. The data demonstrate further that the rate of change in the hardness-load curves gradually approaches a maximum at around 1000 kg. Considering the two extreme hardness values in the table, a maximum difference of about 40% is evident.

Obviously some uncertainties arise in deciding what Brinell hardness value should be assigned to the material under attention in so far as all values are within the specified limits of diameters. The selection is arbitrary, and for this reason it is necessary in reporting a single Brinell hardness value that the diameter of the ball, load, and time be specified, e.g., $H_{10/500/180} = 34.8$.

Table V
The General Effect of Grain Size on the Brinell Hardness Values of Extruded Magnesium Rod at Various Testing Loads

Average Grain Size (in.)	Meyer Constants*		Testing Loads in Kg†			
	n	a_{10}	250	500	750	1000
0.0010	2.30	17.0	29.9	32.0	32.9	33.3
0.0230	2.36	15.0	28.5	30.9	32.3	32.7

*These values were selected as the most probable ones from Figs. 2 and 3.
†Integrated load-time tests were employed with a 180-second time interval. The d/D-values varied between 0.32 and 0.59.

Table VI
Meyer Hardness Values and Corresponding Loads for Annealed Magnesium Rod Under Integrated Load-Time Tests for Various Time Increments

(Average Grain Size Diameter = 0.0010 Inch)

Time Increment (sec.)	Load Ranges in Kg: 250 to 1500				1500 to 3000				250 to 3000			
	L_a	H_a	L_u	H_u	L_a	H_a	L_u	H_u	L_a	H_a	L_u	H_u
15	20.0	25.5	3990	50.8	36.3	46.2	3470	44.2	24.4	31.1	3610	46.0
30	19.6	25.0	3910	49.8	33.8	43.0	3880	43.0	24.7	31.4	3490	44.4
60	19.2	24.4	3830	48.8	37.8	48.1	3290	41.9	24.1	30.7	3410	43.4
120	17.8	22.7	3720	47.4	33.7	42.9	3220	41.0	22.8	29.0	3370	42.9
180	17.7	22.5	3700	47.1	34.7	44.2	3160	40.2	22.9	29.2	3310	42.1

Grain size influences the plastic behavior of magnesium metal, as illustrated in Figs. 2 and 3, and so similar effects can also be expected on Brinell hardness values. In order to ascertain some knowledge of the general effect of grain size on the hardness of extruded magnesium rod, Table V was prepared from the data in Figs. 2 and 3. Notwithstanding the fact that the testing procedure in this instance was different from that employed in obtaining the results recorded in Table IV, the general effect is apparent. Integrated load-time tests give lower Brinell hardness values than the direct tests for reasons already discussed (see also Fig. 7).

In view of the existing shortcomings of the Brinell method Hoyt (19) and many others have suggested the use of the Meyer method for calculating hardness values. By this adoption, variations incident to the geometry of the spherical indentor are avoided, and the values actually represent the mean pressure or the true resistance to penetration. The Meyer hardness numbers are derived from this general equation, using the projected area and the applied load:

$$H = \frac{L}{\frac{\pi d^2}{4}} \qquad \text{Equation 7}$$

In Fig. 10 the mean pressure (or Meyer hardness) curve for magnesium is shown as a smooth curve which increases continuously with load. This behavior reflects the actual increase in hardness from the progressive work hardening effect of indentation.

The initial hardness (or the hardness corresponding to a slight amount of plastic deformation) may be evaluated from the load (L_a) required to produce a 1-mm impression and Equation 7. This load was determined by extrapolating Equation 2 to log d = 0 analytically according to the data in Tables I and III. The results are presented

Table VII
Meyer Hardness Values and Corresponding Loads for Annealed Magnesium Rod Under Direct Load-Time Tests for Various (Total) Times

(Average Grain Size Diameter = 0.0010 Inch)

Total Time (sec.)	Load Ranges in Kg: 250 to 1500				1500 to 3000				250 to 3000			
	L_a	H_a	L_u	H_u	L_a	H_a	L_u	H_u	L_a	H_a	L_u	H_u
15	20.5	26.1	4000	50.9	28.6	36.4	3680	46.8	23.1	29.4	3830	48.8
30	21.5	27.4	3910	49.8	27.4	34.9	3610	46.0	22.6	28.8	3750	47.7
60	19.9	25.3	3970	50.5	36.4	46.3	3560	45.3	23.0	29.3	3730	47.5
120	18.5	23.6	3960	50.4	34.9	44.4	3490	44.4	22.2	28.3	3690	47.0
180	19.1	24.3	3810	48.5	30.4	38.7	3410	43.4	22.6	28.8	3500	44.6

in Tables VI and VII. It is interesting to note that H_a-values, in the lower test range, are approaching the "strainless" or "absolute" hardness value of 22 for annealed magnesium as determined by Mahin and Foss (13) by their removal method. It may be pointed out here that a hypothetical load necessary to produce a 1-mm impression with a 10-mm ball acting for 1 second may be computed from Equation 5, which corresponds to an H_a value of 27.5. Actually this value should be approximately equal to the strainless hardness of magnesium, for it represents conditions of minimal flow and slight plastic deformation.

The ultimate hardness corresponding to the initial hardness plus the maximum attainable plastic deformation with a 10-mm ball was determined from the load (L_u) required to produce a 10-mm impression and Equation 7. For these values Equation 2 was extrapolated to log d = 1.0, and the results are contained in Tables VI and VII. Both mode of loading and time affect the hardness values within any given load-range.

A single number, as Hoyt (20) has pointed out, fails to denote to what extent the hardness value is due to the intrinsic nature of the metal and to what extent to plastic deformation effect during the test. This fundamental information, however, may be obtained from the two constants, a and n, as derived under the Meyer analysis.

Summary and Deductions

Plastic deformational behaviors of extruded magnesium rod have been investigated according to the Meyer and Hargreaves analyses. Certain basic indices were derived from which the capacity for work hardening and plastic flow could be evaluated under a number of conditions. Such variables as magnitude of test load, duration of load, mode of loading, and grain size were all systematically studied, and their effects on the indices were also noted.

Unlike most metals it was found that extruded magnesium rod does not follow the Meyer law throughout the entire testing range. The departure seemed to occur around 1000 to 1500 kg (and $d/D \approx 0.6$) which is above the loading range used in Brinell testing of this material. Even the Hargreaves plastic flow coefficients showed an anomalous behavior within this range. A complex mechanism is suggested which must take into account changes in tri-dimensional stress patterns, or resolved stress components produced by ball indentations of high d/D ratios in a polycrystalline aggregate having a large degree of preferred orientation.

Of supplemental importance was the observation that greater plastic flow at room temperature was obtained in magnesium metal by the intermittent application of a given load than by the continuous action of it over the same duration of time. This finding seems to support the theory of retwinning, the action of which is assumed to occur to a varying degree upon the sudden release of applied stresses.

Some attention was also given to the technical hardness values of pure magnesium metal. The shortcomings of the Brinell test and the importance of load and time were discussed with special reference to magnesium. It was further pointed out that a single number fails to denote to what extent the hardness value is attributable to the intrinsic nature of the metal, and to what extent to plastic deformation effect during test. But, of course, this significant information could be obtained from the two constants, a and n, as derived under the Meyer analysis.

Acknowledgments

The authors are grateful to the National Lead Company, sustainer of the Magnesium Research and Development Program at Mellon Institute, for permission to publish this paper, and to Dr. Alex Stewart, Director of Research for that donor company, for his encouragement and interest in the work.

References

1. E. Schmid and W. Boas, "Kristallplastizität," 1936, J. Springer, Berlin.
2. P. W. Bakarian and C. H. Mathewson, "Slip and Twinning in Magnesium Single Crystals at Elevated Temperatures," *Transactions*, American Institute of Mining and Metallurgical Engineers, Vol. 152, 1943, p. 226-254.
3. E. Meyer, "Untersuchungen über Härte Prüfung und Härte," *Zeitschrift Verein Deutscher Ing.*, Vol. 52, 1908, p. 645-654.

4. F. Hargreaves, "The Ball Hardness and the Cold-Working of Soft Metals and Eutectics," *Journal,* Institute of Metals, Vol. 39, 1928, p. 301-335.
5. Hugh O'Neill, "The Hardness of Metals and Its Measurement," 1934, Chapman and Hall, London.
6. L. G. Morell and J. D. Hanawalt, "X-Ray Study of the Plastic Working of Magnesium Alloys," *Physics,* Vol. 3, 1932, p. 161-168.
7. Z. Jeffries, "Grain-Size Measurements," *Metallurgical and Chemical Engineering,* Vol. 18, 1918, p. 185.
8. H. Moore, "Investigations on the Brinell Method of Determining Hardness," *Transactions,* Fifth Congress, International Association for Testing Materials, 1909, Report II_4, 11 p.
9. S. N. Petrenko, W. Ramberg and B. Wilson, "Determination of the Brinell Number of Metals," *Journal of Research,* National Bureau of Standards, Vol. 17, 1936, p. 59-95.
10. E. J. Rajakowicz and H. O. Maier, "Brinell Tests of Aluminum Alloys," *Aluminium,* Vol. 24, 1942, p. 347; same in *Light Metals,* Vol. 6, 1943, p. 457-466.
11. R. L. Templin, "The Hardness Testing of Light Metals and Alloys," *Proceedings,* American Society for Testing Materials, Vol. 35, pt. II, 1935, p. 283-304.
12. A. G. Worthing and J. Geffner, "Treatment of Experimental Data," 1943, J. Wiley & Sons, Inc., New York.
13. E. G. Mahin and G. J. Foss, Jr., "Absolute Hardness," TRANSACTIONS, American Society for Metals, Vol. 27, 1939, p. 337-362.
14. A. Krupkowski, "Propriètés Mécaniques du Cuivre," *Revue de Metállurgie,* Vol. 29, 1932, p. 16-33.
15. J. E. Dorn and E. Thomsen, "Magnesium; Notes on the Modulus of Elasticity," *Light Metal Age,* Vol. 1, 1943, p. 10-11, 24-25.
16. A. L. Norbury, "The Hardness of Annealed Copper," *Journal,* Institute of Metals, Vol. 29, 1923, p. 407-422; "The Hardness of Certain Copper Solid Solutions," p. 422-444.
17. A. L. Norbury and T. Samuel, "The Recovery and Sinking-in or Piling-up of Material in the Brinell Test . . . " *Journal,* Iron and Steel Institute, Vol. 117, 1928, p. 673-687.
18. R. H. Heyer, "Analysis of the Brinell Hardness Test," *Proceedings,* American Society for Testing Materials, Vol. 37, pt. II, 1937, p. 119-145.
19. S. L. Hoyt, "The Ball Indentation Hardness Test," TRANSACTIONS, American Society for Steel Treating, Vol. 6, 1924, p. 396-420.
20. S. L. Hoyt, "Fundamentals of Hardness Testing," *Proceedings,* American Society for Testing Materials, Vol. 43, 1943, p. 835-842.

DISCUSSION

Written Discussion: By A. L. Norbury, Ministry of Supply, London, England.

The writer believes that the type of nonagreement with the Meyer analysis, found by the authors, could result if the surface layer of a hardness specimen was softer than the interior. It was important to establish that the heating, at 200 C for 1 hour, had not produced this effect on the authors' specimens.

If $(\log a_{10}) + n$ values were calculated for the results in Table A the effects of time and type of loading were more easily compared.

It would be seen that the $(\log a_{10}) + n$ values decreased very systematically with increase in time (suggesting, incidentally, that the results were very accurate) and nonsystematic variations with time of a_{10} and n (due to variations in grain size, etc.) were eliminated.

Table A

Time (seconds)	Load-range 250 to 1500 kg. a_{10}	n	(log a_{10}) + n	Load-range 1500 to 3000 kg. a_{10}	n	(log a_{10}) + n
			Integrated Load-Time Tests			
15*	20.0	2.30	3.60	36.3	1.98	3.54
30*	19.6	2.30	3.59	33.8	2.00	3.53
60*	19.2	2.30	3.58	37.8	1.94	3.52
120*	17.8	2.32	3.57	37.7	1.98	3.51
180*	17.7	3.32	3.57	34.7	1.96	3.50
			Direct Load-Time Tests			
15†	20.5	2.29	3.60	28.6	2.11	3.56
30†	21.2	2.26	3.58	27.4	2.12	3.56
60†	19.9	2.30	3.60	36.4	1.99	3.55
120†	18.5	2.33	3.60	34.9	2.00	3.54
180†	19.1	2.30	3.58	30.4	2.05	3.53

*These values denote time increment.
†These represent total time.

Systematic differences due to type of loading and between load-ranges were also clearly seen.

Written Discussion: By R. L. Dietrich, Process Development Division, Magnesium Laboratories, The Dow Chemical Co., Midland, Mich.

The work done in this paper has been very carefully carried out in such a way as to reduce the number of uncontrolled variables to a minimum, and it is certainly welcome as a contribution to the rather meager information on the plastic deformation of polycrystalline magnesium.

I should like to point out one thing which I feel is rather important in connection with this paper, and that is that all of the work was done on surfaces normal to the extrusion axis, an orientation which is quite favorable for (102) twinning. Twinning on the (102) plane produces a rotation of 86 degrees in the position of the basal planes, a position which is unfavorable to further deformation by slip on the basal or (002) plane which is of course the most active slip plane in magnesium. It would seem that much of the deformation under the ball penetrator must take place by (102) twinning, particularly under the lower loads, and I would like to suggest that perhaps this is the cause of the discontinuity of the Meyer "n" values which the authors found.

This suggestion should be easy to test by running a Meyer analysis in a direction less favorable for twinning, such as a surface parallel to the extrusion direction, and I would like to know whether or not the authors have any data of this type available.

Written Discussion: By F. Hargreaves, Chemical Laboratory, Southern Railway, Eastleigh, England.

The significance of the curious variation of plastic flow index with magnitude of load shown in Fig. 5 is not clear but there is evidently something critical in the value of the load between 1000 and 1500 kilograms. This as the authors mention is coincident with the change in value of the Meyer index "n" within this range as shown in Fig. 1. The relation $L = 21.65k^{2.32}$ (Equation 5) holds over the whole range of loading 250 to 3000 kilograms and this, as mentioned in the text, is just the Meyer relation applied to a duration of loading of 1 second. It is not clear why this holds for all the loads while the ordinary Meyer index

"n" has two values within the range of these loads. It would be of interest to explore the plastic flow within the range of loading 1000 to 1500 kilograms.

In one of my papers[15] I suggested that the flow index "S" might be some measure of the rate of spontaneous annealing after cold working. In a further paper[16] some values for copper were given for both the annealed and cold-worked conditions. The flow index "S" for annealed copper (0.0026) was less than one-tenth of that found for magnesium. It has recently been found[17] that fine-grained copper when severely cold-worked by reducing in thickness by 95% or more by rolling becomes completely annealed on standing at air temperature for about a year.

The effect of mode of loading as shown in Fig. 7 is of great interest, the effect of unloading in the integrated time test being to increase the rate of plastic flow. It is to be presumed that spontaneous annealing is taking place and the effect of unloading is to accelerate this. This draws attention to the difference between a constant load and a variable load in relation to creep.

Regarding the variation in Brinell hardness with variation in magnitude of load shown in Fig. 10, it is this behavior which was the reason for adopting in British Standard Specification 240 definite ratios of load to ball size. For a metal of the hardness of magnesium this ratio is

$$\frac{\text{Load in kilograms}}{(\text{diameter of ball in millimeters})^2} = \frac{5}{1}$$

Written Discussion: By Charles S. Barrett, professor, Institute for the Study of Metals, University of Chicago, Chicago.

The fact that recovered diameters are larger with intermittent loading than with constant "direct" loading of the ball suggests that intermittent loading encounters effectively softer metal, or causes effectively higher stresses on the slip planes.

The possibility that recovery is going on at room temperature to soften the metal either in the loaded or unloaded state, or in both, can be tested by varying the time schedules in the test and observing the resulting values, or by varying the temperature. Presumably the author is investigating this further.

The possibility that there is a higher stress on the slip planes with intermittent loading should be looked into. This might come about during the intermittent unloading, as the author states, by twinning. One can speculate that some of the twins caused by applying the load are untwinned by releasing the load, or perhaps twinning occurs first upon unloading. In either case there will be sharp stress concentrations at certain twin edges, and local flow might occur there. Flow of this sort, which relaxes local stresses while the load is off, would increase the heterogeneity of stress when the load is reapplied. The result would be premature yielding upon reapplication of the load, hence abnormally large diameters of the indent. Metallography and X-ray diffraction could be used to test this idea, for twins can easily be detected.

---

[15] *Journal*, Institute of Metals, Vol. 39, 1928, p. 301.
[16] *Journal*, Institute of Metals, Vol. 41, 1929, p. 257.
[17] M. Cook and T. L. Richards, *Journal*, Institute of Metals, Vol. 70, 1944, p. 159.

Written Discussion: By R. H. Heyer, supervisor, Metallurgical Laboratory, Research Laboratories, The American Rolling Mill Co., Middletown, Ohio.

Thoroughgoing expositions of the ball indentation hardness characteristics of a given material appear infrequently in the literature. The authors have conducted a comprehensive investigation of the hardness of pure magnesium. It is unfortunate that the work appears under a rather unrevealing title which will escape the attention of persons reviewing the literature of indentation hardness testing.

The most important feature of this paper appears to be the information it gives on the effect that testing variables have on the technical hardness of magnesium. The necessity for specifying the load and duration of test is apparent from these data. In general, the results are applicable to other soft metals of high work hardening capacity.

The departure from the Meyer load-impression diameter relationship has been observed by the writer in the case of austenitic stainless steels. The tendency is toward a higher rate of work hardening at the higher loads just as in the case of magnesium. This has been ascribed to a structural phase change in the austenitic steel.

The authors state that the H_a value of 27.5 for a 1-millimeter impression made with a 10-millimeter ball acting for 1 second should be approximately equal to the "strainless" or "absolute" hardness for magnesium, which was found to be 22 by Mahin and Foss. There is little basis for predicting the equality of these values and it can be shown that the H_a value is actually much higher than the "absolute" hardness of the authors' magnesium.

Comparison of the values given below will show that the authors' magnesium is considerably softer than that of Mahin and Foss.

Meyer "a"	Meyer "n"	Brinell	"Absolute" Hardness	Reference
26.2	2.29	48 (1000 Kg.— 60 sec.)	22*	Table III
17.0	2.30	33.3 (1000 Kg.—180 sec.)	15†	Table V

*Mahin and Foss by "strainless indentation" method.

†From Carapella and Shaw data assuming the "absolute" hardness is proportional to the Meyer "a" constant. (This follows from appraisal of the data in Tables II and III of the Mahin and Foss paper.)

Using a test load of 1000 kilograms, as in the Mahin and Foss tests on magnesium, the impression diameter corresponding to an "absolute" hardness of 15 would be about 9.2 millimeters (compared with 7.6 millimeters for the Mahin and Foss annealed magnesium). Thus we are comparing: (a) A test in which a load of 1000 kilograms on a 10-millimeter diameter ball is sustained indefinitely without plastic deformation in a spherical indentation previously machined to a surface diameter of 9.2 millimeters, as against (b) A test in which a load of 17 kilograms on a 10-millimeter diameter ball is applied for 1 second to a flat surface, resulting in a permanent indentation diameter of 1.0 millimeter.

In each case the hardness number is determined as the load divided by the projected area of the indentation. The "absolute" hardness, (a), is approximately 15 and the H_a value, (b), is 27.5.

Of the two methods of obtaining a hardness value with no appreciable strain

hardening, the Meyer procedure is the more practical. It requires indentations at two or more loads and some calculation, whereas the Mahin and Foss method requires machining of spherical indentations into the sample using cut and try methods to determine the proper size of indentation. Although confirmatory experimental data are lacking, it is probable that both methods yield values that are approximately proportional to the compressive yield strengths.

Authors' Reply

The authors are indeed grateful to all those who have so kindly devoted their time and effort in discussing this paper.

Dr. Norbury's contribution is welcomed, and to which we would like to remark that the Norbury values, denoted in the table by the expression, $(\log a_{10}) + n$, are actually the logarithms of the ultimate loads under the conditions described, as this expression results from setting $d = 10$ millimeters in the Meyer equation.

We agree with Dr. Dietrich on the importance of twinning actions in connection with deformational behaviors. Moreover, our theory is that the discontinuities occurring in the Meyer "n" values within the range between 1000 to 1500 kilograms or around the ratio $d/D = 0.6$ can be ascribed to changes in the stress pattern induced by the ball as it penetrated the surface of a metal having a high degree of preferred orientation.

To be more specific about this point, let us direct our attention to the experimental findings of Schmid[18] in which the variation of proof stress over a range of orientations of magnesium crystals was investigated, the results being presented in Fig. 11. Obviously, it matters not whether the stress directions were made to change relative to the orientation of the crystal, or vice versa, the fundamental response to plastic deformation would remain unaltered. Notwithstanding the fact that these findings were the outcome of tensile studies, they, nevertheless, are related to compressive deformational results, for one is the complement of the other.

As outlined in the paper, we have been concerned with results produced by the application of a compressive load through a spherical indenter onto a surface normal to the basal planes. Under this action, the applied load tends to resolve itself more and more into radial stress components as the indenter penetrates the surface. The consequence of this reaction is an array of stress directions having many different orientations relative to the basal planes and varying in magnitude of stress. Here results a compositive effect which, though complex in nature, approximates the simple behaviors depicted by Fig. 11. The contributing feature to the discontinuities in plastic flow constants under consideration is the wide difference prevailing in the results presented in this figure, the two extreme values being in the ratio of 6:1. One reason for not having, hitherto, reported similar discontinuities under the analyses considered may be attributed to the fact that investigations have been confined to metals wherein the differences between the two extreme values of the resolved shear-stress data were in the ratio of 2:1, or less.

---

[18]E. Schmid, *Zeit. Elektrochem.*, Vol. 37, 1931, p. 447.

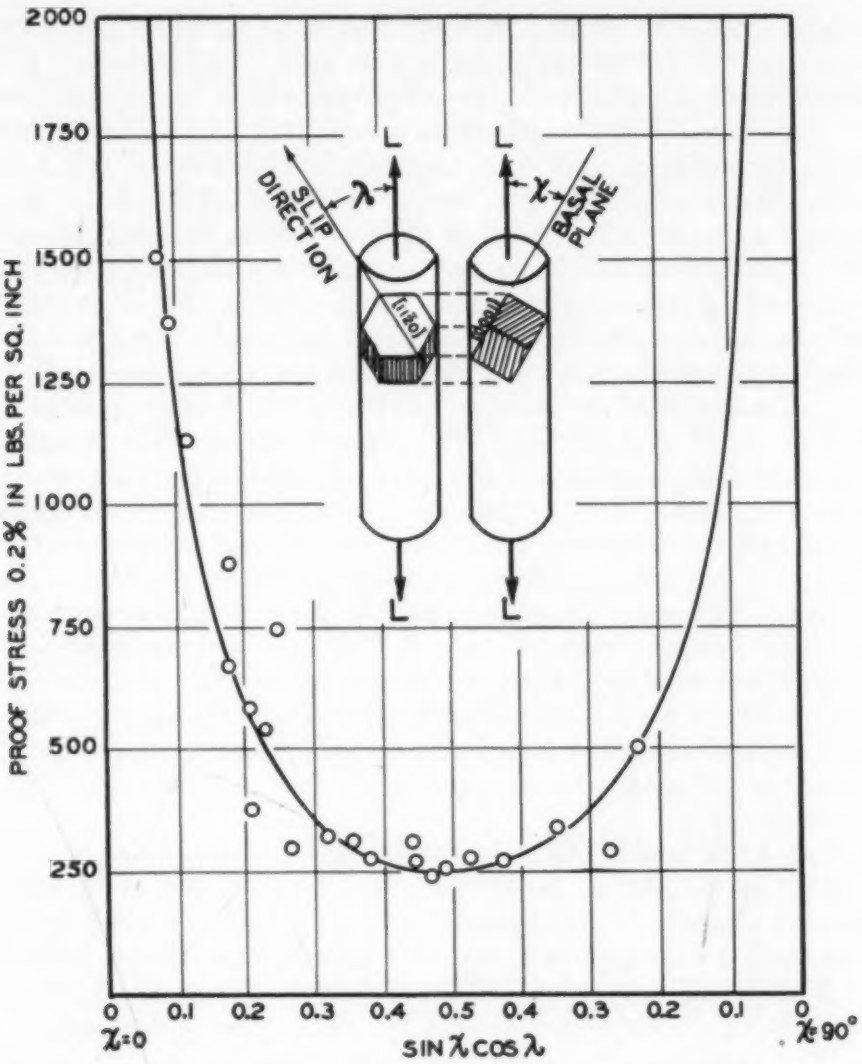


Fig. 11—Variation Proof Stress With Orientation of Magnesium Crystals at Room Temperature.

The foregoing conjectures are also offered as an explanation of the point raised by Dr. Hargreaves concerning the variation of the plastic flow indices with magnitude of test loads. To his next question—why no discontinuity was reported in the Meyer analysis of the k-values (which values may be regarded as diameters produced by loads acting on a 10-millimeter ball for a duration of 1 second), we would like to reply that a slight indication was detected but was too small to regard as significant.

The suggestions of both Drs. Hargreaves and Barrett, as possible explanations to account for the increase noted in the plastic flow rate under the intermittent action of a load over that under the continuous application at room temperature, are certainly appreciated. Further experimentation on this unusual behavior is under progress and our results will be disclosed as soon as possible.

That a departure in the Meyer relationship was also observed by Dr. Heyer

in the case of austenitic stainless steel is a fact of particular concern to us since it was said to parallel the one noted in our work on magnesium. While his observation was attributed to a structural phase change in the austenitic steel, we would like to mention that this explanation is not applicable to our findings.

It was interesting to learn from Dr. Heyer's table that our magnesium was softer than that employed by Drs. Mahin and Foss, but for the sake of consistency, a better comparison between the two Brinell hardness values can be had by selecting results determined under identical test conditions, i.e., $H_{10/1000/60} = 48$ (Mahin and Foss) and 39.5 (see Table IV) respectively.

We realize the controversial nature of the subject dealing with "strainless" or "absolute" hardness, and, therefore, appreciate the comments Dr. Heyer offered. However, it is not clear to us why he has selected a value approximately equal to 15 as the "absolute" hardness of magnesium at room temperature. It is our understanding that this value was taken from Table V, in which case it may be considered as the load required to yield a permanent indentation of 1.0 millimeter after acting for 180 seconds through 10-millimeter ball indenter onto the surface of a material existing in the special condition described in the paper. Whereupon it follows that the Meyer hardness corresponds to 19.1 and has the proper dimensions because it was computed by dividing the load by the projected area of the permanent indentation. By assuming that the "absolute" hardness is proportional to the Meyer constant, a, alone, Dr. Heyer arrived at a value which has only the dimension of load expressed in terms of kilograms; the projected area of the indentation should have also been taken under consideration.

It is apparent that a true "strainless hardness" value cannot be obtained under the Meyer procedure, for by its inherent nature, permanent indentation diameters are required which, of course, implies straining the metal surface with a ball indenter. Our reason for suggesting that the H_a value of 27.5 should be approximately equal to the "strainless" or "absolute" hardness of magnesium was predicated upon the condition that the data, from which the value was derived, represented a state of minimal plastic flow, insofar as the load was regarded as acting on a 10-millimeter ball for 1 second to yield a permanent indentation of 1.0 millimeter.

FOLDING IN THE CUPPING OPERATION

By William M. Baldwin, Jr., and Thomas S. Howald

Abstract

A theoretical and experimental investigation of the tendency of a blank to fold when drawn into a cup is reported. Copper, brass, aluminum in a hard and soft temper, and SAE 1008 steel in a soft temper were investigated. The effect of various die contours, reductions in diameter from blank to cup, and a wide range of blank thicknesses was studied. It was found possible, by purely theoretical means, to predict the tendency of a blank to fold if the stress-strain diagram of the metal is known.

Introduction

THE cupping operation consists in pushing a flat blank or disk of metal through a die, thus forming a hollow shape (Fig. 1). This operation sets up (among other stresses) a compressive "hoop" stress (Fig. 1). Because the upper face of the flange is unconfined, these compressive hoop stresses can form radially disposed buckles or waves (Fig. 2). To prevent this usually undesirable condition, some means of confining the upper face of the flange is employed: this involves the use of pressure applied to a hold-down plate or pad (Fig. 3). Even this expedient, when unjudiciously used, fails to stop buckling. Too generous die radii, for example, can prevent the hold-down plate from confining the flange over a large enough area to stop wrinkling. The effect of this factor, as well as many other factors affecting buckling when a hold-down plate is used, has been investigated a number of times (1) to (7).[1] On the other hand, the factors affecting the limits to which the cupping operation can be carried without a hold-down plate before buckling sets in have not been systematically investigated to the authors' knowledge.

Some meager description of the critical factors affecting folding when no hold-down plate is used can be found in the literature.

[1]The figures appearing in parentheses pertain to the references appended to this paper.

A paper presented before the Twenty-eighth Annual Convention of the Society held in Atlantic City, November 18 to 22, 1946. Of the authors, William M. Baldwin, Jr., is metallurgical engineer and Thomas S. Howald is research assistant, Midwestern Division, Chase Brass and Copper Co., Inc., Cleveland, Ohio. Manuscript received July 12, 1946.

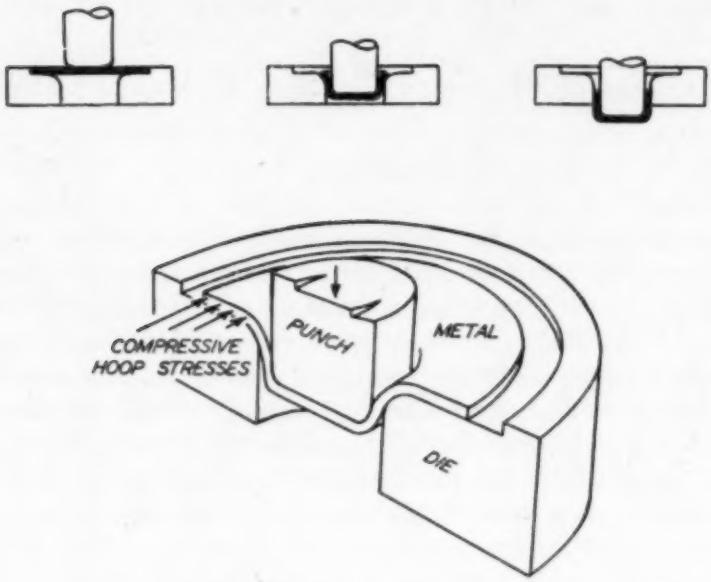


Fig. 1—Upper Sketches Are Cross Sectional Views Showing the Cupping Operation. Lower cut-away sketch shows the compressive hoop stresses developed in the flange of the blank as it is cupped.

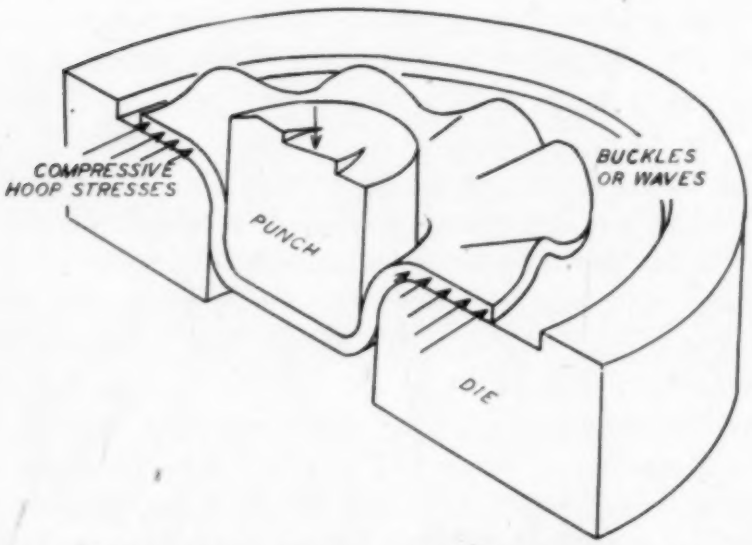


Fig. 2—Cut-Away Sketch Showing Nature of Buckles Formed in Flange by Compressive Hoop Stresses.

Crane (8) and Hinman (9) mention critical blank thicknesses below which folding will occur, but neither of the values is expressed as a function of metal properties, die contours, or reductions in diameter (i.e., $R = (D_o - D_1)100/D_o$ where $D_o =$ blank diameter, $D_1 =$ cup diameter)—factors which might easily affect the critical thickness. Esser and Arend (7) developed an empirical equation to fit data which they obtained with annealed copper, brass and mild steel using

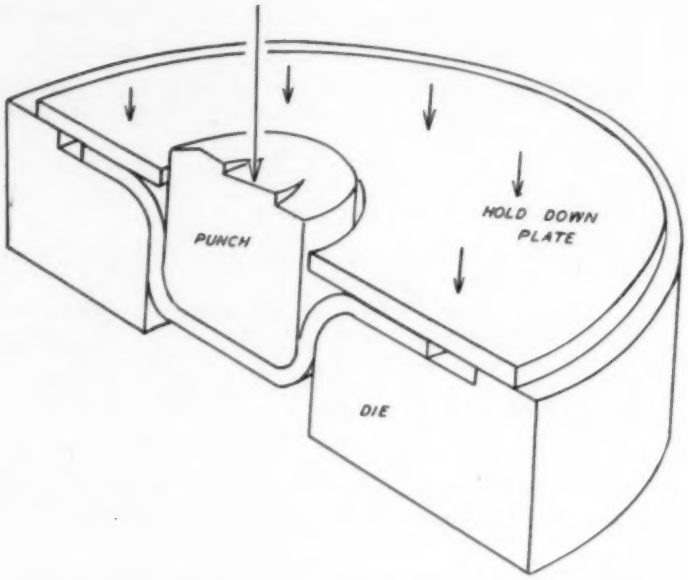


Fig. 3—Cut-Away Sketch Showing Use of a Hold-Down Plate to Repress Buckles.

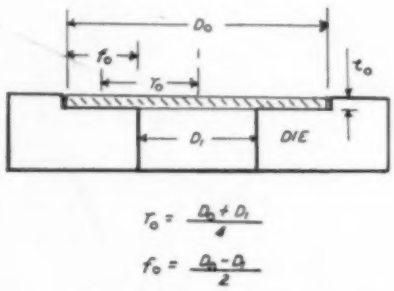


Fig. 4—Sketch Showing Dimensions Used in Geckeler's Equation.

a die with a small (but unreported) radius. Their equation converts to:

$$R = 870\ t_o/D_o \qquad \text{Equation 1}$$

where R is the maximum possible fold-free reduction in diameter expressed as a percentage, t_o is the blank thickness and D_o is the blank diameter.

Jevons (10) gives no quantitative values of a critical blank thickness but does state that "different metals will exhibit a different susceptibility to wrinkles . . . for example, aluminum is unusually liable to wrinkle badly".

The most thorough approach to the problem has been theoretical rather than experimental in nature. Geckeler (11) has carried out a

mathematical analysis for both the case where a hold-down plate is used and the case where no hold-down plate is used.

For the latter case, Geckeler developed an expression giving the critical stress at which buckling will occur:[2]

$$s_e = C_1 \frac{E_o t^2}{f^2} \qquad \text{Equation 2}$$

where f = the width of the flange (see Fig. 4)
t = the blank thickness
s_e = the critical stress in the flange at which folding will occur
C_1 = a constant = 0.46
and E_o = buckling modulus[3] $= \frac{4EP}{(\sqrt{E} + \sqrt{P})^2}$
where E = Young's modulus
and P = the tangent modulus or the slope of the stress-strain diagram of the metal in question.

If the compressive hoop stresses naturally occurring during cupping are less than the critical stress given by Equation 2, then the cupping operation should occur without buckling; if they are greater than the critical stress given by Equation 2, then buckling will occur during cupping.

Geckeler developed a second equation giving the number of waves or lobes into which the flange will buckle if failure does occur. This equation runs:

$$n = C_2 \frac{r}{f} \qquad \text{Equation 3}$$

where r = the mean radius of the flange (see Fig. 4)
C_2 = a constant = 1.65
and n = the number of lobes

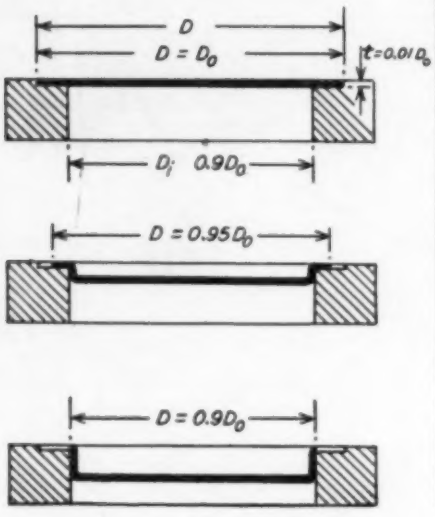
It should be pointed out that the constants C_1 and C_2 appearing in Equations 2 and 3 are interrelated, i.e.,

$$C_1 = \frac{C_2^2}{6}$$

The present investigation had a two-fold purpose: 1—it sought to develop some means of applying Geckeler's equations to the prac-

[2]In deriving these equations, Geckeler assumed that the metal at the inner edge of the flange, where it was bent over the die, behaved as if laterally supported. This assumption is of considerable importance in certain limiting conditions, as will be brought out later in the paper.

[3]The buckling modulus, E_o, is used in the analysis of plastic collapse problems in an analogous manner to the way in which Young's modulus, E, is used in the analysis of elastic collapse problems. Where the tangent modulus, P, equals Young's modulus, E (i.e., where the metal is still in the elastic state), then the buckling modulus reduces to Young's modulus itself. The derivation of the buckling modulus is given in such standard texts as Timoschenko "Strength of Materials," Part II, 2nd Ed., p. 367 et seq., and Nadai "Plasticity" 3rd imp., p. 178 et seq. It has been used in the analysis of the plastic collapse of straight bars subjected to axial load by Engesser (12), Westergaard and Osgood (13), and von Karman (14) and of tubes subjected to radial pressure by Holmquist and Nadai (15).



REDUCTION IN DIAMETER OUTER EDGE $R=\frac{D_0-D}{D_0}100$	FLANGE WIDTH $f=\frac{D-D_i}{2}$	RATIO $\frac{t}{f}$
0 PCT.	$0.1\,D_0$	0.1
5	0.05	0.2
10	0	∞

Fig. 5—Sketches Showing How the Ratio of Blank Thickness, t, to Flange Width, f, Increases in Value as the Cupping Operation Proceeds.

tical end where some prediction of the limiting reductions in diameter for fold-free operation could be made for given conditions of metal, temper, die contour, etc., and 2—to check the results of this theoretical work with experimental data.

Theory

The application of Equation 2 can proceed more easily if it is slightly rearranged:

$$\frac{s_e}{E_o} = 0.46\left(\frac{t}{f}\right)^2 \qquad \text{Equation 3}$$

In this case, the ratio of the compressive hoop stresses, s_h, naturally occurring during cupping to the buckling modulus of the metal should remain less than $0.46\ (t/f)^2$ if buckling is to be avoided; i.e.,

$$\frac{s_h}{E_{o\ \text{cupping}}} < 0.46\left(\frac{t}{f}\right)^2 \text{ for no buckling} \qquad \text{Equation 4}$$

It should be noted that both sides of expression 4 do not remain constant throughout the cupping operation. For example, the ratio of the blank thickness to flange width, t/f, increases during the cupping operation. For the purpose of illustration, let us imagine a cupping operation carried out on a "flat" die, i.e., one in which the width of the flange will be half the difference in blank diameter and die diameter. This is illustrated schematically in Fig. 5. At

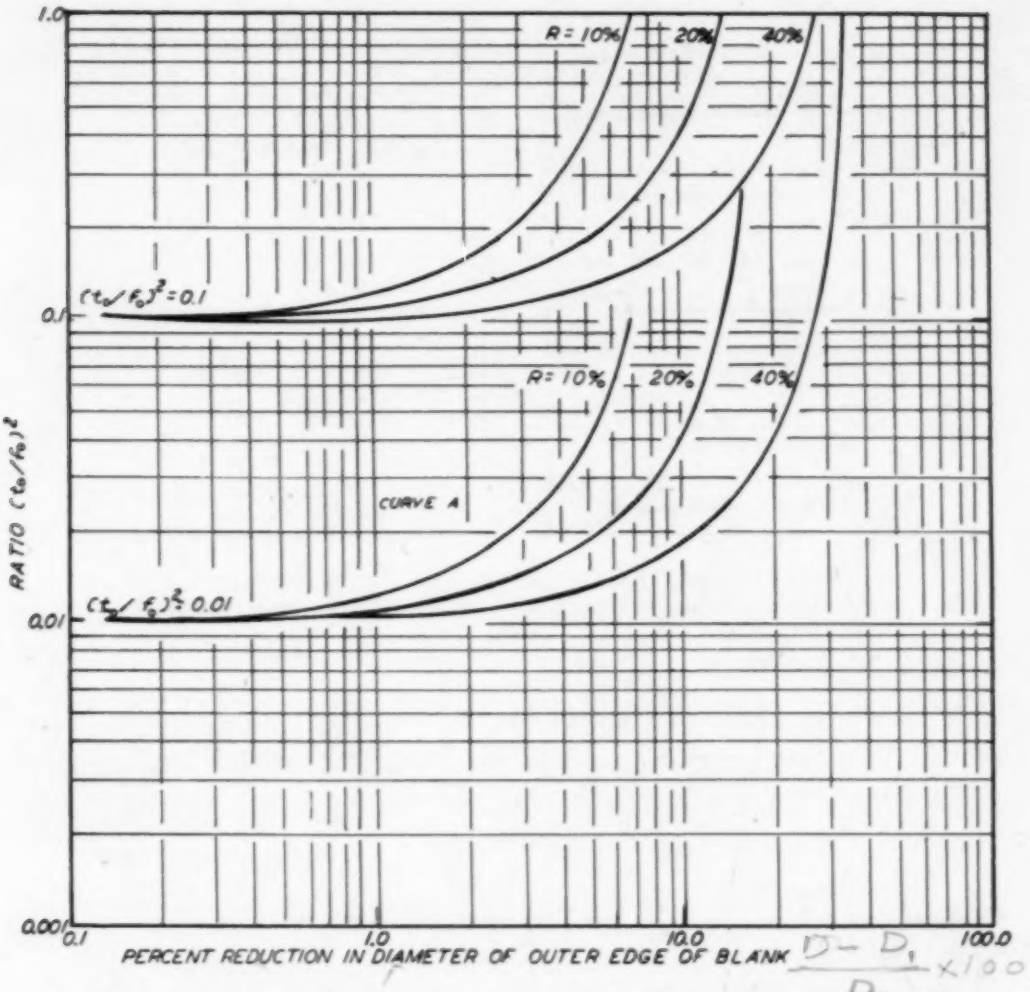


Fig. 6—Graph Showing How the Square of the Ratio of t/f Varies as a Function of the Reduction in Diameter of the Edge of the Blank for Different Starting t_o/f_o Ratios and Different Total Reductions in Diameter from Blank Diameter to Die-Hole Diameter.

the start of the cupping operation, the ratio of blank thickness, t_o, to the flange width, f_o, will have a certain initial value which we may call t_o/f_o. As the blank is drawn in during the cupping operation, the flange width is reduced.[4] Thus the ratio t/f now has a greater value than its initial value t_o/f_o. This trend is continued until the outer edge of the blank is drawn in to the edge of the die-hole, at which point the flange width is reduced to zero, and the ratio t/f assumes an infinite value.

The values of t/f, shown in Fig. 5, have been squared and entered on log-log paper as a function of the reduction in diameter of the outer edge of the flange, giving curve A in Fig. 6. It is seen

[4]Actually, the thickness of the flange increases slightly during the cupping operation, but this has been neglected in the present example and subsequent discussions in the paper.

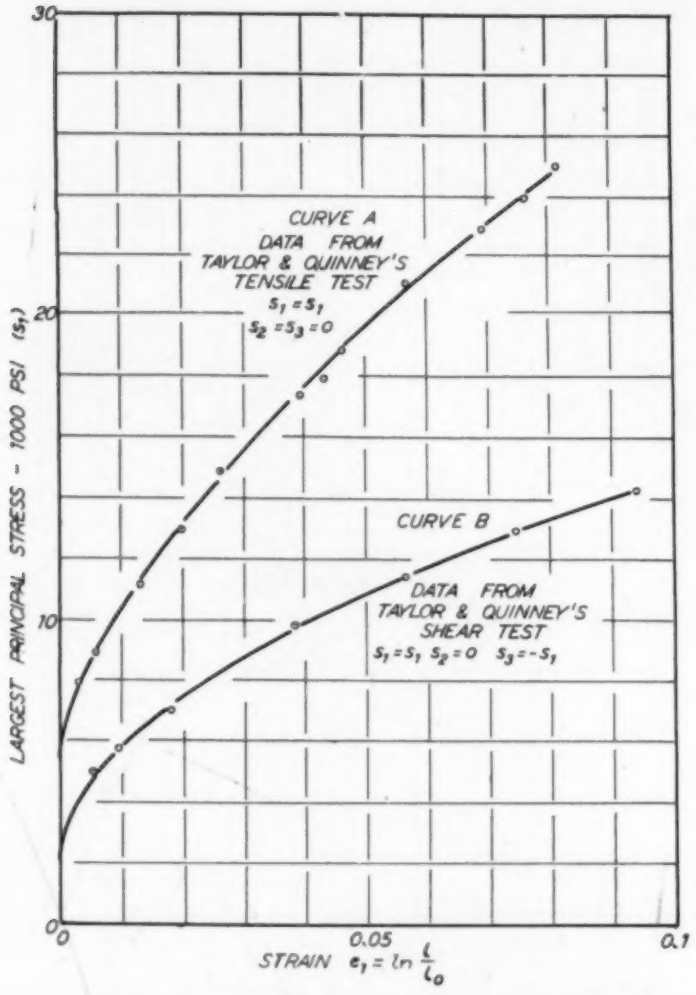


Fig. 7a—Stress-Strain Diagram as Determined by Tensile Test and Torsion Test on Soft Copper.

that this curve has two asymptotes: the horizontal one lying at $(t/f)^2 = 0.01$, which corresponds to the square of the starting value of this ratio; the vertical one lying at 10%, which corresponds to the total reduction in diameter of the outer edge of the flange. Also plotted in Fig. 6 are other curves for different starting ratios and different total reductions. It may be seen that in each case the curve is the same, the only difference being that it is transposed so that its asymptotes lie at the appropriate values of the square of the starting ratio and the total reduction. Curves giving the value of 0.46 $(t/f)^2$ are exactly the same as those given here, except they are dropped vertically so that their horizontal asymptote is at 0.46 $(t_o/f_o)^2$ instead of at (t_o/f_o).[2]

Similarly, the ratio $s_h/E_o)_{\text{cupping}}$ operating in the flange of the blank does not remain constant throughout the cupping operation.

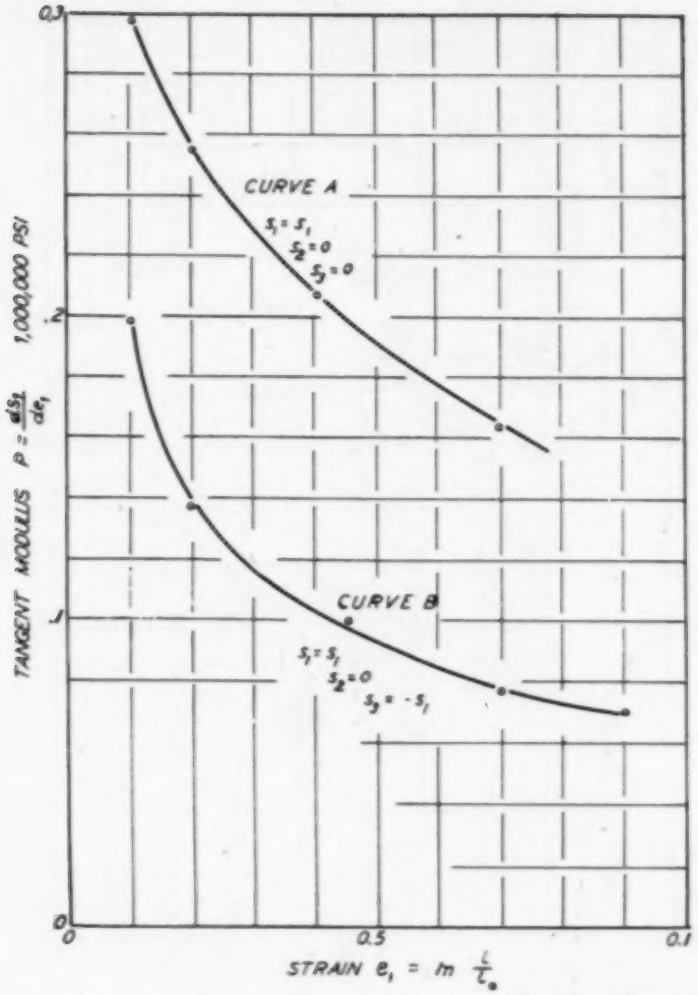


Fig. 7b—Slope of Curves Given in Fig. 7a as a Function of Strain.

The outermost fiber, i.e., the ring of metal represented by the blank circumference, as it is drawn in, is subjected to a simple compressive hoop stress when no hold-down plate is used (cf. Sachs (16), Siebel (17), Fukui (18), et al.). If the stress-strain curve for the metal in tension is known, and if it is assumed that it is the same in compression as it is in tension, then the ratio $s_h/E_o)_{cupping}$ for this fiber may be plotted as a function of the reduction in diameter of the outer edge of the blank. This has been done in Fig. 7a through e (Curve A) using Taylor and Quinney's (19) stress-strain data obtained from a tensile test on soft copper.

It must be remembered that Curve A shows the $s_h/E_o)_{cupping}$ ratio for the outermost fiber only. To determine this ratio for the entire flange, some inquiry must be made into the variation of $s_h/E_o)_{cupping}$ that occurs in any of the interior fibers of the flange,

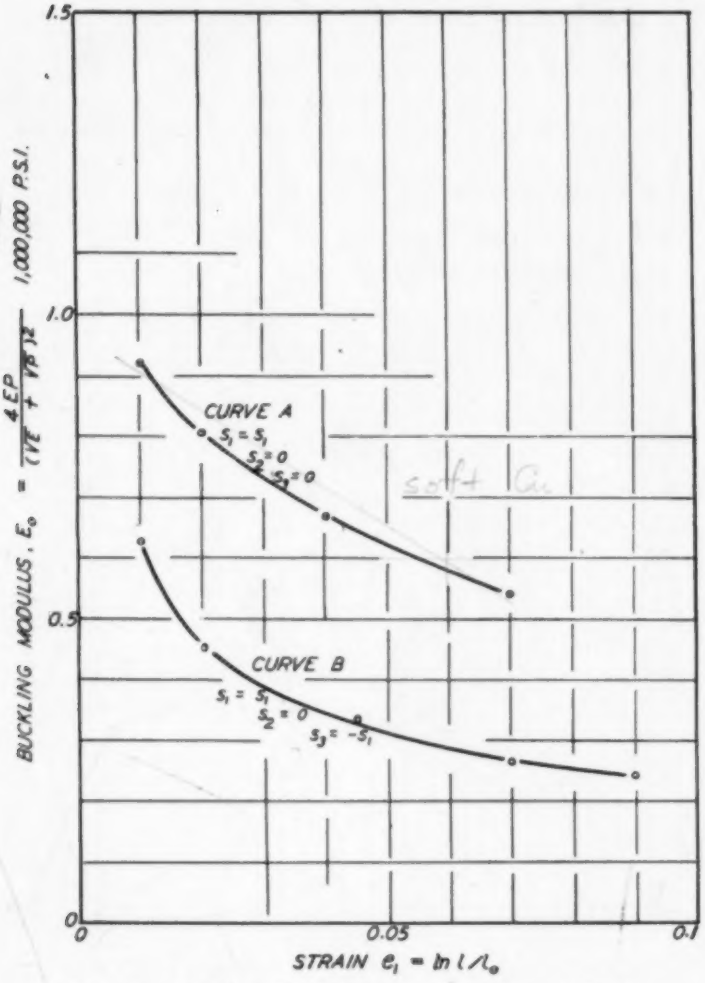


Fig. 7c—Buckling Modulus as a Function of Strain.

i.e., in any ring of metal lying between the outer and inner edges of the flange.

The interior fibers are acted upon by radial tensile stresses as well as compressive hoop stresses. What effect will the presence of these second (radial) stresses have upon the s_h/E_o ratio operating in the hoop direction? A partial answer to this question is obtained from Taylor and Quinney's stress-strain diagram determined from a torsion test on a soft copper tube. During their test, two stresses were developed: a compressive stress, and at right angles to it, a tensile stress equal in magnitude to the compressive stress. The stress-strain diagram labeled Curve B in Fig. 7a is a plot of the tensile stress vs. the strain occurring in the direction in which the tensile stress operated.[5] It is to be remembered that this curve was

[5]Actually this curve also represents a plot of the compressive stress vs. the strain occurring in the direction in which the compressive stress operated since both stresses and strains are equal in magnitude.

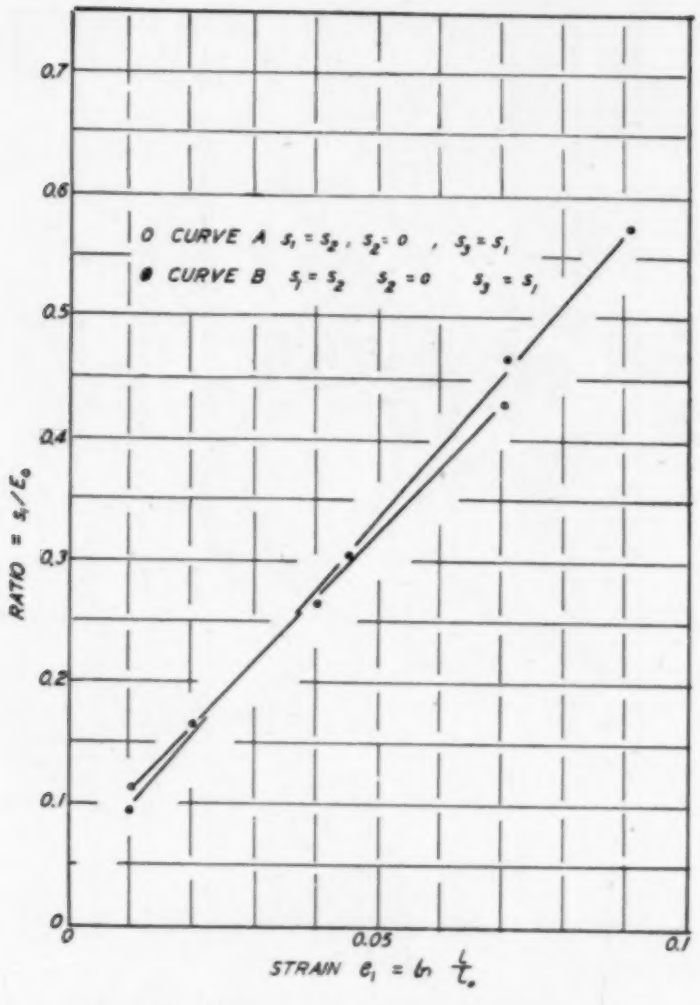


Fig. 7d—Log-Log Plot of the Ratio of Stress to Buckling Modulus as a Function of Strain for the Outermost Fiber of Flange.

determined with the presence of a second stress of opposite sign to the first, and operating at right angles to the first.

Despite the apparent difference between this curve and the stress-strain diagram determined under simple tension (Curve A, Fig. 7a) the curves giving the s_h/E_o ratios as functions of strain derived from both curves A and B[6] are virtually coincident (see Fig. 7d). Similar comparisons made with stress-strain diagrams obtained for a number of different plane stress states by other investigators (20), (21), (22) yielded the same result. It was therefore assumed in the present report that the quantity s_h/E_o as a function of strain remains unchanged by the addition of a second principal stress.

[6]In computing the buckling modulus from the shear data, a value of $E/(1 + \mu)$ was used where μ is Poisson's ratio. This correction was slight, however, leading to differences of about 1 per cent only in the E_o values.

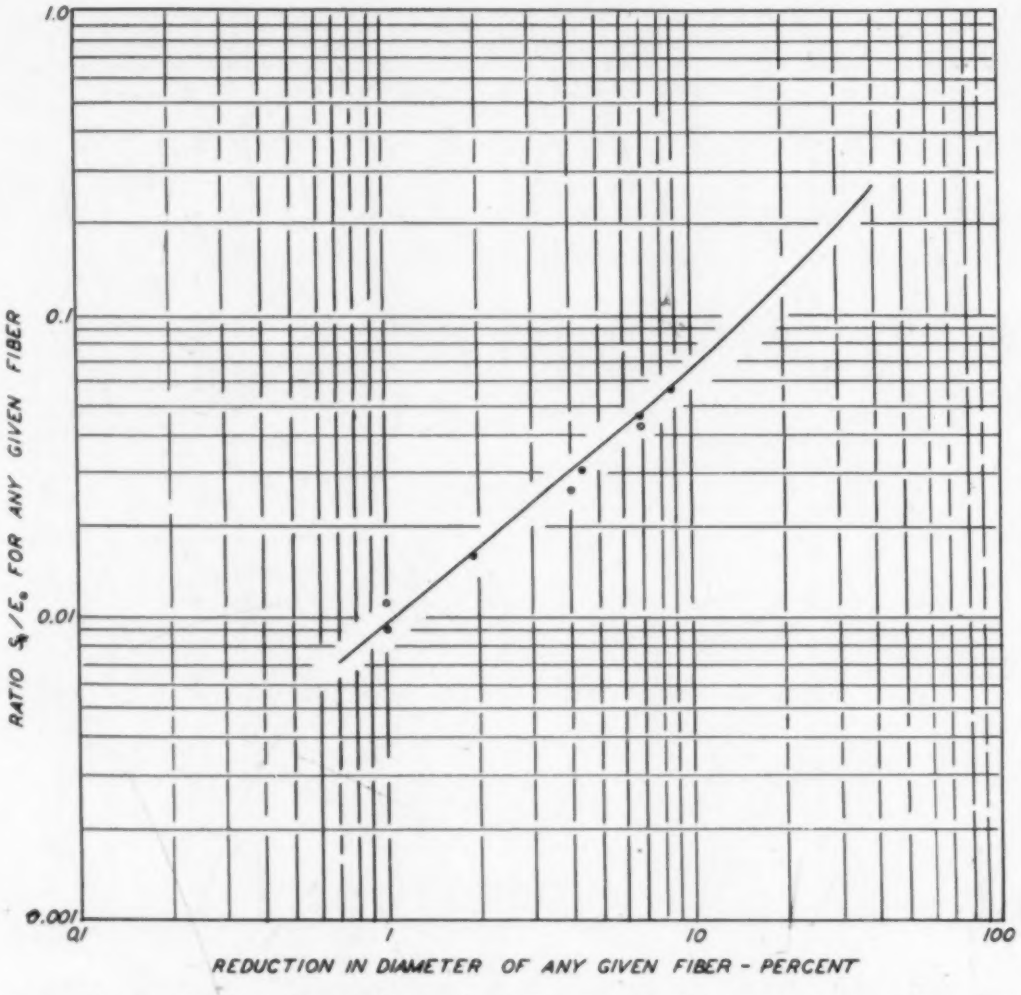


Fig. 7e—Log-Log Plot of the Ratio of Stress to Buckling Modulus as a Function of Strain for Any Given Fiber in Flange (Symbols Represent Taylor and Quinney's Data. Solid line is taken from data presented later in this paper.)

In other words, the curve given in Fig. 7e represents the ratio $s_h/E_o)_{cupping}$ for any given fiber as a function of the reduction in diameter of that fiber. A slight correction must be made, however, if it is desired to express the $s_h/E_o)_{cupping}$ ratio as a function of the reduction in diameter of the outermost fiber or the outside edge of the blank. This is necessitated by the fact that the interior fibers are reduced in diameter at a faster rate than is the outside fiber. This fact arises out of very simple geometric conditions that exist in the flange and equations relating the reduction in diameter of any given interior fiber to a given reduction in diameter of the outermost fiber are given by Sachs (16) and Swift (23). A chart has been prepared (Fig. 8) using these equations which gives the average reduction in diameter over the entire width of the flange for a given reduc-

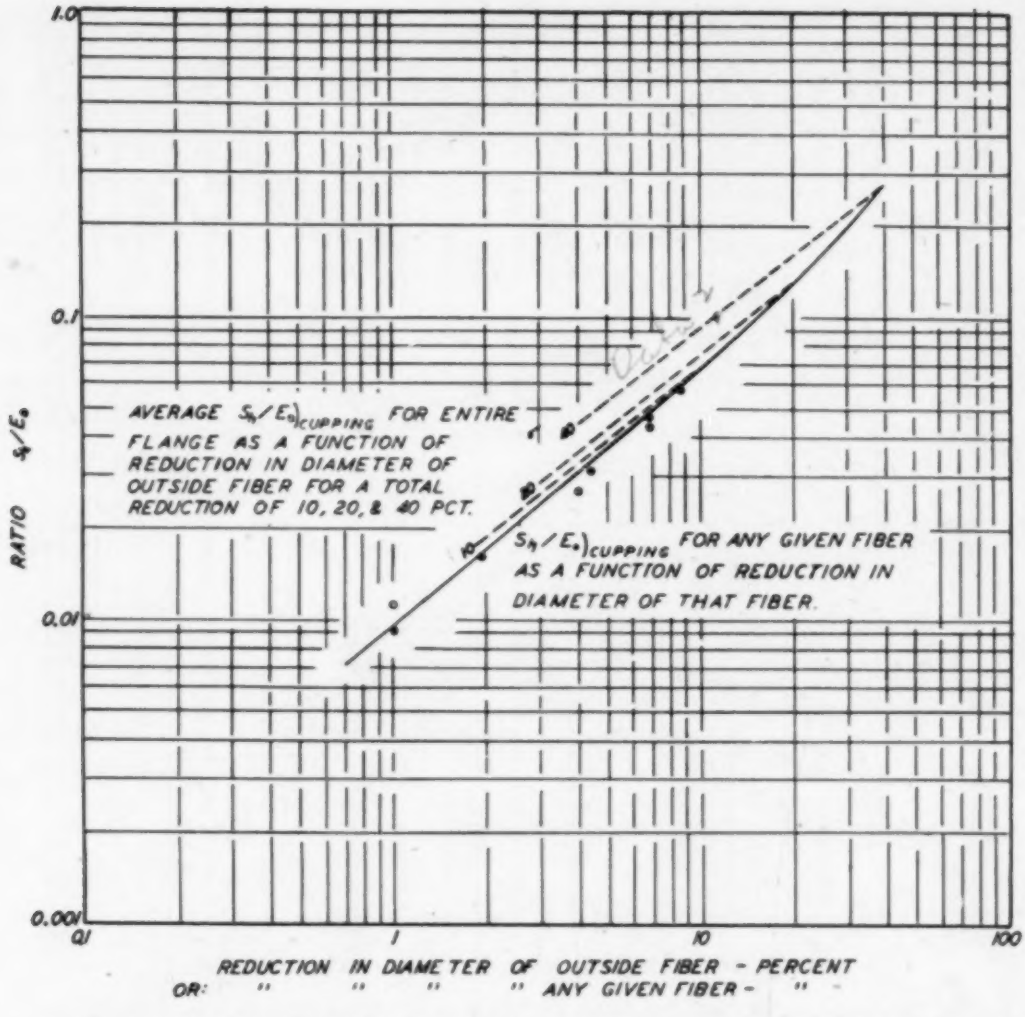


Fig. 7f—Log-Log Plot of the Average Ratio of Stress to Buckling Modulus Throughout Flange as a Function of Strain for the Outermost Fiber of Flange.

tion in diameter of the outermost fiber. It will be noted that a series of curves is given for different total reductions from original blank diameter to cup diameter.

By means of this chart, the desired curves giving the average $s_h/E_o)_{cupping}$ ratio for the entire flange as a function of the reduction in diameter of the outside edge of the blank may be constructed as shown in Fig. 7f.

The curves given in Figs. 7f and 6 can now be treated in accordance with expression 4. It is required that for a given metal (in the present case, soft copper) the curve giving the value $0.46\ (t/f)^2$ as a function of the reduction in diameter of the outermost fiber should not pass below the curve giving the value of s_h/E_o as a function of the reduction in diameter of the outermost fiber at

any point during the cupping operation. For example, in Fig. 9, the s_h/E_o curve for soft copper is shown along with the lowest 0.46 $(t/f)^2$ curve for a 10% total reduction which will not pass below it. The asymptote of this latter curve is 0.46 $(t_o/f_o)^2 = 0.012$, giving a value of t_o/f_o of 0.158.

If it is still presumed that a "flat" die is being used, then $f_o = \frac{1}{2}(D_o - D_1)$. For a 10% reduction in diameter $D_1 = 0.9\ D_o$,

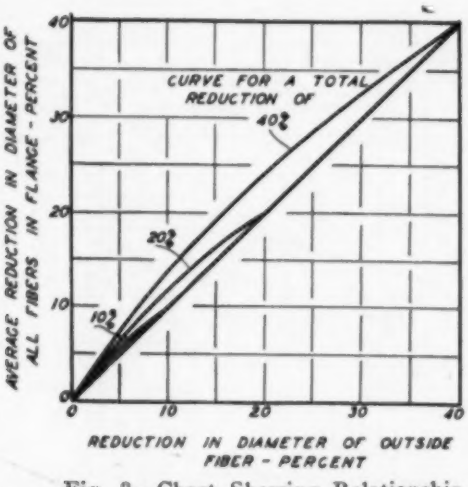


Fig. 8—Chart Showing Relationship Between Average Reduction in Diameter for All Fibers in Flange as a Function of the Reduction in Diameter of the Outside Edge of the Flange. Three curves are given for three different total reductions in diameter (from original blank diameter to final cup diameter).

hence, $f_o = 0.05\ D_o$. If this value is inserted in the ratio of t_o/f_o, we obtain $t_o/D_o = 0.008$. It is thus seen that we can determine a minimum relative blank thickness; i.e., t_o/D_o, above which folding will not occur for a given reduction or relative flange width (since for a "flat" die, reduction $= \dfrac{D_o - D_1}{D_o} = 2f_o/D_o$). This fact is an expression of the principle of geometric similarity.

This procedure, outlined in the preceding two paragraphs, indicates that the number of folds developed during buckling can depend upon the blank thickness, t, despite the fact that this factor does not enter Geckeler's Equation 3. Relatively thick blanks may suffer a definite reduction in diameter before they fold, i.e., the 0.46 $(t/f)^2$ curve may intersect the s_h/E_o curve at a reduction in diameter of several per cent, whereas, relatively thin blanks will suffer an insignificant reduction in diameter before folding occurs. In these two cases, the flange width at the moment when folding occurs is different, leading to different results in Equation 3.

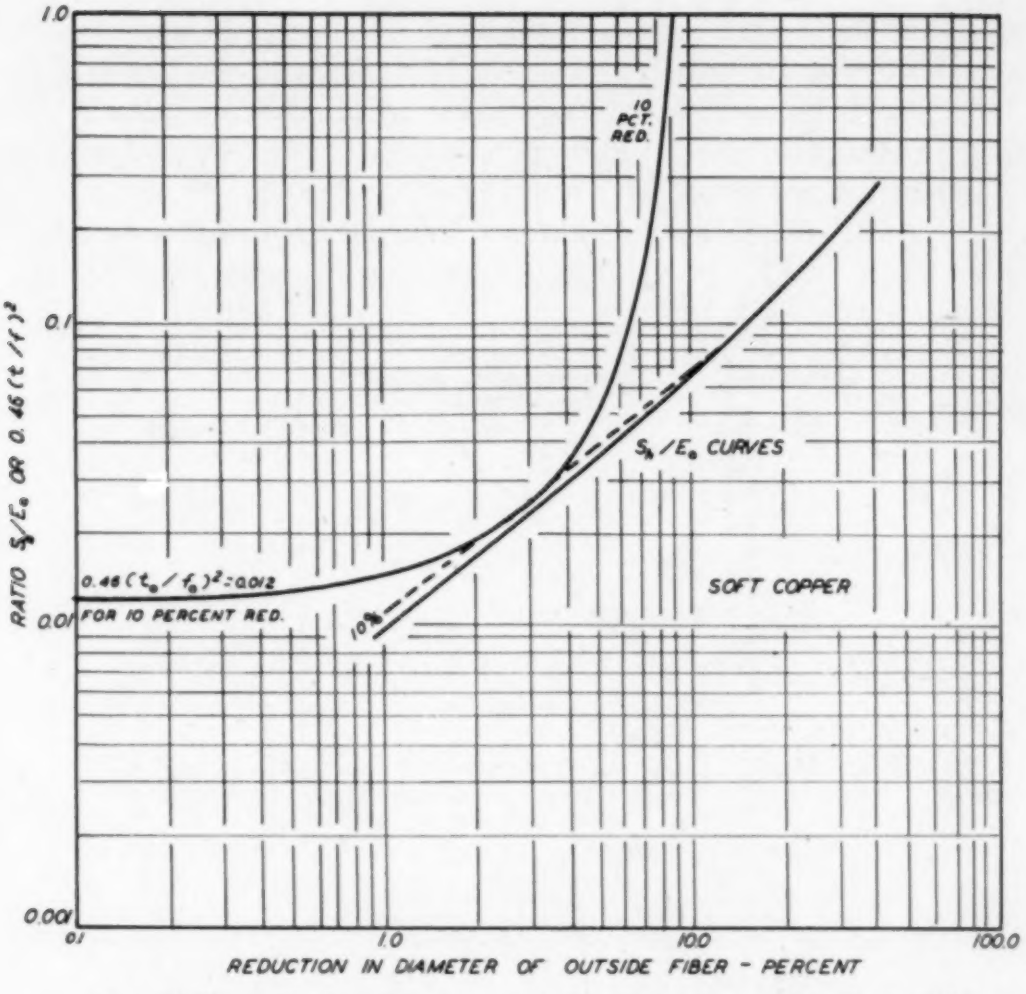


Fig. 9—Chart Showing Lowest 0.46 $(t/f)^3$ Curve for a 10% Total Reduction from Original Blank Diameter to Die-Hole Diameter That Will Not Pass Below the s/E_o Curve for Soft Copper. Horizontal asymptote of former curve lies at a value of 0.46 $(t_o/f_o)^2 = 0.012$.

The above considerations have been confined to "flat" dies, i.e., dies that are of such contours that the flange extends from the outer edge of the blank to the diameter of the die hole, but they can be extended to dies of other contours as well.

The stress state existing in the flange between the outer edge of the blank and some arbitrary diameter, D, is unaffected by any difference in the operation at diameters less than D. (Cf. equations giving the stress state in the flange of cup being formed as deduced by Sachs (16), Siebel (17), Fukui (18), et al.) Thus the stress state existing in the flange lying between diameters D_o and D for the two cupping operations shown in Figs. 10a and 10b is the same despite the fact that the second operation effects a much greater total reduction in diameter from blank to cup. In the second operation,

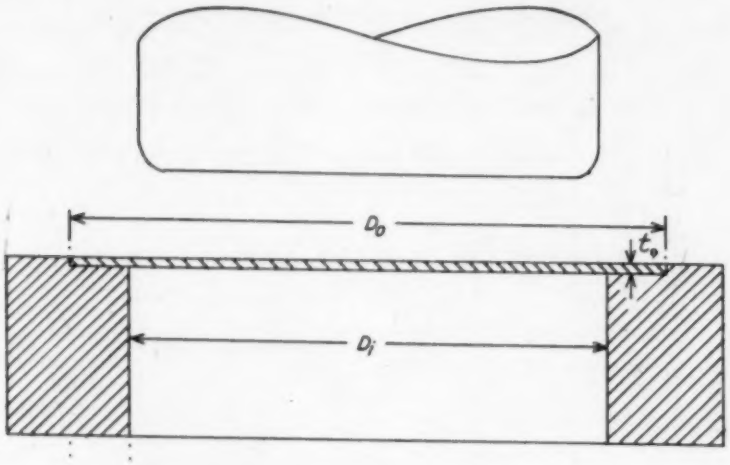


Fig. 10a

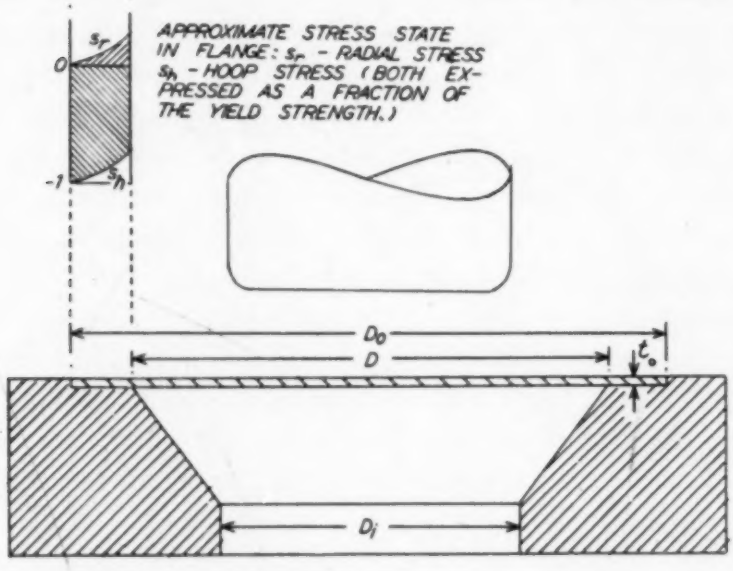


Fig. 10b

Fig. 10a—Flat Die Giving An Arbitrary Reduction from Blank Diameter to Die-Hole Diameter.

Fig. 10b—Conical Die Giving a Different Reduction from Blank Diameter to Die-Hole Diameter but the Same Reduction from Blank Diameter to Shoulder of Die as Given in the Operation Shown in Fig. 10a.

shown in Fig. 10b, it may be presumed that the metal behaves as if laterally supported where it rounds the shoulder of the die (at diameter D) so that the behavior of this flange with regard to buckling should be the same as that of the flange in the first operation shown in Fig. 10a.

If buckling in the flange between diameters D_o and D is the critical factor in the second operation (i.e., if no buckling occurs after the edge of the blank has passed over the shoulder of the conical die),[7] then larger fold-free reductions may be effected with conical dies than with "flat" dies.

[7]This is the case for all but a few conditions, as will be brought out later in the paper.

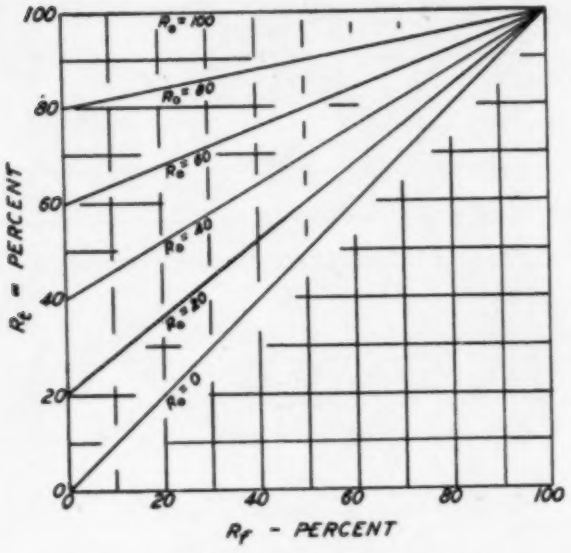


Fig. 11—Chart Showing the Relationship Between Total Reduction, R_t, Affected on Conical Die and Flange Reduction, R_f, for Various "Tare" Reductions, R_o.

To quantitatively relate the total reduction,

$$R_t = \frac{D_o - D_1}{D_o} 100 \qquad \text{Equation 4}$$

to the "flange" reduction,

$$R_f = \frac{D_o - D}{D_o} 100 \qquad \text{Equation 5}$$

and the "tare" reduction of the die,

$$R_o = \frac{D - D_1}{D} 100 \qquad \text{Equation 6}$$

where D_o, D, and D_1 are explained in Figs. 10a and 10b, the following equation may be used:[8]

$$R_t = \left(1 - \frac{R_o}{100}\right) R_f + R_o \qquad \text{Equation 7}$$

---

[8]This equation is derived by adding and subtracting D to the numerator of the fraction on the right-hand side of Equation 4.

$$R_t = \frac{D_o - D + D - D_1}{D_o} 100 = \frac{D_o - D}{D_o} 100 + \frac{D - D_1}{D_o} 100$$

$$= \frac{D_o - D}{D_o} 100 + \frac{D - D_1}{D} 100 \frac{D}{D_o}$$

Inserting Equations 5 and 6 in this expression gives

$$R_t = R_f + R_o - \frac{D}{D_o}$$

$$= R_f + R_o \left(1 - \frac{R_f}{100}\right)$$

which, on rearranging, gives Equation 7.

For a given die R_o is fixed, of course, so that the relation between R_t and R_f is linear, as may be seen in Fig. 11. This chart (or Equation 7) can be used to convert data obtained with a plane circular flange for use on conical dies.

Experimental Procedure

Several series of cupping experiments were conducted to determine the conditions under which folding would or would not occur. In these cupping experiments, the following variables were studies.

Metal—Four different metals (copper, 70/30 brass, 2S aluminum, and SAE 1008 rimmed steel) in various tempers were used. Each metal (with the exception of the steel, which was annealed) was received in the cold-rolled condition and in a definite thickness.

All blanks were prepared from the metal in the as-received condition. In those cases where annealed tempers were investigated, the metal was annealed after blanking. If the blanking operation had followed the anneal, the rim of the blank would have been hardened an indeterminate amount, possibly affecting results. The steel blanks were prepared from annealed stock since it was received in that condition. All anneals were for 1 hour at 1000 F.

Blank Dimensions—Blanks of various diameters up to 1.625 inches were punched out on a blanking die set, while larger sizes were carefully sawed and sanded to size.

Metal of a desired thickness was obtained by pickling the as-received stock to the desired gage. Sufficient web scrap was allowed so that variations in thickness at the edge of the strip resulting from the pickling procedure were not incorporated in the blank itself. Blank thicknesses varied less than plus or minus 5% from a mean value. The pickling process was adopted so as to obtain metal with one fabrication history and thus one set of properties on a wide variety of sizes. Tensile strength and yield strength values on pickled metal indicated that this objective was obtained. These properties also indicated that the pickling procedure used did not introduce any adverse effects.

Tool Dimensions—Two punches were used, one having a diameter of 0.750 inch and the other, a diameter of 1.840 inches. The punch radius was $\frac{3}{16}$ inch in each case. Six dies were used, having diameters of either 0.870 inch or 2.000 inches (see Fig. 12) but having different contours. The tare reductions of the dies were

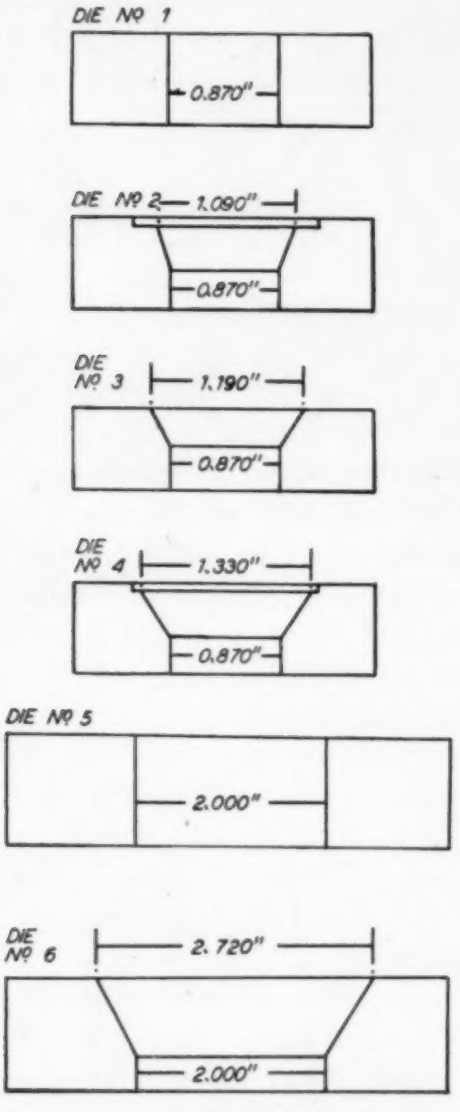


Fig. 12—Sketch Showing Contours of Dies Employed in This Research. Corners on Dies 1 and 5 were sharp. Corners on other dies had radii approximately 0.010 inch.

0% (Nos. 1 and 5), 19% (No. 2), 27% (Nos. 2 and 6), and 34% (No. 3). Blanks were centrally located in the dies by using annular centering rings which fitted between the blank and the set edge of the die.

Procedure—The sequence of experimental operations usually followed one of two patterns: (a) Metal of a given temper was pickled to a range of thicknesses, blanked to a given diameter (and then annealed and flash pickled if a soft temper was being investigated). The blanks were then cupped on a given die fitted with the

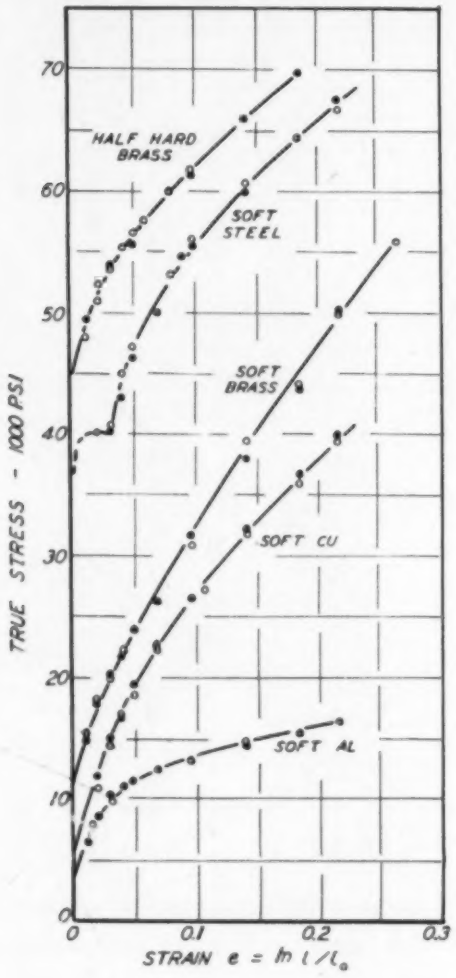


Fig. 13a—Stress-Strain Diagrams of Metals Investigated in This Research.

proper annular centering ring. Usually the range of thickness was broad enough so that some of the thinner blanks folded while some of the thicker blanks did not. A second range of thicknesses was then chosen in the interval between the thickest blank that folded and the thinnest blank that did not, in order to establish more narrowly the critical thickness below which folding would occur. (b) Metal of a given thickness was blanked through a range of diameters and then cupped, starting with the largest blank and proceeding through the smaller sizes until no folds were encountered. These operations were then repeated, each time one of the variables—die contour, blank diameter, blank gage, and die size—being changed.

Stress-Strain Determinations—Stress-strain diagrams were obtained from two separate series of samples. One set of three samples

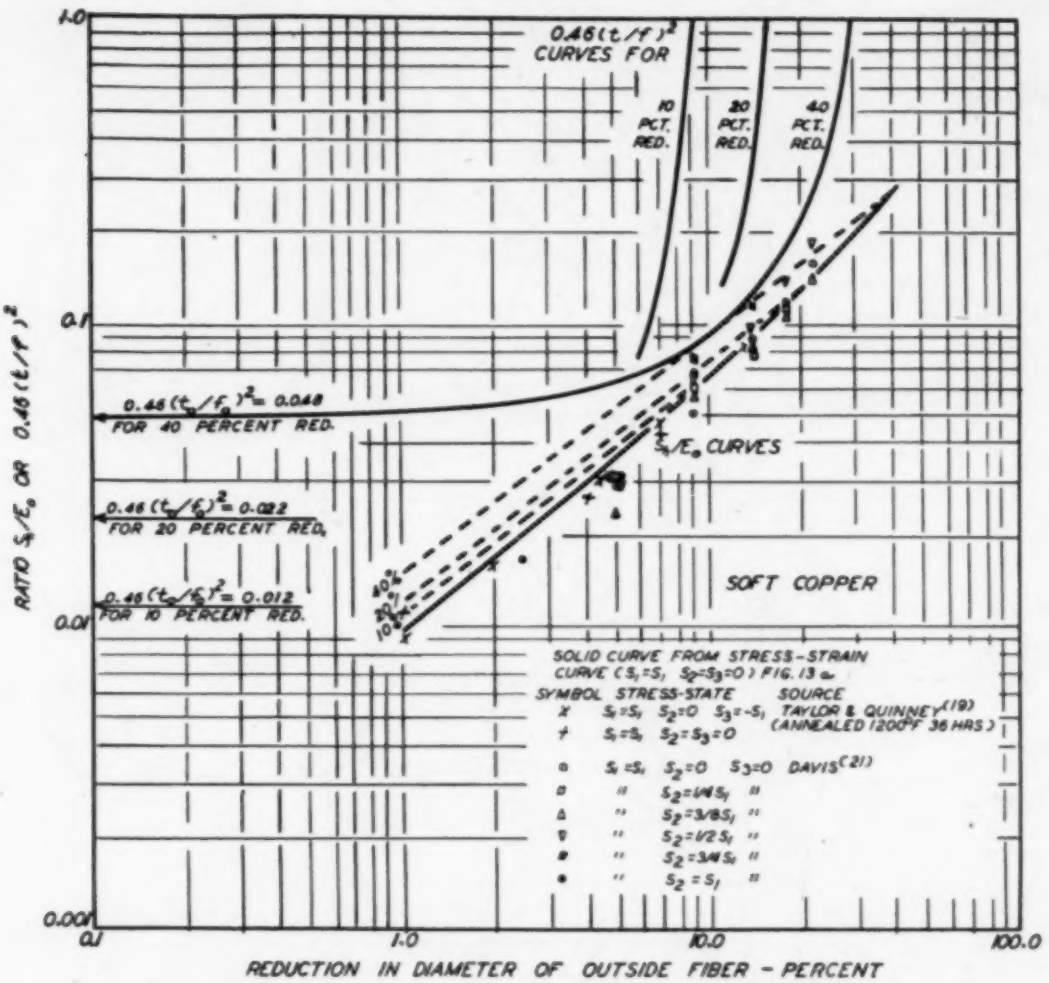


Fig. 13b—s_h/E_o Curves (Solid Curves) Derived from Stress-Strain Diagrams Shown in Fig. 13a. Symbols represent s/E_o values obtained from the literature for various stress states and for similar but not identical experimental conditions.

was tested up to strains of 3% using an automatic stress-strain recorder. Another set of two samples was tested from 1% to fracture using the divider method. There was good agreement in the region where the methods overlapped. The stress-strain curves for hard copper and hard aluminum were not used, since localized necking set in rather quickly, leading to unreliable evaluation of the slopes of the latter (and for the present investigation, the most useful) part of the curves.

Results and Discussion

The stress-strain diagrams of the metals studied are given in Fig. 13a; the $s_h/E_o)_{cupping}$ curves derived from them are given in

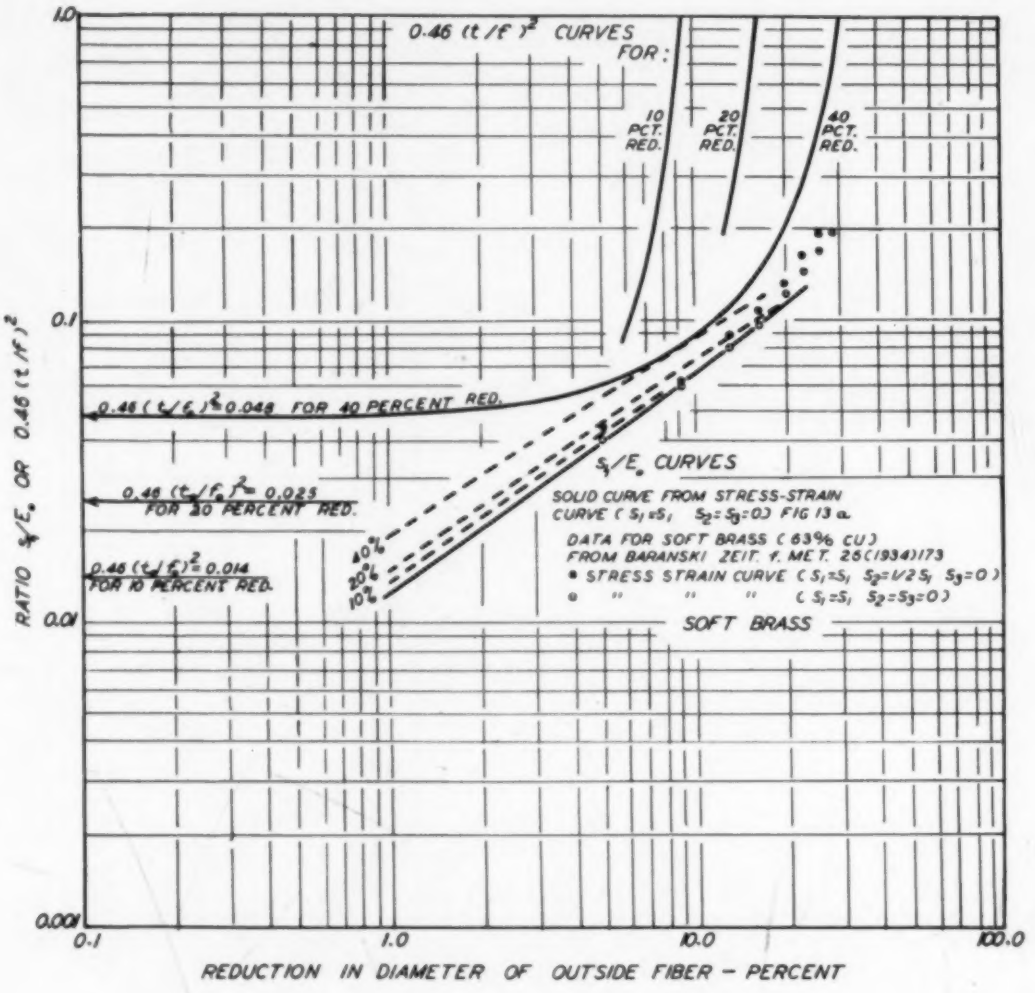


Fig. 13c—See Caption for Fig. 13b.

Figs. 13b through 13f. In addition, values of s/E_o obtained from stress-strain diagrams for not only simple tension but other stress states as well as determined by other investigators are included in these charts. This has been done to show the extent of the variation of these values with (a) stress state, and (b) different experimental conditions (annealing time and temperature, etc.) Also entered in the latter graphs are the lowest $0.46\ (t/f)^2$ curves which do not pass below the $s_h/E_o)_{cupping}$ curves. The horizontal asymptotes of these limiting curves are indicated along the left-hand side of the graphs. In Table I, these asymptotic values have been converted to minimum relative blank thicknesses which can be cupped on a "flat" die for various reductions.

Factors affecting the conditions under which buckling occurs for the case where the flange is a plane circular ring (see Fig. 4).

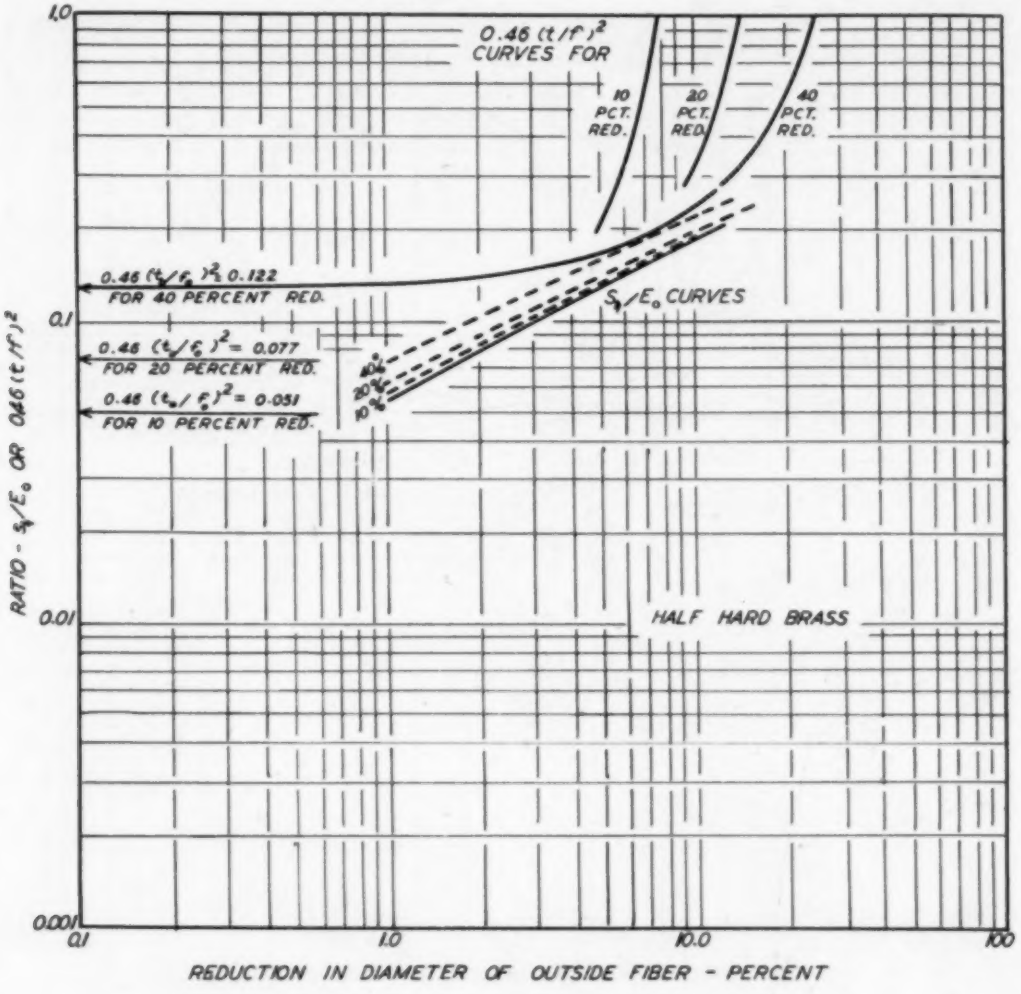


Fig. 13d—See Caption for Fig. 13b.

For these experiments, die Nos. 1 (0.870-inch diameter) and 5 (2.000-inch diameter) were used.

The results are plotted graphically in Figs. 14a to 14g. The co-ordinates have been chosen in accordance with the principle of geometric similarity (see Theory): the abscissae represent the relative blank thickness; i.e., the actual blank thickness, t_o, divided by the actual blank diameter, D_o, while the ordinates represent the per cent reduction in diameter from the outer edge of the blank to the edge of the die hole. The experimental data are represented by bars, the length of the bar indicating the experimental gap between the lowest conditions for folding and the highest conditions for fold-free operation. From the fact that the experimental data for the 0.870 and 2.000-inch dies coincide in all seven graphs, it is evident that the principle of geometric similarity is fulfilled for all metals and tempers studied.

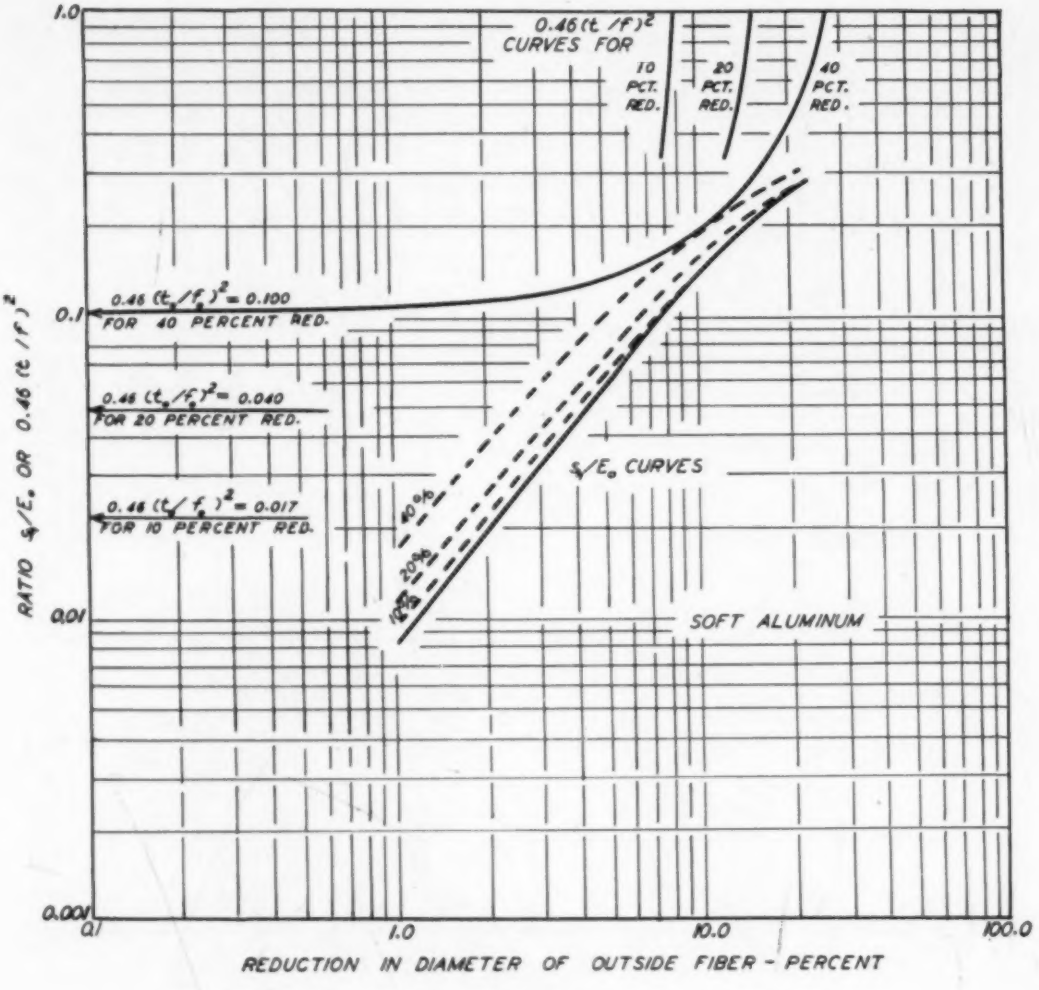


Fig. 13e—See Caption for Fig. 13b.

The limiting reductions in diameter for different relative blank thicknesses, as determined theoretically (see above), are entered in the charts as solid curves. In general, there is very good agreement between experimental and theoretical values. For hard copper and hard aluminum, no theoretical curves were developed (see Experimental Procedure). For these metals, empirical curves, represented by dashed lines, have been drawn through the data.

It appears from these charts that the metal itself has a minor effect on the proneness of a blank to buckle. It might be mentioned that this was found to be true in the case of buckling encountered in tube sinking also (24). Of the four soft metals studied, steel and aluminum are more prone to buckle than the others, the latter fact being in general agreement with Jevons' statement referred to above (10). Esser and Arend's empirical equation (see Introduc-

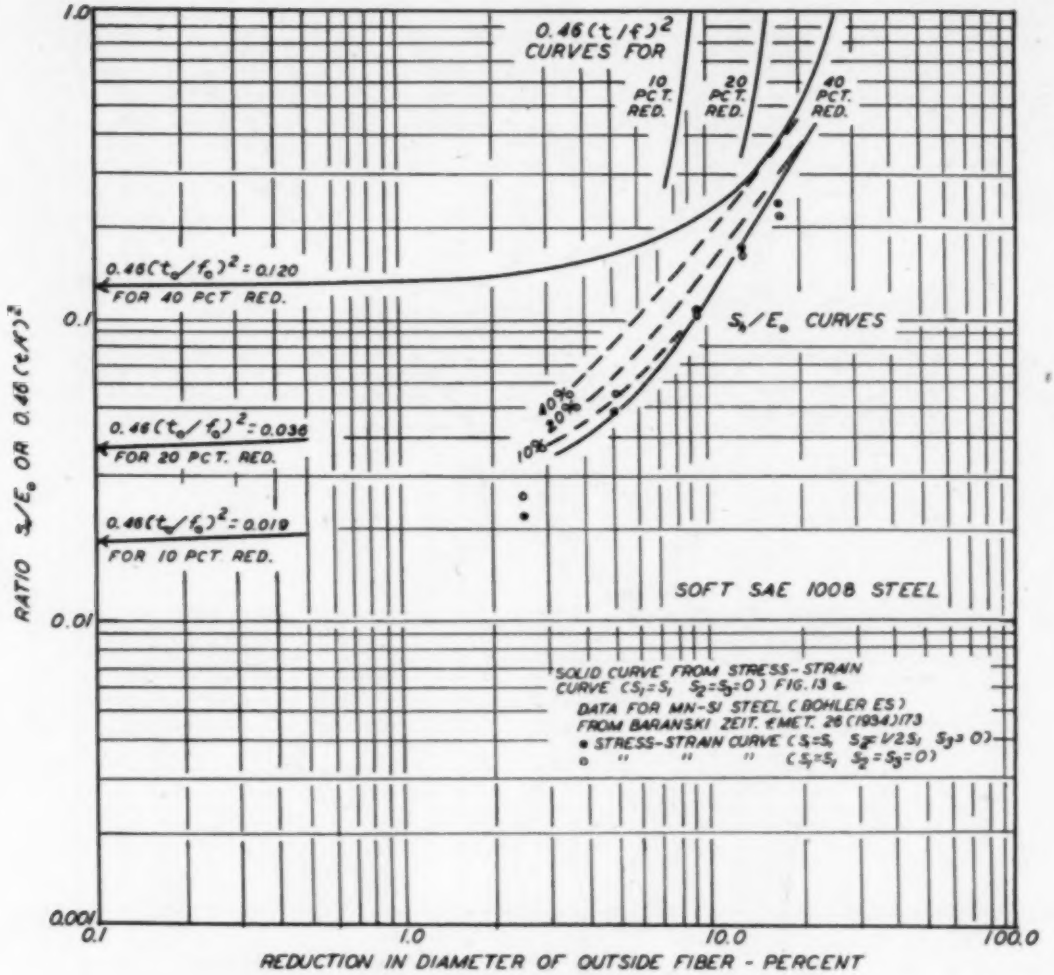


Fig. 13f—See Caption for Fig. 13b.

Table I

Metal	$R = \frac{D_o - D_{100}}{D_o} = \frac{2f}{D}\,100$ Reduction	Asymptotic Value $0.46\,(t_o/f_o)^2$	$(t_o/f_o)^2$	t_o/f_o	t_o/D_o
Soft Copper	10	0.012	0.026	0.16	0.008
	20	0.022	0.038	0.20	0.020
	40	0.048	0.104	0.32	0.064
Soft 70:30 Brass	10	0.014	0.030	0.17	0.009
	20	0.025	0.054	0.23	0.023
	40	0.048	0.104	0.32	0.064
Half Hard 70:30 Brass	10	0.051	0.111	0.33	0.017
	20	0.077	0.167	0.41	0.041
	40	0.122	0.265	0.52	0.104
Soft 2S Aluminum	10	0.017	0.037	0.19	0.010
	20	0.040	0.087	0.30	0.030
	40	0.100	0.217	0.47	0.094
Soft SAE 1008 Steel	10	0.019	0.040	0.20	0.010
	20	0.036	0.078	0.028	0.028
	40	0.120	0.261	0.51	0.102

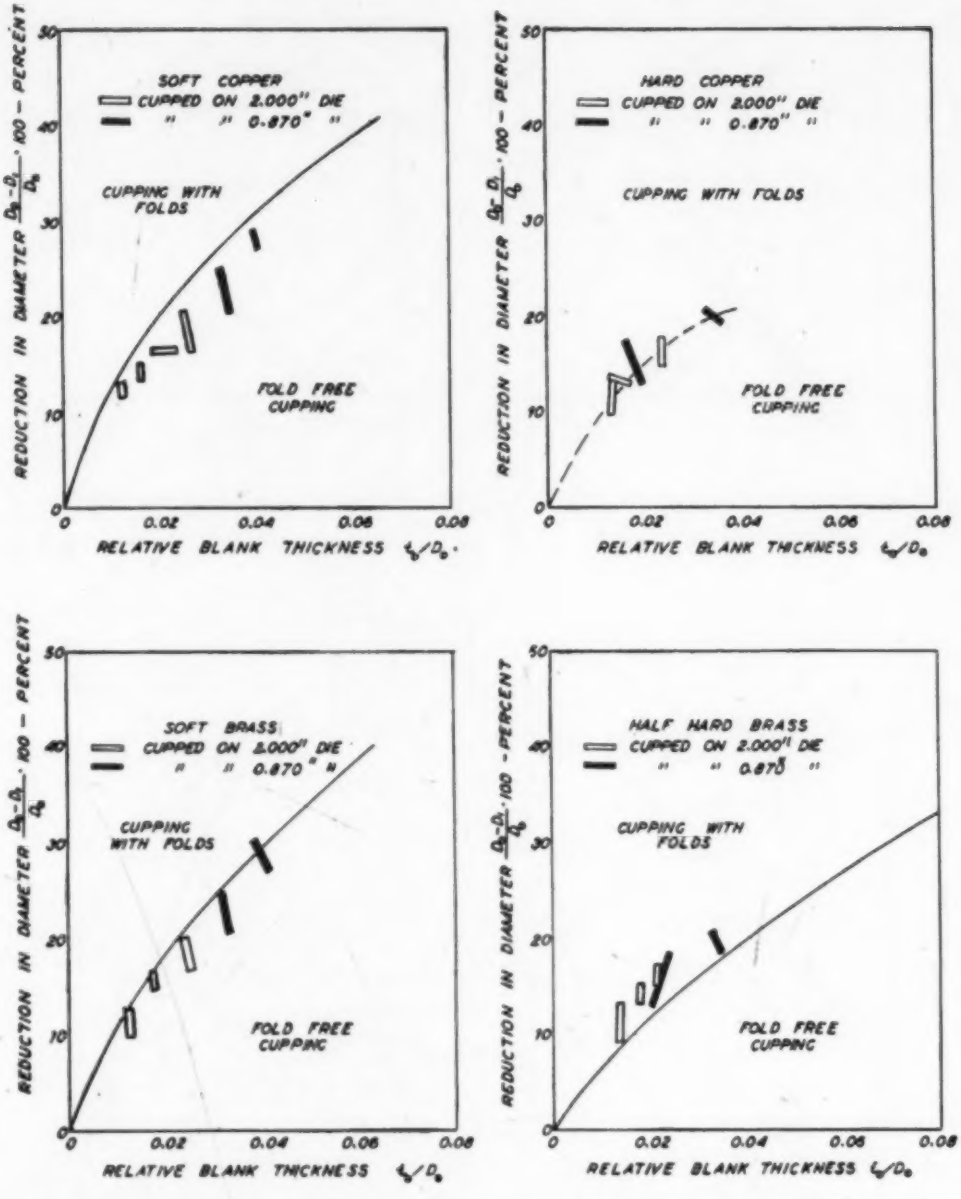


Fig. 14—Maximum Reductions from Blank Diameter to Die-Hole Diameter That May Be Made with "Flat" Dies Without Folding Occurring for Various Relative Blank Thicknesses.

tion) which because of the smallness of their die radius should be roughly applicable to the results obtained here for "flat" dies with virtually no die radius is in surprisingly good agreement with the present data, all things being considered.

Buckling on conical dies. For these experiments, die Nos. 2 ($D_1 = 0.870$ inch, $R_o = 19.0$ %), 3 ($D_1 = 0.870$ inch, $R_o = 28\%$), 4 ($D_1 = 0.870$ inch, $R_o = 34\%$), and 6 ($D_1 = 2.000$ inches, $R_o = 26.5\%$ were used. The results are plotted graphically in Figs. 15a

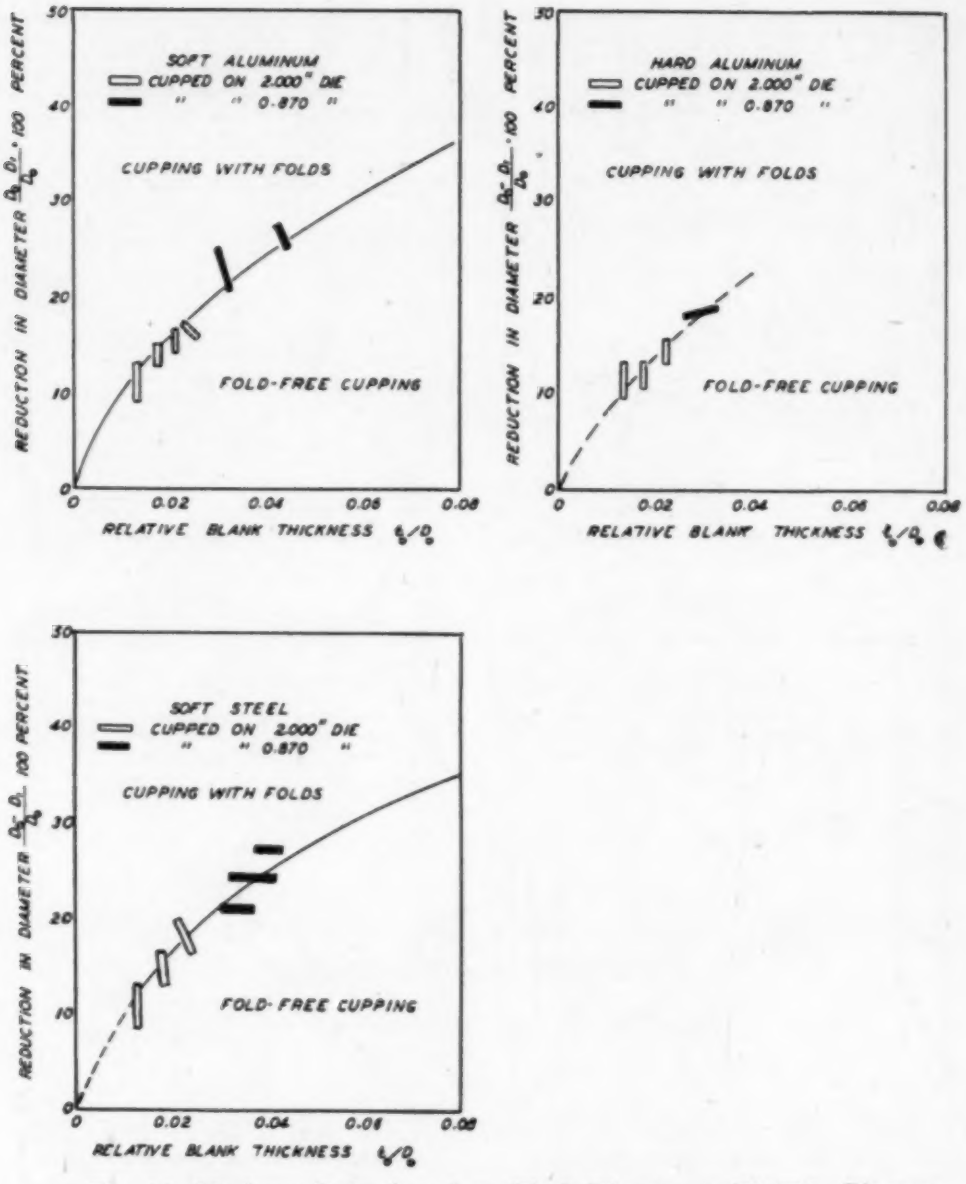


Fig. 14—Maximum Reductions from Blank Diameter to Die-Hole Diameter That May Be Made with "Flat" Dies Without Folding Occurring for Various Relative Blank Thicknesses.

to 15d. The abscissae represent the relative blank thickness, t_o/D_o; the ordinates represent the reduction in diameter from the outer edge of the blank to the diameter, D_1, of the die (see Fig. 10b).

The theoretical curves given in Fig. 14 have been transposed with the aid of the chart given in Fig. 11 as described in the section, "Theory", to R_o values of 19.0, 26.5, 28 and 34%. There is good agreement between the theoretical and experimental data whether the latter were obtained from dies whose land diameter was 0.870 or 2.000 inches. This confirms both the principle of geometric similar-

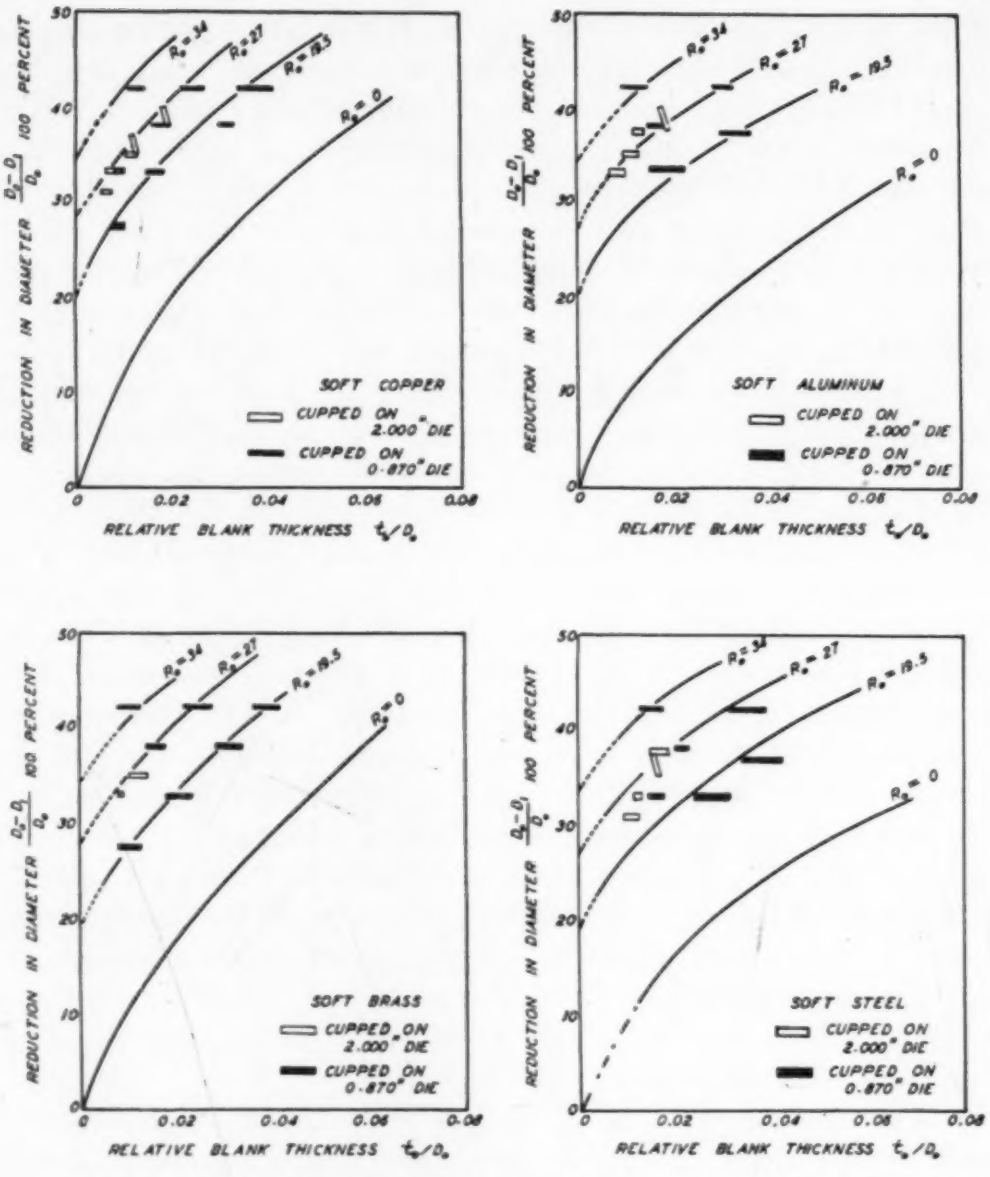


Fig. 15—Maximum Reductions from Blank Diameter to Die-Hole Diameter That May Be Made with Conical Dies Without Folding Occurring for Various Relative Blank Thicknesses.

ity and the method of manipulation used to transpose the curves for all conditions studied. The effect of metal shows the same general trend as in the case of dies giving plane circular flanges.

In the case of conical dies, there are certain limiting conditions already alluded to in the Introduction and Theory, about which certain remarks should be made here. In deriving his original equations, Geckeler assumed that the bending of the metal over the edge of the die at the inner diameter of the flange effected a lateral support at this point on the flange. In the present case, it is quite possible that the

flange may resist buckling up to the point where the outer edge of the blank passes over the shoulder of the die, at which stage the point of support is transferred to the point where the punch contacts the metal, changing the problem completely and again opening up the possibility of buckling. As a matter of fact, buckling was observed to take place in a number of cases after the outer edge of the blank had passed over the corner of the die. This condition occurred in very thin blanks. In Figs. 15a through 15d, this fact is indicated by the dotted lines. In other words, blanks whose dimensions were such as to give a point below the solid line successfully resisted folding throughout the cupping process; those whose dimensions were such as to give a point below the dotted line would resist buckling up to the point where the outer edge of the blank passed over the shoulder of the die, after which stage they collapsed.

Number of lobes into which flange buckles. It was pointed out in the section "Theory" that relatively thick blanks may undergo deformation before folding occurs, thus affecting the value of the flange width, f, in Geckeler's Equation 3. In the following discussion, results obtained with blanks whose thickness was less than a tenth of the flange width only are reported, since it was found in this case that folding occurred after only a fraction of 1% reduction in diameter. This meant that the flange width, f, that was effective at the time of folding was practically the same as the starting flange width, f_o, thus permitting both the experimental results and Geckeler's equation to be plotted as a function of the total flange reduction in diameter. The number of lobes occurring under such conditions have been plotted in Fig. 16.[9]

The data represented in this chart are taken indiscriminantly from results obtained with all metals and tempers studied. Results obtained on 0.870 and 2.000-inch dies as well as "flat" or conical dies are indicated in the chart by different symbols. All of these factors were without significant effect on the results. Also plotted in this graph is a curve giving the theoretical number of lobes according to Geckeler's equation. It will be noted that the experimental values consistently fall above the theoretical curve for the entire range studied. The disagreement between the present data and Geckeler's curve is of interest not only in itself but because of the possible corrections it implies might be required in the equation giving the critical stress, i.e., Equation 2.

[9]Actually the data from thicker blanks differ only slightly from those given here (the corrections required for the thicker blanks being so slight).

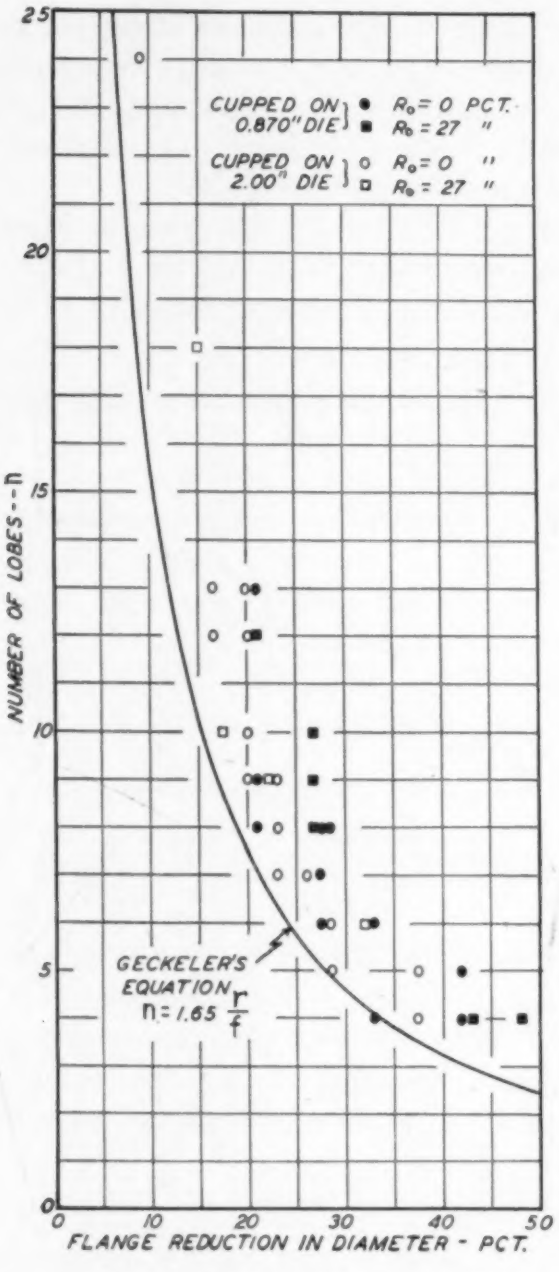


Fig. 16—Number of Lobes Into Which Flange Buckles as a Function of Flange Reduction. Experimental data are for all metals and tempers studied.

Buckling on dies with rounded radius. So far, the discussion has been concerned with results obtained on either "flat" or conical dies. Some mention should be made of the applicability of the data to dies with a rounded radius. Because of the fact that the flange of a blank is thrown up as the punch descends (see Fig. 17), the point of lateral support is moved inward during the cupping opera-

tion. Thus the flange width is not decreased as rapidly as in the case of a conical die. (In fact, the die contour may be so chosen that the flange width actually increases during the cupping operation.) The result of this is that rounded dies, in general, are not so efficient as conical dies in preventing buckling.

General discussion. In the present work, it was assumed (on the basis of stress-strain data from Taylor and Quinney as well as others) that the quantity s/E_o when plotted as a function of strain

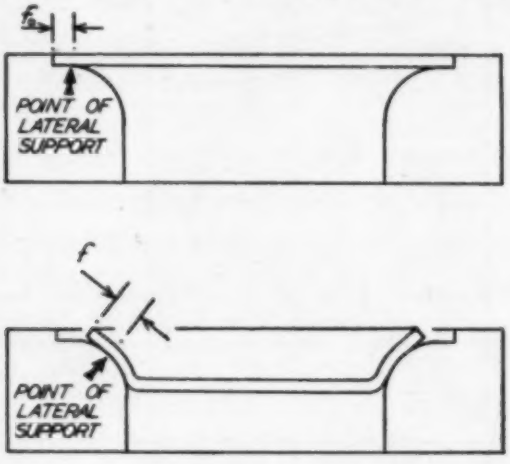


Fig. 17—Change in Flange Width Occurring with Dies of Rounded Radius as Cupping Operation Proceeds.

was insensitive to the stress state occurring in the metal. A point of broader significance, however, is that this assumption may be evoked in the solution of many buckling phenomena encountered in other forming operations. Thus the limiting conditions before buckling occurs for a metal being plastically deformed may be expressed as:

$$\left(\frac{s}{E_o}\right)_{\text{forming}} = f\,(x, y, \ldots\ldots)$$

where x, y,..... represent dimensional or geometric quantities (such as diameters, thicknesses, angles, etc.) involved in the process in question. The left-hand side of this equation will be set by the stress-strain diagram of the metal in question and the appropriate strain rate. No further stress analysis of the forming process need be made. Further, forming operations which are the same with respect to their geometric conditions and the rate at which the ratio $s/E_o)_{\text{forming}}$ is developed should exhibit the same folding tendencies. Thus tube sinking and tube necking, two processes which are very similar in their geometric details, should exhibit very similar

folding tendencies, despite the fact that the stress states existing within the metal during the two processes are quite different.

Acknowledgments

It is a pleasure to acknowledge a debt of gratitude to many people for various services and favors: to Messrs. E. C. Smith and J. J. Bowden of the Republic Steel Corporation for supplying the steel used in this investigation; to Professors K. H. Donaldson and G. Sachs of Case School of Applied Science for supplying the aluminum used; to Mr. A. W. Ross of the Research Department, Midwestern Division, Chase Brase and Copper Company, Inc., for making the drawings; to Mr. A. I. Blank of the Research Department, Chase Brass and Copper Company, Inc., Waterbury, Connecticut, for determining the stress-strain diagrams of the metals; and to Dr. H. P. Croft, Director of Technical Control and Research, Midwestern Division, Chase Brass and Copper Company, Inc., for his encouragement and support of this work.

References

1. M. Sommer, "Experiments on the Drawing of Hollow Bodies," *Maschinenbau,* Vol. 4, 1925, p. 1171-1178; *Forschungsarb. Z. Ver. Deutscher Ing.,* No. 286, 1926.
2. H. Draeger, "Effect of Radii on Drawing of Shells Out of Thin Sheet," *Berichte über Betriebwissenschaftliche Arbeiten,* Vol. 2, 1929, p. 1-21.
3. W. Sellin, "Effect of Draw Die and Punch Radii on the Depth of the Draw in Cupping Sheet Parts," *Berichte über Betriebwissenschaftliche Arbeiten,* Vol. 3, 1930, p. 18-35.
4. E. Ackermann, "The Drawing of Hollow Bodies from Thin Strip with Particular Consideration of the Blank Holding Effect," *Stahl und Eisen,* Vol. 51, 1931, p. 619.
5. L. Herrmann and G. Sachs, "Untersuchungen über das Tiefziehen," *Metallwirtschaft,* Vol. 13, 1934, p. 687-692, 705-710.
6. F. Fischer, "On Stretching and Formation and Prevention of Wrinkles in Drawing Hollow Bodies," *Tech. Hochschule,* Stuttgart, Dissertation, 1927.
7. H. Esser and H. Arend, "Die Tiefziehprüfung von Blechen," *Archiv f. das Eisenhüttenwesen,* Vol. 14, 1940, p. 223-231.
8. E. V. Crane, "Plastic Working of Metals and Power Press Operations," J. Wiley & Sons, New York, 1932, p. 161.
9. C. W. Hinman, "Pressworking of Metals," McGraw-Hill Book Co., New York, 1941, p. 304.
10. J. D. Jevons, "The Metallurgy of Deep Drawing and Pressing," J. Wiley & Sons, New York, 1940, p. 108.
11. J. W. Geckeler, "Plastische Knicken der Wandung von Hohlzylindern und einige Andern Faltungserscheinungen," *Z. Angewandte Mathematik und Mechanik,* Vol. 8, 1928, p. 341-352.
12. Engesser, *Schweizerische Bauzeitung,* Vol. 26, 1895, p. 24-. . .; *Z. f. Architektur und Ingenieurwesen,* 1889, p. 445.

13. H. B. Westergaard and W. R. Osgood, "Strength of Steel Columns," *Transactions,* American Society of Mechanical Engineers, Vol. 49-50, 1928, APM 50-9, p. 65-80.
14. T. von Karman, "Untersuchungen über Knickfestigkeit," *Forschung auf dem Gebiete des Ingenieurwesen*—Beilage, V. D. I. Forschungsheft 81, 1909.
15. J. L. Holmquist and A. Nadai, "A Theoretical and Experimental Approach to the Problem of Collapse of Deep-Well Casing," *Journal,* American Petroleum Institute, 1939, p. 392-420.
16. G. Sachs, "Spanlose Formung der Metalle," Leipzig, Akademische Verlag, 1937, p. 11-38.
17. E. Siebel, "Plastic Forming of Metals," *Steel,* Vol. 94, Oct. 23, 1933, p. 37-40, and continued in subsequent issues.
18. S. Fukui, "Researches on the Deep Drawing Process," Tokyo Institute of Physical and Chemical Research, *Scientific Papers,* Vol. 34, 1938, p. 142-152.
19. G. I. Taylor and H. Quinney, "The Plastic Distortion of Metals," *Philosophical Transactions,* Royal Society, Sec. A, Vol. 230, 1932, p. 323-362.
20. M. Ros and A. Eichinger, "Experimentation Regarding the Clarification of the Problem of the Failure Condition," *Zurich. Eidgenössische Materialprüfungs und Versuchsanstalt,* Report 34, 1929.
21. E. A. Davis, "Increase of Stress with Permanent Strain," *Transactions,* American Society of Mechanical Engineers, Vol. 65, 1943, p. A187-A196.
22. G. Baranski, "Zerreissversuche bei ebener plastischer Verformung," *Zeitschrift für Metallkunde,* Vol. 26, 1934, p. 173-180.
23. H. W. Swift, "Deep Drawing Research," *Proceedings,* Institution of Automobile Engineers, Vol. 34, 1939-40, p. 361-432.
24. G. Sachs and W. M. Baldwin, "Folding in Tube-Sinking," *Transactions,* American Society of Mechanical Engineers, Vol. 68, 1946, p. 647-654.

BEARING PROPERTIES OF 24S-T SHEET AND SHEAR STRENGTH OF 24S-T RIVETS AT ELEVATED TEMPERATURES

By A. E. Flanigan, L. F. Tedsen and J. E. Dorn

Abstract

The shear strength of 24S-T rivets and the bearing properties of 24S-T sheet have been determined at temperatures up to 375 F after exposure times ranging from ¼ hour to 1000 hours. The bearing properties include yield stress (2% offset) and ultimate stress. Compared with the original room temperature values the greatest losses in any of the properties studied are 9% at 212, 15% at 250, 27% at 300 and 40% at 375 F. Curves showing the bearing and shear properties plotted against time at temperature are generally similar in shape to the curves for the corresponding tensile properties. The ratios of ultimate bearing stress and ultimate shear stress to ultimate tensile stress are essentially independent of time and temperature over the range considered. The ratio of bearing yield stress to tensile yield stress is more variable. The data should be used with care in design since the strengths indicated in short-time tests may be greater than those obtainable with steady loading over long periods.

Introduction

THE mechanical properties of high strength aluminum alloy sheet at elevated temperatures are of interest in certain applications. This paper is concerned with the effects of temperature and exposure time on the elevated temperature bearing properties of 24S-T[1] sheet and on the shear strength of 24S-T[1] rivets. The work, performed at the University of California as a portion of project NRC-548, was financed by the War Production Board and was supervised by

[1]This alloy, designated 24S by its producer, the Aluminum Company of America, has the nominal composition: 4.5% copper, 0.6% manganese, 1.5% magnesium. The T condition is obtained by solution heat treatment at 910 to 950 F followed by quenching in water and aging for 4 days or more at atmospheric temperature.

A paper presented before the Twenty-eighth Annual Convention of the Society held in Atlantic City, November 18 to 22, 1946. Of the authors, A. E. Flanigan is assistant professor at the University of California at Los Angeles while L. F. Tedsen and J. E. Dorn are engineer and associate professor, respectively, at the University of California, Berkeley. Manuscript received January 8, 1946.

the Office of Production Research and Development. This paper has been released for publication by the latter agency.

The materials studied are among those popularly employed in high strength sheet construction. The following properties were investigated. They are of interest in connection with the behavior of riveted joints:

A. In bearing tests performed on 0.032-inch bare 24S-T sheet
   1. Bearing yield stress (2% offset)
   2. Ultimate bearing stress
B. In rivet shear tests performed on 1/8-inch D.D. rivets
   1. Ultimate shear stress

In addition to tests at room temperature, specimens were tested at 212, 250, 300 and 375 F after being heated for periods ranging from 15 minutes to 1000 hours.

Specimen Design and Preparation

The shear tests were made on riveted specimens prepared by the Douglas Aircraft Company of Santa Monica, California. Fig. 1

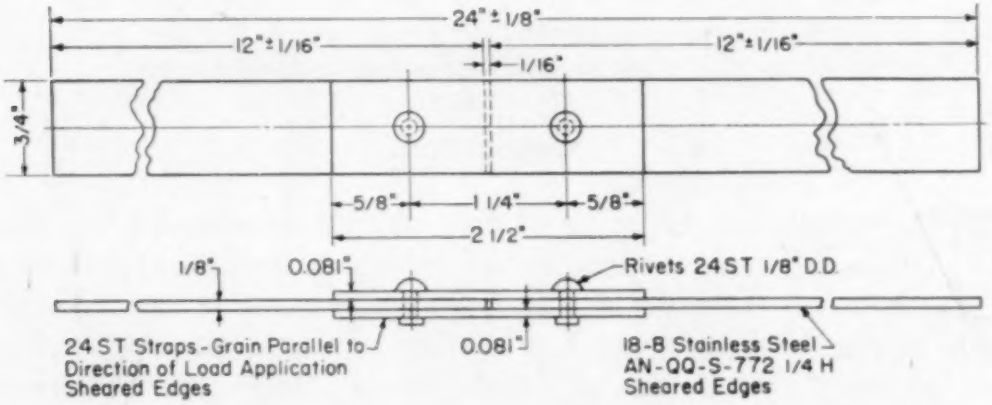


Fig. 1—Elevated Temperature Rivet Shear Specimen.

shows the dimensions of these specimens which were designed to cause double shear of the hand-driven rivets.

Dimensions of the bearing specimen are shown in Fig. 2. Edge distance, width, and thickness were 4D, 4.8D and $\frac{D}{4.9}$ respectively (where D is the diameter of the bearing hole). The loading axis was parallel to the direction of rolling. Specimens were sheared from 0.032-inch thick 24S-T sheet and the $\frac{5}{32}$-inch bearing holes were

reamed to size. The material was obtained from the Douglas Aircraft Company production stock.

The specimens were heated for various lengths of time in carefully controlled oil bath furnaces after which they were stored until required for testing. The storage period ranged from 4 days to several months. A tempering oil (Houghton's No. 80) was used in the oil baths at all temperatures. Temperature variations in the

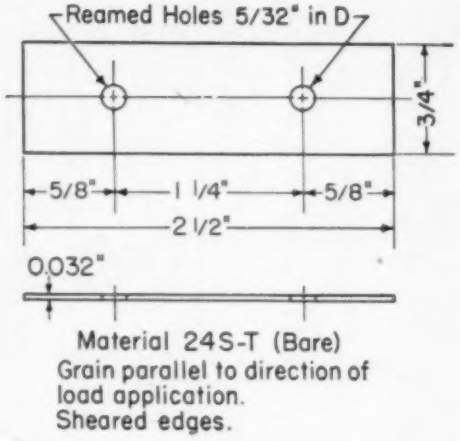


Fig. 2—Elevated Temperature Bearing Specimen.

central 6 inches of specimens in the baths were no greater than ± 2 F temporal and ± 2 F spatial except for brief drops attending the insertion of additional specimens. After removal of specimens from the baths all oil was wiped off before storage.

Heating and Temperature Control During Tests

Preliminary to testing, the stored specimens were reheated and maintained at temperature in a split cylindrical furnace located between the crossheads of the tensile testing machine. Fig. 3 shows the furnace which was 17 inches long and contained 3 banks of heating elements arranged vertically. The voltage across each bank was adjusted independently to minimize spatial temperature variations in the specimens. Any variations which may have occurred are considered unimportant since in each type of specimen the deformation was highly localized. Specimens were brought to the testing temperature in approximately 30 minutes. Temporal variations during the course of a test were no greater than ± 3 F in the bearing tests and ± 6 F in the shear tests.

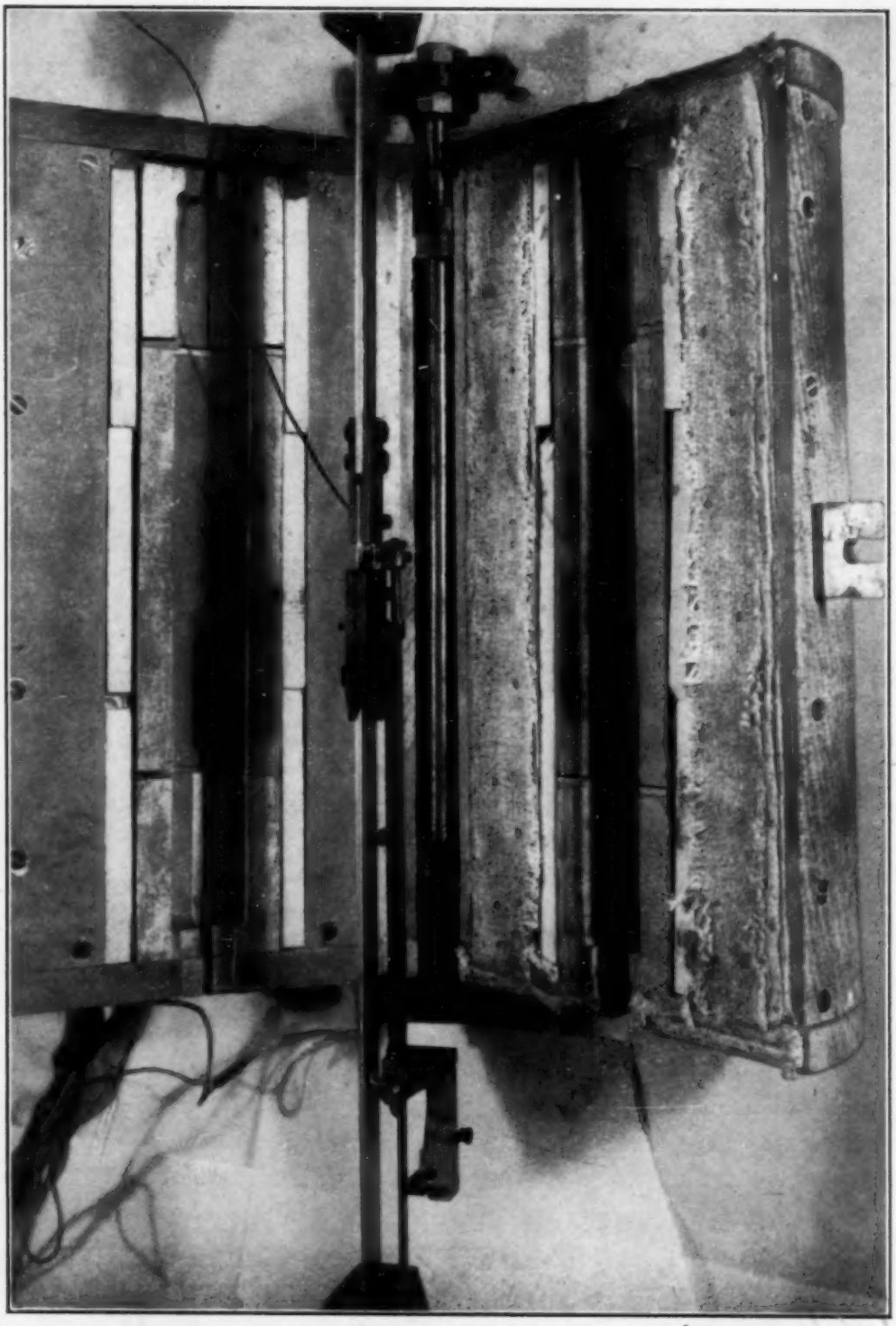


Fig. 3—Photograph of the Furnace in Open Position.

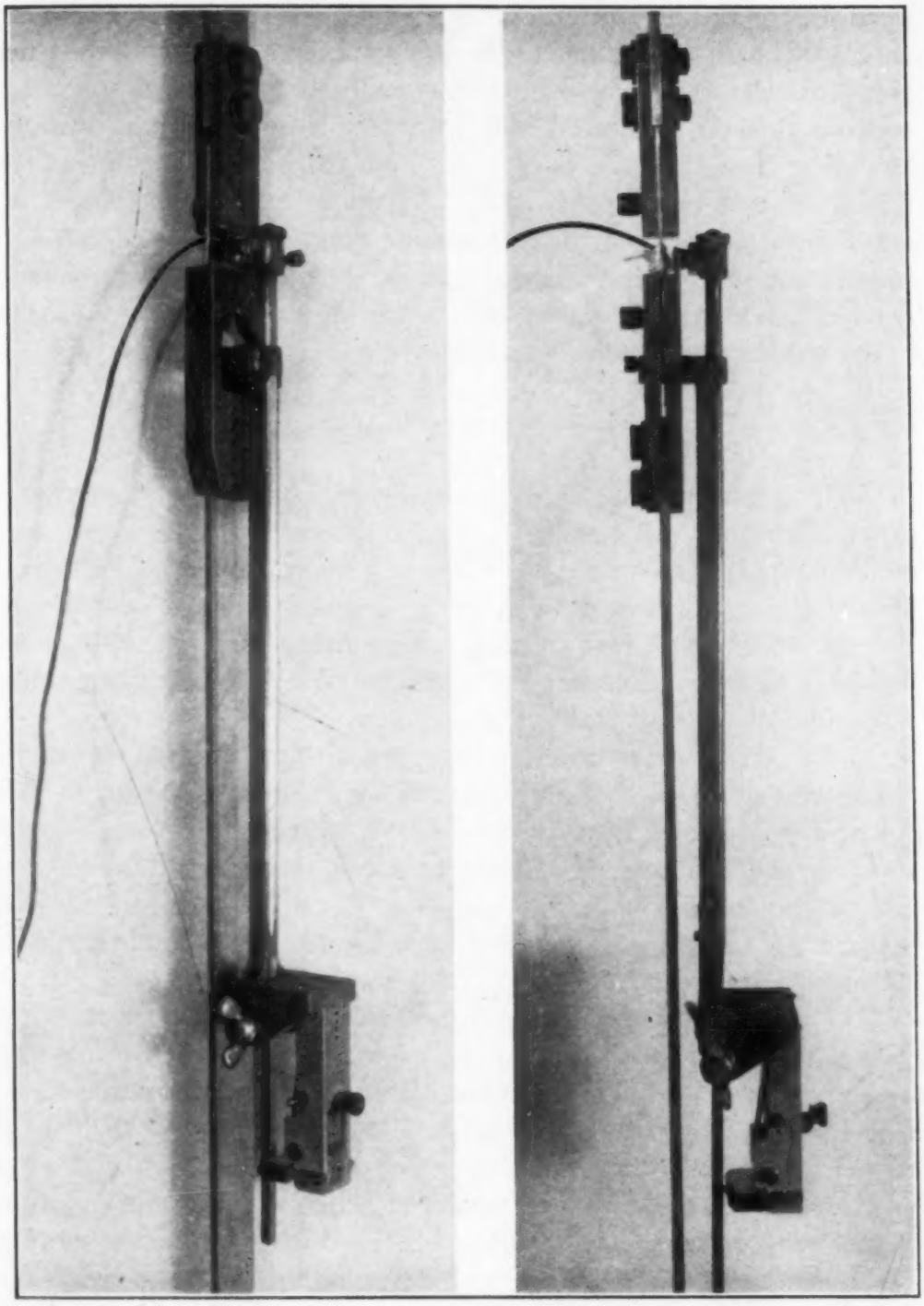


Fig. 4—Extensometer Assembly and Thermocouple Attachment.

In both shear and bearing tests temperature measurements were made by means of a 30-gage glass insulated iron-constantan thermocouple secured firmly at the center of the specimen by several turns

of light, flexible, spun glass sheathing as shown for the bearing specimen in Fig. 4. This couple did not indicate true specimen temperature since it was also in contact with the glass wrapping. The relation between indicated and true temperatures was determined, however, in preliminary tests which involved dummy specimens containing peened-in couples. The correction, which was small, was determined and applied for each testing temperature. The peened-in couples and the dummy specimens were located at the points of greatest interest, namely, at the rivets in the shear tests and adjacent to the hole in the bearing tests.

Load and Deformation Measurements

The load was measured by the deflection of a proving ring in series with the specimen. SR-4, A-11 electric strain gages were mounted in opposition on the inner and outer surfaces of the ring. This unit was calibrated and checked regularly against a calibrated Toledo scale. The load readings were taken on an SR-4 Strain Indicator and the maximum error was thought to be no greater than 3 pounds.

The extensometer developed to permit the evaluation of bearing yield stress at elevated temperatures is shown in Figs. 4 and 5. The device was used to measure the deformation of the lower bearing hole. It incorporates a Tuckerman optical strain gage mounted outside of the furnace on extension arms. The latter extend into the furnace where they are attached to reference points located on the specimen and on the lower grip.

As indicated by Fig. 5, the distance between the upper reference points and the lower loading pin remains very nearly constant throughout the loading period since the intervening portion of the lower grip is essentially stress free. It may also be seen that deformation of the hole during loading causes a shortening of the distance between the pin and the lower reference points. For deformations of the order required to determine bearing yield stress, this shortening is very nearly equal to the hole deformation. Since compression of the pin is entirely elastic and is relatively insignificant, it follows that the hole deformation during loading is described by the relative motion of the upper and lower reference points.

Attachment of the extension arms to the specimen was accomplished by means of sharp conical points. To insure that extensometer and specimen were aligned correctly, the former was mounted

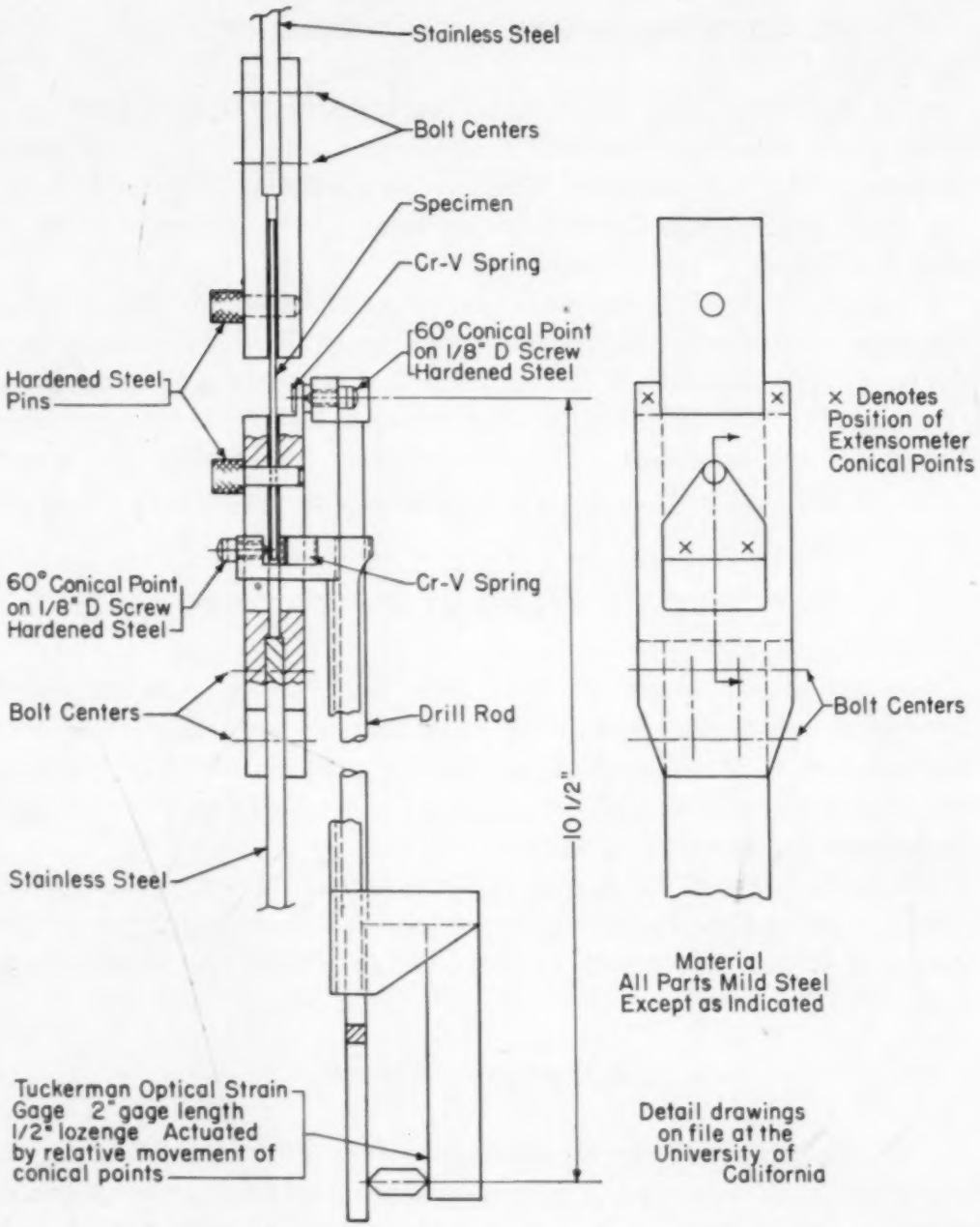


Fig. 5—Schematic Drawing of Elevated Temperature Bearing Test Extensometer Assembly.

with the specimen under a load of approximately 50 pounds (corresponding to a bearing stress of 10,000 psi).

The hardened steel loading pins were 0.0003 inch smaller in diameter than the undeformed bearing holes. The lower grip was designed to allow unrestricted upsetting of the specimen material adjacent to the hole during loading.

Calculation of Bearing and Shear Stresses

In the calculation of ultimate bearing stress and bearing yield stress the bearing area was taken as the product of the pin diameter and the original measured thickness of the specimen. Values of bearing yield stress were determined by means of a 2% offset line as shown in Fig. 6.

Calculations of rivet shear stress were based on the nominal diameter of the hole size recommended by ANC-5(1)[2] for 1/8-inch rivets. (This diameter is 0.1285 inch.) To permit a determination of the actual hole diameter, several untested riveted specimens were dismantled and examined. The average value for 12 holes was found to be 0.1310 ±0.0010 inch. In each case the rivets were found to fill the hole completely.

Strain Rate

A crosshead speed of 0.01 inch per minute was employed throughout the initial portion of each bearing test. This rate was continued up to attainment of the bearing yield stress after which it was increased to 0.06 inch per minute. The latter value was used throughout the rivet shear tests.

It is recognized, of course, that the actual rates of deformation at the rivets and at the bearing holes differed considerably from the crosshead speed. No effort was made to determine the actual strain rates.

Experimental Results

The results are shown by means of curves on the following pages. In general, each point on the curves represents an average value based on two or more tests. Fig. 7 shows the effects of temperature and exposure time on the bearing yield stress and the ultimate bearing stress of 24S-T sheet. The effects of the same variables on the ulimate shear stress of 1/8-inch 24S-T rivets are shown in Fig. 8.

Remarks on the Specimens—Values of the bearing properties determined in tests on sheet materials are known to depend to a considerable extent on the type of specimen employed (1), (2). This is especially true in the case of ultimate bearing stress. The

[2]The figures appearing in parentheses pertain to the references appended to this paper.

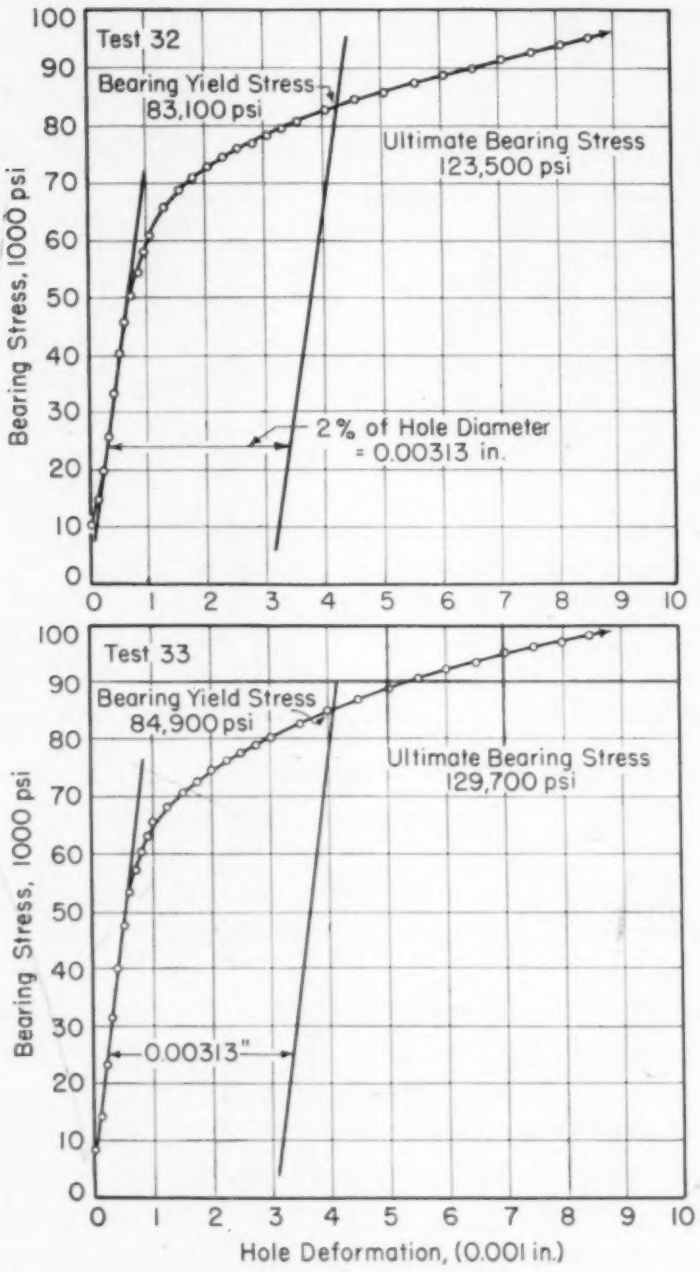


Fig. 6—Typical Bearing Stress-Hole Deformation Curves for 24S-T (Bare) Sheet.

Test temperature—250 F; Crosshead speed—0.01 inch per minute over region indicated, followed by 0.06 inch per minute to ultimate; Hole diameter—5/32 inch; Sheet thickness—0.032 inch; Time at temperature—¼ hour; Direction of stress—with grain.

values obtained with the present specimen, therefore, may differ from those associated with other types.

The rivet shear tests were performed on driven rivets. The actual diameter after driving was 0.131 ± 0.001 inch, a considerable

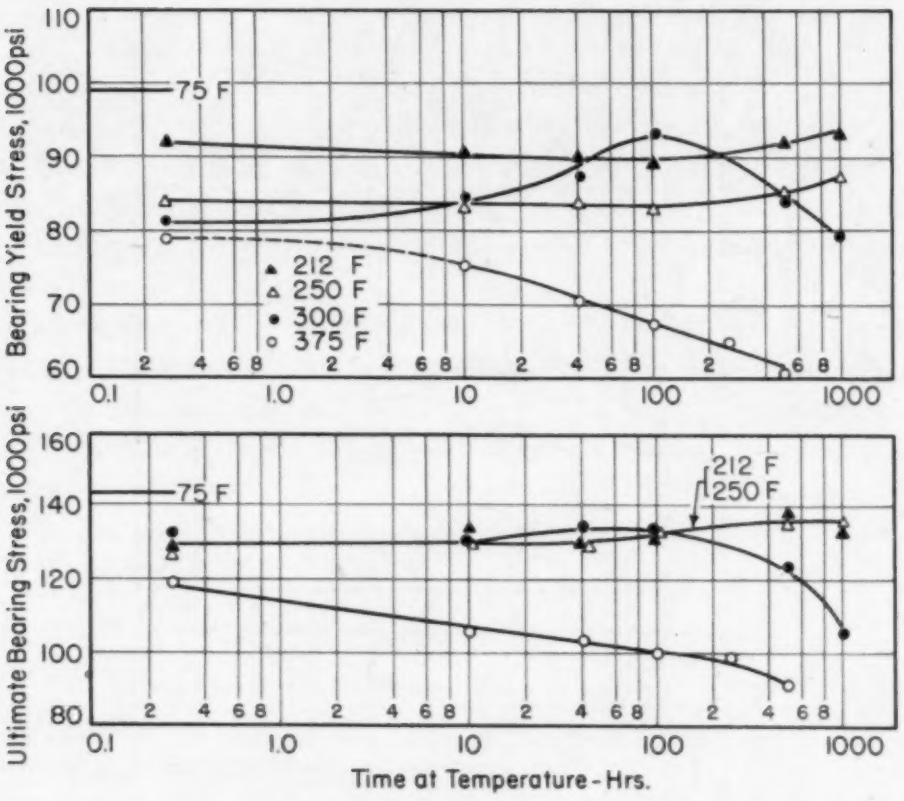


Fig. 7—Effect of Temperature and Time of Exposure on Elevated Temperature Bearing Properties of 24S-T (Bare) Sheet.

Sheet thickness—0.032 inch; Direction of stress—with grain; Crosshead speed—0.01 inch per minute to BYS, followed by 0.06 inch per minute from BYS to ultimate; Bearing hole diameter—5/32 inch; Ratio of edge distance to hole diameter—4.0. (Each point represents average value of two or more tests.)

increase over the original value and 2% in excess of the nominal rivet hole diameter of 0.1285 inch. Since the calculation of ultimate shear stress was based upon a diameter of 0.1285 inch, the calculated values are approximately 4% higher than would have been obtained had the exact diameter of the driven rivets been used.

Effects of Temperature and Time on Bearing and Shear Properties

It was the primary purpose of this investigation to determine the effects of temperature and time on the bearing and shear properties of 24S-T at elevated temperatures. Since the properties depend to some extent on specimen design, and may be expected to vary from one lot of material to another, it is recommended that the values shown in Figs. 7 and 8 be considered in relation to the original room temperature values which are included in the figures and which

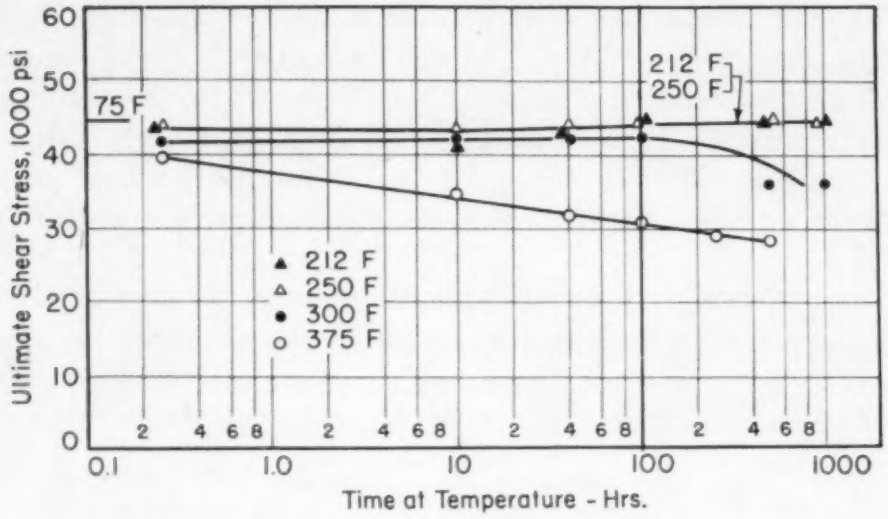


Fig 8—Effect of Temperature and Exposure Time on Ultimate Shear Stress of 24S-T Rivets at Elevated Temperatures.
Rivet diameter—⅛ inch; Crosshead speed—0.06 inch per minute; Rivet type—D.D. (Each point represents average value of two or more tests.)

were determined under the same testing conditions. The changes in properties induced by prolonged exposure at the elevated temperatures are readily understood in view of the susceptibility of 24S-T to "aging" and "overaging".

The values of bearing yield stress at 212 and 250 F are seen to be essentially independent of exposure time for times ranging from ¼ hour to 1000 hours. At 300 and 375 F, however, precipitation effects are apparent. At 300 F a maximum value is reached after approximately 100 hours. Overaging subsequent to the maximum results in a steady decrease in bearing yield stress as a result of which the 1000-hour and ¼-hour values are approximately equal. At 375 F it is possible that a maximum value of bearing yield stress is reached in the interval between ¼ and 10 hours but since no tests were made within the range the only effect noted is that of pronounced overaging attended by a rapid drop in strength.

The behaviors of ultimate bearing stress and ultimate shear stress are quite similar to that of bearing yield stress with the exception that at 300 F the former properties exhibit little evidence of a maximum value before the appearance of overaging.

In the case of both bearing and shear properties the loss of strength at 375 F is so great and so rapid that the use of 24S-T sheet and rivets at this temperature would seem unwise unless accompanied by a drastic reduction in design allowables. Losses in strength over

a 1000-hour period are small at 212 and 250 F and might be tolerated in some cases at 300 F. In this connection it should be remembered that susceptibility to corrosion is known to be increased by exposure of 24S-T to elevated temperatures for periods less than that required for full "aging" (3). Presumably, then, corrosion problems may be a factor in the use of 24S-T at temperatures up to 300 F.

The minimum values of the various properties over a 1000-hour period are summarized in the following table where they are expressed in terms of the original room temperature values. The table was derived from Figs. 7 and 8.

	Bearing Yield Stress, %	Ultimate Bearing Stress, %	Ultimate Shear Stress, %
75 F	100	100	100
212 F	91	91	98
250 F	85	91	98
300 F	80	73	77
375 F*	60	63	63

*At 375 F only times up to 500 hours were considered. Greater losses may be expected in 1000 hours.

Fig. 9, reproduced from reference 4, shows the effects of time and temperature on the elevated temperature tensile properties of 0.040-inch *alclad* 24S-T sheet stressed *transversely*.[3] It may be seen by comparison of Figs. 7 and 8 with Fig. 9 that the curves representing bearing and shear properties are generally similar in shape to the corresponding tensile curves. A further comparison will be made in the following paragraphs.

Comparison of Shear and Tensile Properties

Fig. 10, which was derived from Figs. 8 and 9, shows the effects of time and temperature on the ratio of ultimate shear stress to ultimate tensile stress at elevated temperatures. It may be seen that the ratio is essentially independent of time and temperature for all combinations of the variables investigated. The maximum variation is $\pm 5\%$.

This is an interesting point since it suggests that in the case of other high strength alloys approximate values of the ultimate shear stress at elevated temperatures may be obtained from values of the

[3]Unfortunately the corresponding tensile data for *bare* 24S-T stressed in the *rolling direction* were not available. They would be preferred for direct comparison with the bearing and shear results.

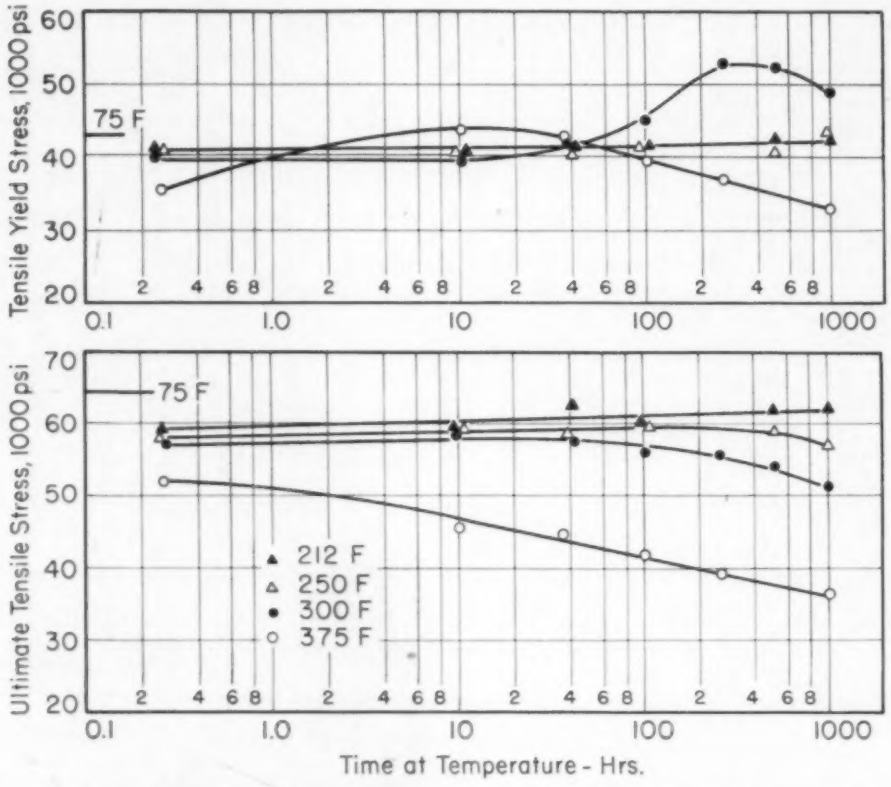


Fig. 9—Effect of Temperature and Time of Exposure on Elevated Temperature Tensile Properties of Alclad 24S-T Sheet.
Sheet thickness—0.040 inch; Direction of stress—cross grain; Crosshead speed—0.06 inch per minute. (Each point represents average value of two or more tests.)

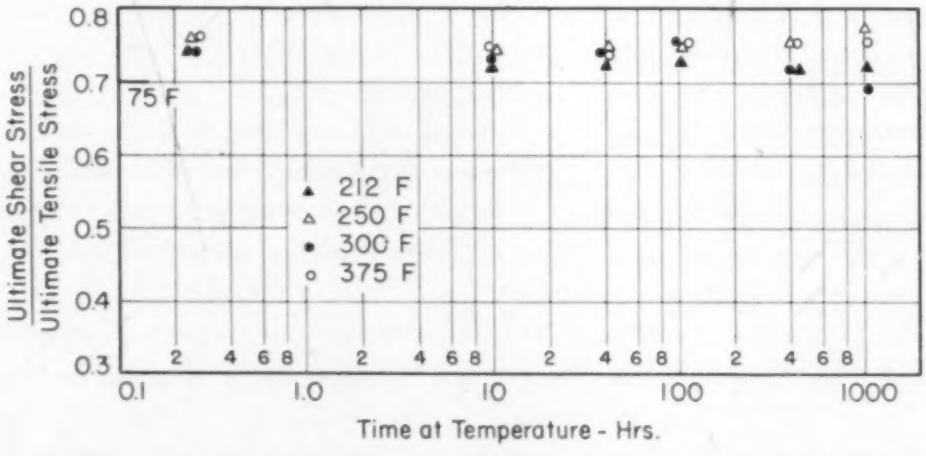


Fig. 10—Effects of Temperature and Time at Temperature on the Ratio of Shear and Tensile Strengths of 24S-T at Elevated Temperatures.
Shear strengths are those of 24S-T ⅛-inch D.D. rivets. (From Fig. 8)
Tensile properties are those of 0.040-inch alclad sheet loaded perpendicular to the grain. (From Fig. 9)

elevated temperature tensile properties if the ratio of the two stresses is known for room temperature. There is no reason, of course, to suppose this possible for all materials and all conditions. In the

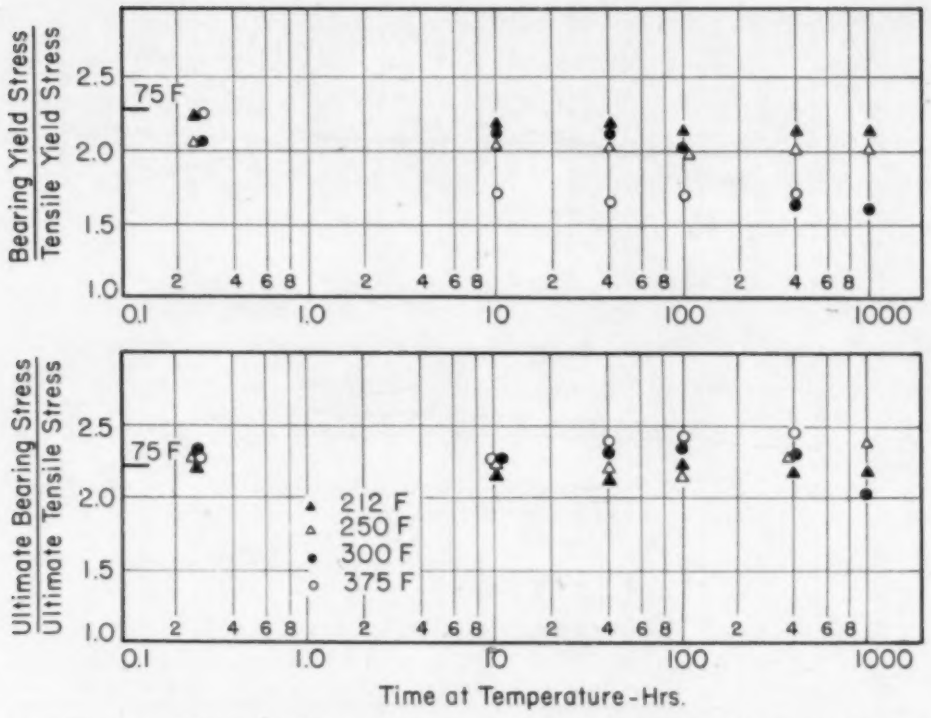


Fig. 11—Effects of Temperature and Time at Temperature on the Ratios of Bearing and Tensile Properties of 24S-T Sheet at Elevated Temperatures.

Bearing properties are those of 0.032-inch bare 24S-T sheet loaded parallel to the grain; edge distance = 4D, width = 4.8D, thickness = D/4.9. (From Fig. 7)

Tensile properties are those of 0.040-inch alclad 24S-T sheet loaded perpendicular to the grain. (From Fig. 9)

cases where elevated temperatures induce extreme changes in ductility, the ultimate tensile stress may be expected to reflect these changes to a greater degree than the shear stress.

In the present case the average value of the ratio is seen to be approximately 0.74. It should be remembered that the shear values were determined for 24S-T ⅛-inch D.D. rivets, whereas the tensile strengths are those of 0.040-inch 24S-T alclad sheet stressed transverse to the direction of rolling.

Comparison of Bearing and Tensile Properties

The ratios of bearing yield stress to tensile yield stress $\frac{BYS}{TYS}$ and ultimate bearing stress to ultimate tensile stress $\frac{UBS}{UTS}$ are shown in Fig. 11, derived from the curves of Figs. 7 and 9. Over the range of temperatures and times investigated there is a maximum variation of $\pm 10\%$ in the ratio of the ultimate strengths. There would seem to be little fundamental reason for constancy of the

ratio, however, since the mechanisms of failure are dissimilar in bearing and tensile tests.

According to Fig. 11, the ratio $\frac{\text{BYS}}{\text{TYS}}$ varies considerably and there seems to be little correlation between the values of bearing and tensile yield stress. It may be noted in this connection, however, that at 300 and 375 F the maximum values of bearing yield stress in Fig. 7 occur after shorter exposure periods than the corresponding values of tensile yield stress in Fig. 9. It will be recalled that the specimens used in the bearing and tensile tests were not taken from the same sheet.

The Problem of Creep

Just as short-time tensile tests at elevated temperatures may indicate strengths greater than those obtainable with steady loading over long periods, similar limitations may be expected in the case of the elevated temperature bearing and shear properties. As a result, such data, especially at the higher temperatures, should be used with caution in design. The importance of creep at elevated temperatures should be borne in mind in connection with the bearing and shear properties listed in Figs. 7 and 8, and also in connection with Figs. 9, 10 and 11 and the related discussion.

Summary and Conclusions

The shear strength of 24S-T rivets and the bearing properties of 24S-T sheet have been determined at temperatures up to 375 F after exposure times ranging from ¼ hour to 1000 hours. These properties have been compared with the corresponding tensile values. The following conclusions may be drawn:

1. The greatest losses in any of the properties studied are found to be 9% at 212, 15% at 250, 27% at 300 and 40% at 375 F. At the latter temperature only times up to 500 hours were considered. Greater losses may be expected in 1000 hours.
2. Since the properties may depend to a considerable extent on specimen design it is recommended that the effects of time and temperature be considered in relation to the original room temperature values determined under the same testing conditions.

3. Shapes of the curves for the bearing and shear properties plotted against time at temperature are in general similar to the shapes of curves for the tensile properties.
4. The ratios of ultimate bearing stress and ultimate shear stress to ultimate tensile stress are each found to be nearly independent of time and temperature over the range considered. The ratio of bearing yield stress to tensile yield stress is more variable.
5. The data obtained at the higher temperatures should be used with caution in design since strengths indicated in short-time tests may be greater than those obtainable with steady loading over long periods.

ACKNOWLEDGMENT

The authors are grateful to the War Production Board and to the Office of Production Research and Development for sponsorship and direction. They wish also to acknowledge the contributions of Bernard P. Faas, James T. Lapaley, Jr. and Allan T. Robinson, NRC-548 engineers, who participated in all phases of the testing program.

References

1. Army-Navy-Civil Committee on Aircraft Design Criteria, "ANC-5, Strength of Aircraft Elements," October 22, 1943.
2. R. A. Miller, "The Bearing Strength of Steel and Aluminum Alloy Sheet in Riveted or Bolted Joints," *Journal of Aero Science,* Vol. 5, No. 1, p. 22-24, November, 1937.
3. E. H. Dix, Jr., "New Developments in High Strength Aluminum Alloy Products," TRANSACTIONS, American Society for Metals, Vol. 35, 1945, p. 130-148.
4. A. E. Flanigan, L. F. Tedsen and J. E. Dorn, "Tensile Properties of Aluminum Alloy Sheet at Elevated Temperatures," to be published in *Metals Technology.*

DISCUSSION

Written Discussion: By R. L. Moore, research engineer, Engineering Design Division, Aluminum Research Laboratories, Aluminum Company of America, New Kensington, Pa.

By presenting data on the effect of elevated temperatures upon the bearing properties of 24S-T sheet and the shearing strength of 24S-T rivets, the authors have provided new information of value to designers of riveted, thin-sheet construction. It is quite convenient, although not entirely unexpected, that the effects of temperature on these properties parallel closely those observed in

elevated temperature tensile tests of the same aluminum alloys. The results of these tests provide a basis for estimating elevated temperature bearing and shearing properties for other aluminum alloys for which elevated temperature tensile data are already available.[1]

The authors have failed to emphasize the interesting fact that the maximum losses of 9% at 212 F and 15% at 250 F, given in conclusion 1, were confined to bearing properties. The losses in shear strength at these temperatures were negligible. It was only at the 300 and 375 F levels that the losses in shear and bearing properties were comparable.

Although the maximum heating times employed were sufficient to indicate useful, general relationships between bearing, shear, and tensile properties at elevated temperatures, care must be exercised, as the authors point out, in using these data in designs involving longer heating periods. The steep gradients shown on the curves for 300 and 375 F in Fig. 7, for example, obviously do not permit much extrapolation beyond the 500-hour and 1000-hour limits investigated. Elevated temperature tensile tests made at Aluminum Research Laboratories on 24S-T have shown losses of as much as 37% in ultimate strength after 10,000 hours' heating at 300 F, as compared to the loss of only 20% observed by the authors after 1000 hours. After 1000 hours' exposure at 300 F, the tensile yield strength was increased about 14%, according to Fig. 9, whereas after 10,000 hours' heating at the same temperature other tests have shown a decrease in tensile yield strength of as much as 22%. These data indicate the possible significance of heating time upon elevated temperature tensile properties. It seems reasonable to expect that bearing and shearing strengths will be influenced in much the same way.

The selection of allowable bearing design stresses for aluminum alloys, such as given in ANC-5,[2] has been based to a large extent upon the use of typical ratios of bearing to tensile properties, obtained from tests[3] similar in many respects to those described by the authors. In view of the considerable emphasis placed upon this type of ratio it should be pointed out that the ratios given in the paper are not directly comparable to those which may be shown to exist between current design values in bearing and tension in ANC-5. The authors' bearing tests were made on specimens having an edge distance of four times the diameter of the bearing hole whereas edge distances of 1.5 and 2.0 times the hole diameter are the only ones covered in ANC-5. The authors' bearing tests, moreover, were made in a with-grain direction on 0.032-inch thick, bare 24S-T sheet, whereas the tensile properties with which the bearing strengths were compared were for 0.040-inch thick Alclad 24S-T sheet, tested across grain. As a result of this questionable procedure, the ratios of bearing to tensile properties shown in Fig. 11 of the paper for 75 F are considerably higher than the ratios used in computing the ANC-5 design values. The constancy of the ratios observed for various temperatures and heating times is the

---

[1] "Alcoa Aluminum and Its Alloys," Published by Aluminum Company of America, 1946.

[2] "Strength of Aircraft Elements," ANC-5, Amendment 1, 1943.

[3] R. L. Moore and C. Wescoat, "Bearing Strengths of Some Wrought-Aluminum Alloys," Technical Note No. 901, N.A.C.A., 1943; R. L. Moore and C. Wescoat, "Bearing Strengths of 24S-T Aluminum-Alloy Plate," Technical Note No. 981, N.A.C.A., 1945; C. Wescoat and R. L. Moore, "Bearing Strengths of 75S-T Aluminum-Alloy Sheet and Extruded Angle," Technical Note No. 974, N.A.C.A., 1945.

significant finding in these tests, not the absolute value of the ratios. The same is true of the ratios given between the shear strength of the 24S-T rivets and the tensile strength of 0.040-inch Alclad 24S-T sheet, shown in Fig. 10.

Authors' Reply

The authors thank Mr. Moore for his comments which undoubtedly add to the value of the paper.

It is true that at temperatures up to 250 F the decreases in bearing properties are greater than those affecting ultimate shear stress.

The comparison of the 10,000-hour tensile properties obtained at the Aluminum Research Laboratories with the corresponding 1000-hour values listed in Fig. 9 illustrates the hazards involved in attempts to extrapolate such data.

For the reasons cited by Mr. Moore, it is proper to emphasize that the absolute values of the ratios of bearing to tensile properties derived in the paper are of less significance than the observations on the response of the ratios to elevated temperature exposure. This, of course, was also the belief of the authors.

THE EFFECTS OF MICROSTRUCTURE ON THE MECHANICAL PROPERTIES OF STEEL

By J. H. Hollomon, L. D. Jaffe, D. E. McCarthy and M. R. Norton

Abstract

The effects of microstructure on the mechanical properties of two steels have been investigated. Specimens of an NE 8735 steel were first heat treated to produce various as-quenched structures, namely, martensite, martensite plus ferrite and pearlite, and martensite plus bainite. These specimens were then tempered before testing. Specimens of an SAE 3135 steel were embrittled various amounts by heating at 450 C for different periods of time after tempering at a higher temperature. Specimens of each steel with each heat treatment were tested in tensile, notched-bar impact, and fatigue tests. Except for the reduction of area (and fracture strength), the tensile properties are unaffected by changes in structure. The impact properties, which reflect the fracture strength at small strains, are very dependent upon structure. The fatigue properties as determined in tests in R. R. Moore machines are affected to a limited extent by changes in structure. The properties of tempered martensitic steels are superior to those of steel having other structures.

Introduction

IT has become recognized that the microstructure of steel plays the predominant role in determining its mechanical properties. Steels of different compositions have very nearly the same properties if they have the same structure. Though the individual references to the effect of structure on the mechanical properties of steel are too numerous to list, it should be pointed out that many years ago Brinell (1)[1] found

The statements or opinions in this article are those of the authors and do not necessarily express the views of the Ordnance Department.

[1]The figures appearing in parentheses pertain to the references appended to this paper.

A paper presented before the Twenty-eighth Annual Convention of the Society held in Atlantic City, November 18 to 22, 1946. At the time this investigation was made, J. H. Hollomon was captain, Ordnance Department, L. D. Jaffe and M. R. Norton were metallurgists, and D. E. McCarthy, corporal, Ordnance Department, Watertown Arsenal Laboratory, Watertown, Mass. Manuscript received March 18, 1946.

quenched and tempered steel to have greater toughness than steel slowly cooled from a high temperature. Furthermore, Bain (2) has discussed the superiority of the properties of steel having a structure consisting of spheroidal carbides in a matrix of ferrite. Wartime experience with guns, armor, and projectiles has indicated that for such applications this structure (tempered martensite) is required. The main impetus to the study of hardenability has been the desire of metallurgists to produce this structure in steel parts so as to obtain the optimum combination of mechanical properties.

Few studies of the effect of microstructure on the mechanical properties have indicated how structure affects all of the different mechanical properties of steels. It is the purpose of this paper to describe the results of a rather comprehensive series of experiments designed to determine the properties of steels having different structures. In these experiments, tensile, impact, and fatigue tests were performed. It is hoped that the effect of structure upon the creep properties will be studied in later experiments.

In practice, five transformations may occur during heat treatment to prevent the formation of a structure that is completely tempered martensite. Upon quenching, ferrite, cementite, pearlite or bainite may form, and during tempering the transformation resulting in temper brittleness may take place.[2] The present study was designed to illustrate how the introduction of pearlite and ferrite in combination, of bainite, and of the constituent responsible for temper brittleness affect the properties of tempered martensitic steel.

Materials and Heat Treatment

Two steels, SAE 3135 and NE 8735, were obtained in the form of hot-rolled, 5/8-inch diameter bar stock. The check analyses of the heats were:

Material	C	Mn	Si	S	P	Ni	Cr	Mo
SAE 3135	0.35	0.87	0.22	0.022	0.029	1.16	0.50	Trace
NE 8735	0.34	0.95	0.26	0.018	0.014	0.66	0.56	0.24

The 8735 steel was chosen for isothermal treatments because it could be quenched to martensite in the 5/8-inch round size and had sufficient pearlitic hardenability to permit complex isothermal treatments. It was not possible, however, to produce severe temper embrittlement in this steel within a reasonable time. It was particularly im-

[2]Austenite also may be retained upon quenching and may subsequently transform upon tempering or remain unaltered.

portant, from the standpoint of the tests herein reported, to include the effect of this variation in structure, since by means of the transformation that leads to temper brittleness a change in impact properties can be effected without inducing any major change in the tensile properties as ordinarily measured at room temperature. To obtain varying degrees of temper brittleness a commercial steel (SAE 3135) not containing molybdenum was selected.

Quenched specimens of the NE 8735 steel were to be tempered to various hardnesses. It was desired to determine the properties of the tempered martensitic specimens over as wide a range of hardness as possible. It was also considered desirable to test the tempered specimens containing (upon quenching) mixtures of martensite, pearlite and ferrite, and of martensite and bainite, at hardnesses used also for the tempered martensitic specimens.

To accomplish these ends, it was necessary to perform certain preliminary experiments. An austenitizing treatment which would result in solution of the carbides and yet not induce undesirable grain growth had to be determined for each steel. The hardness response of each steel to tempering also had to be determined. For these preliminary tests a number of blanks 5/8 inch in diameter and 3 inches long were used. The blanks were quenched after holding 1 hour at various temperatures and disks were then cut from their centers for microscopic examination. Austenitizing the NE 8735 steel above 925 C (1700 F) resulted in marked grain growth, and marked growth took place above 900 C (1650 F) in the SAE 3135 steel. However, since no undissolved carbides were visible upon microscopic examination of the specimens of the NE 8735 steel austenitized at 900 C (1650 F) and the specimens of the SAE 3135 steel austenitized at 870 C (1600 F), these temperatures were chosen for austenitizing.

Additional blanks of each steel were austenitized at the selected temperatures. Disks taken from these blanks were then tempered at various temperatures for 1 hour and quenched in water. The hardnesses of these specimens were determined and plotted as a function of the tempering temperature. For the NE 8735 steel the hardness of these disks increased with increasing temperatures above 690 C (1275 F), indicating that the lower critical had been exceeded. Thus the lowest hardness obtainable in these tests was that produced by tempering at a temperature slightly below 690 C. This minimum hardness was found to be Rockwell C-17. The maximum hardness was limited by the temperatures at which low (tempering) temperature brittleness occurs:

Table I
Heat Treatments to Produce Tempered Martensite and Temper Brittleness

Steel	Series	Rockwell C Hardness	Austenitize* 1 hr. at C	Temper* 1 hr. at C	Embrittle* at 455 C
NE 8735	Y	17	900	685	—
NE 8735	A	25	900	655	—
NE 8735	B	31	900	605	—
NE 8735	C	35	900	575	—
NE 8735	G	39	900	485	—
NE 8735	E	42	900	420	—
SAE 3135	Q	25	870	600	—
SAE 3135	S	25	870	600	5 hours
SAE 3135	T	24	870	600	50 hours
SAE 3135	U	23	870	600	500 hours

*All specimens water-quenched after austenitizing, tempering and embrittling treatments.

230 to 400 C (450 to 750 F) (3). The minimum tempering temperature was set at 420 C (790 F). Tempering at this temperature for 1 hour produced a hardness of Rockwell C-42. Four other tempering temperatures were chosen between these two extremes (Table I). These temperatures produced hardnesses of Rockwell C-25, 31, 35 and 39.

To determine the effect of (tempered) bainite and pearlite it was necessary to obtain specimens having the same hardness as some set of the tempered martensitic specimens. It was thought that tests at the lowest hardness might not be sufficiently severe to distinguish between the impact properties of the steels of various structures at the lowest testing temperature readily available in the laboratory (—78 C, —108 F). Thus the hardnesses common for the specimens of various structures were chosen as Rockwell C-25 and 31. It was desired to study the properties of tempered specimens containing pearlite plus ferrite and those containing bainite, each formed at two temperatures. Preliminary isothermal transformation and tempering treatments were performed to determine the proper treatments. It was found that any wholly pearlitic (and ferrite) structure would be too soft after tempering within the selected range. Thus isothermal treatments were chosen that would produce only partial pearlite and ferrite formation. Tempering temperatures (Table II) were determined that were expected to produce Rockwell C-25 and 31 after partial pearlite (and ferrite) formation at two temperatures.

Since the bainite reaction does not go to completion except at the lowest temperatures of transformation, the possibility of obtaining a completely bainitic structure before tempering was not considered. Two isothermal treatments that would lead to partial bainite formation

were chosen by means of preliminary experiments. After the partial transformation to bainite and before tempering the specimens were cooled in liquid nitrogen to −196 C (−320 F) to minimize retention of austenite. Tempering treatments were selected to produce Rockwell C-25 after transformation at two temperatures in the bainite range (Table II).

To determine the effect of temper brittleness, the SAE 3135 steel was used. A hardness of Rockwell C-25 was chosen because it could

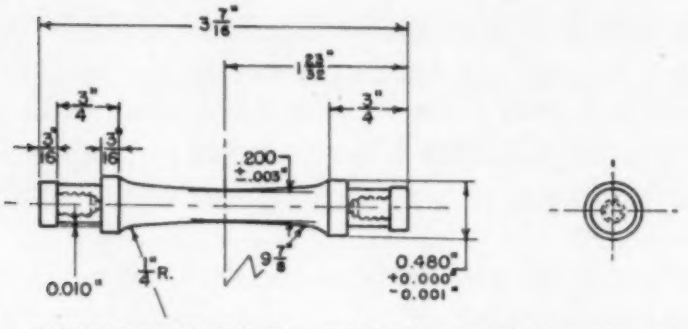
Table II

Isothermal Heat Treatment of NE 8735 Steel to Produce Bainite and Pearlite. All Specimens Austenitized 1 hour at 900 C and Water-Quenched from Tempering Temperature.

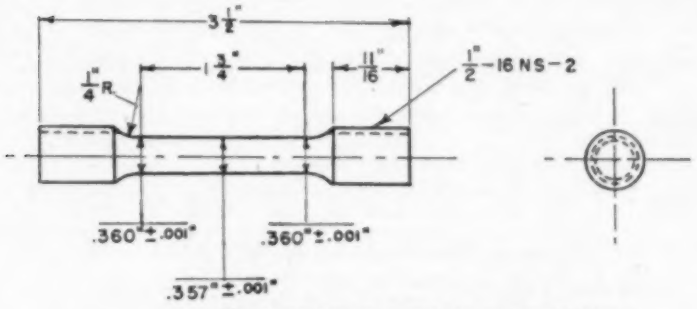
Steel	Series	Rockwell C Hardness	*Isothermal and Tempering Treatment*
			(a) *To Produce Bainite*
NE 8735	L	25	Water-quenched from austenitizing temperature and held for 5 seconds; transferred to salt pot at 400 C and held for 5 minutes; water-quenched to room temperature. Cooled in liquid nitrogen and tempered at 590 C for 1 hour.
NE 8735	Z	22	Water-quenched from austenitizing temperature and held for 4 seconds; transferred to salt pot at 470 C and held for 11 minutes; water-quenched to room temperature. Cooled in liquid nitrogen and tempered at 635 C for 1 hour.
			(b) *To Produce Pearlite and Ferrite*
NE 8735	H	21	Transferred from austenitizing temperature to salt pot at 600 C and held for 115 minutes, then water-quenched. Tempered 1 hour at 625 C.
NE 8735	M	30	Same isothermal treatment as Series H. Tempered 1 hour at 510 C.
NE 8735	P	25	Transferred from austenitizing temperature to salt pot at 550 C and held for 6.5 hours, then water-quenched. Tempered 1 hour at 615 C.
NE 8735	K	30	Same isothermal treatment as Series P. Tempered 1 hour at 570 C.

be obtained at a tempering temperature in excess of 595 C (1100 F) (above which no embrittlement occurs upon tempering). The embrittling temperature and times were chosen on the basis of past experience with other steels.

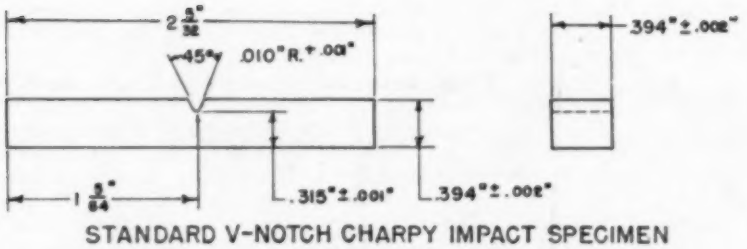
For heat treatment, the 5/8-inch diameter bar stock was cut into 3 9/16-inch lengths for tensile and fatigue specimens, and into 5-inch lengths for Charpy specimens. After heat treatment, two standard V-notched Charpy impact specimens were machined from each 5-inch length. To keep the structure and hardness of the fatigue, impact, and tensile specimens as uniform as possible, all specimens undergoing the same heat treatment were machined from the same length of bar stock and were treated together. Tables I and II list the heat treatments used. All specimens were water-quenched following tempering.



FATIGUE SPECIMEN FOR ROTATING-BEAM MACHINE (R.R. MOORE)



.357" THREADED TENSILE SPECIMEN



STANDARD V-NOTCH CHARPY IMPACT SPECIMEN

Fig. 1—Specimens Used in This Study.

Specimens and Tests

Mechanical Tests—Fig. 1 illustrates the types of specimens used in this investigation. Fatigue specimens were rough machined on a lathe and then ground on an abrasive wheel to approximately 0.205 inch on the minimum diameter, after which they were hand polished with abrasive papers in the following order:

1 Grit No. 150
2 Grit No. 220
3 Grit No. 320
4 Grit No. 00
5 Grit No. 000

Abrasive papers of grit Nos. 150, 320 and 000 were moved along the axis of the specimens while abrasive papers 220 and 00 were moved at

right angles to it. This method of polishing was used to facilitate the removal of scratches left by the previous paper. The longitudinal polishing was done by mounting the specimen between centers and turning it slowly by one hand while moving the abrasive paper back and forth under a medium pressure with the other hand. Circumferential polishing was done by turning the specimen slowly in a bench lathe while holding the abrasive paper against the specimen with a moderate pressure. When polishing was completed the specimens were viewed under a magnifying glass to make certain that all radial scratches and tool marks had been removed. The minimum diameter of the specimen was measured to the nearest ten-thousandth of an inch.

The fatigue tests were performed at a speed of 1750 rpm on R. R. Moore rotating-beam fatigue machines, a description of which may be found elsewhere (4). All stresses were computed by means of the simple beam formula:

$$F = \frac{16WL}{\pi d^3}$$

where F is the maximum fiber stress, W the load applied, d the diameter of the specimen and L the moment arm (4 inches on the R. R. Moore machine).

The V-notch Charpy impact specimens were broken in a standard impact machine of 120 foot-pounds capacity. A mixture of dry ice and acetone was used to cool the specimens to 0, —40 and —78 C (32, —40 and —108 F). Hot water was used for heating the specimens to 50 C (122 F), and an oil bath for temperatures of 100 C (212 F) and above. It was assumed that there was only a negligible change in temperature of the specimens while they were transferred from the heating or cooling medium to the impact machine.

Two 0.357-inch tensile specimens of each heat treatment series were tested. One of these was tested in a hydraulic machine. The yield strength, tensile strength, per cent elongation in 1.4 inch, and per cent reduction of area were determined from this specimen. The second specimen was pulled on a lever-type machine. One person recorded the diameter while a second simultaneously recorded the load. From these data, "true" stress-strain curves were constructed.

Metallographic examinations of the blanks for establishing the treatments to be used were made on disks cut transversely from the midlengths of the blanks. For the final heat treatment a blank was sectioned before tempering and examined microscopically at its midlength. The structures after tempering were observed on transverse

samples cut from one of the broken fatigue specimens of each series. These samples were taken approximately ⅜ inch from the fractured ends of the specimen.

Results

The results of the tensile, fatigue, and impact tests of the specimens of the various structures are presented in Figs. 2 to 17 inclusive. The figures include a description of the heat treatment, the tensile properties, the impact properties over a range of testing temperatures, and the results of the fatigue tests. Included also are the stress-strain curves plotted both on a linear and on a logarithmic scale. Photomicrographs illustrating the structures of the steels after each heat treatment are given in Figs. 18 to 21 inclusive.

Figs. 2 to 7 illustrate the effect of tempering on the properties of martensite (SAE 8735). The specimens were fully martensitic as quenched, as illustrated by Fig. 18a. The photomicrographs of Figs. 18b to 18g show the gradual precipitation and spheroidization of the carbides resulting from the several tempering treatments at increasing temperatures.

The data of Figs. 8 and 9 give the results for specimens transformed at 400 and 470 C (750 and 880 F). The structure resulting from the treatment at 400 C (750 F) is illustrated in Fig. 19a. The structure is essentially bainitic, and as illustrated in the photomicrograph consists of areas of ferrite in which carbides have precipitated and areas of supersaturated ferrite. The ferrite (supersaturated with carbon) is the first product of the bainite reaction from which the carbide later precipitates. The photomicrograph of Fig. 19c illustrates the partial bainite formation that occurred at 470 C (880 F). The structure consists of bainite in a matrix of martensite. The bainite of this structure consists of ferrite with the carbide primarily at its boundaries. The photomicrographs of Figs. 19b and 19d illustrate the effect of the tempering upon the structures shown in Figs. 19a and 19c respectively.

In the pearlitic series (Figs. 10 to 13) it was not possible to permit complete transformation to pearlite and ferrite and still obtain the hardness of the tempered martensitic steels. Pearlite plus ferrite (Figs. 20a and 20d) was produced by isothermal transformation at 600 and 550 C (1110 and 1020 F). Possibly there may be some bainite in the structure of the specimen transformed at 550 C (1020 F). The dark area at the lower left of Fig. 20d differs from the dark nodular

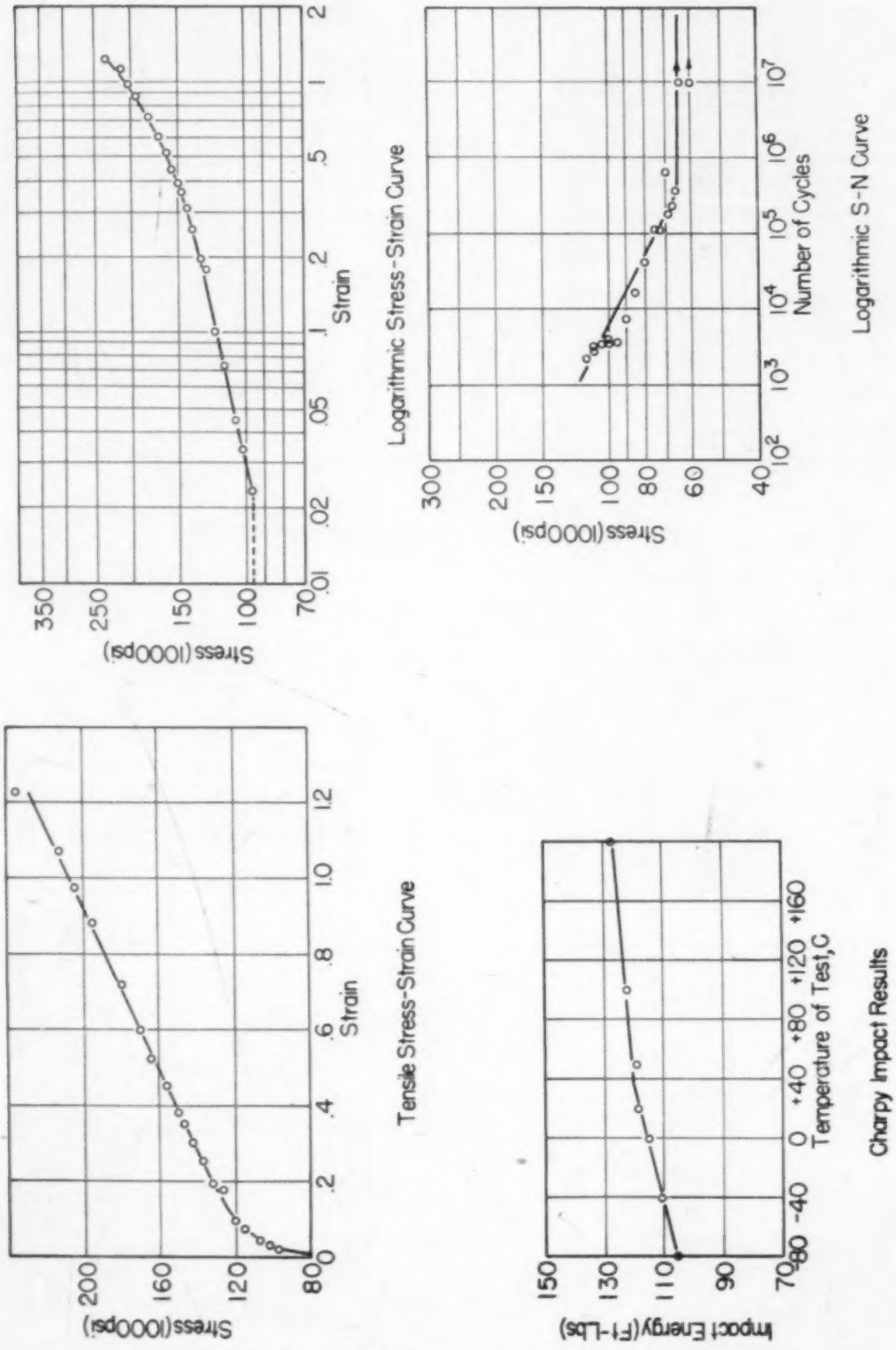


Fig. 2—Test Results for Specimens of Steel NE 8735, Series Y. Structure: tempered martensite. Heat treatment: austenitized at 900 C for 1 hour and water-quenched. Tempered at 685 C for 1 hour and water-quenched. Tensile data: Rockwell C-17; yield strength, psi (0.1%), 94,000; tensile strength, psi, 111,600; elongation, 25.0%; reduction of area, 70.1%.

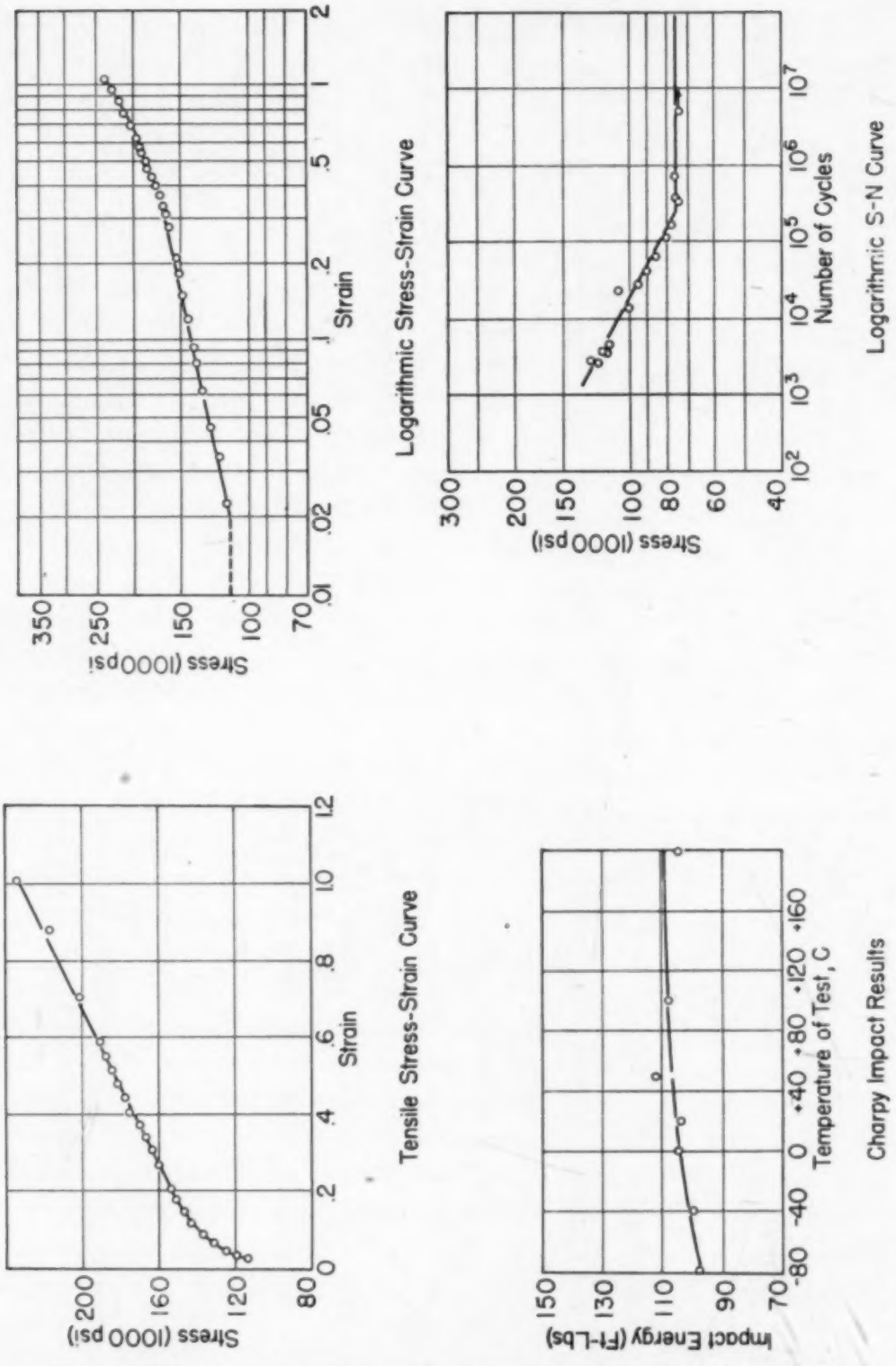


Fig. 3—Test Results for Specimens of Steel NE 8735, Series A. Structure: tempered martensite. Heat treatment: austenitized at 900 C for 1 hour and water-quenched. Tempered at 655 C for 1 hour and water-quenched. Tensile data: Rockwell C-25; yield strength, psi (0.1%), 110,600; tensile strength, psi, 127,500; elongation, 21.4%; reduction of area, 68.9%.

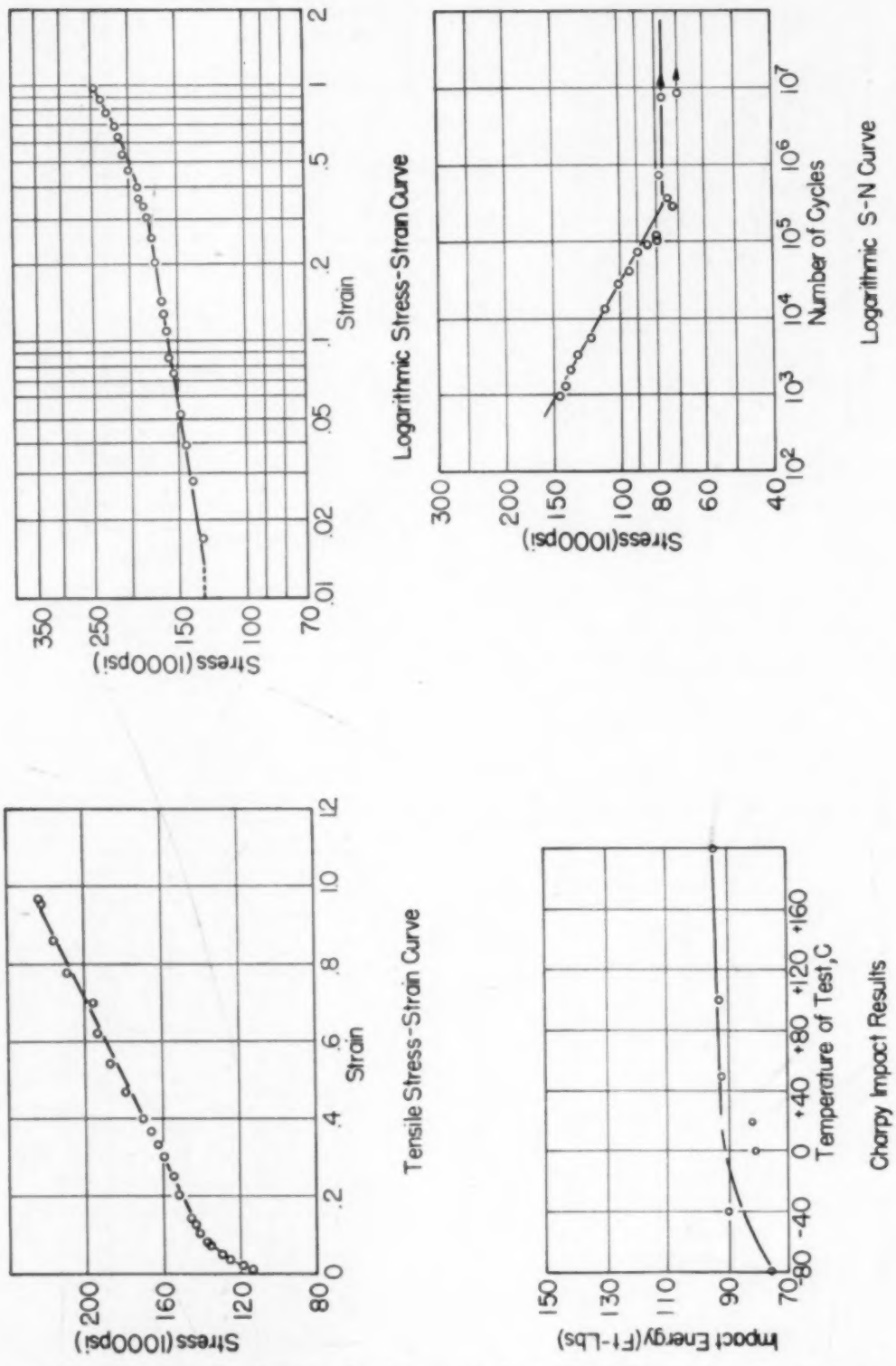


Fig. 4—Test Results for Specimens of Steel NE 8735, Series B. Structure: tempered martensite. Heat treatment: austenitized at 900 C for 1 hour and water-quenched. Tempered at 605 C for 1 hour and water-quenched. Tensile data: Rockwell C-31; yield strength, psi (0.1%), 128,700; tensile strength, psi, 143,500; elongation, 19.3%; reduction of area, 66.0%.

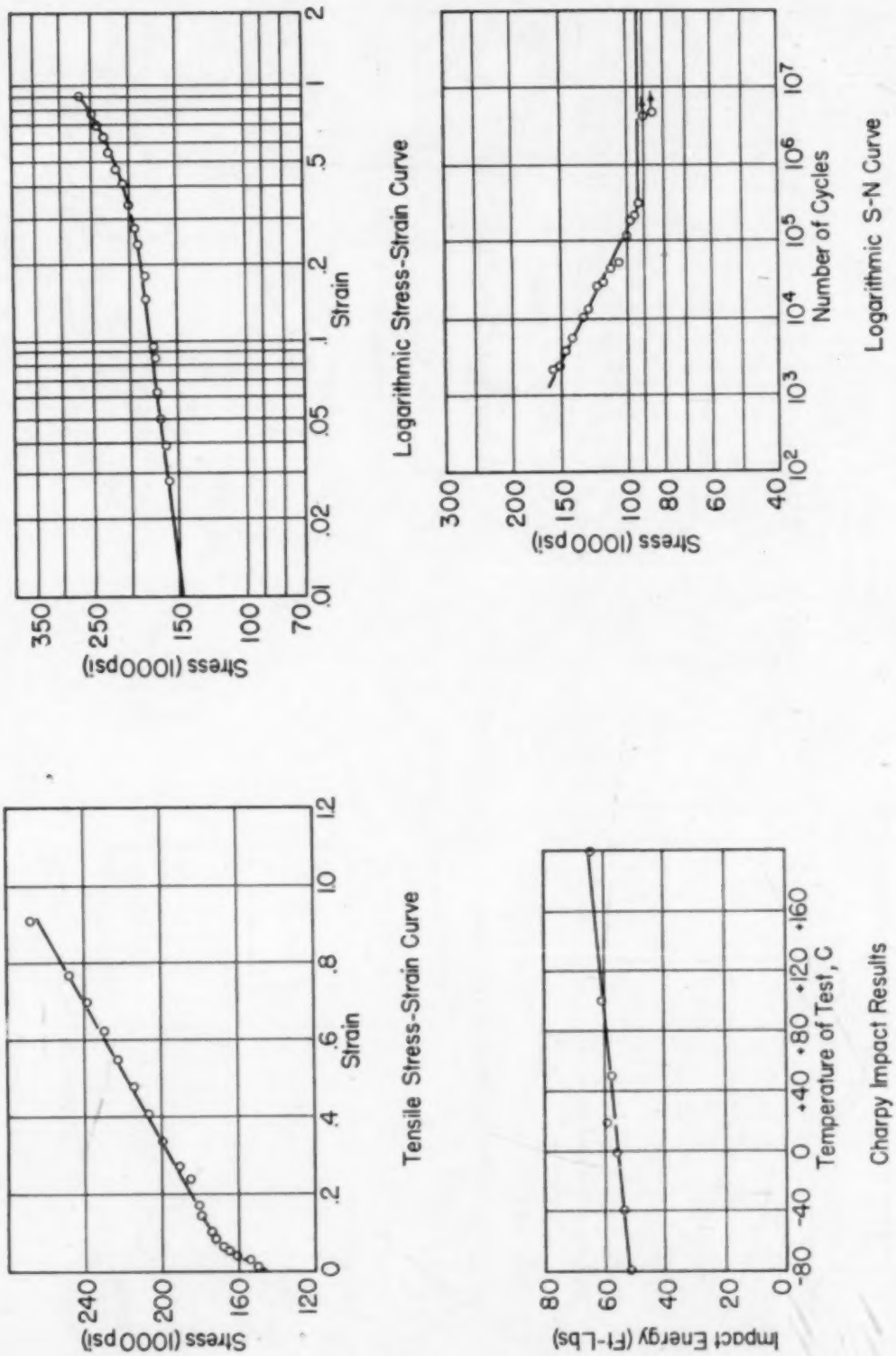


Fig. 5—Test Results for Specimens of Steel NE 8735, Series C. Structure: tempered martensite. Heat treatment: austenitized at 900 C for 1 hour and water-quenched. Tempered at 575 C for 1 hour and water-quenched. Tensile data: Rockwell C-35; yield strength, psi (0.1%), 151,200; tensile strength, psi, 163,000; elongation, 17.1%; reduction of area, 61.3%.

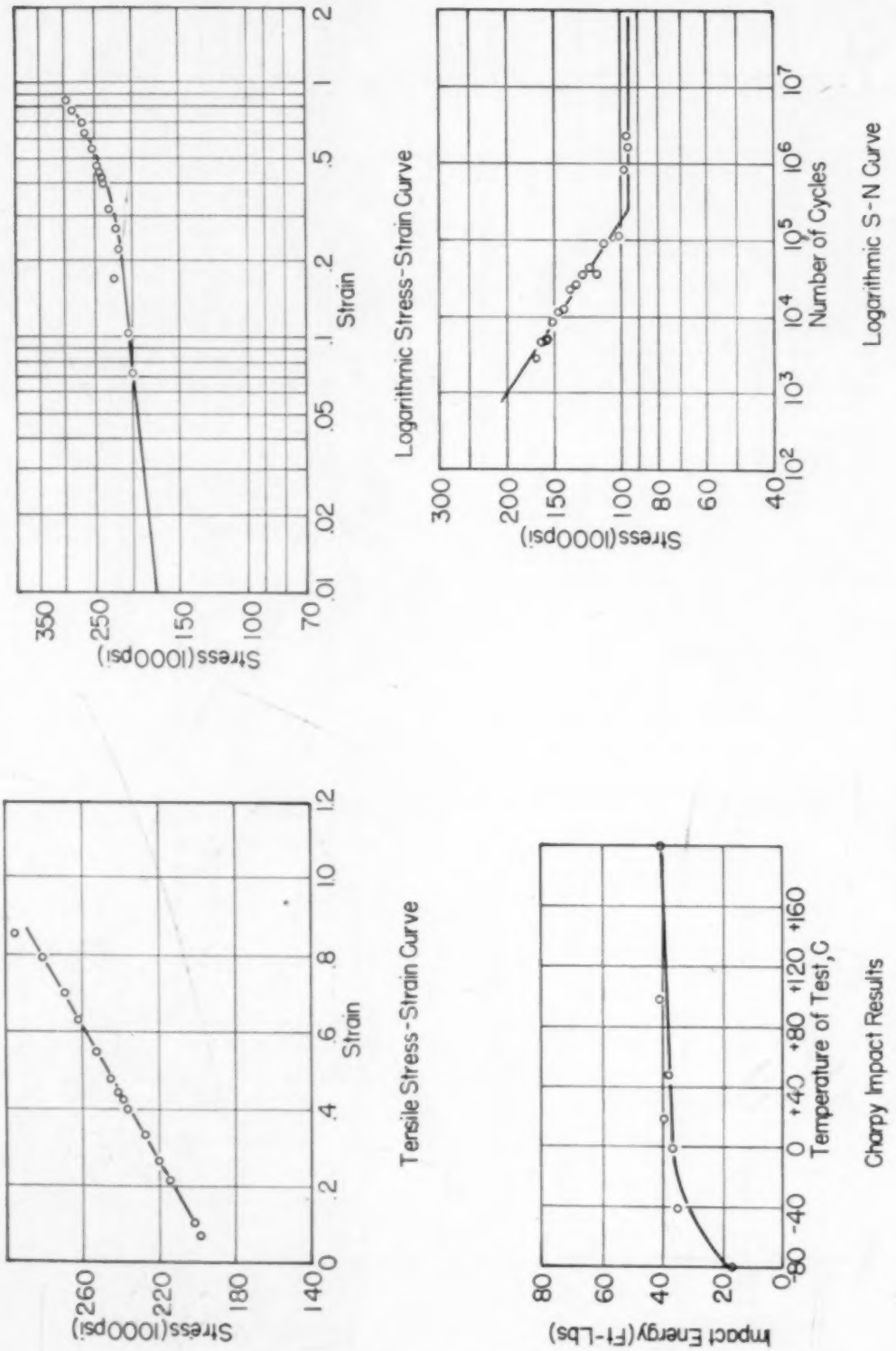


Fig. 6—Test Results for Specimens of Steel NE 8735, Series G. Structure: tempered martensite. Heat treatment: austenitized at 900 C for 1 hour and water-quenched. Tempered at 485 C for 1 hour and water-quenched. Tensile data: Rockwell C-39; yield strength, psi (0.1%), 176,200; tensile strength, psi, 188,000; elongation, 14.3%; reduction of area, 57.8%.

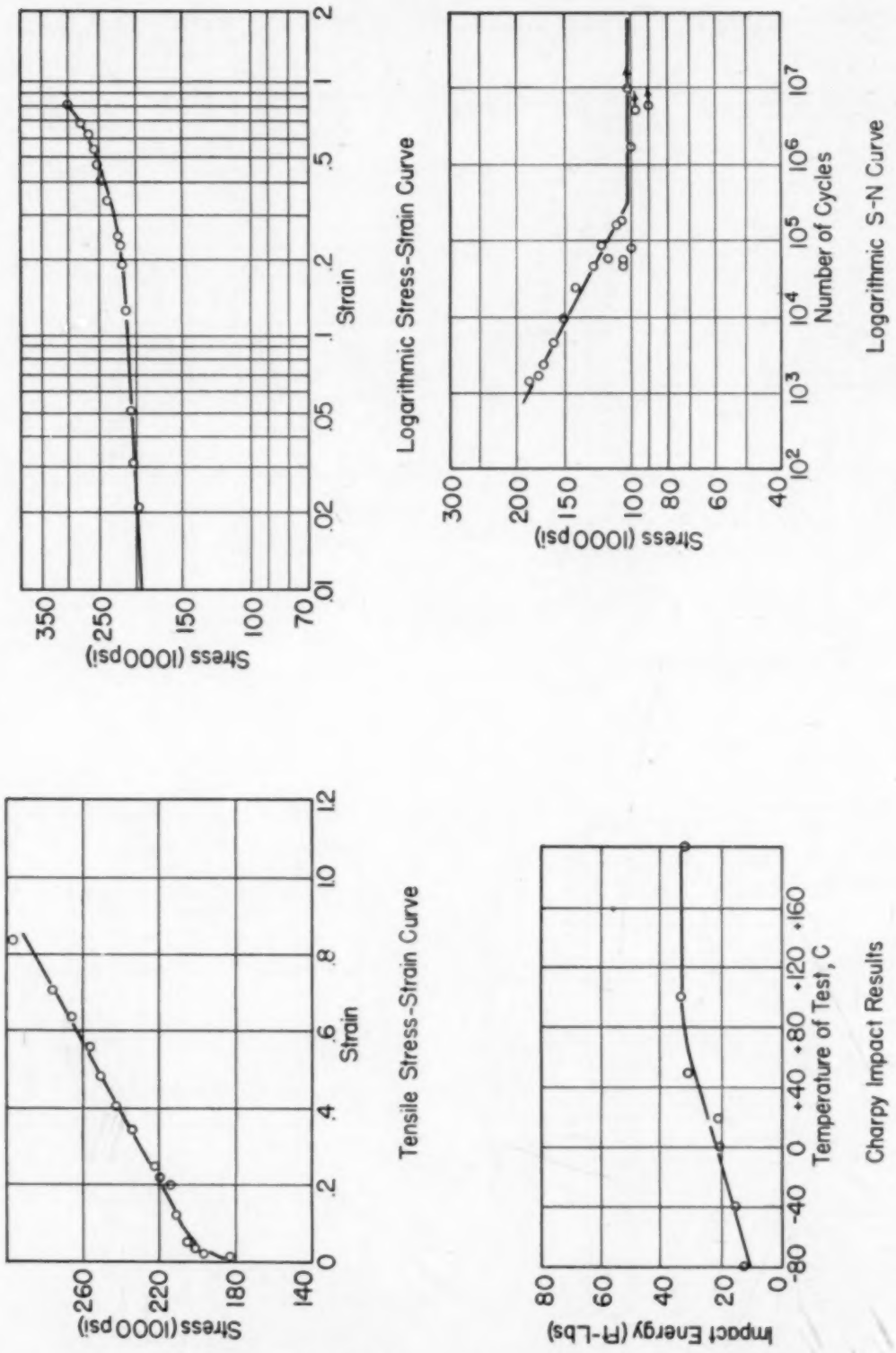


Fig. 7—Test Results for Specimens of Steel NE 8735, Series E. Structure: tempered martensite. Heat treatment: austenitized at 900 C for 1 hour and water-quenched. Tempered at 420 C for 1 hour and water-quenched. Tensile data: Rockwell C-42; yield strength, psi (0.1%), 183,700; tensile strength, psi, 198,500; elongation, 13.6%; reduction of area, 57.8%.

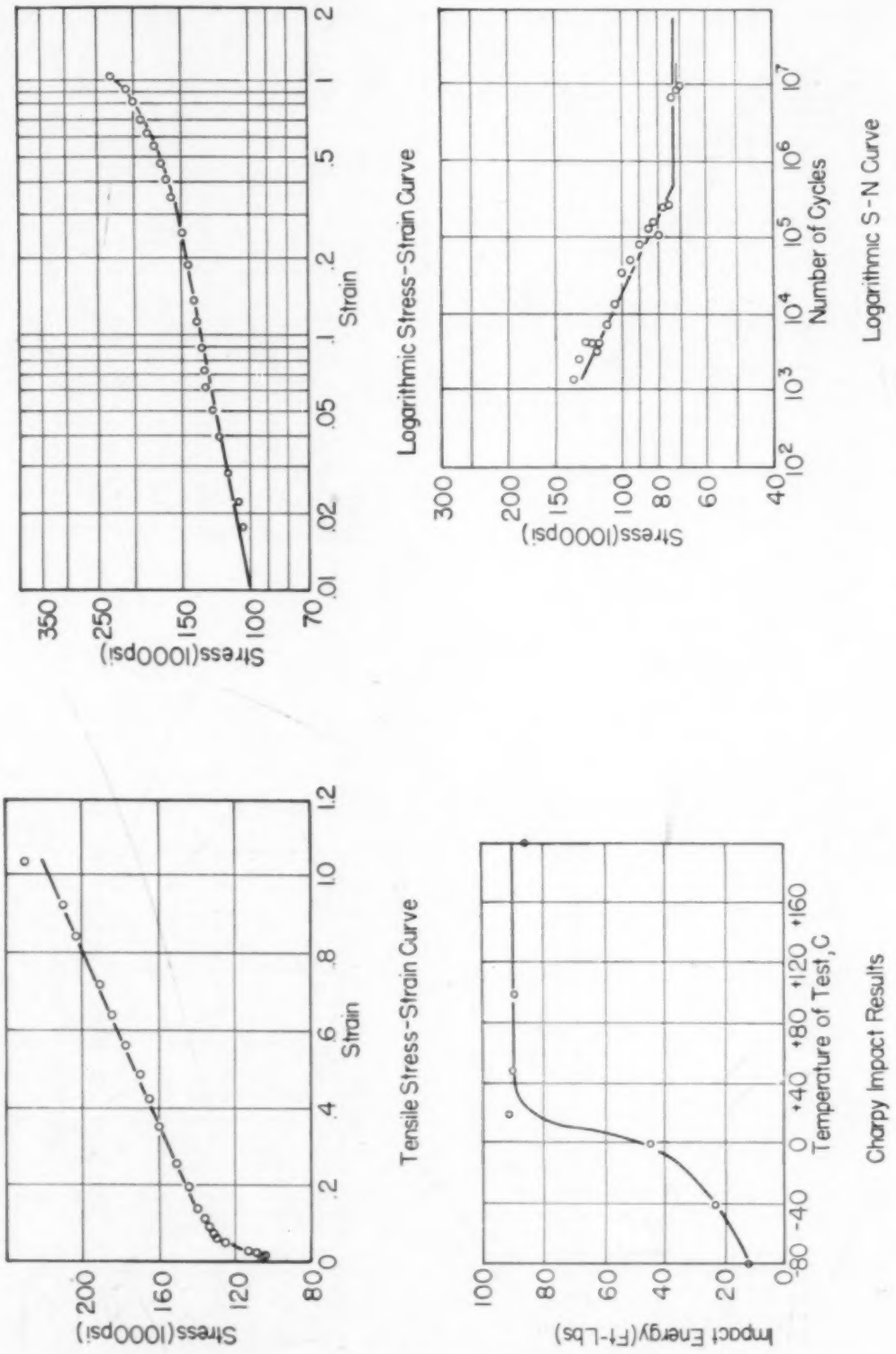


Fig. 8—Test Results for Specimens of Steel NE 8735, Series L. Structure: tempered bainite plus tempered martensite. Heat treatment: austenitized at 900 C for 1 hour and water-quenched for 5 seconds. Transferred to salt pot at 400 C, held for 5 minutes and water-quenched. Cooled in liquid nitrogen and tempered at 590 C for 1 hour. Water-quenched. Tensile data: Rockwell C-25; yield strength, psi (0.1%), 98,000; tensile strength, psi, 126,500; elongation, 21.4%; reduction of area, 63.4%.

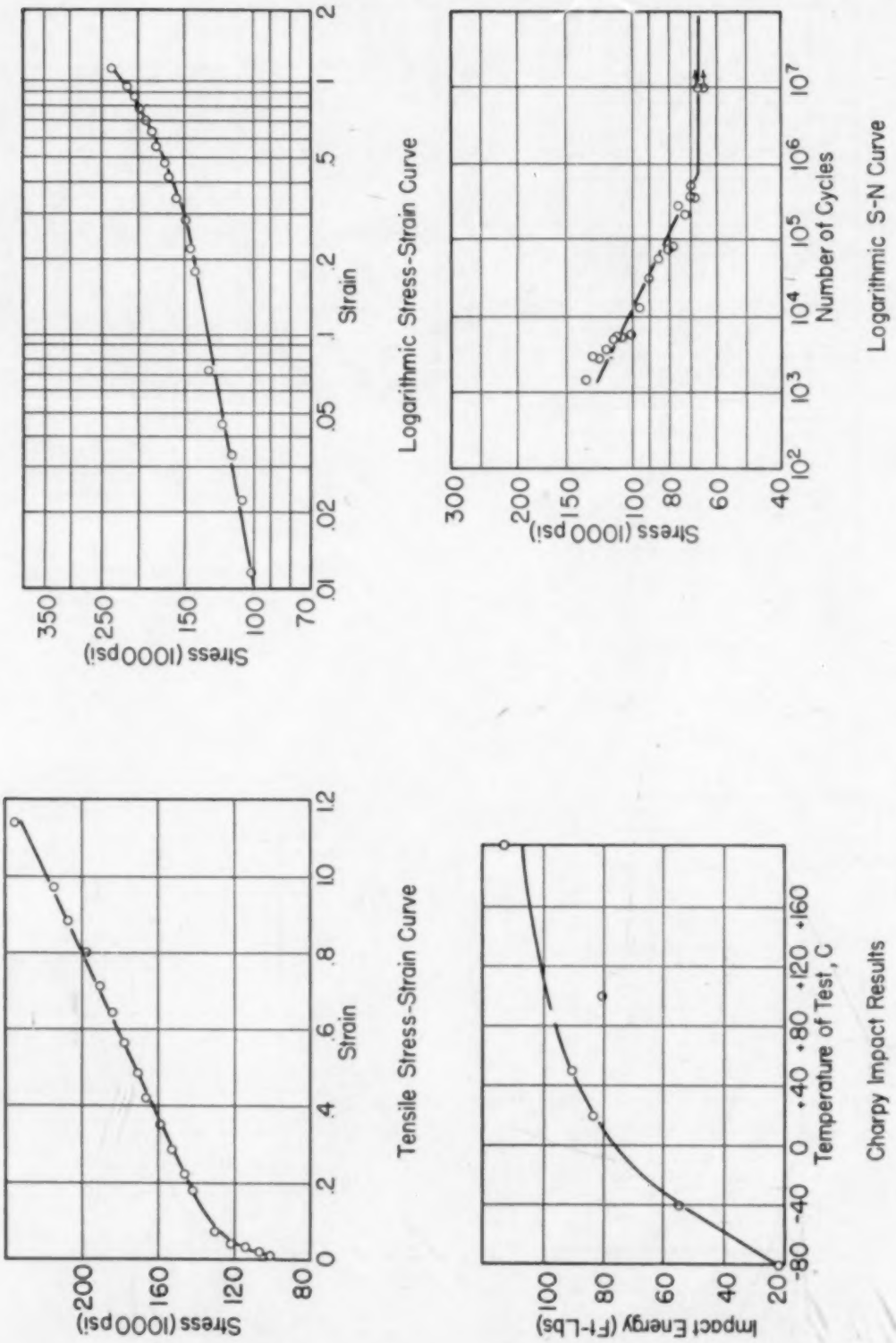


Fig. 9—Test Results for Specimens of Steel NE 8735, Series Z. Structure: tempered bainite plus tempered martensite. Heat treatment: austenitized at 900 C for 1 hour and water-quenched for 4 seconds. Transferred to salt pot at 470 C, held for 11 minutes and water-quenched. Cooled in liquid nitrogen and tempered at 635 C for 1 hour. Water-quenched. Tensile data: Rockwell C-22; yield strength, psi (0.1%), 98,500; tensile strength, psi, 123,500; elongation, 21.4%; reduction of area, 63.4%.

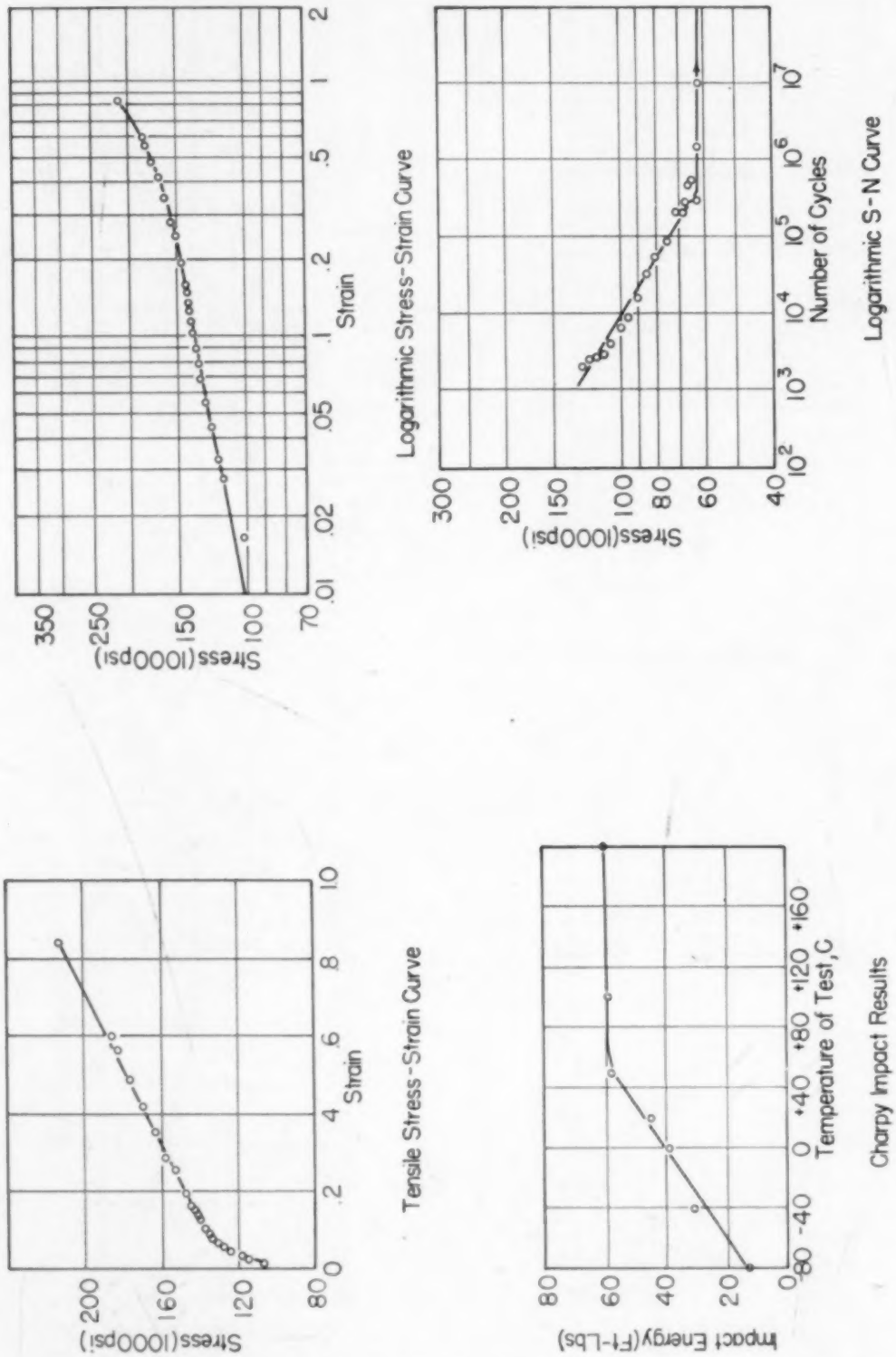


Fig. 10—Test Results for Specimens of Steel NE 8735, Series H. Structure: tempered pearlite, ferrite and martensite. Heat treatment: austenitized at 900 C for 1 hour. Transferred to salt pot at 600 C, held for 115 minutes and water-quenched. Tempered at 625 C for 1 hour and water-quenched. Tensile data: Rockwell C-21; yield strength, psi (0.1%), 96,200; tensile strength, psi, 122,500; elongation, 20.7%; reduction of area, 57.8%.

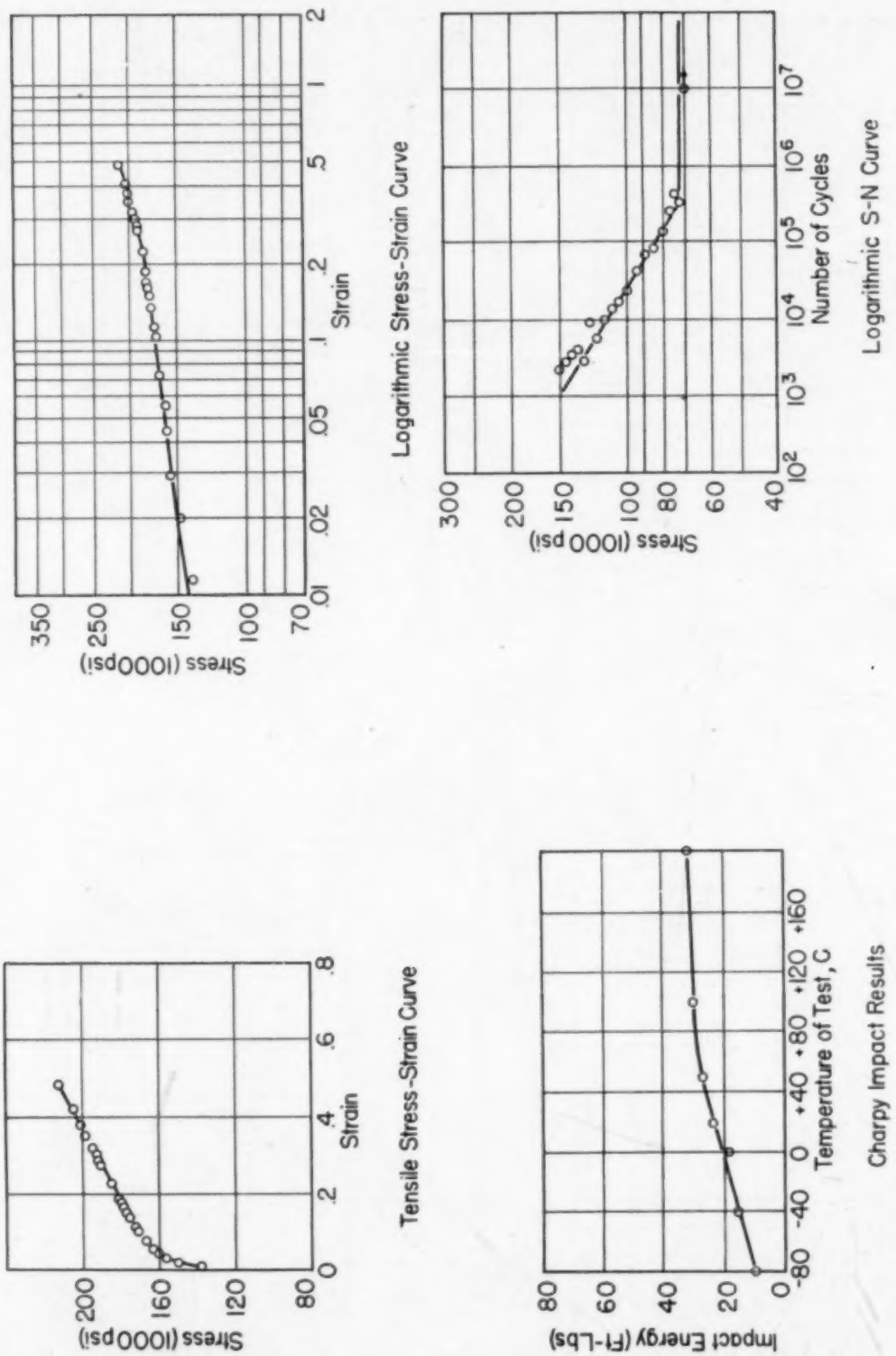


Fig. 11—Test Results for Specimens of Steel NE 8735, Series M. Structure: tempered pearlite, ferrite and martensite. Heat treatment: austenitized at 900 C for 1 hour. Transferred to salt pot at 600 C, held for 115 minutes and water-quenched. Tempered at 510 C for 1 hour. Tensile data: Rockwell C-30; yield strength, psi (0.1%), 111,200; tensile strength, psi, 155,500; elongation, 12.9%; reduction of area, 38.5%.

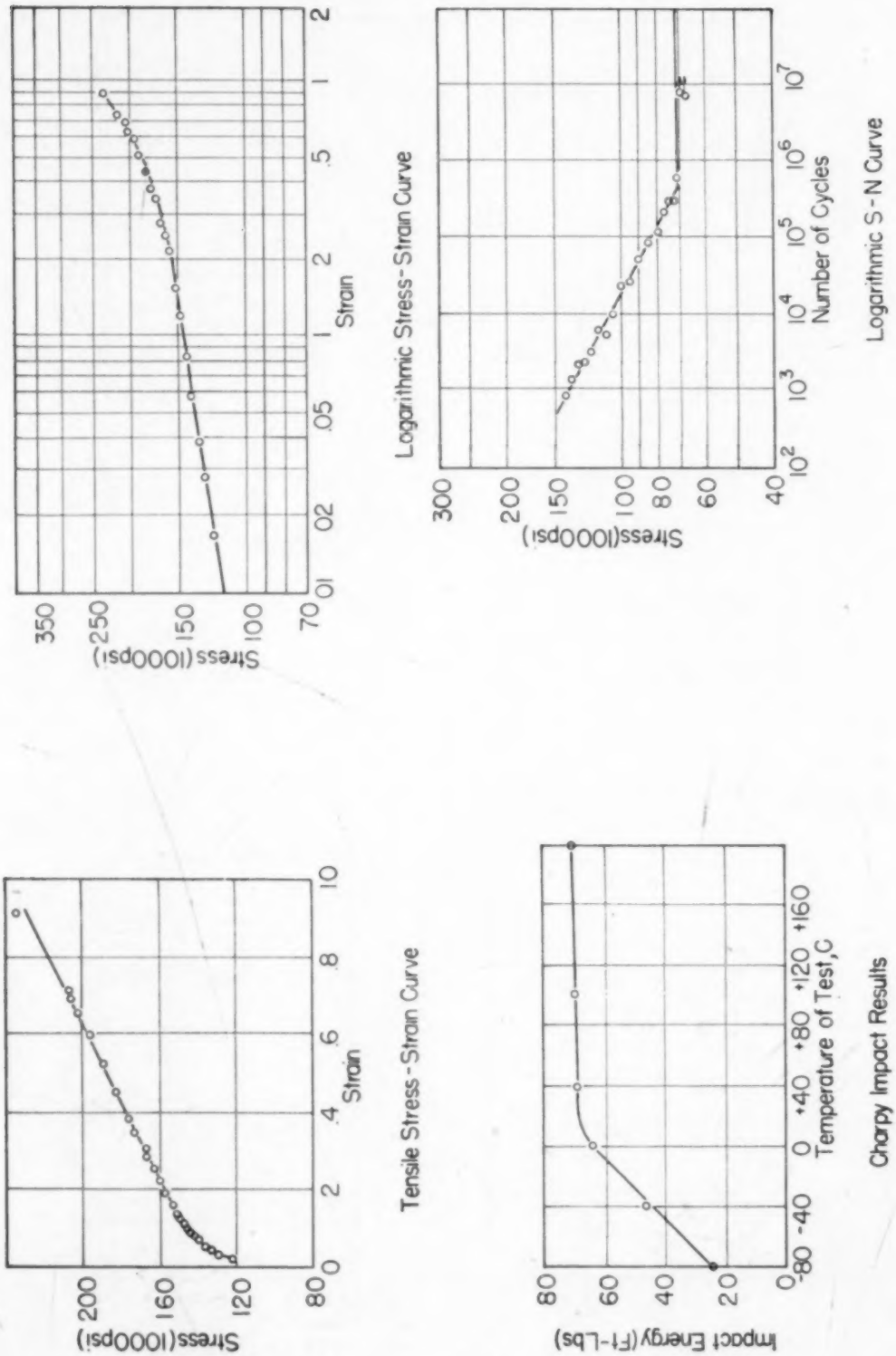


Fig. 12—Test Results for Specimens of Steel NE 8735, Series P. Structure: tempered pearlite, ferrite and martensite. Heat treatment: austenitized at 900 C for 1 hour. Transferred to salt pot at 555 C, held for 6.5 hours and water-quenched. Tempered at 615 C for 1 hour. Tensile data: Rockwell C-25; yield strength, psi (0.1%), 111,200; tensile strength, psi, 134,000; elongation, 19.3%; reduction of area, 57.0%.

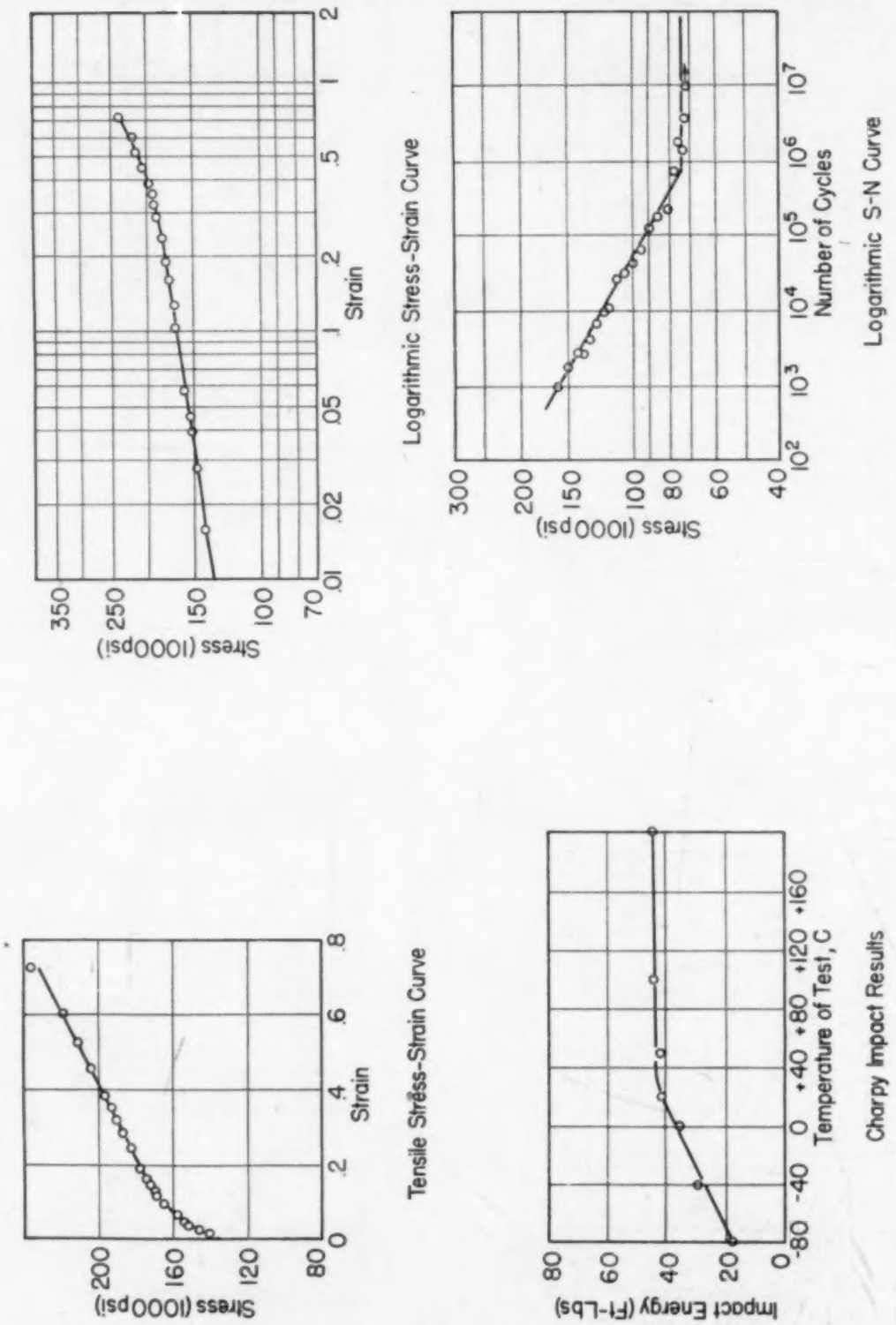


Fig. 13—Test Results for Specimens of Steel NE 8735, Series K. Structure: tempered pearlite, ferrite and martensite. Heat treatment: austenitized at 900 C for 1 hour. Transferred to salt pot at 550 C, held for 6.5 hours and water-quenched. Tempered at 570 C for 1 hour. Tensile data: Rockwell C-30; yield strength, psi (0.1%), 126,200; tensile strength, psi, 154,000; elongation, 17.9%; reduction of area, 54.1%.

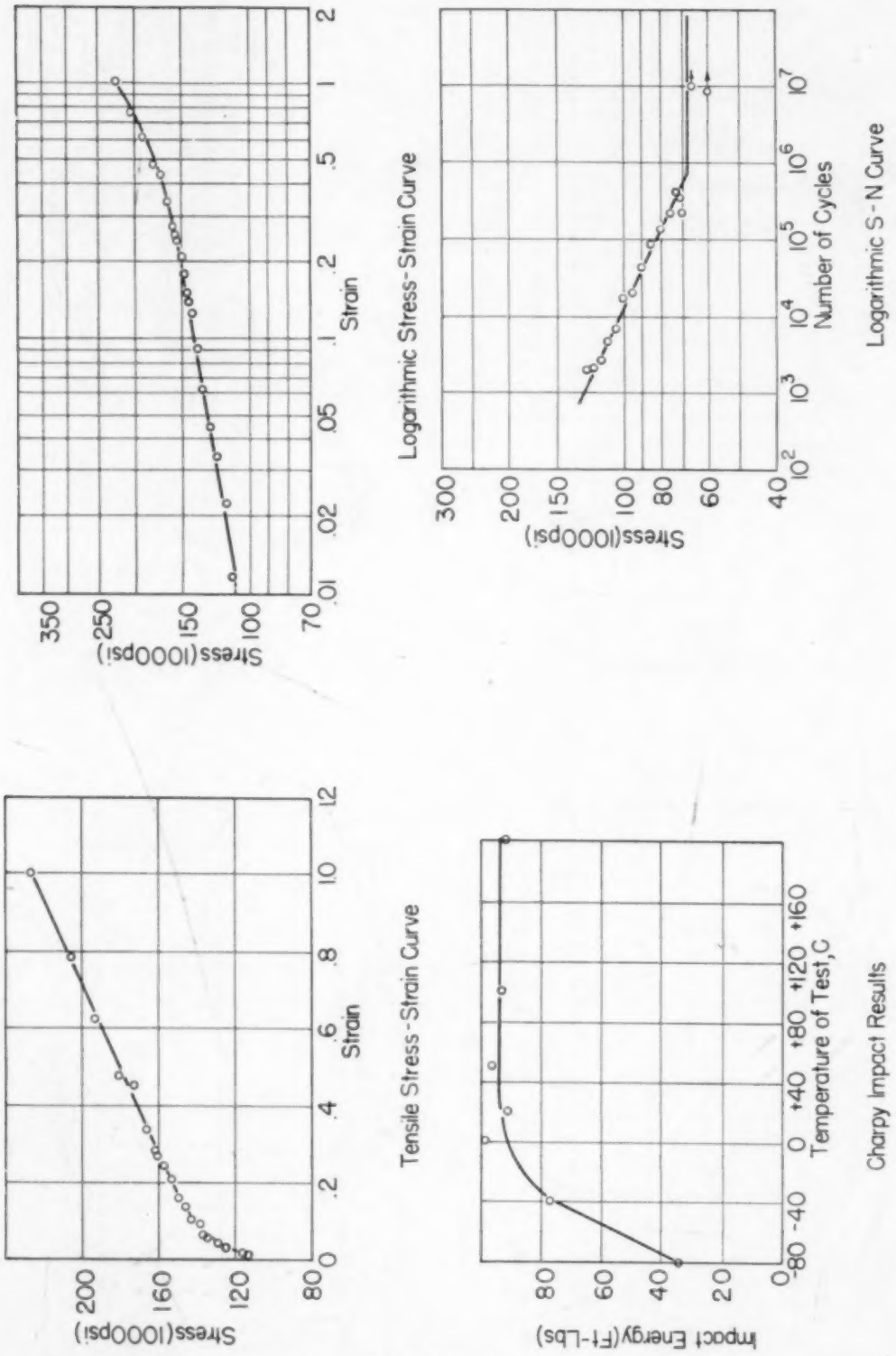


Fig. 14—Test Results for Specimens of Steel SAE 3135, Series Q. Structure: tempered martensite. Heat treatment: austenitized at 870 C for 1 hour and water-quenched. Tempered at 600 C for 1 hour and water-quenched. Not embrittled. Tensile data: Rockwell C-25; yield strength, psi (0.1%), 113,700; tensile strength, psi, 129,000; elongation, 20.7%; reduction of area, 66.3%.

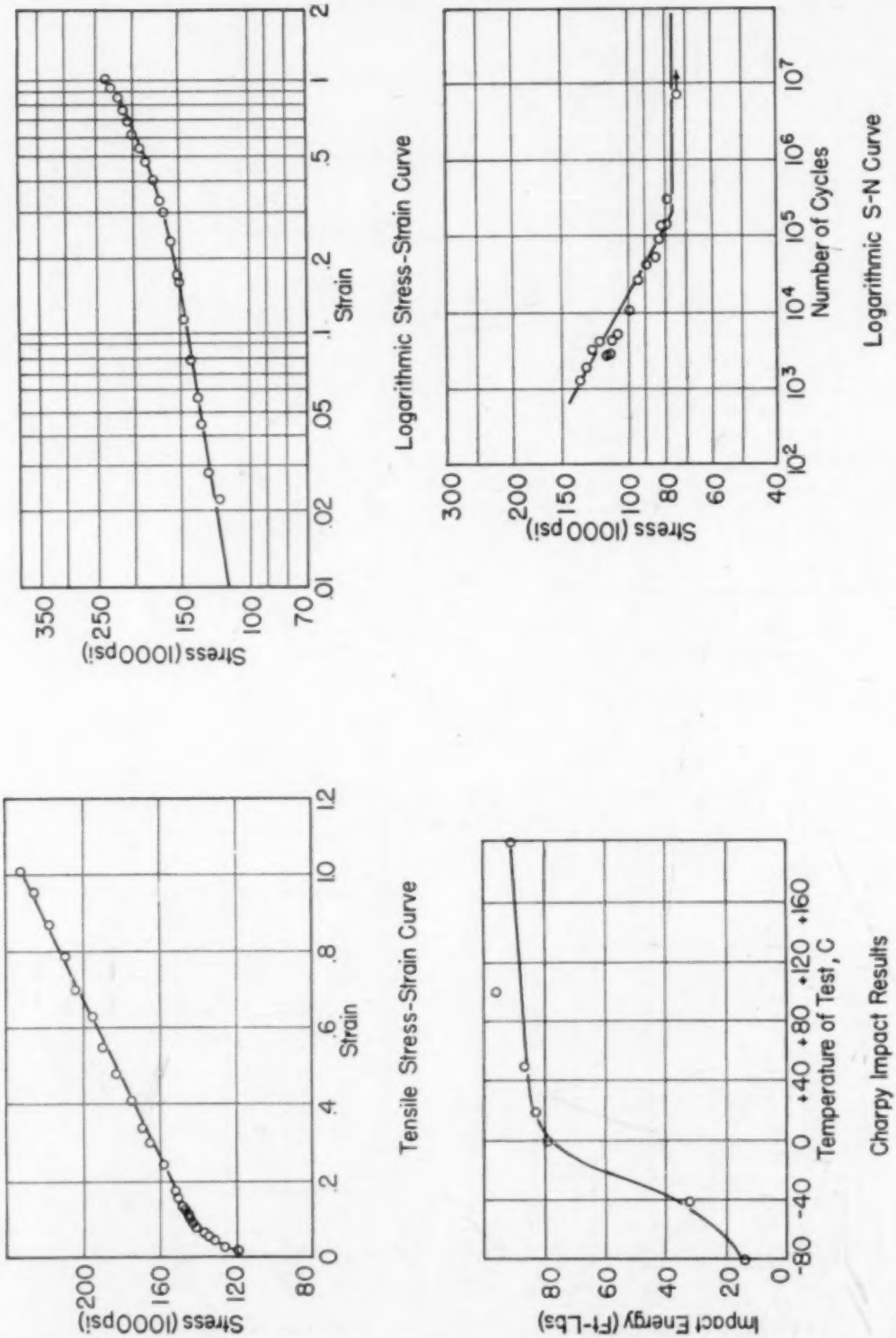


Fig. 15—Test Results for Specimens of Steel SAE 3135, Series S. Structure: tempered martensite plus temper brittleness. Heat treatment: austenitized at 870 C for 1 hour and water-quenched. Tempered at 600 C for 1 hour and water-quenched. Embrittled at 455 C for 5 hours and water-quenched. Tensile data: Rockwell C-25; yield strength, psi (0.1%), 117,500; tensile strength, psi, 130,000; elongation, 21.4%; reduction of area, 64.7%.

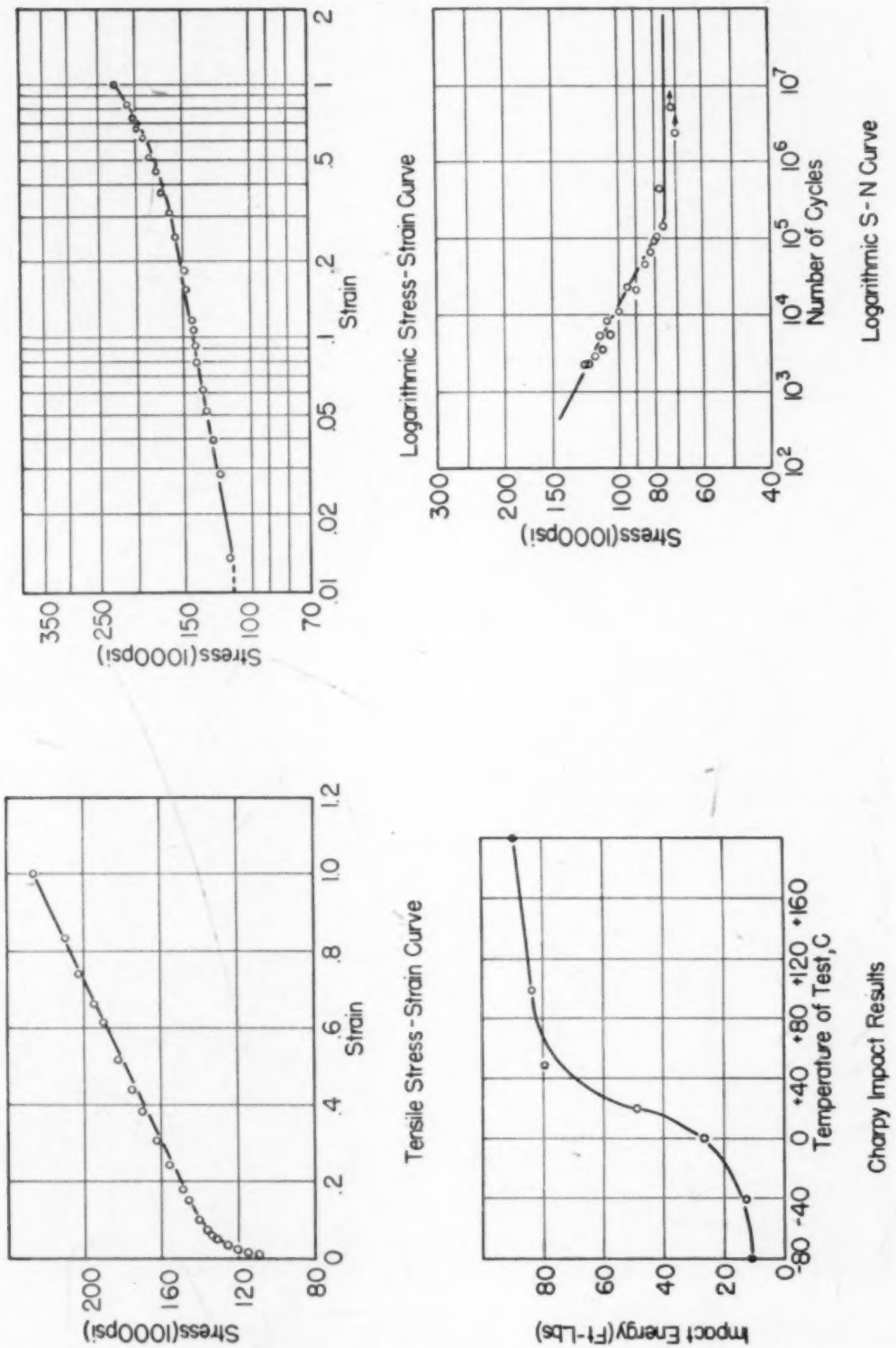


Fig. 16—Test Results for Specimens of Steel SAE 3135, Series T. Structure: tempered martensite plus temper brittleness. Heat treatment: austenitized at 870 C for 1 hour and water-quenched. Tempered at 600 C for 1 hour and water-quenched. Embrittled at 455 C for 50 hours and water-quenched. Tensile data: Rockwell C-24; yield strength, psi (0.1%), 111,200; tensile strength, psi, 126,000; elongation, 20.7%; reduction of area, 64.0%.

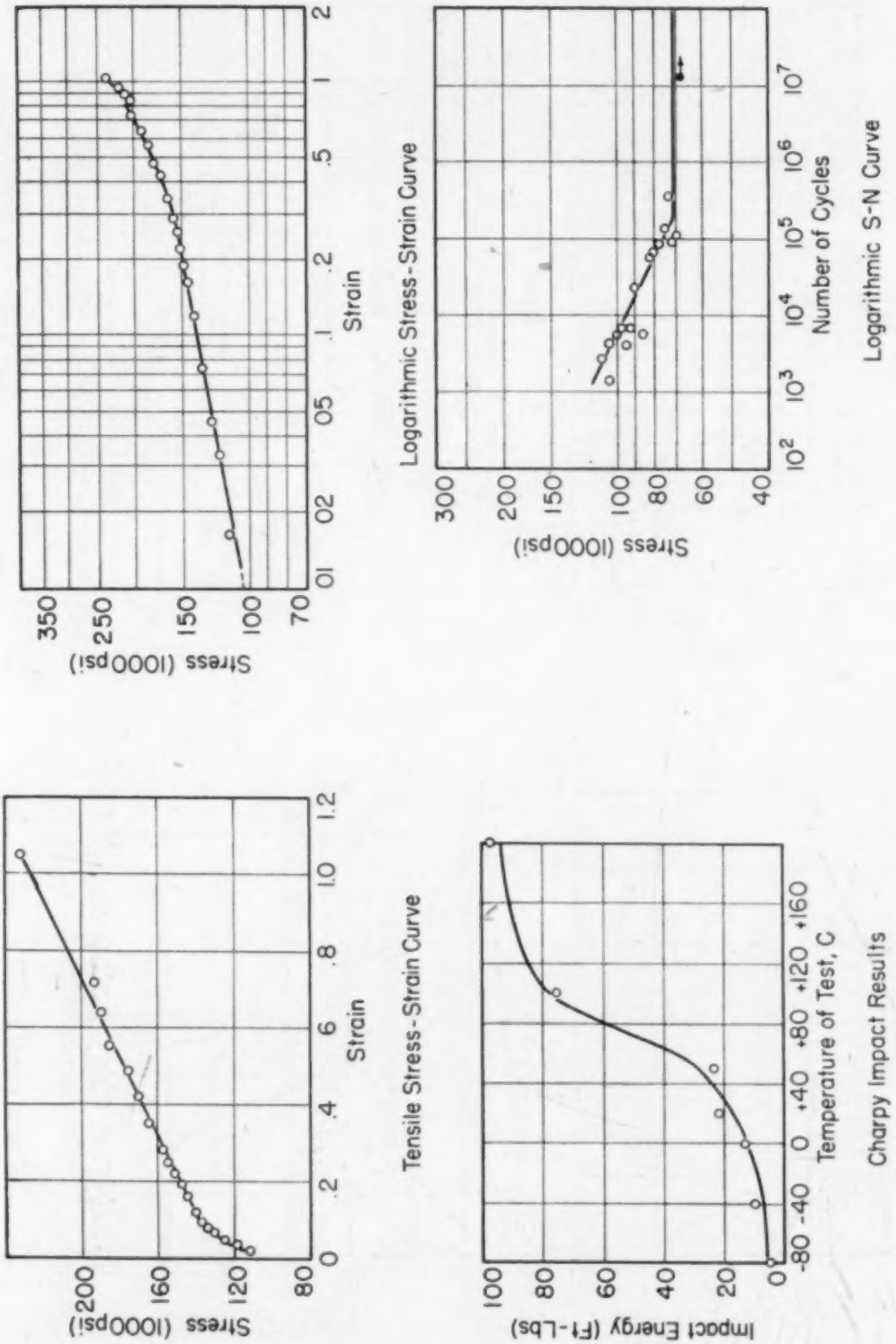


Fig. 17—Test Results for Specimens of Steel SAE 3135, Series U. Structure: tempered martensite plus temper brittleness. Heat treatment: austenitized at 870 C for 1 hour and water-quenched. Tempered at 600 C for 1 hour and water-quenched. Embrittled at 455 C for 500 hours and water-quenched. Tensile data: Rockwell C-23; yield strength, psi (0.1%), 108,700; tensile strength, psi, 123,000; elongation, 21.4%; reduction of area, 64.0%.

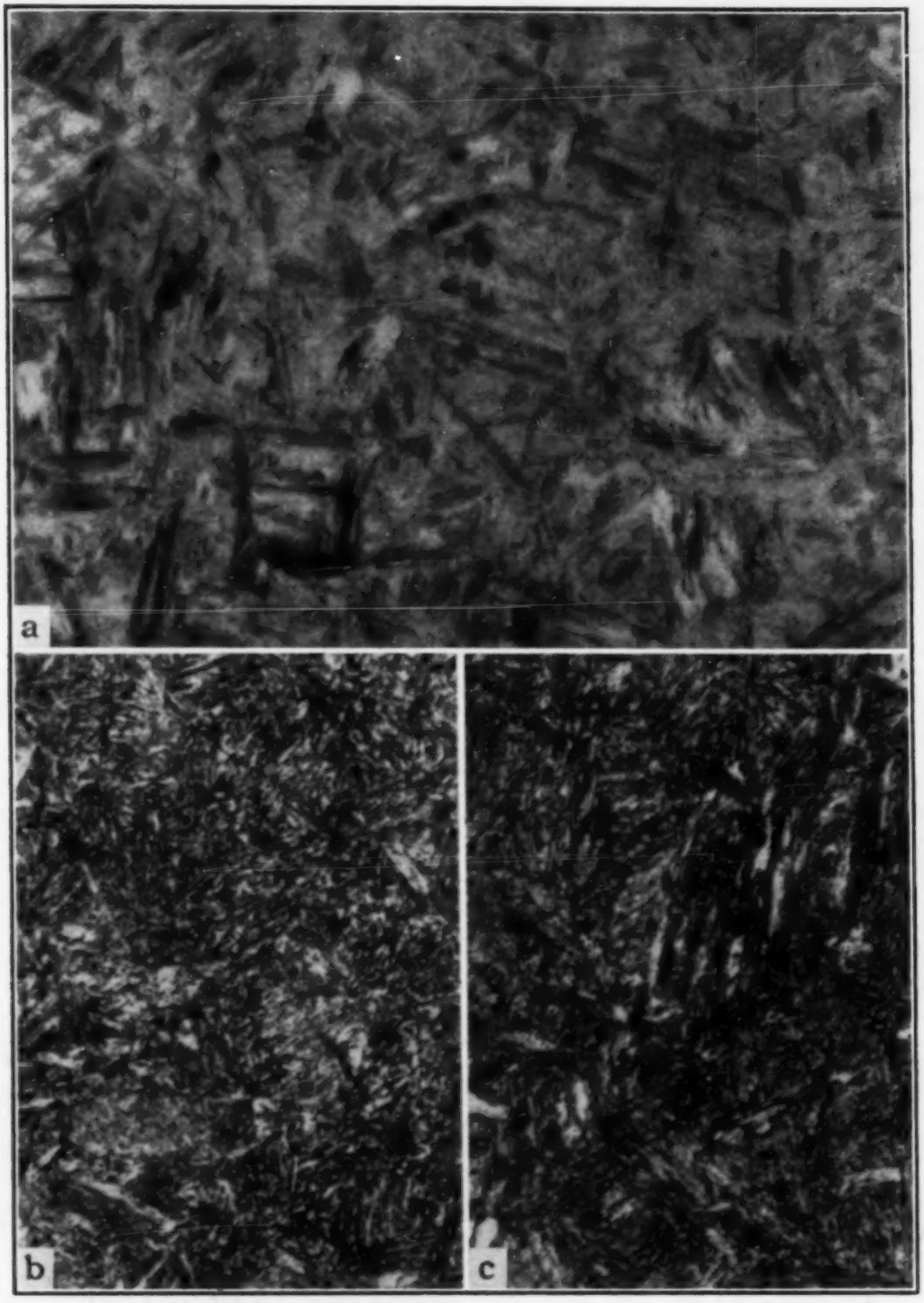


Fig. 18—Photomicrographs of Specimens in Tempered Martensite Series.
See page 836 for complete data.

areas (pearlite) and may be a result of the bainite transformation. The photomicrographs of Figs. 20b, 20c, 20e and 20f illustrate the tempered structures.

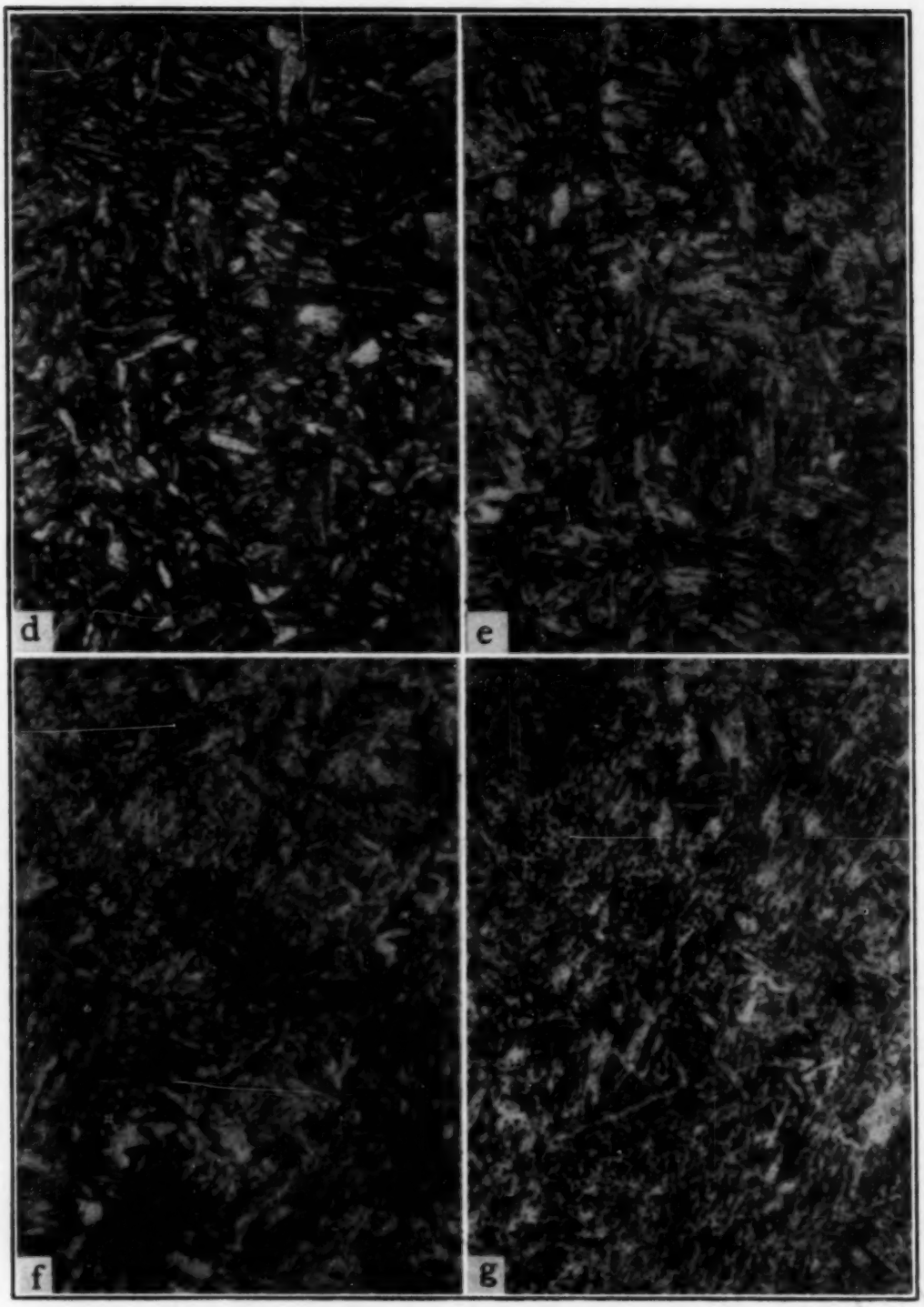


Fig. 18—Photomicrographs of Specimens in Tempered Martensite Series.
See page 836 for complete data.

The 5/8-inch diameter blanks of SAE 3135 could not be quenched to martensite even in violently agitated water. The specimens all contained approximately 10% bainite before tempering. The dark area to

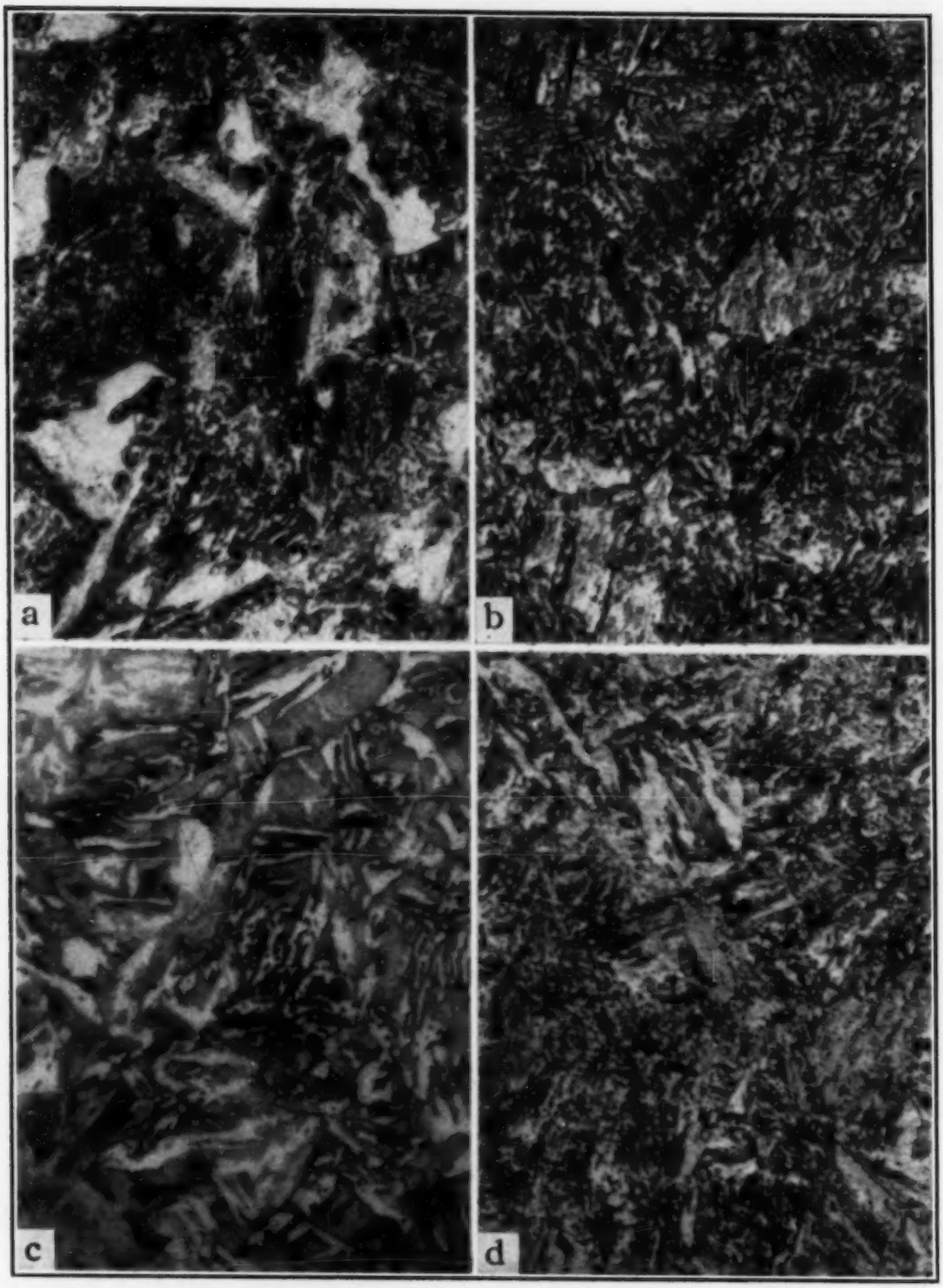


Fig. 19—Photomicrographs of Specimens in Tempered Bainite Series.
See page 836 for complete data.

the right of the center of Fig. 21a typifies the bainite formed upon quenching. In order to secure varying degrees of embrittlement, groups of specimens were heated to 455 C (850 F) for varying times. Some slight additional tempering did occur during the long-time treatments,

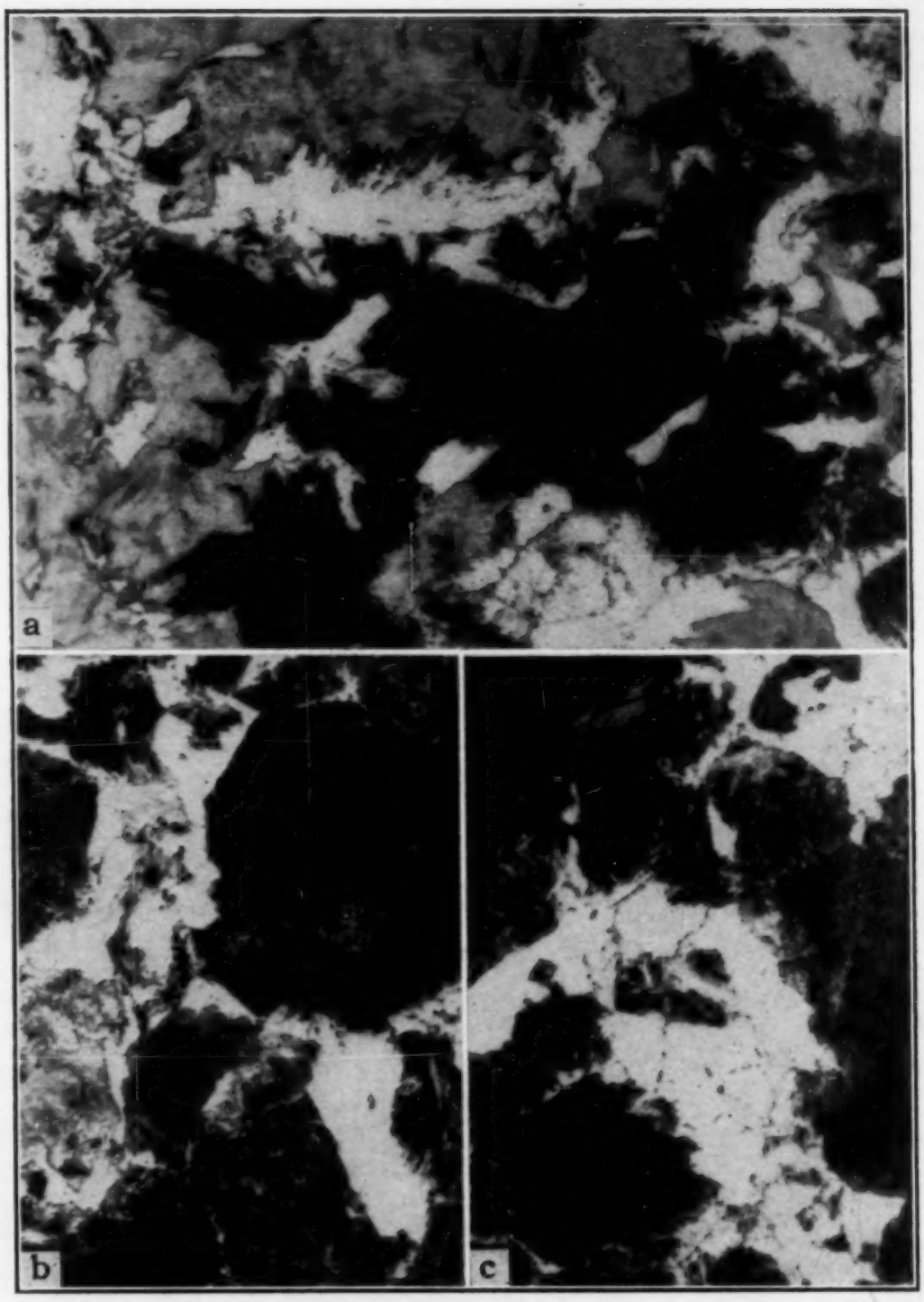


Fig. 20—Photomicrographs of Specimens in Tempered Pearlite Series.
See page 836 for complete data.

but the photomicrograph of Fig. 21b illustrates a typical structure after tempering and embrittlement. The results of the mechanical tests on the temper-brittle specimens are given in Figs. 14 through 17.

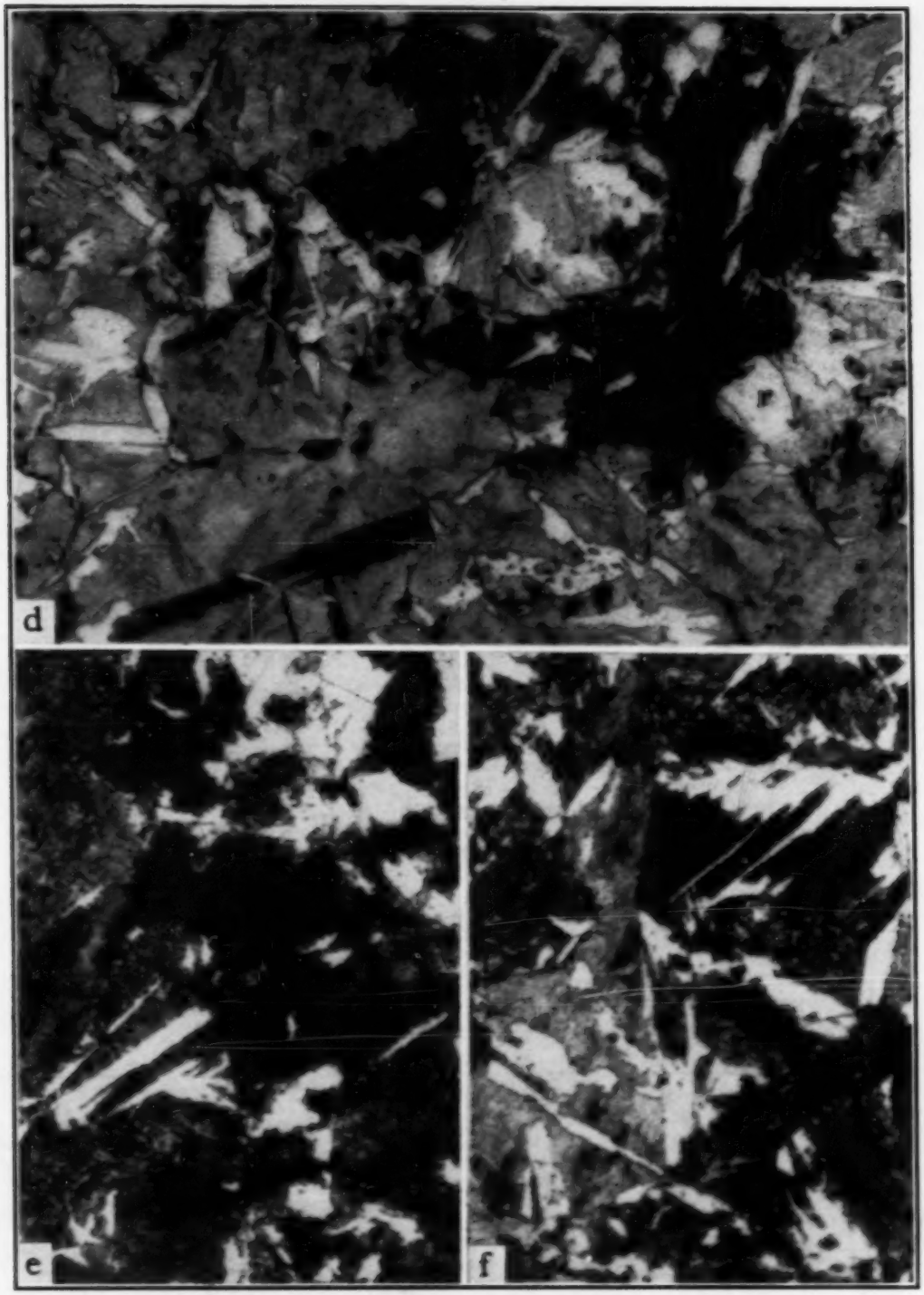


Fig. 20—Photomicrographs of Specimens in Tempered Pearlite Series.
See page 836 for complete data.

Discussion of Results

Tensile and Impact Properties—The slope of the logarithmic stress-strain curve is a measure of the rate of strain hardening (5) and

FIG. 18—PHOTOMICROGRAPHS OF SPECIMENS IN TEMPERED MARTENSITE SERIES

Etchant, 1% Nital. N. A. of Objective: 0.95. × 1000

Fig.	Steel	Heat Treatment	Microstructure
18a	NE8735	900 C, water-quenched.	Martensite.
18b	NE8735	900 C, water-quenched, tempered at 420 C.	Tempered martensite with fine precipitated carbide unresolved at this magnification.
18c	NE8735	900 C, water-quenched, tempered at 485 C.	Similar to Fig. 18b.
18d	NE8735	900 C, water-quenched, tempered at 575 C.	Tempered martensite with unresolved precipitated carbides.
18e	NE8735	900 C, water-quenched, tempered at 605 C.	Similar to Fig. 18d but with occasional resolved carbides.
18f	NE8735	900 C, water-quenched, tempered at 655 C.	Similar to that of Fig. 18e but with more resolved carbides.
18g	NE8735	900 C, water-quenched, tempered at 685 C.	Tempered martensite with most of the precipitated carbides resolved.

FIG. 19—PHOTOMICROGRAPHS OF SPECIMENS IN TEMPERED BAINITE SERIES

Etchant, 1% Nital. N. A. of Objective: 0.95. × 1000

Fig.	Steel	Heat Treatment	Microstructure
19a	NE8735	Transformed isothermally at 400 C, water-quenched.	Mostly bainite.
19b	NE8735	Transformed isothermally at 400 C, water-quenched, tempered at 590 C.	Same as Fig. 19a except that carbides are more readily resolved.
19c	NE8735	Transformed isothermally at 470 C, water-quenched.	Bainite in martensite matrix.
19d	NE8735	Transformed isothermally at 470 C, water-quenched, tempered at 635 C.	Same as Fig. 19c except that carbides precipitated during tempering are present.

FIG. 20—PHOTOMICROGRAPHS OF SPECIMENS IN TEMPERED PEARLITE SERIES

Etchant, 1% Nital. N. A. of Objective: 0.95. × 1000

Fig.	Steel	Heat Treatment	Microstructure
20a	NE8735	Transformed isothermally at 600 C, water-quenched.	Areas of pearlite (dark) and ferrite (white) in background of martensite.
20b	NE8735	Transformed isothermally at 600 C, water-quenched, tempered at 510 C.	Same as Fig. 20a except that martensite regions now reveal carbide precipitated during tempering.
20c	NE8735	Transformed isothermally at 600 C, water-quenched, tempered at 625 C.	Same as Fig. 20b.
20d	NE8735	Transformed isothermally at 550 C, water-quenched.	Similar to Fig. 20a.
20e	NE8735	Transformed isothermally at 550 C, water-quenched, tempered at 570 C.	Same as Fig. 20d except that martensite regions reveal carbide precipitated during tempering.
20f	NE8735	Transformed isothermally at 550 C, tempered at 615 C.	Same as Fig. 20e.

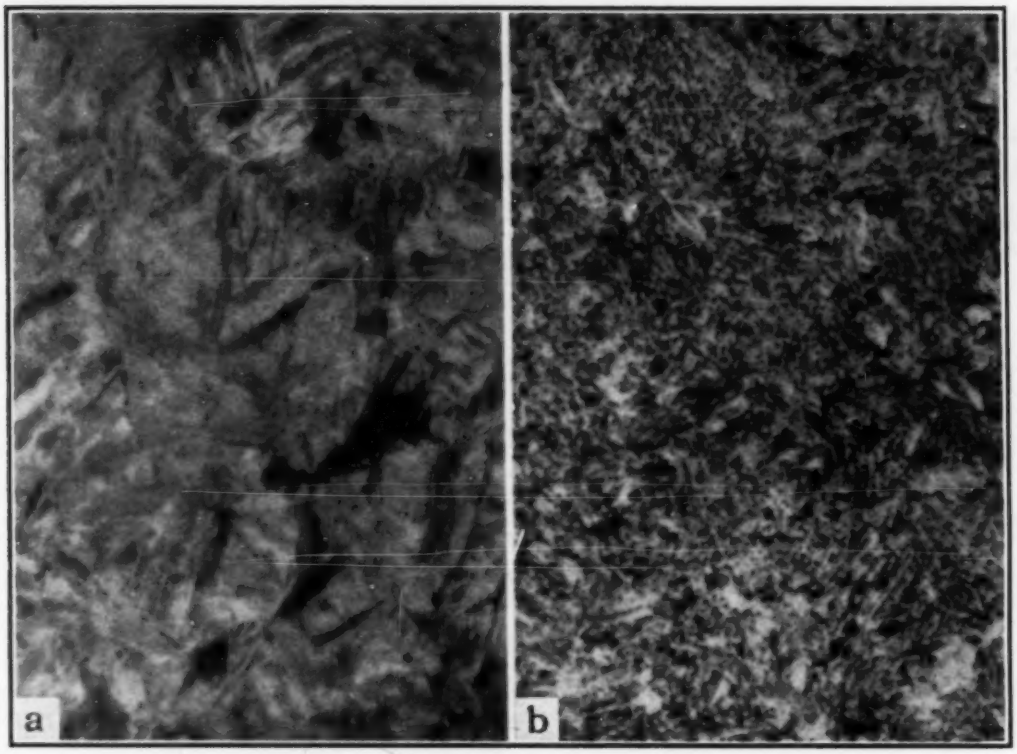


FIG. 21—PHOTOMICROGRAPHS OF SPECIMENS IN TEMPER-BRITTLE SERIES

Etchant, 1% Nital. N. A. of Objective: 0.95. × 1000

Fig.	Steel	Heat Treatment	Microstructure
21a	SAE3135	900 C, water-quenched.	Martensite with small percentage of bainite. Dark area to the right of center is bainite.
21b	SAE3135	900 C, water-quenched, tempered at 600 C, water-quenched, embrittled at 455 C, water-quenched.	Tempered martensite and tempered bainite. Precipitated carbides are just barely resolved.

in Fig. 22 this slope is plotted as a function of the tensile strength. From this plot it is seen that the rate of strain hardening depends only upon the tensile strength. There is no observable difference between the values for the steels of the different structures.[3] However, since the yield-tensile ratios of the (partially) tempered pearlitic specimens and the (partially) tempered bainitic specimens are considerably smaller than those of the tempered martensitic specimens, the strain hardening exponents are larger for these specimens than for the tempered martensitic at the same yield strength. This variation of yield-tensile ratio with structure has been discussed in detail by one of the authors in another paper (5) and has been shown to be due to differences in the

[3]The strain hardening exponent does, however, depend upon carbon content (5).

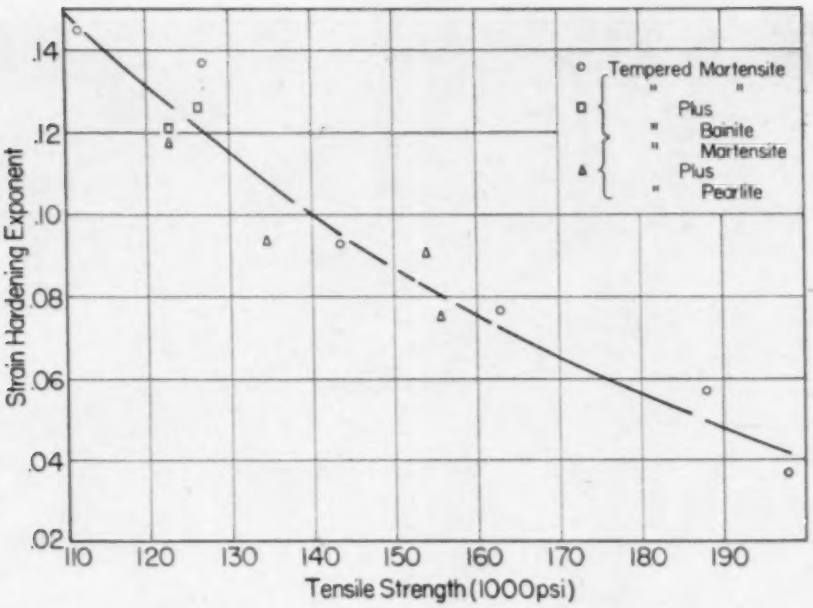


Fig. 22—Relation Between Strain Hardening Exponent and Tensile Strength for the Steels of Various Structures.

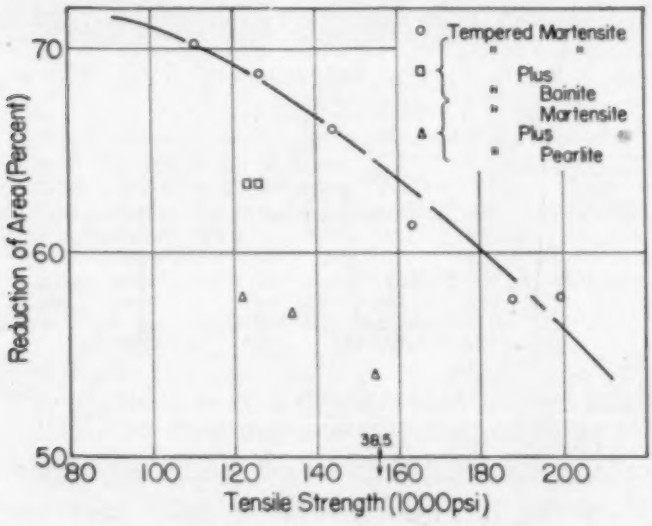


Fig. 23—Relation Between the Reduction of Area and the Tensile Strength for the Steels of Various Structures.

type of initial yielding exhibited by the several steels. Tempered martensitic steels tend to exhibit the drop in load at yielding more readily than do steels of other structures. Thus, the yield strength as measured at small offsets measures the resistance to inhomogeneous yielding and this resistance depends upon structure.

Fig. 23 illustrates that the reduction of areas of the tempered martensitic specimens are higher than those of the specimens of other

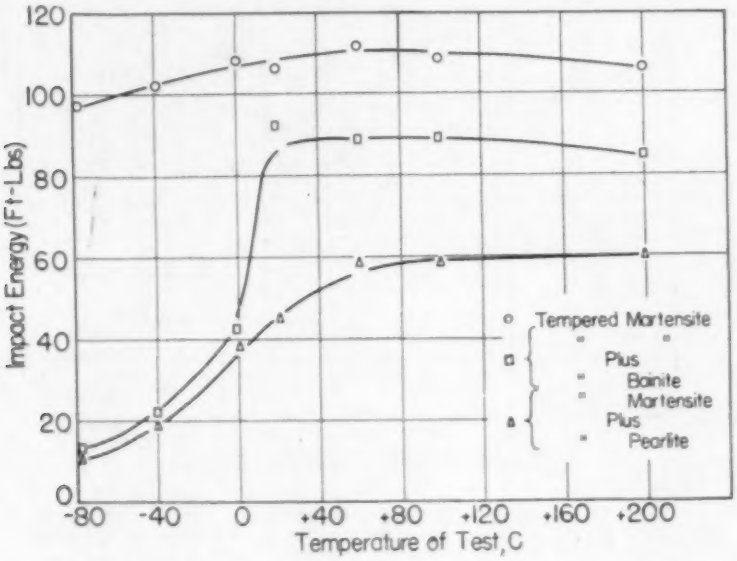


Fig. 24—Impact Properties of Steels of Various Structures at a Tensile Strength of Approximately 125,000 psi.

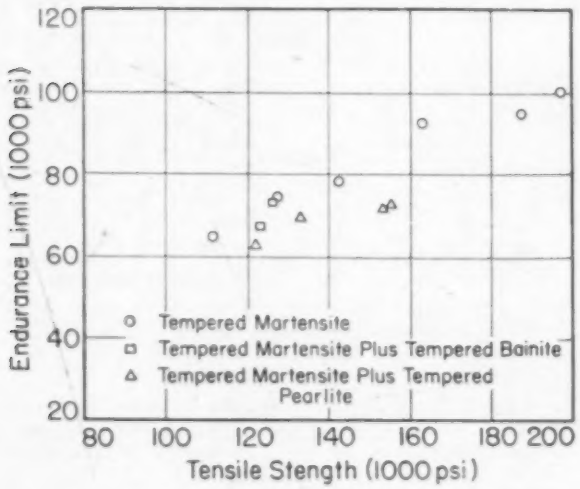


Fig. 25—Relation Between Endurance Limit and Tensile Strength for the Steels of Various Structures.

structures at corresponding tensile strengths. This difference is a result of a lower fracture stress as can be seen by inspection of Figs. 2 to 13. The difference in the fracture properties is much more clearly illustrated by comparison of the impact properties plotted in these same figures. The impact energy of the tempered martensitic steels does not decrease significantly with decreasing testing temperature (above —78 C) except for the specimens of the highest strength (200,000 psi tensile strength). However, the specimens having structures before tempering that were not completely martensitic have lower impact

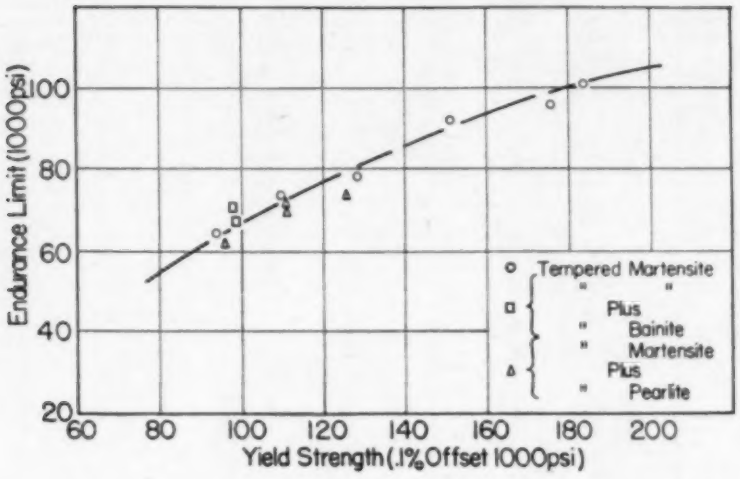


Fig. 26—Relation Between Endurance Limit and Yield Strength (0.1% Offset) for the Steels of Various Structures.

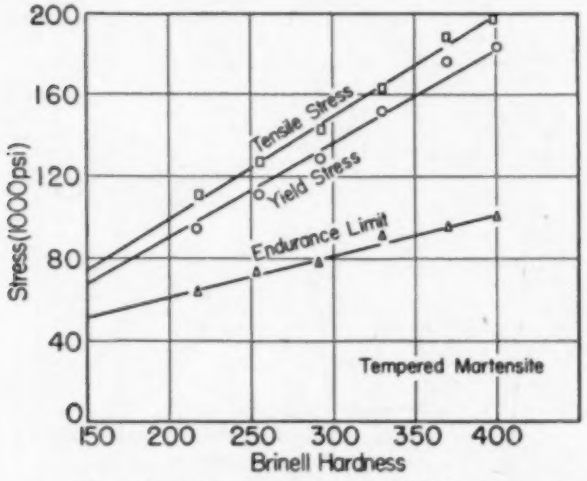


Fig. 27—Relation Between Yield Strength, Tensile Strength, and Endurance Limit and the Brinell Hardness of the Tempered Martensitic Steels.

energies at elevated testing temperatures and the transition temperature is evident in all of the plots. Fig. 24 shows the effect of structure on the impact properties more clearly. The three steels of the graph all had approximately the same tensile strength (125,000 psi). The impact properties of the partially bainitic steel are intermediate between those of the martensitic and those of the partially pearlitic. The difference in impact energy at high testing temperature reflects the difference in fracture stress observed in room temperature tensile tests, whereas the difference in transition temperature is a reflection of a difference in dependence of the fracture stress upon strain for the steels of different structures (6).

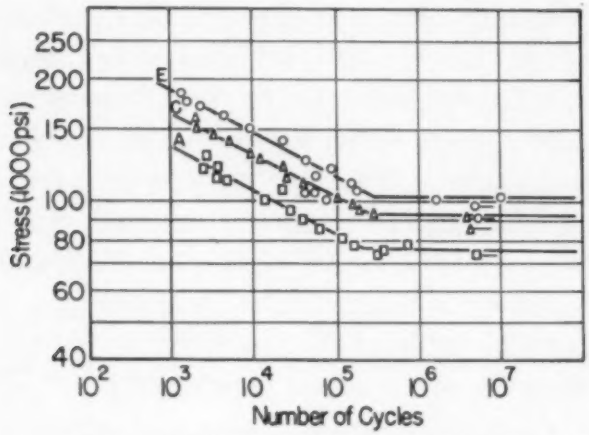


Fig. 28—Effect of Changing Yield Strength on the Logarithmic S-N Curves of Several of the Tempered Martensitic Steels.

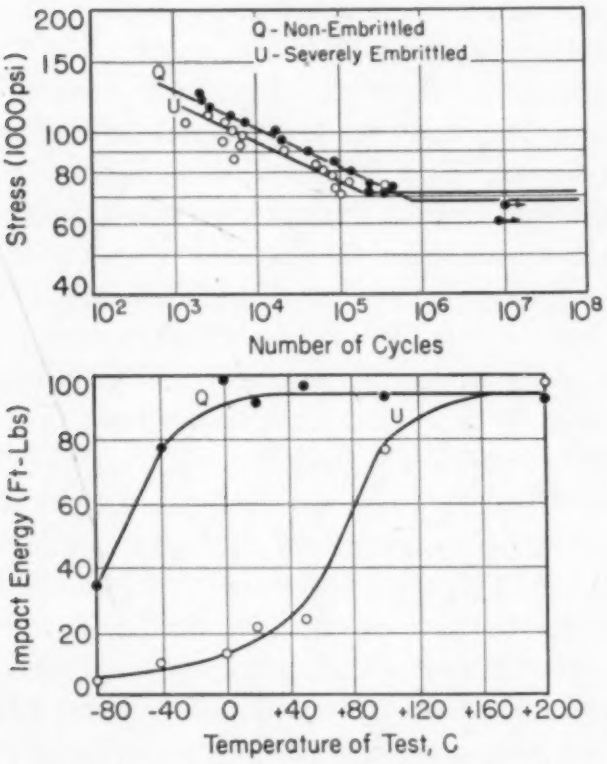


Fig. 29—Fatigue and Impact Properties of Nonembrittled and Severely Embrittled SAE 3130 Steel. Note: Q—Nonembrittled. U—Severely Embrittled.

The effect of temper brittleness upon the tensile and impact properties is illustrated in Figs. 14 to 17. As the amount of the transformation increases, the transition temperature of the impact properties is raised, but the value of the energy above the transition temperature is not affected nor is the reduction of area in the normal tensile

tests (7). The fracture in the tensile test of the severely embrittled specimens (of Figs. 16 and 17) was, however, longitudinal rather than transverse. (Impact curves for the nonembrittled and most severely embrittled specimens are compared in Fig. 29.) This change in properties is slightly different from that effected by the change from tempered martensitic to tempered pearlitic, for, as pointed out above, in the latter both the elevated temperature impact properties and the reduction of area are affected. It must be concluded that the primary effect of the transformation that causes temper brittleness is to decrease the fracture stress at small strains. There is little effect at large strains.

Fatigue Properties—Endurance Limit—The endurance limits of the specimens of SAE 8735 steel having the various structures are plotted in Fig. 25 as functions of the tensile strength and in Fig. 26 as functions of the yield strength (0.1% offset). Fig. 25 indicates that many of the specimens which were not martensitic before tempering have lower endurance limits for a given tensile strength than do the martensitic specimens. This difference in endurance limit is less apparent in the plot of endurance limit versus the yield strength (Fig. 26). Thus, a low yield-tensile ratio is reflected in a low endurance limit. The higher yield strength of the tempered martensitic (and to some extent the tempered bainitic) steels raises the endurance limit at a fixed tensile strength. A summary of the tensile and yield strengths and the endurance limit of the tempered martensitic steels as functions of the Brinell hardness is presented as Fig. 27.

S-N Curve—The S-N curves of tempered martensitic steel at several yield strengths are presented as Fig. 28. As indicated in this figure, the effect of changing the strength of tempered martensitic steels is to shift the entire S-N curve vertically with respect to itself. For the steels of different structures (tempered pearlite, tempered bainite, tempered martensite), the entire S-N curves are very nearly identical when the endurance limits are the same. However, if sufficient alteration in the fracture characteristic is obtained, the S-N curve is affected, as illustrated in Fig. 29. Here the fatigue data for the most severely embrittled and nonembrittled SAE 3135 steel are compared. The effect of the embrittlement is to shift the S-N curve toward smaller number of cycles.

It must be pointed out, however, that under the conditions of the fatigue tests at 1750 rpm, the deformation that occurs at the high stress levels is adiabatic and the temperature of the specimen rises. Thus,

the conditions under which fracture occurs are less severe than they would be if the load were applied so slowly that the heat would have sufficient time to dissipate. No tests except those of P. Kosting (8) seem to have been performed at relatively slow rates. He found considerable difference between the fatigue properties of the steels having different impact properties. Further examination of the properties of steels in isothermal fatigue tests is needed.

Conclusions

The rate of strain hardening is not significantly affected by differences in structure if the height of the stress-strain curve (the tensile strength) is constant. The rate of strain hardening is, however, strongly dependent upon the tensile strength and, as has been shown earlier, upon the carbon content. The initial height of the stress-strain curve, if the yielding is inhomogeneous (Lüders' bands), is greater for tempered martensitic steels.

Pearlite (plus ferrite) and bainite in the quenched structure of tempered specimens are reflected in lower reductions of area in standard tensile tests. The constituent responsible for temper brittleness does not affect the normal tensile properties unless the embrittlement is very severe. The reduction of area is reduced by severe embrittlement and the fracture of the tensile specimens may become, in part at least, longitudinal rather than transverse. The stress at fracture as determined in simple tension is seldom lowered more than a few thousand pounds per square inch by changing the structure from unembrittled tempered martensite (while maintaining a fixed tensile strength).

The impact properties of tempered bainitic steels are intermediate between those of tempered pearlitic and tempered martensitic steels of the same hardness. The effect of temper brittleness on the impact properties is to raise the temperature of transition from ductile to brittle failure. The effect of other changes in structure (from tempered martensite) is to lower the energy level above the transition temperature as well as to raise the transition temperature.

The endurance limit of steels having the same tensile strength depends upon structure through the effect of structure on the yield strength. Steels having a higher yield strength (due to inhomogeneous yielding) have a higher endurance limit. The logarithmic S-N curves of tempered martensitic steels are shifted vertically by changes in hardness: the fractional change in the stress required for fracture at

any fixed number of cycles is constant. There is little or no difference between the S-N curves (obtained by tests in R. R. Moore machines) above the endurance limits of steels partially bainitic or pearlitic before tempering and those of tempered martensitic specimens. Severe temper embrittlement decreases the number of cycles to failure above the endurance limit. The results at high stress values may not be widely applicable, however, because of the temperature rise of the specimens at the high frequency of loading employed in the standard fatigue tests.

Steels having a tempered martensitic structure have mechanical properties superior to those of steels with other structures. At a given tensile strength, they have the highest yield strength, the highest ductility, the highest endurance limit, the greatest toughness under severe conditions and may endure high stresses for the greatest number of cycles. When these steels do fail, the energy absorbed in fracturing is higher than absorbed by steels with other structures.

References

1. A. J. Brinell, "Texture Changes in Steel on Heating and Cooling," *Jernkontorets Annaler,* Vol. 40, 1885, p. 9-38.
2. E. C. Bain, "Functions of the Alloying Elements in Steel," American Society for Metals, Cleveland, 1939, p. 38-40.
3. M. A. Grossmann, "Principles of Heat Treatment," American Society for Metals, Cleveland, 1935, p. 71-73.
4. Research Committee on Fatigue of Metals, "Notes on Fatigue Tests on Rotating-Beam Testing Machine," *Proceedings,* American Society for Testing Materials, Vol. 35, 1935, p. 113-120.
5. J. H. Hollomon, "Tensile Deformation," *Metals Technology,* Vol. 12, No. 4, June 1945.
6. J. H. Hollomon, "The Notched Bar Impact Test," *Transactions,* American Institute of Mining and Metallurgical Engineers, Vol. 158, 1944, p. 298-327.
7. J. H. Hollomon, "Temper Brittleness," TRANSACTIONS, American Society for Metals, Vol. 36, 1946, p. 473.
8. P. R. Kosting, "Progressive Stress Damage," American Society for Metals, Educational Lecture, February 1946.

DISCUSSION

Written Discussion: By Roger Stuart Brown, Ajax Electric Co., Philadelphia.

I certainly agree with the previous speaker that the last sentence of the authors' conclusion, that tempered martensite is always the best structure for best physical properties, covers entirely too much ground. There is no need to review the many investigations to the contrary. I might remind the audience

of the excellent paper by H. J. Elmendorf[3] on the physical properties of various mixtures of bainite and tempered martensite. This showed decided superiority in high carbon steels and one low alloy steel of 30% mixture of bainite and tempered martensite over either bainite alone or tempered martensite alone.

Taking a practical illustration, Roy M. Ellis[4] reported austempering a barrel bushing of the 0.45-caliber automatic pistol, which would produce bainite alone. Subjected to repeated impact in firing tests, it showed a fatigue value 11 times that of the same parts oil-quenched and tempered to the same hardness.

It also seems evident that the benefit of bainitic structures is not confined entirely to high carbon steels. Percussion fuses used in shells for piercing tank armor were made by a quenching process which certainly produced a tempered bainite structure in 0.40% carbon steel, and withstood the shock of hitting armor plate better than the same parts made in quenched and drawn steel (tempered martensite).[4a]

I am in hearty agreement with the authors, that mixed structures containing ferrite or pearlite with or without bainite are inferior to tempered martensite alone. But, I am not convinced that their method of heat treatment produces only a bainite-tempered martensite structure—certainly not in the center of the piece, nor am I convinced the photomicrographs show the structure with bainite and tempered martensite to be free of ferrite.

Written Discussion: By R. A. Grange, United States Steel Corporation Research Laboratory, Kearny, N. J.

The influence of microstructure on the mechanical properties of steel comprises a very large and fruitful field for research; most published data on mechanical properties are not very helpful in this respect since in very few cases has the necessary attention been paid to microstructural details. The authors are to be highly commended for their systematic approach and for their thoroughness in investigating the effect of microstructure on mechanical properties of NE 8735 as tempered to a hardness of Rockwell C-20 to 30. Their data showing the harmful effect of temper brittleness on the S-N curves for SAE 3135 steel having a structure of tempered martensite is also a new and valuable contribution. It is felt, however, that some of the conclusions drawn by the authors may not be applicable to all steels; in particular, it is difficult to reconcile the authors' conclusion that "the properties of tempered martensite are superior to those of steel having other structures" with the well-established superiority in certain respects of untempered bainite over tempered martensite at hardnesses of Rockwell C-50 or over in steel with higher carbon content than the NE 8735 studied by the authors. Furthermore, it should be pointed out that measurement of tensile, impact, or fatigue properties by means of arbitrary laboratory tests cannot always be correlated with actual performance of heat treated parts; this is particularly true of fatigue properties, in which case the distribution of residual stresses in an actual part may have a greater effect than difference in microstructure.

---

[3]H. J. Elmendorf, "The Effect of Varying Amounts of Martensite Upon the Isothermal Transformation of Austenite Remaining After Controlled Quenching," TRANSACTIONS, American Society for Metals, Vol. 33, 1944, p. 236.

[4]Roy M. Ellis, "Isothermal Treatment of Pistol Parts," *Iron Age*, Feb. 8, 1945.

[4a]Harold J. Babcock, "Isothermal Quench Bath Applied to Commercial Practice," *Iron Age*, February 3 and 10, 1944.

The author's statement on page 810 that "the bainite reaction does not go to completion except at the lowest temperatures of transformation" is contrary to the writer's observation on low alloy steels similar to NE 8735 or SAE 3135; we would like to ask the authors to explain the basis for their statement.

Authors' Reply

As Mr. Grange points out and as Mr. Brown infers, the statement that the properties of steel having the tempered martensitic structure are superior to steels having other structures may be too broad. However, there are several mitigating circumstances. In the first place, as is usual in papers of this sort, the authors were basing their conclusions primarily upon evidence they had obtained. Secondly, their own experience during the war, when they were in a position to examine the results of literally thousands of heats of medium carbon alloy steels treated to different structures, completely justifies this conclusion. In no case in which there were data were the properties of tempered bainite superior to those of tempered martensite in the steels used for guns and armor at hardnesses below about Rockwell C-43. It is in this respect that the statement made concerning the properties of tempered martensite should be limited, the experience of the authors being primarily with steels below Rockwell C-50 and having carbon contents below 0.50%.

However, in the experimental comparisons of the properties of steels of different structures, both high and low carbon, there are many pitfalls and it is seldom that they all can be avoided. To cite a specific example, it is unlikely that the pistol parts described in the article by Ellis and referred to by Mr. Brown were tempered martensite before the introduction of the austempering treatment. Not only is the formation of bainite difficult to avoid even in small parts with WD 1075 when quenched in oil, but also the retention of austenite would always be a concomitant of martensite formation. The tests reported by Ellis cannot be construed as proving that the steels of one structure are better than another, but only that one treatment was better than another, neither of which produced structures liable to posterior identification. As for the data of Elmendorf, as Foley[5] points out, the marked improvement of the austempering treatments was very apparent in the two steels of the highest carbon content. Further, although Elmendorf does not give the dimensions of his specimens or the details of the quenching practice, it is possible that the quenched specimens did contain some bainite and without refrigeration treatments they certainly contained some retained austenite.

The above discussion, while not refuting the possible advantage of (untempered) bainitic steels over tempered martensitic steels at hardnesses above about Rockwell C-45 to 50 and at carbon contents above 0.60%, does indicate that this conclusion is by no means well founded. It should also be pointed out that the data of Griffith, Pfeil and Allen[6] are in full agreement with ours. Really significant tests must yet be performed in the high hardness, high carbon range,

[5]G. M. Foley, Discussion to paper of Elmendorf, TRANSACTIONS, American Society for Metals, Vol. 33, 1944, p. 255.

[6]W. T. Griffith, L. B. Pfeil and N. P. Allen, Iron and Steel Institute, Second Report of the Alloy Steels Research Committee, 1939.

but for medium alloy steels at low hardnesses, the superiority of the tempered martensitic structure is, at least in the authors' opinion, well grounded.

Mr. Grange refers to the superiority of (untempered) bainitic steels over tempered martensitic steels at hardnesses of Rockwell C-50 and over. It is quite possible that this difference is due to the presence of retained austenite in the latter steel and that it decomposed in tempering. It is also possible that the brittleness that occurs on tempering some martensitic steels affects adversely the properties of tempered martensites. Although Mr. Grange gives no references, it is assumed that he refers to early experiments made when the austempering process was first developed. If memory serves, these experiments were in the main performed on plain (high) carbon steels with which the obtaining of a completely martensitic structure free of austenite is difficult at best.

Mr. Grange's point on the present unsatisfactory state of knowledge of the science of the behavior of metals is well taken. If we understood, in terms of consistent theory, the mechanical behavior of metals, there would be no question such as he raises concerning correlations between laboratory and field tests. Mr. Grange also asks for references to the lack of completion of the bainite reaction at high temperatures.[7, 8, 9]

---

[7]H. Lange and K. Mathieu, *Mitt., Kaiser-Wilhelm Inst. f. Eisenforsch.*, Vol. 20, 1938, p. 125.

[8]W. T. Griffith, L. B. Pfeil and N. P. Allen, Iron and Steel Institute, Second Report of the Alloy Steels Research Committee, 1939.

[9]H. Döpfer and H. J. Wiester, *Archiv für das Eisenhüttenwesen*, Vol. 8, 1938, p. 541.

METALLURGICAL AND STRUCTURAL INVESTIGATION OF STEEL CASTINGS FOR AIRCRAFT

By L. W. Smith and L. D. Morris

Abstract

Two types of steel castings, statically poured and centrifugally cast, were investigated metallurgically and structurally. Concurrently, forgings of identical components were similarly investigated to provide an additional comparison.

The metallurgical program included the determination of chemical and physical properties and the determination of quality by magnafluxing, etching, radiographic and visual inspection, and metallographic examination. The structural investigation included proof testing, fatigue and repeated load cycling, and static ultimate tests.

In general, the investigation showed that: (a), sound steel castings can be obtained; and (b), castings with sound material and properties can be used in airplane primary structures to supplement and supersede present types of fabricated structural components.

Introduction

IN the last few years under the impetus of wartime urgencies the quality of steel castings increased to a point where their use in airplane prime structure appeared feasible. Therefore, to substantiate such a viewpoint and to warrant consideration of cast steel parts for new models or redesigned parts, the Research Laboratory of the Curtiss-Wright Corporation instituted a program for the evaluation of steel castings for aircraft.

Several statically poured steel castings (Figs. 1 and 2) were obtained from Battelle Memorial Institute where they had been made on an experimental basis under a War Production Board contract in connection with steel castings for aircraft (1), (2), (3).[1] These castings were the upper and lower terminals of the C-46 outboard

[1]The figures appearing in parentheses pertain to the references appended to this paper.

A paper presented before the Twenty-eighth Annual Convention of the Society, held in Atlantic City, November 18 to 22, 1946. Of the authors, L. W. Smith is section head, Metallurgy Section, Materials Department, and L. D. Morris is section head, Structural Test Section, Structures Department, Cornell Aeronautical Laboratory, Buffalo, New York. Manuscript received July 3, 1946.

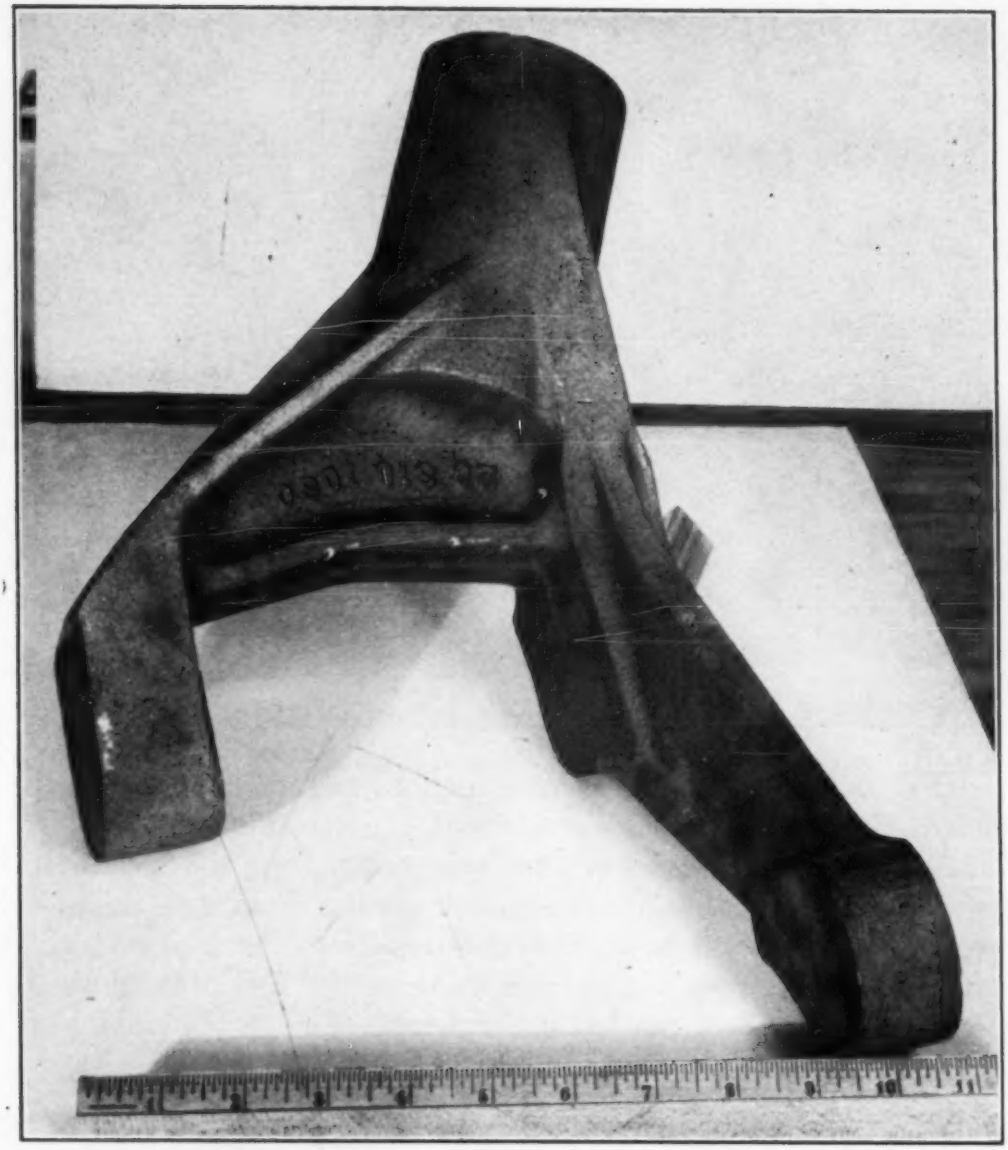


Fig. 1—Upper Terminal Casting of C-46 Outboard Side Brace Strut.

side brace strut and were similar in design to the forged production units. Centrifugal castings were likewise procured in order to make the program more comprehensive since there was the possibility of superior quality and greater ductility from the centrifugally cast type. The selected item (Fig. 3) was the forward fitting for the P-40 engine mount bearer tube since this fitting was of relatively simple design, consisting of a uniformly thick cylindrical wall and a lug, and was particularly suitable for casting centrifugally about its longitudinal axis. These fittings were cast by the American Steel Foundries, Chicago.



Fig. 2—Lower Terminal Casting of C-46 Outboard Side Brace Strut.

The actual program of investigation was undertaken to specifically determine from these castings: (a), metallurgical quality; (b), mechanical properties of specimens taken from the body of the casting and (c), strength characteristics under simulated static and dynamic service loadings. Identical tests were performed on similar forged items in order to appraise the castings for aircraft use by comparison with acceptable and proven (though perhaps overstrength) service units.

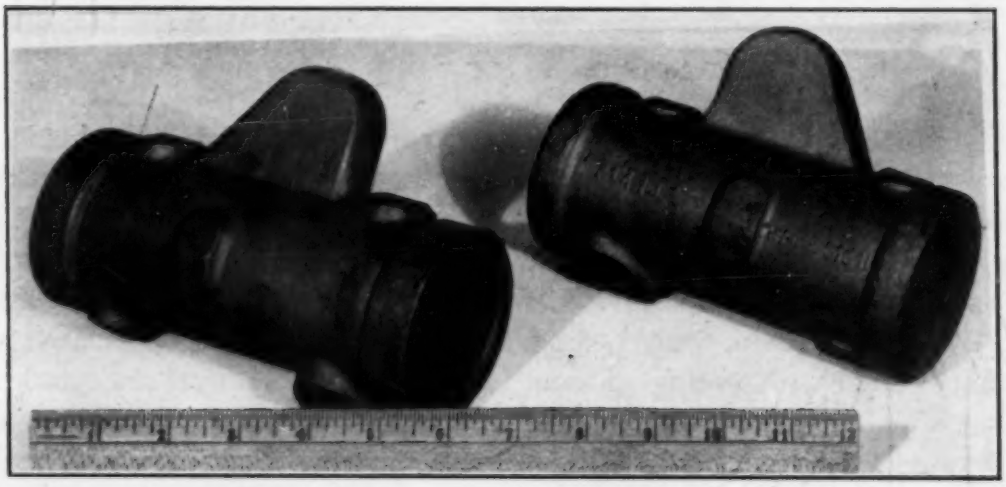


Fig. 3—P-40 Engine Mount Bearer Tube Fitting: Casting on the Left; Forging on the Right.

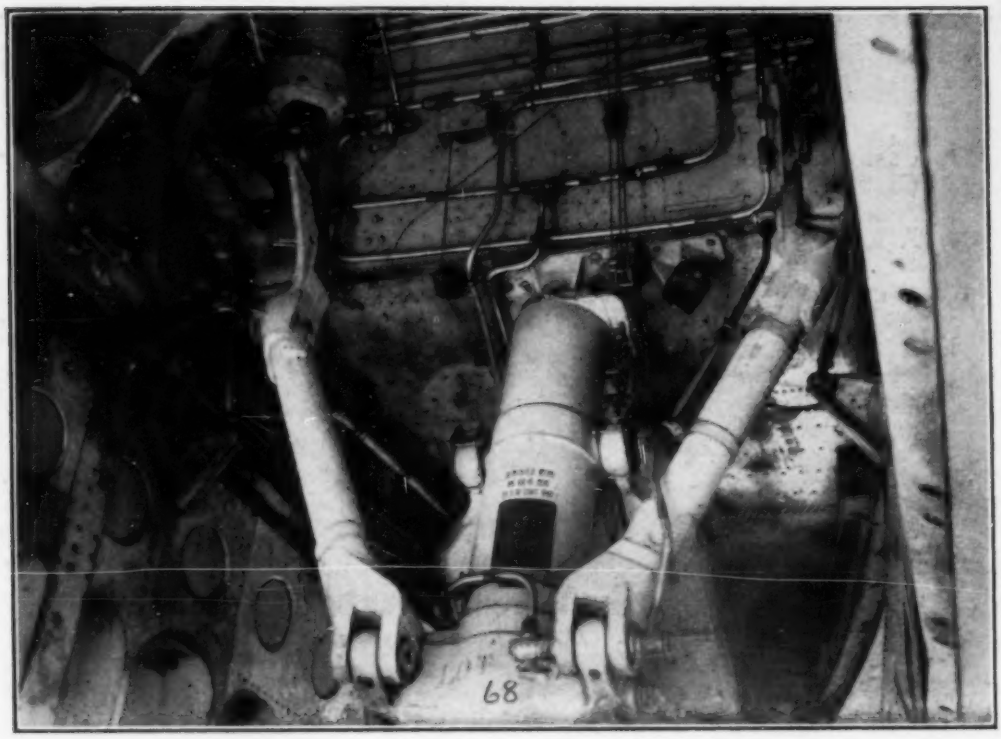


Fig. 4—C-46 Landing Gear Assembly.

For the purpose of clarity, the experimental methods, the results, and the discussion are presented as a unit for each type of casting: Part I of this paper includes information related to statically cast side brace strut terminals, and Part II concerns centrifugally cast P-40 engine mount fittings.

Part I

Statically Cast Terminals For C-46 Outboard Side Brace Strut

Description of Test Item—A service outboard side brace strut for the C-46 landing gear is composed of a forged upper terminal and a forged lower terminal welded to an inserted steel tube and its overall length is approximately 3½ feet. Fig. 4 shows this strut on an airplane. In addition to the function of reacting a side load as its name implies, the outboard side brace strut is also employed to raise and lower the entire landing gear. To allow for this operation, an arm of the upper terminal of the strut is loaded in bending by a piston rod of a hydraulic cylinder as the strut and attached gear pivot on a spar

fitting. Three such strut assemblies but with substituted cast terminals were fabricated by the Curtiss-Wright Kenmore Plant according to regular shop practice which consisted of the following procedure:

1. Casting and tubing normalized
2. Castings rough machined
3. Assembly welded together
4. Assembly heat treated:
   Normalize 1575 F—1½ hrs.—air-cooled
   Quench 1625 F—2 hrs.—oil quench
   Draw 840 F—3 hrs.—air-cooled
5. Assembly finish machined
6. Assembly magnafluxed

Experimental Methods and Results

Inspection—Several sets of castings (upper and lower terminals) as-received were radiographed by an outside agency and later magnafluxed in an assembly but both methods failed to indicate the presence of hot tears in the upper terminal which were subsequently revealed by metallurgical examination. Visual inspection showed the castings to have a rough surface finish only.

Metallographic Examination—One set of castings in the as-received condition was sectioned as shown by Figs. 5 and 6. They were etched in hot 1:1 HCl for 1 hour and examined for defects. The upper terminal was not a high quality casting as shown by Figs. 7 to 11. The casting contained porous spots, hot tears, surface porosity, inclusions, and shrinkage areas. The lower terminal casting was of a better quality. A section of this casting is shown in Fig. 12.

The cast terminals of the strut assembly were sectioned as shown in Figs. 13 and 14 and etched as previously described. The same type of defects were found. The lower terminal was the better of the two castings. Figs. 15 to 17 show defects in castings which were statically tested. Porosity was also noted in and around the welds on both castings.

The microstructures of the two castings in the as-received condition are shown by Figs. 18 and 19. These photographs disclose that both heats of steel gave similar structures in the castings. The desirable structure of the quenched and drawn SAE 4140 cast steel is shown by Fig. 20. The structure obtained from these castings when quenched and drawn is shown by Fig. 21. Free ferrite can be seen. It was noted that the steel was not very clean.

The presence of these defects in both the statically tested and as-received condition castings can be attributed to foundry practice

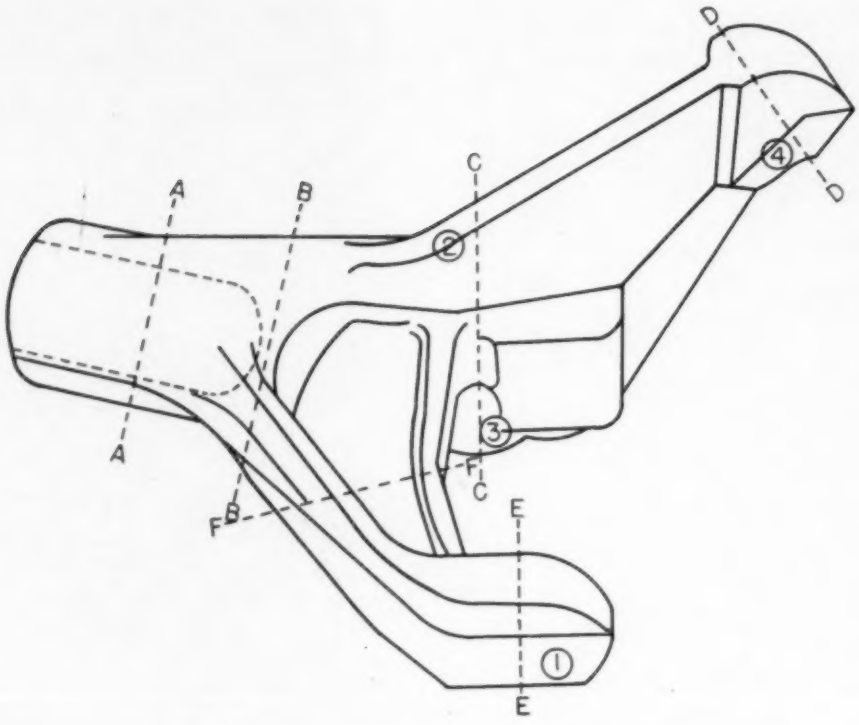


Fig. 5—Upper Terminal: Broken Lines Show Where Casting Was Sectioned. Circles show where micro-specimens were taken.

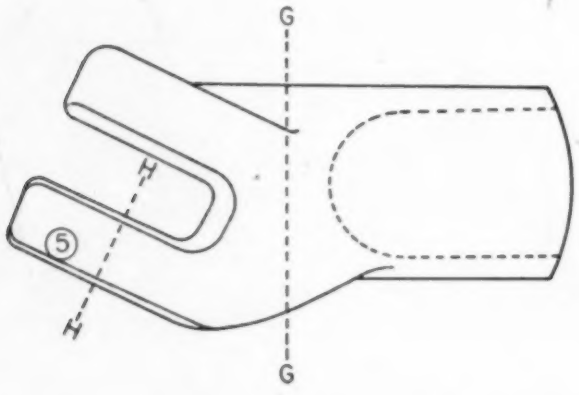


Fig. 6—Lower Terminal: Broken Lines Show Where Casting Was Sectioned. Circle shows where micro-specimen was taken.

procedure. An analysis shows that these defects can be corrected if sufficient development time were allowed. These flaws, however, have little effect, if any, on the strength of the castings and their ability to withstand the severe tests to which they were subjected.

Material Properties—The chemical analyses and mechanical

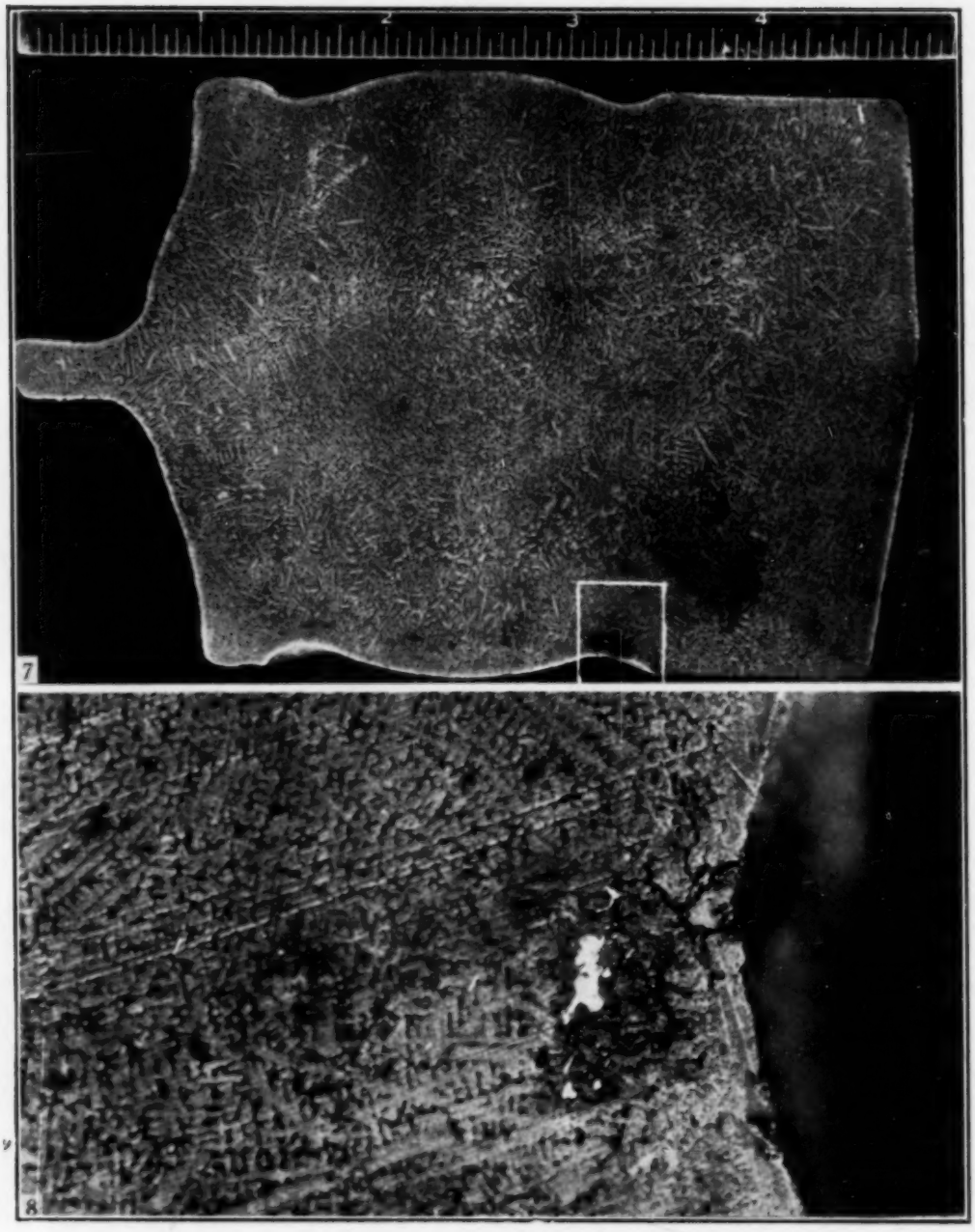


Fig. 7—Photomacrograph Through Section B-B of Fig. 5. Shrinkage and non-metallic inclusion are shown in the square. Fig. 8 shows area at a higher magnification. Part not statically tested

Fig. 8—Photomacrograph of Shrinkage Cracks and Inclusions in Square of Fig. 7; Section B-B of Fig. 5—(10 ×).

properties of test coupons poured with the various heats of steel used in the castings for this investigation are given in Tables I and II. These data were determined at Battelle Memorial Institute where the castings were made. Since additional information in the nature of mechanical properties of material taken from the cast unit was

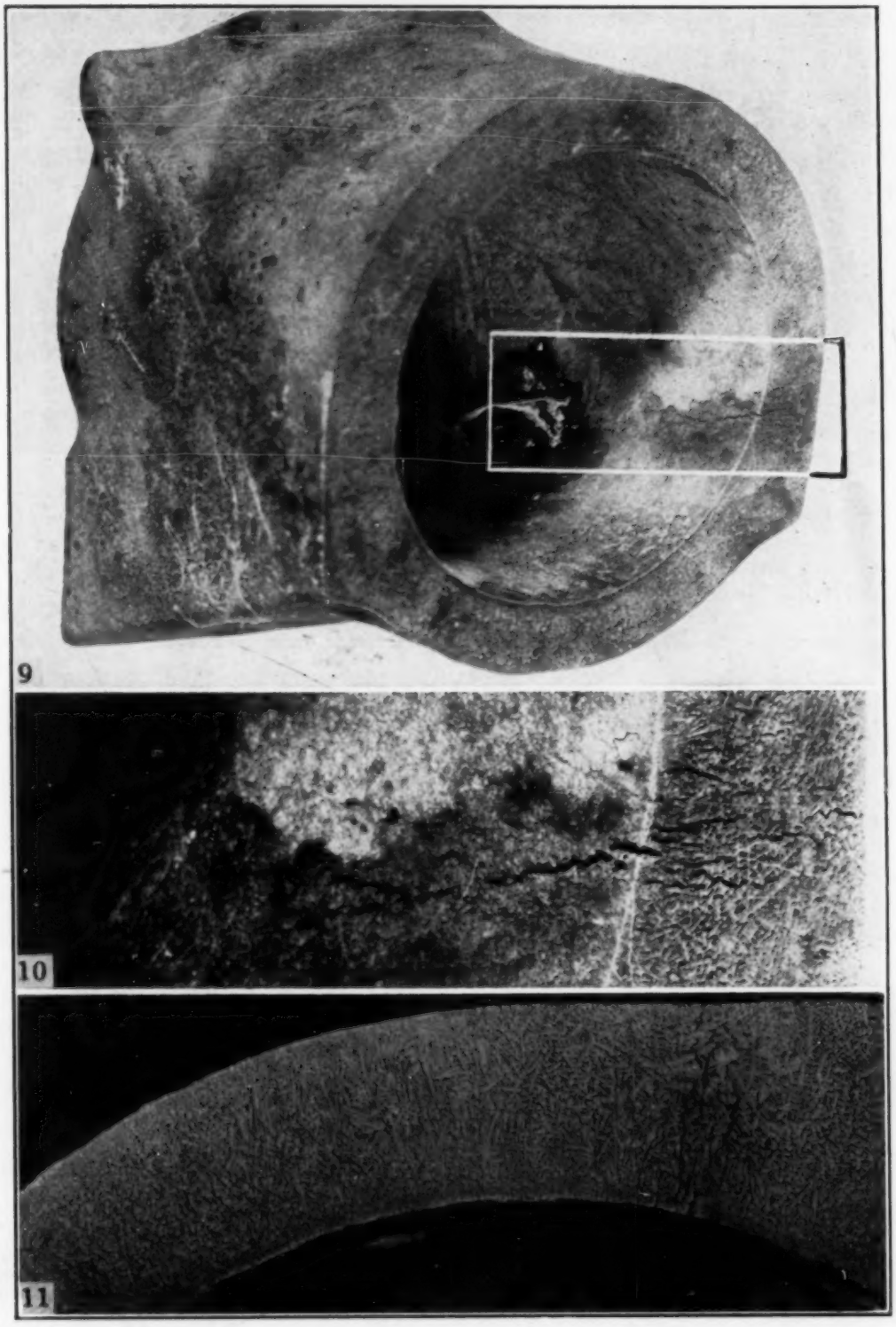


Fig. 9—Oblique View Through Section A-A of Fig. 5 Showing Hot Tears in the Walls of Casting. Area in square shown in Fig. 10 at higher magnification. Full size. Part not statically tested.

Fig. 10—Hot Tears Shown in Square of Fig. 9 Enlarged to 4½×.

Fig. 11—Photomacrograph Through Section A-A of Fig. 5 Showing Hot Tears.

desired for this reported investigation, two tensile coupons, Nos. 1 and 2 of Table III, were machined from the retracting arm of an upper terminal (heat No. 10992) which had been heat treated according to regular shop practice. Other tensile coupons, Nos. 3 and 4, also of Table III, were cut from a similar section of another terminal but heat treated as individual specimens. Comparative data were obtained from forged material by measurements from coupons, Nos. 5 and 6, which were cut from a production forging at the same

Table I
Chemical Composition

Heat No.	Carbon %	Manganese %	Silicon %	Chromium %	Molybdenum %
10986	0.40	0.73	0.35	0.86	0.20
10992	0.37	0.65	0.32	0.79	0.30
10993	0.37	0.74	0.36	0.90	0.32
11000	0.40	0.68	0.32	0.73	0.30
11061	0.40	0.70	0.37	0.91	0.25
11062	0.38	0.69	0.34	0.91	0.25
11113	0.38	0.79	0.33	1.11	0.26
11150	0.39	0.90	0.40	1.11	0.26
11152	0.39	0.87	0.39	1.09	0.27
11153	0.37	0.87	0.36	1.10	0.25

Table II
Mechanical Properties

Heat No.	% Elong. in 2 Inches	% Red. of Area	Yield Strength (psi)	Ultimate Strength (psi)	Charpy Impact (ft.-lbs.) (Keyhole Notch)
10986	7.0	14.0	183,250	197,750	8.5
10992	8.5	27.0	153,250	175,000	8.5
10993	5.0	11.0	152,500	175,500	9.4
11000	8.9	22.9	152,000	173,000	8.9
11061	6.5	14.6	181,750	197,750	9.3
11062	5.8	16.8	187,250	199,750	9.0
11113	7.7	18.6	190,250	205,250	8.6
11150	6.1	12.0	192,500	210,100	...
11152	3.5	6.8	195,000	209,000	6.6
11153	8.1	20.7	195,750	209,500	8.8

Table III
Mechanical Properties, Fabricated Material

Spec. No.	Heat Treatment	Yield Stress (psi)	Ultimate Stress (psi)	% Elong. in 2 In.	% Red. of Area	Remarks
1	Step 4, Shop Processing	121,000	150,000	7.8	21.0	SAE 4140 casting
2	Step 4, Shop Processing	111,000	140,000	6.2	20.0	SAE 4140 casting
3	1625 F, 1 hr., oil quench, 925 F, 1 hr., air cool	173,200	189,000	3.5	4.6	SAE 4140 casting
4	1625 F, 1 hr., oil quench, 840 F, 1 hr., air cool	188,300	205,000	2.0	4.7	SAE 4140 casting
5	1625 F, 1 hr., oil quench, 950 F, 1 hr., air cool	180,000	190,000	13	47.4	NE 8740 forging
6	1625 F, 1 hr., oil quench, 950 F, 1 hr., air cool	177,000	186,000	12	46.5	NE 8740 forging

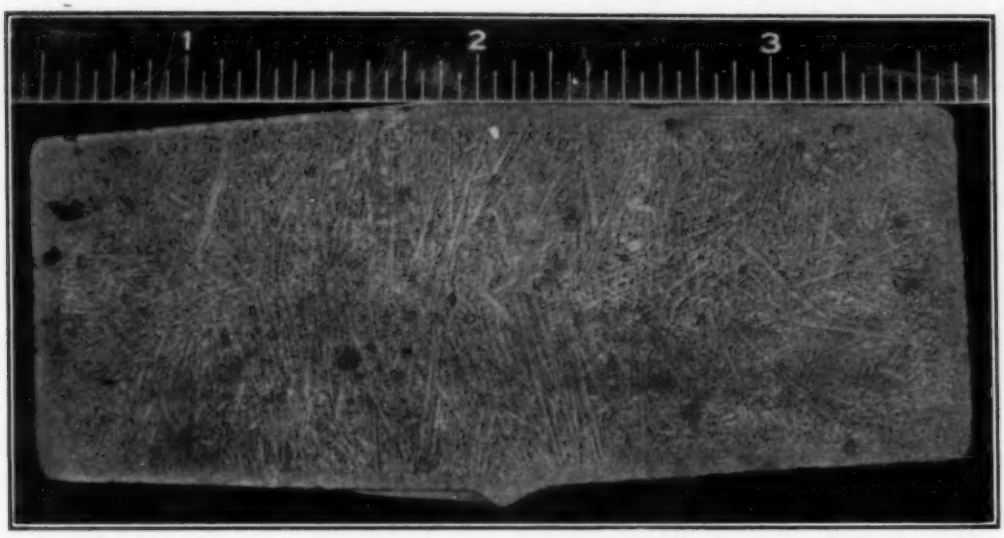


Fig. 12—Photomacrograph Through Section H-H of Fig. 6. Part not statically tested.

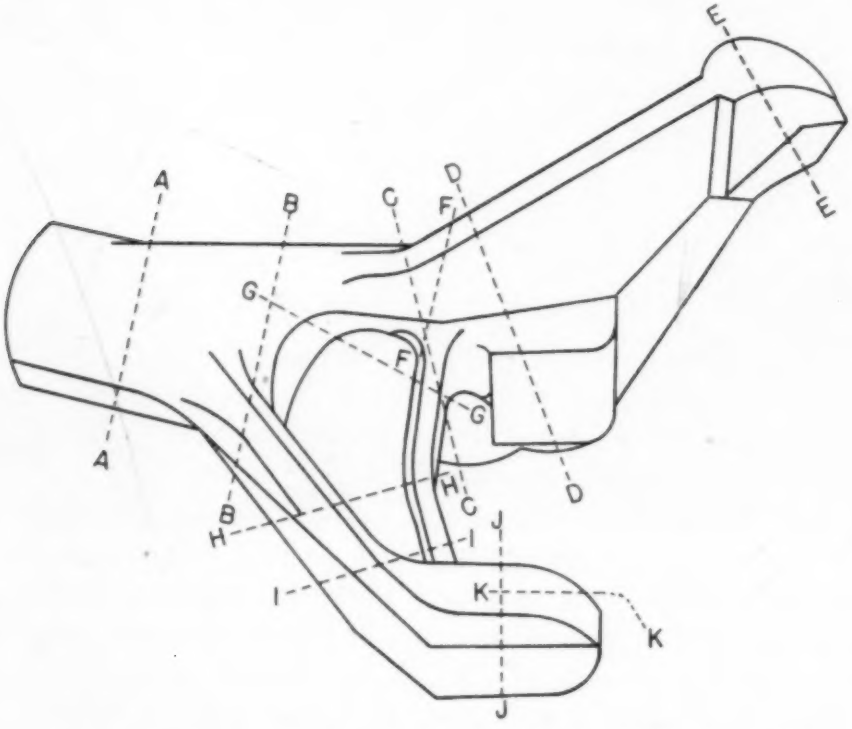


Fig. 13—Upper Terminal: Broken Lines Show Manner in Which Casting Was Sectioned After Static Proof Testing.

location. All tensile specimens were standard 0.500-inch test bars. It is to be noted that the cast material was SAE 4140 whereas the forged material was NE 8740.

Static Proof Tests—A strut assembly with cast terminals which did not show cracks when magnafluxed was supported in a test fix-

ture in a manner simulating its installation in the C-46 airplane (Fig. 22). In this attitude, the two critical service conditions, retracting and side load landing, were duplicated. For the side load landing condition, an axial load from a leverage system with a universal joint at the loading point was transferred through the tube from the lower terminal to the spar attachment fitting and the retracting arm of the upper terminal. In the retracting condition, a force was exerted normal to the upper terminal arm by the piston

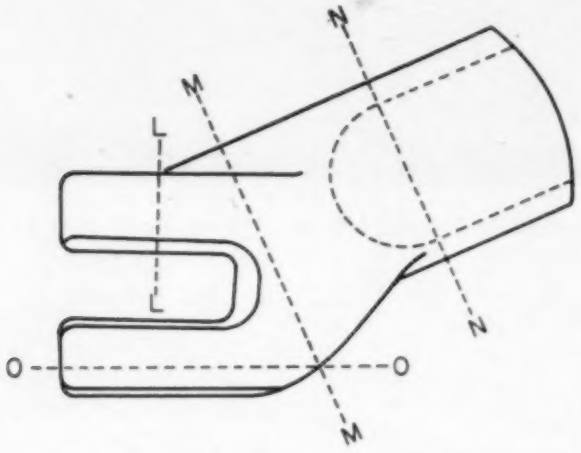


Fig. 14—Lower Terminal: Broken Lines Show Manner in Which Casting Was Sectioned After Static Proof Testing.

rod of a hydraulic cylinder. The magnitude of the hydraulic pressure was observed from pressure gages and applied loads were determined from calibrated loading bars with attached wire resistance strain gages. Since the retracting condition not only produced bending in the upper terminal arm but also bending of the tube, the critical section for this test condition was assumed to be at the intersection of the tube and upper terminal socket. Therefore, wire resistance strain gages were mounted on the tube adjacent to the weld so that permanent deformations could be determined and the stiffness compared to previous similar tests on production units.

During the actual testing procedure, the listed simulated conditions and test loads were successively applied to a strut assembly with cast terminals without producing failure or harmful deformations:

1. Side load landing—112,000 pounds axial tension (design ultimate load).
2. Landing load—1650 psi (tension) cylinder pressure only.
3. Side load landing—112,000 pounds axial tension combined with 1650 psi (tension) cylinder pressure.

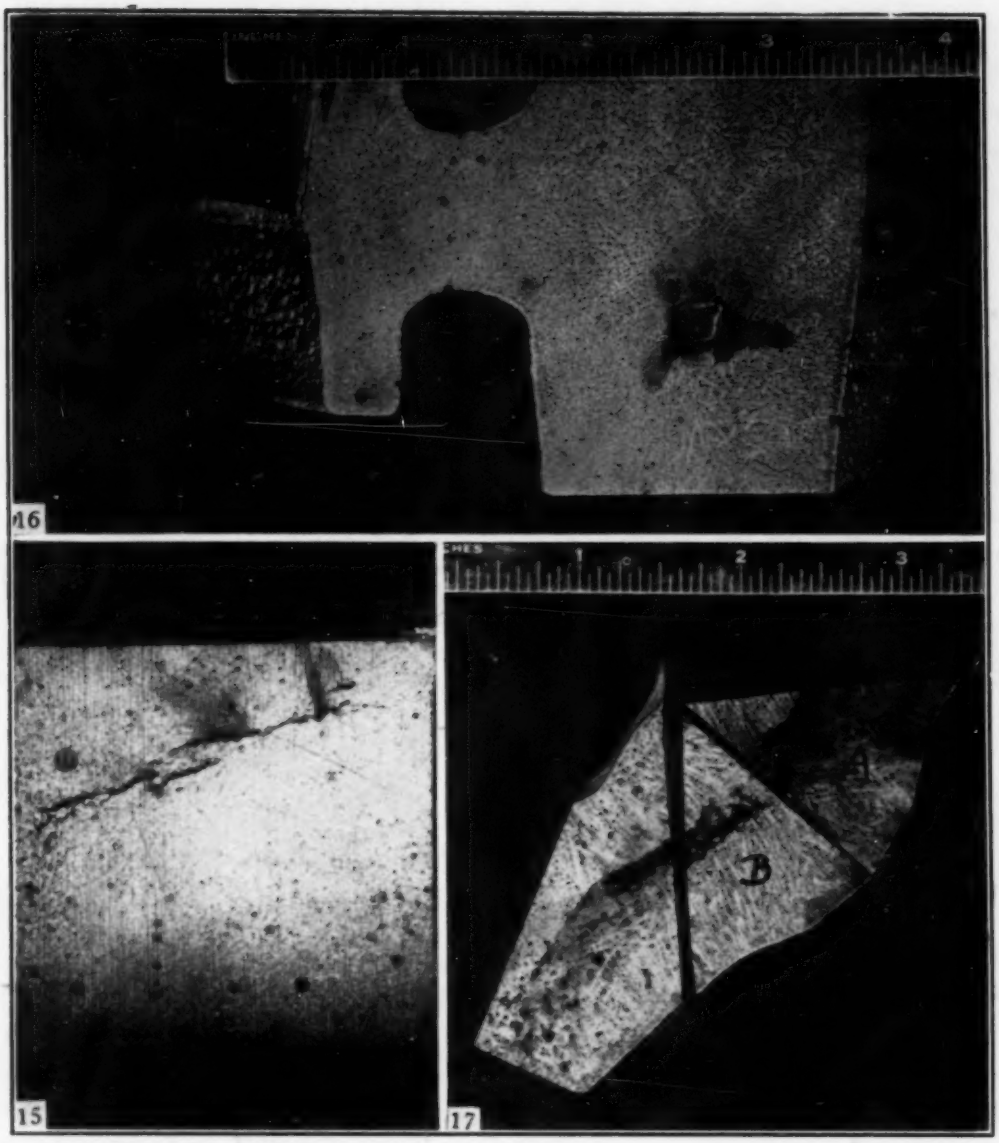


Fig. 15—Photomacrograph of Part of Wall Between Sections A-A and B-B of Fig. 13 Showing Hot Tears. Full size. Tears of this nature were found in the castings before and after static testing. Statically tested.

Fig. 16—Photomacrograph Through Section C-C of Fig. 13. Note large shrinkage hole. The depth of this hole is shown in Fig. 17. Part statically tested.

Fig. 17—Photomacrograph of Shrinkage Area Through Section C-C of Fig. 13. Defect extended for 1¼ inches and its maximum width was ¼ inch. Surface A folds face down on surface B. Part statically tested.

4. Landing load—2475 psi (design ultimate) cylinder pressure only.
5. Side load landing—190,000 pounds axial tension combined with 2475 psi (tension) cylinder pressure.
6. Retracting condition—3000 psi (compression) cylinder pressure acting perpendicular to the retracting arm.

Repeated Load Test—A total of 2000 cycles of retracting load was applied to the upper terminal arm of the outboard side brace strut by a standard C-46 hydraulic retracting cylinder (Fig. 23). A sudden load of 23,800 pounds, 1500 psi compression, acted perpendicular to the retracting arm of the subject strut, thereby developing the maximum bending moment in the arm and producing the critical retracting condition. After every 500 cycles, the strut was removed from the jig and magnafluxed to determine if any cracks had developed. No indication of failure or development of fatigue cracks was observed from these inspections.

In order to experimentally determine the magnitude of the extreme fiber stresses at two locations on the arm of the upper terminal, wire resistance strain gages were employed and the surface strains measured independently by use of an unstrained compensating gage. Strain varied linearly with load and at 1500 psi cylinder pressure, the maximum applied pressure during repeated loading, the extreme fiber stresses were as follows:

Measured Section	Extreme Fiber Stress
Six inches from hydraulic cylinder attachment	85,500 psi tension
	99,000 psi compression
At spar attachment	18,900 psi tension
	135,000 psi compression

Static Ultimate Test—Because the original test fixture was periodically used to test production struts with forged terminals and because it lacked sufficient strength to react the load necessary to produce failure in the upper terminal of the side brace strut, another test fixture was built. The strut again was tested in the critical retracting condition with a bending load applied perpendicular to the retracting arm of the cast upper terminal. In place of a pushing force from a C-46 cylinder as originally applied in initial tests, a leverage pulling force from the opposite side of the arm was devised. This change in no way invalidated the test results, particularly in view of the fact that a forged unit was similarly tested for comparison. Further modification of the testing procedure from the initial method allowed for the reaction of the major portion of the load at the terminal and tube junction and assured failure within the terminal itself. A subsequent similar test was performed on a production strut with the critical section of the forged terminal machined to the approximate dimensions of the cast unit. Both the upper cast and the forged terminals of the investigated outboard side brace strut failed by tension in the "landing" below the spar attachment pin due

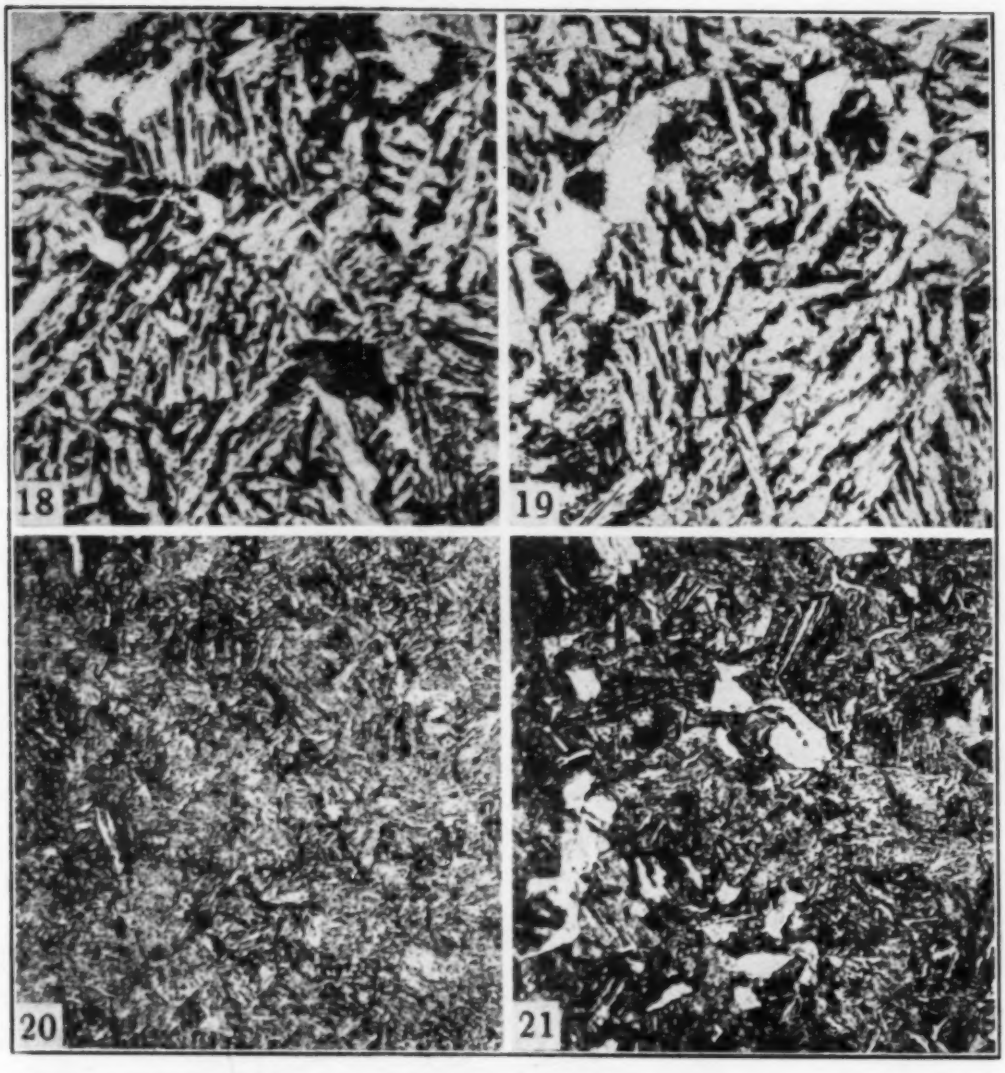


Fig. 18—Upper Terminal: Heat 10992, As-Received (1800 F, 2 Hrs., Ail Cool). 2% nital etch, × 500. Specimen taken at point 1 of Fig. 5.

Fig. 19—Lower Terminal: Heat 11000, As-Received (1800 F, 2 Hrs., Air Cool). 2% nital etch, × 500. Specimen taken at point 1 of Fig. 5.

Fig. 20—Upper Terminal: ¼ x 1 x 1-Inch Piece Cut from Section to Right of Section D-D, Fig. 5, and Then Heat Treated as Follows: 1800 F, 2 Hrs., Air Cool; 1575 F, 1½ Hrs., Air Cool; 1625 F, 2 Hrs., Oil Quench (Houghton No. 2) with Much Agitation; 840 F, 3 Hrs., Air Cool. × 500, 2% nital etch. Shows desirable quenched and drawn structure.

Fig. 21—Upper Terminal: Specimen Taken at Point 4 of Fig. 5 After Part of Arm Between Sections C and D Had Been Heat Treated as Above; Shows Effect of Mass of Casting on Microstructure Obtained. Much free ferrite is present. × 500, 2% nital etch.

to the bending loads imposed. The ultimate load for the casting was 60,500 pounds and for the forging after modification, 77,000 pounds. Even though the location of failure for each type of test unit was identical, these ultimate loads could not be compared directly since unalterable dimensions had produced different section properties.

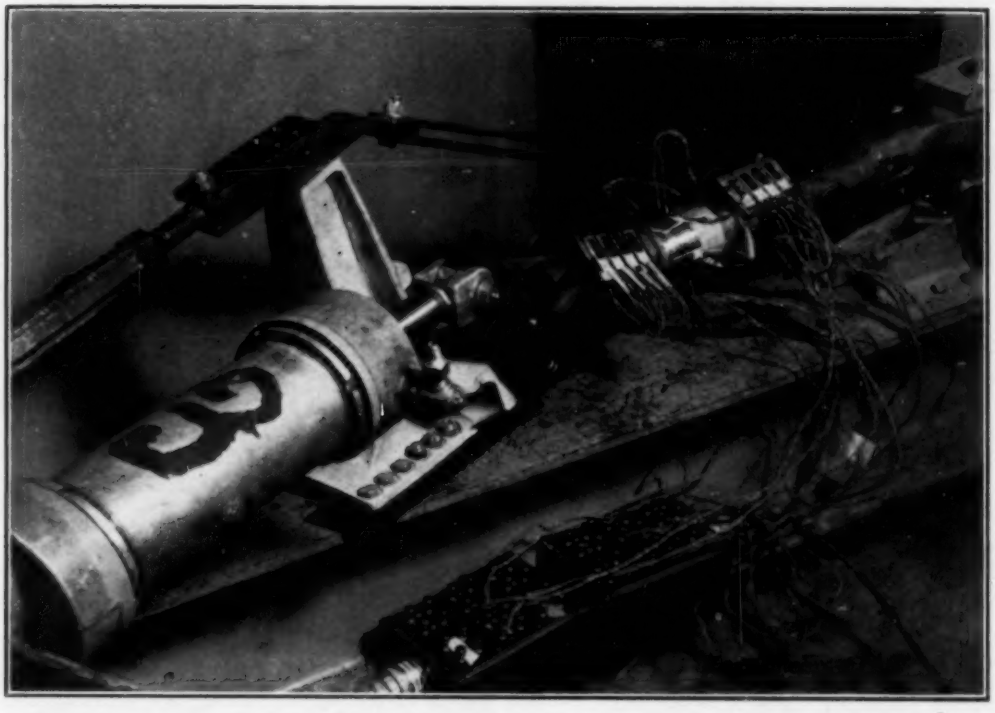


Fig. 22—Static Proof Test of Strut Assembly.

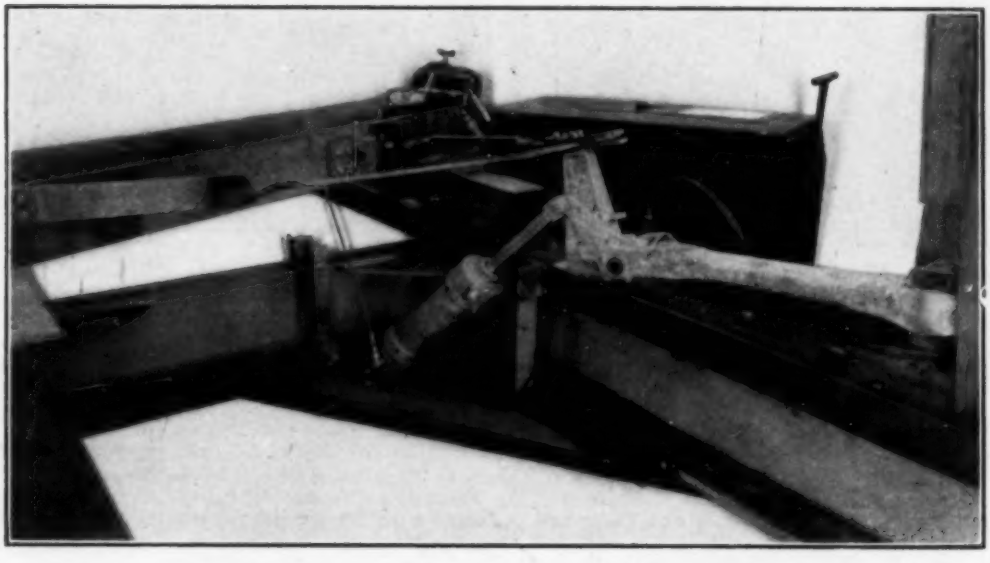


Fig. 23—Repeated Load Test of Strut Assembly.

Hardness tests further indicated that the ultimate strengths were different. Therefore, to obtain an approximate comparison, the ratio of the modulus of rupture to the ultimate strength from hardness tests was devised.

Casting

$$F_{bt} = \frac{M \cdot c}{I} = \frac{60{,}500\#\ (8.55'')\ 2.551''}{4.806\ in^4} = 274{,}000\ psi$$

$$\text{Bending Modulus Factor} = \frac{274{,}000\ psi}{166{,}000\ psi} = 1.65$$
(Rockwell Hardness)

Forging

$$F_{bt} = \frac{M \cdot c}{I} = \frac{77{,}000\#\ (8.55)''\ 2.700''}{5.593\ in^4} = 318{,}000\ psi$$

$$\text{Bending Modulus Factor} = \frac{318{,}000\ psi}{188{,}000\ psi} = 1.64$$
(Rockwell Hardness)

Discussion of Results

Mechanical Properties—Poor ductility was exhibited by standard specimens cut from the retracting arm of the upper cast terminal but since a prominent shrinkage area was found in another casting at a section corresponding to that from which the specimens were taken, the exceedingly low ductility of the test bars was attributed to the deleterious effect of center line shrinkage. Substantiating evidence of poor ductility when cast material is unsound was determined by tests performed at Battelle Memorial Institute as part of another project (3). In this reported investigation, as listed in Table III, only 3.5% elongation in a 2-inch gage length and a reduction of area of about 5% were obtained from the cast material when its ultimate strength was 189,000 psi. In contrast, similar specimens from a production forging had 13% elongation and 47% reduction of area when the ultimate stress was 190,000 psi. An elongation of 3% for a casting does not prohibit its acceptance by licensing and procuring agencies if subsequent static proof and ultimate tests reveal satisfactory factors of safety. Furthermore, with improvement in casting methods and the elimination of material defects in the upper terminal the values of elongation given in Table II should be approached.

Proof Tests—In order to interpret the test loads in terms of the requirements of various licensing and procuring agencies (4), (5), (6) the expression, factor of safety, was advantageously employed. This factor was determined from the ratio of the ultimate test load to the design ultimate load where the design ultimate load was defined as the maximum design applied service load times a factor of 1.5. In general, specifications require a safety factor of 1.5 or 2.0, depending on the agency, with additional evidence of no yielding at the design applied load or 1.15 times the design applied load level.

Thus, even with poor metallurgical quality at the critical section, the strut assembly with cast terminals satisfactorily passed simulated service tests and exhibited without failure safety factors greater than one. Specifically, the experimental assembly withstood: (a), an axial tension load of 190,000 pounds (170% design ultimate) and (b), the load resulting from a hydraulic pressure in the C-46 landing gear in a critical retracting position of 3000 psi (120% design ultimate). In addition to this evidence, neither yielding nor permanent deformation at the weld was produced at either the design applied load level or 1.15 times the design applied load level. At 2800 psi which is 170% of the design applied load nonlinearity of load versus strain was observed but this is well above a regular agency specification.

Repeated Load Test—Repeated load tests were conducted for the critical retracting condition in preference to side load landing because side load landing, a maximum design condition, is not as prevalent in service as is the retracting load produced by normal operation of the C-46 hydraulic system. As a result of the actual applied repeated load, no failure of any part of the strut or signs of fatigue were visible either by physical examination or by magnafluxing after application of 2000 cycles of retracting load. These cycles would correspond to 2000 flights and the applied test load was more severe than the operational hydraulic pressure which varies from 1070 to 1300 psi.

Good agreement between experimental and calculated extreme fiber stresses for the arm at 6 inches from the hydraulic strut was found. Equal tension and compression stresses of 96,000 psi were calculated for a hydraulic cylinder pressure of 1500 psi whereas the actual values independently determined were 85,500 psi tension and 99,000 psi compression. At the spar attachment fitting, an analytical determination was impractical but the experimental values as found from the use of wire resistance strain gages were 18,900 psi tension and 135,000 psi compression.

Ultimate Strength Tests—In order to make the physical dimensions of the forging at the critical section more comparable to those of the casting, the "landing" at the spar attachment section through the retracting arm was machined to 0.477 inch which then was approximately equal to the corresponding dimension, 0.467 inch of the cast terminal. Metallurgical examination after failure showed that the flow lines of the forging had not been cut by machining since the reduction was made along an arc concentric with the contour of

the "landing." Because of this evidence, the reduction was assumed to be an allowable procedure.

Other unalterable dimensions did prevent obtaining equivalent section moduli which, together with dissimilar ultimate strengths from hardness indications, necessitated a valid method of comparison. The ratio of a computed modulus of rupture to the ultimate strength was considered acceptable since factors of equivalent magnitude were obtained by employing the method to strength-modulus of rupture data in ANC-5. By this method, the strength of cast material appears very satisfactory but the possible detrimental effect of lower ductility at the higher ultimate strength is not overlooked. Such a determination was not undertaken due to a lack of fabricated test units.

The influence of the spar attachment was considered to be unimportant at the section which failed, since the bearing reaction was approximately 1.5 inches from the section that failed. Actually, failure occurred behind the pin where compression forces from bearing could have had little effect.

Part II

Centrifugally Cast P-40 Engine Mounting Bearer Tube Fitting

Description of Test Item—The centrifugally cast P-40 engine mounting bearer tube fitting, shown previously in Fig. 3, consists of a uniformly thick cylindrical wall with a raised lug. Its function in the P-40 installation is to transfer load from the horizontal engine support tube which passes through its hollow center to a diagonal tension member which is attached to the lug and the firewall of the airplane. The design ultimate load prescribed for this unit is 47,000 pounds but it is so overdesigned that in a service installation the only possible failure would be the shearing of a pin which holds the diagonal member to the lug.

Four such centrifugally cast fittings were made by the American Steel Foundries of induction melted SAE 4140 steel and, prior to shipment to the Curtiss-Wright Research Laboratory, heat treated as follows:

1650 F—2 hrs.—air cool
1250 F—2 hrs.—air cool

Before the castings were machined according to blueprint specifica-

tions for production forged units, they were X-rayed and magnafluxed and found to be free from internal and external defects.

Experimental Methods and Results

Metallurgical Investigation—Hardness tests taken on a cross section through the lug and part of the wall of casting No. 3627 after heat treatment are as shown in Fig. 24. The walls of the casting were about 5 points Rockwell C harder than the lug. Micro examination showed the steel of this casting to be very clean.

Sectioning and macro-etching of the castings and forgings failed to disclose any internal defects. It was noted, however, that the flow

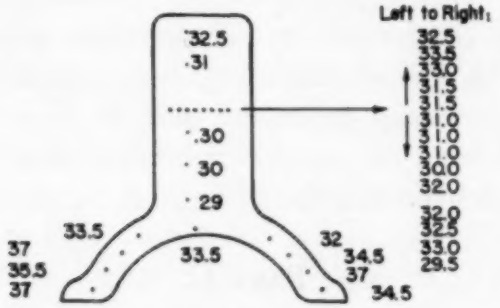


Fig. 24—Hardness Determinations on Cross Section of Lug.

lines of the forgings were poorly oriented with respect to the final contour of the fitting. Figs. 25, 26, 27, 28 and 29 show the macrostructure of the parts.

The castings were found to consist of a relatively coarse microstructure of tempered martensite containing some free ferrite and some very fine primary troostite in those portions away from the edge of the casting. The forgings were of a relatively fine microstructure consisting almost entirely of sorbite. The presence of areas in the lug of the casting exhibiting an incomplete quench may be attributed:

1. To the fact that the castings were heat treated before the lug hole was rough machined while the forgings were heat treated after rough machining and
2. To the superior hardenability of SAE 4340 steel over that of SAE 4140 steel. Grain size control between the castings and forgings was not attempted. Future tests should incorporate this important factor and an attempt should be made to keep the chemical composition of the subject parts the same.

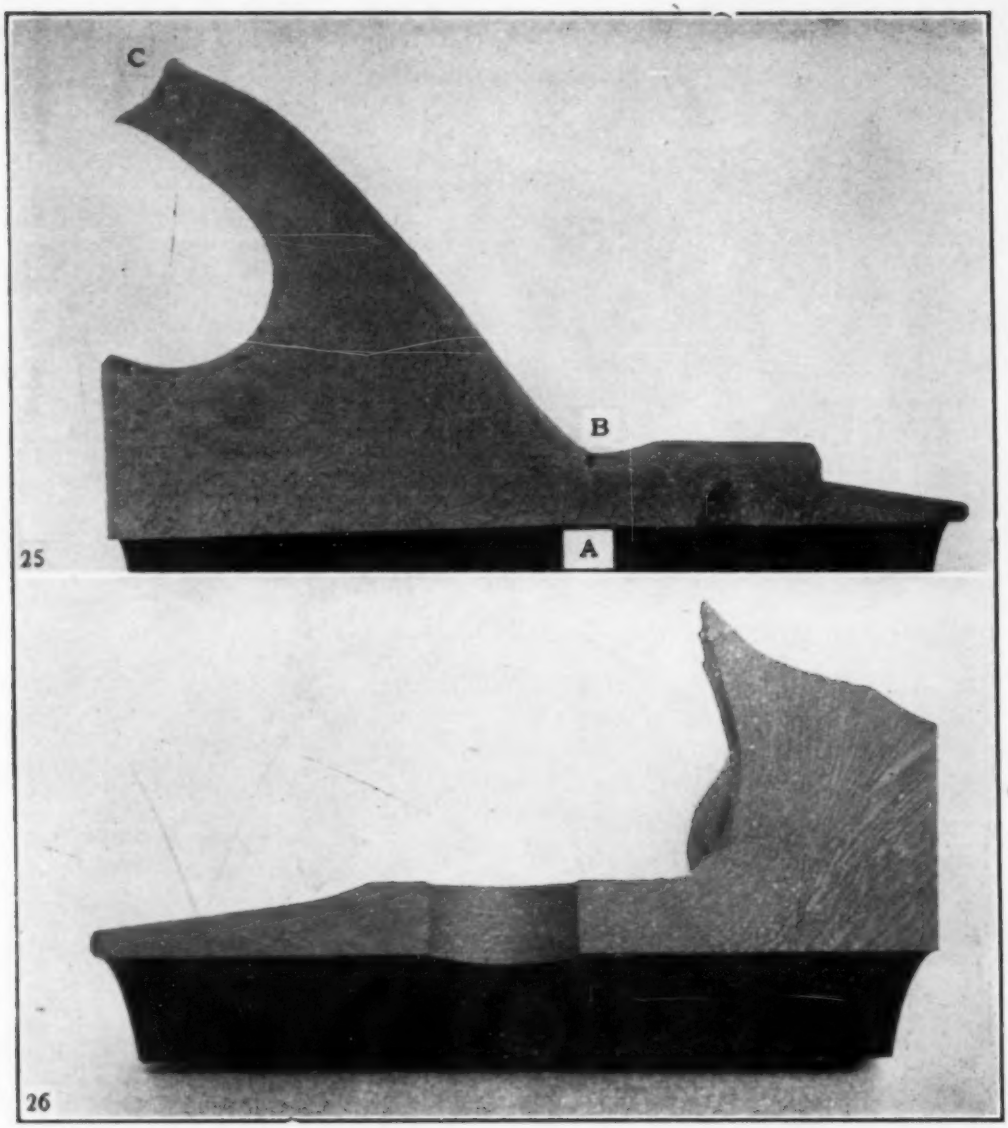


Fig. 25—Photomacrograph of Casting No. 3634 Broken in Static Test. A permanent deformation at A and small crack at B where machining resulted in a stress raiser should be noted. If the lug had not been weakened by increasing the diameter of the hole, the failure would probably have occurred between A and B instead of at C. Stress raisers due to improper machining were more prevalent in the castings than in the forgings. Approximately 1½×. Etched ½ hour in 50% HCl.

Fig. 26—Photomacrograph of the Forging Broken in Static Test Showing Part of the Shear Fracture Which Was Transverse to the Flow Lines. Note that the flow lines of the lug do not form with the flow lines of the wall of the forging. This condition decreases the greater strength which should be derived from properly oriented flow lines in resisting tear-out of the lug from the wall of the forging. Approximately 2×. Etched ½ hour in 50% HCl.

Considering the facts set forth in the preceding paragraph the forgings would be expected to exhibit better physical properties than the castings. However, if greater control had been achieved in the heat treatment of the subject parts, closer comparisons would have been possible.

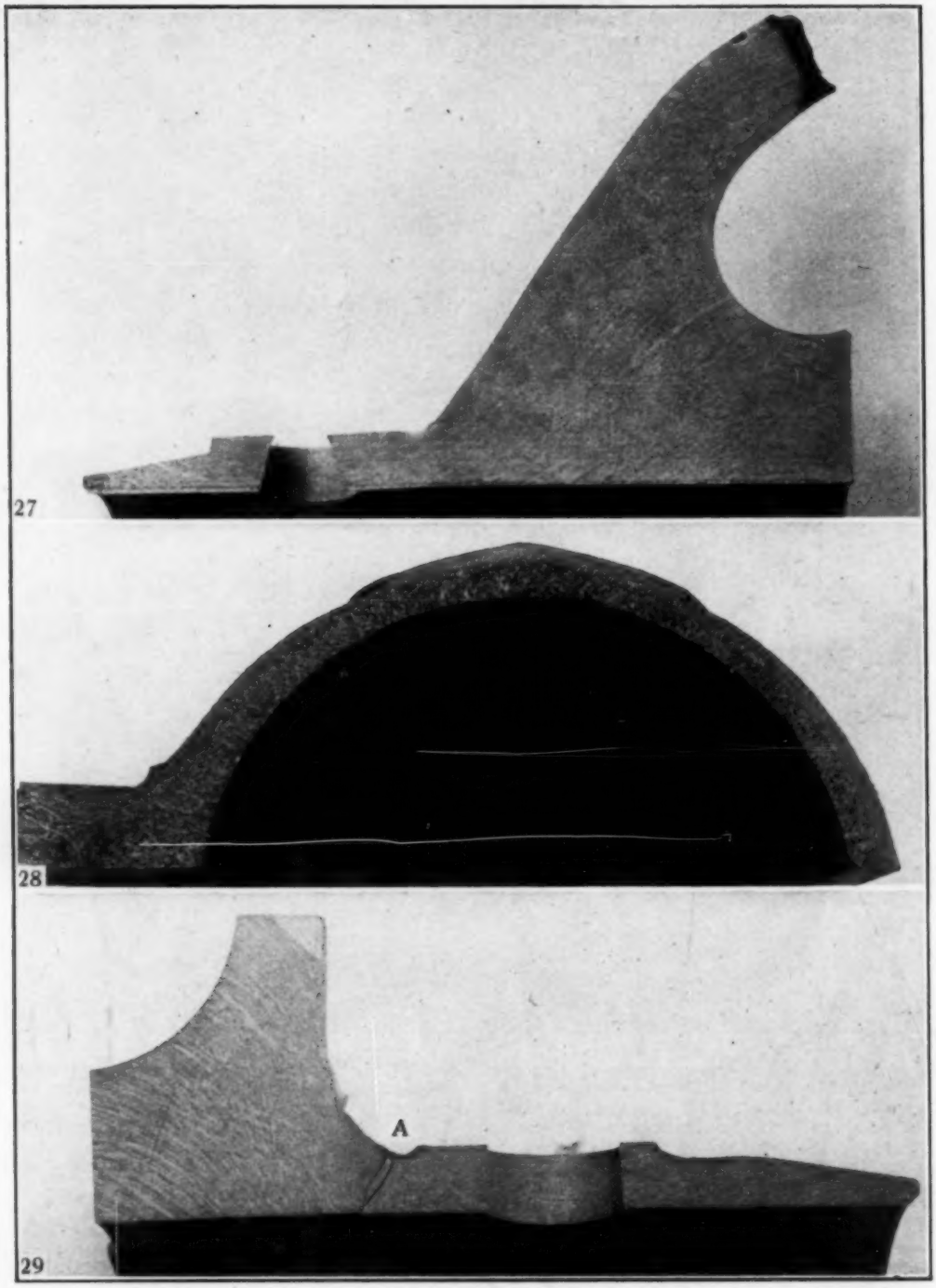


Fig. 27—Photomacrograph of Forging Broken in Static Test Showing Part of the Tension Fracture. Note that the flow lines of the lug do not form well with the flow lines in the wall. Approximately 1¼×. Etched ½ hour in 50% HCl.

Fig. 28—Photomacrograph of Forging Broken in Static Test. Taken transverse through walls and lug. Approximately 1½×. Etched ½ hour in 50% HCl.

Fig. 29—Photomacrograph of Forging Tested in Repeated Load Showing Break at A. Note that flow lines of lug still show some cast structure and do not form with flow lines in the wall. Approximately 1¼×. Etched ½ hour in 50% HCl.

Material Properties—The chemical analyses shown in Table IV were determined by the American Steel Foundries for the steels used in this investigation. In Tables V and VI are given the mechanical properties of centrifugally cast SAE 4140 steel and forged SAE 4340 steel, respectively. Due to the limitations imposed by the wall thickness of the casting, substandard size tensile coupons were necessary for the determination of the mechanical properties.

Static Tests—It was evident from a preliminary strength analysis that, because the P-40 fitting design incorporated so large a factor of safety, the ultimate strength of the fitting as used in production would be impossible to produce. Since development of failure within the fitting was considered to be the primary objective and stimulation of production installation secondary, the 7/8-inch hole in the lug was reamed for a 1-inch pin and the bolt holes for connection to the bearer tube were reamed for high strength 1/2-inch bolts. With these modifications, the fitting and an attached section of the bearer tube were placed in a test fixture which duplicated the geometry of the forward section of the mount installation (Fig. 30). A similar test was performed on a revised production forging.

The ultimate load strength of the modified casting, heat treated to 144,000 psi, was 103,000 pounds and that of the modified forging, heat treated to 166,000 psi, 125,000 pounds.

Repeated Load Test—The fatigue tests of the centrifugally cast and of the forged fitting for the P-40 engine mounting bearer tube were of a comparative nature and did not simulate production installation. The subject fittings were supported by test fixtures in the Laboratory's 50,000-pound repeated load machine (Fig. 31) and pulsating tension loads were applied perpendicular to the axis of the fittings in contrast to the direction of loading in the static test which was in the direction of the forward diagonal.

The fittings were tested simultaneously and each was carried to complete failure as indicated by tripping of the automatic shut-off which stopped the test. A maximum tension load of 25,500 pounds was applied to both units and the load range ratio was about 0.1. Both the forged and cast fittings had been inspected and were of good quality.

Complete failure of the centrifugal casting occurred at 30,900 cycles. Fig. 32 shows the failure of the casting to be primarily a shear failure as compared with the fatigue character of the failure in the forging (Fig. 33). At 34,000 cycles a small fatigue crack

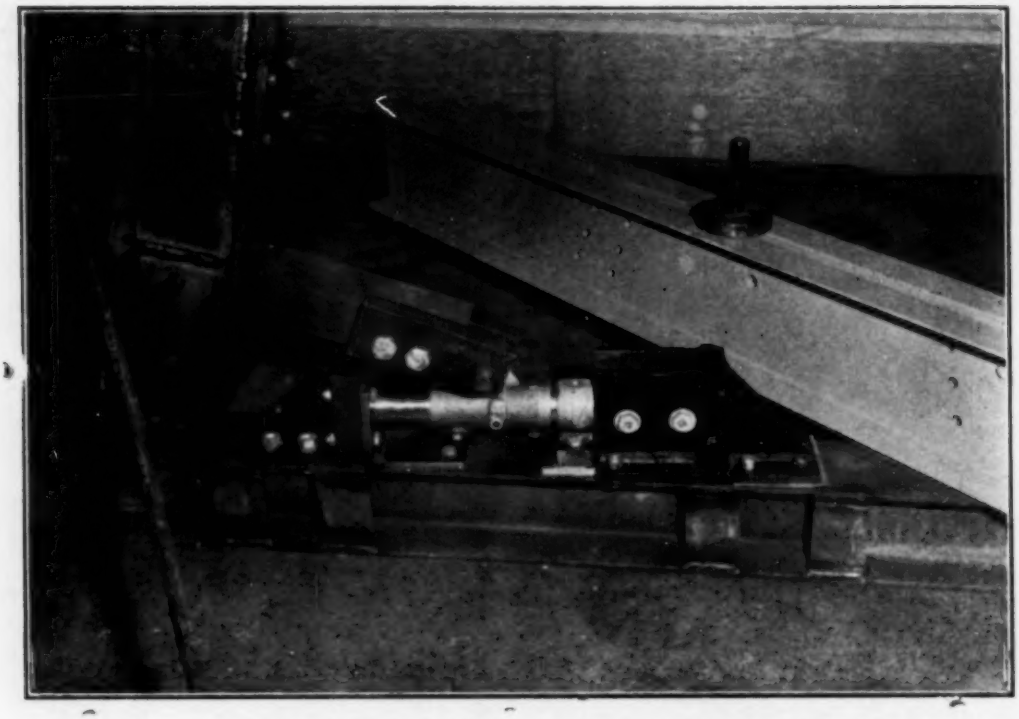


Fig. 30—Static Test of P-40 Engine Mount Bearer Tube Fitting.



Fig. 31—Repeated Load Test of P-40 Casting and Forging.

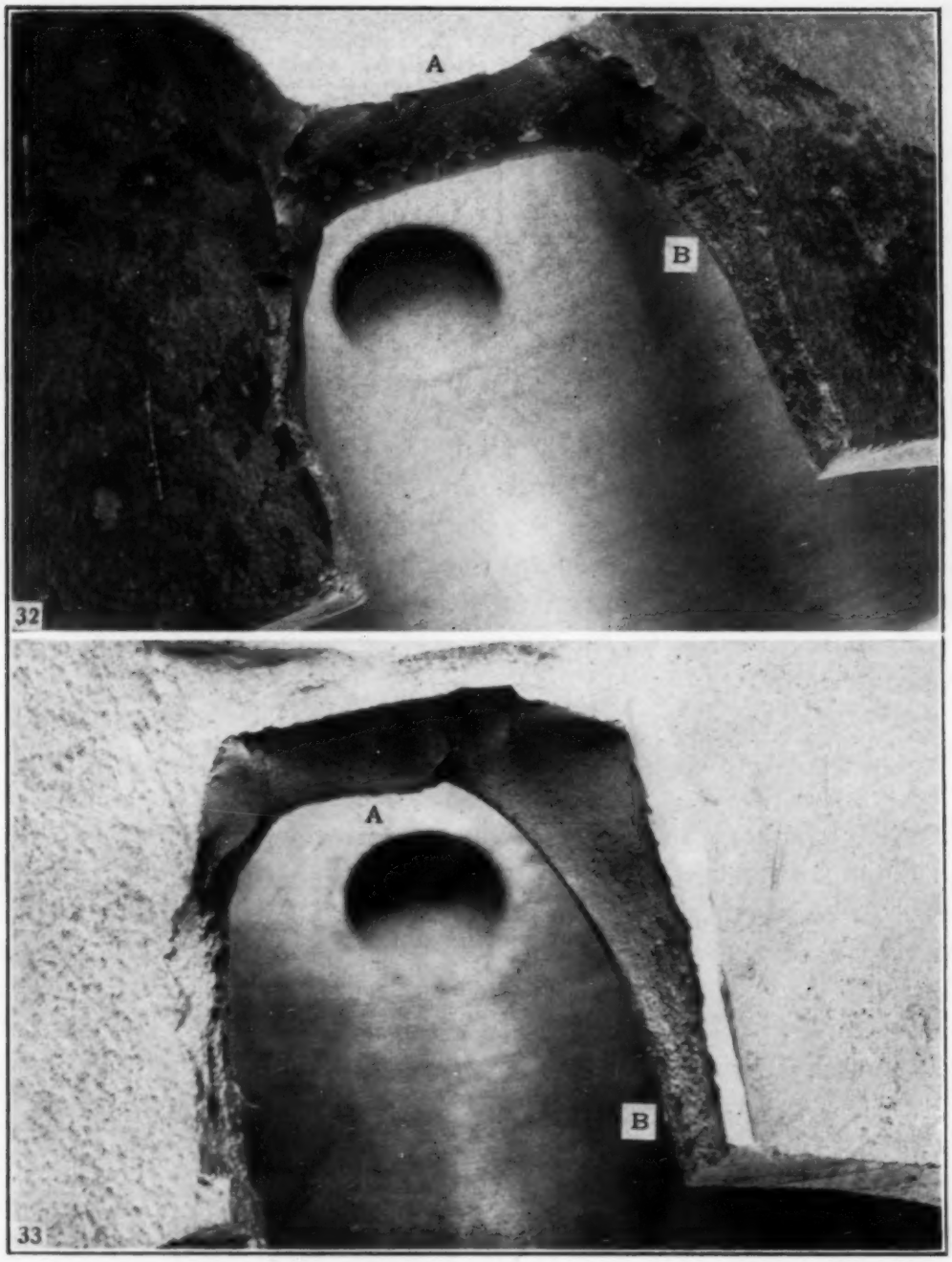


Fig. 32—Photograph of Fracture in the Casting Which Was Subject to Repeated Load Showing Tear-Out of Lug from Wall. The smooth dark gray areas shown near A are due to fatigue cracks while rough dark gray areas like that at point B are shear failures. A stress raiser in the form of a machine cut was present at A. Approximately 3×.

Fig. 33—Photograph of Fatigue Failure in the Forging Between Lug and Wall. Smooth gray areas like that shown at point A are due to fatigue cracks while rough gray areas like that shown at point B are shear failures. Approximately 3×.

became visible in the forging and spread slowly under a decreased load for the next 30,000 cycles. Thereafter, the progressive failure accelerated and at 67,800 cycles complete failure occurred.

Table IV
Chemical Composition

Heat No.	Carbon	Manganese	Silicon	Phosphorus	Sulphur	Chromium	Molybdenum	Special Deox/Ton
3627	0.42	0.81	0.42	0.011	0.027	0.92	0.25	5 lbs. High Carbon Iron
3634	0.40	0.91	0.40	0.011	0.027	0.87	0.26	5 lbs. TI Carbon Iron
3649	0.39	0.91	0.44	0.015	0.029	0.90	0.27	5 lbs. TI Carbon Iron
3653	0.38	0.83	0.43	0.012	0.030	0.96	0.24	5 lbs. TI Carbon Iron

Discussion of Results

Mechanical Properties—Substandard size tensile coupons cut from the wall of the centrifugal cast fitting exhibited better elongation characteristics than those from the statically cast terminal but in no instance were the elongation characteristics of cast material equivalent to those of the forged material. Such results do not, however, prohibit the use of castings for airplane parts since a minimum of 6% which is obtainable from good quality cast material is far more than sufficient to allow for yielding without failure at stress concentrations.

Static Test—From the results of comparable static tests of a centrifugal cast fitting and a similar forged unit, it was determined that in the presence of a stress concentration due to a hole the strength characteristics of each are practically equivalent, at least so much so that any differences could be attributed to experimental error or unmeasurable specimen dimensions. To arrive at a method of comparison, the ratio of the ultimate load to the ultimate stress from hardness tests was used to obtain an equivalent tensile area factor for each. These factors were different by only 2% and it was not considered significant but it is realized that the difference might have been slightly greater if the casting had had a higher heat treatment with a corresponding increase in yield strength and decrease in ductility.

Table V
Mechanical Properties of Centrifugally Cast SAE 4140 Steel

Spec. No.	Heat Treatment	Yield Stress (psi)	Ultimate Stress (psi)	% Elong. in 1 In. $\frac{1}{4}$ Inch Dia. Reduced Section	% Reduction of Area
1	1625 F, 2 hrs., oil quench, 1100 F, 2 hrs., air cool	150,500	165,300	12	45.8
2	Same	150,400	164,000	12	43.0
3	Same	157,100	168,700	13	40.1
4	Same	152,500	167,800	11	39.0

Substandard size specimens were cut from the walls of a heat treated casting.

Table VI
Mechanical Properties of Forged SAE 4340 Steel

Spec. No.	Heat Treatment	Yield Stress (psi)	Ultimate Stress (psi)	% Elong. in 1 In. $\frac{2}{10}$ Inch Dia. Reduced Section	% Reduction of Area
1	1625 F, 1 hr., oil quench, 950 F, 1 hr., air cool	177,000	187,000	....	52.1
2	Same	179,000	189,000	....	52.2
3	Same	178,500	185,500	24.2	51.3
4	Same	175,200	184,200	24.4	51.9

Tensile coupons were heat treated as 1 x 1 x 8-inch bars cut from a forged fitting.

Repeated Load Tests—Due to a lack of additional centrifugally cast test units, further comparative fatigue data were not obtained. On the basis of this one comparative test, it does appear that castings are not quite the equivalent of forgings in fatigue even though the life until the development of a crack may be quite similar. Failure of the centrifugal casting was primarily a shear failure, whereas that of the forging was of a fatigue character and propagated slowly under a decreased load to 67,800 cycles after first becoming visible at 34,000 cycles. The superiority of the forging over the centrifugal casting in resisting the propagation of fatigue failure was evident but was definitely influenced by two factors:

(a) The magnitude of the stress in the casting was greater than that in the forging since an examination of the fittings after failure showed the wall thickness of the forging to be 0.194 inch and of the casting 0.157 inch.

(b) Stress raisers were present in both the centrifugal casting and the forging but one milling machine cut was slightly more severe in the casting.

On the basis of this result and those reported in Part I, the absolute fatigue strength (endurance limit/ultimate strength) of cast material would not be expected to be too much different from forged material. To use steel castings in preference to forgings would therefore require only a small decrease in the average net stress on the critical sections and the avoidance of severe stress concentrations in the design. Both of these considerations would be economically justified in view of the lower expenditure for castings and their fabrication.

Conclusions

From the metallurgical and structural investigation of statically

and centrifugally poured types, it was concluded that:

(a) Aircraft quality steel castings can be made by either of the two methods but judicious foundry practice, particularly in the case of statically poured types, must be followed to obtain this quality.

(b) At a specified ultimate strength, sound cast material (SAE 4140 steel) has a lower ultimate elongation than forged material (SAE 4340 or NE 8740 steel) but, even so, it is sufficiently large to allow for yielding without failure at stress concentrations.

(c) Steel castings of sound quality can be used for the terminals of the C-46 outboard side brace strut. If the critical section at the "landing" is increased, the cast terminals, which fulfill Army requirements, will have the necessary factor of safety of 2 required by Navy and CAA specifications.

(d) If it is economically advisable, the centrifugal method should have preference when excellent metallurgical quality and high ductility are required in a cast unit.

Acknowledgments

The authors wish to acknowledge their appreciation for the capable assistance of Mr. Gordon Olson, Structures Engineer, and Mr. Vernon Pingel, Research Metallurgist, of the Cornell Aeronautical Laboratory who conducted many of the metallurgical, mechanical, and structural tests. Also, the helpful suggestions and assistance of Mr. A. F. Donovan, Mr. W. M. Duke, and Dr. P. K. Porter of the same organization are gratefully acknowledged.

References

1. H. L. Shaw and C. E. Sims, "Steel Castings for Aircraft," WMC Report No. W-95, 1944.
2. D. W. Williams and C. E. Sims, "Steel Castings for Aircraft," WMC Report No. W-149, 1944.
3. C. E. Sims, "Steel Castings for Aircraft," WMC Report No. W-154, 1944.
4. "Specification for Application and Inspection of Castings Used for Aircraft Structural Parts," Navy Department, Bureau of Aeronautics—SR-111A.
5. Army Handbook, Vol. 1—Rev. 7.
6. Civil Aeronautics Manual O4, Airplane Airworthiness.

DISCUSSION

Written Discussion: By N. E. Promisel, chief metallurgist, Navy Department, Bureau of Aeronautics, Washington, D. C.

This article by Messrs. Smith and Morris has been read with great interest

and forms a worthwhile addition to the growing evidence, if more is considered necessary, that castings, under certain conditions, are suitable replacements for forgings in many important structural applications. In my opinion, probably the greatest deterrent to more extensive use of castings in aircraft structures is the lack of assurance of adequate quality, or, conversely, the lack of a suitable, reliable, economical inspection system (which embraces more than merely a specific method) which would insure the rejection of dubious or unsatisfactory castings. The latter part of this statement is made with full recognition of the valuable contribution made to inspection by radiography, but also with a realization of the impracticability of adequately exploring critical parts of all castings by this means. Perhaps techniques currently being developed or refined, such as high intensity fluoroscopy or certain methods of using ultrasonics, will eventually satisfy this inspection need.

With respect to the problem of consistently obtaining castings of satisfactory quality, this present paper itself illustrates the matter. Note, for example, the last two paragraphs under "Metallographic Examination", Part I, pages 852 and 853, or the discussion of "Mechanical Properties" under "Discussion of Results", Part I, page 863. It is essential that foundry practice (including therein grain size control) be suitably adapted to a given design, if necessary after design changes, and that high quality and reliable workmanship be thereafter applied to the production run. Not until such practice and workmanship can be confidently expected will castings be exploited to their full advantage and be able to compete, from a serviceability angle, with the unique advantages in forgings of "designed" flow lines and correction, at least partially, of internal defects by the forging operation.

Of additional significance and importance in obtaining sound castings is the difficulty, in not-so-sound castings, of interpreting the effect of defects on structural integrity. In the present paper, the overdesign of the parts obscured the potential effects of the defects in the static castings as evaluated in the simulated service tests. Such fortuitous circumstances cannot always be expected, however, and the present state of knowledge in general and stress analysis in particular does not permit reliable forecasts of the significance of discontinuities on static and dynamic properties.

With respect to "Conclusion" (d), page 874, it is not believed that centrifugal castings are necessarily better in all cases. Many a design lends itself to a quality and ductility by static casting at least equal to those obtained by centrifugal techniques.

Written Discussion: By J. S. Limage, chief structures engineer, and E. M. Galbreath, chief metallurgist, Bell Aircraft Corp., Buffalo, N. Y.

The authors are to be commended on the timeliness of this paper especially in view of the tremendous experimental program on guided missiles in which steel castings might be substituted for forgings.

The authors have indicated that properly designed and sound steel castings, of approximately the same cross sections as similar forgings, can, when properly heat treated, develop the same static strength as the forgings.

However, the results of the repeated load tests were inconclusive. In Part I the repeated load test of the casting was not run to failure nor was

there any comparison made with a repeated load test of a forging. In Part II only one comparative repeated load test was run. It would seem imperative to have more specific and detailed information before aircraft manufacturers can substitute steel castings for forgings.

This paper does offer interesting possibilities. Provided that the procuring agency would not require too restrictive design factors for the steel castings, it would be possible to use them in experimental jobs where forgings would be used in production.

This substitution would effect a very marked saving not only in dollars and cents but also in time which might be more important than the monetary saving.

It appears that before the average steel foundries could produce satisfactory steel castings for use in aircraft, they must provide more adequate control and inspection than is the general practice.

The aircraft manufacturers must, if they should desire to take advantage of the savings possible with steel castings, exercise extreme care in the design of the castings to insure the absence of stress raisers in the design. Proper foundry control and inspection will insure the absence of stress raisers in the casting.

Written Discussion: By C. W. Briggs, technical and research director, Steel Founders' Society, Cleveland.

There are a number of observations that the writer should like to make regarding the paper by Messrs. Smith and Morris. First, it is wondered if the steel castings obtained from the commercial steel foundry were ordered to nondestructive testing requirements. This is a normal procedure for aircraft castings and usually entails changes in casting procedure.

Steel castings of the type illustrated are normally heat treated by water quenching and tempering. A water quenching heat treatment would have produced a more uniform structure throughout the section with higher properties.

The results of Part I indicated that the steel castings met all the service requirement tests. It is believed that tests made on unit structures such as carried on by the authors are the only way in which it is possible to compare steel castings with products produced by other methods of fabrication. The authors seemed somewhat disturbed over the ductility values obtained from test bars cut from the center of casting sections. This they explained in part. However, it is believed that such values are of little importance in the testing of entire sections. This point was illustrated by the authors. Also if ductility properties of the forging were obtained in a direction transverse to the flow lines it would have been observed that lower values from those shown in Table III would have been recorded. Since the authors were interested in comparing steel castings and steel forgings it was too bad that units of similar dimensions, compositions and heat treatments were not obtained so that a direct comparison could be made. Direct comparisons as carried on at Battelle Memorial Institute indicated no outstanding differences.

Under Section II, it is difficult to see how the centrifugal casting could be compared with a forging when they differed as to composition, heat treatment and dimensions. Also it is believed that sweeping conclusions could hardly be drawn based on one test. It certainly seems reasonable to point out that

the test data were far from sufficient for the authors to advise on changes in average net stress for centrifugal steel castings as compared to forgings.

Also it is believed advisable to point out that there are no outstanding differences in the properties of statically cast and semicentrifugally cast steel castings. True centrifugal castings may have slightly higher ductility values than those found in statically produced castings; however, on tests made on unit structures such variations in ductility are not evident.

Steel castings were, in this country, used for aircraft parts during the war and are being used at the present time. Also steel castings replaced forgings for aircraft parts in Germany during the war in very substantial quantities.

It is hoped that the authors will continue their unit testing of structures and the writer will be glad to offer the assistance of the Steel Founders' Society in aiding them to secure steel castings for test purposes.

Authors' Reply

In replying to the discussion, the authors wish to express their appreciation of the interest shown by the discussers and of the comments related to the general evaluation of steel castings. We do wish to supply the additional information that the castings were obtained in the latter part of 1944 and were supposed to be typical of cast steel quality then available for aircraft parts.

Mr. Promisel has called attention to the fact that the overdesign of the parts obscured the potential effects of the defects in the static castings as evaluated in the simulated service tests. This point is true but sufficient evidence of strength from cast steel was obtained to warrant the consideration by our organization of quality castings for primary aircraft structures. In reply to the second comment concerning the superiority of centrifugal castings, it is doubtlessly true that at the present time statically poured castings may be for many purposes the equivalent of centrifugally cast units. Our previous experience would not substantiate such a viewpoint since the quality of statically poured experimental cast units procured from outside agencies has been decidedly inferior to the centrifugally cast type.

In reply to the comment by Messrs. Limage and Galbreath concerning the lack of complete repeated load data, it is granted that an absolute index was not obtained to compare the fatigue strengths of cast and forged steel units. However, the objective of the program was to appraise available steel castings metallurgically and structurally to determine if they would warrant consideration in new designs or as replacement parts. Two thousand operations of the strut terminal at the maximum design condition was deemed sufficient evidence of fatigue strength particularly since more exhaustive tests were planned if commercially cast terminals were adopted for the landing gear struts. More extensive fatigue testing of the engine mount units was prohibited by the lack of available test units.

In answer to Dr. Briggs' questions, the centrifugal castings from the commercial steel foundry were not specifically ordered to nondestructive testing requirements but were produced by the foundry for experimental use. It is known that the foundry produced them in their research laboratory and made them to the best standards.

Steel parts of a fabricated assembly such as the type which were reported in Part I are usually welded into the assembly before heat treatment. A water quenching heat treatment for such an assembly, as Dr. Briggs states, would have produced a more uniform structure throughout but it would also have produced severe warping and cracking. In fact, we experienced such cracking when parts with the same composition but of a much simpler design were water-quenched as separate units. Furthermore, the lighter construction steel tube would have quenched out to such an extent in water that it would have been impossible to obtain a workable drawing temperature for both the tube and cast steel terminals.

It is probably true that some aircraft manufacturers used steel castings in their models but it is doubtful that many were used for primary structures. The Curtiss-Wright Corporation, Airplane Division, tried to have P-40 motor mounts cast by steel foundries at a time when a major redesign was occurring as a result of a motor change. After considerable search, a steel foundry with a good reputation accepted the order, but the quality of the castings in the first few shipments was so poor that the use of forgings was practically imperative. Because of this experience, the present reported evaluation of steel castings was undertaken at a later date wherein an appraisal of metallurgical quality and of strength based on design loads was made. It is granted that it would have been desirable to have had the same type of steel, heat treatment, and grain structure in the castings as in the forgings but such conditions were neither mandatory nor practical in view of the available units. Sufficient evidence of quality and strength was obtained from a type of cast steel to warrant a recommendation of steel castings for primary aircraft structures.

FACTORS INFLUENCING THE PEARLITIC MICROSTRUCTURE OF ANNEALED HYPOEUTECTOID STEEL

By R. A. Grange

Abstract

The pearlitic microstructure developed by comparable isothermal annealing of each of twelve types of aluminum-killed hypoeutectoid steel was investigated. Its character varied with composition and could be classified in either of two general groups: (a) well-formed lamellar pearlite, and (b) "semipearlite" in which many of the carbides are relatively large and nonlamellar. In the aluminum-killed steels which contained these massive, nonlamellar carbides after they had been austenitized at the temperature ordinarily used in practice, well-formed lamellar pearlite could be developed by annealing, provided the austenitizing temperature was raised to coarsen austenite grains. In steel which had not been killed with aluminum and was moderately coarse-grained at ordinary austenitizing temperatures, the pearlite was always reasonably well formed, even when the steel had been made fine-grained by hot forging. Apparently, the character of pearlite in an annealed steel is somehow controlled by the interrelated factors: composition, thoroughness of deoxidation, and austenite grain size just prior to transformation. In a number of modern types of steel it appears necessary, if an annealed structure of well-formed pearlite is desired, to raise the austenitizing temperature well above that ordinarily used in present commercial practice, at least unless considerable prior cold working is feasible.

Introduction

LAMELLAR pearlite developed by heating above Ac_3 (or Ac_{cm}) followed by slow cooling (full annealing) was one of the first microconstituents recognized in steel, and the usual concept of the structure of annealed[1] steel is thus based upon some of the earliest

[1] As used in this paper, the term "annealed" always refers to steel which has been heated to form austenite and then either slowly cooled, or isothermally transformed, so that austenite transforms at a temperature not more than 100 F below Ae_1.

A paper presented before the Twenty-eighth Annual Convention of the Society held in Atlantic City, November 18 to 22, 1946. The author, R. A. Grange, is associated with the Research Laboratory, United States Steel Corporation of Delaware, Kearny, N. J. Manuscript received May 15, 1946.

recorded metallographic examinations. In the last two decades, however, notable changes have occurred in steelmaking practice; consequently, the structure of modern steels in the annealed condition is not necessarily the same as that observed in steels used in early investigations. The latter were usually plain carbon steels deoxidized in such a way that they were moderately coarse-grained when heated to even a relatively low austenitizing temperature; modern steels, more often than not, are killed with aluminum in order to keep them fine-grained after the austenitizing treatment usually recommended. Moreover, the present large variety of alloy steels were virtually unknown at the time the classical investigations of the structure of annealed steels were conducted. It is of interest, therefore, to make a systematic comparison of the structure of a number of typical modern steels when annealed; with comparable annealing treatment the principal factors to be considered are (a) steel composition, (b) mode of deoxidation (aluminum-killed or "silicon-killed"), and (c) austenite grain size.

In the literature there are many references relative to annealing of steel, but they are concerned almost entirely with the development of a spheroidal or partly spheroidal structure; and, for the most part, they deal with higher-carbon tool steel types. Several recent investigations (1), (2), (3),[2] deal with so-called "cycle annealing" which aims to develop a predominantly spheroidal structure by an essentially isothermal transformation of inhomogeneous austenite. There seems to have been almost no recognition of the fact that in many popular types of commercial steel a structure of well-formed lamellar pearlite is quite difficult to develop by ordinary heat treatment, or that carbides do not always form from reasonably homogeneous austenite by a process of lamellar growth.

The microstructure of annealed steel is of practical interest since it is generally recognized as a factor in machinability; this has induced some users of steel to specify a particular kind of structure for steel to be made into a product requiring extensive machining. The particular structure desired is often a matter of individual preference, and presumably is somewhat influenced by the sort of machining operation contemplated. Difficulty in developing in certain types of low-alloy steel the pearlitic structure sometimes desired led to the suggestion that available data on isothermal transformation be supplemented by a description of the final pearlite in each of a number of representative low-alloy steels. This paper, by means of photo-

[2]The figures appearing in parentheses pertain to the references appended to this paper.

Table I
Nature and Composition of Steels Investigated

Type	Atlas† Reference (Page)	Deoxidized‡ With	C	Mn	P	S	Si	Ni	Cr	Mo	V
SAE 1040 (F.G.)	*	Aluminum	0.40	0.89	0.018	0.046	0.18	...	...	...	...
SAE 1040 (C.G.)	*	Silicon	0.39	0.73	0.022	0.032	0.19	...	...	...	...
SAE 2340 (F.G.)	31	Aluminum	0.37	0.68	0.014	0.021	0.21	3.41	...	...	...
SAE 2340 (C.G.)	*	Silicon	0.39	0.76	0.026	0.021	0.20	3.10	...	...	...
SAE 3140	56	Aluminum	0.38	0.72	0.019	0.033	0.21	1.32	0.49	...	...
SAE 4140	59	Aluminum	0.37	0.77	0.019	0.026	0.15	...	0.98	0.21	...
SAE 4340	64	Aluminum	0.42	0.78	0.018	0.027	0.24	1.79	0.80	0.33	...
SAE 4640	57	Aluminum	0.36	0.63	0.018	0.021	0.19	1.84	...	0.23	...
SAE 5140	35	Aluminum	0.42	0.68	0.026	0.032	0.16	...	0.93	...	...
SAE 6140	62	Aluminum	0.43	0.74	0.019	0.024	0.23	...	0.92	...	0.16
NE 9442	68	Aluminum	0.38	1.08	....	....	0.70	0.34	0.40	0.11	...
SAE 3312	*	Aluminum	0.11	0.45	0.017	0.009	0.18	3.33	1.52	...	...
SAE 4815	96	Aluminum	0.16	0.52	0.009	0.010	0.27	3.36	...	0.19	...
NE 8620	*	Aluminum	0.18	0.79	0.021	0.023	0.31	0.52	0.56	0.19	...

†"Atlas of Isothermal Transformation Diagrams" published by United States Steel Corporation in 1943.

‡Deoxidation with aluminum means that aluminum was added to the steel in the ladle or mold (fine-grain practice); deoxidation with silicon means that no aluminum was added and that the heat was killed principally by silicon ("coarse-grain practice"). Steels deoxidized with titanium, vanadium or other such elements are not considered in this investigation.

*The isothermal transformation diagram for the steel does not appear in the Atlas.

micrographs, supplies such information and demonstrates how the three factors, composition, mode of deoxidation, and austenite grain size, may influence the structure of annealed hypoeutectoid steel.

Material and Procedure

Twelve popular types of hypoeutectoid steel (one plain carbon, eleven low-alloy) were selected for comparison of their pearlitic structure; in most cases the isothermal transformation diagram had been previously determined for identical samples and has been published.[3] Those initially selected are all from heats thoroughly killed with aluminum, as is the usual practice with such grades; that is, they were made according to so-called "fine grain" deoxidation practice and have uniformly small austenite grains unless heated well above the usual austenitizing temperature. Later, samples of types SAE 1040 and 2340 were obtained from heats to which no aluminum had been added, which, unlike most low-alloy steels produced at present, develop moderately coarse grains when austenitized at the temperature ordinarily used in practice. The composition of each of the steels studied is given in Table I; since the results to be described are, in a sense, supplementary to the isothermal transformation diagram, Table I also lists the page in the "Atlas" where the latter may be

[3]In "Atlas of Isothermal Transformation Diagrams", published by United States Steel Corporation in 1943; most of these diagrams have also appeared elsewhere in the literature.

Table II
Details of Heat Treatment and Resulting Austenite Grain Size and Hardness

Structure Illustrated	Type	Austenitized* F	Transformed Temp., F	Transformed Time, Hrs.	Austenite Grain Size ASTM No.	Hardness After Heat Treatment Rb
Fig. 1	SAE 1040 (F.G.)	1550	1290	16	7	80
	SAE 2340 (F.G.)	1450	1130	16	7–8	87
	SAE 3140	1550	1265	16	7–8	85
	SAE 4140	1550	1335	16	7–8	83
	SAE 4340	1550	1250	16	7–8	88
	SAE 4640	1550	1205	16	7–8	88
	SAE 5140	1550	1335	16	6–7	84
	SAE 6140	1550	1335	16	8	87
	NE 9442	1575	1290	16	10–11	89
	SAE 3312	1650	1180	15	9	83
	SAE 4815	1650	1130	16	8–9	87
	NE 8620	1650	1285	16	9–10	82
Fig. 2	SAE 2340 (F.G.)	1450	1130	¼	7–8	(46 Rc)
	SAE 2340 (F.G.)	1450	1130	2	7–8	(43 Rc)
	SAE 2340 (F.G.)	1450	1130	16	7–8	87
Fig. 3	SAE 2340 (F.G.)	1550	1130	48**	7	87
	SAE 2340 (F.G.)	1650	1130	54	4	89
	SAE 2340 (F.G.)	1750	1130	72	3–4	89
Fig. 4	SAE 1040 (F.G.)	1750	1290	84	5	80
	SAE 1040 (F.G.)	2000	1290	96	3	80
	SAE 4640	1750	1205	36	6	86
	SAE 4640	2000	1205	42	2–3	85
	SAE 4815	1750	1130	36	8	87
	SAE 4815	2000	1130	46	4	86
Fig. 5	SAE 1040 (F.G.)	1550	1290	16	7	80
	SAE 1040 (C.G.)	1550	1290	16	4–5	80
	SAE 2340 (F.G.)	1450	1130	16	7–8	87
	SAE 2340 (C.G.)	1450	1130	16	5–6	87

*Austenitized for 10 to 15 minutes at temperature indicated in each case.
**In this and in some other treatments which follow, a longer transformation period was required to complete the transformation of the more sluggish coarse-grained austenite; it was established by experiment that this extra transformation time did not increase the size, shape or number of divorced carbides.

found. In the table and hereafter in the text, the aluminum-killed heats of SAE 1040 and 2340 are designated "SAE 1040 (F.G.)" and "SAE 2340 (F.G.)", and those to which no aluminum had been added, "SAE 1040 (C.G.)" and "SAE 2340 (C.G.)".

Samples from each aluminum-killed heat in the normalized condition were austenitized at about the temperature commonly used in practice, this being the same as was used in determining the isothermal transformation diagram in the "Atlas". After this austenitizing treatment, only one steel, SAE 6140, contained microscopically visible undissolved carbides; in all others, the carbides seemed to be completely dissolved in austenite.[4] A number of preliminary transformation treatments were tried in an attempt to produce in all steels pearlite of comparable interlamellar spacing and, at the same time, a structure reasonably representative of the commercially annealed product.

[4]Payson (1), (2) has shown that austenitizing at a relatively low temperature, such that carbides or small volumes of ferrite remain undissolved in inhomogeneous austenite, favors transformation to a partially spheroidal structure somewhat similar to that which we have designated as containing massive, nonlamellar carbides; in this investigation, however, the austenitizing temperatures are always much higher than those specified by Payson.

The level of transformation temperature finally selected for each steel is that at which the austenite just transformed completely in 16 hours. This temperature, which was never more than 100 F below Ae_1, differs considerably for the several steels in accordance with the differences in Ae_1 and in sluggishness of transformation. By proceeding in this way, pearlite of about the same degree of coarseness was produced in all, thus permitting direct comparison of steels differing in composition. Details of heat treatment may be found in Table II. In a few cases, more than one austenitizing temperature was used as a means of evaluating the influence of austenite grain size.

When this group of comparisons had been made, it was decided to include a number of specimens which would not transform completely in 16 hours at the temperature previously selected for this grade of steel. Consequently, these later specimens were isothermally annealed for a longer time rather than at a different temperature, for direct experiment showed that the appearance of the pearlitic product was not visibly affected by lengthening the 16-hour period several fold, whereas it was altered by change of temperature. In a typical case [SAE 2340 (F.G.)], comparison of transformation product was made on samples isothermally annealed for each of a series of times, including that at which austenite just began to transform. Samples were also prepared from heats of both SAE 1040 and 2340 to which no aluminum had been added for comparison with the aluminum-killed heats of corresponding composition already mentioned. Finally, the influence of austenite grain size alone was studied by developing, by different amounts of forging, a wide range of grain size in a single specimen, which was then transformed to pearlite as before.

Influence of Composition on the Pearlitic Structure of Aluminum-Killed Hypoeutectoid Steels

Each of the twelve types of aluminum-killed steel is from a commercial heat and is, presumably, representative of present production of each. It is assumed, therefore, that the observations on this group of steels, even though limited at present to one sample from a single heat of each grade, apply in principle to other hypoeutectoid steels.

Table II lists the heat treating details, the resulting austenite grain size, and hardness after annealing; the latter is only of incidental interest to the present investigation, but shows that all were thoroughly annealed and did not differ much in hardness. The microstructure of each after isothermal annealing is illustrated in

Fig. 1. It is apparent that in SAE 3140, 4140, 4340, 5140 and 6140, and NE 9442 and 8620, the pearlite is quite well formed, but that in SAE 1040, 2340, 4640 and 4815 it is not, for the most part; the structure of the latter four steels is characterized by massive. largely nonlamellar carbides which are seemingly separated from the true lamellar aggregate and give the structure the appearance of having been partly spheroidized. For convenience, this type of structure will henceforth in this paper be designated "semipearlite".[5] The structure of SAE 3312 is neither well-formed pearlite nor does it comprise massive, nonlamellar carbides; apparently, the somewhat spheroidal appearance of its "pearlite" is due to its relatively high percentage of alloying elements, chromium particularly.

As has been noted, the transformation temperature, selected arbitrarily as that at which transformation was just completed in 16 hours, was considerably different for different compositions. It is believed, however, that the comparison illustrated in Fig. 1 is perfectly valid in its general implication, since at other transformation temperature levels the same trends were evident. For example, it was observed that each steel which developed nonlamellar carbides ("semipearlite") at one temperature level also did so at other levels in the pearlite region, but that these nonlamellar carbides became relatively more prevalent the higher the transformation temperature.

The steels investigated do not comprise a sufficient number or variety to explore adequately all effects of composition upon the structure of annealed aluminum-killed hypoeutectoid steels; nevertheless, it may be significant that in the present group all steels which contain chromium develop well-formed pearlite, while all which do not contain chromium are "semipearlitic". Other strong carbide-forming elements may possibly resemble chromium in this respect, but the range of compositions investigated is insufficient to make certain of this. On the other hand, nickel and other noncarbide formers may possibly increase the tendency toward formation of nonlamellar carbides; yet, SAE 1040, which contains no such alloying elements, shows a decided tendency to form nonlamellar carbides, although not quite so great a tendency as SAE 2340 or 4640.

[5]The term "semipearlite" is used because it connotes the partly nonlamellar, partly lamellar character of such structures; furthermore, it implies that, as shown in Fig. 2, this transformation product forms as such directly from austenite and is not, therefore, some modification of what was once well-formed lamellar pearlite. Of course, there is not always a clear-cut distinction between what we have designated "well-formed lamellar pearlite" and "semipearlite", since the former will usually contain a few nonlamellar carbides, and the latter some areas of lamellar pearlite. In certain relatively high alloy steels, for instance SAE 3312, the pearlitic structure is somewhat finely spheroidal rather than completely lamellar; "semipearlite" is distinguished from such aggregate structures by the presence of nonlamellar carbides which are relatively thick and massive as compared to carbides intimately associated with ferrite in a true aggregate.

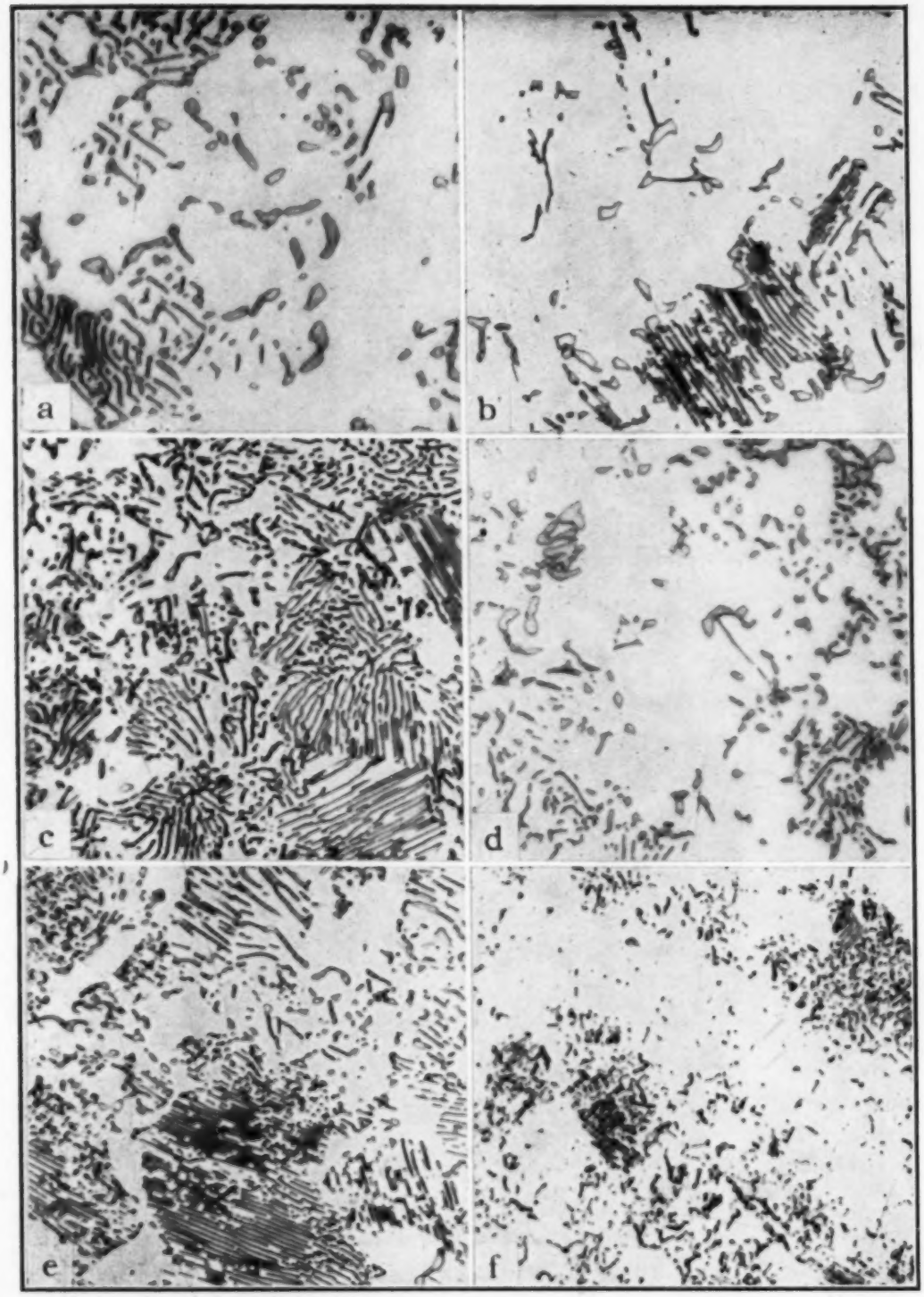


Fig. 1—Microstructure of Isothermally Annealed Aluminum-Killed SAE Steels. Austenitized 100 to 200 F above Ae_3 and transformed at the temperature level where transformation is just completed in 16 hours. Picral etch. × 1000. (a) 1040, (b) 2340, (c) 4340, (d) 4640, (e) 9442, (f) 3312.

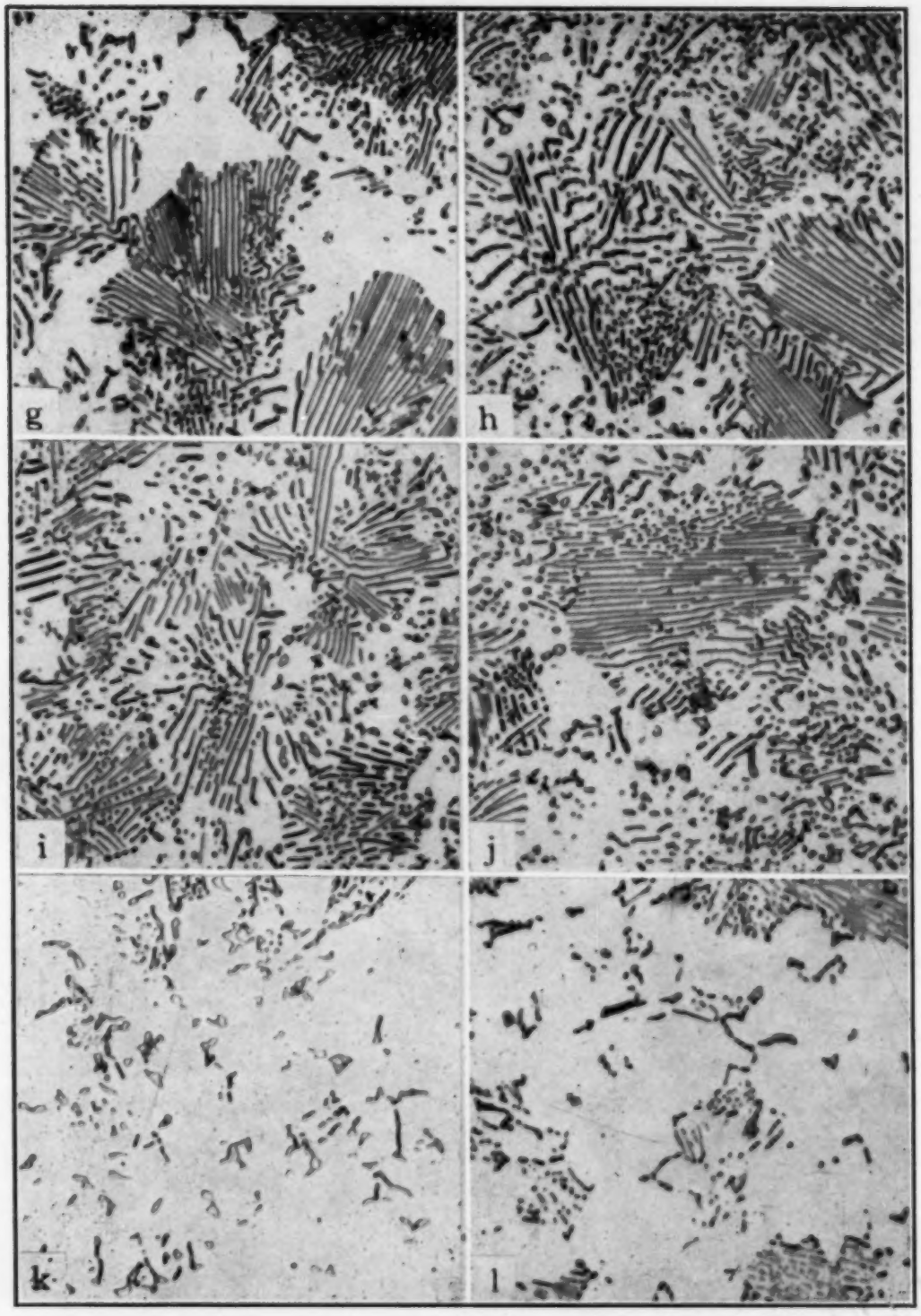


Fig. 1—Microstructure of Isothermally Annealed Aluminum-Killed SAE Steels. Austenitized 100 to 200 F above Ae_3 and transformed at the temperature level where transformation is just completed in 16 hours. Picral etch. × 1000. (g) 3140, (h) 4140, (i) 5140, (j) 6140, (k) 4815, (l) 8620.

Formation of "Semipearlite"

If examination is confined to the structure after transformation is complete, one might infer that the massive, nonlamellar carbides in "semipearlitic" structures result from coalescence of some of the first carbide lamellae to form from austenite. That this is not the case is shown in Fig. 2, which illustrates three stages in the transformation of SAE 2340 steel at 1130 F (610 C). In the first sample, micrograph (a), transformation to ferrite-carbide aggregate has barely begun, yet the carbides are already assuming a massive, nonlamellar appearance (note arrow on the photomicrograph); the other two photomicrographs show that massive, nonlamellar carbides are present in relatively the same proportion throughout the transformation process. Thus, it is clear that these nonlamellar carbides form as such directly from austenite in certain steels, and that carbides do not coalesce to any appreciable degree on holding for a reasonably prolonged period at the transformation temperature level.

We have come to regard well-formed pearlite as the normal structure of slowly cooled steel; yet this may have come about merely because early experience dealt with steels in which the annealed structure happened to be of this type. In recent years, the increased use of alloy steels and of aluminum additions to inhibit grain coarsening has resulted in commercial steels in which "semipearlite" may be just as common as well-formed lamellar pearlite. Apparently, transformation of austenite to a ferrite-carbide aggregate entails at least two modes of carbide growth—lamellar, and the more or less equiaxed type which leads to massive, nonlamellar carbides. In most steels both processes occur to some extent; that is, there are probably few steels in which at least a few nonlamellar carbides do not form, although in the majority lamellar growth apparently predominates so as to produce what we have designated "well-formed lamellar pearlite". In the present instances, we are dealing with samples annealed in such a way that undissolved carbide is not a factor, at least insofar as it is microscopically visible; we recognize, however, that the presence of undissolved carbide favors the formation of the nonlamellar rather than the lamellar type, and thus tends to produce, in almost any steel, a predominantly spheroidal aggregate by direct transformation of austenite.

Influence of Austenitizing Temperature

The samples illustrated in Fig. 1 were all austenitized at about

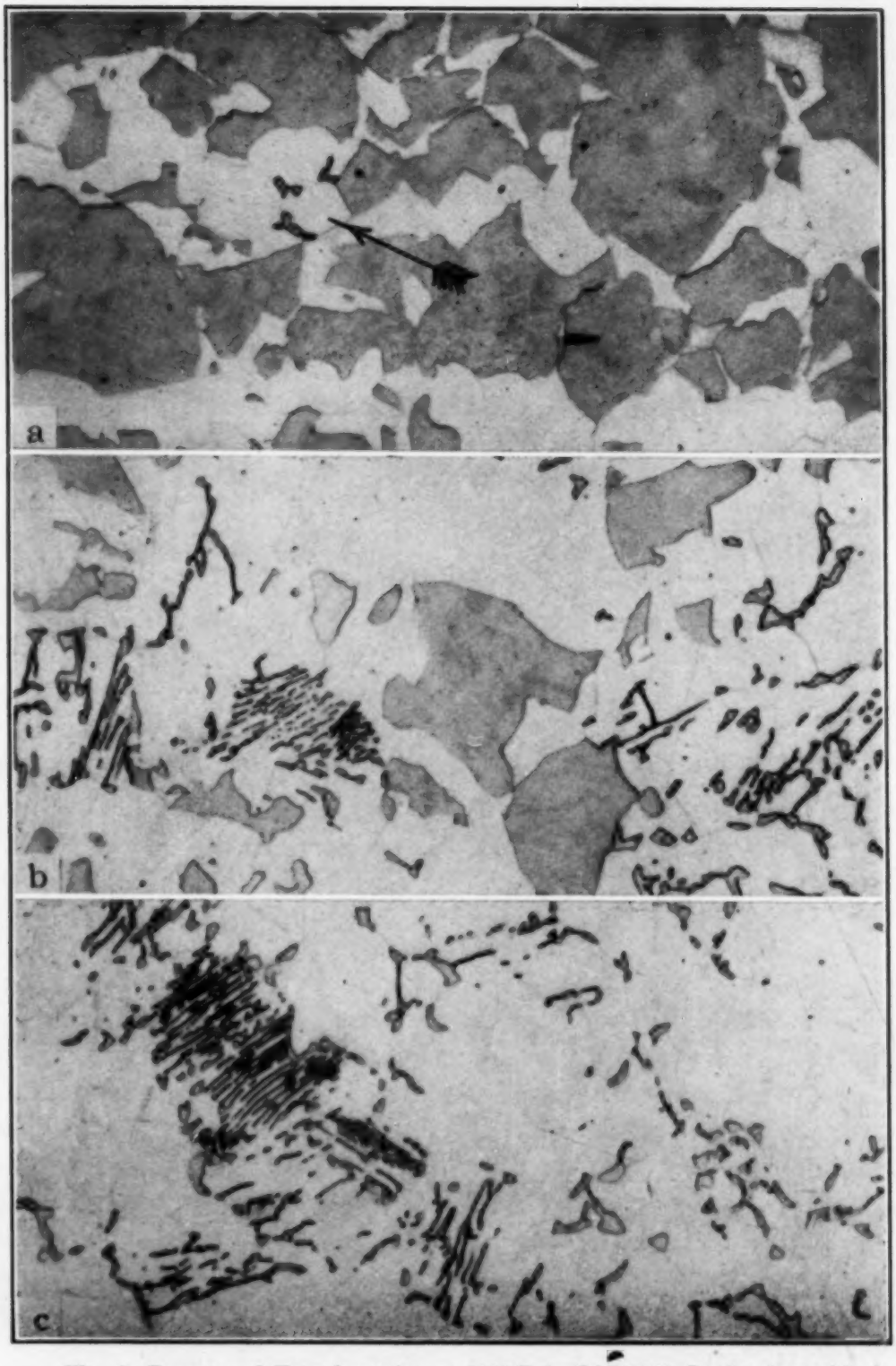


Fig. 2—Progress of Transformation at 1130 F in SAE 2340 Steel. Austenitized at 1450 F, grain size 7-8. Note that massive, nonlamellar carbides form directly from austenite. Picral etch. × 1000. (a) 15 minutes, (b) 2 hours, (c) 16 hours.

the temperature that would ordinarily be used in practice, which is not more than 200 F (95 C) above Ac_3. It is of interest to determine the effect of higher austenitizing temperature upon the tendency of certain steels to form the "semipearlitic" structure on annealing.

Fig. 3 shows the structure of the SAE 2340 (F.G.) steel after it had been austenitized at each of three higher temperatures, and then had transformed as before at 1130 F (610 C), but over a longer time[6] to allow for the slower transformation rate of coarse-grained austenite; the specific treatment in each case is listed in Table II. For comparison with the original austenitizing at 1450 F (790 C), note micrograph (c) of Fig. 2. After austenitizing at 1550 F (845 C) many nonlamellar carbides are present, but only a few when austenitized at 1650 F (900 C), and scarcely any when 1750 F (955 C) was used; it is significant that, as shown in Fig. 3, austenite grains coarsened at 1650 F (900 C) and at 1750 F (955 C), but not at 1550 F (845 C). This particular heat of SAE 2340 steel will therefore contain reasonably well-formed pearlite only after austenitizing at 1650 F (900 C) or higher.

Fig. 4 shows the effect of higher austenitizing temperatures (1750 and 2000 F) on the structure of SAE 1040, 4640, and 4815, in all of which the original annealing treatment developed "semipearlite" (see Fig. 1). In each, well-formed pearlite developed when the austenitizing temperature exceeded some minimum, but this minimum differs for different steels. In these instances there is a definite correlation between this minimum austenitizing temperature and that at which the grains coarsened rapidly. This probably implies that, even among a number of heats of the same type of steel, no precise common limit can be assigned as the minimum austenitizing temperature necessary to develop well-formed pearlite, since the grain-coarsening temperature is likely to vary somewhat among aluminum-killed heats of the same grade.

Influence of Mode of Deoxidation

The foregoing illustrations show that certain grades of steel, when killed with aluminum, have a strong tendency to form nonlamellar carbides after austenitizing at the temperature ordinarily used in practice; in order to determine the effect of mode of deoxidation on the annealed structure, pairs of commercial heats, one killed with alu-

[6]Preliminary experiments demonstrated that a transformation period several times the 16 hours originally used did not alter the appearance of the annealed structure; that is, no massive, nonlamellar carbides were formed by coalescence of lamellar carbides during such a prolonged holding period after transformation was completed.

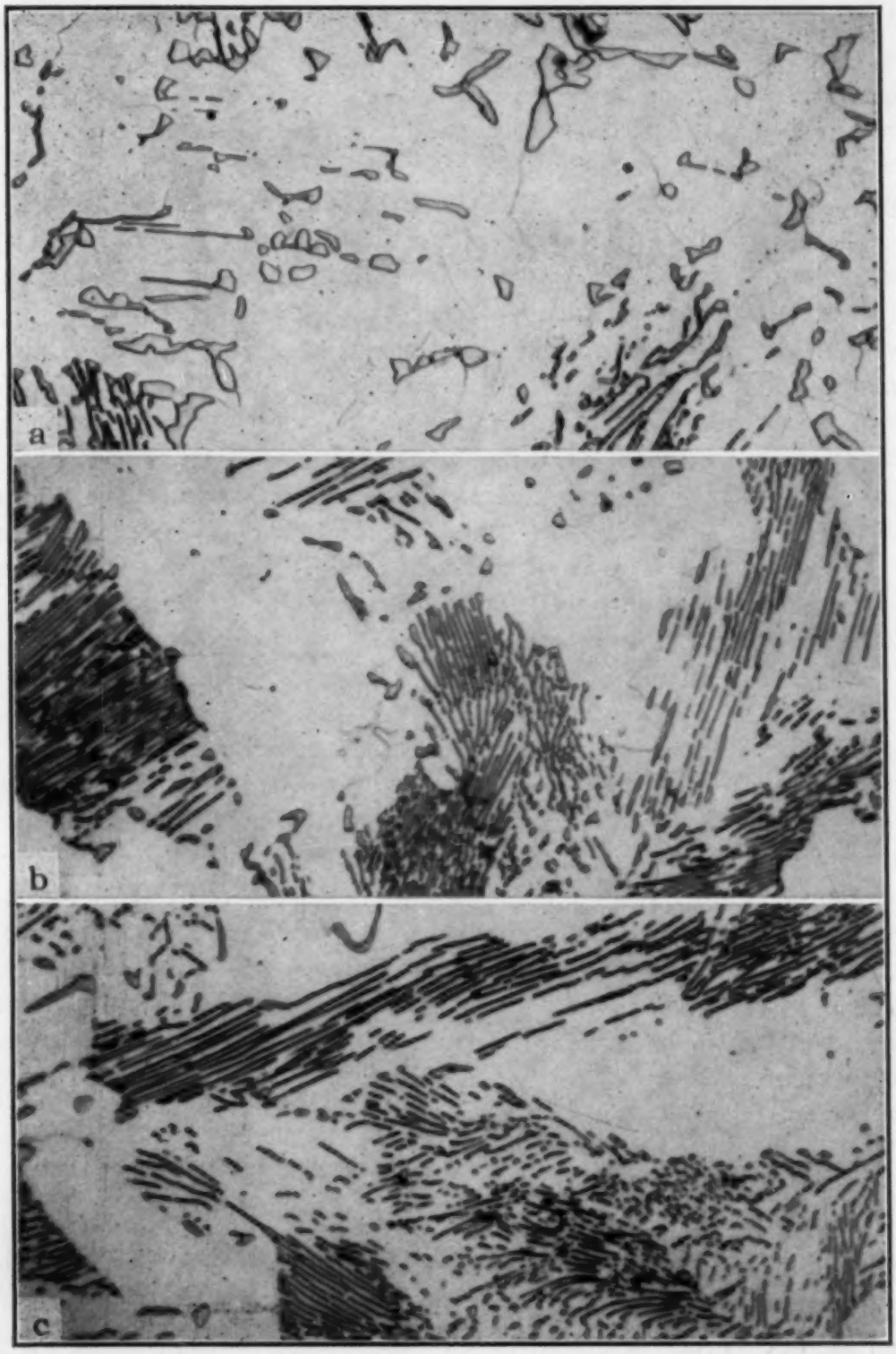


Fig. 3—Influence of Austenitizing Temperature (Grain Size) Upon the Structure of Isothermally Annealed SAE 2340. Picral etch. × 1000. (a) 1550 F, grain size 7, (b) 1650 F, grain size 4, (c) 1750 F, grain size 3-4.

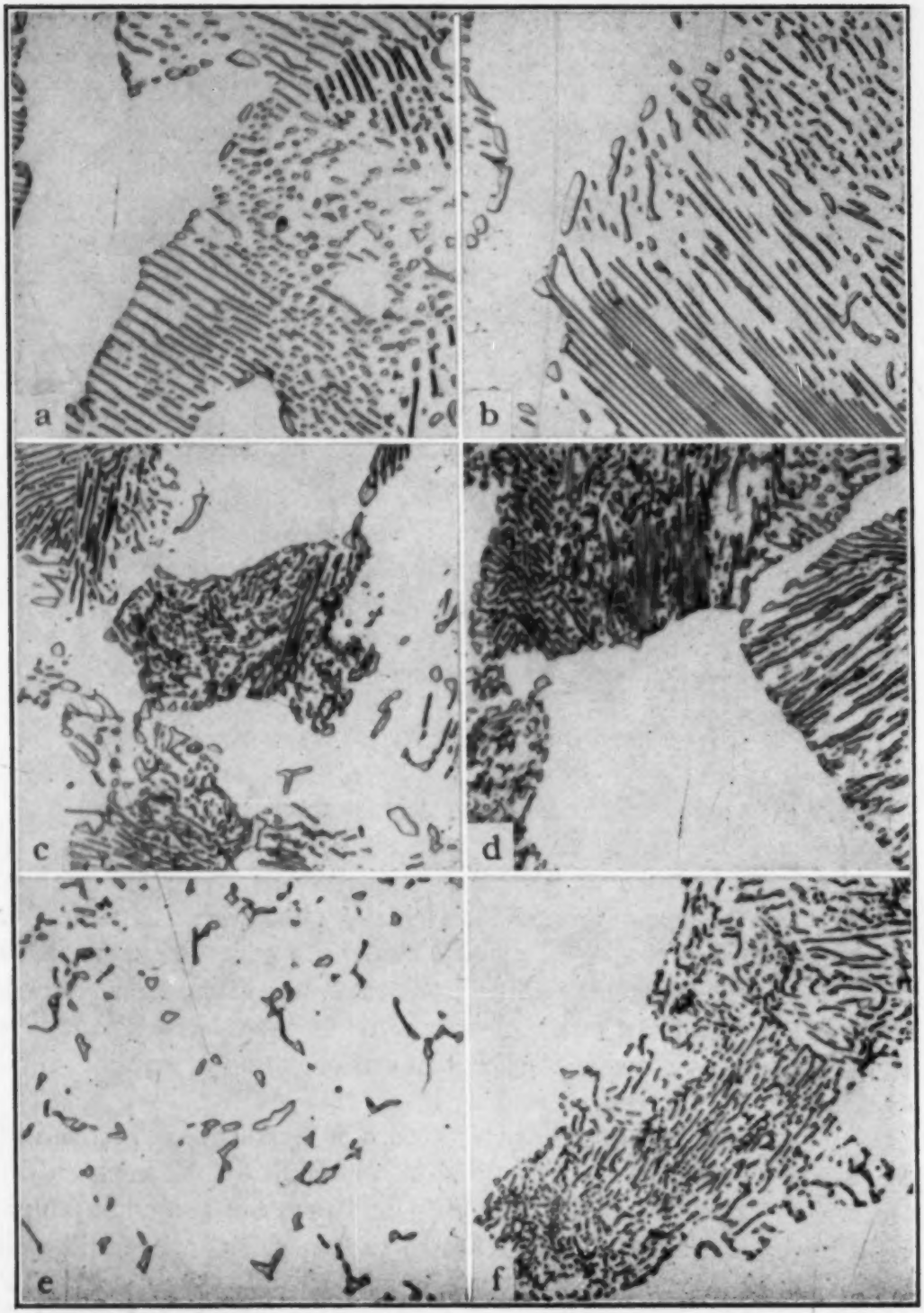


Fig. 4—Influence of Austenitizing Temperature on the Structure of Several Aluminum-Killed Steels. Compare with structure of these steels after austenitizing at lower temperature (Fig. 1). Picral etch. × 1000. (a) SAE 1040, austenitized at 1750 F, grain size 5. (b) SAE 1040, austenitized at 2000 F, grain size 3. (c) SAE 4640, austenitized at 1750 F, grain size 6. (d) SAE 4640, austenitized at 2000 F, grain size 2-3. (e) SAE 4815, austenitized at 1750 F, grain size 8. (f) SAE 4815, austenitized at 2000 F, grain size 4.

minum, the other not, of two such grades were investigated. The heat treating details are given in Table II, and the resulting microstructures illustrated in Fig. 5. Micrographs (a) and (b) represent SAE 1040 steel, micrograph (a) being the aluminum-killed and micrograph (b) the sample from the heat to which no aluminum had been added; both were austenitized at about the temperature used commercially in heat treating this composition, and were then transformed identically. A similar comparison for the pair of SAE 2340 heats is shown in the micrographs (c) and (d). In both these compositions, the samples from heats not treated with aluminum contain reasonably well-formed pearlite in contrast to many massive, nonlamellar carbides ("semipearlite") in the sample from each corresponding aluminum-killed heat; the former are moderately coarse-grained, and the latter fine-grained, as would be expected.

It is thus apparent that mode of deoxidation of a steel may influence its structure when annealed; seemingly, the condition in the austenite which inhibits grain coarsening also promotes formation of nonlamellar carbides in certain types of steel of which SAE 1040 and 2340 are typical.

Influence of Austenite Grain Size

An apparent correlation between austenite grain size and tendency to form "semipearlite" has been shown; that is, massive, nonlamellar carbides were observed in certain steels when fine-grained but never when coarse-grained. In no case, however, was the effect of austenite grain size isolated from that of deoxidation or from the possible effects of other factors associated with treatments at high austenitizing temperatures. In order to study the effect of grain size alone, difference in austenite grain size was produced in a single specimen by forging one end.

In the first experiment of this kind, a wedge-shaped specimen of SAE 2340 (F.G.), ¼ inch thick on one end and $\frac{1}{16}$ inch thick on the other, was heated to 2000 F (1095 C) and then hot-forged to a uniform thickness of $\frac{1}{16}$ inch; this hot-forged specimen, while still well above 1130 F (610 C), was then quenched into lead at 1130 F (610 C) and held at this temperature until completely transformed. The resulting structure at each end of this specimen is shown in photomicrographs (a) and (b), Fig. 6; (a) represents the hot-forged end in which coarse austenite grains produced by heating at 2000 F (1095 C) were broken up by the forging into uniform small grains,

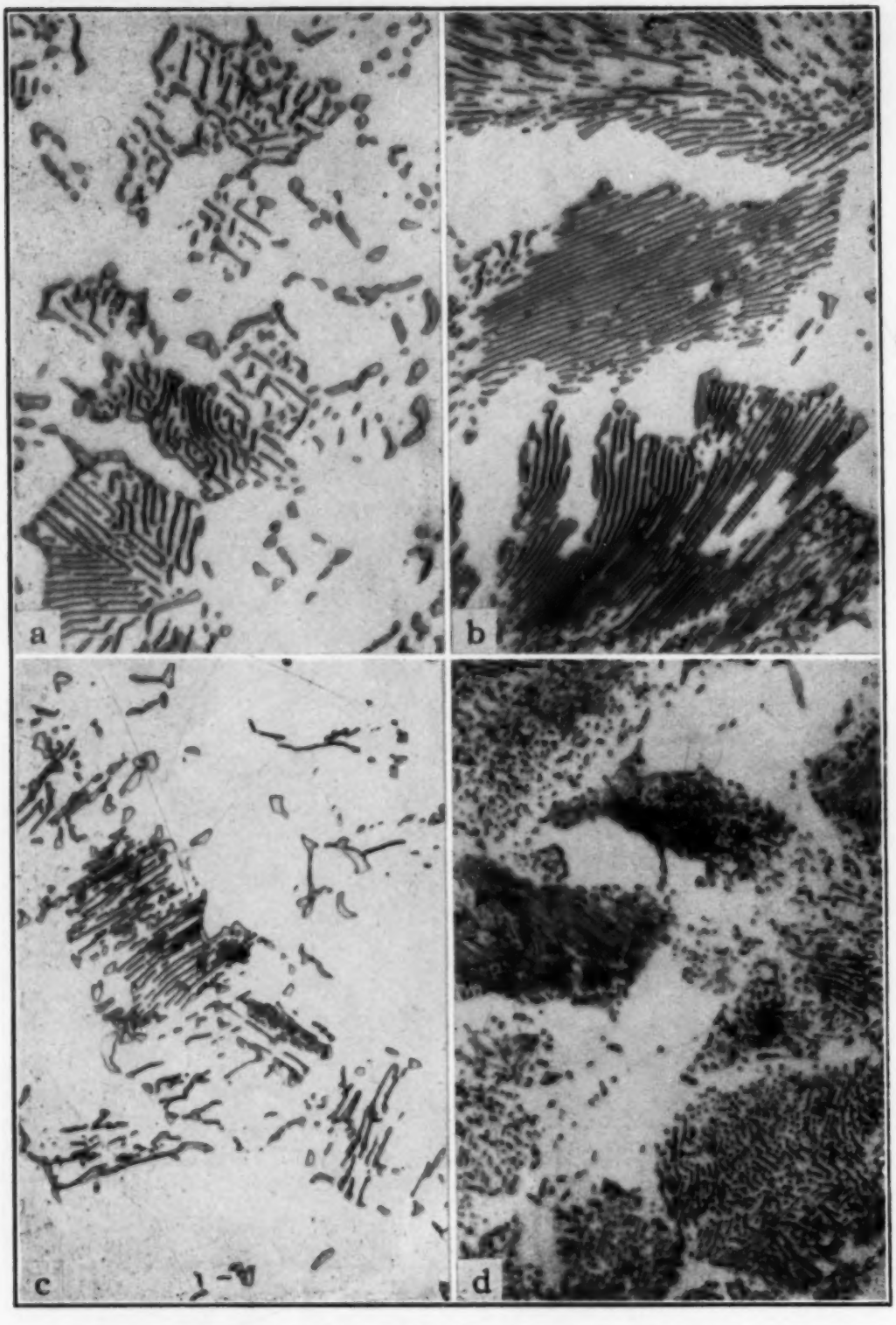


Fig. 5—Influence of Deoxidation Practice on the Structure as Annealed. Picral etch. × 1000. (a) SAE 1040, austenitized at 1550 F and transformed at 1290 F. Aluminum-killed, grain size 7. (b) SAE 1040, austenitized at 1550 F and transformed at 1290 F. No aluminum added, grain size 4.5. (c) SAE 2340, austenitized at 1450 F and transformed at 1130 F. Aluminum-killed, grain size 7.5. (d) SAE 2340, austenitized at 1450 F and transformed at 1130 F. No aluminum added, grain size 5.5.

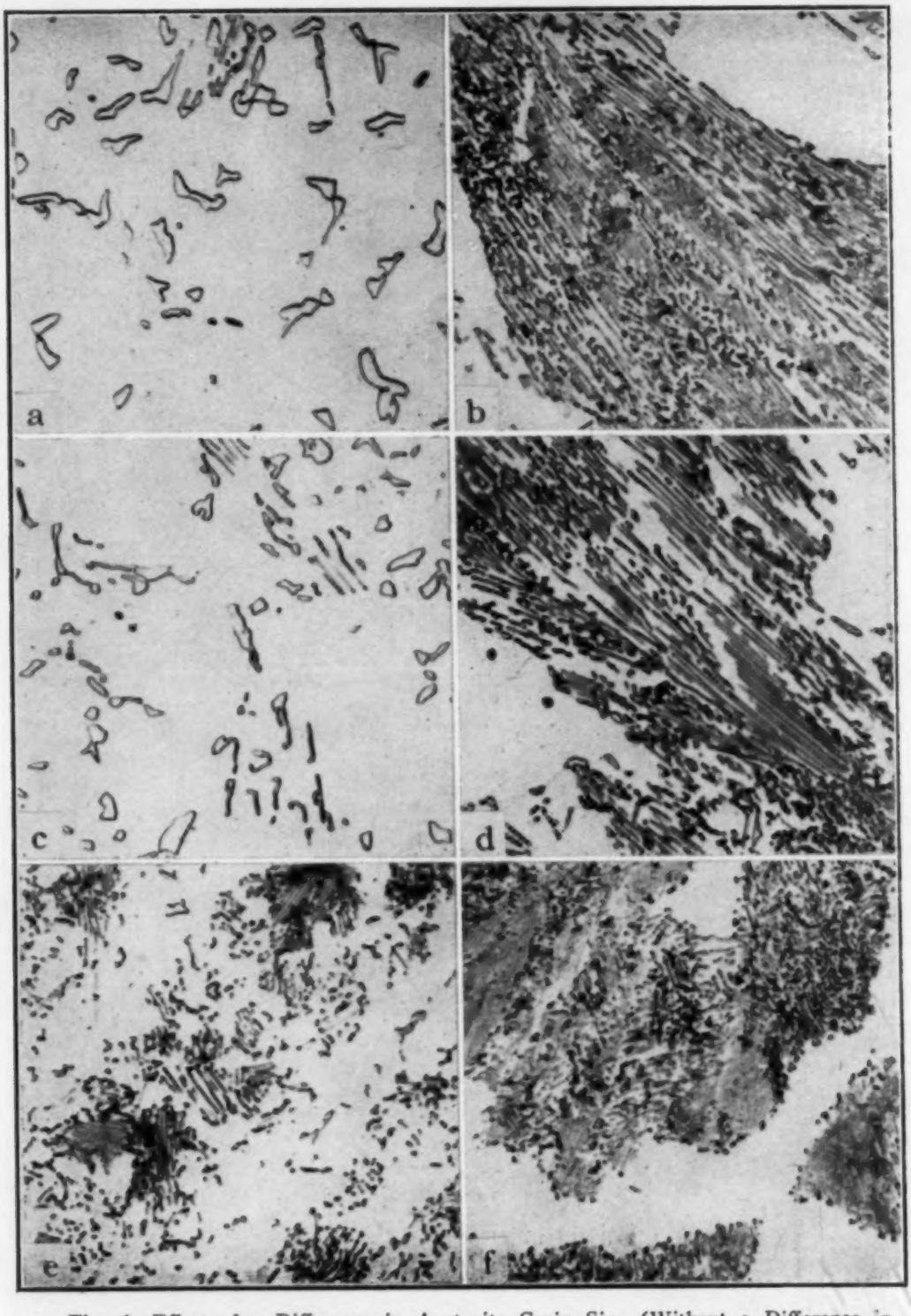


Fig. 6—Effect of a Difference in Austenite Grain Size (Without a Difference in Austenitizing Temperature or Time) on the Character of the 1130 F Transformation Produced in SAE 2340. Picral etch. × 1000. (a and b) (F.G.) Austenitized at 2000 F and transformed at 1130 F, forged end (fine-grained) at left. (b and c) (F.G.) Austenitized at 1600 F and transformed at 1130 F, cold-worked end (coarse-grained) at right. (e and f) (C.G.) Austenitized at 2000 F and transformed at 1130 F, forged end (fine-grained) at left.

while photomicrograph (b) represents the unforged (coarse-grained) end. The difference in structure between these two is a consequence of the difference in grain size, since both had the same austenitizing treatment; in the fine-grained metal the carbides are almost entirely nonlamellar, whereas in the coarse-grained metal they are present as lamellae.

In another experiment, a similar wedge-shaped specimen of SAE 2340 (F.G.) was hammered cold to a $\frac{1}{16}$-inch flat before austenitizing. It was then heated to 1600 F (870 C) (just below its coarsening temperature in absence of cold work), whereupon the cold-worked end became coarse-grained and the opposite end remained fine-grained. This specimen was transformed, as before, at 1130 F (610 C), producing the structures illustrated by photomicrographs (c) and (d) of Fig. 6; (c) represents the fine-grained end, (d) the coarse-grained (cold-worked). Again in this case, "semipearlite" appears where austenite grains are small, but not where they are large.

Finally, hot-forging technique was applied to a similar wedge-shaped specimen of SAE 2340 (C.G.), the whole procedure being identical with that of SAE 2340 (F.G.) just described. In this steel, to which no aluminum had been added, very few massive, nonlamellar carbides were present even though the forged end was extremely fine-grained (micrographs (e) and (f) of Fig. 6); there are, however, a number of small dispersed carbides, but the structure is essentially lamellar pearlite rather than "semipearlite". Apparently, there is not always a direct correlation between austenite grain size and tendency to form "semipearlite"; mode of deoxidation is also an interrelated factor, although it does appear that the massive, nonlamellar carbides characteristic of "semipearlite" never form to any appreciable extent when austenite grains are large.

Discussion of Results

It would seem from these observations that the massive, nonlamellar carbides appear to a marked extent only in aluminum-killed steels of certain compositions, and in these only when austenite grains are relatively small. Nonlamellar carbides may be eliminated from the annealed structure of such compositions by (a) austenitizing them above their grain coarsening temperature at the beginning of the annealing cycle, or (b) avoiding the use of aluminum as a deoxidizer.[7]

[7] It is not known at present whether other powerful deoxidizers such as titanium and vanadium, which are effective in raising the grain-coarsening temperature, behave like aluminum in this respect.

The mode of deoxidation which, in large measure, determines the austenite grain size after the usual anneal also seems to influence the structure of annealed hypoeutectoid steel. While correlation between austenite grain size and the tendency of a given steel to transform to "semipearlite" has been noted, it would appear that the essential factor is the condition in the steel produced by deoxidation with aluminum, rather than grain size directly. This inference is drawn since a steel not killed with aluminum developed reasonably well-formed pearlite even though very fine-grained (see SAE 2340 (C.G.) illustrated in Fig. 6). The usual belief, although somewhat speculative, is that deoxidation with aluminum produces a multitude of submicroscopic particles of aluminum oxide, or aluminum nitride, or both; such particles inhibit grain growth in austenite until, on reaching a sufficiently high temperature, they presumably dissolve and diffuse in austenite. These submicroscopic particles may possibly serve as nuclei on which carbide precipitates from austenite during its transformation to a pearlitic structure; when sufficiently numerous and properly distributed, they may promote formation of the nonlamellar type of carbide which characterizes our "semipearlitic" structures. It is perhaps less surprising that nonlamellar carbides sometimes form than that lamellar growth, taking steels as a whole, occurs as often as it does. The tendency toward lamellar growth must be quite strong, yet not so strong but that it may be replaced to a greater or lesser extent by nonlamellar growth under certain conditions; these conditions are presumably associated with particles capable of nucleating carbide, whether these particles arise from deoxidation with aluminum or are carbides remaining undissolved because of incomplete austenitization; regions of high carbon concentration might have the same effect as undissolved carbides.

It is also possible that lamellar growth is more difficult when the individual volumes of austenite about to transform are very small. This occurs in fine-grained hypoeutectoid steels whenever a large proportion of ferrite is rejected. This viewpoint, if correct, helps to explain why lamellar growth always predominated in our chromium steels but not in the others, chromium being an element which, for a given carbon content, by considerably lessening the proportion of proeutectoid ferrite, increases the size of individual volumes of austenite about to transform to a pearlitic aggregate.

Conclusions

Samples of each of twelve hypoeutectoid steels of standard com-

mercial compositions were austenitized, then completely transformed at a temperature level such that the resulting pearlite was in each steel about equally coarse; comparison of the resulting structure, with particular reference to whether it was largely or only partly lamellar, leads to the following conclusions:

(a) In the aluminum-killed steels containing chromium, the annealed structure was well-formed pearlite, whereas in those without chromium it contained many massive, nonlamellar carbides.

(b) The pearlite was substantially lamellar in those specimens in which the austenite grains just prior to transformation were coarse, whether the coarseness was due to lack of deoxidation with aluminum or to high austenitizing temperature, or was developed by heating after cold working.

(c) In plain carbon, nickel, or nickel-molybdenum steel, when the transforming austenite was fine-grained—whether because of thorough deoxidation with aluminum or low austenitizing temperature or hot forging—the pearlite formed was only partly lamellar, most of the carbide being present as scattered, nonlamellar particles. This "semipearlitic" type of structure is a direct product of transformation of austenite and not, as might be inferred from its final appearance, the result of coalescence of what initially were lamellar carbides.

(d) In a steel of a composition prone to develop nonlamellar carbides, but which had not been killed with aluminum (so-called "silicon-killed"), reasonably well-formed pearlite was developed on annealing, even when the austenite had been made very fine-grained by hot forging.

These conclusions, though strictly valid only for the group of steels included in this investigation, are believed to be generally applicable. They suggest that the mode of formation of the carbides in annealed hypoeutectoid steels is somehow associated with the fineness of grain of the transforming austenite and with the fundamental factors which influence this grain size.

Acknowledgment

This investigation was suggested by representatives of Carnegie-Illinois Steel Corporation from whom the steels were obtained. Asso-

ciates at the United States Steel Corporation Research Laboratory, particularly Drs. R. H. Aborn, R. L. Rickett and G. V. Smith, contributed many valuable suggestions.

References

1. P. Payson, W. L. Hodapp and J. Leeder, "The Spheroidizing of Steel by Isothermal Transformation," TRANSACTIONS, American Society for Metals, Vol. 28, 1940, p. 306-332.
2. P. Payson, "The Annealing of Steel," *Iron Age*, June 24 to July 22, 1943.
3. G. R. Brophy, "Cycle Annealing of Hypoeutectoid Steels," *Iron Age*, Dec. 13, 1945, p. 69-71.

DISCUSSION

Written Discussion: By P. Payson, Research Laboratory, Crucible Steel Company of America, Newark, N. J.

The first steel in which we observed the formation of a nonlamellar structure at high transformation temperatures was a hypoeutectoid steel, SAE 4345, austenitized at 1450 F (790 C), as reported by Payson, Hodapp and Leeder[8] at the annual meeting of the Society 7 years ago. No satisfactory explanation was offered at that time for this unexpected behavior of austenite, although both J. J. B. Rutherford and B. R. Queneau in discussing our paper suggested the possibility of particles other than residual carbides being present to nucleate the formation of nonlamellar carbides. In his excellent Campbell Memorial Lecture in 1941,[9] R. F. Mehl stated that a nonlamellar transformation product was formed at high temperatures only from "heterogeneous austenite containing free carbide or undissipated carbon concentration gradients, or both".

We have found, as has the author, that some hypoeutectoid steels are quite refractory in their transformations at high temperatures and persist in forming nonlamellar products even though they have been austenitized at temperatures well above those at which it is reasonable to expect all carbon concentration gradients would be dissipated. Mr. Grange has, therefore, made a useful contribution in pointing out that deoxidation with aluminum is a factor which plays an important part in determining the transformation product which results during the annealing of these steels.

But the author's discussion of the factors, composition and grain size, is not very convincing. He states that the absence of a lamellar structure in 3312 "is due to its relatively high percentage of alloying elements, chromium particularly". Yet on the same page he states, "all steels which contain chromium develop well formed pearlite". Incidentally we also have found that 3312 does not form a lamellar structure even when the steel is austenitized at temperatures as high as 1800 F (980 C).

Some years ago we made an effort to establish the effects of the various elements (up to about 0.5% concentration) on the tendency of the austenite to

[8] P. Payson, W. L. Hodapp and J. L. Leeder, "The Spheroidizing of Steel by Isothermal Transformation," TRANSACTIONS, American Society for Metals, Vol. 28, 1940, p. 307, Fig. 1.

[9] R. F. Mehl, "The Structure and Rate of Formation of Pearlite," TRANSACTIONS, American Society for Metals, Vol. 29, 1941, p. 827.

transform at high temperatures to a lamellar product. We were primarily interested in developing spheroidal structures and so we used fairly low austenitizing temperatures. We found for steels with about 0.30 to 0.80% carbon that chromium was particularly effective in decreasing the tendency for lamellar carbides to form; that the other carbide formers, molybdenum, tungsten, vanadium and columbium, had a similar effect but to a lesser degree; that manganese, nickel and silicon appeared to be neutral in this respect; and that aluminum definitely favored the formation of lamellar pearlite. In this study, the steels used were made in small induction heats and only very small additions of aluminum were used for deoxidizing them. Our data are not conclusive except in respect to the use of relatively low austenitizing temperatures and on this basis we would expect the carbide formers to limit the formation of lamellar pearlite. Residual carbides and carbon concentration gradients undoubtedly would be the important factor in this behavior.

Mr. Grange points out that his conclusions are based on relatively few heats and that they "are strictly valid only for the group of steels included in this investigation". It is well to emphasize this because it is not unusual to find among different heats of the same grade that the response to annealing, particularly in respect to the formation of lamellar pearlite, is not always the same.

In this discussion of the effects of alloying elements on the formation of pearlite it should be pointed out that the factor in melting practice which causes a steel to be abnormal in the familiar McQuaid-Ehn test is undoubtedly important, because that is how we define abnormality, viz., the tendency of a steel to avoid the formation of a lamellar structure, under the conditions where a lamellar structure is expected. Here the implication is that elements other than those we ordinarily see in an analysis report are responsible for the tendency of the steel not to form a lamellar structure. Furthermore, there is a phenomenon which is opposite in its character to abnormality in that it causes a distinctly lamellar structure to form at the rim of a hypereutectoid steel during an anneal which causes the rest of the bar to be completely spheroidal. At one time it was thought that this "picture-frame" pearlite was merely evidence of decarburization. But it is definitely something in addition to decarburization—something which involves the atmosphere surrounding the bar during the annealing operation.

Finally, the data presented by the author on the effect of grain size are not very helpful. He shows that coarse-grained steels tend to transform to lamellar carbides, but that fine-grained steels also may transform to distinctly lamellar carbides. Here again the effects of the "visible" elements may be overshadowed by the effects of the "invisible" ones. It still appears that the generalization presented as Rule 1 in "The Annealing of Steel"[10] is correct, namely, "The higher the austenitizing temperature, the greater is the tendency for the structure of the annealed steel to be lamellar, whereas, the closer the austenitizing temperature is to the critical (Ae_1) temperature, the greater is the tendency for the structure of the annealed steel to be spheroidal".

The author has made it clear that some steels will have a lamellar product when austenitized at a temperature not far above the critical whereas others will

[10] P. Payson, "The Annealing of Steel," published by Crucible Steel Company of America.

have a semipearlitic structure when austenitized at a temperature way over the critical. But this does not invalidate the rule. If a given austenitizing temperature causes a steel to have a lamellar structure, some lower temperature will cause this steel to have a semipearlitic or spheroidal structure, and if a given austenitizing temperature causes a steel to transform to a spheroidal product, a higher austenitizing temperature in hypoeutectoid steels will cause the transformation product to be more lamellar.

Written Discussion: By Edward A. Loria, Industrial Fellow, Mellon Institute of Industrial Research, Pittsburgh.

This paper is a most useful contribution to the literature on the isothermal annealing of hypoeutectoid steel. The writer is particularly interested in the effects of prior structure, banding and homogenization on the results obtained.

The initial structure of steel prior to austenitizing may be an important factor in this investigation. Normally, various proportions of lamellar and spheroidized carbide, depending upon the machinability characteristics desired, are used as starting structures for the hardening operation while some parts are heat treated from a hot-rolled or as-forged prior condition. Prior structure would be particularly effective where austenitizing temperatures are low enough that undissolved carbides and undissolved carbon concentration gradients would be present. In fact, austenitizing at a temperature that is somewhat lower than is normally used for that particular steel might have an effect, though it may be relatively minor in character. Welchner, Rowland and Ubben[11] studied the effect of spheroidized, annealed and normalized prior structures on the hardenability of several alloy steels and found that the spheroidized and annealed (coarser) structures, which showed the presence of undissolved carbides, gave an inferior depth of hardening. The author points out that on austenitizing at a relatively low temperature, carbides or small volumes of ferrite may remain undissolved in inhomogeneous austenite and favor transformation to a partially spheroidal structure. Also, in employing austenitizing temperatures only 200 to 300 F (95 to 150 C) above Ac_1, it is quite possible that carbon concentration gradients would still be present and would increase the rate of austenite-pearlite reaction at high transformation temperatures. In particular, carbon concentration gradients have an appreciable effect on alloy steels. Of course, it is difficult, if not impossible, to determine this under the microscope for the steel will appear homogeneous in all respects.

Different initial structures would give different TTT-curves, just as austenite grain size affects the type of curve one obtains. The effect of initial structure (i.e., pearlite spacing) on the austenitizing rate was considered by Roberts[12] who showed that, as the pearlite spacing decreases, the rate of nucleation and the rate of growth of austenite increases. In addition, Roberts showed that it is more difficult to form a homogeneous austenite in aluminum-killed steels compared with silicon-killed steels. In his studies on the rate of reaction to austenite he noted that fine-grained steel reacted much more slowly

[11] J. Welchner, E. S. Rowland and J. E. Ubben, "Effect of Time, Temperature and Prior Structure on the Hardenability of Several Alloy Steels," TRANSACTIONS, American Society for Metals, Vol. 32, 1944, p. 521-552.

[12] G. A. Roberts and R. F. Mehl, "The Mechanism and the Rate of Formation of Austenite from Ferrite-Cementite Aggregates," TRANSACTIONS, American Society for Metals, Vol. 31, 1943, p. 613-650.

at the same temperature, the coarse pearlite produced in coarse-grained steel having a slightly faster rate of austenite formation than even the finest structure produced in the fine-grained samples. The rate of austenitizing and the rate of homogenization in steel before quenching is different in each steel and is a variable which will affect subsequent heat treatment. The rate at which steel austenitizes depends on the prior structure. Alloy steels are much more sensitive to austenite heterogeneity since the alloy carbides deplete the austenite of the alloy it might have held in solution so that the steel, in reality, contains a lower alloy content than the over-all chemical analyses indicate. Banded transformation has an analogy in austenitizing. Banded austenite, particularly as to alloy content or impurities, occurs as elongated streaks. Segregation, in turn, affects nucleation and growth since the so-called austenite pools are elongated instead of spherical. It is apparent that practically all commercial hardenable steels, especially the medium carbon, low alloy steels, are banded. The degree of this banded condition may vary from heat to heat or from location to location within the ingot.

The author observes that in the present group all steels containing chromium develop well-formed pearlite, while all which do not contain chromium are "semipearlitic". Also, that other strong carbide-forming elements may possibly resemble chromium in this respect. It is therefore interesting to speculate on the effects of vanadium, titanium, and zirconium which are carbide-stabilizing elements. On the other hand, these elements also promote the formation of a fine grain size in steel. The question that naturally arises is whether vanadium, titanium and zirconium develop well-formed lamellar pearlite since they are strong carbide-forming elements or if there is no apparent effect since these elements, like aluminum, are also grain refiners in steel. The effect of chromium on pearlite formation at 1200 F (650 C) has been studied by Davenport[13] and Austin and Doig.[14] The effect of this element in first increasing and then decreasing the time for pearlite formation at 1200 F can be explained by the fact that chromium raises the Ae_1 point of a steel and also the pearlite nose. Though the nose is continuously pushed to the right by successive additions of chromium, it is also raised toward higher temperatures. Thus, if the 1200 F (650 C) level in the TTT-diagram of a steel of chromium concentration A is on the nearly horizontal portion of the upper side of the pearlite nose, an increase of chromium to concentration B may move the pearlite nose upward enough to produce a decrease in transformation or nucleation time.

Finally, it has been shown that the addition of aluminum to steel (during deoxidation) affects some of the finer details of the structure of the carbide constituent, particularly by tending to spheroidize the carbide and to produce what may be called an "abnormal" structure. It should also be noted that this spheroidal form of carbide is more easily graphitized.

Written Discussion: By James R. Blanchard, Climax Molybdenum Company of Michigan, Detroit.

Mr. Grange is to be congratulated on this very excellent paper. His data

[13]E. S. Davenport, "Isothermal Transformation in Steels," TRANSACTIONS, American Society for Metals, Vol. 27, 1939, p. 837.

[14]C. R. Austin and J. R. Doig, "The Suppression of Pearlite in Manganese-Molybdenum Steels," TRANSACTIONS, American Society for Metals, Vol. 36, 1946, p. 336-360.

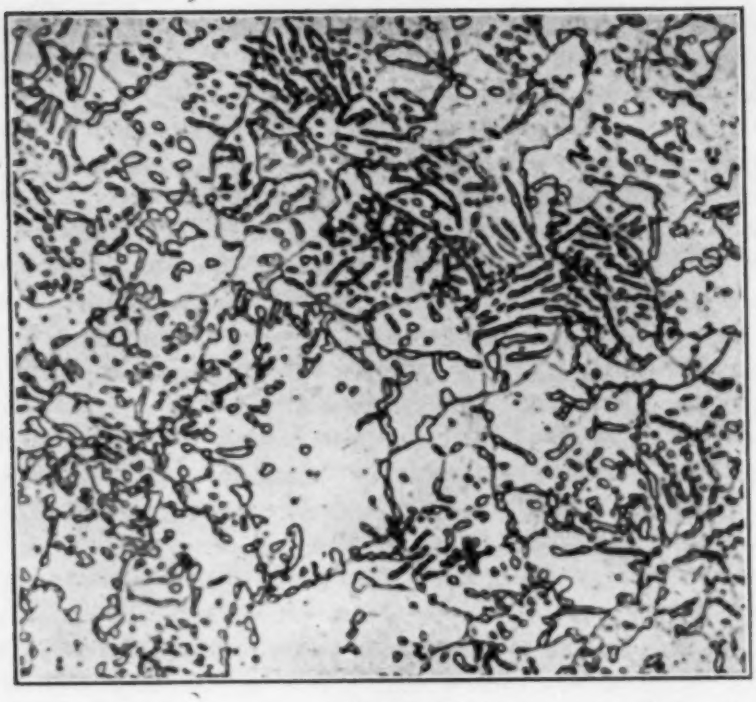


Fig. A—Structure of SAE 4330 Steel, Austenitized for 30 Minutes at 1550 F and Transformed at 1250 F in 8 Hours, Etched in 4% Picral. × 1500.

show that the decomposition of austenite to pearlite is even more complex than was previously supposed by most of us.

The author shows that a lamellar structure is obtained in chromium-bearing steels when they are transformed at temperatures near the Ae_1. This has not always been our experience. For example, we have found that a "semipearlitic" structure is produced in an aluminum-killed, fine-grained, SAE 4330 steel that has been austenitized at 1550 F (845 C) for 30 minutes and transformed at 1250 F (675 C) in 8 hours. This structure is shown in Fig. A. An examination of a water-quenched sample revealed that all the carbides had been dissolved. The heat treatments of the SAE 4330 steel and the author's SAE 4340 steel were nearly identical. There is a difference, however, in the prior condition of the two steels that probably is responsible for the apparently anomalous behavior at 1250 F (675 C). The SAE 4330 steel was in the annealed condition, whereas Mr. Grange's SAE 4340 steel was in the normalized condition. Welchner, Rowland and Ubben[18] found that the prior structure had a considerable effect on the hardenability of SAE 4340 and other steels. It is reasonable, therefore, to expect that the structures obtained on transformation to pearlite might also be affected by prior structure.

The "semipearlitic" structure has also been observed in carbon-molybdenum steels which were in the annealed condition before receiving a normal austenitizing treatment.

[18] J. Welchner, E. S. Rowland and J. E. Ubben, "Effect of Time, Temperature and Prior Structure on the Hardenability of Several Alloy Steels," TRANSACTIONS, American Society for Metals, Vol. 32, 1944, p. 521-551.

These data are presented because it is common practice to slow-cool an SAE 4340 steel after rolling to prevent cracking. A subsequent anneal might not produce a true lamellar structure unless the steel is normalized first.

Mr. Grange found no effect of aluminum on the formation of pearlite in the chromium-bearing steels. Is there an explanation for this?

Written Discussion: By O. W. McMullan, chief metallurgist, Bower Roller Bearing Co., Detroit.

The writer made use of the behavior of steels described in this paper in setting up annealing cycles for shot steels and similar grades during the war. Shot steel of 4150 composition is mentioned particularly because of the large quantity of bar stock mill annealed for high speed machining in automatic screw machines. That work substantially confirms the author's results although there are some points of difference. Mill cycles of course were not subject to such precise control and neither was isothermal annealing but the cooling of a furnace load of 20 to 50 tons approached isothermal conditions in some respects.

Most of the steels in this production work contained chromium but still exhibited the behavior of producing a more or less spheroidized structure after cooling from low annealing temperatures and lamellar when high temperatures were used. The behavior apparently is one of degree rather than totally different, such steels as plain carbon, chromium and manganese tending to be more lamellar than nickel-molybdenum steels, for example.

Neither did the change in commercial cycles appear to be sudden with increase of grain size as reported by the author. When annealed at just above the Ac_3 the structure might more properly be called semispheroidized with the lamellar plates present being short and heavy. Higher annealing temperatures produce increasing percentages of more and more distinctly lamellar structures.

An observation not reported by the author is that as the austenitizing temperature increases the lamellar spacing becomes closer, or at least such is the case with continuous cooling. There is evidence of this also in the author's Fig. 4 (a) and (b) where the lamellar structure is distinct at both temperatures. There is also a change in hardness as might be expected from the structural changes.

Mr. Grange did not discuss the practical side of the structural changes in his paper but the behavior reported is of considerable commercial importance, both as to machinability and physical properties of finished articles. High annealing temperatures to produce coarse-grained structures have long been advocated to provide better machinability. This especially in connection with carburizing steels such as SAE 4620 where improved machinability is claimed to be a result of a coarse grain size with little or no reference being made to the internal grain structure. The writer does not agree with this conclusion and has found it to be a mistake to merely produce a coarse grain size without considering other factors involved. High annealing temperatures improve the machinability of low carbon steels, not because of the coarse austenitic grain size but rather on account of the more brittle structure produced by lamellar rather than spheroidal carbides in a structure in which soft tough ferrite predominates.

With steels such as the shot steels mentioned, wherein lamellar pearlite tends to be considerably over 200 Brinell, the higher hardness produced by

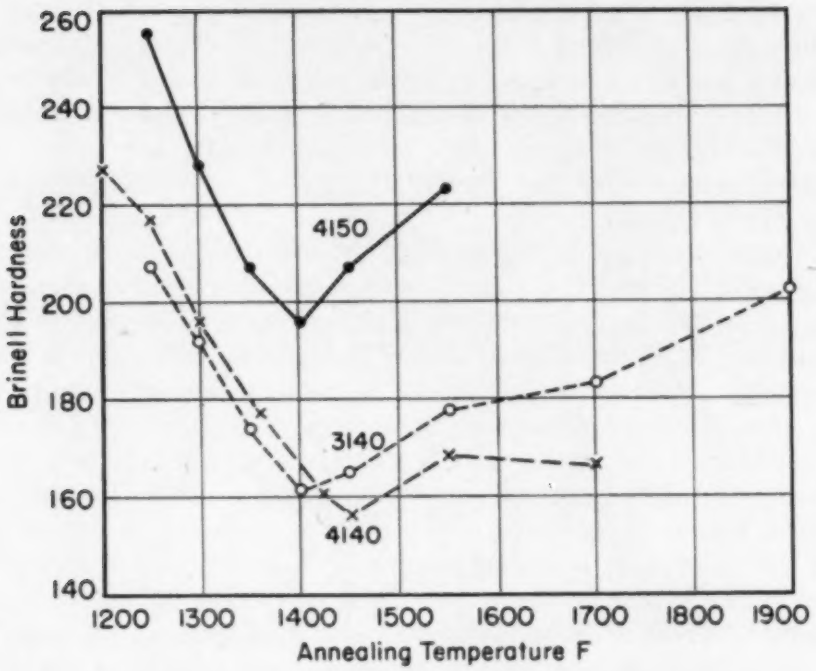


Fig. B—Graph Showing Hardness Results From Annealing Three Grades of Steel at Various Temperatures. The original condition was hot-rolled.

higher annealing temperatures (employing the usual cooling rates in commercial annealing) reduces machinability. Control of the maximum Brinell then becomes more important than obtaining a fully lamellar structure. Lower annealing temperatures which produce a partially spheroidized structure with heavy, widely spaced lamellae in the pearlite provide better machinability because the hardness is lower.

Fig. B shows hardness results from annealing three grades of steel at various temperatures. The original condition was hot-rolled. The increase in hardness in the pearlitic structures varies with alloy composition and carbon content, greater increase being shown as eutectoid composition is approached where hardness is dependent so largely on the condition of the pearlite. With some compositions of lower carbon content little or no increase in hardness occurred with the increase of annealing temperature as ferrite became predominant in the structure.

The annealed structure may influence final physical properties. This was particularly noticeable in induction-hardened shot steels because of the short heating time. The softer tougher structure of the low temperature anneal gave better impact properties to the shot than was obtained following the high temperature, distinctly lamellar anneal.

Written Discussion: By Arthur Levy, Pratt & Whitney Aircraft, East Hartford, Conn.

It struck me rather strongly that no mention was made of increased time at temperature (austenitizing treatment). It almost seems that there was a possibility of the existence of nonhomogeneous austenite at the normal (lower)

austenitizing temperatures. This may be the case because increasing the austenitizing temperature resulted in the formation of a more normal pearlite. It is true that increasing the temperature increased the grain size, yet there is no doubt in my mind that this treatment also increased he homogeneity of the austenite.

The author presented an anomaly on page 891 in the photomicrograph Fig. 4b. Here was SAE 1040 steel, austenitized at 2000 F (1095 C) and exhibiting coarser carbides than the same steel austenitized at 1750 F (955 C). How is this to be accounted for? Similarly, the photomicrograph of SAE 2340; Fig. 6, e and f. The author has previously stated that chromium was associated with the formation of fine spheroids within the pearlite; nevertheless, the nickel steel is shown to be capable of the same effect.

In the discussion of results, it is hypothesized that the submicroscopic particles of aluminum oxide or carbide were responsible for the formation of the semipearlite. Following the author's arguments it would seem more natural for this phenomenon to produce the fine spheroids rather than the coarse semipearlite.

I was very pleased to read this report, particularly because it tends to substantiate my belief that deoxidation and grain coarsening characteristics of steel have an effect on the austenite transformation.

Author's Reply

It is gratifying that most of the discussions accept the general idea that well-formed pearlite is sometimes difficult to develop on conventional annealing in modern commercial hypoeutectoid steels and that this difficulty is associated with deoxidation of the steel with aluminum. There is, however, some disagreement in regard to the influence of composition; in particular, Messrs. Payson and Blanchard both report the occurrence of "semipearlite" in steel containing an appreciable percentage of chromium (SAE 4345 and 4330, respectively), even when the austenitizing temperature was seemingly sufficient to dissolve all carbides in austenite. In view of these additional data, it seems advisable to conclude that "semipearlite" may sometimes result from transformation of fine-grained and reasonably homogeneous austenite containing an appreciable percentage of chromium; nevertheless, the data in the paper, as well as reports from those experienced in commercial annealing, point to the probability that hypoeutectoid steels without chromium, particularly those containing an appreciable percentage of nickel, are far more likely to give trouble in annealing to a structure of well-formed pearlite than steel with about 0.5% or more of chromium.

Our results, which indicate that chromium increases the tendency to develop well-formed pearlite when the austenitizing temperature is high enough to dissolve carbides, are not necessarily inconsistent with Mr. Payson's viewpoint that strong carbide formers promote a spheroidal or partly spheroidal structure when the austenitizing temperature is low. Presumably, development of the spheroidal type of structure is related to the prevalence of undissolved carbides, which are increased for a given austenitizing treatment when strong carbide formers are present, whereas the tendency to develop "semipearlite" from austenite free from undissolved carbides is due to a different basic mechanism.

A difference in the effect of chromium, depending on whether the austenitizing temperature is low or high, is to be expected and is somewhat analogous to the well-established observation that a strong carbide-forming element may decrease hardenability when most of the element and an appreciable part of the carbon in the steel are tied up in the form of carbides which remain undissolved in austenite, whereas it increases hardenability when carbides are dissolved by heating to a higher temperature. That is, depending on whether carbides are dissolved or not, such a carbide former may either increase or decrease hardenability, just as in the present instance chromium appears to decrease the tendency to form lamellar pearlite at low austenitizing temperature at which carbides are not dissolved but to increase this tendency at higher austenitizing temperatures.

The phrases from the paper quoted by Mr. Payson relative to the effect of chromium on the type of pearlite are only portions of sentences; if the entire sentences and the footnote on the page in question are read, the apparent inconsistency he points out will be greatly clarified. Nevertheless, we possibly did not make our view of the effect of chromium entirely clear and consequently welcome this opportunity to discuss it further. The difficulty arises from the inclusion of the SAE 3312 steel in our series of aluminum-killed hypoeutectoid steels; as explained in the text, this steel develops neither well-formed pearlite nor what we call "semipearlite". The structure of SAE 3312 represents a condition quite common in steels containing a relatively large percentage of chromium or molybdenum—namely, one in which well-formed pearlite cannot be developed by any heat treatment because the alloy content seems to preclude formation of perfect carbide lamellae and leads to the development of an aggregate structure in which many carbides are fine spheroids. Our experience indicates that well-formed pearlite forms in comparably annealed SAE 3340; hence it seems likely that less alloy may be required to promote the fine, partly spheroidal aggregate when the carbon content is low. In any event, the structure of the SAE 3312 is quite unlike that in steels we have designated "semipearlitic"; therefore, we regarded the structure of SAE 3312 as being just about as well formed pearlite as can be developed in this particular composition, and hence classified it as "well-formed pearlite" rather than "semipearlite". The classification of the variety of annealed structures into only two arbitrary groups when three types were indicated is the real basis for Mr. Payson's criticism; we feel, however, that such a classification is justified in this case because it so greatly simplifies discussion and, for the reasons given, does not affect conclusions regarding the factors which lead to development of "semipearlite".

We agree with Mr. Payson that the response to annealing of different heats of the same nominal composition is not always identical and believe that this is at least in part due to the difficulty of reproducing from heat to heat exactly the same conditions of deoxidation.

During the investigation it occurred to us, as it has to Mr. Payson, that there might be a correlation between the type of structure (degree of "normality") in the case of carburized steel and the tendency of a particular steel to develop "semipearlite". With this in mind, a sample of each of our steels was carburized and the case examined for type of distribution of ferrite and carbide. No correlation was found in the aluminum-killed steels since two of the steels

which developed "semipearlite" were more "normal" than the eight which did not. It was possible, however, to distinguish in this way between heats which had been deoxidized with aluminum and those which had not.

We believed that in the experiments described last in the text and summarized by the micrographs in Fig. 6 the effect of austenite grain size had been isolated from all other factors, including the effect of what Mr. Payson calls "invisible elements". In these tests, a large difference in grain size was produced in the same small piece of steel; consequently, there could have been no difference in composition and the austenitizing treatment, hence the degree of austenite homogeneity, was identical throughout the sample.[16] The observation that "semipearlite" formed in such a sample where austenite grains were small but not where they were large seems to us to be a reasonably clear-cut demonstration of the effect of austenite grain size isolated from that of any other factor. Judging from Mr. Payson's remarks about the effect of austenite grain size, it seems that he has disregarded the interrelated effect of mode of deoxidation. The generalization cited by Mr. Payson as his "Rule 1" no doubt applies to steels austenitized within the temperature range in which carbides are incompletely dissolved; however, when carbides are dissolved, the data presented in the paper indicate that factors other than the temperature to which steels are heated affect the annealed microstructure.

We agree with Mr. Loria that prior structure may affect the annealed microstructure; however, our investigation dealt with factors which influence the annealed microstructure when carbides were dissolved, at least to the extent that they were not microscopically visible, and the principal effect of a coarse prior structure would be to increase somewhat the minimum temperature necessary to dissolve all carbides. The precise effect of carbon concentration gradients and austenite homogeneity on the annealed microstructure must, of course, remain largely in the realm of speculation since no means are available at present for qualitatively evaluating them. Generally speaking, it seems likely that an austenitizing treatment carried out 100 F or more above the minimum temperature necessary to dissolve microscopically visible carbides in a given sample would produce reasonably homogeneous austenite, although complete homogeneity is probably an ideal state which in practice can be approached but never quite attained.

Mr. Blanchard's observation that "semipearlite" occurs in SAE 4330 steel and also in plain molybdenum steels is a welcome addition to the data in the paper. His data indicate that "semipearlite" may be formed more readily when the steel is initially in the annealed rather than in the normalized condition. We would expect, however, that prior structure would be an important factor only at temperatures within a limited range just above the minimum necessary to dissolve all carbides in a normalized steel. With respect to Mr. Blanchard's question as to why "semipearlite" is less likely to form in steel containing chromium, we can suggest no answer other than the rather inadequate one proposed in the last paragraph of the section of the paper titled "Discussion of Results".

---

[16] It is possible that forging after austenitizing at 2000 F may have slightly increased homogeneity; if so, the "semipearlitic" portion was, if anything, the more homogeneous.

Mr. McMullan very pertinently points out some of the practical implications associated with the character of the annealed structure—a subject on which we have much less experience than he. His observation that in continuously cooled steel the interlamellar spacing of pearlite decreases with increasing austenitizing temperature is confirmed by our experience; it is believed to be due to the fact that an increase in austenite grain size, which accompanies a higher austenitizing temperature, increases the time required for austenite to transform to pearlite and thus causes a given steel, cooled at a particular rate, to transform at a lower average temperature with consequent finer pearlite. Mr. McMullan's observations with respect to annealing SAE 4150 steel would seem to involve, at least in part, austenitizing temperatures too low to dissolve all carbides, since, as ordinarily austenitized, carbides are seldom completely dissolved in this grade of steel.

It is true, as Mr. Levy points out, that no study was made of the effect of varying time of austenitizing; increasing the austenitizing time several fold would, however, probably be equivalent to only a slight increase in austenitizing temperature. In the range of temperature investigated, it is doubtful whether any of the steels were sufficiently inhomogeneous in the austenitic condition to make homogeneity an important factor; certainly the micrograph shown in Fig. 6a demonstrates that "semipearlite" can form from relatively homogeneous austenite, since this sample was austenitized at 2000 F (1095 C).

The micrographs in the paper represent only a portion of a single field at × 1000; any seeming anomaly arising from minute inspection of detail in them is due to the selection of the field rather than to a corresponding real difference in over-all microstructure. With respect to Mr. Levy's suggestion that submicroscopic particles which might serve as nuclei for carbide precipitation ought to promote fine spheroids rather than massive carbides, we should like to point out that the size of the individual carbides is determined by the temperature of their formation rather than by the number of potential nuclei present in the steel.

In conclusion, we wish to thank those who have contributed discussions, all of which help to emphasize in a general way our lack of complete understanding of the process of austenite transformation and of all the factors which influence it. Obviously, a great deal more work remains to be done in this field.

COPPER-TITANIUM ALLOY COATINGS ON MILD STEEL

By Edward J. Chapin and Carle R. Hayward

Abstract

An exploratory study was conducted on the coating of mild steel with copper titanium alloys of several compositions by the application of heat in a protective atmosphere. The methods used in applying the coatings are described. Alloy compositions ranging from about 5% to about 37.5% titanium were investigated to determine the coating composition which would produce the best spreading and surface characteristics. This was found to be of approximately eutectic composition or about 25% titanium content.

The observations made on metallographic examination, microhardness determinations, bend, corrosion, diffusion and nitriding experiments are presented. The results obtained show that copper titanium alloy coatings of eutectic composition have interesting properties which include a high silvery luster, exceptional hardness though somewhat brittle, a dense texture and a possible favorable resistance to corrosion.

Introduction

TITANIUM as a commercially useful metal is best known in its use as a deoxidizer, scavenger, hardener and grain refiner. Its use in the metallic state for purposes other than those mentioned seems to be wholly lacking. It would seem that a greater use of this element should be logical from a standpoint of abundance of raw material. It is estimated (1)[1] that the occurrence of titanium in nature amounts to from 0.3 to 0.45% of the earth's crust. From a standpoint of quantity, it ranks tenth in the list of elements contained therein. Whereas from the standpoint of those elements which in pure metallic form are suitable for mechanical and structural use, it ranks fourth and is exceeded in abundance only by aluminum, iron and magnesium.

In a pure state the element resembles pure iron, while if impure it resembles cast iron in appearance though the hardness is not as

[1]The figures appearing in parentheses pertain to the references appended to this paper.

Of the authors, Edward J. Chapin is metallurgist in the nonferrous section, Naval Research Laboratory, Washington, D. C., and Carle R. Hayward is professor emeritus of process metallurgy, Massachusetts Institute of Technology, Cambridge, Mass. Manuscript received August 26, 1946.

great as that of cast iron. It is only 60% as heavy as wrought iron per unit volume while the physical properties are similar.

The element is characterized by an extreme degree of chemical activity at room temperature when in a finely divided condition. In the massive state this activity is displayed only at high temperatures. The powdered metal burns readily in air with incandescence similar to that displayed by magnesium. It also burns in nitrogen and the halogens and forms quite stable sulphides and carbides, although these are subject to oxidation at high temperatures. Titanium, being a transitional element, also forms hydrides with hydrogen which are stable at ordinary temperatures but which dissociate at red heat liberating the hydrogen and leaving the metallic titanium in a very active condition.

Alloys are formed with such metals as aluminum, manganese, iron, cobalt, nickel, copper, zinc and gallium. Wartman (1) mentions that titanium in alloying with other elements tends to form compounds that are insoluble in the solid state or if solid solutions are formed the tendency is toward those which are stable only in the liquid state. Such conditions favor the formation of brittle alloys of little structural value.

The coating of one metal by another through the application of heat is well known. For example, the commercial processes for coating iron surfaces with copper under the application of heat depend on the fact that a thin layer of copper will spread by capillarity over the iron if the temperature of the latter is above the melting point of copper and in a hydrogen atmosphere. Similarly, titanium will spread over copper by capillarity, as discovered and described by Alexander (2), under suitable conditions of temperature and protective atmosphere to produce a silver-like surface coating on the copper base which is quite resistant to oxidation. It seems that when solid copper and powdered titanium, preferably in the form of titanium hydride, are heated in contact with one another the hydride dissociates liberating hydrogen, while the titanium and copper diffuse one into each other at red heat to form a low melting point alloy, a eutectic, at the point of contact. If the heating is continued for several minutes the titanium will spread by capillarity over the surface of the copper, forming a surface coating consisting of an alloy of copper and titanium. The temperature used governs the composition of the alloy that will form and spread by capillarity, the minimum being the melting point of the eutectic, 878 C. This unusual circumstance is

unique; since copper has a melting point about 700 C lower than titanium it would appear that copper would be reduced to a liquid condition prior to the melting of the titanium.

Titanium does not form low melting alloys with metals of the iron group and therefore will not spread over these metals at low temperature as it does with copper. However, the iron group metals can first be coated with copper and this can then be made to react with titanium to produce an alloy coating of copper-titanium on the iron group base metal. Alexander mentions further in describing his process that, upon prolonged heating of the coating in contact with the base metal, diffusion of the surface alloy into the base metal will take place. This diffusion zone can be further heat treated with carbonaceous material to carburize it or with boron compounds to boronize it thereby producing titanium carbide and titanium boride, both very hard compounds.

The value of protecting iron and steel by various metallic coatings is well recognized. The possibility that copper-titanium alloy coatings on steel might have useful applications and the lack of any data on these coatings led to this investigation. The work undertaken included coating experiments on copper-plated steel samples conducted according to the process outlined by Alexander and already mentioned. Further, coating experiments were conducted on copper-plated and unplated steel samples in which a predetermined copper-titanium content mixture was heated in contact with the base metal. The titanium content of these mixtures ranged from approximately 5 to 37.5% with the balance copper. With this method the steel samples did not have to be copper plated to produce a copper-titanium coating. In addition, experiments were conducted to determine the feasibility of producing a copper-titanium coating on steel using a powdered master alloy that had been previously melted and then crushed. Considerable attention was given to the preparation of samples, especially those factors that contributed toward contamination of the titanium. Microstructures of the various copper-titanium coatings obtained were studied metallographically and the more typical were photographed and are presented in the text. Microhardness tests were made with a Tukon tester and the hardness characteristics of various constituents and zones occurring in both the alloy coatings and base metal were studied. The resistance of the various alloy coatings of titanium copper on steel to a 10% NaCl solution was studied. Some experiments were made on prolonged

heating of copper-titanium alloy coatings on both iron and steel. The results of these were studied metallographically and some interesting photographs were obtained showing the diffusion structure. A qualitative analysis of the extent of diffusion of copper and titanium in the iron-base metal was considered spectrographically and chemically with some X-ray diffraction observations on the interface zone between coating and diffusion structure. Nitriding experiments were conducted on some samples into which copper-titanium had been diffused to observe the effects of such treatment. Several coatings were subjected to bending to determine the effects of this on the stability of the coatings and their adherence to the base metal.

Discussion of Previously Recorded Work

Very little appears in the literature concerning the use of metallic titanium as a coating material on other metals. Alexander's process (2) has already been mentioned. Travers (3) attempted to coat iron with titanium by a high temperature treatment in titanium tetrachloride, $TiCl_4$, but was unsuccessful. A thin film of titanium nitride formed above 1000 C (1830 F) in a hydrogen atmosphere. The nitrogen was present as an impurity in the hydrogen. In hydrogen purified over calcium-magnesium, titanium tetrachloride gave a coating of metallic titanium which only retarded the corrosion of iron.

The properties of the element titanium are of such a nature that a short review of what has been found is considered worthy of mention. Kroll (4) found that oxygen-free titanium in a rolled state had a hardness of Rockwell C-20. After melting it in a 99.6% argon atmosphere the hardness rose to Rockwell C-35 due to absorption of minute quantities of oxygen and nitrogen. The metal is reported to absorb considerable quantities of both gases with a probability of suboxide and nitride formation. These gases cannot be removed by remelting in either hydrogen or a vacuum nor can they be removed by deoxidizing with carbon or thorium. Carbon, like oxygen and nitrogen, renders the metal very hard and brittle. Titanium has a mean coefficient of expansion of 97.9×10^{-7} between 0 C and 850 C (1560 F). It undergoes allotropic transformation at 880 C (1615 F) from hexagonal to cubic symmetry. Fast (5) established the melting point of titanium at 1725 C (3135 F). He also observed the allotropic transformation at 880 C (1615 F) and noted that the metal absorbed oxygen and nitrogen upon heating and became brittle as a result.

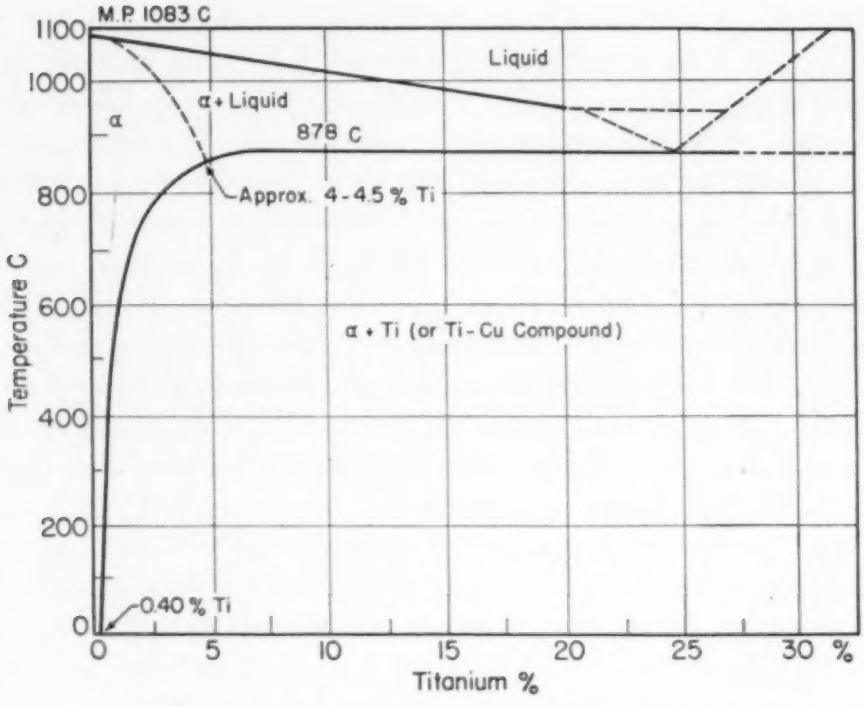


Fig 1—Copper-Titanium Equilibrium Diagram—*Hensel and Larsen.*

The crystal chemistry of several titanium alloys was investigated by Laves and Wallbaum (6) who reported alloys were formed with manganese, iron, cobalt, nickel, copper, zinc and gallium. Those alloys with low titanium content formed the following compounds: $TiMn_2$, $TiFe_2$, $TiCo_2$, $TiNi_3$, $TiCu_3$, $TiZn_3$, and probably $TiGa_3$. The first three are of the 12/6 co-ordination number type while the next three are close-packed structures with $TiCu_3$ being a deformed hexagonal type. Those alloys with intermediate titanium content formed compounds of the CoCl type: FeTi, CoTi, etc., with CuTi nonexistent. With excess titanium content isomorphous compounds were formed: $MnTi_2$, $FeTi_2$, $NiTi_2$, and $CuTi_2$. These are face-centered cubic structures with 96 atoms per cell.

Data on copper-titanium alloys deal almost entirely with the physical properties of copper alloys of low titanium content. The copper-titanium equilibrium diagram is quite incomplete. Kroll (7) determined the copper-titanium eutectic composition to be 24% titanium. Hensel and Larsen (8) constructed a tentative equilibrium diagram from cooling curves obtained from a thermal analysis. This is reproduced in Fig. 1. Their X-ray investigations on copper-titanium alloys ranging from 0.83 to 27.27% titanium showed that lines belonging to a face-centered cube were strongest on all diffrac-

tion pictures. The lattice constant increased from 3.60 Å for pure copper to 3.65 Å for the 20.53% titanium alloy. A solid solution of titanium in copper was indicated with the same space lattice as that of pure copper. With increasing amounts of titanium new lines corresponded mostly to pure titanium with the first alloy to show these new lines containing 7.72% titanium. Not all of the lines could be matched with the titanium structure so that the extra lines may have represented a copper-titanium compound. The age hardening characteristics studied by these investigators showed that copper-titanium alloys would age within certain concentration limits. After quenching from 900 C (1650 F) and aging for 1 hour, aging started at 250 C with the optimum temperature being between 400 and 450 C. Above 500 C (930 F) the hardness decreased.

Jones (9) in investigating the influence of diffusing elements upon the alpha-gamma inversion of iron found that titanium when allowed to diffuse into iron between 1000 and 1300 C (1830 and 2370 F) did so by the production of a diffusion boundary and a columnar ferrite diffusion growth from which he concluded that the binary system Fe-Ti included a gamma loop. That titanium promotes a ferritic structure is indicated by a number of investigators who added titanium to austenitic steels. Kase (10) in a study of metallic cementation examined the penetration of titanium into iron, nickel and copper by means of a ferrotitanium alloy at temperatures from 800 to 1300 C (1470 to 2370 F). He noted that the rate of diffusion increased with increase in temperature and in the case of iron abruptly so at the Ar_3 point. He observed that the cemented surface became harder than the base metal but no advantage resulted regarding corrosion resistance. Laissus (11) obtained diffusion of titanium into iron using ferrotitanium powder containing 33.42% titanium and 8.37% carbon. Microexamination showed the formation of a border of columnar crystals of Fe-Ti solid solution which was less readily attacked by the etching reagent.

Apparatus and Materials Used

The steel used in the experimental work was not of the quality desired but wartime conditions prevented wider choice. The mild steel used included AISI designation C 1020 hot-rolled and C 1022 cold-finished. It was supplied in flats 1 inch wide and in thicknesses of ⅛, ¼ and ½ inch. The suppliers' general analysis for this material was as follows:

	C	Mn	P	S
C 1020	0.18-0.23	0.30-0.50	0.04	0.05
C 1022	0.18-0.23	0.70-1.00	0.04	0.05

Armco iron was used in some experiments to determine the effects of prolonged heating of alloys of copper-titanium in contact with this base metal. The analysis of this was approximately as follows: C, 0.02; FeO, 0.25; S, 0.015; Si, nil; P, 0.005; Cu, 0.165; Mn, 0.025.

The source of powdered titanium used in all of the experiments was powdered titanium hydride about 300 mesh. The formula of this compound was taken as TiH_2 in all computations. This material was also used as a "getter" for oxygen and nitrogen and for a source of hydrogen in some of the earlier work.

Pure copper powder, stearate covered and precipitated copper powder which was deoxidized with hydrogen was used for compounding the copper-titanium-hydride powder mixtures that formed the basis for the various titanium content alloy coatings that were applied to steel. The copper powders were as finely divided as the titanium hydride used in conjuction with them.

The solvents used for the removal of grease from the steel samples included benzine, trichlorethylene and carbon tetrachloride. Mill scale was removed from the samples by making them the cathode in an electrolytic pickling cell containing 25% sulphuric acid by weight and passing a current of 7.5 amperes per square decimeter at 2 volts for about 5 minutes. Distilled water was used for all rinsing and washing purposes and for making up various aqueous solutions used.

The unsatisfactory results obtained in the earlier experiments indicated that the steel surfaces had to be meticulously clean and free from contaminants. Thus the steel samples were bright annealed in a hydrogen atmosphere, some at 750 C (1380 F) and others at 850 C (1560 F). This treatment not only annealed the base metal but it also removed all surface oxidation and slightly decarburized the surfaces as well. This work was done in the same apparatus as that used for the coating experiments which will be described presently and need not be repeated here.

Copper coating of the steel samples was done electrolytically from a Rochelle salts copper-cyanide bath containing 10 liters of solution. This solution contained 260 grams CuCN, 350 grams NaCN, 300 grams Na_2CO_3, and 450 grams $NaKC_4H_4O_6 \cdot 4\ H_2O$. The

plating bath was heated by an electric immersion heater and a temperature of 75 C maintained. The current density nominally employed was 7 amperes per square decimeter at 2.7 volts.

The apparatus used for the coating of steel samples with copper-titanium alloys by the application of heat is shown schematically in Fig. 2. It consisted of a specimen chamber A which was a 1½-inch diameter by 24-inch long fused quartz tube sealed at one end. The open end was stoppered with a two-hole rubber stopper which was

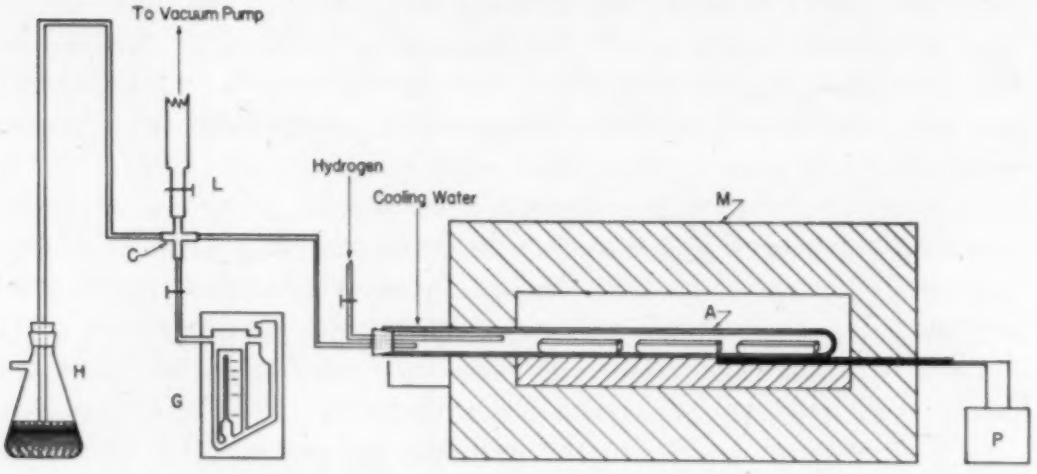


Fig. 2—Schematic Diagram of Apparatus Used for Coating Steel Samples With Copper-Titanium Alloys.

tied securely by strings cemented to the tube and in addition was water-cooled when in operation. The upper outlet of the tube was connected to a hydrogen cylinder. This line contained two drying tubes with one containing calcium chloride and the other a mixture of phosphorous pentoxide and granular pumice with the hydrogen flow passing through the calcium chloride first. The lower outlet of the quartz tube was connected to a 4-way ½-inch pipe fitting, "C". This line was used for evacuating and for the escape of excess hydrogen over the pressure regulated by a mercury seal. A second branch of the 4-way fitting was connected to a Stokes Machine Co. Flosdorf modification McLeod vacuum gage, "G". A third branch of the fitting was connected to a mercury column and seal, "H". This was made up of a ⅜-inch diameter glass tube 36 inches long inserted into a 500-cc. suction flask containing mercury. One end of the glass tube was immersed into the mercury to a depth of 1 inch. This device was used to prevent air from entering the system, yet it afforded a means of excess pressure of hydrogen over that desired to escape. The fourth branch of the 4-way fitting was connected to a rotary oil

vacuum pump with a rated capacity of 12.47 cubic feet per minute at a speed of 430 rpm. A blank-off valve was provided at position "L". Heavy-walled rubber tubing, 3/8-inch hole, was used for all flexible lines.

The furnace "M" had an interior opening 5 inches square by 16 inches long. It was heated by 4 Globar elements placed lengthwise in each corner of the 5-inch square. The power supply for the operation of the furnace was regulated by a switchboard arranged in 10-volt steps from 0 to 220 volts.

Temperature measurement was through a chromel-alumel thermocouple introduced into the back end of the furnace and recessed into the middle of the brick support upon which the quartz tube rested while in the furnace. In position the quartz specimen tube and the thermocouple protecting tube were in contact and the end of the thermocouple was very nearly at a point directly below the midpoint of the two samples. Temperatures were recorded in millivolts by a potentiometer, "P".

Experimental Procedure

Before reasonable results could be obtained suitable procedures had to be worked out experimentally for the preparation of the steel samples prior to coating them and for the actual coating operation.

A 4-inch length was used on all steel samples. Upon removing grease and scale one surface of the 1-inch flat was ground smooth on metallographic grinding belts. This provided the surface which was subsequently coated with a copper-titanium alloy. The samples were then bright annealed in hydrogen, some at 750 C (1380 F) and others at 850 C (1560 F) from 1 to 4 hours, with 1 hour appearing sufficient to thoroughly clean the surfaces of all oxides and to provide slight decarburization. Cooling of the samples was slow and a protective atmosphere was maintained throughout this operation. At this point some of the samples were copper plated while the others were coated directly by heating a powder mixture of copper and titanium hydride.

The samples to be copper plated were first given a dip in a sodium cyanide solution containing 45 grams NaCN per liter and then rinsed in cold distilled water before hanging them in the plating bath. This bath preheated to 75 C and maintained at this temperature deposited 0.0006 inch of copper in 15 minutes quite consistently.

Various thicknesses of copper plate were produced ranging from 0.0005 to 0.0025 inch. The deposits obtained were fine-grained and smooth with little or no blistering in evidence. The thickness of the copper deposited was determined by taking the total weight of the copper deposited and the total surface area into consideration, and calculating the thickness from this.

In those experiments where a copper-titanium coating was to be obtained by the reaction between titanium hydride and copper plate on steel, the method of applying the titanium hydride in a thin, well distributed layer was to first make a suspension of the hydride in a vehicle of reagent alcohol, then to apply this suspension with a small marking brush to the copper surface previously preheated to about 60 C to promote rapid evaporation of the vehicle. Thicker layers of the hydride could be produced by repeating the application of the suspension as many times as was desired. Another method of applying the hydride was tried which was to dust the copper surface with the hydride. However, this proved troublesome from a handling standpoint.

In those experiments where an alloy coating of copper-titanium was produced from heating a copper-titanium hydride powder mixture applied to copper-plated and unplated steel samples a similar technique to that described above was tried but was discarded in favor of a dry method. The compounding of the desired copper powder titanium-hydride mixture consisted of weighing out both ingredients separately then mixing them thoroughly in a mortar. The mixture thus obtained was applied to the surface of the sample by totally enclosing it with a collapsible steel mold leaving only the surface exposed that was to receive the mixture. This exposed surface was adjusted about 1/16 inch below the top of the mold, thus forming a receptacle with the sides of the mold. The mixture was then placed into this receptacle, compacted and smoothed level with the top of the mold. The mold was then removed and the edges of the deposited layer were bevel trimmed. Since this investigation was primarily concerned with the feasibility of producing copper-titanium alloy coatings on steel no attempt was made to restrict the thickness of the coatings to a certain definite amount. The method of applying the powder mixtures to the steel samples was such that no accuracy in thickness or composition could be expected at best.

The formation of the coating of a copper-titanium alloy by the application of heat followed the same procedure in all of the experi-

mental work. It was found that only two samples could be treated at one time. The samples were supported on combustion boats which contained titanium hydride and were placed into position as far as they would go in the tube. In front of the samples a nest of three combustion boats containing titanium hydride was placed to protect the samples against any ingress of oxygen or nitrogen during the crucial heating period. The rubber stopper was then inserted and tied securely. The hydrogen inlet into the tube was normally kept closed off except when it was necessary to supply gas from the cylinder. The tube was then alternately evacuated down to about 20 microns pressure and flushed with hydrogen four times to remove all air. Hydrogen was allowed to fill the system until a pressure of 1 inch of mercury above atmospheric prevailed as regulated by the mercury seal. The hydrogen flow was then cut off and a static atmosphere allowed to prevail.

The tube and its contents was then placed into the furnace which was preheated to the desired temperature. As the tube heated, evolution of hydrogen occurred coming from the titanium hydride being dissociated by heat. This evolution generally was observed to cease when a temperature of 900 C (1650 F) was reached. Usually the hydrogen atmosphere was static during the holding period at the desired temperature which ranged from about 900 C (1650 F) to about 1100 C (2010 F), depending on the nature of the experiment. When cooling of the tube started, the dissociated titanium began to absorb the hydrogen from the system. If this was allowed to continue without supplying gas from the cylinder, vacuum conditions were soon created. Thus to prevent the ingress of air, sufficient gas was allowed to enter the system to maintain the necessary overpressure of hydrogen. When a temperature of about 500 C was reached the tube was removed from the furnace and allowed to cool in air. The tube remained closed and the contents were not removed until the whole had reached room temperature.

Discussion of Results Obtained

Early attempts to produce metallic copper-titanium alloy coatings on copper-plated steel by heating powdered titanium hydride in contact with the copper resulted in the oxidation of the titanium before a metallic coating could be formed. Instead a black layer was produced which could not be rubbed off or dislodged easily. To correct this

condition, an atmosphere excluding air by using hydrogen at a pressure greater than atmospheric was used rather than a vacuum to prevent oxidation from this source. Contaminants which were liable to occur in the copper plate and in the base metal had to be avoided or removed to prevent oxidation of the titanium. Adsorbed gases within the specimen tube had to be removed by alternate evacuation and flushing with hydrogen to prevent oxidation from still another source. When oxygen and nitrogen-free conditions prevailed it was possible to obtain metallic copper-titanium alloy coatings with considerable ease.

The first series of experiments to be considered of which a few are tabulated in Table I were conducted by heating the titanium hydride in contact with copper-plated steel. The method of applying the hydride has already been mentioned and need not be repeated

Table I

Sample Number	Copper Plate Weight Grams	Copper Plate Thickness Inches	TiH_2 Weight Grams	Temperature of Run C	Temperature of Run F	Time Minutes
620	0.374	0.0006	0.165	952	1745	17
652	0.281	0.0005	0.175	1005	1840	17
644	1.033	0.0018	0.265	978	1795	10
650	1.119	0.0019	0.335	975	1785	10
666	1.229	0.0022	0.975	1010	1850	16
646	1.096	0.0019	0.274	907	1665	14
670	0.258	0.0005	0.155	954	1750	22

here. Attempts were made to vary the amount of hydride applied to observe the effects. The temperatures used were commensurate with the fact that at a given temperature only an alloy of definite copper-titanium composition will form and spread by capillarity. To illustrate this and referring to Table I, let us take sample number 620 as an example: with the amount of copper and titanium that is in contact, an alloy coating should form composed of approximately 69% copper and 31% titanium by weight. Likewise the composition of the coating of sample number 646 should be approximately 80% copper and 20% titanium, while that of sample number 666 should be 56% copper and 44% titanium. It should be noted that the temperatures used followed the trend of the alloy formation with the higher temperatures being employed for the higher titanium content. In each of these experiments bright, shiny, silver-colored metallic coatings were produced.

The surface characteristics indicated that spreading of the alloy

formed was not uniform, so that the surfaces upon close scrutiny appeared uneven. In addition, small bumps scattered at random added to this unevenness. Some of these had ruptured tops which gave them the appearance of minute craters. Most of the coatings showed some flaking of the surface which occurred immediately upon removal of the samples from the tube and exposure to atmospheric pressure. These flakes proved to be very hard but also very brittle.

Sample number 646 apparently had insufficient titanium present and the coating produced had not completely spread so that some coppery patches were in evidence, while the coating of sample 666 apparently contained excess titanium with the copper-titanium eutectic wetting the copper plate down the sides, ends and bottom of the sample. The wetted copper plate appeared silver colored in the affected area and no appreciable difference in thickness could be found between that of the unaffected copper plate and the silver-colored wetted areas. This wetting action seemed to have drained the lowest melting point alloy, the eutectic, from the original surface and what was left behind appeared rough and disturbed. This residue apparently was composed of material whose melting point was higher than the temperature employed and therefore it froze immediately after its formation. The formation and fusion of such material under these conditions presents a difficulty in justifying its existence unless the reaction is exothermic. This point will be considered a little later. Generally excess titanium in the coatings was evidenced by the presence of a hard, silvery surface of very high metallic luster. Whereas the copper-titanium eutectic produced a surface that was silver colored yet softer in hardness and in luster. Flaking already mentioned occurred on most of the coatings that were very thin and which displayed a very high metallic luster, and which indicated a compound of high titanium content. This flaking was probably caused by pressure of gas pockets underneath the coating.

The microstructures of these coatings were quite difficult to resolve into definite constituents. They appeared generally as a single white unetched microconstituent which was not attacked by H_2O_2 in NH_4OH and only moderately by $FeCl_3$. Attack was easy with 0.5% HF solution which would indicate free or high titanium content. The brittleness added to the difficulties of microsectioning.

Microhardness measurements made with a Wilson Tukon tester on the various microsections showed in general that titanium in alloying with copper tends to form hard but brittle compounds. As

nearly as could be ascertained the hardness of the material contained in the flakes mentioned above gave a "Knoop" hardness number of 1030. If this value was convertible to Rockwell hardness values it would be in excess of C-70. Hardness measurements, made in places where the coating appeared to have spread smoothly and did not possess the very high luster, gave a "Knoop" number of about 565 or a Rockwell equivalent of C-52. If this hardness could be retained and the brittleness eliminated, these coatings would have considerable merit. In the areas where the copper plate had been wetted by the copper-titanium eutectic alloy, a "Knoop" hardness number of about 250 was obtained or a Rockwell equivalent of C-15. If this wetting action could be promoted to take place on a large scale on copper-plated steel, a desirable coating would be formed which would be decidedly tight and impervious to aqueous solutions and abrasion resistant as well. The unwetted copper plate was of course soft and gave a "Knoop" number of about 85. The intermediate layer between the coating and base metal at the interface appeared to be hard but measurement of this detail was not possible due to its thinness.

Subjecting the coated samples to total immersion for 7 days in a 10% NaCl solution, maintained at 35 C and saturated with air, disclosed that the copper-titanium alloy coatings were resistant to this solution under the conditions used. No appreciable attack of the coatings by the solution could be detected microscopically nor was any electrolytic action apparent between the coating and the thin, hard intermediate layer. However, where the base metal had been exposed through pores in the coatings, caused by ruptured gas bubbles, corrosion of the base metal occurred. This corroding action was of the pitting type with the copper-titanium alloy coatings and the thin intermediate layer decidedly cathodic with respect to the base metal. Susceptibility of a protective coating to this type of corrosive action is of course undesirable where corrosion is a factor.

Although metallic coatings of high luster with appreciable hardness resulted, the tendency for titanium to form brittle compounds with copper rather than extensive solid solutions seemed to be quite evident. The limited solid solubility of titanium in copper and presumably the even more limited solid solubility of copper in titanium would predispose any alloys formed to appear in the form of brittle intermetallic compounds. Since it was difficult to control the amount of titanium hydride in the layer on the copper plate with its limited amount of copper, an excess of titanium over an amount necessary for

a eutectic composition generally prevailed. Thus the resulting surface alloy formed was presumably governed by the amount of titanium present since only a limited amount of copper was available. Where flaking had been observed to occur a very thin surface also prevailed which had a very high metallic luster and also a high hardness accompanied by decided brittleness. It is assumed that these coatings were composed entirely of a high titanium-intermetallic compound. The spreading characteristics of these alloys appeared limited and they appeared to have solidified very quickly after their formation. Where the composition of the alloy formed seemed to be either eutectic or slightly hypereutectic it displayd a great tendency to spread by capillarity if copper was available adjacent to the molten alloy. This characteristic suggests that dipping of copper-plated steel in a molten bath of eutectic composition of copper-titanium alloy should produce a coating in which the copper plate would be readily wetted and its pores sealed tight.

Coatings Obtained With Various Mixtures of Titanium Hydride and Copper Powder Applied to Copper-Plated and Unplated Steel Samples

Since a copper-titanium alloy composition of about eutectic proportions appeared to have the best spreading qualities it was decided to examine this by a series of experiments in which a number of copper powder titanium hydride mixtures were used. This method provided a means of studying the characteristics of various copper-titanium compositions and their structures. It also provided a means of observing the wettability of copper-titanium alloys on unplated steel. The mixtures used included the following percentages of titanium hydride by weight: 5, 10, 15, 20, 25, 28, 30, 36, 37.5%. The manner in which these mixtures were compounded and applied has already been described under the section on experimental procedure. Table II is a tabulation of the pertinent data on the various coatings obtained and is representative of the total work done.

No attempt will be made to discuss the results of each particular TiH_2 copper powder combination tried as this would be uninteresting. The results, however, are discussed according to the factors which seemed to affect the characteristics of the coatings.

The coatings produced from the powder mixtures containing 5, 10 and 15% titanium hydride were generally unsatisfactory. The

Table II-A

Run Number	Temperature C	Temperature F	Time at Temp. Hr.	Time at Temp. Min.	Sample Number	% TiH_2 in Mixture by Weight	Weight Mixture Applied Grams	Thickness Cu Plate Inches	Corrosion Tested in 10% NaCl
15	1072	1960	.	24	500	5.0	0.870	0.002	
					602		0.870	0.002	
27	1083	1980	.	14	408	5.0	1.119	0.002	
					401		1.896	....	
30	1083	1980	.	20	613	5.0	5.245	....	
					612		5.810	0.0005	
40	1070	1960	2	00	515	5.0	4.070	....	
					510		3.760	0.0004	
25	1078	1970	.	30	607	10.0	3.795	....	
					606		2.949	0.002	
39	1050	1920	.	10	514	10.0	4.190	0.0005	
					515		3.550	....	
20	1012	1855	.	25	107	15.0	2.545	....	
					106		2.135	0.001	
38	1037	1900	3	00	512	15.0	3.520	0.0005	X
					511		4.242	....	X
26	1095	1840	.	30	609	15.0	4.055	....	X
					608		4.593	0.0005	X

Table II-B

Run Number	Temperature C	Temperature F	Time at Temp. Hr.	Time at Temp. Min.	Sample Number	% TiH_2 in Mixture by Weight	Weight Mixture Applied Grams	Thickness Cu Plate Inches	Corrosion Tested in 10% NaCl
48	952	1745	.	40	634	30.0	2.690	0.0005	X
12	988	1810	.	20	600	30.0	2.770	0.0019	X
					601		2.775	....	X
36	1005	1840	4	00	508	30.0	....	0.0008	X
					509		....	....	X
43	972	1780	1	07	616	35.0	3.120	0.0025	X
					618		2.790	0.002	X
13	975	1785	.	25	402	36.0	2.270	0.002	X
					400	37.5	2.170	0.0018	X
						Precast Alloy			
46	1062	1995	.	17	626	28% Ti	3.875	0.0005	X
49	1049	1920	1	05	625		3.550	....	X
51	1041	1905	.	15	638		4.438	0.0017	X

Table II-C

Run Number	Temperature C	Temperature F	Time at Temp. Hr.	Time at Temp. Min.	Sample Number	% TiH_2 in Mixture by Weight	Weight Mixture Applied Grams	Thickness Cu Plate Inches	Corrosion Tested in 10% NaCl
19	1008	1850	.	15	202	20.0	1.825	0.002	X
					207		1.580	....	X
31	1006	1845	1	00	614	20.0	4.940	0.0004	X
					615		2.490	....	X
32	1008	1850	2	00	412	20.0	2.740	0.0006	X
					405		3.085	....	X
33	1007	1850	4	00	502	20.0	3.440	0.0005	X
					503		3.765	....	X
16	900	1650	.	30	201	25.0	1.915	....	X
	855	1570	2	00	204		1.790	0.0006	X
24	974	1785	.	10	604	25.0	2.630	0.0018	X
					605		4.790	....	X
34	962	1765	2	00	504	25.0	2.580	0.0018	X
					505		3.615	....	X
14	950	1740	.	15	406	27.0	1.375	0.0017	X
					404	29.0	1.548	0.0018	X
35	1006	1845	2	00	506	28.0	3.400	0.0019	X
					507		4.285	....	X

lowest titanium content coatings were virtually copper coatings in which the titanium was dissolved in the molten copper. These were characterized by surface films which had impaired the wettability of the copper on the unplated samples. It was assumed that some slight oxidation of the titanium was responsible for the existence of these films. In several instances the coatings were noted to be broken into segments with the unplated base metal unwetted between them. The broken segments were coated with surface films which appeared dark colored. This breaking of the coating was not observed in the case of the copper-plated samples used. Apparently the presence of the copper plate provided a protection against contamination, presumably of the titanium, by elements contained in the steel even though eventual melting of the copper plate took place.

With increase of the titanium hydride to 10% the coatings showed a decided tendency to assume a gray color. Thus the strong coloring influence of titanium was noted to manifest itself on copper. The coatings produced appeared dull light gray, grainy and porous. The spreading characteristics were very weak however. The 15% titanium-hydride mixtures produced coatings which showed an increase in luster although the surface was still grainy and somewhat porous. A decided tendency to spread began to become evident. Fusion was observed to take place locally with a limited coalescence of the alloy in evidence. The spreading characteristics, although still weak, showed some improvement with increasing titanium content.

The microstructures of these coatings were generally noted to follow the same pattern. The 5% titanium-hydride mixtures produced coatings which showed a reddish matrix containing a few white unetched stringers scattered through it which were visible only at high magnification. The reddish matrix was very susceptible to etching with H_2O_2 in NH_4OH, being darkened very quickly, so that it was rather difficult to develop the structure. At high magnification a precipitated phase was observed in the reddish matrix that appeared as very fine narrow black particles arranged in parallel wavy rows. The solid solution of titanium in copper at room temperature is very limited, being less than 0.5%. Thus the structure suggested a solid solution of titanium in copper plus a precipitated phase within the grains and a small amount of eutectic that was not very well developed. As the titanium content increased, the microstructure showed an increase in the amount of the white unetched microconstituent. Where the heating had been prolonged a thin interface layer was

observed separating the coating from the base metal and evidence of diffusion by elements of the surface alloy into the base metal was also apparent.

Beginning with a 20% and up to and including 28% titanium-hydride content in the mixtures, the coatings produced gave the most promising results from a standpoint of appearance, smoothness and spreading characteristics. A number of satisfactory results were obtained.

With the 20% TiH_2 content mixture the following gave representative results.

Samples { 202 copper plated, 207 unplated } run at 1008 C for 15 minutes

Samples { 614 copper plated, 615 unplated } run at 1006 C for 1 hour

Samples { 502 copper plated, 503 unplated } run at 1007 C for 4 hours

The coatings of these samples seemed to have been formed by an even spreading of the surface alloy with the copper-plated specimens exhibiting somewhat better characteristics than the unplated ones. The heavier copper-plated specimens showed superior coatings to those thinly plated.

Some tendency for the copper-titanium alloy to wet the sides and ends of the copper-plated samples was observed, while in the unplated samples this characteristic was entirely lacking. This observation indicated that copper-titanium alloys do not wet iron in the manner that they wet copper. The coatings on the unplated samples showed in addition a decided tendency to become discolored at the edges, which was presumably caused by contamination of the titanium by elements in the base metal.

The surfaces produced in the majority of cases appeared smooth, silver colored with a rather soft luster and relatively free from gas blisters and pores. The adhesion of the coatings to the base metal seemed to be satisfactory. The effect of prolonged heating on the coatings seemed to result in their losing their luster to some degree. Generally it was observed that the coatings could be formed satisfactorily in a short period of time at the required temperature and that no advantage was gained by prolonging the heat treatment. In fact, prolonging the heat treatment reduced somewhat the attractive silvery luster.

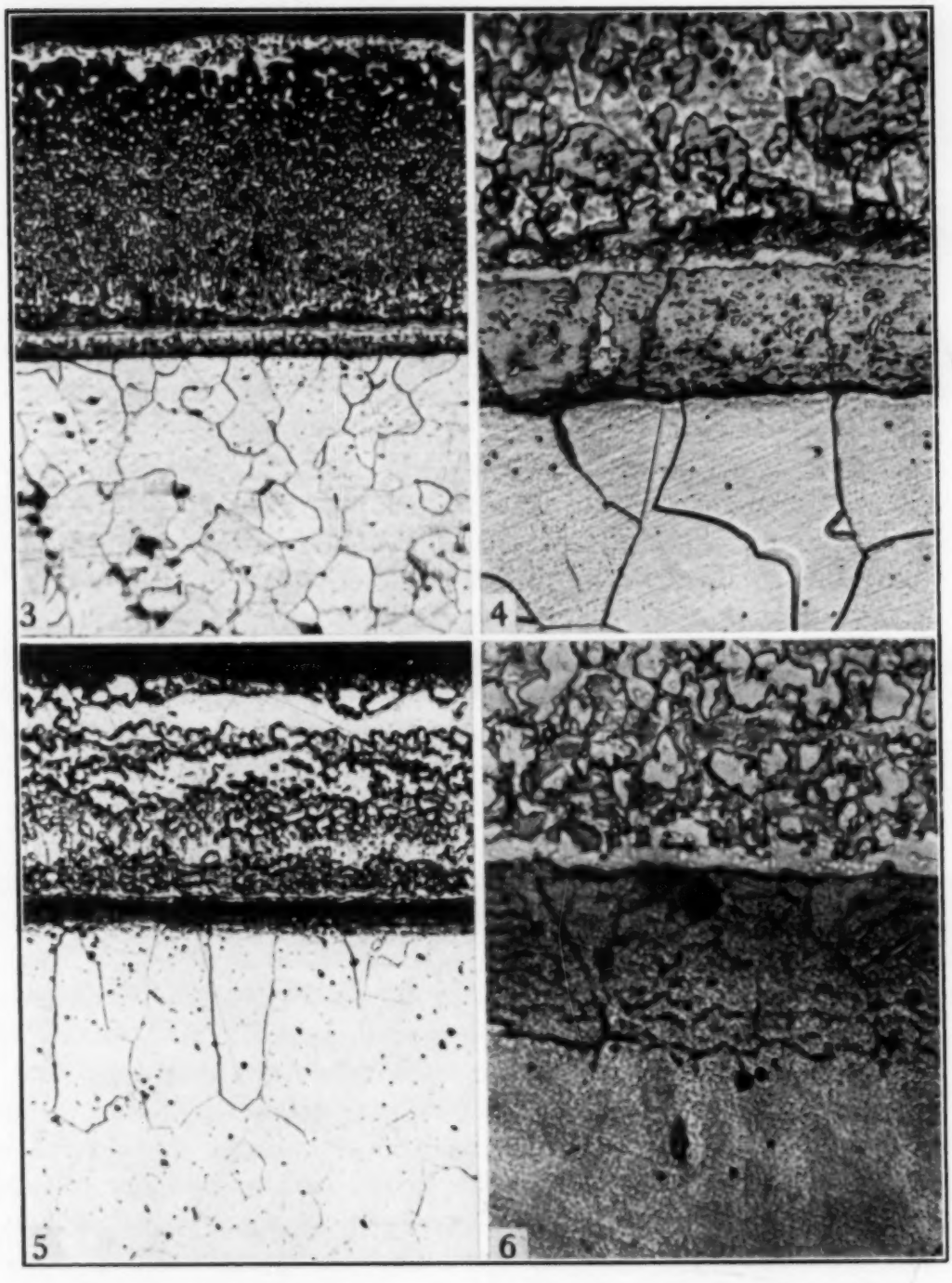


Fig. 3—Sample 502 (Copper Plated) Coating Produced From 20% TiH_2 Mixture. Etch: H_2O_2 in NH_4OH (coating). × 100. 3% Nital (base metal).

Fig. 4—Same as Fig. 3. × 500.

Fig. 5—Sample 503 (Unplated) Coating Produced From 20% TiH_2 Mixture. Etch: H_2O_2 in NH_4OH (coating). × 100. 3% Nital (base metal).

Fig. 6—Same as Fig. 5. × 500.

The microstructures contained the usual two microconstituents with the white unetched one increasing in amount as the titanium content also increased. Fig. 3 is the microstructure of a typical coating obtained with a mixture containing 20% titanium hydride. This was sample number 502 copper plated, run at 1007 C for 4 hours. At the very surface edge the coating appears as an unbroken white unetched layer which apparently is a eutectic, while below this exists a fine aggregate of two microconstituents fairly uniformly dispersed composed of a reddish matrix and a white microconstituent. Some eutectic exists here but it is not well developed and therefore not apparent. At the interface a thin layer separates the coating from the base metal which presumably is a compound composed of copper-titanium-iron, while below the interface a diffusion zone can be seen extending into the base metal the lower extremity appearing as a black line parallel to the interface. Fig. 4, taken at higher magnification, shows these details very clearly. A precipitated phase is apparent in the diffusion zone while the boundary between the lower edge of the diffusion zone and the ferrite grains of the base metal is well defined. It is interesting to note that a columnar ferritic zone seems to be absent. The bond between coating and base metal seems to be well established as a result of prolonged heating.

In Fig. 5 is the microstructure of sample 503 unplated. This sample was run at the same time as sample 502. A somewhat different distribution of the microconstituents seems to be in evidence with the white unetched one arranged in layers more or less parallel to the interface with a matrix of reddish and small white particles. Fig. 6 shows the interface conditions of this sample resolved at higher magnification. The diffusion zone appeared quite different from that of the copper-plated sample and seems to have the precipitated phase arranged in chain-like layers or rows parallel to the interface with some precipitation in evidence along grain boundaries as well. The thin layer separating the coating from the base metal appears as a fringe at the interface. The bond between the coating and the base metal appears well established even though this sample was unplated. It will be noted that a columnar ferrite band is apparent which is characteristic of the process of diffusion, displayed by a number of metals when they diffuse into iron.

As the titanium-hydride content was increased in the mixture the spreading characteristics of the resulting copper-titanium alloys were also noted to increase. A greater tendency of the alloy existed to run

down the sides, ends and to wet even the bottoms of copper-plated samples. On the unplated samples even though the surface alloy spread satisfactorily to form a coating, it showed no tendency to go beyond the edges even when the coatings were quite thick. The high wetting tendency on copper-plated samples seemed to drain the eutectic alloy from the coated surface leaving it enriched in higher melting point material. This generally caused the surface of the coating to become rough and uneven. According to Kroll (7) the eutectic composition in the Cu-Ti system is 24% titanium. Thus, above this titanium content the composition of the system becomes hypereutectic and the copper-titanium compound or compounds will accordingly be expected to have higher melting points, depending on the titanium concentration. This hypereutectic material usually appeared on the high spots of the rough coatings and generally had a very high metallic luster. It also displayed high hardness as well as brittleness.

At 28% titanium-hydride content in the mixtures the tendency toward forming higher melting point copper-titanium compounds became apparent. Beyond this concentration a decided increase in a high metallic luster characterized the formation and increase in these higher melting compositions.

Mixtures containing 25% titanium hydride produced coatings that were quite satisfactory in appearance and showed a maximum amount of spreading. This composition was of course very nearly at a eutectic and fluidity at the lowest possible temperature should have occurred. The draining tendency by wetting down the sides and ends was evident, leaving the surface coating somewhat rough as a result. Some samples which had the copper plate ground off on the sides and ends retained the surface coating intact since the alloy did not have a copper path to follow adjacent to it.

The microstructures of the coatings produced from mixtures containing 25 to 28% TiH_2 did not show very much difference. The eutectic structure was coarse and not very evident. Fig. 7 is the microstructure of sample 504 copper plated, run at 962 C for 2 hours. Although the composition is very nearly eutectic, the structure does not resemble the typical form. The usual two microconstituents are evident in about equal proportions. Diffusion has taken place as is evidenced by the zone which appears in the base metal, the lower boundary appearing as a solid black line below the interface. Some columnar ferritic growth as an outgrowth of the diffusion process is

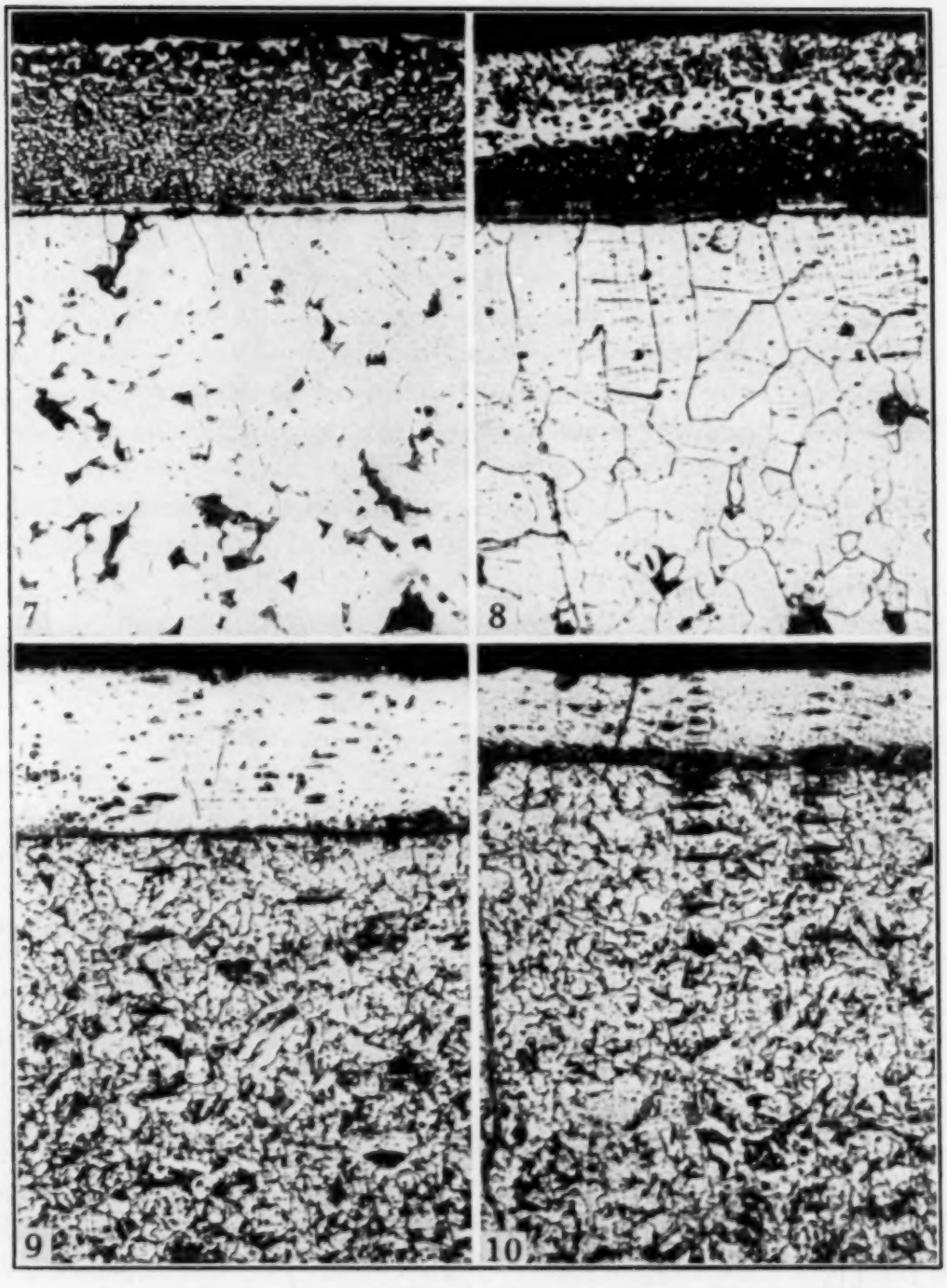


Fig. 7—Sample 504 (Copper Plated) Coating Produced From 25% TiH_2 Mixture. Etch: H_2O_2 in NH_4OH (coating). × 100. 3% Nital (base metal).

Fig. 8—Sample 505 (Unplated) Coating Produced From 25% TiH_2 Mixture. Etch: H_2O_2 in NH_4OH (coating). × 100. 3% Nital (base metal).

Fig. 9—Sample 400 (Copper Plated) Coating Produced From 37.5% TiH_2 Mixture. Etch: H_2O_2 in NH_4OH (coating). × 100. 3% Nital (base metal).

Fig. 10—Sample 402 (Copper Plated) Coating Produced From 36% TiH_2 Mixture. Etch: H_2O_2 in NH_4OH (coating). ×100. 3% Nital (base metal).

evident. This sample was only slightly decarburized. Pearlite can be seen adjoining the diffusion zone. Fig. 8 is the microstructure of sample 505 unplated and run under the same conditions as sample 504. The microstructure is not portrayed very clearly but the upper portion is decidedly eutectic. It will be noted that the structure of this is quite coarse, which seems to be quite a definite characteristic of cast copper-titanium alloys as observed in this work. The diffusion zone is quite dark but its outline can be traced. This zone was susceptible to etching with 3% nital, being darkened very readily by it. A columnar ferritic zone is very evident. This could have been produced during decarburization of the sample although the ferritic structure does not seem to correspond to the depth of the decarburization present.

The coatings produced from mixtures containing from 30 to 37.5% TiH_2 were in general more uneven than those obtained with lower titanium content. This was to be expected since the compositions were hypereutectic and higher melting point constituents would restrict fluidity and spreading. The spreading characteristics, however, seemed to be quite satisfactory but a decided tendency for the hypereutectic material to segregate and crystallize in thin plates was evident. These plates appeared to be oriented normal to the interface so that the surfaces showed them standing on edge. In several instances these plates were observed to be isolated by themselves with no filling in between them. Microexamination showed that these plates were microscopically thin yet were foliated and the surfaces of these crystals were mirror-like. They appeared to be rather soft and were scratched readily with a needle point. With lower titanium content coatings the microconstituents displayed a polyhedral habit but with the higher titanium content a decided tendency toward needle and plate-like formation was evident. Orientation of these plate-like crystals normal to the interface may have resulted from a similar effect to that observed in casting. Cubic metals have casting textures in which a cube axis is the fiber axis oriented normal to the mold surface. In this case the mold surface would correspond to the surface of the steel sample being coated. Further, it is quite possible that the temperature of the steel sample was a little lower than the copper-titanium alloy upon its formation, thus a temperature gradient would produce a fiber texture and satisfy the premise. The presence of hydrogen in the protective atmosphere may have had something to do with this particular structure and this possibility cannot be entirely

overlooked. The isolated plate-like crystals could have been produced from a vapor phase and this possibility cannot be overlooked, although the temperatures employed would rule out such a possibility. The only justification for deposition of these crystals from a vapor phase would be that the alloying between copper and titanium in the presence of atomic hydrogen developed sufficient heat to vaporize the titanium. This assumption would seem untenable; however, the manner in which the isolated crystals seemed to be arranged suggested a vapor phase.

The surfaces of the coatings produced were characterized by a very high metallic luster and appeared to be quite hard and resistant to abrasion; in fact, a file would not scratch them. Even though these coatings contained hypereutectic constituents no spalling or flaking occurred such as was evident in those coatings formed by applying TiH_2 in a thin layer on the copper plate.

The wetting tendencies were still very evident wherever copper was available for the copper-titanium alloy formed to follow. However, it appeared that the coatings solidified very quickly after their formation. This seemed to restrict the spreading qualities so that the wetting was not as extensive as previously noted.

The microstructures of the hypereutectic coatings were generally difficult to develop. They would not etch satisfactorily either with H_2O_2 in NH_4OH or $FeCl_3$. With 0.5% HF considerable staining of the microconstituents took place which obscured the structure. In general the structure consisted of a buff-colored matrix containing white unetched triangular and rod-shaped crystals. The matrix contained some lamellar grains which were not discernible at low magnification. $FeCl_3$ seemed to color the matrix while the 0.5% HF solution seemed to stain the triangular and rod-shaped crystals.

Fig. 9 shows the coating produced on sample 400 copper plated which was treated at 975 C for 25 minutes. The resolution of the microconstituents is lacking. This coating was produced from a mixture containing 37.5% TiH_2. The base metal was not decarburized to any extent, since pearlite can be seen extending right to the interface. There was no tendency displayed by the surface alloy to diffuse into the base metal. In fact, it appears as if the contained carbon in the steel inhibited this action from taking place. From this observation it would appear as if titanium has a preference for carbon and will combine with it rather than enter into solution with the iron. Fig. 10 shows a similar case. This sample is number 402 copper plated and treated under the same conditions as sample 400. The

coating on it was produced from a mixture containing 36% TiH_2. The bond between coating and base metal seems to be well established although the thin intermediate layer was entirely absent. Unplated samples showed a similar trend with the coating at the interface being affected to a greater degree than noted in the copper-plated samples. This occurred in the form of black particles that could not be resolved at high magnification.

Coatings Obtained With a Powdered 28% Copper-Titanium Alloy

The surfaces produced by this material were very dull gray in color and showed no luster. They were unsatisfactory since they were uneven and contained gas blisters. The temperatures required to melt the powder were higher than indicated on the tentative copper-titanium equilibrium diagram shown in Fig. 1 for this composition. The presence of a large number of gas bubbles underneath the coatings indicated either solution of hydrogen into the liquid metal or gases produced by the reduction of oxides in the powder which were trapped in the melt. In either possibility the gases were not expelled and resulted in a very undesirable surface condition. The results obtained seemed to indicate that the copper-titanium alloy upon being finely divided probably suffered some oxidation which would account for the higher melting point and also the large amount of gas bubbles trapped on melting in the presence of hydrogen. The spreading characteristics of this alloy when applied in lump form on copper-plated samples also proved very limited and generally unsatisfactory.

The microstructure of the coatings produced with this alloy appeared to consist of a buff-colored matrix with scattered needles of a white unetched microconstituent. A large amount of microscopic bubbles were in evidence besides the larger ones.

Microhardness Observations—Microhardness measurements revealed that the coatings seemed to have unusual hardness characteristics. The hardness was found to be mainly due to a white microconstituent in the hypoeutectic and eutectic compositions, while in the hypereutectic compositions the hardness seemed mainly due to the triangular and plate-like crystals, although the matrix of the latter compositions displayed high hardness as well. In the hypoeutectic and eutectic compositions the reddish matrix generally gave a Knoop number of from 225 to 255, and the white unetched microconstituent a Knoop number of from 875 to 1080. This wide difference in hard-

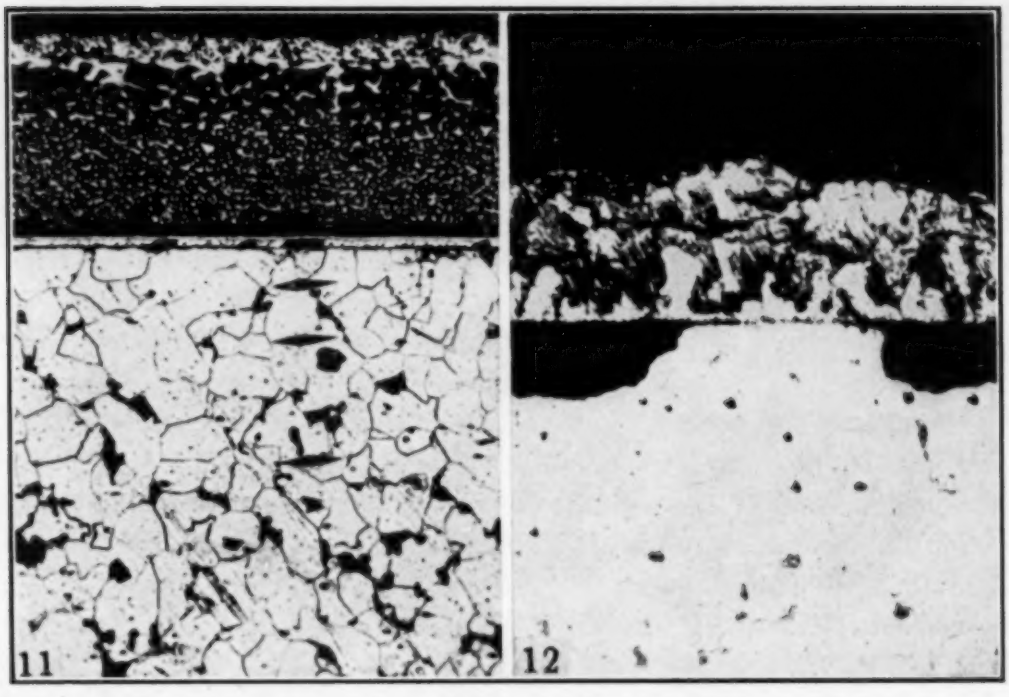


Fig. 11—Sample 504 (Copper Plated) Coated With Mixture Containing 25% TiH_2 Showing Hardness Impressions. Etch: H_2O_2 in NH_4OH (coating). × 100. 3% Nital (base metal).

Fig. 12—Sample 634 (Copper Plated) Coated With Mixture Containing 30% TiH_2 Showing Corrosion. Etch: H_2O_2 in NH_4OH (coating). × 100. 3% Nital (base metal).

ness between the microconstituents made it rather impossible to arrive at a compromise hardness number since no absolutely uniform distribution of the microconstituents occurred and any concentration of the one would show a high hardness while a concentration of the other would show low hardness; see Fig. 11.

In attempting to plot the hardness results, sharp peaks and valleys would invariably occur depending on the distribution of the microconstituents. Where these seemed to be rather uniformly distributed and in fine dispersion the Knoop number obtained was very nearly 500 or a Rockwell equivalent of about C-47. As will be noted from the microphotographs, the surfaces of the coatings generally showed a concentration of the white constituent at that point and a relatively high hardness at the surface resulted. A somewhat similar condition existed in the case of the hypereutectic structures although the difference in the hardness between the buff-colored matrix and the rod-like crystals was not as great; see Figs. 9 and 10. The buff-colored matrix showed a Knoop hardness number of from 500 to 650, while the rod-like crystals gave a Knoop hardness number of from 875

to over 1100. A Knoop number of about 750 appeared to be an average or a Rockwell equivalent of about C-63.

The thin intermediate layer present at the interface also seemed to have high hardness. Generally the Knoop hardness number obtained varied according to titanium content in the coating, with the highest hardness obtained with hypereutectic compositions. Generally, the unplated samples showed this zone to have higher hardness numbers than those that were copper plated. The Knoop hardness numbers ranged from about 350 for 20% TiH_2 mixture coatings to 750 for 36% TiH_2 mixture coatings on copper-plated specimens, while for unplated samples the range included 450 for 20% TiH_2 to 850 for 36% TiH_2 mixtures.

The base metal, except where diffusion had taken place, generally showed no hardening and an abrupt decrease in hardness at the interface resulted. Where diffusion had occurred a hardening of the base metal generally was observed and ranged between a Knoop number of 300 and 400. The base metal consistently displayed a Knoop number of about 200 or about Rockwell C-10.

The general disposition of the microconstituents and the relative high difference in their hardness naturally predisposed the coatings to possess little ductility and therefore to be brittle as a result. The results of a series of bending tests on the coated samples of various compositions confirmed this. The coated samples were on 1/8-inch thick steel and were bent around a 5/8-inch pin. The results showed that the coatings were brittle and possessed little ductility, with the hypoeutectic and eutectic compositions showing better characteristics under bending than the hypereutectic. The greatest internal angle of bend obtained was 152 degrees, while the hypereutectic coatings showed no ductility whatsoever and the coatings cracked very readily. The adhesion of the coatings, however, seemed to be satisfactory and little tendency was observed for flaking to occur as a result of the bending.

No attempt was made to anneal these coatings and whether such heat treatment would reduce the britleness is somewhat problematical. An attempt was made to heat treat a series of coatings by heating them at 800 C for 1 hour in a vacuum then quenching them in water. A general softening over the original hardness prevailed. However, some oxidation of the coatings resulted, due to faulty procedure and the results were not conclusive.

Corrosion Observations—Subjecting a series of coatings formed

from the various TiH_2 mixtures to total immersion for 7 days in a 10% NaCl solution maintained at 35 C and saturated with air showed that in general the coatings were resistant to the solution under the conditions. Those coatings that originally had a high luster and no porosity seemed to be unaffected in every respect. This was quite noticeable in the hypereutectic compositions. The coatings containing hypoeutectic and eutectic compositions generally showed good resistance and showed no appreciable attack except in two cases. Microexamination of these revealed that attack had taken place in the red matrix. Apparently a cell had been formed between it and the white constituent with solution of the red matrix.

Wherever the base metal had been exposed through pores it was apparently vigorously attacked. In these areas microexamination disclosed that the coating was decidedly cathodic with respect to the base metal. Fig. 12 illustrates the action. The coating on this sample was produced from a 30% TiH_2 mixture and it showed porosity through a patch of isolated crystals without a filling between them. The microphotograph plainly shows the cathodic nature of the coating.

Exposure of the coatings to atmospheric conditions for a period of about three months showed a general oxidation of the uncoated base metal while the copper-titanium surfaces retained their brightness and showed no effect of the exposure.

Observations on the Structure of Copper-Titanium Alloy Coatings

The lack of information on the Cu-Ti system makes the analysis of the alloy structures obtained in the coatings somewhat speculative and no attempt can therefore be made to discuss these structures on a quantitative basis. Some interesting observations, however, were made on the alloying habits of titanium with copper under the special conditions of treatment.

In the processes of forming the copper-titanium coatings with heat the first phase was the interdiffusion of the two elements, one into each other to form a low melting alloy at the point of contact. The second phase was the melting of this alloy formed with a rapid reaction resulting between the elements still uncombined. The extent of solid solubility of one element in another is generally conceded to depend on several factors which include: (a) the relative lattice types and atomic sizes of the solute and solvent metals, (b) the chemical

affinity of one for the other and (c) the relative valency effect. Titanium occurs in two allotropic forms, the alpha modification at room temperature is hexagonal close packed and the beta form is body-centered cubic at 880 C, while TiH_2 is considered to have a fluorite (CaF_2) structure. With lesser hydrogen content the structures change somewhat passing to a zinc-blende structure for TiH and to hexagonal close packing for Ti_2H. Whether the structure of titanium hydride changes with evolution of hydrogen is immaterial and only the structure prevalent at the temperature where interdiffusion of titanium and copper takes place is of importance. The structure at this point would appear to be that of the beta form or body-centered cubic. Copper is, of course, face-centered cubic in symmetry. Thus a dissimilar crystal structure exists between the two elements. The atom size factor consideration shows titanium and copper to differ by about 13% in their atomic radii so that this points toward a borderline condition for solubility. Titanium appears on the left side of the first long period of the periodic table included in the group of so-called transition elements and which are considered electropositive. Copper also occurs in the first long period of the periodic table but is to the right of titanium and therefore electronegative with respect to it. Thus a difference exists in the two elements as regards their chemical affinity since the more electropositive the solute and the more electronegative the solvent, or vice versa, the greater is the tendency to restrict solid solubility and to form intermetallic compounds.

A metal of lower valency tends to dissolve a metal of higher valency more readily than vice versa. In the case of copper it dissolves decreasing amounts of a solute as the valency of the solute increases. Titanium is generally considered tetravalent and as such its solubility in copper therefore can be expected to be limited. Considering the reverse of this or the solubility of copper in titanium it would appear that even less copper would dissolve in titanium than vice versa. The general rule that in a binary system the solubility in a higher melting metal is greater than in a low melting metal would thus appear to be an exception in this case as well. Thus a strong tendency is indicated to form stable intermediate compounds at the expense of primary solid solutions. Titanium being strongly electropositive with respect to copper would thus be expected to exhibit this tendency. The formation of a stable compound normally restricts solid solubility and therefore the solubility limit of the restricted solid

solution increases with temperature. This rule seems to be followed in the Cu-Ti system since the solid solubility of titanium in copper increases from a minimum of about 0.4% titanium at room temperature to a maximum of about 4.5% at 878 C. A minimum in the liquidus curve shows the formation of a eutectic which according to Kroll (7) exists at a 24% titanium concentration. According to Laves and Wallbaum (6) in copper alloys of low titanium content the compound Cu_3Ti was formed which had a deformed hexagonal structure while a high titanium content produced an isomorphous compound $CuTi_2$ which was a face-centered structure with 96 atoms per cell, apparently a complex phase. The former would correspond to an "ϵ" phase with an electron atom ratio of 7 : 4 while the latter with its large cell suggests a "γ" phase although $CuTi_2$ does not correspond to an electron atom ratio of 21 : 13 according to Hume-Rothery's rule (12). The crystal structures found in structurally analogous phases that seem to follow the "ϵ" type show a hexagonal close-packed arrangement for an electron atom ratio of 7 : 4 while the "γ" type with a 21 : 13 electron atom ratio shows a cubic complex structure. The copper-titanium compounds Cu_3Ti and $CuTi_2$ seem to follow these analogous structures. If these compounds do exist, then the equilibrium diagram certainly needs modification to include them. The phases present in the microstructures of the copper-titanium alloy coatings showed a part of them to be intermetallic compounds since these generally are more complex and lower in symmetry than their components and therefore exhibit hardness and brittleness which is a condition associated with them.

The structures obtained in the coatings generally showed that titanium was quite soluble in copper under liquid conditions but that this solubility became sharply reduced upon solidification. In most cases a two-phase structure occurred and typified a slowly cooled cast structure with the intermetallic compounds appearing as separate constitutents in polyhedral form. In hypoeutectic copper-titanium compositions a tendency was observed for the alloy formed to display dendritic segregation. An example of this is shown in Fig. 13 which was taken with oblique illumination to reveal the structure. This structure resulted in an attempt to join two OFHC copper strips by heating them with titanium hydride applied to the butted ends at a temperature of 952 C, then furnace cooling at 550 C and then cooling outside the furnace to room temperature. The etched primary dendrites and the well-defined white edging appearing at the interface

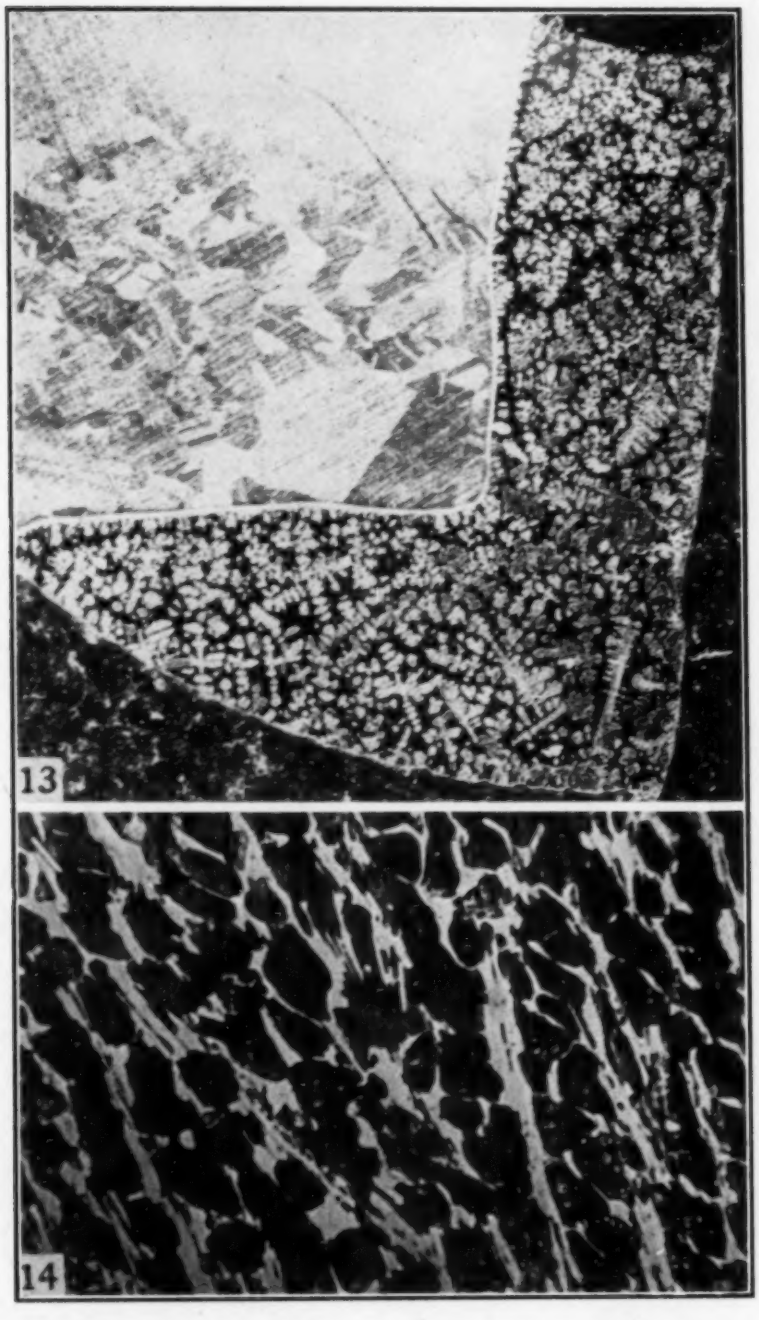


Fig. 13—Cored Structure of Copper-Titanium Alloy Obtained by Heating OFHC Copper and TiH_2. × 10, oblique illumination. Etch: H_2O_2 in NH_4OH.

Fig. 14—Structure Cast 20% Titanium-Copper Alloy. Etch: H_2O_2 in NH_4OH. × 100.

between solid copper and the cored alloy appeared to be the same phase. The filling, appearing black in the microphotograph, is a massive white unetched phase. There is a striking similarity between

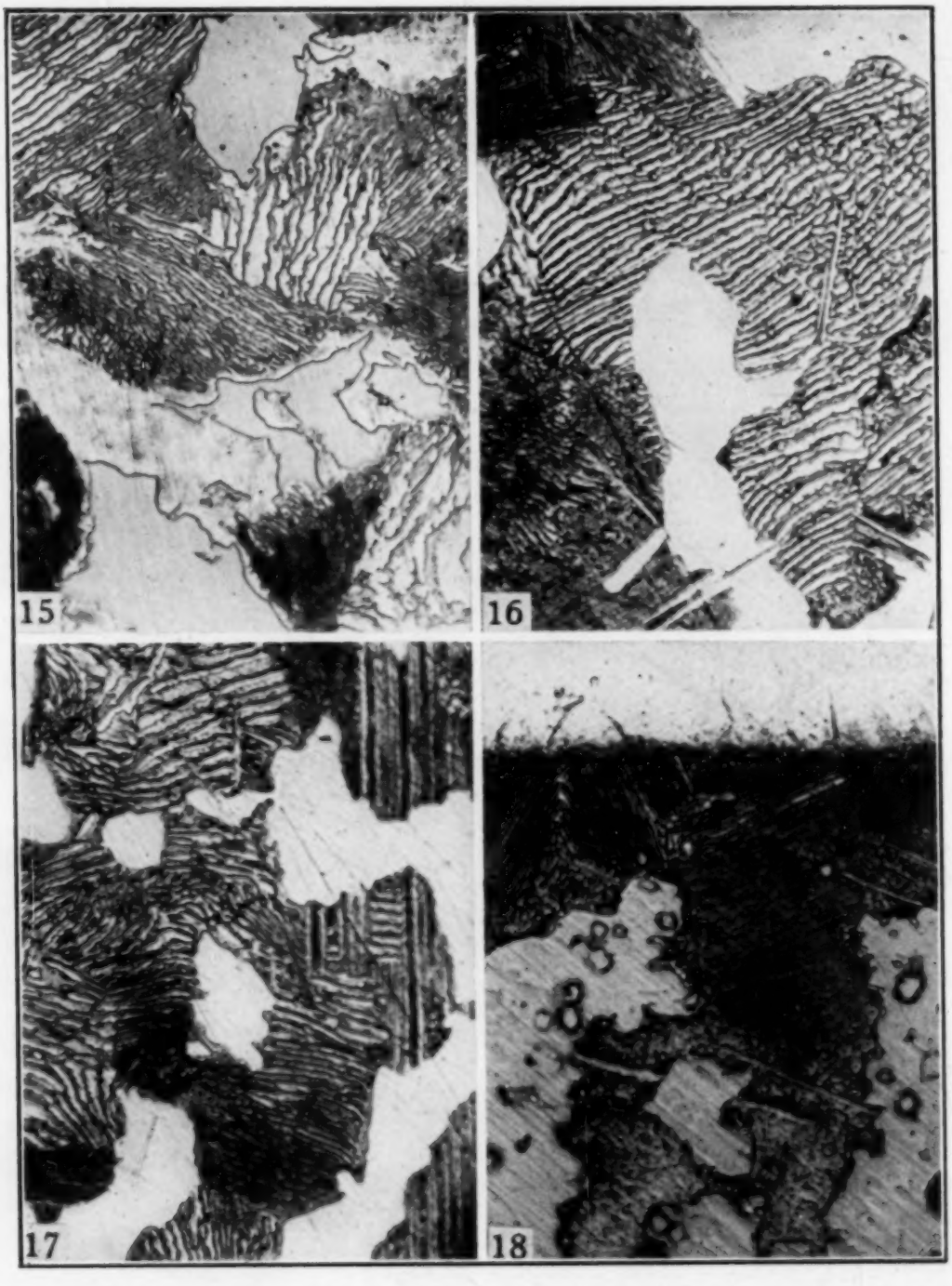


Fig. 15—Showing Incomplete Eutectoid Formation in Primary Alpha. Etch: very light with H_2O_2 in NH_4OH. × 500.

Fig. 16—Showing Eutectoid Background With Massive Beta Phase Plainly Evident. Etch: very light with H_2O_2 in NH_4OH. × 500.

Fig. 17—Showing Eutectoid and Network Structure Formed by Precipitation of Beta Phase From Primary Alpha. Etch: very light with H_2O_2 in NH_4OH. × 500.

Fig. 18—Interface Conditions Between Copper and Cored Alloy of Fig. 13. Etch: very light with H_2O_2 in NH_4OH. × 500.

this structure and that of a hypoeutectic cast iron. Fig. 14 shows a very good example of this similarity. This structure is of a 20% titanium-copper alloy produced in one of the coating experiments. The dark gray corresponds to the austenite while the white massive material corresponds to Fe_3C. The eutectic structure like that in cast iron is not very evident and the reason for this is that the "α" part of

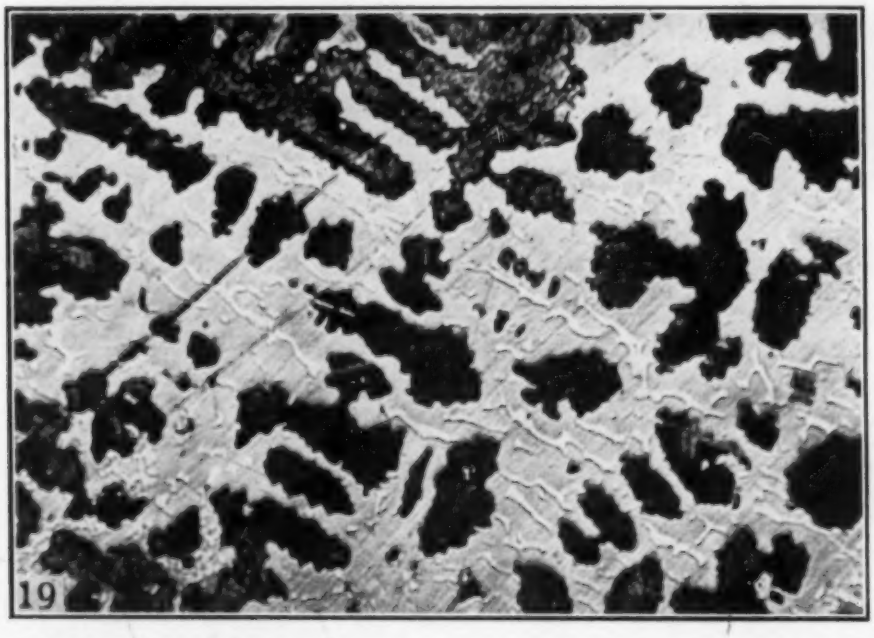


Fig. 19—Cored Structure of Fig. 13 Showing 3 Phases Present. Etch: H_2O_2 in NH_4OH; $FeCl_3$; 0.5% HF. × 100.

the eutectic was alongside the primary "α" and therefore was indistinguishable from it. For the purposes of discussion it is advisable to assign an identifying symbol to the various phases, thus "α" will stand for the solid solution of titanium in copper, "β" for the intermetallic compound Cu_3Ti and "γ" for the compound $CuTi_2$. It is, of course, to be understood that this is purely an arbitrary designation merely selected for convenience. Thus "α" corresponds to austenite and "β" corresponds to Fe_3C.

Primary "α", like its counterpart in austenite, apparently undergoes a similar change with the development of a similar structure to that of the eutectoid, pearlite. At what temperature this decomposition takes place is not known. However, a eutectoid in the copper-titanium system is indicated.

Fig. 15 shows primary "α" which has been nearly converted to a eutectoid structure, while Fig. 16, at the same magnification, shows

the details of the eutectoid background with the massive "β" plainly visible. Presumably the "β" phase separating out from primary "α" formed on the eutectiferous "β" already present rather than at the primary "α" grain boundaries. This appears to be a form of preferred nucleation or a growth of large nuclei that are present.

In Fig. 17, a network structure appears in addition to the eutectoid. Here the "β" phase apparently was present in rather large amounts in the "α" and separated out in the form of plates. Since lattice matching is quite necessary during nucleation of this phase, the orientation of it must be related to the "α" solid phase. The new structure chose to appear in the form of plates and thus formed a Widmanstätten pattern. A closer look at the interface conditions of the cored structure of Fig. 13 shown in Fig. 18 reveals a similar circumstance in which the dark gray or "α" contains precipitated "β" in the form of plates.

In the cored structure of Fig. 13, etching of the "β" phase with 0.5% HF solution revealed another phase illustrated in Fig. 19 which is believed to be a higher titanium-content compound, possibly $CuTi_2$ or "γ". The presence of this phase suggests a peritectic reaction from which the "β" phase is derived. Evidence of this phase was also seen in the copper-titanium alloy coatings in excess of 30% titanium. These structures generally appeared as consisting of a buff-colored matrix, probably Cu_3Ti plus rod-shaped crystals of $CuTi_2$. These rod-shaped crystals were probably plates which would appear as rods or needles when viewed on edge. A well-developed eutectic structure was almost entirely lacking; however, evidence points to a similar structure to that of ledeburite wherever it occurred.

Influence of Hydrogen—The direct influence of hydrogen and the extent to which it may have affected the structures of the alloys of the coatings cannot be appraised with any degree of certainty. Its presence at a pressure slightly greater than atmospheric certainly caused it to be dissolved in the molten metal. Some porosity observed in the coatings showed that hydrogen probably had been dissolved and had not been expelled during solidification but remained trapped. The cored structure of Fig. 13 seemed to contain quite an amount of microscopic bubbles. The presence of tiny blisters in the coatings was evidence of the solubility of gas in the alloy. Hydrogen also probably provided a means of momentary superheating of the alloy in the coating during its formation, as will be discussed presently.

The occurrence of copper-titanium compositions whose melting

points apparently were higher than the temperatures employed suggested that to justify their existence superheating of the alloys formed had to occur. This superheating had to be supplied from heat from some source during the reaction between titanium and copper. Evidence of a heat generation within the quartz tube during the experimental work was obtained in the fact that a suddent slight temperature rise was noted on several occasions when the temperature of the tube had reached about 880 C. Subsequent attempts to remelt some of the coatings at the temperatures employed from their formations were unsuccessful and seemed to verify the observation that additional heat had been generated. It did not seem reasonable to assume that the alloying action between copper and titanium would be exothermic nor was the possibility of a thermite reaction probable. However, the hydrogen contained in the titanium hydride seemed to offer a possible reason for the generation of heat. It is an established fact that a large amount of heat is generated when hydrogen atoms unite to form molecules. This process takes place readily when atomic hydrogen comes in contact with a metal in a suitable condition with the liberation of about 100,000 calories per gram molecule (2 grams of H_2) of hydrogen. The conditions for the generation of heat by hydrogen when copper and titanium alloyed to form the coatings appeared to be in accord with this fact.

When titanium hydride is heated it liberates the combined hydrogen which is presumably in an atomic form as it evolves. The appropriate metallic surface condition for hydrogen atoms to unite into molecules apparently occurred when the alloy formed by the interdiffusion of copper and titanium started to melt. Once the proper metal surface is provided, the available atomic hydrogen can quickly be converted to the molecular state releasing heat. The amount of TiH_2 usually contained in the mixtures from which the coatings were produced was usually too small to produce much atomic hydrogen but the amount of TiH_2 used as a "getter" was present in sufficient amounts to supply a sizable amount. Generally about 50 grams of TiH_2 was used for this purpose and this amount totally dissociated could supply a gram molecule of hydrogen with its equivalent of heat.

The surfaces of many of the coatings which had been produced both from the heating of the TiH_2 in contact with copper plate and from mixtures containing more than 28% TiH_2 appeared as if fusion had taken place rapidly but momentarily with little opportunity for equalization of the surface by much spreading to take place. This

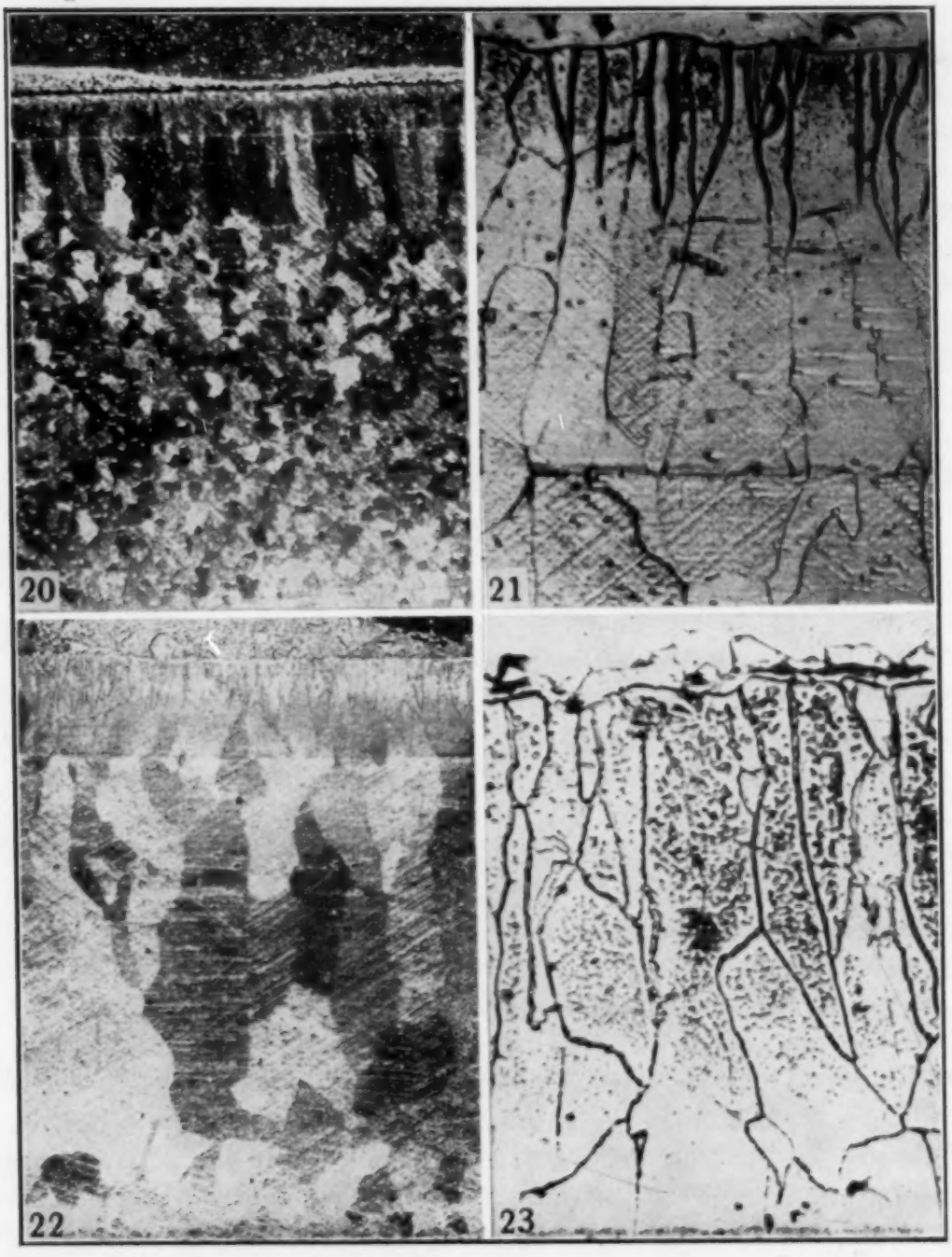


Fig. 20—48-Hour Diffusion of Copper-Titanium Into Armco Iron. Etch: 3% Nital. × 10.

Fig. 21—Hardened Diffusion Zone 48-Hour Diffusion Copper-Titanium Into Armco Iron Same as Fig. 20. Etch: 3% Nital. × 100.

Fig. 22—96-Hour Diffusion 25% Titanium-Copper Alloy Into Armco Iron. Etch: 3% Nital. × 10.

Fig. 23—Structure Immediately Below Interface of 96-Hour Diffusion Specimen. × 100.

observation indicated that superheating of the alloy formed must have taken place. This, coupled with the fact that it was not possible to remelt these coatings at the temperature of their formation, bears out the assumption that they could not have been produced without the aid of additional heat from somewhere.

Diffusion of Copper-Titanium into Armco Iron

The results of the experimental work in producing surface coatings of copper-titanium alloys on steel indicated a strong tendency on the part of the surface alloy to penetrate into the base metal by diffusion, upon prolonged heating and when the base metal did not contain appreciable amounts of inhibiting elements. It was observed that when the base metal contained carbon at the interface, diffusion of the surface alloy was inhibited as was seen in Figs. 9 and 10. In the case of Figs. 3 and 4, diffusion appeared to have taken place when carbon seemed to be present only in small quantities. While in the case illustrated by Figs. 5 and 6, diffusion had occurred in a similar fashion although the appearance of the precipitated phase in the diffusion zone looked radically different from that of Fig. 4. The tendency for diffusion to occur uniformly is evidenced by the uniform width of the zones formed. The precipitated phase of Figs. 4 and 6 could not be determined with certainty. However, it appeared that copper and titanium had penetrated into the base metal in the case of Fig. 4, but that titanium seemed to be predominant as the diffusing element in Fig. 6.

Since it was observed that diffusion seemed to progress better in a carbon-free medium it was decided to use Armco iron for diffusion observations rather than a decarburized steel. Consequently, specimens 2 inches long by 1 inch wide by ½ inch thick were prepared. One surface was slotted to a depth of ⅛ inch, and by using metal pieces across the ends, a receptacle was formed. A powdered mixture of titanium hydride and copper was packed into this receptacle and a coating formed by heating. This coating constituted the supply of the diffusing elements.

Two experiments were conducted as follows: (a) 48-hour diffusion run with a coating composed of 6.45 grams containing 30% TiH_2 at an average temperature of 1062 C (1945 F). The results obtained showed a columnar ferritic band, the upper part of which showed as a hardened band 0.021 inch in width, as shown in Fig. 20,

taken with oblique illumination. (b) 96-hour diffusion run with a coating composed of 15 grams containing 25% TiH_2 at an average temperature of 1102 C (2015 F). The results obtained showed a very deep columnar ferrite band with the upper part as a hardened band 0.041 inch in width, as shown in Fig. 22 with oblique illumination. Both diffusion experiments were conducted in a protective atmosphere of dry hydrogen. The iron specimens were bright annealed in hydrogen prior to the diffusion experiments.

The general structure produced by the prolonged heating of the surface alloys of copper-titanium in contact with the iron followed a similar pattern to that formed by the diffusion of other metals into iron. A columnar band of ferritic crystals resulted in each case which started at the interface and extended into the base metal for quite some distance. Immediately below the interface a hardened band was observed in each case parallel to the interface and uniform in width. These bands stood out in relief upon polishing with the lower edges appearing as lines of demarcation. Separating the coating alloy from the iron a fringe of, presumably, a compound of iron-copper-titanium occurred which served to feed the diffusion process. The hardened diffusion zones showed a precipitated phase in the upper portions that occurred along grain boundaries and within the grains themselves, decreasing in particle size with depth. Generally the lower half of the hardened zone showed the precipitated phase only at high magnification. This phase showed a tendency to drag out after etching during subsequent polishing. It showed considerable susceptibility to etching with 3% nital as well and was darkened very quickly by it, suggesting that this was due to the contained titanium.

The general structure obtained with the 48-hour diffusion experiment is illustrated in Fig. 20. The hardened diffusion band with its line of demarcation appeared well defined and quite uniform in thickness. The columnar diffusion zone likewise appeared uniform in depth. Fig. 21 shows a resolution of the hardened zone and clearly illustrates the fissuring effect produced by the copper-titanium diffusion. Some discontinuity of the columnar grains existed above and below the boundary line between the hardened and unhardened zones although the major grain boundaries seem to persist across this boundary.

The same general structure was obtained in the 96-hour diffusion experiment as is pictured in Fig. 22. The hardened zone is thicker and the columnar zone is much deeper in proportion to that obtained

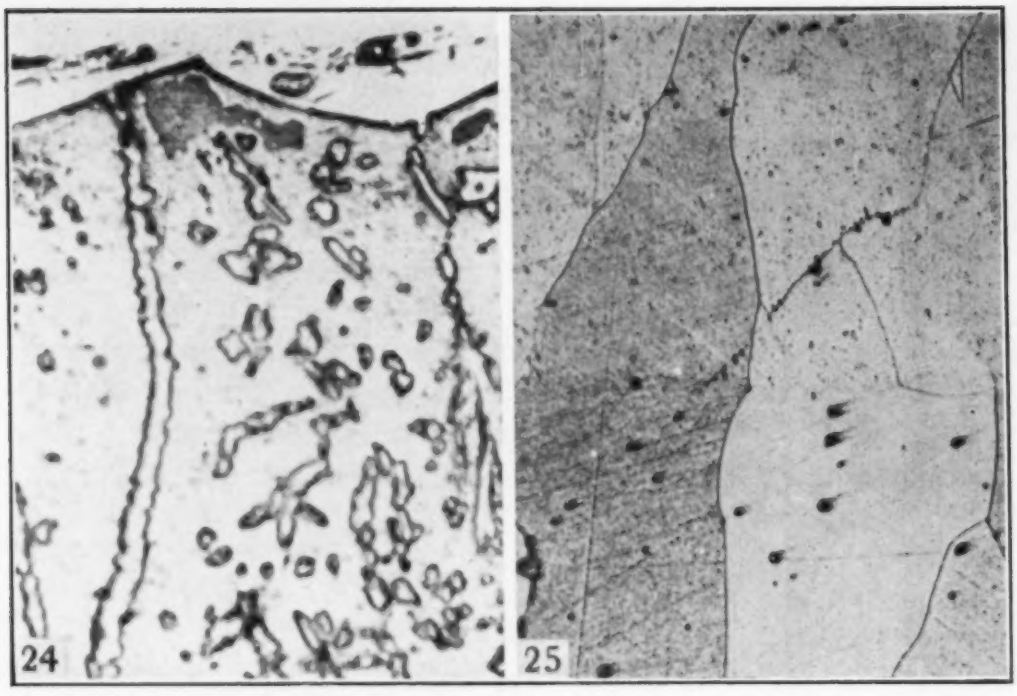


Fig. 24—Structure Showing Resolution of Precipitated Phase—96-Hour Diffusion Specimen. Etch: 3% Nital. × 500.

Fig. 25—Boundary Conditions Between Hardened Diffusion Zone and Rest of Columnar Zone—96-Hour Diffusion. Etch: 3% Nital. × 100.

in the 48-hour experiment. The heavier, deeper and more pronounced precipitation at fissure grain boundaries and within the grains is illustrated in Fig. 23. A further enlargement of the precipitated phase is shown in Fig. 24. The distribution of the precipitated phase in the hardened zone suggested the existence of a definite concentration gradient within this zone with an abrupt drop at the lower boundary line. This concentration gradient was characterized by a gradual decrease in the size of the precipitated particles as the lower edge of the zone was approached. Once across the line of demarcation the precipitated phase disappeared from view. This condition and sequence is clearly illustrated in Fig. 25. On the upper side of the hardened zone boundary a fine dispersal of precipitated particles can be seen while below this boundary they are entirely lacking. The columnar grains also show unconformities above the boundary line although the major grain boundaries seem to persist across the line of demarcation. The grains on the upper side seemed to be influenced by the fissuring effect exerted higher up. A change of orientation or a strong lattic distortion in the hardened diffusion zone as compared to the rest of the columnar zone seems to be indicated.

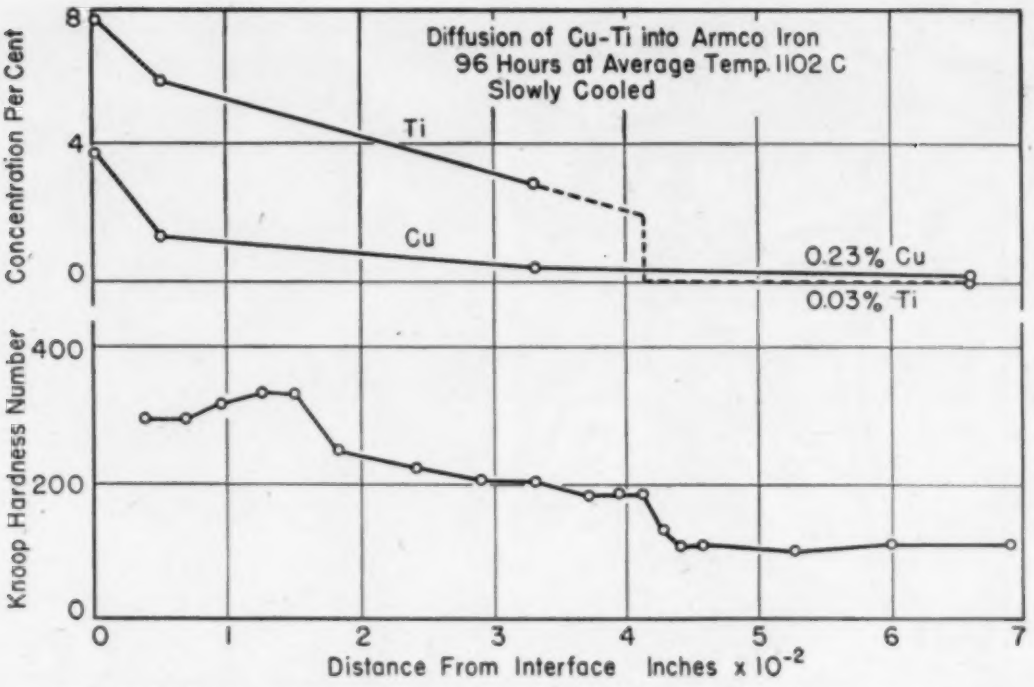


Fig. 26—Diffusion of Copper-Titanium Into Armco Iron—96 Hours at Average Temperature, 1100 C (2010 F). Slowly cooled.

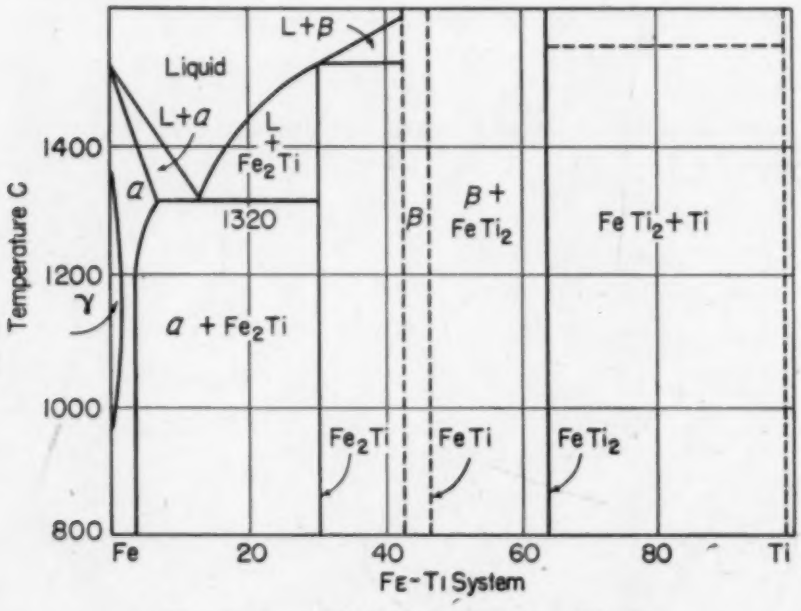


Fig. 27—Iron-Titanium Equilibrium Diagram.

Fig. 26 shows data of microhardness measurements and a comparative plot of copper and titanium concentration that was found with depth of diffusion.

The concentration data were secured by first cutting steps in the

diffusion specimen 1⅛ inches long by 11/16 inch wide by 0.265 inch thick beginning with the interface and continuing through the hardened diffusion zone into the columnar zone below. Step number 2 was 0.005 inch below step 1; step 3 was 0.028 inch below step 2; step 4 was 0.033 inch below step 3. The short length of the specimen prevented a greater number of steps from being cut, however. The information sought was only qualitative so that the results obtained were rather limited. However, sufficient data were obtained to indicate the trend of the diffusion of copper-titanium into iron. The chips from the various steps were collected and those chips from cutting step 2 and step 4 were analyzed chemically. The steps themselves were analyzed spectrographically by sparking. These data were collected in the form of ratios based on densitometer readings. The chemical results were correlated with the spectrographic analysis to arrive at the concentrations of both copper and titanium in the diffusion structure.

From Fig. 26 it will be observed that a sharp change in hardness values occurred at the boundary line between the hardened and unhardened zones. It was assumed that this sharp change in hardness was caused by a corresponding change in concentration of titanium. This assumption seemed to be justified by the extremely small titanium content found below the hardened zone. The role of copper does not seem to be exactly clear here except that there is a noticeable indication that titanium restricts the solubility of copper in iron. The original copper content of the specimen was 0.165% so that an increase of 0.065% occurred below the hardened zone, showing that copper was able to penetrate iron in spite of the apparent restricting influence of titanium.

To arrive at some possible explanation for the abrupt change in hardness and the formation of a hardened zone immediately below the interface a glance at the iron-titanium equilibrium diagram shown in Fig. 27 shows that the system contains a closed gamma loop, followed by a narrow alpha solid solution region and then a large region where the iron-titanium compound Fe_2Ti and alpha solid solution exist together presumably with Fe_2Ti as a precipitated phase. The presence of an intermetallic compound generally produces hardening effects and it appears quite logical to assume that the hardened zone was produced by the precipitation of the compound Fe_2Ti. This premise seems to be borne out by the details shown in Fig. 25. The extremely small amount of titanium content found below this hardened zone

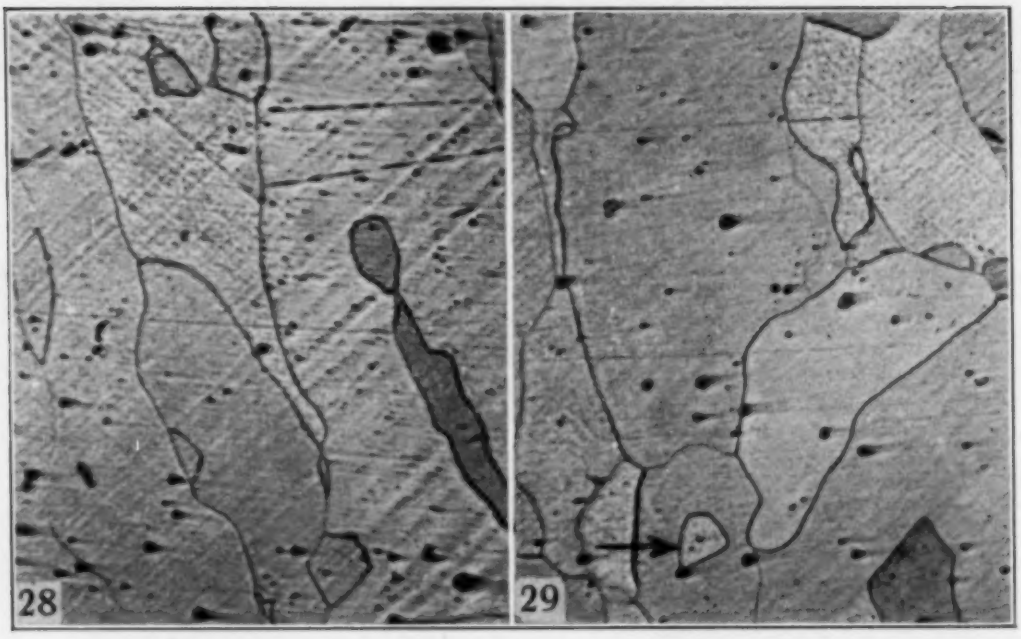


Fig. 28—Showing Isolated Grains in Lower Part of Columnar Ferritic Zone—96-Hour Diffusion of Copper-Titanium Into Armco Iron. Etch: 3% Nital. × 100.

Fig. 29—Showing Isolated Grains in Lower Part of Columnar Ferritic Zone—96-Hour Diffusion of Copper-Titanium Into Armco Iron. Etch: 3% Nital. × 100.

seemed to indicate that the solubility of titanium in alpha iron was indeed limited and much less than indicated in the equilibrium diagram shown in Fig. 27. The ferritic columnar structure formed in both the 48 and 96-hour diffusion specimens indicated the formation of a new phase by diffusion. This phase was, of course, the alpha solid solution of titanium in iron. As the temperatures at which the two diffusion experiments were conducted should have included diffusion of titanium into gamma iron actual evidence of this seemed to be lacking or it was not apparent microscopically. With the minute quantity of titanium present in the ferritic alpha iron the titanium content would be indeed minute in gamma iron.

X-ray diffraction pictures of samples obtained from the interface showed lines belonging to the characteristic body-centered iron lattice with practically no change in the lattice parameter from that obtained in the original sample. This observation would seem to verify the limited solid solubility of titanium in alpha iron. Some extra lines appeared on the diffraction pictures that fitted into a hexagonal system which would support the existence of the compound Fe_2Ti as the precipitated phase in this case. No copper lines were observed which would indicate that at least a part of the copper had entered the iron

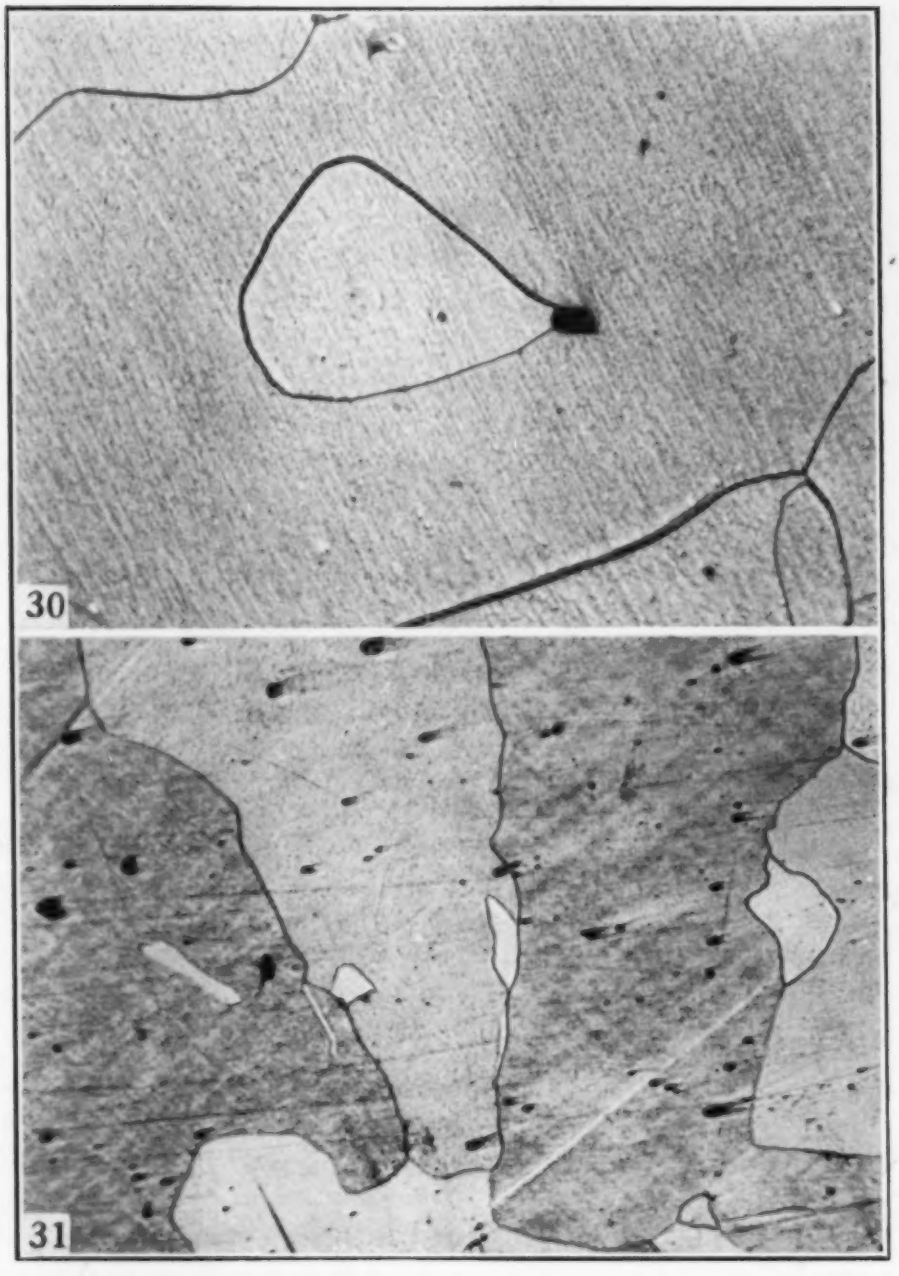


Fig. 30—Showing Isolated Grain in Lower Part of Columnar Ferritic Zone—96-Hour Diffusion of Copper-Titanium Into Armco Iron. Etch: 3% Nital. × 500.

Fig. 31—Showing Isolated Grain Remnants Within Columnar Ferritic Grains—96-Hour Diffusion of Copper-Titanium Into Armco Iron. Etch: 3% Nital. × 100.

in solution and a part probably reporting also in the iron-titanium compound. The fissuring effect strongly indicates a definite influence of copper in this respect so that it must occur in the iron-titanium

compound, probably as a third element to form a ternary iron-copper-titanium compound.

Where the lower extremity of the columnar band merged with the equiaxed grains some rather curious outgrowths of the columnar formation resulted. Fig. 28 shows isolated grains within the ferritic columnar grains that appear as islands. These have apparently resisted the ferritic preferred orientation and represent areas in which either no diffusion of titanium has occurred or else they represent the material included in the gamma loop. A grain can be seen in the center of the microphotograph being enveloped by the columnar grain above it with its long finger reaching down along the boundary and with a small grain nucleating ahead of the finger. On the opposite side another grain seems to be started. Fig. 29 shows a similar condition with incompletely enveloped grains. In the lower left-hand corner of this figure an interesting isolated grain occurs within another grain. This is shown at higher magnification in Fig. 30. It will be noted that an Fe_2O_3 inclusion occurs at one corner of this isolated grain which may have had something to do with its isolation. Fig. 31 shows the lower extremities of well-formed columnar grains which contain isolated grain remnants.

Nitriding of 48-Hour Diffusion Specimen

A portion of the 48-hour diffusion specimen shown in Fig. 20 was cut into a ½ by ½ by ¾-inch sample. The coating which supplied the diffusion elements was removed and the interface polished. This specimen was nitrided for 24 hours at 523 C in 30% dissociated ammonia gas. The specimen, after this treatment, showed a nitrided case where the diffusion of copper-titanium had taken place. The microsection showed the case to be about one-half the thickness of the originally hardened diffusion band of 0.021 inch. Some needles were observed near the fissured surface and occurred between the fissured grains. The case showed exfoliation which had not been apparent prior to microsectioning of the sample. The nitrided portion of the diffusion zone seemed to be very hard but also very brittle. Penetration of nitrogen was observed also to occur laterally in from the sides of the specimen following preferentially along the lower boundary of the hardened diffusion zone. Immediately below this boundary line no hardening effects due to nitrogen were observed.

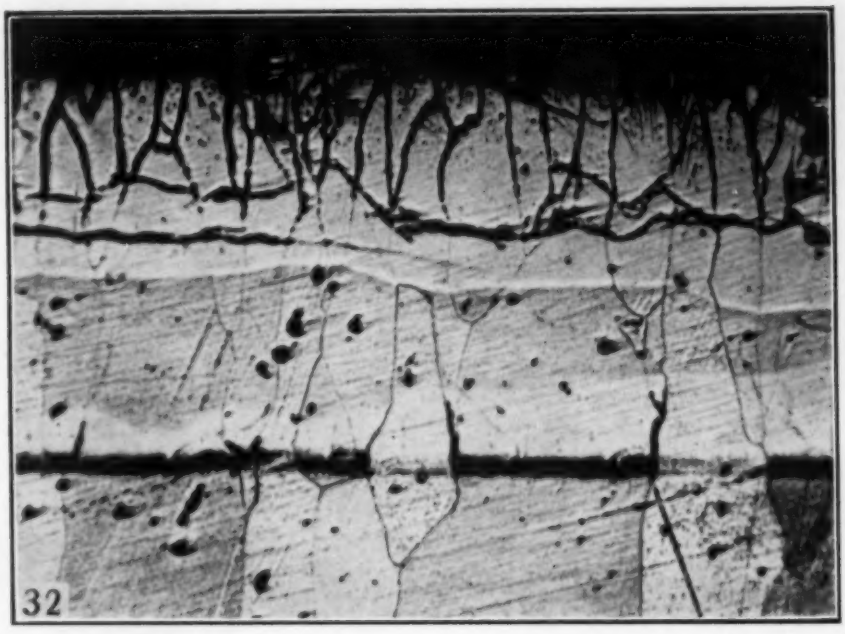


Fig. 32—Nitrided Sample of 48-Hour Diffusion of Copper-Titanium Into Armco Iron Showing Normal and Lateral Penetration of Nitriding Gas. Etch: 3% Nital. × 100.

Microhardness measurements showed an abrupt difference in hardness between the hardened diffusion side of the boundary line and the unhardened ferritic zone below. Apparently the lattice condition of the diffusion-hardened zone, especially along its lower edge, seemed to be in such a state of looseness as to allow the nitriding gas to penetrate readily. This condition is illustrated in Fig. 32 with the dark horizontal line below the center of the photograph forming the boundary line between the diffusion hardened zone and the unhardened ferritic zone. The penetration of nitrogen normal to the surface of the diffusion zone can clearly be seen and the lateral penetration from the right side and following the upper side of the boundary line is also quite evident. It is quite interesting to note that although the columnar crystals cross the boundary line they were not hardened by nitrogen below the boundary line, nor was any penetration by the nitrogen evident below the boundary line. This would indicate that titanium had been converted to a nitride in the diffusion-hardened zone. The white appearing nitrided material directly above the boundary line gave a Knoop hardness number of 890 while directly across this boundary the Knoop number obtained was 146, while the nitrided portion where penetration of nitrogen was normal to the diffusion zone and where exfoliation occurred gave a Knoop number

of 1161, while at the zone in between where penetration of nitrogen had not reached, a Knoop number of 240 was obtained. The difference in hardness between the case parallel to the interface and that at the diffusion-hardened boundary is probably due to the lower titanium concentration at the latter point. This would then indicate that the titanium had been converted to a nitride and that the concentration affected the hardness values obtained. The exfoliation was probably caused by the growth of the nitrided structure causing a strong outward force to develop. With the structure quite weak, in this case due to the columnar ferrite grains, spalling of the case is an inevitable result. Some nitride needles along the surfaces of the sides of the sample were observed but no appreciable hardening of the iron and no hard case was formed outside the diffusion-hardened zone.

Summary

(a) Metallic coatings were formed on copper-plated steel by heating a thin layer of TiH_2 in contact with the copper to a minimum temperature of about 900 C (1650 F) in a protective atmosphere of pure dry hydrogen. The resulting coatings had a surface of high metallic luster, a silver color and a dense texture. They were hard and showed brittle skin tendencies by flaking. The surface characteristics were difficult to control due to the tendency of titanium to form high-melting and brittle compounds with copper which retarded spreading of the alloy formed.

(b) Metallic coatings were produced by heating intimate mixtures of copper powder and powdered titanium hydride spread in a layer on both copper-plated and unplated steel samples. The mixtures containing from 20 to 28% TiH_2 gave satisfactory results with 25% TiH_2 content being the best. This composition being nearly a eutectic displayed the best spreading characteristics when applied to copper-plated samples and showed decided wetting tendencies. This wetting tendency was lacking in the unplated samples although satisfactory coatings were produced.

(c) Coatings were produced by melting a powdered precast 28% titanium-copper alloy spread thinly on copper-plated and unplated samples. These coatings displayed evidences of sluggish spreading characteristics and large amounts of entrapped gas in the form of blisters, causing uneven surfaces.

(d) Structures of the coatings showed as a cast type with a close resemblance to that of white cast iron with a chilled surface

skin. Hypoeutectic copper-titanium compositions showed tendency toward dendritic segregation. Hypereutectic compositions showed a tendency for one phase, presumably the higher titanium content compound, to crystallize in the form of plates normal to the surface. Eutectic structure was generally ill defined and it resembled closely one that looked like ledeburite when it occurred.

A eutectoid similar to that of pearlite was observed in the alpha solid solution of titanium in copper. The transformation temperature of this was not determined.

Evidence points toward a peritectic reaction which generates a lower titanium content copper compound on the order of Cu_3Ti from a higher titanium-copper compound $CuTi_2$.

(e) Hardness measurements showed that a white unetched microconstituent, presumably a copper-titanium intermetallic compound, produced the hardness observed in the coatings. A high difference was found between the primary solid solution and the intermetallic compound. Brittleness also was caused by the presence of this constituent. Bend tests conducted on coatings revealed that hypereutectic compositions showed no ductility and near eutectic ones showed limited internal angles of bend. The best internal angle of bend obtained was 152 degrees.

(f) Diffusion experiments showed that copper and titanium diffused into iron with production of a hardened zone within a columnar ferritic band. The boundary between the hardened zone and the unhardened columnar zone was characterized by a sharp drop in hardness and in titanium concentration as well, suggesting the hardening agent to be a precipitated iron-titanium-copper compound. The solid solubility of titanium in alpha iron was found to be quite small, 0.03%. A decided fissuring effect, characteristic of copper, occurred in the upper part of the hardened zone.

(g) The hardened diffusion zone was found to nitride while the unhardened ferritic zone appeared unaffected. A difference in hardness in the nitrided zone indicated that a lower titanium concentration produced less hardness as this ranged from a Knoop hardness number of 1161 near the surface of the 48-hour copper-titanium diffusion specimen to 890 at the boundary line.

Acknowledgment

Grateful appreciation is expressed to Dr. P. P. Alexander of Metal Hydrides, Inc., for sponsoring this research; to Dr. V. O.

Homerberg of the Massachusetts Institute of Technology for his interest in reviewing the manuscript; to Professor Rosenthal of Massachusetts Institute of Technology for his advice on X-ray diffraction studies.

References

1. F. S. Wartman, U. S. Bureau of Mines Conference on Metallurgical Research, Salt Lake City, May 21, 1940.
2. P. P. Alexander, U. S. Patent 2,351,798.
3. A. Travers, *Chimie et Industrie,* special number, March 1932, p. 345.
4. W. Kroll, *Metallwirtschaft,* Vol. 18 (4), 1939, p. 77-80.
5. J. D. Fast, *Zeitung Anorg. Chem.,* Vol. 241 (1), 1939, p. 42-56.
6. F. Laves and H. J. Wallbaum, *Naturwiss.,* Vol. 27 (4), 1939, p. 674-675.
7. W. Kroll, *Zeitschrift für Metallkunde,* Vol. 23 (33), 1931.
8. F. R. Hensel and E. I. Larsen, American Institute of Mining and Metallurgical Engineers Technical Publication 432, 1931.
9. W. J. Jones, *Journal,* Iron and Steel Institute, No. II, 1934, p. 429.
10. T. Kase, *Kinzoku No Kenkyu,* Vol. 13, 1936, p. 50.
11. J. Laissus, *Revue de Metallurgie Memoirs* (24), 1927, p. 764.
12. Wm. Hume-Rothery, Structure of Metals and Alloys, 1939, p. 100. Revised.

CAST HEAT RESISTANT ALLOYS OF THE 16% CHROMIUM-35% NICKEL TYPE

By Howard S. Avery and Norman A. Matthews

Abstract

The "HT"-type cast alloy is described in detail, with data covering mechanical properties at room temperature, as cast and after aging at 1400 F; elevated temperature strength and ductility from 1400 to 2200 F (760 to 1205 C); stress-rupture properties; creep strength from 1400 to 2150 F (760 to 1175 C); suggested working stresses; magnetic permeability; thermal expansion; elastic modulus at 1400 to 1800 F (760 to 980 C); resistance to carburization and hot gas corrosion; and the effect of temperature fluctuations on creep rates.

The relationship between yield strength and hindered contraction stresses is indicated and discussed in connection with thermal fatigue, with a hypothetical description of its mechanism.

These data are correlated with those from another parallel research program, which also provides information on hot gas corrosion resistance, Charpy impact strength, hot hardness and melting ranges.

Pertinent comparisons with the "HH" (26% Cr-12% Ni) alloys are included to differentiate their characteristics and permit choice between them for high temperature service.

HEAT resistant alloys of the "HT" type, with the nominal composition of 16% Cr and 35% Ni, are one of the first two in tonnage and importance of the cast Cr-Ni-Fe grades employed for high temperature service. They are widely used under carburizing conditions and for parts that are subjected to alternate heating and cooling. The related "HU" type, nominally 18% Cr-38% Ni, has similar properties with added hot gas corrosion resistance.

There is a dearth of metallurgical literature about the creep strength of these alloys and of explanations why they are superior to others for certain kinds of service. The purpose of this paper is to

A paper presented before the Twenty-eighth Annual Convention of the Society held in Atlantic City, November 18 to 22, 1946. Of the authors, Howard S. Avery is research metallurgist, American Brake Shoe Co., Mahwah, N. J., and Norman A. Matthews is works metallurgist, Electro-Alloys Division, American Brake Shoe Co., Elyria, Ohio. Manuscript received June 22, 1946.

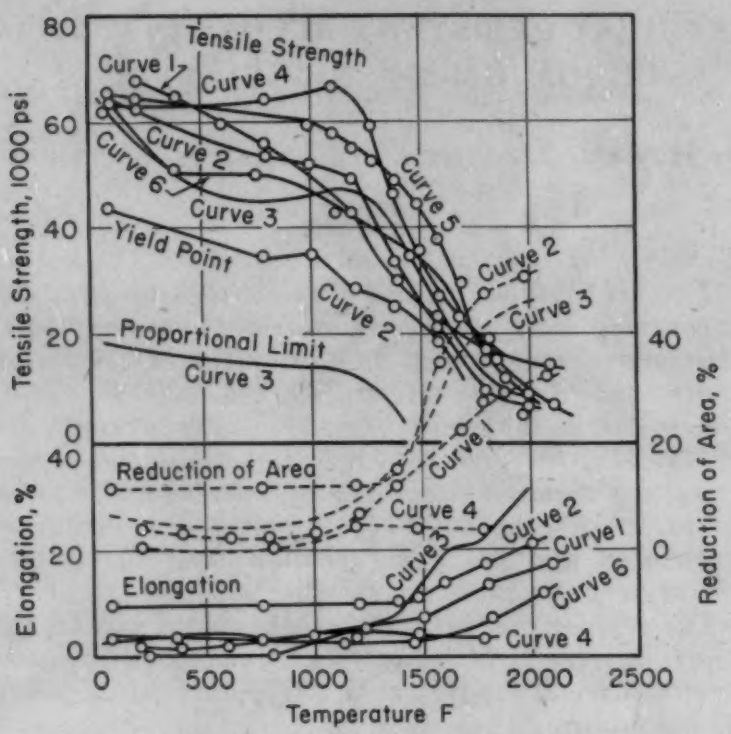


Fig. 1—Effect of Temperature on Tensile Properties of Cast Iron-Chromium-Nickel Alloys (3).

Curve	Chemical Composition, % Cr	Ni	C	Si	Mn	P	S		
1	17.0	35.0	0.50	...	...	....	...		Type composition
2	15.0	35.0	...	...	...	....	...		Type composition
3	14.95	35.55	0.50	1.52	0.70	0.045	0.04	Al	
4	20.0	8.0	1.20	...	...	....	...	1.0	Type composition
5	26.0	11.0	0.4	0.8	...	....	...	Cu	Type composition
6	13.0	60.7	0.7	0.5	0.6	....	...	0.8	Typical analysis

present data that will provide at least base line properties covering the temperature range of maximum usefulness and will permit a rational selection of the alloy for service in which its characteristics indicate suitability. Pertinent comparisons with the popular 26% Cr-12% Ni grade (A.C.I. Designation: "HH"), which has been previously described (1), (2),[1] are included. As the "HH" type is less expensive, it is important to recognize the conditions where the "HT" alloy promises superior performance.

Pilling and Worthington (3) have reported hot tensile test data on a wrought 0.10% C-16.1% Cr-36.5% Ni alloy, a cast 0.50% C-15% Cr-35% Ni, and a rolled 0.52% C-19.6% Cr-39.5% Ni grade (Figs. 1, 2, and 3). They note that cast alloys have received little study. This type is mentioned as a commercial grade for carburizing containers and general structural purposes. Design stresses (Table I)

[1]The figures appearing in parentheses pertain to the references appended to this paper.

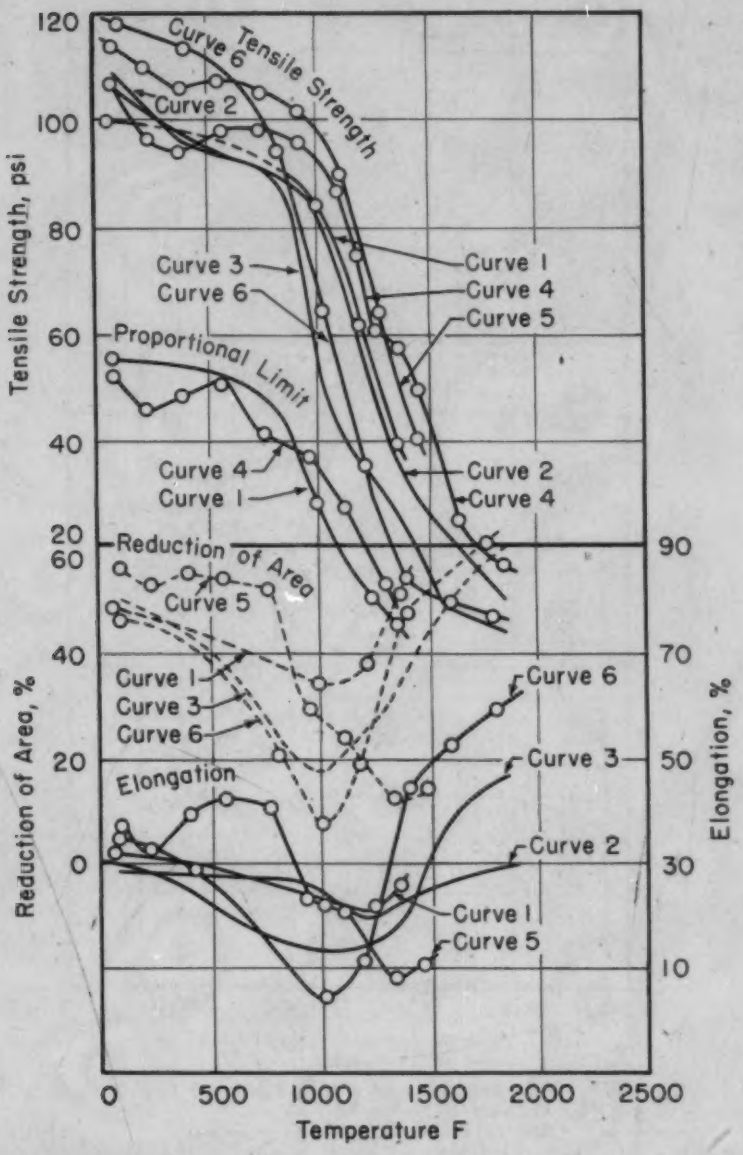


Fig. 2—Effect of Temperature on Tensile Properties of High Nickel Content Alloys (3).

Curve	Chemical Analysis, % Cr	Ni	C	Si	Mn	P	S		Heat Treat.
1	10.20	34.50	0.29	0.03	1.10	0.028	0.034		As rolled
2*	16.1	36.5	0.10	0.05	1.3	....	....		
3*	15.9	60.3	0.14	0.09	2.4	....	....		
4	11.7	65.05	0.29	0.87	1.80	0.018	0.050	Fe	W.Q.
5	19.04	79.7	0.09	0.10	..	....	0.012	0.88	As rolled
6*	19.8	bal.	0.13	0.3	2.3	....	....	0.48	

*Typical analysis.

show a wide range and are presented without substantiating creep data.

Fahrenwald (4), (5) gives a variety of data on a 17% Cr-35% Ni alloy, including ultimate strength versus temperature with a variation from 100,000 psi at 32 F to 19,000 psi at 2000 F; thermal

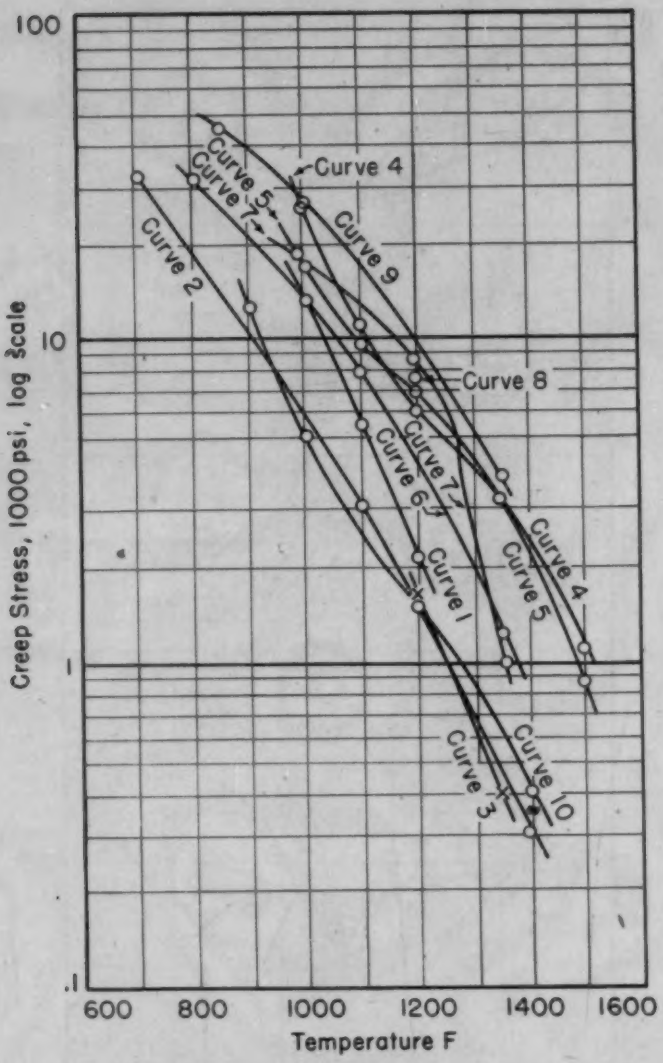


Fig. 3—Effect of Temperature on Creep Stress of Iron-Chromium-Nickel Alloys (1% per 10,000-Hour Basis) (3).

Curve	Chemical Analysis, % Cr	Ni	C	Si	Mn	P	S	Cu		Heat Treatment
1	13.22	0.14	0.11	0.30	0.45	0.020	0.028	...		
2	20.5	...	0.28	0.17	0.38	0.026	0.013	0.98		1830 F water; 1200 F
3	26.94	0.51	0.20	0.36	0.80	0.025	0.019	...		
4	6.37	19.01	0.14	1.09	0.43	0.017	0.023	...		
5	18.11	8.12	0.09	0.43	0.38	0.026	0.030	...		
6	18.10	23.4	0.21	2.96	0.53	....	....	...		Annealed
7	11.12	35.9	0.28	0.003	1.45	0.032	0.027	...		1650 F Annealed
8	24.90	19.67	0.12	0.76	0.53	0.008	0.026	...		
9	27.52	22.50	0.59	2.22	0.32	....	....	...	Fe	
10	18.8	76.0	0.31	0.27	2.79	....	....	0.66	0.80	1900 F Annealed

expansion coefficients from 7.7×10^{-6} per degree F at 32 F to 11.7×10^{-6} at 2000 F; specific heat from 0.106 at 32 F to 0.182 at 2000 F; thermal conductivity of 120 btu/sq. ft/in./hr./F at 70 F; an average emissivity at temperatures up to 1300 F of 0.25 for bright

Table I
Suggested Design Stresses for 16% Cr-35% Ni Alloys

	(Stress in Psi) Temperature				
	1400 F	1600 F	1800 F	2000 F	Reference
A ASTM-ASME—1931	5000	2000	600	300	(3)
B ASTM-ASME—1931	1800	750	290	140	(3)
C ASTM-ASME—1931	2500	1700	1250	1250	(3)
D ASTM-ASME—1931	4500	2000	500	160	(3), (4)
Wilcox—1935	....	760	300	140	(7)
Metals Handbook—1939	3600	1500	400	100	(11)
Suggested in this paper	3900	2500	1000	240	

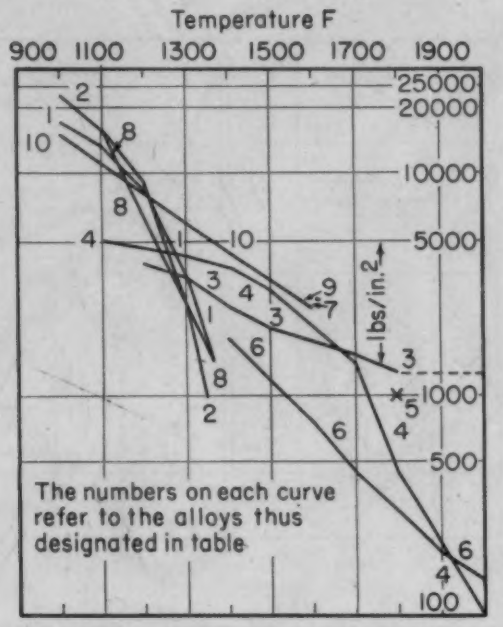


Fig. 4—Elevated Temperature Strength of "HT" Type Alloys as Summarized by Stanbery in *Metals & Alloys*, September 1933.

Composition

1. 11% Cr, 35% Ni, 0.28% C, 0.34% W
2. 13% Cr, 35% Ni, 0.32% C
3. 15% Cr, 35% Ni, 0.50% C
4. 15% Cr, 35% Ni
5. 17% Cr, 40% Ni, 0.40% C
6. 16% Cr, 36% Ni, 0.60% C
7. 19% Cr, 40% Ni, 0.95% C
8. 27% Cr, 35% Ni, 0.11% C
9. 31% Cr, 33% Ni, 0.26% C
10. 46% Cr, 50% Ni, 0.24% C

and 0.75 for oxidized metal; and an air oxidation rate of 0.01 inch per 100 hours (0.9 inch per year) at 2300 F. The sources of these data are obscure and descriptions of experimental techniques are generally lacking.

Stanbery (6) approximately defines the type composition as 0.30 to 0.50% C, 15 to 20% Cr, and 35 to 45% Ni. He gives the expansion coefficient as 11.0×10^{-6} per degree F from 1000 to 2100 F;

the weight as 495 lbs./cu. ft. or 0.288 lbs./cu. in.; and the thermal conductivity of 35% that of 0.20% C steel. His summary of hot strength data appears as Fig. 4.

Wilcox (7) in describing the 29% Cr-9% Ni alloy gives short-time tensile strength and recommended design stress values of 15% Cr-35% Ni for comparison, with the remark that the high temperature characteristics and design values of 28% Cr-10% Ni are only slightly lower than those for 15% Cr-35% Ni (Fig. 5). (This generalization should be accepted with extreme caution, as the "HE"

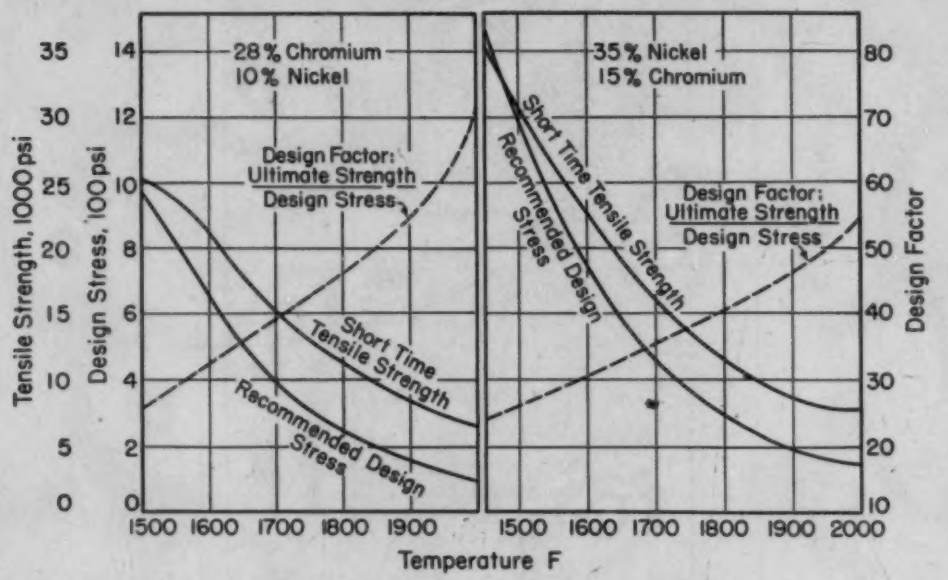


Fig. 5—Design Stress Values and Hot Tensile Strength of "HT" and "HE" Types of Heat Resistant Alloys as Given by Wilcox in METAL PROGRESS for May 1935.

and "HH" alloys involved cover a very wide range of properties. It is approximately true only if the "HH" alloy is properly balanced to produce a stable austenite.)

During the past nine years, close contact through committee action has been maintained with the research program sponsored by the Alloy Casting Institute at Battelle Memorial Institute under the direction of Dr. O. E. Harder and Mr. J. T. Gow. The 16% Cr-35% Ni alloy has received considerable attention recently. Detailed reports, which are useful supplements to the original data reported herein, are available only to members of the A.C.I. but summaries of important results have been published (2), (8), (9), (10), (12), (20) and where pertinent have been included in the text of this paper.

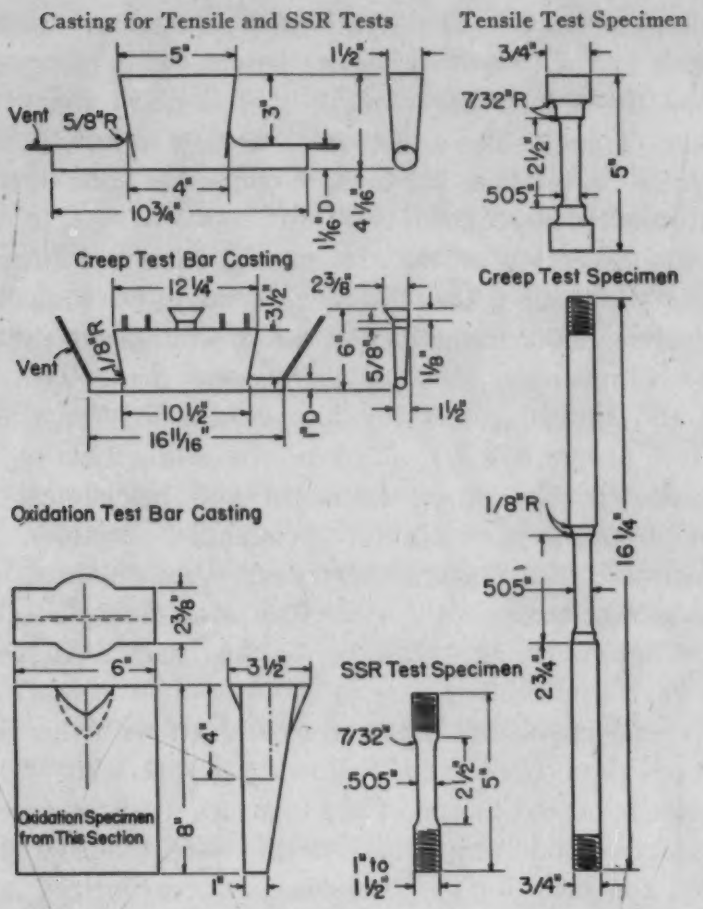


Fig. 6—Heat Resistant Alloy Test Castings and Specimens.

Experimental Procedure

The data herein are part of those obtained during a broad program of research on the cast heat resistant alloys, which has been in progress for about 12 years.[2] Creep and stress-strain-rupture tests, which require careful and critical control to obtain consistent and reproducible data, have followed in general the previously described procedures (13) as standardized at the American Brake Shoe Company Metallurgical Laboratory. The test specimens and the castings from which they are obtained appear in Fig. 6. The patterns were developed after considerable experiment to produce sound cast bars. The 10-inch bar design was subsequently adopted as standard for ASTM B-4 specification B190-44T and for Alloy

[2]This program was originally sponsored by the American Manganese Steel Company while a subsidiary of the American Brake Shoe and Foundry Company, and at present is co-ordinated with the production practices of the Electro-Alloys Division and the American Manganese Steel Division of the American Brake Shoe Company. Organizational consolidation has not affected the continuity of the research.

Casting Institute work. The stress-rupture tests are usually made on the 5-inch bar with a 2-inch gage length, while long-term creep tests employ the 4-inch gage length that doubles the precision of measurement. There is also a distinct advantage in having the threads of the specimen on the long bar outside of the hot zone of the furnace at temperatures above 1800 F (980 C).

With the exception of the commercial basic arc furnace heats, which are so designated, the alloys were made by conventional induction furnace practice in the Experimental Foundry of the American Brake Shoe Company. Most of them were made with the same equipment and procedure as the alloys supplied for the hot gas corrosion test program (20), (21) of the Alloy Casting Institute, which permits correlation of oxidation and mechanical test data without complications from different production variables.

The basic direct arc furnace specimens were obtained from commercial production heats in the American Manganese Steel Division foundry at Chicago Heights, Illinois, or the Electro-Alloys Division foundry at Elyria, Ohio.

The thermal expansion data were obtained with the dilatometer described by Flinn, Cook and Fellows (14) on flat, 4-inch gage length specimens heated in one of the furnaces used for creep testing.

Laboratory carburizing experiments were made with ⅞-inch diameter by 2½-inch long specimens pack carburized at 1800 F (980 C) in small heat resistant alloy boxes. Estimates of carburization were obtained from microscopical examination of cross sections, weight gain, diameter increase, and carbon determinations on successive lathe cut samples. The carburizing agent was renewed for each 24-hour carburizing cycle.

Some low carbon 16% Cr-35% Ni alloys were also field tested in an industrial carburizing environment. The specimens, in the form of 1 by 1 by 2-inch blocks, were welded to the bottom surface of carburizing box tops, and underwent a total of 1500 hours inside the boxes, presumably in contact with the carburizing compound and certainly exposed to carburizing gases, while heated to approximately 1775 F (970 C). Carburization was evaluated by microscopic examination.

These same low carbon alloys were exposed intermittently, as similar blocks, in an industrial heat treating furnace at 1940 F (1060 C). Oxidation was evaluated by periodic measurements of thickness.

Another group of specimens from the heats supplied for the A.C.I. hot gas corrosion test program were similarly exposed in a furnace controlled at 1940 F (1060 C). These permit direct comparisons of data from the two programs.

The hindered contraction tests were conducted by heating a specimen 16 by 7/8-inch diameter with a 0.505-inch diameter by 1-inch long gage length to a high temperature (using conventional hot tensile test equipment), applying a small load to remove any slack in the system, and then slowly cooling the test bar. The unrelieved stress characteristic of each temperature during the cooling period appears on the load indicator of the machine and is plotted as in Fig. 20.

Magnetic tests were made in a special permeameter described in AIME T.P. No. 1443 (13), employing machine ground 1.00-inch long by 0.250-inch diameter specimens and a magnetizing force of 24 oersteds. The short, straight specimen, which was adopted to permit sampling the gage length of tested creep bars, militates against obtaining correct absolute values at high permeability levels. Near unity the data are believed to be dependable; above Mu = 2.0, they should be considered as relative.

Composition

The "HT"[3] alloys range from 13 to 17% Cr and 34 to 37% Ni. The "HU" grade covers 17 to 21% Cr and 37 to 40% Ni. There is as yet no clear evidence that variations within the extremes established by both of these ranges, or of manganese between 0.50 and 1.25%, exert any serious effect on mechanical properties or elevated temperature strength. In contrast, carbon and silicon exert important effects and must be carefully considered in the specification and utilization of these grades.

Chemical behavior, especially in hot gases, does not follow the same pattern. Chromium is the most potent protective element, with nickel contributing about one-third the same influence (on a weight percentage basis) in oxidizing atmospheres. In the presence of appreciable hydrogen sulphide, nickel is ineffective and may be a liability. Carbon content is apparently not critical, while silicon

[3]The Alloy Casting Institute designations are coded as follows: (a) The initial letter indicates service; "H" for heat resistance and "C" for corrosion resistance; (b) The second letter represents the specific type, such as "HH" for 26% Cr-12% Ni, "HT" for 16% Cr-35% Ni, "HU" for 18% Cr-38% Ni, "HW" for 12% Cr-60% Ni, etc.; (c) Numerals following the letters imply the midpoint of a 0.10% C range. For specific heats in this paper they indicate the actual carbon content in hundredths of a per cent.

tends to reinforce the protective effect of chromium. Silicon also confers resistance to carburization. Nickel probably exerts a similar but lesser effect, perhaps operating in opposition to the carbide-forming tendencies of chromium.

Usual foundry production will fall within the limits:

C, %	Mn, %	Si, %	Ni, %	Cr, %
0.35	2.0	2.0	33	13
0.75	max.	max.	37	17

which are being considered for a tentative ASTM specification. The similar "HU" grade differs only in chromium and nickel. There is some tendency to merge the two grades and to produce within an intermediate specification.

The distinct role of nitrogen in this alloy has not been established but it is undoubtedly of considerably less importance than in the 26% Cr-12% Ni alloy. The "HT" alloy is stably austenitic by a wide margin, whereas the "HH" alloy may be shifted from a stable austenite to a partially ferritic alloy by variations in nitrogen content. The usual range of nitrogen is from 0.02 to 0.06% in commercial practice and thus, assuming potency equivalent to carbon, may be neglected as a variable.

The latitude in carbon should not be accepted as assurance that properties do not vary appreciably within the 0.35 to 0.75% limits. Room temperature ductility is particularly affected. Manufacturers work to closer limits within this range when applications require specific properties. However, other variables, such as pouring temperature and cooling rate, sometimes overshadow the effect of carbon on elevated temperature properties.

Room Temperature Mechanical Properties

Carbon exerts a pronounced influence on ductility at ordinary temperature, as shown in Fig. 7. The corresponding as-cast tensile strength varies little, any definite trend being masked by the normal experimental errors. An ultimate strength of 70,000 psi $\pm$ 5000 psi is probably representative. The Brinell hardness range is about 150 to 185.

Aging of even the low carbon compositions at temperatures that permit carbide precipitation will develop a moderate increase in tensile strength and a drop in ductility (Fig. 7). This has no established significance for industrial utilization other than to indicate the

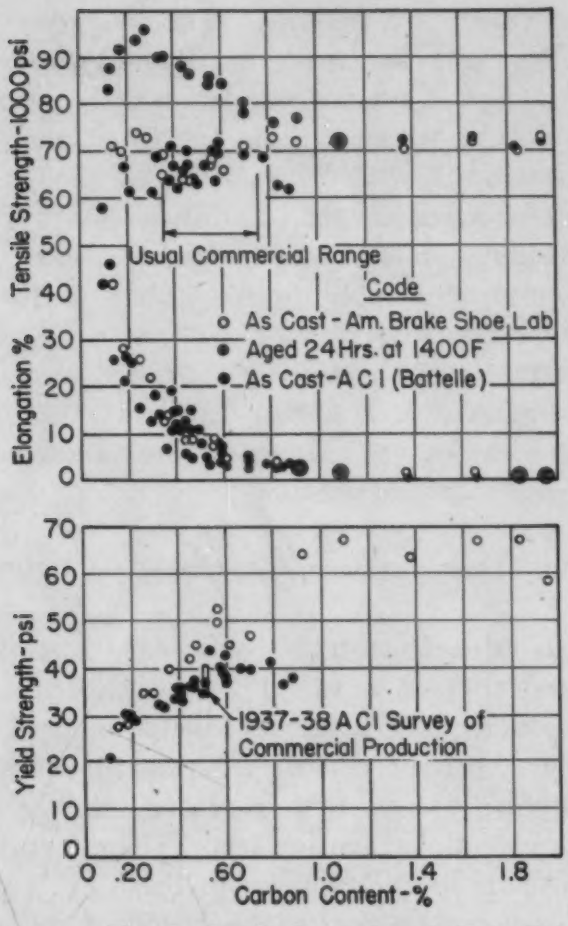


Fig. 7—Tensile Properties of 15% Chromium-35% Nickel Alloys. As cast and aged 24 hours at 1400 F (815 C).

	Composition Range, %				
	Mn	Si	Ni	Cr	N
American Brake	0.67	1.17	34.4	15.9	0.03
Shoe Co.	0.83	1.43	35.0	16.5	0.05
A.C.I.	0.60	0.53	29.9	14.4	0.02
	1.11	2.26	40.8	19.1	0.08

mechanism of a slight dimensional change. Contraction accompanies carbide precipitation. If high dimensional precision at a single elevated temperature is required it is advisable to age at this temperature before putting castings in service.

Ductility after aging has been used as an acceptance test for the 26% Cr- 12% Ni alloys, with designation of two grades, having 4 and 9% minimum elongation after 24 hours at 1400 F (15) respectively. The 9% elongation material is intended as the premium grade. The 16% Cr-35% Ni alloys in the commercial carbon range would not meet this requirement, yet they are considered better for severe service where cyclic heating, hindered thermal contraction, and asso-

ciated thermal stresses are serious. This suggests a critical re-examination of the merits of tensile test ductility after aging, which has the disadvantage of a negative correlation with creep strength (1).

The tensile data as shown here do not differ much from those of substantially austenitic 26% Cr-12% Ni alloys, though the latter are usually somewhat stronger as cast. Both have adequate strength and toughness for handling, fabrication, and performance at room temperature in appropriate applications. They differ at elevated temperatures, however.

There is a trend toward greater yield strength as carbon increases, which may be seen in Fig. 7 and in Tables II and III, which are condensed summaries from A.C.I. work, the values being generally reported to two significant figures.

Elevated Temperature Strength and Ductility

Hot strength on a short-term basis may be evaluated by hot tensile tests, stress-rupture tests, or by an experimental hindered contraction procedure. The last two have been used in this work as they are believed to more closely represent service conditions, which seldom involve a load that increases steadily until fracture occurs as in the conventional tension test. The effect of temperature on short-time tensile properties appears in Table IV.

A standardized load in the neighborhood of the yield strength will permit the same comparison of ductility as tensile tests, though the values are usually lower. In addition, creep rate and fracture time data are obtained for plotting with other stress-rupture and creep tests. For comparison purposes, the values of 20,000 psi at 1400 F (760 C), 10,000 psi at 1600 F (870 C), and 6000 psi at 1800 F (980 C) have been selected.

In Table V, the effect of carbon on both the 16% Cr-35% Ni and 26% Cr-12% Ni alloys is shown at two temperatures. The 26% Cr-12% Ni alloy becomes more brittle at 1400 F (760 C) above 0.40% C and at 1800 F above about 0.45%. The transition from partially ferritic to wholly austenitic structure occurs at about 0.43% C in the 26% Cr-12% Ni series given (1). If other composition changes are invoked to stabilize austenite, such as increased nickel or decreased chromium, the point at which 16% Cr-35% Ni hot ductility becomes greater may be around 0.30% C or below. (A 0.32% C ferrite-free 24% Cr-13% Ni alloy exhibited 15.5 hours' life and 3.5% elonga-

Table II
Summary of A.C.I. Tensile Test Data on "HT" Alloys (12)

Specimens supplied by various manufacturers.

Heat No.	Chemical Analysis, %							Room Temperature — As Cast						Room Temp.—Aged 1600 F—48 Hrs.						Tested at 1600 F						Tested at 1800 F					
	C	Mn	Si	Ni	Cr	N	Mo	PL	YS	TS	EL	RA	EM	PL	YS	TS	EL	RA	EM	PL	YS	TS	EL	RA	EM	PL	YS	TS	EL	RA	EM
A	0.50	0.81	1.34	35.8	15.3	0.059	...	14	36	66	5.5	6.6	25	16	38	68	3.0	2.8	25	...	..	..	..	..	...	5.1	7.6	11.0	42	45	...
C	0.48	0.67	1.14	35.3	15.9	0.032	...	13	36	63	5.5	7.2	26	16	36	70	4.0	4.6	25	...	..	..	..	..	...	5.2	8.0	12.0	29	42	...
D	0.49	0.74	0.77	35.6	15.3	0.052	...	13	36	64	5.5	6.1	23	17	38	76	3.5	7.4	23	...	..	..	..	..	...	4.7	8.5	12.0	27	40	...
E	0.54	0.99	0.91	34.6	15.1	0.018	...	14	37	63	4.0	4.9	23	17	39	75	4.0	4.2	26	...	..	..	..	..	...	4.7	8.0	12.0	35	42	...
F	0.49	0.93	0.93	35.4	15.2	0.060	...	13	34	63	5.5	5.8	22	15	35	22	6.0	7.3	23	...	..	..	..	..	...	5.2	7.5	10.0	39	55	...
G	0.50	0.83	0.99	35.3	14.9	0.025	...	16	35	56	6.5	7.2	25	17	43	73	3.5	3.8	24	...	..	..	..	..	...	5.2	9.1	12.0	21	42	...
H	0.52	0.74	0.53	34.9	15.2	0.035	...	18	41	65	4.0	4.2	26	19	42	78	4.0	5.3	26	...	..	..	..	..	...	5.6	8.5	12.0	42	48	...
I	0.46	0.92	0.92	34.7	15.7	0.024	...	14	35	65	6.0	7.4	21	17	38	72	5.5	7.1	23	...	..	..	..	..	...	5.0	8.8	11.0	28	57	...
J	0.54	0.74	1.06	34.5	14.9	0.05	0.076	15	39	67	4.5	5.3	24	18	41	74	4.0	5.1	24	...	..	..	..	..	...	5.0	8.2	11.0	29	46	...
																				Pre-aged 48 Hrs.—1600 F											
B	0.41	0.71	1.59	35.0	14.9	0.03	...	19	33	62	11.0	12.0	21	19	50	79	3.5	4.1	20	7.8	12	17	25	38	11.9	4.8	7.0	8.5	27	53	9.8
L	0.58	0.92	1.31	34.4	17.3	0.08	...	19	39	64	4.0	4.0	21	18	51	77	2.5	3.1	21	7.1	14	19	24	32	15.3	6.2	8.9	10.2	28	40	10.5
K	0.84	1.03	1.95	40.8	14.4	0.03	...	17	37	63	2.5	2.1	20	18	53	79	2.5	4.1	21	5.8	12	19	22	32	14.0	4.3	7.2	8.8	23	44	8.9
ZG	0.10	0.75	1.59	34.0	15.7	0.04	...	13	22	58	42.0	48.0	19	21	25	71	32.0	42.0	22	6.6	10	15	33	75	9.5	...	...	...	..	..	...
U	0.17	0.60	0.53	37.1	17.6	0.02	...	22	30	83	46.0	38.0	..	19	33	88	35.0	36.0	..	6.5	15	20	13	12	15.0	6.4	7.8	10.8	13	13	9.2
N	0.19	1.11	1.41	38.1	18.5	0.04	...	18	30	67	26.0	28.0	19	19	34	77	13.0	12.0	27	5.5	12	19	19	24	12.8	3.8	8.2	10.1	25	37	10.5
R	0.33	1.00	1.34	36.2	15.3	0.03	...	15	34	69	14.0	20.0	26	20	38	70	5.0	89.0	25	6.7	13	19	31	54	15.5	5.5	9.4	13.2	35	59	12.5
ZB	0.39	1.06	0.66	34.8	16.7	0.08	...	16	36	71	11.0	13.0	21	18	..	74	3.5	4.8	23	7.5	16	22	28	43	17.5	4.6	7.2	10.2	35	42	10.0
ZD	0.39	0.77	1.39	35.1	19.1	0.04	...	16	34	71	15.0	14.0	22	20	40	72	4.0	6.2	24	6.8	12	17	25	26	15.0	4.6	8.2	12.2	29	31	10.0
Z	0.40	0.71	1.95	29.9	16.8	0.05	Cu	18	36	67	12.0	12.0	23	17	40	72	4.0	6.2	29	6.0	13	19	26	35	15.0	6.1	8.8	12.2	21	42	9.6
O	0.46	0.97	1.31	37.1	15.9	0.04	0.23	22	36	70	15.0	12.0	20	27	46	75	2.5	2.7	..	7.5	15	15	34	42	17.0	6.0	9.6	11.3	31	39	12.7
T	0.50	0.65	1.94	32.2	17.7	0.04	...	18	37	63	8.0	10.0	24	21	45	70	2.5	1.7	26	8.0	15	20	21	34	18.0	5.6	9.0	13.4	23	25	7.3
S	0.53	0.74	1.09	36.3	15.4	0.06	...	..	44	67	5.0	7.0	25	29	49	76	2.5	4.7	23	8.8	16	21	26	37	18.5	6.0	12.0	13.8	22	38	13.5
Y	0.57	0.94	1.30	35.1	18.0	0.06	...	20	40	70	7.5	8.1	28	21	47	73	1.5	2.1	28	8.2	17	22	24	29	13.5	4.7	8.0	10.9	27	37	8.0
ZC	0.59	0.88	1.77	34.8	15.9	0.06	...	21	43	72	5.5	4.3	22	18	40	71	4.0	3.9	26	9.2	15	18	31	46	16.5	6.7	8.9	11.6	30	40	10.8
W	0.66	0.76	1.34	37.1	15.6	0.05	1.36	18	40	67	3.5	3.3	27	..	40	73	3.5	4.3	..	6.5	13	18	24	35	16.5	5.4	9.0	12.9	31	30	9.3
M	0.70	0.84	1.72	35.6	16.3	0.03	...	19	40	78	5.0	5.8	21	22	41	76	3.0	3.9	24	6.8	14	20	18	28	13.5	4.5	9.4	12.8	19	28	11.0
ZF	0.78	1.05	1.54	36.9	16.8	0.03	0.23	20	41	69	3.5	3.9	20	16	41	75	4.5	5.0	22	8.5	16	22	23	38	15.0	...	...	...	..	..	...
ZE	0.88	0.97	2.26	33.4	18.5	0.02	...	21	38	62	3.5	4.7	19	18	41	73	3.0	3.1	31	...	12	20	37	39	11.2	4.5	6.5	10.5	38	48	8.5

Code: PL = Proportional Limit in 1000 Psi. YS = Yield Strength for 0.2% Offset, in 1000 Psi. TS = Ultimate Tensile Strength in 1000 Psi.
EL = Elongation in 2 in., %. RA = Reduction in Area in %. EM = Elastic Modulus in Million Psi.

Table III
Summary of A.C.I. Tensile Test Data on "HT" Alloys (12)

Specimens produced under laboratory conditions

Heat No.	Chemical Analysis, %						Room Temperature — As Cast						Room Temp.—Aged 1600 F—48 Hrs.						Pre-aged 48 Hrs. at 1600 F						Tested at 1800 F					
	C	Mn	Si	Ni	Cr	N	PL	YS	TS	EL	RA	EM	PL	YS	TS	EL	RA	EM	PL	YS	TS	EL	RA	EM	PL	YS	TS	EL	RA	EM
B-1*	0.52	5.08	1.06	29.9	15.2	0.034	25	42	63	8.5	11.0	23	26	50	79	3.5	4.1	22	...	...	..	..	..	...	5.3	8.8	13	31	43	...
B-2*	0.52	9.21	1.19	24.6	15.2	0.054	25	41	64	9.0	10.0	27	26	51	77	2.5	3.1	23	...	...	..	..	..	...	4.8	8.2	12	24	31	...
B-3*	0.52	14.4	1.27	20.3	15.4	0.035	27	41	61	9.0	14.0	24	21	53	79	2.5	4.1	27	...	...	..	..	..	...	5.4	9.2	12	17	23	...
																			Tested at 1600 F											
B-77	0.21	0.72	1.13	35.6	16.7	0.020	19	29	61	25.0	26.0	24	23	37	83	2.5	30.0	27	6.0	13.1	17	8	20	14.3	7.5	9.2	10	8	12	8.9
B-78	0.31	0.82	1.12	35.4	16.0	....	21	32	61	18.0	24.0	24	23	42	78	6.5	10.0	25	9.4	14.4	18	17	44	13.5	5.0	9.6	12	24	60	7.3
B-83	0.38	0.79	1.16	36.3	16.8	0.018	19	34	64	20.0	16.0	22	24	47	77	4.6	4.3	22	9.0	15.8	20	20	33	14.5	6.9	11.0	12	20	55	10.4
B-79	0.40	0.77	1.16	34.8	16.5	....	19	35	67	15.0	14.0	23	21	39	72	4.0	3.9	20	8.2	14.7	18	26	53	13.5	6.1	9.0	12	21	60	8.4
B-84	0.44	0.84	1.21	35.3	16.2	0.020	20	36	66	13.0	15.0	25	19	39	78	4.9	6.3	19	8.5	13.4	18	24	44	11.5	5.0	9.2	12	25	56	11.0
B-80	0.46	0.70	1.22	36.5	16.2	....	21	38	67	11.0	10.0	23	20	39	76	5.8	8.2	21	7.7	...	19	33	49	15.5	5.3	8.8	11	30	50	10.0
B-81	0.49	0.80	1.13	35.9	16.1	....	18	35	64	11.0	12.0	24	22	41	79	5.7	6.2	21	6.0	12.5	18	25	59	14.5	5.1	...	11	27	62	10.2
B-82	0.59	0.74	0.98	36.3	16.4	....	19	38	68	7.5	8.5	24	17	40	84	6.2	5.4	22	7.0	14.0	19	25	53	14.6	6.4	10.0	12	21	49	9.8
B-56	0.59	0.78	1.10	35.3	16.1	....	16	38	69	7.5	3.5	21	20	41	81	4.2	5.1	21	7.6	13.6	19	27	51	15.5	5.7	10.1	12	32	46	8.4
B-57	0.70	0.70	1.07	36.0	16.0	....	..	..	69	4.8	5.1	21	22	43	81	5.0	7.9	20	9.2	15.2	20	29	41	11.5	7.9	10.2	14	21	50	7.8

Code: RT = Room Temperature. PL = Proportional Limit in 1000 Psi. YS = Yield Strength for 0.2% Offset, in 1000 Psi. TS = Ultimate Tensile Strength in 1000 Psi. EL = Elongation in 2 in., %. RA = Reduction in Area in %. EM = Elastic Modulus in Million Psi.
*A.C.R.I. Test Block Specimens (8). All other tests on specimens from Fig. 6 type castings.
Note: The original data are reported in greater detail; they have been generally condensed to two significant figures here.

tion at 1400 F with 20,000 psi; and 13.4 hours with 9.0% elongation at 1800 F with 6000 psi.)

The occurrence of high ductility above 1400 F thus appears to depend on the presence of ferrite in 26% Cr-12% Ni. In the absence of ferrite, there is a definite lowering of elongation as carbon increases, while the 16% Cr-35% Ni alloy, in sharp contrast, shows the opposite trend. This absence of a negative correlation between carbon content and hot ductility for the latter alloy is noteworthy; it does not parallel the room temperature behavior and is a significant point of superiority over 26% Cr-12% Ni. As most of the carbon is in combination as chromium carbides and not in solid solution in the austenite matrix, it is possible that the mechanism involves lowering the matrix chromium content. This cannot be done by direct composition control without impairing oxidation resistance.

The relation between carbon and hot ductility has an important bearing on behavior under carburizing conditions. Austenitic heat resistant alloys in the form of muffles, retorts, boxes, etc., absorb carbon much more slowly than the ferritic steels being processed in them, but eventually they will carburize deeply to about 2% carbon. There is some field evidence that ultimate failure of 16% Cr-35% Ni alloys, if sound and not overstressed by static loading, is associated with attainment of approximately this carbon level throughout the cross section of a casting. Brittleness without high elastic strength confers vulnerability to stresses induced by thermal gradients, which are common under the cyclic heating condition of heat treating and carburizing practice. From Table V, it is reasonable to conclude that such vulnerability occurs much earlier in the life of a 26% Cr-12% Ni alloy part. This, together with equal or greater tendency to absorb carbon, as will be shown later, explain its unsuitability and the generally acknowledged superiority of 16% Cr-35% Ni for carburizing service.

For convenience, the A.C.I. tensile test data at 1600 and 1800 F are assembled in Tables II and III and the corresponding stress-rupture data in Table VI. The tensile values for the first nine heats are averages from four individual tests; the over-all average of them, representing a survey of commercial production in 1937, appears in Table VII.

The short life and high creep rates of alloys below 0.35% C are noteworthy, justifying the recommendation that this be the commercial minimum for alloys to be used at elevated temperatures where

Table IV
Effect of Temperature on Tensile Properties*

Composition, %					
C	Mn	Si	Ni	Cr	N
0.33	0.60	1.29	35.8	16.3	0.04

Temperature F	Temperature C	Ultimate Tensile Strength psi	Elongation % in 2 in.	Reduction in Area %
80	26	68,750	14.0	18.9
1400	760	34,800	13.5	18.5
1400	760	34,380	13.5	20.4
1472	800	27,560	17.5	29.3
1600	870	19,350	26.0	42.3
1600	870	18,200	27.5	35.0
1670	910	15,100	25.5	40.2
1800	982	10,850	19.0	40.3
1800	982	10,700	23.0	31.4
1905	1040	8,020	30.0	33.2
2000	1093	5,720	37.0	45.1
2282	1250	2,970	42.5	65.7

*The rate of load application strongly influences elevated temperature test results. These data were obtained with loading corresponding to a free crosshead speed of 0.03 inch per minute. The specimens were held at temperature an hour before loading. Approximate yield strength values were obtained but are not reported here as the data in Table V are considered more useful.

Table V
Comparative Stress-Rupture Properties

16% Cr-35% Ni (HT) and 26% Cr-12% Ni (HH) Alloys

Alloy	Composition, % C	Mn	Si	Ni	Cr	N	Structure
			26% Cr-12% Ni Series				
HH-31	0.31	0.42	0.42	11.4	26.5	0.07	Partially Ferritic
HH-42	0.42	0.45	0.45	11.3	26.1	0.06	Partially Ferritic
HH-52	0.52	0.53	0.47	11.4	26.4	0.07	Wholly Austenitic
HH-61	0.61	0.31	0.48	11.4	26.3	0.07	Wholly Austenitic
			16% Cr-35% Ni Series				
HT-35	0.35	0.67	1.28	34.9	16.0	0.05	Austenitic
HT-36	0.36	0.81	1.19	34.8	16.0	0.04	Austenitic
HT-44	0.44	0.74	1.17	35.0	16.2	0.05	Austenitic
HT-47	0.47	0.82	1.23	34.9	16.0	0.04	Austenitic
HT-56	0.56	0.71	1.22	34.7	16.4	0.04	Austenitic
HT-56	0.56	0.80	1.27	34.8	15.9	0.04	Austenitic
HT-61	0.61	0.76	1.29	34.6	16.1	0.05	Austenitic
HT-70	0.70	0.81	1.26	34.7	16.5	0.05	Austenitic
HT-92	0.92	0.78	1.17	34.6	16.2	0.05	Austenitic

Alloy	1400 F—20,000 psi Life in Hours 16-35	26-12	Elong.—% 16-35	26-12	1800 F—6000 psi Life in Hours 16-35	26-12	Elong.—% 16-35	26-12
HH-31	..	3	..	20	..	3	..	56
HT-35	29	..	16	..	..	..	..	..
HT-36	32	..	23	..	24	..	9	..
HH-42	..	10	..	10	..	21	..	11
HT-44	60	..	14	..	70	..	7	..
HT-47	50	..	14	..	50	..	6	..
HH-52	..	36	..	3	..	52	..	1
HT-56	37	..	14	..	22	..	17	..
HT-56	52	..	21	..	52	..	11	..
HH-61	..	42	..	2	..	47	..	2
HT-61	14	..	19	..	..	..	..	..
HT-70	16	..	19	..	..	..	..	..
HT-92	16	..	19	..	..	..	..	..

strength is an important factor. The decrease in strength as silicon is raised (alloys D-20, D-21, and D-22) is also significant. This trend is frequently encountered in experimental work with both 16% Cr-35% Ni and 26% Cr-12% Ni alloys, though it is usually less

Table VI-A
Summary of A.C.I. Stress-Rupture Data on "HT" Alloys

Specimens Supplied From Commercial Production
Aged 48 Hours at 1600 F Before Testing

Heat	Chemical Analysis, %							Stress-Strain-Rupture Properties: 1600 F—12,000 psi				1800 F—7000 psi			
No.	C	Mn	Si	Ni	Cr	N	Cu	Life Hrs.	Min. Creep Rate %/Hr.	Elong. %	Red. Area %	Life Hrs.	Min. Creep Rate %/Hr.	Elong. %	Red. Area %
ZG	0.10	0.75	1.59	34.0	15.7	0.04	...	0.14	12.0	28	27	1.4	5.0	8	12
U	0.17	0.60	0.53	37.1	17.6	0.02	...	0.8	8.1	10	9	1.5	5.5	13	16
N	0.19	1.11	1.41	38.1	18.5	0.04	...	1.1	9.5	17	26	8.3	0.35	15	27
R	0.33	1.00	1.34	36.2	15.3	0.03	...	4.2	1.1	18	44	8.7	0.4	9	27
ZB	0.39	1.06	0.66	34.8	16.7	0.08	...	8.1	1.2	22	40	5.0	1.0	18	23
ZD	0.39	0.77	1.39	35.1	19.1	0.04	...	4.2	1.8	20	28	7.4	0.7	15	20
Z	0.40	0.71	1.95	29.9	16.8	0.05	...	5.3	2.0	21	30	11.0	0.17	9	22
O	0.46	0.97	1.31	37.1	15.9	0.04	0.23	15.0	0.42	15	33	13.0	0.13	5	9
T	0.50	0.65	1.94	32.2	17.7	0.04	...	11.0	0.55	14	16	30.0	0.04	6	11
S	0.53	0.74	1.09	36.3	15.4	0.06	...	0.42	0.05	6	17	9.6	0.39	9	20
Y	0.57	0.94	1.30	35.1	18.0	0.06	...	11.0	0.76	17	29	4.9	2.8	27	32
ZC	0.59	0.88	1.77	34.8	15.9	0.06	...	4.2	4.5	28	42	5.8	1.6	19	23
W	0.66	0.76	1.34	37.1	15.6	0.05	1.36	6.1	1.8	24	48	3.5	2.2	16	30
M	0.70	0.84	1.72	35.6	16.3	0.03	...	8.2	1.2	19	33	5.4	1.3	13	17
ZF	0.78	1.05	1.54	36.9	16.8	0.03	0.23	7.5	1.5	20	35	4.2	3.0	30	34
ZE	0.88	0.97	2.26	33.4	18.5	0.02	...	2.2	7.7	27	39	6.5	1.0	19	17
B	0.41	0.71	1.59	35.0	14.9	0.03	...	3.0	3.5	15	32	2.5	3.5	17	31
L	0.58	0.92	1.31	34.4	17.3	0.08	...	3.1	5.5	27	43	5.2	2.7	26	43
K	0.84	1.03	1.95	40.8	14.4	0.03	...	2.4	7.5	26	43	1.8	12.0	39	50

prominent in short-time tensile tests. The effect does not always occur, and some data support the idea that it diminished for long-term creep tests on "HT" alloys. Studies are in progress on this; the current conclusion is that silicon probably will decrease high temperature strength. Additional data appear in Table X.

Creep Strength

The creep strength of the 16% Cr-35% Ni alloys has been established with reasonable accuracy over the range from 1400 to 2000 F The Alloy Casting Institute data have been obtained chiefly at 1600 F, though 1800 F tests are in progress. The 1600 F results provide a survey of Cr and Ni variations on the base alloy. As carbon content has been included as a variable in the American Brake Shoe Company program it is probable that the values in Fig. 15 are representative of commercial production that is under good technical control.

The conventional designation of load carrying ability for 16% Cr-

Table VI-B
Summary of A.C.I. Stress-Rupture Test Data on "HT" Alloys

Specimens Produced Under Laboratory Conditions
Aged 48 Hours at 1600 F Before Testing

Heat No.	Chemical Analysis, % C	Mn	Si	Ni	Cr	W	Stress-Strain Rupture Properties: 1600 F—12,000 psi Life Hrs.	Min. Creep Rate %/Hr.	Elong. %	Red. Area %	1600 F—9000 psi Life Hrs.	Min. Creep Rate %/Hr.	Elong. %	Red. Area %	1600 F—7000 psi Life Hrs.	Min. Creep Rate %/Hr.	Elong. %	Red. Area %
B-77	0.21	0.72	1.13	35.6	16.7	0.020	0.5	6.7	7.0	9.2	..	....	...	...	...	....	..	...
B-78	0.31	0.82	1.12	35.4	16.0	....	2.5	2.8	18.0	21.0	..	....	...	...	...	....	..	...
B-83	0.38	0.79	1.16	36.3	16.8	0.018	19.0	0.08	6.7	15.0	..	....	...	...	...	....	..	...
B-79	0.40	0.77	1.16	34.8	16.5	....	7.6	1.1	16.0	31.0	82	0.0040	2.1	4.7	...	....	..	...
B-84	0.44	0.84	1.21	35.3	16.2	0.020	5.4	1.3	13.0	39.0	73	0.0070	3.8	8.1	81	0.016	7.0	11.0
B-80	0.46	0.70	1.22	36.5	16.2	....	7.3	1.7	22.0	38.0	81	0.016	7.0	11.0	...	....	..	...
B-81	0.49	0.80	1.13	35.9	16.1	....	10.0	0.99	20.0	46.0	..	....	...	...	...	....	..	...
B-82	0.59	0.74	0.98	36.3	16.4	....	15.0	0.33	11.0	37.0	..	....	...	...	...	....	..	...
B-56	0.59	0.78	1.10	35.3	16.1	....	16.0	0.33	15.0	55.0	..	....	...	...	...	....	..	...
B-57	0.70	0.70	1.07	36.0	16.0	....	24.0	0.26	17.0	23.0	..	....	...	...	...	....	..	...
D-1	0.06	0.75	1.25	35.7	16.1	....	0.23	53.0	20.8	21.7	..	....	...	...	...	....	..	...
D-2	0.16	0.95	1.18	35.9	16.0	....	0.21	23.0	6.0	7.0	..	....	...	...	...	....	..	...
D-3	0.12	0.84	1.32	35.7	16.3	....	0.18	31.0	11.1	6.7	..	....	...	...	...	....	..	...
D-4	0.43	0.90	1.38	34.0	14.2	....	5.7	1.7	19.0	24.0	70	0.010	3.5	6.6	260	0.0010	2.2	2.3
D-5	0.40	0.80	1.38	32.9	15.7	....	7.6	1.3	17.0	27.0	126	0.0037	3.0	3.1	...	....	..	...
D-6	0.41	0.81	1.23	32.5	18.2	....	7.3	1.5	26.0	27.0	89	0.026	6.4	8.4	...	....	..	...
D-7	0.44	0.86	1.31	33.8	20.1	....	5.9	2.0	32.0	45.0	112	0.016	7.4	12.0	397	0.0013	3.9	8.5
D-8	0.44	0.85	1.41	37.3	15.7	....	5.4	2.1	21.0	36.0	99	0.015	6.1	11.0	...	....	..	...
D-9	0.44	0.83	1.22	34.5	18.3	....	11.4	1.0	25.0	34.0	91	0.022	5.4	12.0	...	....	..	...
D-10	0.43	0.84	1.36	36.8	19.8	....	5.9	2.0	21.0	31.0	65	0.051	7.8	17.0	...	....	..	...
D-11	0.41	0.84	1.29	37.1	13.8	....	7.9	1.9	29.0	42.0	71	0.045	9.1	14.0	...	....	..	...
D-12	0.42	0.90	1.35	37.3	16.0	....	5.9	2.2	24.0	29.0	52	0.017	5.0	8.9	...	....	..	...
D-13	0.43	0.82	1.47	37.3	18.1	....	4.9	2.2	30.0	44.0	69	0.037	6.3	11.0	...	....	..	...
D-14	0.38	0.93	1.30	37.5	19.9	....	5.7	1.8	24.0	46.0	62	0.050	6.9	13.0	...	....	..	...
D-15	0.42	0.85	1.36	38.5	14.1	....	12.5	0.91	24.0	29.0	79	0.012	5.5	16.0	383	0.0011	2.2	2.4
D-16	0.40	0.84	1.36	40.1	16.6	....	7.2	1.7	21.0	33.0	89	0.019	4.6	5.7	...	....	..	...
D-17	0.44	0.84	1.32	39.8	18.3	....	5.6	2.3	21.0	33.0	62	0.050	10.0	17.0	...	....	..	...
D-18	0.44	0.77	1.29	34.4	20.0	....	5.2	2.6	27.0	48.0	49	0.110	16.0	26.0	413	0.0020	4.7	7.4
D-20	0.46	1.02	0.43	34.9	15.3	....	...	...	...	...	151	0.008	4.3	7.0	504	0.0008	1.8	2.4
D-21	0.43	0.95	1.60	34.9	16.6	....	...	...	...	...	62	0.087	10.0	20.0	320	0.0020	4.0	6.6
D-22	0.45	0.91	2.57	35.6	16.0	....	...	...	...	...	23	0.580	18.0	21.0	119	0.025	9.3	8.2

D-1 to D-18 poured at 2750 F ± 10 F, except D-1, D-2, D-5.

39.4 % see p. 981

Table VII
Average Mechanical Properties of Nine Heats of "HT" 15% Cr-35% Ni-Type Heat Resistant Alloy

Composition Range, %					
C	Mn	Si	Ni	Cr	N
0.48 to 0.54	0.67 to 0.99	0.55 to 1.34	34.5 to 35.8	14.9 to 15.9	0.02 to 0.06

	Tested at Room Temperature		Tested at
	As Cast	Aged 48 Hrs.—1600 F	1800 F
Proportional Limit, psi	14,200	16,800	5,100
Yield Strength 0.2%, psi	36,500	38,800	8,200
Ultimate Tensile Strength, psi	63,500	73,100	11,300
Elongation in 2 inches, %	5.2	4.4	32.3
Reduction in Area, %	6.1	5.3	46.3
Elastic Modulus in Million, psi	23.9	23.1	...
Brinell Hardness Number	168	187	178 R.T.

35% Ni alloys is in terms of Limiting Creep Stress (L.C.S.) for 1% elongation per 10,000 hours, excluding the initial stage of creep. More precisely defined, it is the maximum stress that will produce a minimum deformation rate below 0.0001% per hour.

The L.C.S. value is obtained by plotting data from two or more tests on either logarithmic or semilogarithmic paper and interpolating or extrapolating to the desired creep rate co-ordinate. Both methods of plotting yield similar L.C.S. values because one or more data points are usually close to the 0.0001%/Hr. rate, but the extrapolated values may differ considerably. The semilog plot is more conservative. Present evidence does not establish which of these or other proposed mathematical treatments (16), (17) of the data is most valid.

For 26% Cr-12%Ni, the weight of evidence favors the log-log straight-line relationship, which for some of the weaker alloys of this type seems to hold over at least six cycles on the creep rate co-ordinate (1). The stronger alloys with higher carbon contents appear less consistent, while concurrently there is more scatter in the experimental data. Some duplicate tests differ considerably. As pronounced differences in creep rate can be produced by heat treatments that change the carbide distribution it has been tentatively considered that departures from the straight-line relationship may be attributed to variations in strength due to carbide habit.

The influence of carbides on strength undoubtedly applies to 16% Cr-35% Ni also, but whether this is a satisfactory explanation of departures from a straight line on either log-log or semilog plots is not clear. Creep and stress-strain-rupture data for four 16% Cr-35% Ni compositions are presented by plotting on log-log co-ordinates herein (Figs. 8, 9, 10, and 11), but the relationship is considered

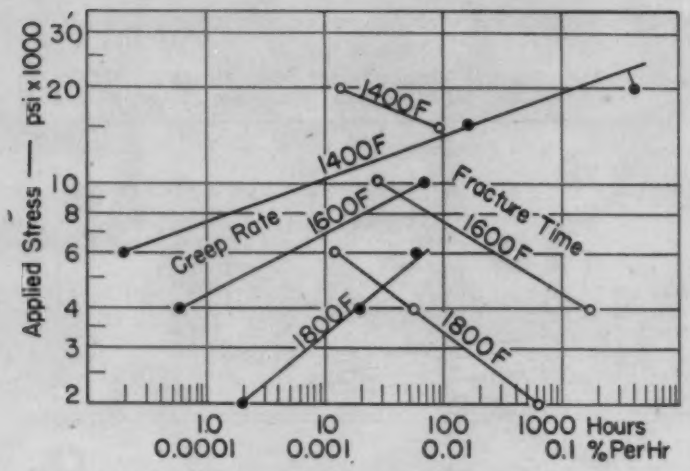


Fig. 8—Log-Log Plot of Creep Characteristics of 16% Chromium-35% Nickel-0.29% Carbon Type. Alloy HT-29.

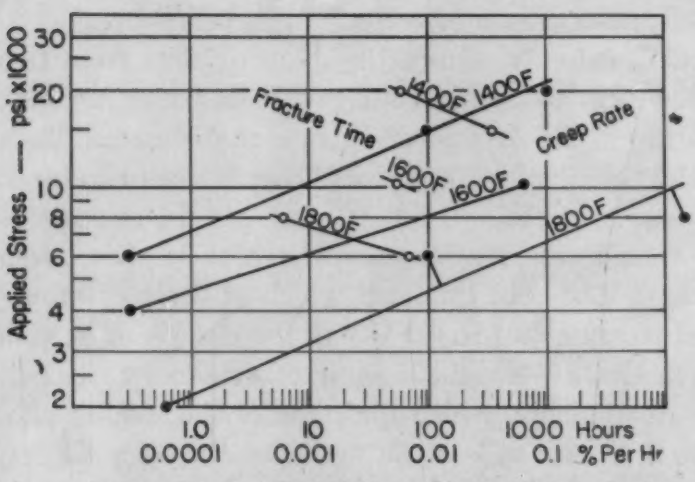


Fig. 9—Log-Log Plot of Creep Characteristics of 16% Chromium-35% Nickel-0.44% Carbon Type. Alloy HT-44.

tentative. Harder and Gow (Figs. 12 and 13) have used the semi-log method with satisfaction (12). There is a need for long-term creep data that will extend the plots for one or two cycles beyond the 1000-hour co-ordinate and thereby provide additional illumination of the relationship and of the behavior that may be expected in service up to perhaps 10 years. The considerable difference between the log-log and semilog methods is shown in Fig. 14, wherein the data from one A.C.I. composition is plotted on a log-log straight line and the lines from Fig. 12 are added for comparison.

A circumstance that should receive consideration is the slow establishment of the secondary stage minimum creep rate when

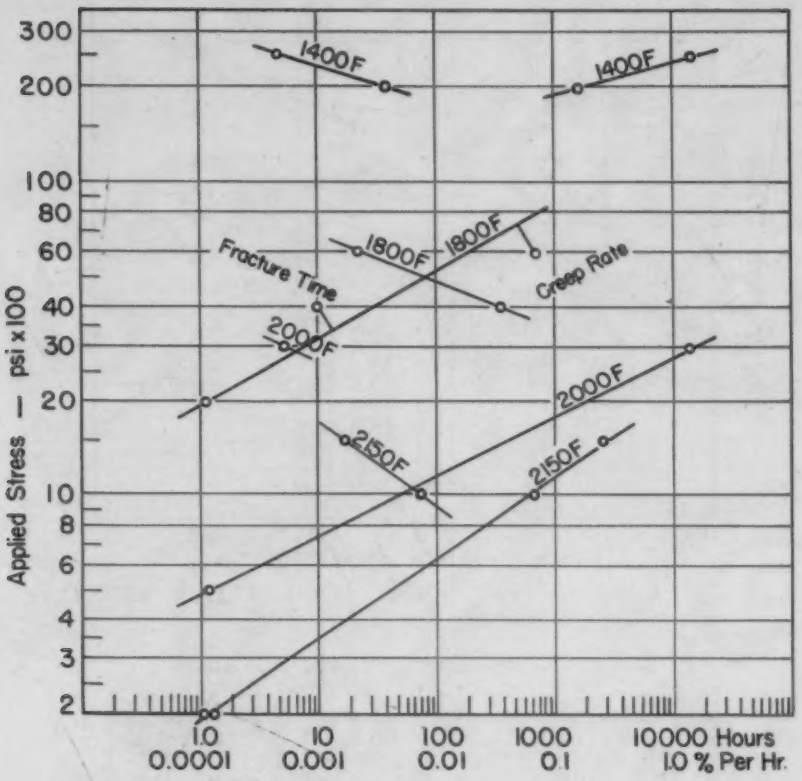


Fig. 10—Log-Log Plot of Creep Characteristics of 16% Chromium-35% Nickel-0.56% Carbon Type. Alloy HT-56.

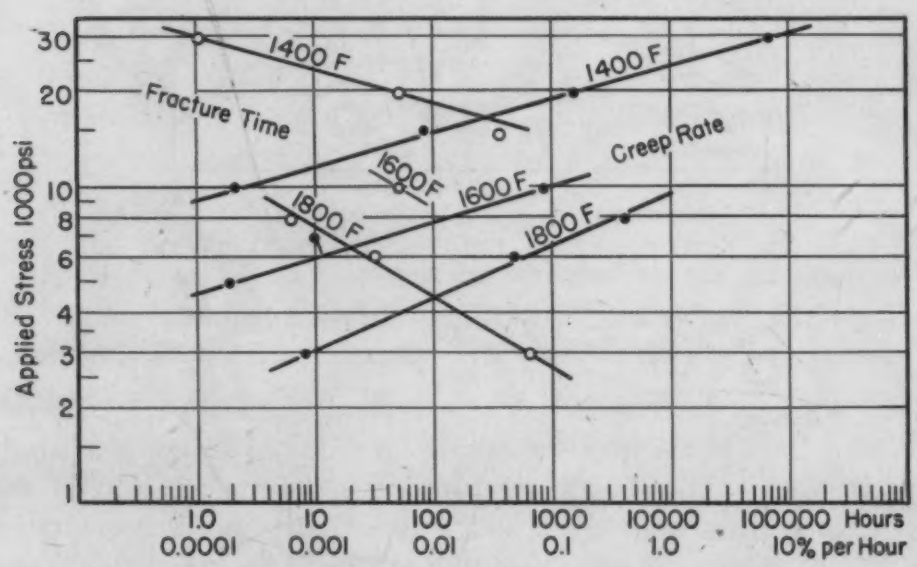


Fig. 11—Log-Log Plot of Creep Characteristics of 16% Chromium-35% Nickel-0.56% Carbon Type. Alloy HT-56, a duplicate heat for comparison with Fig. 10.

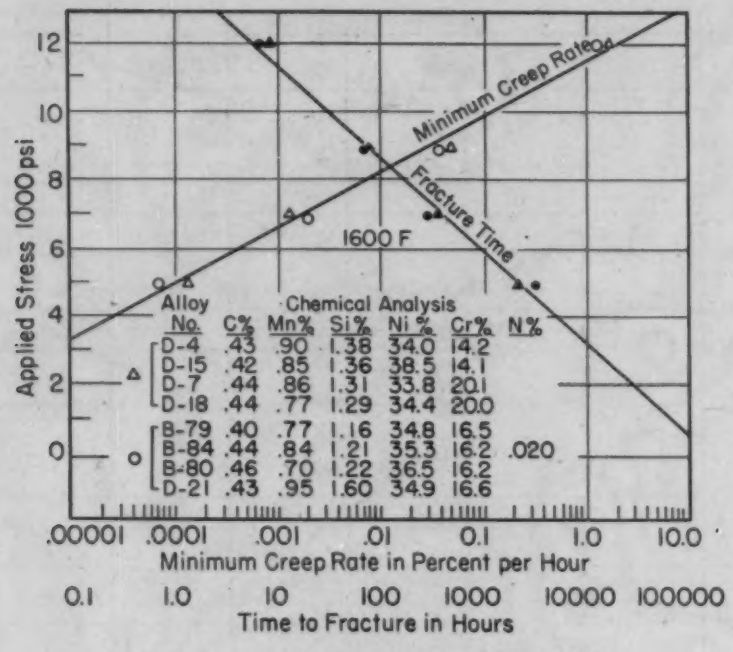


Fig. 12—Creep Characteristics of HT Alloys.

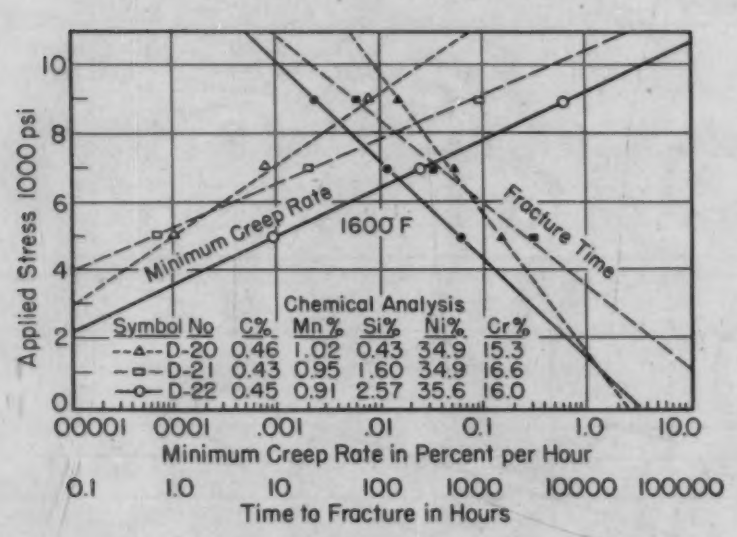


Fig. 13—Creep Characteristics of HT Alloys With Variable Silicon Contents.

stresses are low. At, and especially beyond, the 0.0001%/Hr. rate more than 1000 hours may sometimes be required to reach a steady Stage II rate. Unless high precision of measurement is used this behavior may pass undetected and a rate that is not representative be plotted. Such values are probably too high, and tend to curve a log-log plot downward, thereby suggesting erroneously that the semi-log relationship is more valid. Here again long-term stress-rupture

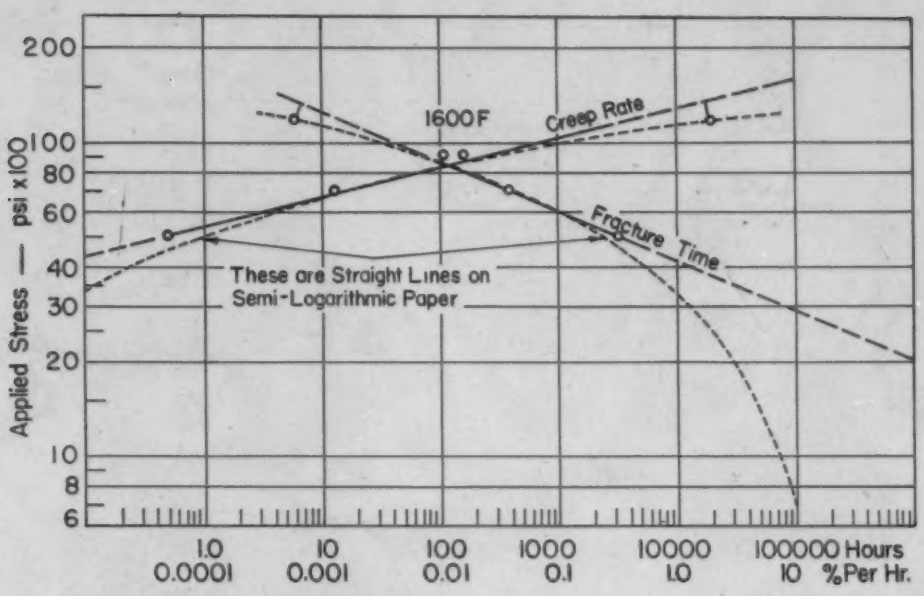


Fig. 14—Comparison of Log-Log and Semilog Plotting of Creep and Stress Rupture Data. Alloy D-7, 0.44% carbon, 33.8% nickel, 20.1% chromium.

tests with unmistakable delineation of the three stages and involving secondary rates below 0.00001%/Hr. would be helpful.

For many industrial applications, this discussion is academic, since the "HT" alloy is used principally for carburizing service around 1750 F and in heat treating furnaces that operate above 1600 F. Operation is characteristically intermittent. The cyclic acceleration of creep rate that is observed above 1600 F will be important in these applications, and considerably lower the allowable working stress if deformation is to be kept within close limits. A comparison of steady temperatures and cyclic temperature creep is presented in Table VIII.

The data in Table IX-A are tentatively limited to the silicon range from 1.0 to 1.5%, as represented by the midpoint of 1.25%. For carburizing resistance it may be desirable to employ the alloys from 1.5 to 2.2% silicon. The data in Table X are assembled to permit an estimate of the effect on hot strength; a pronounced weakening effect in stress-rupture tests at 1400 and 1800 F is noticeable. The absence of the trend at 1600 F is puzzling and at present unexplained except as a fortuitous example of erratic carbide distribution as described later under metallography. For comparison the A.C.I. silicon series in Tables VI-B and IX-B indicates a definite shortening of fracture time and lowering of creep resistance at 1600 F.

Table VIII
Comparison of Cyclic and Constant Temperature Creep Tests

		Chemical Composition, %					
		C	Mn	Si	Ni	Cr	N
A		0.45	0.97	1.32	36.6	17.9	0.06
B		0.21	1.11	1.21	34.2	18.0	0.03

	Temp. F	Cycle*	Stress psi	Duration Hours	Min. Rate % per Hr.	Elong. %
A	1800	4–20–24	255	1010 d	0.00010 / 0.00016 a	0.130
A	1800	4–20–24	1000	1006 d	0.00046	0.487
A	1800	none	1250	1060 d	0.00002	0.046
A	1800	none	2100	1008 d	0.00016	0.205
B	1800	4–20–24	1000	1030 d	0.00013	....
B	1800	3–1	1000	1056 d	0.00011	0.124
B	1800	none	1500	1056 d	0.00003	0.039
B	1800	none	2100	1273 br.	0.0001	0.340

a = 0.000095% per hour up to 535 hours, 0.00016% per hour thereafter.
d = Discontinued at time indicated.
br. = Broke at time indicated.
*The conventional creep tests were conducted at constant temperature. The cyclic test involves heating to 1800 F in 4 hours, holding at 1800 F for 20 hours (during which creep measurements are made), and slow cooling to room temperature in 24 hours; the cycle being repeated continuously. In one case, designated the 3-1 cycle, the specimen was heated to 1800 F in 4 hours, held at 1800 F for 68 hours, furnace-cooled to 70 F in 4 hours and held at 70 F for 20 hours.

Table IX-A
Summary of Creep Test Data on 16% Cr-35% Ni Alloys

Constant Temperature Conditions

	Alloy	Item	Chemical Analysis, % C	Mn	Si	Ni	Cr	N	Melting Practice
	HT-21	A	0.21	1.11	1.21	34.2	18.0	0.03	Basic Arc Fce.
	HT-29	B	0.29	0.72	1.28	34.4	16.2	0.044	Basic Ind. Fce.
	HT-35	C	0.35	0.67	1.21	37.6	16.5	0.07	Basic Arc Fce.
	HT-44	D	0.44	0.74	1.17	35.0	16.2	0.047	Basic Ind. Fce.
	HT-45	E	0.45	0.97	1.32	36.6	17.9	0.06	Basic Arc Fce.
	HT-56	F	0.56	0.71	1.22	34.7	16.4	0.036	Basic Ind. Fce.
	HT-56	G	0.56	0.80	1.27	34.8	15.9	0.037	Basic Ind. Fce.

	Creep Test Data: Temp. F	Stress psi	Duration Hours	Min. Rate % per Hr.	Elong. %	Residual Room Temp. Properties: Tens. Str. psi	Elong. %	R.A. %
A (HT-21)	1600	3,000	312	nil ?	?	Load increased to 5000 psi		
	1600	5,000	384	0.00011	0.11	Broke in creep test		
	1600	3,500	624	0.00004?	0.03	Broke in creep test		
	1800	1,500	1,056	0.00003	0.04	58,500	5.5	...
	1800	2,100	1,273	0.00010	0.34	Broke in creep test		
B (HT-29)	1400	6,000	1,002	0.00002	0.09	76,250	5.0	7.0
	1600	4,000	1,844	0.00006	0.9?	Broke in creep test		
	1800	2,000	632	0.0002	1.0?	Broke in creep test		
C (HT-35)	1800	2,000	1,224	0.00008	0.33	14,600 (In 3rd stage at 1224 hrs.)	..	...
D (HT-44)	1400	6,000	1,005	0.00003	0.14	71,500	3.0	2.7
	1400	15,000	356	0.0096	7.0	Broke in creep test		
	1600	4,000	1,001	0.00002	0.09	57,250	1.5	1.1
	1800	2,000	1,013	0.00006	0.08	69,000	4.0	6.6
E (HT-45)	1600	3,500	1,320	0.00002	0.107	53,200	2.0	0.8
	1800	1,250	1,060	0.00002	0.046	65,000	3.0	4.4
	1800	2,100	1,008	0.00016	0.205	44,000	1.0	1.2
F (HT-56)	1400	15,000	....	.....	...			
	1800	2,000	1,003	0.00011	0.13	67,500	4.0	4.3
	2000	500	1,025	0.00012	0.30	57,150	7.5	8.9
	2150	200	1,001	0.00012	0.20	55,125	7.0	10.6
G (HT-56)	1400	15,000	392	0.0086	7.0	Broke in creep test		
	1400	10,000	1,002	0.00031	0.70	68,200	2.5	3.5
	1600	7,000	....	.....	...			
	1600	5,000	1,002	0.00019	0.31	47,500	1.0	0.8

Table IX-B

A.C.I. Data from the Battelle Memorial Institute Creep Laboratory for Comparison (12)

Alloy	Chemical Analysis, % C	Mn	Si	Ni	Cr
D-4	0.41	0.90	1.38	34.0	14.2
D-15	0.40	0.85	1.27	38.5	14.1
D-7	0.44	0.86	1.31	33.8	20.1
D-18	0.44	0.77	1.29	39.4	20.0
D-20	0.45	1.02	0.43	35.1	15.4
D-21	0.43	0.95	1.60	35.1	16.6
D-22	0.44	0.91	2.57	35.6	16.1

	Creep Test Data: Temp. F	Stress psi	Duration Hours	Min. Rate % per Hr.	Elong. %	
D-4	1600	5,000	997	0.00027	2.2	Broke in creep test
D-15	1600	5,000	1,193	0.00018	..	Broke in creep test
D-7	1600	5,000	3,258	0.00005	2.1	Broke in creep test
D-18	1600	5,000	1,129 d	0.000065	..	
D-20	1600	5,000	1,520	0.00010	2.2	Broke in creep test
D-21	1600	5,000	2,900	0.00007	3.2	Broke in creep test
D-22	1600	5,000	603	0.00090	1.7	Broke in creep test
D-4	1800	3,500	105	0.0095	12.7	Broke in creep test
D-21	1800	3,500	380	0.00065	..	Broke in threads
D-21	1800	3,500	595	0.00061	1.3	Broke in creep test
D-18	1800	3,500	340	0.0015	3.2	Broke in creep test

d = Discontinued at time indicated.

Table X

Effect of Silicon in 16% Cr-35% Ni Alloys

Alloy	Si %	Chemical Analysis, % C	Mn	Si	Ni	Cr	N	Melting Practice
HT-56	1.22	0.56	0.71	1.22	34.7	16.4	0.04	Basic Ind. Fce.
HT-56	1.27	0.56	0.80	1.27	34.8	15.9	0.04	Basic Ind. Fce.
HT-57	2.13	0.57	0.81	2.13	34.9	16.0	0.02	Basic Ind. Fce.

Alloy	Si %	As-Cast Tensile Properties: Yield Strength psi	Ult. Tens. Strength psi	Elong. % in 2 in.	R.A. %	Hardness BHN
HT-56	1.22	50,000	66,500	8.0	7.3	187
HT-56	1.27	52,500	67,500	8.5	10.7	...
HT-57	2.13	38,300	70,750	7.0	7.0	183

Alloy	Si %	Stress-Rupture and Creep Properties: Temp. F	Stress psi	Duration Hours	Min. Creep Rate % per Hr.	Elong. %	Red. Area %	Room Temp. Properties After Creep Testing: Ult. Tens. Strength psi	Elong. %	Red. Area %
HT-56	1.22	1400	20,000	36.9	0.16	14.0	38.5	.....	..	..
HT-56	1.27	1400	20,000	52.1	0.16	20.5	24.1	.....	..	..
HT-57	2.13	1400	20,000	7.6	1.5	21.0	42.0	.....	..	..
HT-56	1.27	1400	10,000	1002.0	0.00031	0.70	...	68,200	2.5	3.5
HT-57	2.13	1400	10,000	...	0.00034	...	...	.....	..	..
HT-56	1.27	1600	10,000	52.0	0.088	11.0	24.4	.....	..	..
HT-57	2.13	1600	10,000	48.0	0.058	8.0	14.0	.....	..	..
HT-56	1.27	1600	7,000	506.0	0.00098	2.0	...	.....	..	..
HT-57	2.13	1600	7,000	361.0	0.0008	1.0	...	.....	..	..
HT-56	1.27	1600	5,000	1002.0	0.00019	0.31	...	47,500	1.0	0.8
HT-57	2.13	1600	5,000	1668.0	0.00021	3.0	...	Broke in creep test		
HT-56	1.22	1800	6,000	21.9	0.06	16.5	38.8	.....	..	..
HT-56	1.27	1800	6,000	31.6	0.053	15.0	30.0	.....	..	..
HT-57	2.13	1800	6,000	11.2	0.25	24.0	33.0	.....	..	..
HT-56	1.22	1800	4,000	353.5	0.0010	3.5	7.0	.....	..	..
HT-56	1.27	1800	3,000	645.0	0.00081	2.0	...	Broke in creep test		
HT-57	2.13	1800	4,000	104.0	0.005	5.0	22.0	.....	..	..
HT-56	1.22	1800	2,000	1003.0	0.00012	0.13	...	67,500	4.0	4.3
HT-57	2.13	1800	2,000	1633.0	0.00031	13.0	8.0	Broke in creep test		

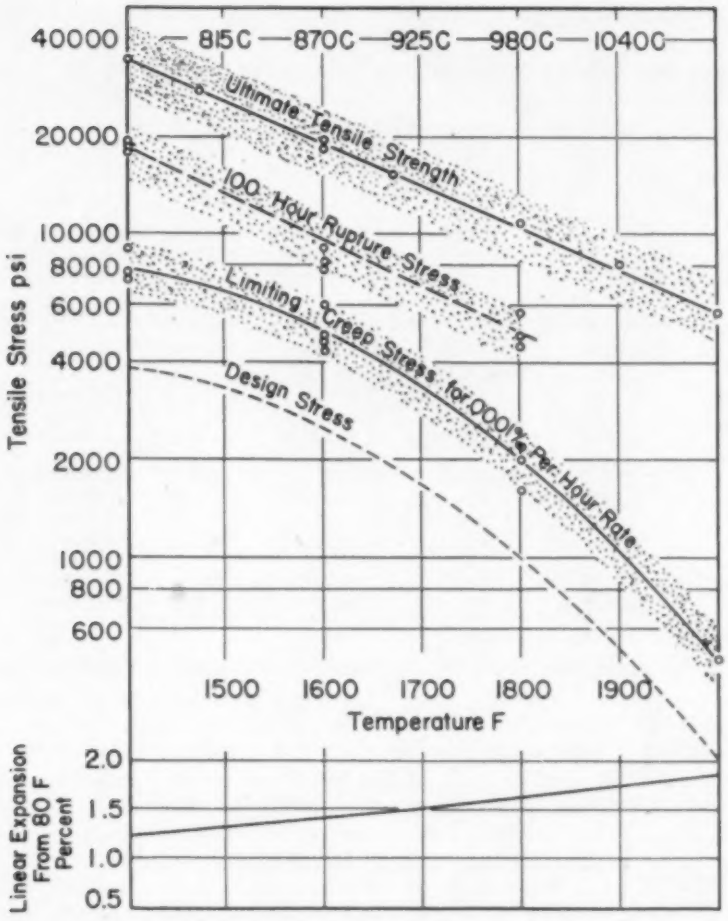


Fig. 15—Elevated Temperature Characteristics of 16% Chromium-35% Nickel Alloys Under Constant Temperature Conditions. Type HT.

Working Stresses

The range of design stresses that has been suggested is surprising (Table I). Field experience, with its uncontrolled variables and usual lack of accurate quantitative data, is responsible for the variation. Laboratory tests provide considerable clarification.

Discouragement of field testing is not intended; it is a valuable procedure for checking laboratory conclusions or for illuminating new problems. While the variables may be under poor control there is less chance that an important service factor may be omitted because it is unsuspected, and thereby invalidate the end result. Perhaps the sanest attitude is to recognize the limitation of field tests and to consider laboratory data more accurate (and certainly more precise) unless there is qualitative disagreement. A major discrepancy should be the signal for a critical review of experimental procedure and a

more rigorous analysis of the factors that may be involved.

An arbitrary but generally satisfactory basis for design is to consider 50% of the Limiting Creep Stress (for 0.0001%/Hr. or 1% in 10,000 hours) as a safe tensile working stress for sound material. A useful life of from 2 to 8 years (17,000 to 70,000 hours) should be generally acceptable. Examination of stress-rupture data suggests that 50% of the L.C.S. may provide a maximum life expectancy of from 20,000 to 400,000 hours, depending on whether semilog or log-log extrapolation is accepted. If constant temperature conditions are maintained, if the critically stressed areas involved are sound, and if a logarithmic stress-time relationship is valid, the following stresses are tentatively recommended.

Table XI
Suggested Tensile Working Stresses for 16% Cr-35% Ni Alloys

	Carbon: 0.35 to 0.75% Silicon: 0.50 to 1.75%								
Temp., F:	1400	1500	1600	1700	1800	1900	2000	2100	2150
Stress, psi:	3900	3300	2500	1600	1000	520	240	130	90

At 1400 F and perhaps 1500 F, the cyclic acceleration of creep rate is probably negligible. Above 1600 F, it can be serious. The fact that the values above depend on constant temperature conditions deserves re-emphasis. If fluctuations are involved safety factors of about $\times$ 2.5 at 0.45% C and perhaps up to $\times$ 10 for 0.21% C may be required, as indicated by Table VIII.

Considerable new data will be required to establish the safe but economical working loads for cyclic temperature service. While the greater deformation rates are known the effect on life expectancy is not, which suggests a fertile field for experiment.

The design stresses in Table XI generally will provide a creep rate below 0.00001%/Hr. or 1% in 100,000 hours. Since 1% per year deformation may be tolerable in furnace construction or carburizing service it might be suggested that heavier loads, corresponding to the L.C.S. for example, are practical. This neglects a general characteristic of austenitic alloys (1). As loads decrease, the total elongation that will be exhibited before fracture also decreases, and low loads sustained for long periods may produce sudden fracture with very little apparent ductility. This is an important reason why stress-rupture as well as creep data should be studied in the selection of design stresses.

Magnetic Permeability

The relationship between magnetic permeability and creep strength that has been observed for the 26% Cr-12% Ni alloys, and which makes magnetic analysis valuable as an acceptance test, does not apply to the "HT" alloys. They exhibit magnetism in the higher carbon ranges but satisfactory correlation with creep is not apparent.

Permeability data from ¼-inch diameter by 1-inch long specimens are presented in Table XII. Magnetism is apparently a function of the matrix composition, which can be changed by carbide segregation and by heat treatment. Carbide precipitation increases

Table XII
Magnetic Permeability of "HT" Alloys

Alloy	Chemical Analysis, % C	Mn	Si	Ni	Cr	N		Thermal History	Permeability H=24	H=30*
HT-29	0.29	0.72	1.28	34.4	16.2	0.04		1800 F— 630 Hrs.	1.38	...
								1600 F—1844 Hrs.	1.26	...
								1400 F—1002 Hrs.	1.20	...
HT-44	0.44	0.74	1.17	35.0	16.0	0.05		1800 F—1013 Hrs.	1.73	...
								1600 F—1001 Hrs.	5.26	...
HT-56	0.56	0.80	1.27	34.8	15.9	0.04		1400 F—1002 Hrs.	15.7	...
C-14	0.45	0.80	1.24	32.2	16.0	0.08		As Cast	3.08	3.86
								1600 F—48 Hrs.	1.17	1.21
								2100 F—2 Hrs.—W.Q.	1.15	1.21
C-15	0.45	0.80	1.24	36.4	16.0	0.08		As Cast	5.64	...
								1600 F—48 Hrs.	8.59	...
								2100 F—2 Hrs.—W.Q.	1.42	1.51
C-16	0.46	0.80	1.24	40.3	16.0	0.08		As Cast	8.42	...
								1600 F—48 Hrs.	16.6	...
								2100 F—2 Hrs.—W.Q.	6.5	3.78
The Group Below Consists of Commercial Heats Used in A.C.I. Studies										
ZG	0.10	0.75	1.59	34.0	15.7	0.04		1600 F—48 Hrs.	1.003	1.02
U	0.17	0.60	0.53	37.1	17.6	0.02		1600 F—48 Hrs.	1.16	1.32
N	0.19	1.11	1.41	38.1	18.5	0.04		1600 F—48 Hrs.	1.003	1.02
R	0.33	1.00	1.34	36.2	15.3	0.03		1600 F—48 Hrs.	1.62	1.74
ZB	0.39	1.06	0.66	34.8	16.7	0.08		1600 F—48 Hrs.	7.69	...
ZD	0.39	0.77	1.39	35.1	19.1	0.04		1600 F—48 Hrs.	1.012	1.07
Z	0.40	0.71	1.95	29.9	16.8	0.05	Cu	1600 F—48 Hrs.	1.003	1.03
O	0.46	0.97	1.31	37.1	15.9	0.04	0.23	1600 F—48 Hrs.	16.3	...
T	0.50	0.65	1.94	32.2	17.7	0.04	...	1600 F—48 Hrs.	1.057	1.12
S	0.53	0.74	1.09	36.3	15.4	0.06	...	1600 F—48 Hrs.	15.9	...
Y	0.57	0.94	1.30	35.1	18.0	0.06	...	1600 F—48 Hrs.	15.5	...
ZC	0.59	0.88	1.77	34.8	15.9	0.06	...	1600 F—48 Hrs.	1.99	2.12
W	0.66	0.76	1.34	37.1	15.6	0.05	1.36	1600 F—48 Hrs.	16.0	...
M	0.70	0.84	1.72	35.6	16.3	0.03	...	1600 F—48 Hrs.	6.4	...
ZF	0.78	1.05	1.54	36.9	16.8	0.03	0.23	1600 F—48 Hrs.	15.2	...
ZE	0.88	0.97	2.26	33.4	18.5	0.02	...	1600 F—48 Hrs.	1.42	1.58
The Group Below are Laboratory Heats Used in A.C.I. Studies										
							W			
B-77	0.21	0.72	1.13	35.6	16.7	...	0.020	1600 F—48 Hrs.	1.07	1.09
B-78	0.31	0.82	1.12	35.4	16.0	...	...	1600 F—48 Hrs.	1.34	1.50
B-83	0.38	0.79	1.16	36.3	16.8	...	0.018	1600 F—48 Hrs.	1.71	1.86
B-79	0.40	0.77	1.16	34.8	16.5	...	...	1600 F—48 Hrs.	1.35	1.54
B-84	0.44	0.84	1.21	35.3	16.2	...	0.020	1600 F—48 Hrs.	2.16	2.40
B-80	0.46	0.70	1.22	36.5	16.2	...	...	1600 F—48 Hrs.	2.78	3.58
B-81	0.49	0.80	1.13	35.9	16.1	...	...	1600 F—48 Hrs.	7.23	...
B-82	0.59	0.74	0.98	36.3	16.4	...	...	1600 F—48 Hrs.	13.9	...

*Where two values for permeability appear, the same specimens were tested at the American Brake Shoe Company laboratory and at Battelle Memorial Institute in co-operative research. The Battelle apparatus is similar in principle but differs in design.

permeability. That this affects the matrix by removing chromium and carbon rather than because the carbides are magnetic is confirmed by observing the surface covered with a magnetic colloid suspension in a magnetic field (19). The austenite in high carbon alloys and the austenite zone adjacent to massive carbides in lower carbon alloys exhibit most intense magnetization.

Some of the alloys in this Cr-Ni-Fe field have Curie points near room temperature. When this occurs very erratic test values may be obtained unless temperature is controlled.

Permeability can be used as a crude index of carbon content. After carburizing service the face of a casting that has absorbed carbon is usually magnetic and can be readily differentiated from the opposite face with a small magnet. Even at high carbon contents the alloy is not strongly magnetic; it is not held satisfactorily for machining by a magnetic chuck, for example.

Thermal Expansion

The austenitic Cr-Ni-Fe alloys exhibit only small differences in expansion coefficients, even over a wide composition range. A trend toward lower values as nickel increases is apparent, however. The 16% Cr-35% Ni alloy has an intermediate position (Fig. 16).

Thermal gradients will produce internal stresses whose magnitudes are proportional to thermal expansion provided they do not produce plastic flow. Thus low expansion is favorable under conditions of hindered thermal contraction or cyclic heating. The field experience ranking of the three important alloys in Table XIII follows the same trend as their expansion coefficients. This property undoubtedly contributes but there is other evidence that indicates that it is not the only factor involved.

There is good agreement between laboratories on expansion studies; the accuracy of the data need not be a matter of concern,

Table XIII
Experience Ranking of Three Heat Resistant Alloys for Cracking Tendencies in Intermittent Heating and Cooling Service

Alloy Type	Nominal Composition	Merit Ranking	Thermal Expansion Coefficient Micro Inches per Inch—80 to 1800 F per F	per C
HW	12% Cr-60% Ni	Best	8.7	15.7
HT	16% Cr-35% Ni	Good	9.5	17.1
HH	26% Cr-12% Ni	Poorest	10.4	18.7

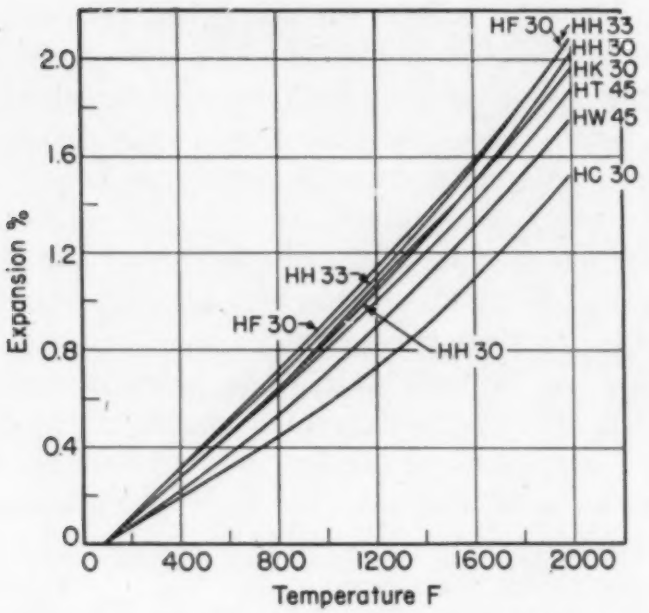


Fig. 16—Thermal Expansion Characteristics of Thermalloy Heat Resistant Alloys.

A.C.I. Type	Nominal Composition	Average Expansion Coefficients Microinches per Inch per F: 80 to 1200 F	80 to 1600 F	80 to 2000 F	100 to 800 F	800 to 1500 F	1500 to 2000 F
HC-30	27% Cr	6.3	7.0	7.7	6.1	7.7	11.1
HH-30	26% Cr-12% Ni	9.4	9.9	10.5	9.1	10.0	13.0
HH-33	26% Cr-12% Ni	10.0	10.3	10.6	9.6	11.0	13.0
HK-30	26% Cr-20% Ni	9.4	9.7	10.1	9.0	10.0	12.0
HF-30	21% Cr- 9% Ni	10.1	10.4	10.9	10.0	11.0	12.0
HT-45	16% Cr-35% Ni	9.0	9.3	9.8	8.6	9.7	12.0
HW-45	12% Cr-60% Ni	8.0	8.6	9.2	7.9	9.3	11.0

therefore. The chief probable source of experimental error is the contraction that accompanies carbide precipitation. This may slightly complicate determinations above 1200 F, as indicated in Fig. 17 from A.C.I. work.

Melting Points

Gow, Brasunas and Harder (9) have reported data from cooling curves obtained with silica-tube-protected platinum thermocouples. The indicated liquidus values correspond to the temperature of maximum thermal arrest; the solidus temperatures represent a much less prominent discontinuity in the cooling curves (Table XIV).

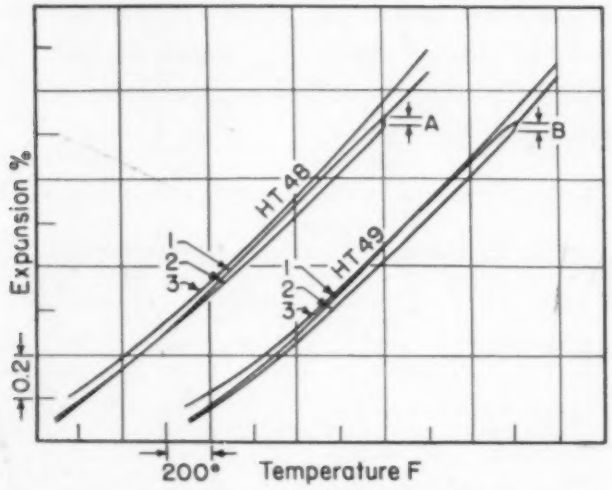
Carbon, silicon, nickel, and chromium are all reported to decrease solidus and liquidus temperatures. For the commercial "HT" alloys a generalized melting range from 2310 to 2525 F appears appropriate. At 0.29% C the solidus temperature is close to 2400 F. Holding at this temperature produced scattered areas where incipient fusion

Table XIV
Melting Ranges for 10 to 20% Cr and 30 to 40% Ni Alloys (9)

	High Purity Ternary Cr-Ni-Fe Alloys (9)					
	10% Cr		15% Cr		20% Cr	
	Liquidus	Solidus	Liquidus	Solidus	Liquidus	Solidus
30% Ni	2655 F	2575 F	2620 F	2550 F	2595 F	2510 F
35% Ni	2645 F	2565 F	2610 F	2530 F	2585 F	2505 F
40% Ni	2630 F	2555 F	2600 F	2515 F	2575 F	2495 F

	Commercial Purity HT-45 and Related Alloys (9)							
	14% Cr		16% Cr		18% Cr		20% Cr	
	Liquidus	Solidus	Liquidus	Solidus	Liquidus	Solidus	Liquidus	Solidus
33 to 34% Ni	2520 F	2335 F	2495 F	2325 F	2490 F	2310 F	2485 F	2335 F
35 to 36% Ni	....	....	2500 F	2330 F	2495 F	2335 F	2490 F	2345 F
37 to 38% Ni	2495 F	2315 F	2480 F	2310 F	2480 F	2315 F	2475 F	2320 F
39 to 40% Ni	2495 F	2315 F	2480 F	2320 F	2480 F	2330 F	2475 F	2320 F

	Effects of Carbon and Silicon						
Alloy:	HT-46	HT-46	HT-43	HT-45	HT-17	HT-36	HT-56
Si:	0.44	1.38	1.64	2.61	3.06	2.99	3.64
Liquidus—F:	2505	2500	2475	2440	2500	2475	2420
Solidus—F:	2330	2330	2320	2240	2392	2250	2250



Chemical Analysis								
Alloy	C%	Mn%	Si%	Ni%	Cr%	P%	S%	N%
HT-48	0.48	0.67	1.14	35.3	15.9	-	.015	.032
HT-49	0.49	0.74	0.77	35.6	15.3	.034	.014	-

Fig. 17—A.C.I. Thermal Expansion Tests on HT (16% Chromium-35% Nickel) Alloys. Heating and cooling rate—5 F per minute. Curve 1—heating 75 to 1800 F. Cooling—1800 to 1600 F. Curve 2—cooling—1600 to 75 F after aging 15 hours at 1600 F. Curve 3—reheating—75 to 1800 F. A—Actual contraction on aging. B—Contraction on aging not measured.

is apparent (Fig. 39). With the higher carbon commercial alloys, fusion is more pronounced at 2400 F and the melted portions solidify as typical eutectic structures.

Optical pyrometer emissivity corrections were obtained during this research. The calculated emissivity for "HT" alloys ranged

from 0.34 to 0.49 on the pouring stream to about 0.44 to 0.60 on the open bath, which usually is covered with a thin oxide film. Apparent optical pyrometer temperatures (black body calibration) are about 200 F low on the pouring stream, but oxide filmed surfaces below 2800 F give nearly correct values, corresponding to an emissivity approximating 1.0 between 2600 and 2800 F. Conversion charts are included in the paper (9).

Hindered Contraction Stresses

If thermal contraction of an alloy is hindered, either by fixed anchorages or by the rigidity of a casting subjected to differential cooling, serious stresses will appear. Plastic flow will rapidly reduce high initial values to those comparable with the stresses in the vicinity of the conventional yield strength. Thereafter, or for stresses below this, stress relief is slow and is dependent upon the creep characteristics of the material. The limits for rapid stress relief at various temperatures have been determined experimentally, as described under the previous section on procedure.

Table XV
Hindered Contraction Stresses in "HT" Alloys

Temp. F	Tensile Stress in Psi		
	HT-29*	HT-44*	HT-56*
2000	4,125	4,250	4,500
1950	4,750	4,800	5,500
1900	5,750	5,500	5,750
1850	6,500	6,250	6,300
1800	7,500	7,350	7,250
1750	9,000	8,350	8,250
1700	10,600	9,750	9,300
1650	12,750	11,400	10,650
1600	15,250	13,300	12,350
1550	18,250	15,400	14,500
1500	22,000	18,250	16,700
1450	25,250	21,700	19,700
1400	29,000	24,750	22,900
1350	32,125	28,250	26,250
1300	35,125	31,000	29,700
1250	37,875	33,750	33,400
1200	40,450	36,300	37,100
1100	44,600	40,750	43,500
1000	48,250	44,750	48,750
900	51,300	48,100	53,650
800	54,500	51,000	56,250
700	57,000	53,500	broke at 800 F
600	59,400	56,250	
500	61,075	58,350	
480	broke	broke	
Elong. at Fracture:†	17%	17%	14%
True Stress at Fracture:†	74,500	73,000	68,500

*For detailed analyses see Table IX-A.

†Stresses in table are based on original 0.505-inch diameter gage length. The true stress at fracture is based on the final reduced area at room temperature. The elongation value was measured at room temperature.

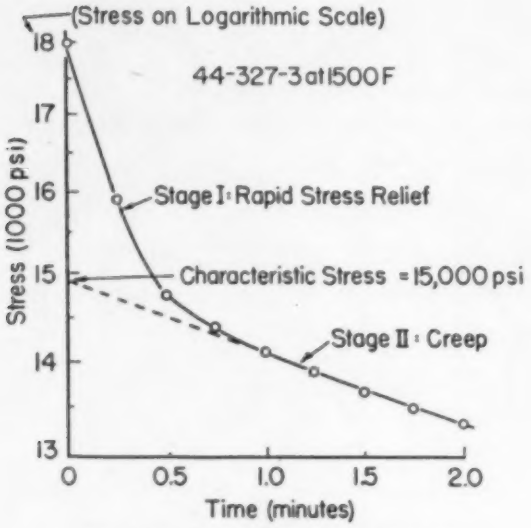


Fig. 19—Time-Stress Curve, Temperature and Strain Constant, Initial Stress Greater Than Characteristic Stress.

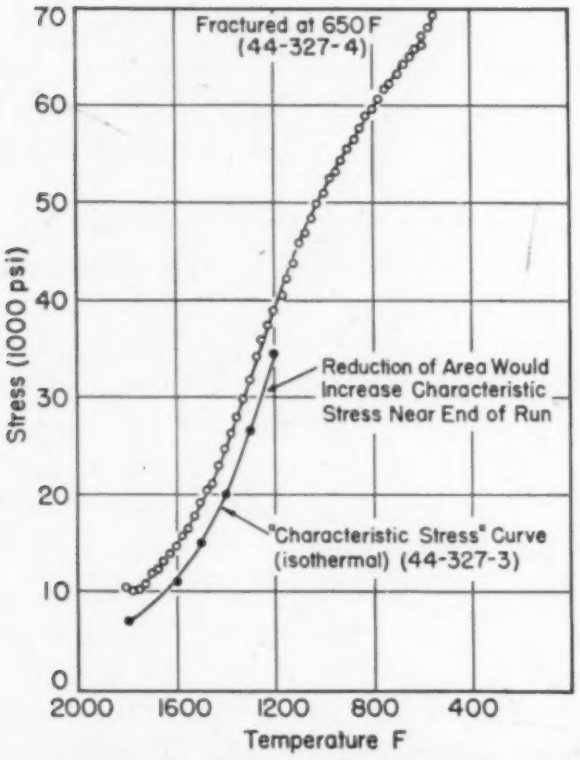


Fig. 20—Heat Resistant Alloys. Hindered thermal contraction test. Spec. No. 44-327. 0.42% carbon, 34.9% nickel, 16.3% chromium. Stresses shown are based on cross section at beginning of run. Initial stress at 1800 F—10,500 psi. Cooling rate (1200 to 1000 F)—20 F per minute. 10% total R.T. elongation. 14% total R.T.-R.A.

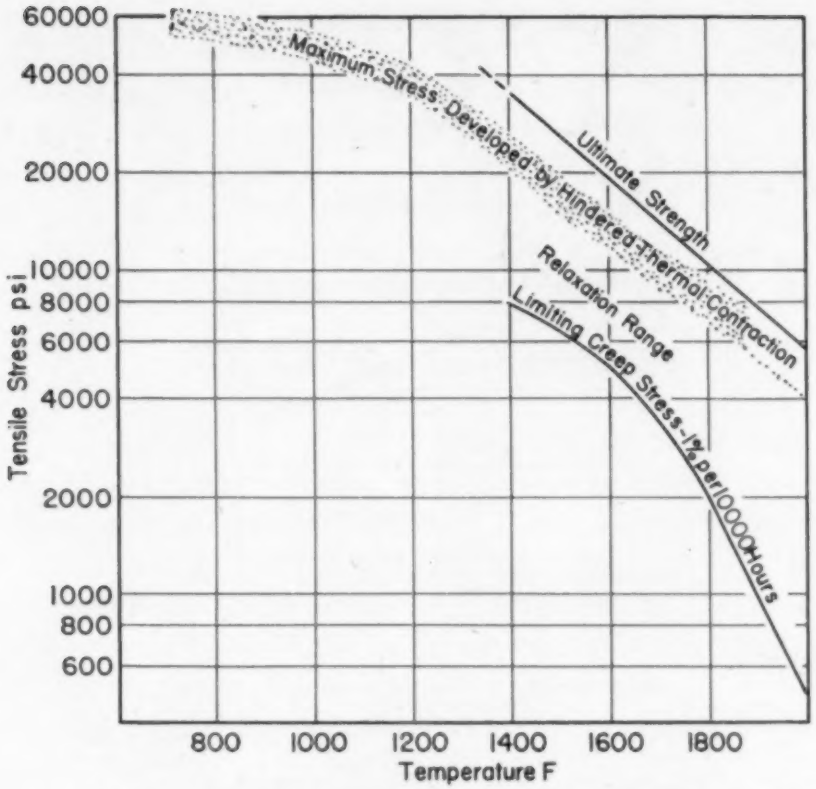


Fig. 21—Hindered Contraction Stresses in 15% Chromium-35% Nickel Alloys and Their Relation to Ultimate Strength and Limiting Creep Stress.

The tensile stresses from hindered contraction are especially important because they are believed to be the final cause of thermal fatigue failure. Representative values for 26% Cr-12% Ni alloys have been previously reported (1). To these are added data from three 16% Cr-35% Ni alloys in Table XV. Between 1800 and 1400 F these stresses are similar to those obtained for yield strength in hot tensile tests. The testing technique has the advantage of providing a stress versus temperature plot over a wide temperature range. Disadvantages are the lack of ultimate strength or creep range values and of isothermal ductility data, though the resulting elongation is a unique summation of ductility and plastic flow over the whole cooling range.

Unfortunately, the values reported here are closely related to furnace and specimen design and the rate of cooling during the test. The stresses would probably be approximated in any apparatus that provided sufficient contraction to exceed elastic properties, but the precise values and the elongation observed are expected to be a function of the test equipment constants. To permit better definition of test conditions, a brief study of isothermal relaxation has been

correlated with hindered contraction stresses on a single material (Figs. 19 and 20). It is believed that the extrapolated value termed "characteristic stress" should be duplicatable in different laboratories.

Fig. 21 is a plot of the range delineated by several tests, covering 0.29 to 0.56% C, against temperature. Hindered contraction stresses thus appear as intermediate between ultimate strength and limiting creep stresses. The coincidence of the ranges for yield strength at 1600 and 1800 F from Table II is significant. Since both yield strength and hindered contraction stresses are arbitrary values based on definition and testing procedure, it is probable that both indicate the same mechanical property. The possibility that strain hardening may affect the two values differently at lower temperatures should be considered, however.

It is noteworthy that the 16% Cr-35% Ni alloys usually break before reaching room temperature, while certain more ductile compositions, such as partially ferritic 26% Cr-12% Ni, may reach room temperature and even endure a second cycle without fracture. This suggests that high hindered contraction stresses in the lower end of the range may be dangerous to the former alloys, and implies the need for caution in using the material for heat treating parts that are alternately heated and quenched.

Thermal Fatigue

The foregoing has demonstrated the magnitude of thermal stresses and indicated that they can produce early failure. The mechanism of service deterioration from this source is more obscure and operates more insidiously. A series of temperature cycles is considered necessary, producing a succession of events somewhat as described below.

A casting, assumed to be originally stress-free,[4] is locally heated, producing thermal expansion. This is resisted by either fixed anchorages or the rigidity and strength of the colder portion. The resistance builds up elastic stress until the yield strength is exceeded, with consequent plastic flow (upsetting) in compression of this hottest portion. When the heating portion of the cycle is complete, the upset portion will retain a residual compressive stress approximating the values shown in Figs. 20 and 21 for the maximum temperature

[4]Some heat resistant alloy castings exhibit residual stresses (from mold cooling) ranging up to more than 20,000 psi, but this probably does not materially alter the analysis of thermal fatigue given here.

attained. The amount of relaxation from this stress (see Fig. 19 for an example) will depend on the time the temperature is constant. When cooling occurs the residual compression declines by elastic recovery until zero stress is reached at some intermediate temperature. Further cooling develops tension. Under severe conditions, this tensile stress will increase until the elastic limit is exceeded before room temperature is attained, and tensile plastic flow will result. If this flow is not excessive, thereby avoiding the fracture that occurred in Fig. 20, the upset area will return apparently intact to its initial temperature, but with the important difference that it contains high residual tensile stress.

The second and subsequent cycles differ in that heating and consequent expansion first relieves the tensile stress, passing zero at some moderately elevated temperature, and then builds up compressive stress. It is possible, because of the different zero stress location, that the maximum temperature can be attained without plastic flow on this cycle. If so, the return to room temperature may also take place without producing additional plastic flow in tension. Under these circumstances, a long life in cyclic service may be expected.

If the second cycle includes so much expansion that upsetting occurs again at the maximum temperature, tensile flow will be induced as the subsequent minimum temperature is approached. Each following similar cycle will also involve both compressive and tensile flow. It is postulated that the alteration of these will eventually exhaust the inherent ductility of the material and finally produce cracking. This result is termed "thermal fatigue". The failure will naturally occur on the tensile portion of a cycle. As precisely uniaxial stresses are rare, compressive flow portions of the cycles generally will be associated with warping and buckling, which usually accompany thermal fatigue cracks.

The number of cycles before failure, provided some flow takes place at each temperature extreme, will depend on the amount of such flow, which in turn depends on the part design and thermal gradient complex. The susceptibility of a given alloy to thermal fatigue will also depend on thermal expansion (a low coefficient will lessen the tendency for a given set of conditions to cause stresses reaching the plastic flow points), on strength at both high and low temperatures (elastic limits must be exceeded before the damaging flow occurs), and on ductility near the temperature extremes. Values for the latter

differ considerably for different alloys and at different temperatures, making prediction of behavior based on one set of conditions very uncertain of application to another case with a different temperature range. Ductility at the lowest temperature of a thermal cycle is probably critical.

The "HT" alloy has three possible advantages over the "HH" grade for some cyclic service conditions. It has lower expansion coefficients (Fig. 16); it has higher creep strength near 1400 F (Table XVI) than most "HH" alloys, and thus can attain higher stress levels with a minimum of plastic flow; and has greater ductility at 1400 F in the strong grades. This last advantage probably holds only when the cycle minimum is in this range. Adequate data are not available to indicate how far below 1400 F this favorable circumstance continues. The advantage of greater creep strength disappears above ± 1500 F in comparison with some balanced wholly austenitic 26% Cr-12% Ni alloys.

The complex of factors contributing to thermal fatigue makes experimental study difficult. A valid accelerated test would be valuable, but it should be recognized that its practical significance will probably be confined to an individual set of conditions. Data from one such empirical technique (12) are becoming available, which rank four alloys in the order: (a) HH-30, (b) HT-32, (c) HH-57, and (d) HT-54, for cycles involving successive water quenches from 1600 F by alternate flame and water impingement on a ⅜-inch thick by 4-inch diameter disk containing eight ¼-inch diameter holes as stress raisers. There was a considerable difference between the high and low carbon grades of each type in the number of cycles sustained before cracking.

These data suggest that carbon content is more important than the alloy type, and that room temperature ductility may be significant under the specific test conditions. They should also provoke a careful examination of service applications and an attempt to check the results in the field, as they differ sharply from the current experience ranking of the alloys (Table XIII). Experience with the 26% Cr-12% Ni grade may have been influenced by utilization of unbalanced alloys susceptible to sigma embrittlement, however.

The study of thermal fatigue is a fertile field for future research and for the careful correlation of field and laboratory data.

Table XVI
Comparison of "HT" (16% Cr-35% Ni) and "HH" (26% Cr-12% Ni) Alloys At Two Carbon Levels

	Chemical Composition, %						
Alloy	C	Mn	Si	Ni	Cr	N	Structure†
HH-31*	0.31	0.42	0.42	11.4	26.5	0.07	A + F + C
HH-32*	0.32	0.48	0.46	11.5	25.9	0.16	A + C
HH-42	0.42	0.45	0.45	11.3	26.1	0.06	A + F + C
HH-44	0.44	0.54	0.60	12.8	26.9	0.08	A + C
HT-29	0.29	0.72	1.28	34.4	16.2	0.04	A + C
HT-44	0.44	0.74	1.17	35.0	16.2	0.05	A + C

	Room Temperature Properties After Aging 24 Hours at 1400 F				
Alloy	Yield Strength psi	Ult. Tens. Strength psi	Elong. %	R.A. %	Hardness BHN
HH-31	55,000	86,000	25.0	29.0	179
HH-32	50,000	87,800	6.8	7.8	202
HH-42	73,000	89,000	13.0	15.0	210
HH-44	64,000	89,125	4.3	4.3	...
HT-29	51,000	95,500	13.0	19.0	207
HT-44	49,000	88,000	5.5	9.2	210

	Limiting Creep Stress—psi			Hindered Contraction Stress*—psi			
Alloy	1400 F	1600 F	1800 F	1200 F	1400 F	1600 F	1800 F
HH-31	3,400	....	1,150	30,200	20,500	10,950	....
HH-32	5,950	3,200	1,750	39,500	28,000	16,200	....
HH-42	6,300	....	2,200	.....	.....	.....	....
HH-44	7,800	4,500	3,000	46,250	31,000	15,750	....
HT-29	7,600	4,400	1,600	40,500	29,000	15,000	7,500
HT-44	7,200	4,800	2,200	36,300	24,500	13,200	7,500

*For the HH-31 and HH-32 alloys, hindered contraction data were obtained on companion heats with very similar analyses. The HH-32 alloys were wholly austenitic.
†A = austenite; F = ferrite; C = carbide.

Miscellaneous Properties

Evidence of elastic behavior diminishes as temperatures increase. The concept of creep has replaced elastic limit and its more practical associated properties, proportional limit and yield strength, in high temperature design. There is occasional need for elastic modulus values, however. The experimental values, such as those in Tables II and III, are affected by testing procedure, as in Table XVII.

It is thus questionable if the modulus values from tensile tests can be used for long-term loading. To obtain an estimate of such behavior the elastic recovery of some unfractured creep specimens as the load is removed while at the testing temperature (at the end of the test) is assembled in Table XVIII.

Hot hardness (12) and Charpy impact values (12) from A.C.I. research are summarized in Tables XIX and XX.

The available heat conductivity data are not accepted with confidence and are therefore omitted here. This property may have an important bearing on the temperature gradients that develop in cyclic

Table XVII
Effect of Loading Rate on Tensile Properties (12)

Heat No.*	Alloy	Loading Rate† psi per min.	Tested at 1800 F: Prop. Limit psi	Yield Strength 0.1% def. psi	Yield Strength 0.2% def. psi	Ultimate Tensile Strength psi	Elong. in 2 in. %	R.A. %	Elastic Modulus Million psi
B-77	HT-21	1250	7,500	9,000	9,200	10,300	7.8	11.5	8.9
B-77	HT-21	125	3,950	7,000	7,400	9,200	13.3	19.5	8.7
B-56	HT-59	1250	5,700	9,200	10,100	12,400	31.7	46.0	8.4
B-56	HT-59	125	5,000	7,500	7,900	10,800	29.0	53.5	7.5
B-57	HT-70	1250	7,900	9,800	10,200	13,500	21.4	50.0	7.8
B-57	HT-70	125	4,800	8,000	9,150	13,200	29.2	51.3	5.7

*See Table VI-B for analyses.
†to 0.2 deformation Yield Strength—0.03 inch per minute thereafter.

Table XVIII
Modulus Values from Elastic Recovery After Creep Testing

Alloy‡	Temperature F	Temperature C	Creep Stress psi	Indicated Elastic Modulus psi
HT-29	1400	760	6,000	15,000,000
HT-36	1800	982	3,000	11,000,000
HT-44	1400	760	6,000	17,500,000
HT-44	1600	870	4,000	16,000,000
HT-44	1800	982	2,000	15,000,000
HT-56	1400	760	10,000	18,000,000
HT-56	1600	870	5,000	17,500,000
HT-70	1800	982	2,000	11,000,000

‡See Table IX-A for analyses and creep test details.

heating and may therefore contribute to the thermal fatigue problem. This represents a gap in present knowledge.

The density of the "HT" alloys is 7.94 grams per cc, corresponding to 0.286 pound per cubic inch. It varies little over the commercial composition range. Over a wider zone of analyses it increases with nickel and decreases with chromium content. (The specific gravity of 26% Cr-12% Ni is about 7.72; of 12% Cr-60% Ni, about 8.14.)

Resistance to Carburization

The "HT" alloy is popular for carburizing service because it is considered resistant to deterioration incident to the temperature cycles of carburizing, because it maintains hot ductility even after absorbing considerable carbon, and because it resists carbon absorption.

A ranking in carburizing tendencies of several important heat resistant alloys, with SAE 1020 steel for comparison, appears in Fig. 22. A test in actual service is detailed in Table XXI. Quantitatively,

the estimation of carburizing from microscopic examination, as in the table, is considered less satisfactory than the chemical analysis of successive layer samples. Additional work to clarify the difference between results in Fig. 22 and Table XXI has been in progress. Pack carburizing experiments have suggested that the carburizing potential under these conditions is very close to some borderline value,

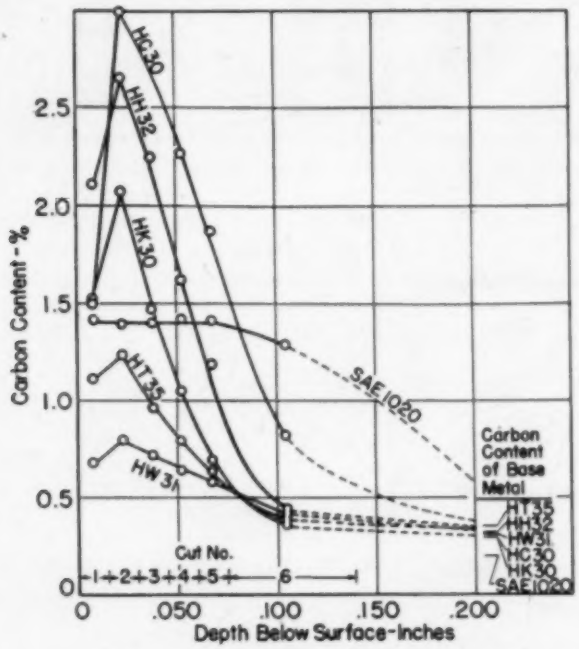


Fig. 22—Heat Resistant Alloys. Carbon penetration after pack carburizing at 1800 F for 100 hours in Houghton's "pearlite carburizing material." (Dodge Specification 5021)

Four Cycles of 25 Hours at 1800 F

Grade	Cr, %	Ni, %	Si, %
SAE 1020	..	..	...
HC-30	27	2	1.17
HH-32	26	12	1.18
HK-30	26	20	1.21
HT-35	16	35	1.28
HW-31	12	58	0.80

with the result that sometimes very little carburization of the Cr-Ni-Fe alloys occurs while the control of SAE 1020 steel reacts normally. The merits of gas carburizing as a laboratory technique are now under investigation; this is more pertinent to the present trend in commercial practice.

Much more rapid carburization occurs in a natural gas atmosphere (12). (Table XXII.)

Carburization is accompanied by a gain in weight and an increase in diameter. These data for the test in Fig. 22 appear in Table XXIII. Very rapid carburization in service may thus cause serious

Table XIX
Hot Hardness of 16% Cr-35% Ni Alloys

30-sec. load, mutual indentation method with 1-cm. dia. x 1-cm. cylinders

Heat No.	Chemical Analysis, % C	Mn	Si	Ni	Cr	N	Tens. Str.—psi R.T.	1800 F	Brinell Hardness 75	1200	1400	1600	1800
							Temperature—F:		75	1200	1400	1600	1800
							Load—Kilograms:		3000	2000	1500	1000	500
A	0.50	0.81	1.34	35.8	15.3	0.06	68	10.8	169	127	86	36	32
H	0.52	0.74	0.53	34.9	15.2	0.04	67	11.8	167	109	97	58	37
F	0.49	0.93	0.93	35.4	15.2	0.06	65	10.4	166	117	86	55	34
E	0.54	0.99	0.91	34.6	15.1	0.02	64	11.7	169	122	101	58	40
I	0.46	0 92	0.92	34.7	15.7	0.02	65	11.5	167	109	82	58	43
F	0.49	0.93	0.93	35.4	15.2	0.06	65	10.0	168	111	82	51	34

Table XX
Charpy Impact Resistance of 16% Cr-35% Ni Alloys

V-notched Charpy Specimens, Superheated 30 to 70 F to Compensate Temperature Drop Before Impact

Heat No.	Chemical Analysis, % C	Mn	Si	Ni	Cr	N	Mo		Impact in Ft-Lbs. Temperature, F 75	1200	1400	1600	1800
E	0.54	0.99	0.91	34.6	15.1	0.02	...	As Cast	3.5	6.0	6.5	7.0	7.5
I	0.46	0.92	0.92	34.7	15.7	0.02	...	As Cast	5.5	8.5	10.5	11.0	13.5
J	0.54	0.74	1.06	34.5	14.9	0.05	0.76	As Cast	3.0	7.0	7.0	7.5	10.0
								As Cast—Average	4.0	7.0	8.0	8.5	10.5
E				(Same heats as above except					3.5	6.5	6.0	6.5	7.0
I				aged 48 Hrs. at 1600 F					7.0	10.0	10.5	13.0	12.0
J				before testing.)					4.0	7.0	7.5	7.0	7.5
								Aged 1600 F—48 Hrs.—Average	5.0	8.0	8.0	9.0	9.0

Table XXI
Depths of Carburization of Heat Resistant Alloys After Use

Service: 1500 Hours at 1775 F in Carbo X Compound Supplied by the Rodman Chemical Company of Verona, Pa.

Alloy	Chemical Analysis, % C	Mn	Si	Ni	Cr	N	Depth of Heavy Carburization, In. Average	Maximum	Total Depth of Carburization, In. Average	Maximum
					16% Cr-35% Ni Alloys					
HT-14	0.14	0.72	1.22	34.7	16.4	0.05	0.094	0.109	0.150	0.166
HT-18	0.18	0.74	1.31	34.5	16.2	0.04	0.099	0.107	0.148	0.161
HT-25	0.25	0.75	1.31	34.4	16.3	0.04	0.094	0.098	0.141	0.161
HT-29	0.29	0.72	1.28	34.4	16.2	0.04	0.131	0.139	0.131	0.146
					26% Cr-12% Ni Alloys					
HH-32	0.32	0.49	0.46	11.2	26.6	0.16	0.045	0.057	0.099	0.104
HH-31	0.31	0.55	1.20	11.2	26.8	0.16	0.036	0.064	0.122	0.152
HH-32	0.32	0.54	1.18	12.8	26.7	0.16	0.056	0.084	0.100	0.131
					26% Cr-20% Ni Alloys					
HI-32	0.32	0.55	1.21	15.9	26.7	0.17	0.063	0.074	0.121	0.137
HK-33	0.33	0.53	1.25	18.7	26.7	0.16	0.035	0.050	0.119	0.132
HK-31	0.31	0.54	1.26	21.6	26.7	0.17	0.021	0.062	0.093	0.122

growth, and if local, cause such large stresses that warping or rupture occurs.

Decarburization may occur during the heating and cooling portion

Table XXII
Carburization of "HT" Alloys in Natural Gas (12)

Exposure at 1700 F for 100 Hours
(Specimens ⅜-inch dia. by 1 inch, weighing about 14 grams)

Alloy Grade	Chemical Composition, % C	Mn	Si	Ni	Cr	N	Weight Gain, Gms.	Carbon Increase, %
HT	0.49	0.93	0.93	35.4	15.2	0.06	0.043	0.30
Mn HT	0.52	9.21	1.19	24.6	15.3	0.05	0.023	0.16
HH	(For comparison)			12.0	24.0	...	0.028 to 0.054	0.20 to 0.38
HW	(For comparison)			59.0	13.0	...	0.017	0.12

(Carbon increase is based on over-all weight change)

Nominal Gas Composition CO_2	CH_4	C_2H_6	C_3H_8	N_2
1.2	69.8	9.9	4.2	15.2

of a carburizing cycle. When this occurs it is evident microscopically. To this is attributed the lower surface carbon contents in Fig. 22 in comparison with the metal about 0.030 inch below the surface.

Table XXIII
Weight and Volume Changes During Carburization

Original Avg.	Alloy:	SAE 1020	HC-30	HH-32	HK-30	HT-35	HW-31
210.0 grams	Weight Increase:	2.0	1.7	0.90	0.55	0.55	0.55
0.87 inch	Diameter Increases:	0.008	0.012	0.005	0.004	0.004	0.001

In addition to the inhibiting effect of nickel on carburization, as implied in Fig. 22, silicon usually reduces the carbon absorption rate. Effective prevention of carburization above 1.50% Si for 16% Cr-35% Ni and 1.25% Si for 26% Cr-12% Ni has been reported (12) for pack carburizing at 1700 F.

Hot Gas Corrosion Resistance

Adequate resistance to surface attack by hot gases is a primary requirement of heat resistant alloys. The 16% Cr-35% Ni level is an economical balance of the two elements for satisfactory scaling resistance at 1600 F. However, practical experience long ago established that the same surface stability was not obtained in sulphur-bearing gases. This is frequently attributed to the 35% Ni content, since high nickel alloys are known to be vulnerable to sulphidation. Recent evidence indicates, however, that the comparatively low chromium content is at least partly responsible. A number of alloys made on a 0.4% C, 0.8% Mn and 1.2% Si base, with various nickel, chromium and iron contents, were supplied by the American Brake

Shoe Company to the Alloy Casting Institute in a co-operative research program. These alloys were tested at Battelle Memorial Institute and the results partially reported (12), (20), (21). Some of them bracket the 16% Cr-35% Ni range as detailed in Table XXIV. Additional alloys made at Battelle or supplied by commercial foundries were also tested in the same apparatus.

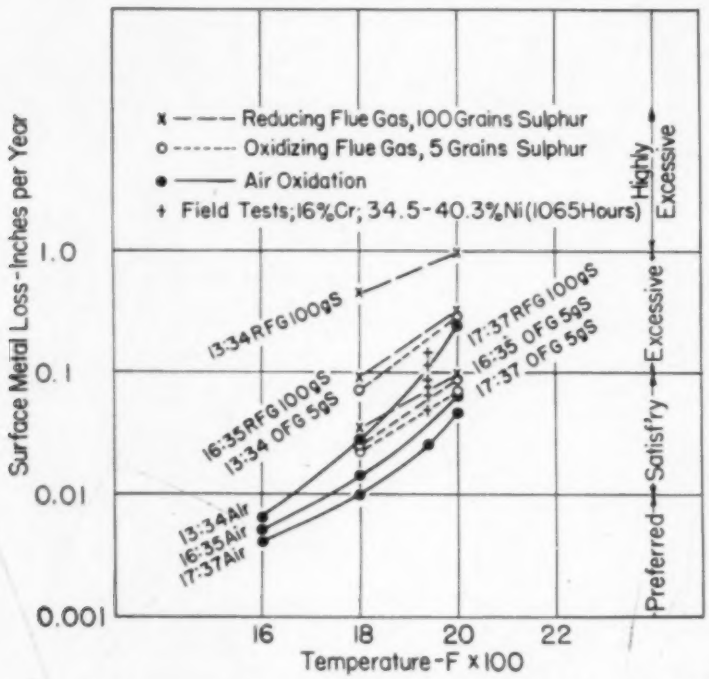


Fig. 23—Hot Gas Corrosion Resistance of Selected HT and HU Alloy Combinations (Based on 100-Hour Tests).

From this considerable amount of data, corrosion rates for several alloy combinations have been calculated and are shown below in Table XXV. The figures for 13% Cr-34% Ni and 17% Cr-37% Ni are particularly significant since they represent the minimum chromium and nickel contents for the "HT" and "HU" alloys respectively. Some of these data have been plotted in Fig. 23 for air oxidation, low sulphur oxidizing and high sulphur reducing flue gas conditions, representing severe and mild conditions to be encountered in normal commercial heat treating operations. From the plotted curves, estimates of corrosion rates may be made for intermediate temperatures.

An interesting comparative series of longer-term field tests was conducted by the American Manganese Steel Division of the American Brake Shoe Company. In these experiments, ½ by 1 by 2-inch

Table XXIV

Hot Gas Corrosion—Analyses of Alloys, Test Conditions and Test Results

Alloy No.	Chemical Analysis, % C	Mn	Si	Ni	Cr	N	Cu	Corrosion Penetration in Inches per Year — Air 1600 F	Air 1800 F [1]	Air 1800 F [2]	Air 1800 F [3]	Air 1800 F [4]	Air 2000 F	Air 2200 F	Flue Gas Oxidizing 1800 F 5gS	Flue Gas Oxidizing 1800 F 100gS	Flue Gas Oxidizing 2000 F 5gS	Flue Gas Oxidizing 2000 F 100gS	Flue Gas Reducing 1800 F 5gS	Flue Gas Reducing 1800 F 100gS	Flue Gas Reducing 2000 F 5gS	Flue Gas Reducing 2000 F 100gS
"C" Series of Alloys—Variable Ni and Cr																						
C-4	0.35	0.82	1.28	31.8	11.1	0.04		0.069*	0.073	0.013	0.062	0.066	1.20 *	....	0.095	0.479*	....	0.854	0.102	0.572	....	....
C-5	0.35	0.82	1.28	35.6	11.1	0.04		0.008	....	0.013	0.032	....	0.849*	0.998	0.088	0.090	....	....	0.108	0.762	0.162	0.787
C-6	0.39	0.82	1.28	39.3	10.8	0.04		0.008*	0.013	....	....	....	0.303*	....	0.061	....	0.315	0.153	....	0.825	0.058	0.944
C-14	0.45	0.80	1.24	32.2	16.0	0.08		0.004*	0.024	0.018	....	....	0.197*	0.256	0.042	0.019	....	....	0.047	0.260	....	....
C-15	0.45	0.80	1.24	36.4	16.0	0.08		0.004*	0.010	0.007	0.012	....	0.080*	0.172	0.015	....	....	....	....	0.151	....	....
C-16	0.46	0.80	1.24	40.3	16.0	0.08		0.004*	0.011	....	....	0.016	0.033*	0.099	0.015	0.022	....	....	0.011	....	....	0.823
C-34	0.47	0.77	1.21	32.3	20.9	0.06		0.006	0.011	....	....	....	0.031	0.201*	0.020	0.022	....	....	0.015	0.009	....	....
C-35	0.47	0.77	1.31	36.0	21.0	0.06		0.004	0.010	0.006	0.005	....	0.038	0.141	0.019	0.017	0.045	0.038	0.011	0.011	0.027	0.023
C-36	0.46	0.76	1.29	40.1	21.0	0.06		0.001*	0.009	....	....	0.008	0.040	0.131*	0.013	0.039	....	....	0.021	0.012	....	....
Carbon Series—HT Alloy																						
D-1	0.06	0.75	1.25	35.7	16.1	...		....	0.045	....	....	....	....	....	0.013	0.009	....	....	0.038	0.005	....	....
D-3	0.12	0.84	1.27	35.3	16.4	...		....	0.022	....	....	....	....	....	0.063	0.008	....	....	0.041	0.027	....	....
D-2	0.15	0.90	1.12	35.8	16.1	...		....	0.045	....	....	....	....	....	0.006	0.012	....	....	0.040	0.005	....	....
B-77	0.21	0.72	1.13	35.6	16.7	...		....	0.046	....	....	....	....	....	0.005	0.013	....	....	0.037	0.005	....	....
B-79	0.40	0.77	1.16	34.8	16.5	...		....	0.049	....	....	....	....	....	0.037	0.006	....	....	0.069	0.009	....	....
B-80	0.46	0.70	1.22	36.5	16.2	...		....	0.019	....	....	....	....	....	0.072	0.007	....	....	0.024	0.004	....	....
B-81	0.50	0.80	1.13	35.9	16.1	...		....	0.039	....	....	....	....	....	0.014	0.012	....	....	0.017	0.007	....	....
B-56	0.57	0.78	1.11	35.3	16.1	...		....	0.046	....	....	....	....	....	0.058	0.012	....	....	0.030	0.005	....	....
Silicon Series—HT Alloy																						
C-27	0.46	1.02	0.44	34.9	15.3	...		....	0.070*	....	....	....	....	....	0.118	0.061	....	....	0.031	0.105	....	....
C-28	0.43	0.95	1.60	34.9	16.6	...		....	0.013*	....	....	....	....	....	0.059	0.035	....	....	0.035	0.008	....	....
C-29	0.45	0.91	2.57	35.6	16.0	...		....	0.013*	....	....	....	....	....	0.025	0.024	....	....	0.010	0.006	....	....
Miscellaneous Alloys																						
CA-10	0.46	1.02	0.48	34.9	15.3	...	1.38	0.006	0.039	....	....	....	0.054	....	0.019*	0.013*	....	....	0.017*	0.051*	....	....
CA-8	0.45	0.88	1.83	35.4	15.7	...	As	....	0.011	....	....	....	0.031	....	....	....	....	....	....	....	....	....
CA-9	0.45	0.88	1.83	35.4	15.7	...	0.09	....	0.011	....	....	....	0.039	....	....	....	....	....	....	....	....	....
Control Alloy—HT																						
C-22	0.48	0.80	1.33	35.5	16.2	0.07	...	0.006	0.016	....	....	....	0.044*	0.136*	....	....	0.048	0.072	....	....	0.026	0.271
For Comparison—HH (26% Cr-12% Ni) Alloy																						
C-26	0.44	0.68	1.28	11.6	26.2	0.07	...	0.003	0.040	....	....	....	0.036	....	....	....	....	....	....	....	....	....
C-88	0.47	0.77	1.23	12.1	25.6	0.05	...	0.004	0.017	0.005	....	....	0.053	....	0.015	0.014	....	....	0.008	0.009	....	....
C-21	0.33	0.49	0.56	11.5	26.0	0.12	...	0.014	0.027*	0.007	....	....	0.051*	0.043*	0.030	0.029	....	....	0.037	0.046	....	....

[1] 100-Hr. tests; [2] 1000-Hr. continuous tests; [3] 1000-Hr. intermittent tests; [4] 1000-Hr. intermittent tests with periodic tumbling to remove scale.

*Average of two or more tests.

Table XXV
Calculated Corrosion Rates of "HT" and "HU" Alloys in Inches per Year

Alloy Combination Ni, %	Cr, %	Air 1600 F	Air 1800 F	Air 2000 F	Air 2200 F	Oxidizing Flue Gas 5gS (a) 1800 F	Oxidizing Flue Gas 5gS (a) 2000 F	Oxidizing Flue Gas 100gS (b) 1800 F	Oxidizing Flue Gas 100gS (b) 2000 F	Reducing Flue Gas 5gS (a) 1800 F	Reducing Flue Gas 5gS (a) 2000 F	Reducing Flue Gas 100gS (b) 1800 F	Reducing Flue Gas 100gS (b) 2000 F
34	13	0.006	0.029	0.26	0.50	0.075	0.30	0.085	0.25	0.056	0.15	0.46	1.0
35	16	0.005	0.014	0.065	0.14	0.028	0.10	0.028	0.08	0.032	0.05	0.09	0.25
37	17	0.004	0.010	0.048	0.14	0.025	0.07	0.024	0.04	0.026	0.04	0.036	0.10
38	18	0.004	0.009	0.045	0.13	0.024	0.06	0.020	0.04	0.020	0.04	0.020	0.05
40	21	0.004	0.008	0.038	0.13	0.022	0.05	0.018	0.03	0.018	0.03	0.018	0.04

(a) 5gS— 5 grains sulphur per 100 cubic feet; representing atmospheres from low sulphur fuel.
(b) 100gS—100 grains sulphur per 100 cubic feet; representing atmospheres from high sulphur fuel.

Table XXVI
Field Test Hot Gas Corrosion Data

Exposure in Commercial Heat Treating Furnace (a) at 1940 F (1060 C)
Under Oxidizing Conditions

Alloy	Chemical Composition, % C	Mn	Si	Ni	Cr	N	Total Test Period Hrs. (b)	Total Surface Metal Loss, In. (c)	Corrosion as Surface Metal Loss—In./Yr. Furnace Fuel Data 50* 50† (d)	95* 5† (d)	100* 0† (e)	0* 100† (e)
HT-14	0.14	0.72	1.2	34.7	16.4	0.05	8,100	0.083	0.135	0.060	0.052	0.219
HT-35	0.35	0.67	1.3	34.9	16.0	0.05	8,100	0.125	0.235	0.080	0.063	0.408
HT-44	0.44	0.74	1.2	34.9	16.4	0.05	8,100	0.118	0.210	0.085	0.071	0.349
HH-32	0.32	0.54	1.2	12.8	26.7	0.16	8,100	0.068	0.155	0.040	0.027	0.283
HH-31	0.31	0.55	1.2	11.2	26.8	0.16	8,100	0.068	0.095	0.065	0.062	0.129
HT-47	0.47	0.82	1.2	34.9	16.0	0.04	5,150	0.060	0.125	....	....	....
HT-56	0.56	0.80	1.3	34.8	15.9	0.04	5,150	0.070	0.163	....	....	....
HT-61	0.61	0.76	1.3	34.6	16.1	0.05	5,150	0.083	0.173	....	....	....
HT-70	0.70	0.81	1.3	34.7	16.5	0.05	5,150	0.070	0.155	....	....	....
C-4	0.35	0.82	1.28	31.8	11.1	0.04	2,110	0.085	0.390	....	....	....
C-14	0.45	0.80	1.24	32.2	16.0	0.08	2,110	0.028	0.120	....	....	....
C-16	0.46	0.80	1.24	40.3	16.0	0.08	2,110	0.015	0.070	....	....	....
C-34	0.47	0.77	1.21	32.3	20.9	0.07	2,110	0.010	0.040	....	....	....

*% Time on Gas.
†% Time on Oil.

Notes: (a) Furnace can be either gas or oil fired and operation is shifted from one to the other as supplies warrant. Fuel gas is essentially free from sulphur (natural gas from Texas Panhandle). Fuel oil is either No. 350 or No. 125 Industrial Fuel Oil from Standard Oil Company of Indiana with general specification of not more than 1.5% sulphur.
(b) Tests still in progress.
(c) % time on gas and % time on oil are not accurately known for several periods during tests. These figures are total surface metal losses and not rates (inches/year) as shown in subsequent columns.
(d) Rates calculated from test periods totaling 2000 to 2500 hours in each case where accurate fuel records are available.
(e) Extrapolated from (d).

Table XXVII
Corrosion by Gaseous Sulphur Compounds (12)

Specimens, ⅜-inch dia. by 1 inch, Exposed for 1 Hour

Alloy Type	No. Heats	Chemical Composition, % C	Mn	Si	Ni	Cr	N	Weight Gain in Grams/dm²/Hour In Hydrogen Sulphide 1400 F	1800 F	2000 F	In Sulphur Dioxide 1400 F	1800 F	2000 F
HH	2 to 7	0.30	0.68	0.34	10.4	23.0	0.09	1.25	4.6	11.6	0.023	0.011	0.037
		0.41	0.95	1.80	12.7	26.7	0.12	1.38	5.7	14.2	0.028	0.015	0.046
HT	1	0.49	0.93	0.93	35.4	15.2	0.06	2.13	8.8	51.5	0.347	0.373	0.630
HW	1	0.59	0.86	1.02	59.1	13.1	0.02	3.34	36.4	50.0	0.414	0.469	0.893

Table XXVIII
Hot Gas Corrosion in a Sulphur-Bearing Atmosphere

Chemical Analysis of HT (Center) Specimen, %					
C	Mn	Si	Ni	Cr	N
0.43	0.38	1.23	34.4	17.2	0.06

Type Alloy	Chemical Analysis of Corrosion Products S% as Sulphide	S% as Sulphate	SO_4, %	Ni, %	Cr, %
26% Cr-12% Ni	Scale too thin for sampling				
26% Cr-32% Ni	2.83	0.58	1.74	13.4	9.74
16% Cr-35% Ni	2.96	1.33	3.99	16.6	13.28
13% Cr-65% Ni	2.22	1.07	3.21	37.9	12.34
17% Cr-63% Ni	0.48	2.00	6.00	31.8	13.98

Temperature = 1675 to 1700 F. Exposure time = 300 hours, intermittent.

specimens, tack welded to a suitable heat resistant alloy tray, were installed in an industrial heat treating furnace operating intermittently at 1940 F (1060 C). Direct flame impingement was avoided and the tray was rotated at intervals to equalize possible differences in exposure due to position. The furnace was fired with low sulphur content natural gas, with the burners adjusted for an oxidizing atmosphere. Metal loss was calculated from periodic thickness measurements since weight loss determinations, necessitating descaling, were impractical. However, the longer periods of the tests compensate for the lack of precise measurements and metallographic examinations that are possible when the specimens are descaled and sectioned after a single exposure interval. These results are shown in Table XXVI and pertinent comparative values have been superimposed on the plotted results of the 100-hour laboratory tests of Fig. 23.

The greater attack by high sulphur-bearing reducing gases, apparent in Table XXIV, is further emphasized in Table XXVII wherein the corrosion rates in undiluted H_2S and SO_2 (12) are presented. Fusion of the corrosion product was visible on the "HT" and "HW" alloys in conjunction with weight gains above 25 grams per dm^2 per hour. The much greater rate of corrosion in H_2S as compared to SO_2 confirms that hydrogen sulphide is the agent responsible for the rapid attack of high nickel heat resistant alloys in sulphurous flue gas atmospheres.

A visual comparison of the relative attack on five different type alloys exposed for 300 hours in a pack carburizing furnace operated at 1675 to 1700 F appears in Fig. 24. The furnace was fired with Bunker "C" fuel oil which usually contains 0.50 to 0.75% sulphur. Table XXVIII gives the composition of the "HT" alloy, the type analyses of the remaining alloys, and analyses of the corrosion products.

The available data on hot gas corrosion resistance permits a fairly satisfactory description of the utility and limitations of the "HT" type alloy from this standpoint. The alloy is stable in air at temperatures up to and including 1800 F over its complete analysis range. It is also stable at 2000 F provided the nickel, chromium and silicon contents are at or above the mean or 35.0, 16.0 and 1.2% respectively. Silicon is extremely effective in minimizing scaling loss in oxidizing atmospheres and should be maintained as high as feasible (1 to 1.5%) without sacrificing strength. The alloy is not sufficiently stable in air at 2200 F to be commercially satisfactory in service approaching this temperature.

With respect to oxidizing flue gases, the alloy is adequately stable at 1800 F in the presence of sulphur up to 100 grains per 100 cubic feet. In the vicinity of 16% Cr and above, the alloy is borderline at 2000 F in the presence of appreciable sulphur and stable in the presence of low sulphur. With chromium contents of 18% and higher, the alloy may be considered for general applications in oxidizing atmospheres at 2000 F.

In reducing or neutral flue gas atmospheres, in which carbon monoxide (CO) and hydrogen (H_2) gases are present, and in which the sulphur exists essentially as hydrogen sulphide (H_2S), the alloy is stable at 1800 F with low sulphur content gases. The alloy is only stable with high sulphur content gases when the chromium content is above the mean of the commercial range of the "HT" type. Stability at 2000 F is generally unsatisfactory in reducing atmospheres.

Carbon apparently does not have an important effect on hot gas corrosion resistance. The effects of manganese and nitrogen have not been precisely determined but are presumed to be slight within present commercial ranges.

The surface metal loss data, however, do not permit the complete analysis of the hot gas corrosion problem when appreciable stress is involved. Grain boundaries are particularly susceptible to attack, probably because the carbide segregated there partially divests the adjacent matrix of protective chromium. Even in air atmosphere, the vulnerability of grain boundaries is apparent (Figs. 25 and 26). Research has not yet provided an evaluation of the effect of stress, due to either mechanical or thermal circumstances, combined with hot gas corrosion, but it would be anticipated that with such a combination grain boundary attack may be serious.

The sensitivity to chromium and nickel content demonstrates

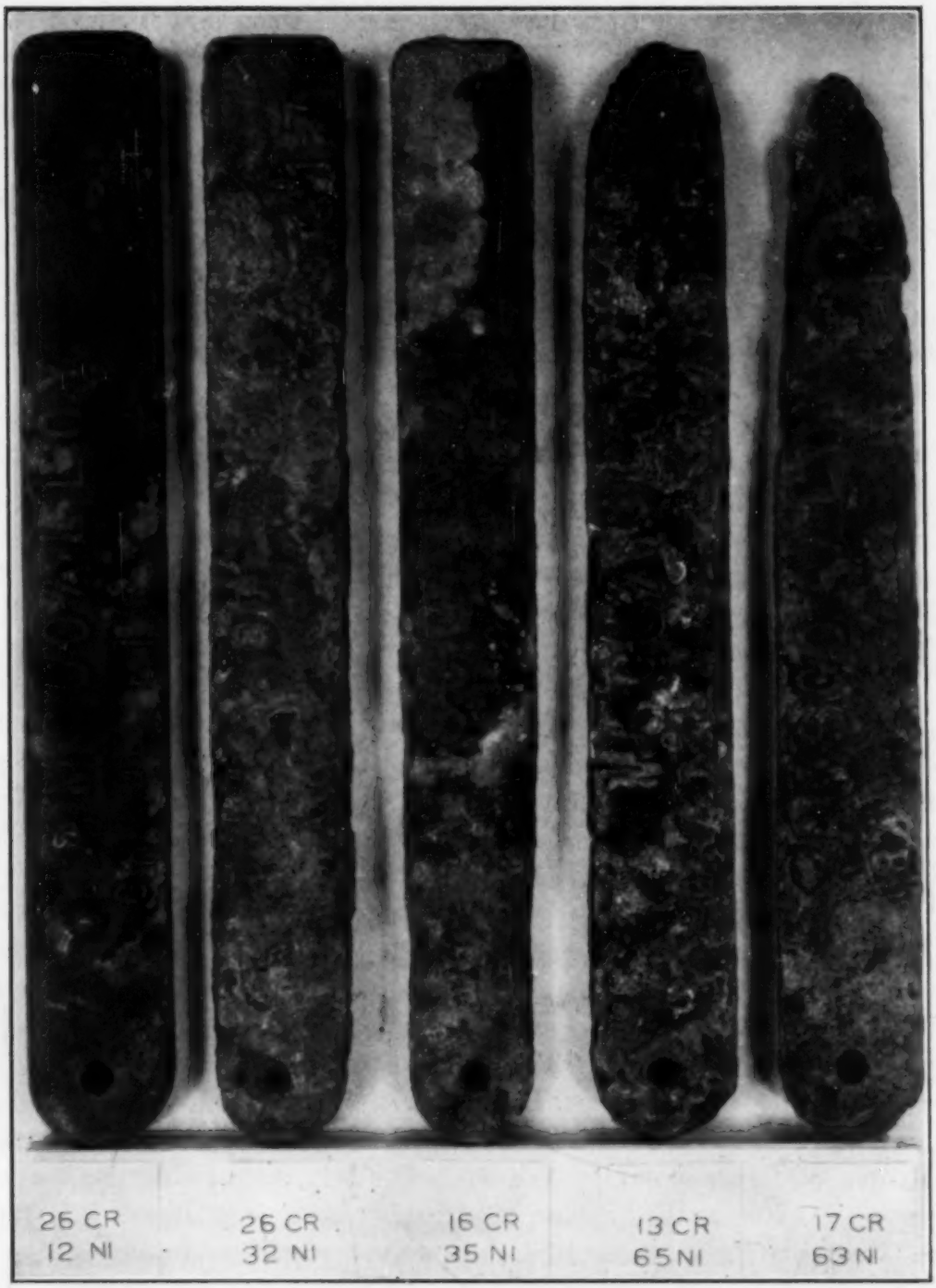


Fig. 24—Relative Attack of Five Heat Resistant Alloys in Sulphurous Furnace Gases.

the desirability of employing the "HU" (18% Cr-38% Ni) alloy range in place of "HT" when high temperature corrosion may be severe. Where considerable hydrogen sulphide may be encountered

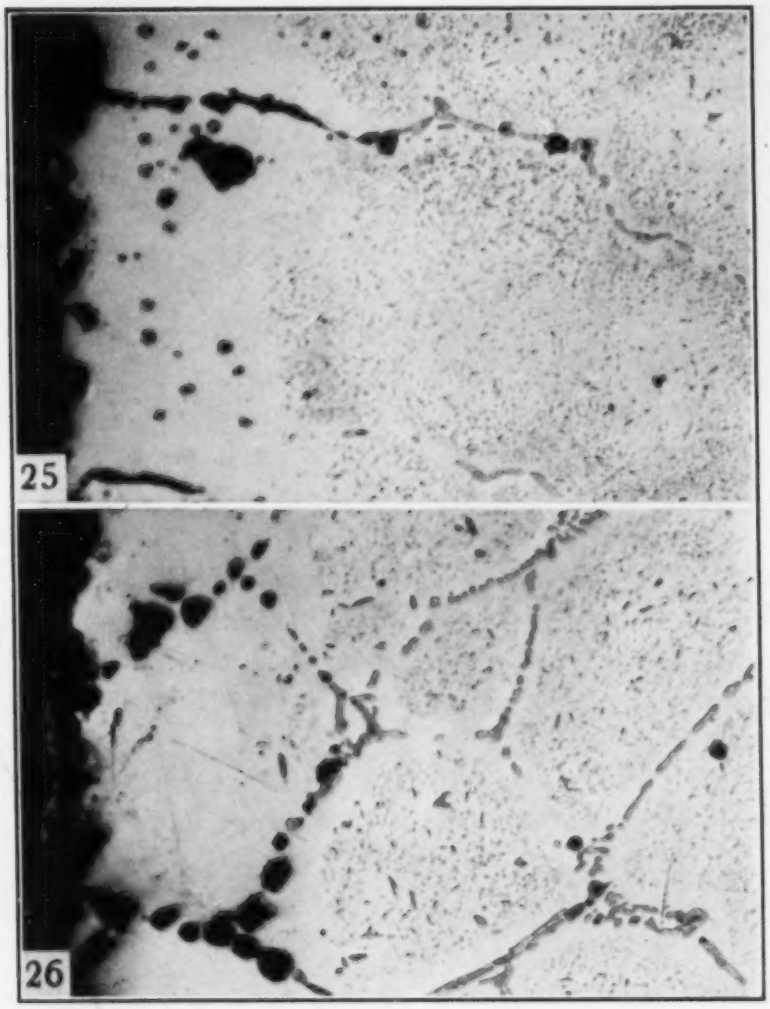


Fig. 25—Grain Boundary Attack After 630 Hours at 1800 F Under Stress of 2000 psi. × 250.
Fig. 26—Grain Boundary Attack After 1003 Hours at 1800 F Under Stress of 2000 psi. × 250.

the selection of the "HH" (26% Cr-12% Ni) grade may be advisable in preference to either of the two above.

Recent developments in the A.C.I. program indicate that when conditions alternate, as when reducing and oxidizing atmospheres are employed, successively, the gas composition of maximum destructiveness is the controlling factor. This implies that an alloy should be selected to withstand the most severe circumstances that may be encountered rather than the most probable or even average conditions.

Metallography

The metallography of the 16% Cr-35% Ni grade is relatively

simple, but certain factors are involved that are difficult to evaluate quantitatively. The matrix is a stable austenite; there are no complications from sigma or ferrite development as in the case of 26% Cr-12% Ni and other borderline alloys (HF, HI, etc.). The austenite contains carbides in solid solution, as a fine granular precipitate, and as masses in eutectiform arrangement. The amount of free carbide present, which is controlled by composition and temperature, apparently exerts a considerable influence on mechanical properties.

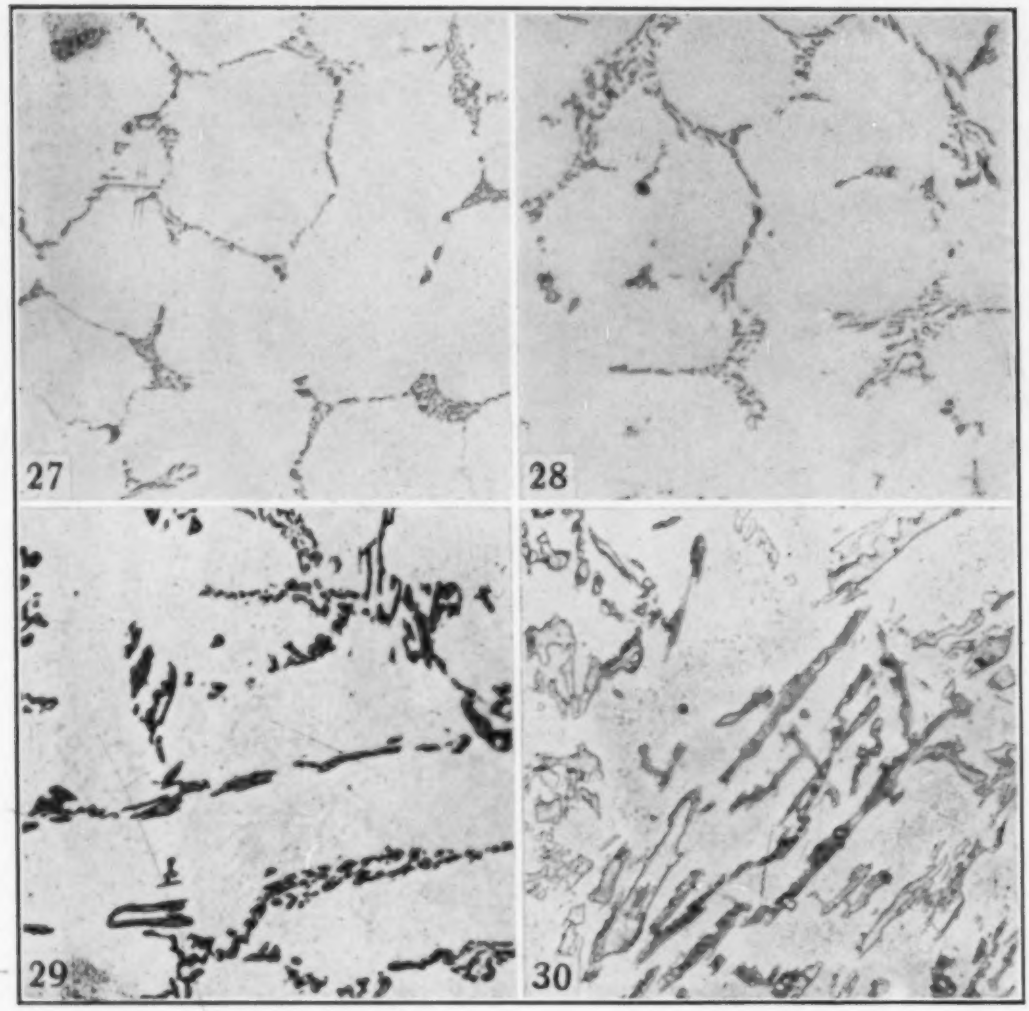
Free carbides tend to fix chromium in combination thereby impoverishing the matrix. Thus a carbon series, such as in Table V, is theoretically also an inverse matrix chromium series. The significance of this has not been thoroughly explored. Fortunately this fixation of chromium does not seriously affect general oxidation resistance as might be expected.

The form, amount, and distribution of carbide are important factors; they constitute the major variables influencing strength and ductility. As cast, the commercial alloys exhibit a network of eutectic carbides in a matrix that contains few if any of the fine granular type (Figs. 27, 28, 29 and 30). Subsequent exposure to elevated temperature will precipitate the excess held in supersaturated solution. Low temperatures (1400 to 1600 F) will produce many fine particles (Figs. 31, 32, 33 and 34); as temperatures rise the particles become fewer and coarser (Figs. 35, 36, 37 and 38). It is apparent that the as-cast austenite is not homogeneous, carbon gradients caused by the dendritic progress of solidification being prominent after carbide precipitation.

The amount of carbon that is soluble in the matrix just under the solidus is probably near 0.30% C. In Fig. 39, 2 hours at 2400 F has apparently dissolved all free carbide except traces at the grain boundaries. At 2300 F, with 0.18 and 0.25% C, grain boundary carbide is present but the grains themselves are carbide-free (Figs. 40 and 41).

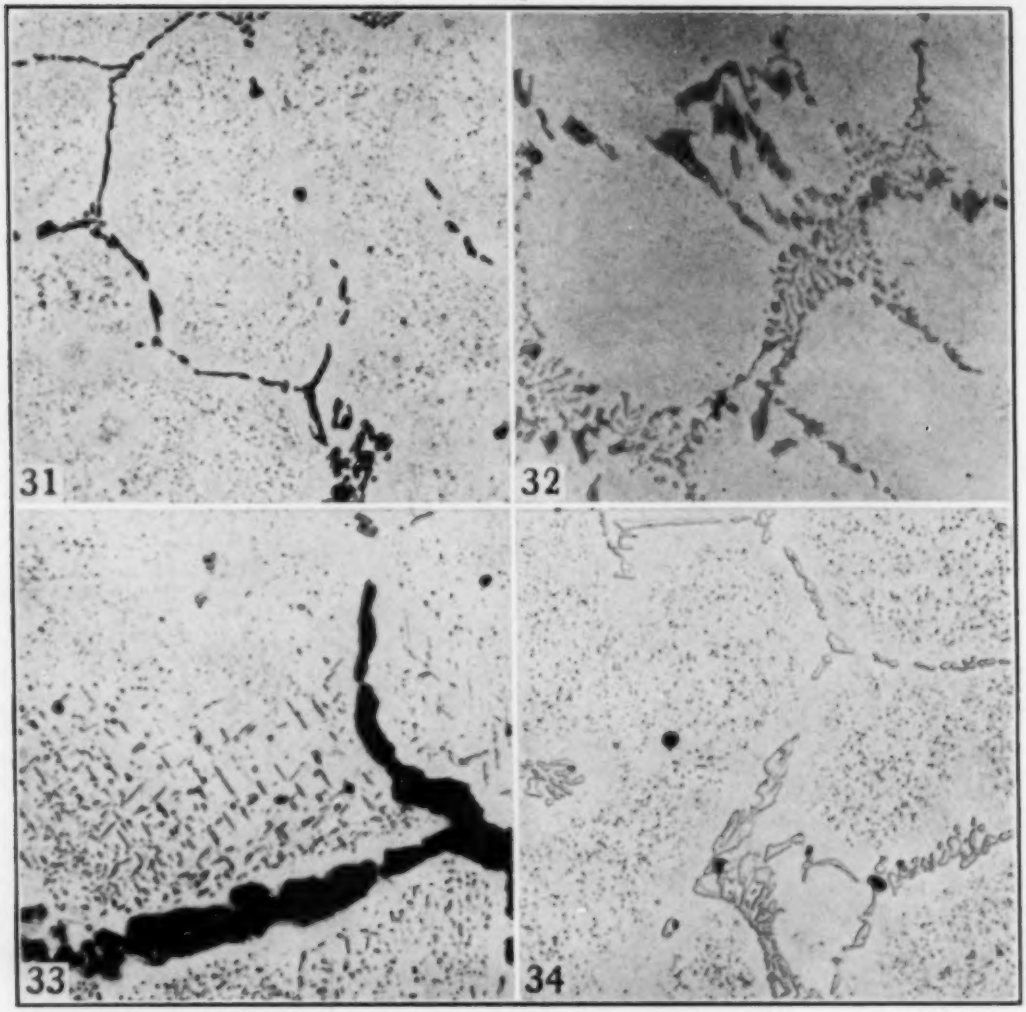
At the lower elevated temperatures there is little diffusion of carbon and the cast dendritic structure persists for long periods. Above 1800 F diffusion becomes apparent; at 2000 F some agglomeration will occur during a 1000-hour creep test, and at 2150 F even the eutectic carbides exhibit spheroidization. At 2300 F diffusion is sufficient to erase matrix carbon gradients in 12 hours. Subsequent exposure at 1800 F will precipitate the excess carbide in the now homogenized matrix as a quite uniform dispersion (Fig. 42).

The change from segregated to uniform carbide distribution has a pronounced effect on properties. In Table XXIX, the tensile



Figs. 27 to 30—As-Cast Structures of 16% Chromium-35% Nickel "HT" Type Alloys. Etched in hot alkaline $K_3Fe\ Cy_6$. × 250. Fig. 27—0.44% carbon. Fig. 28—0.57% carbon. Fig. 29—1.09% carbon. Fig. 30—1.95% carbon.

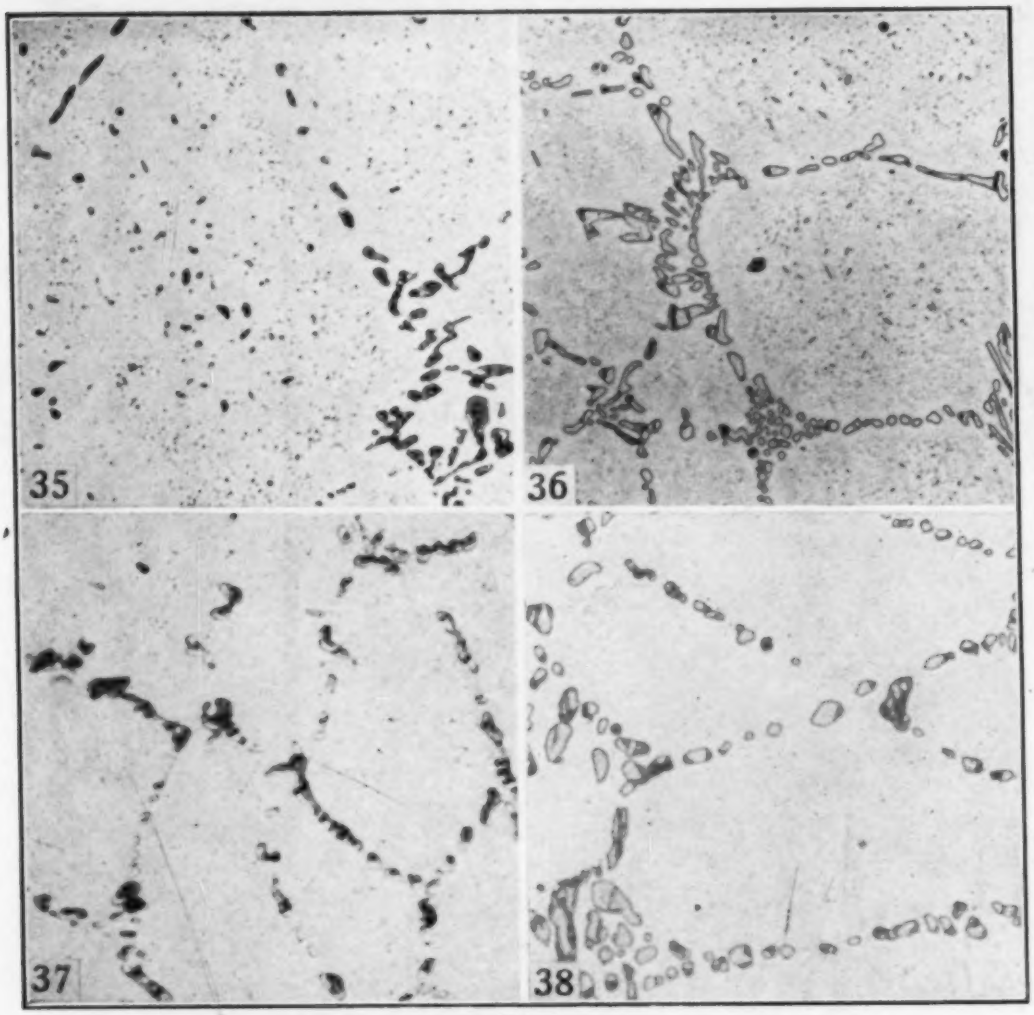
properties after aging, before and after homogenization at 2300 F, are presented. Strength is increased with some decrease in ductility. Parallel experiments with stress-rupture tests suggest a similar strengthening up to about 0.45% C but the data are erratic. The A.C.I. program has also included comparisons after various heat treatments, as detailed in Table XXX. An increase in life expectancy and creep resistance generally occurs after diffusion is promoted, though exceptions (see Alloy "S") are possible. A pronounced drop in ductility, which is undesirable, also results. The significance of these phenomena is believed to be the proof they provide that a wide range of properties may appear in a single alloy, depending on carbide habit. Thus, between 0.35 and 0.60% C in the commercial alloys,



Figs. 31 to 34—Carbide Precipitation in 16% Chromium-35% Nickel "HT" Alloys Tested at 1400 to 1600 F. Etched in hot alkaline $K_3Fe\ Cy_6$. × 250. Fig. 31—0.44% carbon. Creep tested 1005 hours at 1400 F. Fig. 32—0.57% carbon. Stress-rupture tested 8 hours at 1400 F. Fig. 33—0.29% carbon. Creep tested 1884 hours at 1600 F. Note heavily oxidized grain boundaries. Fig. 34—0.44% carbon. Creep tested 1001 hours at 1600 F.

considerable variations are possible and have been noted experimentally. At about 0.60 to 0.75% carbon the austenite is probably nearly saturated despite dendritic segregation (the excess carbide appearing as a network) and more uniformity in elevated temperature strength might be expected.

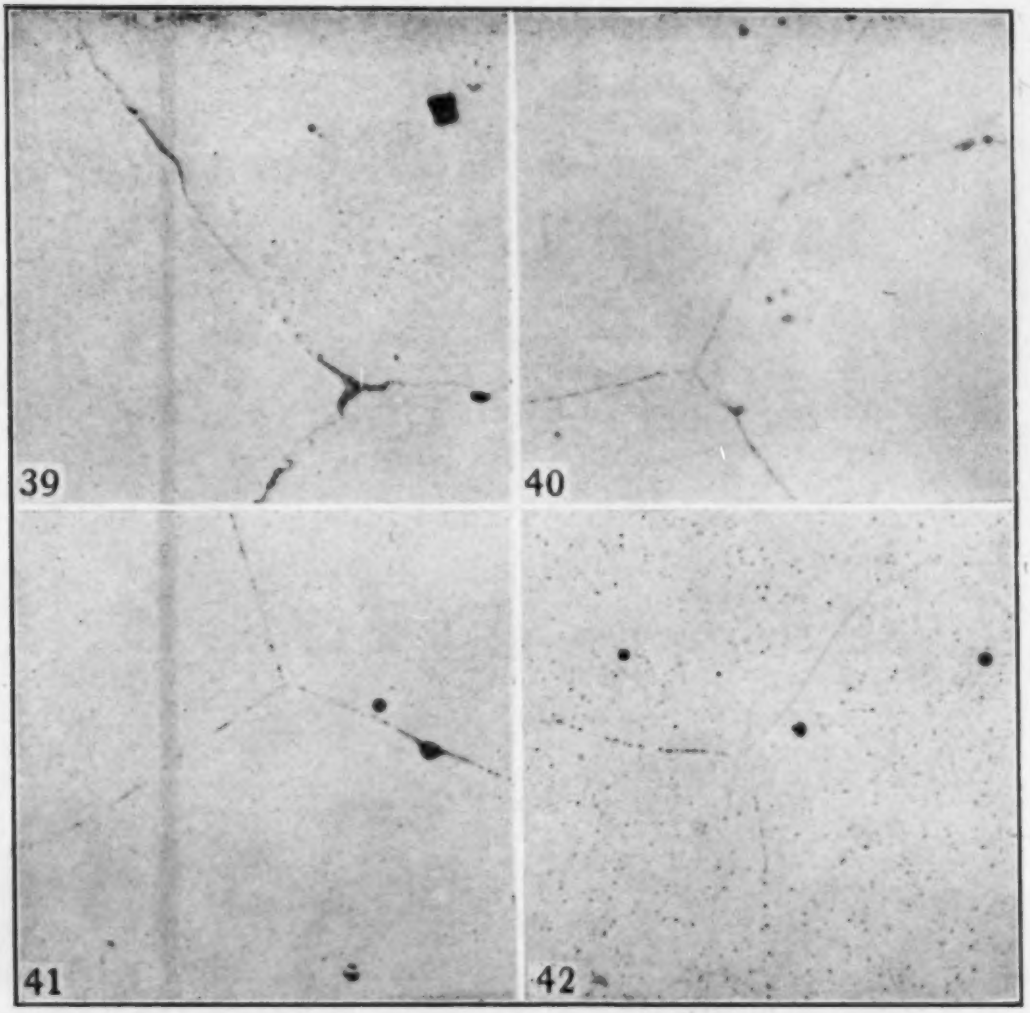
There is a possibility that homogenization and subsequent aging might be used to increase the hot strength of the weaker alloys below 0.35% C. This does not seem commercially feasible, however, as it involves expensive heat treatment and the same strength may be readily obtained with a moderate increase in carbon.



Figs. 35 to 38—Structures of 16% Chromium-35% Nickel "HT" Alloys Creep Tested From 1800 to 2150 F. Etched in hot alkaline $K_3Fe\ Cy_6$. × 250. Fig. 35—0.44% carbon. Creep tested 1013 hours at 1800 F. Fig. 36—0.56% carbon. Creep tested 1003 hours at 1800 F. Fig. 37—0.56% carbon. Creep tested 1025 hours at 2000 F. Fig. 38—0.56% carbon. Creep tested 1001 hours at 2150 F.

Stress-rupture results from a single heat, but reflecting two pouring temperatures and two rates of cooling after solidification, appear in Table XXXI (12). The spread from 3 to 10 hours in life (1600 F and 12,000 psi) and 0.43 to 3.5% per hour in minimum creep rate is large in comparison with the total range covered by the compositions in Tables VI and VII. This is considered to reflect the influence of carbide habit as modified by production variables.

In the graphs of Figs. 7 and 15, scatter bands for the principal properties are shown; these are intended to include the variations typified above provided no diffusion heat treatment, as in Tables XXIX and XXX, is employed. Their widths are based on the data



Figs. 39 to 42—Structures of 16% Chromium-35% Nickel "HT" Alloys After Homogenizing Heat Treatments. Etched in hot alkaline $K_3Fe\ Cy_6$. × 250. Fig. 39—0.29% carbon. Water-quenched from 2 hours at 2400 F. Note evidence of incipient fusion. Fig. 40—0.18% carbon. Air-cooled from 12 hours at 2300 F. Fig. 41—0.27% carbon. Air-cooled from 12 hours at 2300 F. Fig. 42—0.27% carbon. Carbide precipitation at 1800 F after 12 hours at 2300 F.

available, with omission of occasional extreme tensile test values. General experience with high temperature testing has also been invoked for the Limiting Creep Stress bands; statistical treatment would be very desirable for this important property but not enough data are available.

The freedom from ferrite and sigma phases has an important bearing on the range of expected properties. The "HE" (28% Cr-10% Ni), "HF" (21% Cr-9% Ni), "HH" (26% Cr-12% Ni), "HI" (28% Cr-14% Ni), and sometimes the "HK" (26% Cr-20% Ni) types are borderline in this respect; certain combinations

Table XXIX

The Effect of Homogenization and Consequent Carbide Redistribution on the Properties of 16% Cr-35% Ni Alloys

C variable	Composition Range, % Mn	Si	Ni	Cr	N
	0.67 to 0.75	1.17 to 1.31	34.4 to 35.0	16.0 to 16.4	0.043 to 0.052

	Room Temperature Tensile Properties After Aging									
	As Cast + Furnace Cool from 24 Hours at 1400 F					2300 F—12 Hours—Air Cool + Furnace Cool from 24 Hours at 1400 F				
C, %	Yield Strength psi	Tensile Strength psi	Elong. in 2 in. %	Red. Area %	Hardness BHN	Yield Strength psi	Tensile Strength psi	Elong. in 2 in. %	Red. Area %	Hardness BHN
0.14	48,000	87,750*	25.8	35.9	168	59,000	95,750*	14.5	17.0	196
0.18	48,000	91,750*	21.0	34.5	187	67,000	99,500	10.0	23.4	217
0.25	53,000	93,500	16.0	30.8	207	75,000	113,250*	10.8	19.0	262
0.29	25,000	95,500*	13.0	19.4	207	78,000	110,500*	6.3	14.4	262
0.35	59,000	90,250*	7.5	9.8	199	78,000	116,750*	7.0	10.6	262
0.44	49,000	88,000	5.5	9.2	210	58,000	105,250	4.8	6.8	241

*Average of two tests.
The yield strength values are approximate, from load increase observation.

Table XXX

Effect of Heat Treatment (12) on Stress-Strain-Rupture Properties at 1600 F and 12,000 psi

(For Compositions, See Table XII)

		As Cast + 48 Hrs. at 1600 F				2100 F—2 Hrs.—W.Q. + 48 Hrs. at 1600 F				2200 F—2 Hrs.—W.Q. + 48 Hrs. at 1600 F			
Alloy	C	Life Hrs.	Min. Rate %/Hr.	Elong. %	R.A. %	Life Hrs.	Min. Rate %/Hr.	Elong. %	R.A. %	Life Hrs.	Min. Rate %/Hr.	Elong. %	R.A. %
R	0.33	4.2	1.1	18.0	44	..	..	...	..	9.0	0.40	9.9	27.0
ZB	0.39	8.1	1.2	22.0	40	..	..	...	..	45.1	0.014	2.9	12.0
ZD	0.39	4.2	1.8	20.0	28	5.4	1.3	15.0	19	14.5	0.004	4.2	7.7
Z	0.40	5.3	2.0	21.0	30	..	..	...	..	21.9	0.016	2.0	5.0
O	0.46	14.5	0.42	15.0	33	4.7	0.72	6.9	11	27.4	0.04	3.0	3.9
S	0.53	41.6	0.052	5.9	17	..	..	...	..	24.5	0.08	5.4	3.6
ZC	0.59	4.2	4.5	28.0	42	11.4	1.6	25.0	34	50.2	0.012	3.2	13.0

Table XXXI

The Effect of Casting Variables on Stress-Rupture Properties (12)

Specimens from a Single Heat of HT Alloy

Casting Variables		Stress-Strain Rupture Properties (Preaged 48 Hours at 1600 F) 1600 F and 12,000 psi			
Pouring Temp. F	Mold Cooling	Life Hrs.	Min. Creep Rate % per Hr.	Elong. % in 2 In.	Red. Area %
2870	Slow to R.T.	3.0	3.5	23	45
2870	Quick shakeout	6.8	0.85	19	32
2695	Slow to R.T.	7.7	1.2	21	28
2695	Quick shakeout	10.0	0.43	10	13
	From Tables VI-A and VI-B for Comparison				
4 Commercial heats:	0.33 to 0.40% C	4.2 to 8.1	1.1 to 2.0	18 to 22	28 to 44
4 Commercial heats:	0.46 to 0.57% C	11.0 to 42.0	0.05 to 0.76	6 to 17	16 to 33
4 Commercial heats:	0.59 to 0.78% C	4.2 to 8.2	1.2 to 4.5	19 to 28	33 to 48
1 Laboratory heat:	0.38% C	5.7	1.8	24	46
1 Laboratory heat:	0.38% C	19.0	0.08	6.7	15
18 Laboratory heats:	0.40 to 0.49% C	4.9 to 12.5	0.91 to 2.6	13 to 32	24 to 48
3 Laboratory heats:	0.59 to 0.70% C	15.0 to 24.0	0.26 to 0.33	11 to 17	23 to 55

of the constituent elements may produce only partially austenitic alloys that may be weak at high temperatures and subject to sigma embrittlement around 1600 F. Composition control to produce definite properties may thus require intimate knowledge, adequate technical control and exceptional melting skill. In contrast, the "HT" alloy has much latitude. Despite the effects of carbide habit there is less variation expected in creep strength over the range from 0.35 to 0.75% C, 34 to 40% Cr, and 13 to 21% Ni than has been observed experimentally between 0.25 and 0.35% C in 23 to 27% Cr-10 to 13% Ni alloys. The same applies to hot ductility.

This latitude is stressed here for comparison with "HH" alloys and not to imply that "HT" alloys are uniform even if carelessly made. Room temperature ductility is a sensitive property and others, such as resistance to carburization, hot gas corrosion, and thermal fatigue require informed technical control to produce consistent results.

Summary

The foregoing assembly of data indicates that the creep strength (for 0.0001% per hour minimum rate) of 16% Cr-35% Ni alloys ranges from around 8000 psi at 1400 F to 180 psi at 2150 F. Using working stresses based on half of these values, life expectancy before fracture, from extrapolation, ranges upward from 20,000 hours. Unit stresses can be calculated on metal sections that remain after service by considering the expected metal loss from hot gas corrosion.

The limitation of the 16% Cr-35% Ni (HT) grade to temperatures below 1900 F in air, 1800 F in oxidizing and low sulphur reducing flue gases, and to below perhaps 1400 F in high sulphur (100 grains per 100 cu. ft.) reducing flue gases is indicated. The maximum temperatures for the more resistant 18% Cr-38% Ni (HU) grade are similarly about 2050 F in air and oxidizing flue gases; and 2000 F for reducing flue gas with high sulphur. The most damaging agent is apparently hydrogen sulphide.

The quantitative effects of intergranular oxidation and stress corrosion are not yet defined and may require additional safety factors.

Carbon reduces room temperature ductility, thereby probably influencing thermal fatigue resistance. It does not impair hot ductility, however. In conjunction with good resistance to carburization, especially if silicon is above 1.5%, this carbon effect is favorable for

carburizing service, which is an important application for these alloys.

Silicon generally lowers high temperature strength and should be balanced against the need for carburizing resistance. The two ranges, 0.50 to 1.5% and 1.5 to 2.3% Si, might be differentiated for general structural and carburizing service respectively.

Cyclic temperature service may accelerate creep, thus requiring a safety factor from 2.5 to × 10 imposed on the constant temperature working stresses above 1500 to 1600 F (185 to 870 C), or may induce damaging thermal stresses. These are an important cause of service failures. Hindered contraction stresses have been determined as a contribution to the problem of "thermal fatigue", which has been discussed from a hypothetical and analytical perspective to provoke further experimental study.

Comparisons with the 26% Cr-12% Ni (HH) alloys indicate that the "HT" grade is generally superior in creep strength at 1400 F and similar to the balanced grades above 1600 F; has somewhat less thermal expansion; has better resistance to carburization, but less resistance to attack in reducing sulphurous hot gases; much superior hot ductility as carbon increases, thereby having a distinct advantage in carburizing service; and much less sensitivity to composition over a broad commercial manufacturing range.

Acknowledgments

The contributions of many associates to the research partially reported here is acknowledged with appreciation. Mr. W. G. Hoffman, President of the Electro-Alloys Division, has been especially helpful in guiding the direction and sponsoring the economic support of the work. The metallographic skill of Mrs. Eva Rule and Mr. Robert Gray, the careful high temperature testing by Miss Mary A. Moran, Mr. John Ward, Mr. Monroe Bester, and Dr. J. G. Beckerley, and the secretarial assistance of Miss Mary Dunko have been invaluable. Permission of the Technical and Publications Committees of the Alloy Casting Institute to quote freely from A.C.I. data is also appreciated.

References

1. Howard S. Avery, Earnshaw Cook and J. A. Fellows, "Engineering Properties of Heat Resistant Alloys," American Institute of Mining and Metallurgical Engineers Technical Publication No. 1480, *Metals Technology*, August 1942, and *Transactions*, American Institute of Mining and Metallurgical Engineers, Vol. 150, 1942, p. 373-400.

2. J. T. Gow and O. E. Harder, "Balancing the Composition of Cast 26% Cr-12% Ni Type Alloys," TRANSACTIONS, American Society for Metals, Vol. 30, 1942, p. 855-935.
3. N. B. Pilling and Robert Worthington, "The Effect of Temperature on Some Properties of Iron-Chromium-Nickel Alloys," in "Symposium on Effect of Temperature on Metals," American Society for Testing Materials-American Society of Mechanical Engineers, 1931, p. 495-556. (Includes 76 references.)
4. F. A. Fahrenwald, "Some Principles Underlying the Successful Use of Metals at High Temperatures," *Proceedings,* American Society for Testing Materials, Vol. 24, Part II, 1924, p. 310.
5. "The Book of Stainless Steels," 2nd Edition, American Society for Metals, 1935, Cleveland, Ohio, p. 458, 462-469, 643.
6. L. J. Stanbery, "Heat Resisting Chromium-Nickel-Iron Alloys for Furnace Construction," *Metals and Alloys,* Vol. 4, No. 9, September 1933, p. 127; Vol. 4, No. 10, October 1933, p. 159.
7. R. J. Wilcox, "Notes on 29-9 Alloy Castings to Resist Heat and Corrosion," METAL PROGRESS, Vol. XXVII, No. 5, May 1935, p. 49.
8. O. E. Harder, "The Alloy Casting Research Institute Test Block for Heat Resisting Alloys; Its History, Selection and Utilization," American Society for Testing Materials, Technical Papers, Vol. 39, 1939, p. 626-636.
9. J. T. Gow, A. S. Brasunas and O. E. Harder, "The Liquidus-Solidus Temperatures and Emissivities of Some Commercial Heat Resistant Alloys," American Institute of Mining and Metallurgical Engineers Technical Publication No. 1838, 1945.
10. E. A. Schoefer, "Temperature Measurements of Molten Alloys," Alloy Casting Bulletin, No. 2, July 1944.
11. J. D. Corfield, "Heat Resisting Castings," Metals Handbook, 1939, p. 550-553, published by American Society for Metals.
12. Howard S. Avery, "Properties of 'HT' Type Alloys—A Summary," Alloy Casting Bulletin, No. 9, October 1946.
13. J. A. Fellows, Earnshaw Cook and H. S. Avery, "Precision in Creep Testing," American Institute of Mining and Metallurgical Engineers Technical Publication No. 1443-C, 1942, No. 303.
14. R. A. Flinn, E. Cook and J. A. Fellows, "A Quantitative Study of Austenite Transformation," TRANSACTIONS, American Society for Metals, Vol. 31, 1943, p. 41-70.
15. American Society for Testing Materials, Designation: B190-44T, "Tentative Specifications for Chromium-Nickel-Iron Alloy Castings (25-12 class) for High Temperature Service," American Society for Testing Materials Standards, 1944, Part I, p. 1778-1782.
16. A. Nadai and P. G. McVetty, "Hyperbolic Sine Chart for Estimating Working Stresses of Alloys at Elevated Temperatures," *Proceedings,* American Society for Testing Materials, Vol. 43, 1943, p. 735-748.
17. P. G. McVetty, "Interpretation of Creep Test Data," *Proceedings,* American Society for Testing Materials, Vol. 43, 1943, p. 707-734.
18. C. H. M. Jenkins, E. H. Bucknall, C. R. Austin and G. A. Mellor, "Some Alloys for Use at High Temperatures: Part IV. The Constitution of the Alloys of Nickel, Chromium, and Iron," *Journal* (British), Iron and Steel Institute, 1937, p. 136.
19. H. S. Avery, V. O. Homerberg and Earnshaw Cook, "Metallographic Identification of Ferro-Magnetic Phases," *Metals and Alloys,* Vol. 10, No. 11, November 1939, p. 353-355.

20. Anton deS. Brasunas, James T. Gow and Oscar E. Harder, "Resistance of Iron-Nickel-Chromium Alloys to Corrosion in Air at 1600 to 2200 F," *Proceedings,* American Society for Testing Materials, June meeting, 1946.

21. E. A. Schoefer, "Corrosion of Nickel-Chromium-Iron Alloys—The Influence of Nickel and Chromium Content on Penetration Rates in Air and Flue-Gas at High Temperatures," Alloy Casting Bulletin, No. 4, March 1945.

DISCUSSION

Written Discussion: By C. T. Evans, Jr., chief metallurgist, Elliott Co., Jeannette, Pa.

The authors are to be commended for such a thorough treatment of such a complex subject. Data on these older compositions are particularly welcome to the metallurgist concerned with the new gas turbine structures. Such parts as rotor casings, inlet and exhaust casings and duct work flanges can often be cast to good advantage, and the design stresses can be readily kept within the limitations which the data indicate. Furthermore, the indications are that above 1600 F (870 C), for long-time service, the new "super" alloys of the vitallium class are no longer "super", and that the older compositions come back into their own.

It is to be hoped that this work will continue unabated with emphasis on the tests which shed some light on the intricate problem of thermal fatigue. A more extended comparison of the "HT" (16% chromium-35% nickel) and "HH" (25% chromium-12% nickel) types with the 25% chromium-20% nickel "HK" type is badly needed, since this latter alloy gives many indications of combining the better features of both the more widely used compositions.

It is regrettable that no reference is made to the serious problem of weldability. Designing engineers tend to think of all austenitic alloys as highly weldable, whereas this is far from the case, particularly where these relatively high carbon cast compositions are concerned. In the writer's experience, whether or not an alloy is readily weldable can be the determining factor in its acceptability from either a structural or a repair viewpoint.

Only a few years ago, it was thought that all heat resisting alloys of the austenitic type tended to become brittle under load at temperatures in excess of 1200 F (650 C). Since then, several high strength compositions have been formulated which, in the wrought form, retain their ductility as measured by elongation to fracture in the rupture test. These same alloys, in cast form, exhibit the characteristic progressive brittleness mentioned by the authors. It has been further observed that the presence of ferrite and/or sigma tends to promote this hot ductility to fracture in the wrought alloys, although its presence is not absolutely necessary. Even in the cast compositions, the authors have taken note of the fact that when ferrite or sigma is present in the 25% chromium-12% nickel "HH" type, the hot ductility goes up.

It might be postulated that the absence of segregation in the alloys in wrought form is responsible for the improved and retained ductility characteristics. This would suggest that solution heat treatments might be helpful to

the cast alloys and perhaps the authors have some comments on this point.

In any case, a major mystery needs to be cleared up as to why the wrought and cast forms behave so differently. If cast alloys or treatments could be developed which would give structures retaining high ductility under load, it is the writer's opinion that a chief objection to the use of castings in critical gas turbine parts would be eliminated. As suggested by the authors, high factors of safety in castings are often required only because of their brittleness characteristic. Furthermore, it is reasonably certain that such structures would have a much higher level of resistance to thermal fatigue.

Written Discussion: By Alfred R. Bobrowsky, head of high temperature materials section, National Advisory Committee for Aeronautics, Cleveland.

Messrs. Avery and Matthews have presented an interesting paper on a number of properties of certain heat resistant alloys. It was mentioned that the semilogarithmic method of plotting rate of creep and time for rupture at constant temperature yields more nearly a straight-line plot than does the logarithmic method. It may be noted that a theory suitable for application to creep and stress rupture tests has been derived recently at the Aircraft Engine Research Laboratory of the National Advisory Committee for Aeronautics at Cleveland, which uses the concept of dislocations and rate-process theory to develop relations between the elevated-temperature test properties and fundamental characteristics of the materials such as crystal structure and modulus of rigidity. The theory predicts that creep and stress rupture data will be linear more readily on semilogarithmic plots than on log-log plots, a hyperbolic-sine relationship is the rigorous starting point for the semilogarithmic approximation. Two papers published by the National Advisory Committee for Aeronautics contain this theory.[1, 2]

Written Discussion: By Roger Sutton, General Alloys Co., Boston.

The authors are to be commended, not only on a noteworthy presentation of data, but particularly on the fact that this is the first logical interpretation of such data that it has been my opportunity to hear. Unfortunately, in the past it has been the practice of those engaged in research to accept such laboratory data as might be available to them, and compare it directly with similar data on other alloys. When such comparison has been at variance with known field performance records, it has been generally assumed by these research men that the performance data were either wrong, or biased.

These authors have looked beyond the actual data itself, correlated the information obtained, and applied an extremely clear logic with the end result that their conclusions are verified by the experience of the heat resistant alloy casting users of the country.

I can find no statements in this paper with which I am in disagreement. I would like to call your attention to certain facts confirming the conclusion of these authors, which facts are based on many years of experience with these alloys in the industrial field. It has been the experience of the General Alloys Company that in all cases where alternate heating and cooling, or thermal shock,

[1] A. S. Nowick and E. S. Machlin, "Quantitative Treatment of the Creep of Metals by Dislocation and Rate-Process Theories," NACA TN No. 1039, April 1946.

[2] E. S. Machlin and A. S. Nowick, "Stress Rupture of Heat Resisting Alloys as a Rate Process," NACA TN No. 1126, September 1946.

are encountered, the nickel-chromium types of alloy are vastly superior to the chromium-nickel grades. Moreover, it has been our experience that in the over-all picture, the alloys containing approximately 38% nickel-18% chromium have a life of approximately 50% more than the 35% nickel-15% chromium alloys where these conditions of thermal shock, temperature differential, alternate heating, and cooling, etc., are encountered. Moreover, based on our own experience, we have found the 38% nickel-18% chromium grade of material to be much more resistant to hot gas corrosion, particularly at temperatures above 1800 F. The beneficial effects of increasing nickel are further borne out in our experience by the vastly increased life of the 60% nickel-12% chromium, and 68% nickel-18% chromium alloys, whose ultimate service lives are found three to five times that of 35% nickel-15% chromium—in the case of the 60% nickel-12% chromium alloys—and five to ten times, in the case of 68% nickel-18% chromium.

It is to be hoped that additional papers on this same subject will be presented by these authors in the near future.

Written Discussion: By H. M. German, metallurgical assistant to the president, Driver-Harris Co., Harrison, N. J.

The Driver-Harris Company, one of the pioneer makers of heat resisting castings, has confined its casting activities to three types of alloys, namely—Nichrome,[3] an alloy of substantially 60% nickel, 15% chromium, balance iron; Chromax,[3] an alloy of substantially 35% nickel, 15% chromium, balance iron; and Cimet,[3] an alloy of substantially 12% nickel, 25% chromium and balance iron. The last named alloy is recommended only for applications where the alloy is to operate in sulphur atmospheres, as the higher nickel content alloys do not withstand the attack of sulphur satisfactorily. This alloy, however, does not resist carburization or nitriding as well as the higher nickel alloys, and in many cases becomes brittle in service due to the formation of sigma phase. We have never found the presence of brittle sigma phase in either the 35% nickel-15% chromium, or the 60% nickel-15% chromium alloys.

Experience over many years has proven that the 60% nickel-15% chromium alloy is the best analysis to resist high temperatures, erosion and corrosion of furnace atmospheres (except those containing sulphur), carburization and nitriding. For lower temperatures and where strength is required, the 35% nickel-15% chromium alloy is very satisfactory.

The high nickel alloys can be improved greatly by the addition of molybdenum and columbium or titanium. In order to determine the effect of these elements, standard production heats were made in a 1000-pound Ajax electric furnace. Analyses of the heats are shown below:

	I	II	III
Carbon	0.57	0.57	0.50
Manganese	1.09	1.10	1.18
Silicon	1.50	1.49	1.56
Nickel	35.83	36.19	35.58
Chromium	15.89	16.17	15.47
Columbium	None	1.91	2.03
Molybdenum	None	None	1.85
Iron	Balance	Balance	Balance

[3]Registered Trademark.

Standard creep test pieces and carburizing trays for service tests were made from the above heats. The creep test samples were sent to the International Nickel Company laboratory at Bayonne, N. J., for creep test. A quotation from their report is as follows:

"The creep resistance of cast heat resisting alloys of the 35/15 type is greatly improved by the presence of columbium, while still further improvement is obtained by an addition of columbium and molybdenum. A direct comparison can be made between the three alloys tested at 1800 F under 2000 psi. The straight 35/15 alloy entered the third stage of creep within 50 hours after the 2000-psi stress was applied, while an addition of 1.91% columbium delayed the entrance into the final stage for 600 hours. The alloy containing 2.04% columbium and 1.85% molybdenum, however, had not entered the third stage of creep even after 1500 hours under stress. The increase in creep resistance at 2000 psi is roughly eight-fold for the columbium addition, and eighty-fold for the columbium-molybdenum addition.

"Further, even to approximate the low creep rate of the columbium-molybdenum alloy, it is necessary to reduce the stress on the 35/15 alloy to less than one-half at 1800 F. The columbium alloy is evidently of intermediate load carrying ability."

A report by one of our field engineers on the service tests of the carburizing trays, which were subject to heating and quenching, is given below:

"The customer had set up an average of about 3150 hours for the standard Chromax analysis which was quite acceptable. In this experiment the two No. 1 ran 2870 hours and 3415 hours, bracketing the average. One of the No. 2 was returned after 2870 hours, due obviously to the wreck in the furnace and not to a usual failure. The second No. 2 has failed at 3700 hours and both of the No. 3 ran 4500 hours and are now through and being returned for examination. This is an extremely long life by any comparison for this use and as will be seen is about 50% greater than the average of the standard Chromax."

Heats were also made in which titanium and molybdenum were added to standard 35/15 analyses. Analyses of two of these heats are shown below:

	23044	9145	19144
Carbon	0.53	0.61	0.55
Manganese	1.15	1.20	1.36
Silicon	1.57	1.40	1.55
Chromium	15.61	18.33	16.31
Nickel	35.50	37.68	36.13
Titanium	1.61	2.24	1.95
Molybdenum	1.79	1.55	2.24
Iron	Balance	Balance	Balance

Standard creep test samples were sent to the University of Michigan for creep testing and the following results were reported. Tests were made at 1800 F (980 C) under a load of 3000 psi. Heat 9145 reached the second stage at 25 hours with an elongation of 0.00055 inch. At the end of the test, at 1025 hours, it was still in the second stage and had an elongation of 0.001275 inch/inch.

Heat 23044 reached the second stage at 25 hours with an elongation of 0.0001 inch and at the end of 650 hours, when the test was discontinued, it was

still in the second stage and had an elongation of only 0.00016 inch/inch. Heat 19144 reached the second stage in 25 hours with an elongation of 0.0006 inch. At the end of the test, in 1010 hours, it was still in the second stage and had an elongation of 0.00122 inch/inch. Tests have been run which actually showed a minus creep. This shrinkage is due to the precipitation of carbides and of columbium or titanium phases when they are in excess of amounts required to satisfy the carbon contents.

By some small variations in analysis, malleable alloys of the 35% nickel-15% chromium type have shown good creep results. For example, a heat of the following analysis: carbon 0.36%, manganese 1.10%, silicon 1.58%, nickel 35.66%, chromium 16.25%, molybdenum 1.96%, columbium 2.52%, and iron balance, when tested at 1800 F (980 C) under a load of 2500 psi gave the following results.

The test reached second stage in 25 hours with an elongation of 0.00025 inch. At the end of the test in 1125 hours, it was still in the second stage and had an elongation of 0.0025 inch/inch.

From the foregoing data, it will be recognized that the 35% nickel-15% chromium type alloy with molybdenum and with titanium or columbium is a superior alloy and should have extensive applications.

Messrs. Avery and Matthews are to be congratulated for their excellent paper and method of presentation. The data given are a distinct contribution to the understanding and application of heat resisting castings.

Authors' Reply

The comments of those who have discussed this paper are appreciated. Several of them have raised interesting points that we hope will be covered by future work.

Mr. Evans has mentioned the desirability of data covering the 25% chromium-20% nickel or "HK" type of cast alloys. Research on these has been in progress for several years and it is planned to present pertinent engineering data in a future paper. Some preliminary information has been made available for the new METALS HANDBOOK.

The "HT" alloys are commercially weldable and machinable. No comment on this was included as it has been common knowledge for years, the occasional difficulties encountered being related chiefly to shop procedures. Acceptable quantitative data, which would have been desirable for this paper, are apparently lacking. There is some possibility that such information will be developed in the future by co-operation between the Alloy Casting Institute and the American Welding Society if the industrial need is great enough.

The comment on solution heat treatment is very pertinent as it has played an important part in wartime research on the gas turbine alloys. However, it has not yet been established as a practical means of increasing the service ductility of the cast chromium-nickel-iron heat resistant alloys. Tables XXIX and XXX include some data on solution heat treated material. It will be noted that in comparison with as-cast properties the effectively heat treated alloys develop greater strength but lower ductility at room temperature and at 1600 F

(870 C). This experience has been general; solution heat treatment, especially when carried out at a temperature high enough to produce homogenization, increases creep strength but not hot ductility. Thus the data do not confirm the hypothesis that segregation is responsible for the lower ductility of cast alloys.

There is a distinct difference in microscopic structure. Wrought alloys have a relatively uniform distribution of constituents while the cast material, whether coarse or fine-grained, is a mosaic of tiny cells, each of which consists of a periphery of relatively strong austenite containing considerable precipitated carbide surrounding a core of more plastic austenite with a lower carbon content. Undoubtedly this three-dimensional mosaic influences high temperature properties, which change considerably when it is destroyed by homogenization. The exact role of these segregation cells in determining properties is not clear, however.

Mr. Bobrowski probably misunderstood our comments on the relative merits of logarithmic and semilogarithmic plotting of creep data. We are trying to remain open-minded on the subject, believing as Dr. Gillett has pointedly remarked[4] that the great need is for more experimental data before mathematical analyses are accepted. In this paper our own data are presented by logarithmic plotting; the Battelle Memorial Institute results are on semilogarithmic paper, and one A.C.I. heat is presented in both ways. The data at 1800 F (980 C) in Fig. 8, 2150 F (1175 C) in Fig. 10, and 1800 F (980 C) in Fig. 11 coincide rather well with straight lines on the log-log paper. The poor agreement of some of the other points is tentatively attributed to experimental error, which is sometimes quite large on these alloys because of the potent variable of carbide habit.

We strongly suspect that when data follow the semilogarithmic behavior best (assuming the absence of erratic factors) there are two variables involved. Besides the normal stress versus creep or life relationship that we wish to determine, the factors of growth, intergranular oxidation, sluggishness in attaining the stage of minimum creep rate, and change in stress because of reduction in area during progress of the test all may operate singly or together to curve the logarithmic plots downward. In creep testing cast irons the factor of growth is quite important. In much of the published data on ferritic steels at lower temperatures, and in our own laboratory testing of austenitic alloys at and above 1800 F (980 C), intergranular oxidation apparently causes an abrupt change in the logarithmic relationship. If data points are few the breaks may be obscured, making a semilogarithmic plot seem more appropriate.

In some cases, we have found a rather sharp break in creep curves for rates near or below the 1% per 10,000-hour range, the lower load tests exhibiting an unexpectedly high creep rate. Very careful plotting of such data on a magnified scale suggests that the value being used is actually in Stage I and that the creep mechanism is so sluggish that Stage II will require longer than the usual 1000-hour test to establish it with certainty.

Elimination of many of these factors by careful selection of the material

[4]H. W. Gillett, "Some Things We Don't Know About the Creep of Metals," *Transactions*, American Institute of Mining and Metallurgical Engineers, Vol. 135, 1939, p. 15.

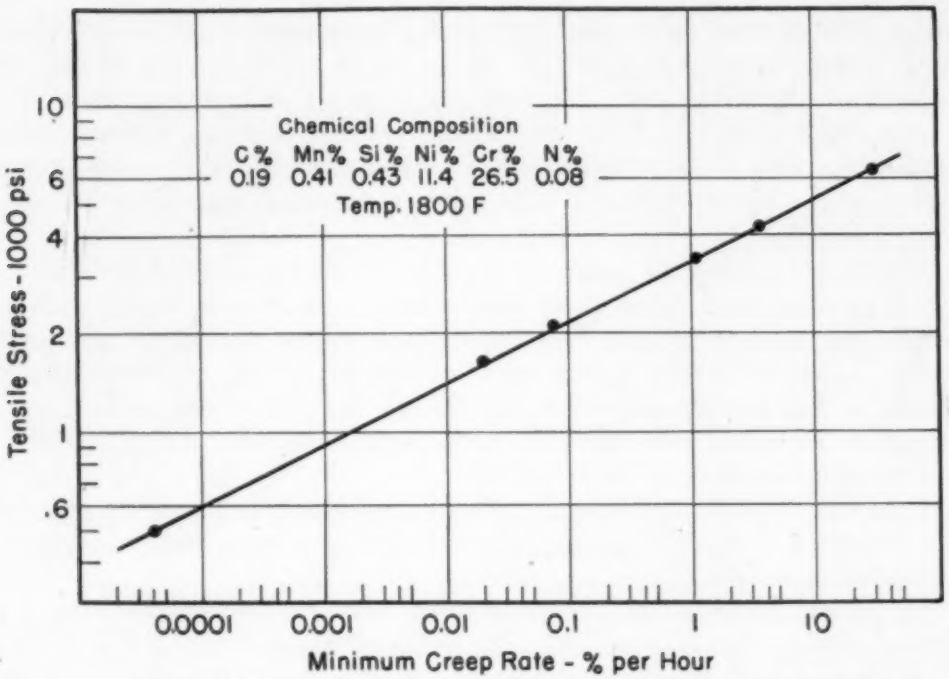


Fig. A—Typical Evidence Justifying the Straight-Line Log-Log Plot of Creep Data.

has some promise of clarifying the situation. Fig. A presents the results of such an experiment. This is a quite weak alloy that is very little influenced by carbide precipitation, it has excellent hot gas corrosion resistance and surface stability with very little tendency toward intergranular oxidation, it is not subject to growth as is the case with cast iron, and the relatively low strength permits rather rapid establishment of Stage II rates. The data points have been corrected for the reduction in area near the end of Stage II. It will be noted that this conforms very well to a logarithmic plot over six logarithmic cycles of strain rate. It is this type of evidence that leads us to use log-log plots until the controlling laws have been more clearly established.

Mr. Sutton's remarks represent confirmation by field experience of the superiority in hot gas corrosion resistance of the "HU" type in comparison with the "HT" compositions. As there is little difference in final cost for the two, the "HU" grade should become increasingly popular.

Mr. German has suggested a relationship between thermal fatigue resistance and creep strength and has indicated that titanium and molybdenum (U. S. Patent 2,408,771) or columbium additions benefit both.

The figures for the occurrence of the third stage of creep for the three alloys tested at 1800 F (980 C) and 2000 psi are not consistent with the data from our Laboratory and Battelle. It is possible that the test conditions permitted control temperature cycling to accelerate the creep rates.

The information on the titanium modifications tested at 1800 F (980 C) and 3000 psi permits conversion to the form of presentation in this paper, with indicated minimum creep rates of 0.00007, 0.00001 and 0.00006% per hour respectively for heats 9145, 23044 and 19144. Assuming stress-creep rate slopes parallel to those tested for the HT-55 type a limiting creep-stress range of

perhaps 3300 to 4200 psi is probable, which is consistent with known effects of strong carbide-forming elements in the Cr-Ni-Fe heat resistant alloys. The comments on eight-fold and eighty-fold improvement in creep resistance should be interpreted carefully. Note that a hundred-fold decrease in creep rate at constant load may mean only a doubling of load-carrying ability, and even this relation is dependent on associated fracture behavior and on the slope of plotted creep data.

The idea that thermal fatigue and creep are related is compatible with the analysis presented in our paper. If plastic flow occurs on each heating cycle it is expected that ordinary tensile ductility will control the occurrence of cracking. The A.C.I. test at Battelle represents these conditions. If the short-time creep strength is high enough to prevent plastic flow, however, a reversal of behavior is expected and good resistance to cyclic thermal stresses, without regard to room temperature ductility, is anticipated.

Note that, in contrast to many applications, short-time strength is apparently more important to thermal fatigue behavior than long-term creep data, as heat treating cycles seldom exceed a few hours.

It was not intended that this paper cover unusual alloy modifications of the "HT" type but as a contribution to the study of thermal fatigue the following data indicating the influence of columbium on relatively short-time creep properties are presented (Table A).

Table A
Columbium In "HT" (16% Cr-35% Ni) Alloys

Alloy No.	Chemical Analysis, % C	Mn	Si	Ni	Cr	N	Cb	As-Cast Tensile Properties Ult. Strength psi	Elongation % in 2 in.
HT-56 a	0.56	0.71	1.22	34.7	16.4	0.036	..	66,500	8.0
HT-56 b	0.56	0.89	1.27	34.8	15.9	0.037	..	67,500	8.5
HT-56 Cb1	0.56	0.88	1.29	33.7	16.6	0.029	0.94	67,500	7.0
HT-55 Cb2	0.55	0.88	1.29	33.5	16.5	0.033	1.90	75,000	7.0

		Stress-Strain-Rupture Properties					
		At 1400 F & 30,000 Psi		At 1400 F & 20,000 Psi		At 1800 F & 6000 Psi	
Alloy	Cb %	Fracture Time Hours	Min. Creep Rate % per Hour	Fracture Time Hours	Min. Creep Rate % per Hour	Fracture Time Hours	Min. Creep Rate % per Hour
HT-56 a	..	..	...	37	0.16	22	0.07
HT-56 b	..	1.1	7.2	52	0.16	32	0.05
HT-56 Cb1	0.94	0.78	14.0	46	0.17	123	0.025
HT-55 Cb2	1.90	1.9	5.4	85	0.044	165	0.010

It is not usually possible for an engineer to determine by analysis whether strength at the maximum or ductility at the minimum of a thermal cycle is controlling the tendency to crack. The possibility of obtaining a clear-cut answer (unless the maximum temperature is too low) is presented by a service trial of the HT-55 Cb2 above against HT-20 or a similar low carbon modification with high room temperature ductility and relatively low hot strength.

INDEX OF AUTHORS

VOLUME XXXVIII

TRANSACTIONS OF AMERICAN SOCIETY FOR METALS

1947

A

Ansel, G. 709
Austin, J. B. 28
Avery, Howard S. 437, 957

B

Baldwin, William M., Jr. 757
Barnett, M. K. 471
Bens, Frederick P. 505
Boyer, Howard E. 209

C

Carapella, Louis A. 729
Cavanagh, P. E. 517
Chapin, Edward J. 909
Chen, Hsin-Min 70
Chipman, John 70
Clark, C. L. 148
Cook, Earnshaw 437
Cullen, O. E. 659

D

Dean, R. S. 577
de Coriolis, E. G. 659
Dietrich, R. L. 709
Dorn, J. E. 789

F

Flanigan, A. E. 789
Fredrickson, Jay W. 593
Freeman, J. W. 148

G

Geil, G. W. 551
George, P. F. 686
Goldsmith, J. R. 398
Graham, T. R. 577
Grange, R. A. 879

H

Hayward, Carle R. 909
Hollomon, J. H. 807
Howald, Thomas S. 757
Huebler, Jack 659

J

Jaffe, L. D. 807

K

Kahles, John F. 618

L

Liedholm, C. A. 180
Long, J. R. 577

M

Matthews, Norman A. 957
McAdam, D. J., Jr. 551
McCarthy, D. E. 807
Meinhart, W. L. 398
Morris, L. D. 848

N

Norton, M. R. 807
Nyquist, Helen L. 271

P

Paschkis, Victor 117

S

Segsworth, R. S. 517
Shaw, William E. 729
Shepherd, B. F. 354
Smith, L. W. 848
Sugden, D. P. 577

T

Tarasov, L. P. 331
Tedsen, L. F. 789
Thibault, N. W. 271, 331

U

Udy, M. C. 471

V

Valentine, K. B. 488

W

Wilks, Charles R. 437
Woodard, D. H. 551

Z

Zapffe, Carl A. 239
Ziegler, N. A. 398

INDEX OF SUBJECTS AND AUTHORS OF PAPERS

VOLUME XXXVIII

TRANSACTIONS OF AMERICAN SOCIETY FOR METALS

1947

A

Age Hardening Copper-Cobalt-Manganese Alloys—*By Jay W. Fredrickson* 593
Aircraft Steel Castings; Metallurgical and Structural Investigation of—*By L. W. Smith and L. D. Morris* 848
Aluminum Sheet Bearing Properties and Shear Strength of 24S-T Rivets at Elevated Temperatures—*By A. E. Flanigan, L. F. Tedsen and J. E. Dorn* 789
Annealed and Cold-Worked Alloys Containing 2 to 20% Manganese; The Properties of—Copper-Manganese Alloys—*By R. S. Dean, J. R. Long, T. R. Graham and D. P. Sugden* 577
Annealed Hypoeutectoid Steel; Factors Influencing the Pearlitic Microstructure of—*By R. A. Grange* 879
Annual Address of the President 9
Annual Dinner of ASM 23
Annual Meeting of ASM 8
Annual Report of the Secretary 15
Annual Report of the Treasurer 13
Apparent Influence of Grain Size on the High Temperature Properties of Austenitic Steels—*By C. L. Clark and J. W. Freeman* 148
Austenitic Steels; Apparent Influence of Grain Size on the High Temperature Properties of—*By C. L. Clark and J. W. Freeman* 148

B

Bearing Properties of 24S-T Sheet and Shear Strength of 24S-T Rivets at Elevated Temperatures—*By A. E. Flanigan, L. F. Tedsen and J. E. Dorn* 789

C

Calculation of Press Forging Pressures and Application to Magnesium Forgings—*By R. L. Dietrich and G. Ansel* 709
Campbell Memorial Lecture—21st; The Effect of Changes in Condition of Carbides on Some Properties of Steel—*By J. B. Austin* 28
Carbides on Some Properties of Steel; The Effect of Changes in Condition of—*By J. B. Austin* 28
Carbon Concentration Control—*By E. G. de Coriolis, O. E. Cullen and Jack Huebler* 659
Carbon-Molybdenum and Cast Carbon Steels; The Effect of Manganese on the Properties of—*By N. A. Ziegler, W. L. Meinhart and J. R. Goldsmith* 398
Cast Alloy Steels; A Laboratory Study of Quench Cracking in—*By M. C. Udy and M. K. Barnett* 471
Cast Alloy Steels; Relation of Quenching Rate and Hardenability to the Mechanical Properties of Several Heat Treated—*By Charles R. Wilks, Howard S. Avery and Earnshaw Cook* 437
Cast Carbon and Carbon-Molybdenum Steels; The Effect of Manganese on the Properties of—*By N. A. Ziegler, W. L. Meinhart and J. R. Goldsmith* 398
Cast Heat Resistant Alloys of the 16% Chromium-35% Nickel Type—*By Howard S. Avery and Norman A. Matthews* 957

Chromium (16%)-35% Nickel Type; Cast Heat Resistant Alloys of the—*By Howard S. Avery and Norman A. Matthews* 957
Chromium-Oxygen Equilibrium in Liquid Iron—*By Hsin-Min Chen and John Chipman* 70
Cobalt-Copper-Manganese Alloys; Age Hardening—*By Jay W. Fredrickson* 593
Cold-Worked and Annealed Alloys Containing 2 to 20% Manganese; The Properties of—Copper-Manganese Alloys—*By R. S. Dean, J. R. Long, T. R. Graham and D. P. Sugden* 577
Continuous Cooling Transformations; Experimental Studies of—*By C. A. Liedholm* 180
Cooling Transformations; Experimental Studies of Continuous—*By C. A. Liedholm* 180
Copper-Cobalt-Manganese Alloys; Age Hardening—*By Jay W. Fredrickson* 593
Copper; Influence of the Strain Rate and the Stress System on the Mechanical Properties of—*By D. J. McAdam, Jr., G. W. Geil and D. H. Woodard* 551
Copper-Manganese Alloys; The Properties of Cold-Worked and Annealed Alloys Containing 2 to 20% Manganese—*By R. S. Dean, J. R. Long, T. R. Graham and D. P. Sugden* 577
Copper-Titanium Alloy Coatings on Mild Steel—*By Edward J. Chapin and Carle R. Hayward* 909
Cupping Operation; Folding in the—*By William M. Baldwin, Jr., and Thomas S. Howald* 757

D

Determination of Knoop Hardness Numbers Independent of Load—*By L. P. Tarasov and N. W. Thibault* 331

E

Effect of Changes in Condition of Carbides on Some Properties of Steel—*By J. B. Austin* 28
Effect of Manganese on the Properties of Cast Carbon and Carbon-Molybdenum Steels—*By N. A. Ziegler, W. L. Meinhart and J. R. Goldsmith* 398
Effects of Microstructure on the Mechanical Properties of Steel—*By J. H. Hollomon, L. D. Jaffe, D. E. McCarthy and M. R. Norton* 807
Election of Officers of ASM 22
Electroplated Lockwashers; Stress Cracking of—*By K. B. Valentine* 488
Elevated Temperatures; Bearing Properties of 24S-T Sheet and Shear Strength of 24S-T Rivets at—*By A. E. Flanigan, L. F. Tedsen and J. E. Dorn* 789
Elevated Temperatures; Hardness Testing of Metals and Alloys at—*By Frederick P. Bens* 505
Equilibrium in Liquid Iron; Chromium-Oxygen—*By Hsin-Min Chen and John Chipman* 70
Experimental Studies of Continuous Cooling Transformations—*By C. A. Liedholm* 180

F

Factors Influencing the Pearlitic Microstructure of Annealed Hypoeutectoid Steel—*By R. A. Grange* 879
Folding in the Cupping Operation—*By William M. Baldwin, Jr., and Thomas S. Howald* 757
Formation and Transformation Studies of Iron-Carbon Powder Alloys—*By John F. Kahles* 618

G

Grain Size on the High Temperature Properties of Austenitic Steels; Apparent Influence of—*By C. L. Clark and J. W. Freeman* 148

H

Hardenability and Quenching Rate Relation to the Mechanical Properties of Several Heat Treated Cast Alloy Steels—*By Charles R. Wilks, Howard S. Avery and Earnshaw Cook* 437
Hardenability of Shallow Hardening Steels Determined by the P-V Test—*By B. F. Shepherd* 354
Hardness Testing of Metals and Alloys at Elevated Temperatures—*By Frederick P. Bens* 505
Heat Resistant Alloys (Cast) of the 16% Chromium-35% Nickel Type—*By Howard S. Avery and Norman A. Matthews* 957
Heat Treated Cast Alloy Steels; Relation of Quenching Rate and Hardenability to the Mechanical Properties of Several—*By Charles R. Wilks, Howard S. Avery and Earnshaw Cook* 437
High Temperature Properties of Austenitic Steels; Apparent Influence of Grain Size on the—*By C. L. Clark and J. W. Freeman* 148
Hypoeutectoid Steel (Annealed); Factors Influencing the Pearlitic Microstructure of—*By R. A. Grange* 879

I

Influence of the Strain Rate and the Stress System on the Mechanical Properties of Copper—By *D. J. McAdam, Jr., G. W. Geil and D. H. Woodard* 551
Interrupted Quench and Its Practical Aspects—*By Howard E. Boyer* 209
Iron-Carbon Powder Alloys; Formation and Transformation Studies of—*By John F. Kahles* 618

K

Knoop Hardness of Hard Substances and Factors Affecting Its Determination; Measured—*By N. W. Thibault and Helen L. Nyquist* 271
Knoop Hardness Numbers Independent of Load; Determination of—*By L. P. Tarasov and N. W. Thibault* 331

L

Laboratory Study of Quench Cracking in Cast Alloy Steels—*By M. C. Udy and M. K. Barnett* 471
Liquid Iron; Chromium-Oxygen Equilibrium in—*By Hsin-Min Chen and John Chipman* 70
Lockwashers (Electroplated); Stress Cracking of—*By K. B. Valentine* .. 488

M

Magnesium Alloys; Some Special Metallographic Techniques for—*By P. F. George* 686
Magnesium Forgings; Calculation of Press Forging Pressures and Application to—*By R. L. Dietrich and G. Ansel* 709
Magnesium (Pure); Plastic Deformational Analyses on—*By Louis A. Carapella and William E. Shaw* 729
Manganese (2 to 20%); The Properties of Cold-Worked and Annealed Alloys Containing—Copper-Manganese Alloys—*By R. S. Dean, J. R. Long, T. R. Graham and D. P. Sugden* 577
Manganese-Copper Alloys—The Properties of Cold-Worked and Annealed Alloys Containing 2 to 20% Manganese—*By R. S. Dean, J. R. Long, T. R. Graham and D. P. Sugden* 577
Manganese-Copper-Cobalt Alloys; Age Hardening—*By Jay W. Fredrickson* 593
Manganese Effect on the Properties of Cast Carbon and Carbon-Molybdenum Steels—*By N. A. Ziegler, W. L. Meinhart and J. R. Goldsmith* 398
Measured Knoop Hardness of Hard Stubstances and Factors Affecting Its Determination—*By N. W. Thibault and Helen L. Nyquist* 271
Mechanical Properties of Copper; Influence of the Strain Rate and the Stress System on the—*By D. J. McAdam, Jr., G. W. Geil and D. H. Woodard* 551

Mechanical Properties of Steel; Effects of Microstructure on the—*By J. H. Hollomon, L. D. Jaffe, D. E. McCarthy and M. R. Norton* 807
Metallographic Techniques for Magnesium Alloys; Some Special—*By P. F. George* 686
Metallurgical and Structural Investigation of Steel Castings for Aircraft—*By L. W. Smith and L. D. Morris* 848
Metals and Alloys at Elevated Temperatures; Hardness Testing of—*By Frederick P. Bens* 505
Microstructure Effects on the Mechanical Properties of Steel—*By J. H. Hollomon, L. D. Jaffe, D. E. McCarthy and M. R. Norton* 807
Mild Steel; Copper-Titanium Alloy Coatings on—*By Edward J. Chapin and Carle R. Hayward* 909
Mine Hoist Cable; Nondestructive Inspection of—*By P. E. Cavanagh and R. S. Segsworth* 517

N

Nickel (35%)-16% Chromium Type; Cast Heat Resistant Alloys of the—*By Howard S. Avery and Norman A. Matthews* 957
Nondestructive Inspection of Mine Hoist Cable—*By P. E. Cavanagh and R. S. Segsworth* 517

O

Oxygen-Chromium Equilibrium in Liquid Iron—*By Hsin-Min Chen and John Chipman* 70

P

Pearlitic Microstructure of Annealed Hypoeutectoid Steel; Factors Influencing the—*By R. A. Grange* 879
Periodic Chart for Metallurgists—*By Carl A. Zapffe* 239
Plastic Deformational Analyses on Pure Magnesium—*By Louis A. Carapella and William E. Shaw* 729
Powder Alloys (Iron-Carbon); Formation and Transformation Studies of—*By John F. Kahles* 618
President's Annual Address 9
Press Forging Pressures and Application to Magnesium Forgings; Calculation of—*By R. L. Dietrich and G. Ansel* 709
Pure Magnesium; Plastic Deformational Analyses on—*By Louis A. Carapella and William E. Shaw* 729
P-V Test; Hardenability of Shallow Hardening Steels Determined by the —*By B. F. Shepherd* 354

Q

Quench Cracking in Cast Alloy Steels; Laboratory Study of—*By M. C. Udy and M. K. Barnett* 471
Quenching (Interrupted) and Its Practical Aspects—*By Howard E. Boyer* 209
Quenching Rate and Hardenability Relation to the Mechanical Properties of Several Heat Treated Cast Alloy Steels—*By Charles R. Wilks, Howard S. Avery and Earnshaw Cook* 437

R

Relation of Quenching Rate and Hardenability to the Mechanical Properties of Several Heat Treated Cast Alloy Steels—*By Charles R. Wilks, Howard S. Avery and Earnshaw Cook* 437
Rivets (24S-T) at Elevated Temperatures; Bearing Properties of 24S-T Sheet and Shear Strength of—*By A. E. Flanigan, L. F. Tedsen and J. E. Dorn* 789

S

Secretary's Annual Report 15
Shallow Hardening Steels Determined by the P-V Test; Hardenability of —*By B. F. Shepherd* 354
Shear Strength of 24S-T Rivets at Elevated Temperatures; Bearing Properties of 24S-T Sheet—*By A. E. Flanigan, L. F. Tedsen and J. E. Dorn* 789
Sheet (24S-T) and Shear Strength of 24S-T Rivets at Elevated Temperatures; Bearing Properties of—*By A. E. Flanigan, L. F. Tedsen and J. E. Dorn* 789
Solidification; Theoretical Thermal Studies of Steel Ingot—*By Victor Paschkis* 117
Some Special Metallographic Techniques for Magnesium Alloys—*By P. F. George* 686
Steel Castings for Aircraft; Metallurgical and Structural Investigation of —*By L. W. Smith and L. D. Morris* 848
Steel Ingot Solidification; Theoretical Thermal Studies of—*By Victor Paschkis* 117
Strain Rate and the Stress System Influence on the Mechanical Properties of Copper—*By D. J. McAdam, Jr., G. W. Geil and D. H. Woodard* .. 551
Stress Cracking of Electroplated Lockwashers—*By K. B. Valentine* 488
Stress System and Strain Rate Influence on the Mechanical Properties of Copper—*By D. J. McAdam, Jr., G. W. Geil and D. H. Woodard* 551
Structural and Metallurgical Investigation of Steel Castings for Aircraft—*By L. W. Smith and L. D. Morris* 848

T

Technical Program and Reports of Officers, ASM—28th Annual Convention, Atlantic City, November 18 to 22, 1946 1
Theoretical Thermal Studies of Steel Ingot Solidification—*By Victor Paschkis* 117
Titanium-Copper Alloy Coatings on Mild Steel—*By Edward J. Chapin and Carle R. Hayward* 909
Transformation and Formation Studies of Iron-Carbon Powder Alloys—*By John F. Kahles* 618
Treasurer's Report 13